

# Conceptual Model Report: Central and Southern Portions of Gulf Coast Aquifer System in Texas



*Report By:*

*Jianyou (Jerry) Shi, Ph.D., P.G.*

*Radu Boghici, P.G.*

*Roberto Anaya, P.G.*

## **Texas Water Development Board**

P.O. Box 13231

Austin, Texas 78711-3231

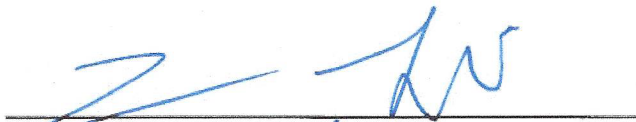
April 19, 2022

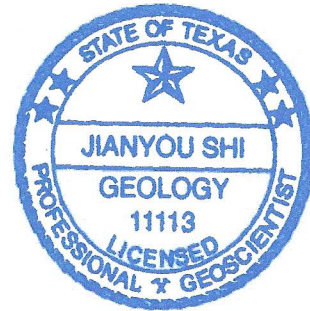
## Geoscientist Seals

The following professional geoscientists contributed to this conceptual model report and associated data compilation and analyses:

Jianyou (Jerry) Shi, P.G.

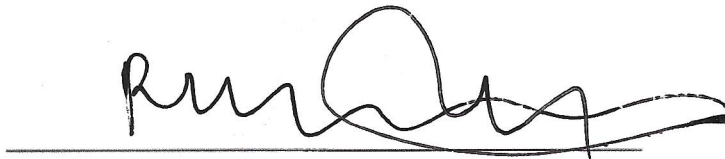
Dr. Shi was the project manager and responsible for oversight on the project and technical aspects not covered by the co-authors of this report.

  
4/19/2022



Radu Boghici, P.G.


Mr. Boghici was responsible for compiling groundwater water level, groundwater quality, digital specific capacity test, and groundwater pumping.

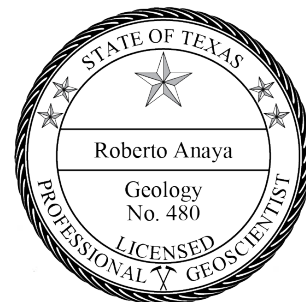
  
4/19/2022



Roberto Anaya, P.G.

Mr. Anaya was responsible for collecting hydrogeologic framework picks from previous studies.

  
4/19/2022



*This page is intentionally blank.*

## Table of Contents

<b>CONCEPTUAL MODEL REPORT: CENTRAL AND SOUTHERN PORTIONS OF GULF COAST AQUIFER SYSTEM IN TEXAS</b>		<b>1</b>
<b>EXECUTIVE SUMMARY:</b>		<b>23</b>
<b>1.0</b>	<b>INTRODUCTION</b>	<b>26</b>
<b>2.0</b>	<b>STUDY AREA</b>	<b>32</b>
2.1	PHYSIOGRAPHY AND CLIMATE .....	42
2.2	GEOLOGY.....	62
2.2.1.	<i>Structural Setting</i> .....	62
2.2.2.	<i>Geologic History</i> .....	63
2.2.3.	<i>Faults</i> .....	66
2.2.4.	<i>Salt Domes</i> .....	66
2.2.5.	<i>Surface Geology</i> .....	67
<b>3.0</b>	<b>PREVIOUS INVESTIGATIONS</b>	<b>74</b>
3.1	RECONNAISSANCE INVESTIGATIONS AND LOCAL STUDIES.....	74
3.2	SINGLE COUNTY STUDIES .....	74
3.2.1	<i>Aransas County</i> .....	74
3.2.2	<i>Bee County</i> .....	75
3.2.3	<i>Brooks County</i> .....	75
3.2.4	<i>Cameron County</i> .....	75
3.2.5	<i>DeWitt County</i> .....	75
3.2.6	<i>Duval County</i> .....	76
3.2.7	<i>Fayette County</i> .....	76
3.2.8	<i>Goliad County</i> .....	76
3.2.9	<i>Jackson County</i> .....	77
3.2.10	<i>Jim Wells County</i> .....	77
3.2.11	<i>Karnes County</i> .....	77
3.2.12	<i>Live Oak County</i> .....	78
3.2.13	<i>Matagorda County</i> .....	78
3.2.14	<i>Refugio County</i> .....	78
3.2.15	<i>Starr County</i> .....	79
3.3	MULTIPLE COUNTY STUDIES .....	79

3.4	REGIONAL STUDIES .....	82
3.5	GROUNDWATER FLOW MODELING STUDIES .....	84
<b>4.0</b>	<b>HYDROLOGIC SETTING</b> .....	<b>90</b>
4.1	HYDROSTRATIGRAPHY .....	90
4.2.	GROUNDWATER LEVELS AND FLOWS .....	115
4.2.1.	<i>Lateral Groundwater Flow</i> .....	115
4.2.2.	<i>Water-Level Change over Time</i> .....	116
4.2.3.	<i>Cross-Formation Flow</i> .....	117
4.3.	GROUNDWATER RECHARGE.....	150
4.3.1	<i>Estimate of Groundwater Recharge from Stream Baseflow</i> .....	150
4.3.2	<i>Correlation between Groundwater Recharge and Precipitation</i> .....	153
4.3.3	<i>Recharge Distribution</i> .....	154
4.4	RIVERS, STREAMS, LAKES, SPRINGS, AND CANALS .....	163
4.4.1	<i>Gain or Loss of Rivers and Streams</i> .....	163
4.4.2	<i>Lakes and Reservoirs</i> .....	164
4.4.3	<i>Springs</i> .....	165
4.4.4	<i>Diversion from Lower Rio Grande</i> .....	165
4.5	HYDRAULIC PROPERTIES .....	188
4.5.1	<i>Transmissivity and Hydraulic Conductivity from Pumping Tests</i> .....	189
4.5.2	<i>Transmissivity and Hydraulic Conductivity from Specific Capacity Tests</i> .....	191
4.5.3	<i>Comparison of Hydraulic Conductivity Values between Pumping Tests and Specific Capacity Tests</i> .....	191
4.5.4	<i>Summary of Hydraulic Conductivity Values from Pumping Tests and Specific Capacity Tests</i> .....	191
4.5.5	<i>Correlation between Hydraulic Conductivity and Sand Fraction</i> .....	192
4.5.6	<i>Storativity and Specific Yield</i> .....	196
4.6	AQUIFER DISCHARGE.....	229
4.6.1.	<i>Evapotranspiration</i> .....	229
4.6.2.	<i>Aquifer Discharge through Pumping</i> .....	230
4.7	GROUNDWATER QUALITY .....	244
4.7.1	<i>Chicot Aquifer</i> .....	248
4.7.2	<i>Evangeline Aquifer</i> .....	249
4.7.3	<i>Burkeville Unit</i> .....	251
4.7.4	<i>Jasper Aquifer</i> .....	252
4.8	SUBSIDENCE .....	304
4.8.1	<i>Correlation between Compaction and Groundwater Level Decline</i> .....	304

4.8.2	<i>Subsidence in Study Area</i> .....	306
<b>5.0</b>	<b>CONCEPTUAL GROUNDWATER FLOW MODEL FOR CENTRAL AND SOUTHERN PORTIONS OF THE GULF COAST AQUIFER SYSTEM</b>	<b>314</b>
5.1	PRE-DEVELOPMENT CONDITIONS (STEADY STATE) .....	316
5.2	POST-DEVELOPMENT CONDITIONS (TRANSIENT STATE) .....	318
5.3	IMPLEMENTATION OF GROUNDWATER RECHARGE.....	318
<b>6.0</b>	<b>FUTURE IMPROVEMENTS</b>	<b>321</b>
	<b>ACKNOWLEDGMENTS</b>	<b>323</b>
	<b>REFERENCES</b>	<b>325</b>
	<b>APPENDIX A: GROUNDWATER LEVEL HYDROGRAPHS</b>	<b>333</b>
	<b>APPENDIX B: GROUNDWATER LEVEL AT WELL CLUSTERS TO SHOW CROSS FORMATION FLOW</b>	<b>452</b>
	<b>APPENDIX C: ESTIMATED GROUNDWATER RECHARGE FROM STREAM BASEFLOW-PRECIPIATION CORRELATION FOR YEARS BETWEEN 1981 AND 2014</b>	<b>489</b>
	<b>APPENDIX D: SUMMARY OF STREAM GAIN OR LOSS</b>	<b>521</b>
	<b>APPENDIX E: SUMMARY OF HYDRAULIC CONDUCTIVITY AND STORATIVITY/SPECIFIC YIELD VALUES</b>	<b>534</b>
	<b>APPENDIX F: HYDROGRAPH OF TOTAL DISSOLVED SOLIDS</b>	<b>546</b>

**LIST OF FIGURES AND TABLES**

Figure 1.0.1 Location of major aquifers in Texas..... 29

Figure 1.0.2 Location of minor aquifers in Texas..... 30

Figure 1.0.3 Location of the central and southern portions of the Gulf Coast Aquifer System in Texas.....31

Figure 2.0.1 Locations of highways, cities, and towns in central and southern portions of the Gulf Coast Aquifer System in Texas (TNRIS, 2018). ..... 34

Figure 2.0.2 Locations of river basins and major streams and rivers in central and southern portions of the Gulf Coast aquifer System in Texas (TNRIS, 2018). 36

Figure 2.0.3 Locations of existing reservoirs and lakes greater than one square mile in central and southern portions of the Gulf Coast aquifer System in Texas (TNRIS, 2018). ..... 37

Figure 2.0.4 Texas River Authorities in study area. .... 38

Figure 2.0.5 Texas Regional Water Planning Areas in study area. .... 39

Figure 2.0.6 Texas Groundwater Conservation Districts (GCDs), Underground Water Conservation Districts (UWCD), and Aquifer Storage and Recovery Conservation District (ASRCD) in study area. .... 40

Figure 2.1.1 Physiographic provinces in study area (Wermund, 1996). ..... 44

Figure 2.1.2 Level III ecological regions in study area (U. S. Environmental Protection Agency, 2013). ..... 45

Figure 2.1.3 Elevation of land surface and bathymetry of Gulf of Mexico. Land surface elevation data are from U. S. Geological Survey National Elevation Dataset. Bathymetry of Gulf of Mexico (w98e78n31s18\_bathy.img) is downloaded from <http://gcoos.tamu.edu/products/topography/SRTM30PLUS.html>. .... 46

Figure 2.1.4 Climate classifications of study area (based on Larkin and Bomar, 1983)..... 47

Figure 2.1.5 Average annual air temperature for time period 1981 to 2010 (based on PRISM 30-year normal downloaded from <https://prism.oregonstate.edu/normals/>). ..... 48

Figure 2.1.6 Average annual precipitation for time period 1980 to 2015 (PRISM, 2018). 49

Figure 2.1.7 Measured annual precipitation at stations in Calhoun (Point Comfor0.00), Dewitt (Yoakum), Lavaca (Hallettsville 2 N), Matagorda (Palacios Municipal Airport), and Victoria (Victoria Regional Airport) counties (National Climatic Data Center, 2018). ..... 50

Figure 2.1.8 Measured annual precipitation at stations in Karnes (Runge), Live Oak (George West 2 SSW), Nueces (Corpus Christi International Airport), Jim Wells (Mathis 4 SSW), and Refugio (Welder Wlfe Foundation) counties (National Climatic Data Center, 2018). ..... 52

Figure 2.1.9 Measured annual precipitation at stations in Cameron (Brownsville South Padre Island International Airport), Hidalgo (McAllen Miller International Airport), and Kleberg (Kingsville) counties (National Climatic Data Center, 2018). ..... 54

Figure 2.1.10 Measured average monthly precipitation between 1980 and 2015 at stations in Calhoun (Point Comfor0.00), Dewitt (Yoakum), Lavaca (Hallettsville 2 N), Matagorda (Palacios Municipal Airport), and Victoria (Victoria Regional Airport) counties (National Climatic Data Center, 2018). ..... 55

Figure 2.1.11	Measured average monthly precipitation between 1980 and 2015 at stations in Karnes (Runge), Live Oak (George West 2 SSW), Nueces (Corpus Christi International Airport), Jim Wells (Mathis 4 SSW), and Refugio (Welder Life Foundation) counties (National Climatic Data Center, 2018).....	56
Figure 2.1.12	Measured average monthly precipitation between 1980 and 2015 at stations in Cameron (Brownsville South Padre Island International Airport), Hidalgo (McAllen Miller International Airport), and Kleberg (Kingsville) counties (National Climatic Data Center, 2018). .....	57
Figure 2.1.13	Average annual lake evaporation rate (inch per year) between 1971 and 2000 in study area (Narasimhan and others, 2007).....	58
Figure 2.1.14	Average lake evaporation difference between August and January for the period 1971 through 2000 in study area (based on monthly data from Narasimhan and others (2007))......	59
Figure 2.1.15	Estimated actual evapotranspiration in study area (Scanlon and others, 2012). .....	60
Figure 2.1.16	Soils in study area based on Soil Survey Geographic Database (SSURGO) downloaded from <a href="https://www.arcgis.com/apps/View/index.html?appid=cdc49bd63ea54dd2977f3f2853e07fff">https://www.arcgis.com/apps/View/index.html?appid=cdc49bd63ea54dd2977f3f2853e07fff</a> .....	61
Table 2.2.1.	Stratigraphy and hydrogeologic classification of geologic units in study area (modified from Baker, 1995). .....	68
Figure 2.2.1	Major structures in central and southern portions of the Gulf Coast aquifer System in Texas and surrounding regions (modified from Young and others (2014))......	69
Figure 2.2.2	Locations of major deltaic deposition centers and coastline for selected depositional episodes (modified from Young and others (2010). .....	70
Figure 2.2.3	Locations of major faults in the study area and its vicinity (based on Tectonic Map of Texas by Bureau of Economic Geology of The University of Texas at Austin, 1997)......	71
Figure 2.2.4	Locations of shallow salt domes in the study area and its vicinity (location based on Bureau of Economic Geology (1997); depth to salt dome cap based on Young and others (2014))......	72
Figure 2.2.5	Surface geology of the study area (based on Bureau of Economic Geology (2013))......	73
Figure 3.5.1	Areal coverage of previous groundwater flow models.....	89
Figure 4.1.1	Locations of well logs and control points.....	94
Figure 4.1.2	Control points along and behind western perimeters of the hydrostratigraphic layers.....	95
Figure 4.1.3	Elevation of ground surface and Gulf of Mexico bottom (top of Layer 1). The ground surface elevation is based on U. S. Geological Survey’s National Elevation Dataset (NED). The bathymetry of the Gulf of Mexico bottom is based on the U. S. Geological Survey’s SRTM3_PLUS V6.0.....	96
Figure 4.1.4	Thickness of Layer 1 (alluvium/eolian deposits and Chicot Aquifer). .....	97
Figure 4.1.5	Bottom elevation of Layer 1 (Alluvium/Eolian deposits and Chicot Aquifer). .....	98
Figure 4.1.6	Thickness of Layer 2 (Evangeline Aquifer). .....	99



Figure 4.1.7	Bottom elevation of Layer 2 (Evangeline Aquifer).....	100
Figure 4.1.8	Thickness of Layer 3 (Burkeville Unit). ....	101
Figure 4.1.9	Bottom Elevation of Layer 3 (Burkeville Unit).....	102
Figure 4.1.10	Thickness of Layer 4 (Jasper Aquifer).....	103
Figure 4.1.11	Bottom elevation of Layer 4 (Jasper Aquifer).....	104
Figure 4.1.12	Location of hydrostratigraphic cross sections. ....	105
Figure 4.1.13	Hydrostratigraphic cross section 01 along west-east direction. Vertical lines represent well logs and horizontal bars are hydrostratigraphic picks. ....	106
Figure 4.1.14	Hydrostratigraphic cross section 02 along west-east direction. Vertical lines represent well logs and horizontal bars are hydrostratigraphic picks. ....	107
Figure 4.1.15	Hydrostratigraphic cross section 03 along west-east direction. Vertical lines represent well logs and horizontal bars are hydrostratigraphic picks. ....	108
Figure 4.1.16	Hydrostratigraphic cross section 04 along west-east direction. Vertical lines represent well logs and horizontal bars are hydrostratigraphic picks. ....	109
Figure 4.1.17	Hydrostratigraphic cross section 05 along west-east direction. Vertical lines represent well logs and horizontal bars are hydrostratigraphic picks. ....	110
Figure 4.1.18	Hydrostratigraphic cross section 06 along west-east direction. Vertical lines represent well logs and horizontal bars are hydrostratigraphic picks. ....	111
Figure 4.1.19	Hydrostratigraphic cross section 01 along south-north direction. Vertical lines represent well logs and horizontal bars are hydrostratigraphic picks. ....	112
Figure 4.1.20	Hydrostratigraphic cross section 02 along south-north direction. Vertical lines represent well logs and horizontal bars are hydrostratigraphic picks. ....	113
Figure 4.1.21	Hydrostratigraphic cross section 03 along south-north direction. Vertical lines represent well logs and horizontal bars are hydrostratigraphic picks. ....	114
Figure 4.2.1	Number of average annual water level measurements in Gulf Coast Aquifer System.....	119
Figure 4.2.2	Water levels in alluvium/eolian and Chicot Aquifer (1980). ....	120
Figure 4.2.3	Water levels in alluvium/eolian and Chicot Aquifer (1990). ....	121
Figure 4.2.4	Water levels in alluvium/eolian and Chicot Aquifer (2000). ....	122
Figure 4.2.5	Water levels in alluvium/eolian and Chicot Aquifer (2010). ....	123
Figure 4.2.6	Water levels in alluvium/eolian and Chicot Aquifer (2015). ....	124
Figure 4.2.7	Water levels in Evangeline Aquifer (1980). ....	125
Figure 4.2.8	Water levels in Evangeline Aquifer (1990). ....	126
Figure 4.2.9	Water levels in Evangeline Aquifer (2000). ....	127
Figure 4.2.10	Water levels in Evangeline Aquifer (2010). ....	128
Figure 4.2.11	Water levels in Evangeline Aquifer (2015). ....	129
Figure 4.2.12	Water levels in Burkeville Unit (1980). ....	130
Figure 4.2.13	Water levels in Burkeville Unit (1990). ....	131
Figure 4.2.14	Water levels in Burkeville Unit (2000). ....	132
Figure 4.2.15	Water levels in Burkeville Unit (2010). ....	133
Figure 4.2.16	Water levels in Burkeville Unit (2015). ....	134
Figure 4.2.17	Water levels in Jasper Aquifer (1980).....	135
Figure 4.2.18	Water levels in Jasper Aquifer (1990).....	136

Figure 4.2.19	Water levels in Jasper Aquifer (2000).....	137
Figure 4.2.20	Water levels in Jasper Aquifer (2010).....	138
Figure 4.2.21	Water levels in Jasper Aquifer (2015).....	139
Figure 4.2.22	Water level hydrographs at selected wells in alluvium/eolian and Chicot Aquifer. ....	140
Figure 4.2.23	Water level hydrographs at selected wells in alluvium/eolian and Chicot Aquifer. ....	141
Figure 4.2.24	Water level hydrographs at selected wells in Evangeline Aquifer.....	142
Figure 4.2.25	Water level hydrographs at selected wells in Evangeline Aquifer.....	143
Figure 4.2.26	Water level hydrographs at selected wells in Evangeline Aquifer and Burkeville Unit.....	144
Figure 4.2.27	Water level hydrographs at selected wells in Jasper Aquifer.....	145
Figure 4.2.28	Water level difference between two adjacent wells (less than 2,640 feet apart) screened in Chicot and Evangeline aquifers. Positive and negative values represent upward and downward groundwater flow, respectively. ....	146
Figure 4.2.29	Water level difference between two adjacent wells (less than 2,640 feet apart) screened in Evangeline Aquifer and Burkeville Unit. Positive and negative values represent upward and downward groundwater flow, respectively.....	147
Figure 4.2.30	Water level difference between two adjacent wells (less than 2,640 feet apart) screened in Evangeline and Jasper aquifers. Positive and negative values represent upward and downward groundwater flow, respectively. ....	148
Figure 4.2.31	Water level difference between two adjacent wells (less than 2,640 feet apart) screened in Burkeville Unit and Jasper Aquifer. Positive and negative values represent upward and downward groundwater flow, respectively. ....	149
Figure 4.3.1	Estimated groundwater recharge for Gulf Coast Aquifer System (Scanlon and others, 2012).....	155
Figure 4.3.2	Selected river basins, river gages, and permitted historical discharge locations. ....	156
Figure 4.3.3	Observed correlation between overall average groundwater recharge and overall average precipitation at selected river basins (shown in dots) and simulated regression using a logistics growth model (shown as solid line). ....	157
Figure 4.3.4	Groundwater recharge estimated from stream baseflow-precipitation correlation (1980).....	158
Figure 4.3.5	Groundwater recharge estimated from stream baseflow-precipitation correlation (1990).....	159
Figure 4.3.6	Groundwater recharge estimated from stream baseflow-precipitation correlation (2000).....	160
Figure 4.3.7	Groundwater recharge estimated from stream baseflow-precipitation correlation (2010).....	161
Figure 4.3.8	Groundwater recharge estimated from stream baseflow-precipitation correlation (2015).....	162
Figure 4.4.1	Locations of river gages and basins used for evaluating surface water and groundwater interaction. Basins are indexed for identification and discussion purposes.....	167

Figure 4.4.2	Stream gain (positive values) or loss (negative values) results in Basin 4 across Austin, Colorado, Fort Bend, and Wharton counties. ....	168
Figure 4.4.3	Stream gain (positive values) or loss (negative values) results in Basin 12 across DeWitt, Jackson, and Lavaca counties. ....	169
Figure 4.4.4	Stream gain (positive values) or loss (negative values) results in Basin 21 across Bee and Refugio counties. ....	170
Figure 4.4.5	Stream gain (positive values) or loss (negative values) results in Basin 27 across Jim Wells, Nueces, and San Patricio counties. ....	171
Figure 4.4.6	Stream gain (positive values) or loss (negative values) results in Basin 29 across Duval, Jim Wells, Live Oak, and McMullen counties. ....	172
Figure 4.4.7	Stream gain (positive values) or loss (negative values) results in Basin 31 across Duval, Jim Wells, and Webb counties. ....	173
Figure 4.4.8	Results of river gain/loss study by Slade and others (2002). ....	174
Figure 4.4.9	Locations of lakes and reservoirs greater than one square mile in study area. ....	175
Figure 4.4.10	Water level elevation at Coletto Creek Reservoir. ....	176
Figure 4.4.11	Water level elevation at Lake Corpus Christi. ....	177
Figure 4.4.12	Water level elevation at Lake Texana. ....	178
Figure 4.4.13	Distribution of springs in study area. ....	179
Figure 4.4.14	Distribution of canals and diversion reaches along Rio Grande in study area. ....	180
Figure 4.4.15	Diversion from Rio Grande to Anzalduas Canal in Mexico. ....	181
Figure 4.4.16	Diversion from Rio Grande along the U. S. side between Rio Grande City and Anzalduas Dam. ....	182
Figure 4.4.17	Diversion from Rio Grande along the U. S. side between Anzalduas Dam and Progreso City. ....	183
Figure 4.4.18	Diversion from Rio Grande along the U. S. side between Progreso City and San Benito City. ....	184
Figure 4.4.19	Diversion from Rio Grande along the U. S. side between San Benito City and Brownsville City. ....	185
Figure 4.4.20	Diversion from Rio Grande along the U. S. side between Brownsville City and Gulf of Mexico. ....	186
Figure 4.4.21	Total diversion from Rio Grande along the U. S. side. ....	187
Figure 4.5.1	Distribution of average horizontal hydraulic conductivity values from pumping tests in the study area. ....	199
Figure 4.5.2	Distribution of average horizontal hydraulic conductivity values from specific capacity tests in Chicot Aquifer in the study area. ....	200
Figure 4.5.3	Distribution of average horizontal hydraulic conductivity values from specific capacity tests in Evangeline Aquifer in the study area. ....	201
Figure 4.5.4	Distribution of average horizontal hydraulic conductivity values from specific capacity tests in Burkeville Unit in the study area. ....	202
Figure 4.5.5	Distribution of average horizontal hydraulic conductivity values from specific capacity tests in Jasper Aquifer in the study area. ....	203
Figure 4.5.6	Distribution of wells with pumping tests and specific capacity tests. ....	205
Figure 4.5.7	Correlation of horizontal hydraulic conductivity values between pumping tests and specific capacity tests. ....	206

Figure 4.5.8	Distribution of average horizontal hydraulic conductivity values from pumping tests and specific capacity tests in Chicot Aquifer in the study area.	207
Figure 4.5.9	Distribution of average horizontal hydraulic conductivity values from pumping tests and specific capacity tests in Evangeline Aquifer in the study area.	208
Figure 4.5.10	Distribution of average horizontal hydraulic conductivity values from pumping tests and specific capacity tests in Burkeville Unit in the study area.	209
Figure 4.5.11	Distribution of average horizontal hydraulic conductivity values from pumping tests and specific capacity tests in Jasper Aquifer in the study area.	210
Figure 4.5.12	Histograms of logarithmic hydraulic conductivity values from Chicot Aquifer, Evangeline Aquifer, Burkeville Unit, and Jasper Aquifer in the study area.	211
Figure 4.5.13	Sand fraction in Chicot Aquifer based on new framework.	212
Figure 4.5.14	Sand fraction in Evangeline Aquifer based on new framework.	213
Figure 4.5.15	Sand fraction in Burkeville Unit based on new framework.	214
Figure 4.5.16	Sand fraction in Jasper Aquifer based on new framework.	215
Figure 4.5.17	Correlation between horizontal hydraulic conductivity and sand fraction in Chicot Aquifer. $R^2$ value indicates some linear correlation.	216
Figure 4.5.18	Correlation between horizontal hydraulic conductivity and sand fraction in Evangeline Aquifer. $R^2$ value indicates moderate linear correlation.	217
Figure 4.5.19	Correlation between horizontal hydraulic conductivity and sand fraction in Jasper Aquifer. $R^2$ value indicates weak linear correlation.	218
Figure 4.5.20	Distribution of horizontal hydraulic conductivity value for Chicot Aquifer in the study area.	219
Figure 4.5.21	Distribution of horizontal hydraulic conductivity value for Evangeline Aquifer in the study area.	220
Figure 4.5.22	Distribution of horizontal hydraulic conductivity value for Burkeville Unit in the study area.	221
Figure 4.5.23	Distribution of horizontal hydraulic conductivity value for Jasper Aquifer in the study area.	222
Figure 4.5.24	Distribution of storativity and specific yield values from pumping tests in the study area.	223
Figure 4.5.25	Distribution of storativity coefficient from pumping test, sand fraction, and depth for Chicot Aquifer in the study area.	224
Figure 4.5.26	Distribution of storativity coefficient from pumping test, sand fraction, and depth for Evangeline Aquifer in the study area.	225
Figure 4.5.27	Distribution of storativity coefficient from pumping test, sand fraction, and depth for Burkeville Unit in the study area.	226
Figure 4.5.28	Distribution of storativity coefficient from pumping test, sand fraction, and depth for Jasper Aquifer in the study area.	227
Table 4.5.1	Summary of horizontal hydraulic conductivity values from pumping tests and specific capacity tests.	228
Table 4.5.2	Summary of horizontal hydraulic conductivity values from rasters produced using pumping test, specific capacity test, and sand fraction.	228

Figure 4.6.1	Vegetation types in study area (McMahan and others, 1984). .....	234
Figure 4.6.2	Estimated maximum evapotranspiration in study area (Scanlon and others, 2005). .....	235
Figure 4.6.3	Trend analysis of total groundwater pumping from 2000 to 2011 in Mexico. ....	237
Figure 4.6.4	Annual groundwater pumping between 1980 and 2015 in Austin, Brazoria, Fort Bend, Matagorda, Washington, and Wharton counties.....	238
Figure 4.6.5	Annual groundwater pumping between 1980 and 2015 in Calhoun, Colorado, Fayette, Jackson, Lavaca, and Victoria counties.....	239
Figure 4.6.6	Annual groundwater pumping between 1980 and 2015 in Aransas, Bee, DeWitt, Goliad, Karnes, and Refugio counties. ....	240
Figure 4.6.7	Annual groundwater pumping between 1980 and 2015 in Duval, Jim Wells, Live Oak, McMullen, Nueces, and San Patricio counties. ....	241
Figure 4.6.8	Annual groundwater pumping between 1980 and 2015 in Brooks, Jim Hogg, Kenedy, Kleberg, Webb, and Willacy counties. ....	242
Figure 4.6.9	Annual groundwater pumping between 1980 and 2015 in Cameron, Hidalgo, and Starr counties and Mexico. ....	243
Figure 4.7.1	Arsenic average concentrations in groundwater samples collected from Chicot Aquifer between 1980 and 2015.....	254
Figure 4.7.2	Barium average concentrations in groundwater samples collected from Chicot Aquifer between 1980 and 2015.....	255
Figure 4.7.3	Cadmium average concentrations in groundwater samples collected from Chicot Aquifer between 1980 and 2015.....	256
Figure 4.7.4	Nitrate and nitrite average concentrations in groundwater samples collected from Chicot Aquifer between 1980 and 2015.....	257
Figure 4.7.5	Selenium average concentrations in groundwater samples collected from Chicot Aquifer between 1980 and 2015.....	258
Figure 4.7.6	Thallium average concentrations in groundwater samples collected from Chicot Aquifer between 1980 and 2015.....	259
Figure 4.7.7	Total dissolved solids average concentrations in groundwater samples collected from water wells in Chicot Aquifer between 1980 and 2015 and geophysical logs. ....	260
Figure 4.7.8	Hydrograph of total dissolved solids in groundwater from the Chicot Aquifer. ....	261
Figure 4.7.9	Synthetic organics concentrations in groundwater samples collected from Chicot Aquifer between 1980 and 2015.....	262
Figure 4.7.10	Volatile organic compound concentrations in groundwater samples collected from Chicot Aquifer between 1980 and 2015.....	263
Figure 4.7.11	Gross alpha particle activity in groundwater samples collected from Chicot Aquifer between 1980 and 2015.....	264
Figure 4.7.12	Uranium concentrations in groundwater samples collected from Chicot Aquifer between 1980 and 2015.....	265
Figure 4.7.13	Piper diagram of groundwater samples collected from Chicot Aquifer.....	266
Figure 4.7.14	Arsenic average concentrations in groundwater samples collected from Evangeline Aquifer between 1980 and 2015. ....	267

Figure 4.7.15	Barium average concentrations in groundwater samples collected from Evangeline Aquifer between 1980 and 2015. ....	268
Figure 4.7.16	Cadmium average concentrations in groundwater samples collected from Evangeline Aquifer between 1980 and 2015. ....	269
Figure 4.7.17	Nitrate and nitrite average concentrations in groundwater samples collected from Evangeline Aquifer between 1980 and 2015.....	270
Figure 4.7.18	Selenium average concentrations in groundwater samples collected from Evangeline Aquifer between 1980 and 2015. ....	271
Figure 4.7.19	Thallium average concentrations in groundwater samples collected from Evangeline Aquifer between 1980 and 2015. ....	272
Figure 4.7.20	Total dissolved solids average concentrations in groundwater samples collected from water wells in Evangeline Aquifer between 1980 and 2015 and geophysical logs.....	273
Figure 4.7.21	Hydrograph of total dissolved solids in groundwater from the Evangeline Aquifer. ....	274
Figure 4.7.22	Synthetic organics concentrations in groundwater samples collected from Evangeline Aquifer between 1980 and 2015. ....	275
Figure 4.7.23	Gross alpha particle activity in groundwater samples collected from Evangeline Aquifer between 1980 and 2015. ....	276
Figure 4.7.24	Uranium concentrations in groundwater samples collected from Evangeline Aquifer between 1980 and 2015.....	277
Figure 4.7.25	Piper diagram of groundwater samples collected from Evangeline Aquifer. ....	278
Figure 4.7.26	Arsenic average concentrations in groundwater samples collected from Burkeville Unit between 1980 and 2015. ....	279
Figure 4.7.27	Barium average concentrations in groundwater samples collected from Burkeville Unit between 1980 and 2015. ....	280
Figure 4.7.28	Cadmium average concentrations in groundwater samples collected from Burkeville Unit between 1980 and 2015. ....	281
Figure 4.7.29	Nitrate and nitrite average concentrations in groundwater samples collected from Burkeville Unit between 1980 and 2015.....	282
Figure 4.7.30	Selenium average concentrations in groundwater samples collected from Burkeville Unit between 1980 and 2015. ....	283
Figure 4.7.31	Thallium average concentrations in groundwater samples collected from Burkeville Unit between 1980 and 2015. ....	284
Figure 4.7.32	Total dissolved solids average concentrations in groundwater samples collected from water wells in Burkeville Unit between 1980 and 2015 and geophysical logs. ....	285
Figure 4.7.33	Hydrograph of total dissolved solids in groundwater from the Burkeville Unit.....	286
Figure 4.7.34	Synthetic organics concentrations in groundwater samples collected from Burkeville Unit between 1980 and 2015. ....	287
Figure 4.7.35	Gross alpha particle activity in groundwater samples collected from Burkeville Unit between 1980 and 2015. ....	288
Figure 4.7.36	Uranium concentrations in groundwater samples collected from Burkeville Unit between 1980 and 2015. ....	289

Figure 4.7.37 Piper diagram of groundwater samples collected from Burkeville Unit. ....	290
Figure 4.7.38 Arsenic average concentrations in groundwater samples collected from Jasper Aquifer between 1980 and 2015. ....	291
Figure 4.7.39 Barium average concentrations in groundwater samples collected from Jasper Aquifer between 1980 and 2015. ....	292
Figure 4.7.40 Cadmium average concentrations in groundwater samples collected from Jasper Aquifer between 1980 and 2015. ....	293
Figure 4.7.41 Nitrate and nitrite average concentrations in groundwater samples collected from Jasper Aquifer between 1980 and 2015. ....	294
Figure 4.7.42 Selenium average concentrations in groundwater samples collected from Jasper Aquifer between 1980 and 2015. ....	295
Figure 4.7.43 Thallium average concentrations in groundwater samples collected from Jasper Aquifer between 1980 and 2015. ....	296
Figure 4.7.44 Total dissolved solids average concentrations in groundwater samples collected from water wells in Jasper Aquifer between 1980 and 2015 and geophysical logs. ....	297
Figure 4.7.45 Hydrograph of total dissolved solids in groundwater from the Jasper Aquifer. ....	298
Figure 4.7.46 Synthetic organics concentrations in groundwater samples collected from Jasper Aquifer between 1980 and 2015. ....	299
Figure 4.7.47 Volatile organic compound concentrations in groundwater samples collected from Jasper Aquifer between 1980 and 2015. ....	300
Figure 4.7.48 Gross alpha particle activity in groundwater samples collected from Jasper Aquifer between 1980 and 2015. ....	301
Figure 4.7.49 Uranium concentrations in groundwater samples collected from Jasper Aquifer between 1980 and 2015. ....	302
Figure 4.7.50 Piper diagram of groundwater samples collected from Jasper Aquifer. ....	303
Table 4.8.1 Summary of groundwater decline or stress increase and compaction. ....	308
Figure 4.8.1 Correlation between compaction and groundwater stress change. ....	310
Figure 4.8.2 Total compaction/subsidence between 1908 and 1973 in the study area. ....	311
Figure 4.8.3 Total compaction/subsidence between 1908 and 2015 in the study area. ....	312
Figure 4.8.4 Total compaction/subsidence between 1980 and 2015 in the study area. ....	313
Figure 5.1.1 Schematic groundwater flow of pre-development conditions. ....	319
Figure 5.1.2 Schematic groundwater flow of post-development conditions. ....	320
Figure A1 Groundwater level hydrograph at State Well 8019503. ....	334
Figure A2 Groundwater level hydrograph at State Well 8019802. ....	335
Figure A3 Groundwater level hydrograph at State Well 8027601. ....	336
Figure A4 Groundwater level hydrograph at State Well 8858502. ....	337
Figure A5 Groundwater level hydrograph at State Well 6614703. ....	338
Figure A6 Groundwater level hydrograph at State Well 6630103. ....	339
Figure A7 Groundwater level hydrograph at State Well 6637601. ....	340
Figure A8 Groundwater level hydrograph at State Well 6660205. ....	341
Figure A9 Groundwater level hydrograph at State Well 6660401. ....	342
Figure A10 Groundwater level hydrograph at State Well 6660707. ....	343
Figure A11 Groundwater level hydrograph at State Well 6660708. ....	344
Figure A12 Groundwater level hydrograph at State Well 8003909. ....	345

Figure A13 Groundwater level hydrograph at State Well 8004601. ....	346
Figure A14 Groundwater level hydrograph at State Well 8005102. ....	347
Figure A15 Groundwater level hydrograph at State Well 8005502. ....	348
Figure A16 Groundwater level hydrograph at State Well 8005701. ....	349
Figure A17 Groundwater level hydrograph at State Well 8006101. ....	350
Figure A18 Groundwater level hydrograph at State Well 8006703. ....	351
Figure A19 Groundwater level hydrograph at State Well 8011201. ....	352
Figure A20 Groundwater level hydrograph at State Well 8011301. ....	353
Figure A21 Groundwater level hydrograph at State Well 8012502. ....	354
Figure A22 Groundwater level hydrograph at State Well 8326701. ....	355
Figure A23 Groundwater level hydrograph at State Well 6549901. ....	356
Figure A24 Groundwater level hydrograph at State Well 8007102. ....	357
Figure A25 Groundwater level hydrograph at State Well 8007404. ....	358
Figure A26 Groundwater level hydrograph at State Well 8014801. ....	359
Figure A27 Groundwater level hydrograph at State Well 8014901. ....	360
Figure A28 Groundwater level hydrograph at State Well 8024201. ....	361
Figure A29 Groundwater level hydrograph at State Well 8111901. ....	362
Figure A30 Groundwater level hydrograph at State Well 8322801. ....	363
Figure A31 Groundwater level hydrograph at State Well 6541401. ....	364
Figure A32 Groundwater level hydrograph at State Well 6631504. ....	365
Figure A33 Groundwater level hydrograph at State Well 6638202. ....	366
Figure A34 Groundwater level hydrograph at State Well 6638304. ....	367
Figure A35 Groundwater level hydrograph at State Well 6638801. ....	368
Figure A36 Groundwater level hydrograph at State Well 6639801. ....	369
Figure A37 Groundwater level hydrograph at State Well 6645802. ....	370
Figure A38 Groundwater level hydrograph at State Well 6646402. ....	371
Figure A39 Groundwater level hydrograph at State Well 6646601. ....	372
Figure A40 Groundwater level hydrograph at State Well 6647101. ....	373
Figure A41 Groundwater level hydrograph at State Well 6648701. ....	374
Figure A42 Groundwater level hydrograph at State Well 6648802. ....	375
Figure A43 Groundwater level hydrograph at State Well 6652304. ....	376
Figure A44 Groundwater level hydrograph at State Well 6652603. ....	377
Figure A45 Groundwater level hydrograph at State Well 6653307. ....	378
Figure A46 Groundwater level hydrograph at State Well 6653804. ....	379
Figure A47 Groundwater level hydrograph at State Well 6654108. ....	380
Figure A48 Groundwater level hydrograph at State Well 6656302. ....	381
Figure A49 Groundwater level hydrograph at State Well 6661305. ....	382
Figure A50 Groundwater level hydrograph at State Well 6662104. ....	383
Figure A51 Groundwater level hydrograph at State Well 6662307. ....	384
Figure A52 Groundwater level hydrograph at State Well 6662603. ....	385
Figure A53 Groundwater level hydrograph at State Well 6662805. ....	386
Figure A54 Groundwater level hydrograph at State Well 6663105. ....	387
Figure A55 Groundwater level hydrograph at State Well 8454806. ....	388
Figure A56 Groundwater level hydrograph at State Well 8455203. ....	389
Figure A57 Groundwater level hydrograph at State Well 8455204. ....	390
Figure A58 Groundwater level hydrograph at State Well 8455310. ....	391



Figure A59 Groundwater level hydrograph at State Well 8455901. ....	392
Figure A60 Groundwater level hydrograph at State Well 8707802. ....	393
Figure A61 Groundwater level hydrograph at State Well 8713503. ....	394
Figure A62 Groundwater level hydrograph at State Well 6612204. ....	395
Figure A63 Groundwater level hydrograph at State Well 6619804. ....	396
Figure A64 Groundwater level hydrograph at State Well 6622201. ....	397
Figure A65 Groundwater level hydrograph at State Well 8415702. ....	398
Figure A66 Groundwater level hydrograph at State Well 8422801. ....	399
Figure A67 Groundwater level hydrograph at State Well 8429306. ....	400
Figure A68 Groundwater level hydrograph at State Well 8430501. ....	401
Figure A69 Groundwater level hydrograph at State Well 8431102. ....	402
Figure A70 Groundwater level hydrograph at State Well 8437301. ....	403
Figure A71 Groundwater level hydrograph at State Well 8437901. ....	404
Figure A72 Groundwater level hydrograph at State Well 8438701. ....	405
Figure A73 Groundwater level hydrograph at State Well 8438903. ....	406
Figure A74 Groundwater level hydrograph at State Well 8444601. ....	407
Figure A75 Groundwater level hydrograph at State Well 8445304. ....	408
Figure A76 Groundwater level hydrograph at State Well 8446701. ....	409
Figure A77 Groundwater level hydrograph at State Well 8301605. ....	410
Figure A78 Groundwater level hydrograph at State Well 8309703. ....	411
Figure A79 Groundwater level hydrograph at State Well 8416407. ....	412
Figure A80 Groundwater level hydrograph at State Well 8423204. ....	413
Figure A81 Groundwater level hydrograph at State Well 8424104. ....	414
Figure A82 Groundwater level hydrograph at State Well 8439701. ....	415
Figure A83 Groundwater level hydrograph at State Well 8447313. ....	416
Figure A84 Groundwater level hydrograph at State Well 8325701. ....	417
Figure A85 Groundwater level hydrograph at State Well 8325801. ....	418
Figure A86 Groundwater level hydrograph at State Well 8326401. ....	419
Figure A87 Groundwater level hydrograph at State Well 8326901. ....	420
Figure A88 Groundwater level hydrograph at State Well 8327801. ....	421
Figure A89 Groundwater level hydrograph at State Well 8327802. ....	422
Figure A90 Groundwater level hydrograph at State Well 8334701. ....	423
Figure A91 Groundwater level hydrograph at State Well 8335201. ....	424
Figure A92 Groundwater level hydrograph at State Well 8336401. ....	425
Figure A93 Groundwater level hydrograph at State Well 8342701. ....	426
Figure A94 Groundwater level hydrograph at State Well 8432501. ....	427
Figure A95 Groundwater level hydrograph at State Well 6634201. ....	428
Figure A96 Groundwater level hydrograph at State Well 6634202. ....	429
Figure A97 Groundwater level hydrograph at State Well 6635901. ....	430
Figure A98 Groundwater level hydrograph at State Well 6641903. ....	431
Figure A99 Groundwater level hydrograph at State Well 6642902. ....	432
Figure A100 Groundwater level hydrograph at State Well 6643803. ....	433
Figure A101 Groundwater level hydrograph at State Well 6649901. ....	434
Figure A102 Groundwater level hydrograph at State Well 6740301. ....	435
Figure A103 Groundwater level hydrograph at State Well 7863101. ....	436
Figure A104 Groundwater level hydrograph at State Well 8301901. ....	437

Figure A105 Groundwater level hydrograph at State Well 8310602.....	438
Figure A106 Groundwater level hydrograph at State Well 8317901.....	439
Figure A107 Groundwater level hydrograph at State Well 8329201.....	440
Figure A108 Groundwater level hydrograph at State Well 7950909.....	441
Figure A109 Groundwater level hydrograph at State Well 8834601.....	442
Figure A110 Groundwater level hydrograph at State Well 6746704.....	443
Figure A111 Groundwater level hydrograph at State Well 6746705.....	444
Figure A112 Groundwater level hydrograph at State Well 6753401.....	445
Figure A113 Groundwater level hydrograph at State Well 5951802.....	446
Figure A114 Groundwater level hydrograph at State Well 5951806.....	447
Figure A115 Groundwater level hydrograph at State Well 6603806.....	448
Figure A116 Groundwater level hydrograph at State Well 6731604.....	449
Figure A117 Groundwater level hydrograph at State Well 6739518.....	450
Figure A118 Groundwater level hydrograph at State Well 6739603.....	451
Figure B1 Groundwater levels at State Well 6618501 and State Well 6618502. ....	453
Figure B2 Groundwater levels at State Well 6622203 and State Well 6622201. ....	454
Figure B3 Groundwater levels at State Well 6627802 and State Well 6627704. ....	455
Figure B4 Groundwater levels at State Well 6627802 and State Well 6627803. ....	456
Figure B5 Groundwater levels at State Well 6631904 and State Well 6631906. ....	457
Figure B6 Groundwater levels at State Well 6635206 and State Well 6627801. ....	458
Figure B7 Groundwater levels at State Well 7840201 and State Well 7840203. ....	459
Figure B8 Groundwater levels at State Well 7840201 and State Well 7840204. ....	460
Figure B9 Groundwater levels at State Well 7840309 and State Well 7840301. ....	461
Figure B10 Groundwater levels at State Well 7840610 and State Well 7840601.....	462
Figure B11 Groundwater levels at State Well 7840612 and State Well 7840601.....	463
Figure B12 Groundwater levels at State Well 7906604 and State Well 7906605.....	464
Figure B13 Groundwater levels at State Well 7912206 and State Well 7912205.....	465
Figure B14 Groundwater levels at State Well 7913802 and State Well 7913510.....	466
Figure B15 Groundwater levels at State Well 7918603 and State Well 7918602.....	467
Figure B16 Groundwater levels at State Well 7922206 and State Well 7922201.....	468
Figure B17 Groundwater levels at State Well 7923201 and State Well 7915802.....	469
Figure B18 Groundwater levels at State Well 7925506 and State Well 7925505.....	470
Figure B19 Groundwater levels at State Well 7930401 and State Well 7930402.....	471
Figure B20 Groundwater levels at State Well 7937918 and State Well 7937919.....	472
Figure B21 Groundwater levels at State Well 7938413 and State Well 7938407.....	473
Figure B22 Groundwater levels at State Well 7938704 and State Well 7938706.....	474
Figure B23 Groundwater levels at State Well 8001601 and State Well 8001602.....	475
Figure B24 Groundwater levels at State Well 8001703 and State Well 8001704.....	476
Figure B25 Groundwater levels at State Well 8326702 and State Well 8326711.....	477
Figure B26 Groundwater levels at State Well 8334302 and State Well 8334303.....	478
Figure B27 Groundwater levels at State Well 8433202 and State Well 8433201.....	479
Figure B28 Groundwater levels at State Well 8439405 and State Well 8439404.....	480
Figure B29 Groundwater levels at State Well 8440704 and State Well 8440701.....	481
Figure B30 Groundwater levels at State Well 8440704 and State Well 8440703.....	482
Figure B31 Groundwater levels at State Well 8446801 and State Well 8446907.....	483
Figure B32 Groundwater levels at State Well 8447910 and State Well 8447808.....	484

Figure B33 Groundwater levels at State Well 8455615 and State Well 8455603.....	485
Figure B34 Groundwater levels at State Well 8455616 and State Well 8455602.....	486
Figure B35 Groundwater levels at State Well 8455616 and State Well 8455603.....	487
Figure B36 Groundwater levels at State Well 8707608 and State Well 8707607.....	488
Figure C1 Estimated groundwater recharge from stream baseflow-precipitation correlation (1981). .....	490
Figure C2 Estimated groundwater recharge from stream baseflow-precipitation correlation (1982). .....	491
Figure C3 Estimated groundwater recharge from stream baseflow-precipitation correlation (1983). .....	492
Figure C4 Estimated groundwater recharge from stream baseflow-precipitation correlation (1984). .....	493
Figure C5 Estimated groundwater recharge from stream baseflow-precipitation correlation (1985). .....	494
Figure C6 Estimated groundwater recharge from stream baseflow-precipitation correlation (1986). .....	495
Figure C7 Estimated groundwater recharge from stream baseflow-precipitation correlation (1987). .....	496
Figure C8 Estimated groundwater recharge from stream baseflow-precipitation correlation (1988). .....	497
Figure C9 Estimated groundwater recharge from stream baseflow-precipitation correlation (1989). .....	498
Figure C10 Estimated groundwater recharge from stream baseflow-precipitation correlation (1991).....	499
Figure C11 Estimated groundwater recharge from stream baseflow-precipitation correlation (1992).....	500
Figure C12 Estimated groundwater recharge from stream baseflow-precipitation correlation (1993).....	501
Figure C13 Estimated groundwater recharge from stream baseflow-precipitation correlation (1994).....	502
Figure C14 Estimated groundwater recharge from stream baseflow-precipitation correlation (1995).....	503
Figure C15 Estimated groundwater recharge from stream baseflow-precipitation correlation (1996).....	504
Figure C16 Estimated groundwater recharge from stream baseflow-precipitation correlation (1997).....	505
Figure C17 Estimated groundwater recharge from stream baseflow-precipitation correlation (1998).....	506
Figure C18 Estimated groundwater recharge from stream baseflow-precipitation correlation (1999).....	507
Figure C19 Estimated groundwater recharge from stream baseflow-precipitation correlation (2001).....	508
Figure C20 Estimated groundwater recharge from stream baseflow-precipitation correlation (2002).....	509
Figure C21 Estimated groundwater recharge from stream baseflow-precipitation correlation (2003).....	510

Figure C22 Estimated groundwater recharge from stream baseflow-precipitation correlation (2004).....	511
Figure C23 Estimated groundwater recharge from stream baseflow-precipitation correlation (2005).....	512
Figure C24 Estimated groundwater recharge from stream baseflow-precipitation correlation (2006).....	513
Figure C25 Estimated groundwater recharge from stream baseflow-precipitation correlation (2007).....	514
Figure C26 Estimated groundwater recharge from stream baseflow-precipitation correlation (2008).....	515
Figure C27 Estimated groundwater recharge from stream baseflow-precipitation correlation (2009).....	516
Figure C28 Estimated groundwater recharge from stream baseflow-precipitation correlation (2011).....	517
Figure C29 Estimated groundwater recharge from stream baseflow-precipitation correlation (2012).....	518
Figure C30 Estimated groundwater recharge from stream baseflow-precipitation correlation (2013).....	519
Figure C31 Estimated groundwater recharge from stream baseflow-precipitation correlation (2014).....	520
Figure D1 Stream gain or loss at Basin 3. ....	522
Figure D2 Stream gain or loss at Basin 5. ....	523
Figure D3 Stream gain or loss at Basin 7. ....	524
Figure D4 Stream gain or loss at Basin 8. ....	525
Figure D5 Stream gain or loss at Basin 10.....	526
Figure D6 Stream gain or loss at Basin 11.....	527
Figure D7 Stream gain or loss at Basin 13.....	528
Figure D8 Stream gain or loss at Basin 14.....	529
Figure D9 Stream gain or loss at Basin 19.....	530
Figure D10 Stream gain or loss at Basin 20.....	531
Figure D11 Stream gain or loss at Basin 22.....	532
Figure D12 Stream gain or loss at Basin 25.....	533
Table E1 Summary of hydraulic conductivity values from pumping tests.....	535
Table E2. Summary of hydraulic conductivity values from pumping tests and specific capacity tests.....	544
Table E3. Summary of storativity and specific yield values from pumping tests.....	545
Figure F1 Hydrograph of total dissolved solids at State Well 8049702.....	547
Figure F2 Hydrograph of total dissolved solids at State Well 6616407.....	548
Figure F3 Hydrograph of total dissolved solids at State Well 6543707.....	549
Figure F4 Hydrograph of total dissolved solids at State Well 6551915.....	550
Figure F5 Hydrograph of total dissolved solids at State Well 6559810.....	551
Figure F6 Hydrograph of total dissolved solids at State Well 6614403.....	552
Figure F7 Hydrograph of total dissolved solids at State Well 6525106.....	553
Figure F8 Hydrograph of total dissolved solids at State Well 6544104.....	554
Figure F9 Hydrograph of total dissolved solids at State Well 6640606.....	555
Figure F10 Hydrograph of total dissolved solids at State Well 6651704.....	556

Figure F11 Hydrograph of total dissolved solids at State Well 6660401.....	557
Figure F12 Hydrograph of total dissolved solids at State Well 8002606.....	558
Figure F13 Hydrograph of total dissolved solids at State Well 8004610.....	559
Figure F14 Hydrograph of total dissolved solids at State Well 8012202.....	560
Figure F15 Hydrograph of total dissolved solids at State Well 8013104.....	561
Figure F16 Hydrograph of total dissolved solids at State Well 8325501.....	562
Figure F17 Hydrograph of total dissolved solids at State Well 6642205.....	563
Figure F18 Hydrograph of total dissolved solids at State Well 6557904.....	564
Figure F19 Hydrograph of total dissolved solids at State Well 8007308.....	565
Figure F20 Hydrograph of total dissolved solids at State Well 8008201.....	566
Figure F21 Hydrograph of total dissolved solids at State Well 8015113.....	567
Figure F22 Hydrograph of total dissolved solids at State Well 8015602.....	568
Figure F23 Hydrograph of total dissolved solids at State Well 8023102.....	569
Figure F24 Hydrograph of total dissolved solids at State Well 8101201.....	570
Figure F25 Hydrograph of total dissolved solids at State Well 8110901.....	571
Figure F26 Hydrograph of total dissolved solids at State Well 8111902.....	572
Figure F27 Hydrograph of total dissolved solids at State Well 6541804.....	573
Figure F28 Hydrograph of total dissolved solids at State Well 6632809.....	574
Figure F29 Hydrograph of total dissolved solids at State Well 6638704.....	575
Figure F30 Hydrograph of total dissolved solids at State Well 6638906.....	576
Figure F31 Hydrograph of total dissolved solids at State Well 6640803.....	577
Figure F32 Hydrograph of total dissolved solids at State Well 6646815.....	578
Figure F33 Hydrograph of total dissolved solids at State Well 6647904.....	579
Figure F34 Hydrograph of total dissolved solids at State Well 6648402.....	580
Figure F35 Hydrograph of total dissolved solids at State Well 6656401.....	581
Figure F36 Hydrograph of total dissolved solids at State Well 6607502.....	582
Figure F37 Hydrograph of total dissolved solids at State Well 8455328.....	583
Figure F38 Hydrograph of total dissolved solids at State Well 6612204.....	584
Figure F39 Hydrograph of total dissolved solids at State Well 6612603.....	585
Figure F40 Hydrograph of total dissolved solids at State Well 6619804.....	586
Figure F41 Hydrograph of total dissolved solids at State Well 6626202.....	587
Figure F42 Hydrograph of total dissolved solids at State Well 6627905.....	588
Figure F43 Hydrograph of total dissolved solids at State Well 6628607.....	589
Figure F44 Hydrograph of total dissolved solids at State Well 6628804.....	590
Figure F45 Hydrograph of total dissolved solids at State Well 6630101.....	591
Figure F46 Hydrograph of total dissolved solids at State Well 6635201.....	592
Figure F47 Hydrograph of total dissolved solids at State Well 7906102.....	593
Figure F48 Hydrograph of total dissolved solids at State Well 8415704.....	594
Figure F49 Hydrograph of total dissolved solids at State Well 8436601.....	595
Figure F50 Hydrograph of total dissolved solids at State Well 8438703.....	596
Figure F51 Hydrograph of total dissolved solids at State Well 6526812.....	597
Figure F52 Hydrograph of total dissolved solids at State Well 6533304.....	598
Figure F53 Hydrograph of total dissolved solids at State Well 7914102.....	599
Figure F54 Hydrograph of total dissolved solids at State Well 6660907.....	600
Figure F55 Hydrograph of total dissolved solids at State Well 8003303.....	601
Figure F56 Hydrograph of total dissolved solids at State Well 8431202.....	602

Figure F57 Hydrograph of total dissolved solids at State Well 8329702.....	603
Figure F58 Hydrograph of total dissolved solids at State Well 8432501.....	604
Figure F59 Hydrograph of total dissolved solids at State Well 6641904.....	605
Figure F60 Hydrograph of total dissolved solids at State Well 6756601.....	606
Figure F61 Hydrograph of total dissolved solids at State Well 7949905.....	607
Figure F62 Hydrograph of total dissolved solids at State Well 7957605.....	608
Figure F63 Hydrograph of total dissolved solids at State Well 7907703.....	609
Figure F64 Hydrograph of total dissolved solids at State Well 7916602.....	610
Figure F65 Hydrograph of total dissolved solids at State Well 8834601.....	611
Figure F66 Hydrograph of total dissolved solids at State Well 5960703.....	612
Figure F67 Hydrograph of total dissolved solids at State Well 5962403.....	613
Figure F68 Hydrograph of total dissolved solids at State Well 6604302.....	614
Figure F69 Hydrograph of total dissolved solids at State Well 7925608.....	615
Figure F70 Hydrograph of total dissolved solids at State Well 6754204.....	616
Figure F71 Hydrograph of total dissolved solids at State Well 7904402.....	617
Figure F72 Hydrograph of total dissolved solids at State Well 8411201.....	618
Figure F73 Hydrograph of total dissolved solids at State Well 8412705.....	619
Figure F74 Hydrograph of total dissolved solids at State Well 6603807.....	620
Figure F75 Hydrograph of total dissolved solids at State Well 8727803.....	621
Figure F76 Hydrograph of total dissolved solids at State Well 5954505.....	622

## **EXECUTIVE SUMMARY:**

The Texas State legislature mandated that the Texas Water Development Board (TWDB) obtain or develop groundwater availability models for all major and minor aquifers in Texas. To develop a groundwater availability model (also known as a numerical groundwater flow model), a conceptual groundwater model must be constructed first to lay the foundation for the groundwater availability model to be built upon. A conceptual model is a simplified version of the “real world”, which the groundwater availability model can handle through a computer program.

This report summarizes a groundwater conceptual model developed for the central and southern portions of the Gulf Coast Aquifer System in Texas. The Gulf Coast Aquifer System is a major aquifer in Texas. The central portion coincides with Groundwater Management Area 15. The southern portion coincides with Groundwater Management Area 16. The conceptual model extends beyond the boundaries of Groundwater Management Areas 15 and 16 into surrounding areas (collectively called the “study area”).

The Gulf Coast Aquifer System in the study area occupies more than 26,405 square miles in 33 counties in Texas: Aransas, Austin, Bee, Brazoria, Brooks, Calhoun, Cameron, Colorado, DeWitt, Duval, Fayette, Fort Bend, Goliad, Hidalgo, Jackson, Jim Hogg, Jim Wells, Karnes, Kenedy, Kleberg, Lavaca, Live Oak, Matagorda, McMullen, Nueces, Refugio, San Patricio, Starr, Victoria, Washington, Webb, Wharton, and Willacy.

This conceptual model provides the geologic framework and interpretation of the groundwater flow system within the study area. This evaluation includes previous studies; climate; physiography (the study of physical features of the Earth’s surface); geology; hydrostratigraphy (the layering of aquifers and other hydrogeological units); water levels and groundwater flow; groundwater recharge; surface water; hydraulic properties (flow characteristics) of the aquifers; groundwater discharge (evapotranspiration and pumping); water quality; and land subsidence (gradual or sudden sinking of the Earth’s surface due to subsurface movement of Earth materials).

The conceptual flow model for the Gulf Coast Aquifer System contains four hydrostratigraphic units (from shallowest to deepest): the Chicot Aquifer and the overlying alluvium deposits (Model Layer 1); the Evangeline Aquifer (Model Layer 2); the Burkeville Unit (Model Layer 3); and the Jasper Aquifer (Model Layer 4). In this study, the Jasper Aquifer includes the upper sandy portion of the Catahoula Formation. The Burkeville Unit could be clayey as a confining layer or sandy as an aquifer. All four units thicken and dip toward the Gulf of Mexico.

The conceptual model domain is confined by the ground surface at the top and the Jasper Aquifer at the bottom. The Jasper Aquifer is in direct contact and connected with the underlying Yegua-Jackson Aquifer in the updip area where the Catahoula Formation is mainly sand. In the downdip area, the Jasper Aquifer is separated from the Yegua-Jackson Aquifer by the clayey Catahoula Formation and deeper in the subsurface by the Anahuac Formation, thus, zero flow through the bottom of the Jasper Aquifer is assumed in the downdip area. The lateral extent of the conceptual flow model is bounded by the Brazos River to the north, the updip boundary of the Gulf Coast Aquifer System to the west, about 10 miles into Mexico from the Rio Grande to the south, and about 10 miles into the Gulf of Mexico to the east. Along the northern perimeter of the model domain, the Brazos River is in Model Layer 1 and Model Layers 2 through 4 are assumed zero flow or no flow. This assumption is most likely sufficient because of the width of the geographic buffer between the Brazos River and Groundwater Management Area 15 northern boundary. The groundwater flow through the model domain perimeter to the west, south, and east is assumed to depend on water levels across the perimeter and will be addressed during numerical model construction.

The conceptual flow model includes two hydrogeologic conditions: the pre-development conditions (prior to the 1940s) and the post-development conditions (after the 1940s). Because of limited groundwater withdrawal prior to the 1940s, the Gulf Coast Aquifer System in the study area was under long-term dynamic equilibrium (groundwater inflow equals groundwater outflow). During the pre-development conditions, groundwater levels and flows fluctuated over time due to seasonal and annual changes in precipitation.



However, the natural groundwater discharge such as spring flow and baseflow to rivers was balanced by the natural recharge such as infiltration due to precipitation. As a result, the water levels and storage in the aquifers showed little long-term variation.

After the 1940s, groundwater withdrawal changed the aquifer system in the study area. These changes included falling water level or aquifer storage, reducing discharge to surface water, and even sea water intrusion.

In summary, this conceptual model identifies the unique hydrostratigraphic units and the associated structures, the characteristics of the groundwater flow, and the factors that control the flow. The information from the conceptual model will be used to construct a numerical groundwater flow model or groundwater availability model for the Gulf Coast Aquifer System in the study area. Although the TWDB has made the best efforts during the development of this conceptual model, uncertainties still exist due to the lack of data for certain areas and the complexity of the study area. These uncertainties include, but are not limited to, the hydrostratigraphic structure to the far downdip area, the distribution of sand and clay, the variation of true groundwater recharge, and the impacts of faults on groundwater flow. The TWDB will update the conceptual model, if warranted, by additional information through the continued stakeholder process and the development of the numerical model. If this occurs, the TWDB will inform the stakeholders.

## 1.0 INTRODUCTION

The Texas Water Development Board (TWDB) has designated nine major and twenty-two minor aquifers in Texas (Figures 1.0.1 and 1.0.2). Major aquifers supply large quantities of water over large areas and minor aquifer supply relatively small quantities of water over large areas or supply large quantities of water over small areas. The characteristics of these aquifers, except the Cross Timbers Aquifer, are discussed by George and others (2011). The characteristics of the Cross Timbers Aquifer are highlighted in Blandford and others (2021).

This report documents the development of a conceptual groundwater model for the central and southern portions of the Gulf Coast Aquifer System in Texas (Figure 1.0.3). The central portion coincides with Groundwater Management Area 15. The southern portion coincides with Groundwater Management Area 16. This conceptual model extends beyond the boundaries of Groundwater Management Areas 15 and 16 into surrounding areas (collectively called the “study area”). This conceptual model lays the foundation for a numerical groundwater availability model that will be developed and documented in a separate report.

According to the TWDB Water Use Survey 2015 summaries, the groundwater from the Gulf Coast Aquifer System in Groundwater Management Areas 15 and 16 was mainly used for irrigation (237,931 acre-feet per year), municipal (51,421 acre-feet per year), livestock (12,407 acre-feet per year), manufacturing (7,173 acre-feet per year), steam electric power (3,097 acre-feet per year), and mining (2,090 acre-feet per year) purposes. The 2017 State Water Plan indicated the annual groundwater existing supplies from the Gulf Coast Aquifer System in Texas declining from 1,234,093 acre-feet in 2020 to 1,186,458 acre-feet in 2070.

Senate Bill 2 passed by the Texas Senate in 2001 mandated that the TWDB, in coordination with groundwater conservation districts and regional water planning groups, obtain or develop groundwater availability models for all major and minor aquifers in Texas. As a result, the TWDB has developed or adopted groundwater availability models for all the major aquifers and nearly all of the minor aquifers in Texas.

Groundwater availability models provide a great tool for assessing groundwater availability and the effects of water management strategies during different climatic conditions. A groundwater availability model is a numerical representation of the aquifer system capable of simulating historical conditions and predicting future aquifer conditions using various climatic and pumping scenarios.

To fulfill the legislature mandate and help the groundwater conservation districts in the study area manage their groundwater resources, TWDB developed two groundwater availability models for the central portion (Chowdhury and others, 2004) and the southern portion (Chowdhury and Mace, 2007) of the Gulf Coast Aquifer System and an alternative model for Groundwater Management Area 16. These models have been used for estimating groundwater recharge, discharge to surface water, lateral flow between adjacent regions, flow between aquifers, flow between fresh water and brackish water, total aquifer recoverable storage, desired future conditions, and modeled available groundwater. The simulation results from the models have helped the groundwater conservation districts and regional water planning groups to plan and manage the groundwater resources located within their respective boundaries. The models have also been used by industries, private citizens, and river authorities for understanding the flow dynamics of the aquifer system, both historically and predictively.

A groundwater flow model is a living tool that requires constant update upon availability of new information. For example, the U. S. Geological Survey has developed numerous models for the northern portion of the Gulf Coast Aquifer System in Texas. Since the development of the groundwater availability models for the central and southern portions of the Gulf Coast Aquifer System, the TWDB has collected or received a significant amount of new data including groundwater levels, groundwater quality, pumping tests, surface water fluxes, groundwater recharge, and stratigraphic studies for the Gulf Coast Aquifer System in Texas. This new information significantly improved our understanding of the complex groundwater flow system in the Gulf Coast Aquifer System, which, combined with advanced modeling tools, warrants an update of the existing groundwater availability models. Furthermore, advances in computing power provides the opportunity to combine the

central and the southern portions of the Gulf Coast Aquifer System in a single model to improve the simulation of the groundwater flow in the aquifer and to eliminate the inconsistency along the overlapped area between the existing models.

The precursor of such a groundwater availability model is the development of a conceptual groundwater model. A conceptual groundwater model is a simplified version of the “real world”, which the groundwater availability model can handle through a computer code. This report and its associated database provided the fundamental geologic framework, structure, and properties of the Gulf Coast Aquifer System in the study area, including physiographic provinces, climate, geology, previous studies, hydrologic setting, water levels, groundwater flow, aquifer recharge, surface water features, aquifer properties, pumping, water quality, and subsidence.

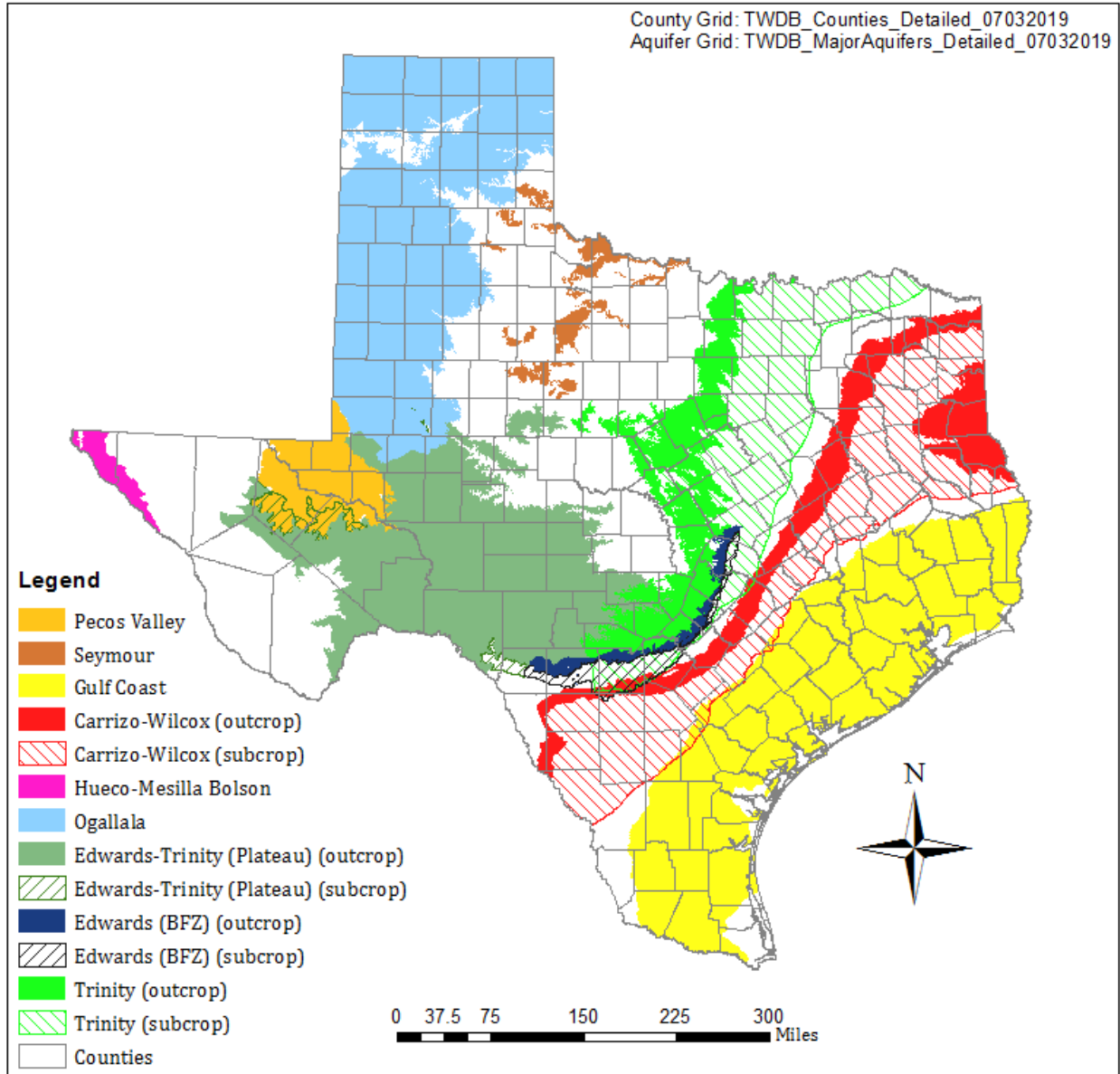


**Figure 1.0.1** Location of major aquifers in Texas.

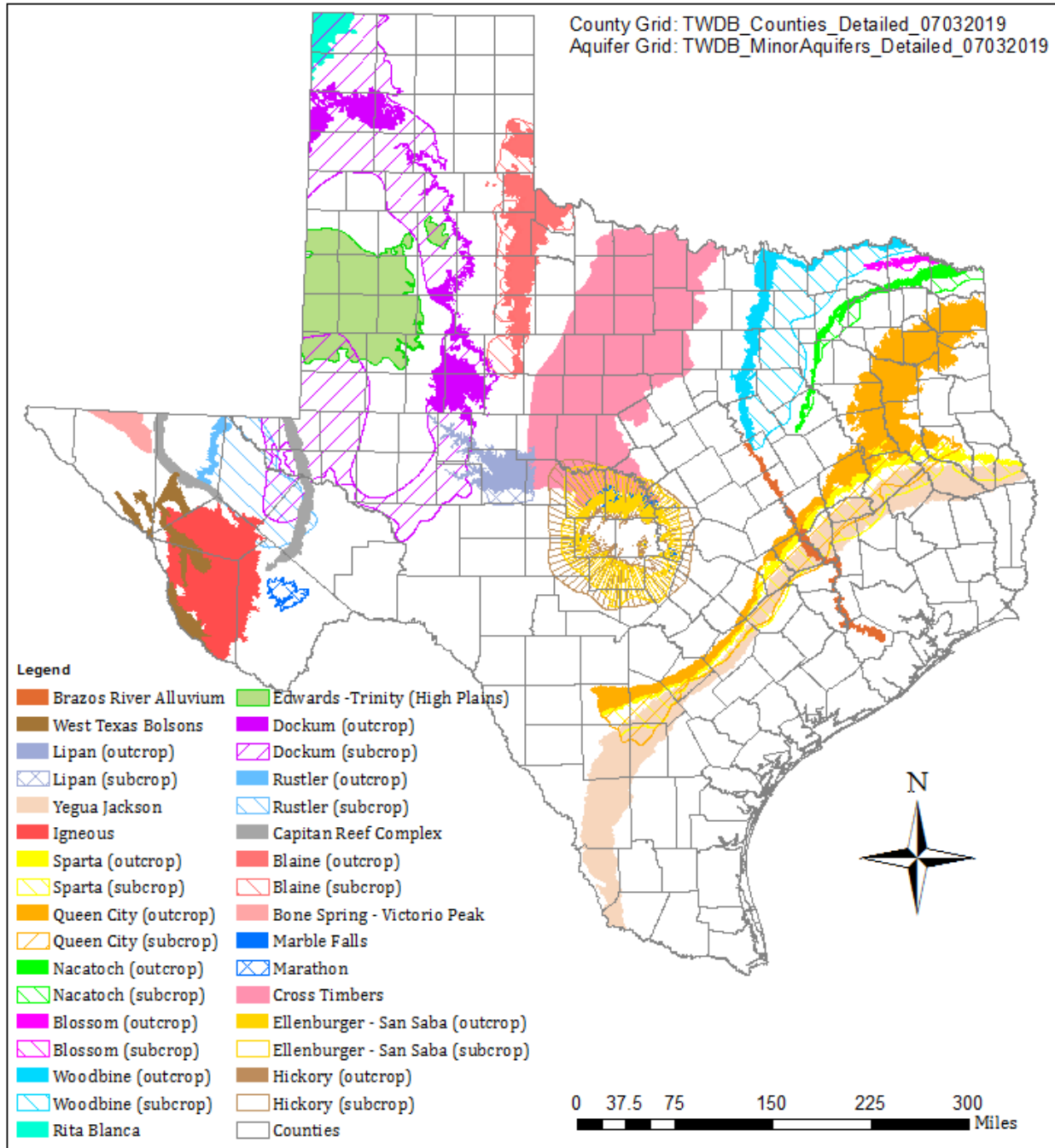


**Figure 1.0.2 Location of minor aquifers in Texas.**

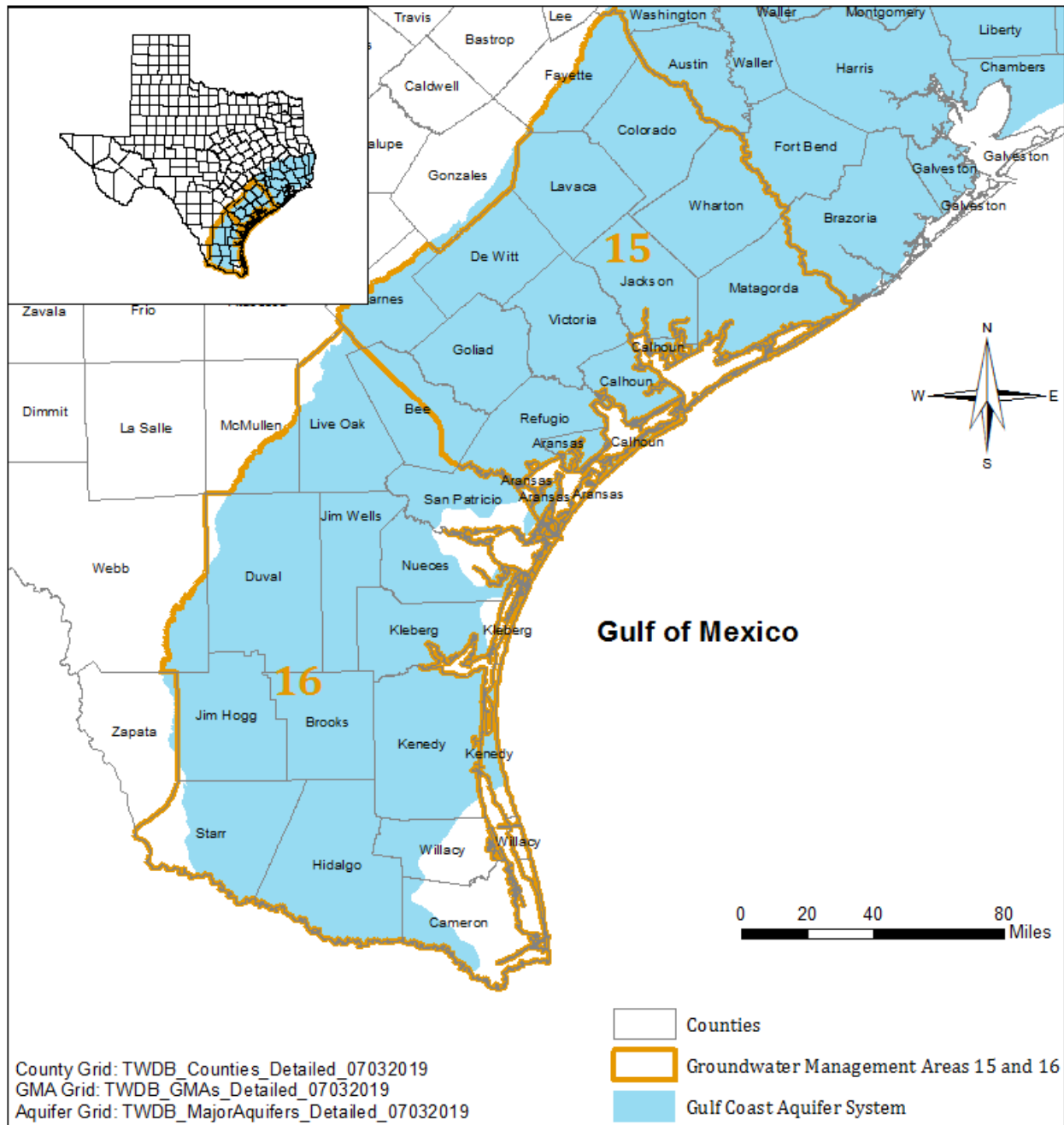


**Figure 1.0.3** Location of the central and southern portions of the Gulf Coast Aquifer System in Texas.

## 2.0 STUDY AREA

The Gulf Coast Aquifer System in the study area occupies 26,405 square miles in 33 counties in Texas: Aransas, Austin, Bee, Brazoria, Brooks, Calhoun, Cameron, Colorado, DeWitt, Duval, Fayette, Fort Bend, Goliad, Hidalgo, Jackson, Jim Hogg, Jim Wells, Karnes, Kenedy, Kleberg, Lavaca, Live Oak, Matagorda, McMullen, Nueces, Refugio, San Patricio, Starr, Victoria, Washington, Webb, Wharton, and Willacy (Figure 1.0.3).

Figure 2.0.1 shows the counties, roadways, cities, and towns in the study area. The study area contains rivers, streams, lakes, and reservoirs in 11 river basins (from north to south): Brazos-Colorado River Basin, Colorado River Basin, Lavaca River Basin, Colorado-Lavaca River Basin, Lavaca-Guadalupe River Basin, Guadalupe River Basin, San Antonio River Basin, San Antonio-Nueces River Basin, Nueces River Basin, Nueces-Rio Grande River Basin, and Rio Grande Basin (Figure 2.0.2). The six major rivers in the study area are (from north to south): Colorado River, Lavaca River, Guadalupe River, San Antonio River, Nueces River, and Rio Grande (Figure 2.0.2). Major lakes or reservoirs (area greater than one square mile) are presented in Figure 2.0.3. Figure 2.0.4 shows the river authorities associated with the study area: Lower Colorado River Authority, Lavaca-Navidad River Authority, Guadalupe-Blanco River Authority, San Antonio River Authority, and Nueces River Authority. The study area falls into the Lower Colorado Regional Water Planning Area, the Lavaca Regional Water Planning Area, the South-Central Texas Regional Water Planning Area, the Coastal Bend Regional Water Planning Area, and the Rio Grande Regional Water Planning Area (Figure 2.0.5). The study area includes whole or part of the following groundwater conservation districts: Bee Groundwater Conservation District, Brush Country Groundwater Conservation District, Calhoun County Groundwater Conservation District, Coastal Bend Groundwater Conservation District, Coastal Plains Groundwater Conservation District, Colorado County Groundwater Conservation District, Corpus Christi Aquifer Storage & Recovery Conservation District, Duval County Groundwater Conservation District, Evergreen Underground Water Conservation District, Fayette County Groundwater Conservation District, Goliad County Groundwater Conservation District, Kenedy County Groundwater Conservation District, Live Oak



Underground Water Conservation District, McMullen Groundwater Conservation District, Pecan Valley Groundwater Conservation District, Red Sands Groundwater Conservation District, Refugio Groundwater Conservation District, San Patricio Groundwater Conservation District, Starr County Groundwater Conservation District, Texana Groundwater Conservation District, and the Victoria County Groundwater Conservation District ([Figure 2.0.6](#)).

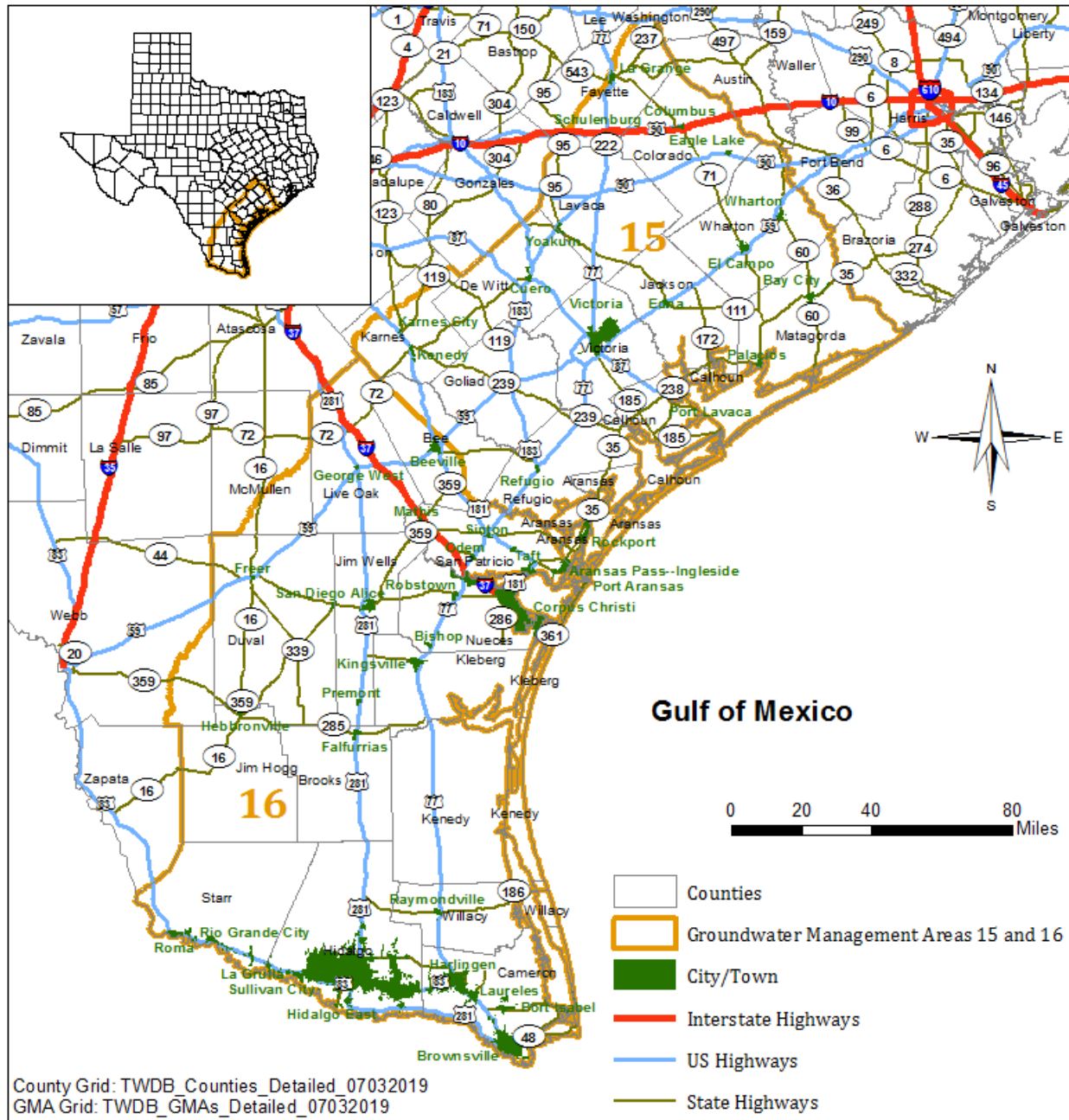


**Figure 2.0.1** Locations of highways, cities, and towns in central and southern portions of the Gulf Coast Aquifer System in Texas (TNRIS, 2018).

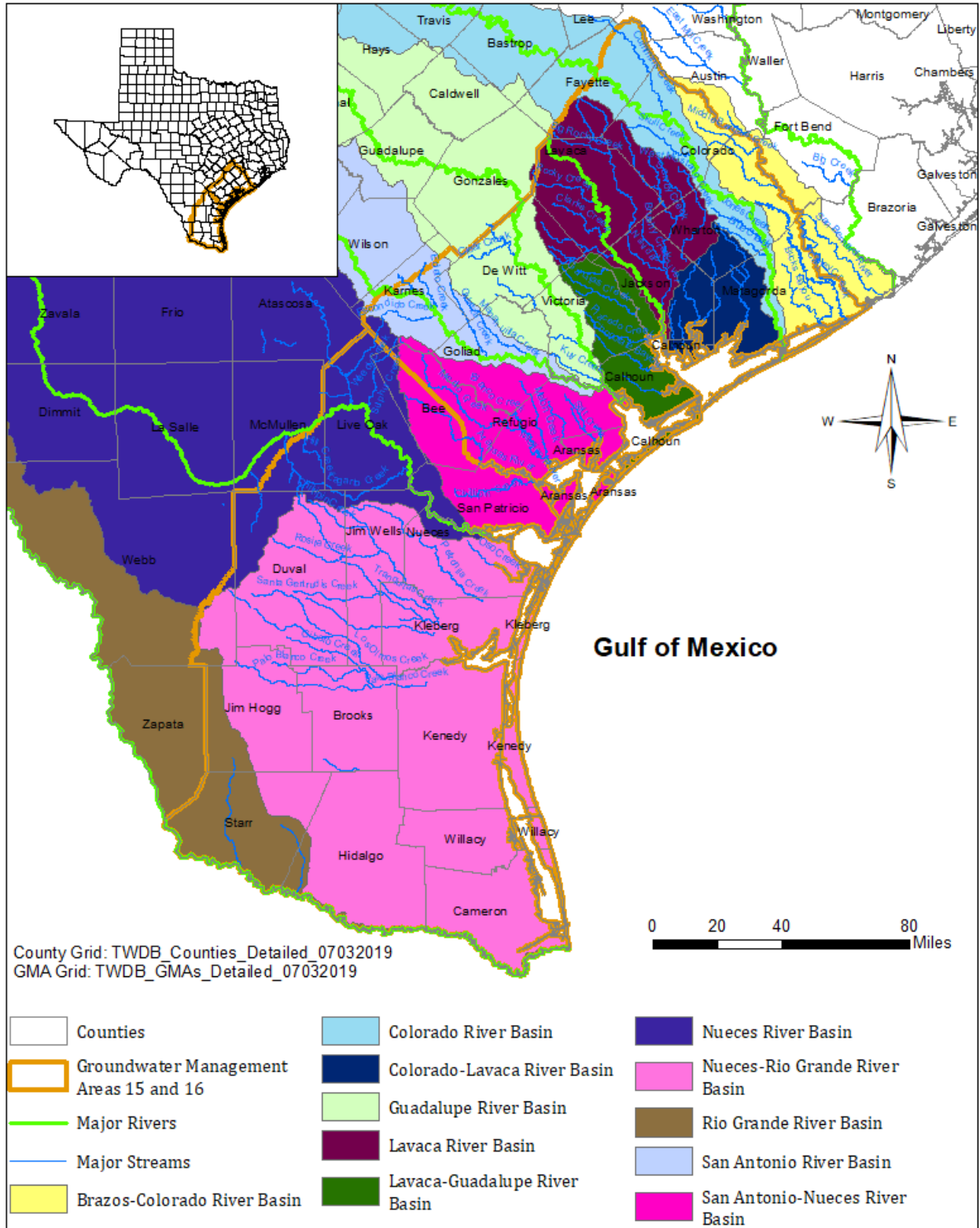


**Figure 2.0.1      Locations of river basins and major streams and rivers  
in central and southern portions of the Gulf Coast aquifer  
System in Texas (TNRIS, 2018).**

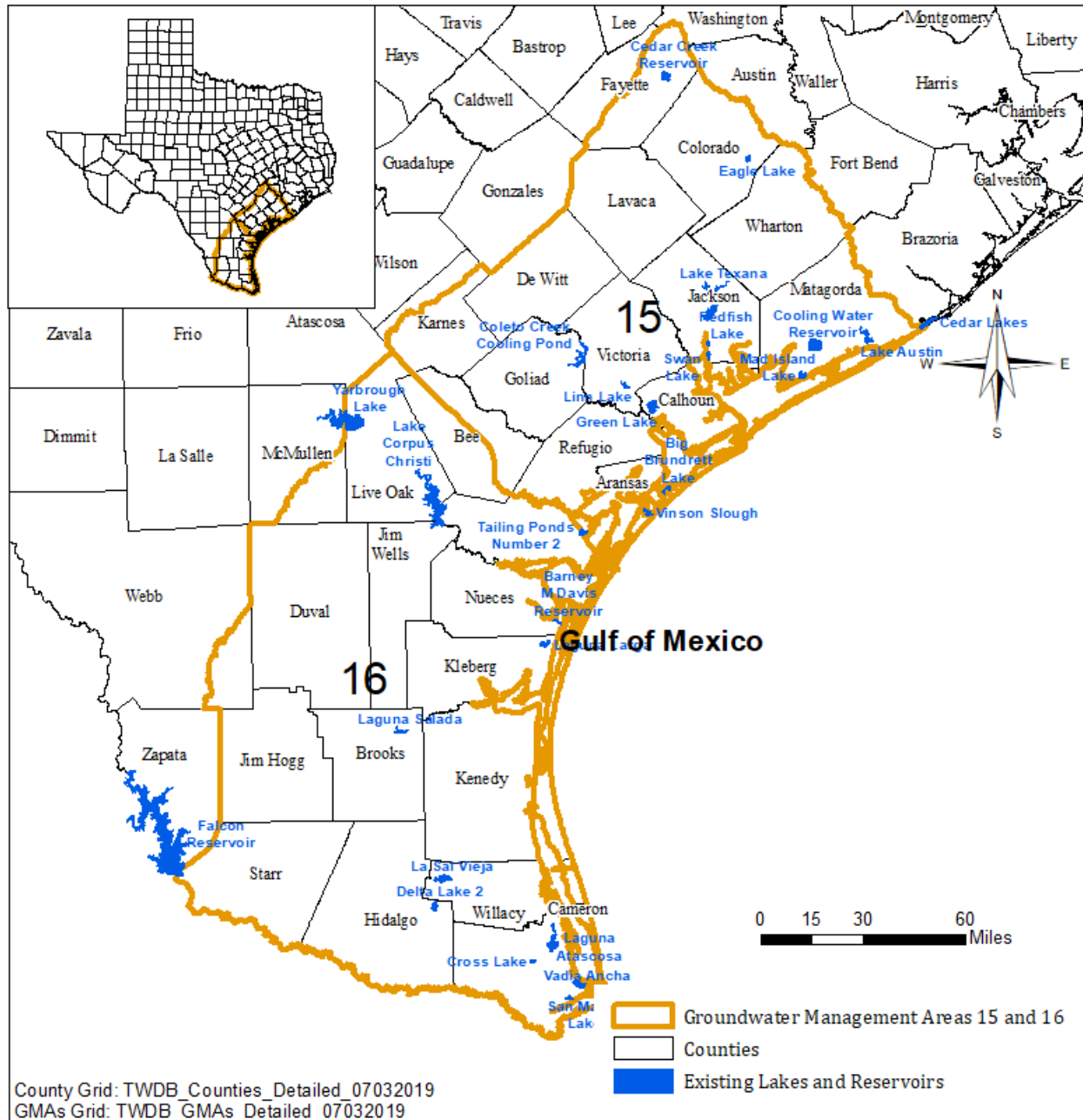


**Figure 2.0.2** Locations of existing reservoirs and lakes greater than one square mile in central and southern portions of the Gulf Coast aquifer System in Texas (TNRIS, 2018).

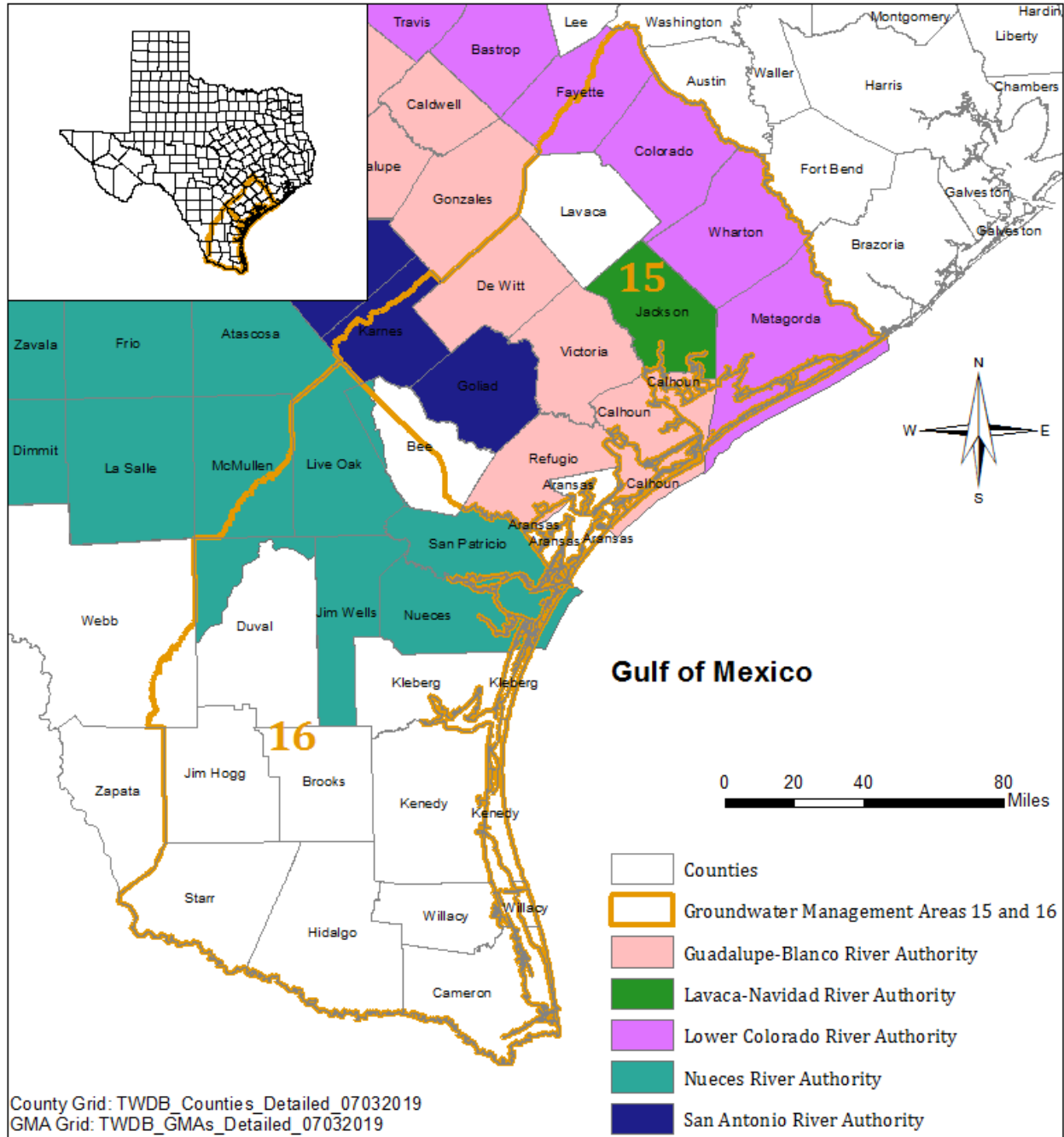


**Figure 2.0.3 Texas River Authorities in study area.**

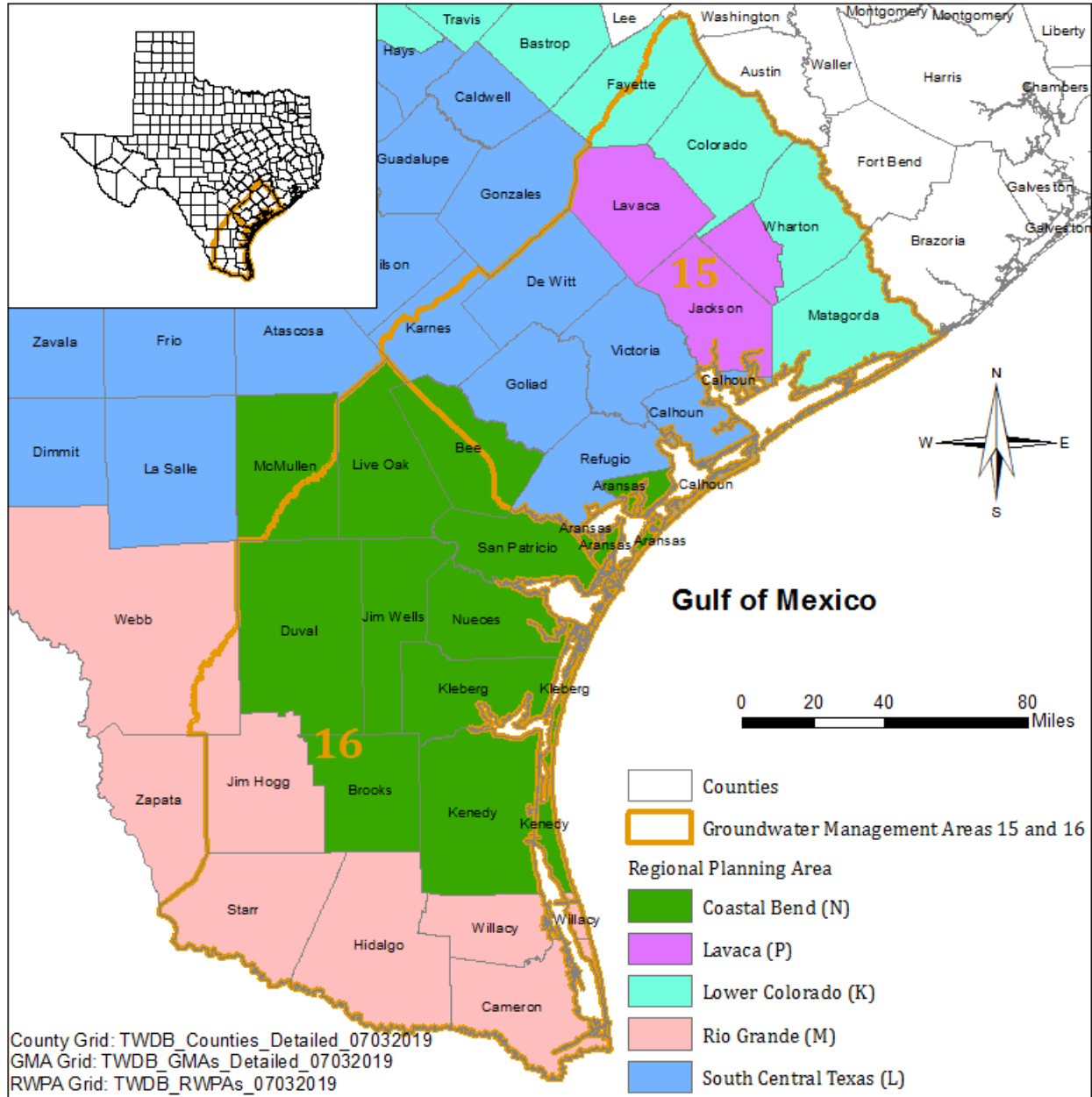


**Figure 2.0.4 Texas Regional Water Planning Areas in study area.**

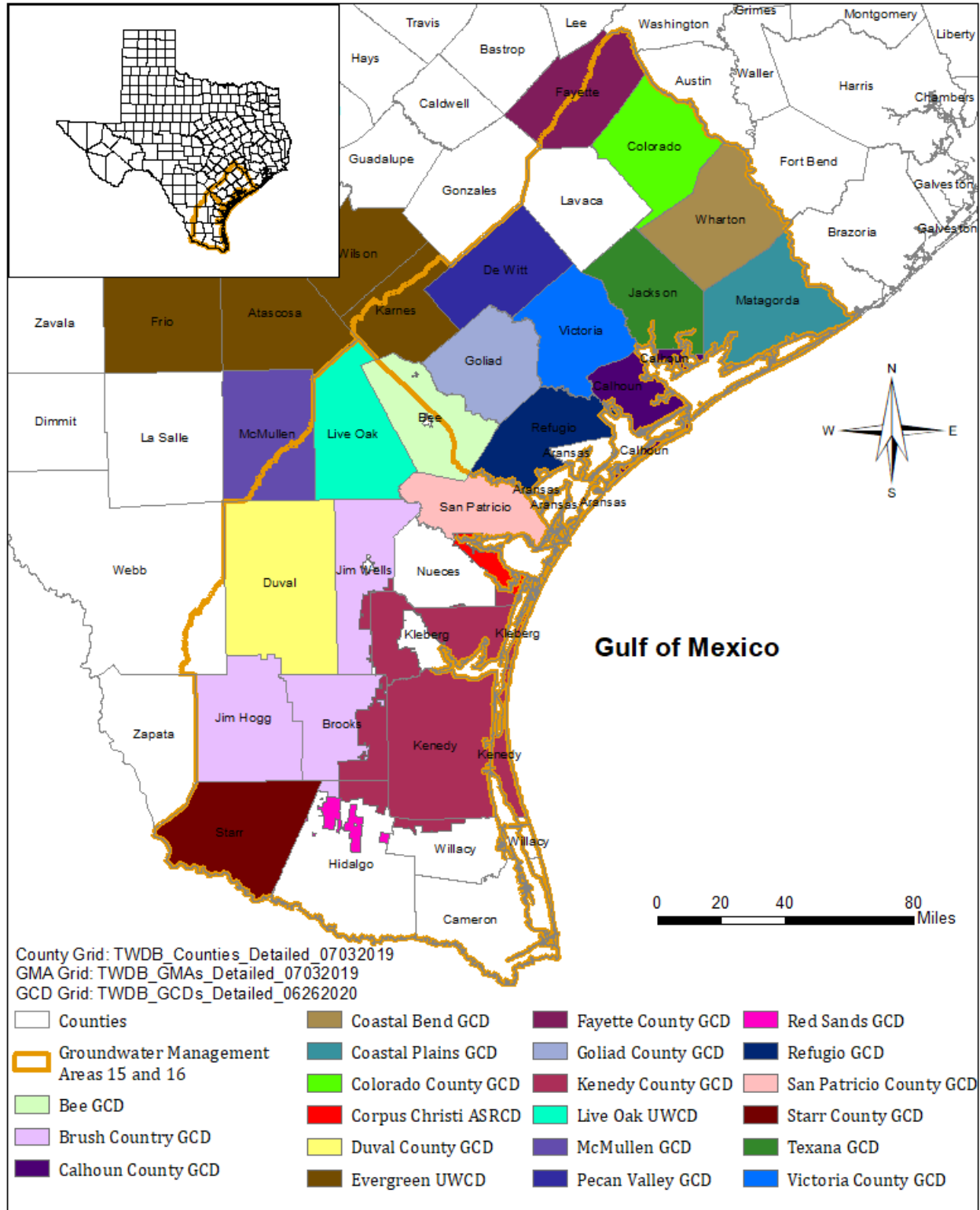


**Figure 2.0.5 Texas Groundwater Conservation Districts (GCDs), Underground Water Conservation Districts (UWCD),**



**and Aquifer Storage and Recovery Conservation District  
(ASRCD) in study area.**

## 2.1 Physiography and Climate

The study area sits on two physiographic provinces: the Coastal Prairies and the Interior Coastal Plains (Figure 2.1.1). Physiographic provinces are areas with similar landforms that distinguish them from adjacent areas. According to Wermund (1996), the Coastal Prairies is comprised of deltaic sands, silts, and clays with flat grasslands and broad sand sheets pocked by low dunes and blowouts forming ponds, while the Interior Coastal Plains is characterized by alternating belts of uncemented but resistant sand ridges among weaker shales. Except along streams and in oak mottes, large trees are sparse, and the study area is dominated by chaparral brush and grass with decreasing density toward the southwest.

The study area is in four Level III ecological regions (Figure 2.1.2). Ecological regions have distinct assemblages of natural communities and species. The Western Gulf Coastal Plains is mainly grassland and cropland. Pasture and range are common in the East Central Texas Plains with a spread of underlying dense, lower permeable clay pans. The Texas Blackland Prairies is composed of clayey soils and is dominated with cropland and pasture and forage production for livestock. Thorny brush such as mesquite is the predominant species in the Southern Texas Plains.

The ground surface increases from zero along the Gulf Coast towards the inland and reaches over 1,000 feet above mean sea level in Webb County (Figure 2.1.3). Elongated depressions exist along rivers and streams. The bottom of the Gulf of Mexico deepens in the eastern portion of the study area to more than 100 feet below sea level. Sand barriers separate the shallower estuaries from the deeper open ocean.

The climate in the study area is classified as Subtropical Humid, Subtropical Subhumid, and Subtropical Steppe with warm summers and decreasing humidity, decreasing precipitation, and greater daily temperature change from northeast to southwest (Larkin and Bomer, 1983) (Figure 2.1.4). The average annual temperature from 1981 to 2010 in the study area calculated from Parameter-elevation Relationships on Independent Slopes Model (PRISM) data (30-year normal from <https://prism.oregonstate.edu/normals/>) ranges from upper

60s (Fahrenheit) to middle 70s (Fahrenheit) with an increasing trend from northeast to southwest (Figure 2.1.5).

The 36-year (1980 to 2015) average annual precipitation based on PRISM (2018) shows an opposite trend ranging from about 54 inches per year at the northern coastal area to less than 20 inches per year at the southwest of the study area (Figure 2.1.6). Data collected from the study area between 1980 and 2015 show that precipitation could vary significantly from year to year (Figures 2.1.7 through 2.1.9). Please note the annual precipitation data were calculated using monthly data and any years without the complete 12-month data were not used for the annual precipitation calculation. The average monthly precipitation calculated from the same dataset shows moderate bimodal distribution with two relatively high precipitation periods: May through June and September through October (Figures 2.1.10 through 2.1.12).

The average annual lake evaporation rate between 1971 and 2000 increases from north to south and from the Gulf to inland ranging from about 40 to 70 inches per year (Figure 2.1.13). The annual lake evaporation rate significantly exceeds the annual average rainfall in the southern inland. Figure 2.1.14 shows the average lake evaporation difference between August and January for the period 1971 through 2000, which, like the annual evaporation rate, also indicates an increasing trend from north to south and from the Gulf to inland. Using vegetation type information from satellite images Scanlon and others (2012) estimated actual evapotranspiration in the study area ranging from about 12 to 58 inches per year (Figure 2.1.15).

Based on the Soil Survey Geographic Database (SSURGO) (Natural Resources Conservation Service, 2020), the soils in the study area are dominated by clays and other fine-grained materials in the north (Groups C and D) and transition to sand and gravels in the south (Groups A and B) (Figure 2.1.16). If other factors such as precipitation, landscape, temperature, and vegetation are the same, coarser soils (Groups A and B) tend to have higher infiltration rate or lower surface runoff potential than finer soils (Groups C and D).

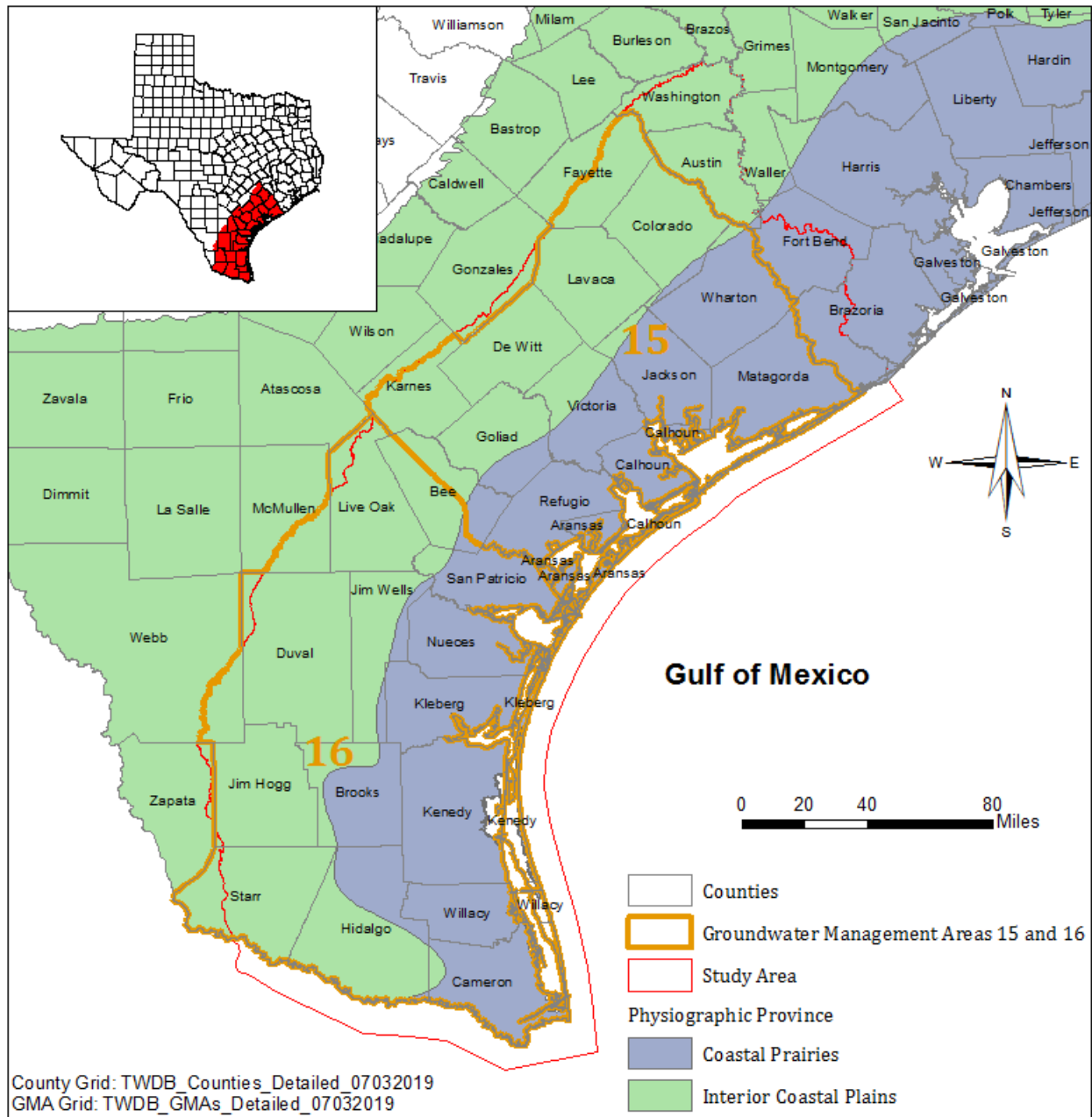


**Figure 2.1.1** Physiographic provinces in study area (Wermund, 1996).

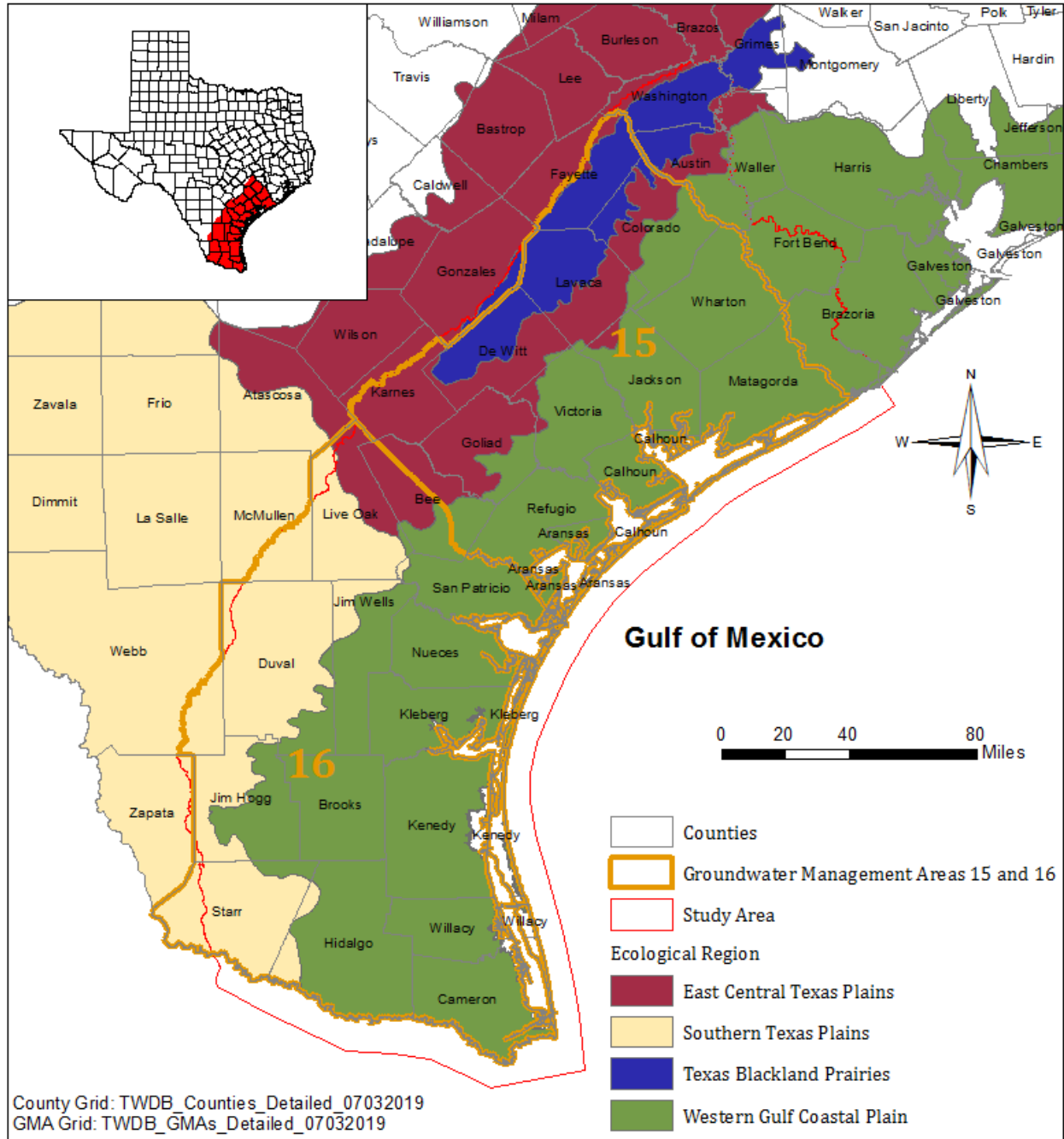


**Figure 2.1.2 Level III ecological regions in study area (U. S. Environmental Protection Agency, 2013).**

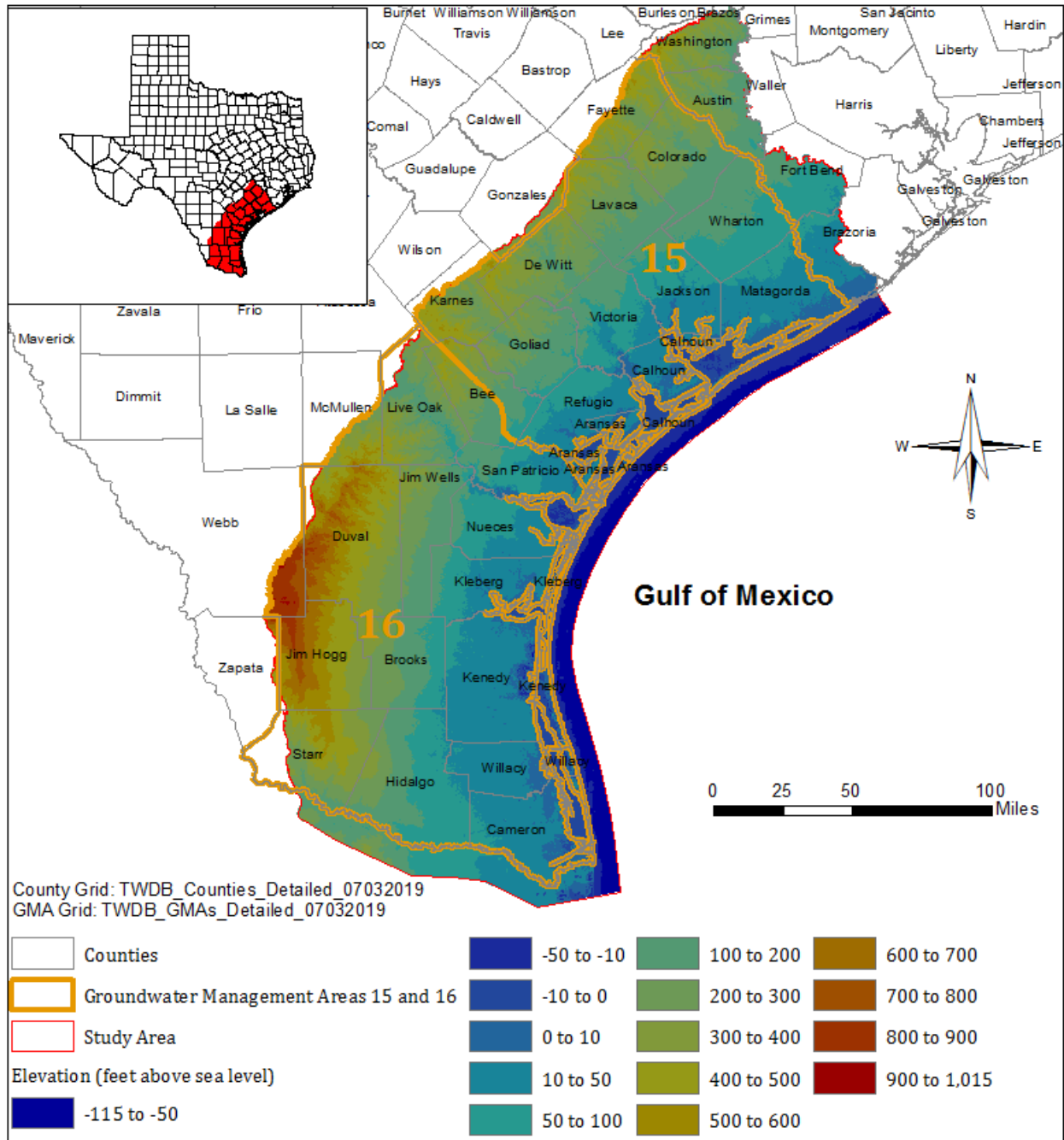


**Figure 2.1.3** Elevation of land surface and bathymetry of Gulf of Mexico. Land surface elevation data are from U. S. Geological Survey National Elevation Dataset. Bathymetry of Gulf of Mexico (w98e78n31s18\_bathy.img) is downloaded from <http://gcoos.tamu.edu/products/topography/SRTM30PLUS.html>.

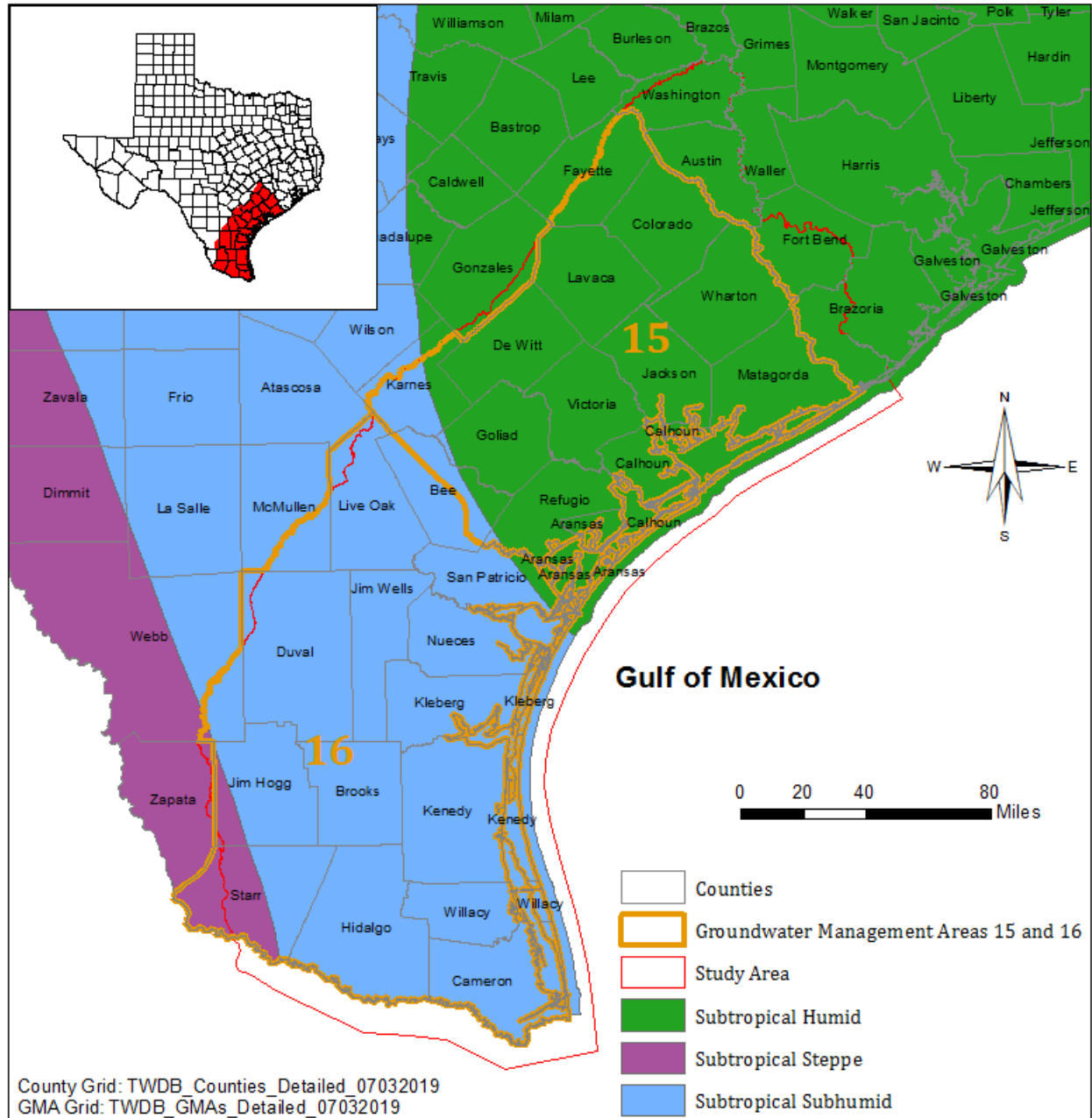


**Figure 2.1.4 Climate classifications of study area (based on Larkin and Bomar, 1983).**

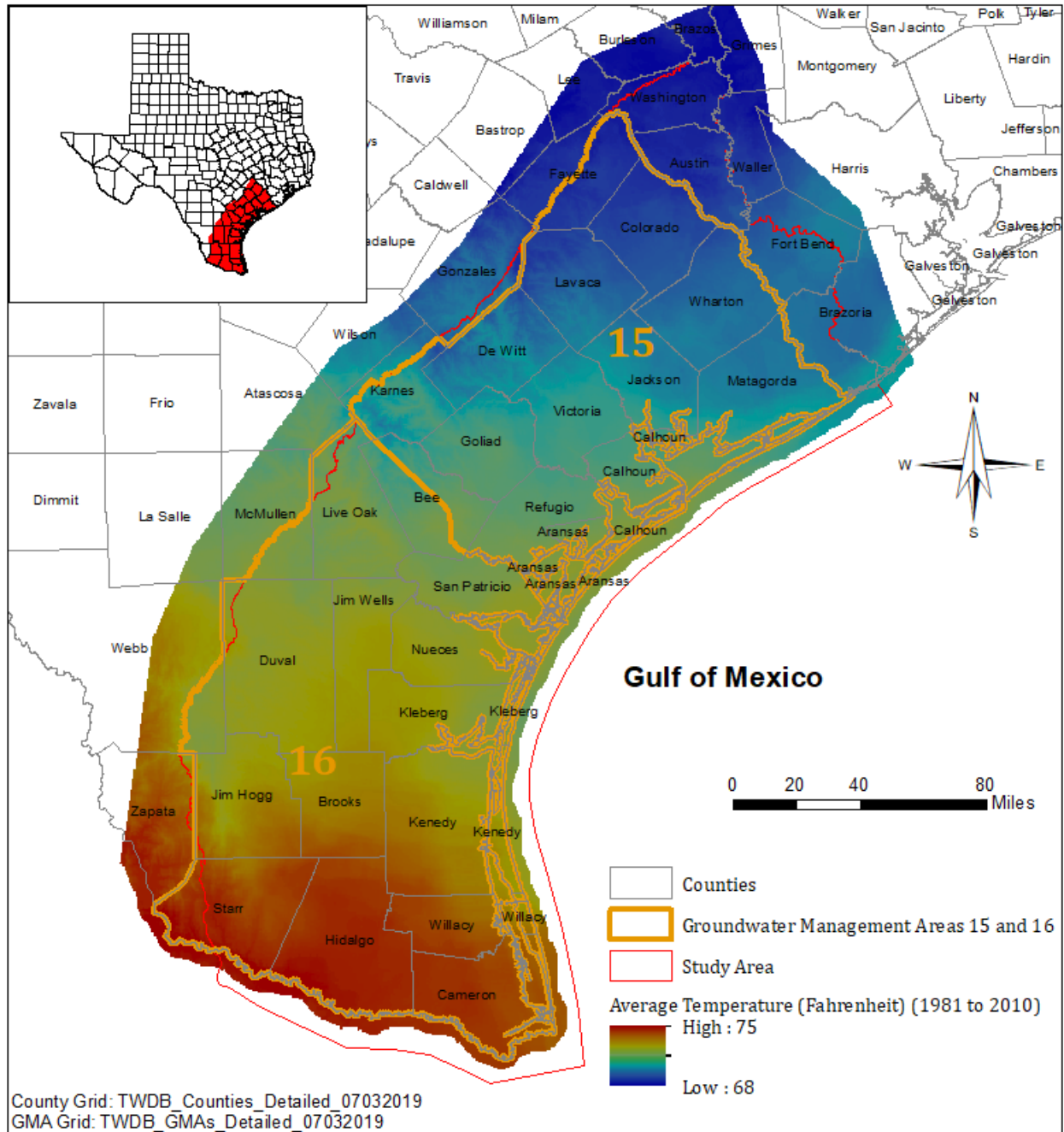


**Figure 2.1.5** Average annual air temperature for time period 1981 to 2010 (based on PRISM 30-year normal downloaded from <https://prism.oregonstate.edu/normals/>).



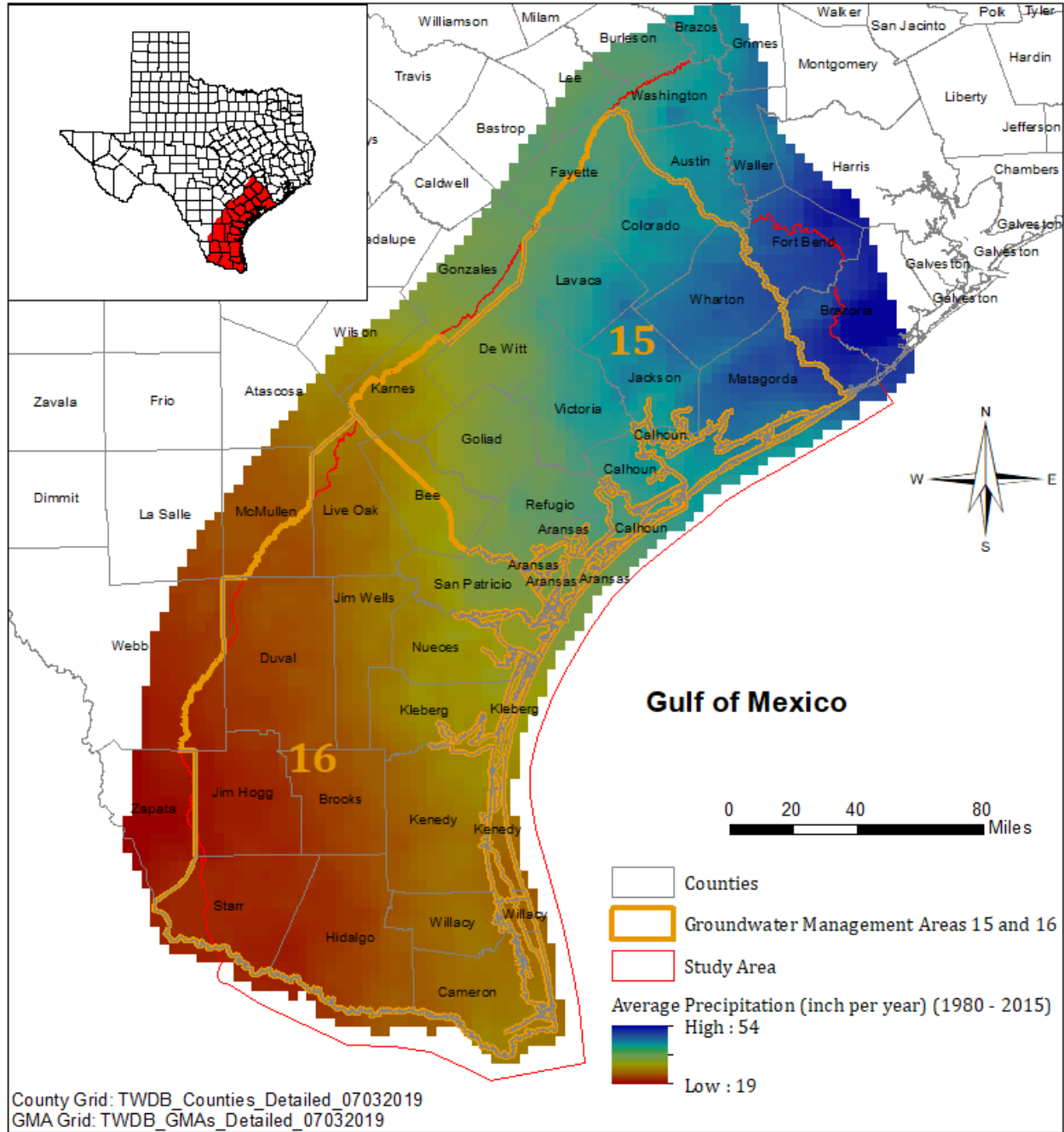


**Figure 2.1.6 Average annual precipitation for time period 1980 to 2015 (PRISM, 2018).**

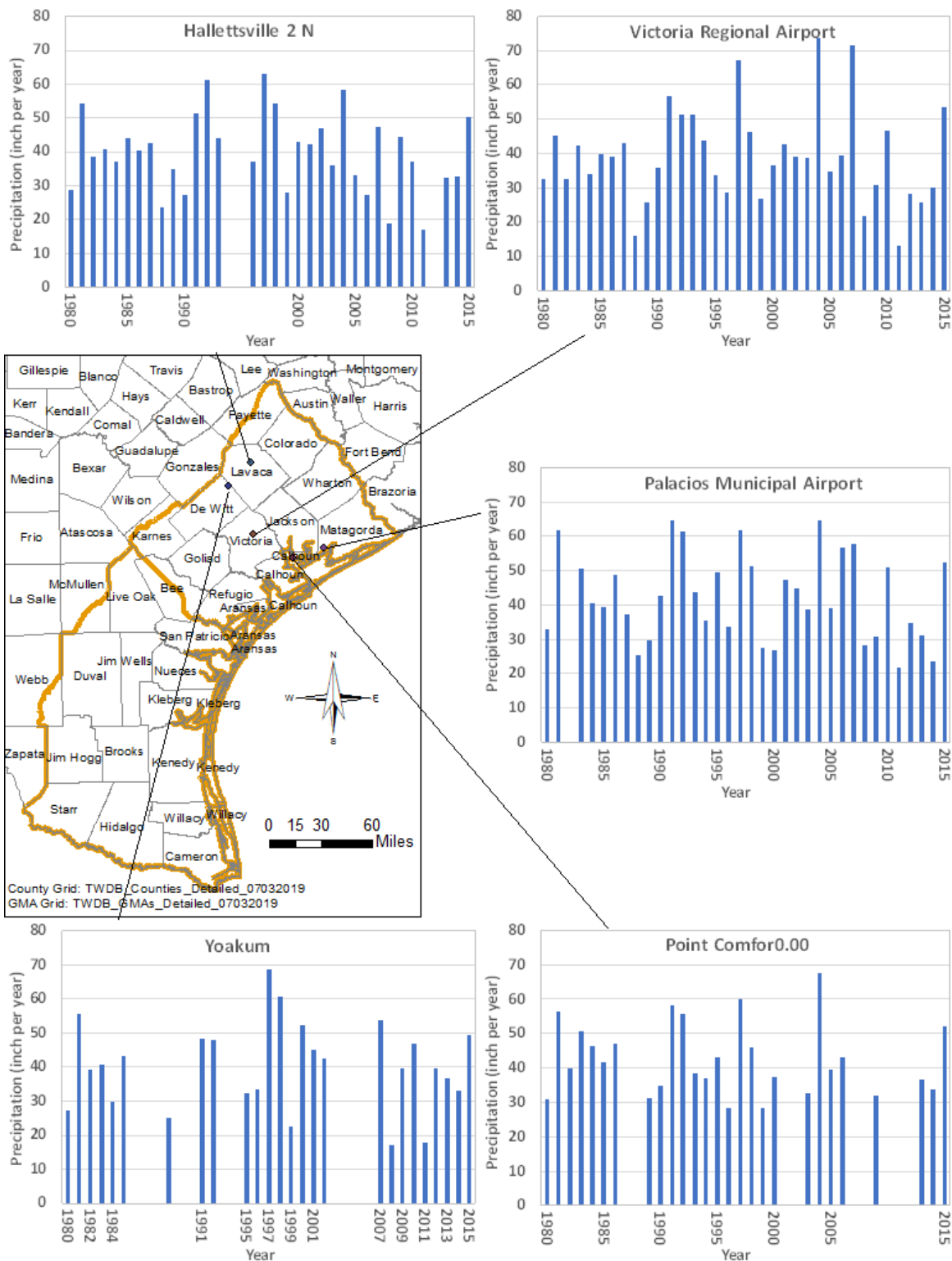


**Figure 2.1.7 Measured annual precipitation at stations in Calhoun (Point Comfor0.00), Dewitt (Yoakum), Lavaca (Hallettsville 2 N), Matagorda (Palacios Municipal Airport), and Victoria**

**(Victoria Regional Airport) counties (National Climatic Data Center, 2018).**

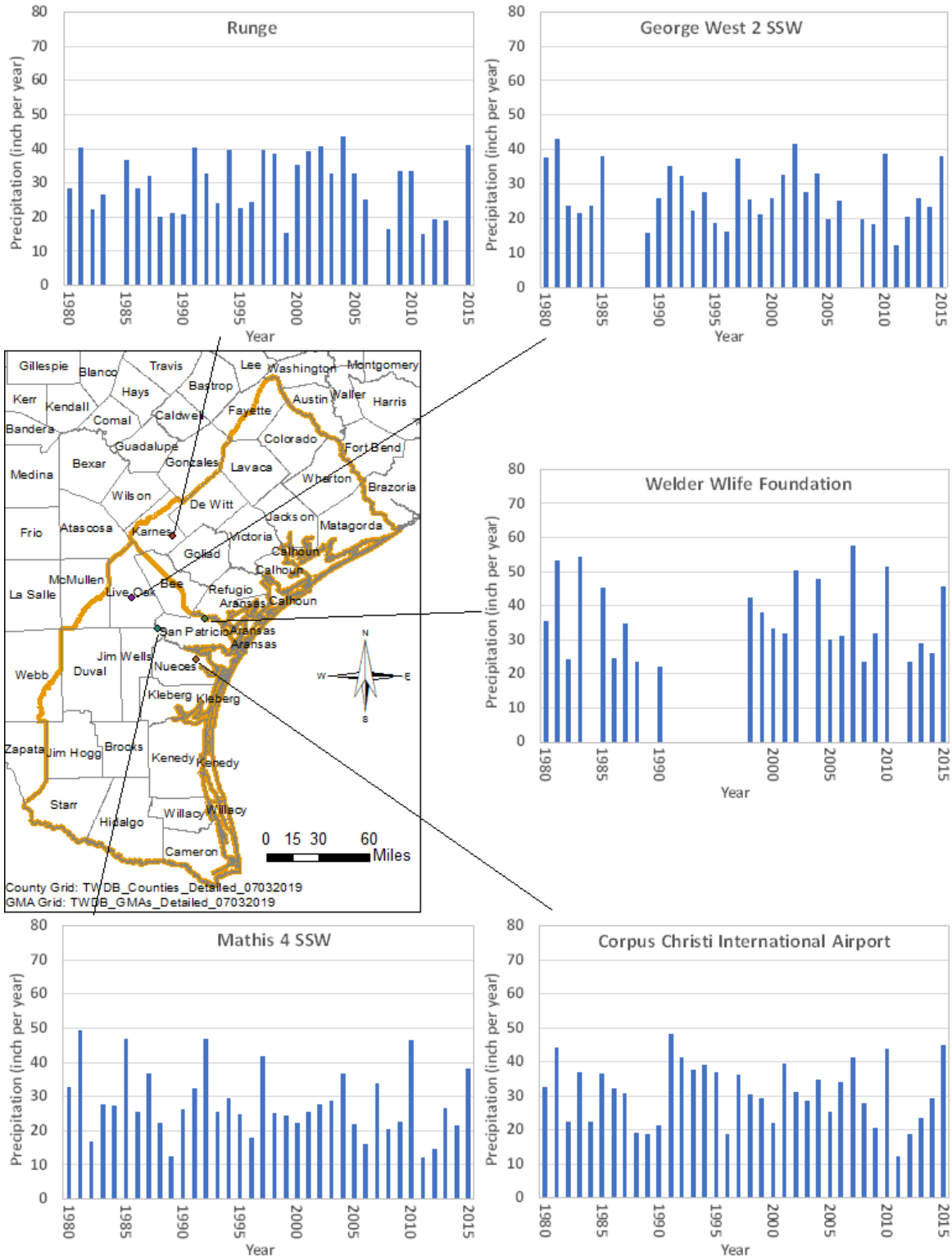


**Figure 2.1.8 Measured annual precipitation at stations in Karnes (Runge), Live Oak (George West 2 SSW), Nueces (Corpus Christi International Airport), Jim Wells (Mathis 4 SSW), and**

**Refugio (Welder Wliffe Foundation) counties (National Climatic Data Center, 2018).**

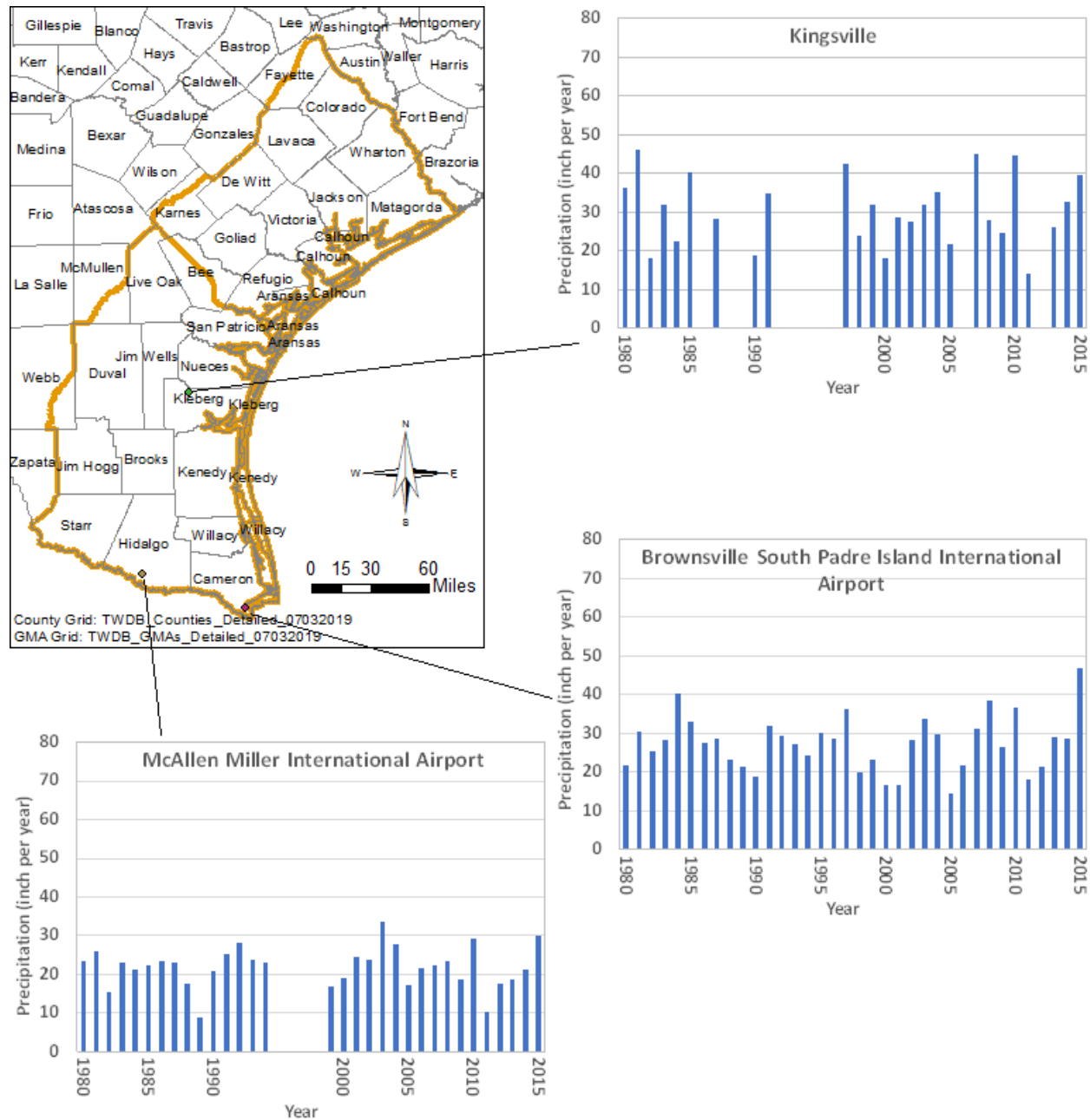


**Figure 2.1.9 Measured annual precipitation at stations in Cameron (Brownsville South Padre Island International Airport), Hidalgo (McAllen Miller International Airport), and Kleberg (Kingsville) counties (National Climatic Data Center, 2018).**

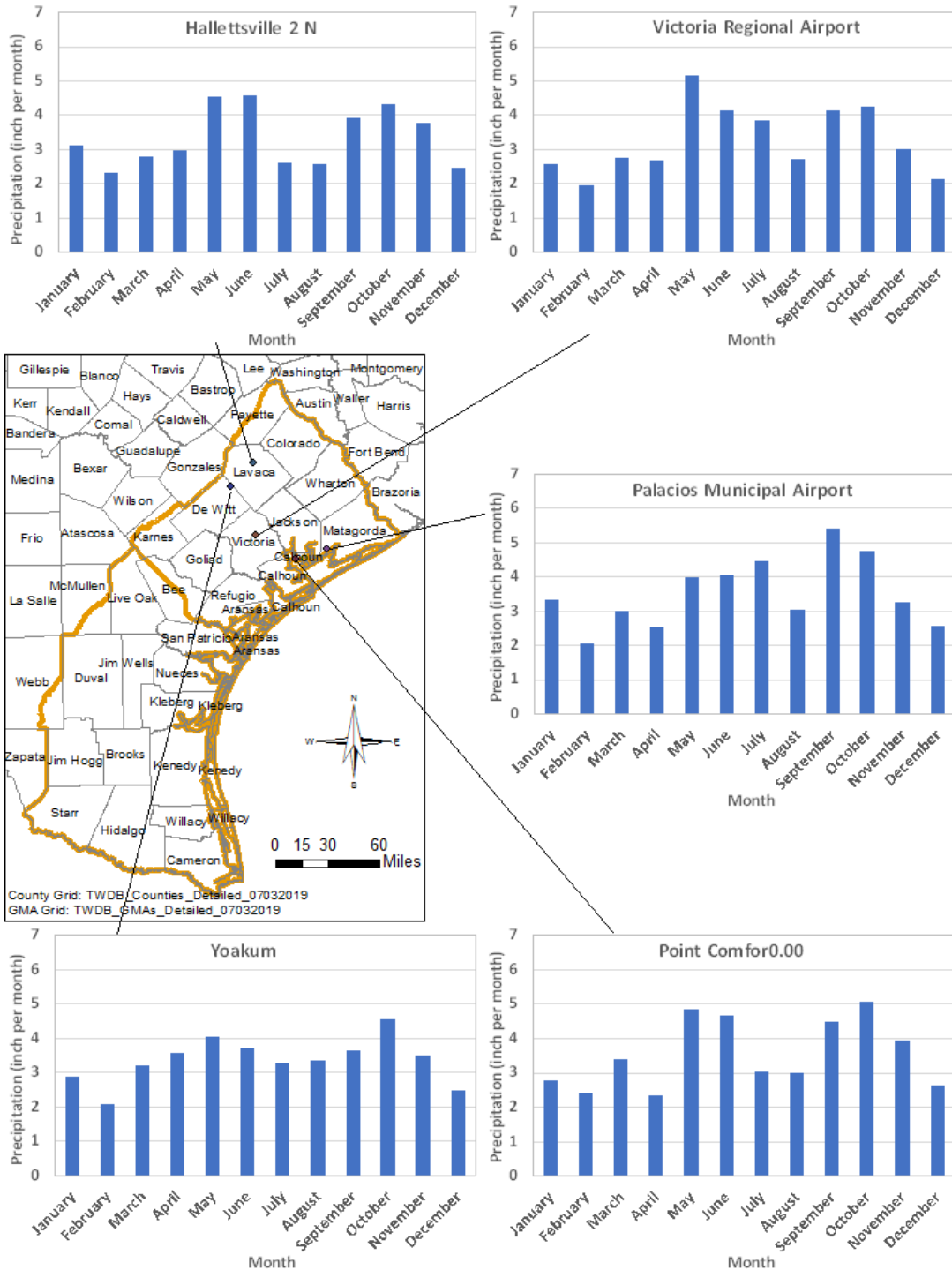


**Figure 2.1.10 Measured average monthly precipitation between 1980 and 2015 at stations in Calhoun (Point Comfor0.00), Dewitt (Yoakum), Lavaca (Hallettsville 2 N), Matagorda (Palacios Municipal Airport), and Victoria (Victoria Regional Airport) counties (National Climatic Data Center, 2018).**

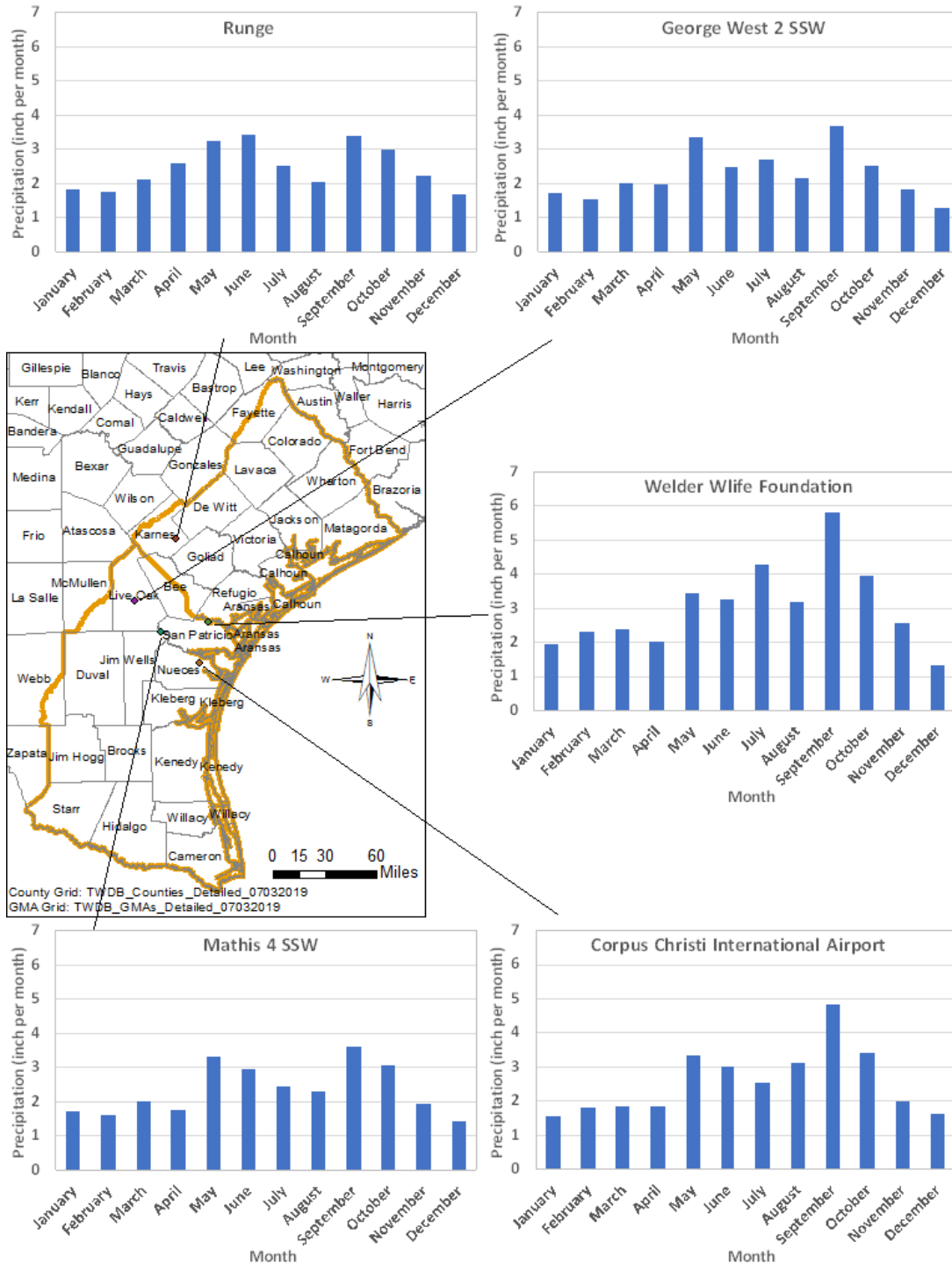


**Figure 2.1.11 Measured average monthly precipitation between 1980 and 2015 at stations in Karnes (Runge), Live Oak (George West 2 SSW), Nueces (Corpus Christi International Airport), Jim Wells (Mathis 4 SSW), and Refugio (Welder Life Foundation) counties (National Climatic Data Center, 2018).**



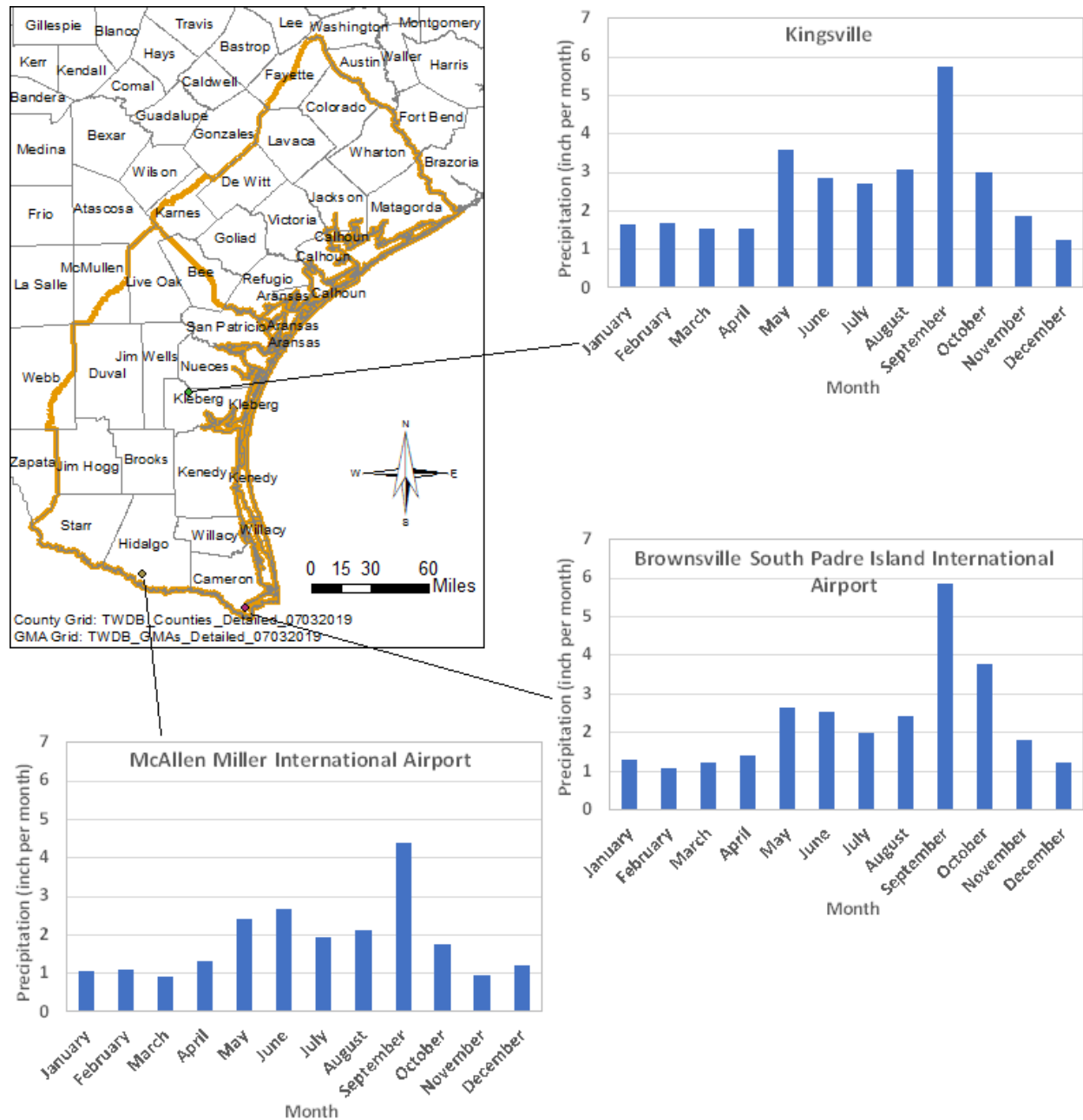


**Figure 2.1.12** Measured average monthly precipitation between 1980 and 2015 at stations in Cameron (Brownsville South Padre Island International Airport), Hidalgo (McAllen Miller International Airport), and Kleberg (Kingsville) counties (National Climatic Data Center, 2018).

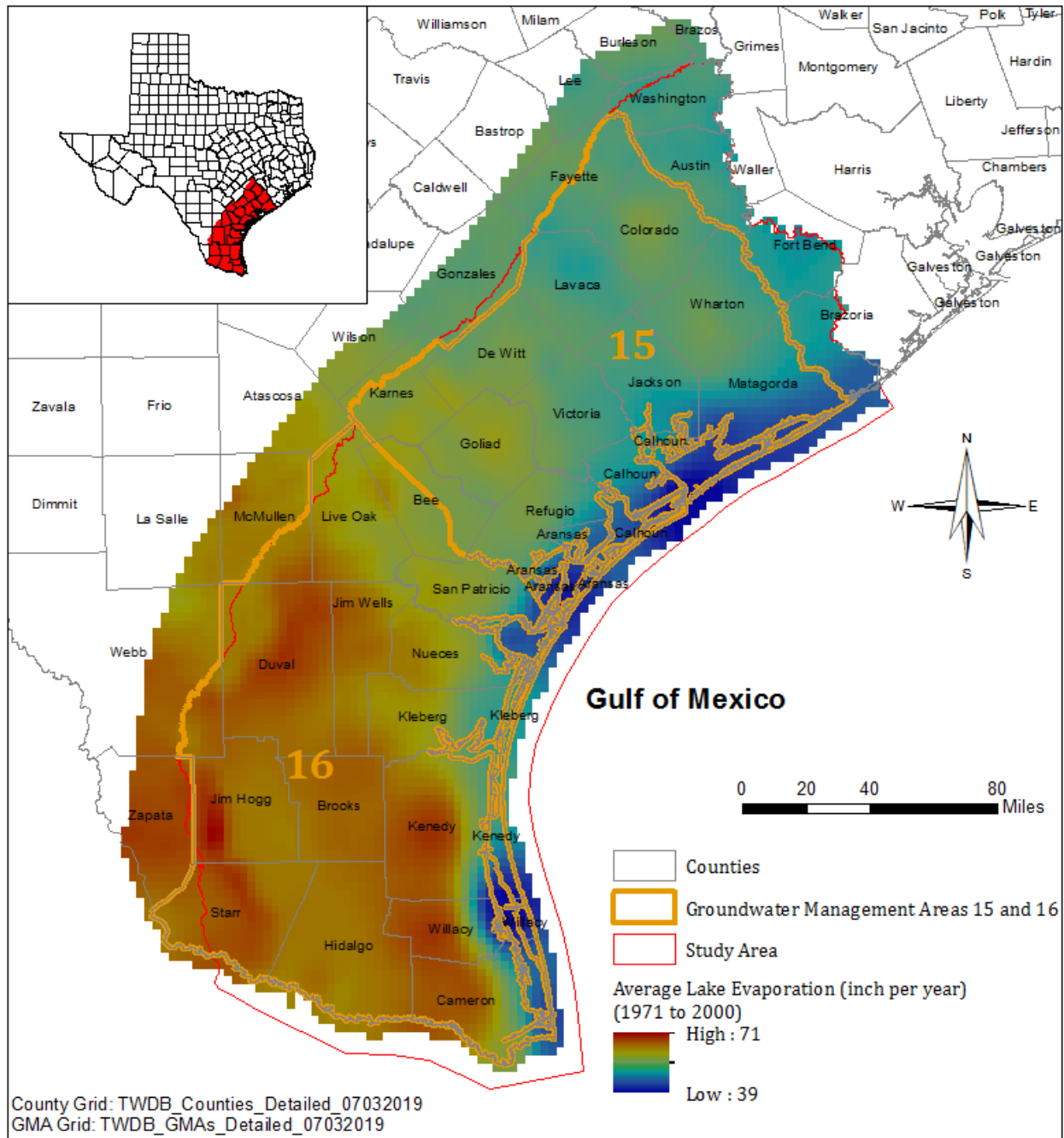


**Figure 2.1.13 Average annual lake evaporation rate (inch per year) between 1971 and 2000 in study area (Narasimhan and others, 2007).**

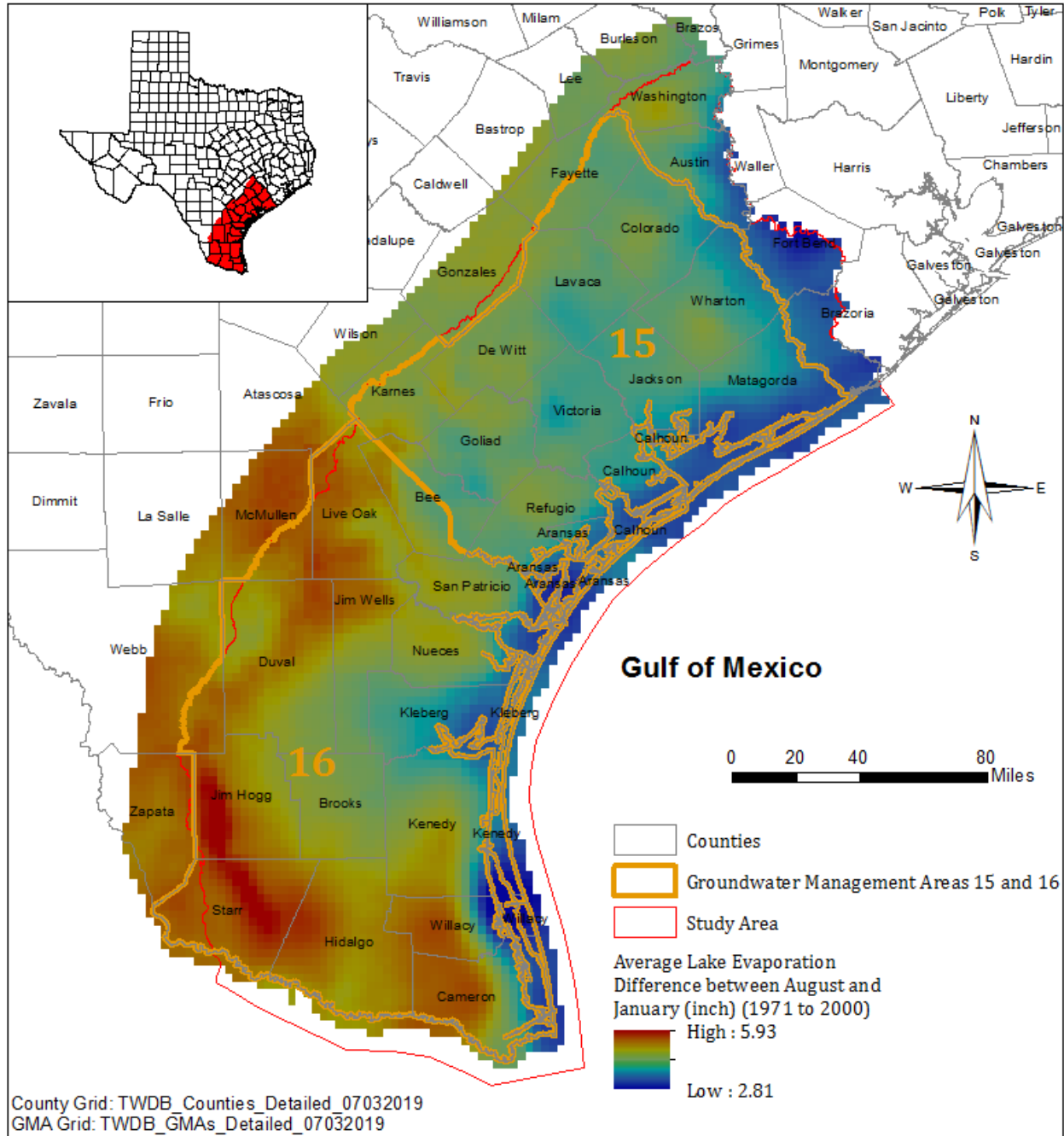


**Figure 2.1.14 Average lake evaporation difference between August and January for the period 1971 through 2000 in study area (based on monthly data from Narasimhan and others (2007)).**

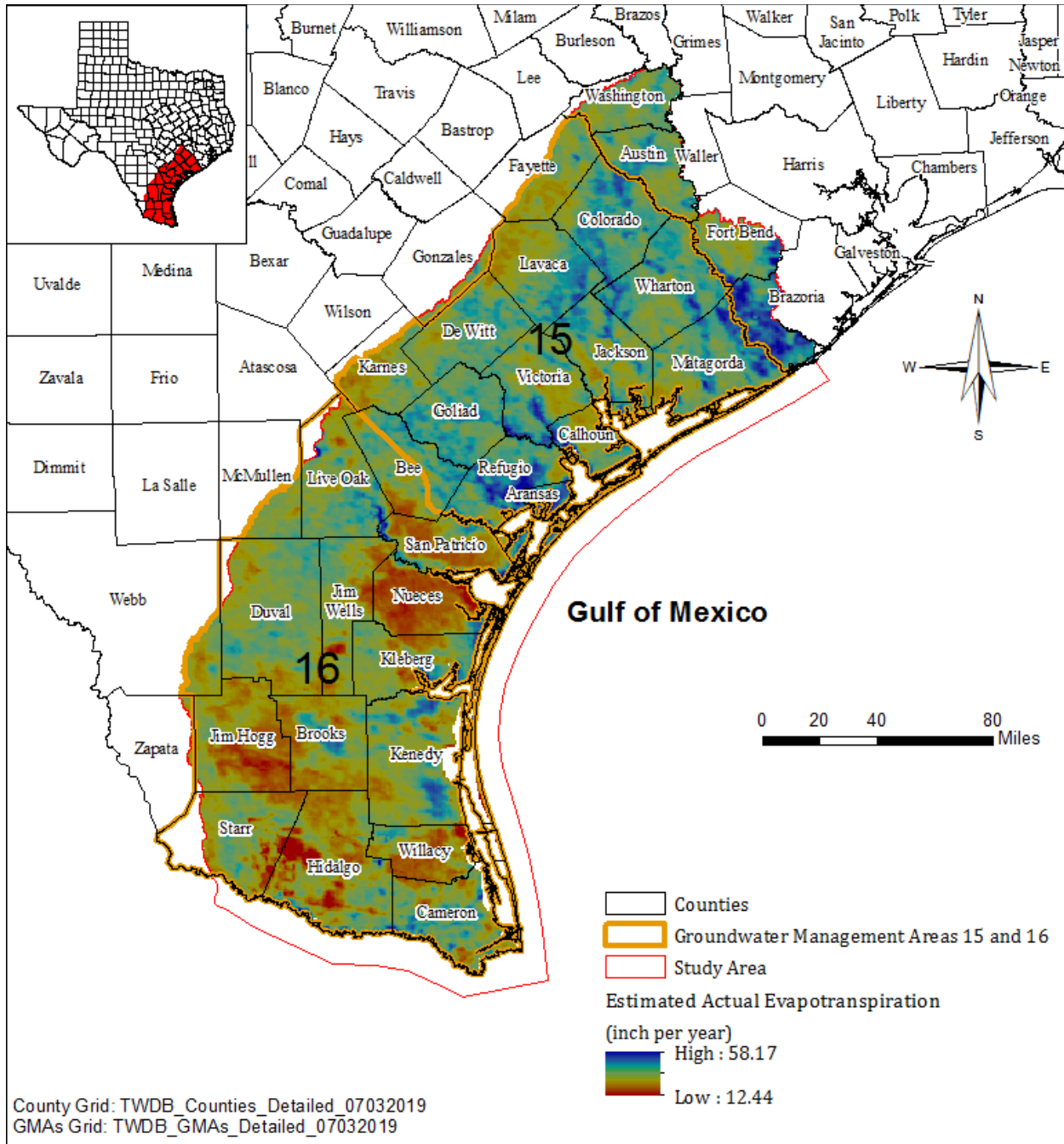


**Figure 2.1.15 Estimated actual evapotranspiration in study area (Scanlon and others, 2012).**

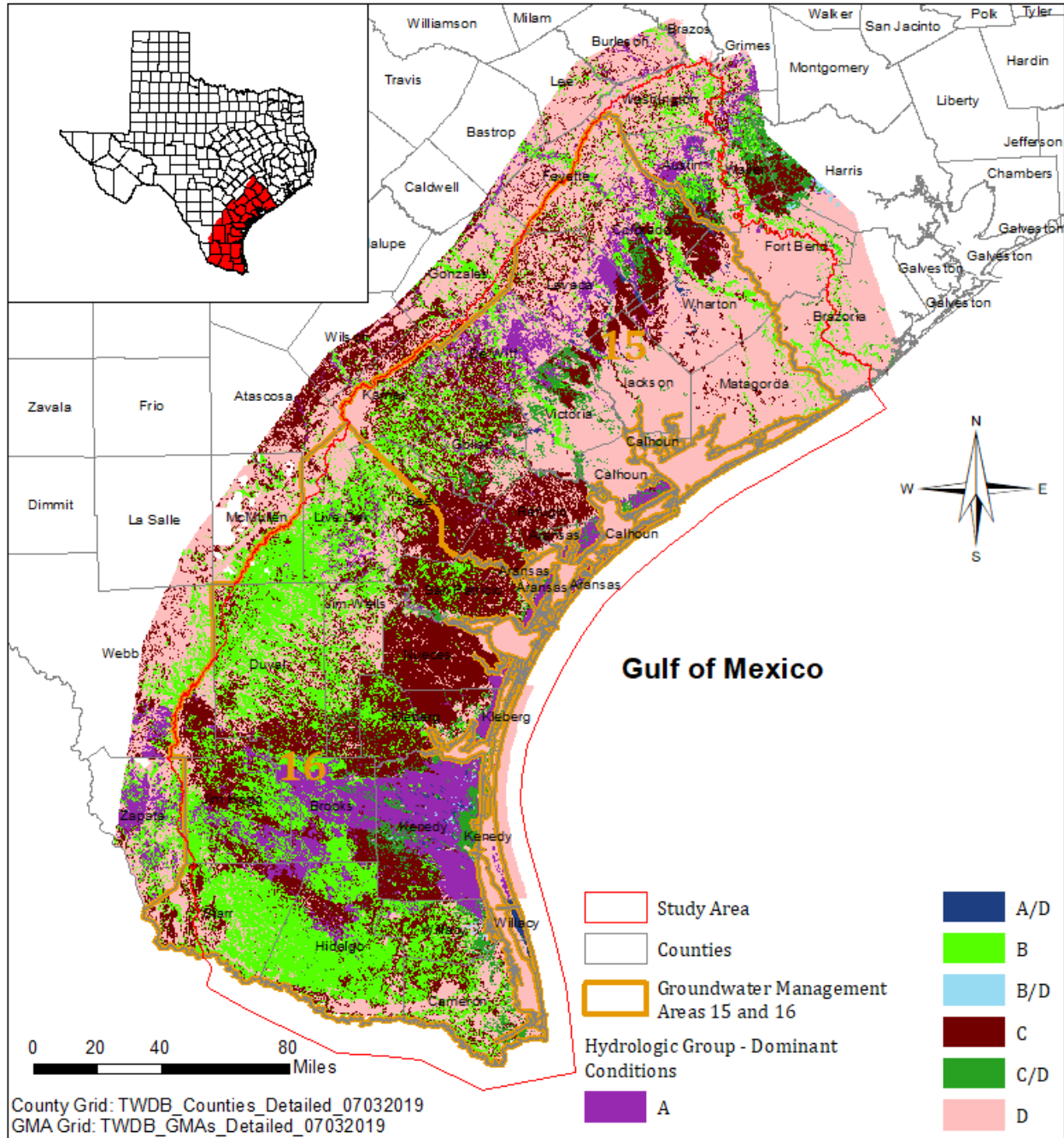


**Figure 2.1.16** Soils in study area based on Soil Survey Geographic Database (SSURGO) downloaded from <https://www.arcgis.com/apps/View/index.html?appid=cdc49bd63ea54dd2977f3f2853e07fff>.

## **2.2 Geology**

The Gulf Coast Aquifer System in the study area contains the following geological units (from the oldest to the youngest): the sandy portion of the Catahoula Formation near the outcrop area, the Oakville Formation, the Fleming Formation, the Goliad Formation, the Willis Formation, the Lissie Formation, the Beaumont Formation, and the Holocene alluvium and Eolian sand (Table 2.1.1). Young and others (2010, 2014) combined the Oakville and the Lagarto formations into Fleming Group. In this study, the Fleming Formation is treated as the equivalent of the Lagarto Formation. This section provides a brief discussion of the geology of the study area. The discussion is divided into the structural setting, geologic history, faults, salt domes, and surface geology through the study area. Details about the Gulf Coast Aquifer System can be found in Young and others (2010, 2014) and Mace and others (2006).

### **2.2.1. Structural Setting**

The study area sits on the northern coastal zone of the Gulf of Mexico, which originated during the early Mesozoic Era due to separation of the South American continent (part of the Gondwana) from the North American continent (the Laurentia). Intermittent marine flooding formed extensive evaporite deposits along rift valleys during the Jurassic period. During early Cretaceous, transgressive seas intruded the study area and its northwest with deposition of carbonate rocks, which formed the foundation for subsequent terrigenous clastic sedimentation during the Cenozoic period (Winker and Buffler, 1988). These terrigenous clastic sediments formed (from the oldest to the youngest): the Carrizo-Wilcox Aquifer, the Queen City Aquifer, the Sparta Aquifer, the Yegua-Jackson Aquifer, and the Gulf Coast Aquifer System. The study area is underlain predominantly by the Gulf Coast Aquifer System. Other older aquifers mainly exist to the northwest of the study area, though geologic units equivalent to the older aquifers are present under the Gulf Coast Aquifer System in the study area.

Ewing (1991) and Galloway and others (1991) classified the study area as part of the northwestern margin of terrigenous clastic sedimentation of the Gulf of Mexico basin.

Specifically, the study area was considered by Ewing (1991) and Young and others (2010) as a coastal zone extending from the early Cretaceous shelf margin to the base of the modern continental slope (Figure 2.2.1). The deposition of the clastic sequences on the Cretaceous carbonate platform was controlled by the climate, the source area, and the San Marcos Arch (Figure 2.2.1). The climate mainly controlled the sea level fluctuation which caused the phase change between nearshore deltaic and shallow marine deposition environments. The change of source area to the northwest of the study area shifted the deposition center along the Gulf Coast. The San Marcos Arch was a structural high that separated two structure-low areas: the Houston Embayment to the east and the Rio Grande Embayment to the west. In the coastal zone, the Cenozoic clastic sequences got thicker towards the embayments and southeast due to subsidence. According to Young and others (2014), the Gulf Coast Aquifer System of Texas was located within the onshore non-marine Neogene sediments.

### **2.2.2. Geologic History**

The Gulf Coast Aquifer System in the study area was composed of deposits from fluvial-deltaic non-marine environments ranging from gravel, sand, silt, to clay. In the deltaic environment, river channels were often filled with sand and gravel and bounded by silt and clay in flood plains, which limited the extent of each lithological unit (Young and others, 2014). These fluvial deltas were the deposition centers and were mainly controlled by the source area of the sediments. Changes in the source area location caused the shift of the deposition centers.

During and prior to the sedimentation of the Catahoula Formation, the deposition centers were around the Houston Embayment and Rio Grande Embayment due to the large volumes of sand, silt, and clay from the southern Rocky Mountains and volcanos in West Texas and Mexico (Winker, 1982; Morton and Galloway, 1991; Galloway, 2005) (Figure 2.2.2(A)). The Catahoula Formation is mainly composed of non-marine sands, clays, and volcanic deposits interbedded with alluvium sediments. In general, the Catahoula Formation unconformably overlies the Jackson Group (sandstone) in the north and the Frio Formation (clay) in the south of the study area. The Catahoula Formation grades finer with

increasing thickness ranging from about 200 feet to 1000 feet from north to south (Mace and others, 2006). Further downdip, the Catahoula Formation grades to the Frio and Anahuac formations.

The Rio Grande Rift in New Mexico reduced the sediment supply to the Rio Grande Embayment and shifted the deposition center at the Houston Embayment to the Mississippi Embayment when the Oakville Formation (sandstone) was deposited (Winker, 1982) (Figure 2.2.2(B)). However, during the Miocene (Oakville, Fleming (Lagarto), and Goliad formations), the Edwards Plateau along the Balcones Fault Zone in Central Texas supplied abundant Cretaceous calcareous detritus to smaller fluvial systems in the study area (Galloway and others, 1986; Morton and others, 1988). The Oakville Formation, unconformably overlying the Catahoula Formation, is mainly sandstone with some clay (Sellards and others, 1932). The Oakville Formation was formed in the lower progradational part of a major fluvial-deltaic depositional episode with a thickness ranging from 300 to 700 feet at outcrop area to 1,000 to 2,000 feet along the coast (Baker, 1979; Galloway and others, 1982 and 1986).

The major deposition center for the Cretaceous calcareous sediments was on the San Marcos Arch during middle-late Miocene (Fleming (Lagarto) and Goliad) (Figure 2.2.2(C)). Lithologically, the Fleming (Lagarto) Formation is similar to the Oakville Formation, but with higher clay content, especially in the south of the study area (Baker, 1979; Mace and others, 2006). Like the Oakville Formation, the Fleming Formation was formed in the upper retrogradational part of the same fluvial-deltaic depositional episode (Baker, 1979; Galloway and others, 1982 and 1986). According to Baker (1979) and Galloway and others (1982, 1986), the thickness of the Fleming Formation ranges from about 700 to 1,400 feet in outcrop area to 2,000 to 3,000 feet along the coast.

The Goliad Formation was deposited in a fluvial environment, which contained sands and gravels along river channels and muds in floodplains (Hoel, 1982). In general, the sediments in the Goliad Formation show an upward fining trend with caliche on top (Hosman, 1996). The Goliad Formation does not display significant thickness changes except locally across the major growth fault zones (Hoel, 1982). The thickness of the Goliad



Formation ranges from 200 feet at outcrop area to about 1,400 feet near the coast (Young and others, 2010).

During the Pliocene (Willis Formation) and Pleistocene (Lissie and Beaumont formations), the major deposition center had moved to the Mississippi Embayment. As a result, the study area was characterized by relatively thin deposits with channel fills along alluvial valleys due to the lack of tectonic activity and high-frequency glacio-eustatic fluctuations (Blum and Price, 1998) (Figure 2.2.2(D) and (E)). In the northern part of the study area, the Willis Formation consists of unfossiliferous sand, or sand not containing fossils, with gravels overlying the Fleming Formation (Solis, 1981). In the south of the study area, the Willis Formation is mainly gravelly sand with clay (Plummer, 1932). The thickness of the Willis Formation ranges from about 100 feet in the outcrop area to 500 feet along the coast (Knox and others, 2006).

The Lissie Formation unconformably overlies the Willis Formation, or the Goliad Formation where the Willis Formation is absent. The Lissie Formation was deposited in floodplain or deltaic environments (Sellards and others, 1932) and consists of fine to coarse sand (Mace and others, 2006; Knox and others, 2006) often with a caliche bed at the base (Price, 1934). The sand deposits are often found along fluvial channels and shallow shelf with fine-grained sediments in between (Young and others, 2010). The Lissie Formation is, in general, less sandy than the Willis Formation (Young and others, 2010). In comparison with underlying formations such as Willis and Goliad, the Lissie Formation shows a gentle dipping towards the Gulf (Mace and others, 2006; Solis, 1981). According to Knox and others (2006), the thickness of the Lissie Formation increases from about 100 feet at outcrop to more than 700 feet along the modern coast.

Overlying the Lissie Formation unconformably is the Beaumont Formation. The formation is dominated by fine-grained sediments such as clay and silt with sand or gravel patches along paleo-river channels, beaches, and barrier islands. The Beaumont Formation increases in thickness to about 500 feet near the modern coast and dips coastward from 1 to 10 feet per mile (Solis, 1981). Individual sand and clay layers range from 20 to 50 feet thick (Knox et al., 2006). Thicknesses of individual sands increase updip, whereas

thicknesses of individual shales increase downdip (Young and others, 2010). Along river channels, the Beaumont is 50% to 65% sand (Solis, 1981).

The Holocene sediments consist mainly of channel fills along river valleys and barrier islands (DuBar and others, 1991). According to Young and others (2010), the river valleys were first filled with bay-estuary muds as the sea level rose. Sandy alluvial deposits then filled the updip parts of the valleys when the fluvial-deltaic systems prograded seaward. Today, only the Colorado, Brazos, and Rio Grande rivers have filled their valleys to the coast. Other river valleys in the study area are still partly occupied by bays and lagoons. The Holocene fluvial sands along the Rio Grande and Brazos rivers could reach 30 feet thick (Wood and others, 1963). The deltaic silty and clayey sands range 100 to 300 feet in thickness near the mouth of the Rio Grande River (Brown and others, 1980). The eolian deposits cover large areas to the south and could reach 30 feet thick in Kenedy County (Wood and others, 1963). Details of the hydrogeologic units in the study area are summarized in [Table 2.2.1](#).

### **2.2.3. Faults**

Faults in the Gulf Coast Aquifer System are mainly growth faults parallel to the Gulf Coast. These growth faults created vertical preferential pathways for groundwater flow due to coarser deposits along the downthrown sides of the faults. In addition, the faulting also produced a thicker downthrown block and displaced lithological units against each other. Displacement by growth faults decreases upward ranging from a few hundred feet to only a few feet in the Gulf Coast Aquifer System (Verbeek, 1979). The displacement could hinder lateral groundwater flow due to juxtaposition of a permeable unit against a less permeable unit (Young and others, 2014). [Figure 2.2.3](#) shows the major normal faults in the Gulf Coast Aquifer System (Bureau of Economic Geology, 1997).

### **2.2.4. Salt Domes**

According to Young and others (2014), a salt dome typically includes a vertical, cylindrical salt stock consisting of 90 to 99 percent halite, sulfate, and carbonate cap rock on top of the salt stock, and uplifted sediments surrounding the salt stock. Salt-dome crests in the study

area are generally one to three miles in diameter. Salt dissolution by groundwater impacts water quality. The cap rock and high density of the salt stock can act as barriers and change the groundwater flow pattern. The location and depth to the cap rocks of the shallow salt domes in the study and their vicinities are presented in [Figure 2.2.4](#). Please note the locations of the salt domes are digitized from the Tectonic Map of Texas by Bureau of Economic Geology (1997) and the depths to the crests of the salt domes are from Young and others (2014), except the one located at northwestern Brooks County.

### ***2.2.5. Surface Geology***

The surface geology of the study area and its vicinity is presented in [Figure 2.2.5](#), showing the outcrops of geological formations approximately parallel to the Gulf Coast. Please note, in Mexico, the Catahoula/Frio Formation, Fleming/Oakville Formation, and Goliad Formation are separated. The Catahoula Formation's outcrop defines the Gulf Coast Aquifer System's western boundary, as shown in [Figure 2.2.5](#). It extends over the whole study area, except in Webb County where part of the formation does not crop out. Near the outcrop, the Catahoula Formation is in contact with the Yegua-Jackson Aquifer. This connection may introduce significant groundwater flow between the Gulf Coast Aquifer System and Yegua-Jackson Aquifer.

The Oakville and Fleming formations extend all the way south to Duval County and pinch out thereafter. The Goliad Formation pinches out to the north in Austin and Colorado counties and crops out for the rest of the study area. The Willis Formation crops out to the north in Austin, Colorado, Lavaca, Duval, and Victoria counties, and pinches out to the south. The Lissie and Beaumont formations crop out across the whole study area except in Brooks, Jim Hogg, Kennedy, and Kleberg counties to the south where the ground surface is covered by eolian deposits. The alluvium and terrace deposits occupy the current and past river valleys and along the barrier islands in the Gulf.

The surface geology will be incorporated into hydrogeologic unit configuration, groundwater recharge, and groundwater-surface water interaction during the conceptual and numerical model constructions.

**Table 2.2.1. Stratigraphy and hydrogeologic classification of geologic units in study area (modified from Baker, 1995).**

ERA	Period		Epoch	Stratigraphic Unit	Hydrogeologic Unit		
Cenozoic	Quaternary		Holocene	Alluvium and Eolian Sand	Alluvium /Eolian Aquifer	Model Layer 1	Gulf Coast Aquifer System
			Pleistocene	Beaumont Formation	Chicot Aquifer		
				Lissie Formation			
				Willis Formation			
	Tertiary	Neogene	Pliocene	Goliad Formation	Evangeline Aquifer	Model Layer 2	
			Miocene	Upper Fleming Formation			
				Middle Fleming Formation	Burkeville Unit	Model Layer 3	
				Lower Fleming Formation	Jasper Aquifer	Model Layer 4	
				Oakville Formation			
			Paleogene	Oligocene	Catahoula Formation (sand)		

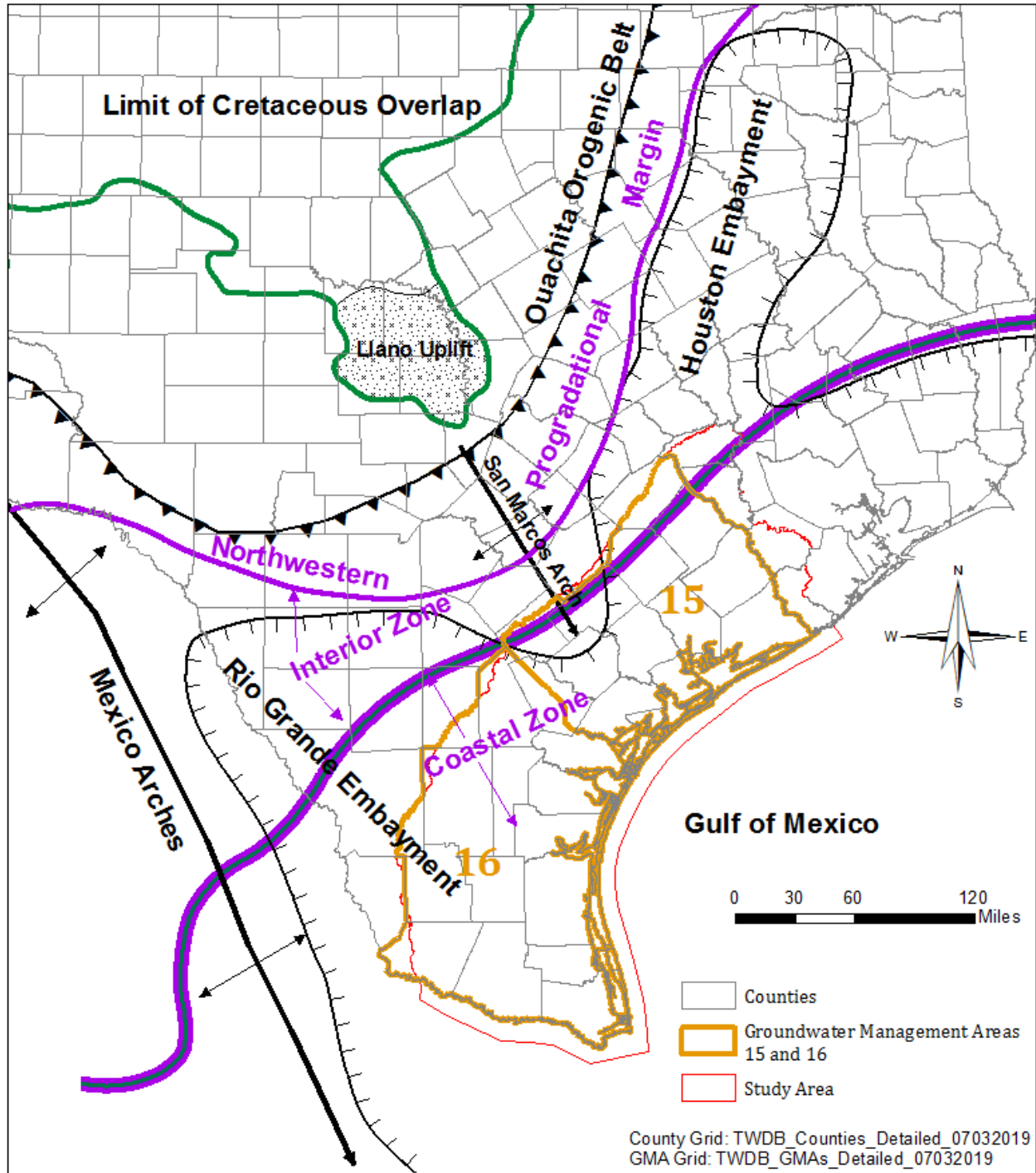


**Figure 2.2.1 Major structures in central and southern portions of the Gulf Coast aquifer System in Texas and surrounding regions (modified from Young and others (2014)).**

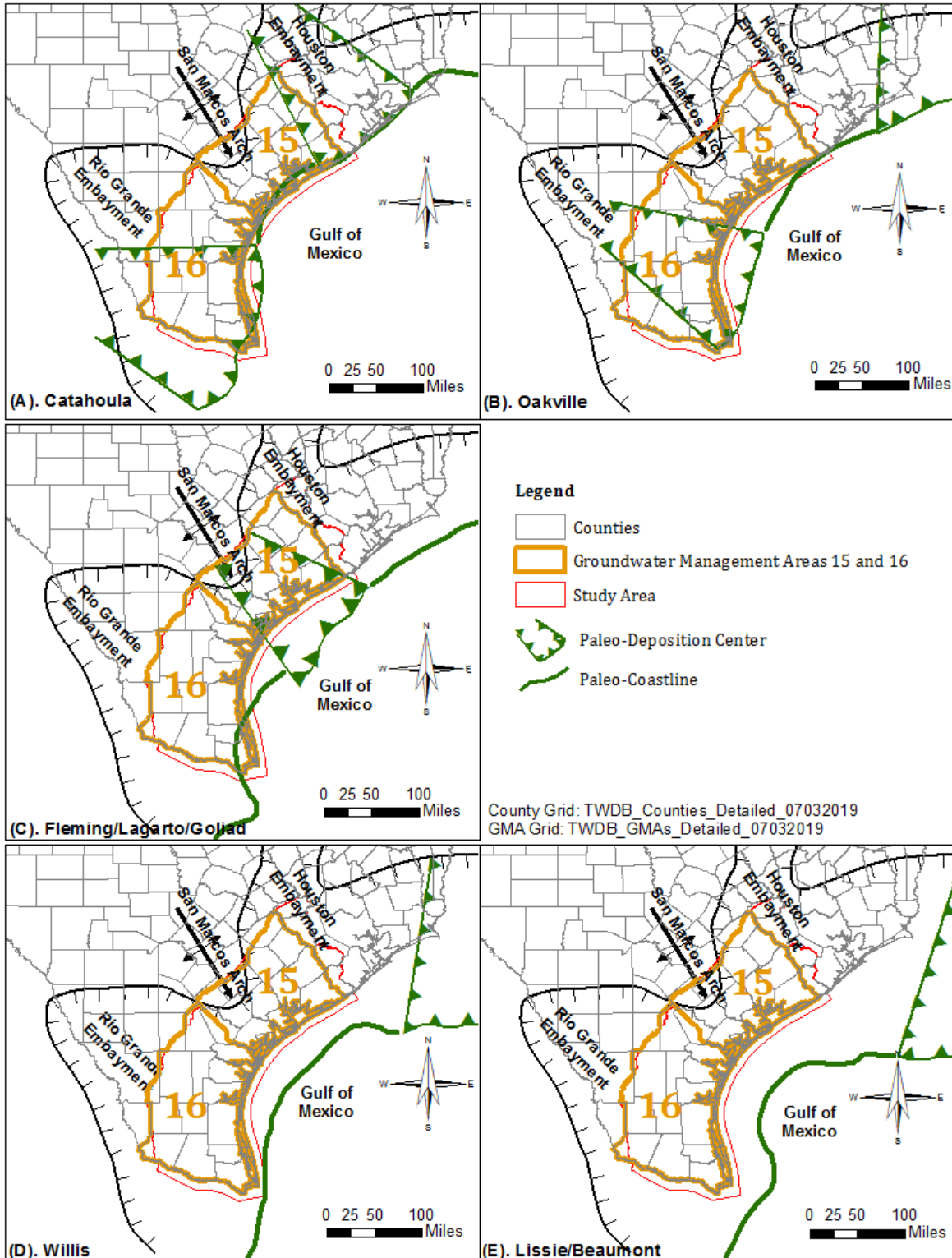


**Figure 2.2.2** Locations of major deltaic deposition centers and coastline for selected depositional episodes (modified from Young and others (2010)).

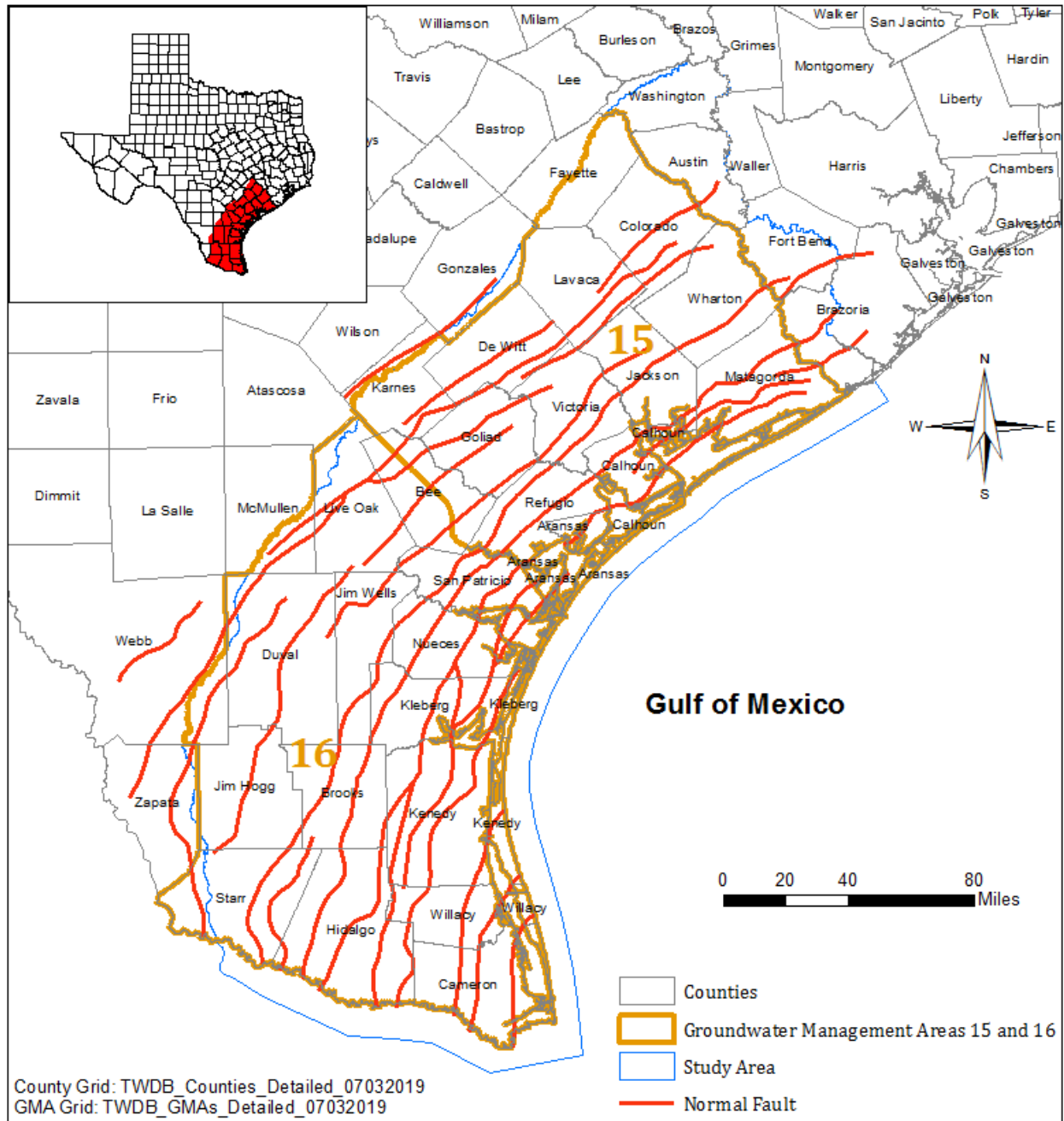


**Figure 2.2.3** Locations of major faults in the study area and its vicinity (based on Tectonic Map of Texas by Bureau of Economic Geology of The University of Texas at Austin, 1997).

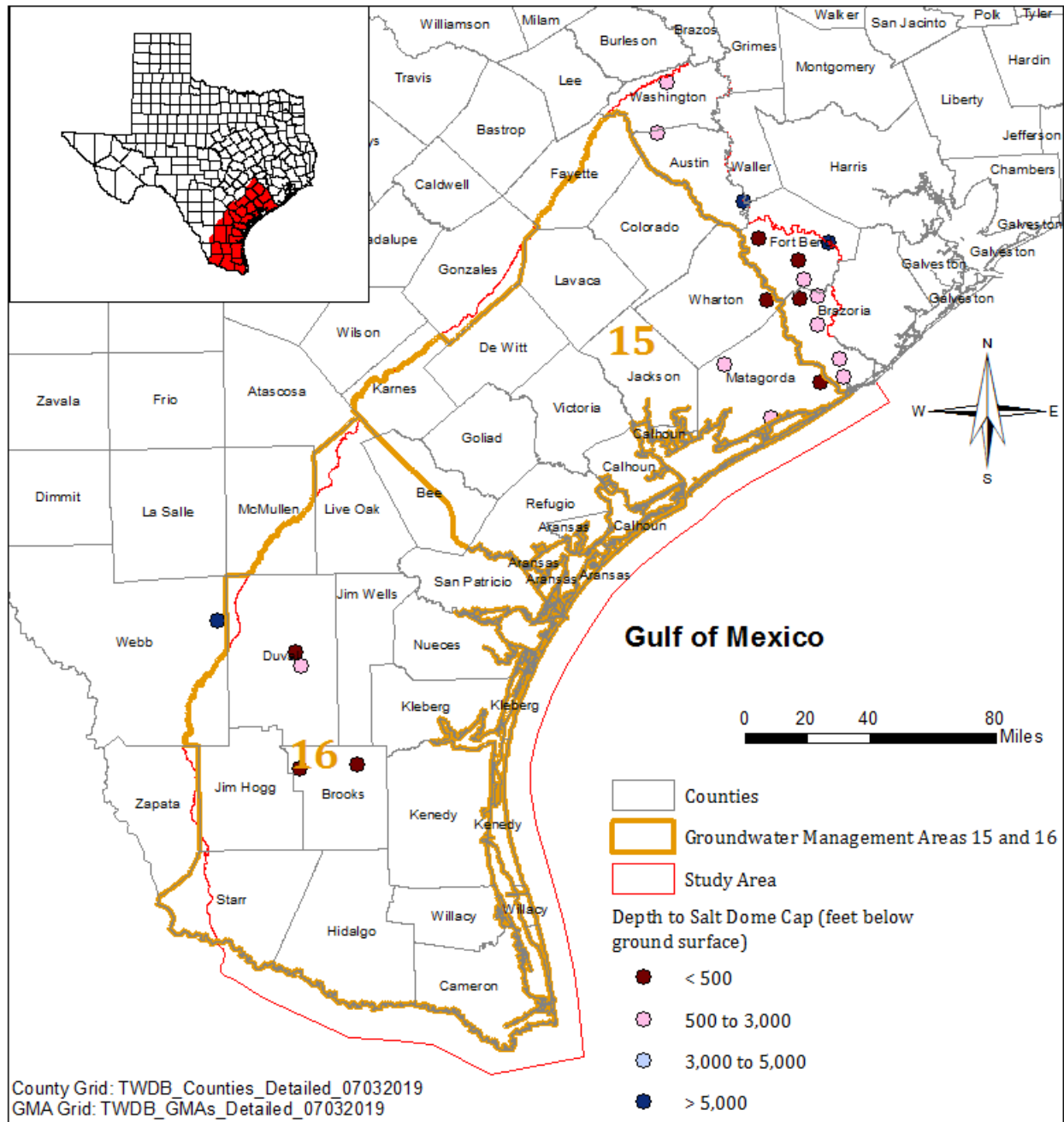


**Figure 2.2.4** Locations of shallow salt domes in the study area and its vicinity (location based on Bureau of Economic Geology (1997); depth to salt dome cap based on Young and others (2014)).



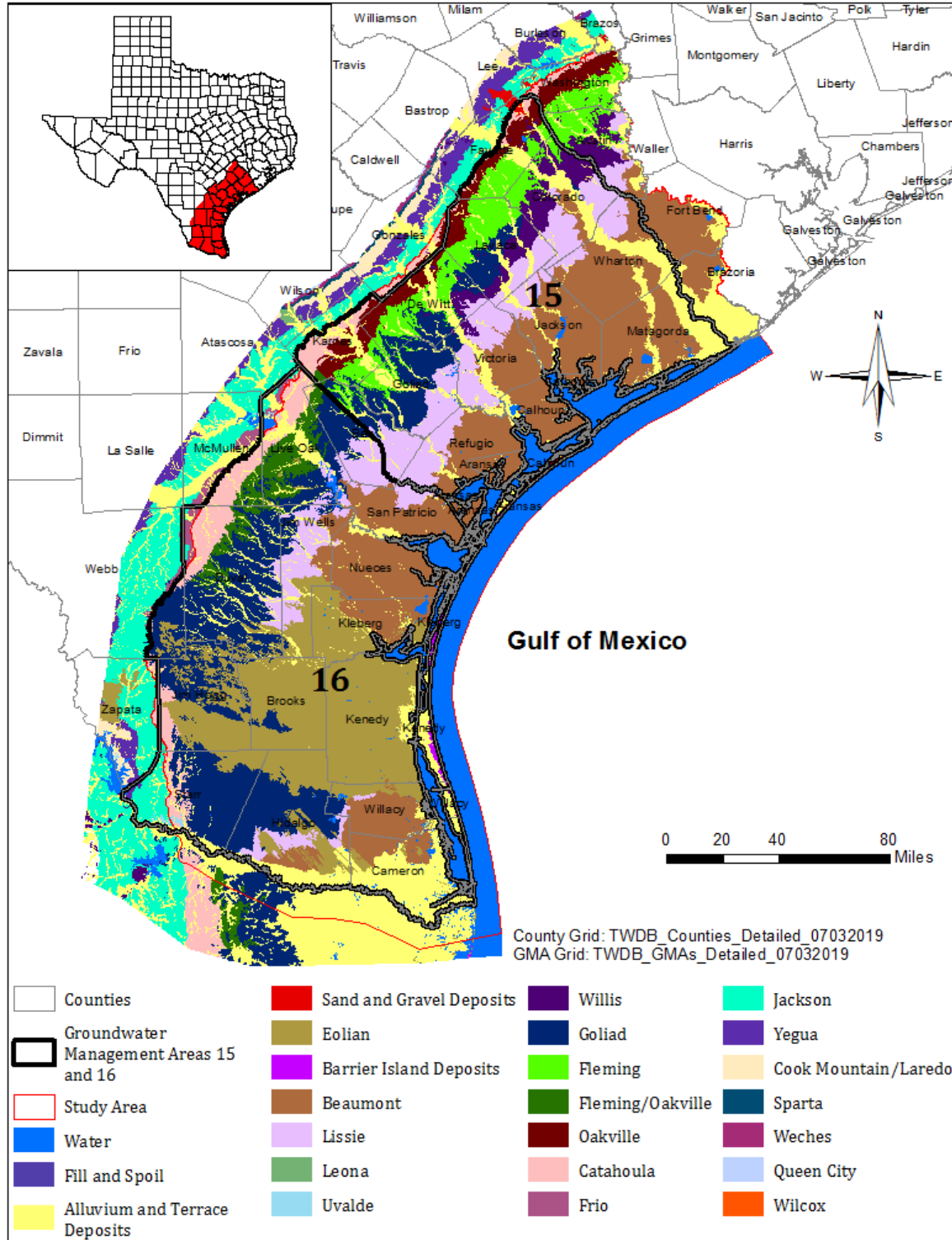


**Figure 2.2.5** Surface geology of the study area (based on Bureau of Economic Geology (2013)).

### **3.0 Previous Investigations**

This section focuses on previous hydrogeologic investigations in the study area. The studies are organized by reconnaissance investigations, single county studies, multiple county studies, large regional studies, and groundwater flow modeling studies.

#### **3.1 Reconnaissance Investigations and Local Studies**

Reconnaissance investigations are the first phase of water resources planning. These reconnaissance investigations only determined general groundwater quality, first-order estimate of water availability, existing water use, and areas for further studies of major water-bearing units. For example, Alexander and others (1964) performed a reconnaissance study of the groundwater resources and quality in the Guadalupe, San Antonio, and Nueces river basins, which covered part of the Gulf Coast Aquifer System in the study area. Adidas (1991) calculated groundwater through the Catahoula Formation using assumed hydraulic properties in the vicinity of Bruni, Webb County.

#### **3.2 Single County Studies**

The single county studies are arranged by alphabetic order of the county names and described as follows:

##### ***3.2.1 Aransas County***

According to Shafer (1970), Aransas County was dominated by brackish water, though fresh groundwater also existed in the shallow portion of the Gulf Coast Aquifer System. The study suggested a limited withdrawal of the fresh groundwater, less than 11,000 acre-feet per year, to avoid saltwater intrusion. Pumping tests performed at the Live Oak Peninsula indicated that the Gulf Coast Aquifer System in this area was not able to transmit a significant amount of fresh groundwater with relatively low transmissivity values ranging from 1,500 to 3,900 gallons per day per foot and specific yield values ranging from 0.00071 to 0.0096.

### **3.2.2 *Bee County***

Sufficient fresh and slightly saline groundwater existed in the shallow portion of the Gulf Coast Aquifer System in Bee County (Myers and Dale, 1966). The most promising area for further development was around the southeast region of the county where the Gulf Coast Aquifer System was relatively thick. Aquifer tests showed that the transmissivity of the Gulf Coast Aquifer System ranged from 7,500 to 30,000 gallons per day per foot with storativity values ranging from 0.00047 to 0.0011.

### **3.2.3 *Brooks County***

Myers and Dale (1967) studied the groundwater resources in the Oakville Formation, Fleming (Lagarto) Formation, Goliad Formation, Lissie Formation, Beaumont Formation, and wind-blown deposits in Brooks County. The pumping tests indicated the Goliad Formation's transmissivity ranging from 10,700 to 18,500 gallons per day per foot with an average storativity of 0.000019.

### **3.2.4 *Cameron County***

Dale and George (1954) studied the groundwater resources in Cameron County. Their study showed that fresh groundwater only existed in alluvium deposits and shallow wells, while the deep groundwater was highly mineralized.

### **3.2.5 *DeWitt County***

Follett and Gabrysch (1965) evaluated the groundwater resources in DeWitt County. Their study indicated the presence of about 65 million acre-feet of fresh to slightly saline water in the sands ranging from the Catahoula to the alluvium deposits. However, only a small portion of the total was economically recoverable. Aquifer pumping tests showed the transmissivity ranging from 3,350 to 35,000 gallons per day per foot with storativity values ranging from 0.007 to 0.01.

### **3.2.6 Duval County**

A study by Shafer (1974) identified the major geologic formations bearing fresh to moderately saline groundwater in Duval County - the Catahoula, Oakville, and Goliad formations. Historical pumping had caused water level decline in the Goliad Formation. However, Shafer (1974) suggested additional groundwater development from the Oakville and Goliad formations could provide enough for the future use. Aquifer tests indicated that the Goliad Formation had transmissivity ranging from 270 to 990 square feet per day with a storativity value of 0.00062 and the Oakville Formation had a transmissivity of 2,000 square feet per day.

### **3.2.7 Fayette County**

Rogers (1967) studied the groundwater resources and quality in Fayette County. Fresh and slightly saline groundwater occurred in aquifers within the Gulf Coast System (Catahoula, Oakville, and Fleming (Lagarto) formations). The Gulf Coast Aquifer System could provide 19,000 acre-feet of water annually. Groundwater quality tended to deteriorate downdip. The pumping tests indicated that the Catahoula Formation had transmissivity values ranging from 4,125 to 5,290 gallons per day per foot with a storativity of 0.018, and the Oakville and Fleming (Lagarto) formations from 3,816 to 5,910 gallons per day per foot with a storativity of 0.00013.

### **3.2.8 Goliad County**

Dale and others (1957) studied the groundwater resources in Goliad County. They estimated about 100 million acre-feet of fresh water available in the Oakville, Lagarto (Fleming), Goliad, and Lissie formations of the Gulf Coast Aquifer System. The freshwater-bearing units could go as deep as 1,200 to 2,000 feet below ground surface. Pumping tests indicated that the hydraulic conductivity of the water-bearing aquifers ranges from about 70 to 240 gallons per day per square foot with a storativity value of 0.0002 to 0.0006.

Uranium Energy Corp (2008) performed a hydrogeologic investigation at a site located on the northside of FM-1961, about one mile east of Highway 77/183. The investigation

included drilling, pumping tests, and groundwater quality sampling. The average hydraulic transmissivity and storativity at observation wells related to pumping well PTW-1 were 747 square feet per day and 0.0006, respectively. The average hydraulic transmissivity and storativity at observation wells related to pumping well PTW-6 were 968 square feet per day and 0.00024, respectively.

### ***3.2.9 Jackson County***

Baker (1965) evaluated the groundwater resources in the Gulf Coast Aquifer System in Jackson County. His study indicated about 95 million acre-feet of fresh water was available, but heavy pumping had caused water level decline. Pumping tests showed the hydraulic conductivity ranging from 59 to 885 gallons per day per square foot with an average of about 300. The storativity values generally increased upward due to less compaction ranging from 0.000018 to 0.0042.

### ***3.2.10 Jim Wells County***

Mason (1963a) evaluated the groundwater resources of the Goliad sand in the Alice area which covers most of Jim Wells County. His study indicated that groundwater withdrawal lowered the water table by more than 100 feet. Groundwater from the Goliad sand was fresh to slightly saline. Pumping test results indicated the transmissivity of the aquifer ranging from 2,500 to 8,700 gallons per day per foot, with a storativity value of 0.00025.

### ***3.2.11 Karnes County***

Anders (1960) evaluated groundwater resources in Karnes County. The water-bearing units included the Catahoula Formation, Fleming (Lagarto) Formation, Goliad Formation, and alluvium deposits. Pumping tests indicated that the Catahoula Formation had a transmissivity value of about 1,400 gallons per day per foot and the Oakville Formation was around 10,000 to 14,000 gallons per day per foot.

Wet Rock Groundwater Services, LLC. (2017) installed a well screened in the Burkeville Unit about 10 miles southeast of the City of Kenedy. Pumping test yielded a hydraulic

conductivity value of 0.3 feet per day at the pumping well and storativity ranging from 0.000067 to 0.00024 at observation wells.

### ***3.2.12 Live Oak County***

Anders and Baker (1961) evaluated the groundwater resources in Live Oak County. Their study indicated that the main water-bearing formations were the Carrizo, Oakville, Fleming (Lagarto), and Goliad formations. They estimated 20 million acre-feet of fresh and slightly saline water in the water-bearing formation located above the depth of 2,000 feet. Pumping tests indicated the transmissivity of the Oakville Formation ranging from 28,000 to 55,000 gallons per day per foot and the Goliad and younger formations from 10,000 to 32,500 gallons per day per foot. The storativity values ranged from 0.00057 to 0.0012.

According to Mr. Kevin Spencer (personal communication, February 23, 2015), R. W. Harden & Associates, Inc. performed a site investigation in City of Three River. This investigation included drilling, well installation, geophysical logging, water level measurement, and pumping tests.

### ***3.2.13 Matagorda County***

Hammond (1969) studied the groundwater resources in the Gulf Coast Aquifer System in Matagorda County. Pumping tests showed the hydraulic conductivity ranging from 103 to 3,950 gallons per day per square foot.

### ***3.2.14 Refugio County***

Mason (1963b) studied the groundwater resources in Refugio County. His study indicated that the Goliad Formation was the best water-bearing unit with good water quality. From the Goliad to Lissie to Beaumont formations, the water became more saline with decreasing transmissivity.

### **3.2.15 Starr County**

Dale (1952) studied the groundwater resources in Starr County. His study indicated that the Goliad Formation was the principal aquifer in the county.

### **3.3 Multiple County Studies**

The summary of the multiple county studies is arranged from the earliest to the most recent and described as follows:

Swartz (1957) compiled water levels in wells between 1938 and 1956 in Aransas and San Patricio counties. Rayner (1958) compiled the water levels between 1934 and 1958 in Jackson, Matagorda, and Wharton counties. Stearman (1960) compiled water levels in wells between 1950 and 1959 located in Cameron, Hidalgo, and Starr counties.

Marvin and others (1962) evaluated groundwater resources, use, and quality in Calhoun and Victoria counties. In Victoria County, fresh groundwater was abundant and groundwater withdrawal occurred mainly in the Lissie and Goliad formations. However, fresh groundwater was limited in Calhoun County and groundwater withdrawal was mainly in the Lissie or younger formations. Hydraulic conductivity values from pumping and recovery tests ranged from 247 to 570 gallons per day per square foot in Calhoun County and from 100 to 276 gallons per day per square foot in Victoria County.

Per the request from the Attorney General of Texas, the Texas Water Commission performed a study to determine the amount of water necessary to satisfy domestic, municipal, and industrial requirements in Cameron, Hidalgo, Starr, and Willacy counties (Vandertulip and others, 1964). This study also projected the total acres of land which could be irrigated each year from the available water supply of the Rio Grande. Another study by Baker and Dale (1964) covered the same region, but its focus was the historic groundwater use and characteristics of the major water-bearing aquifers.

Shafer (1968) did the groundwater resources evaluation in Nueces and San Patricio counties. The principal water-bearing units were the Goliad, Lissie, and Beaumont

formations. Aquifer tests showed the transmissivity ranging from 1,500 to 24,000 gallons per day per foot.

Shafer and Baker (1973) studied the groundwater resources in the Gulf Coast Aquifer System in Kleberg, Kenedy, and southern Jim Wells counties. Their study indicated that the major freshwater-bearing unit was the Goliad Formation, but pumping had caused groundwater level decline significantly around Kingsville and southern Jim Wells County from early 1930s to late 1960s. Pumping tests showed a transmissivity of 6,000 gallons per day per foot with a storativity of 0.0007 for the Oakville Formation and transmissivity ranging from 24,100 to 30,500 gallons per day per foot with a storativity of 0.0002 for the Goliad Formation. Another test in the Goliad Formation showed an average transmissivity of 31,500 gallons per day per foot between a drawdown test and a recovery test.

Loskot and others (1982) evaluated the groundwater resources in Colorado, Lavaca, and Wharton counties. The study pointed out that the Chicot (Willis Formation and younger units) and Evangeline (Goliad Formation and upper portion of the Fleming (Lagarto) Formation) aquifers were the main freshwater-bearing units in the study area. Pumping tests showed that the Jasper (lower portion of the Fleming Formation, Oakville Formation and sandy part of the Catahoula Formation) Aquifer in Lavaca County had transmissivity values ranging from 500 to 1,250 square feet per day. The hydraulic conductivity values ranged from 5.5 to 24 feet per day with an average of 12 feet per day for the Evangeline Aquifer and from 29 to more than 200 feet per day with an average of 80 feet per day for the Chicot Aquifer.

Enacted by Texas House Bill 2, Texas Water Development Board performed another evaluation of the groundwater resources in Cameron, Hidalgo, Starr, and Willacy counties (McCoy, 1990). This study indicated that enough groundwater could be developed from the Gulf Coast Aquifer System to meet the demands until 2010.

In 1999, Parsons Engineering Science, Inc. did a qualitative study on the interaction between surface water and groundwater in 22 river basins in Texas, including the study area.



Lizárraga and Ockerman (2010) simulated stream flow, groundwater recharge, and evapotranspiration in Lower San Antonio River Watershed between 2000 and 2007 using the Hydrological Simulation Program – FORTRAN (HSPF). Their study indicated that the rainfall exited the watershed as evapotranspiration (82 percent), stream flow (less than 10 percent), and groundwater recharge (about nine percent). The average evapotranspiration and groundwater recharge were about 27.6 and 2.3 inches per year, respectively, in central Karnes County (Zone 7 in their study), 30.6 and 2.5 inches per year, respectively, in southeastern Karnes and Goliad counties (Zone 8 in their study), and 32.8 and 1.5 inches per year, respectively, in far southeast Goliad and adjacent Refugio and Victoria counties (Zone 9 in their study).

Braun and Lambert (2011) investigated the stream flow and stream/aquifer interaction in the Upper Coletto Creek Watershed in DeWitt, Goliad, and Victoria counties between 2009 and 2010. Their study indicated that most streams were gaining when flow existed in the streams and all but two reaches experienced no flow during dry seasons.

Lizárraga and Wehmeyer (2012) calculated stream gain and loss along the Lower San Antonio Watershed between 2000 and 2010. The watershed is spread from the City of San Antonio to Refugio and Victoria counties. All the evaluated stream segments across the Gulf Coast Aquifer System showed as gaining during the study period, except one between Floresville and Fall City along San Antonio River, which is across the Yegua-Jackson Aquifer to the northwest of the study area.

Using Light and raDAR (LIDAR), National Geodetic Survey (NGS) benchmarks, and old topographic maps, Young (2016) calculated land subsidence from prior to and during the 1950s to present in seven counties in Groundwater Management Area 15: Calhoun, DeWitt, Jackson, Matagorda, Refugio, Victoria, and Wharton. His study showed that much of study area had experienced land subsidence of over two feet.

Lopez and others (2018) performed radon ( $^{222}\text{Rn}$ ) and radium ( $^{226}\text{Ra}$ ) surveys at 12 stations in the Buffin Bay between Kenedy and Kleberg counties to evaluate temporal and spatial changes of groundwater discharge to the bay. Their study indicated that the average

groundwater discharge rate (difference between  $^{222}\text{Rn}$  and  $^{226}\text{Ra}$  rates) was about 15 to 50 centimeters per day or 180 to 610 feet per year.

### 3.4 Regional Studies

The regional studies cover at least the whole study area and are arranged from the earliest to the most recent and described as follows:

Myers (1969) compiled and calculated the hydraulic properties of the aquifers in Texas which included the Gulf Coast Aquifer System in the study area. In his report, the Gulf Coast Aquifer System was called “gulf coast sands”.

Building on stratigraphic interpretations from both petroleum and groundwater resources, Baker (1979) published a series of well log cross sections covering the entire Texas Gulf Coast and stratigraphic designations for the Gulf Coast Aquifer System, which have been used as standard reference by other researchers for aquifer stratigraphy in the region (Chowdhury and Turco, 2006; Knox and others, 2006; Young and others, 2006).

As part of their Regional Aquifer-System Analysis (RASA) Program (started in 1978), the U. S. Geological Survey published a series of reports on major aquifer systems across the Gulf Coastal Plain from Texas to Alabama. The Gulf Coast Aquifer System in our study is equivalent to the coastal lowland aquifer system, one of the three aquifer systems in the RASA Program. During the RASA Program, Weiss (1987) applied electric logs to estimate the total dissolved solids in the groundwater out of the coastal aquifer systems. Prudic (1991) estimated the hydraulic conductivity values of the aquifers using pumping tests and specific capacity tests. His study covered the Tertiary and younger sandy sediments which included the Gulf Coast Aquifer System. Weiss (1992) divided the Gulf Coast Aquifer System into five permeable zones and two confining units based on geophysical logs. Hosman (1996) divided the Gulf Coast Aquifer System into time-stratigraphic units.

During the Source Water Assessment and Protection (SWAP) Program required by the Safe Drinking Water Act Amendments of 1996, the U. S. Geological Survey developed the stratigraphic surfaces for the Chicot and Evangeline aquifers using the data primarily from

Carr and others (1985) supplemented by the information from Baker (1979, 1986) and the Geology Atlas of Texas. The SWAP aquifer surfaces were used in developing conceptual models for TWDB groundwater availability models of the Gulf Coast Aquifer System (Waterstone Environmental Hydrology and Engineering, Inc., 2003; Chowdhury and others, 2004; Kasmarek and Robinson, 2004).

Slade and others (2002) compiled the streamflow gain and loss results along rivers in Texas, which covered some segments along the Colorado, Lavaca, Nueces, Atascosa, Frio, and Navidad rivers in the study area.

Based on review of published data and type of vegetations, Scanlon and others (2005) performed a reconnaissance study. The study estimated maximum groundwater evapotranspiration rate and extinction depth across Texas.

Scanlon and others (2012) estimated the groundwater recharge at the outcrop areas of the Gulf Coast Aquifer System using the chloride mass balance approach and stream baseflow data. Their study indicated that the regional groundwater recharge rate increased from less than 0.1 inch per year near Rio Grande to about 2 inches per year along the boundary between Groundwater Management Areas 15 and 16. As noted in the report, the recharge values from the chloride mass balance approach likely under-estimated the true groundwater recharge.

A framework study by Young and others (2010) further refined the hydrostratigraphy of the aquifer system. This study used the chronostratigraphic approach to define the bottom of the following units: the Oakville Formation, the lower, middle, and upper portions of the Fleming (Lagarto) Formation, the lower and upper portions of the Goliad Formation, the Willis Formation, the Lissie Formation, and the Beaumont Formation. As part of the study, the sand fraction for each of the units described above was also estimated using geophysical logs.

Young and others (2014) did a hydrogeochemical study of the Gulf Coast Aquifer System. Using the framework by Young and others (2010), this study focused on the chemical quality of the groundwaters in the Gulf Coast Aquifer System subunits. This study also

estimated the age of the groundwater and travel time using existing groundwater flow models and isotope data.

To fulfill the requirement of the Texas HB 30 from the 84<sup>th</sup> Legislative Session, Young and others (2016) delineated the potential brackish groundwater production areas in the Gulf Coast Aquifer System in the study area. A first-order groundwater flow model was also developed as part of the study to estimate the impacts of potential groundwater withdrawal in the production areas.

### **3.5 Groundwater Flow Modeling Studies**

The following list discusses regional modeling studies conducted in the study area and is arranged from the earliest to the most recent. Models with unique approaches, such as use of constant head to simulate groundwater recharge and models covering only part of the Gulf Coast Aquifer System, are excluded from the discussion.

1) As part of their Regional Aquifer-System Analysis (RASA) Program (started in 1978), the U. S. Geological Survey developed several three-dimensional, variable density, finite difference models for the Gulf Coast Aquifer System. Of them, the largest ones covered the whole Gulf Coast from Texas to Alabama (Kuiper, 1994; Williamson and Grubb, 2001). These models included 10 aquifer layers and 5 confining layers with a uniform grid of 10 miles by 10 miles. The models covered the upland Gulf Coast Aquifers such as the Wilcox, Queen City, Sparta, and Yegua-Jackson formations, and lowland Gulf Coast Aquifers such as the Jaspers, Evangeline, and Chicot aquifers. Model parameters such as water table on the top, flow from the geopressured zone at the bottom, and aquifer properties (hydraulic conductivity and specific storage) were adjusted using regression approach to match the measured water levels. The models predicted poorly on the deep heads and flow (Kuiper, 1994) but did show that the groundwater withdrawal had increased the groundwater recharge, reduced groundwater discharge, and changed groundwater flow directions from the predevelopment conditions (1925) (Williamson and Grubb, 2001).

2) Also for the Regional Aquifer-System Analysis (RASA) program, the U. S. Geological Survey developed sub-regional models using the same layer structure but with a grid of

five miles by five miles. The Gulf Coast Aquifer System in Texas was covered by a sub-regional model (Ryder, 1988). Application of the model was detailed in Ryder and Ardis (1991).

3) A three-dimensional, steady-state MODFLOW-88 model was developed by HDR, Inc. (2000) to evaluate the groundwater resources in the south Gulf Coast Aquifer System in Region N. This model contains five numerical layers representing the Chicot Aquifer (Layers 1 and 2), the Evangeline Aquifer (Layer 3), the Burkeville confining unit (Layer 4), and the Jasper Aquifer (Layer 5). The model was calibrated to pre-development water levels and verified to pseudo-steady state pumping. However, no predictive simulation was performed.

4) Kuchanur and others (2003) developed a steady-state MODFLOW-2000 model to help manage groundwater resources in Refugio County. The model contains two layers representing the Beaumont and Lissie sand in Layer 1 and the Lissie and Goliad sand in Layer 2. Layer 1 extended from the ground surface to 500 feet below ground surface and the bottom of Layer 2 was set at 1,100 feet below mean sea level. The model was calibrated to water levels using PEST (a parameter estimation program). The model was then used to estimate maximum pumping rate with certain constraints.

5) Uddameri and Kuchanur (2006) developed a steady-state MODFLOW-2000 model covering the Coastal Bend Region from DeWitt, Victoria, and Calhoun counties to the north to Nueces and Live Oak counties to south. The model contained seven numerical layers: the Chicot Aquifer (Layers 1 and 2), the Evangeline Aquifer (Layers 3 and 4), the Burkeville confining unit (Layer 5), the Jasper Aquifer (Layer 6), and the Catahoula Formation (Layer 7). The model was calibrated to water levels using PEST. No predictive simulation was performed.

6) Chowdhury and others (2004) developed one steady-state and one transient three-dimensional MODFLOW-96 models for the Central Gulf Coast Aquifer System. The models covered the Groundwater Management Area 15, portion of the Groundwater Management Area 16, and a sliver of the Groundwater Management Area 14. The models include four

model layers representing (from shallowest to deepest) the Chicot Aquifer, the Evangeline Aquifer, the Burkeville confining unit, and the Jasper Aquifer. The steady-state model simulated the pre-development groundwater flow conditions from 1910 through 1940 without groundwater withdrawal and was calibrated to water levels collected in 1940. The steady-state model was used to quantify groundwater recharge, boundary conditions, and aquifer properties. The transient model simulated the groundwater flow from 1981 to 1999 with groundwater pumping and varied groundwater recharge. The transient model used initial water levels from the steady-state model and contained transitional period from 1940 to 1980 with the pumping information from 1980. The calibrated transient model was used to predict groundwater level change and discharge to surface water under different future pumping scenarios.

7) Similar to the central Gulf Coast Aquifer System model, Chowdhury and Mace (2007) developed another three-dimensional MODFLOW-96 model for the Gulf Coast Aquifer System in the Lower Rio Grande Valley of Texas. This model also contained four layers (from shallowest to deepest): the Chicot Aquifer, the Evangeline Aquifer, the Burkeville confining unit, and the Jasper Aquifer. The model included a pseudo-steady state period representing pre-1980 aquifer conditions and transient period from 1981 through 1999.

8) As part of the Lower Colorado River Authority – San Antonio Water System Project, Young and others (2009) developed two MODFLOW-SURFACT models to estimate the impacts of pumping and sustainable long-term water needs from irrigation in Colorado, Wharton, and Matagorda counties. The models contained six model layers representing the following hydrogeological units: the surficial layer (Layer 1), the Beaumont Formation (Layer 2), the Lissie Formation (Layer 3), the Willis Formation (Layer 4), the Upper Goliad Formation (Layer 5), and the Lower Goliad Formation (Layer 6). The surficial layer was used to better simulate the interaction between the surface water and the groundwater. The first model was a steady-state model representing the pre-development conditions (1900). The second model represented the development period from 1901 to 1997 using

154 variable transient stress periods. The models were calibrated to water levels and stream baseflow using PEST.

9) To support the joint groundwater conservation district planning process in the Groundwater Management Area 16, Hutchison and others (2011) developed a three-dimensional MODFLOW-2000 model to evaluate the impacts of groundwater pumping in the Gulf Coast Aquifer System. This model contained the Chicot Aquifer (Layer 1), the Evangeline Aquifer (Layer 2), the Burkeville confining unit (Layer 3), the Jasper Aquifer (Layer 4), the Yegua-Jackson Aquifer (Layer 5), and the Queen-City, Sparta, and Carrizo-Wilcox aquifers (Layer 6). The model included a steady-state period representing pre-1963 conditions and 37 transient periods representing years 1963 through 1999. The model was calibrated to measured water levels.

10) Brackish groundwater pumping in the Lower Rio Grande Valley is expected to increase in response to increased municipal demands. To evaluate the impacts of potential brackish groundwater withdrawal, Panday and others (2017) developed a three-dimensional MODFLOW-USG flow and transport model to simulate changes in groundwater levels, total dissolved solids concentrations, and surface-water/groundwater interactions. The model included density dependent flow to evaluate the impact of salt density on groundwater flow and solute migration. The model consisted of 12 numerical layers with the Gulf Coast Aquifer System simulated as Layers 1 through 10 (Beaumont, Lissie, Willis, Upper Goliad, Lower Goliad, Upper Fleming (Lagarto), Middle Fleming (Lagarto), Lower Fleming (Lagarto), Oakville, and Upper Catahoula formations). The model contains a grid of 2,640 feet by 2,640 feet (half a mile by half a mile) with the Rio Grande and irrigation canals refined to 330 feet by 330 feet. The model included a steady state period to representing year 1984 and 29 transient annual periods to represent years 1985 through 2013. The model was calibrated to measured water levels in wells and compared with measured flows along the Rio Grande.

Figure 3.5.1. shows the areal coverage of the previous groundwater models, except the one by the U. S. Geological Survey during the RASA Program that covered multiple Gulf states. Please note the coverage represents the model domains, which may contain inactive areas.

In summary, all the existing groundwater flow models are either outdated, localized, poorly refined, or not calibrated. For the last ten years or so, additional investigations have produced a significant amount of new data which greatly improved our understanding of the groundwater flow in the Gulf Coast Aquifer System. The groundwater conservation districts and other groundwater users expect a more robust tool to help their groundwater resources management and planning. This requires a refined vertical layer structure so that major hydrostratigraphy and its influence on groundwater flow can be reasonably quantified. Maintaining a healthy stream baseflow is important not only to surface water users but also to wildlife. Groundwater withdrawal and climate are the greatest impacts to baseflow. Use of a groundwater flow model to estimate baseflow can be improved by applying a finer grid along rivers and streams. Groundwater pumping lowers water levels and induces land subsidence. Depressions by high groundwater withdrawal could be as large as miles wide. One way to minimize the impacts of adjacent pumping is to increase model domain so the adjacent pumping can be included in the model. Land subsidence is a slow process but varies spatially due to pumping location and clay content. A finer grid and use of analytical wells can certainly improve the simulation of water level decline and the resulted subsidence. Finer grids and increased model domains demand more computing power and memory. Fortunately, tremendous progress has been made on both in the last ten years using computer clusters and cloud computing. In addition, groundwater modeling techniques and tools have also significantly improved, including parameter estimates and paralleling processes. Today, it is possible to combine the central and southern portions of the Gulf Coast Aquifer System in a refined groundwater flow model.



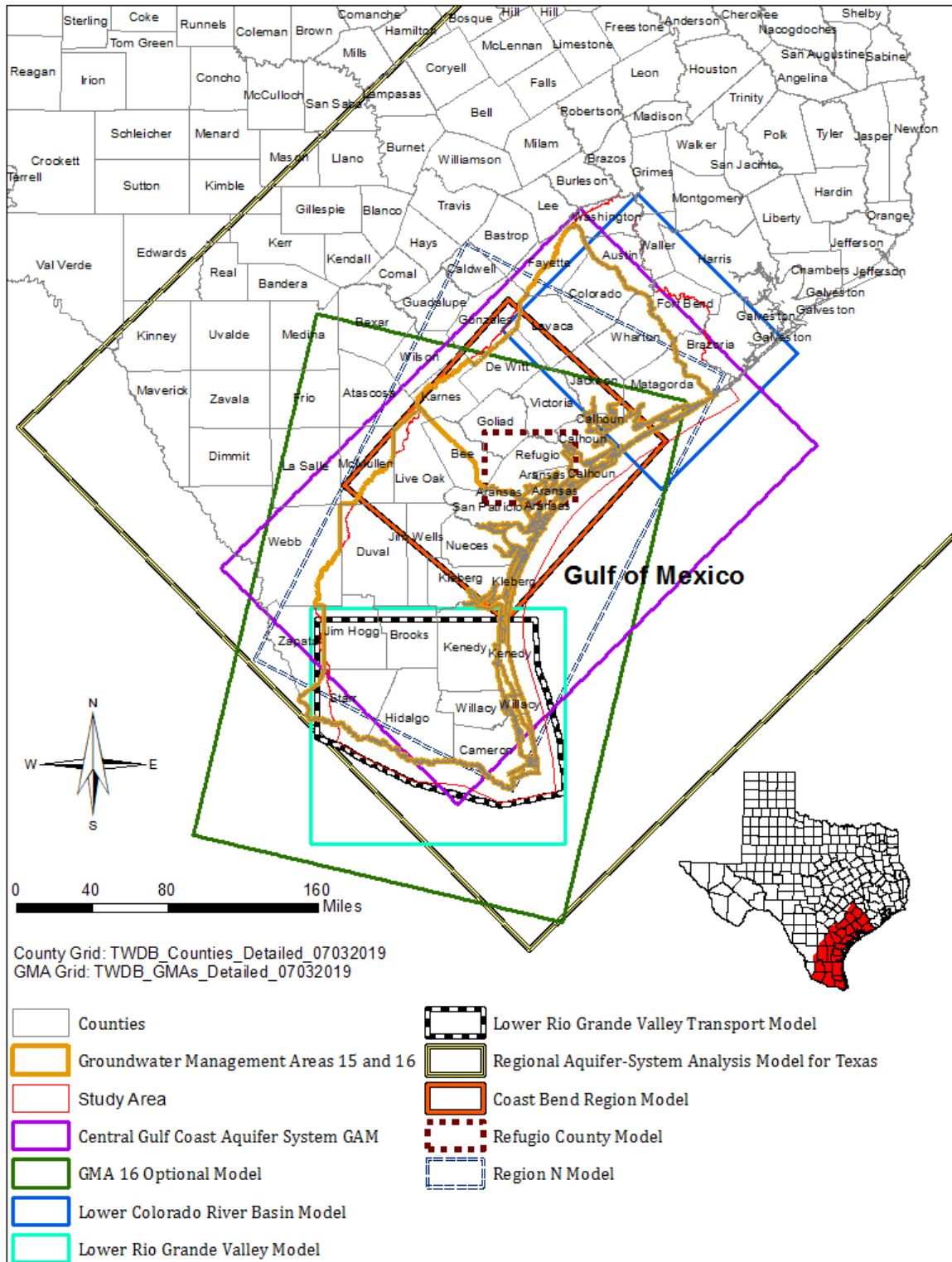


**Figure 3.5.1 Areal coverage of previous groundwater flow models.**

## 4.0 Hydrologic Setting

This section summarizes the information needed for the development of the conceptual groundwater flow model. Specifically, this section includes the layering framework, water levels, recharge, surface water-aquifer interaction, discharge, hydraulic properties, water quality, and subsidence.

### 4.1 Hydrostratigraphy

The Gulf Coast Aquifer System contains the following stratigraphic units (from shallowest to deepest): the alluvium and eolian sand, the Beaumont Formation, the Lissie Formation, the Willis Formation, the Goliad Formation, the Fleming (Lagarto) Formation, the Oakville Formation, and the sand part of the Catahoula Formation. The sand part of the Catahoula Formation is mainly located in and near its outcrop area. For this study, the above stratigraphic units are further categorized into four hydrostratigraphic layers (from shallowest to deepest):

- Layer 1 – the alluvium/eolian deposits and the Chicot Aquifer (the Beaumont Formation, the Lissie Formation, and the Willis Formation)
- Layer 2 – the Evangeline Aquifer (the Goliad Formation and the Upper Fleming Formation)
- Layer 3 – the Burkeville Unit (the Middle Fleming Formation)
- Layer 4 – the Jasper Aquifer (the Lower Fleming Formation, the Oakville Formation, and the sand part of the Catahoula Formation)

Details of the hydrogeologic units in the study area are presented in [Table 2.2.1](#).

The hydrostratigraphic layer structure involves the definition of the top and bottom or thickness of each hydrostratigraphic layer. Using the chronostratigraphic approach, Young and others (2010) developed layer structures for ten units (from shallowest to deepest): Beaumont, Lissie, Willis, Upper Goliad, Lower Goliad, Upper Lagarto, Middle Lagarto, Lower

Lagarto, Oakville, and Catahoula (sand). Since then, the TWDB brackish water studies has updated some previous stratigraphic picks and collected additional information. After review of existing hydrostratigraphic studies, 792 well logs from the following studies were used to construct the layer structure:

- Hydrostratigraphy of Gulf Coast Aquifer – Brazos to Rio Grande (Young and others, 2010)
- Brackish Resources Aquifer Characterization System (BRACS) database (TWDB, 2018)
- Hydrogeologic Framework for Northern Gulf Coast Aquifer (Young and others, 2012)

In addition, the Geologic Atlas of Texas (GAT) by the Bureau of Economic Geology of the University of Texas at Austin and the National Elevation Dataset (NED) by the U. S. Geological Survey were also used to define layer boundary, elevation, and thickness.

The general procedure to produce the framework involved the following steps:

- Step 1 – estimate the contact elevation at the well logs where it was missing based on the Geologic Atlas of Texas, the National Elevation Dataset, surrounding logs, and locations of salt domes and faults;
- Step 2 – convert contact elevations to layer thickness;
- Step 3 – add points along the western perimeter of the layer with a thickness of five feet for every 660 feet;
- Step 4 – grid the thickness dataset using SURFER with the kriging method and grid size of 330 feet;
- Step 5 – transform the grid file under SURFER with a minimum thickness of five feet;
- Step 6 – apply Gaussian filter 30 times to the grid file;

- Step 7 – add control points behind the western perimeter and between well logs;
- Step 8 – import the SURFER grid file to ArcGIS as a raster;
- Step 9 – sample the raster at the control points to obtain thickness at those locations; and
- Step 10 – repeat Steps 4 through 9 until difference between iterations at the control points is less than two feet.

The well logs and control points are shown in [Figures 4.1.1.](#) and [4.1.2.](#) Gridding thickness instead of elevation has two advantages: 1) avoiding artificial pinch-outs, and 2) fully using the western perimeter as a control line regardless whether a layer crops out to ground surface or pinches out underground. Top elevation of Layer 1 is defined using the U. S. Geological Survey's National Elevation Dataset (land area) and SRTM3\_PLUS V6.0 bathymetry (Gulf of Mexico). The top elevation of Layer 1, with the layer thickness, is then used to calculate the bottom elevation of Layer 1. The bottom elevation of each of the other layers can then be calculated using its thickness and the bottom elevation of the layer above.

[Figure 4.1.3](#) shows the ground surface elevation or the top of Layer 1 (alluvium/eolian deposits and Chicot Aquifer) which ranges from 102 feet below mean sea level in the Gulf of Mexico to 943 feet above mean sea level in Webb County. The increasing trend is clear from the Gulf towards the inland with local depressions along major rivers and streams. The thicknesses of the four layers are presented in [Figures 4.1.4, 4.1.6, 4.1.8, and 4.1.10,](#) respectively. [Figures 4.1.5, 4.1.7, 4.1.9, and 4.1.11](#) show the bottom elevations of the four layers, respectively. Cross sections were also produced perpendicular and parallel to the coastline ([Figure 4.1.12](#)) and shown in [Figures 4.1.13 through 21.](#) As shown in the figures, the four layers dip towards the Gulf of Mexico about 80 feet per mile. Layers 1 (alluvium, eolian, and Chicot Aquifer) and 2 (Evangeline Aquifer) thicken towards the Gulf to more than 3,000 and 5,000 feet, respectively. Layer 3 (Burkeville Unit) remains relatively consistent in thickness at about 500 to 1,000 feet. The thickness of Layer 4 (Jasper Aquifer) varies, but generally increases to 2,000 to 4,000 feet along a band about 30 to 50 miles

from the western perimeter ([Figures 4.1.10](#)). This local thickening is due to the addition of the Catahoula sand to the Jasper Aquifer under and near the outcrop areas. The thickest and the deepest parts for each layer are generally consistent with the deltaic deposition centers near the mouths of the Rio Grande, the Brazos River, and the Colorado River (see [Figure 2.2.2](#)).

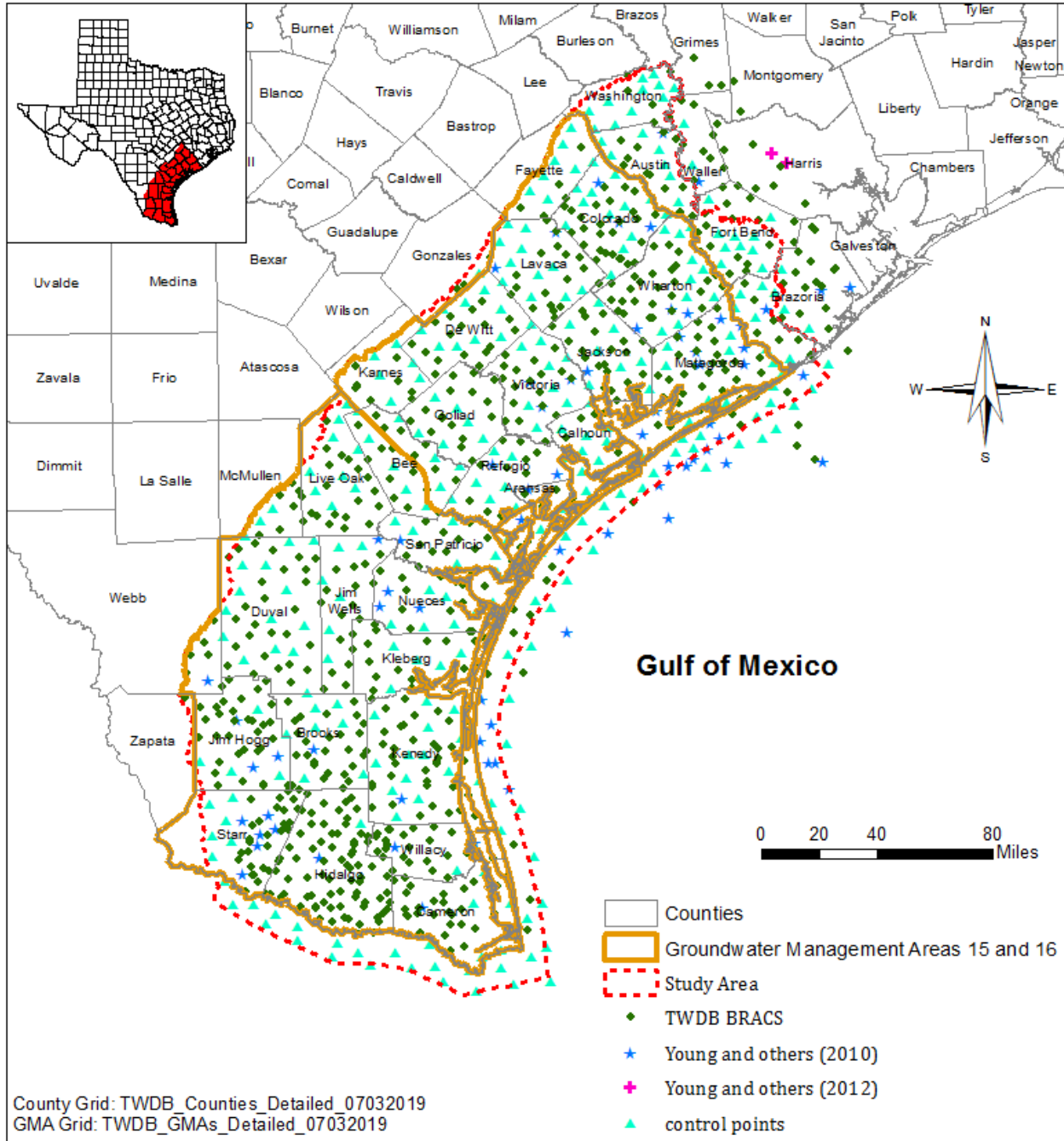


**Figure 4.1.1** Locations of well logs and control points.

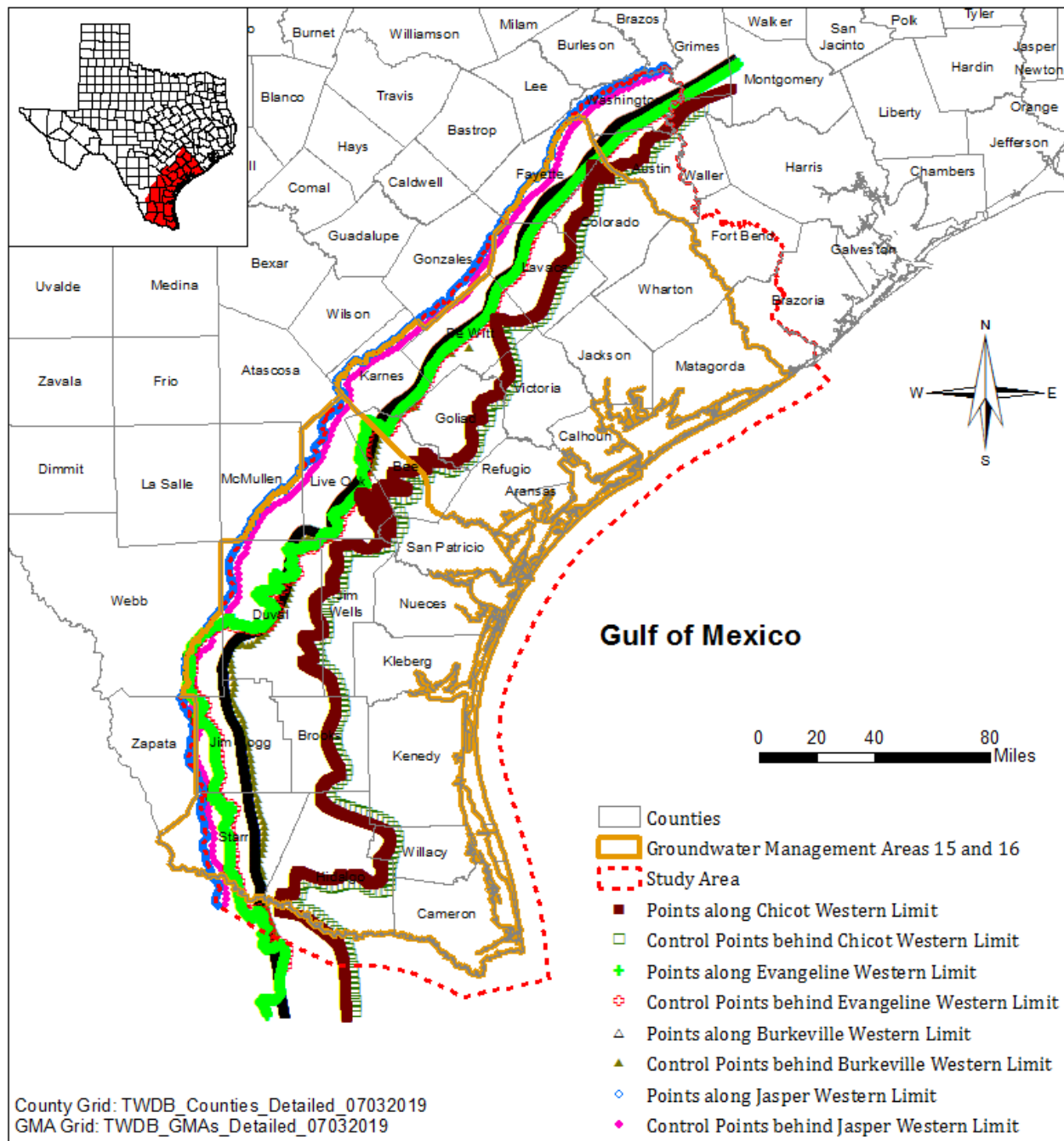


**Figure 4.1.2 Control points along and behind western perimeters of the hydrostratigraphic layers.**

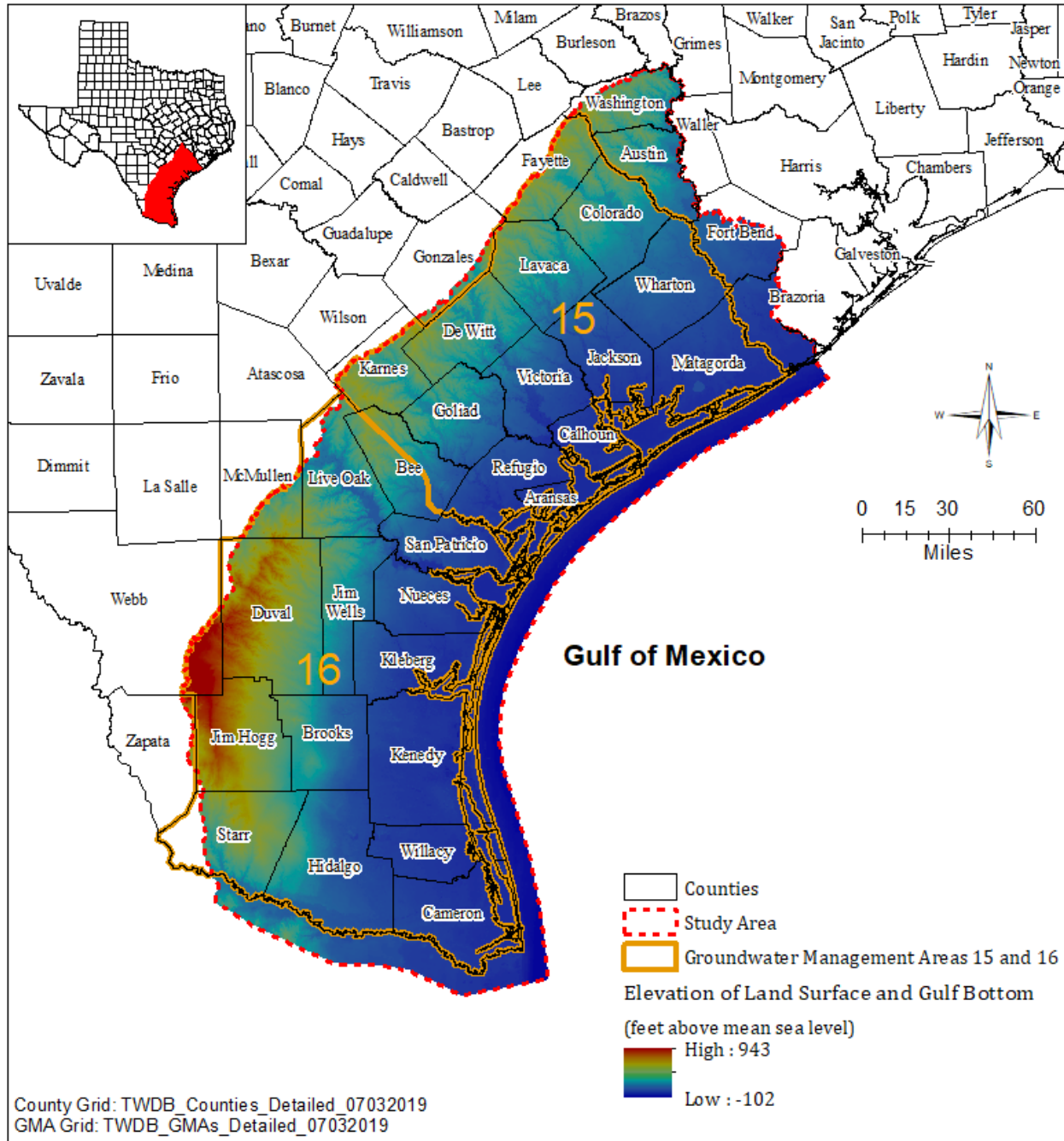


**Figure 4.1.3 Elevation of ground surface and Gulf of Mexico bottom (top of Layer 1). The ground surface elevation is based on U. S. Geological Survey’s National Elevation Dataset (NED). The bathymetry of the Gulf of Mexico bottom is based on the U. S. Geological Survey’s SRTM3\_PLUS V6.0.**



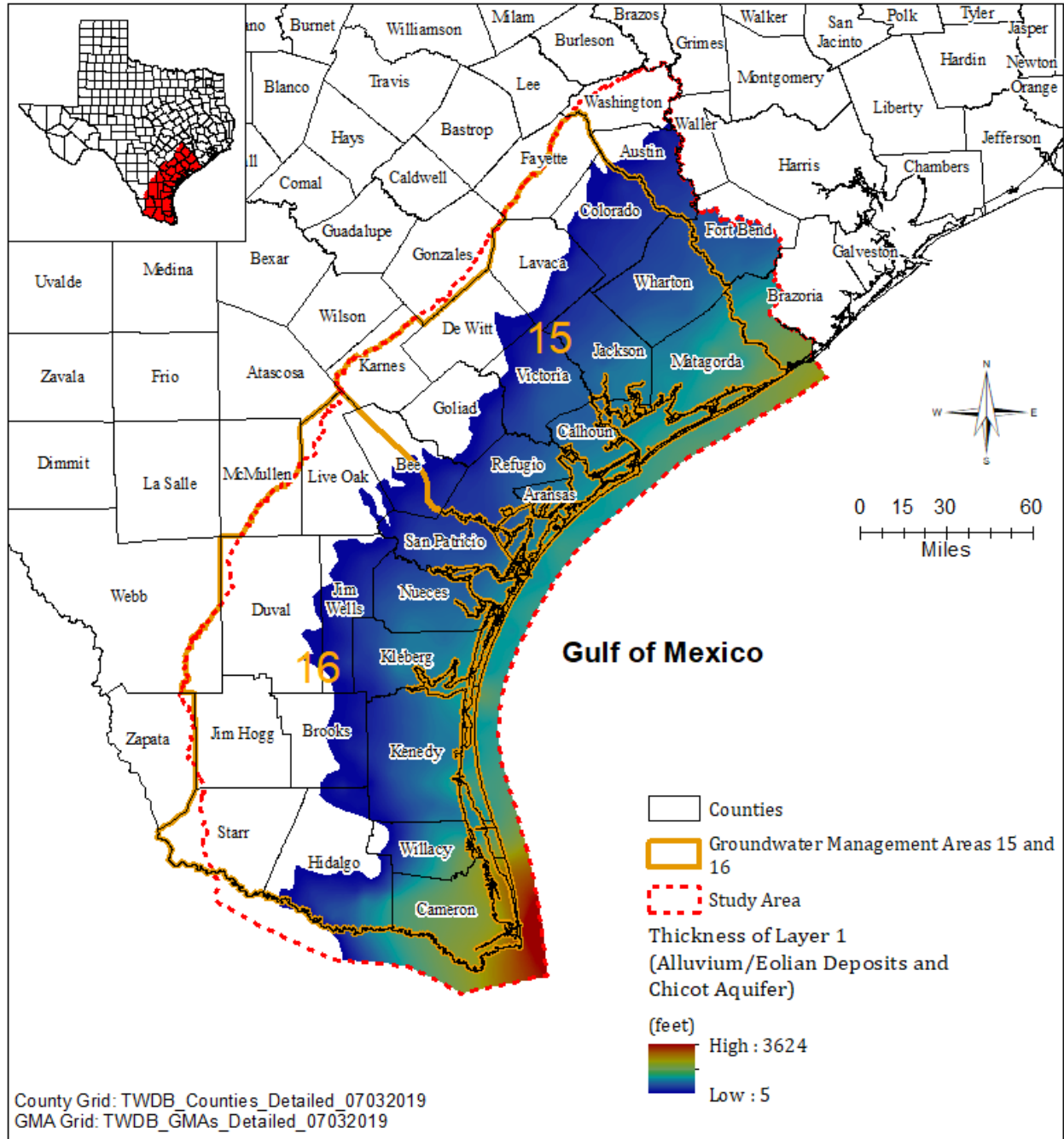


**Figure 4.1.4 Thickness of Layer 1 (alluvium/eolian deposits and Chicot Aquifer).**

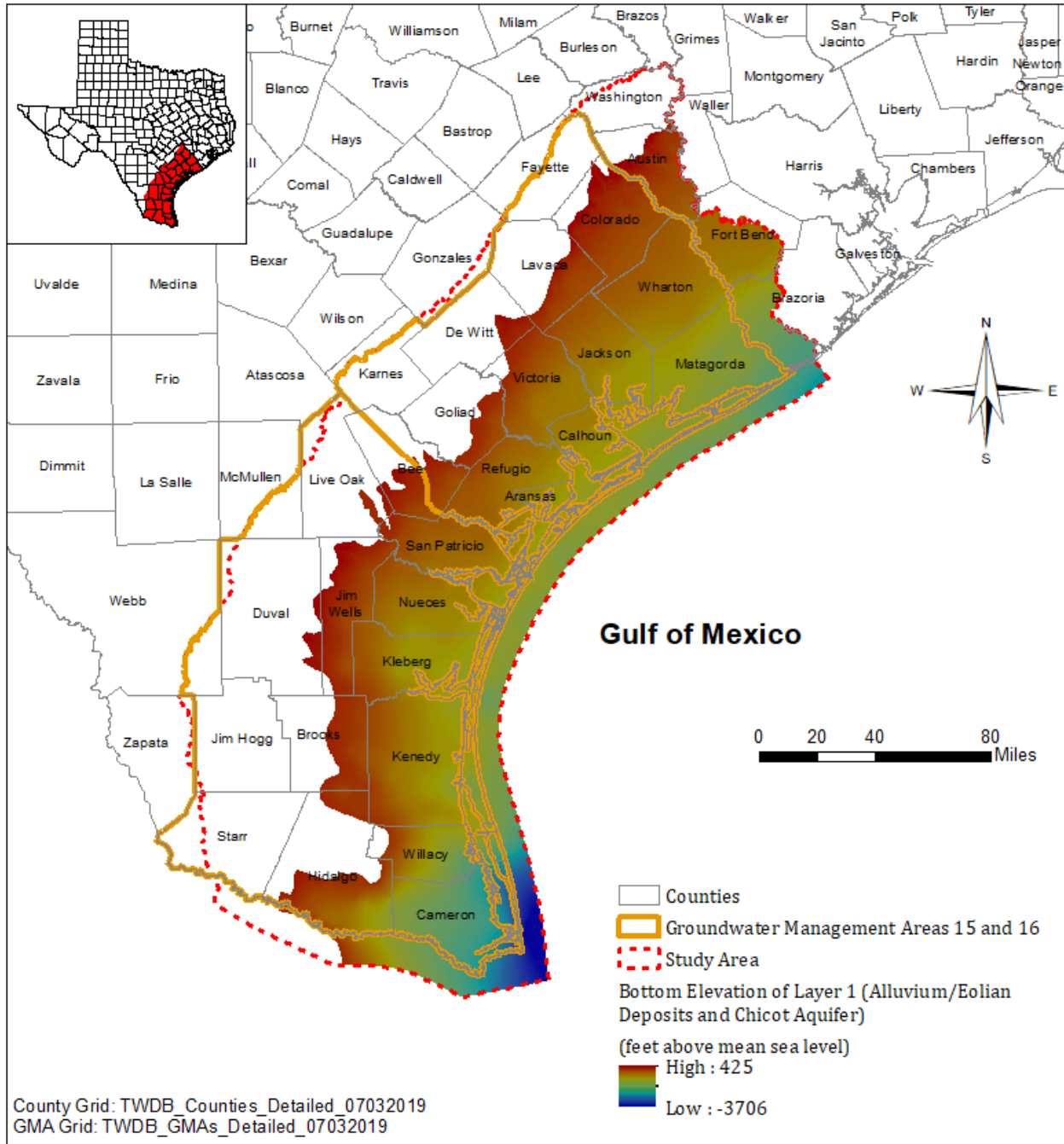


**Figure 4.1.5 Bottom elevation of Layer 1 (Alluvium/Eolian deposits and Chicot Aquifer).**

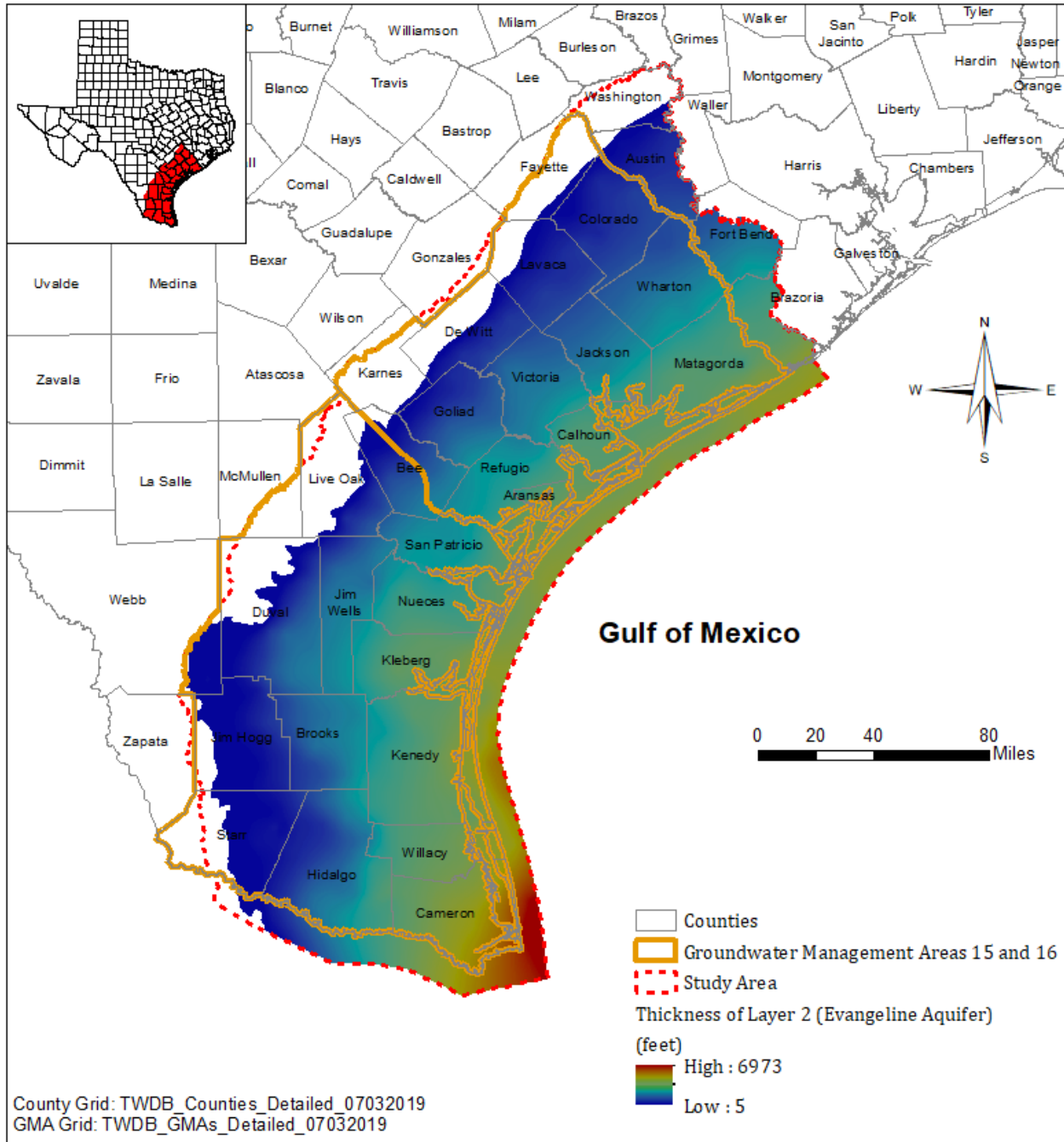


**Figure 4.1.6 Thickness of Layer 2 (Evangeline Aquifer).**

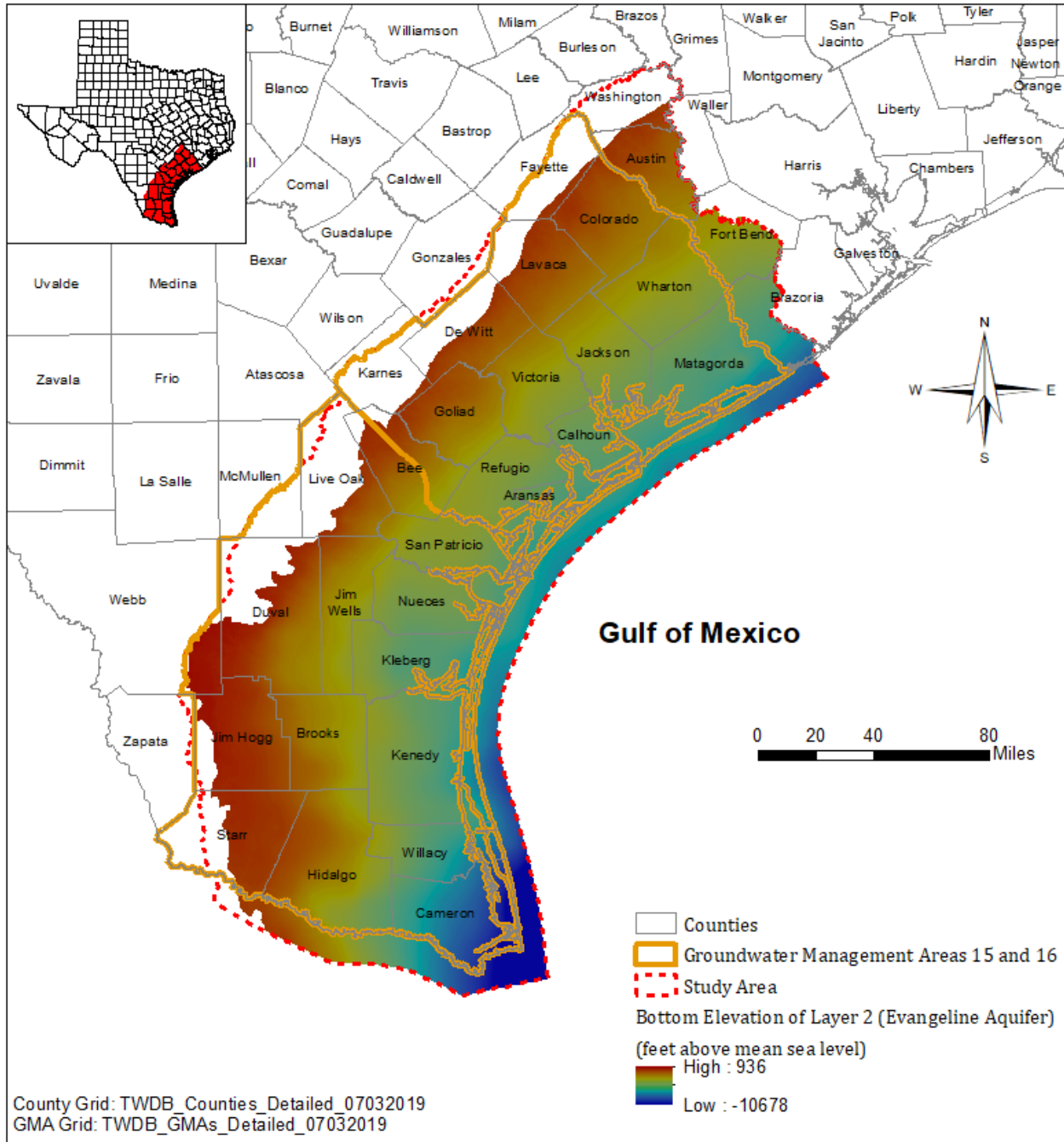


**Figure 4.1.7 Bottom elevation of Layer 2 (Evangeline Aquifer).**

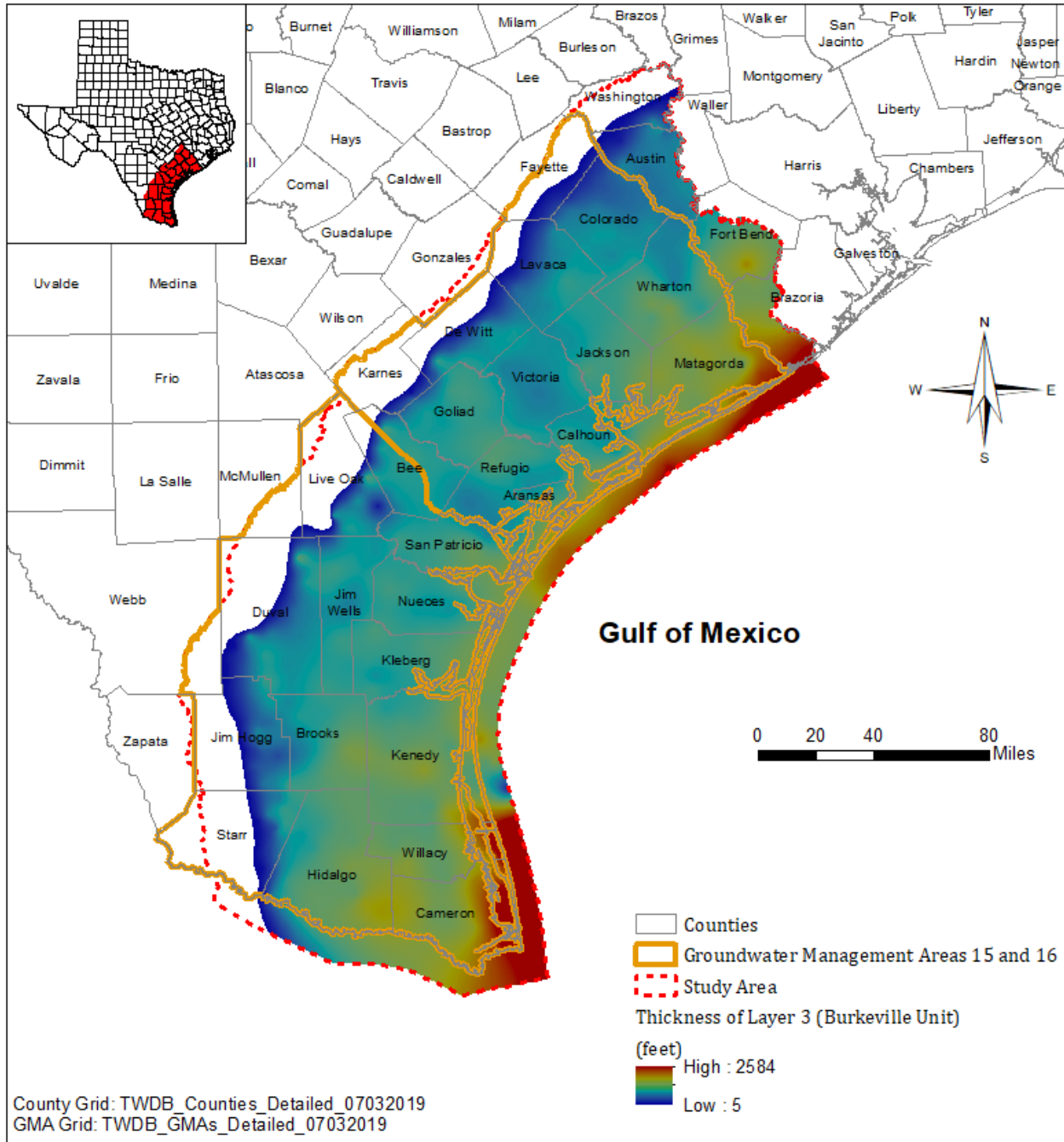


**Figure 4.1.8 Thickness of Layer 3 (Burkeville Unit).**

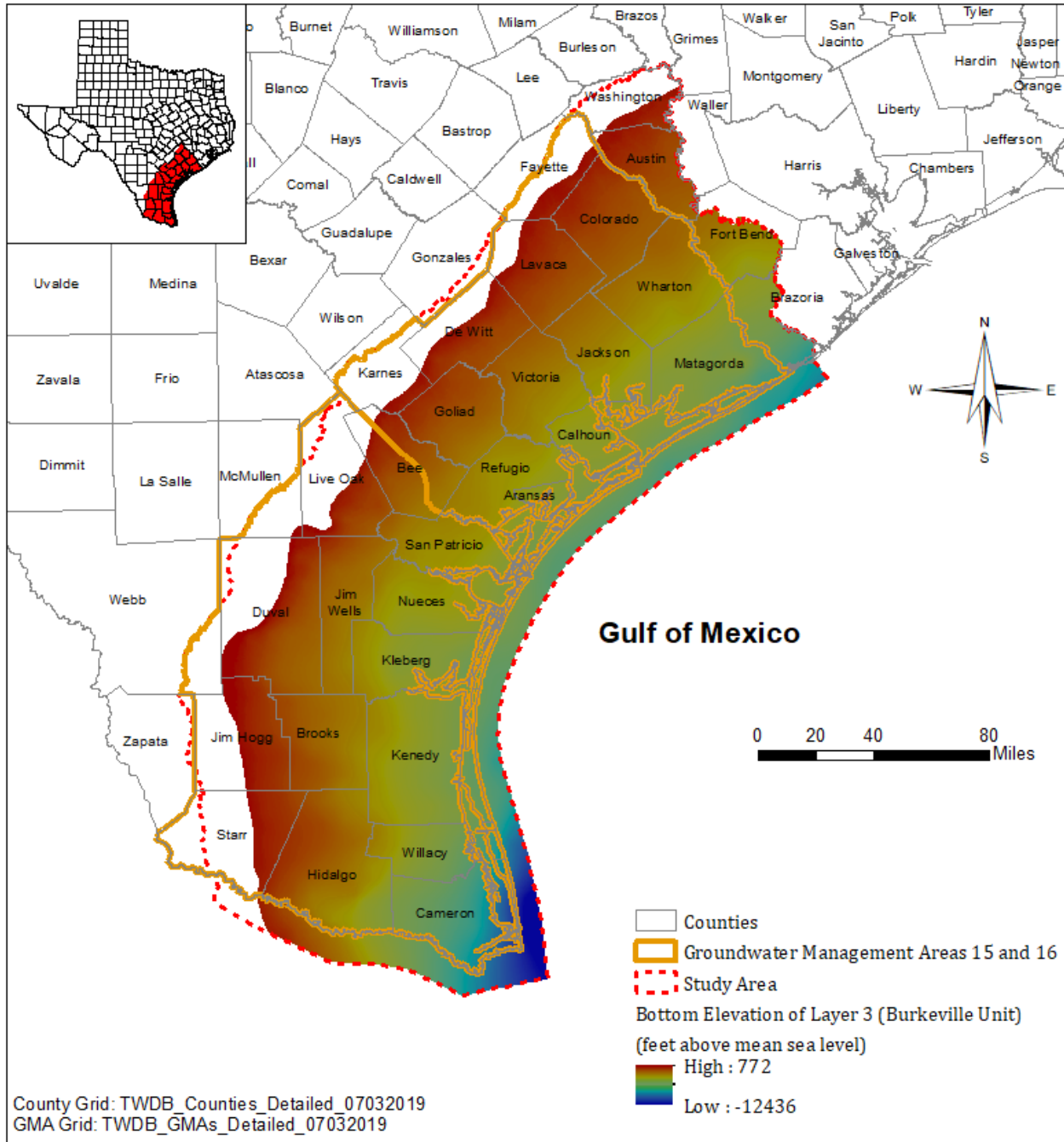


**Figure 4.1.9 Bottom Elevation of Layer 3 (Burkeville Unit).**

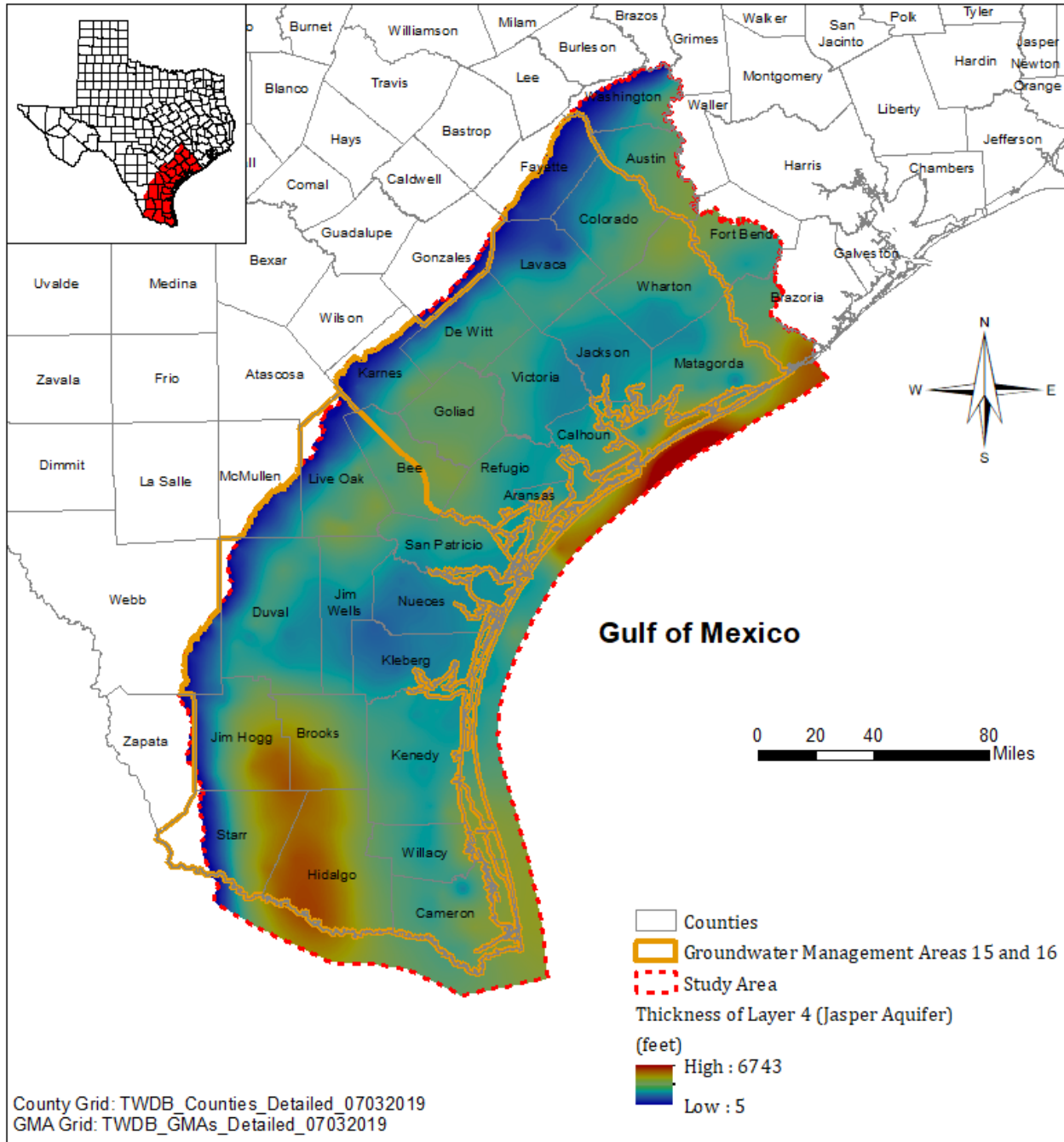


**Figure 4.1.10 Thickness of Layer 4 (Jasper Aquifer).**

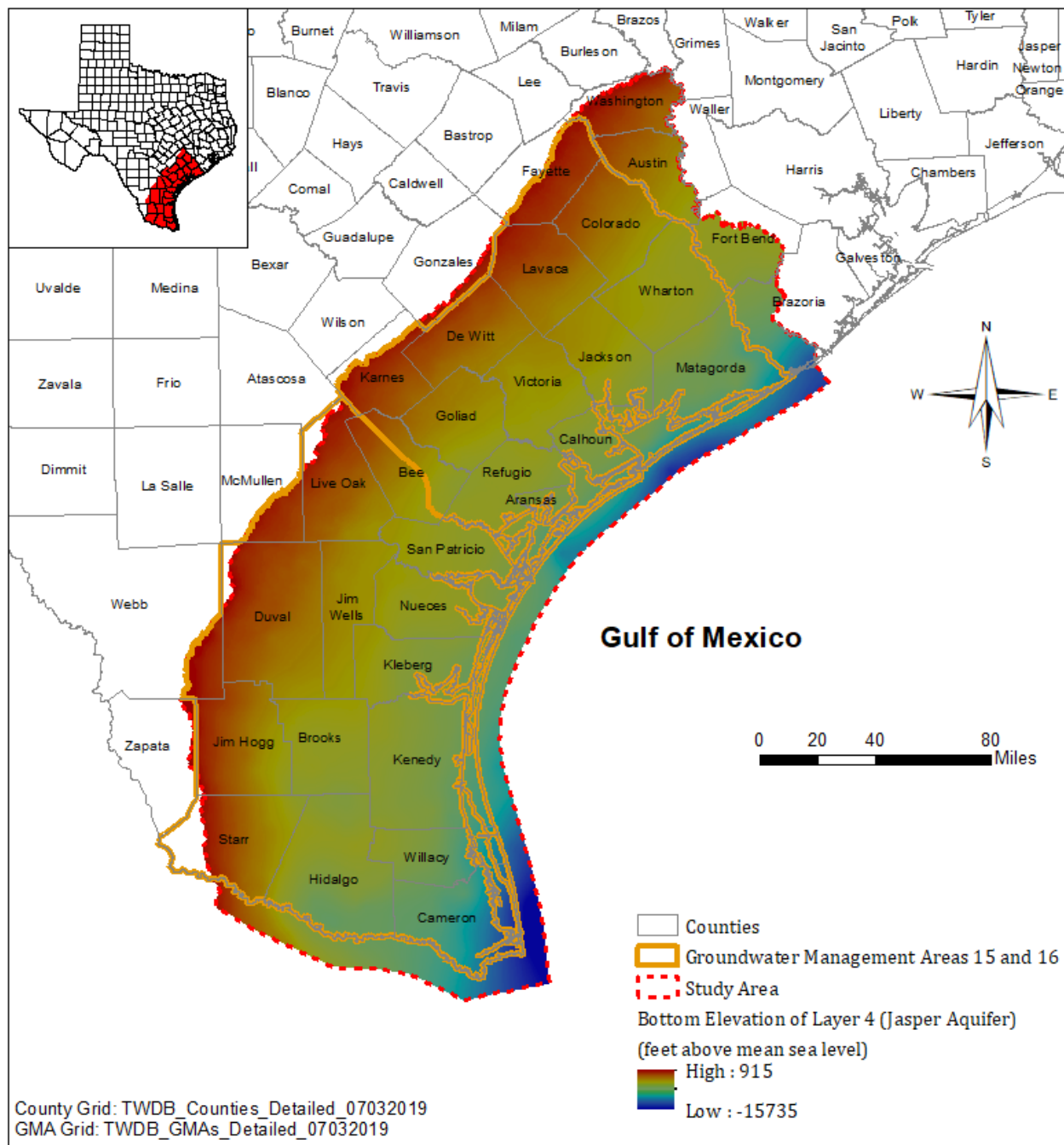


**Figure 4.1.11 Bottom elevation of Layer 4 (Jasper Aquifer).**



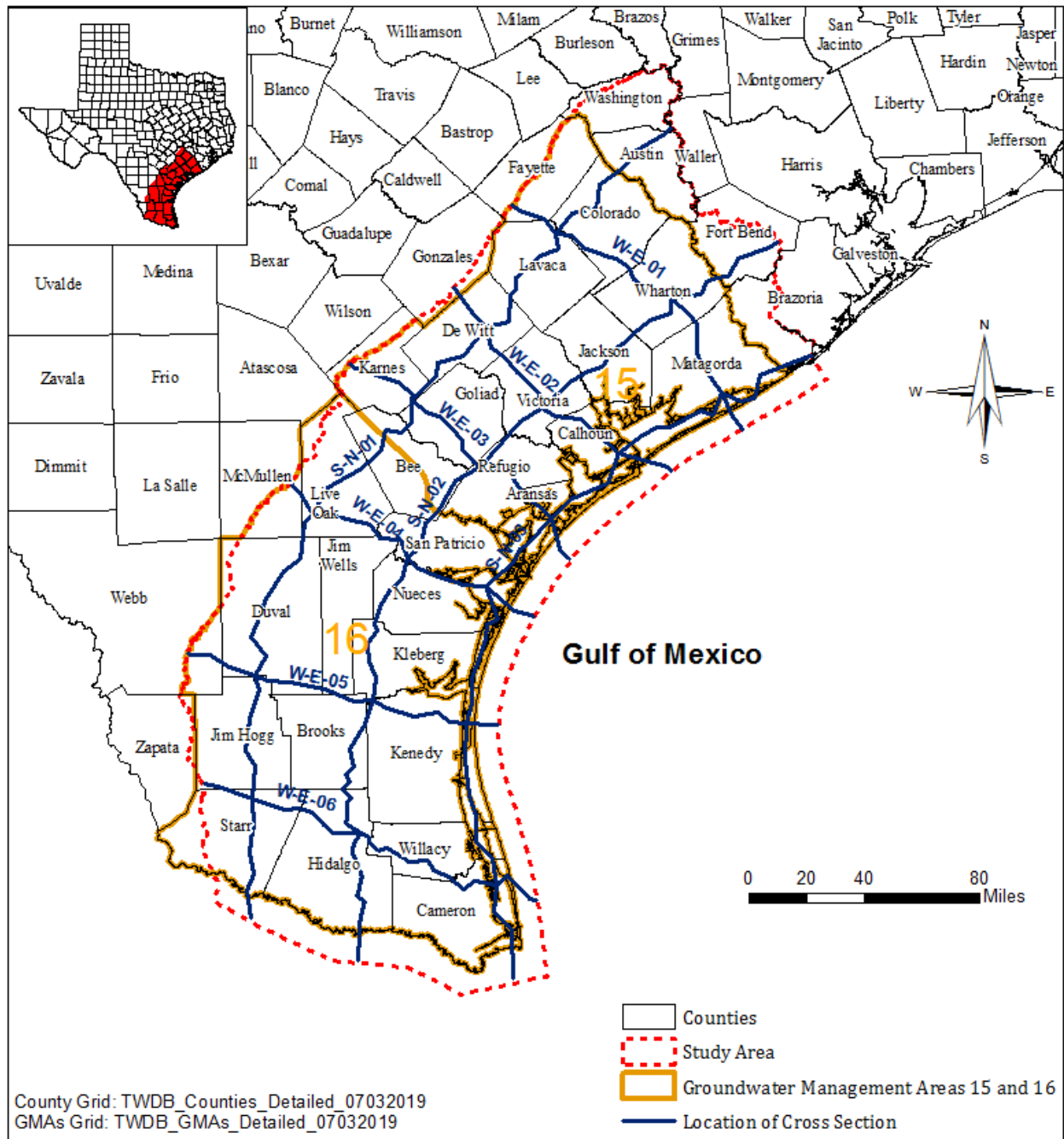


**Figure 4.1.12** Location of hydrostratigraphic cross sections.

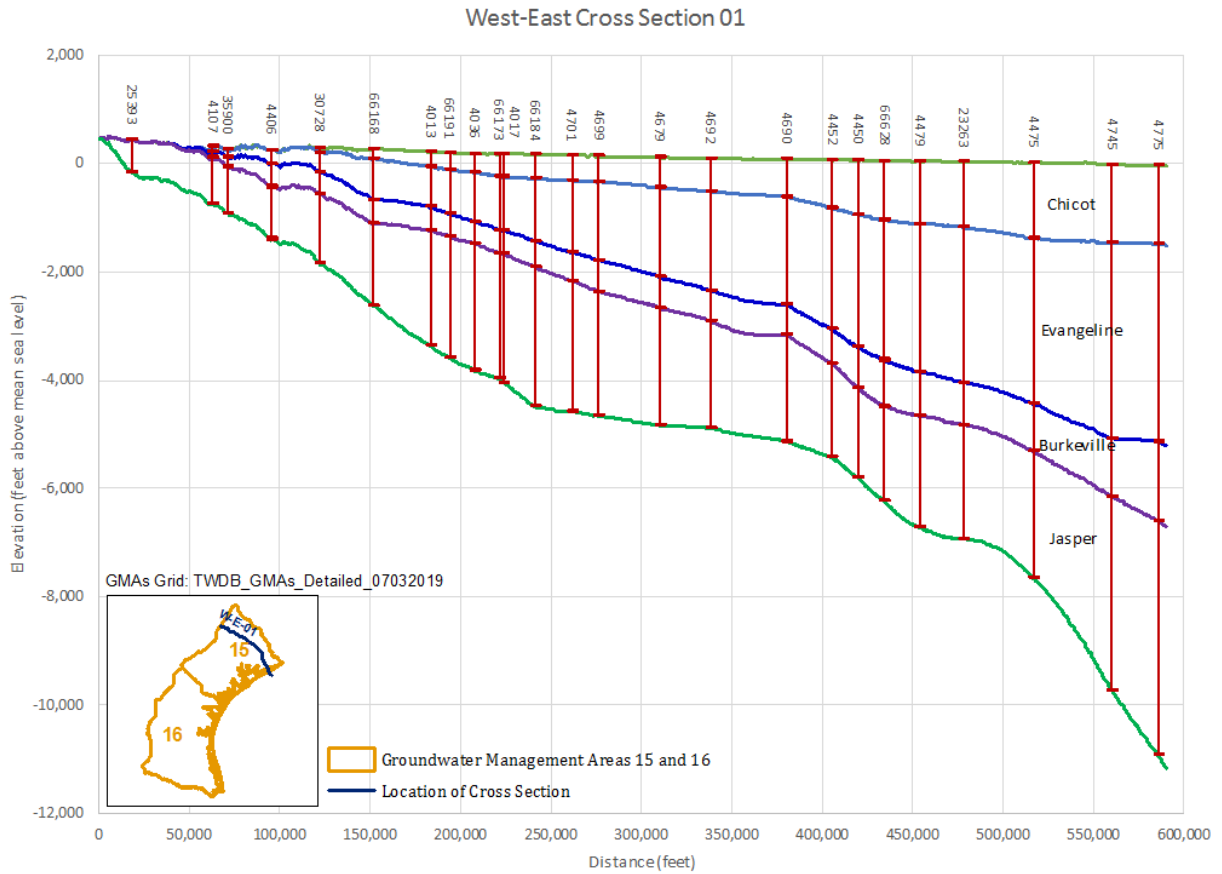


**Figure 4.1.13 Hydrostratigraphic cross section 01 along west-east direction. Vertical lines represent well logs and horizontal bars are hydrostratigraphic picks.**

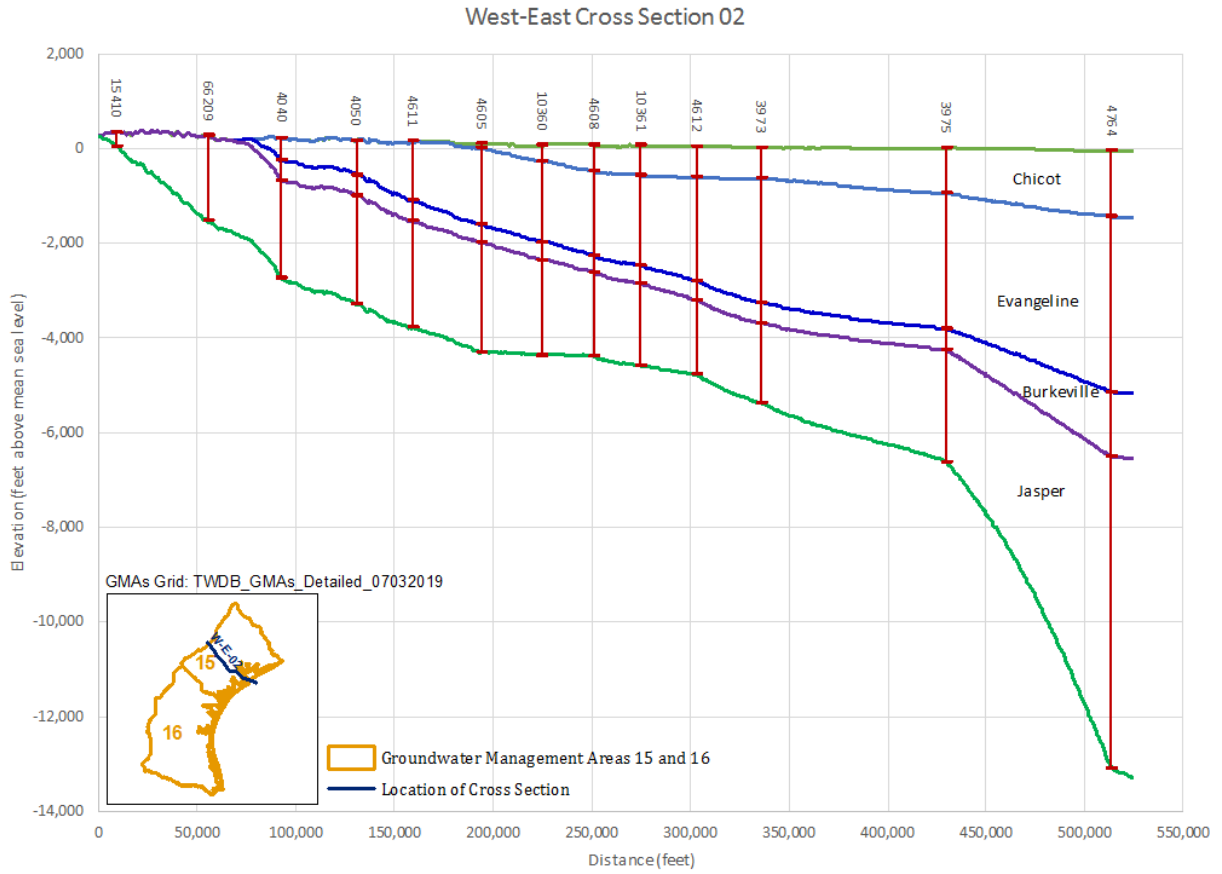


**Figure 4.1.14 Hydrostratigraphic cross section 02 along west-east direction. Vertical lines represent well logs and horizontal bars are hydrostratigraphic picks.**

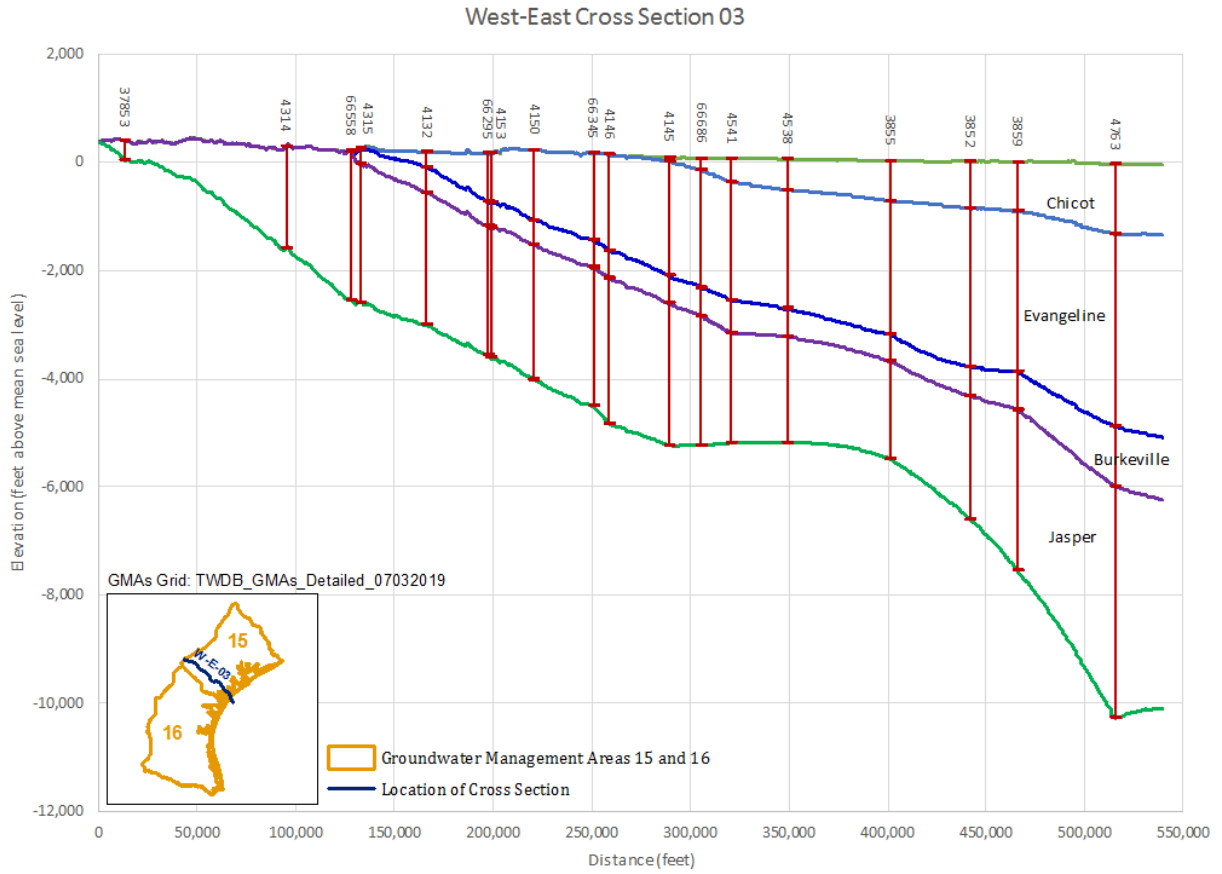


**Figure 4.1.15 Hydrostratigraphic cross section 03 along west-east direction. Vertical lines represent well logs and horizontal bars are hydrostratigraphic picks.**

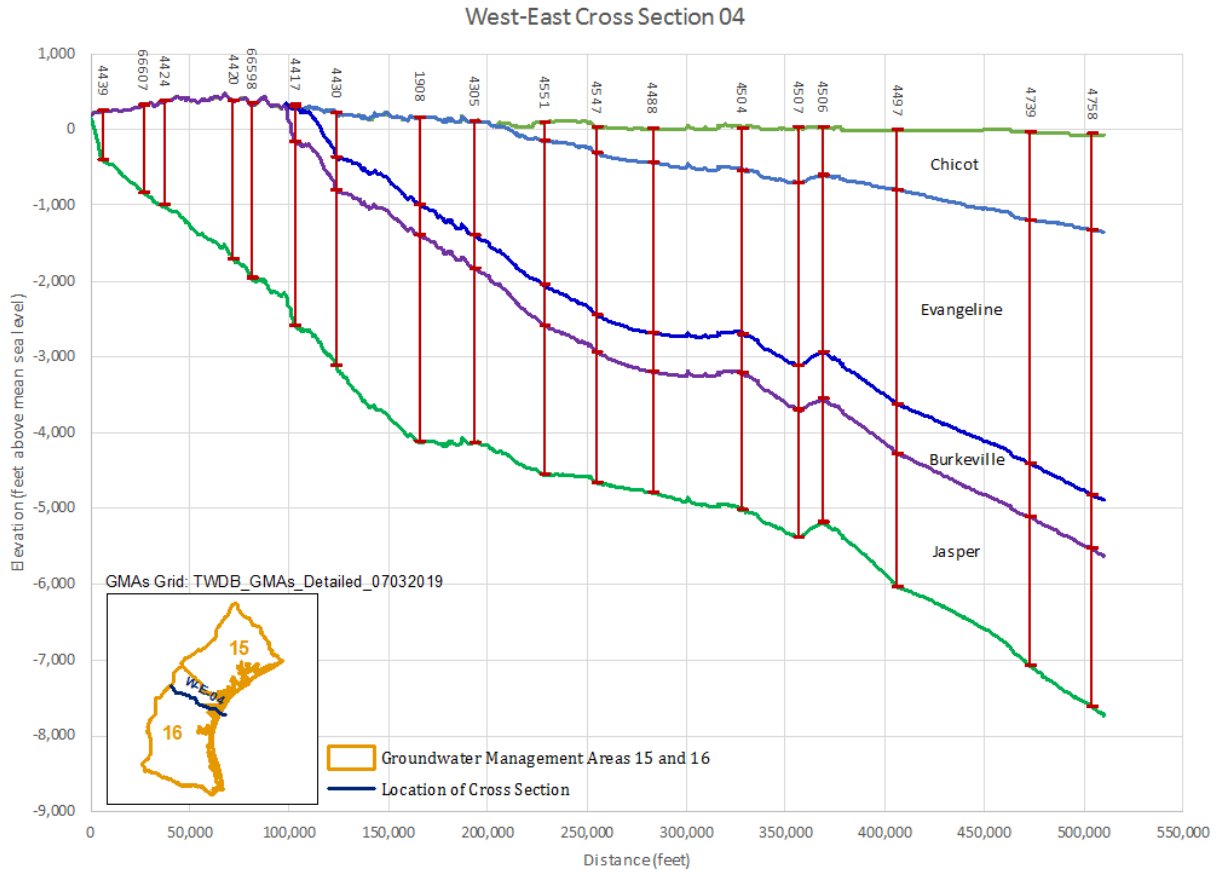


**Figure 4.1.16 Hydrostratigraphic cross section 04 along west-east direction. Vertical lines represent well logs and horizontal bars are hydrostratigraphic picks.**

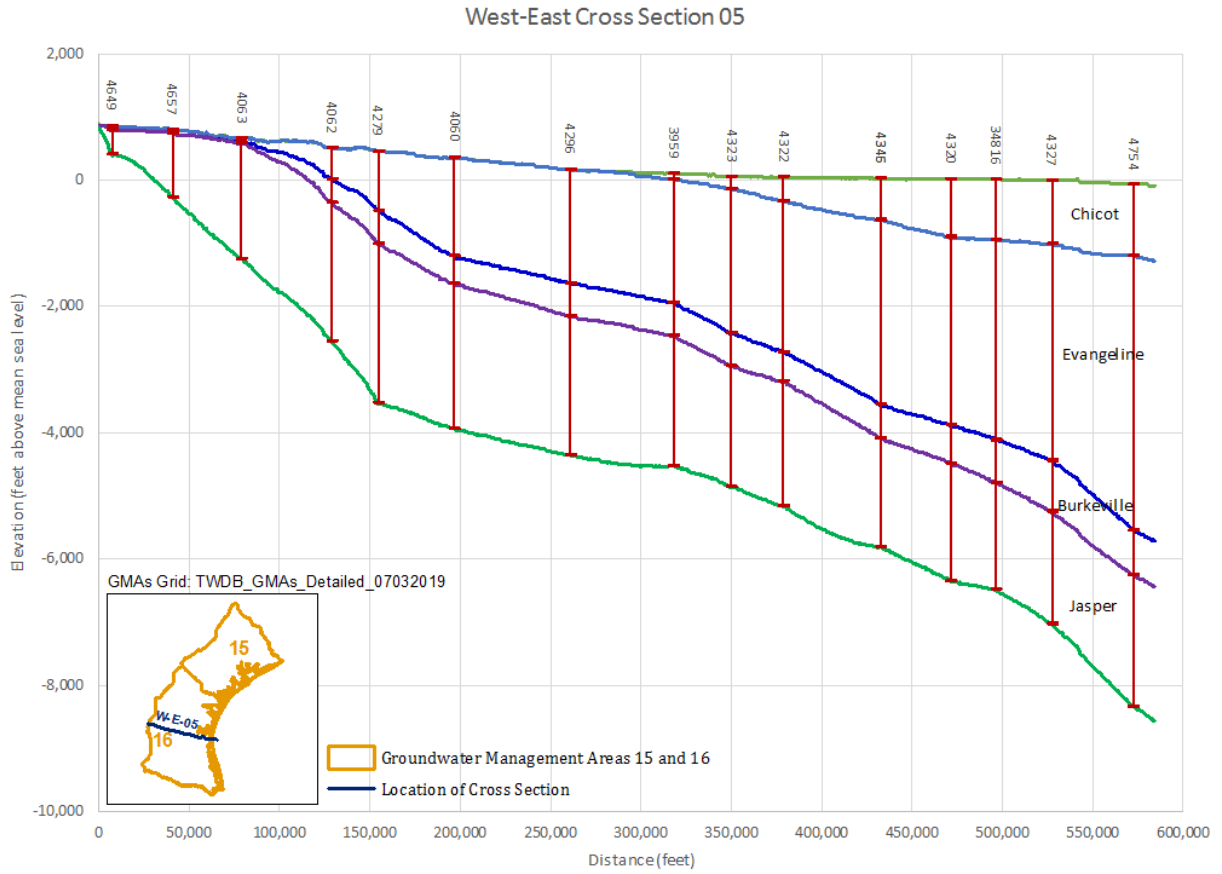


**Figure 4.1.17 Hydrostratigraphic cross section 05 along west-east direction. Vertical lines represent well logs and horizontal bars are hydrostratigraphic picks.**

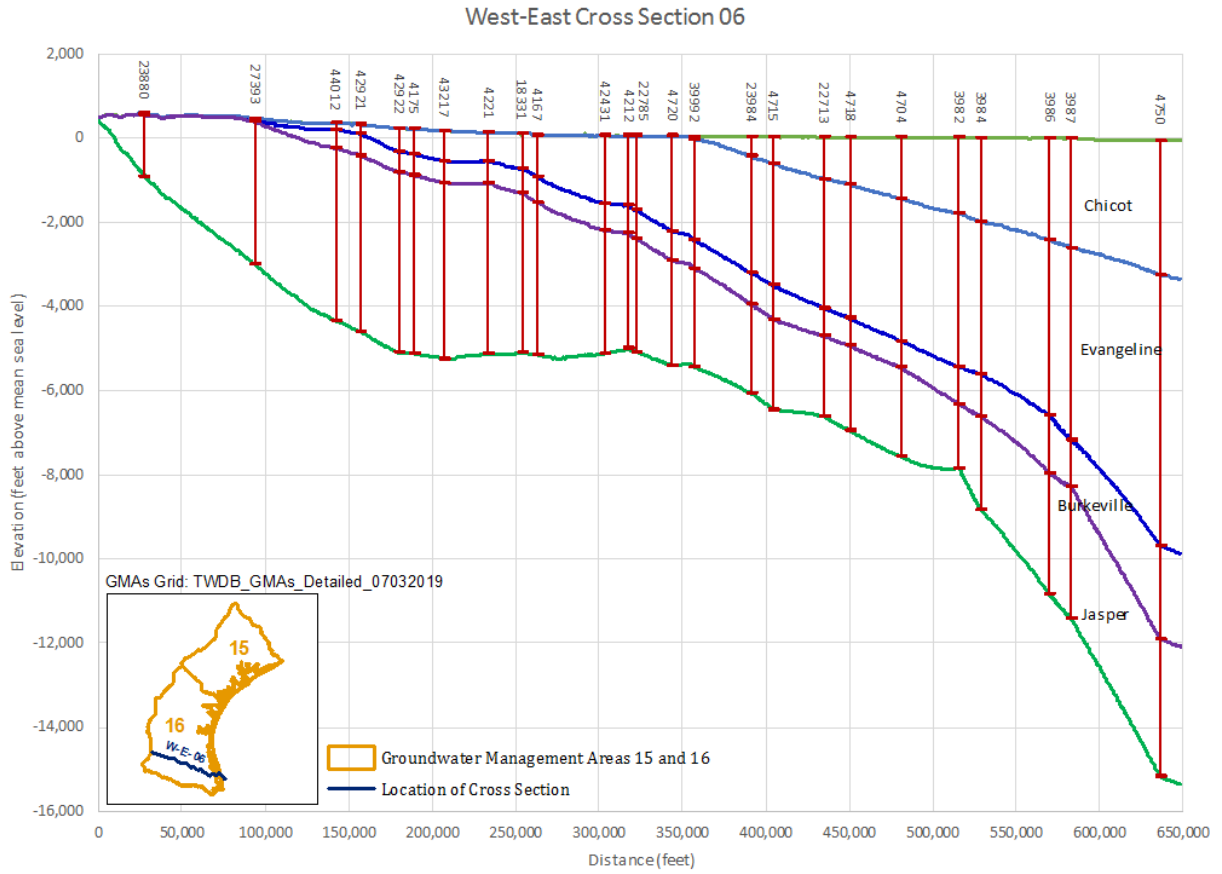


**Figure 4.1.18 Hydrostratigraphic cross section 06 along west-east direction. Vertical lines represent well logs and horizontal bars are hydrostratigraphic picks.**

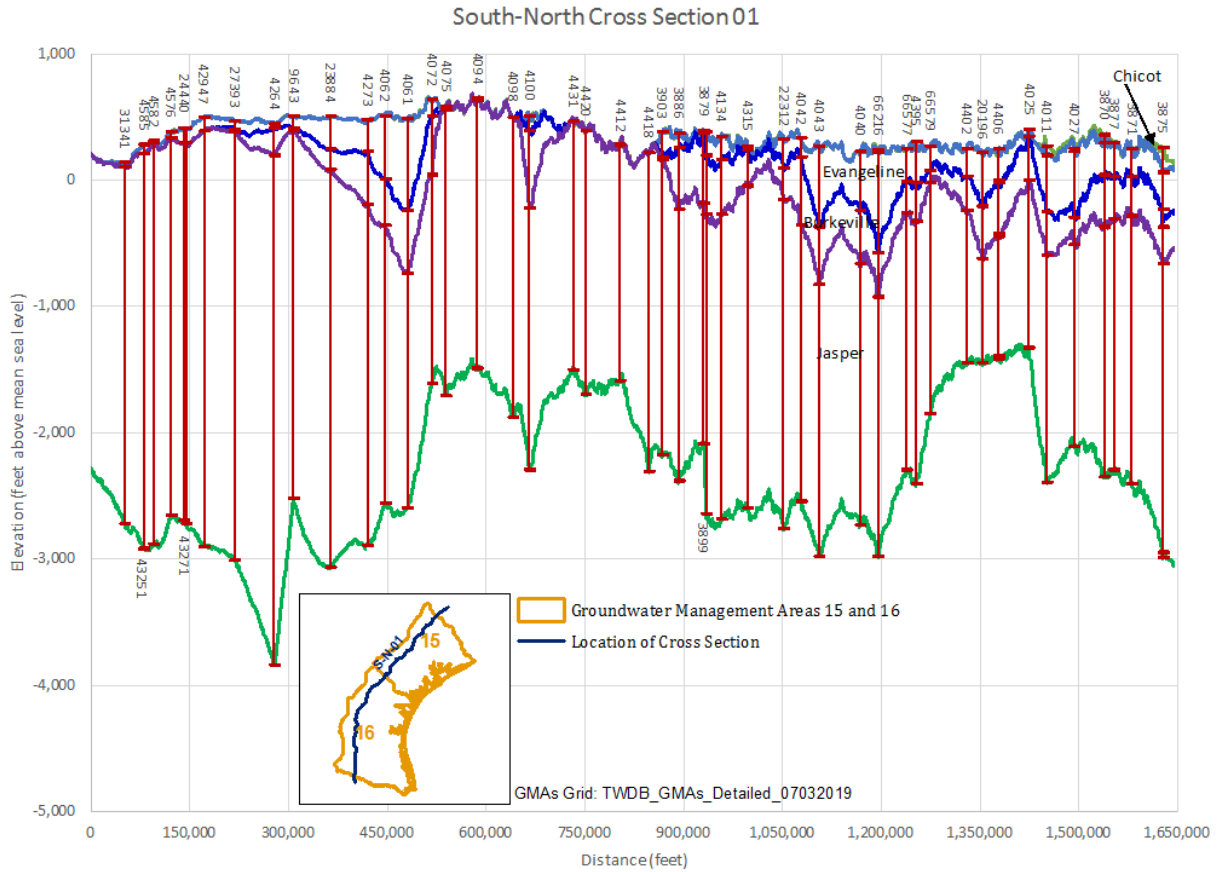


**Figure 4.1.19 Hydrostratigraphic cross section 01 along south-north direction. Vertical lines represent well logs and horizontal bars are hydrostratigraphic picks.**



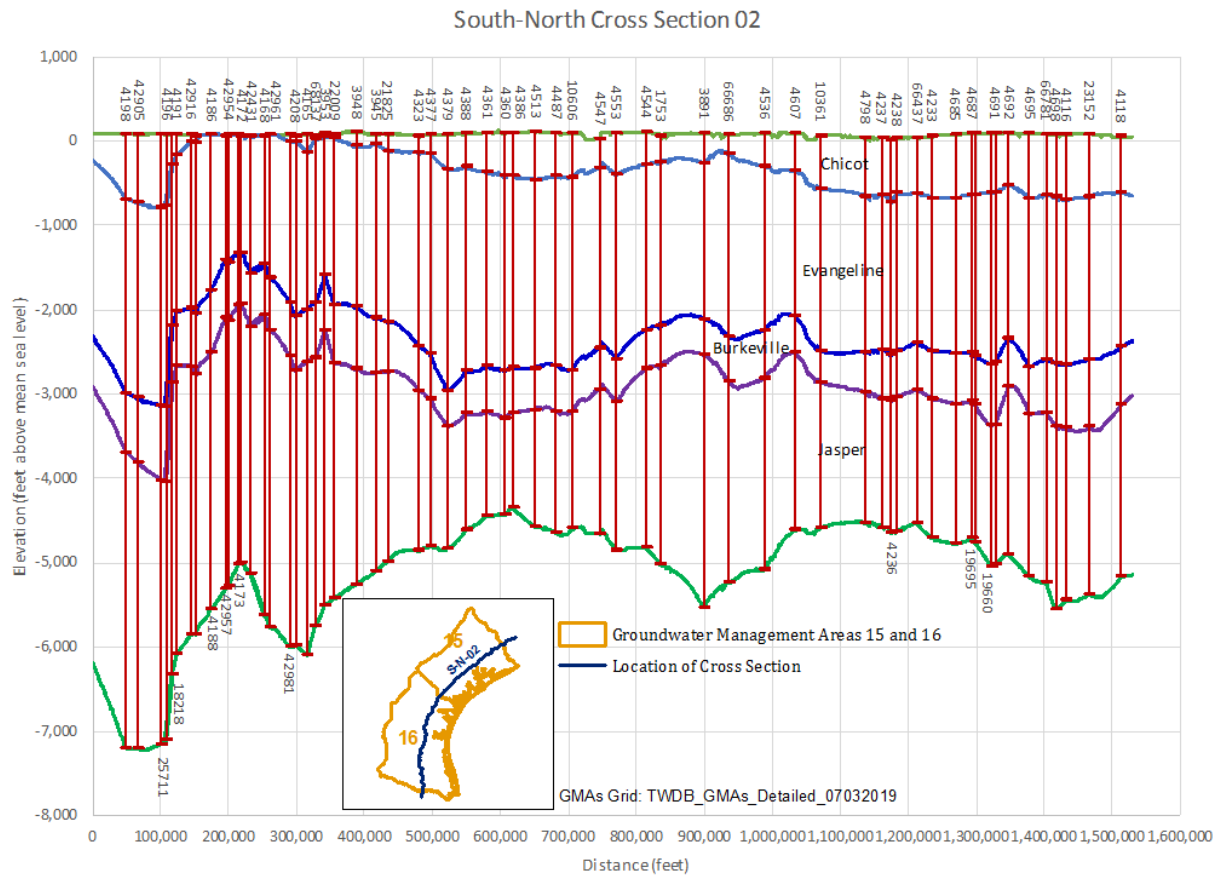


**Figure 4.1.20 Hydrostratigraphic cross section 02 along south-north direction. Vertical lines represent well logs and horizontal bars are hydrostratigraphic picks.**

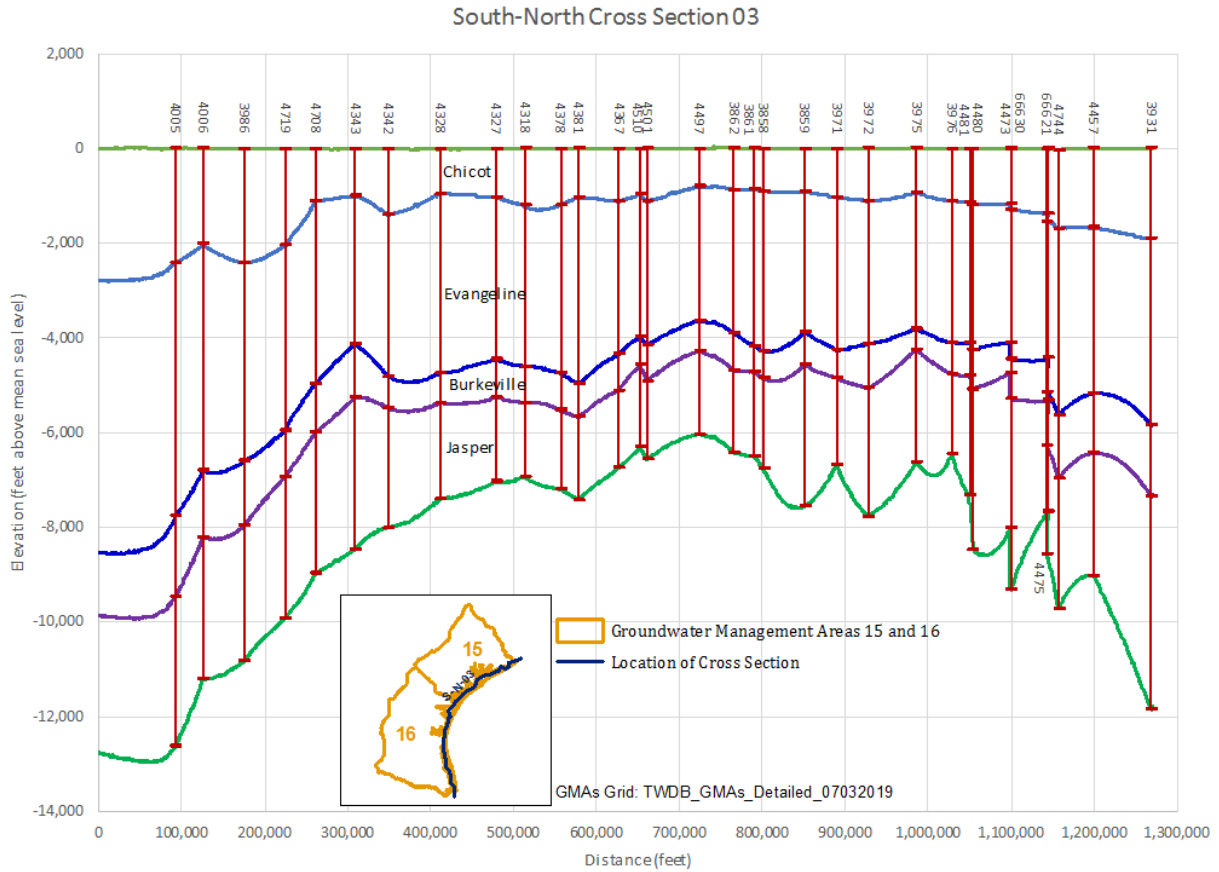


**Figure 4.1.21 Hydrostratigraphic cross section 03 along south-north direction. Vertical lines represent well logs and horizontal bars are hydrostratigraphic picks.**

## **4.2. Groundwater Levels and Flows**

The TWDB groundwater database (TWDB, 2019a) was used to extract water level measurements in wells in the study area. Wells with available screen interval information were compared with the hydrostratigraphic structure to determine which hydrogeologic unit(s) these wells belong to. Wells screened in multiple layers were not included in the study. The hydrogeologic units of wells without screen interval information were determined by their available hydrostratigraphic codes.

Annual water levels were calculated based on average of measurements from January, February, November, and December to minimize impacts of pumping. For example, water levels from November and December of 1980 and from January and February of 1981 were averaged to represent the end of 1980.

Groundwater extraction from the Gulf Coast Aquifer System in the study area has been occurring for more than a century. In addition, water level measurements prior to 1933 are scarce (Figure 4.2.1). It is thus impossible to reproduce a true pre-development condition. As a result, this section only provides water level contours in 1980, 1990, 2000, 2010, and 2015. These contours are used to evaluate lateral groundwater flow for each hydrogeological unit during these years. To assess groundwater level change over time, hydrographs were produced at wells with at least 30 years of annual data. Annual water level differences between well clusters were used to examine cross-formation flow. Each cluster contains two wells from different hydrogeological units but with lateral distance less than half a mile (2,640 feet).

### **4.2.1. Lateral Groundwater Flow**

In general, the groundwater in the Chicot Aquifer flows towards the Gulf of Mexico, with local potentiometric surface depressions along north-central Matagorda County, central Jackson County, east-central Victoria County, and northeastern Kleberg County (Figures 4.2.2 through 4.2.6). These depressions are correlated to major population centers in these counties and, thus, likely related to groundwater extraction even during winter months.

Like the Chicot Aquifer, the Evangeline Aquifer also shows a groundwater flow towards the Gulf of Mexico (Figures 4.2.7 through 4.2.11). The depression in northeastern Kleberg County is also likely due to groundwater withdrawal. It is worthwhile to note the lack of water level data in the coastal counties in Groundwater Management Area 15 for the Evangeline Aquifer.

Very few water level data exist for the Burkeville Unit in Bee, DeWitt, Goliad, Karnes, and Live Oak counties (Figures 4.2.12 through 4.2.16). The limited water level data also indicated a groundwater flow trend towards the Gulf of Mexico.

Figures 4.2.17 through 4.2.21 show the water level contours for the Jasper Aquifer. The groundwater flow within the narrow band on or close to the outcrop area of the aquifer varied from place to place. Some places showed a regional flow towards the Gulf of Mexico such as counties in Groundwater Management Area 15 (Figures 4.2.18 and 4.2.20), while others indicated flow towards the pumping centers (Figures 4.2.17 and 4.2.19).

#### ***4.2.2. Water-Level Change over Time***

The groundwater level change over time was evaluated using transient water level measurements collected from wells. Only those wells screened in a single hydrogeologic unit and with more than 30 annual water level data were used to create the water level hydrographs.

Of 3,074 wells screened in a single aquifer, 151 wells meet the criteria listed above. Of them, 66 wells are in the alluvium/eolian and Chicot Aquifer, 68 in the Evangeline Aquifer, two in the Burkeville Unit, and 15 in the Jasper Aquifer.

Some of the hydrographs are shown in Figures 4.2.22 and 4.2.23 for the wells in the Chicot Aquifer, Figures 4.2.24 and 4.2.25 for the wells in the Evangeline Aquifer, Figure 4.2.26 for the wells in the Evangeline Aquifer and the Burkeville Unit, and Figure 4.2.27 for the wells in the Jasper Aquifer. The rest of the hydrographs are presented in Appendix A.

The hydrographs show very little water level fluctuation at most of the selected wells with exceptions at the wells located at or near the population centers in Jackson, Kleberg, and

Victoria counties where groundwater withdrawal may have occurred during the winter and, thus, caused the larger water level change over time. At several locations, the water level experienced a significant drop from 1930s/40s to 1980s and then showed a moderate recovery afterwards (Figures 4.2.24 and 4.2.25), which may be due to the conversion from groundwater to surface water supplies.

#### **4.2.3. Cross-Formation Flow**

Cross-formation flow is the groundwater flow between different hydrogeological units and is controlled by nature and human activity. Landscape change can influence the groundwater recharge and, in turn, modify groundwater flow patterns. Groundwater withdrawal can change or even reverse cross-formation flow.

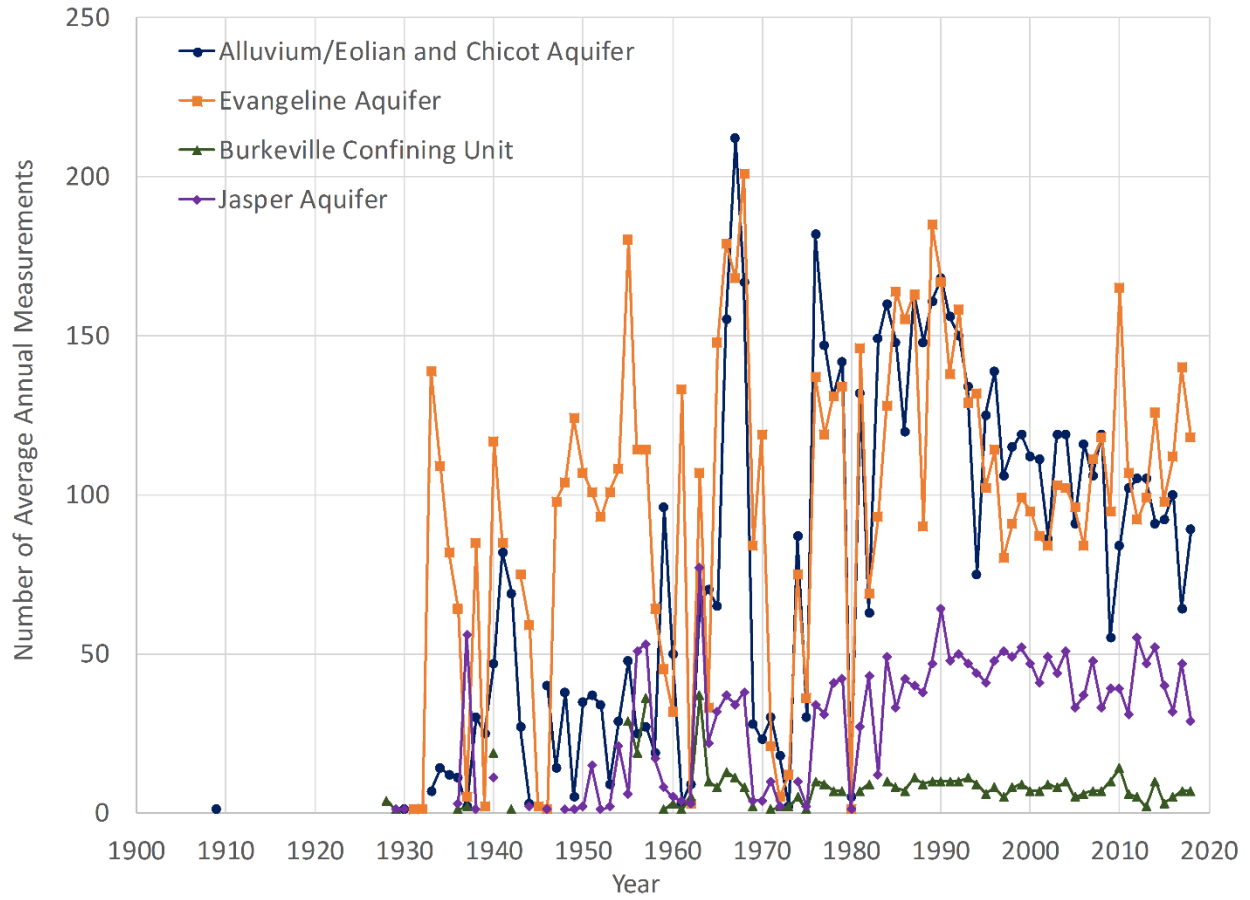
In this section, the water level difference between two adjacent wells completed in different hydrogeological units but less than half mile (2,640 feet) apart was used to evaluate the cross-formation flow. Due to the potential error introduced by well locations and water level measurements, a water level difference between -5 and 5 feet was considered neutral or no significant cross-formation flow; less than -5 feet downward flow; and more than 5 feet upward flow. The water level difference was only calculated when both wells had the water level data at the same year using all historical annual average water level data. As a result, the same pair may have multiple difference values correlated to different years.

Figure 4.2.28 shows the water level difference between the Chicot and Evangeline aquifers. Figure 4.2.29 shows the water level difference between the Evangeline Aquifer and the Burkeville Unit. Figure 4.2.30 shows the water level difference between the Evangeline and Jasper aquifers. Figure 4.2.31 shows the water level difference between the Burkeville Unit and the Jasper Aquifer. The details of the calculations are presented in Appendix B.

As shown in these figures, the water level difference indicated that the cross-formation flow changed from downward near or at the outcrop area to neutral or upward flow towards the Gulf. An exception does exist in Goliad County (Figure 4.2.28). It is not clear what caused the upward flow in Goliad County. It might be due to a local hydrogeological

heterogeneity or groundwater use. The upward flow next to the Colorado River in Colorado and Wharton counties is consistent with the river being a major discharging point.

Overall, the groundwater levels have been relatively stable for most of the wells with more than 30 historical annual average water level data. This indicates that groundwater in the Gulf Coast Aquifer System has been able to bounce back during winter from groundwater withdrawal over the summer. However, continual groundwater pumping at some of the wells near the major population centers in the study area may have over-drafted the aquifer and caused water level decline even during winter. Groundwater withdrawal can modify the groundwater flow direction locally, but the regional flow direction has remained towards the Gulf. As a result, the cross-formation flow often occurs downward at and near the outcrop area and upward further hydraulically downgradient towards the Gulf of Mexico and near major rivers.



**Figure 4.2.1** Number of average annual water level measurements in Gulf Coast Aquifer System.

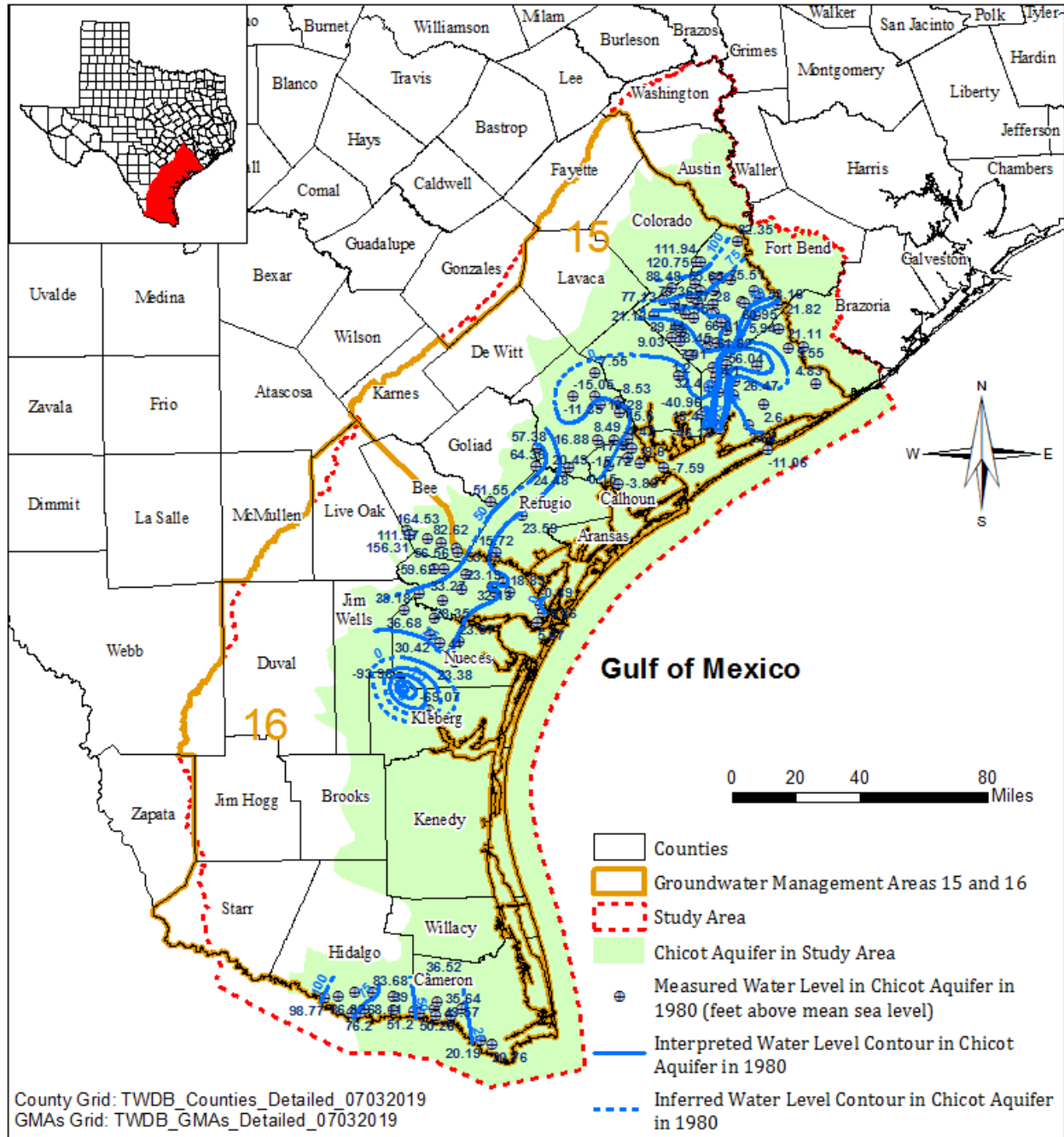


**Figure 4.2.2 Water levels in alluvium/eolian and Chicot Aquifer (1980).**



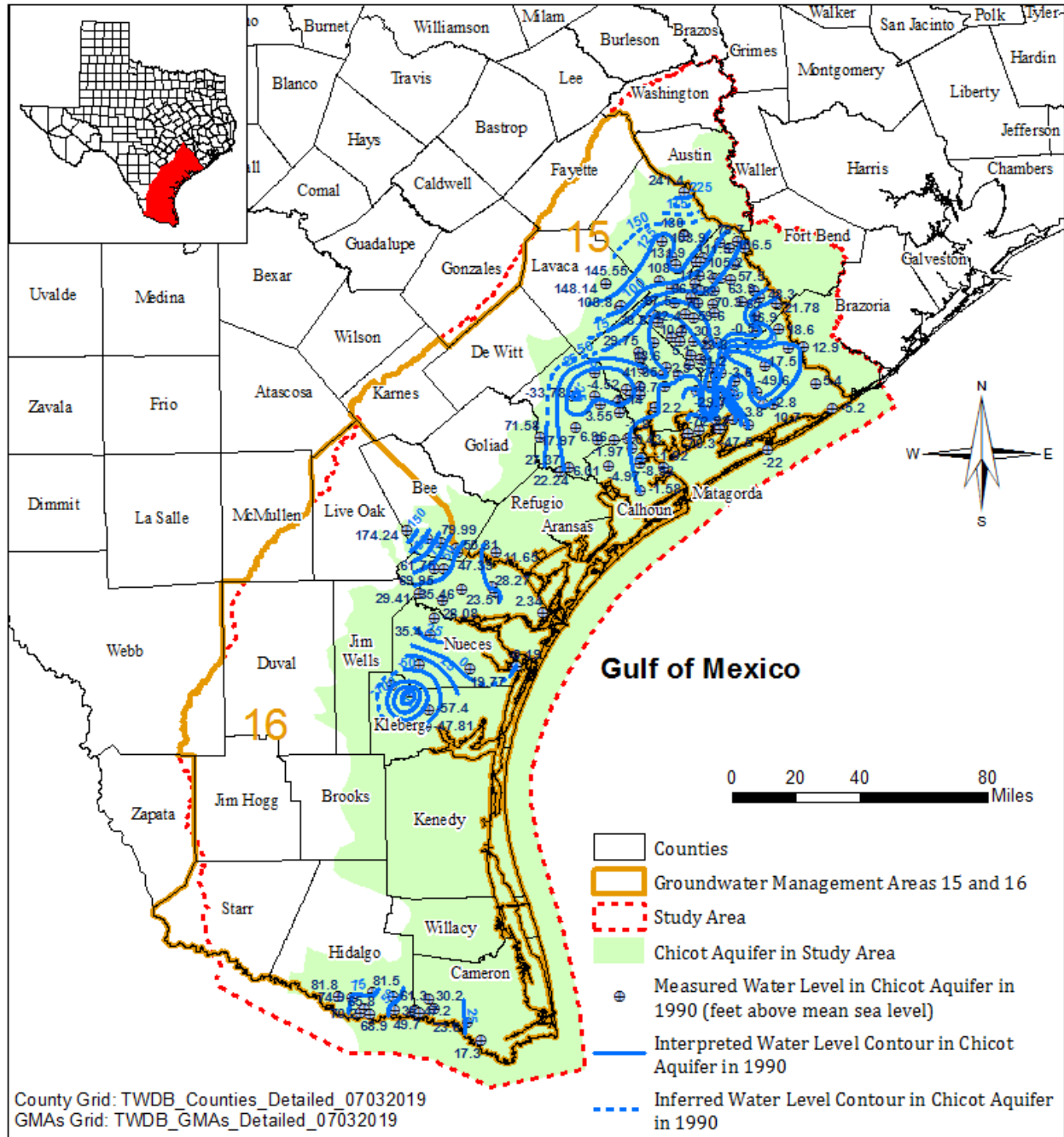


**Figure 4.2.3 Water levels in alluvium/eolian and Chicot Aquifer (1990).**

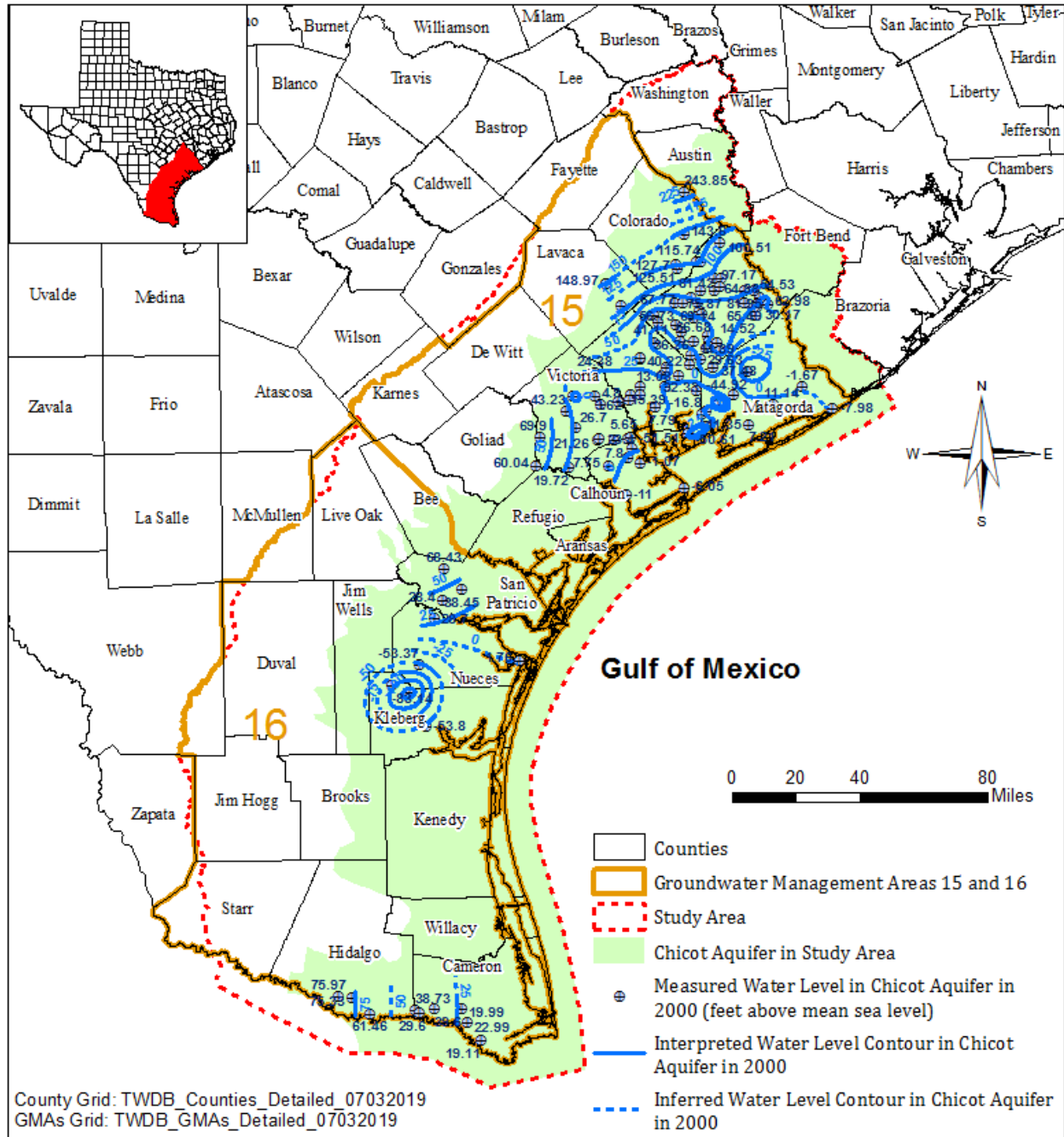


**Figure 4.2.4 Water levels in alluvium/eolian and Chicot Aquifer (2000).**

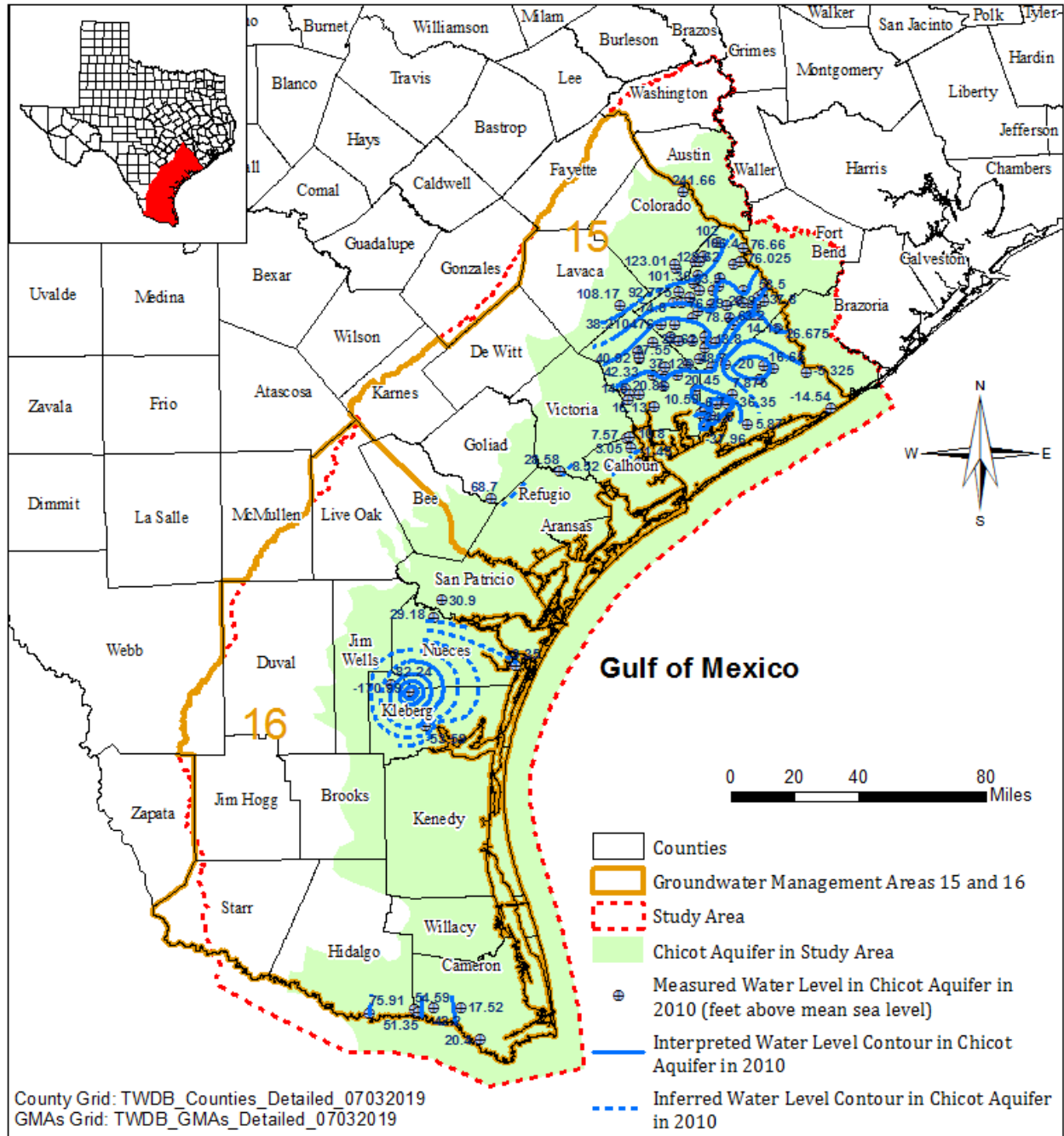


**Figure 4.2.5 Water levels in alluvium/eolian and Chicot Aquifer (2010).**

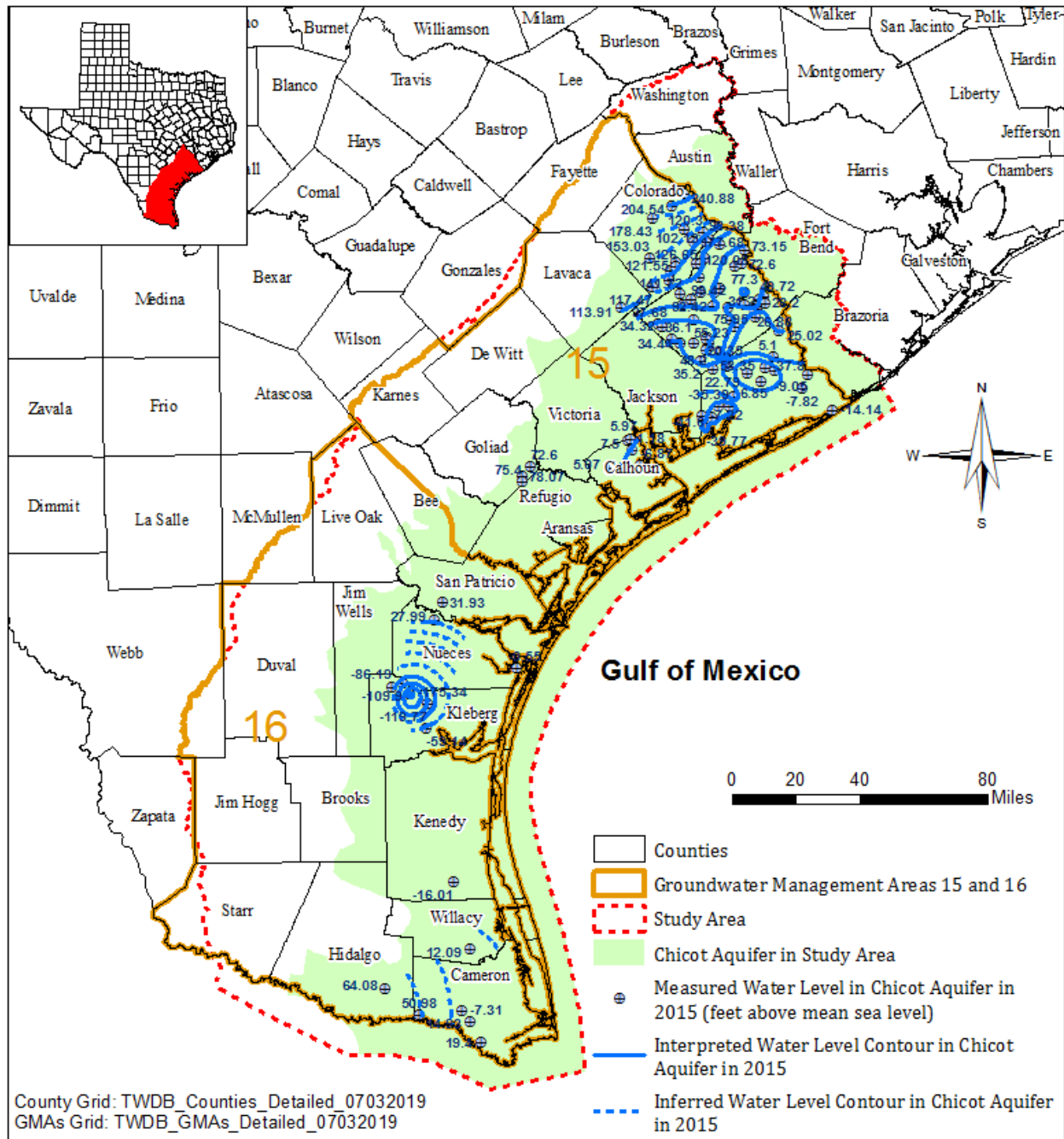


**Figure 4.2.6 Water levels in alluvium/eolian and Chicot Aquifer (2015).**

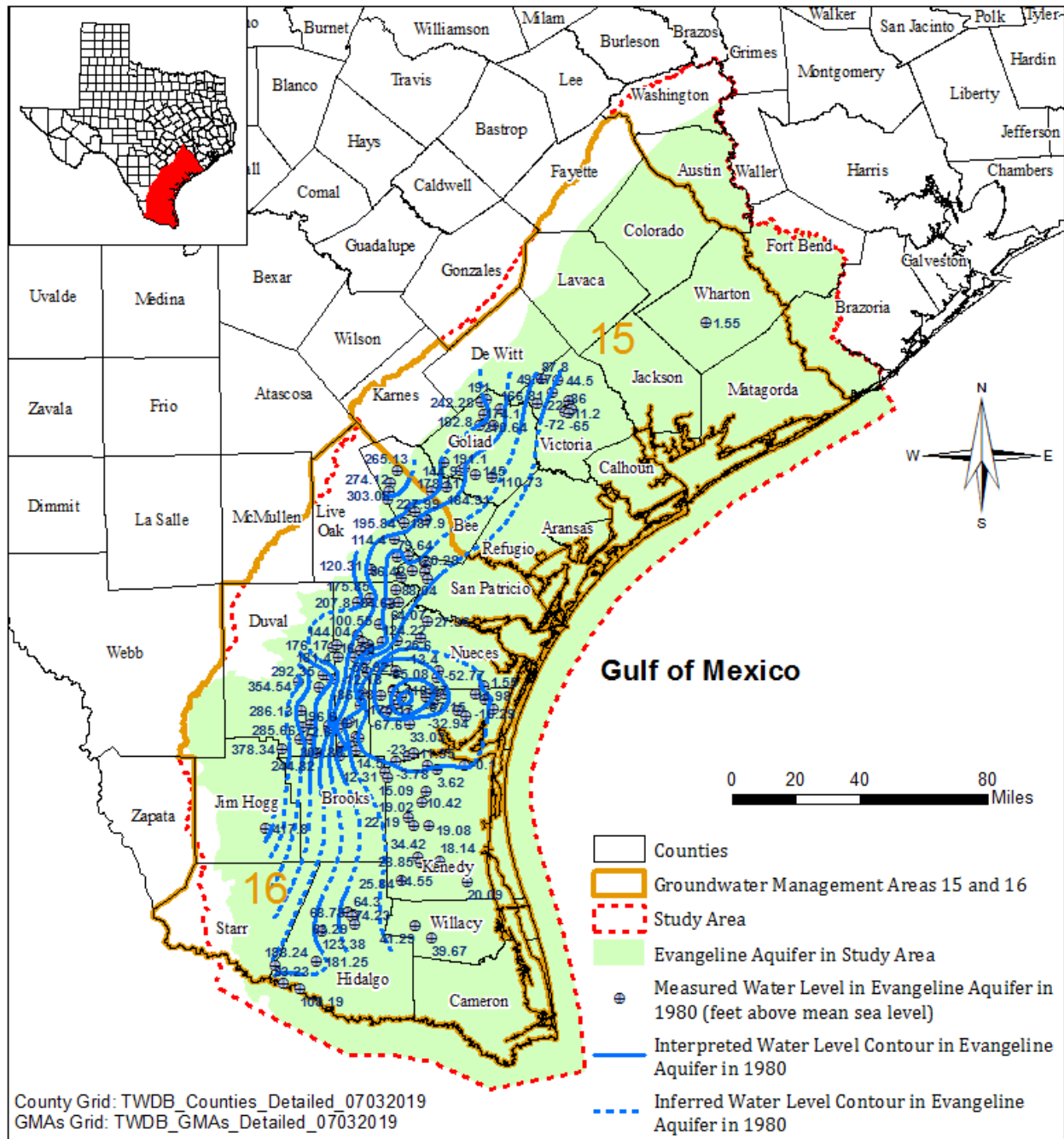


**Figure 4.2.7 Water levels in Evangeline Aquifer (1980).**

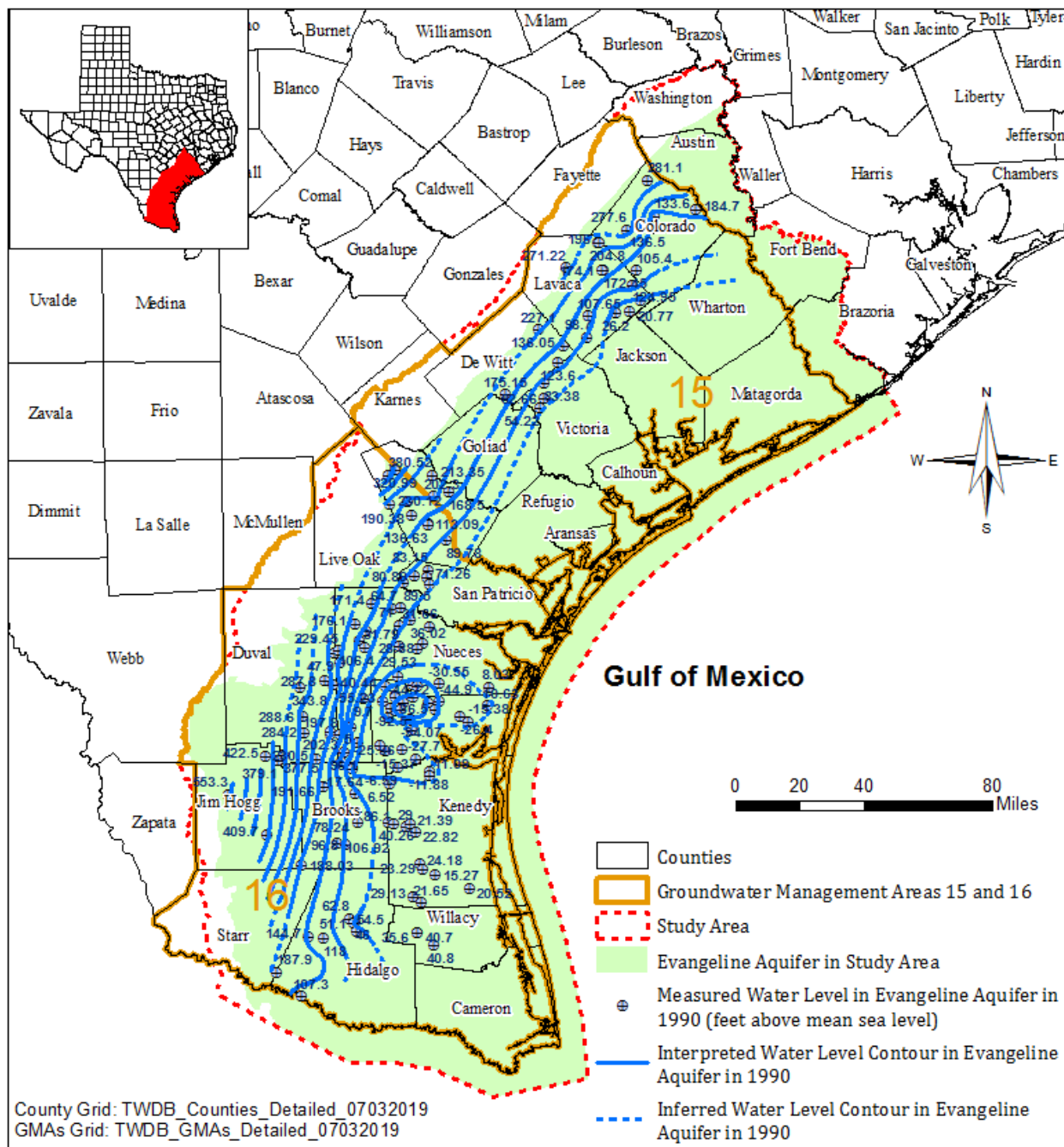


**Figure 4.2.8 Water levels in Evangeline Aquifer (1990).**

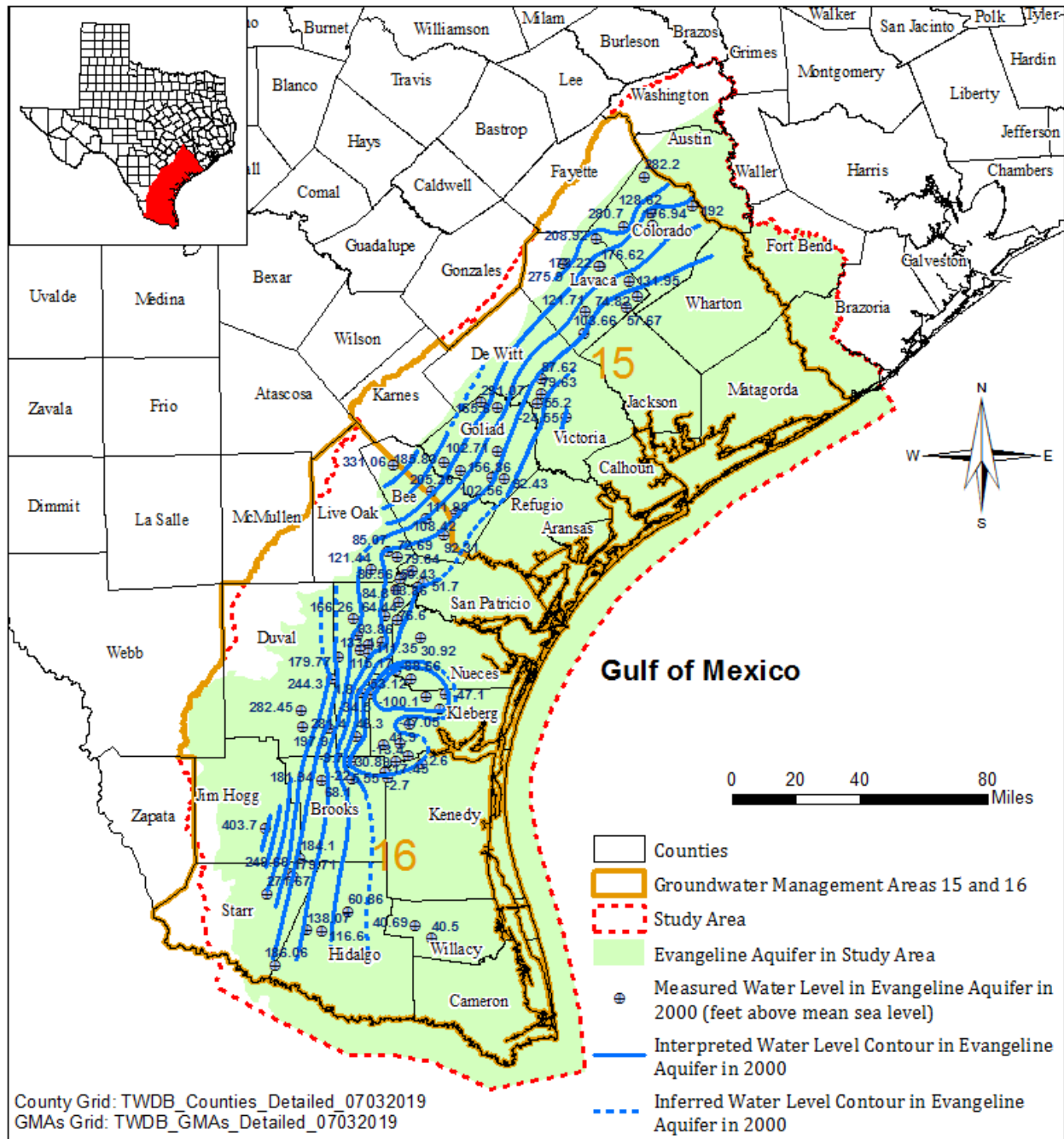
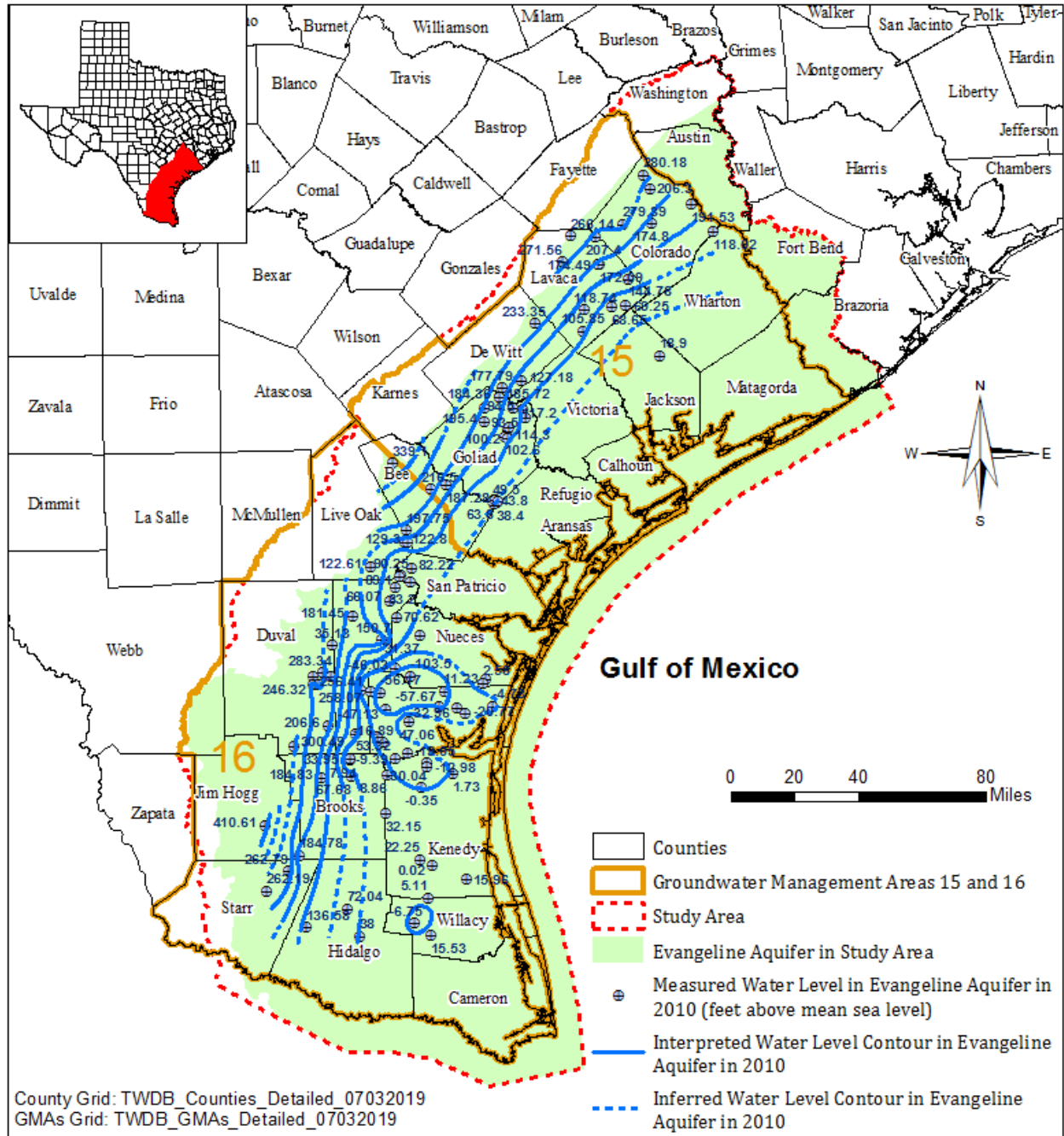
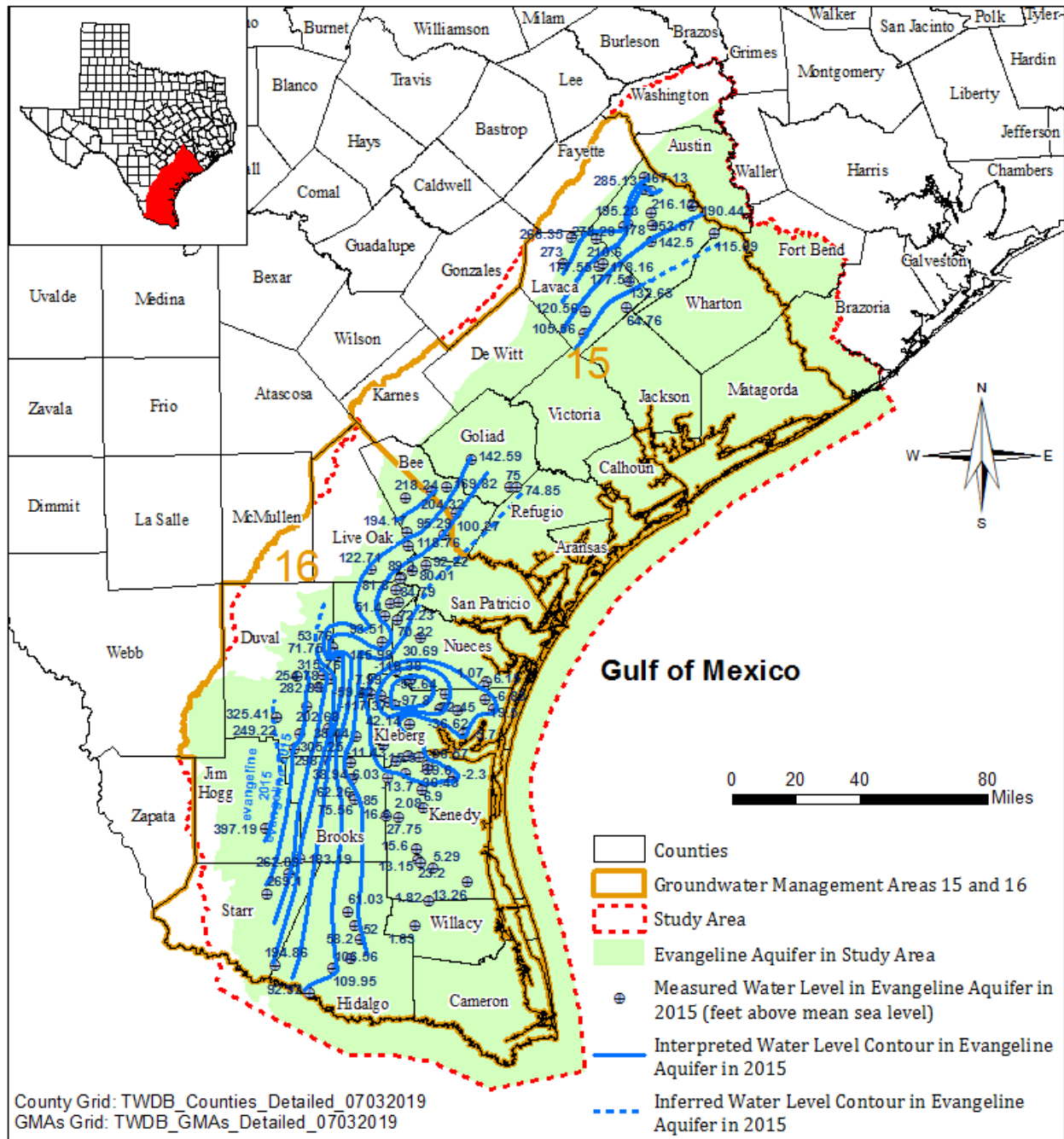


Figure 4.2.9 Water levels in Evangeline Aquifer (2000).



**Figure 4.2.10 Water levels in Evangeline Aquifer (2010).**





**Figure 4.2.11 Water levels in Evangeline Aquifer (2015).**

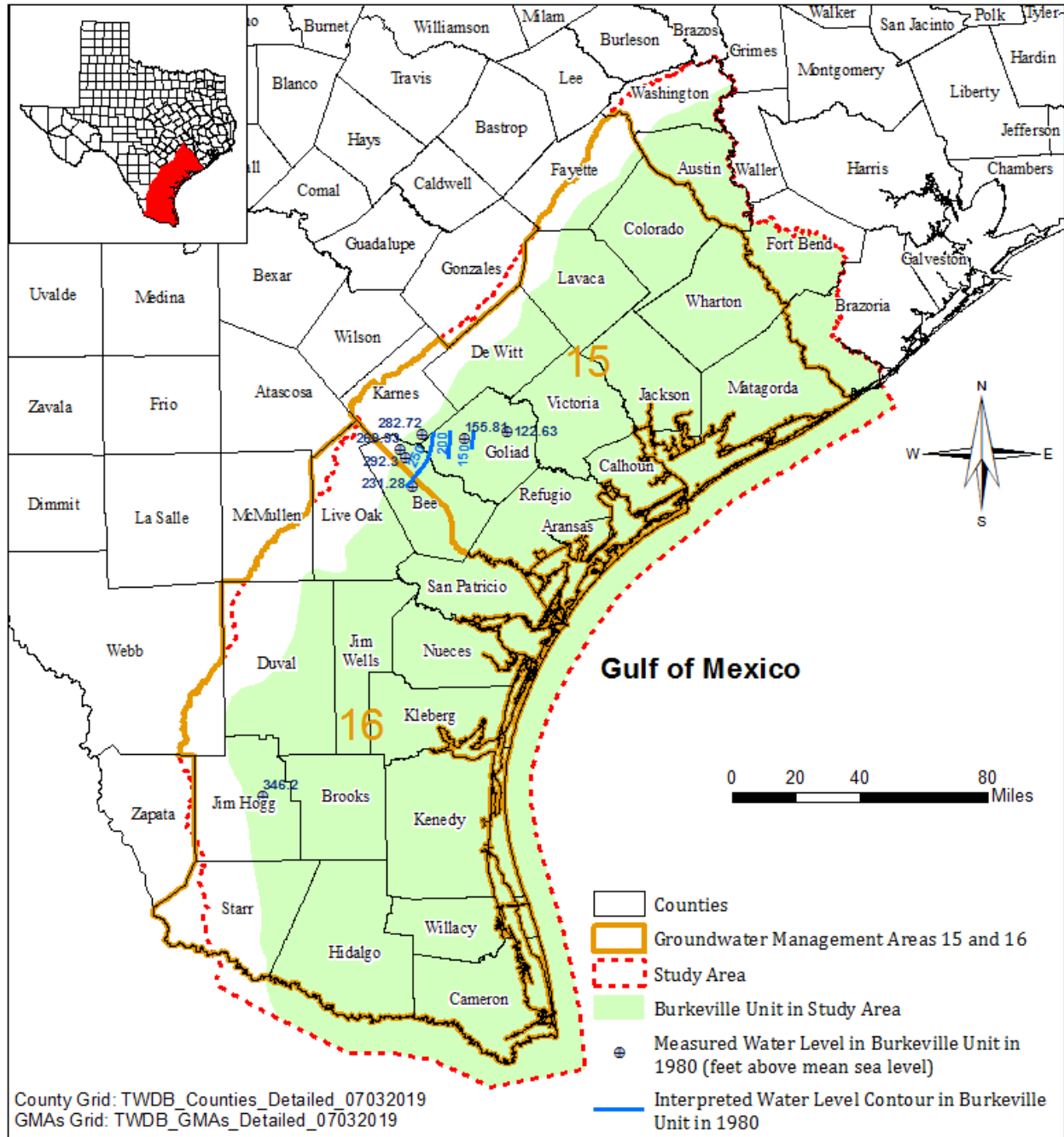


**Figure 4.2.12 Water levels in Burkeville Unit (1980).**

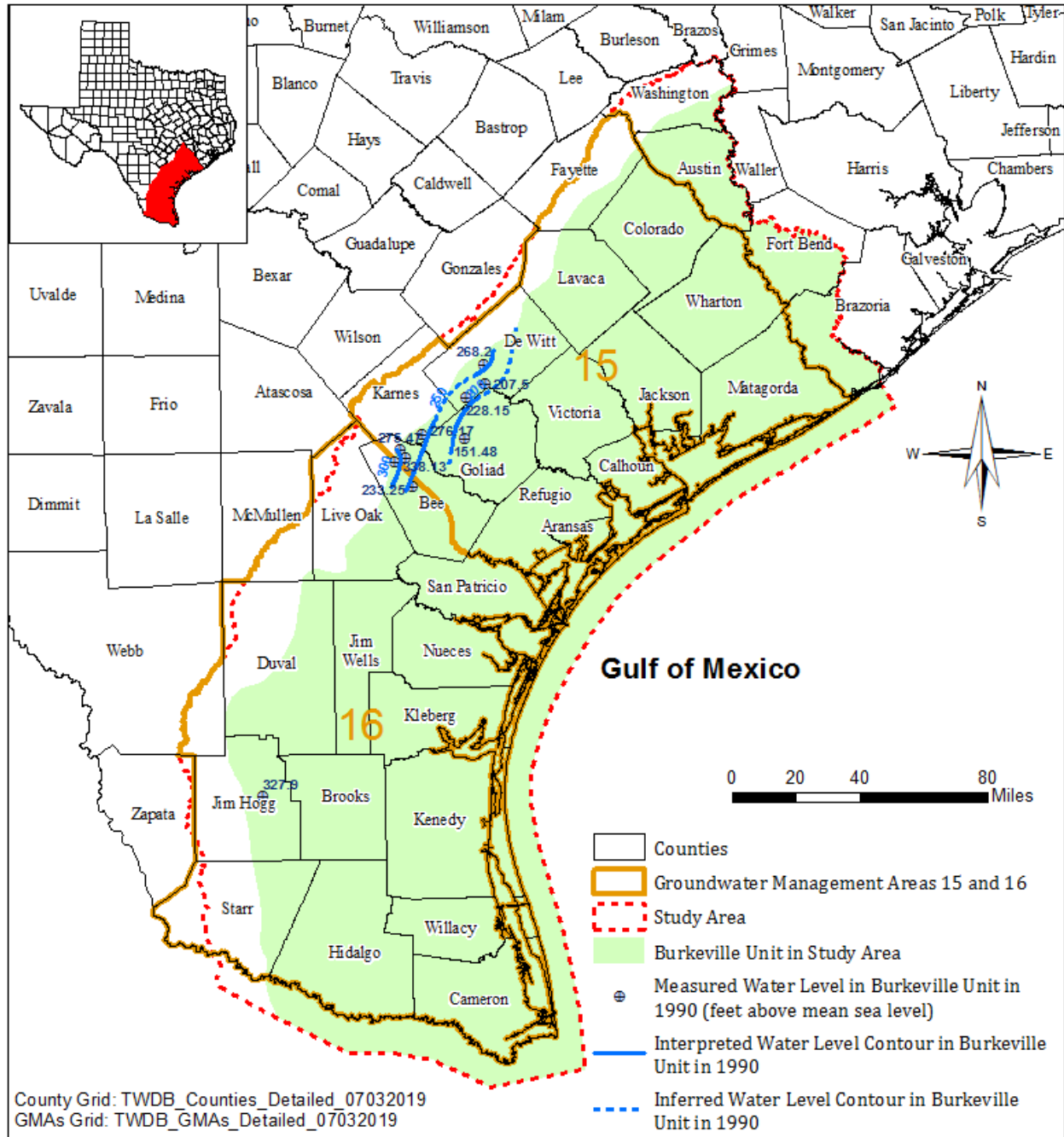


**Figure 4.2.13 Water levels in Burkeville Unit (1990).**

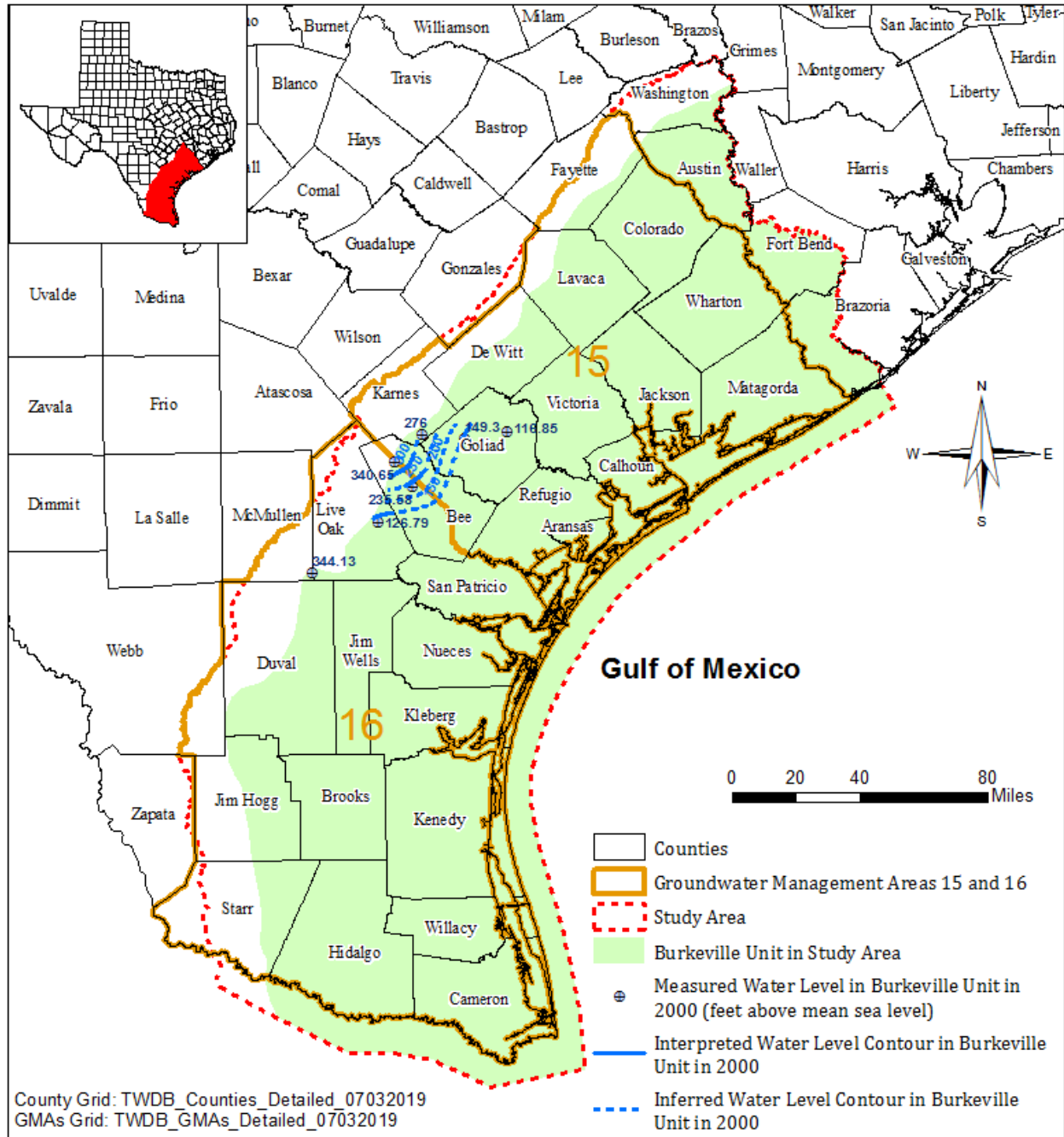
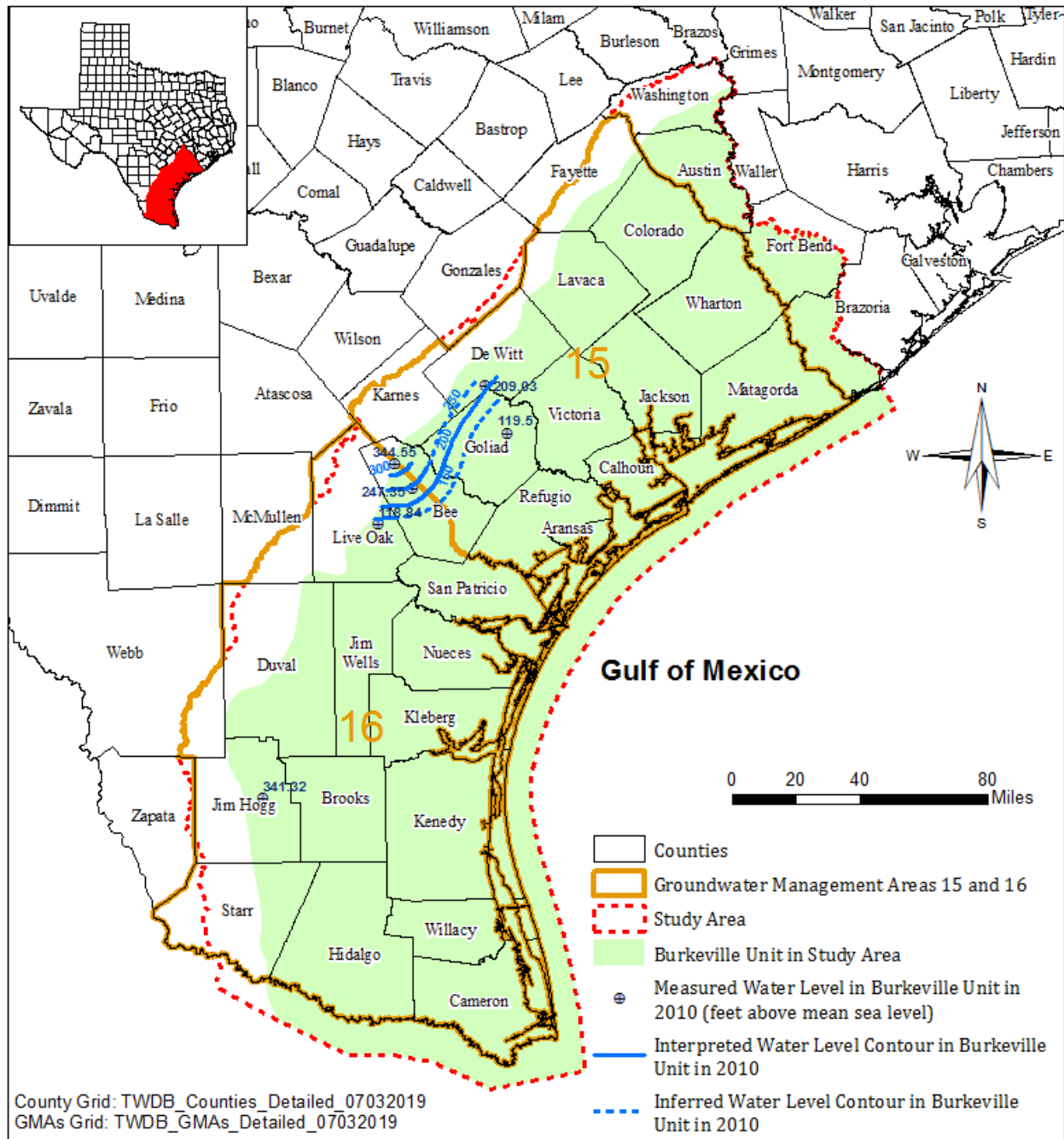
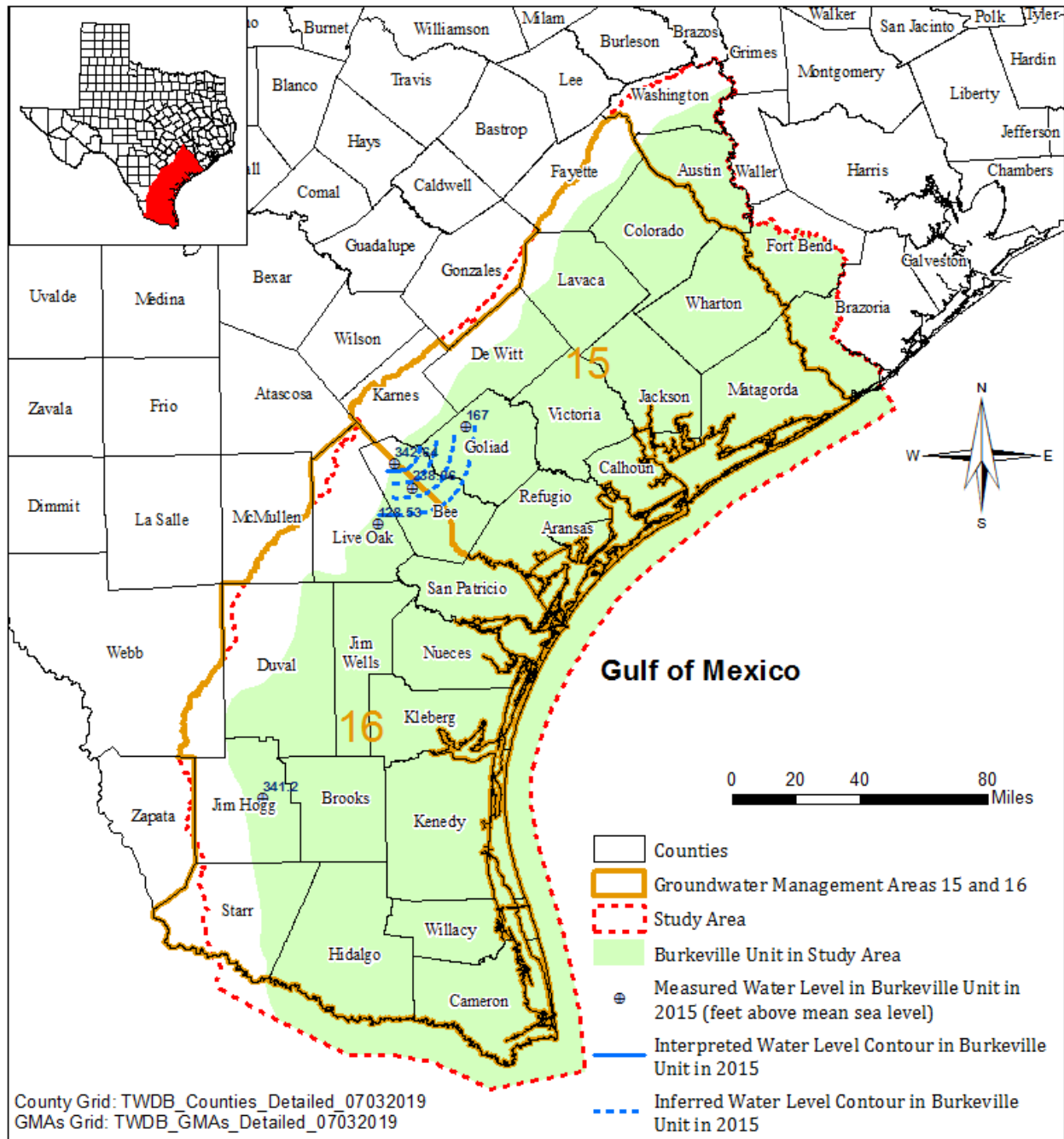


Figure 4.2.14 Water levels in Burkeville Unit (2000).



**Figure 4.2.15 Water levels in Burkeville Unit (2010).**



**Figure 4.2.16 Water levels in Burkeville Unit (2015).**

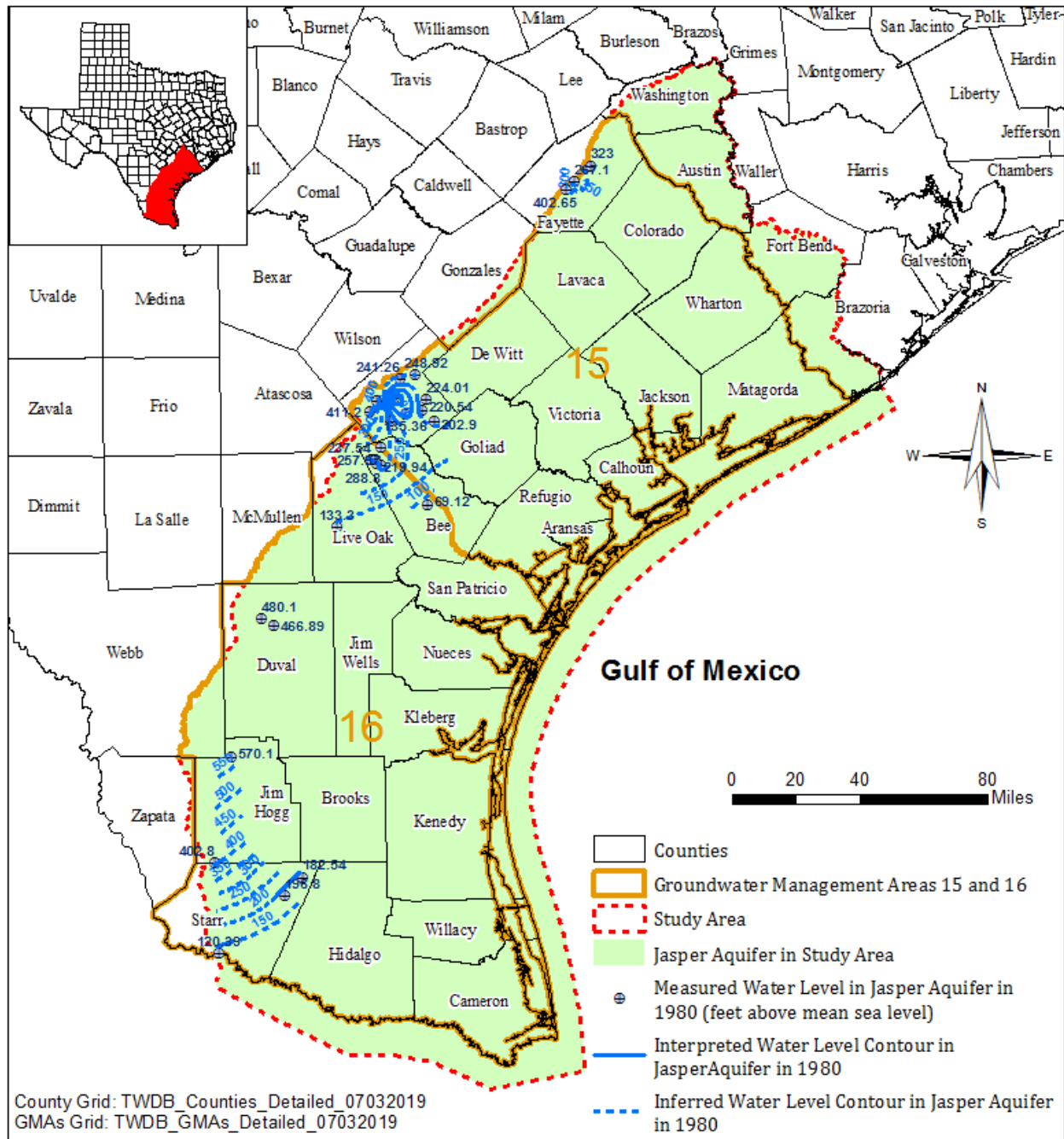
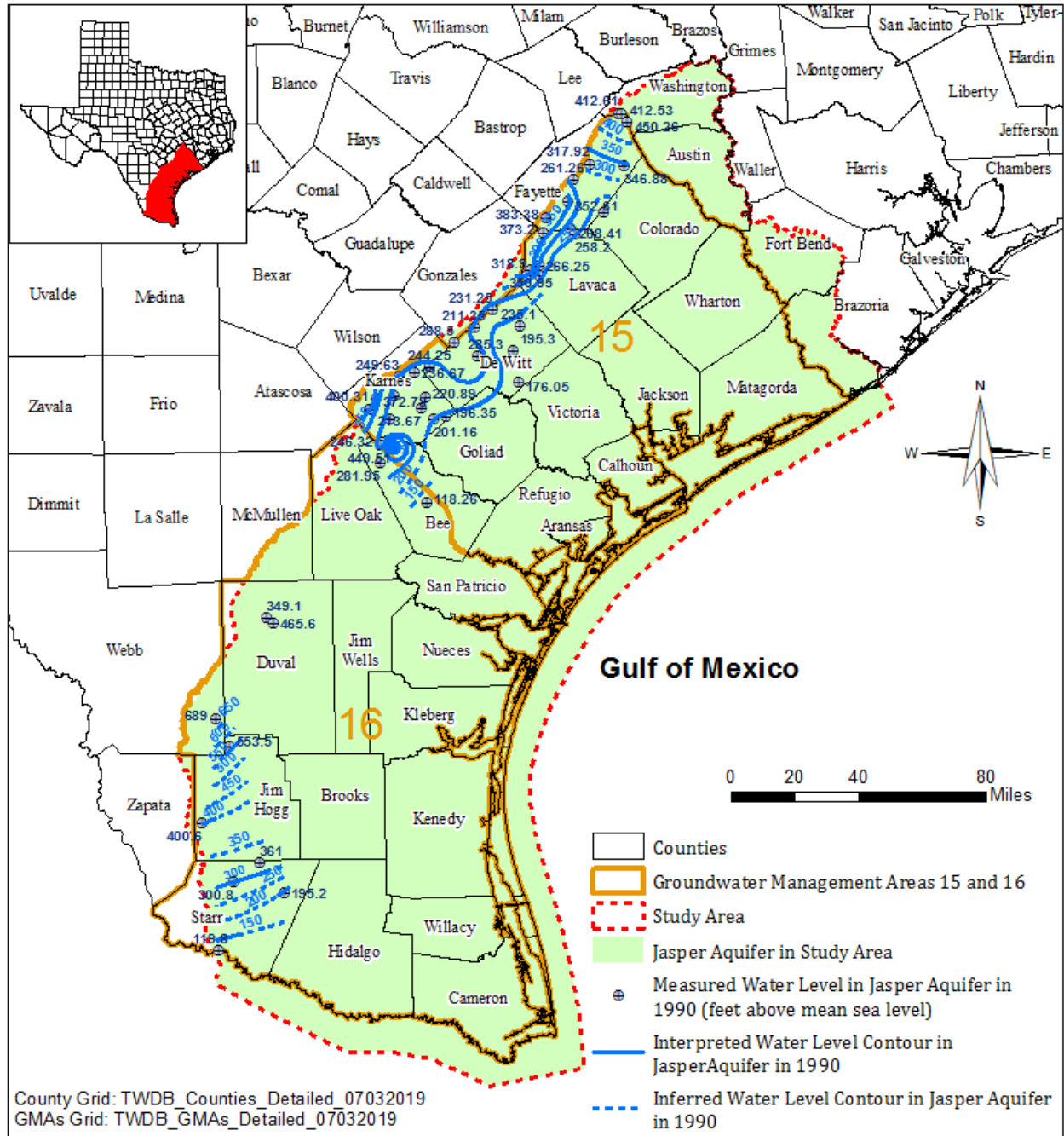


Figure 4.2.17 Water levels in Jasper Aquifer (1980).



**Figure 4.2.18 Water levels in Jasper Aquifer (1990).**



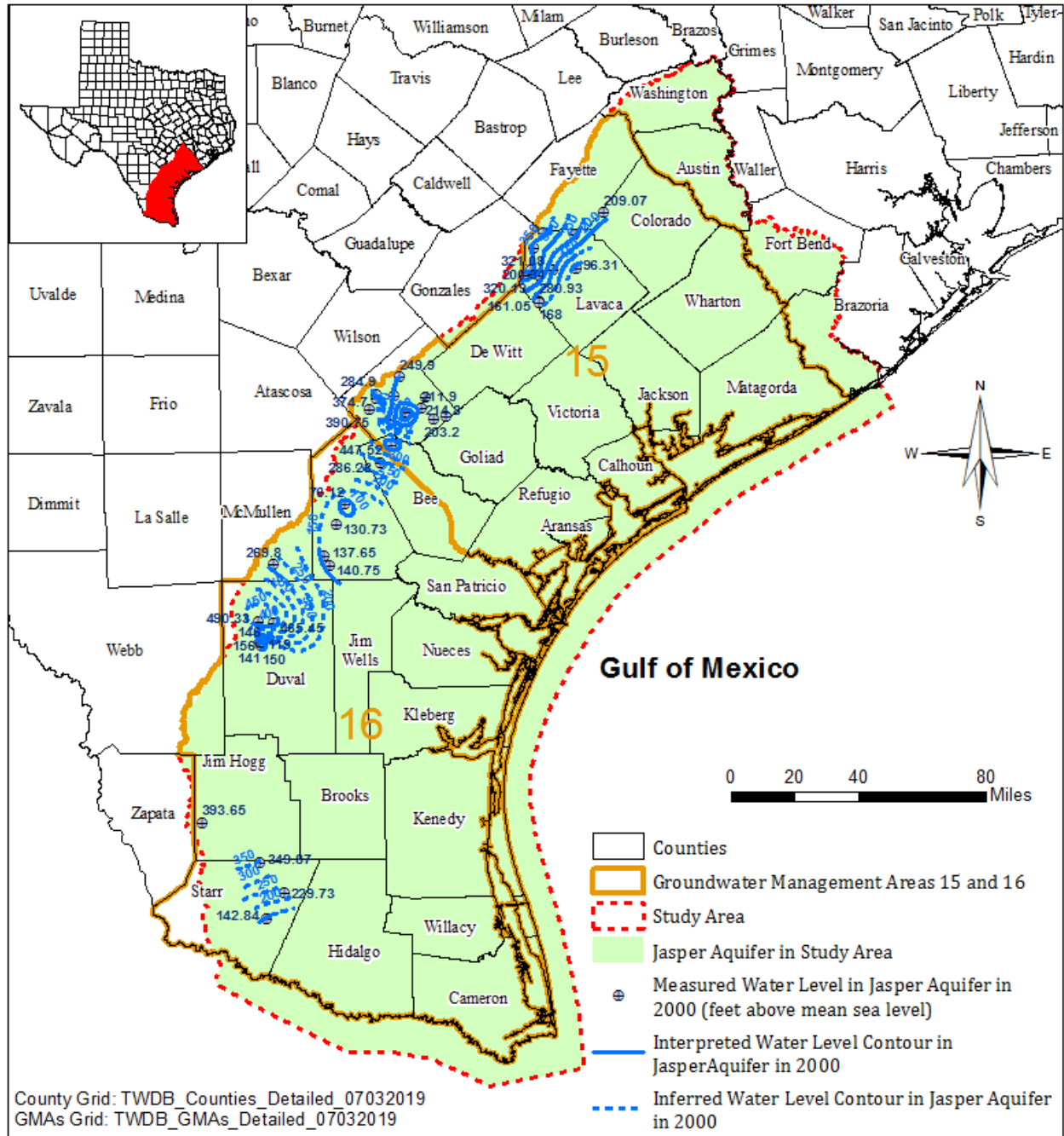
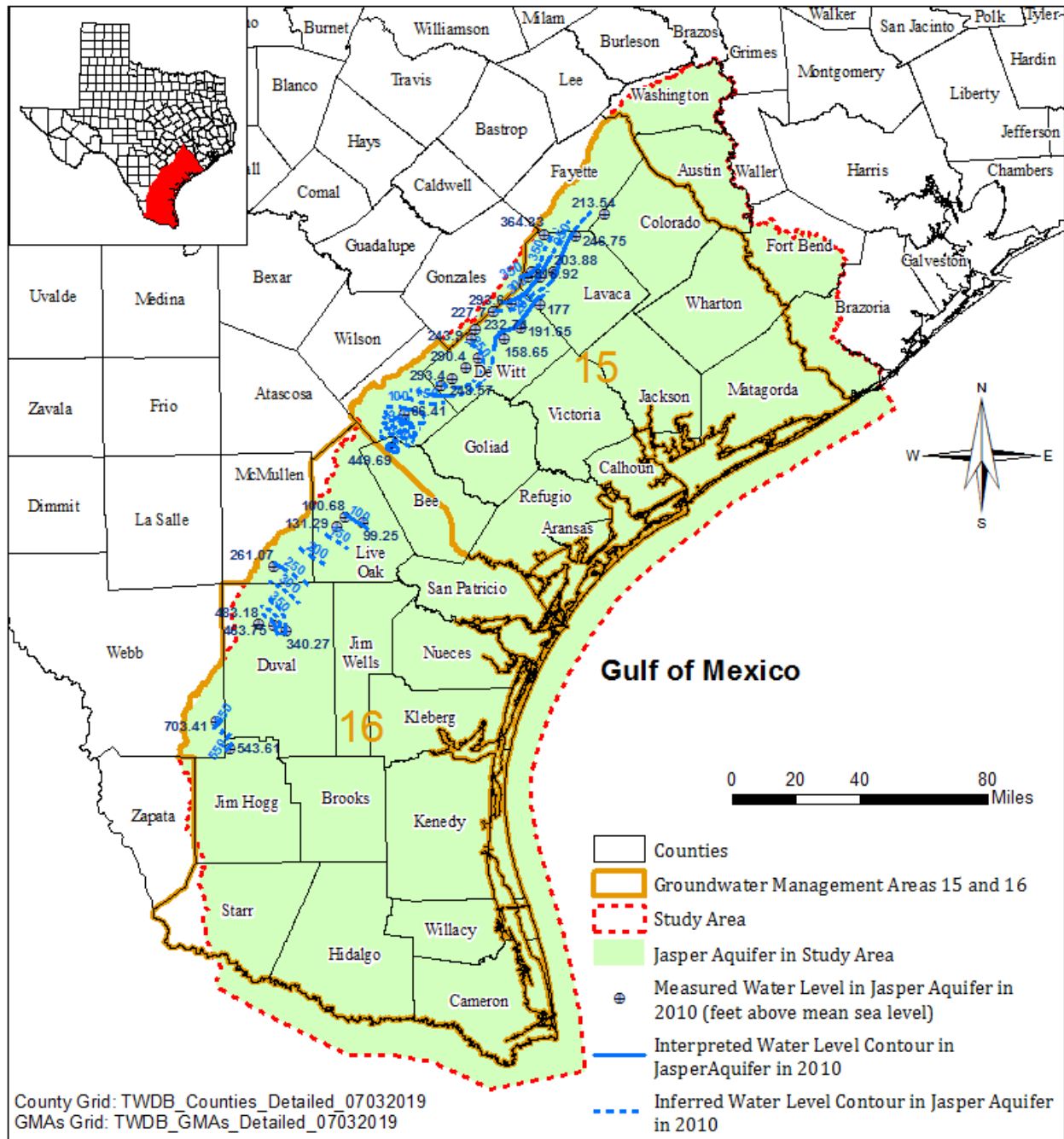


Figure 4.2.19 Water levels in Jasper Aquifer (2000).



**Figure 4.2.20 Water levels in Jasper Aquifer (2010).**

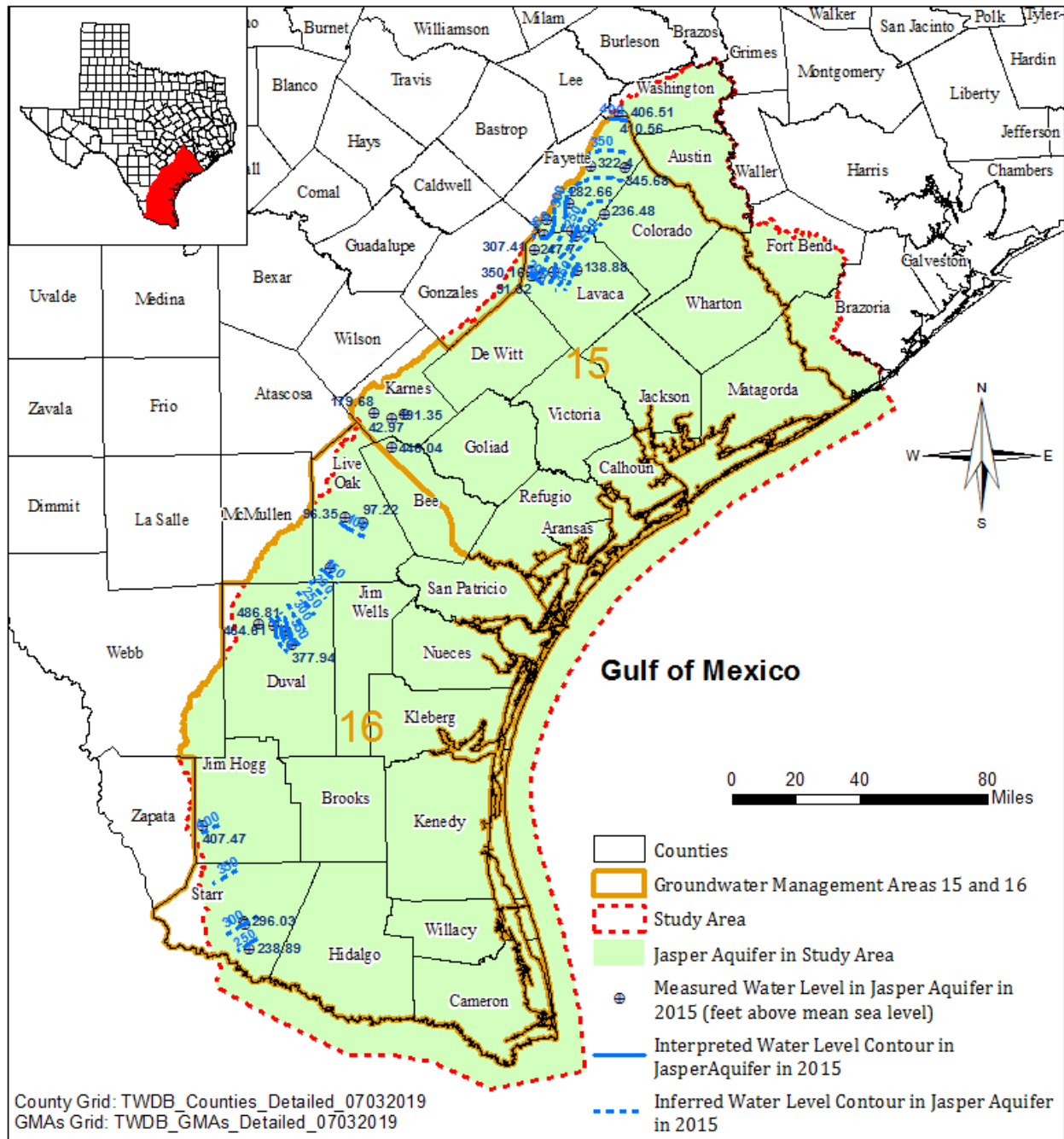
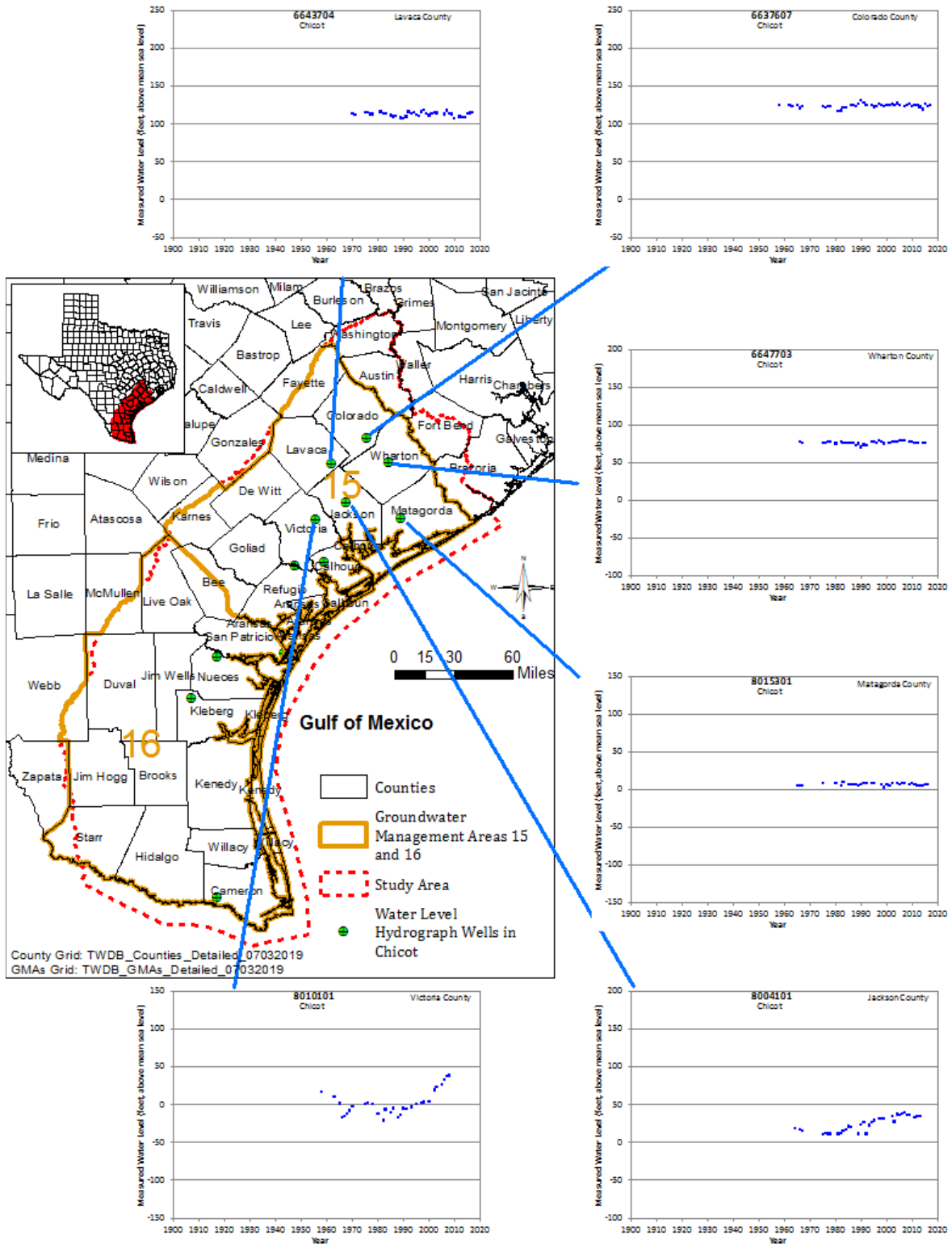
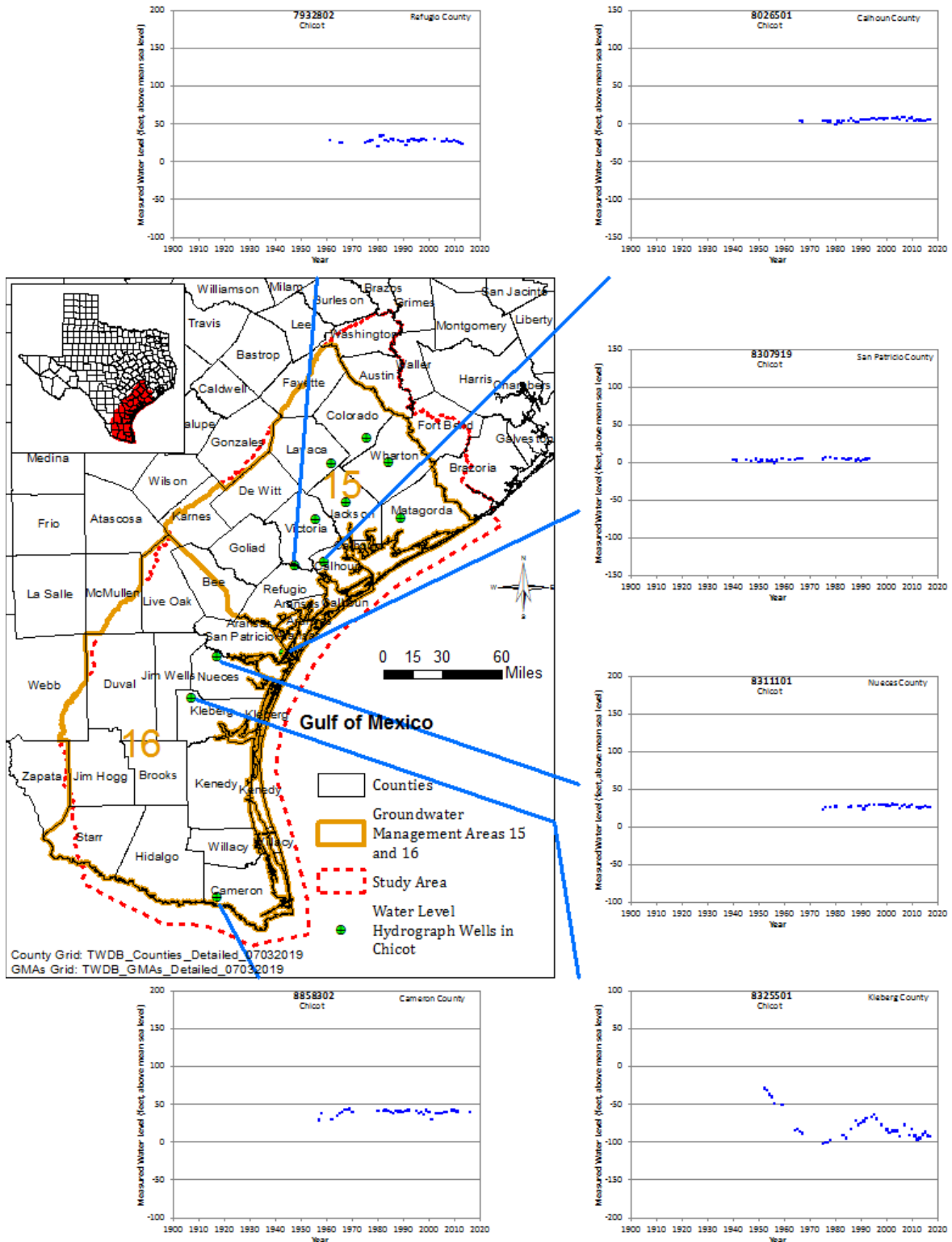


Figure 4.2.21 Water levels in Jasper Aquifer (2015).



**Figure 4.2.22** Water level hydrographs at selected wells in alluvium/eolian and Chicot Aquifer.



**Figure 4.2.23** Water level hydrographs at selected wells in alluvium/eolian and Chicot Aquifer.

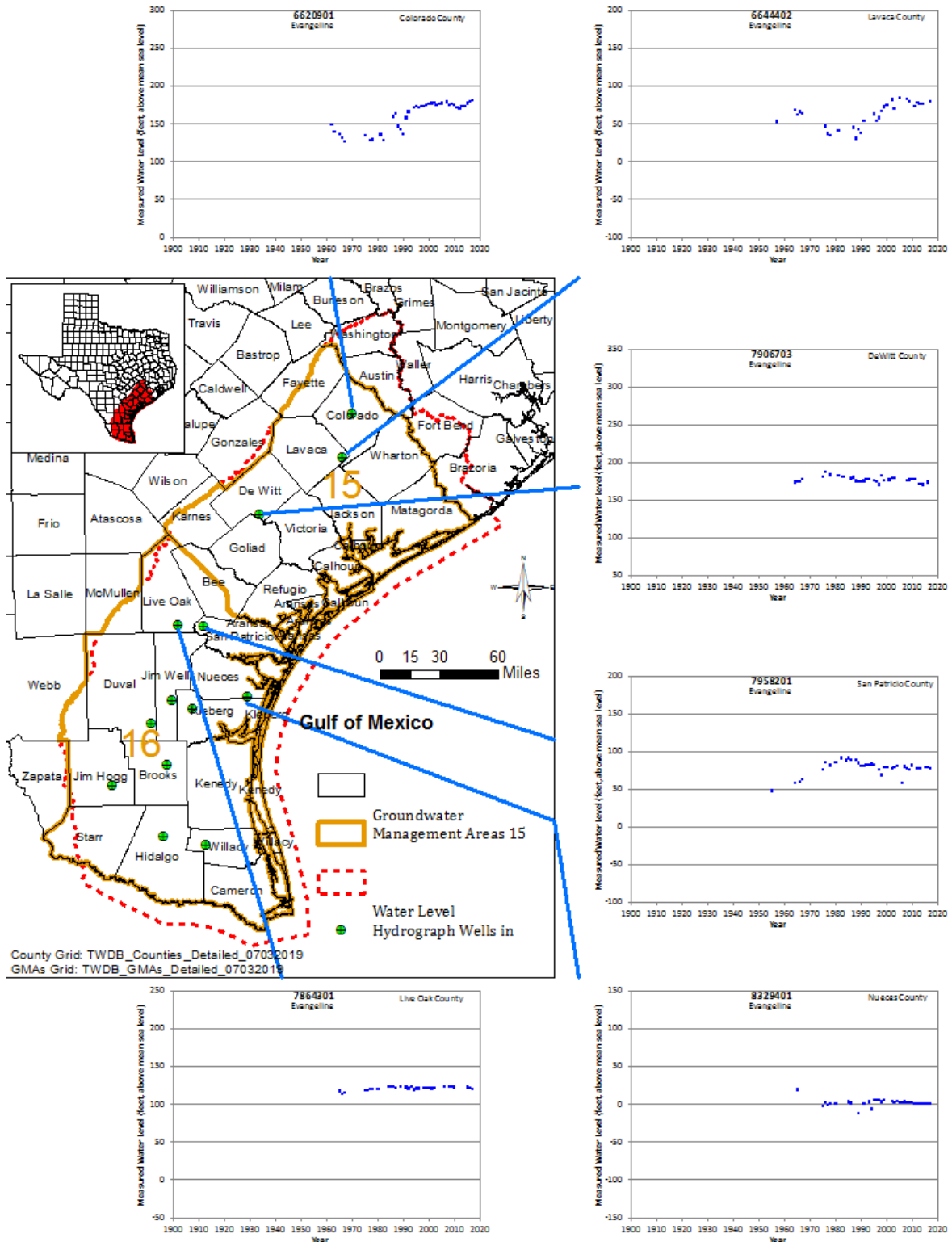


**Figure 4.2.24 Water level hydrographs at selected wells in Evangeline Aquifer.**

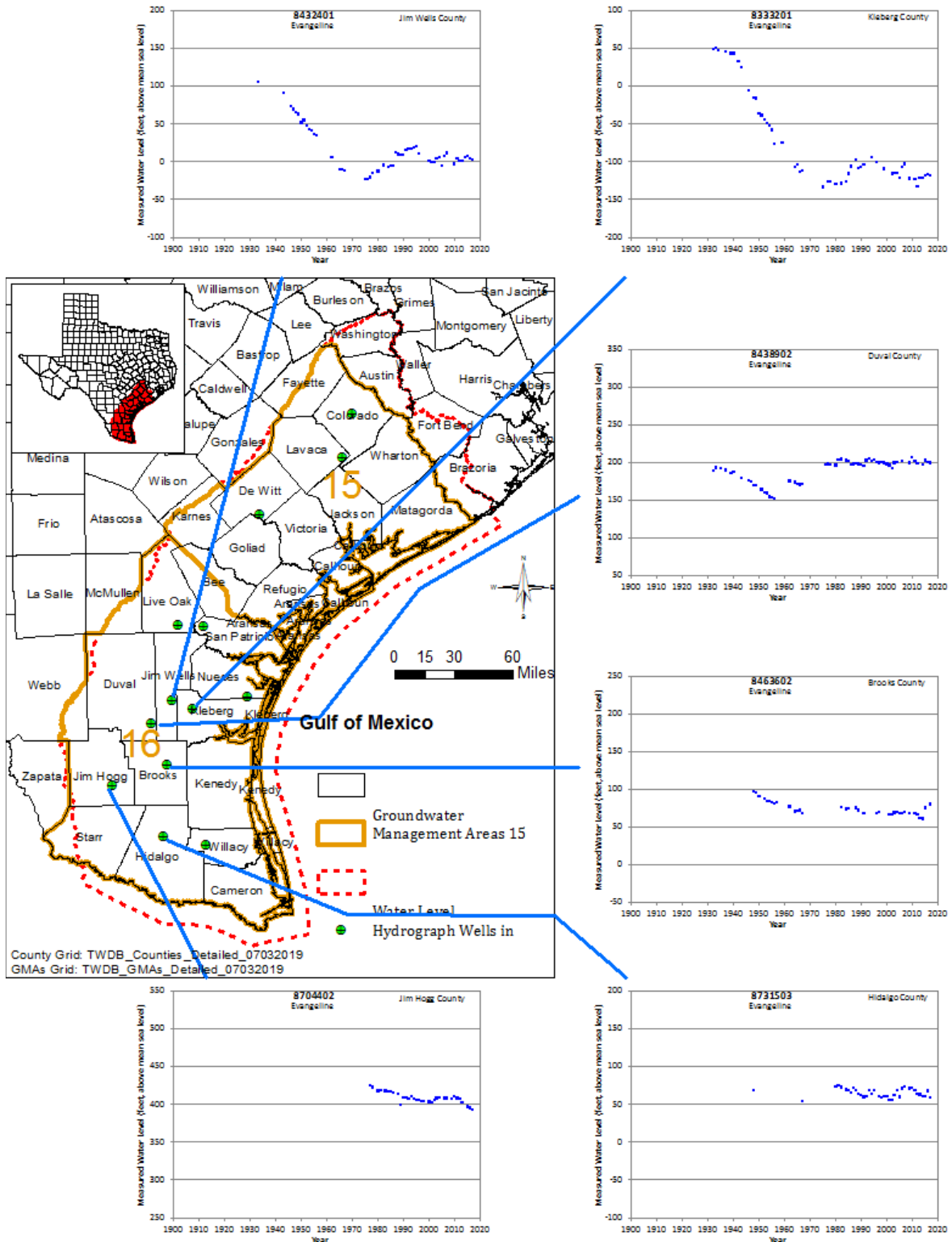


**Figure 4.2.25 Water level hydrographs at selected wells in Evangeline Aquifer.**

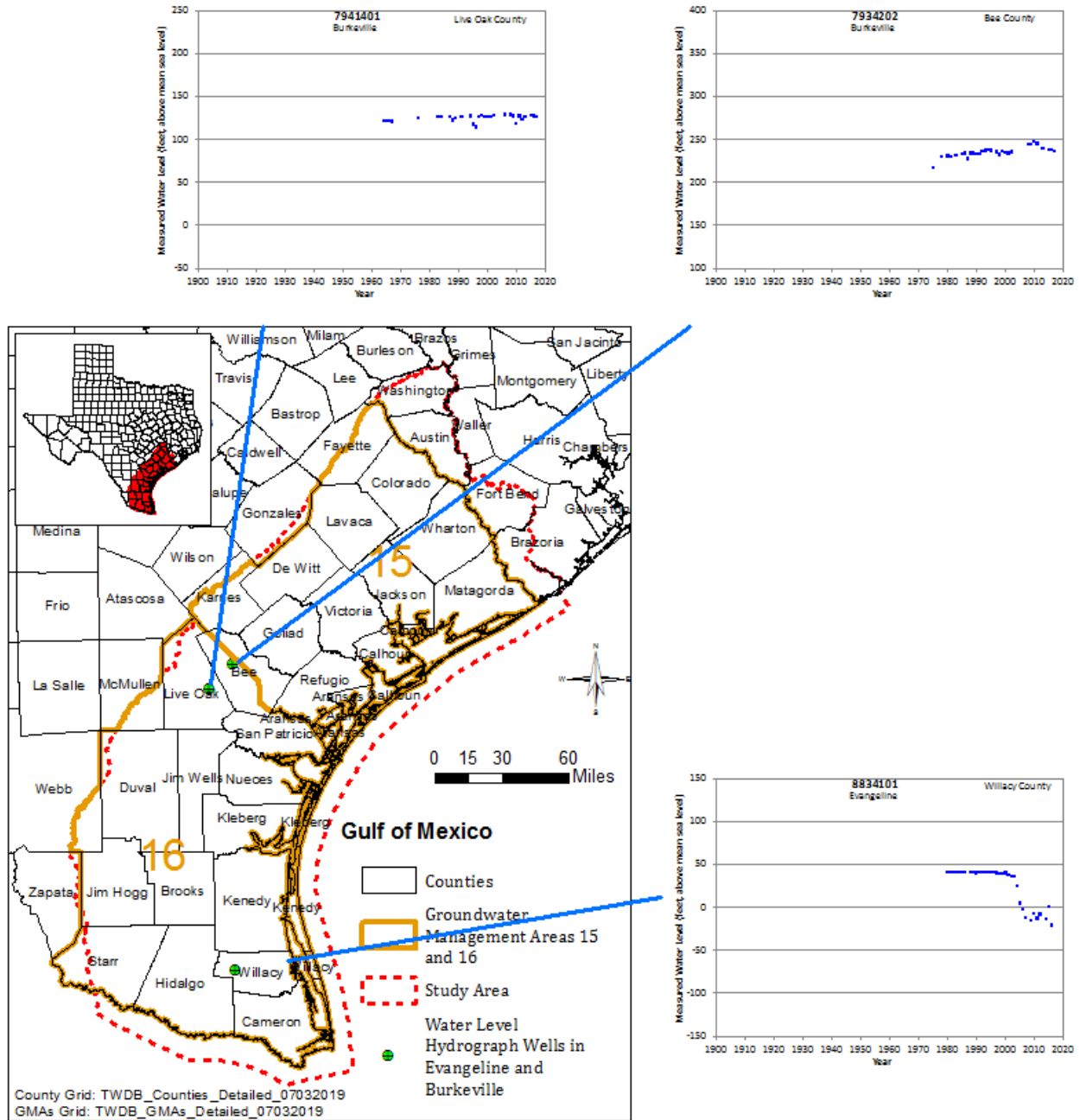


**Figure 4.2.26 Water level hydrographs at selected wells in Evangeline Aquifer and Burkeville Unit.**



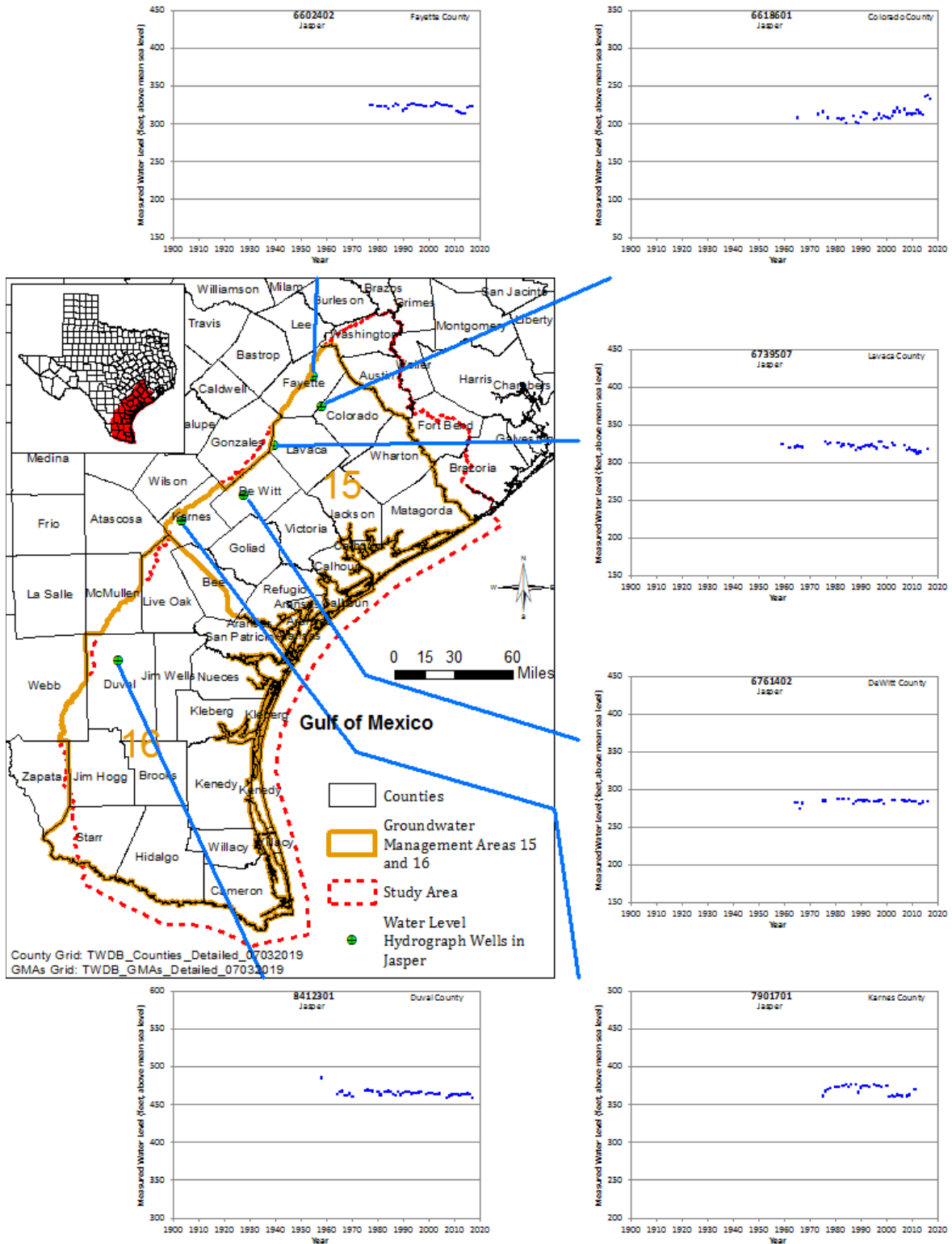


**Figure 4.2.27** Water level hydrographs at selected wells in Jasper Aquifer.

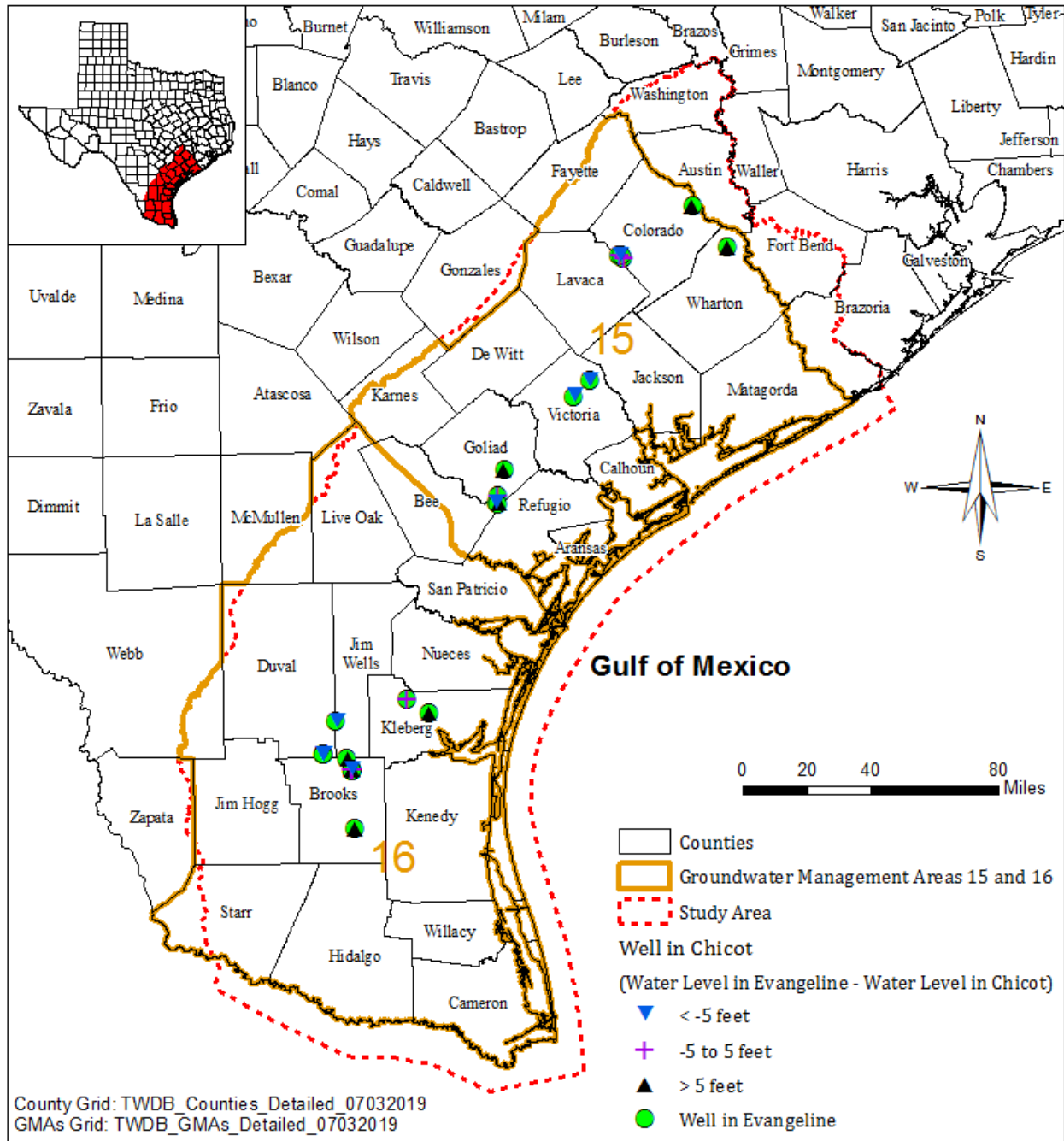


**Figure 4.2.28** Water level difference between two adjacent wells (less than 2,640 feet apart) screened in Chicot and Evangeline aquifers. Positive and negative values represent upward and downward groundwater flow, respectively.

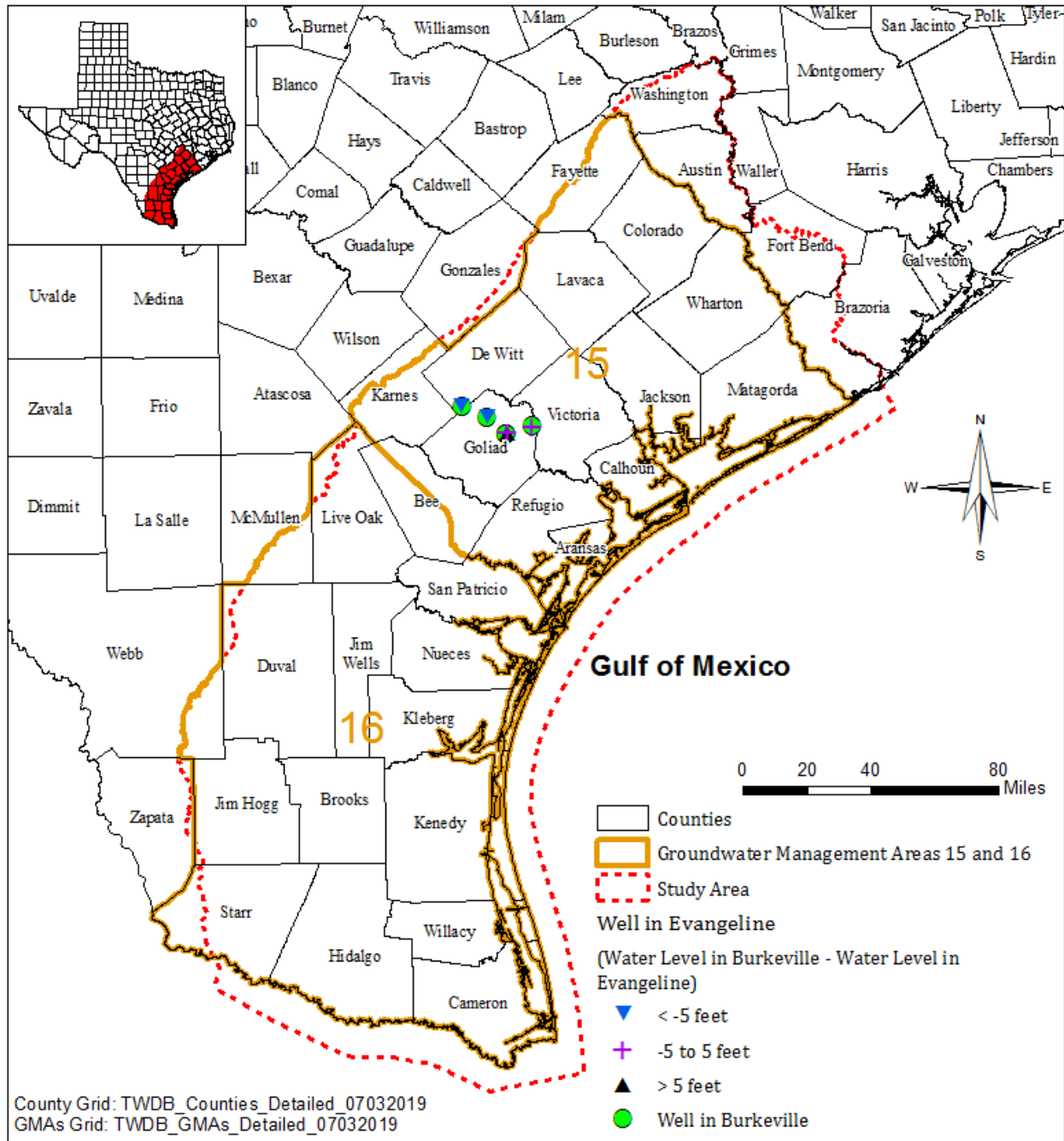


**Figure 4.2.29** Water level difference between two adjacent wells (less than 2,640 feet apart) screened in Evangeline Aquifer and Burkeville Unit. Positive and negative values represent upward and downward groundwater flow, respectively.

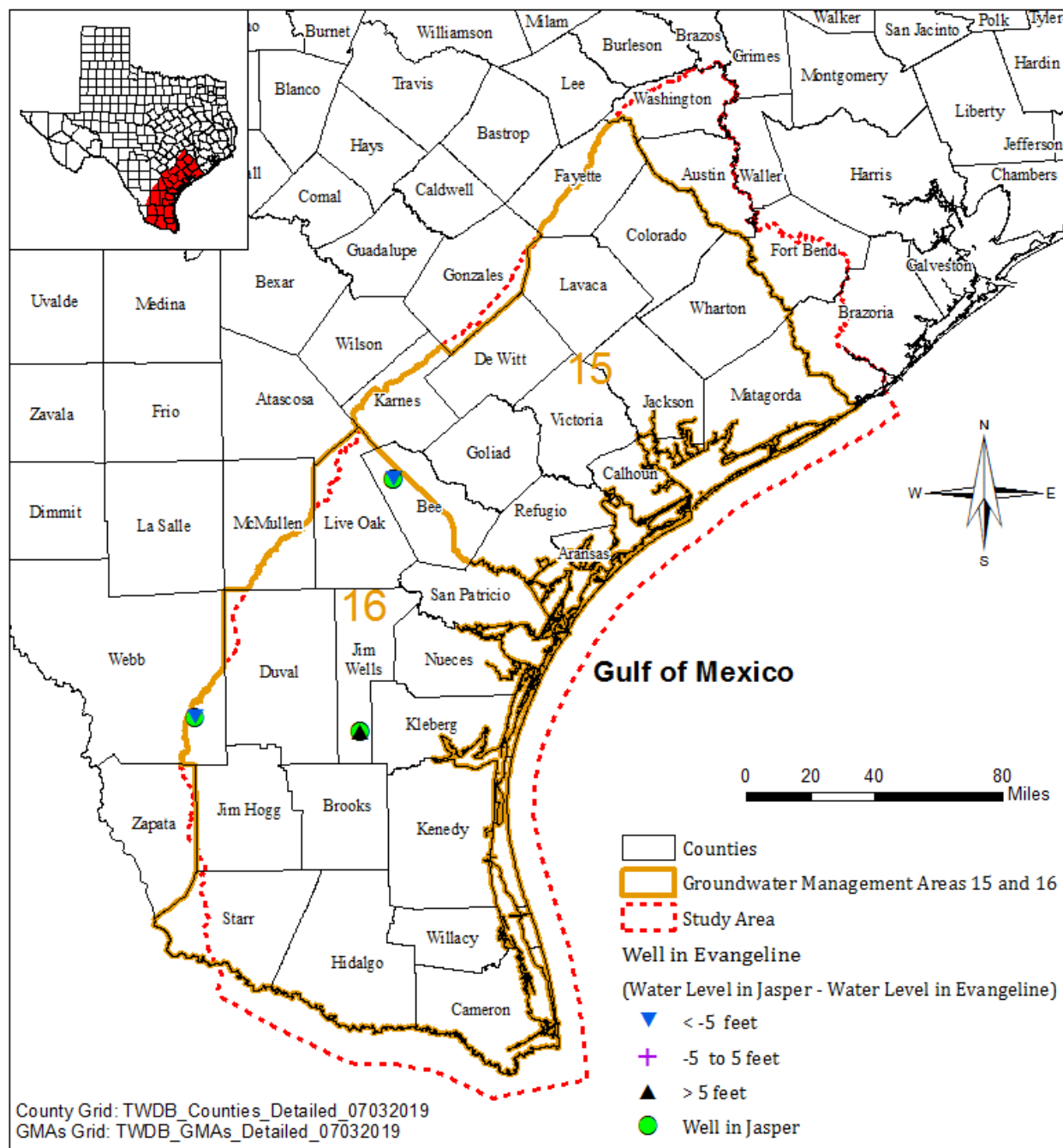


**Figure 4.2.30** Water level difference between two adjacent wells (less than 2,640 feet apart) screened in Evangeline and Jasper aquifers. Positive and negative values represent upward and downward groundwater flow, respectively.

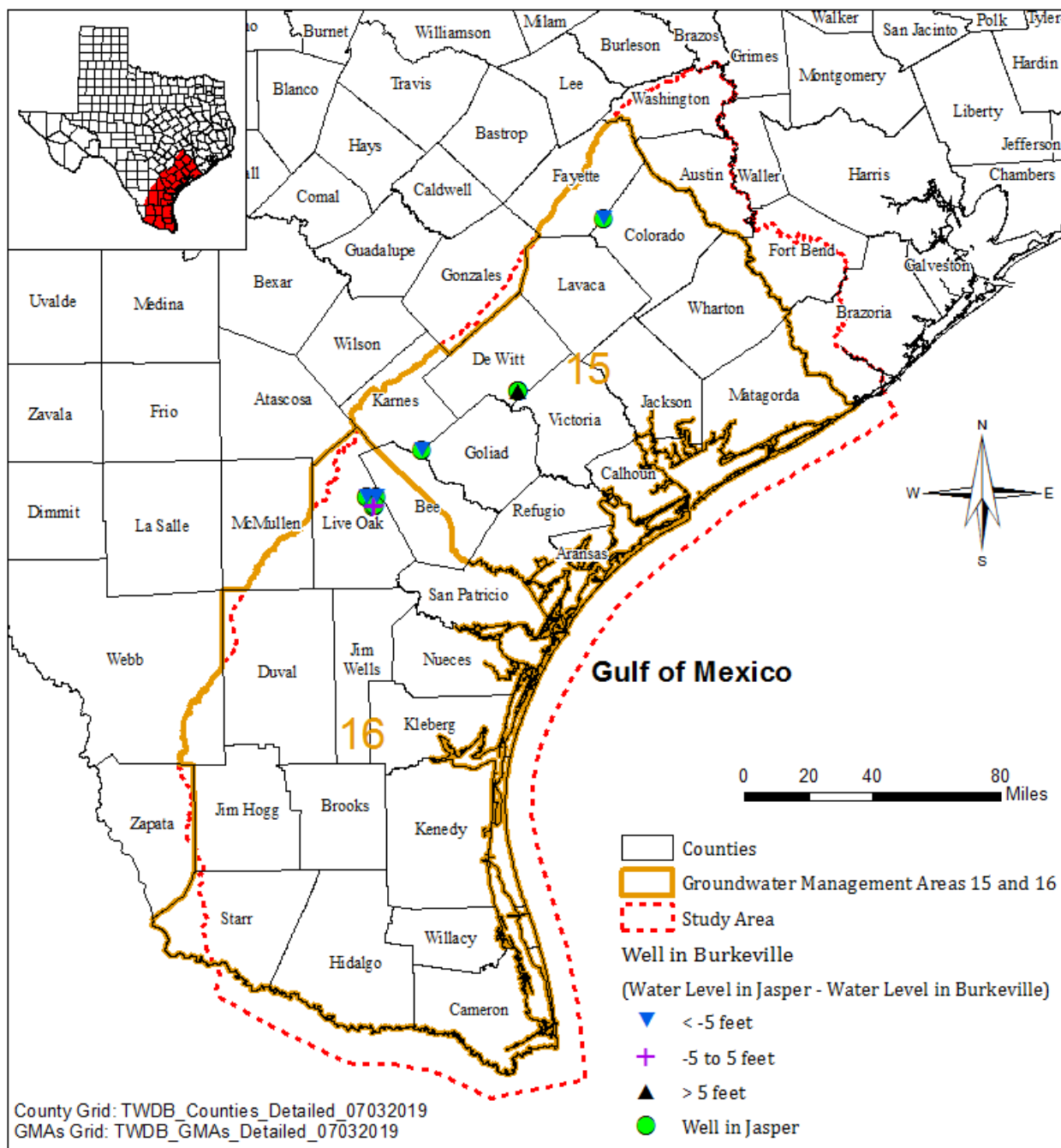


**Figure 4.2.31** Water level difference between two adjacent wells (less than 2,640 feet apart) screened in Burkeville Unit and Jasper Aquifer. Positive and negative values represent upward and downward groundwater flow, respectively.

### 4.3. Groundwater Recharge

Total groundwater recharge is the water that reaches the aquifer by means of precipitation, return flow from irrigation, leakage of surface water, and cross-formational flow from other aquifers. Recharge is rarely measured directly, but groundwater recharge from precipitation can be estimated by several methods. For example, Scanlon and others (2012) used chloride mass balance to estimate the groundwater recharge in the Gulf Coast Aquifer System in Texas. Their study indicated that the recharge ranged from 0.022 inches per year to the south to 3.12 inches per year to the north in this study area (Figure 4.3.1).

Another approach to estimate the groundwater recharge is based on stream baseflow. Stream baseflow is the groundwater discharge to a stream. This section discusses how to estimate groundwater recharge based on stream baseflow and how to correlate groundwater recharge to precipitation.

#### 4.3.1 Estimate of Groundwater Recharge from Stream Baseflow

Once water enters an aquifer as recharge, there are many ways in which it might exit the aquifer as outflow. Water can flow out of an aquifer through evapotranspiration, pumping, flowing into deeper or adjacent aquifers (cross-formational flow), or into surface water as stream baseflow. Based on mass conservation, the total groundwater recharge ( $R$ ) in a river basin can be expressed by the following equation:

$$R = F_b + P + EVT + E + S$$

Where:

$F_b$  = baseflow

$P$  = pumping

$EVT$  = evapotranspiration

$E$  = exchange with other units

$S$  = aquifer storage change

As a result, the groundwater recharge estimated from stream baseflow is often less than the total groundwater recharge.

Other than stream baseflow, surface runoff, permitted discharge, and release from reservoirs also contribute to stream flow. Because it is almost impossible to separate baseflow from the latter two, river basins with significant permitted discharge and reservoir release should not be used for baseflow separation from stream flow. In addition, stream flow data should cover long enough time to minimize the impacts of short-term extremes. As a result, the following criteria were used to select river basins and associated flow gages for baseflow separation:

- Streams in each basin must gain groundwater;
- Each gage must contain flux measurements covering most of the years between 1980 and 2015;
- Each basin must not contain releases from reservoir(s); and
- Permitted discharge contributing more than 30 percent of the total stream flow to each basin must be no more than two years.

The river basin boundary for this study was based on the U. S. Geological Survey's Watershed Boundary Dataset (Version 2.1) HUC\_10 attribute. A more recent version can be downloaded from [https://www.usgs.gov/core-science-systems/ngp/national-hydrography/watershed-boundary-dataset?qt-science\\_support\\_page\\_related\\_con=4#qt-science\\_support\\_page\\_related\\_con](https://www.usgs.gov/core-science-systems/ngp/national-hydrography/watershed-boundary-dataset?qt-science_support_page_related_con=4#qt-science_support_page_related_con). Historical stream flow data at gages were downloaded from the U. S. Geological Survey ([https://waterdata.usgs.gov/nwis/uv/?referred\\_module=sw](https://waterdata.usgs.gov/nwis/uv/?referred_module=sw)). The permitted discharge information was downloaded from the U. S. Environmental Protection Agency (EPA) Enforcement and Compliance database (<https://echo.epa.gov/facilities/facility-search>), which covers years from 2004 onward.

A total 14 basins/gages passed the selection criterion and are shown in [Figure 4.3.2](#). A computer code developed by Arnold and others (1995) was modified to calculate the daily baseflow from the daily stream flow data at gages. This computer code produced three declining daily baseflow values under three passes. Because baseflow often underestimates the groundwater recharge, the baseflow value under the first pass was used to calculate groundwater recharge for this study. The daily groundwater recharge ( $R_d$ ) was calculated using the following equation:

$$R_d = \frac{B_d}{A_b}$$

Where:

$B_d$  = daily baseflow

$A_b$  = basin area

Because daily stream flow data may be missing for certain days, annual groundwater recharge ( $R_b$ ) is calculated using the following equation:

$$R_b = \frac{AB_d * D_y}{A_b}$$

Where:

$AB_d$  = average daily baseflow in a year

$D_y$  = days in a year

$A_b$  = basin area

The annual groundwater recharge values from 1980 through 2015 were then used to calculate the overall average groundwater recharge for each of the selected river basins.



### **4.3.2 Correlation between Groundwater Recharge and Precipitation**

The annual precipitation (1980) and monthly precipitation (1981 through 2015) raster data were downloaded from the PRISM Climate Group (<http://www.prism.oregonstate.edu/>). The monthly precipitation data were then summed up to calculate the annual data for 1981 through 2015. The overall average precipitation for each of the selected river basins was then calculated from the annual raster images. This overall average precipitation was used to correlate to the overall average groundwater recharge as discussed above (Figure 4.3.3).

Studies have shown that precipitation recharges groundwater when infiltration rate is greater than soil residual porosity. As a result, low rainfall events may not contribute groundwater recharge at all. In this study, it was assumed that groundwater recharge would be zero when annual total rainfall is ten inches or less. Groundwater recharge generally increases with increasing precipitation. However, this increasing trend will slow down once the soil moisture approaches its capacity. In this study, a revised logistics growth model was used to correlate the groundwater recharge to the precipitation. The model is represented by the following equation (Figure 4.3.3):

$$R_c = 6.4976139 / (1 + 4270.1954e^{-0.20319653*P}) + 0.0115878$$

Where:

$R_c$  = recharge

$P$  = precipitation

How well the model fits the recharge/precipitation data can be quantified by the coefficient of determination,  $R^2$ . The  $R^2$  value for this study was 0.86 which indicates a very good correlation between the overall average groundwater recharge and the overall average precipitation for the selected river basins/gages. Using this equation, annual precipitation raster data from PRISM can be converted to groundwater recharge for the study area, and the result is discussed in next section.

### **4.3.3 Recharge Distribution**

Figures 4.3.4 through 4.3.8 show the estimated groundwater recharge from the stream baseflow-precipitation correlation for the selected years: 1980, 1990, 2000, 2010, 2015. The groundwater recharge rates for the other years between 1981 and 2014 are presented in Appendix C. As shown in the figures, the maximum recharge ranges from 0.41 inches per year in 2011 to 6.51 inches per year in 2002 with a decreasing trend from north to south, a reflection of decreasing precipitation. The lowest groundwater recharge could totally diminish at certain areas in relative dry years. It is worthy to point out that, along the Lower San Antonio Watershed in Karnes, Goliad, Refugio, and Victoria counties, the calculated groundwater recharge rates are consistent with the simulated results of Lizárraga and Ockerman (2010).

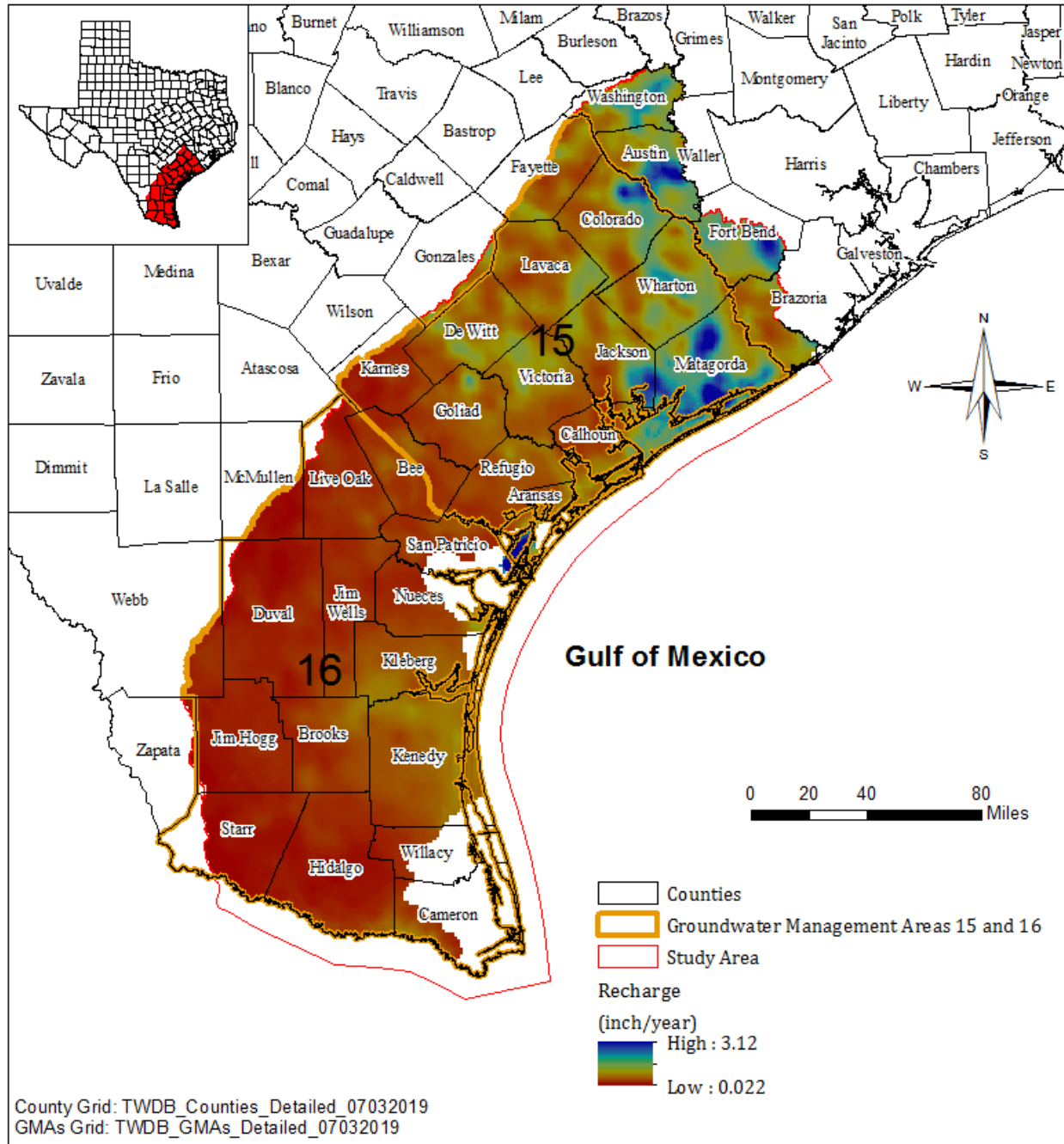


**Figure 4.3.1 Estimated groundwater recharge for Gulf Coast Aquifer System (Scanlon and others, 2012).**

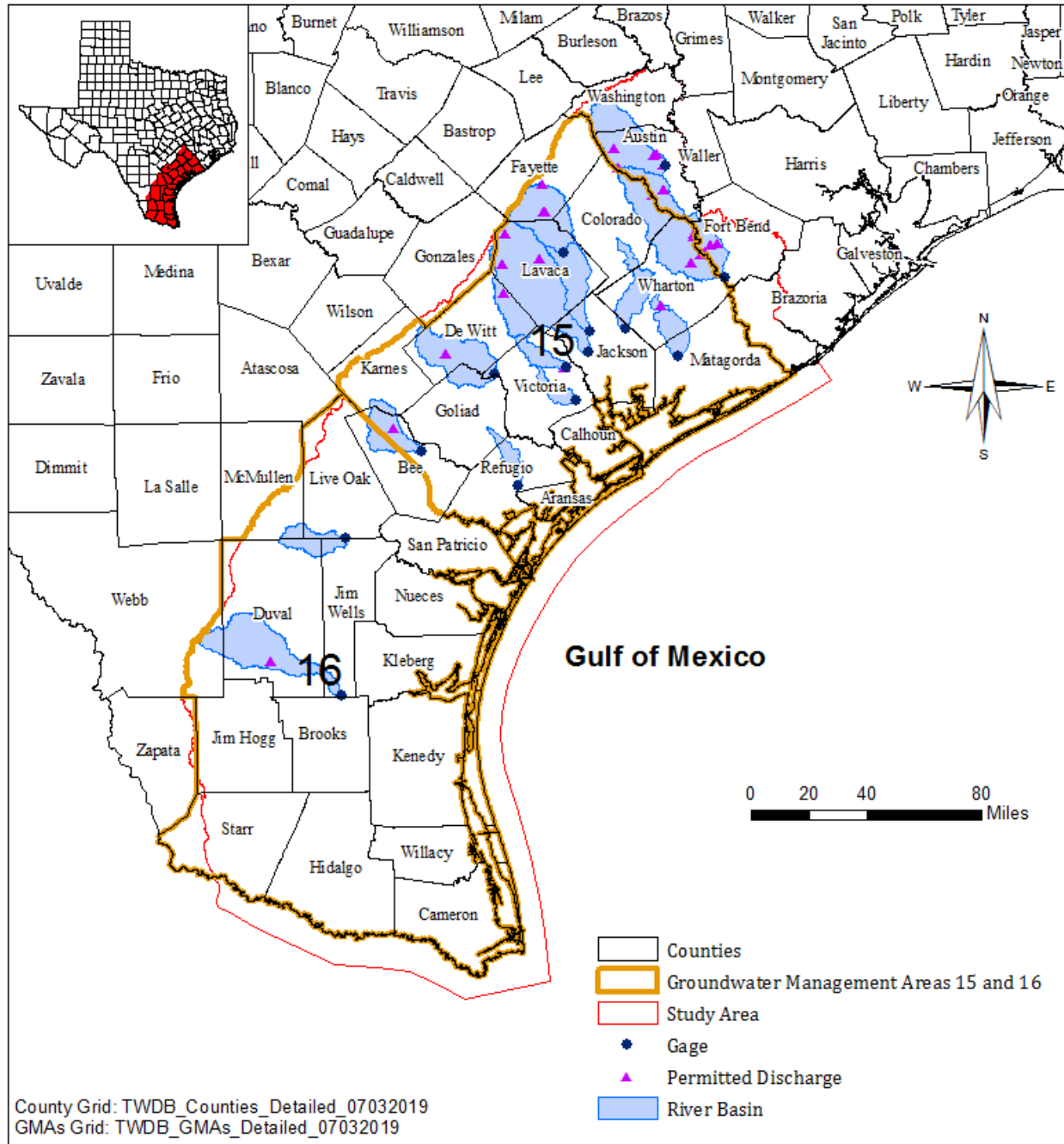


**Figure 4.3.2 Selected river basins, river gages, and permitted historical discharge locations.**

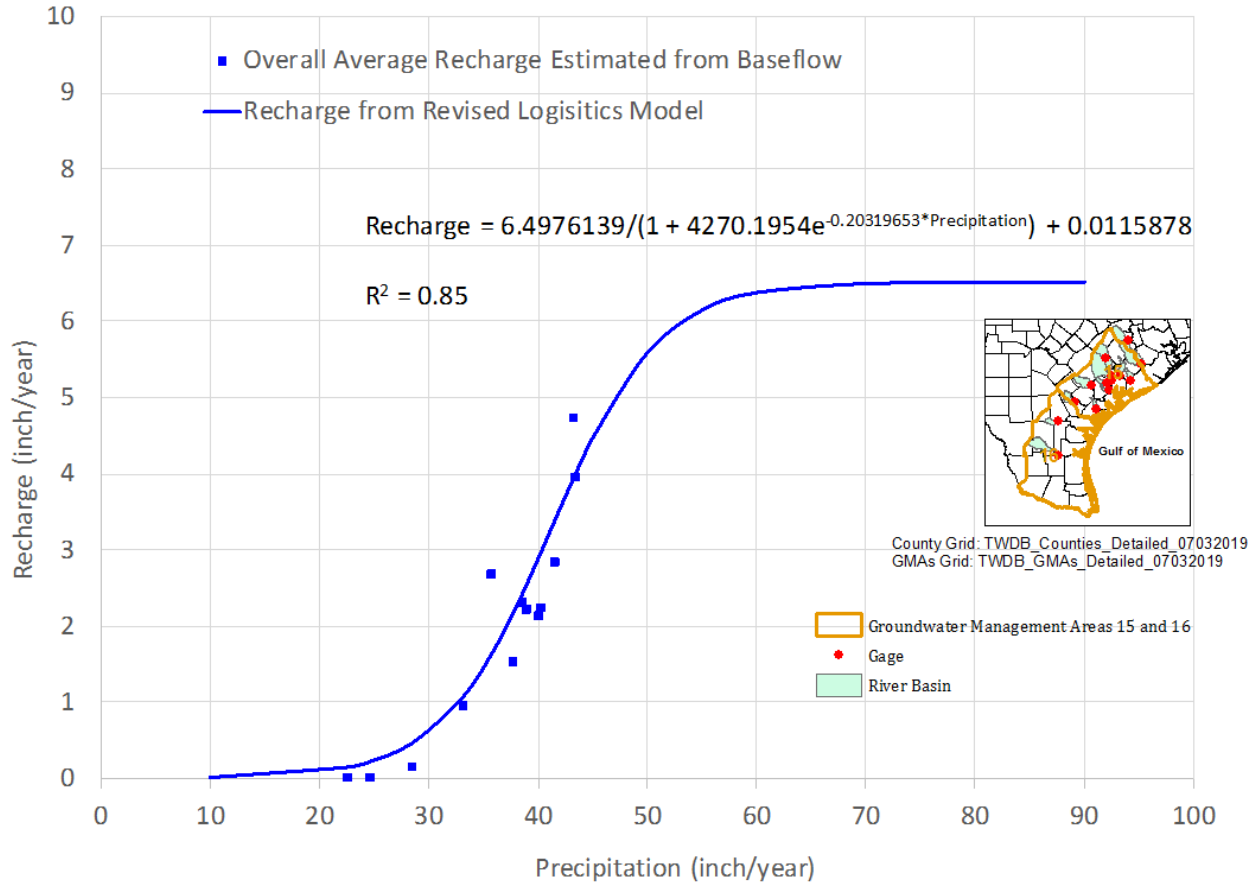


**Figure 4.3.3** Observed correlation between overall average groundwater recharge and overall average precipitation at selected river basins (shown in dots) and simulated regression using a logistics growth model (shown as solid line).

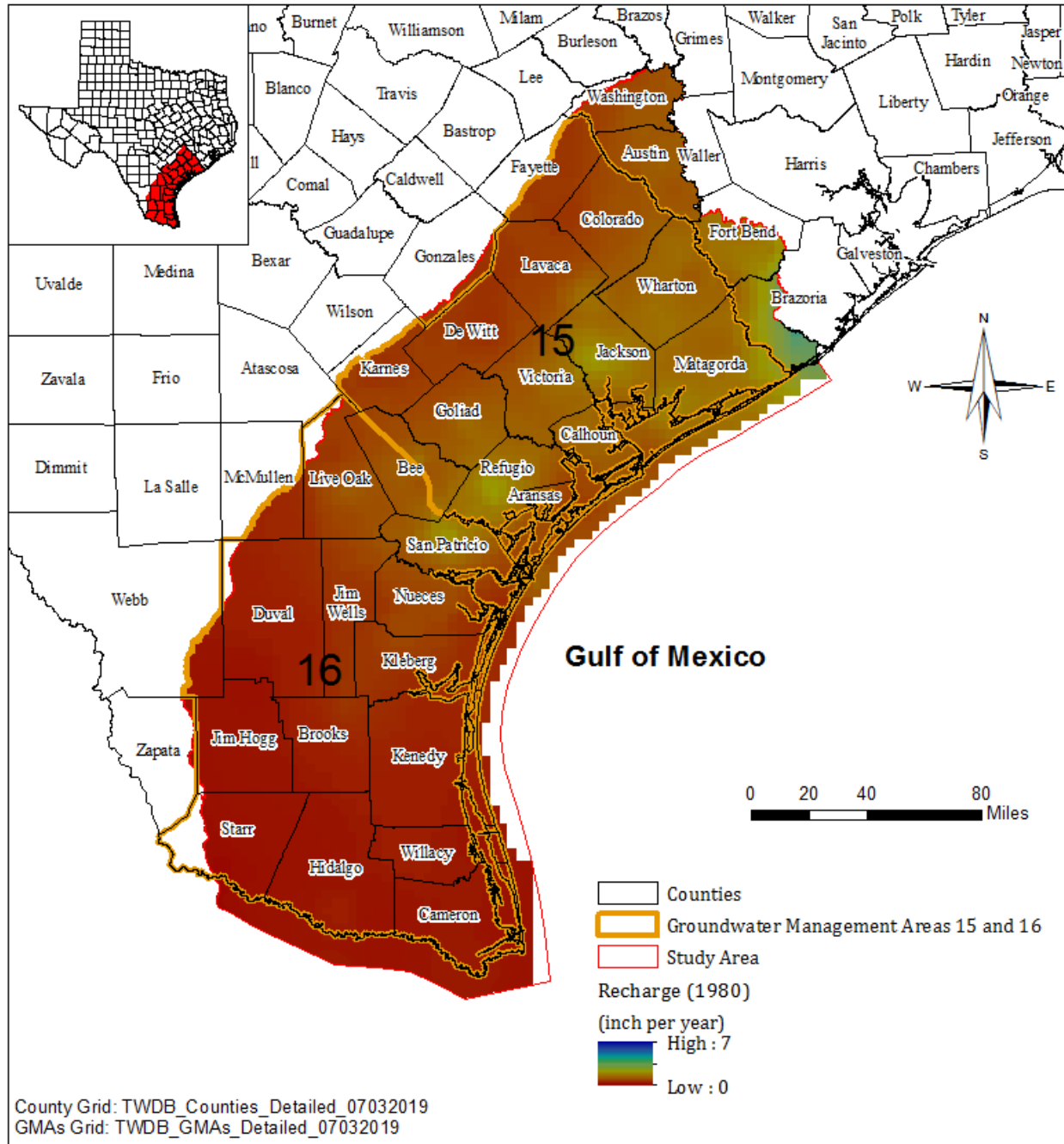


**Figure 4.3.4 Groundwater recharge estimated from stream baseflow-precipitation correlation (1980).**

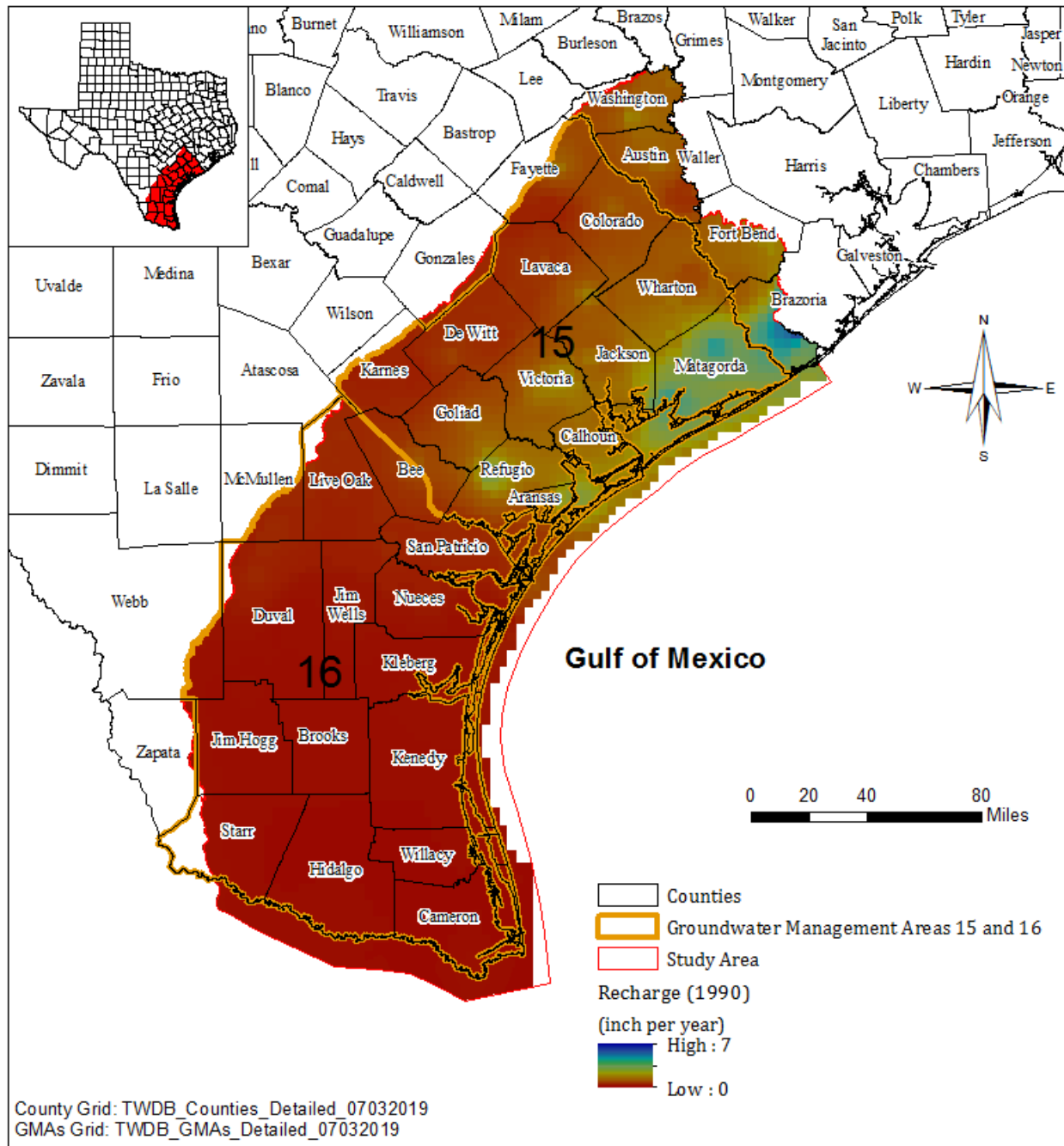


**Figure 4.3.5 Groundwater recharge estimated from stream baseflow-precipitation correlation (1990).**

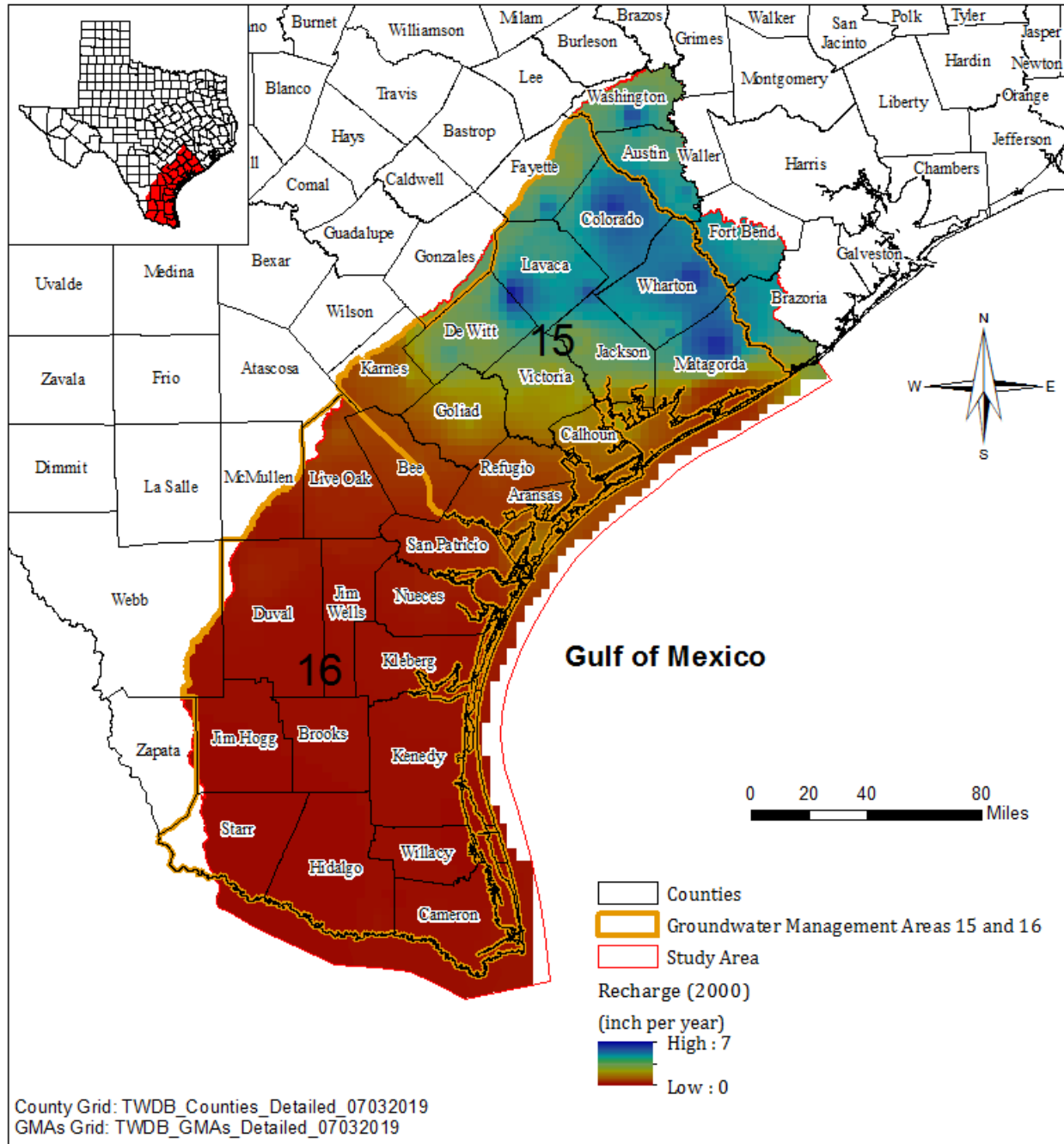


**Figure 4.3.6** Groundwater recharge estimated from stream baseflow-precipitation correlation (2000).



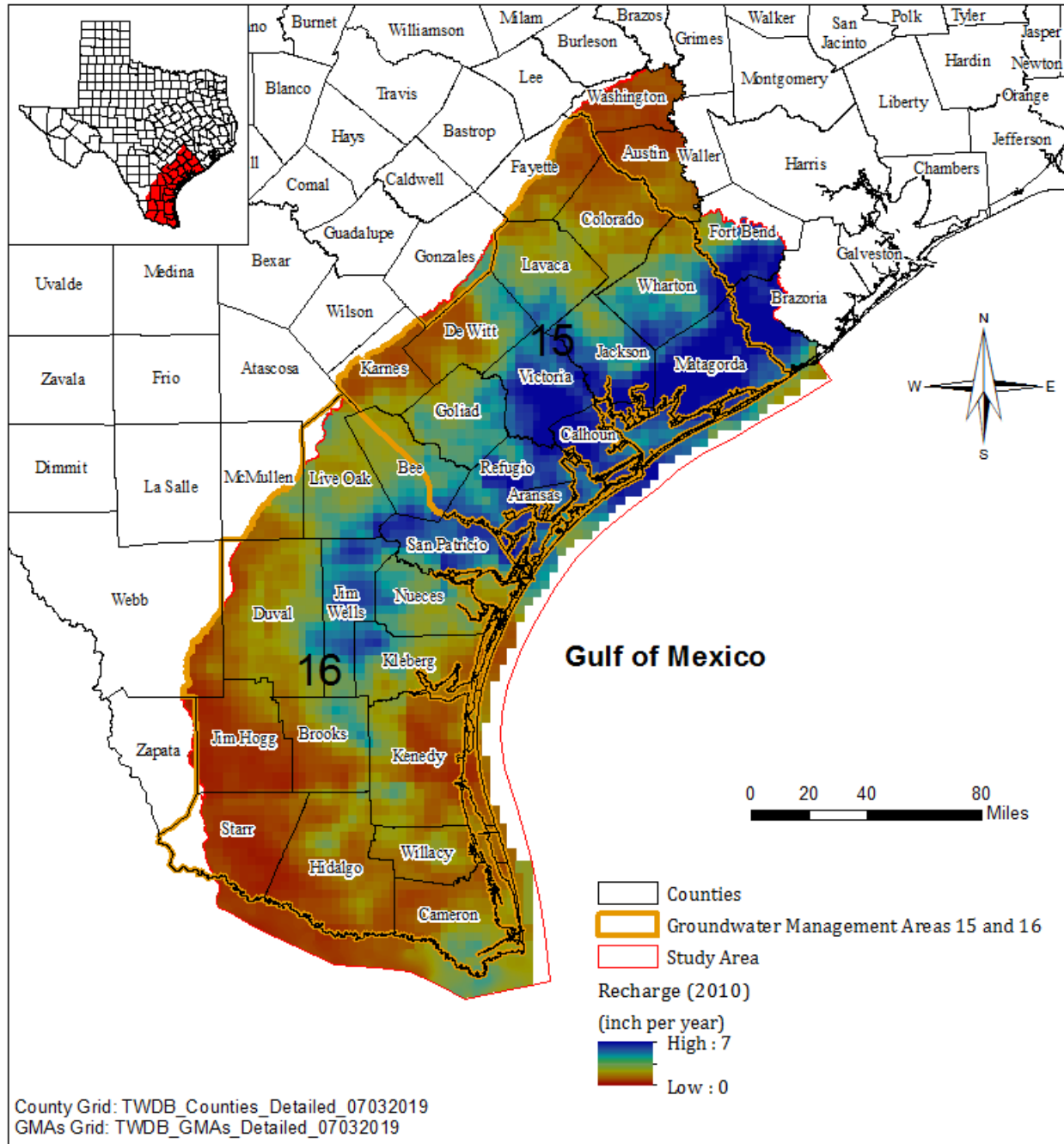


**Figure 4.3.7** Groundwater recharge estimated from stream baseflow-precipitation correlation (2010).

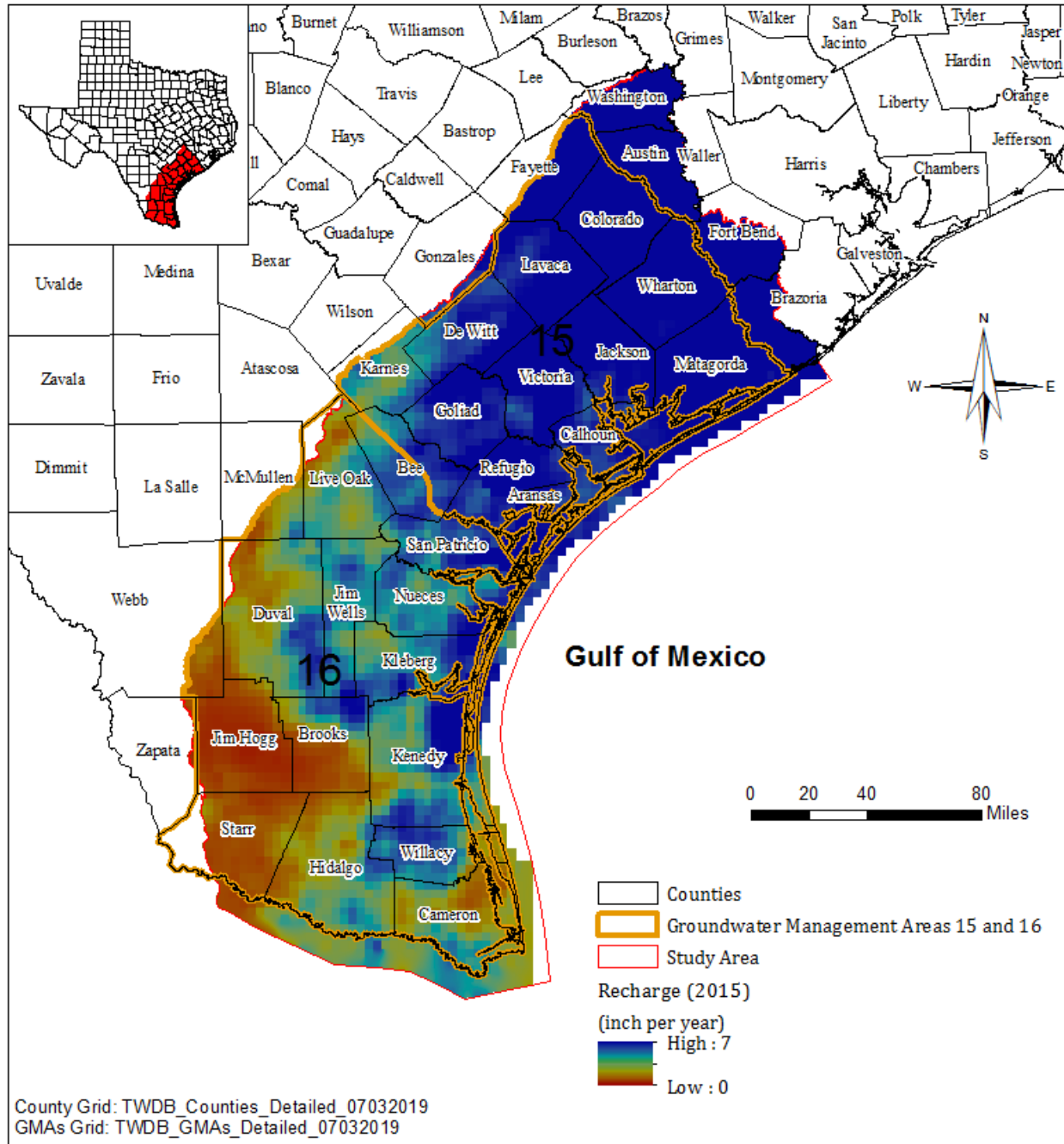


**Figure 4.3.8** Groundwater recharge estimated from stream baseflow-precipitation correlation (2015).

#### **4.4 Rivers, Streams, Lakes, Springs, and Canals**

Groundwater can interact with surface water such as rivers, streams, and lakes. Such interaction could involve gaining water from, or losing water to, the surface water bodies. In a numerical groundwater flow model, surface water bodies are often defined as boundary conditions. In this section, the interaction between groundwater and surface water is evaluated and, if possible, quantified. The information from this analysis will be used for the numerical model development.

##### ***4.4.1 Gain or Loss of Rivers and Streams***

The interaction between groundwater and surface water is often treated as a calibration criterion during the numerical model development. The interaction is quantified as stream gain or loss. When the water level in an aquifer is higher than the riverbed, the groundwater flows into the river. In this case, the river gains water from the aquifer. The opposite could happen when the water level in an aquifer is lower than the riverbed. In this case, the river loses water to the aquifer. A river flux measured at a stream gage often represents the total flow at that station. This total flow includes flow from upstream including any releases from reservoirs or surface water right permits, baseflow, and runoff. Runoff is the flow above land surface that usually occurs during and after rainfall events. Baseflow is the flow from groundwater to a river or vice versa. Thus, the analysis of baseflow is typically used to evaluate stream gains or losses with respect to groundwater.

[Figure 4.4.1](#) shows the locations of the river gages and basins used for the evaluation of the interaction between groundwater and surface water (see [Figure 2.0.2](#) for locations of rivers and streams). Please note 14 of the 18 river basins are also used for estimating the groundwater recharge in the previous section. The other four river basins were added for the groundwater/surface water interaction study due to low permit discharge relative to stream baseflow. Unlike the river basins used for the recharge estimate, these four river basins contain losing streams at times and only have limited baseflow data between 1980 and 2015.

Figures 4.4.2 through 4.4.7 and Appendix D show the stream gain or loss information at the river basins. Several conclusions can be drawn from the figures:

- Most of the basins in the study area contain gaining streams. Two basins, one across Colorado and Wharton counties (labeled as 5 in Figure 4.4.1) and one in Jim Wells, Nueces, and San Patricio counties (labeled as 27 in Figure 4.4.1), shows both gaining and losing (Appendix D). Possible cause for the streams to lose water to the groundwater system may have been the groundwater withdrawal;
- River gain or loss could change dramatically from year to year; and
- River gain or loss decreases in magnitude from north to south.

Slade and others (2002) summarized previous river gain/loss studies in Texas. Most of the studies were outside the conceptual model study area and were performed before 1980, with two exceptions: one along the Colorado River in Colorado and Wharton counties, and the other along the Nueces River (and its tributary Frio River) in Live Oak County (Figure 4.4.8). The study along the Colorado River were performed in August 1985. All but one of the gages fall in Basin 5, discussed above, and were all dominated by river loss to groundwater, which is consistent with the finding of Basin 5 (Appendix D). The study along the Nueces and Frio rivers was performed in November 1991. Some of the gages showed the rivers gaining from the groundwater and the other losing to groundwater (Figure 4.4.8).

#### **4.4.2 Lakes and Reservoirs**

Within the study area, there are 41 lakes or reservoirs with area greater than one square mile. Lake Corpus Christi across Jim Wells, Live Oak, and San Patricio counties is the largest with an area of about 28 square miles (Figure 4.4.9). Twenty-five of the lakes and reservoirs are natural. Fourteen lakes and reservoirs were impounded before 1980. Lake Texana in Jackson County was impounded in May 1980. The power plant cooling water reservoir in Matagorda County was constructed between 1975 and 1988. Falcon International Reservoir and Choke Canyon Lake are only partially located in the study area.

TWDB has collected or compiled water level data at three reservoirs in the study area: Coletto Creek Reservoir, Lake Corpus Christi, and Lake Texana. [Figures 4.4.10 through 4.4.12](#) show the annual reservoir/lake levels calculated from daily values for the three reservoirs, respectively. Other lakes/reservoirs do not have continuous historical level data. Estimates based on the U. S. Geological Survey's topographic map show varied water levels ranging from zero feet above mean sea level near the Gulf to 390 feet above mean sea level in Cedar Creek Reservoir in Fayette County.

#### **4.4.3 Springs**

When the water level in an aquifer is above the ground, it can discharge to the surface as springs. Springs typically occur in topographically low areas such as river valleys. Along with groundwater levels and stream gain/loss data, the spring flow information can be used as calibration targets during the numerical model development.

According to Heitmuller and Reece (2003), there were 23 historical springs in the study area that originated from the Gulf Coast Aquifer System or younger alluvium/fluvium/dune sands ([Figure 4.4.13](#)). Many of the springs ceased to flow and few had flow measurements. None of the flow measurements occurred after 1969. Overall, groundwater discharge by springs was small and varied significantly over time.

#### **4.4.4 Diversion from Lower Rio Grande**

Water from the Rio Grande have been diverted by both the U. S. and Mexico through canals for irrigation, municipal, and industrial uses. Diversion on the Mexico side was through the Anzalduas Canal. Diversion on the U. S. side was primarily through a canal system. [Figure 4.4.14](#)) shows the distribution of canals and diversion reaches along the Rio Grande in the study area.

The International Boundary & Water Commission has daily diversion data and can be downloaded from [https://www.ibwc.gov/Water\\_Data/rtdata.htm](https://www.ibwc.gov/Water_Data/rtdata.htm). The diversion to the Anzalduas Canal in Mexico ranges from about 38,000 acre-feet per year to 1.5 million acre-feet per year with an average of about 800,000 acre-feet per year between 1980 and 2011

(Figure 4.4.15). On the U. S. side, the diversion between Rio Grande City and the Anzalduas Dam ranges from about 112,000 to 344,000 acre-feet per year with an average of about 206,000 acre-feet per year between 1980 and 2010 (Figure 4.4.16). The diversion between the Anzalduas Dam and Progreso City ranges from about 147,000 to 323,000 acre-feet per year with an average of about 206,000 acre-feet per year between 1980 and 2010 (Figure 4.4.17). The diversion between Progreso City and San Benito City ranges from about 280,000 to 704,000 acre-feet per year with an average of about 458,000 acre-feet per year between 1980 and 2010 (Figure 4.4.18). The diversion between San Benito City and Brownsville City ranges from about 42,000 to 139,000 acre-feet per year with an average of about 101,000 acre-feet per year between 1980 and 2010 (Figure 4.4.19). The diversion between Brownsville City and the Gulf of Mexico ranges from 310 to 4,245 acre-feet per year with an average of 2,339 acre-feet per year between 1980 and 2010 (Figure 4.4.20). The total diversion on the U. S. side ranges from about 618,000 to 1.5 million acre-feet per year with an average of about 974,000 acre-feet per year between 1980 and 2010 (Figure 4.4.21).

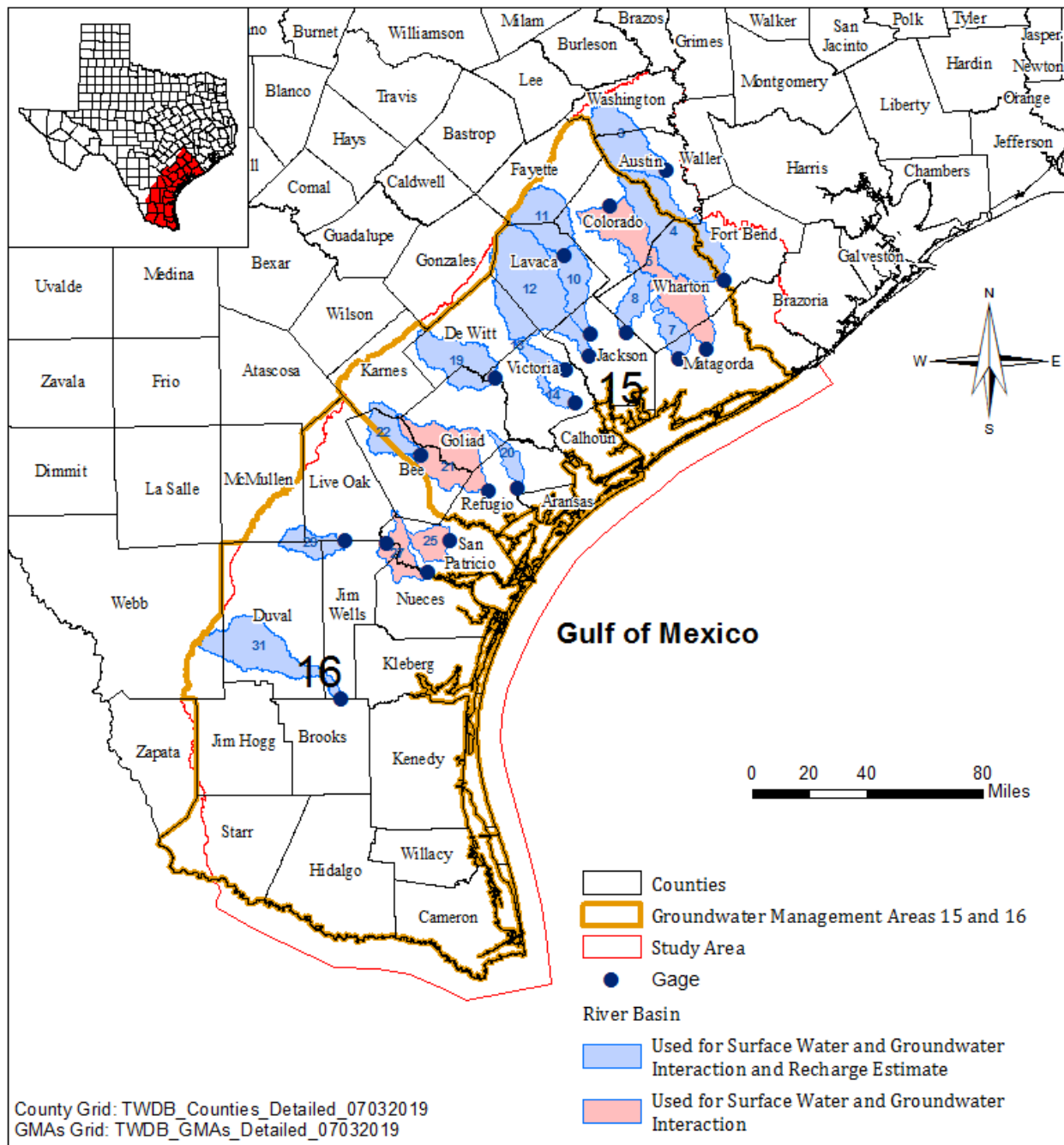


**Figure 4.4.1** Locations of river gages and basins used for evaluating surface water and groundwater interaction. Basins are indexed for identification and discussion purposes.

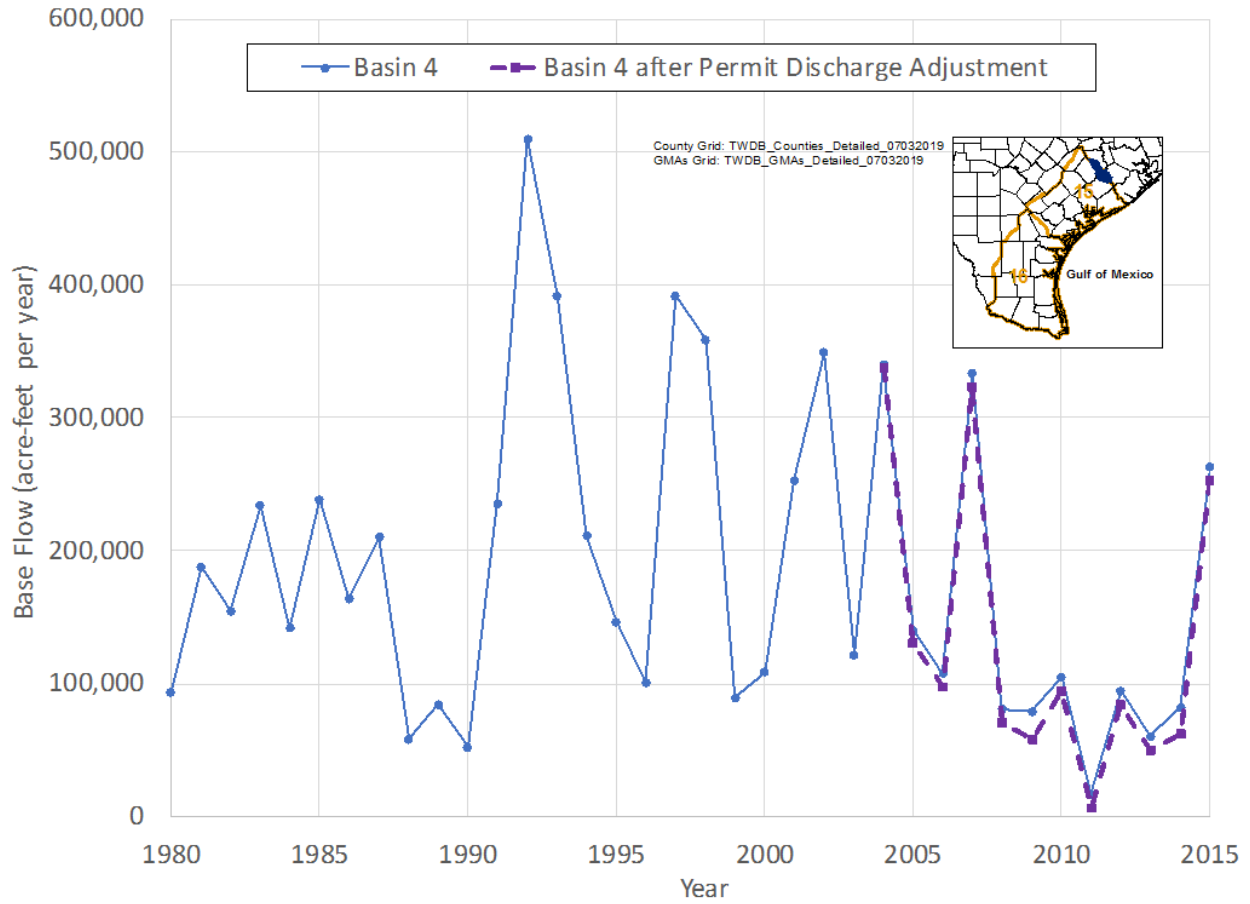


**Figure 4.4.2 Stream gain (positive values) or loss (negative values) results in Basin 4 across Austin, Colorado, Fort Bend, and Wharton counties.**



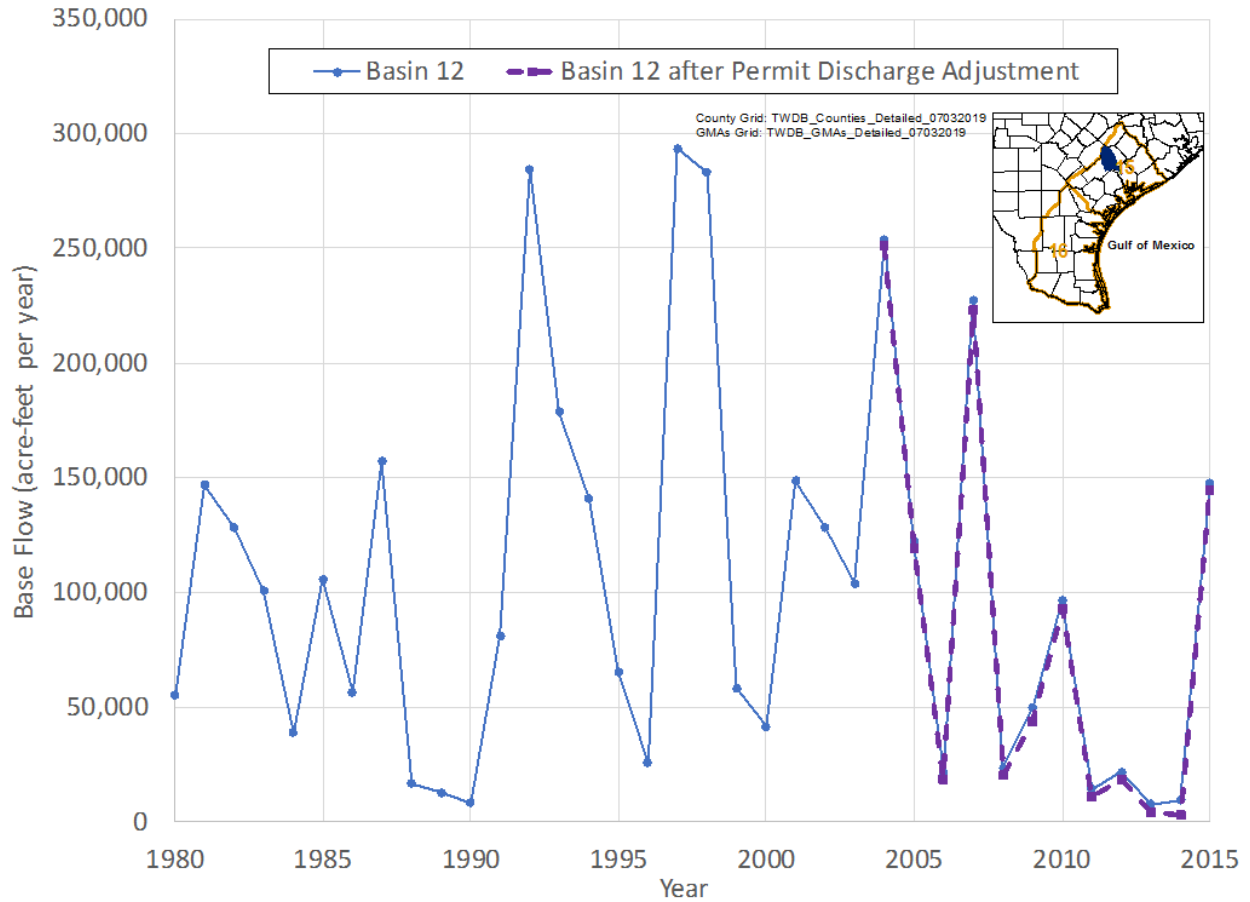


**Figure 4.4.3 Stream gain (positive values) or loss (negative values) results in Basin 12 across DeWitt, Jackson, and Lavaca counties.**

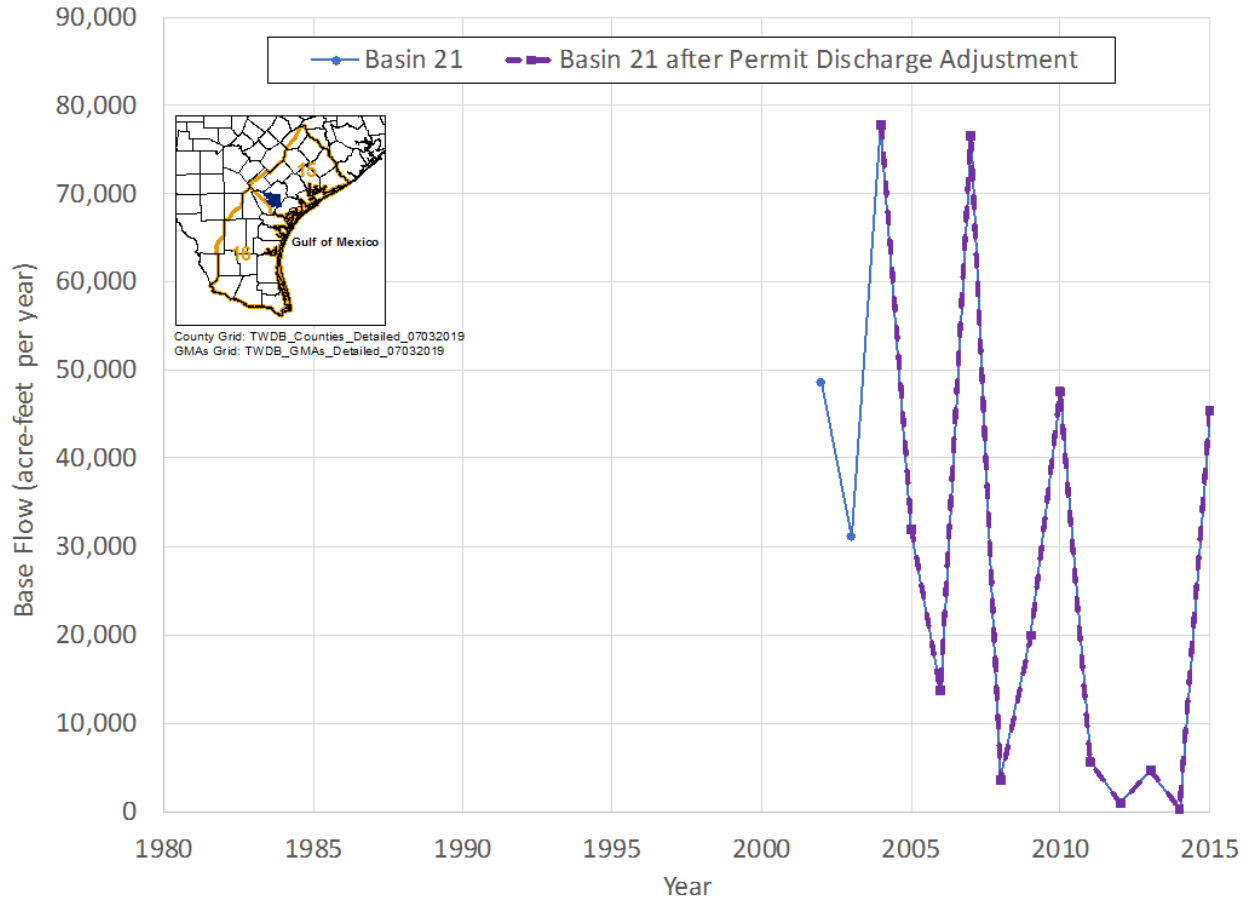


**Figure 4.4.4 Stream gain (positive values) or loss (negative values) results in Basin 21 across Bee and Refugio counties.**

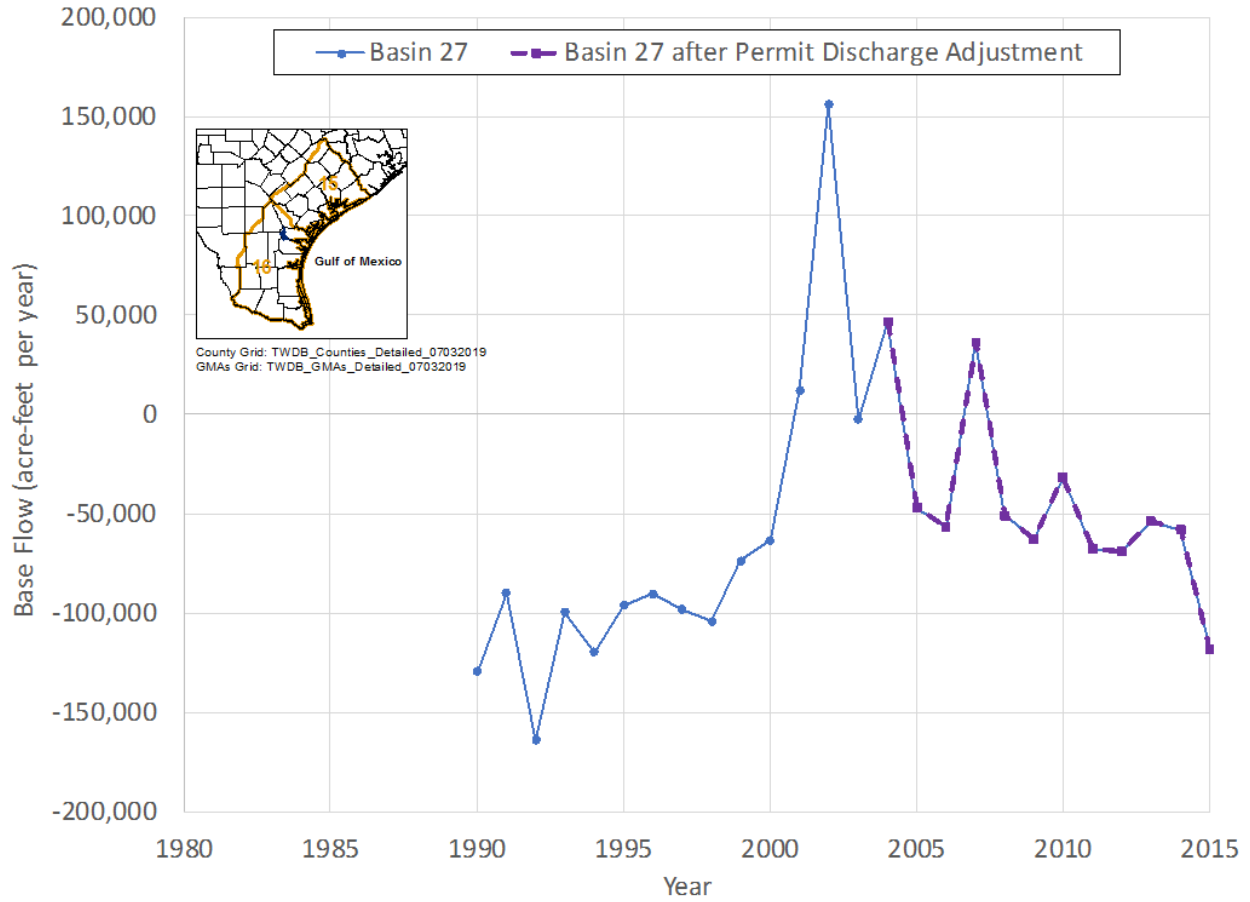


**Figure 4.4.5 Stream gain (positive values) or loss (negative values) results in Basin 27 across Jim Wells, Nueces, and San Patricio counties.**

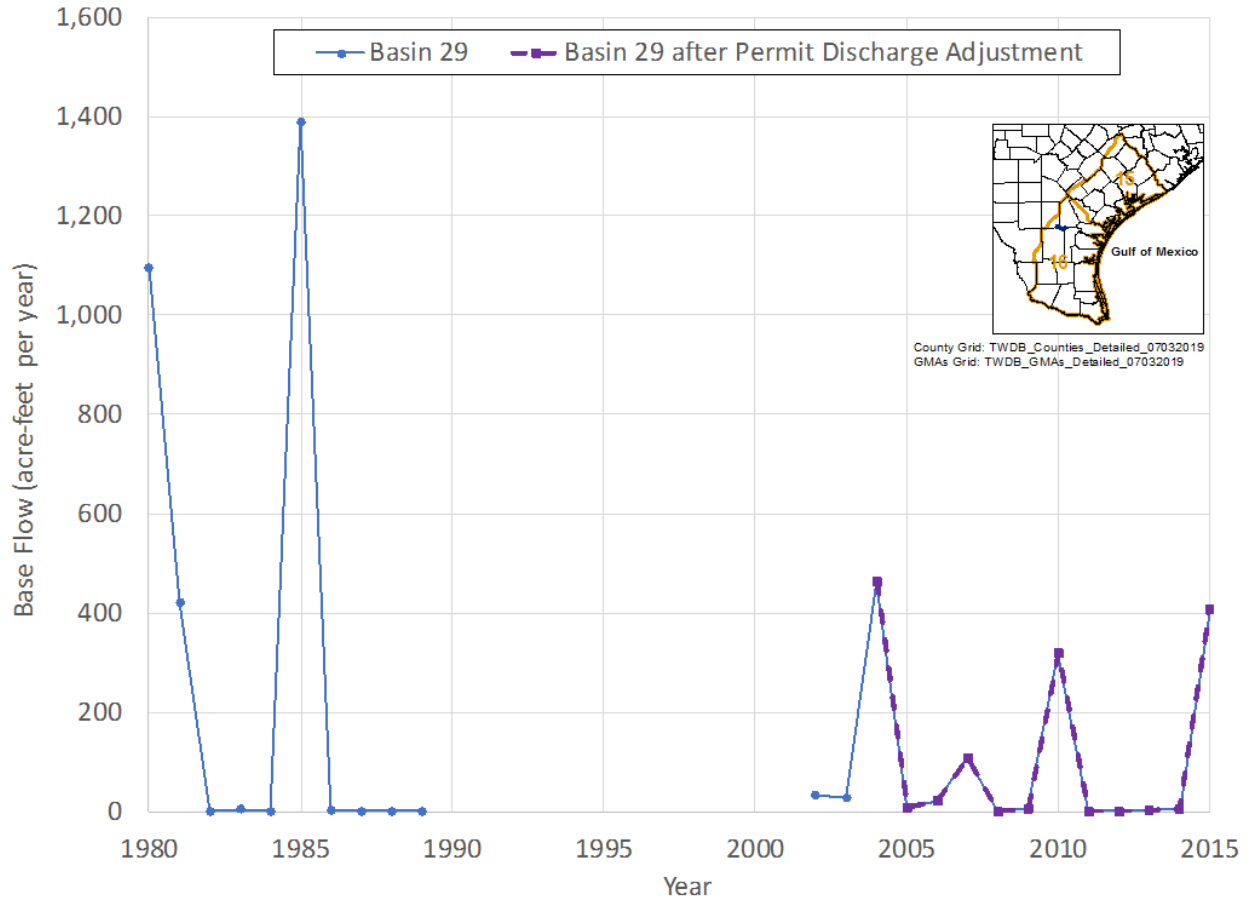


**Figure 4.4.6 Stream gain (positive values) or loss (negative values) results in Basin 29 across Duval, Jim Wells, Live Oak, and McMullen counties.**

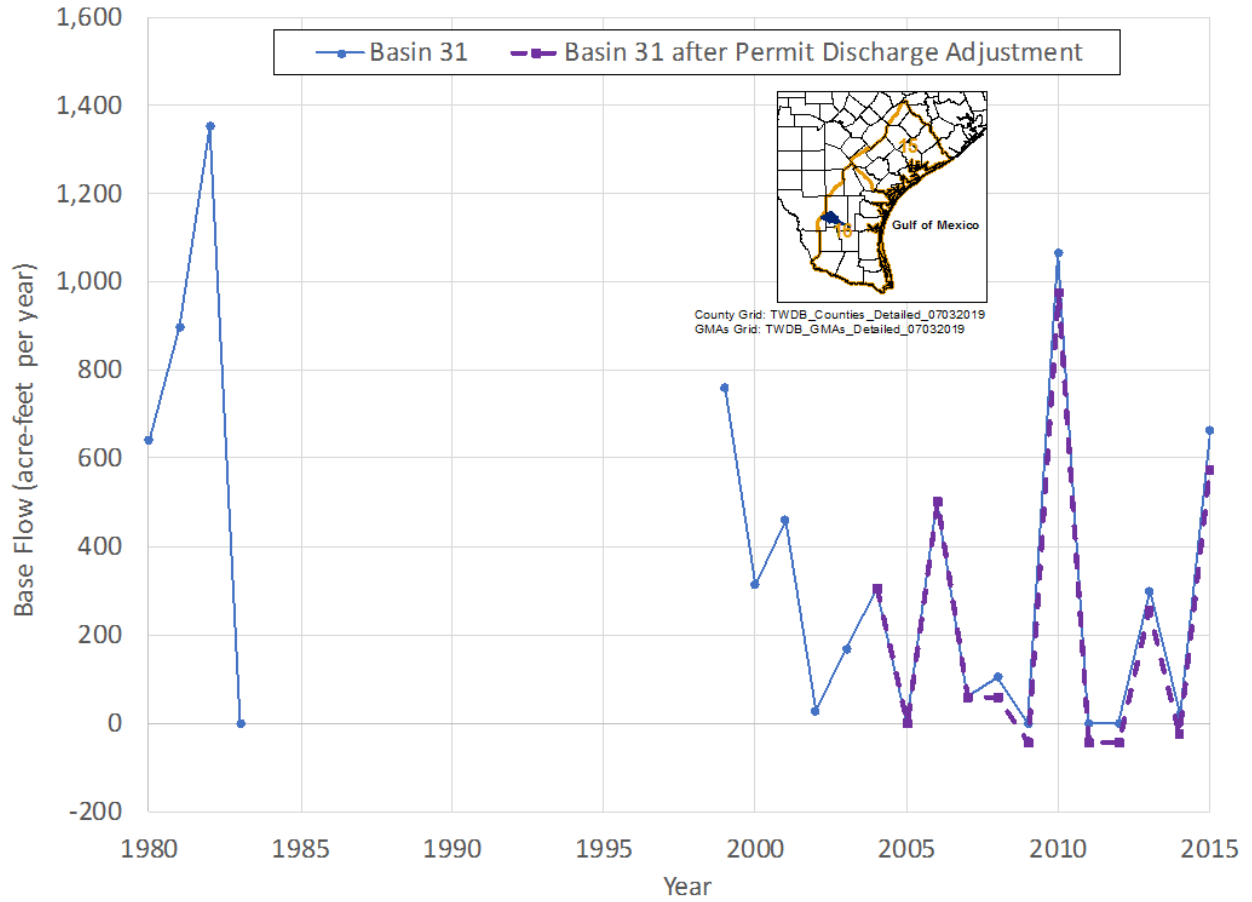


**Figure 4.4.7 Stream gain (positive values) or loss (negative values) results in Basin 31 across Duval, Jim Wells, and Webb counties.**

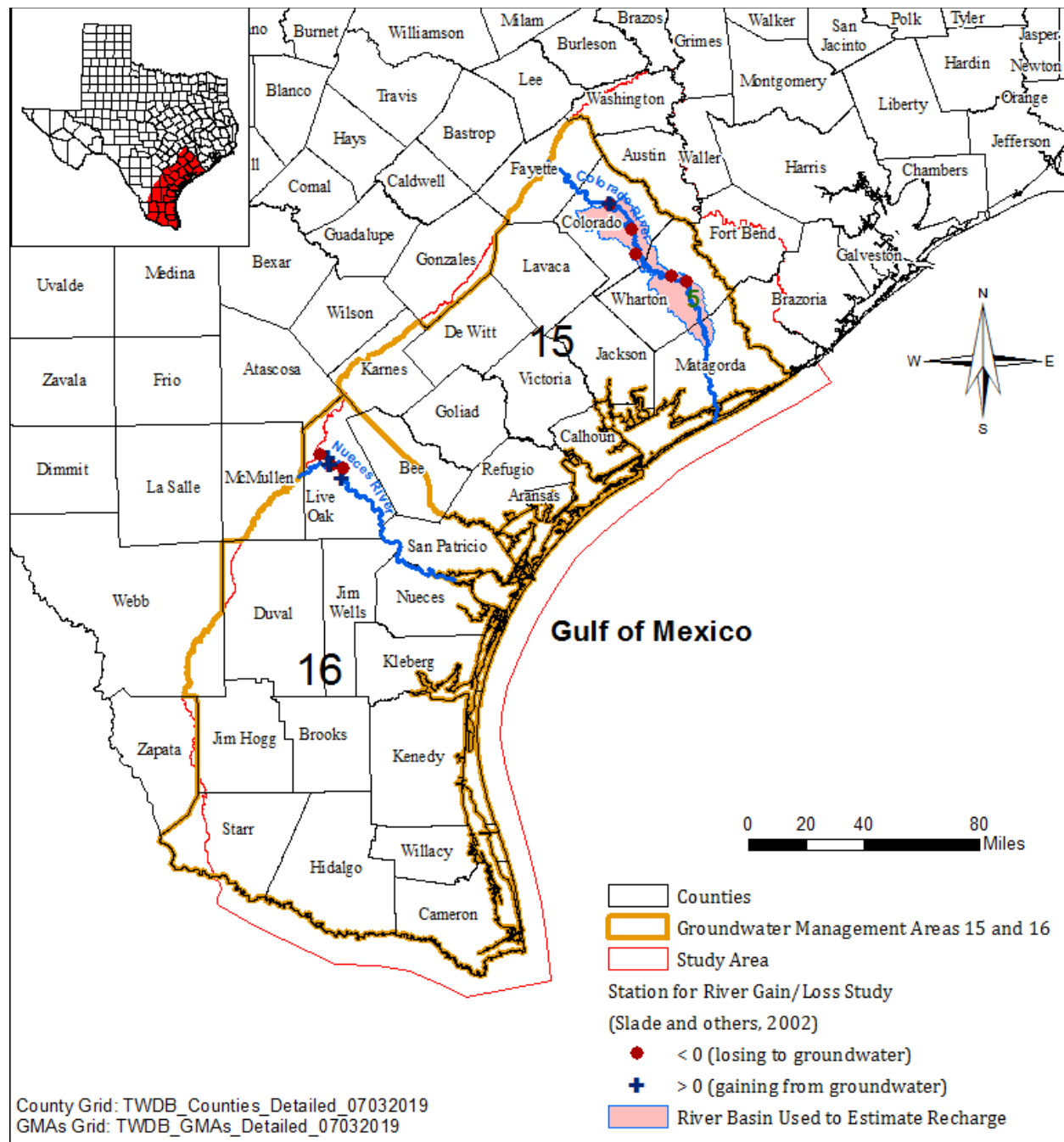


**Figure 4.4.8 Results of river gain/loss study by Slade and others (2002).**

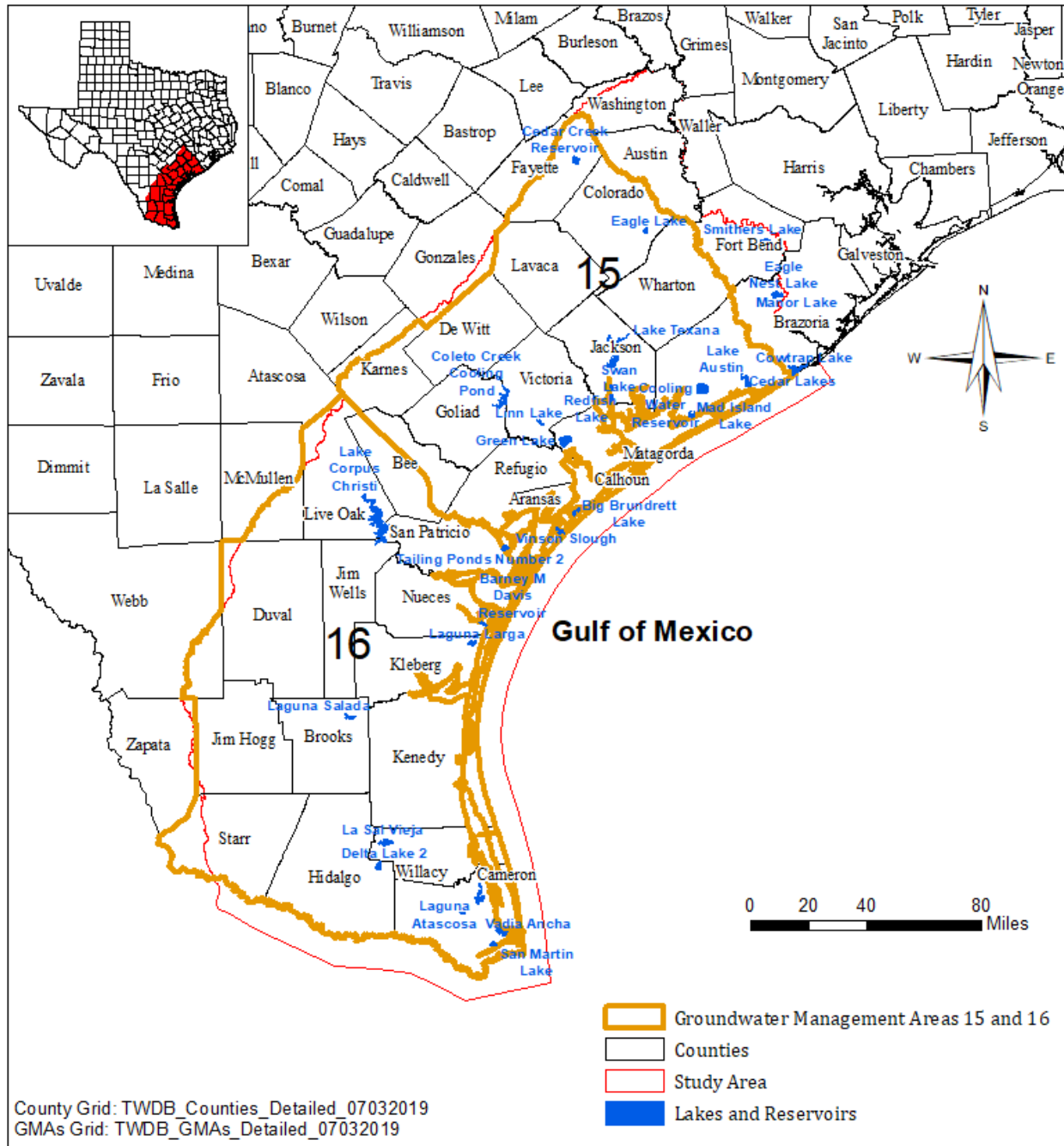


**Figure 4.4.9** Locations of lakes and reservoirs greater than one square mile in study area.

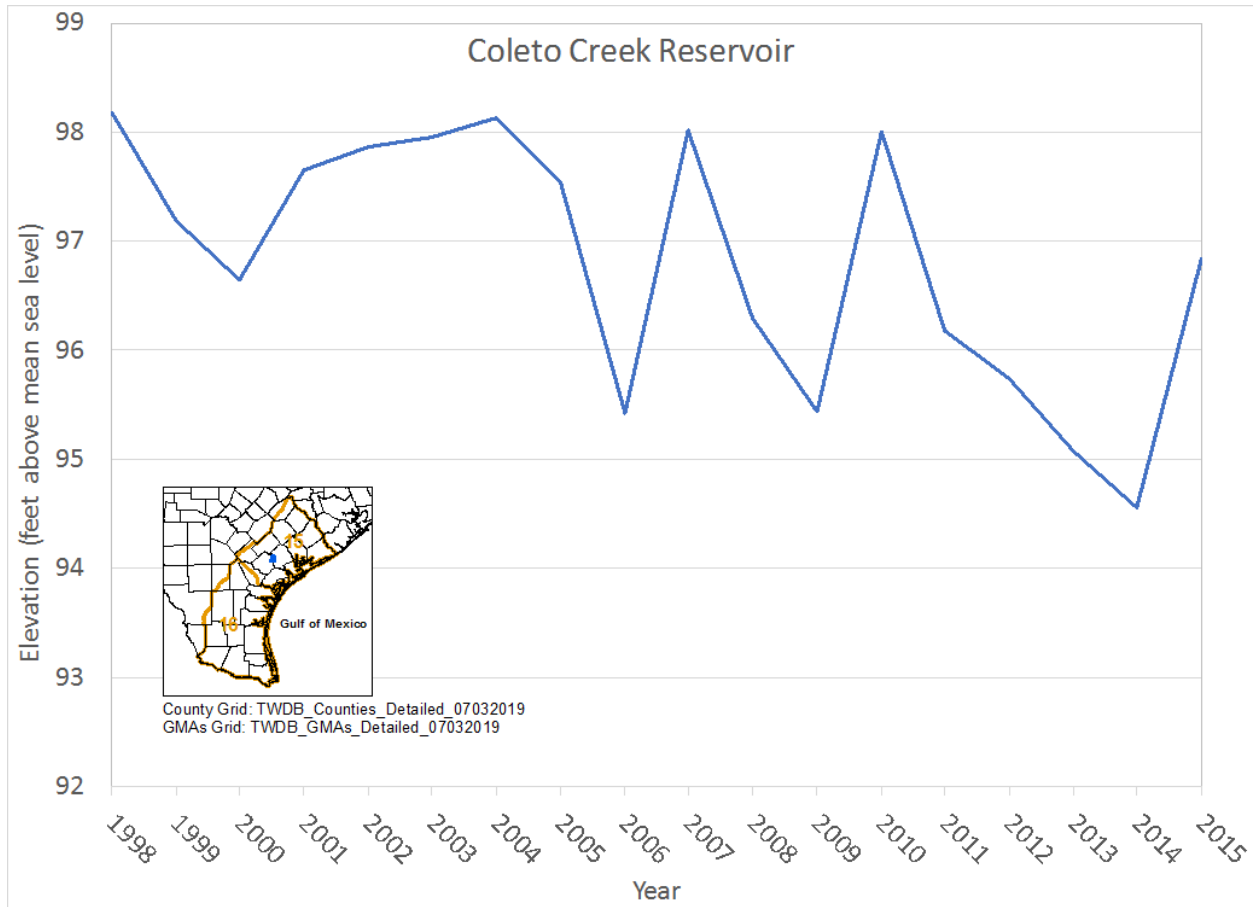


**Figure 4.4.10 Water level elevation at Coletto Creek Reservoir.**



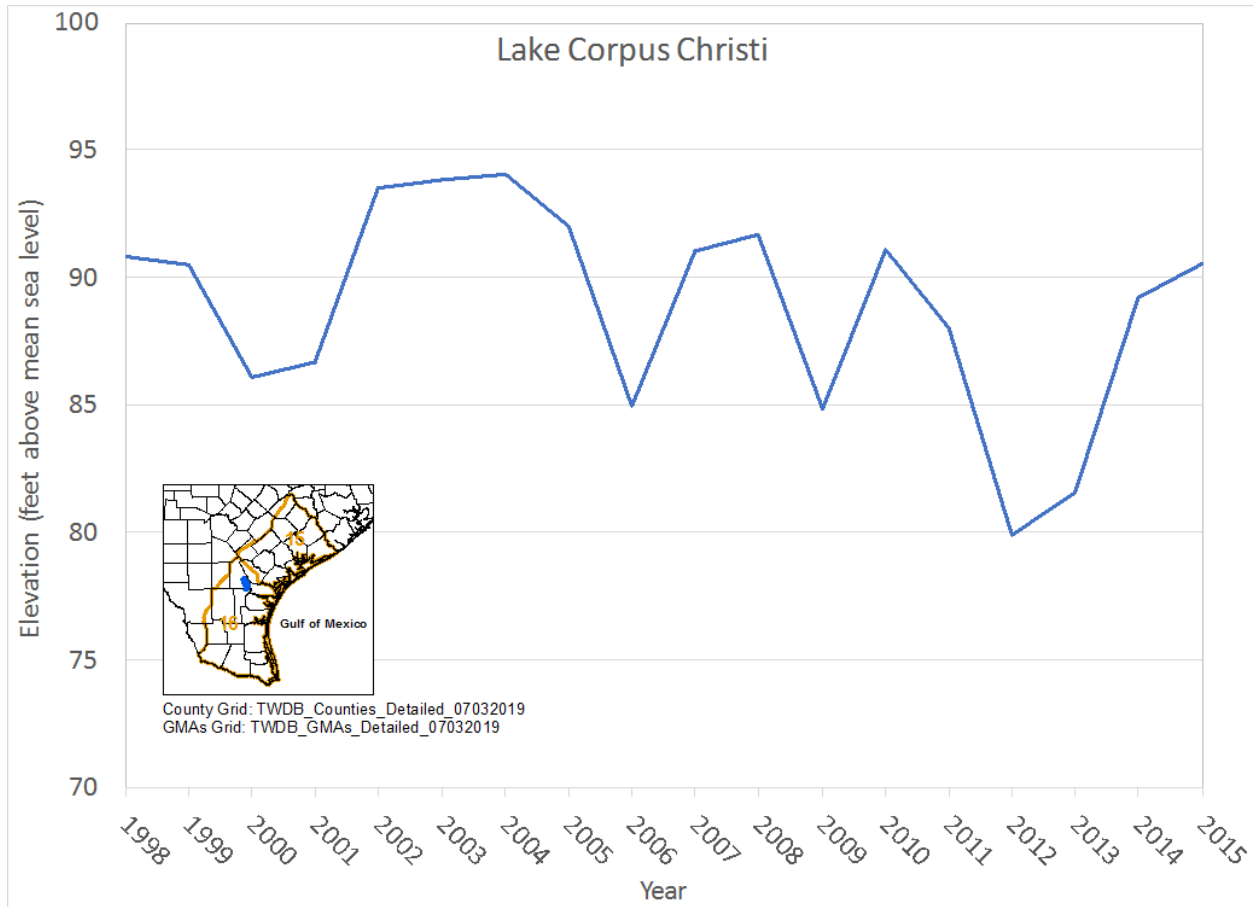


**Figure 4.4.11 Water level elevation at Lake Corpus Christi.**

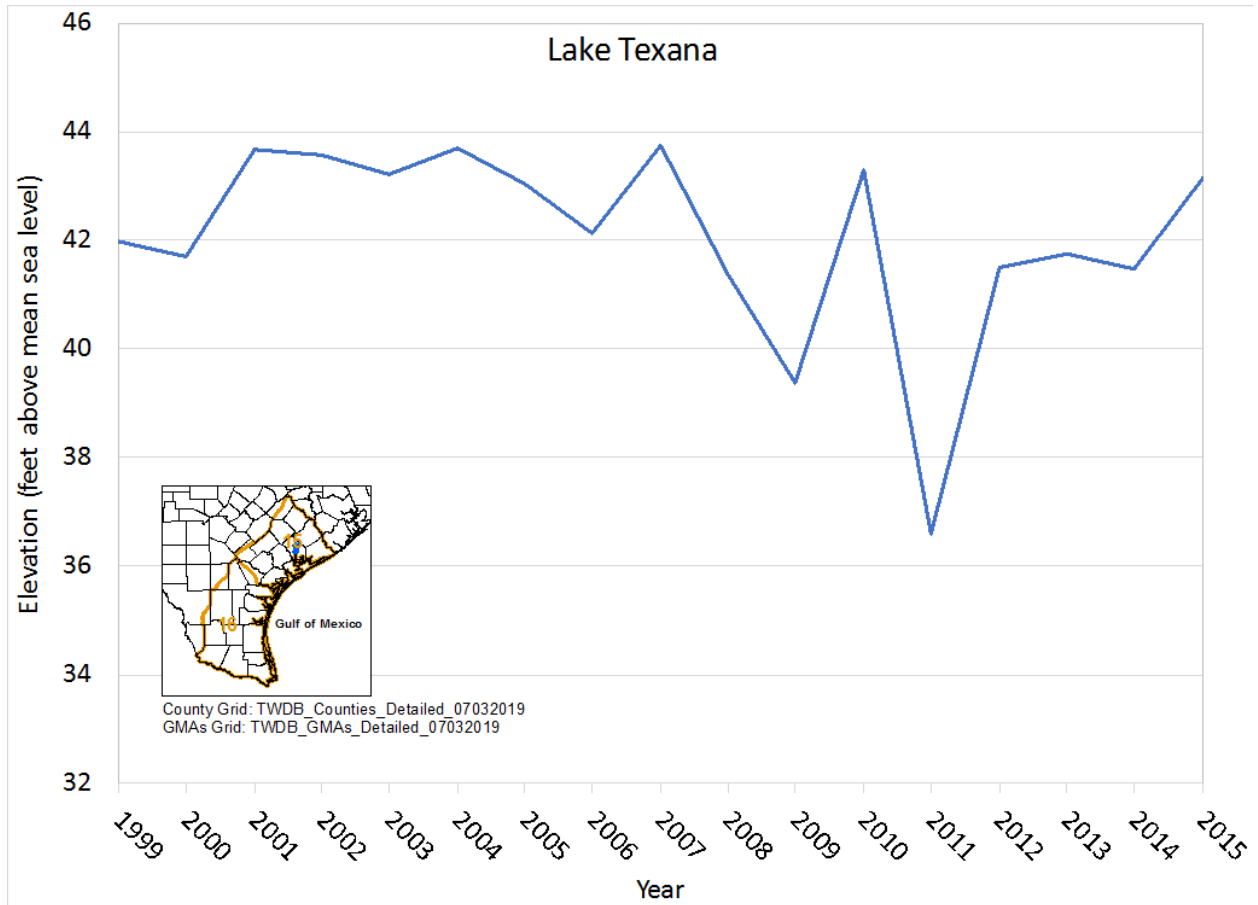


**Figure 4.4.12 Water level elevation at Lake Texana.**

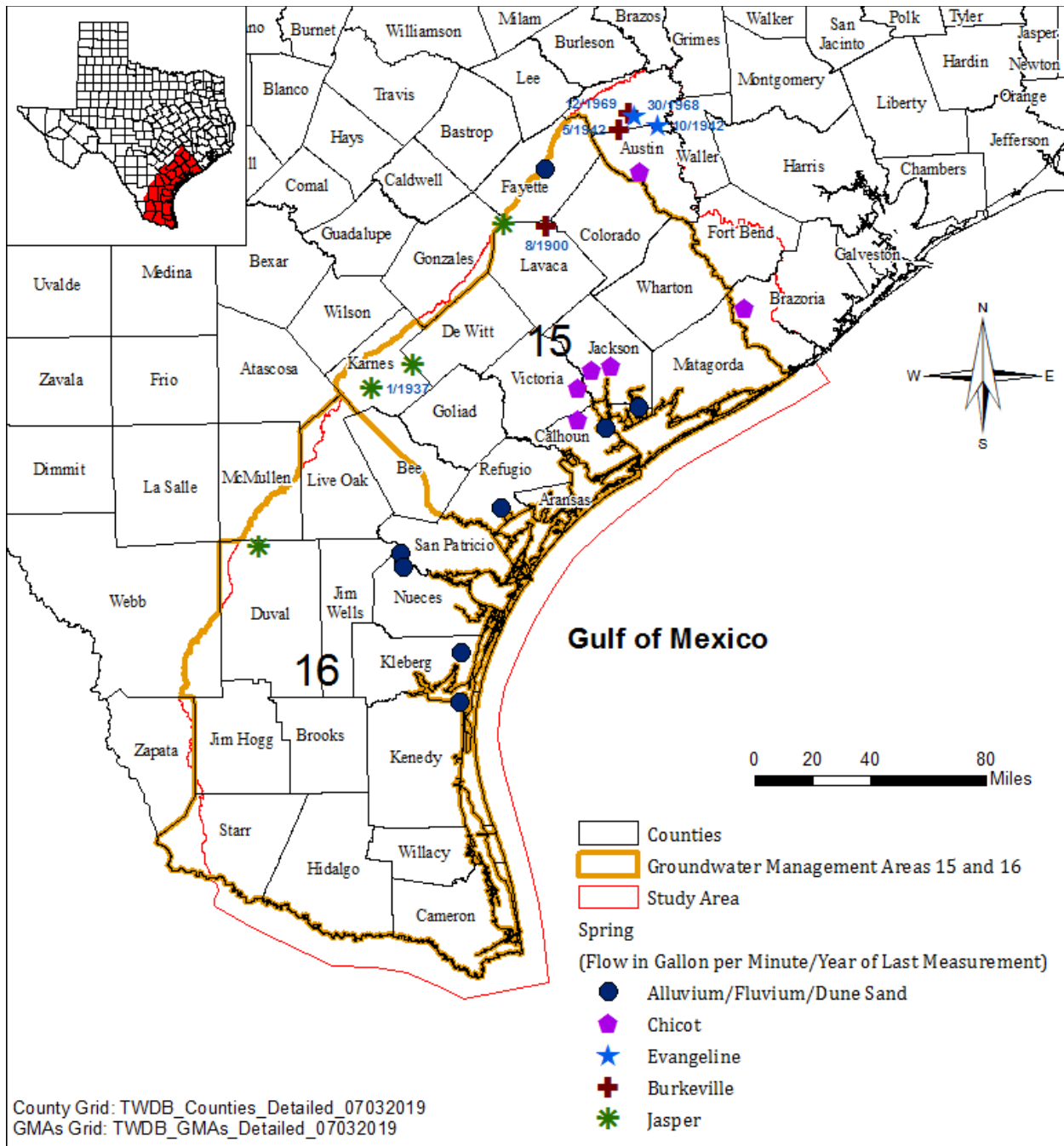


**Figure 4.4.13** Distribution of springs in study area.

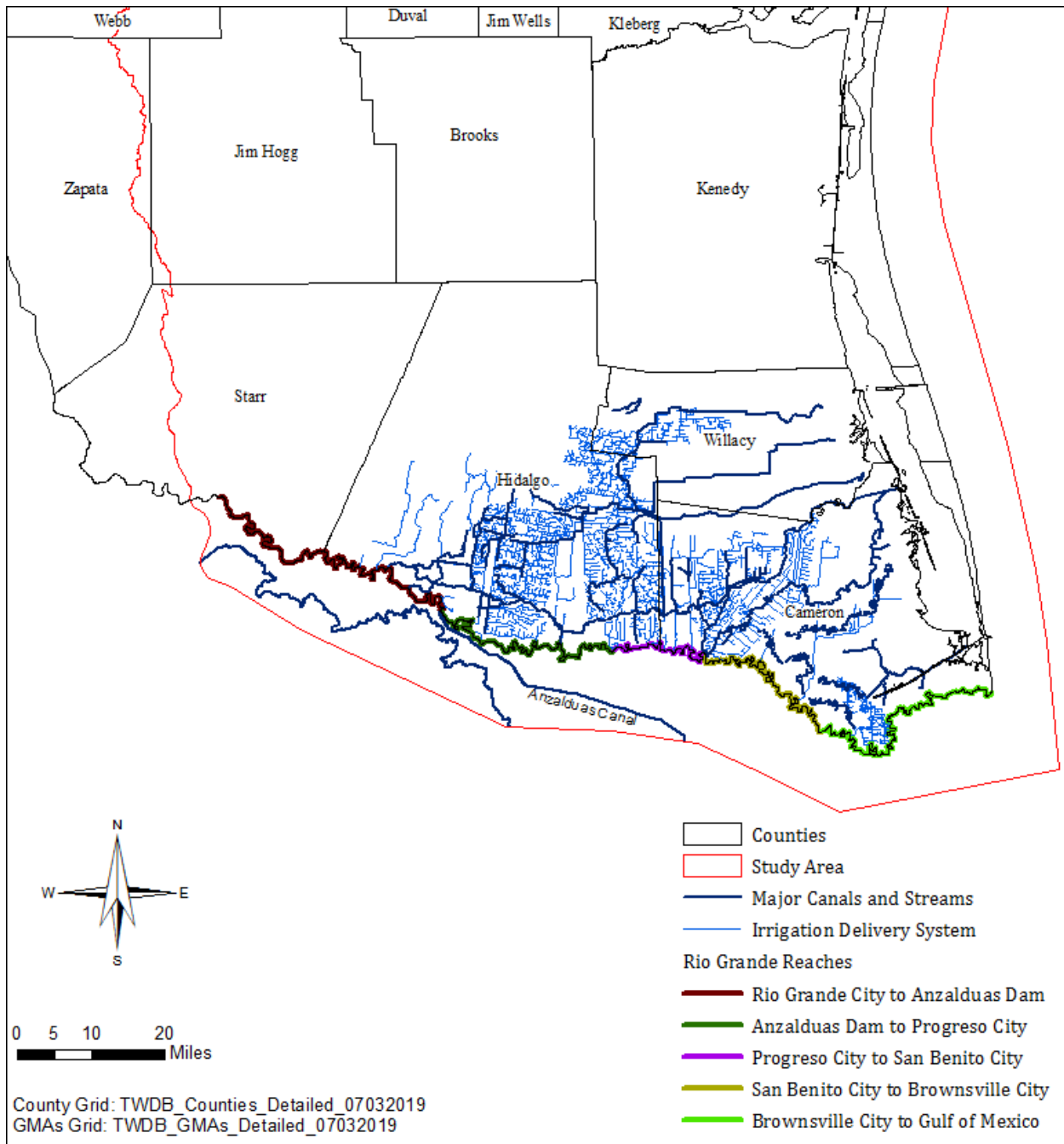


**Figure 4.4.14 Distribution of canals and diversion reaches along Rio Grande in study area.**

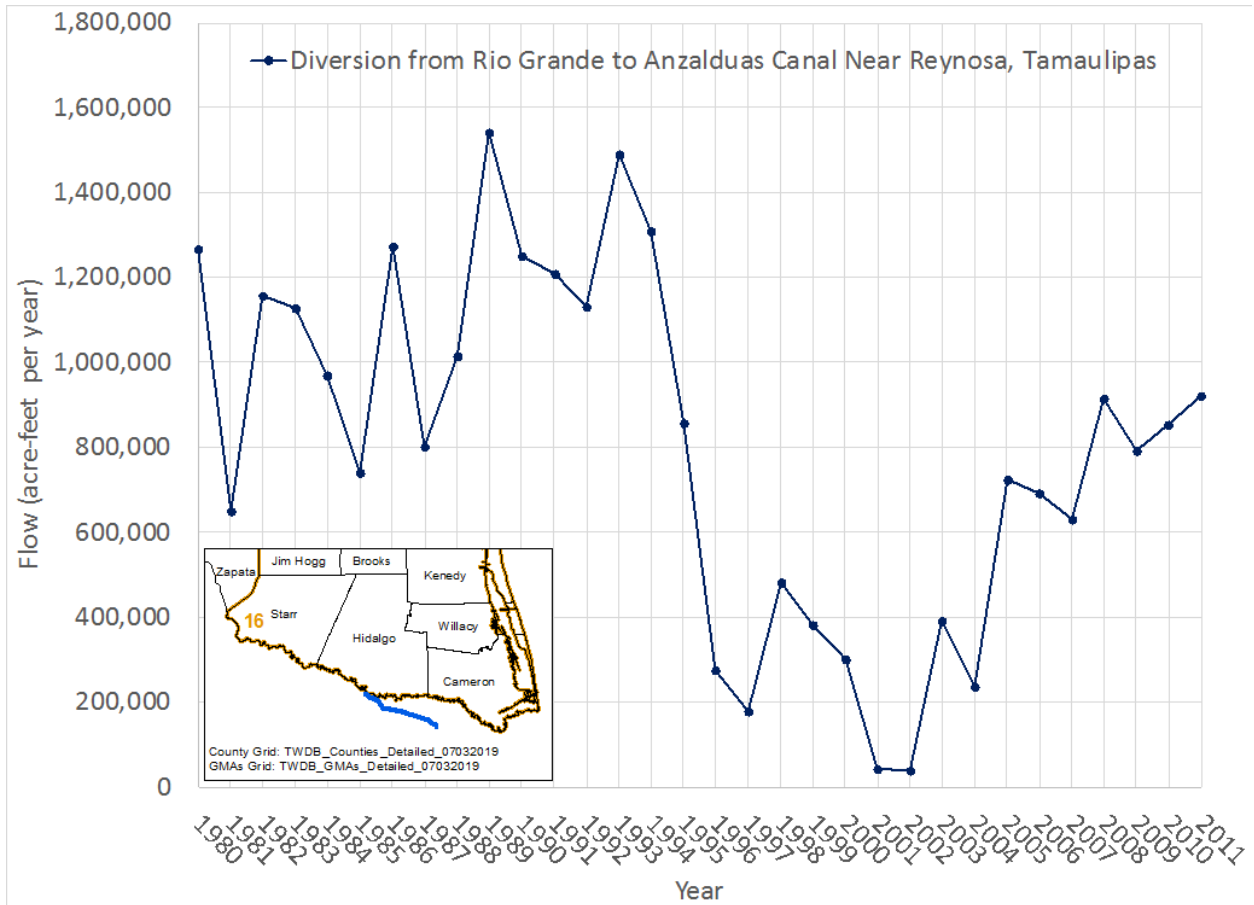


**Figure 4.4.15 Diversion from Rio Grande to Anzalduas Canal in Mexico.**

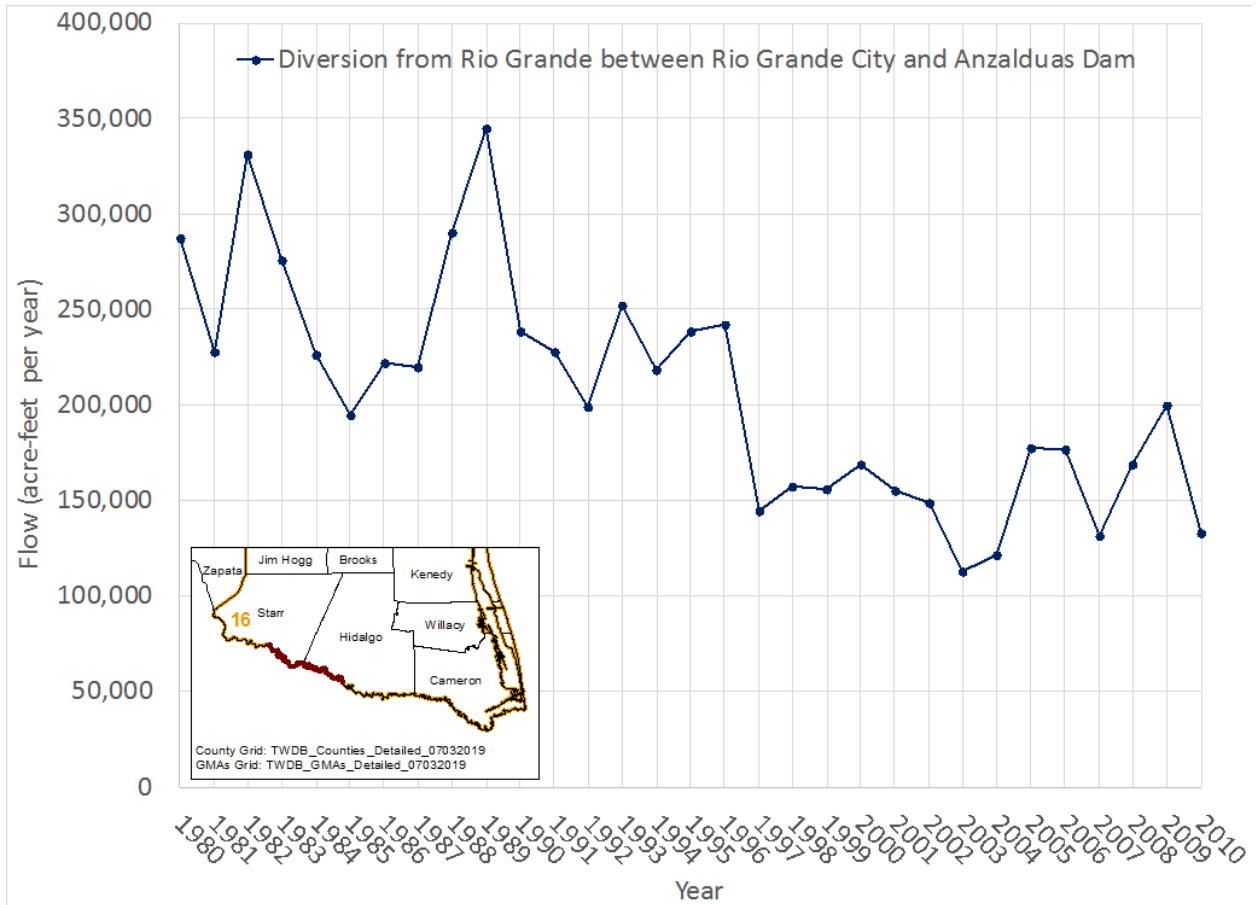


**Figure 4.4.16 Diversion from Rio Grande along the U. S. side between Rio Grande City and Anzalduas Dam.**

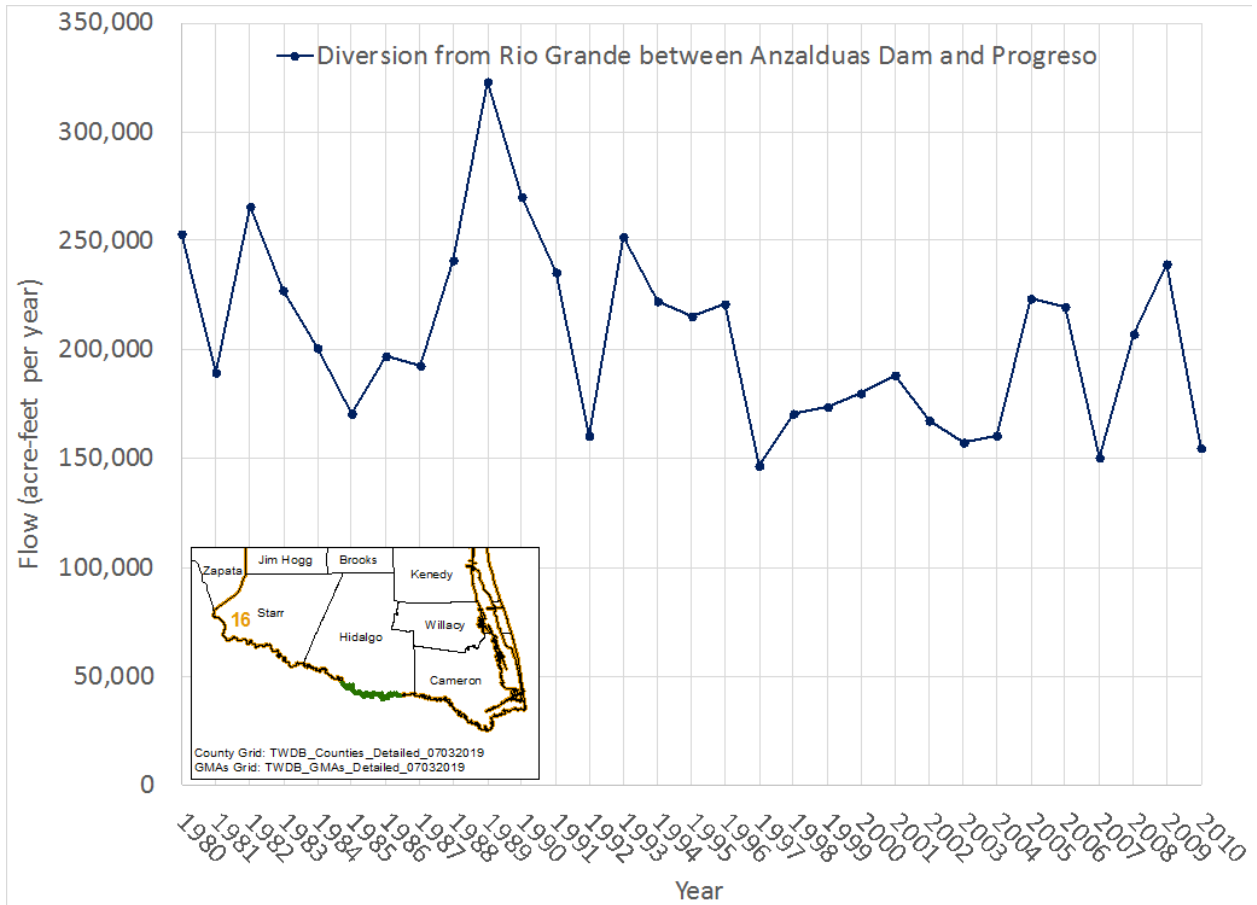


**Figure 4.4.17 Diversion from Rio Grande along the U. S. side between Anzalduas Dam and Progreso City.**

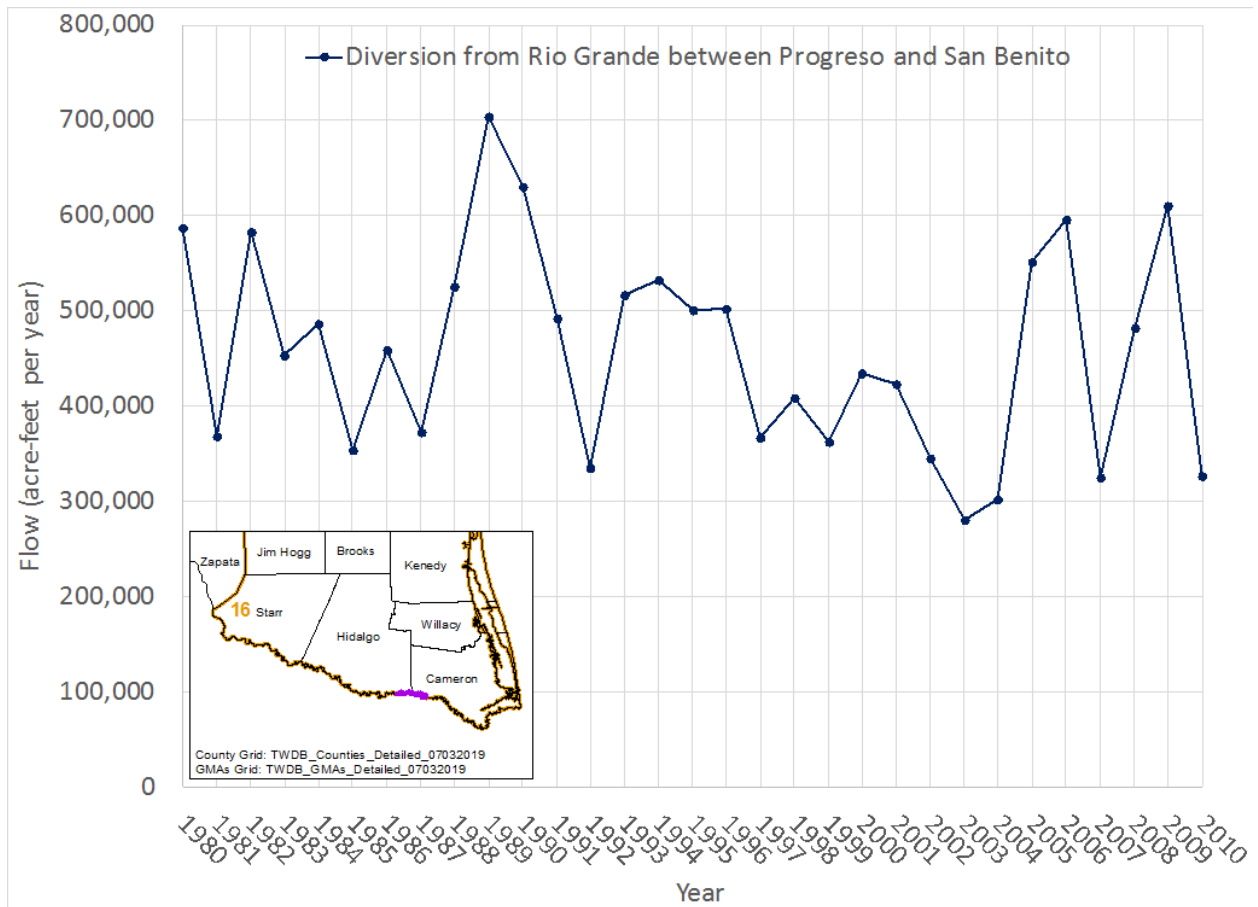


**Figure 4.4.18 Diversion from Rio Grande along the U. S. side between Progreso City and San Benito City.**



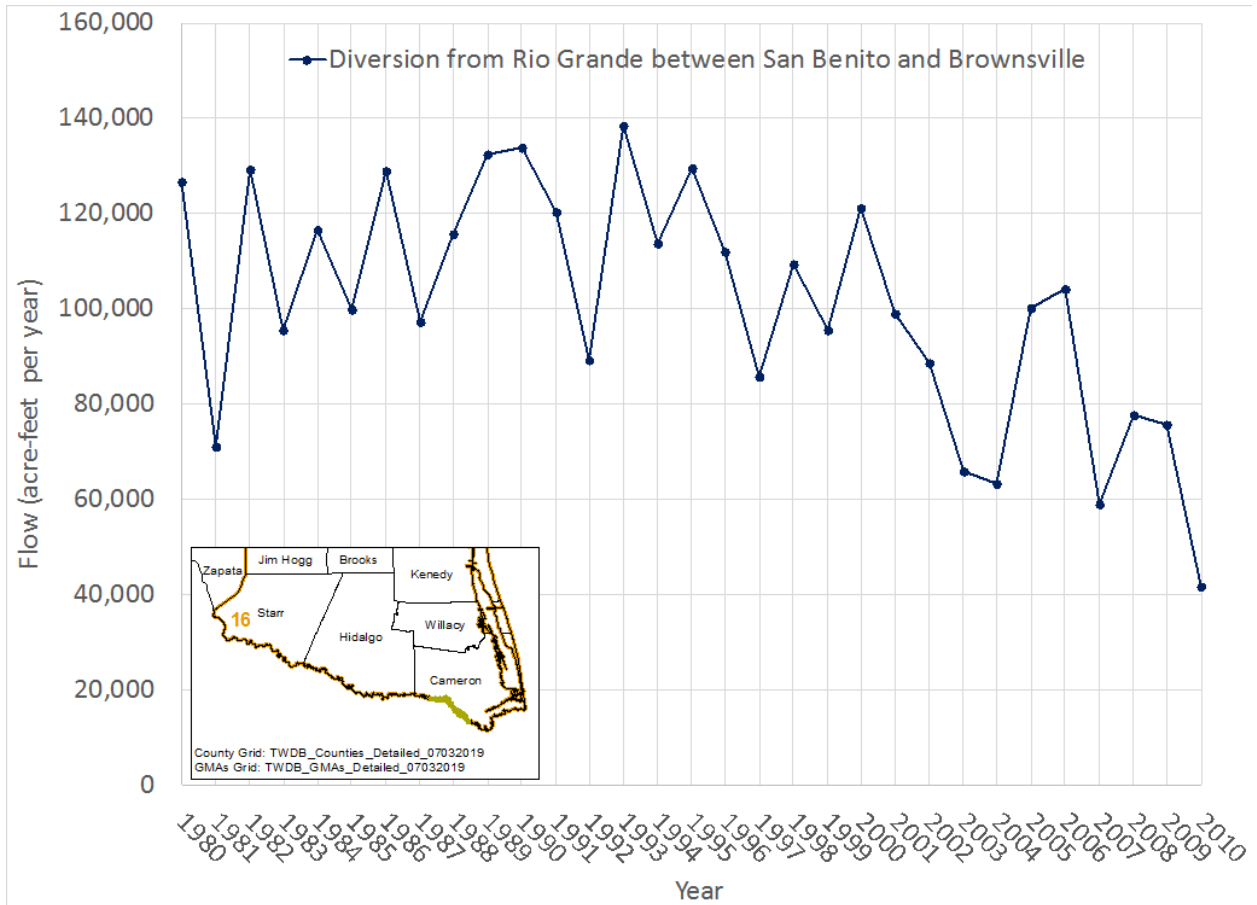


**Figure 4.4.19 Diversion from Rio Grande along the U. S. side between San Benito City and Brownsville City.**

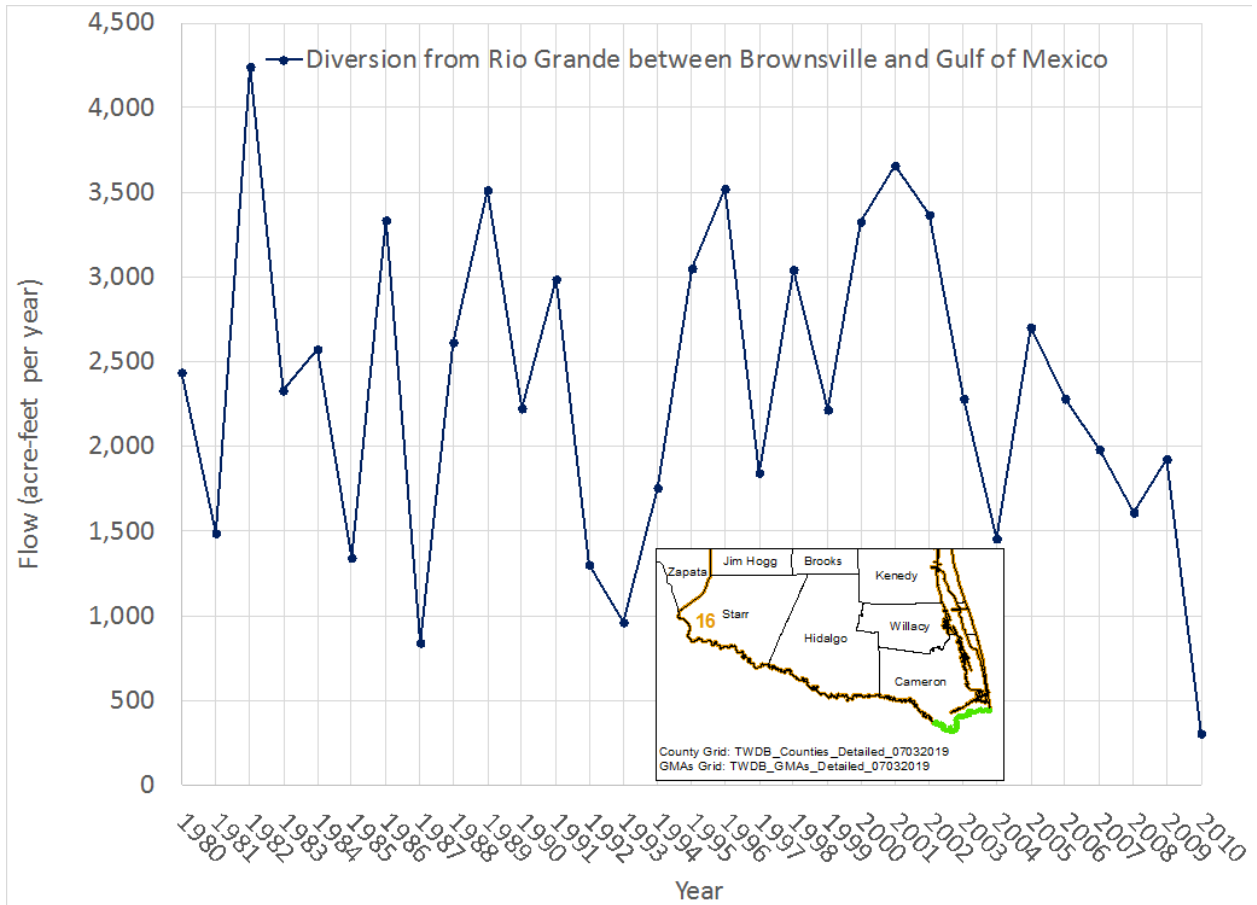


**Figure 4.4.20 Diversion from Rio Grande along the U. S. side between Brownsville City and Gulf of Mexico.**

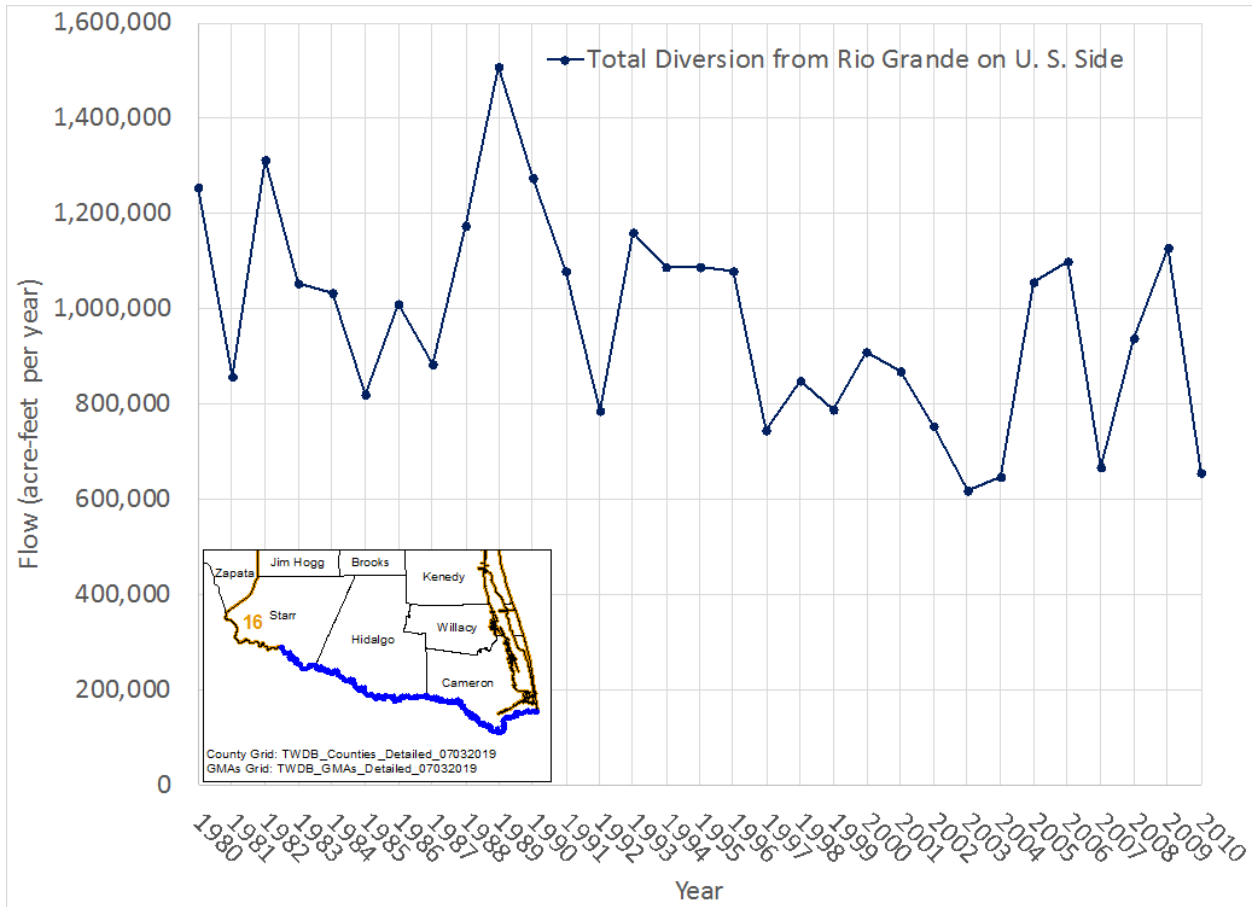


**Figure 4.4.21 Total diversion from Rio Grande along the U. S. side.**

#### 4.5 Hydraulic Properties

Several parameters are used to describe aquifer hydraulic properties including hydraulic conductivity, transmissivity, specific yield, storativity, and specific capacity. Each of these terms is briefly described below.

*Transmissivity (T)* is a measure of groundwater flow through the entire thickness of an aquifer. An aquifer with a higher transmissivity tends to transmit more water than an aquifer with lower transmissivity. Transmissivity may be expressed in square feet per day or gallons per day per foot.

*Hydraulic Conductivity (K)* is a parameter representing how easily groundwater can flow through an aquifer. A higher hydraulic conductivity value means that the groundwater can flow through the aquifer more easily than an aquifer with lower hydraulic conductivity. Hydraulic conductivity may be expressed in feet per day or gallons per day per square foot.

*Specific Yield (Sy)*, also called drainable porosity, is the volume of water released per unit volume of aquifer under the force of gravity. It approximates the effective porosity when the voids in the aquifer are large and well connected. For aquifers with finer materials, the specific yield is usually less than the effective porosity. Specific yield is dimensionless.

*Storativity (S)*, also called coefficient of storage, is the volume of water released per unit area of aquifer when the water level in the aquifer is lowered by a unit of length. In a confined (or artesian) aquifer, storativity can be used to calculate aquifer specific storage by dividing the aquifer thickness. In an unconfined (water table) aquifer, storativity is essentially equal to the specific yield. The storativity of a confined aquifer is often lower than the specific yield of an unconfined aquifer; given both aquifers contain the same materials. As a result, for the same aquifer, the outcrop area yields more water than downdip portion with the same head loss or drawdown. Storativity is dimensionless.

*Specific Capacity (Sc)*, the discharge of a well divided by the drawdown, is a measure of well yield. Specific capacity depends on aquifer property, well construction, and pumping rate. Specific capacity increases with increasing aquifer transmissivity and well diameter. Well

specific capacity is often hindered by poor well design and construction as well as increasing pumping rate, which reduces well efficiency. Specific capacity may be expressed in gallons per minute per foot of drawdown in the well.

Pumping test is considered the best method to obtain transmissivity and storage values. Specific capacity can also be used to estimate transmissivity using the Cooper-Jacob approximation of the Theis equation,

$$T = \frac{Q}{4\pi s_m} \left[ \ln \left( \frac{2.25Tt}{r_w^2 S} \right) \right]$$

Where:

$Q$  = mean pumping rate

$S$  = storativity (assumed 0.0001 in this study)

$r_w$  = borehole radius

$T$  = transmissivity

$t$  = pumping duration

Conductivity is then calculated using the following equation,

$$K = T/B$$

Where:

$B$  = total well screen length

#### **4.5.1 Transmissivity and Hydraulic Conductivity from Pumping Tests**

Previous studies have produced 323 hydraulic transmissivity or/and conductivity values from pumping tests in the study area. These studies include:

- Former Texas Board of Water Engineers bulletins: Dale and others (1957); Anders (1960); Anders and Baker, Jr. (1961); and Marvin and others (1962);
- Texas Water Development Board reports: Myers and Dale (1966, 1967); Rogers (1967); Hammond, Jr. (1969); Myers (1969); Sandeen (1972); Shafer and Baker, Jr. (1973); Shafer (1974); Loskot and others (1982); and Christian and Wuerch (2012);
- Evergreen Underground Water Conservation District pumping test in City of Kenedy;
- Corpus Christi Aquifer Storage and Recovery Conservation District feasibility study (HDR Engineering Inc., INTERA Inc, Geochemical Solutions LLC, and Wellspec, 2019); and
- Pumping tests performed by drillers and U. S. Geological Survey that were recorded in TWDB groundwater database scanned driller reports.

This study also calculated 212 hydraulic transmissivity values based on previous pumping test data collected from:

- Confidential site in City of Three Rivers (personal communication with Mr. Kevin Spencer of R. W. Harden & Associates, Inc., February 23, 2015);
- Texas Commission on Environmental Quality public supply well records (via Dr. Steve Young of INTERA, Inc.); and
- TWDB groundwater database scanned driller reports.

After comparing the well construction with the hydrogeological framework, only those wells completely screened in a single hydrogeological unit (Chicot, Evangeline, Burkeville, or Jasper) were selected. Wells with multiple pumping tests were averaged. As a result, a total of 302 unique hydraulic transmissivity/conductivity values were obtained in the

study area: 157 in the Chicot, 91 in the Evangeline, five in the Burkeville, and 49 in the Jasper (Figure 4.5.1). Details of the pumping tests are presented in Table E1 of Appendix E.

#### **4.5.2            *Transmissivity and Hydraulic Conductivity from Specific Capacity Tests***

Specific capacity tests from the following sources were used to estimate hydraulic transmissivity/conductivity values in the study area:

- TWDB groundwater database scanned driller reports for old wells (<https://www.twdb.texas.gov/groundwater/data/drillersdb.asp>);
- TWDB groundwater database digital driller reports for new wells (<https://www.twdb.texas.gov/groundwater/data/drillersdb.asp>); and
- Texas Commission on Environmental Quality plotted well logs (<https://gisweb.tceq.texas.gov/waterwellpublic/>).

Like the pumping test, only wells completely screened in a single hydrogeological unit (Chicot, Evangeline, Burkeville, or Jasper) were selected. Wells with multiple specific capacity tests were averaged. A total of 10,970 unique hydraulic conductivity values were obtained in the study area: 4,440 in the Chicot (Figure 4.5.2), 3,424 in the Evangeline (Figure 4.5.3), 596 in the Burkeville (Figure 4.5.4), and 2,510 in the Jasper (Figure 4.5.5).

#### **4.5.3            *Comparison of Hydraulic Conductivity Values between Pumping Tests and Specific Capacity Tests***

Wells with both pumping tests and specific capacity tests were selected to evaluate the quality of the hydraulic conductivity values from specific capacity tests (Figure 4.5.6) and results are shown in Figure 4.5.7. Figure 4.5.7 indicates that the specific capacity tests generally produced comparable hydraulic conductivity values as the pumping tests.

#### **4.5.4            *Summary of Hydraulic Conductivity Values from Pumping Tests and***

### ***Specific Capacity Tests***

Figures 4.5.8 through 4.5.11 show wells with hydraulic conductivity values from pumping tests and specific capacity tests for the Chicot, Evangeline, Burkeville, and Jasper, respectively, in the study area. If a well had hydraulic conductivity from both types of tests available, only the pumping test was retained. The combination gives a total of 11,174 unique hydraulic conductivity values in the study area: 4,545 in the Chicot, 3,489 in the Evangeline, 600 in the Burkeville, and 2,540 in the Jasper (Table 4.5.1). Details of the pumping tests and specific capacity tests are presented in Table E2 of Appendix E. As shown in Table 4.5.1, the Chicot Aquifer has slightly higher mean and geometric mean horizontal hydraulic conductivity values than the other three, though the Burkeville Unit shows a much lower maximum value.

The distributions of logarithmic hydraulic conductivity values for the Chicot Aquifer, the Evangeline Aquifer, the Burkeville Unit, and the Jasper Aquifer are normal with dominated values ranging from  $10^{1.0}$  or 10 to  $10^{1.5}$  or 32 feet per day (Figure 4.5.12). In comparison with the Evangeline and Burkeville units, however, the Chicot and Jasper aquifers also show higher frequency of hydraulic conductivity values of three to 10 feet per day and 32 to 100 feet per day.

#### ***4.5.5 Correlation between Hydraulic Conductivity and Sand Fraction***

Though pumping tests and specific capacity tests provided many horizontal hydraulic conductivity values in the study area, data gaps still exist. This is especially true for the Burkeville Unit and Jasper Aquifer (Figures 4.5.10 and 4.5.11). To fill the data gaps, sand fraction data derived from Young and others (2010) were used to estimate hydraulic conductivity values at location where pumping tests and specific capacity tests were not available.

Since the framework in this study differs from the one by Young and others (2010) in some locations, new sand fraction associated with the new framework was calculated from the old sand fraction associated with the framework by Young and others (2010) using the following equation:



$$F = \frac{\sum_{n=1}^4 \{F_n * \text{Max}[\text{Min}(B, B_n) - \text{Max}(T, T_n), 0]\}}{(B - T)}$$

Where:

$F$  = new sand fraction (dimensionless)

$B$  = bottom of new framework (feet below ground)

$T$  = top of new framework (feet below ground)

$F_n$  = old sand fraction from Young and others (2010) (dimensionless)

$B_n$  = bottom of old framework from Young and others (2010) (feet below ground)

$T_n$  = top of old framework from Young and others (2010) (feet below ground)

$n = 1$  (Chicot),  $2$  (Evangeline),  $3$  (Burkeville), and  $4$  (Jasper)

Figures 4.5.13 through 4.5.16 show the new sand fraction in the Chicot Aquifer, Evangeline Aquifer, Burkeville Unit, and Jasper Aquifer, respectively.

To convert the new sand fraction data to horizontal hydraulic conductivity, a correlation between these two must be found first. Since the sand fraction data from Young and others (2010) were from geophysical log interpolation, they might not reflect the true sand fraction of well screens where pumping test or specific capacity test were performed. In addition, well screens are rarely consistent with the framework. As a result, the sand fraction from Young and others (2010) was not used to correlate the hydraulic conductivity. Rather a selected group of wells were used for this study. These wells must meet the following criteria:

- reliable hydraulic conductivity from pumping test;
- clear lithological description; and

- simple screens in a single hydrogeologic unit (Chicot, Evangeline, Burkeville, and Jasper).

Clear lithologic description means that only wells with sand and clay/shale across screens were selected. Wells with simple screens means that only wells with single, double, or triple screens and enough separation between screens were selected to minimize impacts from packers. This yielded 67 wells: 44 in the Chicot, six in the Evangeline, one in the Burkeville, and 16 in the Jasper.

The new sand fraction ( $F$ ) across well screens was calculated using the following equation:

$$F = B_s/B$$

Where:

$B_s$  = total thickness of sand across well screen(s)

$B$  = total length of screen(s)

Figure 4.5.17 indicates some linear correlation between horizontal hydraulic conductivity and sand fraction in the Chicot Aquifer. A moderate linear correlation is observed in the Evangeline Aquifer (Figure 4.5.18). The Jasper Aquifer shows a weak or no linear correlation between the two (Figure 4.5.19). Because only one well exists in the Burkeville Unit, correlation between horizontal hydraulic conductivity and sand fraction could not be evaluated for the unit. As a result, the regression equations from the Evangeline and Jasper aquifers were averaged to represent Burkeville. The regression equations between horizontal hydraulic conductivity ( $K_h$ ) and sand fraction ( $F$ ) for the four hydrogeologic units are as follows:

- Chicot:  $K_h = 71.238 * F + 0.1$
- Evangeline:  $K_h = 28.244 * F + 0.05$
- Burkeville:  $K_h = 27.973 * F + 0.026$

- Jasper:  $K_h = 27.702 * F + 0.002$

The equation intercept was selected to be slightly lower than the minimum horizontal hydraulic conductivity value for the unit from pumping tests and specific capacity tests as shown in [Table 4.5.1](#). This produces  $K_h$  value equal to the intercept when the sand fraction is zero.

After converting the new sand fraction to horizontal hydraulic conductivity, values within one mile of pumping tests and specific capacity tests were removed, and the rest were combined with the hydraulic conductivity values from the pumping tests and specific capacity tests. This dataset, combined with control points in Mexico, was gridded using SURFER and then converted to the horizontal hydraulic conductivity raster under ArcGIS 10.7 ([Figures 4.5.20](#) through [4.5.23](#)). [Table 4.5.2](#) shows the rasters representing the horizontal hydraulic conductivity fields across the study area had consistent values as the pumping test and specific capacity test as shown in [Table 4.5.1](#). However, areas with pumping tests and specific capacity tests do show greater heterogeneity than the rest where the hydraulic conductivity was defined by the sand fraction. In addition, [Tables 4.5.1](#) and [4.5.2](#) indicate no significant difference between the Burkeville Unit and the other three aquifers.

As a preliminary verification, the horizontal hydraulic conductivity from this study was compared with the result from the pumping tests by Uranium Energy Corp (2008) in northern Goliad County. The pumping tests by Uranium Energy Corp were located on the northern side of FM-1961 about one mile east of Highway 77/183 and performed in Middle Goliad Formation (Sand Zone B). The pumping tests produced average transmissivity values of 747 and 968 square feet per day or hydraulic conductivity values of 37 and 48 feet per day at observation wells related to pumping wells PTW-1 and PTW-6, respectively. In comparison, the hydraulic conductivity at the same location from this study as shown in [Figure 4.5.21](#) is about 20 feet per day. It is likely the lower value was a result of including the lower permeable Upper Fleming (Lagarto) Formation as part of the Evangeline Aquifer in this study. The pumping tests by Uranium Energy Corp (2008) also produced average storativity values of 0.00024 and 0.0006, while [Figure 4.5.26](#) shows 0.0005 from this study.

Though the one-point verification cannot be expanded to the whole study area, it does provide some confidence about the method that was used to estimate hydraulic conductivity and storativity values in this study.

#### **4.5.6            *Storativity and Specific Yield***

Previous studies have produced 66 storativity or specific yield values from pumping tests in the study area. These studies included:

- Former Texas Board of Water Engineers bulletins: Dale and others (1957); Anders (1960); and Anders and Baker, Jr. (1961);
- Texas Water Development Board reports: Baker, Jr. (1965); Rogers (1967); Myers and Dale (1967); Hammond, Jr. (1969); Myers (1969); Sandeen (1972); and Shafer (1974);
- Evergreen Underground Water Conservation District pumping test in the City of Kenedy;
- Corpus Christi Aquifer Storage and Recovery Conservation District feasibility study (HDR Engineering Inc., INTERA Inc, Geochemical Solutions LLC, and Wellspec, 2019); and
- Pumping tests performed by drillers and the U. S. Geological Survey that were recorded in TWDB groundwater database scanned driller reports.

This study also calculated 52 storativity or specific yield values based on previous pumping test data collected from:

- Confidential site in the City of Three Rivers (personal communication with Mr. Kevin Spencer of R. W. Harden & Associates, Inc., February 23, 2015);
- Texas Commission on Environmental Quality public supply well records (via Dr. Steve Young of INTERA, Inc.); and,

- TWDB groundwater database scanned driller reports.

After comparing the well construction with the hydrogeological framework, only those wells completely screened in a single hydrogeological unit (Chicot, Evangeline, Burkeville, or Jasper) were selected. Results of multiple pumping tests in the same wells were averaged. As a result, a total of 100 unique values were obtained in the study area: 38 in the Chicot Aquifer, 39 in the Evangeline Aquifer, three in the Burkeville Unit, and 20 in the Jasper Aquifer (Figure 4.5.24). Details of the pumping tests are presented in Table E3 of Appendix E.

Figure 4.5.24 indicates huge data gaps for all four units. As described in previous section, storage is primarily controlled by aquifer type (confined versus unconfined). Since the Gulf Coast Aquifer System is mainly composed of sand layers interbedded with clay/shale, the storage should show a trend from unconfined to confined conditions or decrease with increasing depth due to increasing clay/shale layers and farther away from water table. In addition, coarser medium such as sand and gravels tend to have greater storage values than fine-grained sediments such as silty sand and clay. As a result, storage is expected to decrease with depth and increase with sand fraction.

Of 100 storage values from pumping tests, only 20 have reliable sand fraction data across well screens. As a result, the sand fraction data for the new framework recalculated from Young and others (2010) were used for this study (see Figures 4.5.13 through 4.5.16). In addition, only a single correlation (regression) between storage ( $S$ ) and sand fraction ( $F$ ) and well middle screen depth ( $D$ ) was made for all four units and shown in the following equation:

$$S = 2.48436612382925 * F - 0.00108223982277531 * D - 4.42489275454066$$

After calculating storage from sand fraction and depth, values within one mile of pumping tests with available storage values were removed, and the rest were combined with the pumping test values. This dataset, combined with control points in Mexico, was gridded using SURFER and then converted to the storage raster under ArcGIS 10.7. As shown in Figures 4.5.25 through 4.5.28, the storage values decrease from outcrop to downdip area

for all four units. In the Chicot outcrop area, the maximum storage was about 0.13, which is close to the specific yield of a sand-clay interbedded medium (Figure 4.5.25). The maximum storage values for the other three units were much lower than Chicot (Figures 4.5.26 through 4.5.28), showing a combination of unconfined and confined conditions in the outcrop area. Further downdip, all four units indicate confined conditions with storage values close to  $1.0E-4$  to  $1.0E-6$ . The low storage for the Chicot is more likely due to wells screened in the deeper sections that are separated from water table by clay, and therefore act more confined than unconfined. For the Evangeline Aquifer, the Burkeville Unit, and the Jasper Aquifer with similar geologic composition (sand interbedded with clay), the specific yields of these units are expected to range from 0.1 to 0.2. The values likely go down with increasing clay content and up with higher sand and gravel.

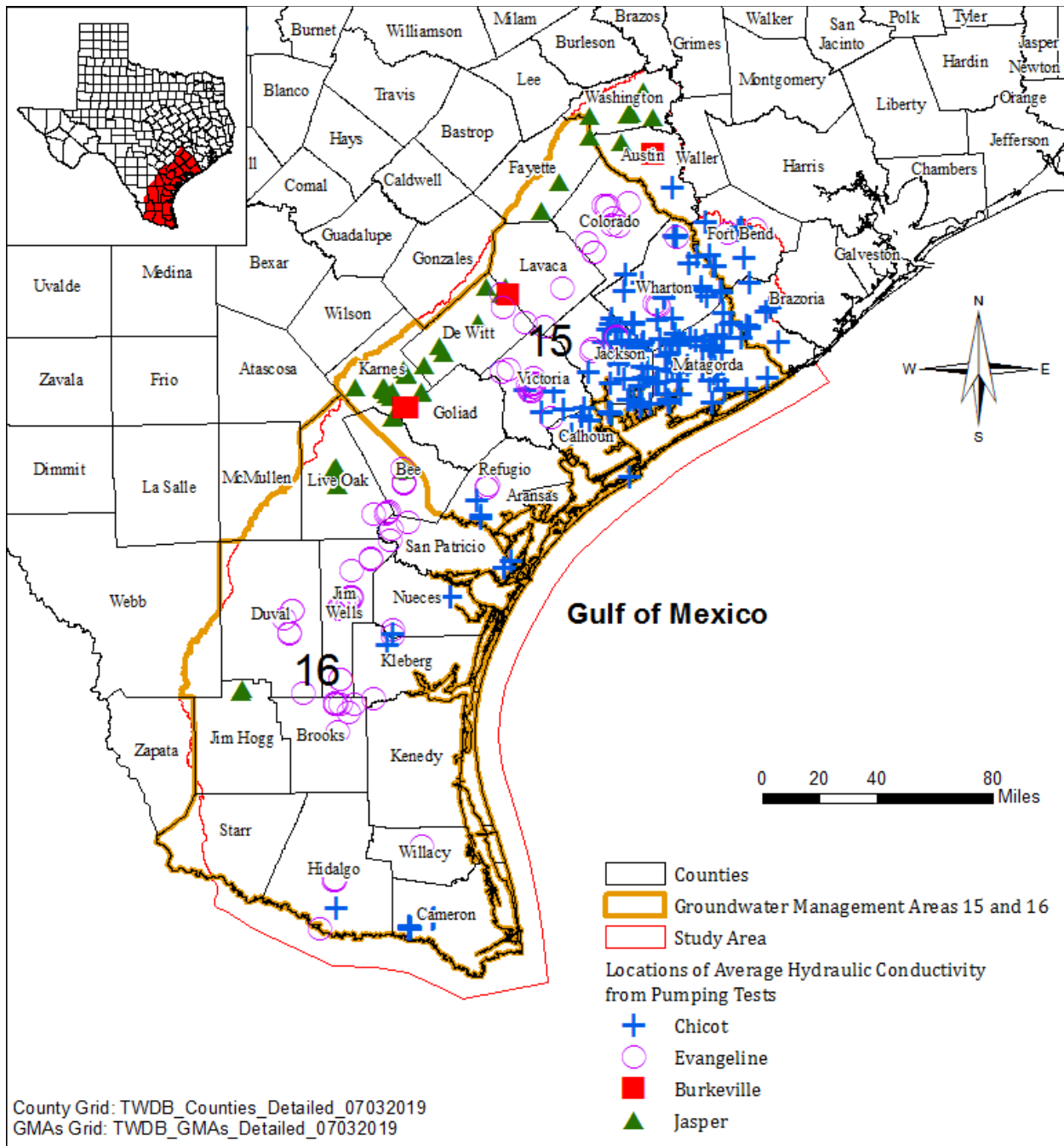


**Figure 4.5.1** Distribution of average horizontal hydraulic conductivity values from pumping tests in the study area.

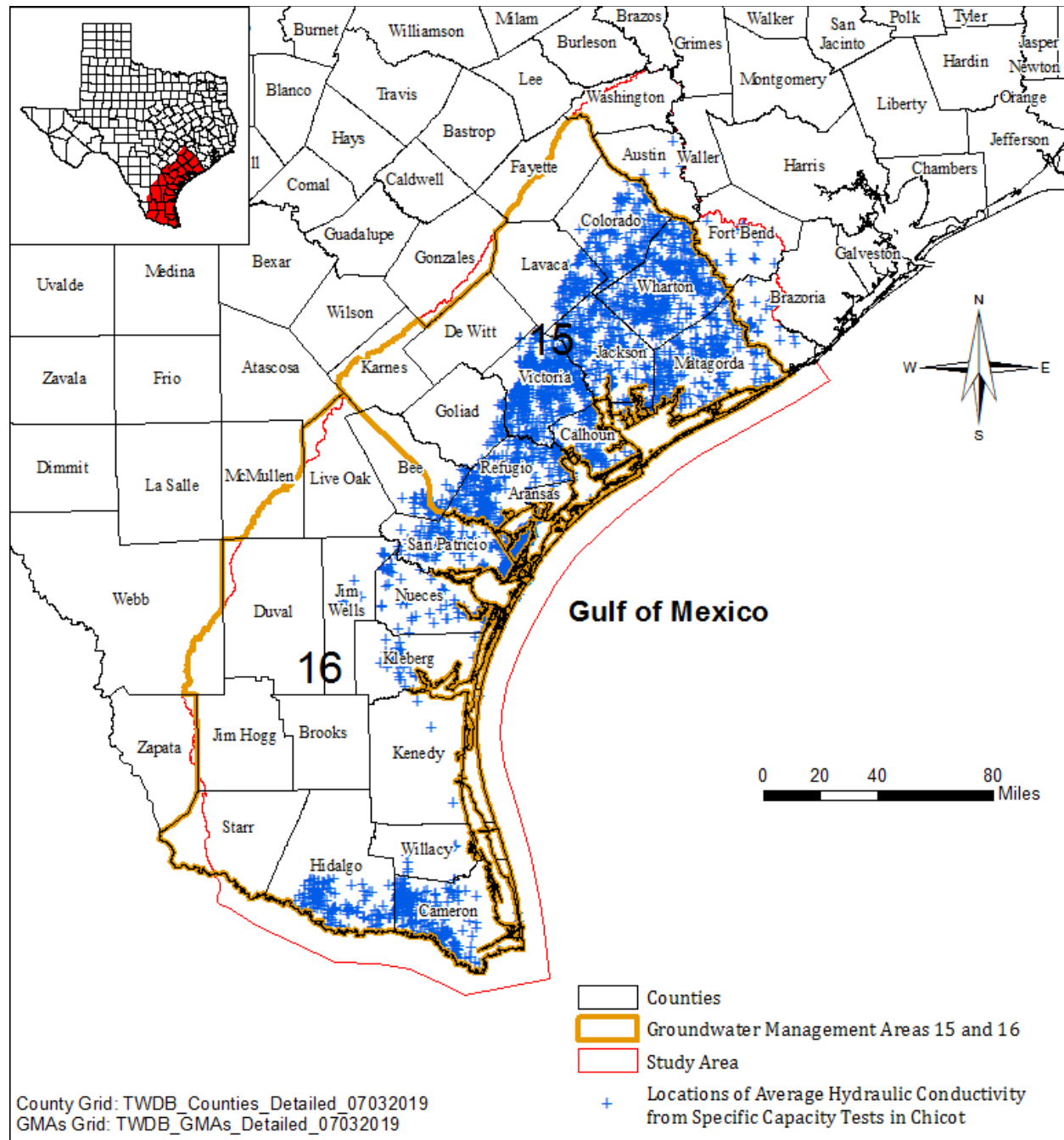


**Figure 4.5.2** Distribution of average horizontal hydraulic conductivity values from specific capacity tests in Chicot Aquifer in the study area.



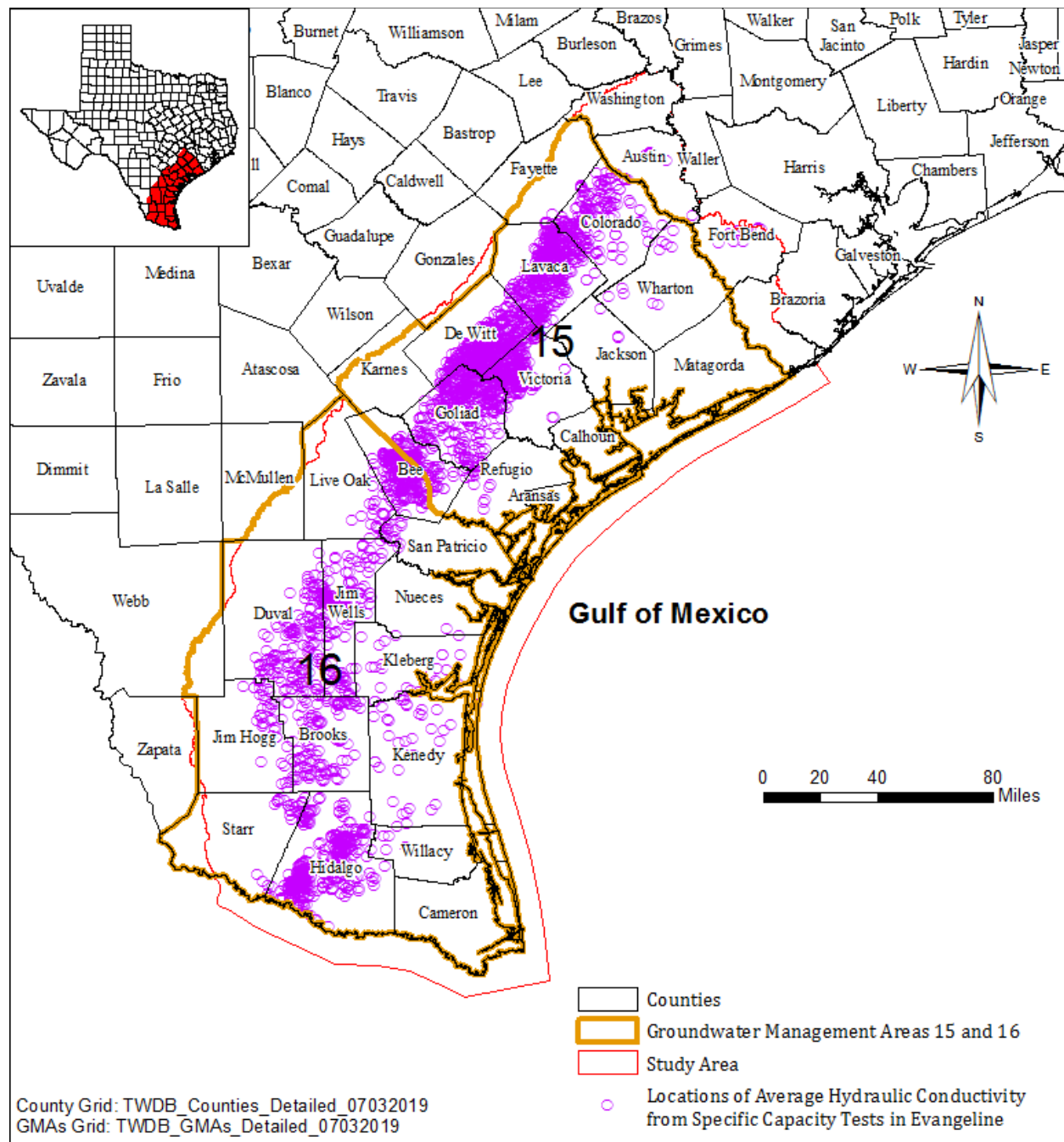


**Figure 4.5.3** Distribution of average horizontal hydraulic conductivity values from specific capacity tests in Evangeline Aquifer in the study area.

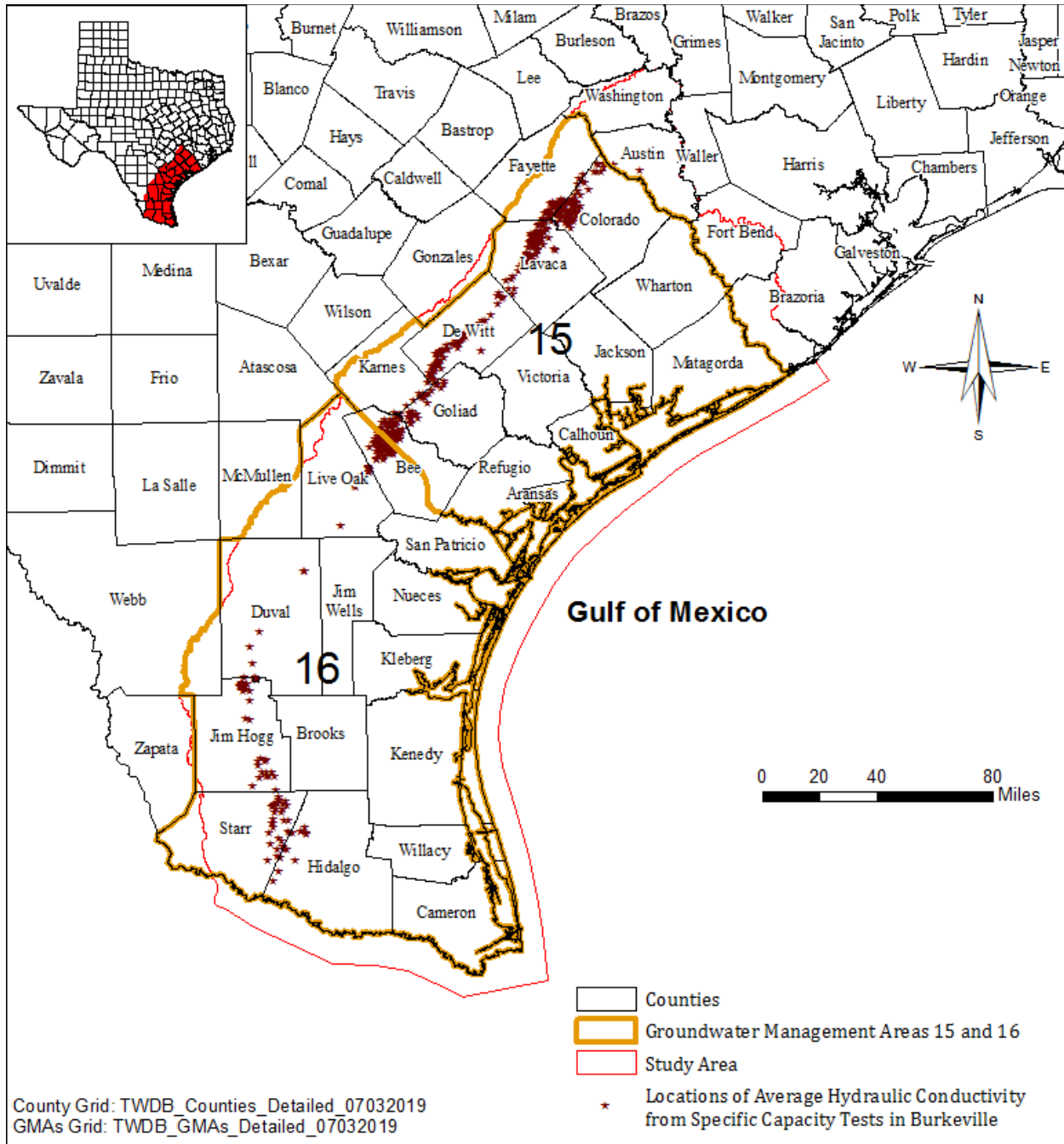


**Figure 4.5.4** Distribution of average horizontal hydraulic conductivity values from specific capacity tests in Burkeville Unit in the study area.

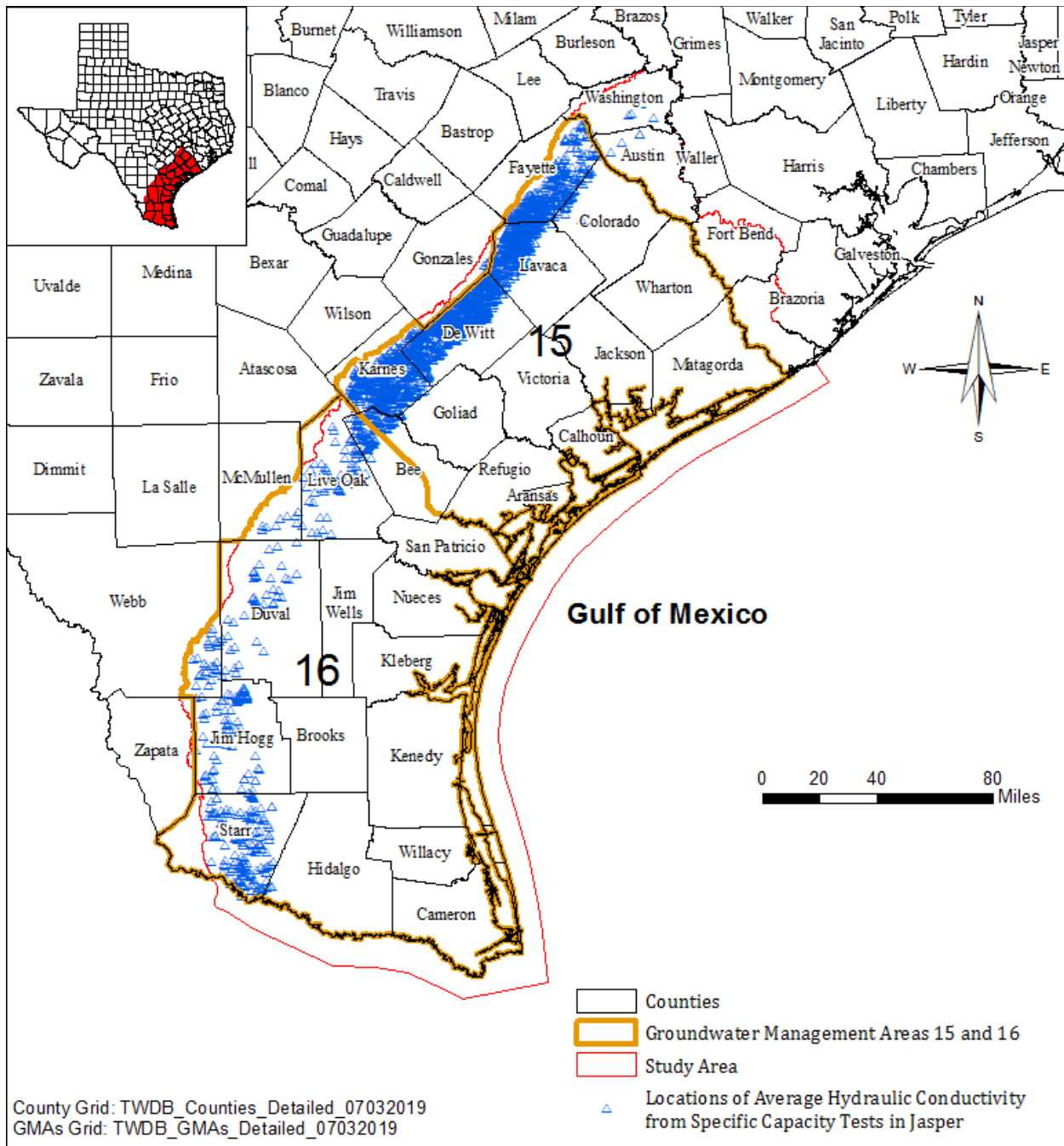


**Figure 4.5.5 Distribution of average horizontal hydraulic conductivity values from specific capacity tests in Jasper Aquifer in the study area.**

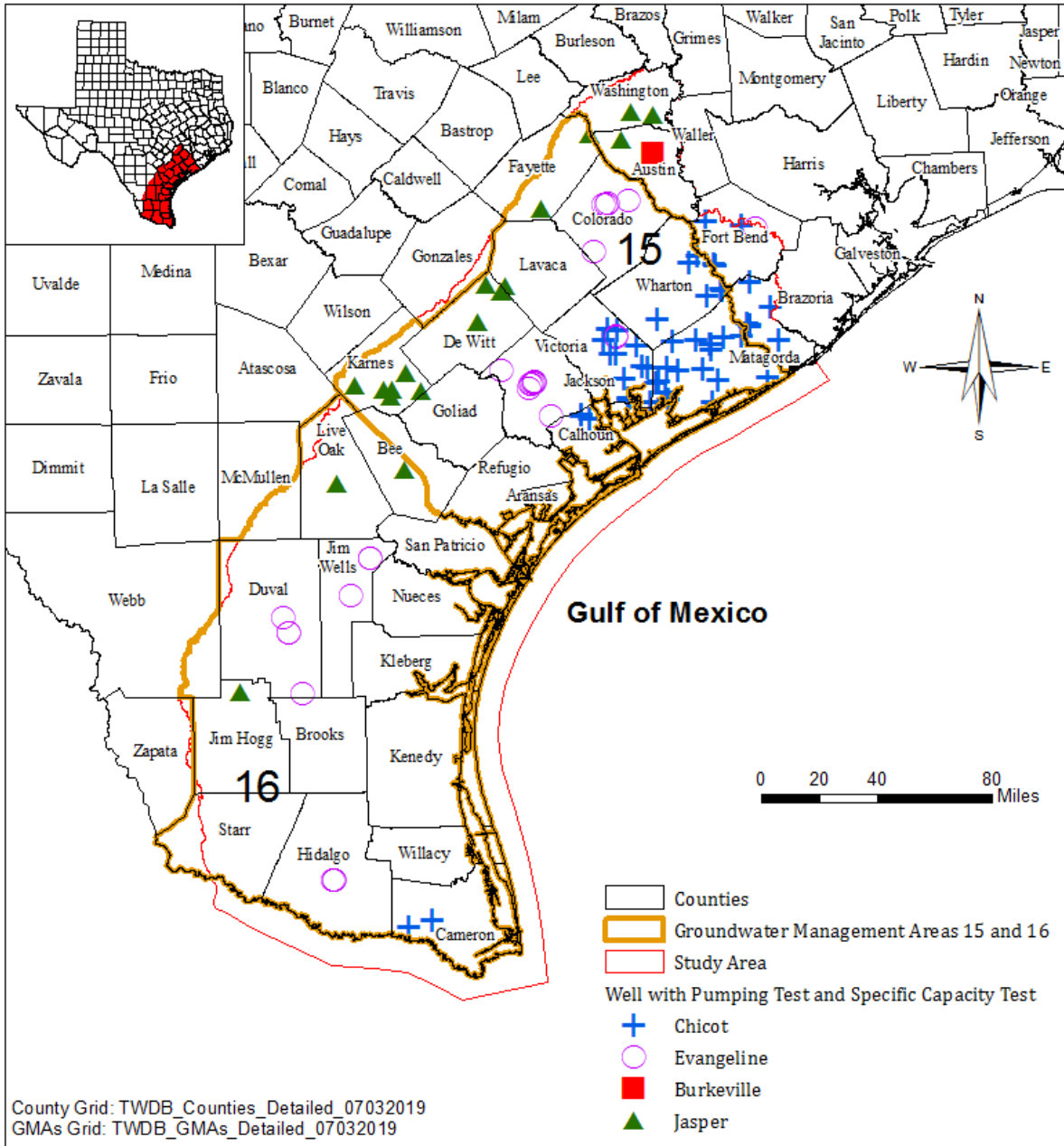


**Figure 4.5.6      Distribution of wells with pumping tests and specific capacity tests.**

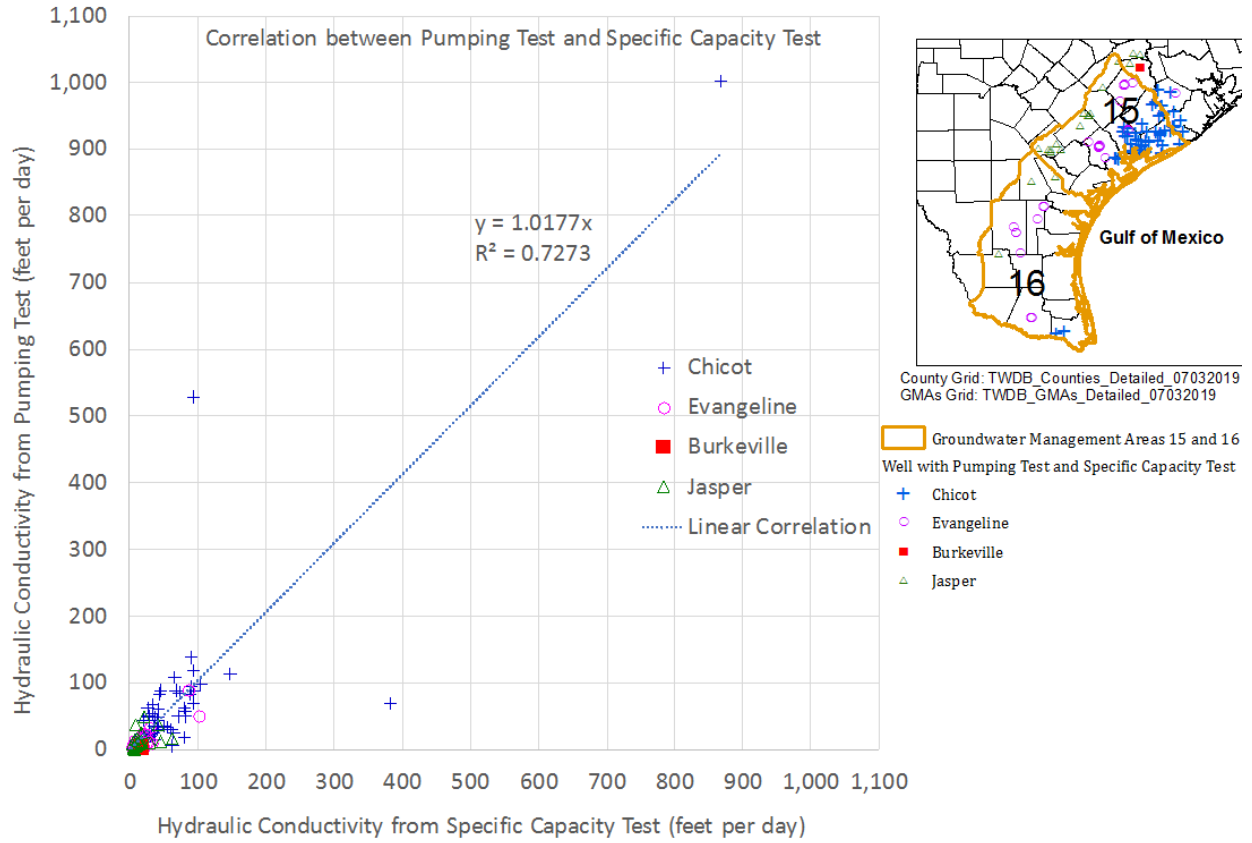


**Figure 4.5.7 Correlation of horizontal hydraulic conductivity values between pumping tests and specific capacity tests.**

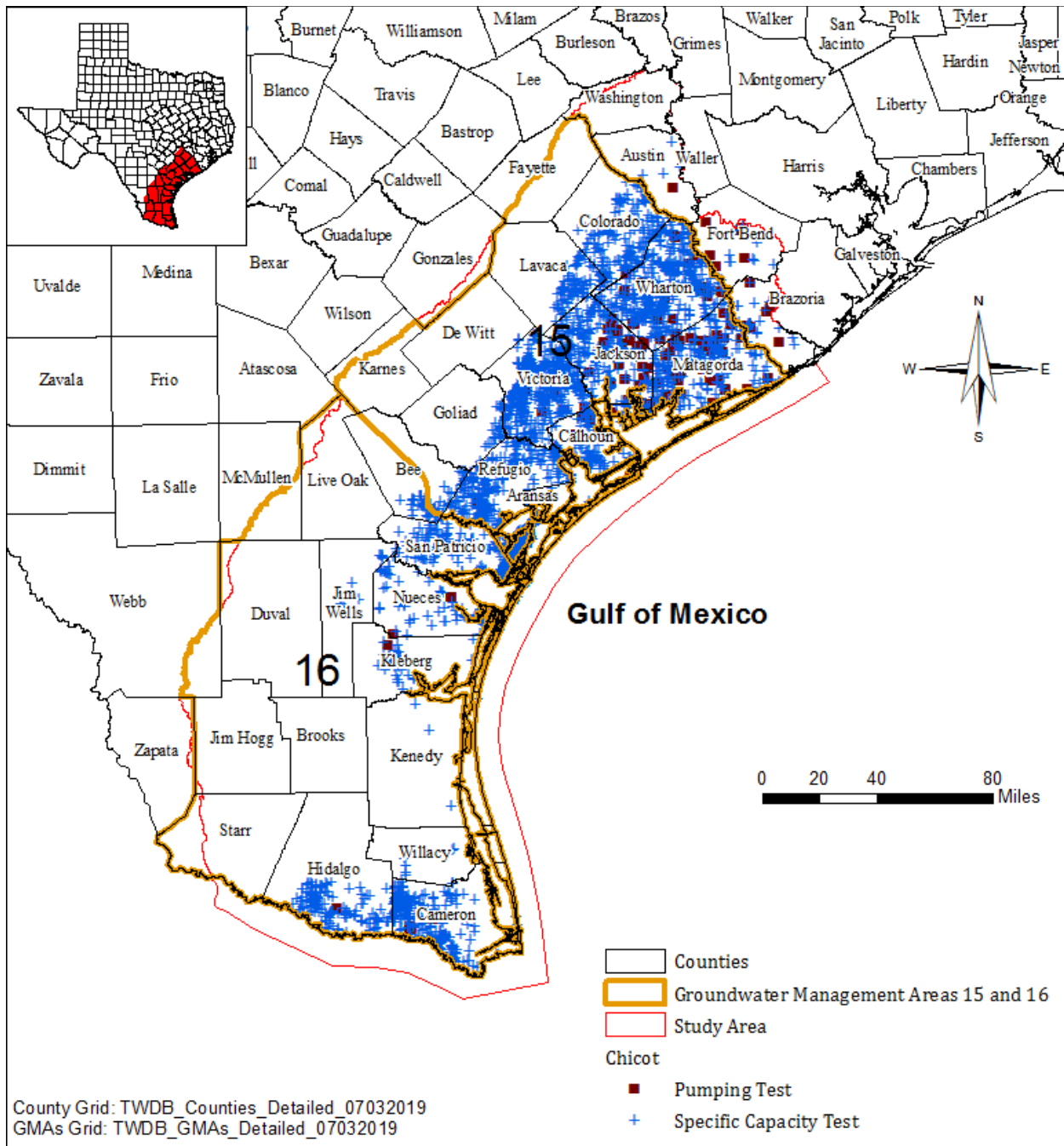


**Figure 4.5.8** Distribution of average horizontal hydraulic conductivity values from pumping tests and specific capacity tests in Chicot Aquifer in the study area.

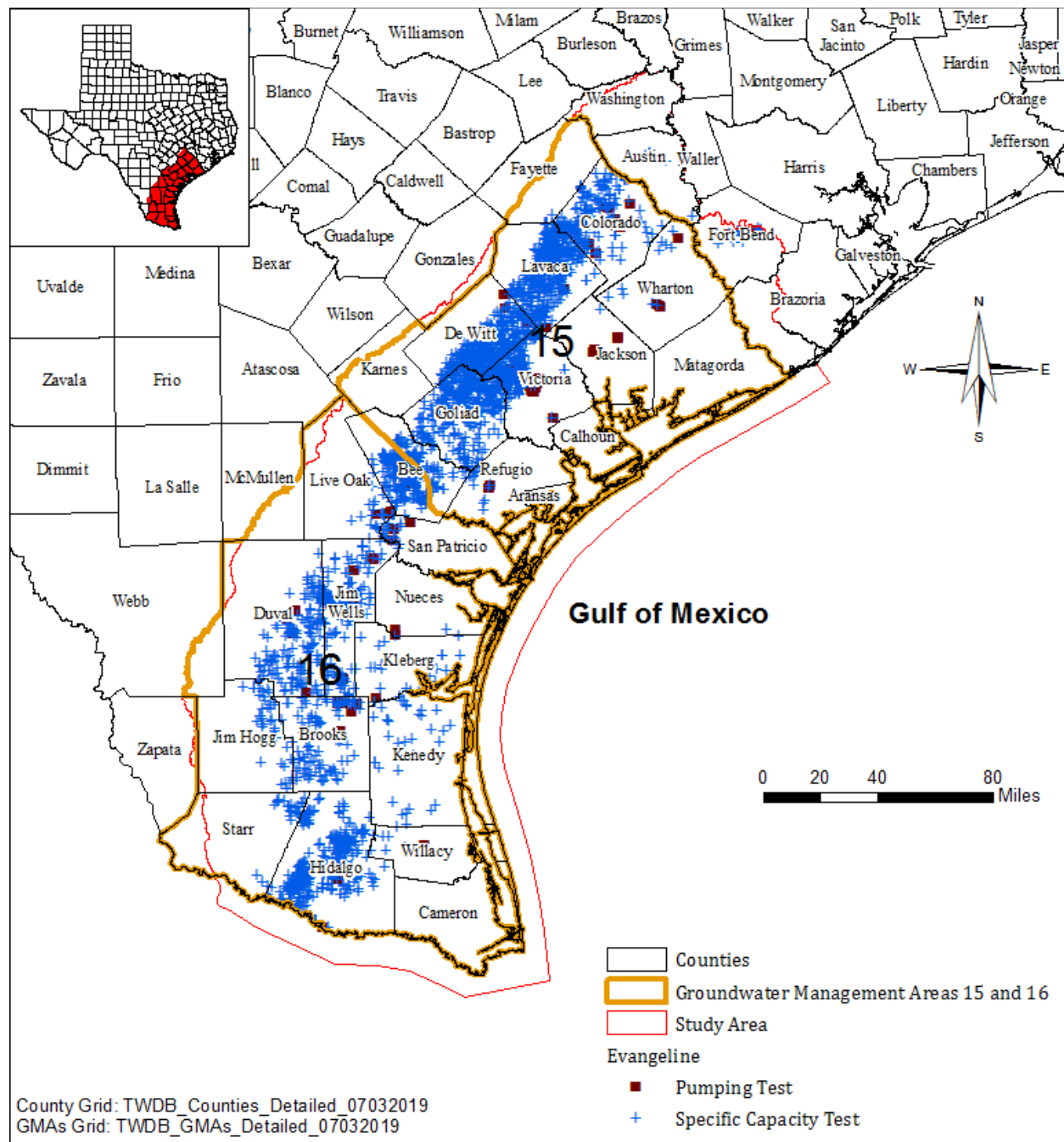


**Figure 4.5.9** Distribution of average horizontal hydraulic conductivity values from pumping tests and specific capacity tests in Evangeline Aquifer in the study area.



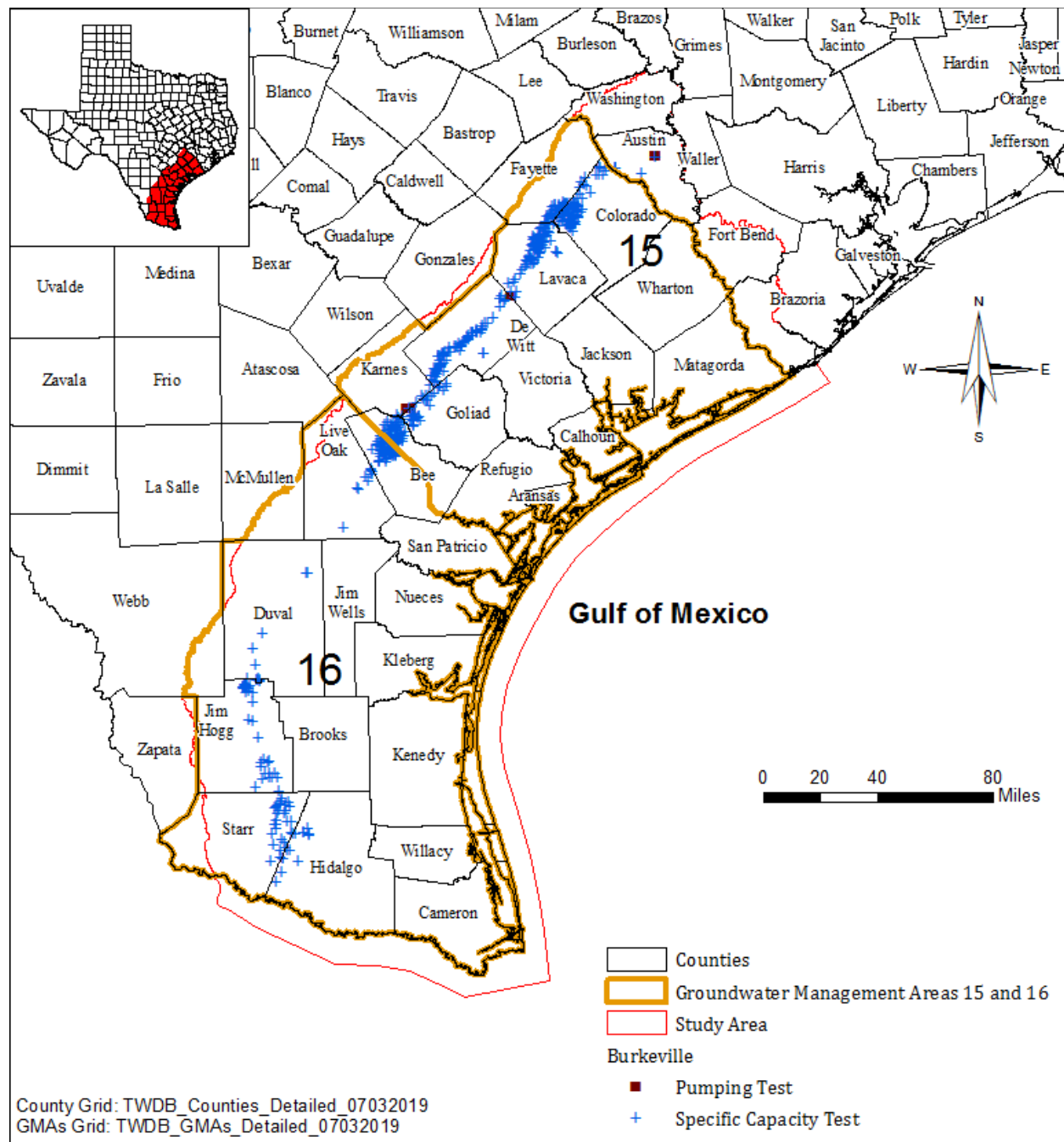


**Figure 4.5.10** Distribution of average horizontal hydraulic conductivity values from pumping tests and specific capacity tests in Burkeville Unit in the study area.

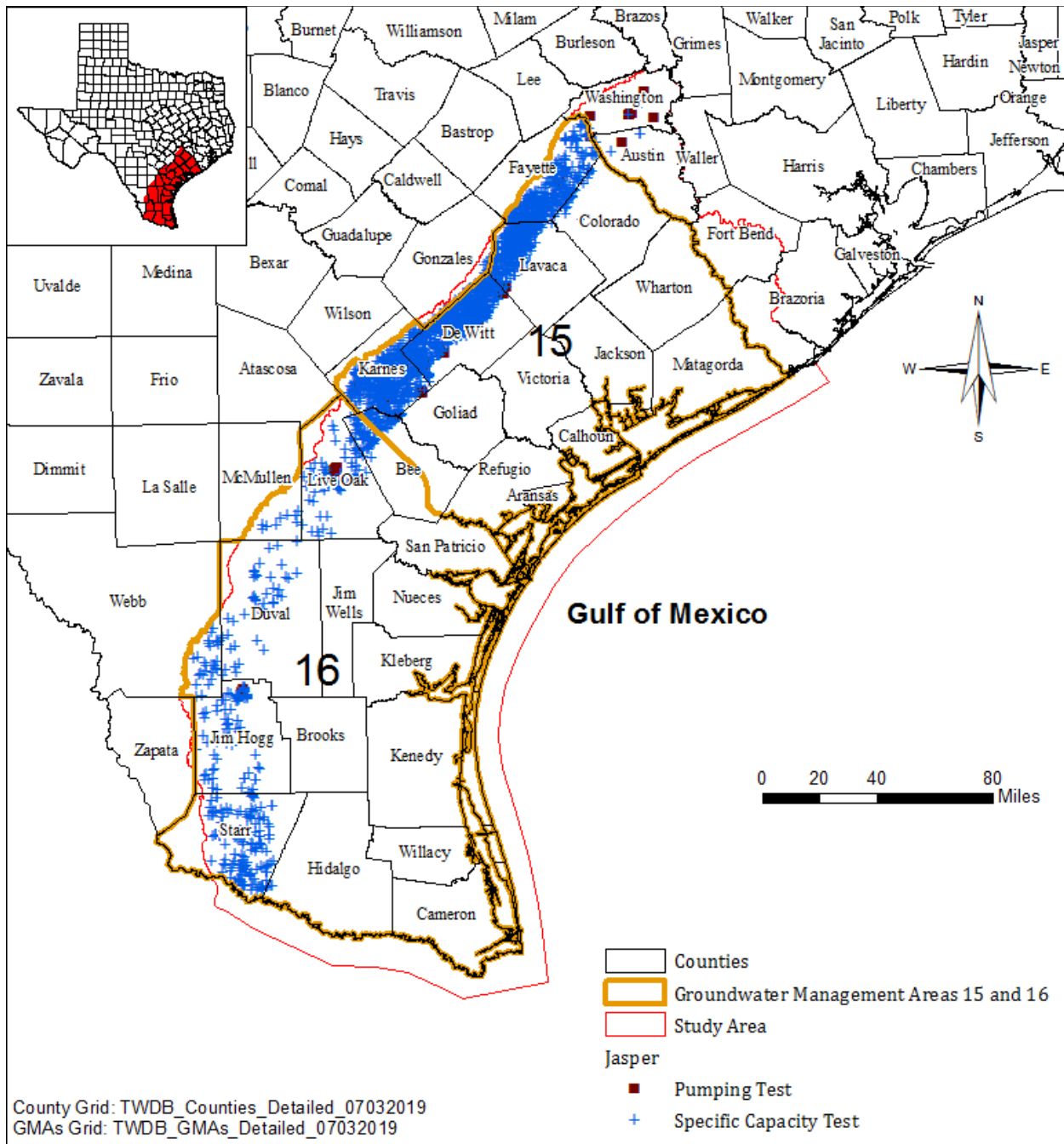


**Figure 4.5.11** Distribution of average horizontal hydraulic conductivity values from pumping tests and specific capacity tests in Jasper Aquifer in the study area.

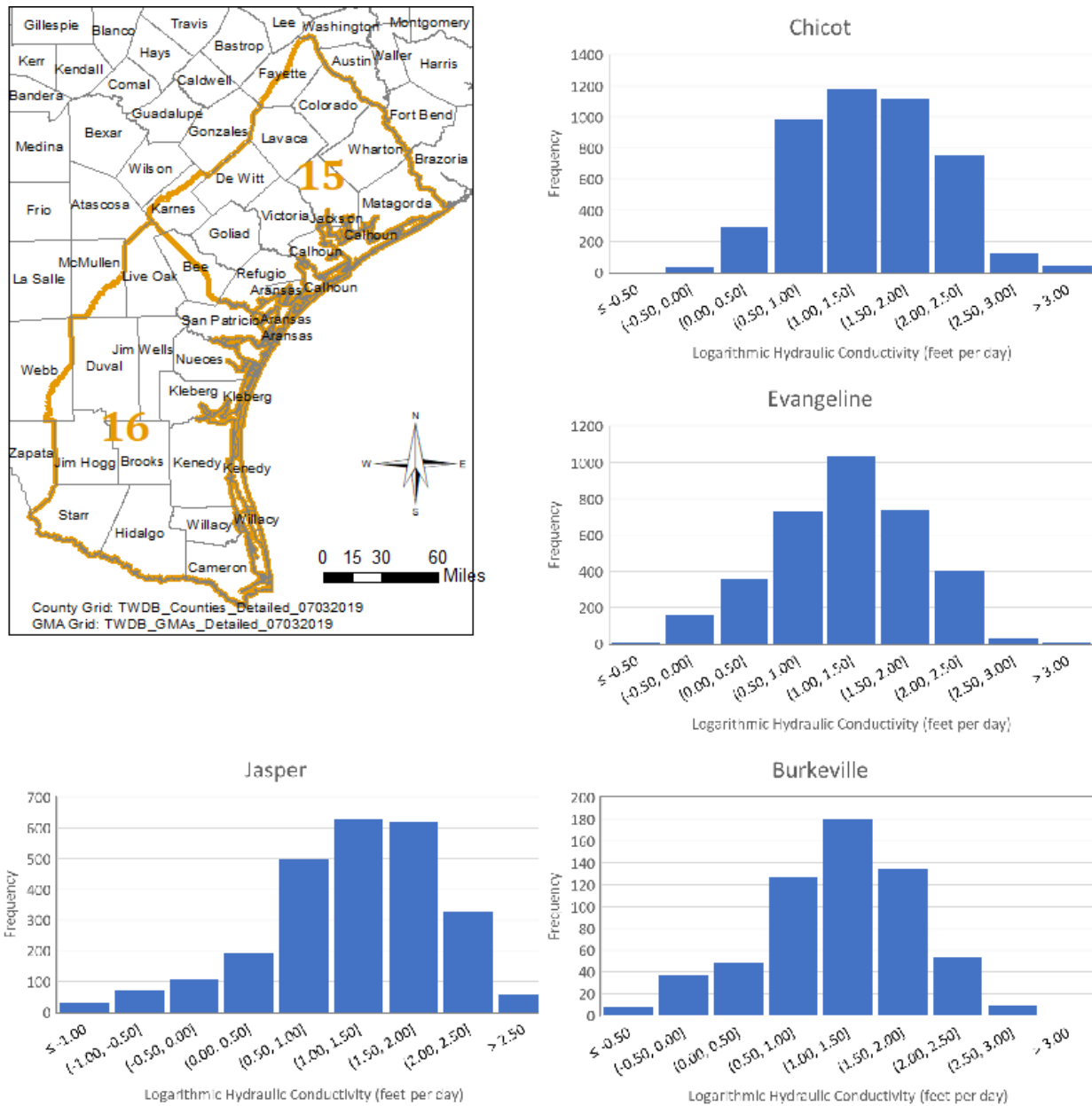


**Figure 4.5.12** Histograms of logarithmic hydraulic conductivity values from Chicot Aquifer, Evangeline Aquifer, Burkeville Unit, and Jasper Aquifer in the study area.

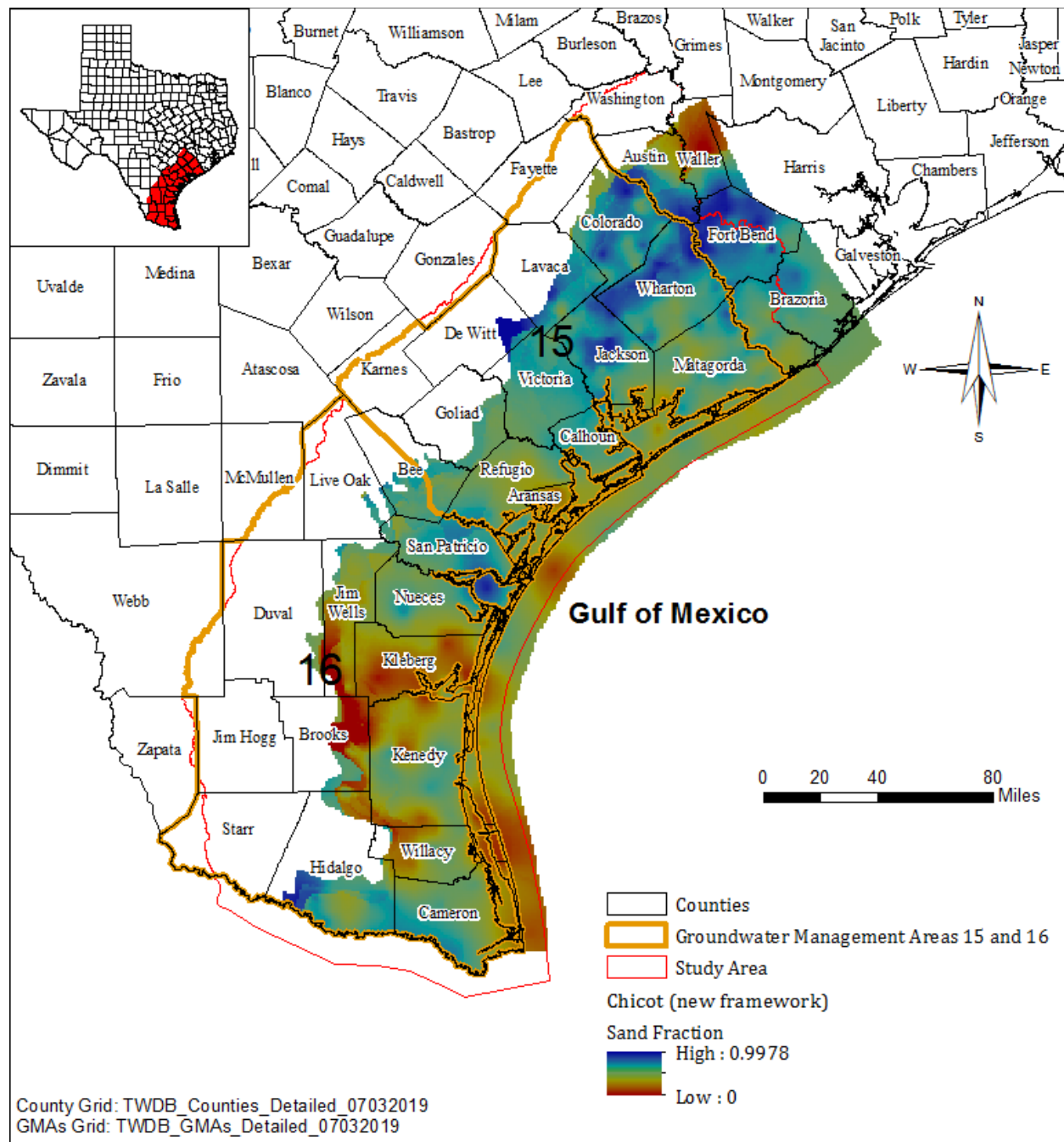


**Figure 4.5.13 Sand fraction in Chicot Aquifer based on new framework.**

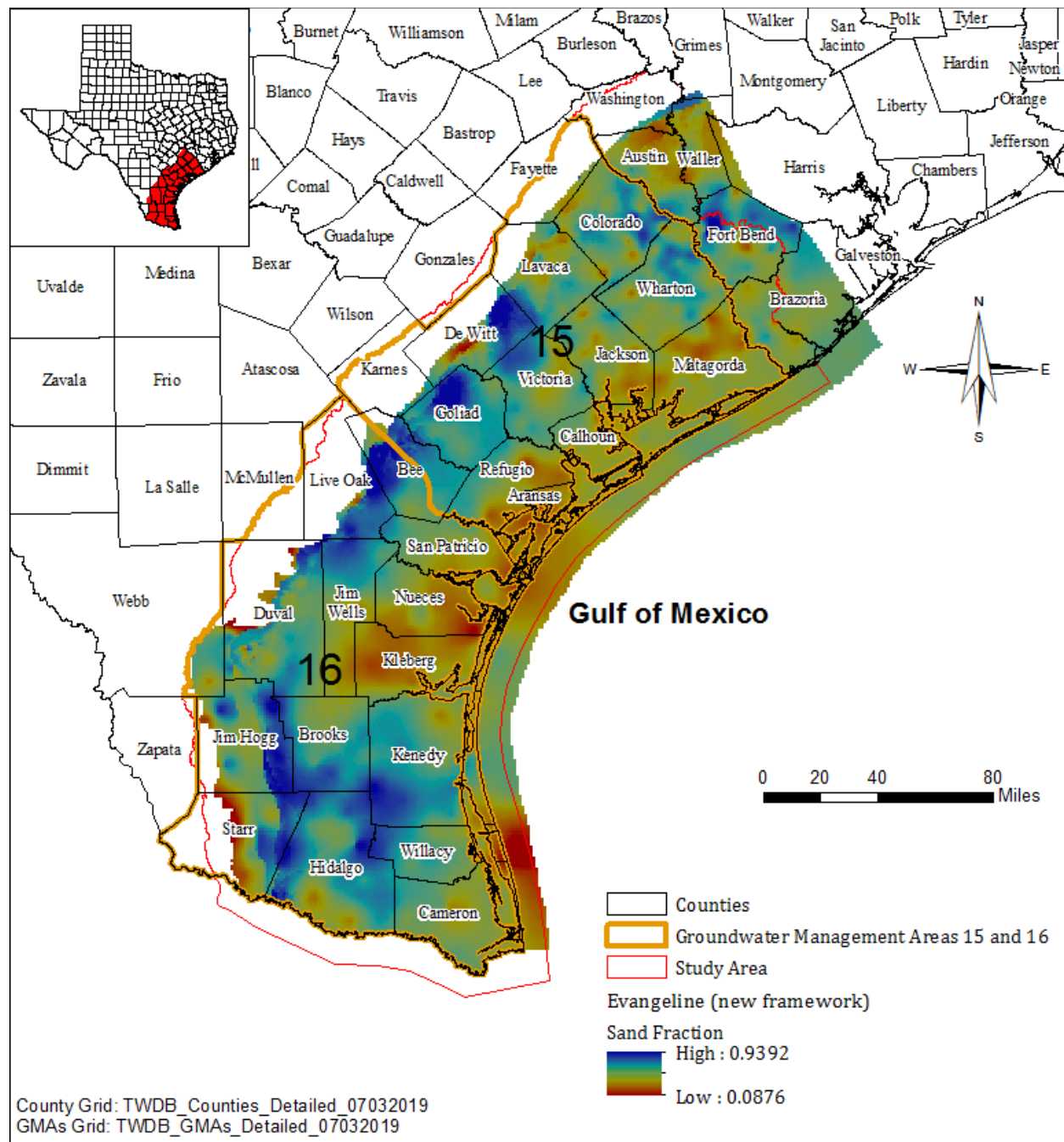


**Figure 4.5.14 Sand fraction in Evangeline Aquifer based on new framework.**

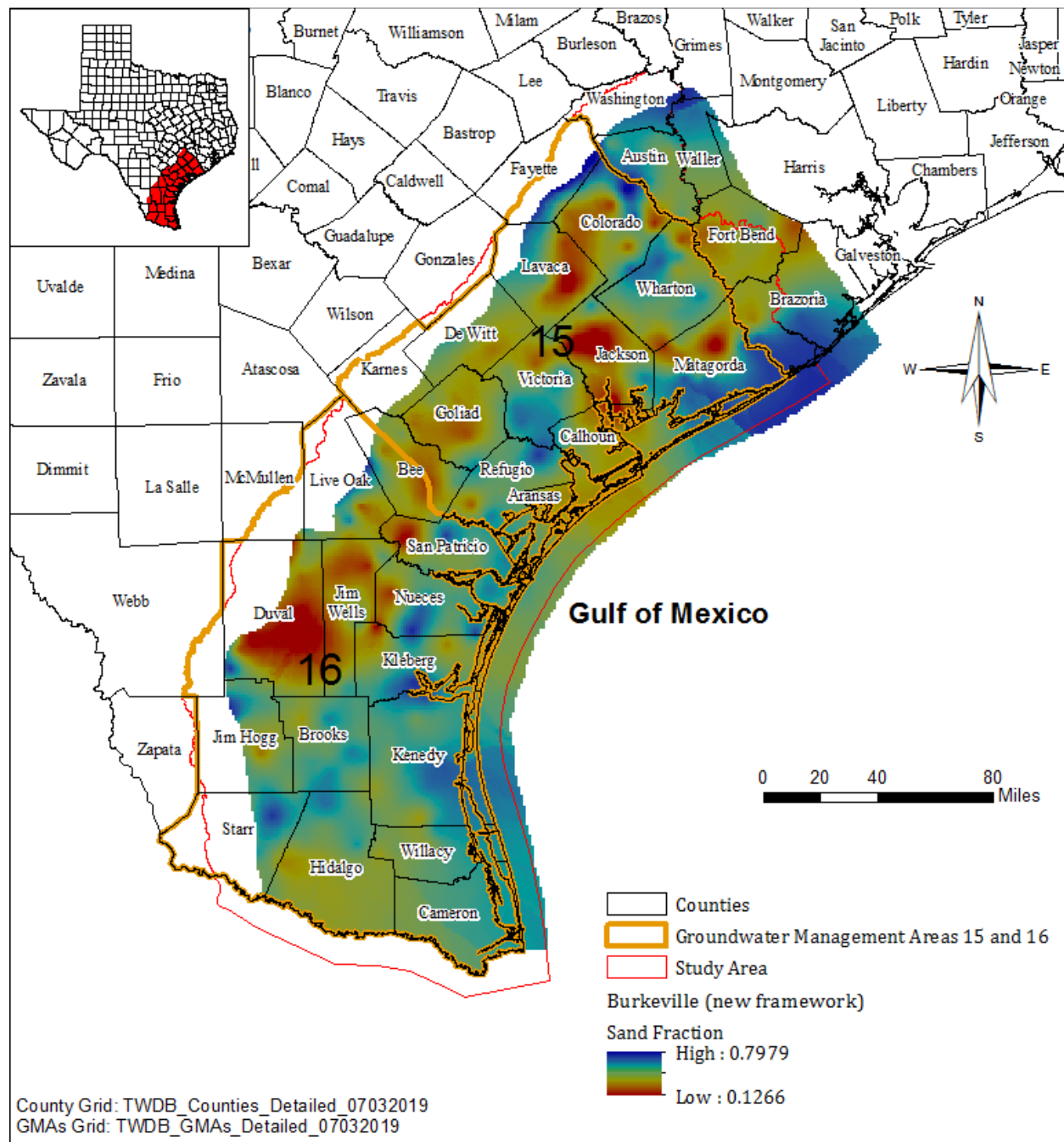


**Figure 4.5.15 Sand fraction in Burkeville Unit based on new framework.**

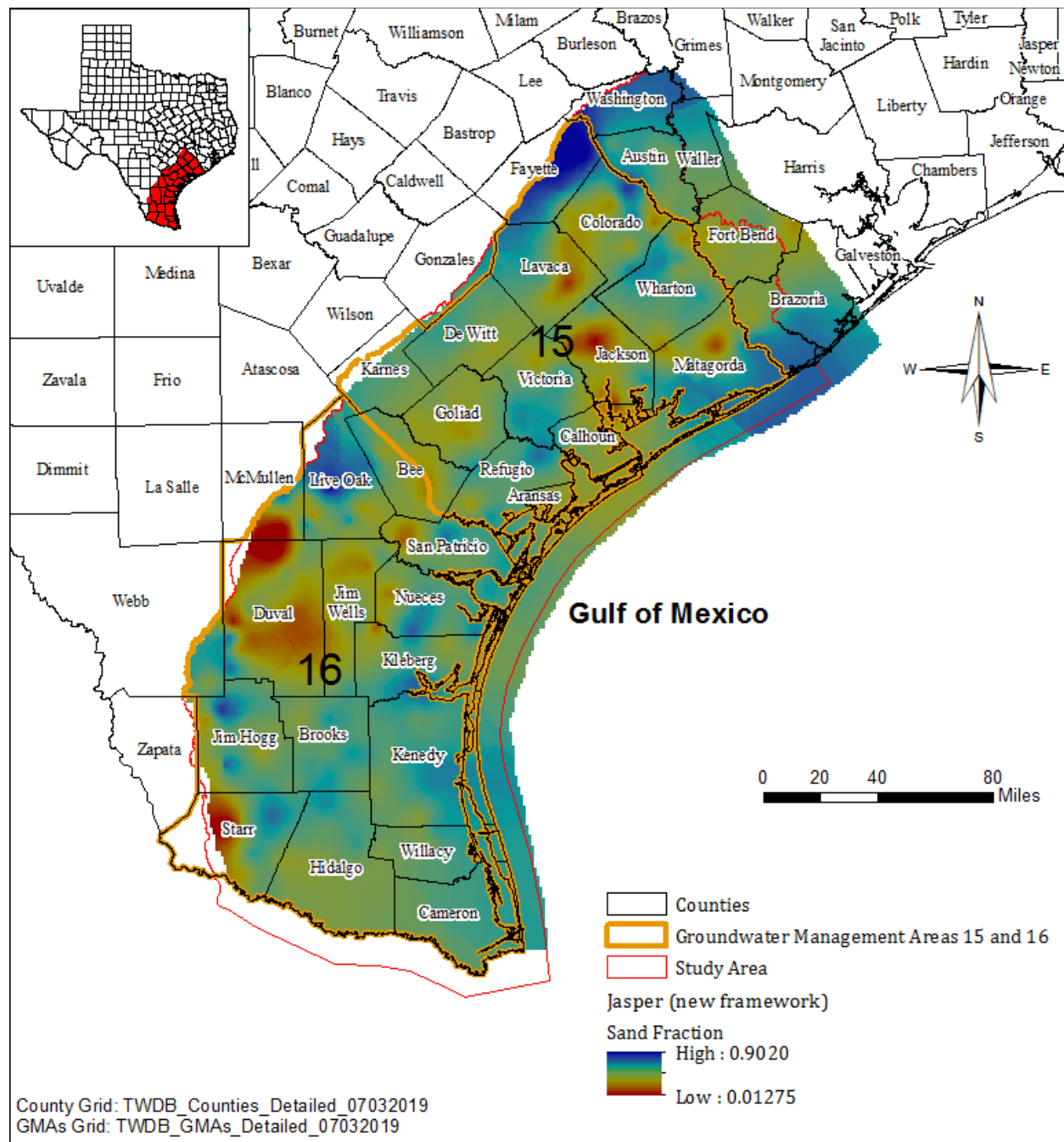


**Figure 4.5.16 Sand fraction in Jasper Aquifer based on new framework.**

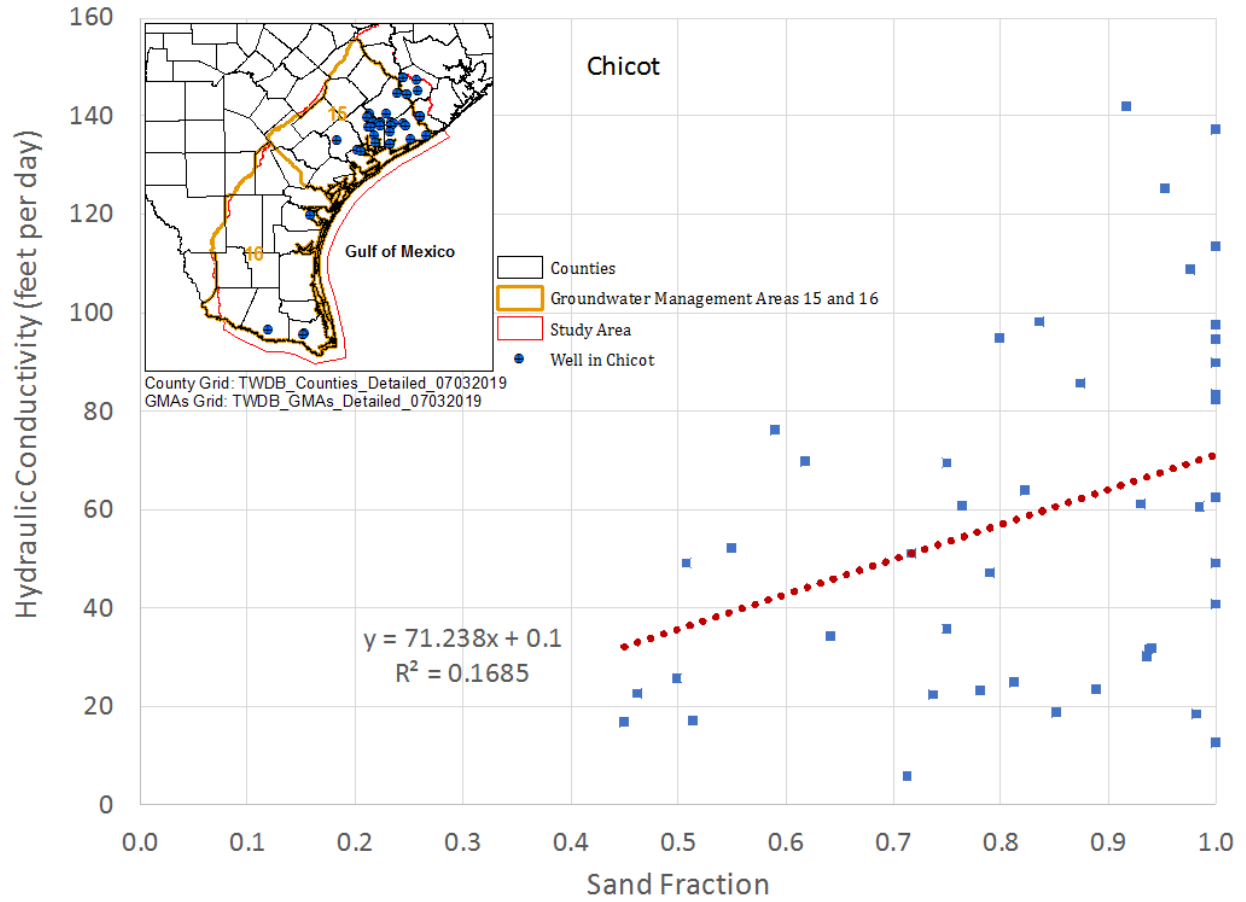


**Figure 4.5.17 Correlation between horizontal hydraulic conductivity and sand fraction in Chicot Aquifer.  $R^2$  value indicates some linear correlation.**



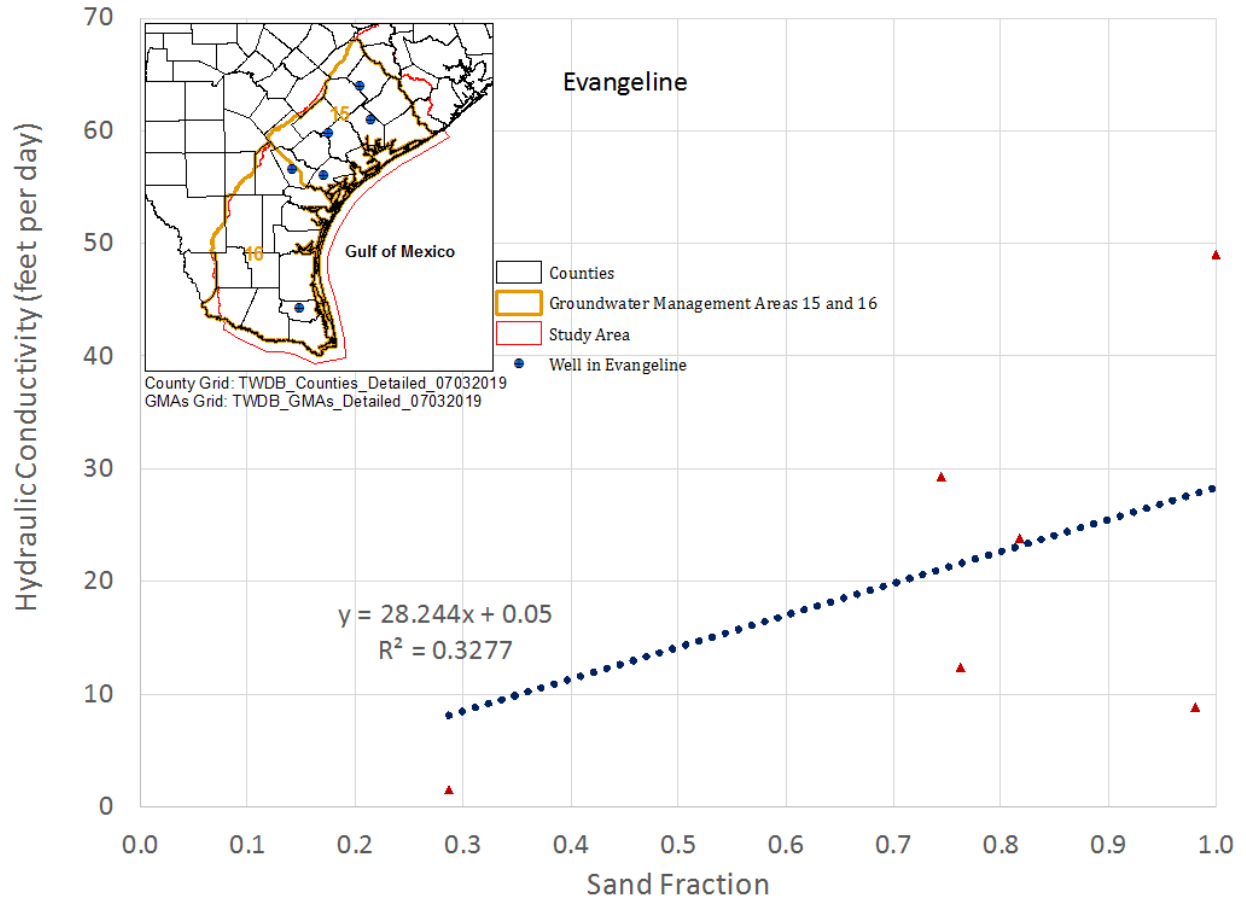


**Figure 4.5.18** Correlation between horizontal hydraulic conductivity and sand fraction in Evangeline Aquifer.  $R^2$  value indicates moderate linear correlation.

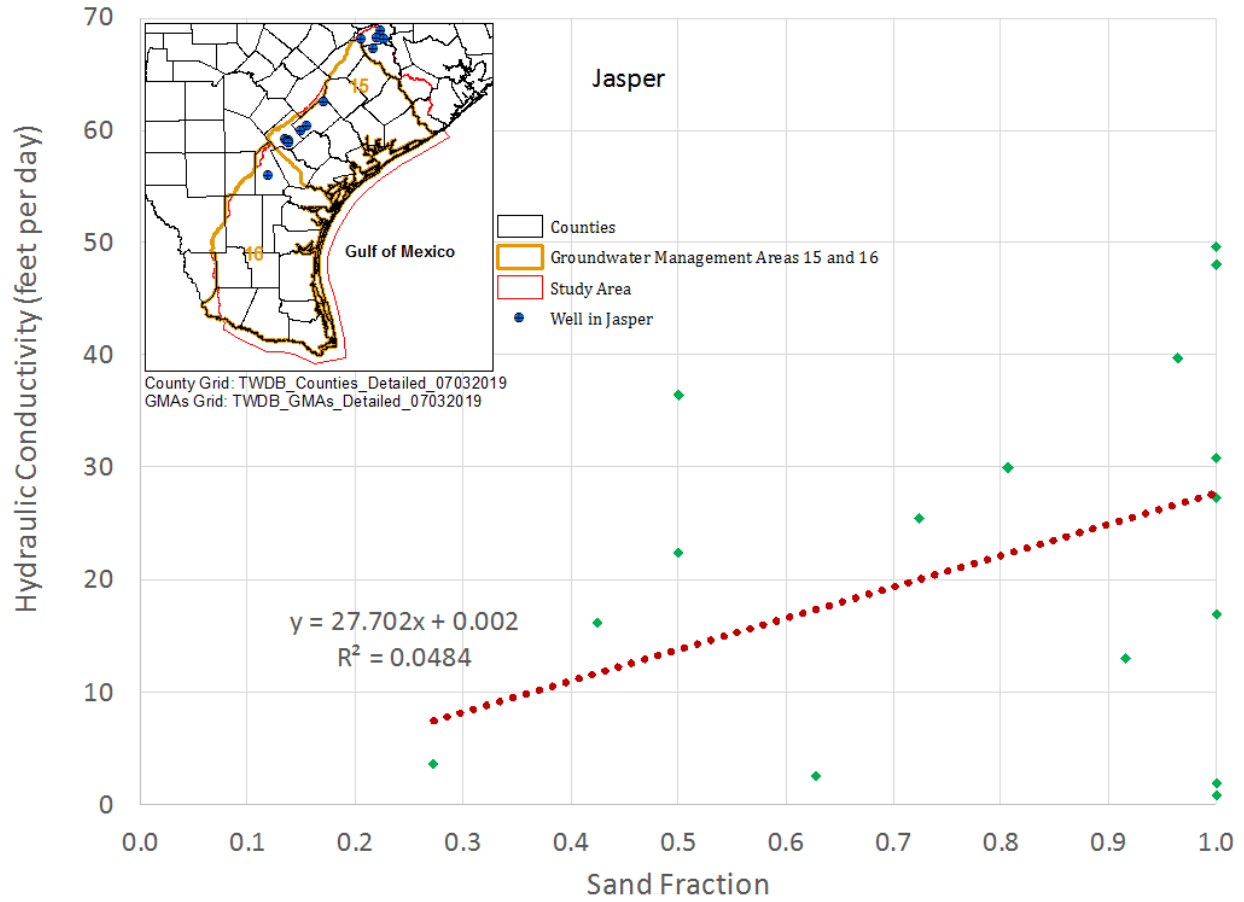


**Figure 4.5.19 Correlation between horizontal hydraulic conductivity and sand fraction in Jasper Aquifer. R<sup>2</sup> value indicates weak linear correlation.**

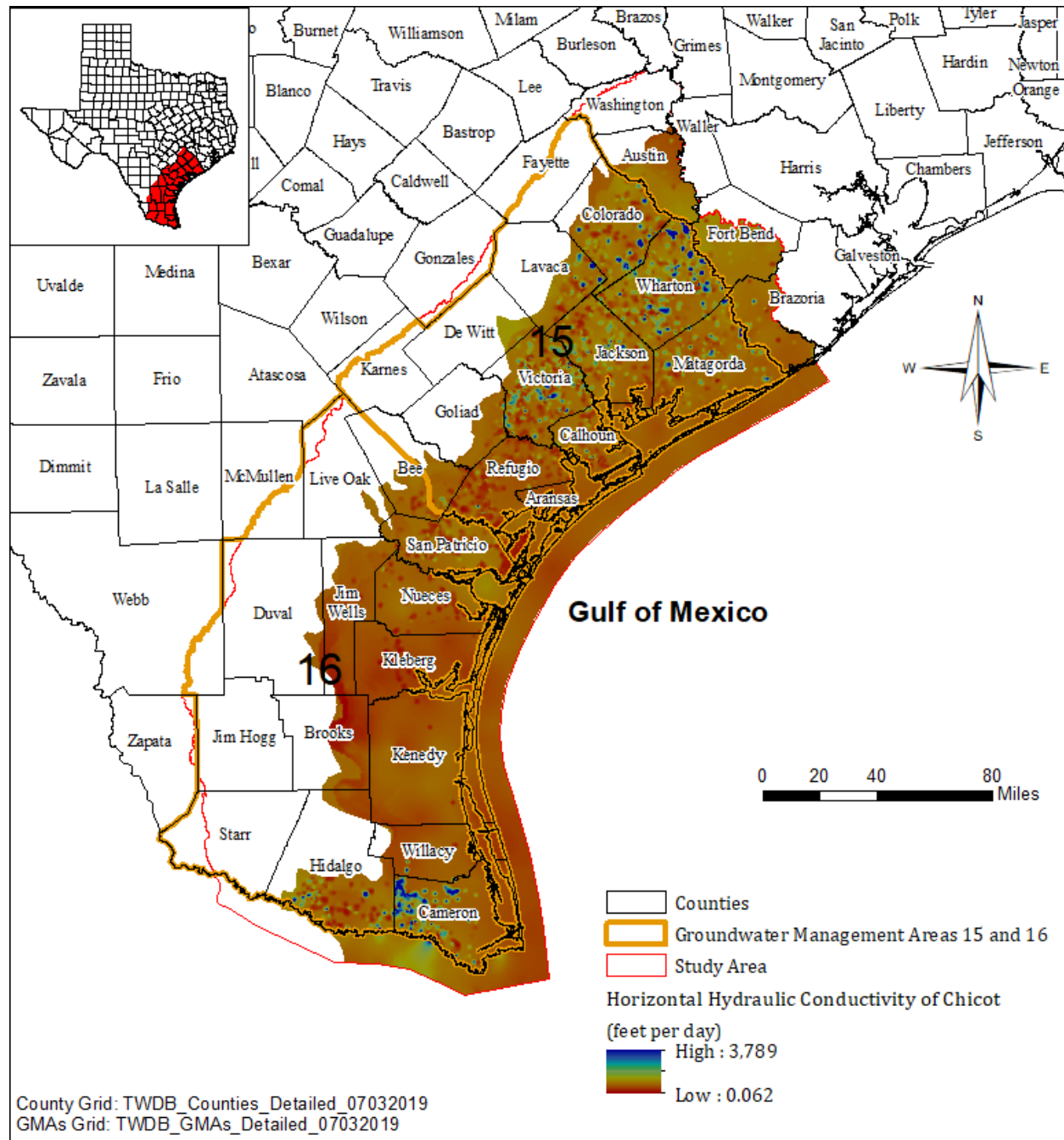


**Figure 4.5.20** Distribution of horizontal hydraulic conductivity value for Chicot Aquifer in the study area.

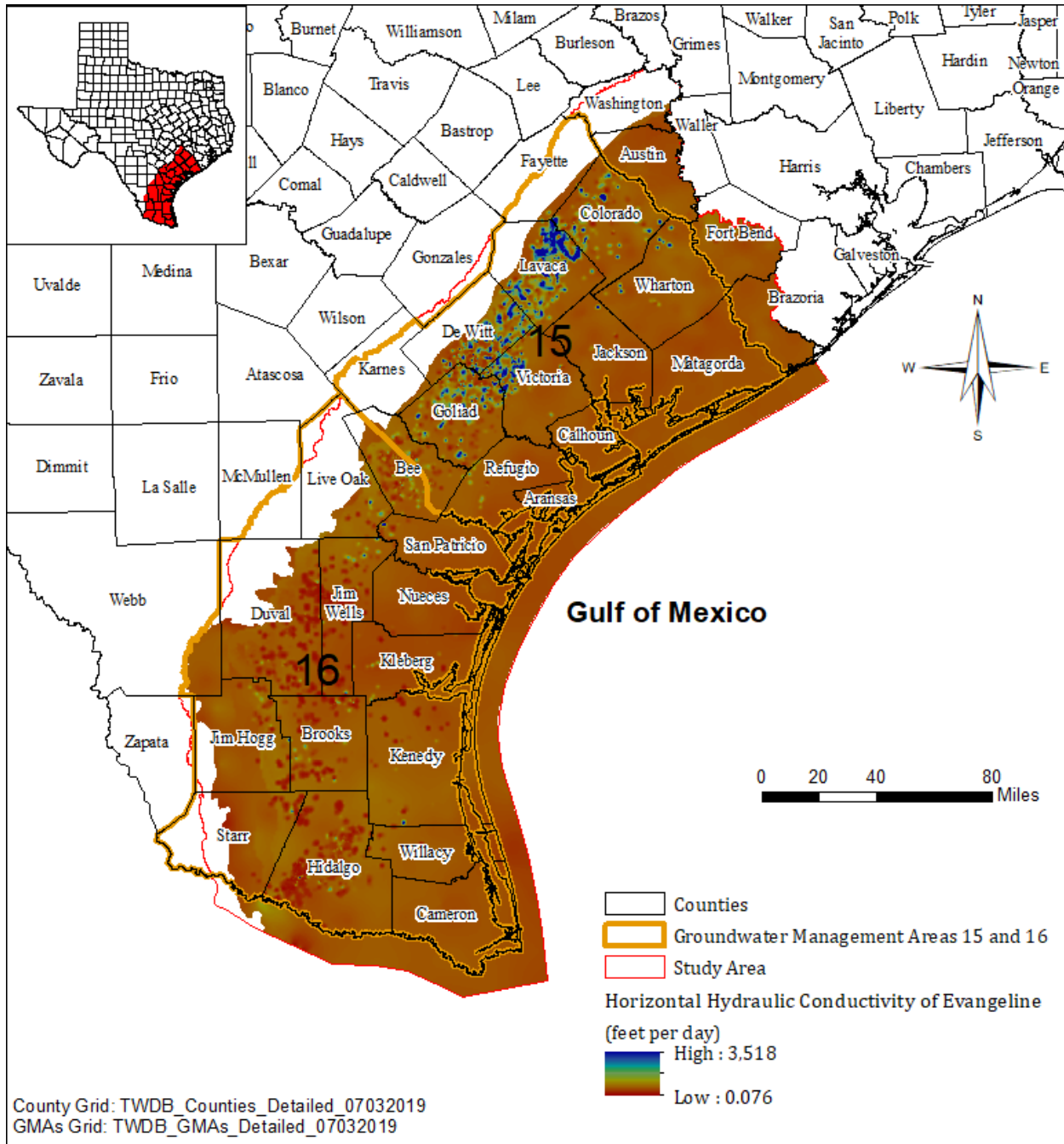


**Figure 4.5.21** Distribution of horizontal hydraulic conductivity value for Evangeline Aquifer in the study area.

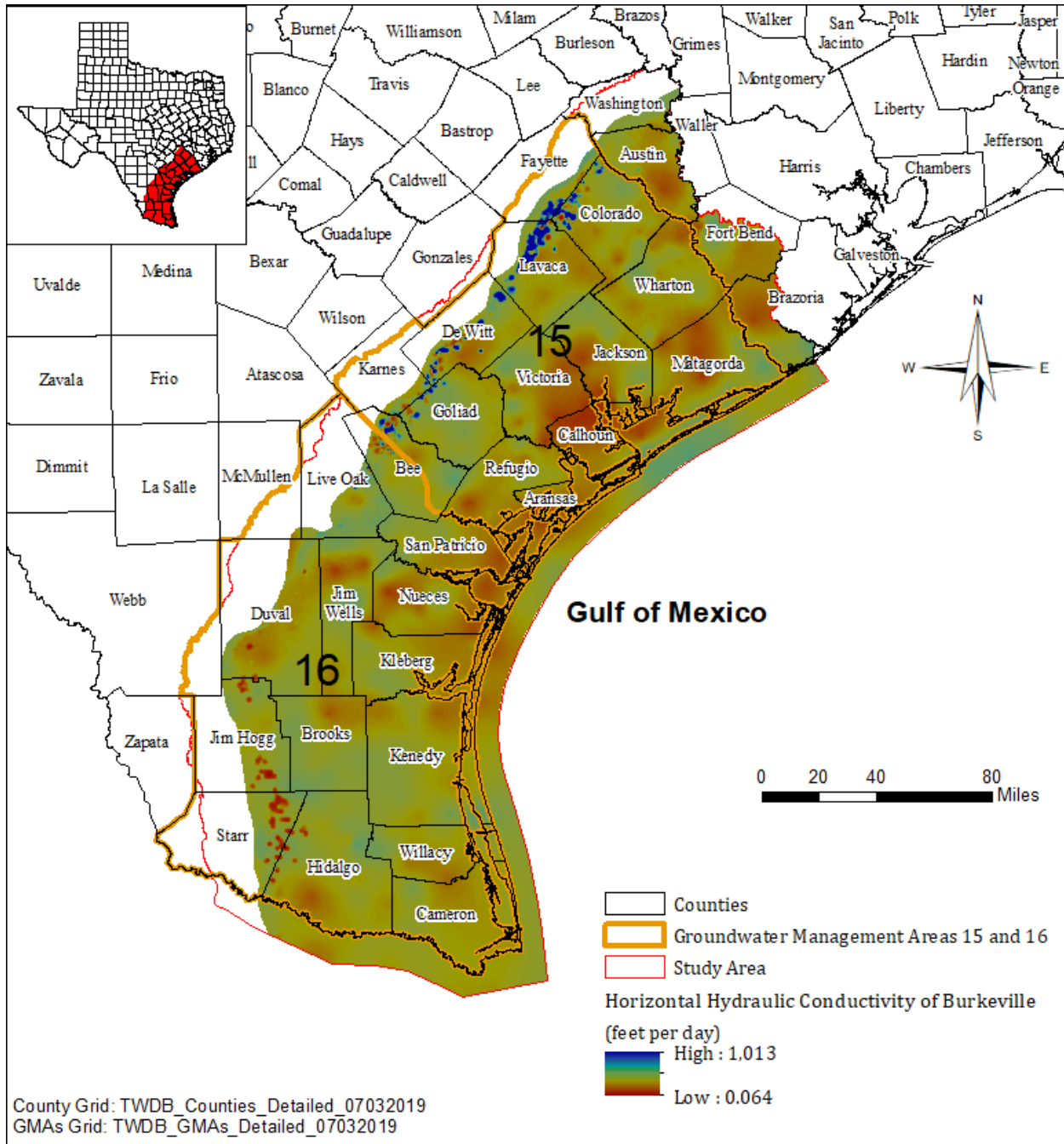


**Figure 4.5.22 Distribution of horizontal hydraulic conductivity value for Burkeville Unit in the study area.**

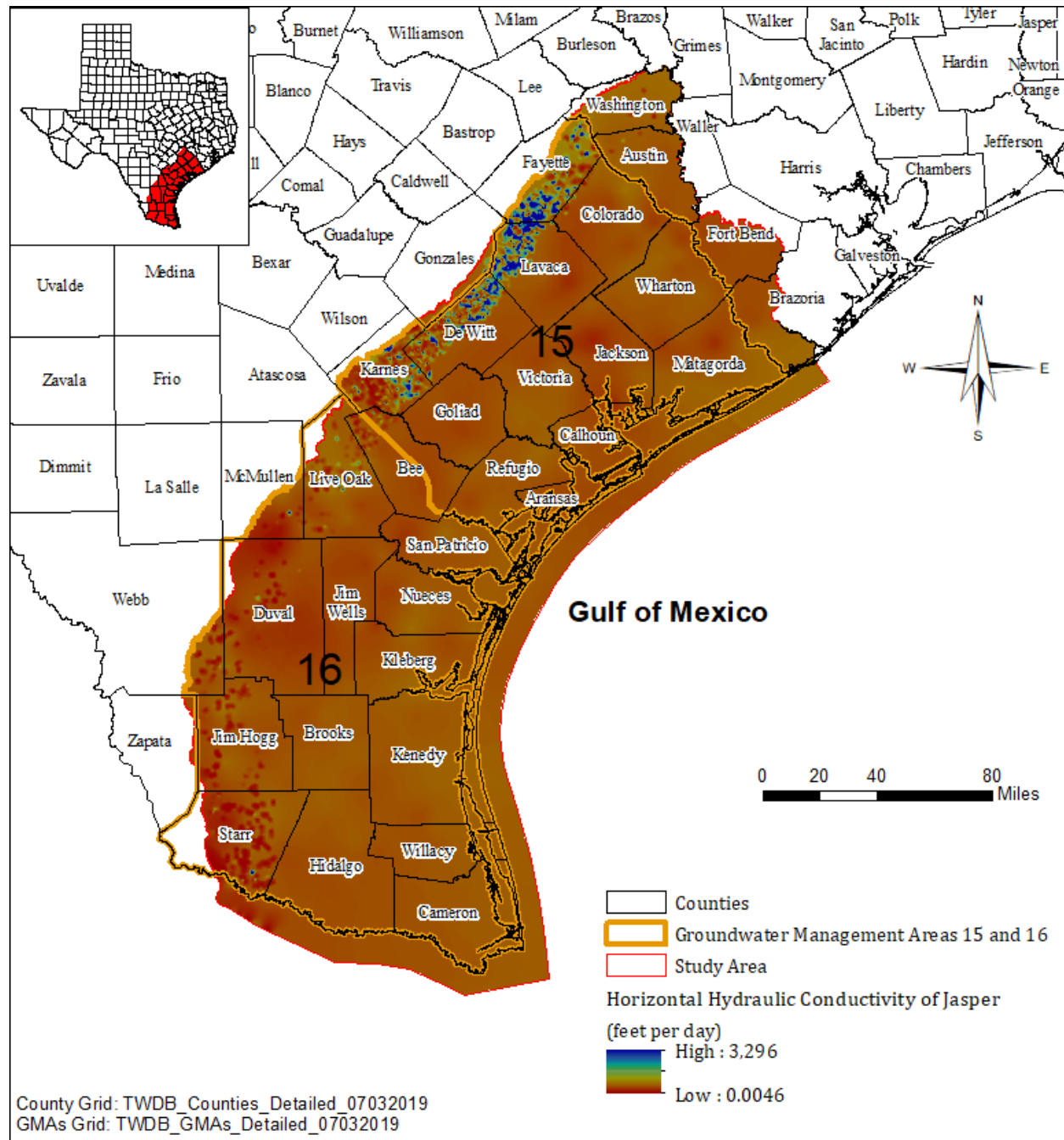


**Figure 4.5.23** Distribution of horizontal hydraulic conductivity value for Jasper Aquifer in the study area.

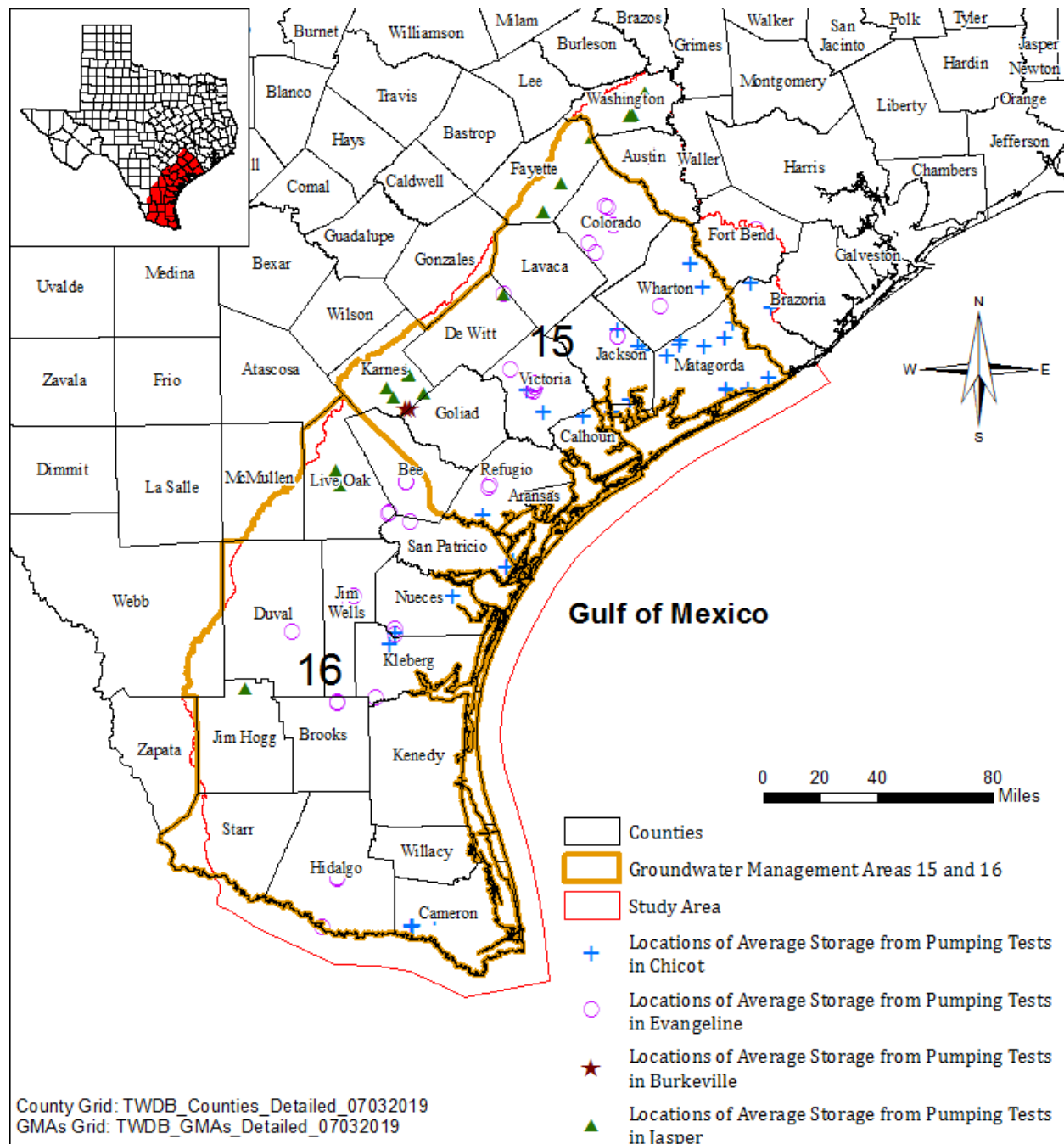


**Figure 4.5.24** Distribution of storativity and specific yield values from pumping tests in the study area.

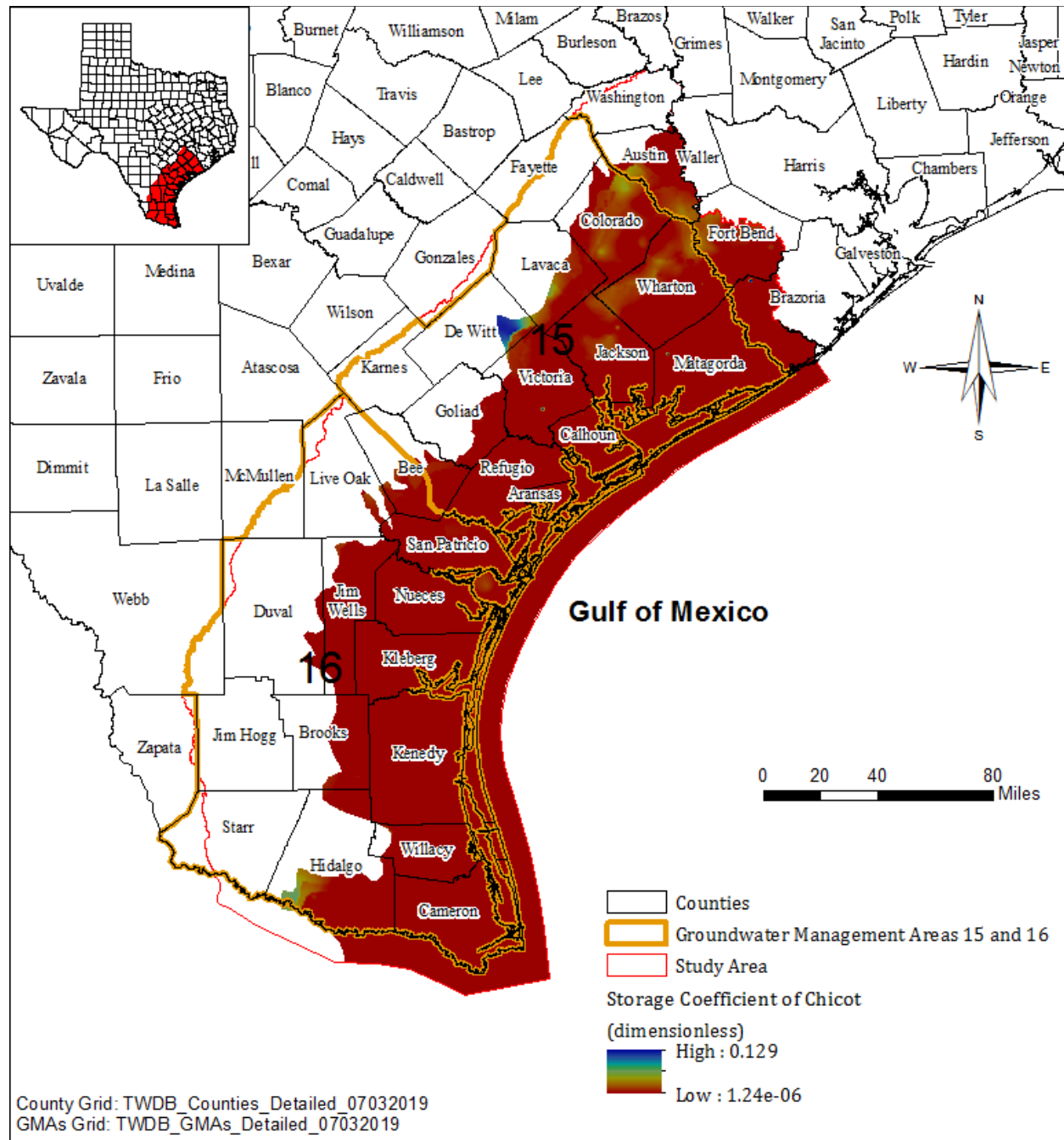


**Figure 4.5.25** Distribution of storativity coefficient from pumping test, sand fraction, and depth for Chicot Aquifer in the study area.



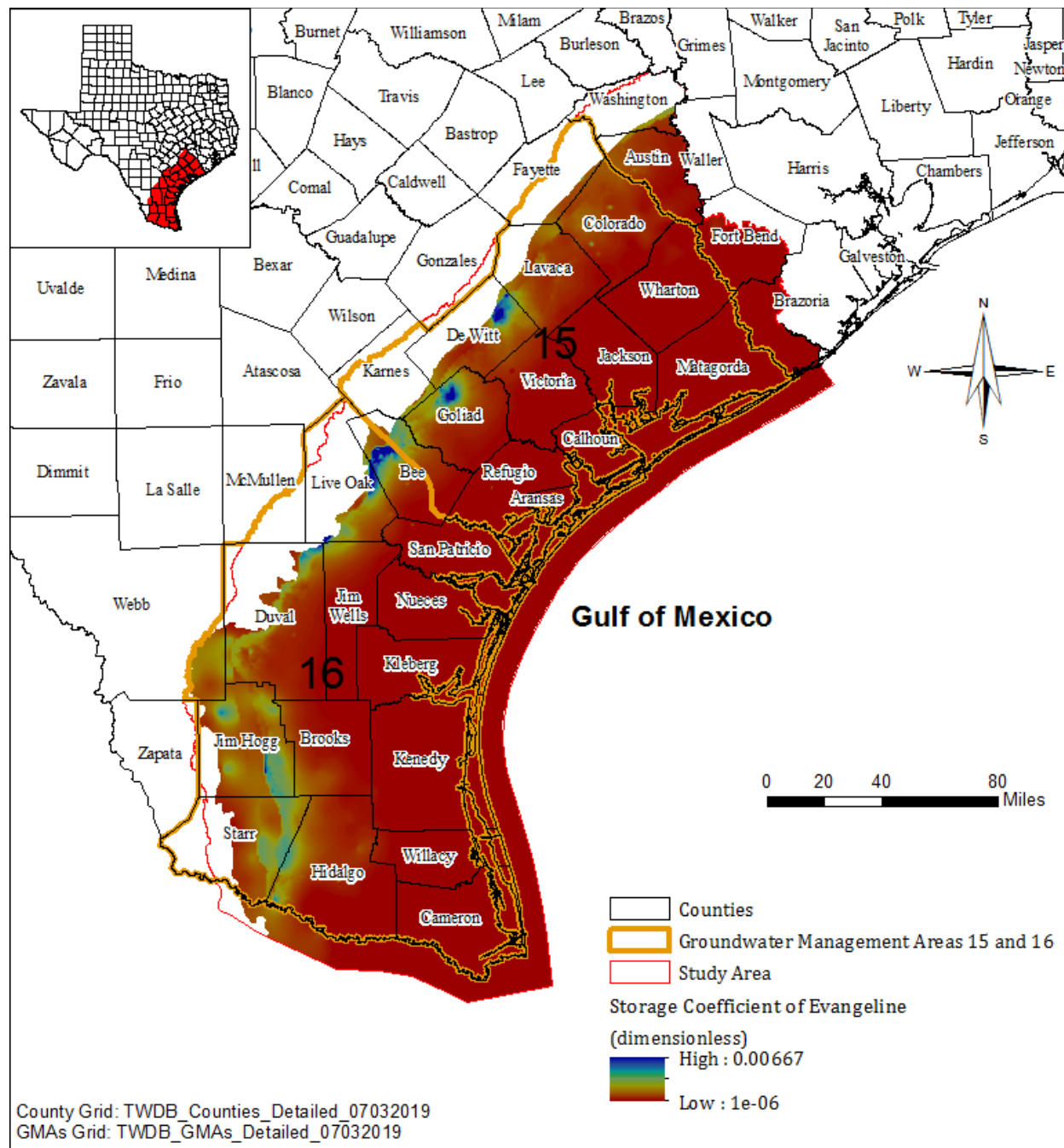


**Figure 4.5.26** Distribution of storativity coefficient from pumping test, sand fraction, and depth for Evangeline Aquifer in the study area.

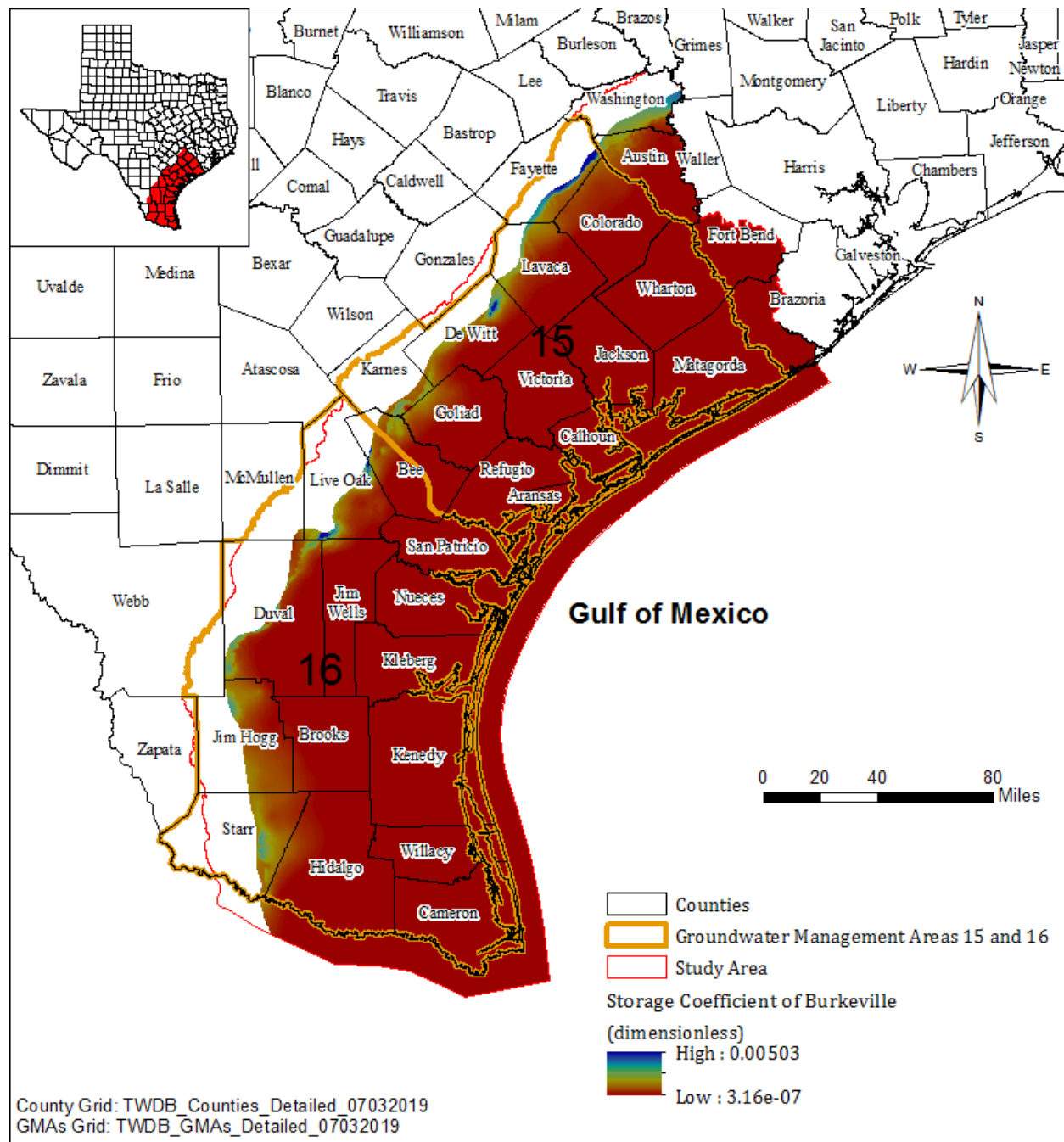


**Figure 4.5.27** Distribution of storativity coefficient from pumping test, sand fraction, and depth for Burkeville Unit in the study area.

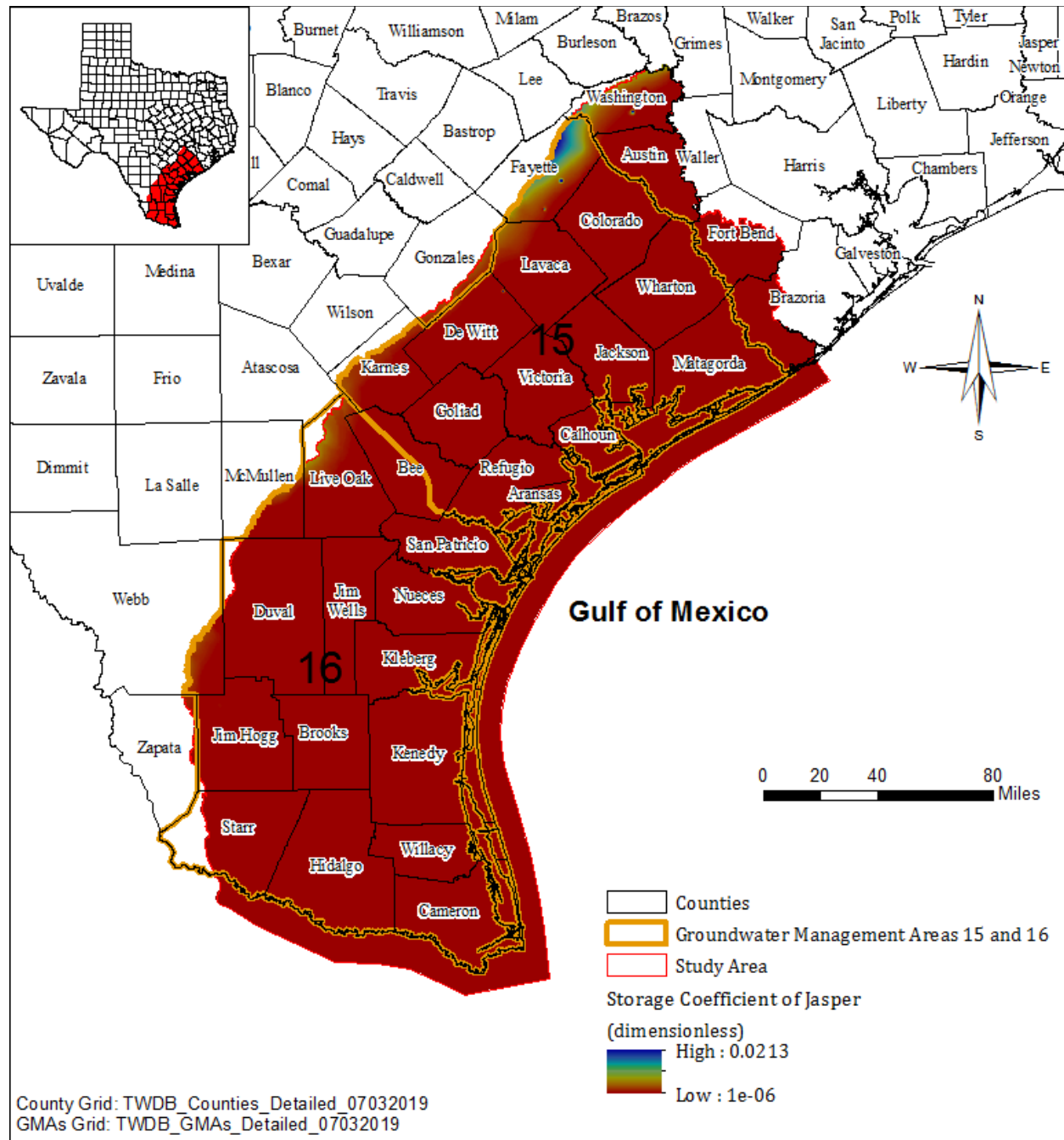


**Figure 4.5.28** Distribution of storativity coefficient from pumping test, sand fraction, and depth for Jasper Aquifer in the study area.

**Table 4.5.1 Summary of horizontal hydraulic conductivity values from pumping tests and specific capacity tests.**

Unit	Count of Pumping Tests	Count of Specific Capacity Tests	Total Count	Minimum	Maximum	Mean	Geomean
Chicot	157	4388	4545	0.16	3830	78.52	25.53
Evangelina	91	3398	3489	0.069	3805	46.70	16.09
Burkeville	5	595	600	0.059	1350	45.46	15.38
Jasper	49	2491	2540	0.0037	4060	57.89	16.37

**Table 4.5.2 Summary of horizontal hydraulic conductivity values from rasters produced using pumping test, specific capacity test, and sand fraction.**

Unit	Minimum	Maximum	Mean	Geomean
Chicot	0.062	3789	44.32	38.79
Evangelina	0.076	3518	16.47	14.86
Burkeville	0.064	1013	13.54	12.77
Jasper	0.0046	3296	14.62	13.13

## **4.6 Aquifer Discharge**

Discharge refers to the groundwater leaving a groundwater system by flow to surface water, to land surface, or to atmosphere. Groundwater discharge can occur naturally through flow to springs, streams, lakes, reservoirs, and evapotranspiration. Groundwater can also be removed from the groundwater system by pumping. For information on groundwater discharge through springs, streams, lakes, and reservoirs please refer to Section 4.4 entitled “Rivers, Streams, Lakes, Springs, and Canals”. The following sections will discuss natural discharge through evapotranspiration and groundwater pumping through anthropogenic means.

### ***4.6.1. Evapotranspiration***

Evapotranspiration is the total amount of groundwater removed by evaporation and transpiration of plants. Evapotranspiration is controlled by the depth of water table, soil texture, and vegetation such as the density, root depth, and type of plants. Greater density and root depth enhance evapotranspiration. Coniferous forests tend to remove more groundwater than deciduous forests.

The study area is dominated by grassland, crop field, shrubs, and small trees ([Figure 4.6.1](#)). The roots for such plants in Texas are usually less than 20 feet deep ([Table 4.6.1](#)). If the water table falls below this depth, the evapotranspiration from the groundwater is expected to be zero. Evapotranspiration starts when the water table rises to the root zone and increases with the rising water table. Evapotranspiration reaches the maximum when the water table is at ground surface. In general, the maximum groundwater evapotranspiration rates are the total amount of water lost to evaporation and transpiration. In the numerical flow model, the maximum evapotranspiration rates can be used to estimate the groundwater evapotranspiration when the water table fluctuates.

In a study presented to the TWDB by Scanlon and others (2005), Deeds and Kelley estimated long-term maximum evapotranspiration rates across Texas. As shown in [Figure 4.6.2](#), the maximum groundwater evapotranspiration rate increases from about 20 inches

per year in the northern portion of the study area to over 50 inches per year in southern portion of the study area.

#### **4.6.2. *Aquifer Discharge through Pumping***

Since 1984, Texas Water Development Board has conducted an annual historical water use survey which includes six categories: municipal, manufacturing, steam-electric generation, irrigation, mining, and livestock. Water use estimates for municipal, manufacturing, and steam-electric power categories come from an annual survey of public water suppliers, major manufacturing and power entities. Response to this survey is mandatory (Section 16.012(m) of the Texas Water Code, as amended by the 78th Texas Legislature in 2003). Municipal water use is reported by public water suppliers. In general, public water supply systems provide water to areas with relative high population density. Water use for mining is based on the annual water-use survey and estimated from water use in secondary processes for oil and gas recovery. Water use for livestock is derived from annual livestock population estimates produced by the U. S. Department of Agriculture's National Agriculture Statistics Service. Estimated water use per animal unit is based on research conducted by the Texas Agricultural Experiment Station. Irrigated agriculture water-use estimates are based on annual crop acreage from the Natural Resources Conservation Service (prior to 2001) and the Farm Service Administration (2001 and later). Irrigation rates per acre are estimated based on potential evapotranspiration, with final estimates reviewed by local authorities.

Domestic groundwater use is not included in the TWDB water use survey. However, the domestic groundwater use can be estimated from population density of rural areas, where a public water system is not available. In this study, the U. S. census block data from 2000 was used as baseline to estimate the population and pumping in rural area. The procedure is described below:

- Step 1 - eliminate the largest population blocks gradually until total population in remaining blocks is close to the rural population for each county from TWDB water use survey;

- Step 2 - adjust block population from Step 1 to calculate new block population for 1980, 1990, and 2010 using the following equation:

$$PN_b = P0_b \frac{PN_c}{P0_c}$$

Where:

$PN_b$  = block population for 1980, 1990, or 2010

$P0_b$  = block population for 2000

$PN_c$  = county rural population for 1980, 1990, or 2010

$P0_c$  = county rural population for 2000

- Step 3 - calculate daily domestic pumping for each block in rural area by multiplying block population from Step 2 by 100 gallons per person per day; and
- Step 4 – convert daily to annual domestic pumping for each block by multiplying 365 or 366 days.

Since census block data for 2015 have errors, the domestic pumping for each block in rural areas for 2015 and other years between 1981 and 2014 without census data is linearly interpolated or extrapolated as follows:

- Domestic Pumping between 1981 and 1989 – use 1980 and 1990;
- Domestic Pumping between 1991 and 1999 – use 1990 and 2000; and
- Domestic Pumping between 2001 and 2015 – use 2000 and 2010.

Total domestic pumping for each county is then calculated by summing the pumping at each block in the county.

For Goliad County, the groundwater pumping data for all categories, except domestic, were from Goliad County Groundwater Conservation District. For Wharton County, industrial,

irrigation, and municipal pumping from 2005 to 2015 and domestic and livestock pumping from 2005 to 2010 were from the Coastal Bend Groundwater Conservation District's website. Mr. Andy Garza, General Manager of Kenedy County Groundwater Conservation District, sent the pumping data for the district to Jerry Shi. Exact comparison between the TWDB groundwater use survey and the district pumping data is impossible, because the district contains Kenedy County and part of the surrounding counties. However, pumping data from the district appeared consistent with the TWDB groundwater use survey.

No groundwater use was recorded prior to 1994 on the Mexico side of the study area. However, pumping permit values have been available since, and were downloaded for this study from <https://app.conagua.gob.mx/consultarepda.aspx>. After review, it was assumed that pumping in a specific year was the sum of pumping from previous years and current year. For example, pumping in 2010 was the sum of pumping from 1994 to 2010. Further review indicated that pumping data from 1994 to 1999 was less reliable. As a result, annual pumping for all categories from 1980 to 1999,  $Q_n$ , were linearly extrapolated from total pumping between 2000 and 2011 by trend analysis as shown in Figure 4.6.3 using the following equation:

$$Q_n = 519.10208 * n - 1010970.79527$$

Where:

$$n = 1980, 1981, \dots, 1999$$

Annual pumping for each category,  $q_n$ , was then calculated using the following equation:

$$q_n = \frac{Q_n}{Q_{n+1}} * q_{n+1}$$

Where:

$$Q_n = \text{total pumping for Year } n$$

$$Q_{n+1} = \text{total pumping for Year } n+1$$

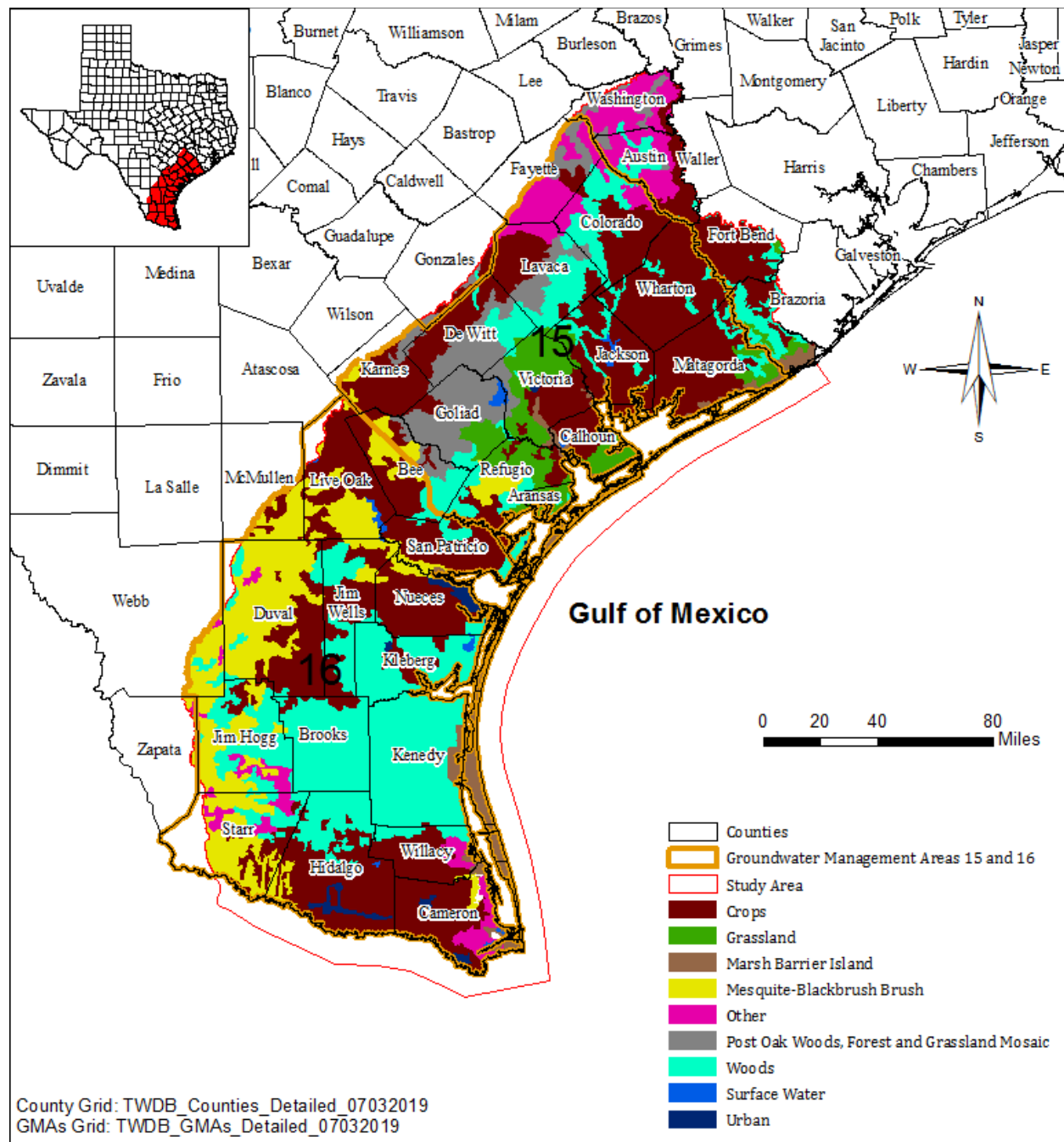


$n = 1999, 1998, \dots, 1980$

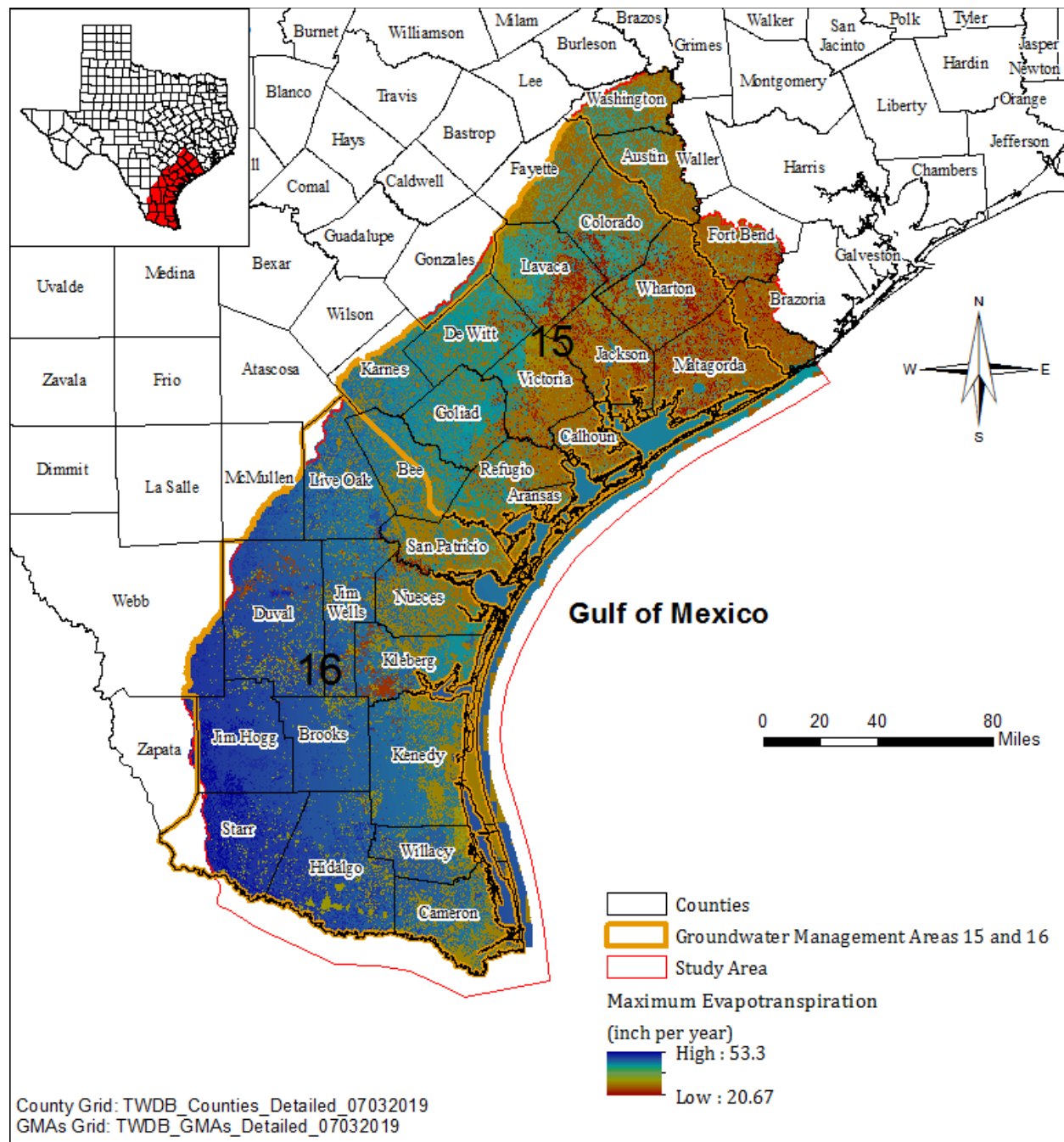
The annual groundwater use for each county and Mexico between 1980 and 2015 from the Gulf Coast Aquifer System is presented in [Figures 4.6.4](#) through [4.6.9](#). For this study, pumping by manufacturing, steam-electric generation, and mining was lumped together as industrial pumping.

In general, counties with large crop production, such as Colorado, Fort Bend, Jackson, Matagorda, Victoria, and Wharton, tended to use large amount of groundwater, ranging from about 24,000 to 140,000 acre-feet per year. These counties are within or adjacent to northern Groundwater Management Area 15. In contrast, Aransas, Calhoun, Kenedy, Webb, and Willacy counties used less than 1,000 acre-feet per year. Each of the rest used about 1,000 to 10,000 acre-feet per year.

Pumping location and aquifer association for the municipal and industrial groundwater uses will be determined using the TWDB groundwater database and specific well locations. Distribution of livestock pumping will be based on land cover data from the National Land Cover Dataset (Fry and others, 2011). Distribution of irrigation pumping will be based on the irrigation farmland distribution (U. S. Department of Agriculture, 2020) and the locations of irrigation wells. Location of domestic pumping will be based on census blocks or the TWDB groundwater database.



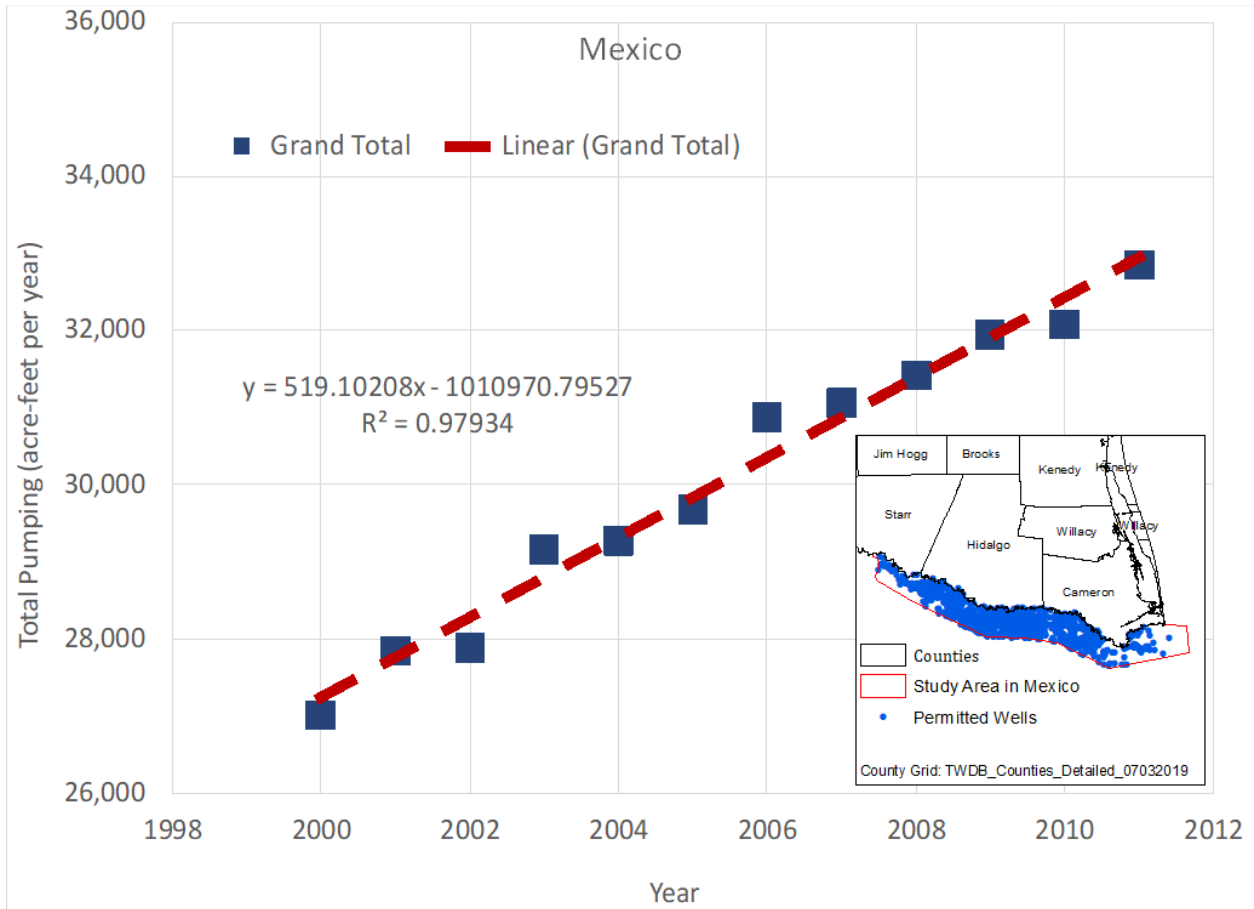
**Figure 4.6.1** Vegetation types in study area (McMahan and others, 1984).



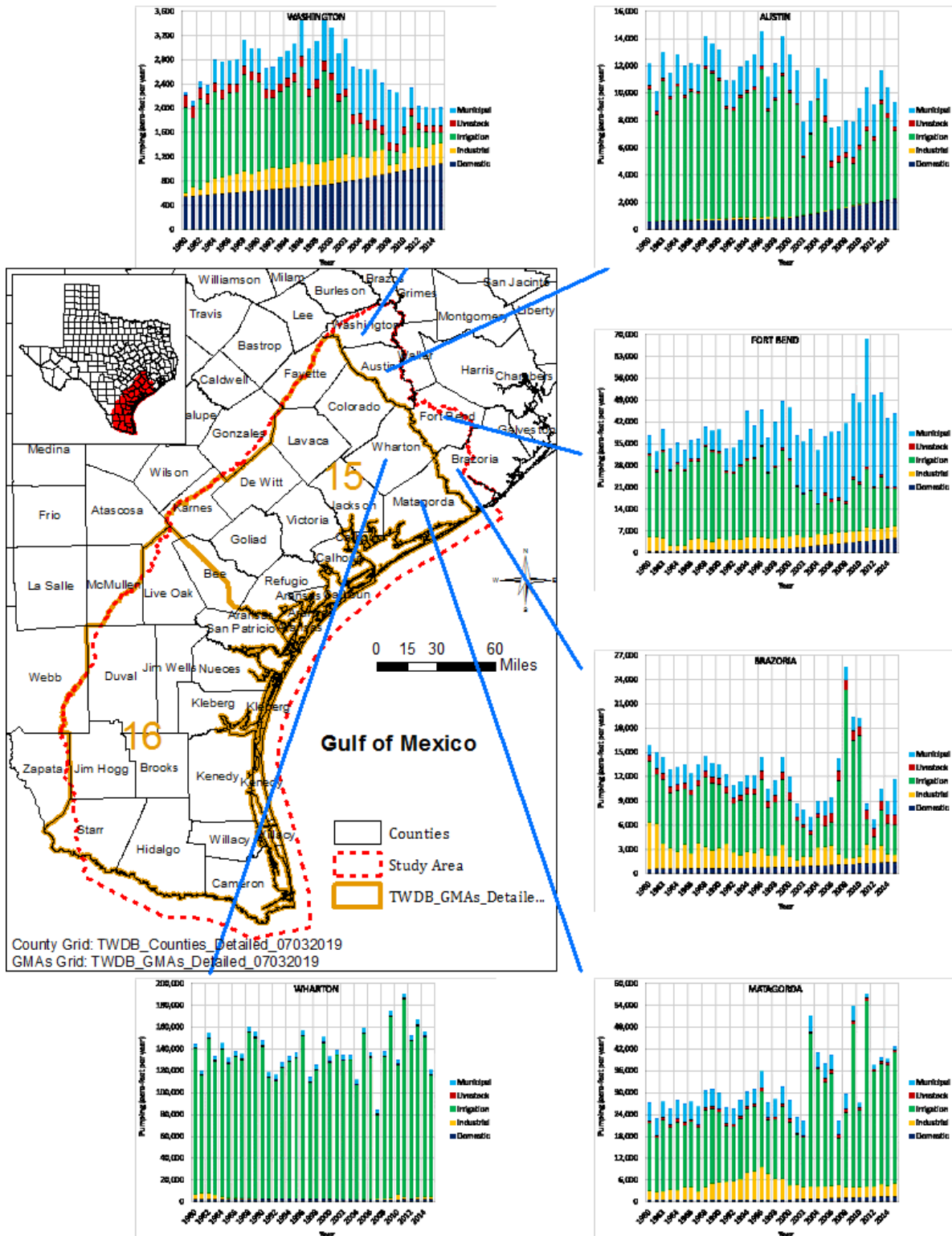
**Figure 4.6.2** Estimated maximum evapotranspiration in study area (Scanlon and others, 2005).

Table 4.6.1 Depth of plant roots (revised from Schenk and Jackson, 2003).

<b>Vegetation</b>	<b>Root Depth (feet)</b>	<b>Location</b>	<b>Soil Type</b>
American Elm	23	Edwards Plateau, Texas, USA	shallow, calcareous overlying fractured
Ashe Juniper	26	Edwards Plateau, Texas, USA	shallow, calcareous overlying fractured limestone
Cedar Elm	29	Edwards Plateau, Texas, USA	shallow, calcareous overlying fractured limestone
Crops	6.9	various	various
Grassland	2 to 3.1	Texas, USA	various
Honey Mesquite	6.6	Texas, USA	Nuvalde clay loam
Live Oak	60	Edwards Plateau, Texas, USA	shallow, calcareous overlying fractured limestone
open shrubland	8.6 to 19.7	Texas, USA	various
Sugarberry	19	Edwards Plateau, Texas, USA	shallow, calcareous overlying fractured limestone
White Shin Oak	23	Edwards Plateau, Texas, USA	shallow, calcareous overlying fractured limestone
Wooded grassland	3.6 to 7.6	Texas, USA	various



**Figure 4.6.3      Trend analysis of total groundwater pumping from 2000 to 2011 in Mexico.**



**Figure 4.6.4** Annual groundwater pumping between 1980 and 2015 in Austin, Brazoria, Fort Bend, Matagorda, Washington, and Wharton counties.

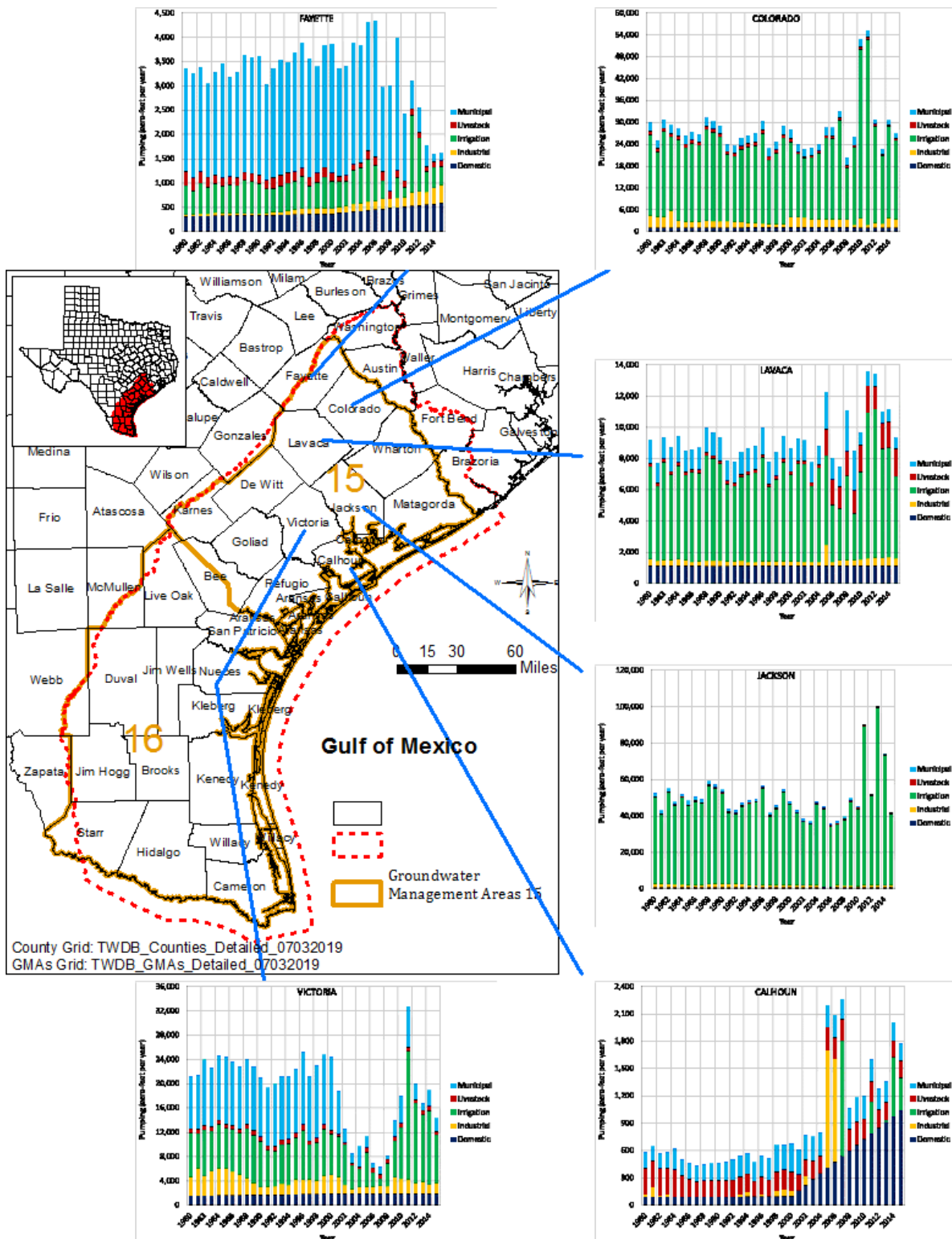


**Figure 4.6.5 Annual groundwater pumping between 1980 and 2015 in Calhoun, Colorado, Fayette, Jackson, Lavaca, and Victoria counties.**

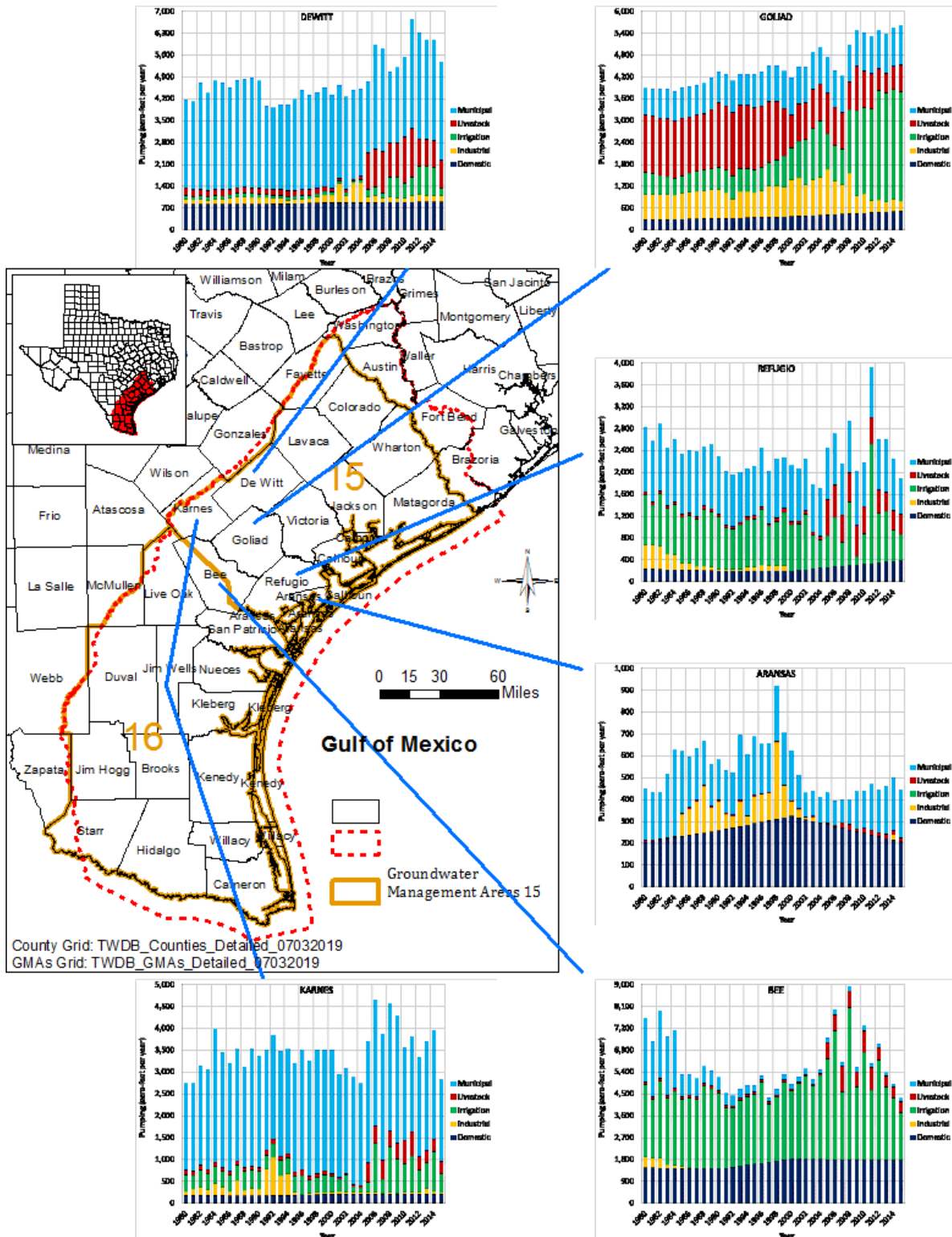


**Figure 4.6.6 Annual groundwater pumping between 1980 and 2015 in Aransas, Bee, DeWitt, Goliad, Karnes, and Refugio counties.**



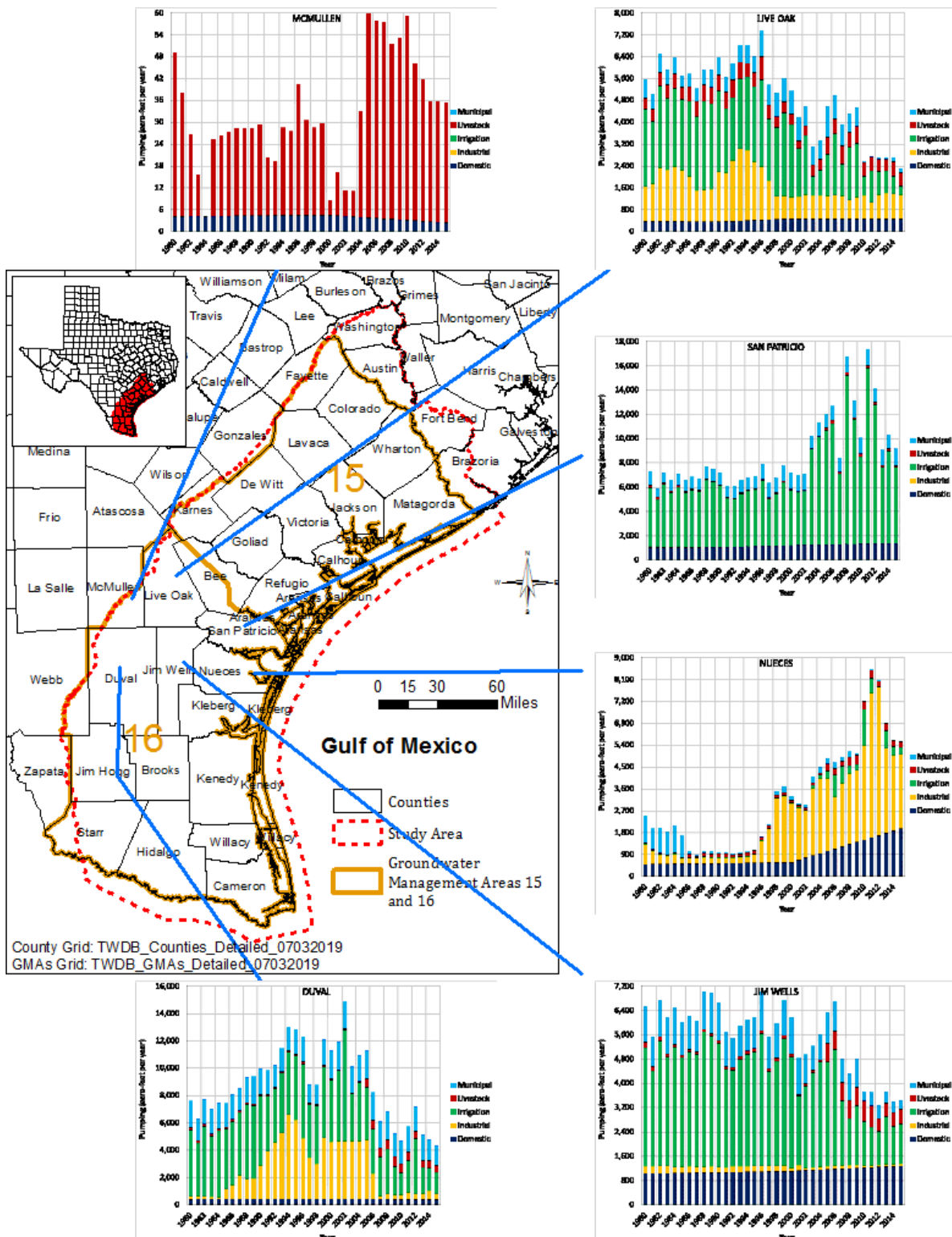


**Figure 4.6.7 Annual groundwater pumping between 1980 and 2015 in Duval, Jim Wells, Live Oak, McMullen, Nueces, and San Patricio counties.**

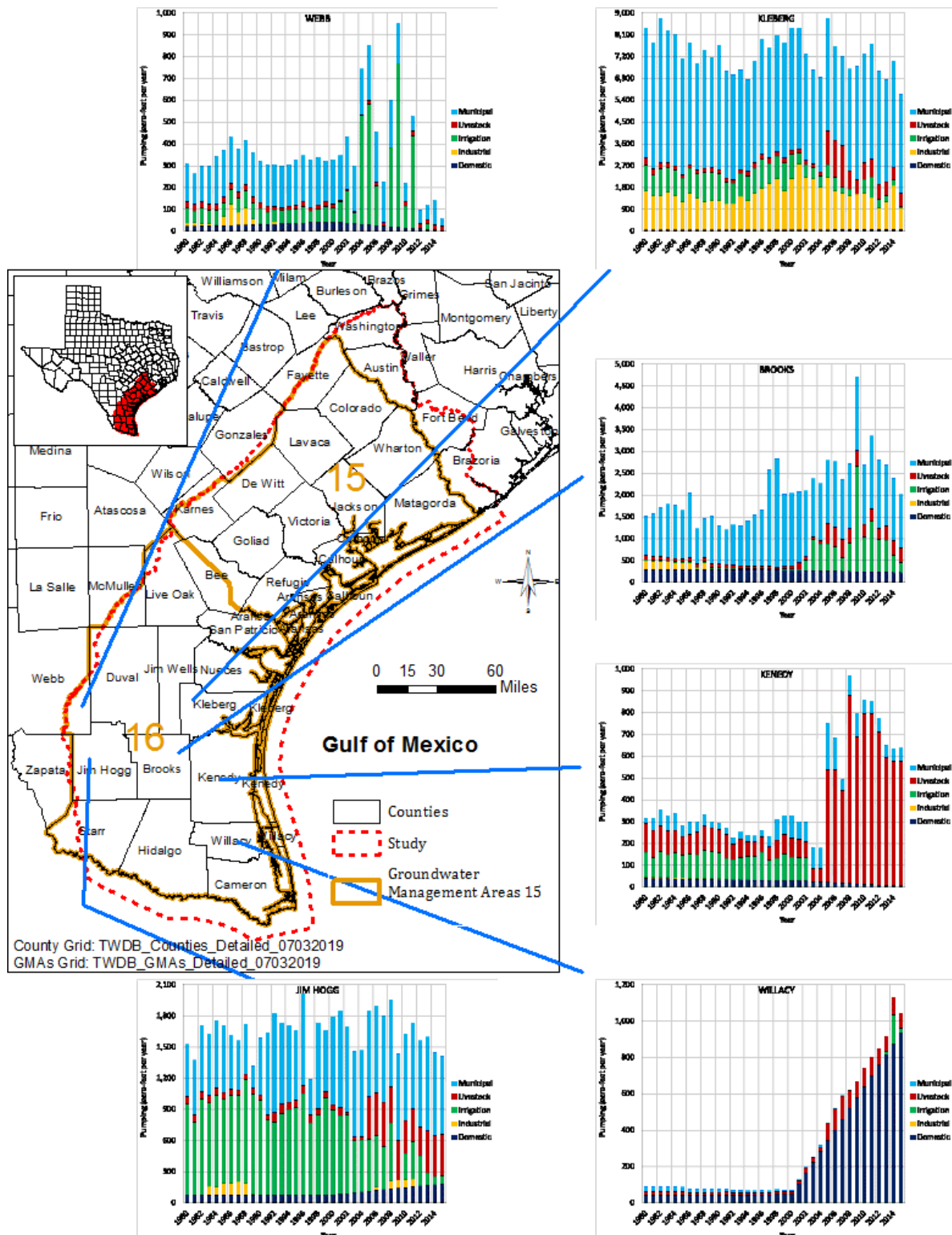


**Figure 4.6.8** Annual groundwater pumping between 1980 and 2015 in Brooks, Jim Hogg, Kenedy, Kleberg, Webb, and Willacy counties.

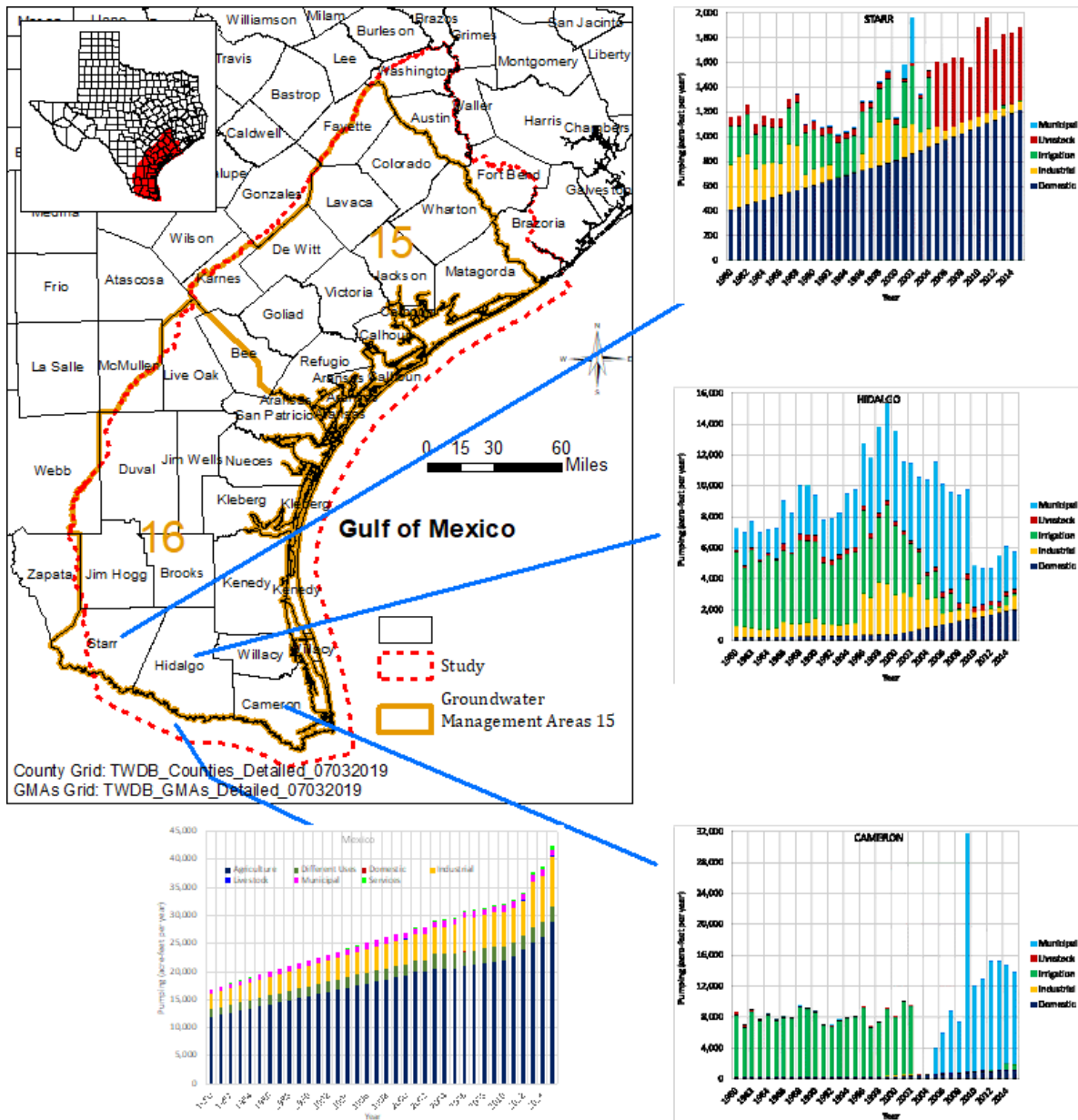


**Figure 4.6.9 Annual groundwater pumping between 1980 and 2015 in Cameron, Hidalgo, and Starr counties and Mexico.**

## 4.7 Groundwater Quality

Groundwater quality is a key factor to determine its usage. Groundwater contains solids and dissolved matters. Some of the constituents, when exceeding certain levels, may pose threats to humans and the environment. In Texas, the drinking water standards (30 TAC Chapter 290, Subchapter F) enforced by the Texas Commission on Environmental Quality (TCEQ) govern the drinking water quality and reporting requirements for public water systems. Water with any chemical constituents over the drinking water standards is considered unsafe for human consumption. The Texas drinking water standards include several criteria:

- Maximum Contaminant Levels (MCLs): MCLs define the maximum allowable concentrations for chemical in a public water supply system. The chemicals could be natural or man-made;
- Maximum Residual Disinfectant Levels (MRDLs): MRDLs define the highest levels of disinfectants allowed in drinking water. The disinfectants are the byproducts of water treatment process; and
- Action Levels (ALs): ALs are the maximum allowable concentrations of copper and lead in drinking water. If ten percent (10%) of tap water exceed the action levels, the water system must take additional steps.

Of the drinking water criteria, only Maximum Contaminant Levels (MCLs) are enforceable standards. As a result, this study only focuses on chemicals defined by MCLs. These chemicals are divided into the following categories:

- Inorganics: antimony, arsenic, asbestos, barium, beryllium, cadmium, chromium, cyanide, fluoride, mercury, nitrate, nitrite, nitrate and nitrite, selenium, and thallium;
- Synthetic Organics: alachlor, atrazine, benzopyrene, carbofuran, chlordane, dilepton, dibromo chloropropane, di(2-ethylhexyl)adipate, di(2-ethylhexyl)phthalate,

dinoseb, diquat, endothall, endrin, ethylene dibromide, glyphosate, heptachlor, heptachlor epoxide, hexachlorobenzene, hexachlorocyclopentadiene, lindane, methoxychlor, oxamyl (vydate), pentachlorophenol, picloram, polychlorinated biphenyls (PCBs), simazine, toxaphene, 2,3,7,8-TCDD (dioxin), 2,4,5-TP, and 2,4-D;

- Volatile Organic Compounds (VOCs): 1,1-dichloroethylene, 1,1,1-trichloroethane, 1,1,2-trichloroethane, 1,2-dichloroethane, 1,2-dichloropropane, 1,2,4-trichlorobenzene, benzene, carbon tetrachloride, cis-1,2-dichloroethylene, dichloromethane, ethylbenzene, monochlorobenzene, o-dichlorobenzene, para-dichlorobenzene, styrene, tetrachloroethylene, toluene, trans-1,2-dichloroethylene, trichloroethylene, vinyl chloride, and xylenes (total);
- Naturally Occurring Radionuclides: radium-226 and radium-228, gross alpha particle activity, and uranium;
- Man-Made Radionuclides: beta particle activity and photon radioactivity; and
- Microbial Contaminants: escherichia coli (E. Coli).

For this conceptual model report, chemical concentrations in a dissolved phase collected at water wells on different dates are from the following sources:

- TWDB groundwater database (TWDB, 2019b); and,
- Brackish Resources Aquifer Characterization System (BRACS) database (TWDB, 2018).

Only wells screened completely or predominantly within one of the Chicot Aquifer, the Evangeline Aquifer, the Burkeville Unit, and the Jasper Aquifer were used for this study. Annual average was based on individual samples from different dates within the same year. The overall average was based on annual averages between 1980 and 2015. Please note that the underlined chemicals above, such as 1,1,1-trichloroethane, were below their maximum contaminant levels for all individual annual averages. Chemicals double-underlined such as carbofuran were not available from the TWDB groundwater database.

In this study, only chemicals with at least one concentration or one annual average concentration greater than its maximum contaminant level were presented (i.e. those neither underlined nor double-underlined above). The inorganics were sampled and analyzed both temporally and spatially. These chemicals were presented individually as an overall average between 1980 and 2015 at wells. For example, the dissolved concentration of arsenic was presented as an overall average between 1980 and 2015 at different wells in the Chicot, Evangeline, Burkeville, and Jasper, respectively. Because nitrate, nitrite, and the combination of nitrate and nitrite all have the same maximum contaminant level, only the combination of nitrate and nitrite were presented in this study.

The synthetic organics and volatile organic compounds had limited data temporally and spatially. These chemicals were presented based on the maximum annual average concentration among all chemicals in that category at each well. For example, if any of the synthetic organics collected from the same well has an annual average concentration greater than its maximum contaminant level, the well was labelled as greater than maximum contaminant level for the synthetic organics.

The naturally occurring radionuclide category (alpha particle activity and uranium) had even fewer data available. If any annual average concentration at a well was greater than its maximum contaminant level, the chemical was labelled as maximum greater maximum contaminant level for that chemical at the well.

For total dissolved solids, Texas only has a secondary, non-enforceable drinking water maximum contaminant level (1,000 milligrams per liter). However, the total dissolved solids are important to groundwater users, planners, and developers. As a result, the total dissolved solids in the groundwater from the Gulf Coast Aquifer System in the study area are discussed and presented in this section.

In addition to the analytical data from water wells listed above (TWDB, 2019b; TWDB, 2018), total dissolved solids can also be estimated from resistivity of geophysical logs. Geophysical logs generally produce much more data laterally and vertically and, combined with data from water wells, provide much better representation of the total dissolved

solids in groundwater system. The total dissolved solids calculated from geophysical logs are from the following studies:

- Brackish Resources Aquifer Characterization System (BRACS) database (TWDB, 2018);
- Hydrogeochemical Evaluation of the Texas Gulf Coast Aquifer System and Implications for Developing Groundwater Availability Models (Young and others, 2014); and
- Hydrostratigraphy of Gulf Coast Aquifer – Brazos to Rio Grande (Young and others, 2010).

In this study, the groundwater is classified into the following categories:

- Fresh – Total dissolved solids less than 1,000 milligrams per liter;
- Brackish
  - Slightly Saline – Total dissolved solids 1,000 to less than 3,000 milligrams per liter;
  - Moderately Saline – Total dissolved solids 3,000 to less than 10,000 milligrams per liter;
- Very Saline – Total dissolved solids 10,000 to less than 35,000 milligrams per liter; and
- Brine – Total dissolved solids greater than 35,000 milligrams per liter (ocean water belongs to this category).

Only total dissolved solids completely within one of the Chicot Aquifer, the Evangeline Aquifer, the Burkeville Unit, and the Jasper Aquifer were used for this study. Average total dissolved solids for a formation at a geophysical log location were calculated using all values within the formation at the location. The average total dissolved solids from

geophysical logs were then combined with the overall average calculated from analytical data collected at water wells between 1980 and 2015 to study the change of total dissolved solids at different locations.

Pumping can accelerate or even reverse natural groundwater flow pattern and change the water quality at wells. To evaluate this temporal variation, water wells with at least five annual average total dissolved solids between 1980 and 2015 are selected to produce hydrographs and the results are described in the following sections.

#### **4.7.1 Chicot Aquifer**

Average dissolved arsenic concentration between 1980 and 2015 were mostly below the maximum contaminant level (10 micrograms per liter) in the Chicot Aquifer in the northern part of the study area (Figure 4.7.1). However, its concentration increased to the south and exceeded its maximum contaminant level at some wells in Groundwater Management Area 16. Average dissolved barium concentration exceeded its maximum contaminant level only at one well in San Patricio County (Figure 4.7.2), while average dissolved cadmium concentration was above its maximum contaminant level at many locations (Figure 4.7.3). Nitrate and nitrite combined had several locations in Hidalgo and Victoria counties with average concentrations exceeding its maximum contaminant level (Figure 4.7.4). Two wells showed average dissolved selenium concentration above its maximum contaminant level in Hidalgo and Nueces counties near Corpus Christi (Figure 4.7.5). Average dissolved thallium concentration was above its maximum contaminant level in Calhoun (three wells) and Hidalgo (several locations) counties (Figure 4.7.6).

Average total dissolved solids were lower than 1,000 milligrams per liter at most of the locations located in Austin, Colorado, Fort Bend, Jackson, Matagorda, and Wharton counties, but increased toward the Gulf of Mexico (such as in Brazoria County) and the south (Figure 4.7.7). The groundwater in Groundwater Management Area 15 was generally either fresh or slightly saline. In Groundwater Management Area 16, the groundwater was basically brackish except in Kenedy and Willacy counties where the groundwater could be very saline. The distribution of the total dissolved solids from this study was consistent



with the pattern of freshwater fraction from Young and others (2010). For example, low total dissolved solids were generally coincided with high freshwater fraction while high total dissolved solids were with low freshwater fraction.

The total dissolved solids in groundwater from the Chicot Aquifer changed over time but mainly remained within the same category at the selected wells (Figure 4.7.8 and Appendix F), with exception of three wells: State Well 6543707 (Figure F3 of Appendix F), State Well 6551915 (Figure F4 of Appendix F), and State Well 8012202 (Figure F14 of Appendix F). At these three wells, the total dissolved solids changed from fresh water to slightly saline water or verse versa.

One well in Colorado County showed several synthetic organic compounds above their maximum contaminant levels (Figure 4.7.9). The same well also had vinyl chloride (a volatile organic compound) exceeding its maximum contaminant level (Figure 4.7.10).

Gross alpha particle activity (an indicator of naturally occurred radioactivity) was above its maximum contaminant level at several wells in Hidalgo County (Figure 4.7.11). Average dissolved Uranium, another naturally occurred radioactive element, showed average dissolved concentration above its maximum contaminant level at several wells in Hidalgo and Nueces counties (Figure 4.7.12).

The piper diagram indicates the groundwater in the Chicot Aquifer originated as calcium-bicarbonate facies and then gradually evolved into sodium-chloride-sulphate facies in more saline samples along groundwater pathway (Figure 4.7.13).

#### **4.7.2            *Evangeline Aquifer***

Average dissolved arsenic concentration between 1980 and 2015 were below its maximum contaminant level in the Evangeline Aquifer in northern Groundwater Management Area 15 (Figure 4.7.14). However, its concentration increased to the south and exceeded its maximum contaminant level at many wells in the rest of the study area. Average dissolved barium concentration exceeded its maximum contaminant level at only one well in Victoria County (Figure 4.7.15), while average dissolved cadmium concentration was above its

maximum contaminant level at many locations (Figure 4.7.16). Nitrate and nitrite combined had several locations in Brooks, Duval, Hidalgo and Starr counties with average concentrations exceeding its maximum contaminant level (Figure 4.7.17). Three wells showed average dissolved selenium concentration above its maximum contaminant level in Colorado, Hidalgo, Kenedy, and San Patricio counties (Figure 4.7.18). Average dissolved thallium concentration was above its maximum contaminant level at two wells in Hidalgo County (Figure 4.7.19).

The groundwater in the outcrop area was either fresh or slightly saline (Figure 4.7.20). The total dissolved solids increased downdip and the groundwater became very saline along coastal line. The total solids could be over 35,000 milligrams per liter in Brazoria, Cameron, Hidalgo, Matagorda, and Willacy counties (Figure 4.7.20). Like the in Chicot, the distribution of the total dissolved solids from analytical data at wells and geophysical logs was consistent with the pattern of freshwater fraction from Young and others (2010).

The total dissolved solids in groundwater from the Evangeline Aquifer remained at the same category over time at the selected wells (Figure 4.7.21 and Appendix F). Only one well (State Well 8436601) changed from fresh water to slightly saline water (Figure F49 of Appendix F).

Several wells in outcrop area showed some synthetic organic compounds above their maximum contaminant levels (Figure 4.7.22). No analyses were taken for volatile organic compounds in the Evangeline Aquifer.

Gross alpha particle activity was above its maximum contaminant level at more wells in the Evangeline Aquifer than in the Chicot Aquifer (Figure 4.7.23). This was especially true in Groundwater Management Area 16. Several wells in Groundwater Management Area 16 showed dissolved uranium average concentration above its maximum contaminant level (Figure 4.7.24).

Like the Chicot Aquifer, the piper diagram for the Evangeline Aquifer indicates the groundwater originated as calcium-bicarbonate facies and then gradually evolved into sodium-chloride-sulphate facies in more saline samples (Figure 4.7.25).

### **4.7.3            *Burkeville Unit***

Average dissolved arsenic concentration between 1980 and 2015 was below its maximum contaminant level in the Burkeville Unit except at two wells in Lavaca and Live Oak counties (Figure 4.7.26). Average dissolved barium concentration was all below its maximum contaminant level (Figure 4.7.27), while average dissolved cadmium concentration was above its maximum contaminant level at about half of the wells (Figure 4.7.28). Nitrate and nitrite combined was below its maximum contaminant level (Figure 4.7.29). The average dissolved selenium and thallium concentrations were also below their respective maximum contaminant levels in the study area (Figures 4.7.30 and 31).

The Burkeville Unit was dominated by brackish groundwater with the total dissolved solids ranging from 1,000 to 10,000 milligrams per liter in the outcrop area and adjacent subcrop area (Figure 4.7.32). The total dissolved solids increased quickly toward the Gulf of Mexico and reached very saline in those counties along costal line. Brine groundwater existed in Brazoria and Matagorda counties, and dominated Hidalgo and likely Cameron and Willacy counties in the lower Rio Grande region (Figure 4.7.32). It appeared that the average total dissolved solids were generally lower at wells where the freshwater fraction was higher or vice versa (Figure 4.7.32). All four selected wells installed in the Burkeville Unit showed decreasing trend in the total dissolved solids but remained in the same category over the monitored years (Figure 4.7.33).

No synthetic organic compounds were found above their maximum contaminant levels (Figure 4.7.34). Figure 4.7.35 showed the gross alpha particle activity exceeding its maximum contaminant level at one well in Live Oak County. One well in Hidalgo County also had uranium exceeding its maximum contaminant level (Figure 4.7.36).

The Piper diagram indicates the groundwater in the Burkeville Unit originated as calcium-bicarbonate facies and then gradually evolved into sodium-chloride-sulphate facies in more saline samples (Figure 4.7.37).

#### 4.7.4 *Jasper Aquifer*

Average dissolved arsenic concentration between 1980 and 2015 were above its maximum contaminant level at almost half of the wells in Jasper Aquifer with an increasing trend from north to south (Figure 4.7.38). Average dissolved barium concentrations were all below its maximum contaminant level (Figure 4.7.39). Average dissolved cadmium concentration was above its maximum contaminant level at many wells (Figure 4.7.40). This was especially obvious in Karnes, Live Oak, and Washington counties. Nitrate and nitrite combined was below its maximum contaminant level in Groundwater Management Area 15 but above its maximum contaminant level at some wells in Groundwater Management Area 16 (Figure 4.7.41). One well in Starr County showed the average dissolved selenium concentration above its maximum contaminant level (Figure 4.7.42). Several wells in Duval, Jim Hogg, Starr, and Washington counties had average dissolved thallium concentration above its maximum contaminant level (Figure 4.7.43).

The groundwater from the Jasper Aquifer showed a very similar pattern in total dissolved solids as that from the Burkeville Unit, except the outcrop area in Groundwater Management Area 15 where fresh groundwater was dominant (Figure 4.7.44). A similar increasing trend in total dissolved solids can be found from the outcrop area to the Gulf of Mexico. The groundwater quickly became brackish from the outcrop area to the subcrop area with total dissolved solids ranging from 1,000 to less than 10,000 milligrams per liter, and further transitioned to very saline in those counties along the coastal line with total dissolved solids ranging from 10,000 to less than 35,000 milligrams per liter. Brine groundwater was observed in Brooks, eastern Matagorda, and eastern and southern Hidalgo (and mostly likely Cameron and Willacy) counties. The distribution of total dissolved solids in the groundwater from the Jasper Aquifer also correlated well to the freshwater fraction by Young and others (2010) (Figure 4.7.44). Like the groundwater from the Evangeline Aquifer, the groundwater from the Jasper Aquifer also remained at the same category over time at the selected wells (Figure 4.7.45 and Appendix F), except at State Well 7925608 in Bee County where the groundwater changed from slightly saline to fresh (Figure F69 of Appendix F).

Synthetic compounds were found with concentration above their maximum contaminant levels at several wells in Duval, Fayette, and Karnes counties (Figure 4.7.46). Two wells in Fayette County showed some volatile organic compounds collected in 1989 exceeding their respective maximum contaminant levels (Figure 4.7.47). Several wells had gross alpha particle activity exceeding its maximum contaminant level (Figure 4.7.48). Most of these wells are in Karnes County and Groundwater Management Area 16. Uranium was found above its maximum contaminant level at one well in Lavaca County (Figure 4.7.49).

Like that in the Chicot and Evangeline aquifers, the groundwater in the Jasper Aquifer showed calcium-bicarbonate facies near recharge zone and then gradually evolved into sodium-chloride-sulphate facies in more saline samples (Figure 4.7.50).

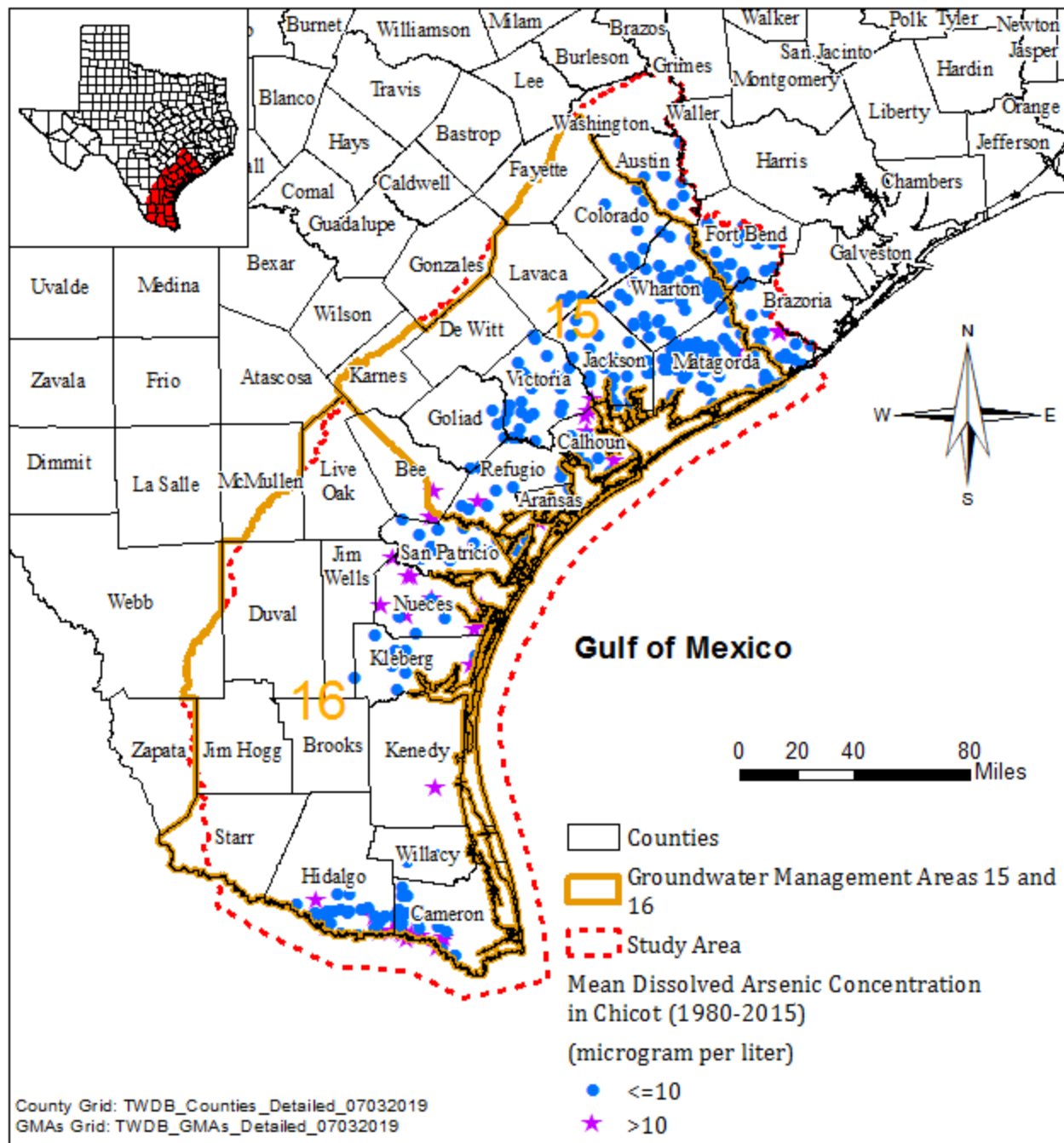


**Figure 4.7.1 Arsenic average concentrations in groundwater samples collected from Chicot Aquifer between 1980 and 2015.**

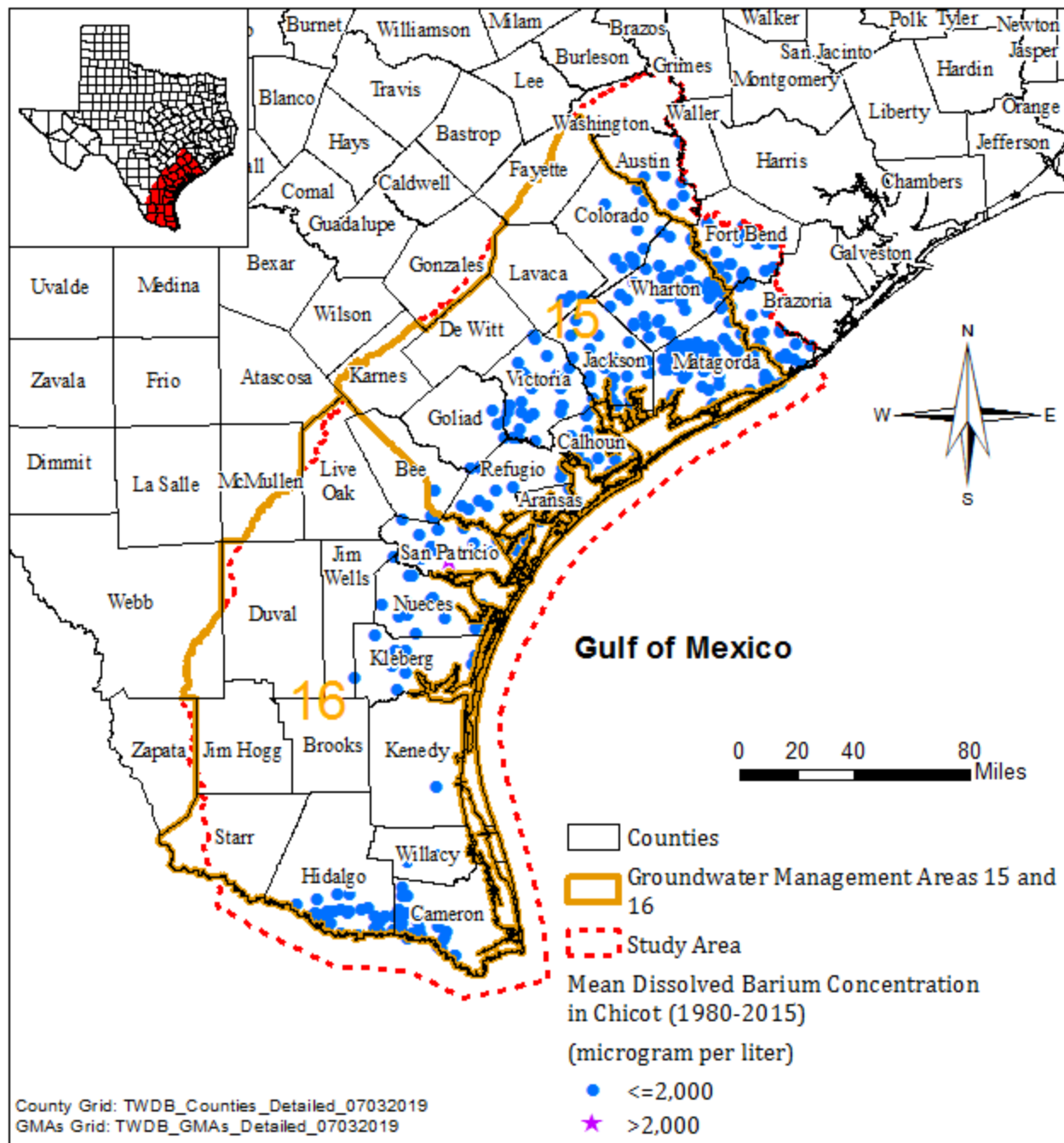


**Figure 4.7.2 Barium average concentrations in groundwater samples collected from Chicot Aquifer between 1980 and 2015.**

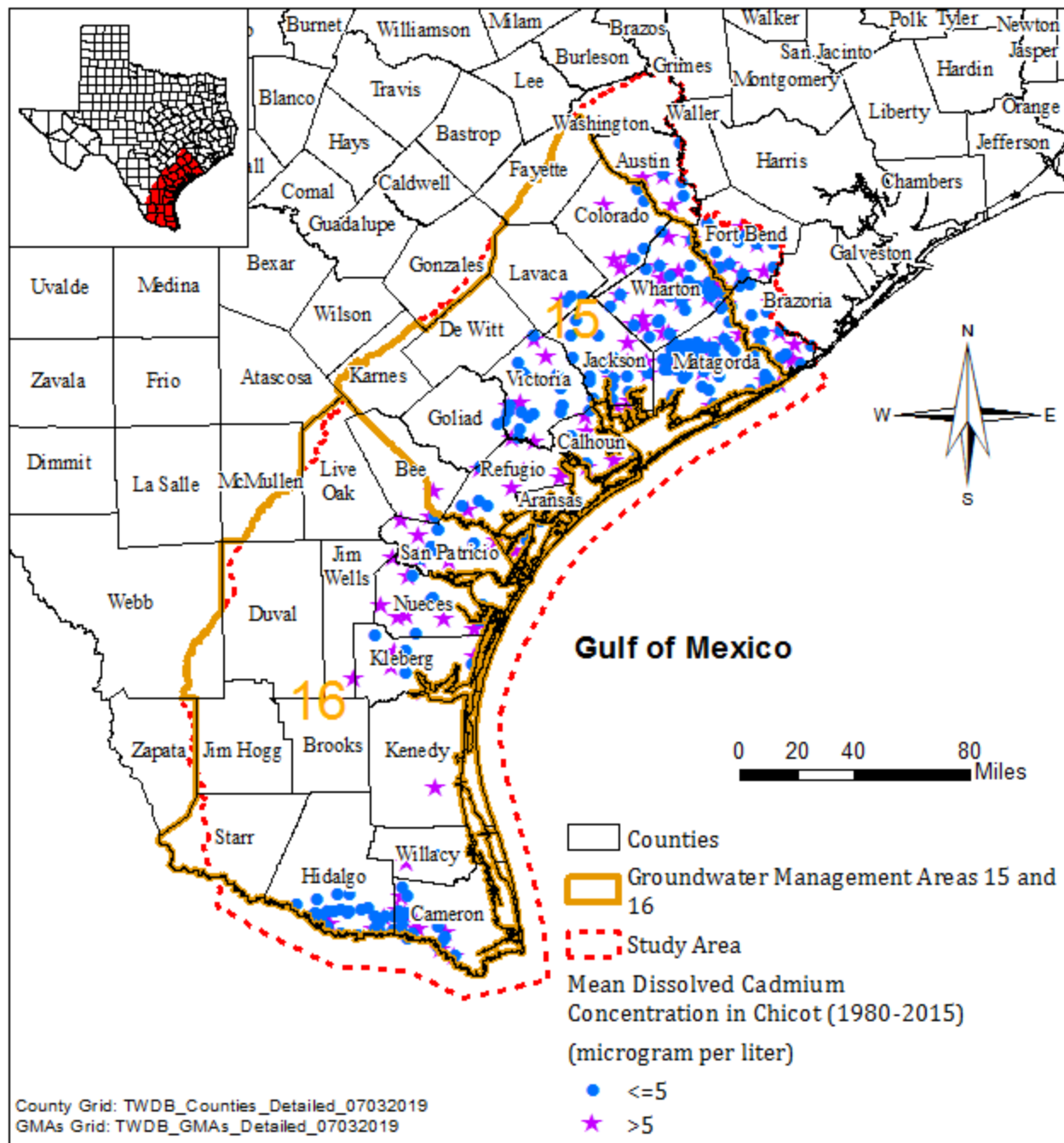


**Figure 4.7.3 Cadmium average concentrations in groundwater samples collected from Chicot Aquifer between 1980 and 2015.**



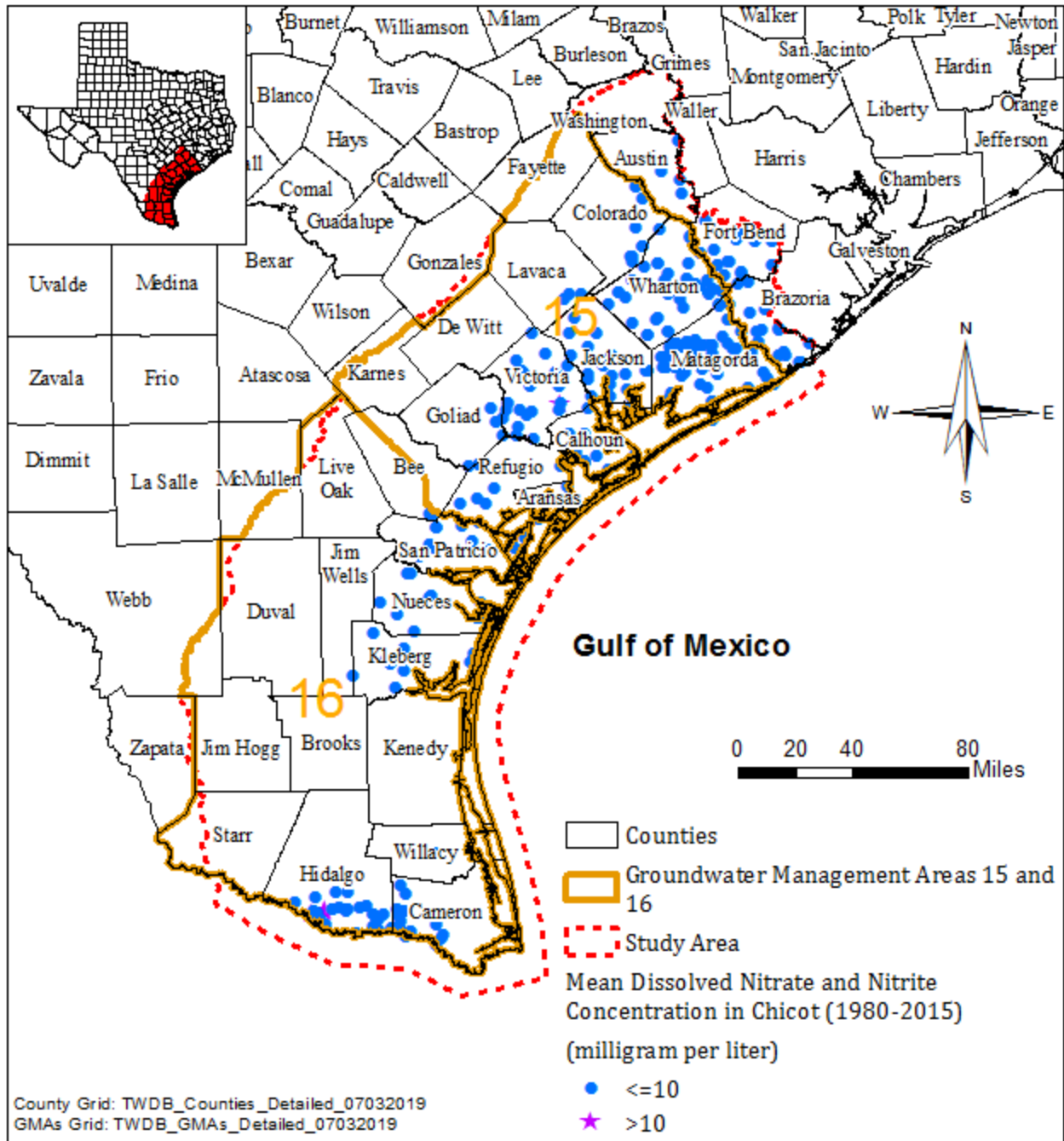


**Figure 4.7.4 Nitrate and nitrite average concentrations in groundwater samples collected from Chicot Aquifer between 1980 and 2015.**

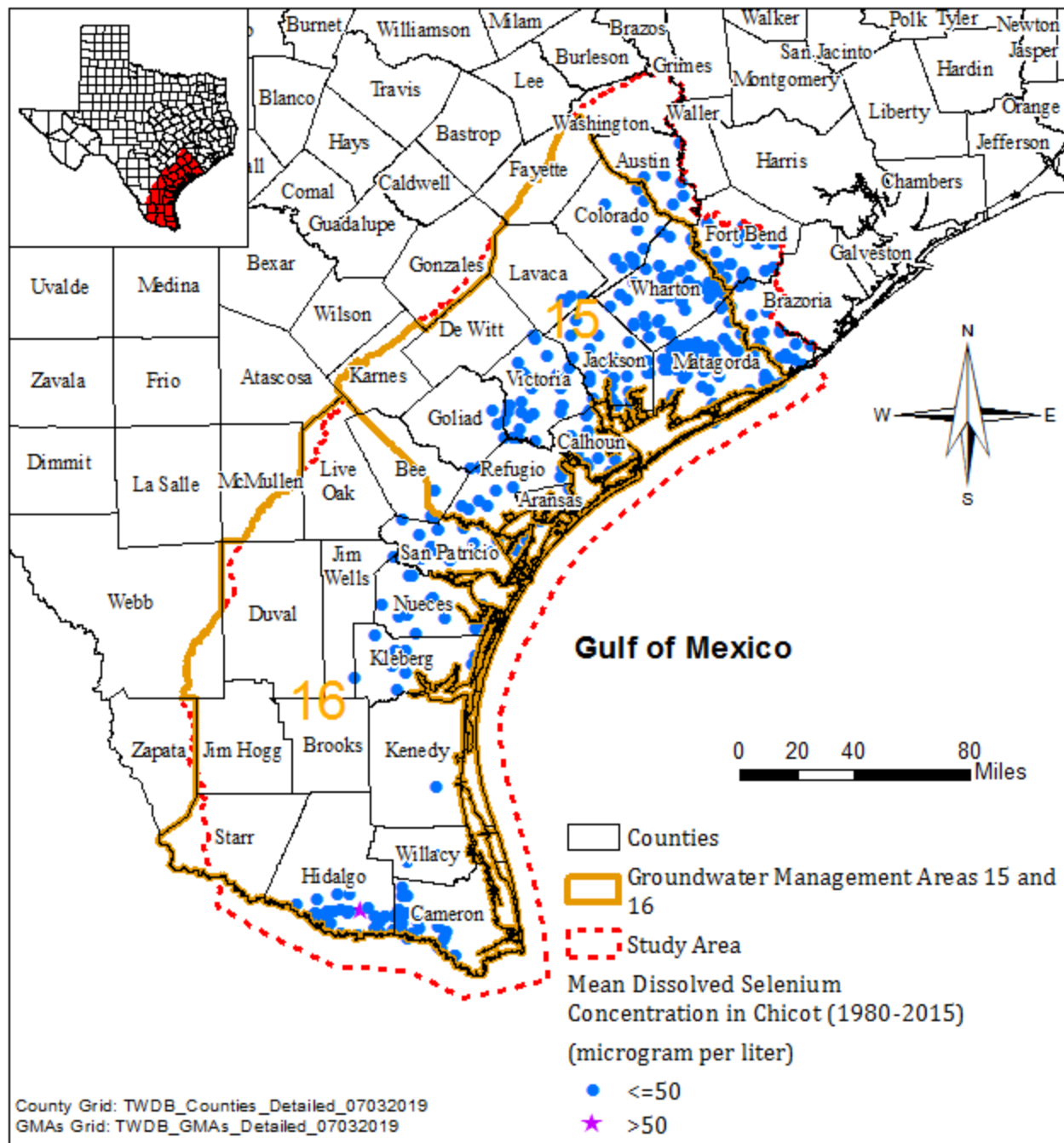


**Figure 4.7.5 Selenium average concentrations in groundwater samples collected from Chicot Aquifer between 1980 and 2015.**

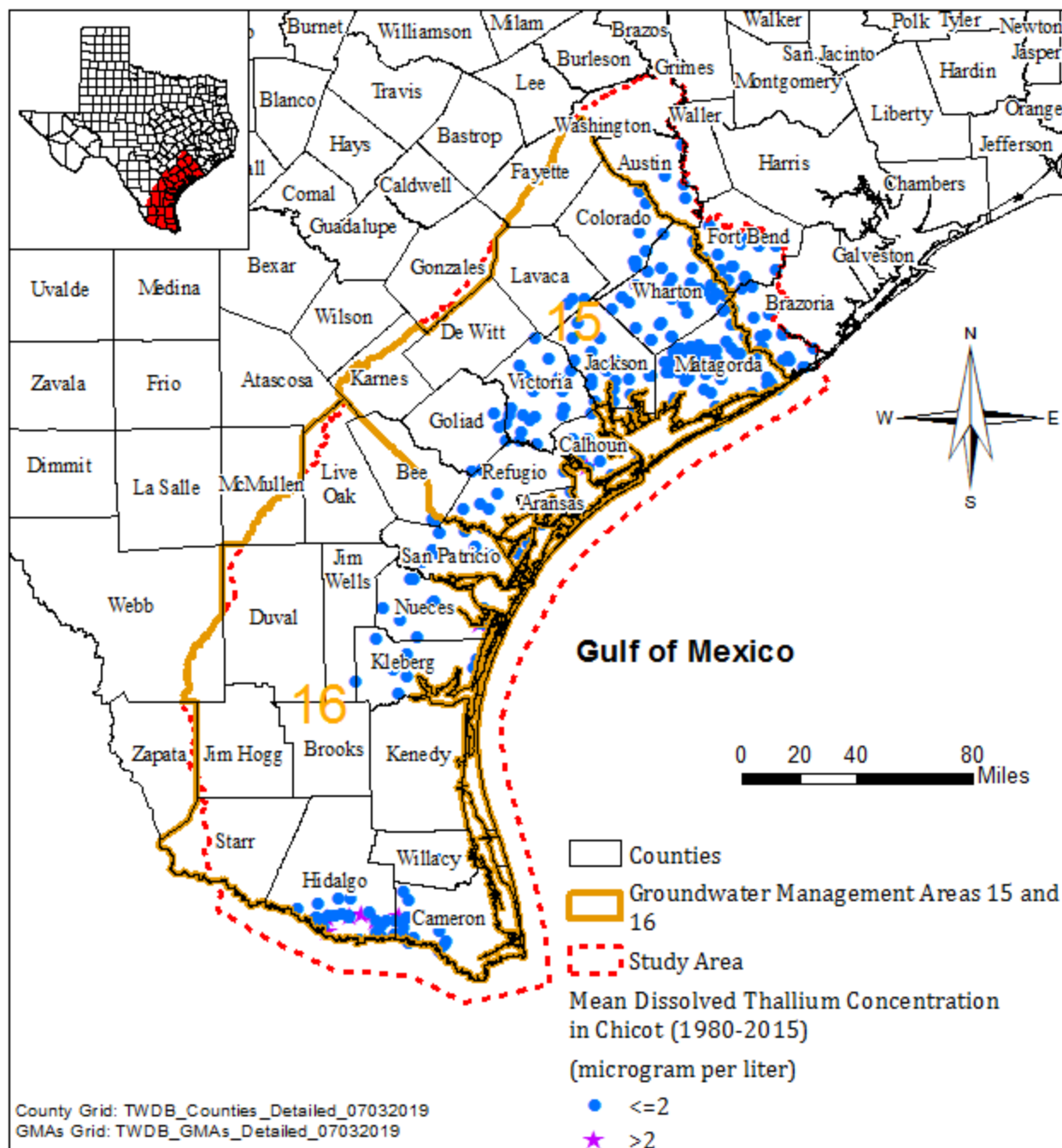


**Figure 4.7.6** Thallium average concentrations in groundwater samples collected from Chicot Aquifer between 1980 and 2015.

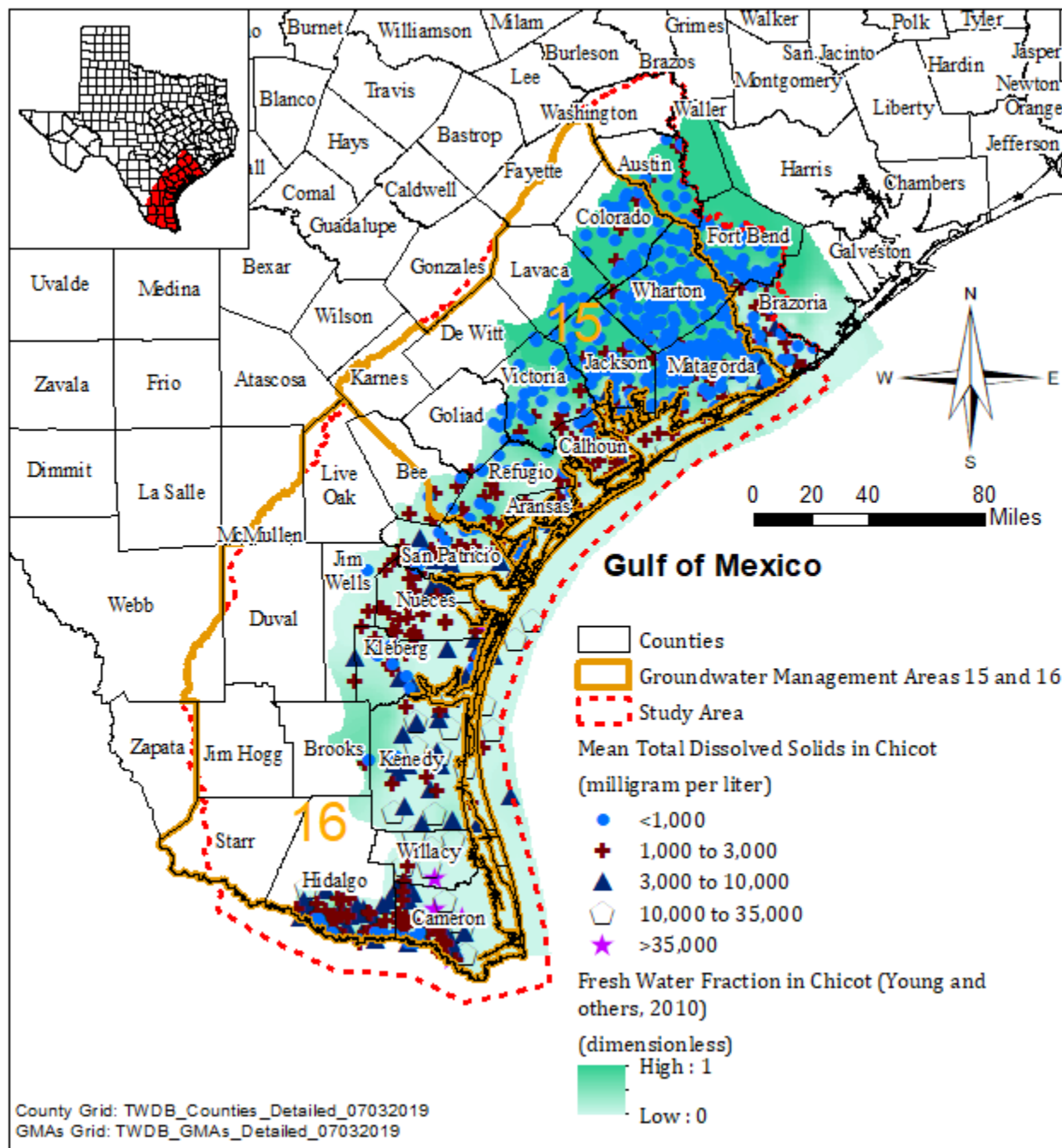


**Figure 4.7.7** Total dissolved solids average concentrations in groundwater samples collected from water wells in Chicot Aquifer between 1980 and 2015 and geophysical logs.

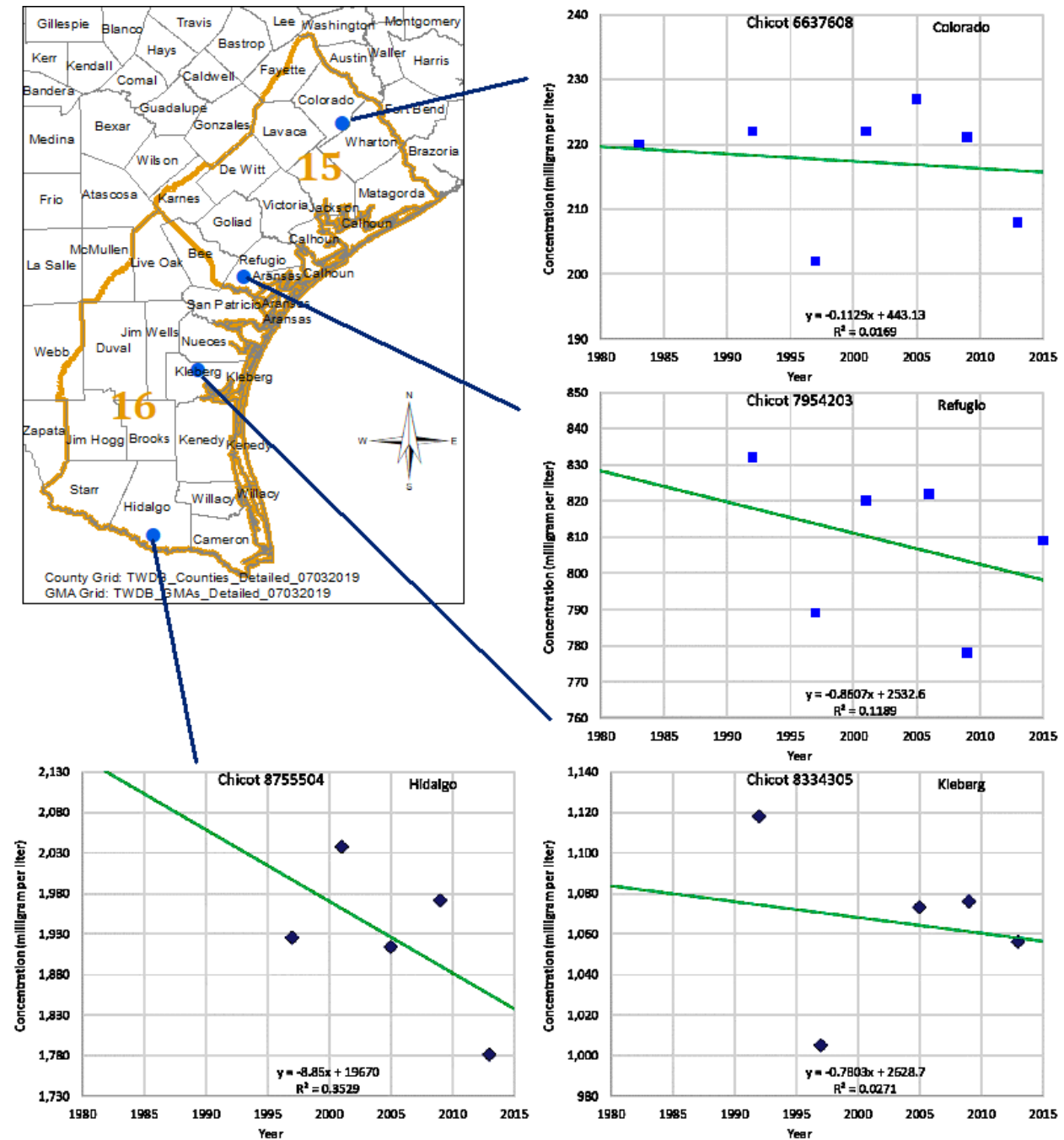


**Figure 4.7.8 Hydrograph of total dissolved solids in groundwater from the Chicot Aquifer.**

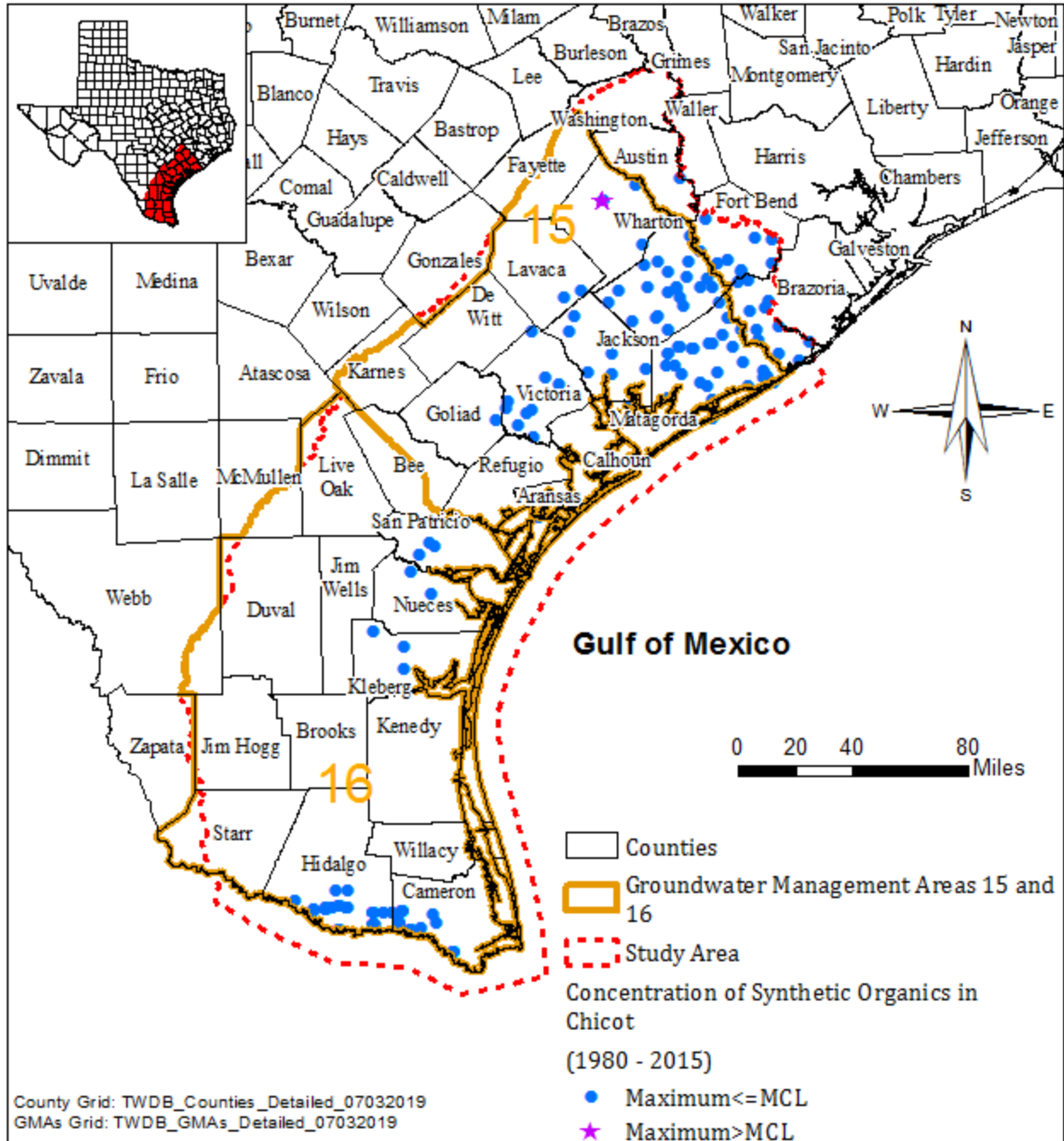


**Figure 4.7.9 Synthetic organics concentrations in groundwater samples collected from Chicot Aquifer between 1980 and 2015.**

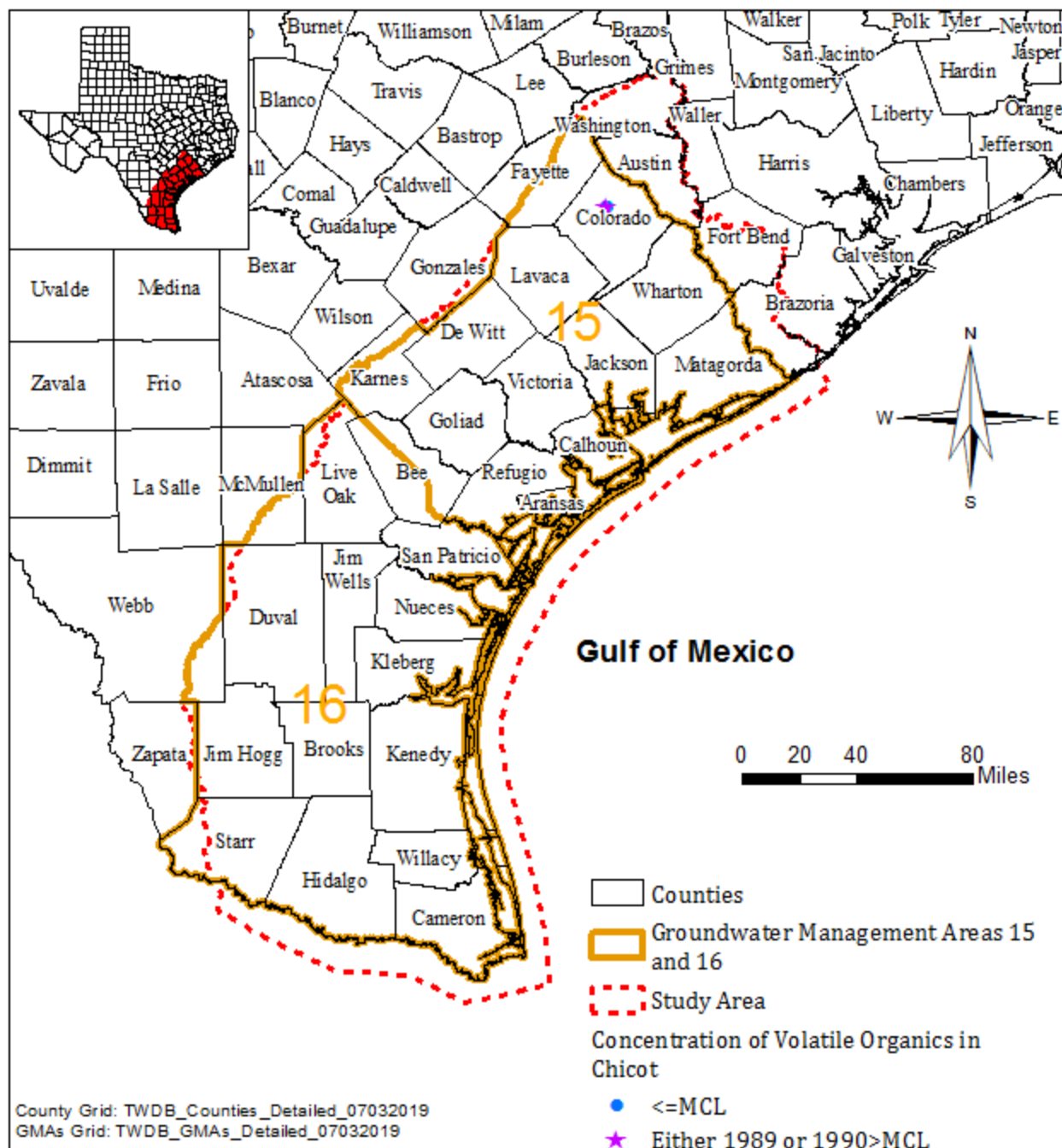


**Figure 4.7.10** Volatile organic compound concentrations in groundwater samples collected from Chicot Aquifer between 1980 and 2015.

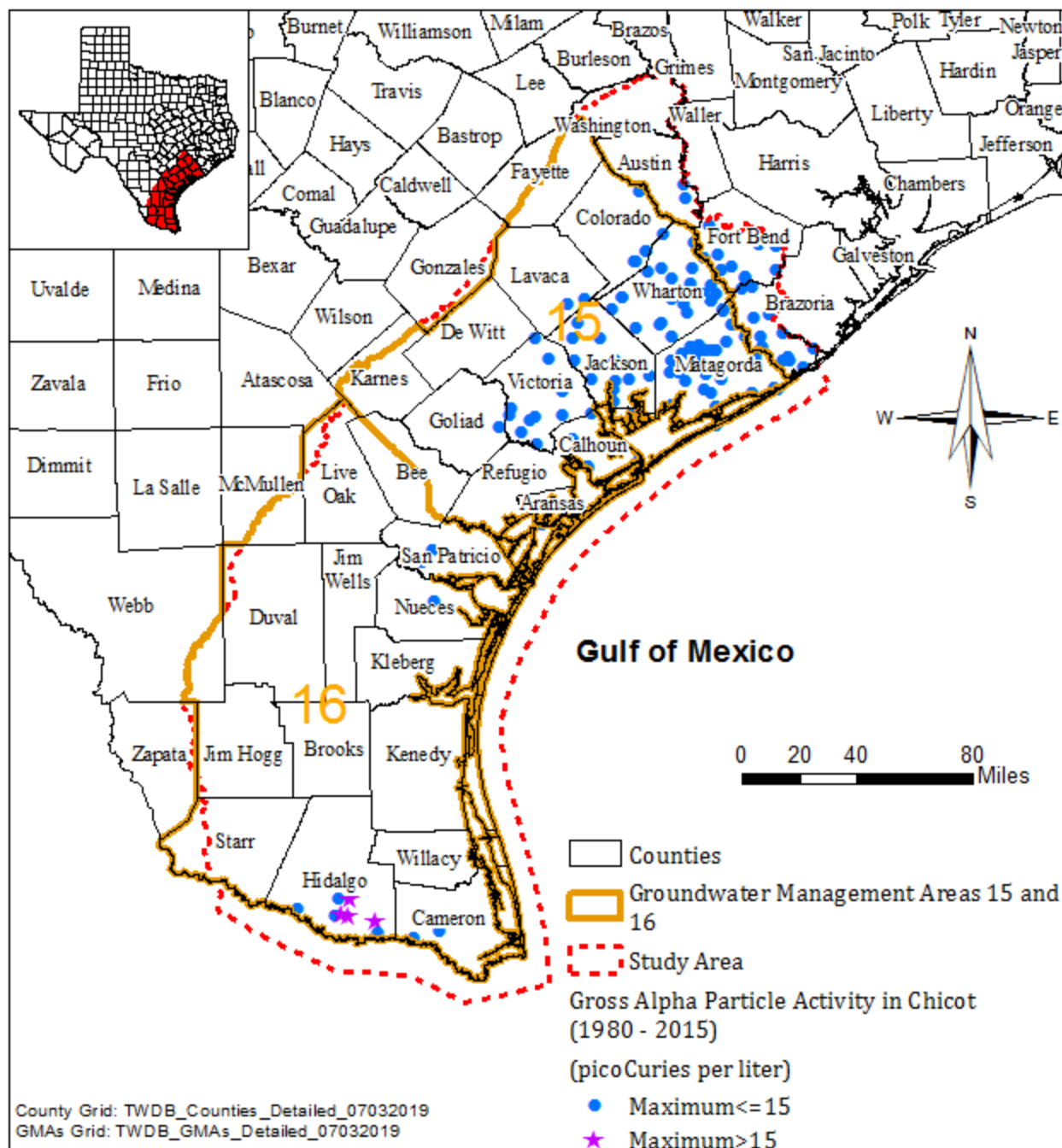


**Figure 4.7.11** Gross alpha particle activity in groundwater samples collected from Chicot Aquifer between 1980 and 2015.



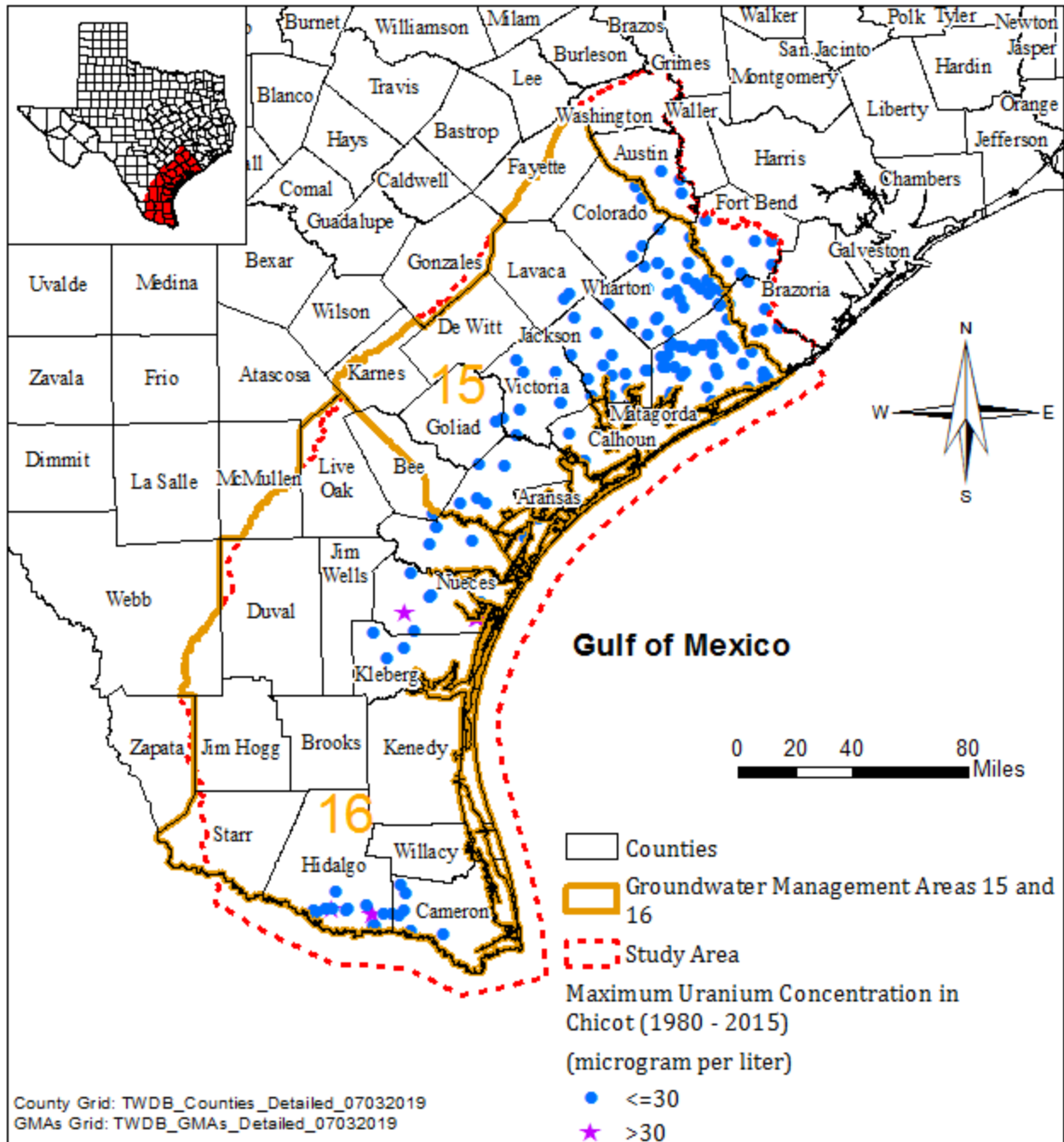


**Figure 4.7.12 Uranium concentrations in groundwater samples collected from Chicot Aquifer between 1980 and 2015.**

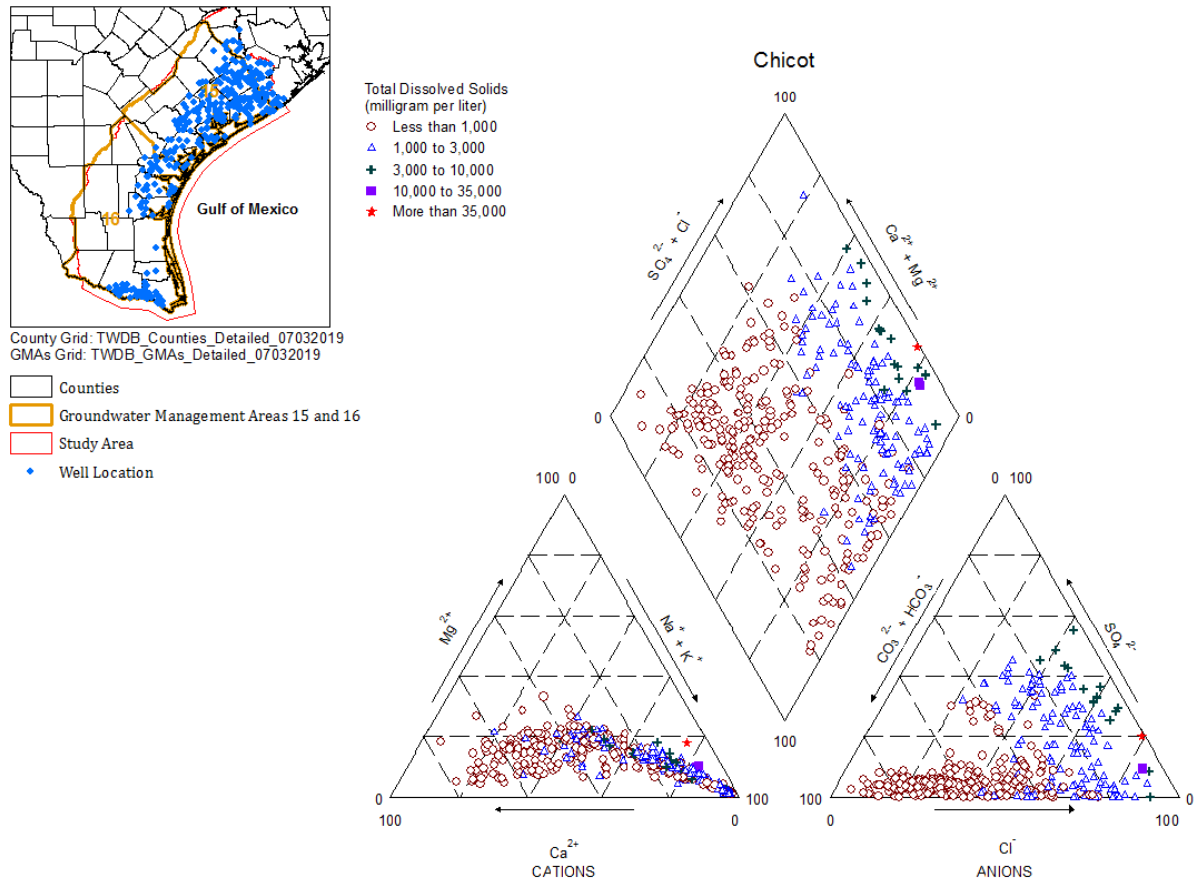


**Figure 4.7.13 Piper diagram of groundwater samples collected from Chicot Aquifer.**

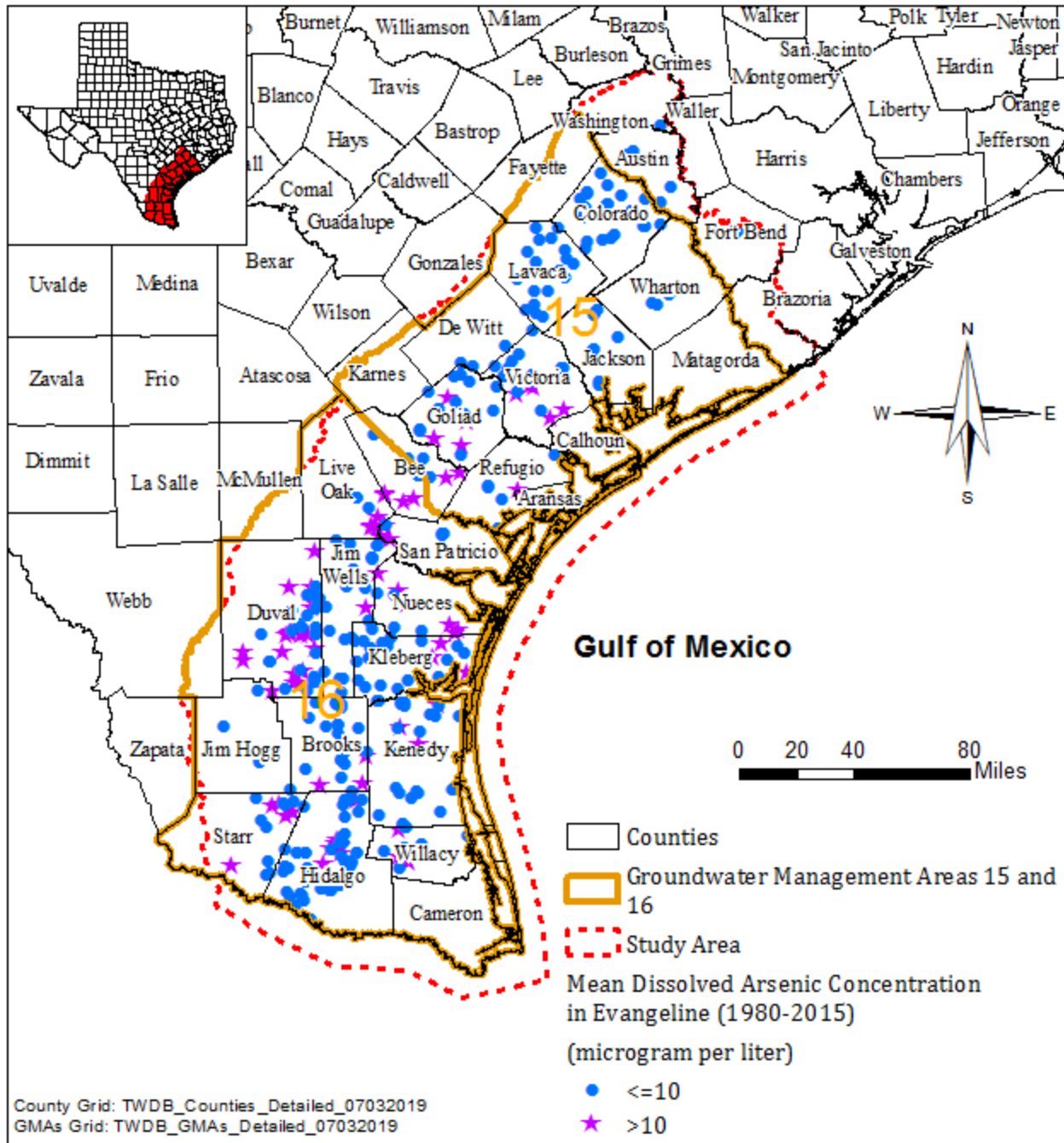


**Figure 4.7.14** Arsenic average concentrations in groundwater samples collected from Evangeline Aquifer between 1980 and 2015.

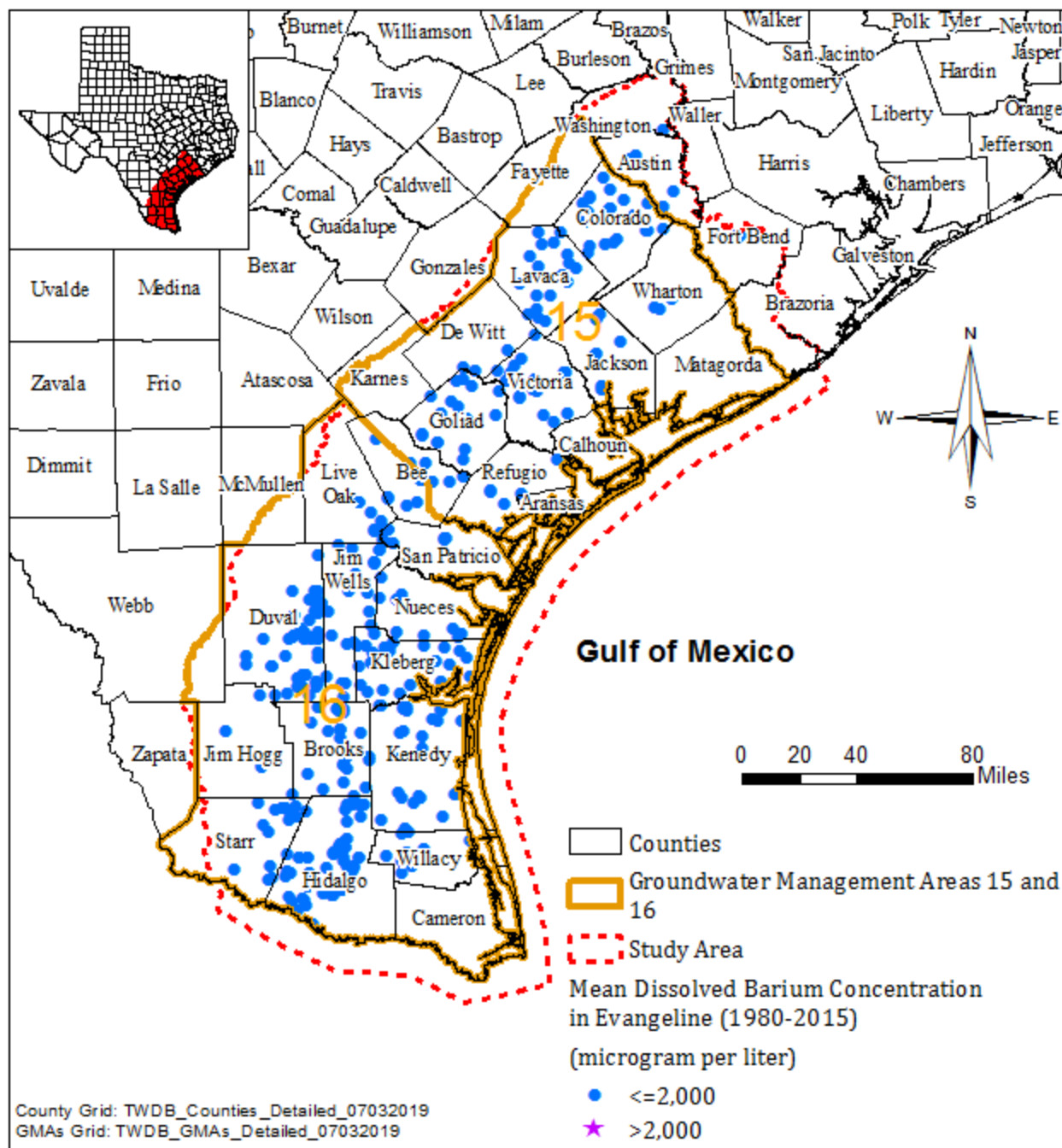


**Figure 4.7.15 Barium average concentrations in groundwater samples collected from Evangeline Aquifer between 1980 and 2015.**

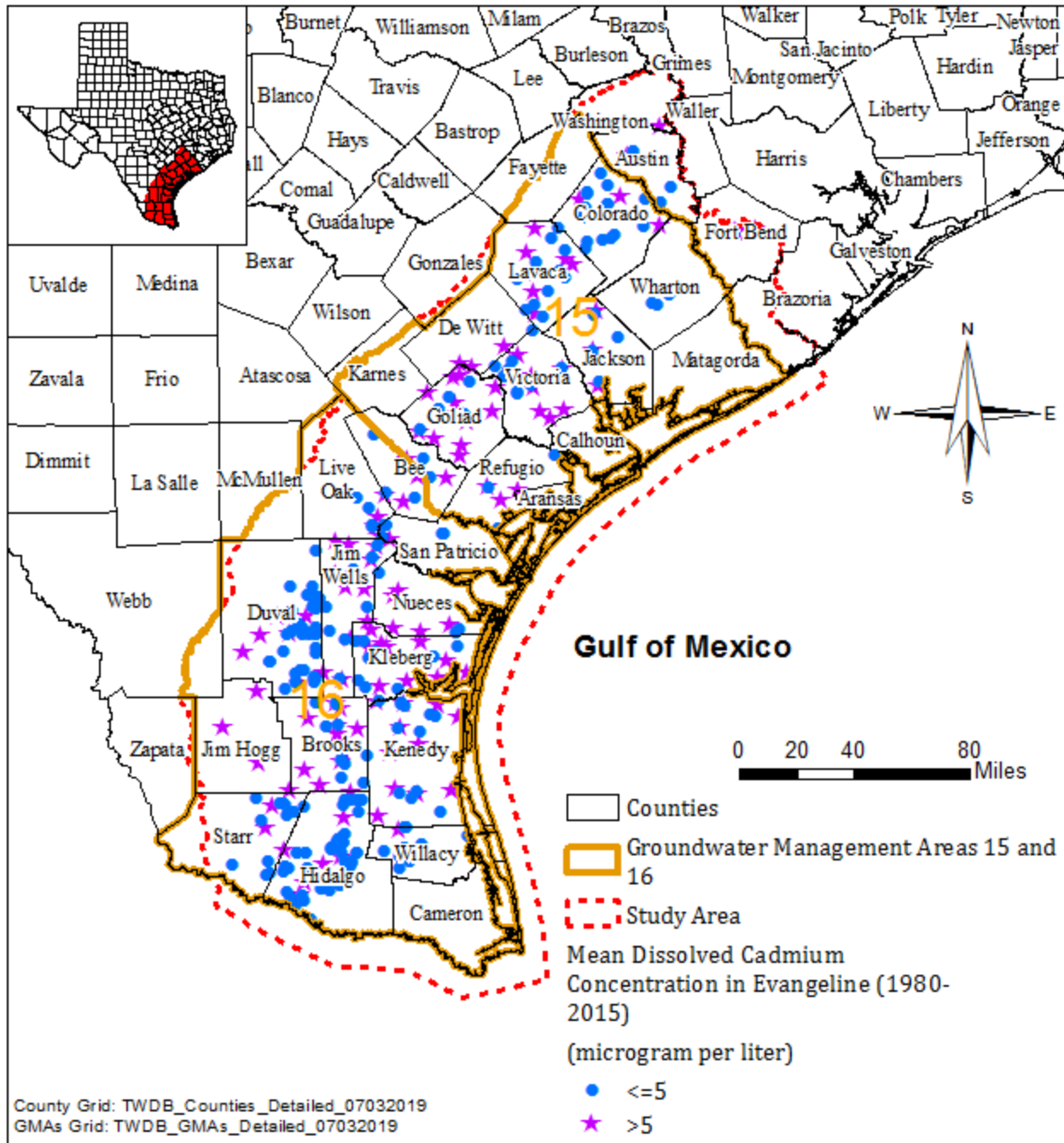


**Figure 4.7.16 Cadmium average concentrations in groundwater samples collected from Evangeline Aquifer between 1980 and 2015.**

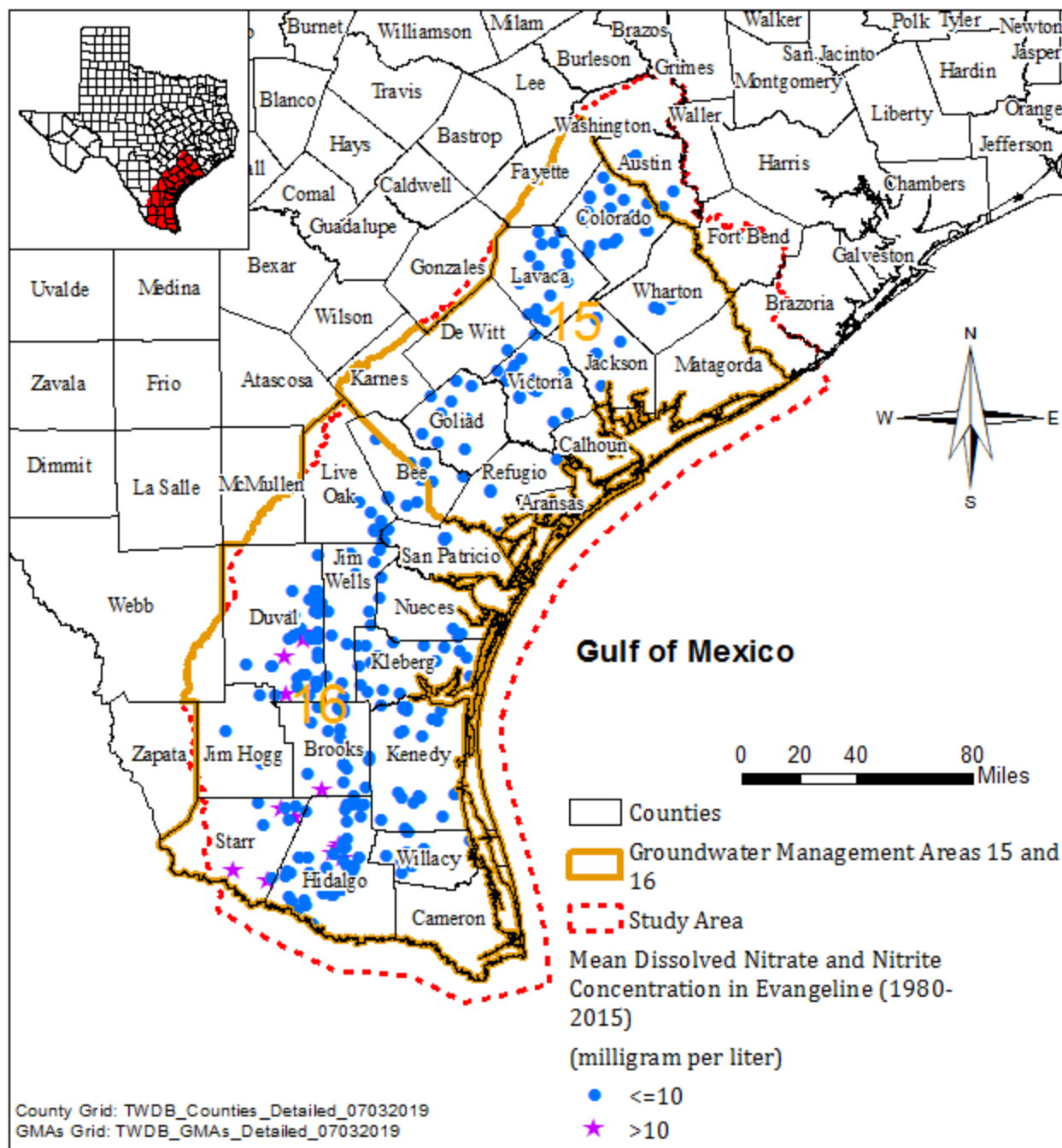


**Figure 4.7.17 Nitrate and nitrite average concentrations in groundwater samples collected from Evangeline Aquifer between 1980 and 2015.**

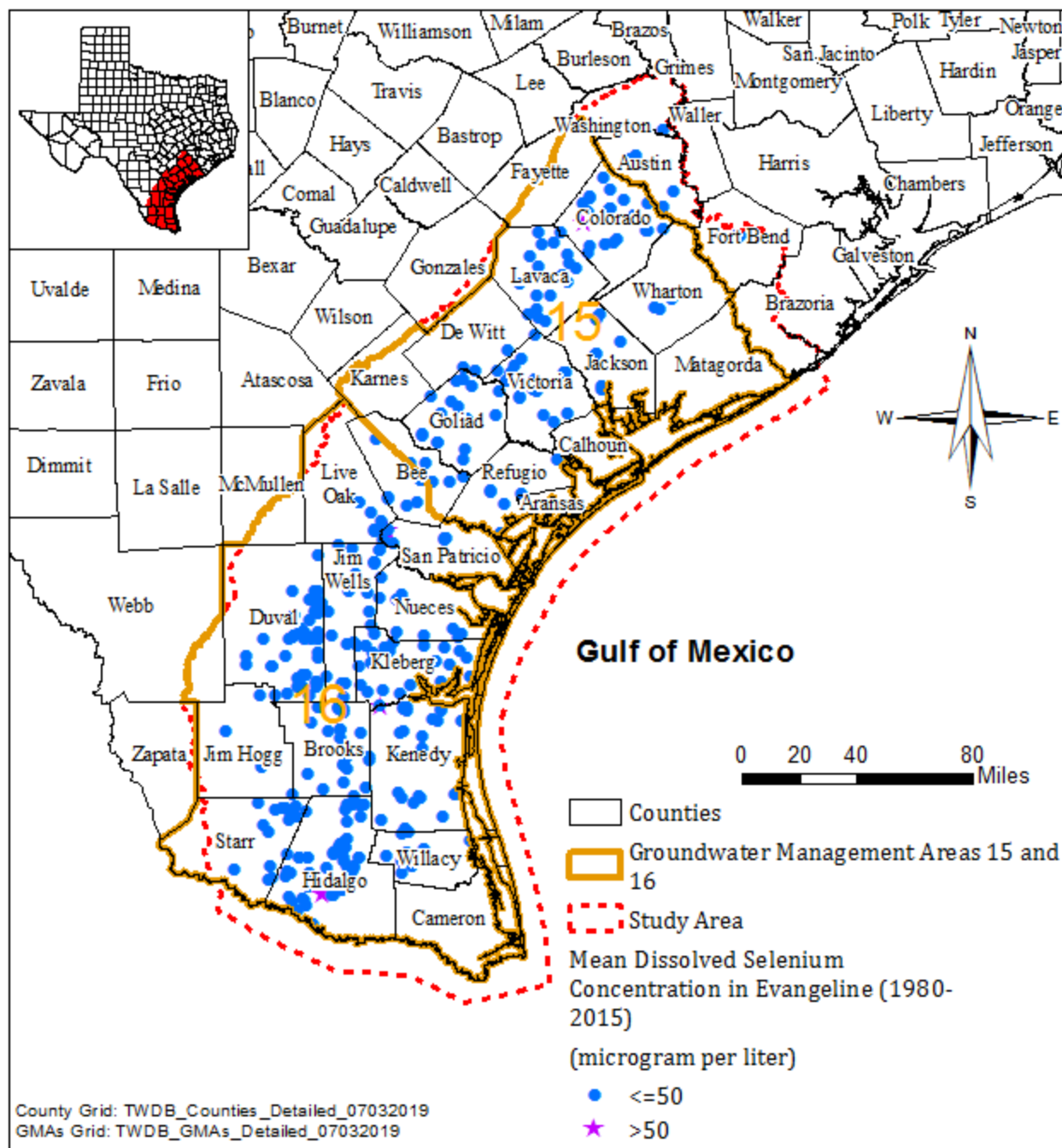


**Figure 4.7.18** Selenium average concentrations in groundwater samples collected from Evangeline Aquifer between 1980 and 2015.

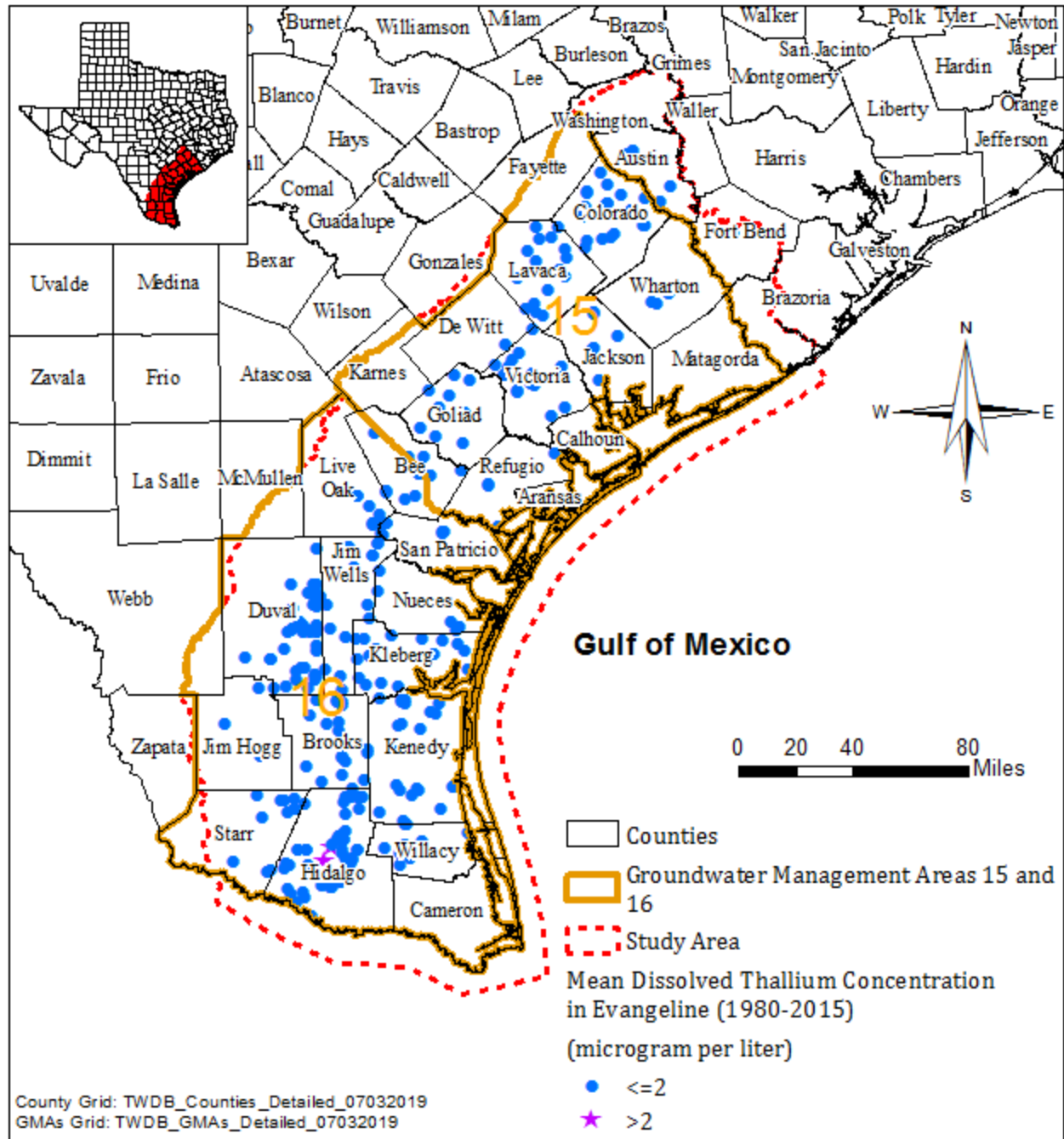


**Figure 4.7.19** Thallium average concentrations in groundwater samples collected from Evangeline Aquifer between 1980 and 2015.



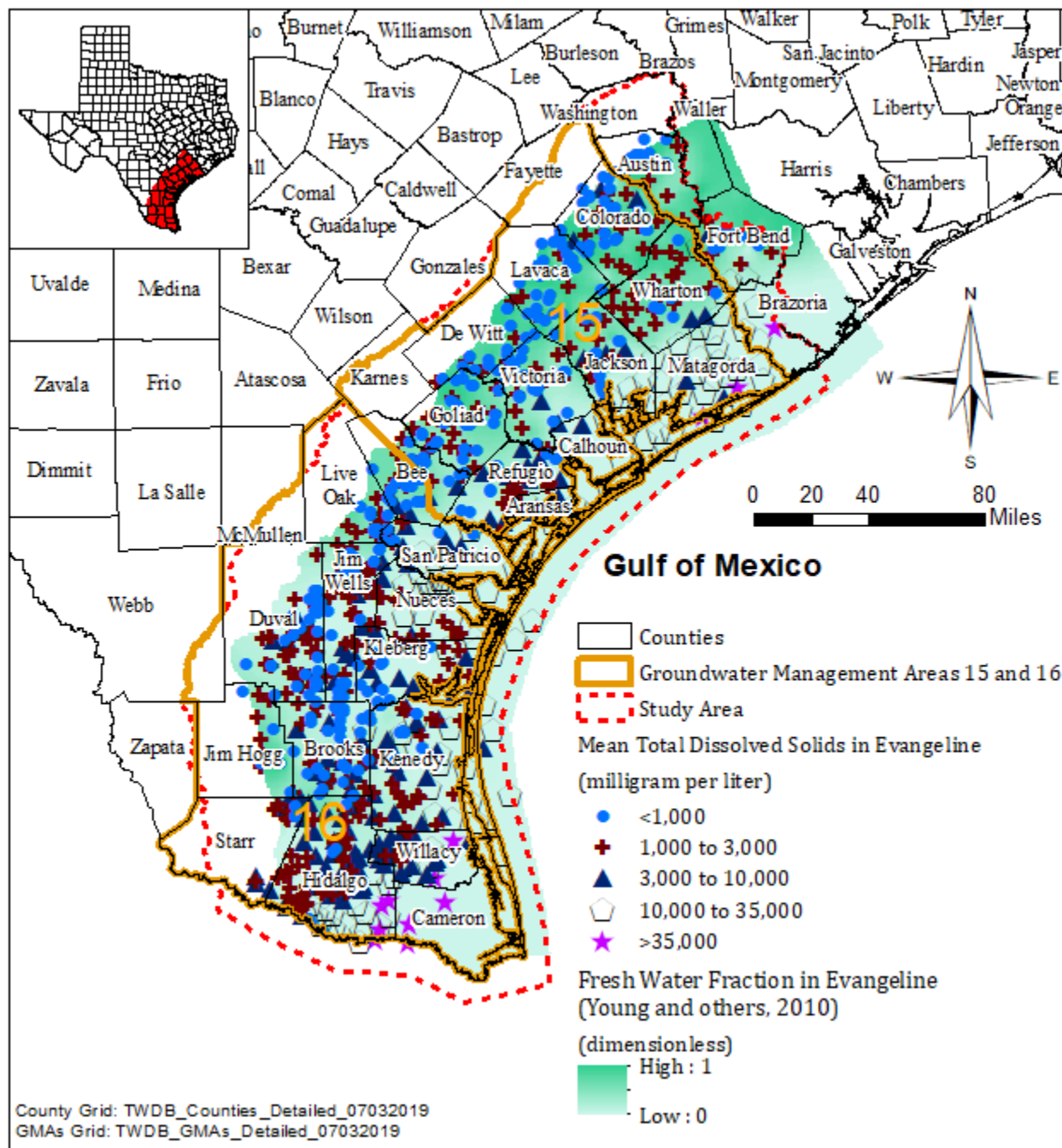


**Figure 4.7.20** Total dissolved solids average concentrations in groundwater samples collected from water wells in Evangeline Aquifer between 1980 and 2015 and geophysical logs.

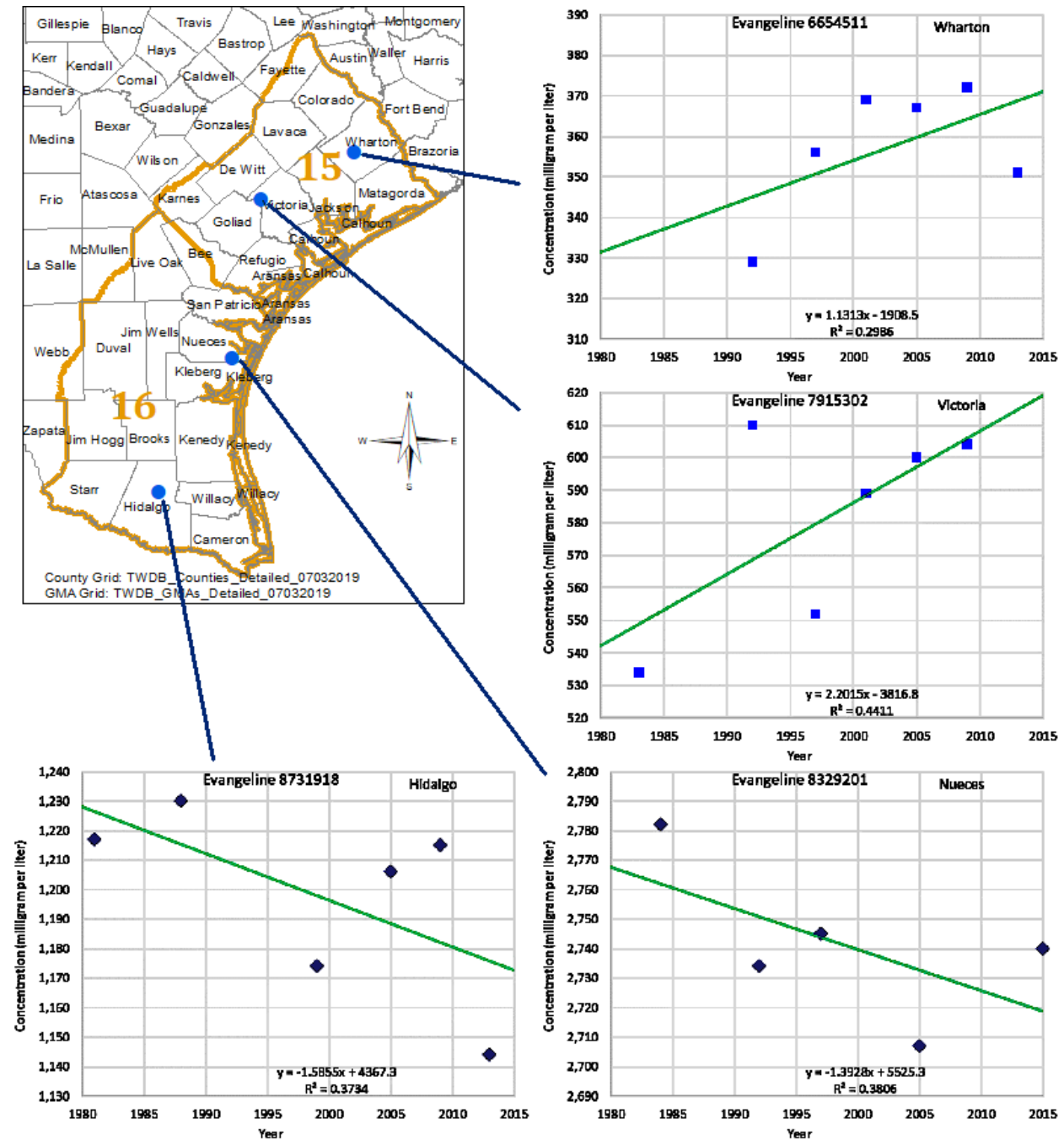
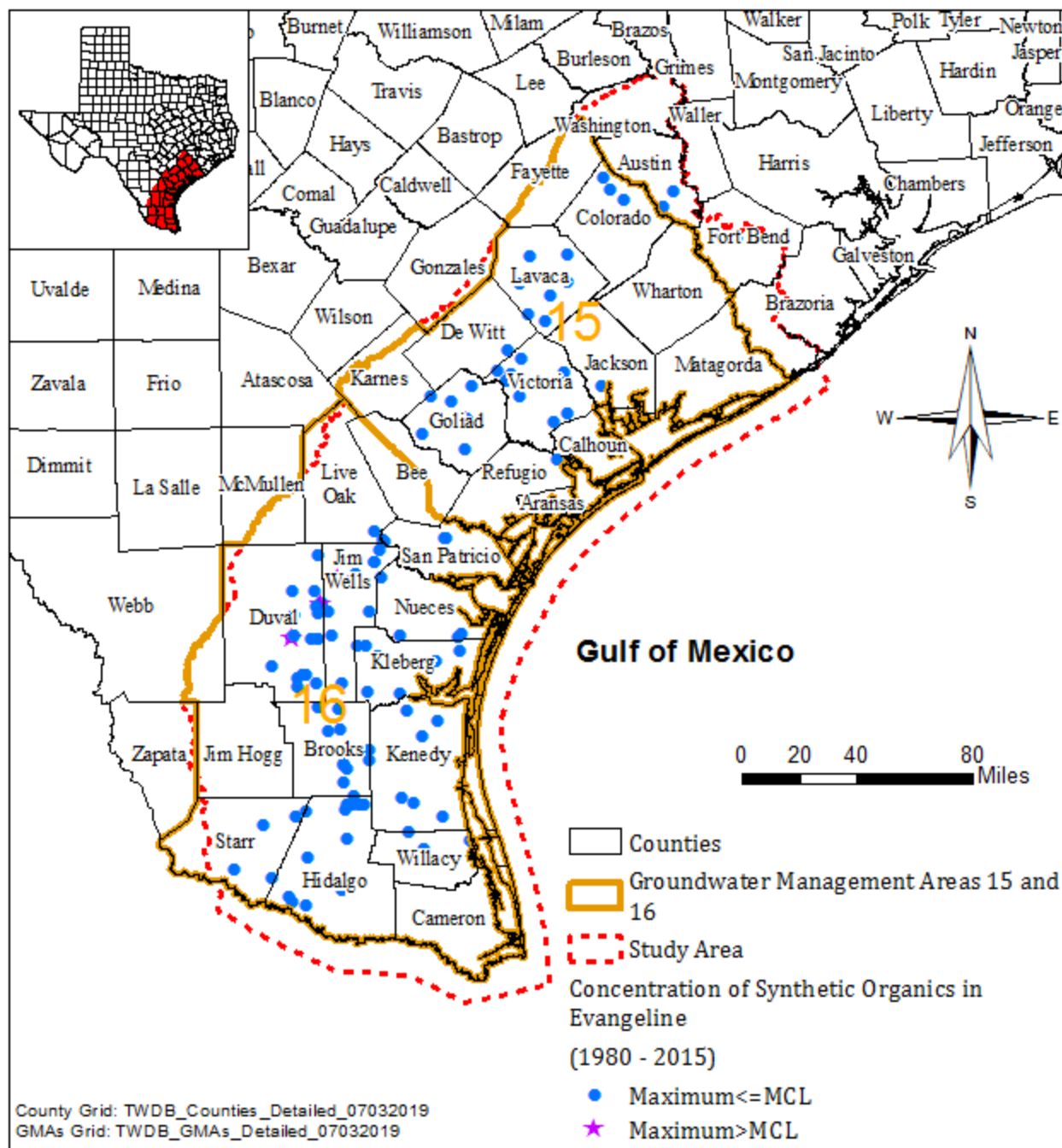
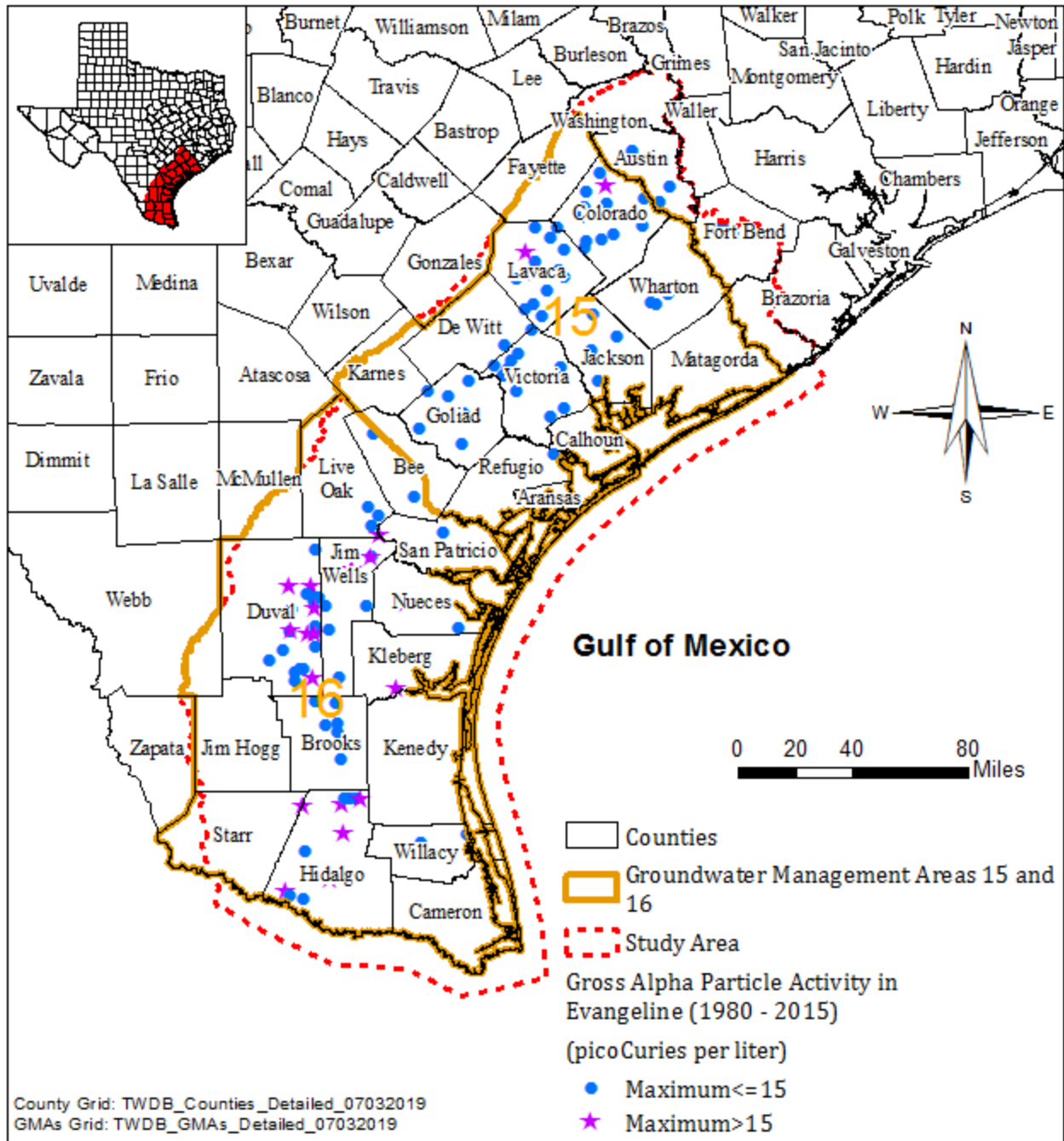


Figure 4.7.21 Hydrograph of total dissolved solids in groundwater from the Evangeline Aquifer.



**Figure 4.7.22 Synthetic organics concentrations in groundwater samples collected from Evangeline Aquifer between 1980 and 2015.**



**Figure 4.7.23** Gross alpha particle activity in groundwater samples collected from Evangeline Aquifer between 1980 and 2015.

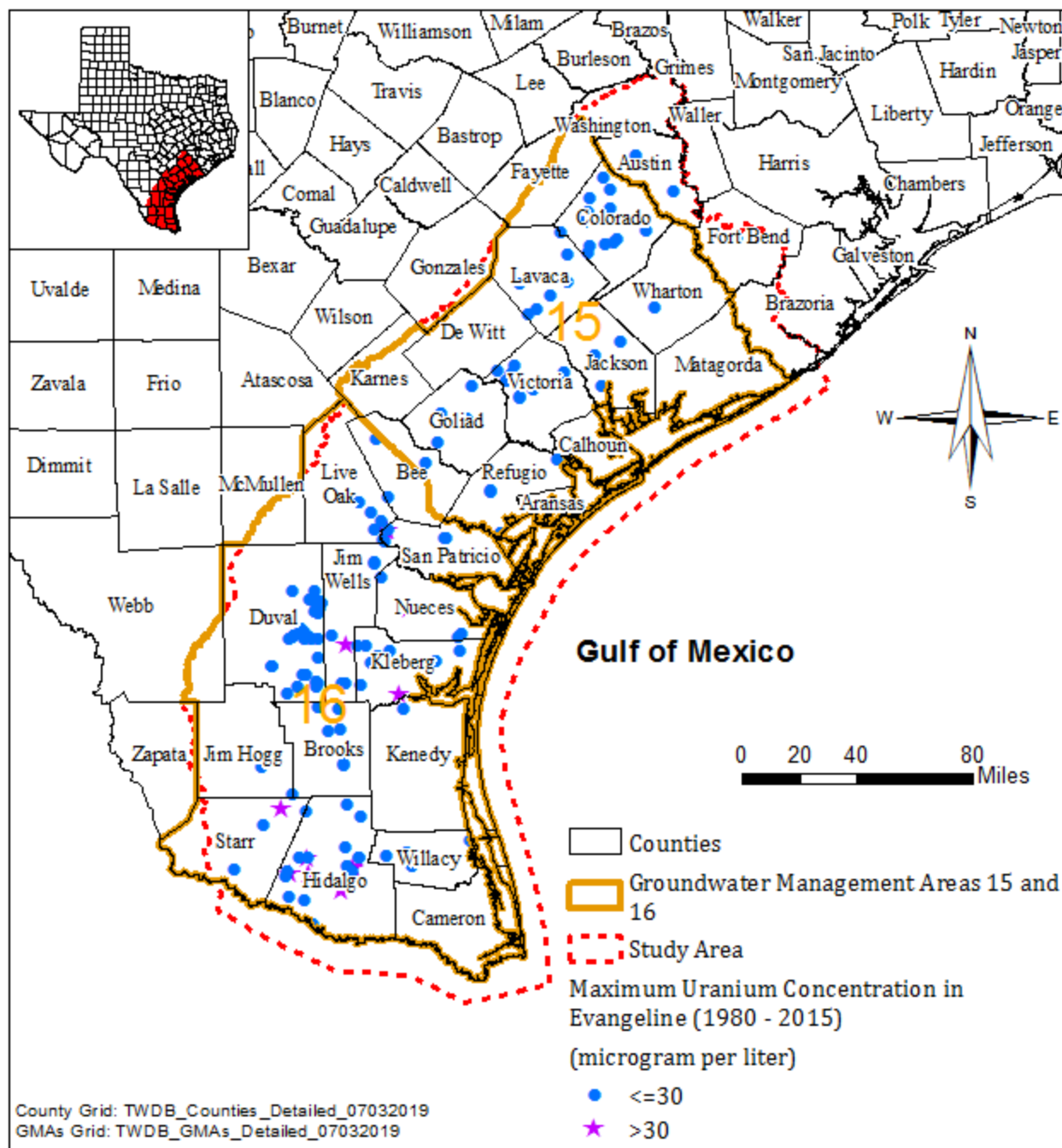


**Figure 4.7.24** Uranium concentrations in groundwater samples collected from Evangeline Aquifer between 1980 and 2015.

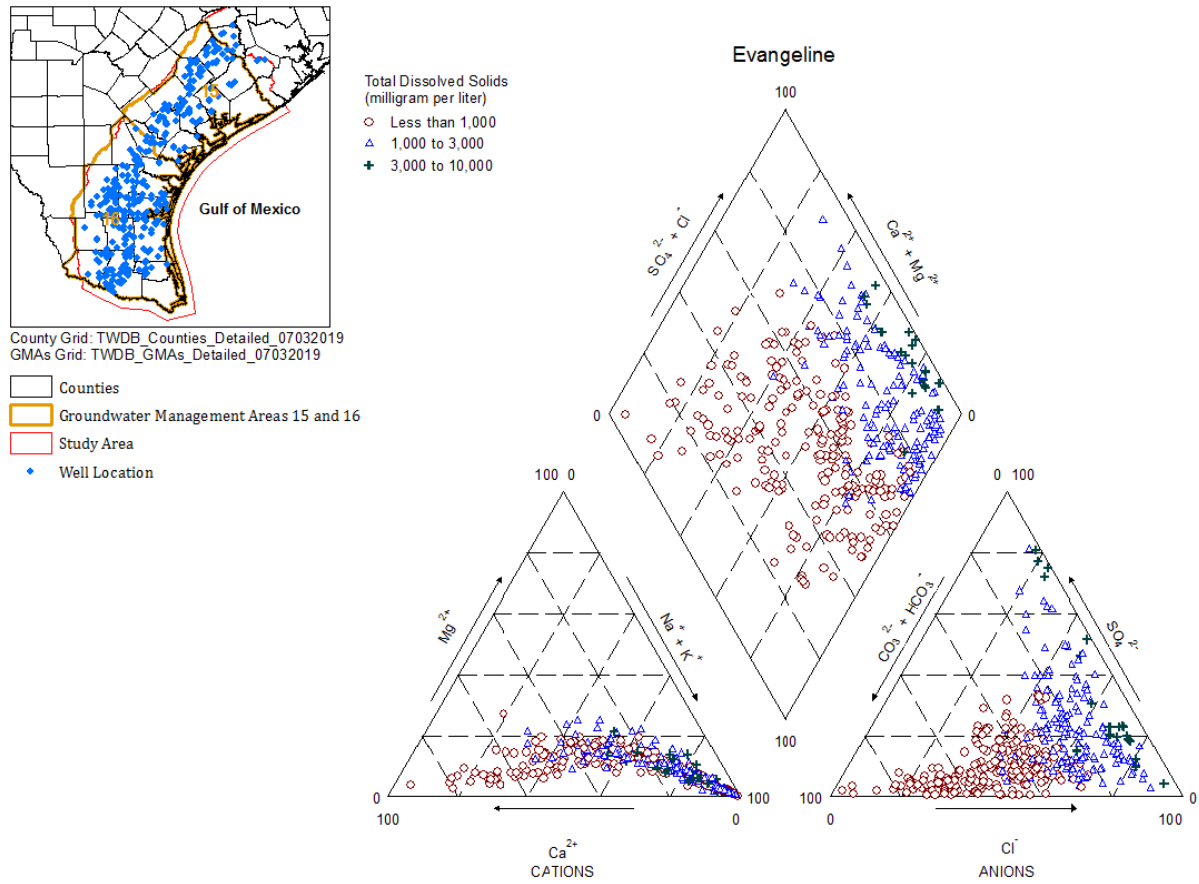


**Figure 4.7.25 Piper diagram of groundwater samples collected from Evangeline Aquifer.**

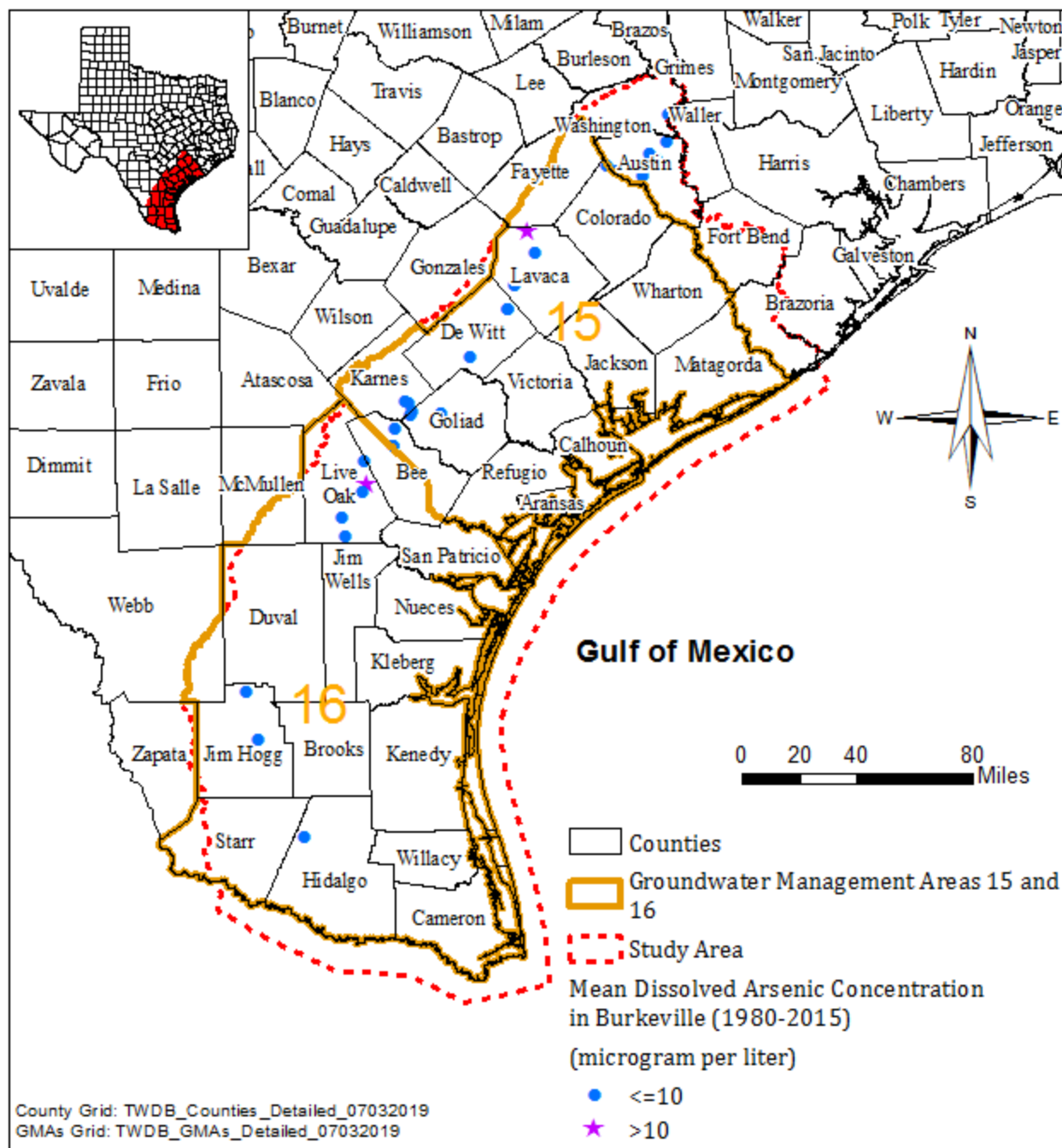


**Figure 4.7.26** Arsenic average concentrations in groundwater samples collected from Burkeville Unit between 1980 and 2015.

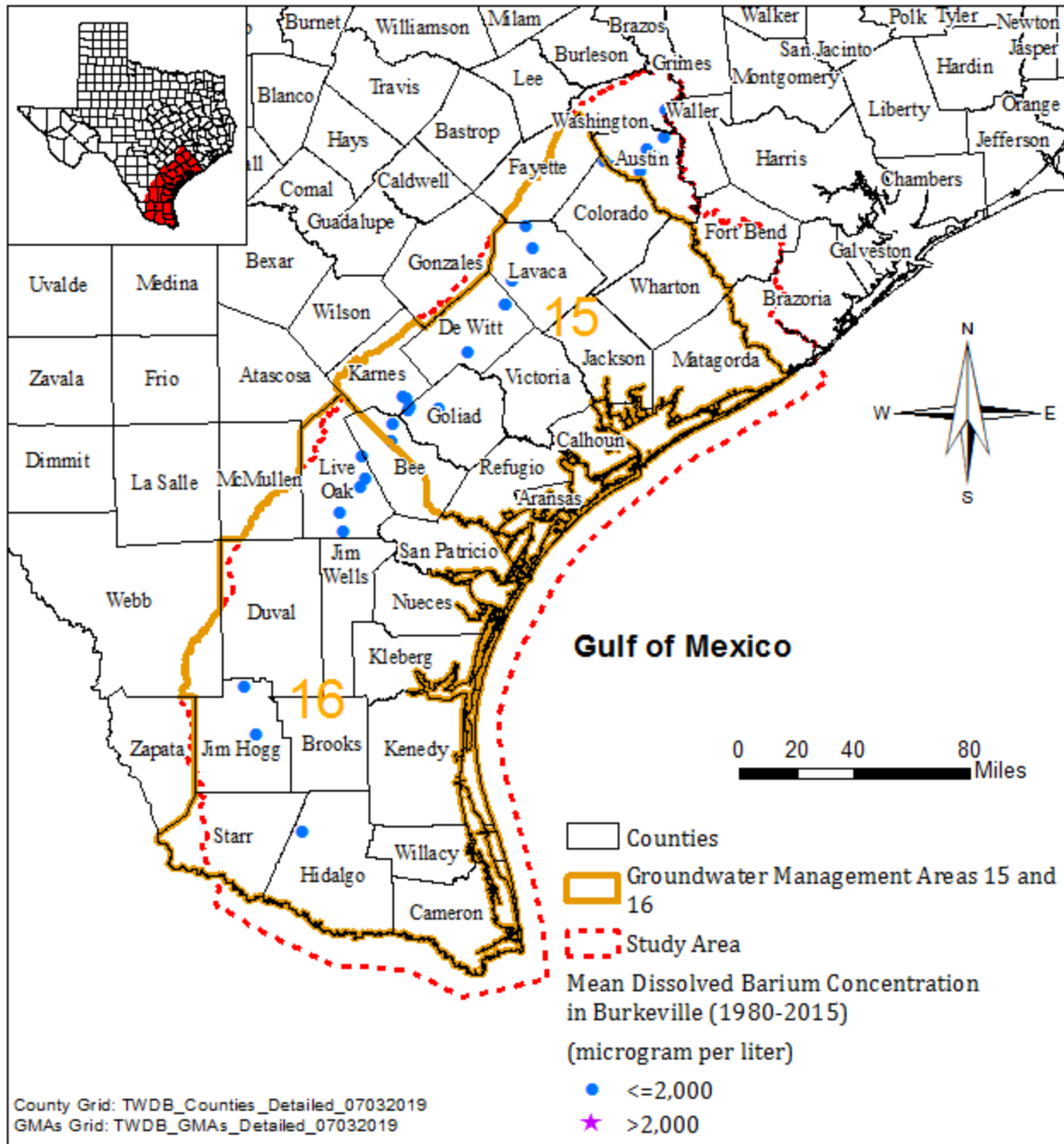


**Figure 4.7.27 Barium average concentrations in groundwater samples collected from Burkeville Unit between 1980 and 2015.**



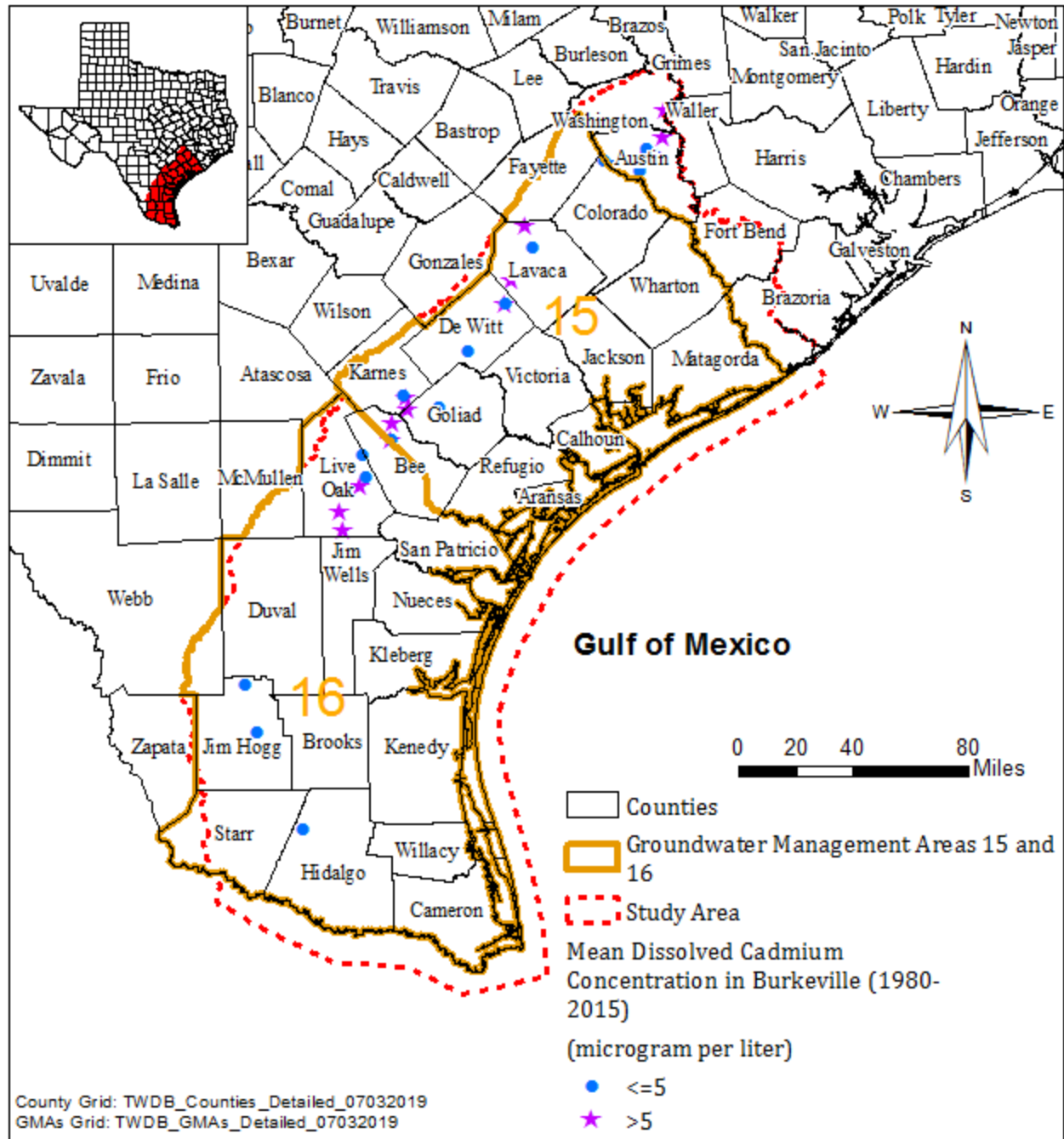


**Figure 4.7.28 Cadmium average concentrations in groundwater samples collected from Burkeville Unit between 1980 and 2015.**

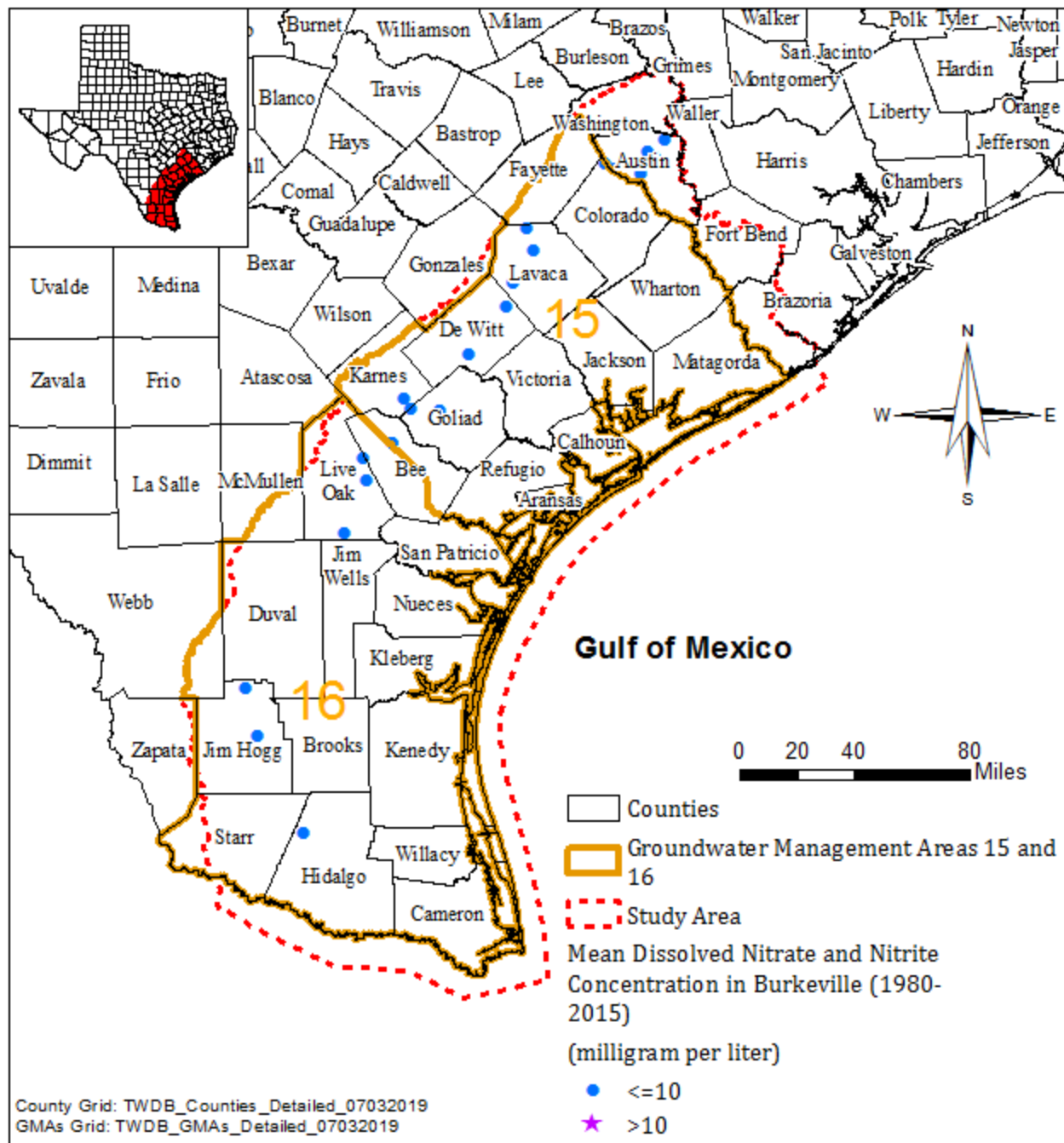


**Figure 4.7.29 Nitrate and nitrite average concentrations in groundwater samples collected from Burkeville Unit between 1980 and 2015.**

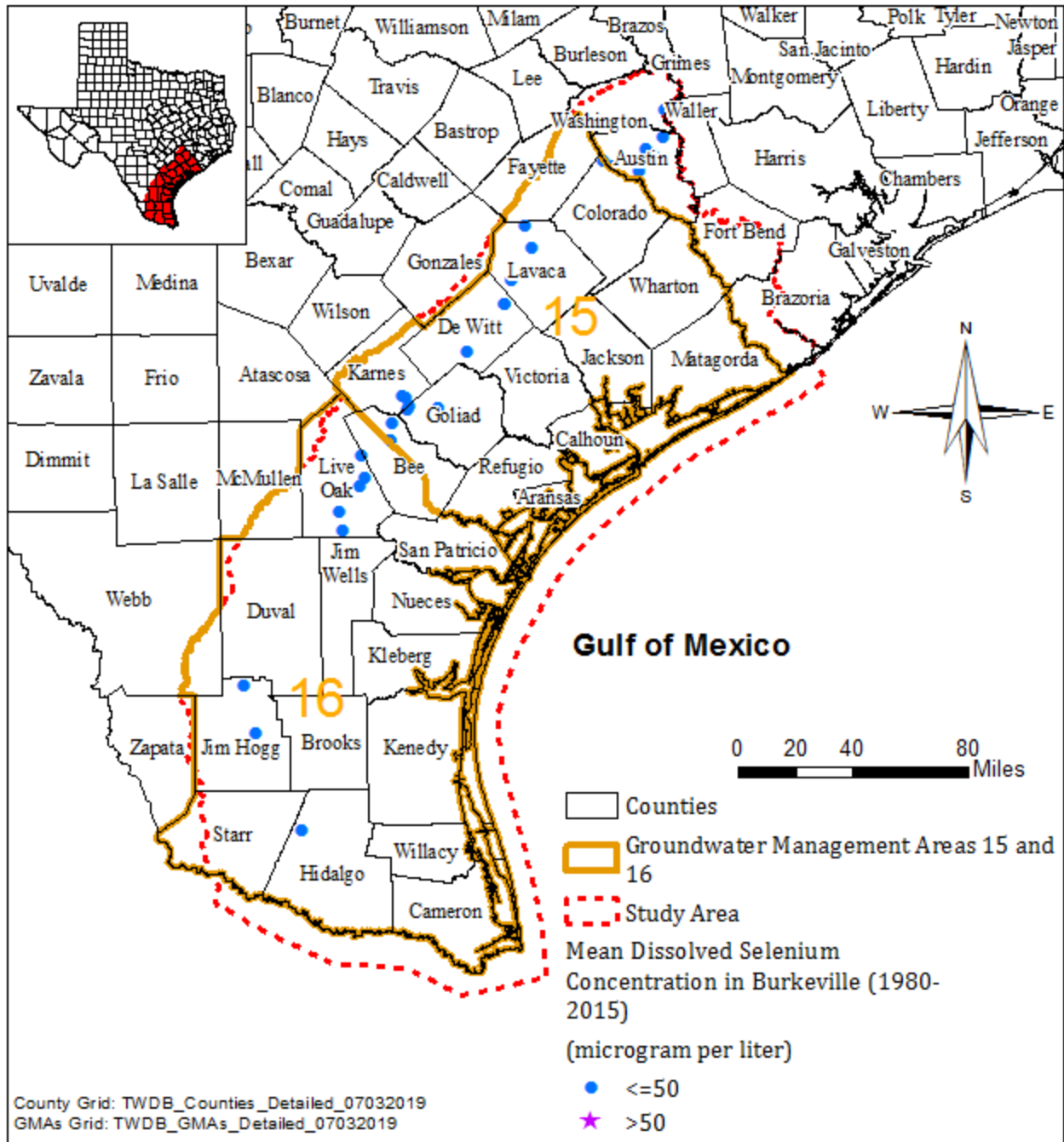


**Figure 4.7.30 Selenium average concentrations in groundwater samples collected from Burkeville Unit between 1980 and 2015.**

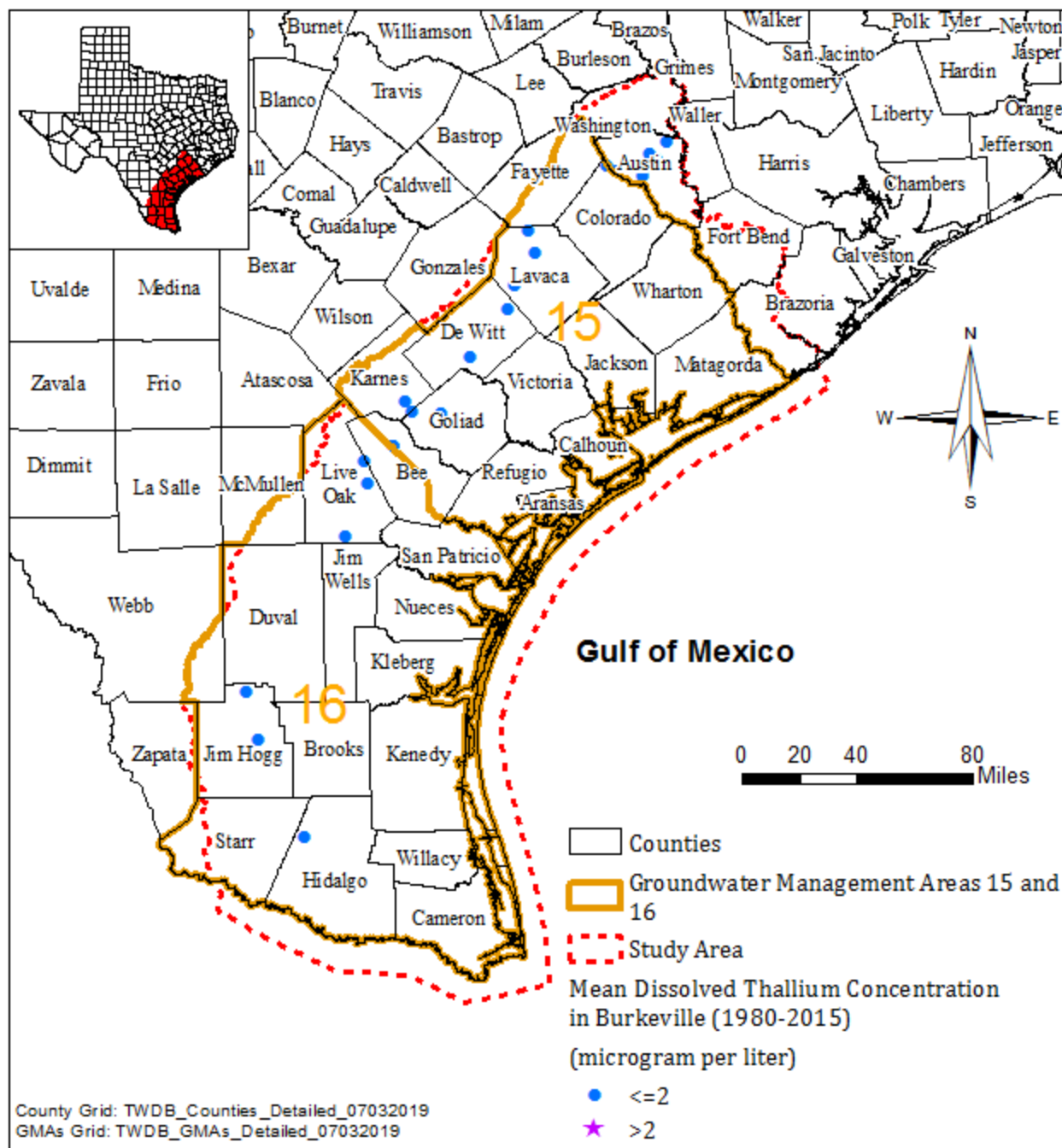


**Figure 4.7.31** Thallium average concentrations in groundwater samples collected from Burkeville Unit between 1980 and 2015.

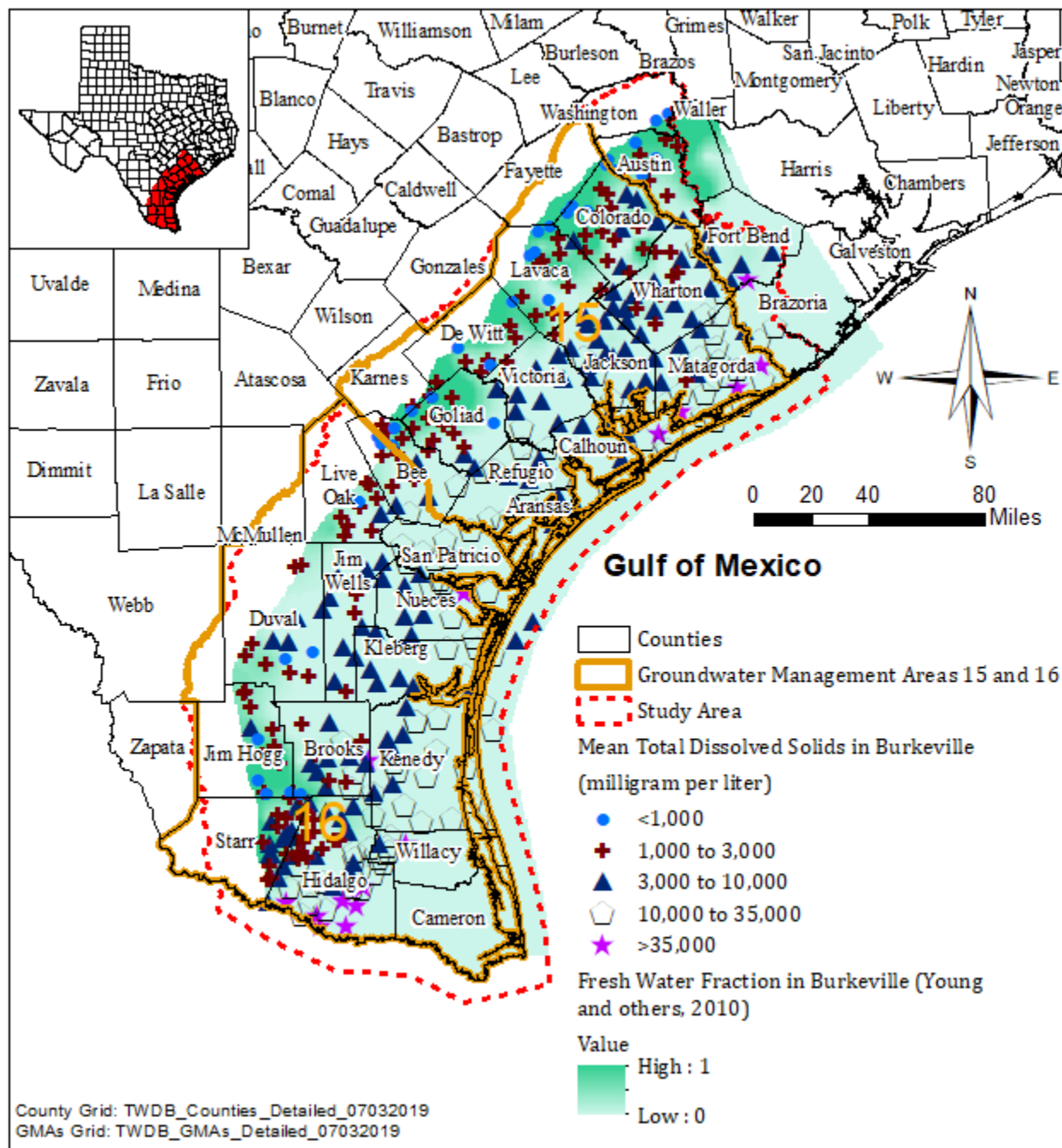


**Figure 4.7.32** Total dissolved solids average concentrations in groundwater samples collected from water wells in Burkeville Unit between 1980 and 2015 and geophysical logs.

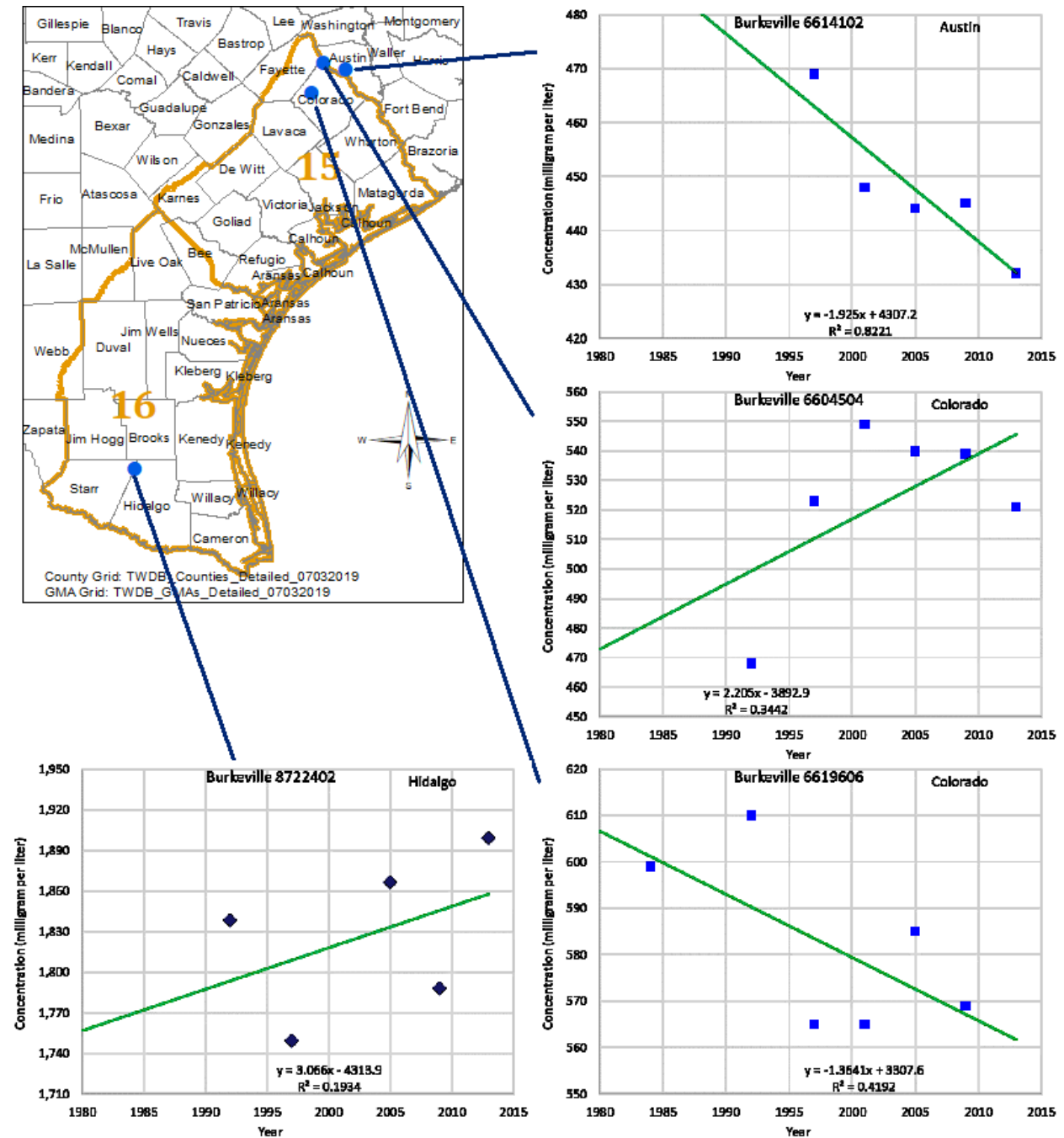
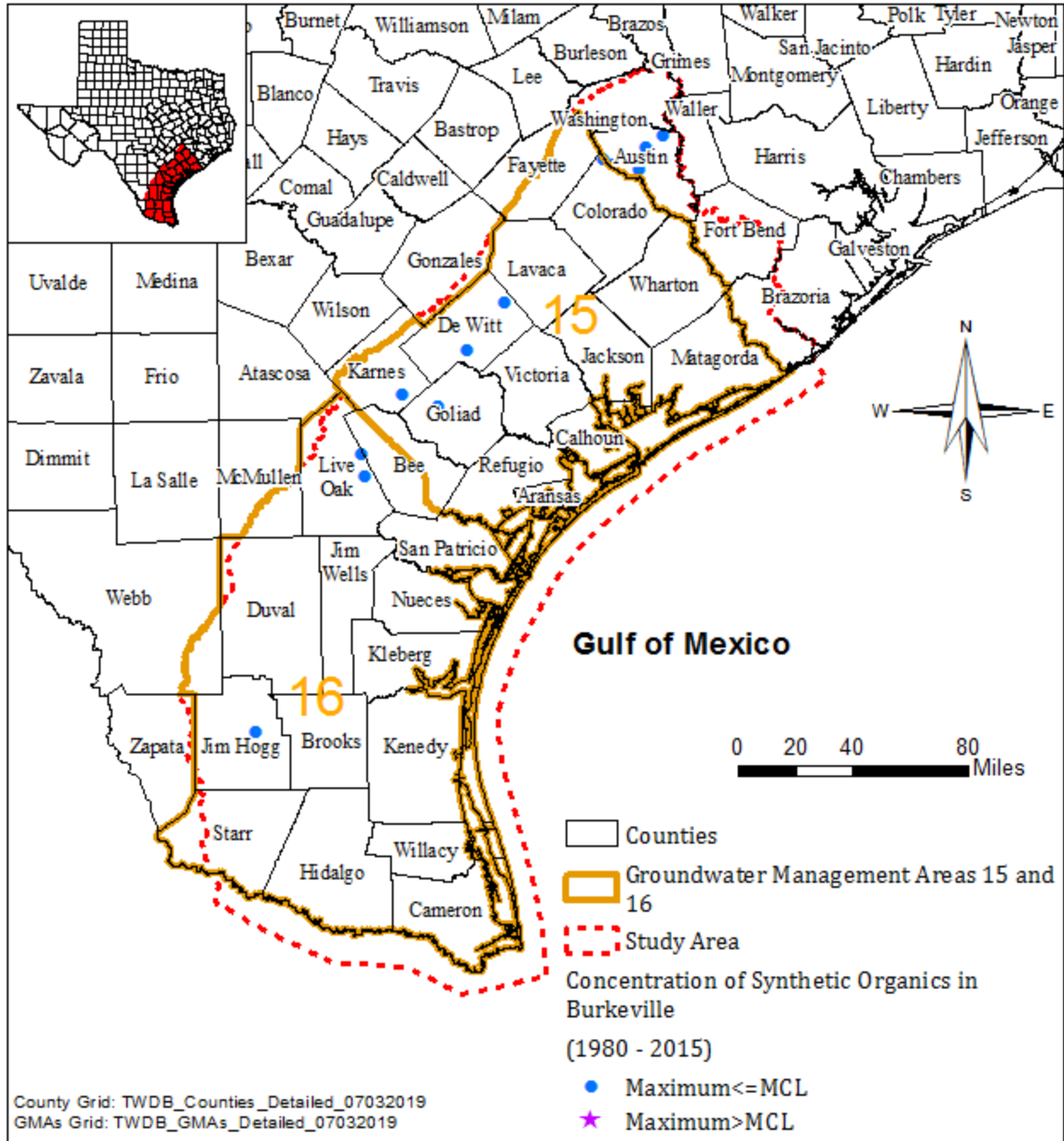
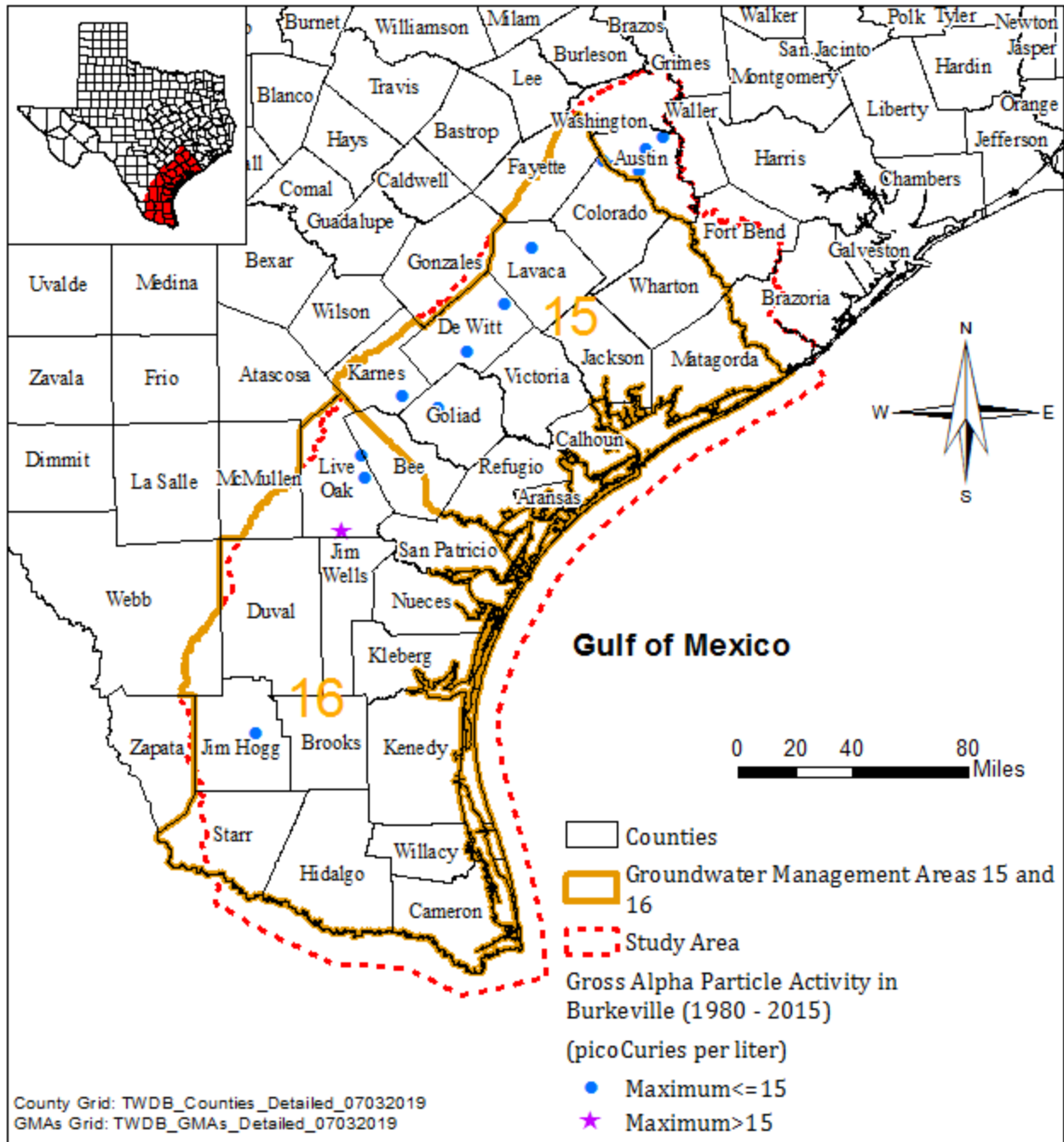


Figure 4.7.33 Hydrograph of total dissolved solids in groundwater from the Burkeville Unit.



**Figure 4.7.34 Synthetic organics concentrations in groundwater samples collected from Burkeville Unit between 1980 and 2015.**



**Figure 4.7.35** Gross alpha particle activity in groundwater samples collected from Burkeville Unit between 1980 and 2015.



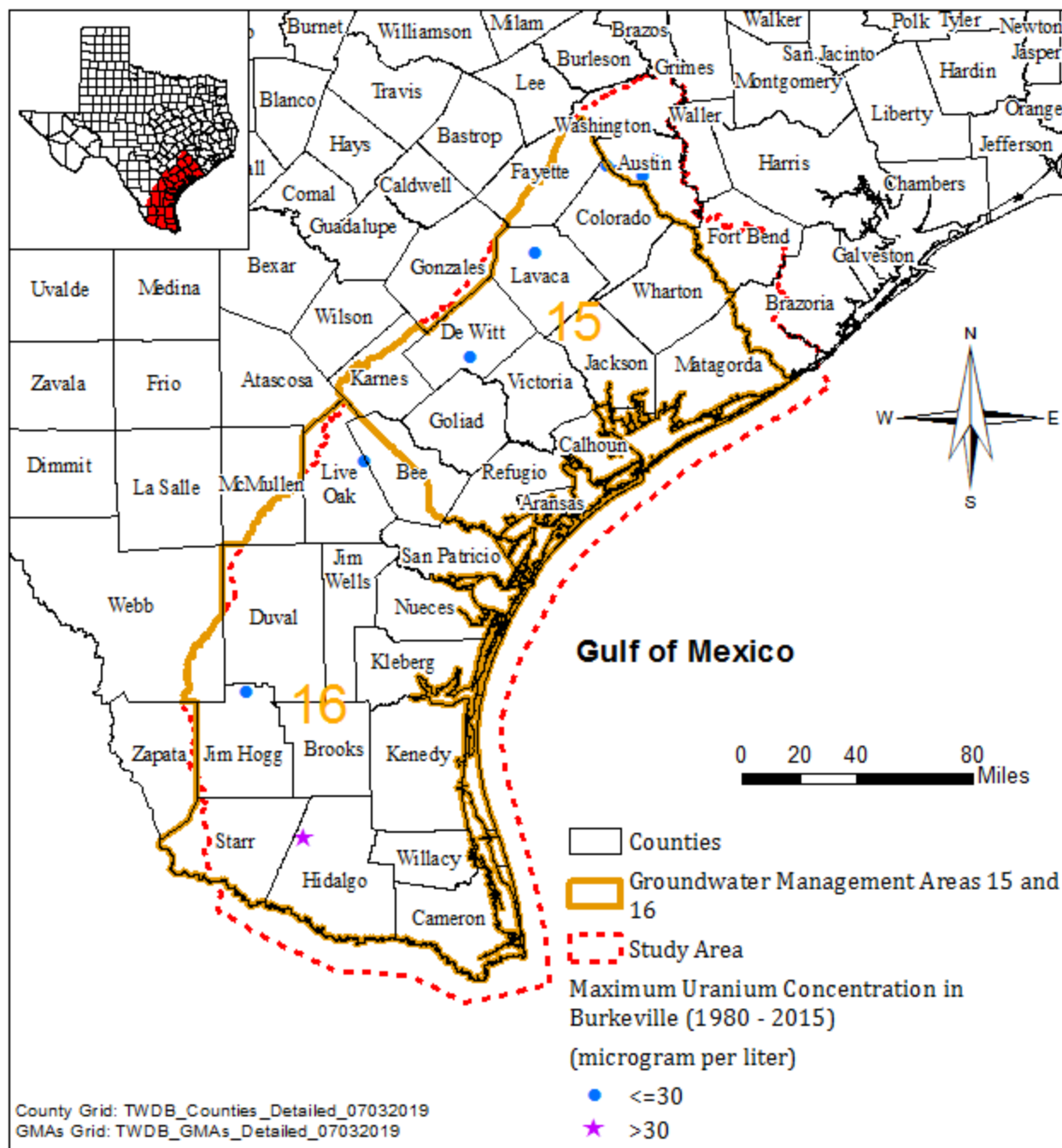


**Figure 4.7.36 Uranium concentrations in groundwater samples collected from Burkeville Unit between 1980 and 2015.**

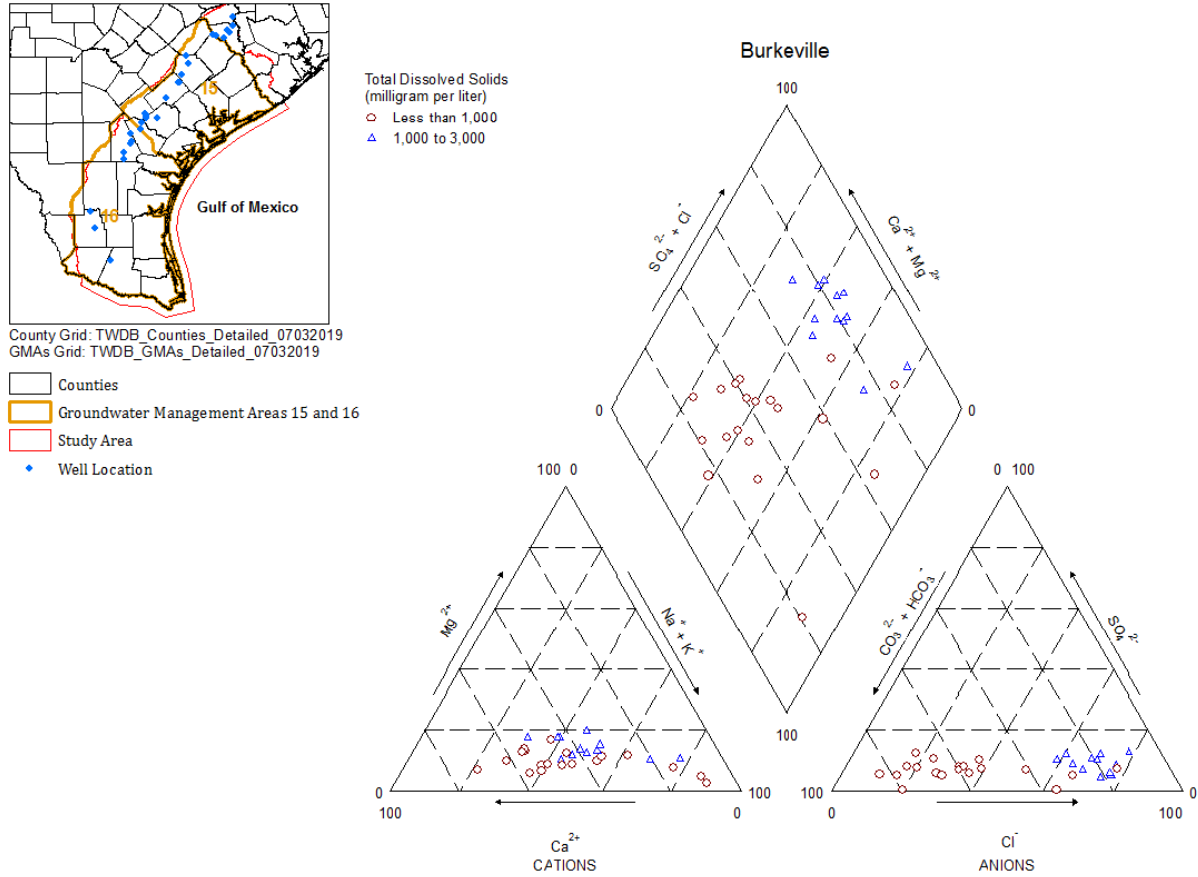


**Figure 4.7.37 Piper diagram of groundwater samples collected from Burkeville Unit.**

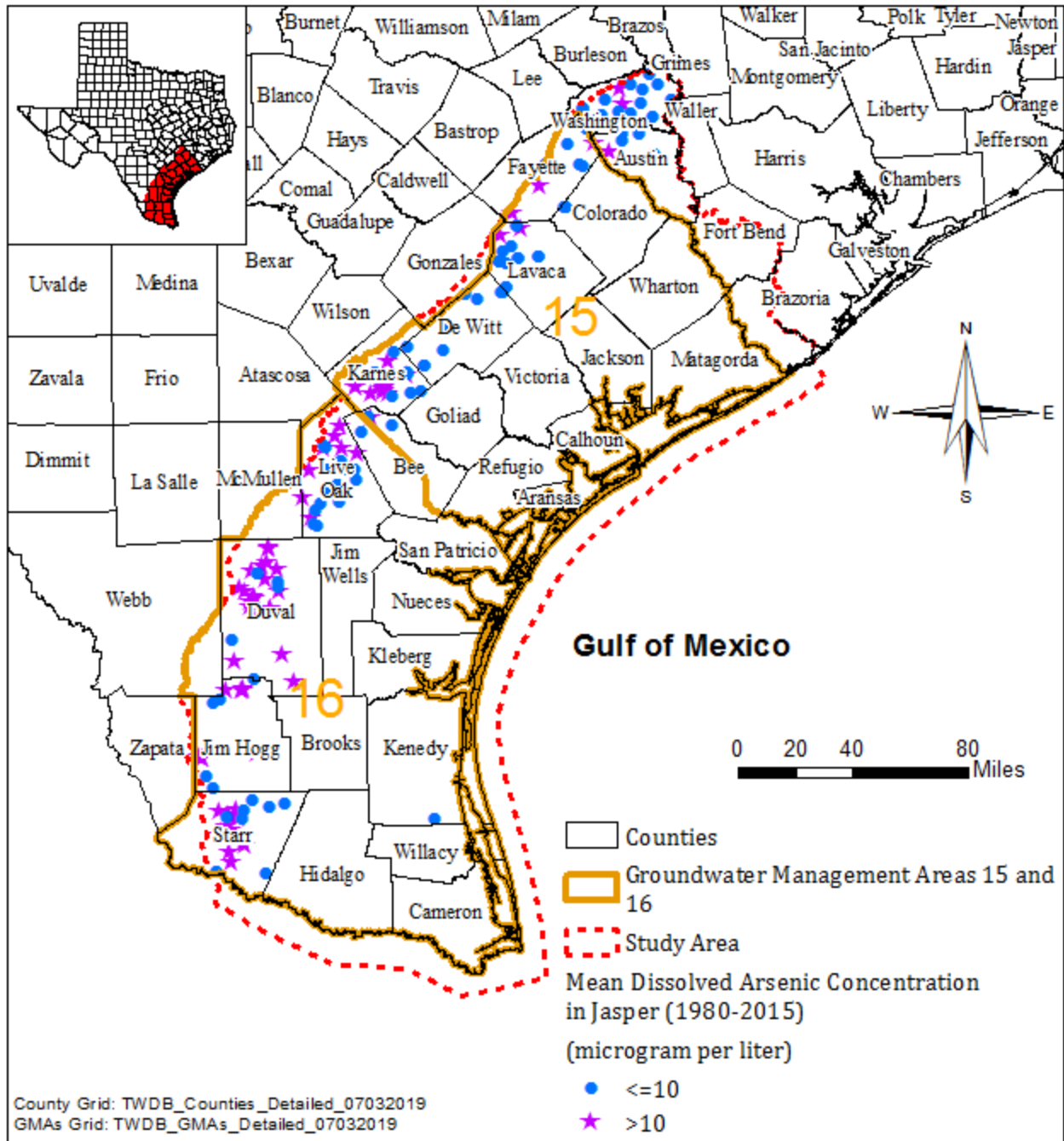


**Figure 4.7.38** Arsenic average concentrations in groundwater samples collected from Jasper Aquifer between 1980 and 2015.

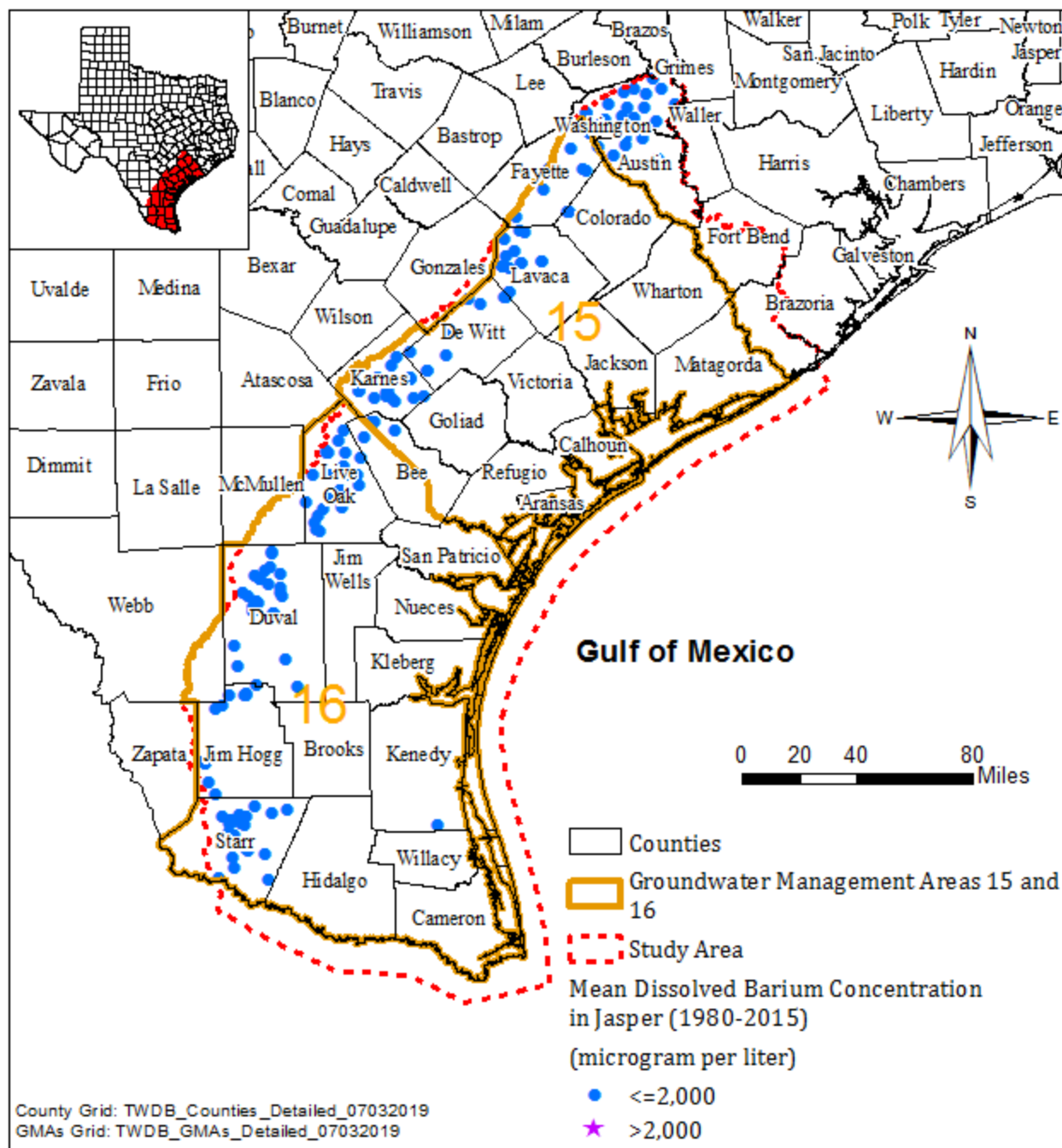


**Figure 4.7.39 Barium average concentrations in groundwater samples collected from Jasper Aquifer between 1980 and 2015.**

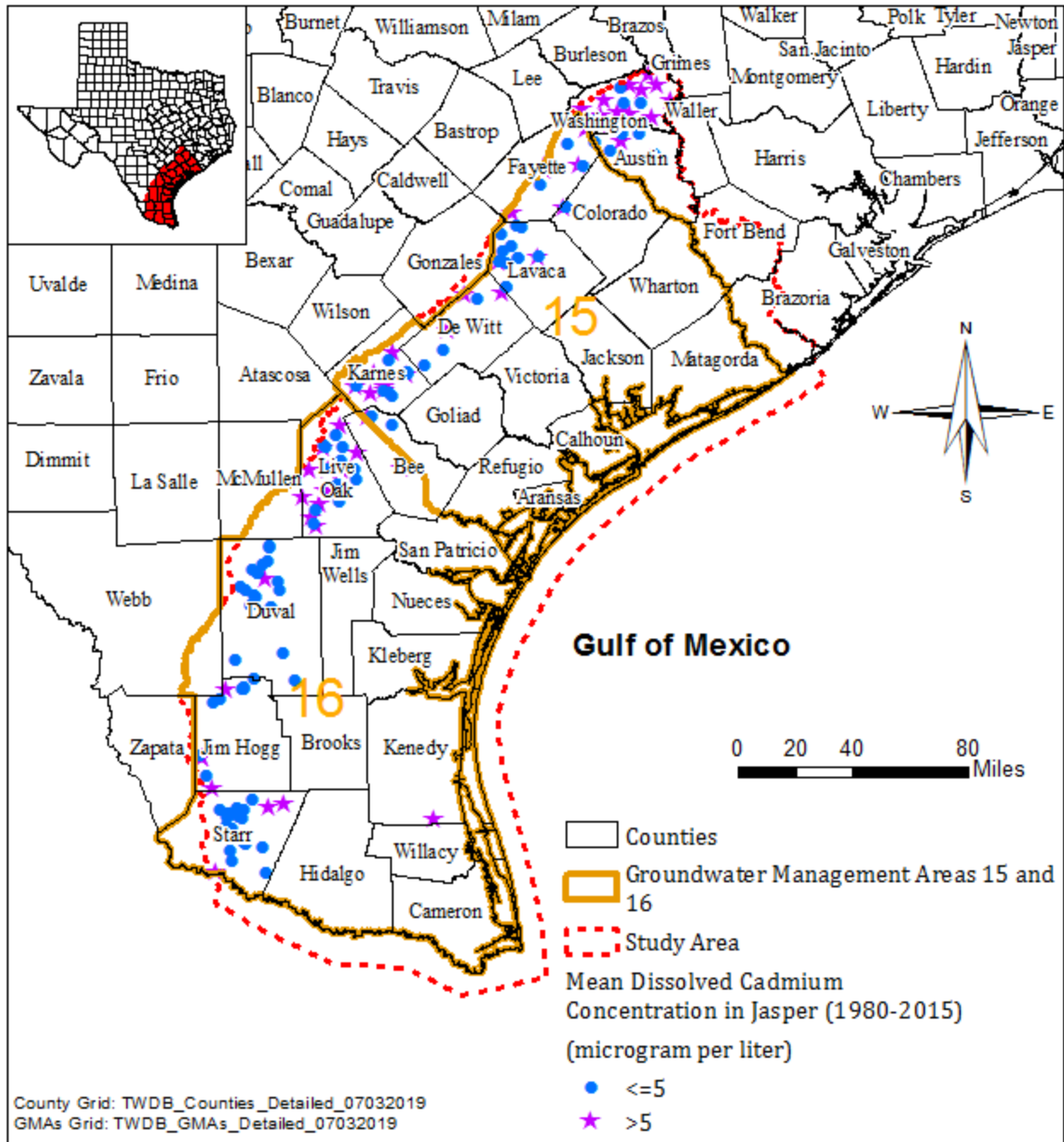


**Figure 4.7.40 Cadmium average concentrations in groundwater samples collected from Jasper Aquifer between 1980 and 2015.**

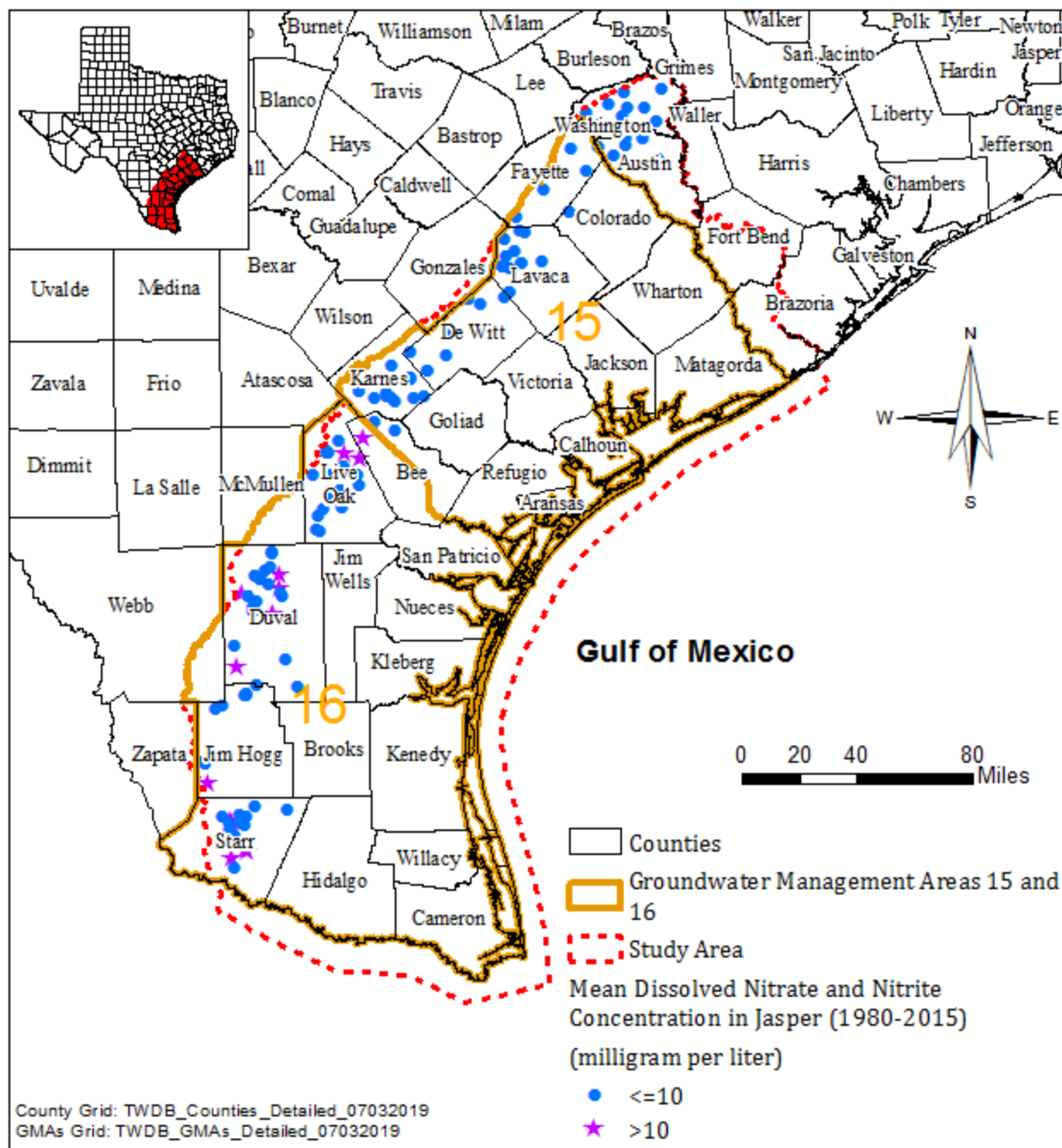


**Figure 4.7.41 Nitrate and nitrite average concentrations in groundwater samples collected from Jasper Aquifer between 1980 and 2015.**

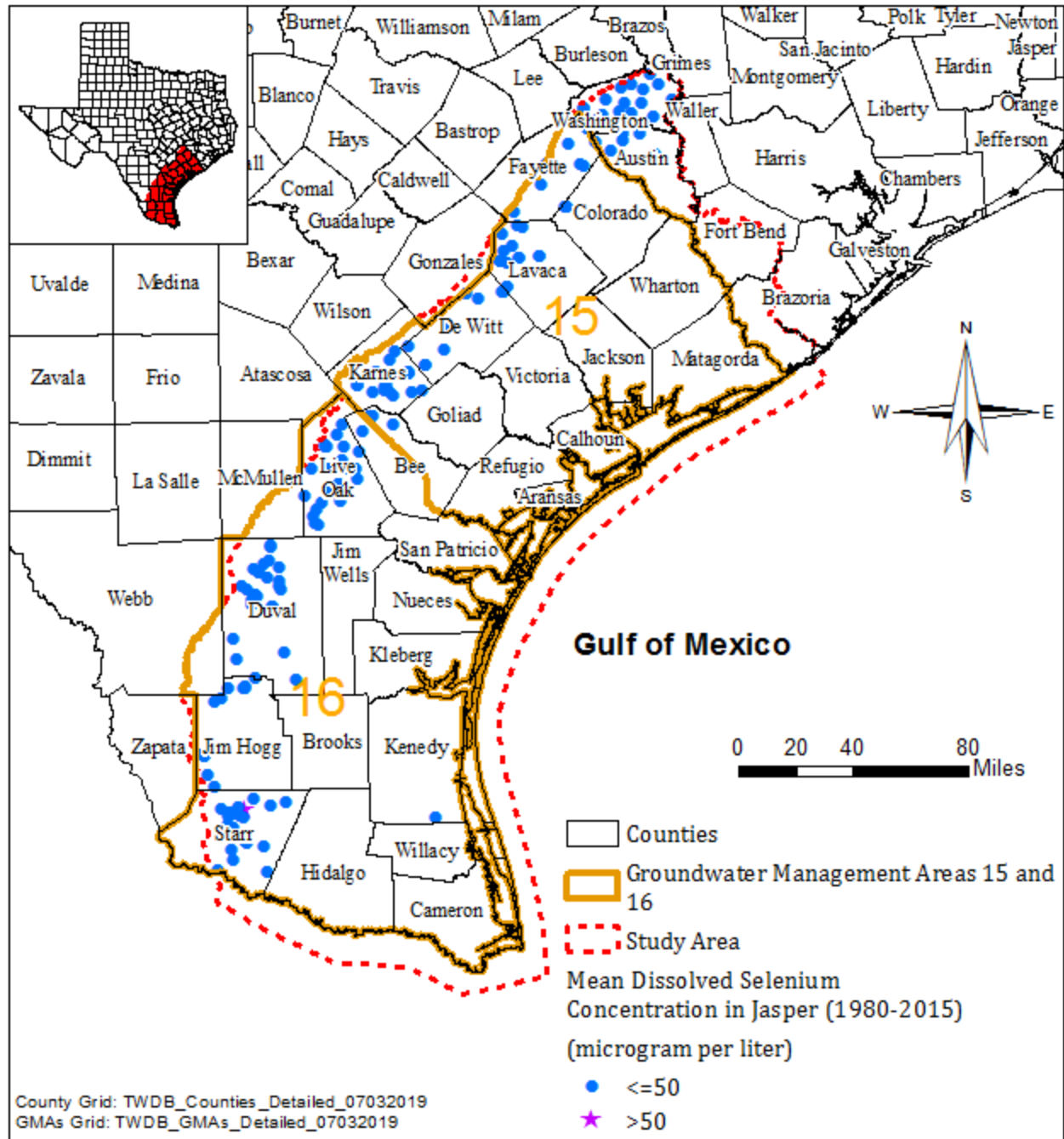


**Figure 4.7.42 Selenium average concentrations in groundwater samples collected from Jasper Aquifer between 1980 and 2015.**

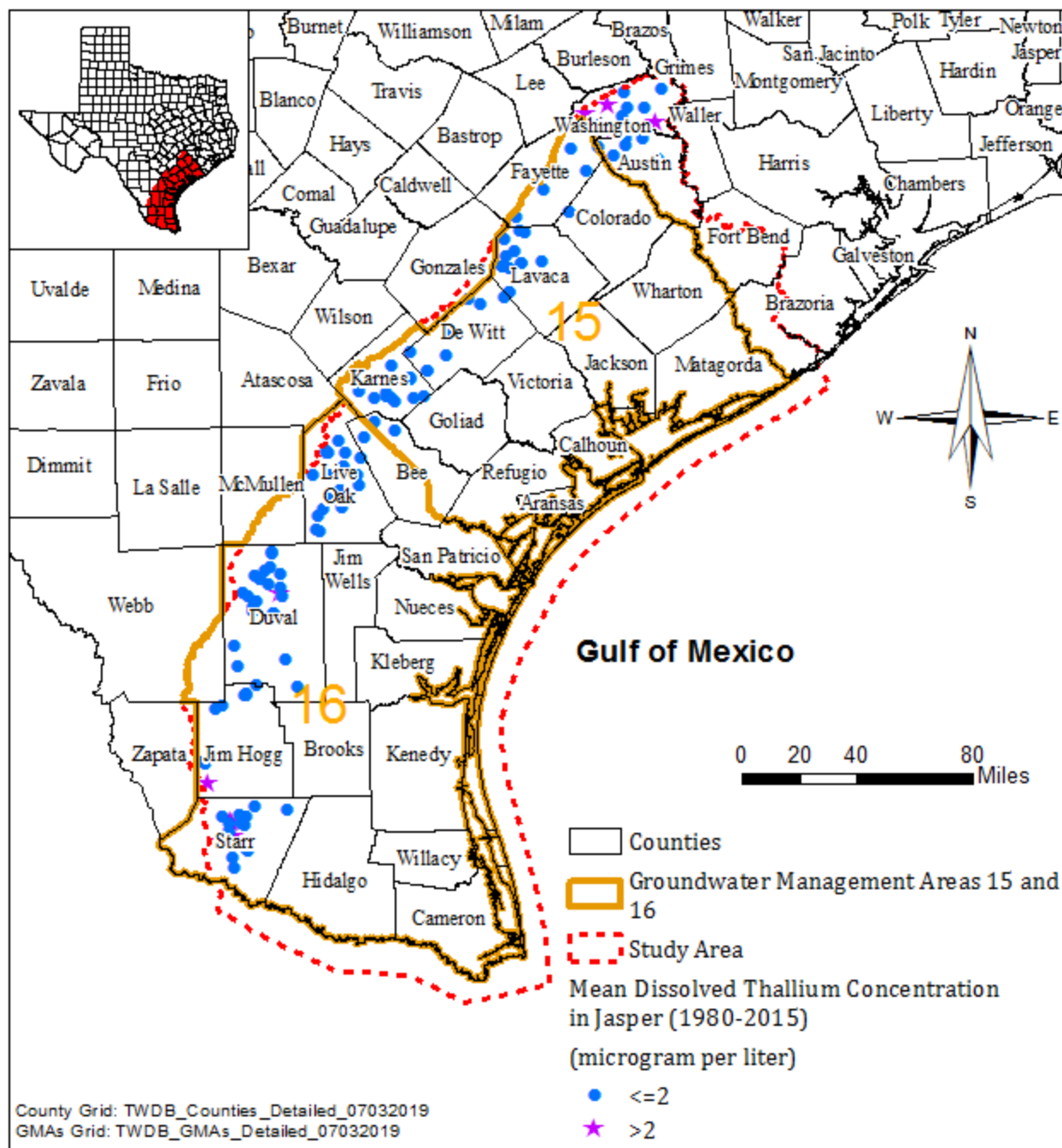


**Figure 4.7.43** Thallium average concentrations in groundwater samples collected from Jasper Aquifer between 1980 and 2015.



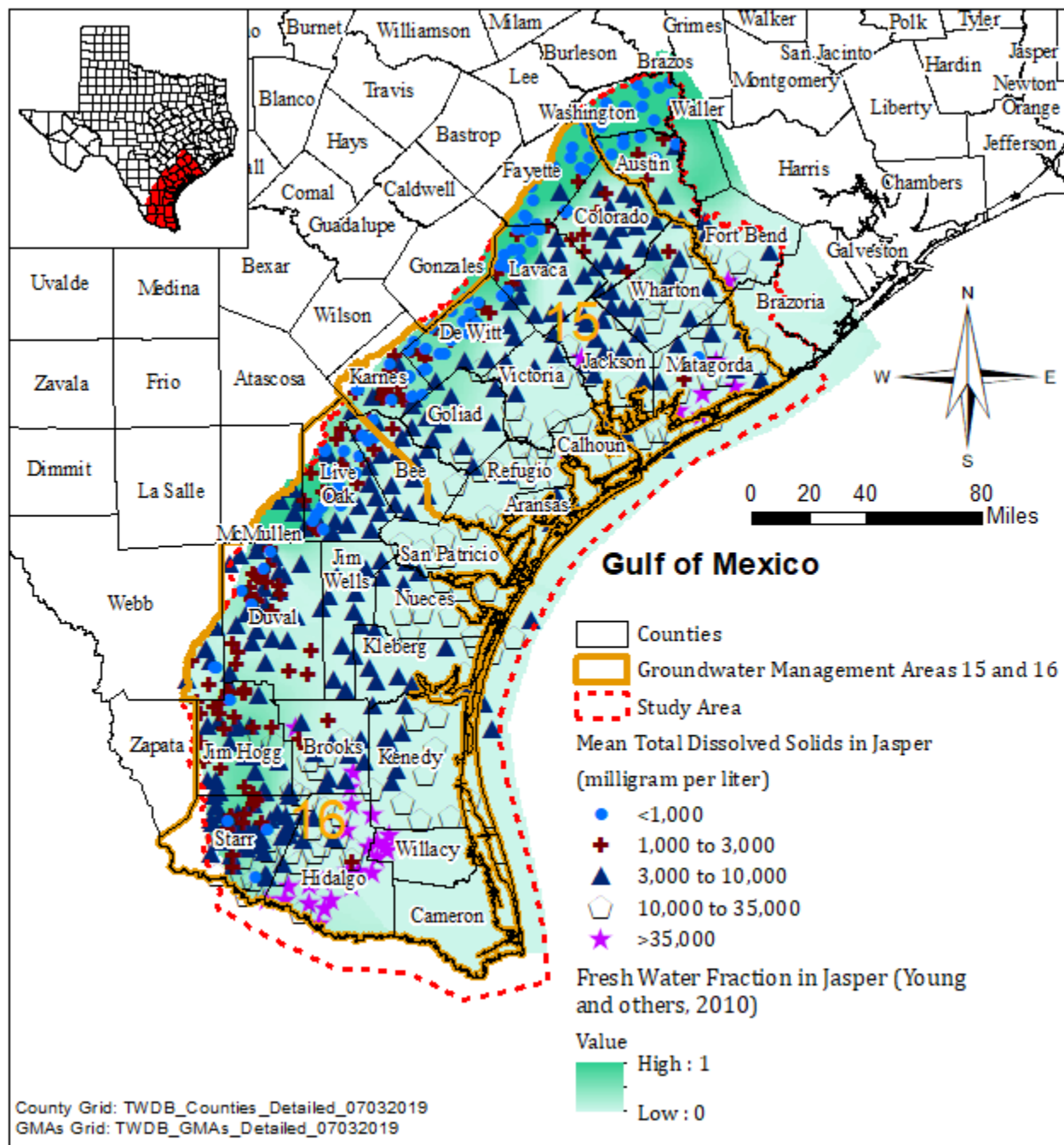


**Figure 4.7.44** Total dissolved solids average concentrations in groundwater samples collected from water wells in Jasper Aquifer between 1980 and 2015 and geophysical logs.

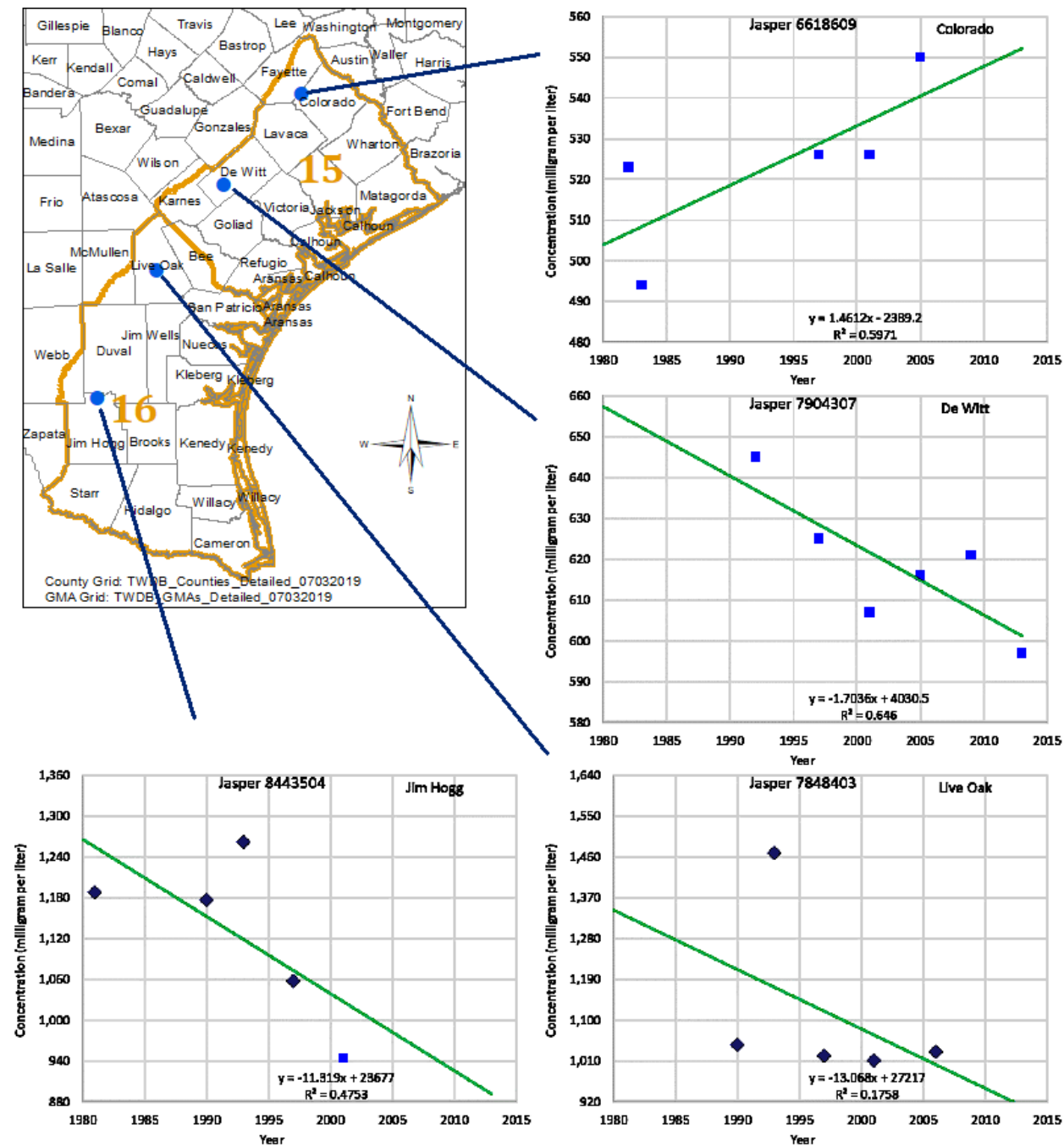


**Figure 4.7.45 Hydrograph of total dissolved solids in groundwater from the Jasper Aquifer.**

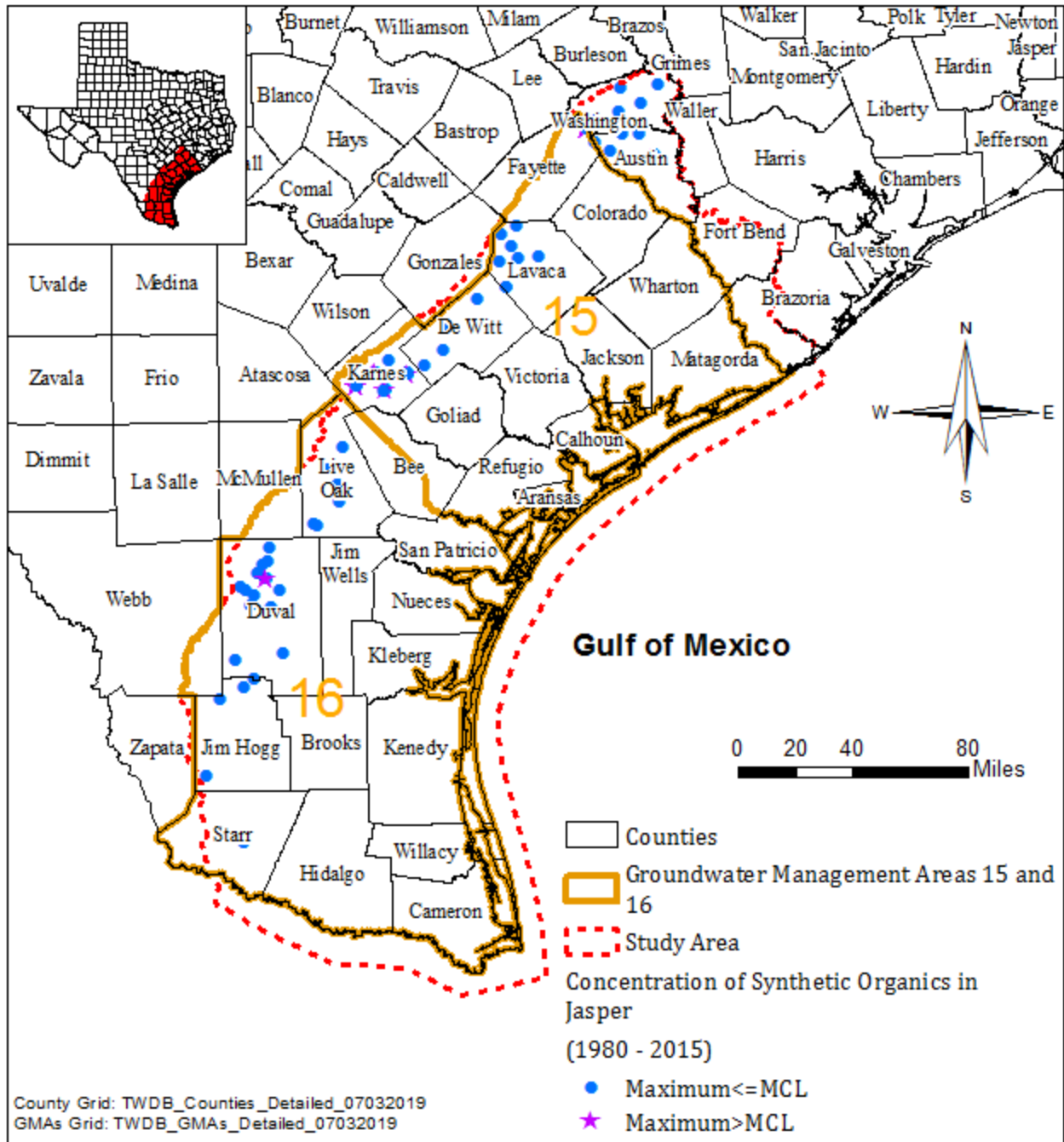


**Figure 4.7.46 Synthetic organics concentrations in groundwater samples collected from Jasper Aquifer between 1980 and 2015.**

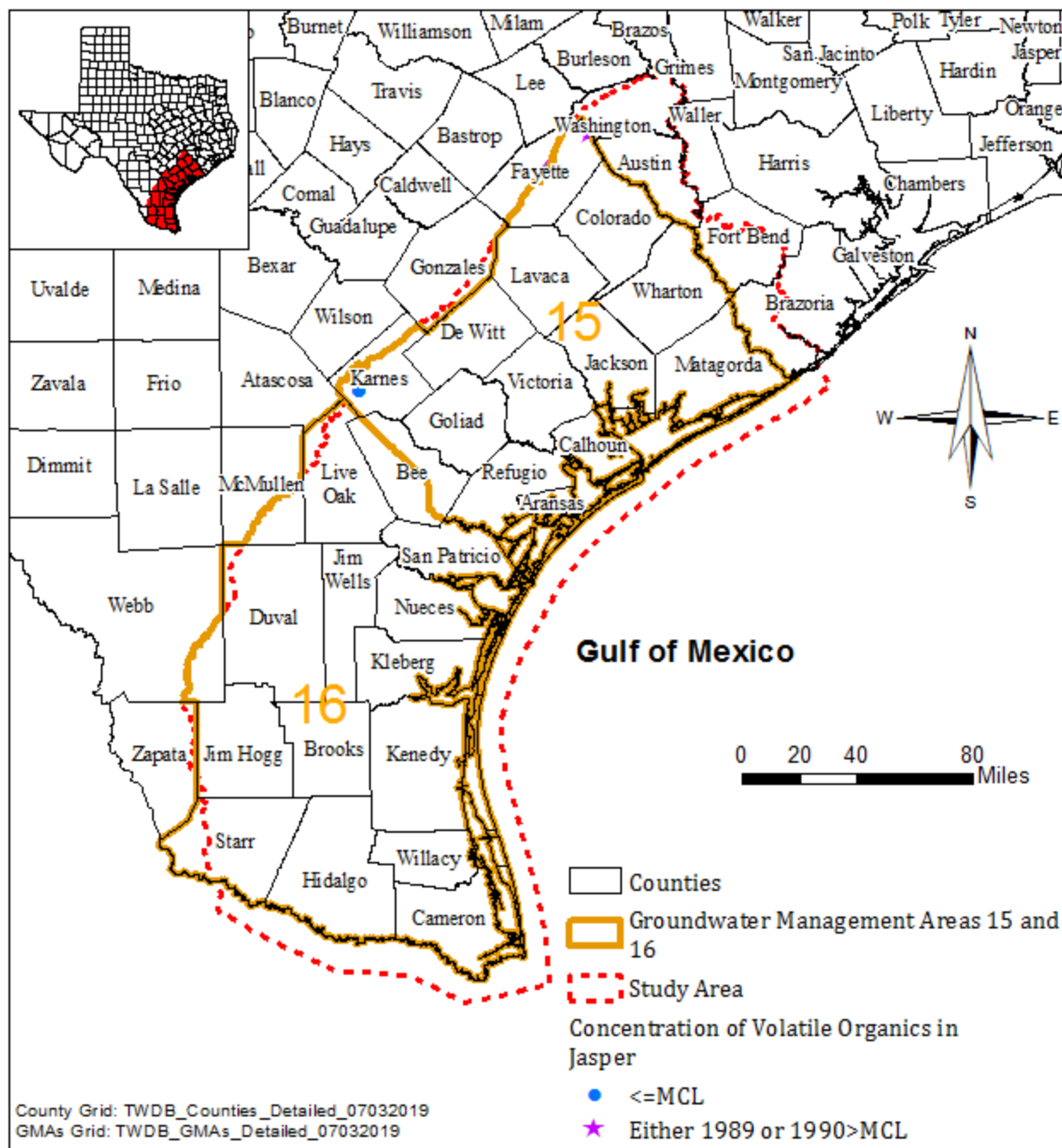


**Figure 4.7.47 Volatile organic compound concentrations in groundwater samples collected from Jasper Aquifer between 1980 and 2015.**

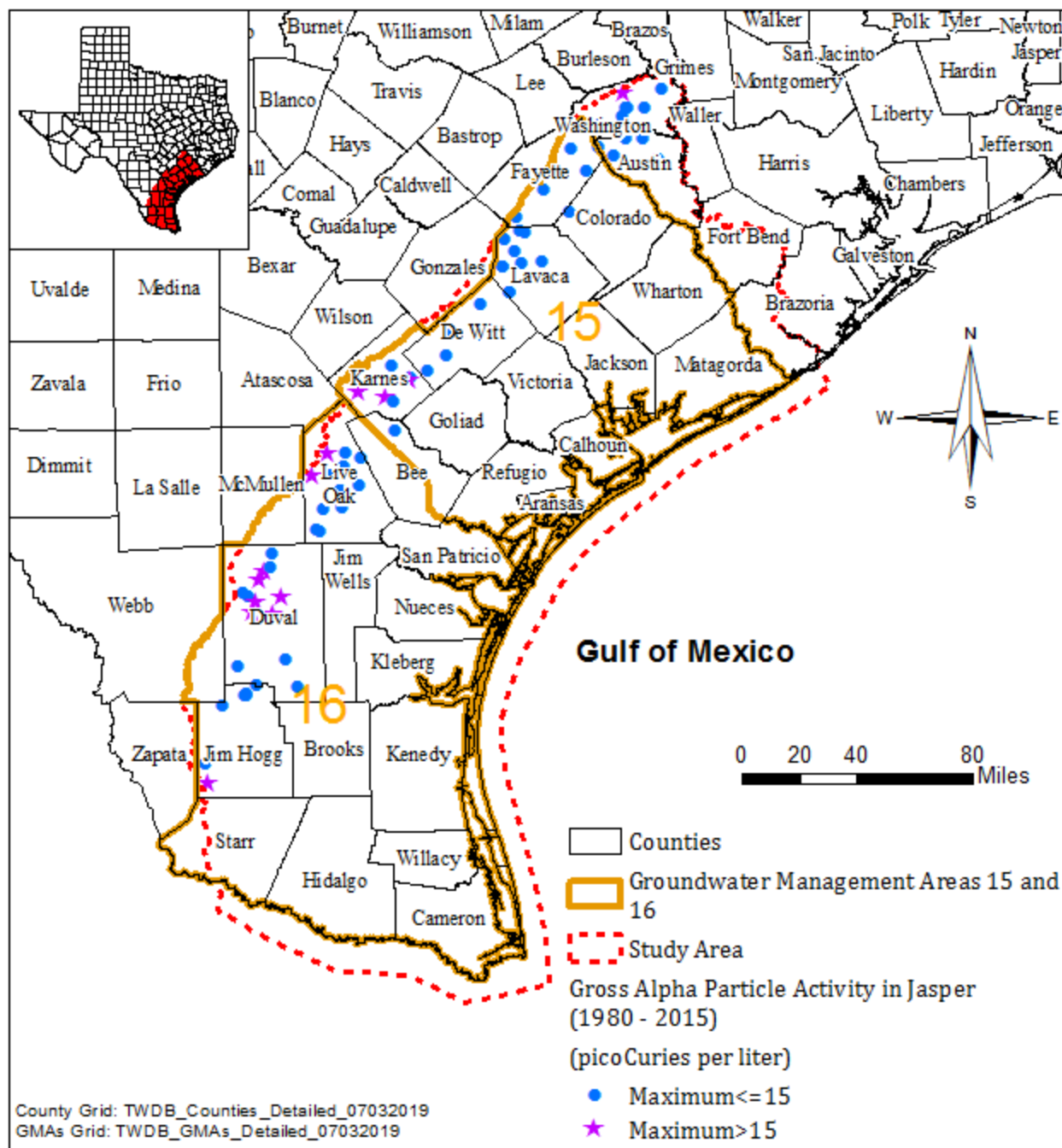


**Figure 4.7.48** Gross alpha particle activity in groundwater samples collected from Jasper Aquifer between 1980 and 2015.

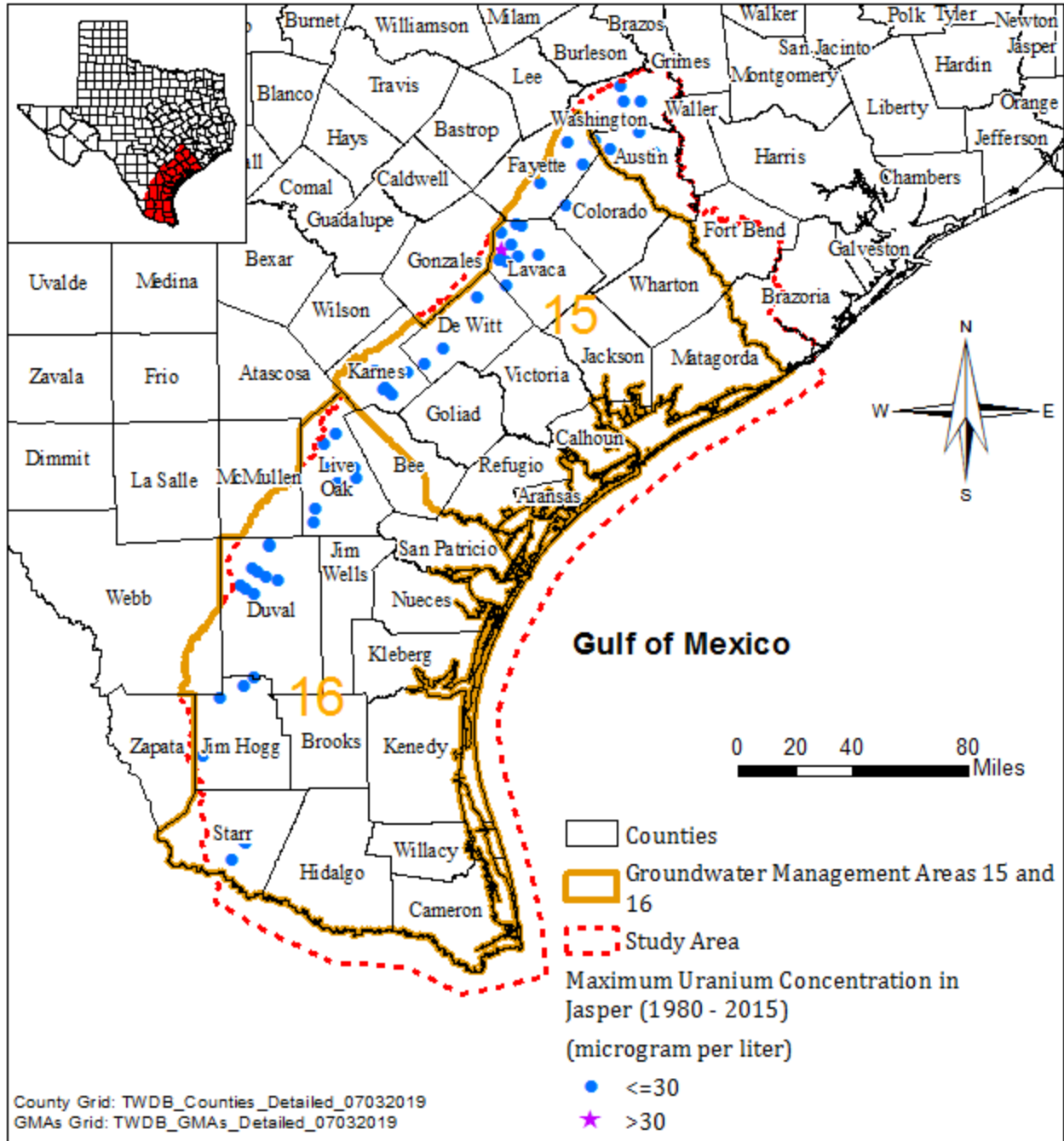


**Figure 4.7.49 Uranium concentrations in groundwater samples collected from Jasper Aquifer between 1980 and 2015.**

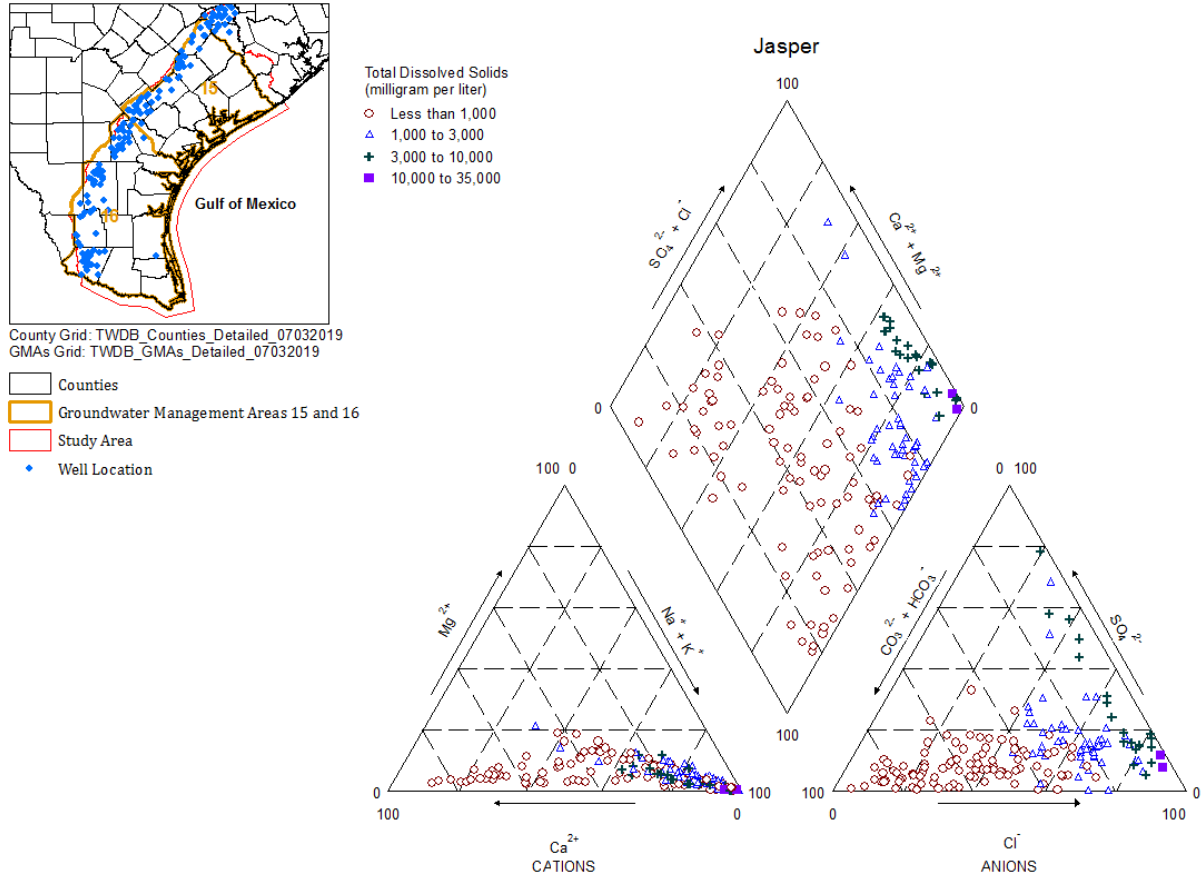


**Figure 4.7.50 Piper diagram of groundwater samples collected from Jasper Aquifer.**

## **4.8 Subsidence**

Due to withdrawal of groundwater, oil, and gas, land surface subsidence has been observed in the Texas coastal region. The Houston-Galveston region north of the study area has experienced the greatest subsidence (more than nine feet) (Kasmarek and others, 2016; Gabrysch, 1982). Based on releveling of benchmarks, Ratzlaff (1980) calculated the subsidence at limited locations in the study area. His study showed that the subsidence was generally less than 0.5 feet, except northern Matagorda and southern Jackson counties (> 1.5 feet between 1918 and 1973), west of Corpus Christi (5.28 feet between 1942 and 1975), and central Refugio County (0.74 feet between 1918 and 1951).

Young (2016) estimated land subsidence in seven counties in Groundwater Management Area 15: Calhoun, DeWitt, Jackson, Matagorda, Refugio, Victoria, and Wharton counties. The land surface difference calculation between Light and raDAR (LIDAR) and National Geodetic Survey (NGS) benchmarks indicated more than two feet of land subsidence in DeWitt, Jackson, Matagorda, Refugio, Victoria, and Wharton counties, and at least 1.5 feet in Calhoun County from before 1950 to present. The LIDAR and old topographic maps indicated at least two feet of subsidence in all seven counties between 1950/60 and present. The joint data by LIDAR, survey benchmarks, and old topographic maps indicated more than two feet of land subsidence in southwest Wharton, southeast Jackson, and northwest Matagorda counties.

Because the study by Ratzlaff (1980) only covered limited locations and the one by Young (2016) had a relatively long-time interval, a regression approach was developed to apply the studies by Kasmarek and others (2016) and Gabrysch (1982) in the Houston-Galveston region to the study area. This approach is described in the following section.

### ***4.8.1 Correlation between Compaction and Groundwater Level Decline***

Common methods to estimate subsidence include releveling of benchmarks, use of extensometers, tide record, and, more recently, interferometric synthetic-aperture radar (InSAR) images. Since 1960s, the U. S. Geological Survey has installed extensometers in the Houston-Galveston region to monitor the compaction of the Chicot and Evangeline aquifers



(Kasmarek and others, 2016). These extensometers were placed at approximately the bottom of the aquifers and recorded the change of thicknesses. Because the compaction of the older units (older than Evangeline) is neglectable, the compaction from the extensometers can be used to approximate the land surface subsidence. The early extensometer data combined with releveling of benchmarks were used by Gabrysch (1982) to study the specific-unit compaction and groundwater level decline in several time intervals: 1906 to 1943, 1943 to 1964, 1943 to 1973, 1943 to 1978, 1964 to 1973, 1973 to 1978, and 1906 to 1978. More recent extensometer data contain monthly compaction from the 1970s/80s to present days (Kasmarek and others, 2016).

According to Gabrysch (1982), subsidence prior to 1943 was small and mainly due to natural process. As a result, only the compaction and water level decline from the following time intervals by Gabrysch (1982) were used for the correlation study: 1943 to 1964, 1964 to 1973, and 1973 to 1978.

The following equation was used to convert the specific-unit compaction in Gabrysch (1982) to compaction:

$$C = C_s * S * B$$

Where:

$C$  = compaction (feet)

$C_s$  = specific-unit compaction (feet<sup>-1</sup>)

$S$  = average stress change (feet of water)

$B$  = clay thickness (feet)

To be consistent with the time intervals by Gabrysch (1982), the extensometer data from Kasmarek and others (2016) were first averaged for each year, and then the annual data were used to calculate the compaction for the following time intervals: 1978 to 1983, 1983 to 1988, 1988 to 1993, 1993 to 1998, 1998 to 2003, 2003 to 2008, and 2008 to 2013.

Kasmarek and others (2016) did not provide water level data. As a result, the water levels at the extensometer locations since 1978 were downloaded from the TWDB website (<https://www.twdb.texas.gov/groundwater/data/gwdbbrpt.asp>). The water levels were first averaged to calculate the annual data. The annual data were then used to calculate groundwater level decline (i.e. stress increase) for the intervals listed above.

Only compaction data due to groundwater decline from Kasmarek and others (2016) and Gabrysch (1982) were used for the study. During the data review, it was found that the compaction was not impacted by depth and clay thickness in these two studies. As a result, the compaction was only correlated to the groundwater decline (stress increase). However, extensometer depth and clay thickness, with compaction and stress change, were summarized in [Table 4.8.1](#) for readers' convenience. The correlation between the compaction and stress change was presented in [Figure 4.8.1](#), which indicated a moderate correlation.

#### **4.8.2 Subsidence in Study Area**

The equation on [Figure 4.8.1](#) was used to calculate compaction from water level decline for the study area. First, individual water levels at a well from a single year were averaged to calculate annual water level. If the annual water level was higher than a following water level, compaction would then be calculated. Two consecutive water levels could be one or multiple years apart. The individual compactations were then summarized to estimate the total compaction. Please note the total compaction may be under-estimated due to lack of water levels at some time intervals.

[Figure 4.8.2](#) shows the total compaction between 1908 and 1973. This time interval is comparable to the interval 1918 to 1973 by Ratzlaff (1980). Although a direct comparison between these two is impossible because both studies did not cover the exact same locations, it is still clear that the compaction/subsidence between the two studies are very close in the Matagorda and Jackson counties (1 to 2 feet).

Lack of water level data at west of Corpus Christi between 1942 and 1975, as well as at central Refugio County between 1918 and 1951, made the comparison impossible between this regression study and the study by Ratzlaff (1980).

Figure 4.8.2 also indicates a subsidence between 2 and 3 feet prior to 1973 in northern Kleberg, northern Brooks, southern Jim Wells, and central Victoria counties, with the largest (more than 5 feet) near Kingsville in Kleberg County.

Figure 4.8.3 shows the total compaction between 1908 and 2015, which approximately represents the total compaction/subsidence up to date. In comparison with Figure 4.8.2, it suggests that the compaction/subsidence have continued and extended to other areas since 1973. The compaction/subsidence in the City of San Diego in Duval County and Karnes City and the City of Kenedy in Karnes County occurred after 1960s. The compaction/subsidence in these locations and others near the western perimeter of the Gulf Coast Aquifer System may have been over-estimated.

As described in Section 4.6, significant groundwater pumping in the study area started in 1940s. It is thus expected that obvious land subsidence also started around 1940s. As a result, the subsidence shown in Figure 4.8.3 should have occurred mainly after 1940s. This timeframe is about the same as the time interval used by Young (2016). In comparison with Young (2016), Figure 4.8.3 indeed shows very similar values in Calhoun, DeWitt, Jackson, Matagorda, Refugio, Victoria, and Wharton counties.

Since the numerical model may have a time frame of 1980 to 2015, the compaction/subsidence for this period is presented in Figure 4.8.4, ranging from less than one foot to more than five feet. Again, the subsidence near the western perimeter of the Gulf Coast Aquifer System may have been over-estimated.

**Table 4.8.1 Summary of groundwater decline or stress increase and compaction.**

Site	Well	Extensometer Depth (feet)	Period	Average Stress Change (feet of water)	Clay Thickness (feet)	Compaction (feet)	Note
Addicks	LJ-65-12-726	1802	1943-1964	76	730	7.77E-01	Gabrysch (1982)
Addicks	LJ-65-12-726	1802	1964-1973	138	730	1.01E+00	Gabrysch (1982)
Addicks	LJ-65-12-726	1802	1973-1978	34	730	4.96E-01	Gabrysch (1982)
Addicks	LJ-65-12-726	1802	1978-1983	68	730	8.08E-01	Kasmarek and others (2016)
Addicks	LJ-65-12-726	1802	1983-1988	17	730	6.47E-01	Kasmarek and others (2016)
Addicks	LJ-65-12-726	1802	1988-1993	17	730	5.74E-01	Kasmarek and others (2016)
Addicks	LJ-65-12-726	1802	1993-1998	16	730	4.52E-01	Kasmarek and others (2016)
Addicks	LJ-65-12-726	1802	1998-2003	24	730	5.59E-01	Kasmarek and others (2016)
Addicks	LJ-65-12-726	1802	2008-2013	8	730	1.48E-01	Kasmarek and others (2016)
Baytown	LJ-65-16-931	1475	1943-1964	64	1000	3.71E+00	Gabrysch (1982)
Baytown	LJ-65-16-931	1475	1964-1973	50	1000	2.50E+00	Gabrysch (1982)
Baytown	LJ-65-16-931	1475	2008-2013	4	1000	2.27E-01	Kasmarek and others (2016)
Clear Lake	LJ-65-32-424	1740	1943-1964	105	590	1.98E+00	Gabrysch (1982)
Clear Lake	LJ-65-32-424	1740	1964-1973	17	590	2.01E+00	Gabrysch (1982)
Clear Lake	LJ-65-32-424	1740	1973-1978	15	590	7.97E-01	Gabrysch (1982)
Houston-Northeast	LJ-65-14-746	2170	2008-2013	15.48	1020	8.57E-02	Kasmarek and others (2016)
Lake Houston	LJ-65-07-909	1940	1983-1988	5.40	1300	1.87E-01	Kasmarek and others (2016)
Lake Houston	LJ-65-07-909	1940	1988-1993	7.49	1300	1.50E-01	Kasmarek and others (2016)
Lake Houston	LJ-65-07-909	1940	1993-1998	4.75	1300	6.71E-02	Kasmarek and others (2016)
Lake Houston	LJ-65-07-909	1940	1998-2003	2.57	1300	2.98E-02	Kasmarek and others (2016)
Lake Houston	LJ-65-07-909	1940	2008-2013	4.50	1300	5.93E-02	Kasmarek and others (2016)
Moses Lake	KH-64-33-920	800	1943-1964	21	500	8.19E-01	Gabrysch (1982)

Site	Well	Extensometer Depth (feet)	Period	Average Stress Change (feet of water)	Clay Thickness (feet)	Compaction (feet)	Note
Moses Lake	KH-64-33-920	800	1964-1973	19	500	6.18E-01	Gabrysch (1982)
Moses Lake	KH-64-33-920	800	2008-2013	0.56	500	4.12E-03	Kasmarek and others (2016)
Pasadena	LJ-65-23-322	2831	1943-1964	93	1140	4.03E+00	Gabrysch (1982)
Pasadena	LJ-65-23-322	2831	1964-1973	67	1140	3.28E+00	Gabrysch (1982)
Pasadena	LJ-65-23-322	2831	1973-1978	5	1140	9.12E-01	Gabrysch (1982)
Pasadena	LJ-65-23-322	2831	2008-2013	1.38	1140	3.75E-01	Kasmarek and others (2016)
Seabrook	LJ-65-32-625	1381	1943-1964	68	800	1.80E+00	Gabrysch (1982)
Seabrook	LJ-65-32-625	1381	1964-1973	59	800	1.18E+00	Gabrysch (1982)
Seabrook	LJ-65-32-625	1381	2008-2013	6.78	800	9.26E-02	Kasmarek and others (2016)

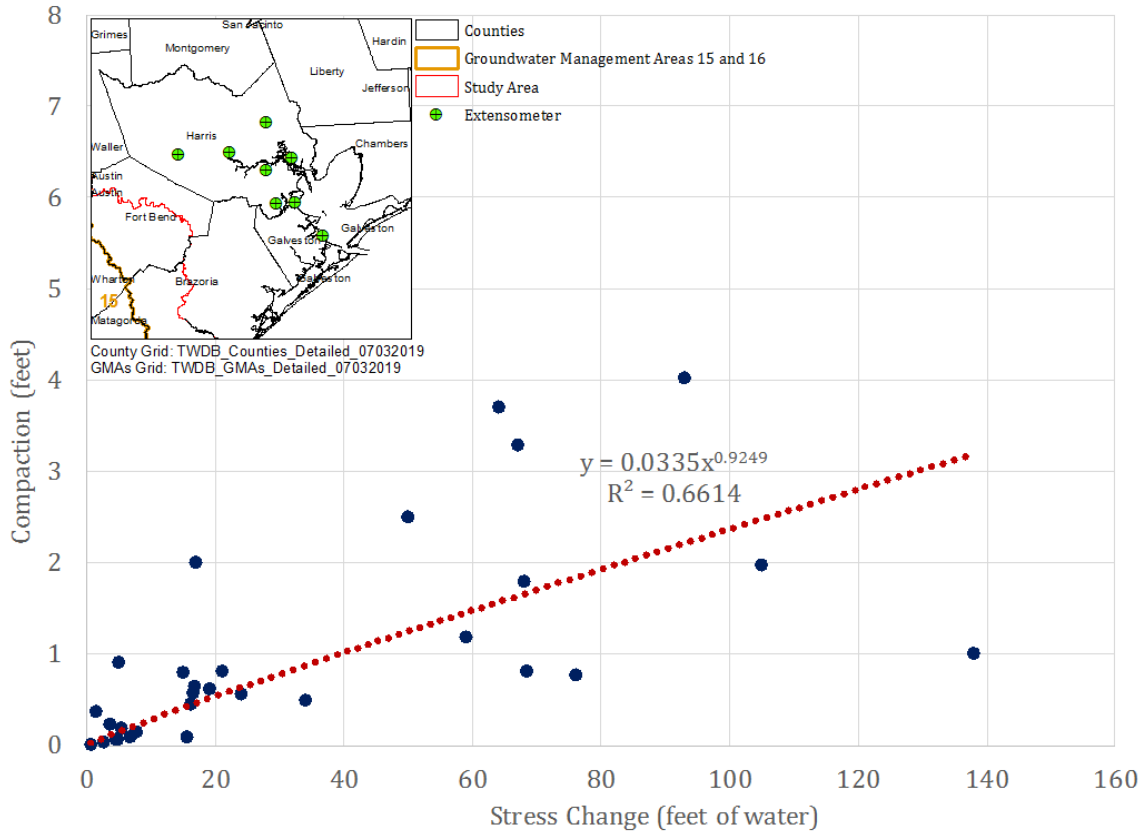


**Figure 4.8.1 Correlation between compaction and groundwater stress change.**

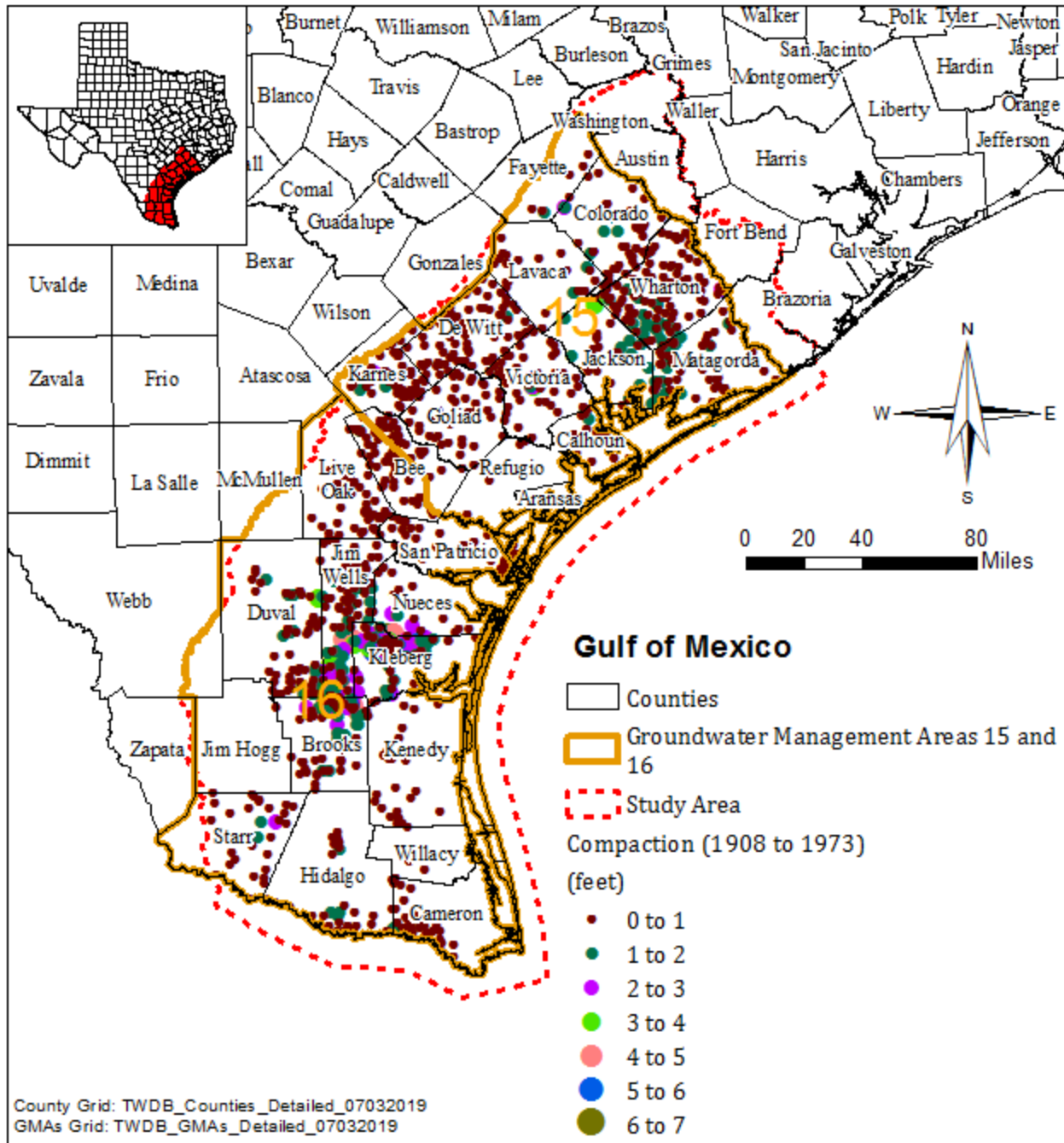


**Figure 4.8.2 Total compaction/subsidence between 1908 and 1973 in the study area.**

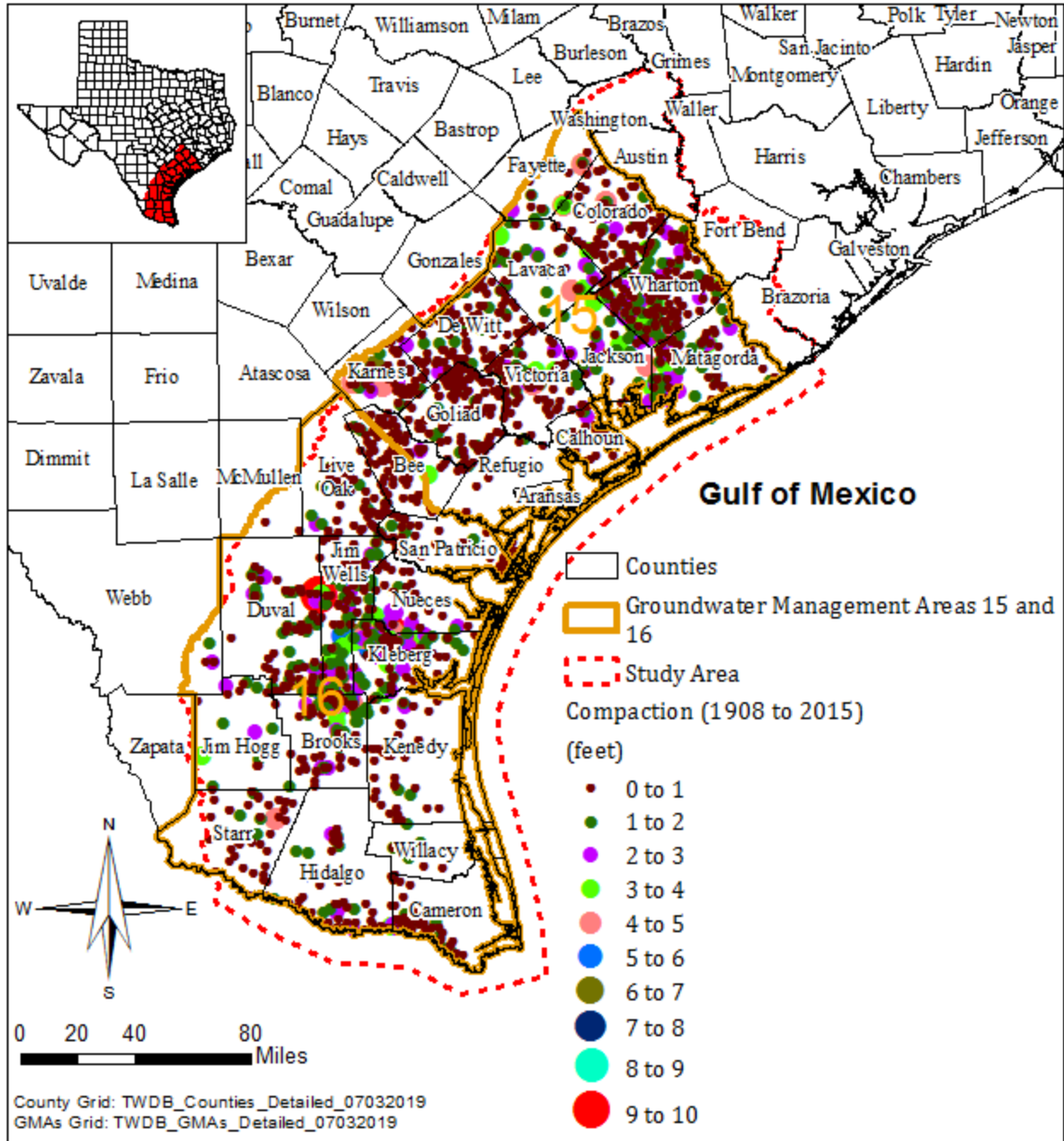


**Figure 4.8.3 Total compaction/subsidence between 1908 and 2015 in the study area.**



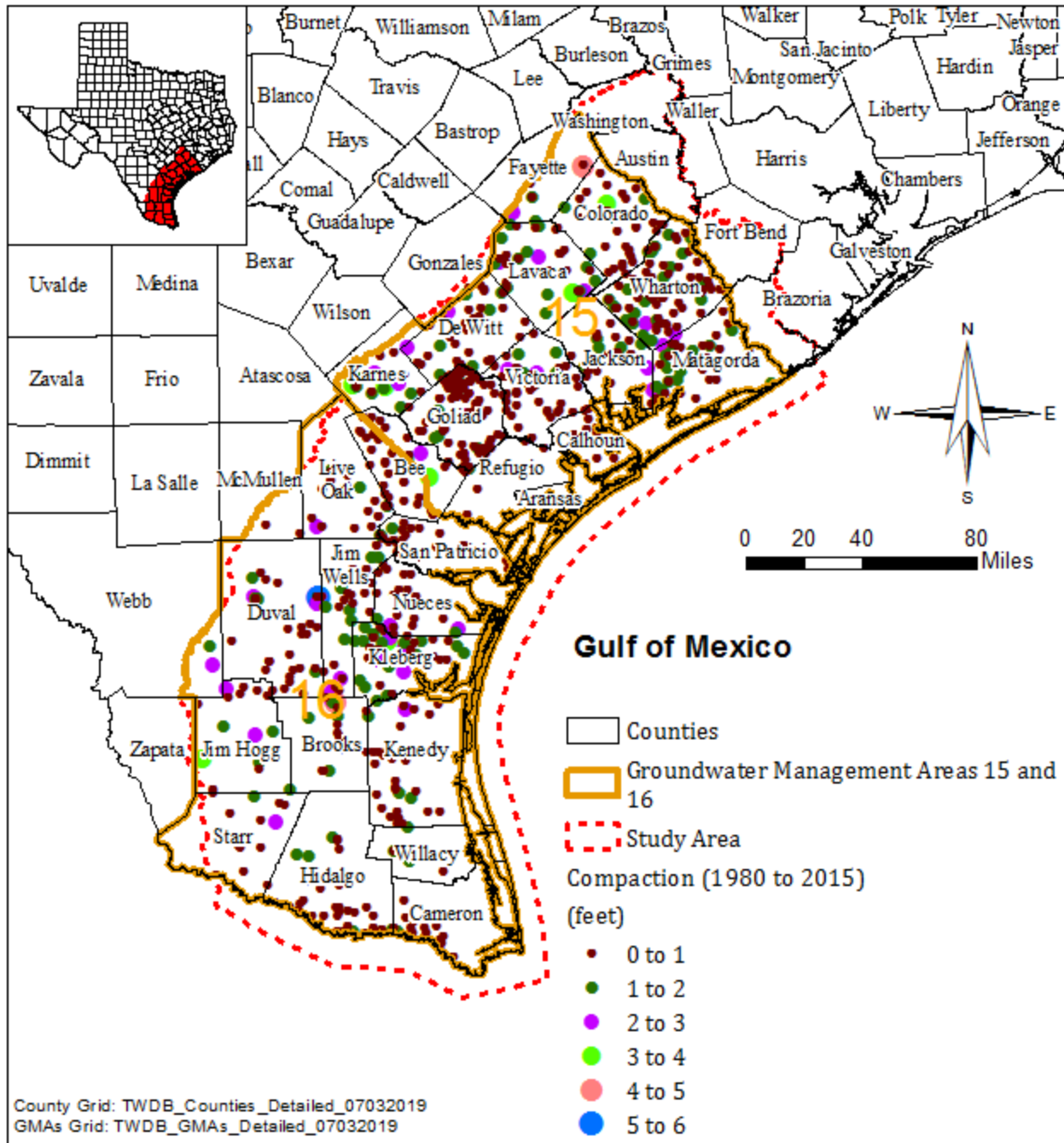


**Figure 4.8.4 Total compaction/subsidence between 1980 and 2015 in the study area.**

## **5.0 Conceptual Groundwater Flow Model for Central and Southern Portions of the Gulf Coast Aquifer System**

A conceptual groundwater flow model is a simplified version of the real groundwater flow system. A conceptual model includes identifying unique hydrostratigraphic units that host the groundwater, characteristics of the groundwater flow, and factors that control the flow.

First, the characteristics of the geologic units must be investigated and simplified to unique hydrostratigraphic units. Each hydrostratigraphic unit shares similar hydrogeologic properties and can be distinguished from adjacent hydrostratigraphic units. This step involves understanding the geologic history and using field data (such as geophysical logs and pumping tests) to determine the lateral and vertical extent of each of the hydrostratigraphic units. The result of this step is a simplified, intuitive hydrogeologic framework that can be handled using a computer code during the numerical model development.

The characteristics of the groundwater flow, such as flow direction, flow quantity, recharge zone, and discharge zone, are then identified using the hydrostratigraphic framework, precipitation data, water levels, stream baseflow, reservoir information, spring flow, and hydrogeologic properties of the hydrostratigraphic units.

Many factors influence groundwater flow. Some of the processes are natural, such as the infiltration of recharge from precipitation. Others may be associated with anthropogenic activities, such as groundwater pumping. The dominant processes (inflow and outflow components) must be identified and, if possible, quantified so that a numerical model can realistically simulate the flow system and minimize the uncertainty during model calibration and prediction.

The groundwater in the Gulf Coast Aquifer System ranges from fresh water (total dissolved solids less than 1,000 milligrams per liter) to brine/ocean water (total dissolved solids greater than 35,000 milligrams per liter). In general, the total dissolved solids increase downward and toward the Gulf of Mexico with fresh water mainly in the outcrop area and

shallow portion and brine water adjacent to the coastal line. Groundwater density increases with increasing total dissolved solids. Density difference could influence groundwater flow. A groundwater flow model without simulating density, if designed properly, can still be a valuable tool to identify the pathways and travel times of brackish, saline, and brine waters.

The conceptual flow model for the central and southern portions of the Gulf Coast Aquifer System consists of four hydrostratigraphic units (from shallowest to deepest): the Chicot Aquifer and younger units, the Evangeline Aquifer, the Burkeville Unit, and the Jasper Aquifer. The top and bottom of the conceptual model domain are the ground surface and the bottom of the Jasper Aquifer, respectively. In this model domain, the interaction with the underlying Yegua-Jackson Aquifer is assumed zero due to the low permeability of the Catahoula/Frio/Anahuac Formation which separates these two, except the upper portion near the outcrop area where the sandy Catahoula Formation is contained in the Jasper Aquifer. The lateral extent of the conceptual flow model is bounded by the Brazos River to the north, the perimeter of the Gulf Coast Aquifer System to the west, about 10 miles into Mexico to the south, and approximately 10 miles into the Gulf of Mexico to the east. The lateral groundwater flow across the model domain perimeter below the Brazos River is assumed zero. This assumption is justified due to the presence of the Brazos River and the buffer between the river and Groundwater Water Management Area 15. As described above, lateral groundwater flow from the Yegua-Jackson Aquifer to the Jasper Aquifer along the updip to the west of the model domain can be represented by a head-dependent boundary. Similarly, the lateral groundwater flow across the southern perimeter in Mexico can also be simulated using a head-dependent boundary. In addition, the buffer south of the Rio Grande further minimizes the impacts of the boundary conditions. Due to its immense size relative to the study area, the Gulf of Mexico along the east domain perimeter can be represented by constant head. However, the Gulf of Mexico is expected to extend only into the Chicot Aquifer within the model domain. As a result, head-dependent boundary may be used to quantify the groundwater discharge from the Evangeline Aquifer, the Burkeville Unit, and the Jasper Aquifer into the Gulf of Mexico.

Aquifers are more permeable than confining units. Groundwater flow and storage occur mainly in aquifers. Cross formation flow between aquifers can happen when water levels are different between the aquifers. Cross formation flow can occur directly where a confining unit is absent or through the confining unit. In the study area, the Gulf Coast Aquifer System is mainly composed of sand interbedded with clay. According to Young and others (2010; 2014), even the Burkeville Unit is sandy in its outcrop area. The sand fraction for the Burkeville Unit in the downdip area is also very similar to the Chicot, Evangeline, and Jasper aquifers (Young and others, 2010). Therefore, these units can be well connected hydraulically. Low permeable clay could extend miles in some areas, which causes even the Chicot Aquifer to be confined, and influence the groundwater flow pattern.

The conceptual flow model includes two hydrogeologic conditions: steady state and transient state. The steady state represents the pre-development conditions prior to 1940s when the groundwater use was limited in the study area. The steady state represents a time when inflows and outflows are balanced, and the system is at equilibrium. Once groundwater was withdrawn from the aquifers, either by pumping or flowing wells, the aquifer system was not at steady state anymore. Thus, the hydraulic conditions prior to 1940s were a “pseudo” steady state. In general, the real steady state should have a higher water level and greater natural discharge to streams and springs. The transient state represents the time period after 1940s when the groundwater use was significant.

### **5.1 Pre-Development Conditions (Steady State)**

Because of limited groundwater withdrawal prior to the 1940s, the Gulf Coast Aquifer System in the study area was under long-term dynamic equilibrium. Groundwater levels and flows fluctuated over time due to seasonal and annual changes in precipitation. However, the total discharge was balanced by the total recharge. As a result, the water levels and storage in the system showed little long-term variation. [Figure 5.1.1](#) shows the schematic groundwater flow under pre-development conditions. The major groundwater inflow components under pre-development conditions are: (1) recharge through precipitation infiltration, and (2) regional flow from the Yegua-Jackson Aquifer. The

outflow components include discharges to the Gulf of Mexico, rivers, and springs, and groundwater loss by evapotranspiration.

The infiltration recharge occurred over the whole study area except groundwater discharge points such as surface water bodies and riparian zone. Once the water reached the aquifer, part of it likely took the preferential pathways to return to the ground surface as river baseflow and springs. This flow system is shallow and short with relatively fast groundwater flow. The groundwater under such a flow system is often young and fresh with very low total dissolved solids. However, some of the infiltration could travel further vertically and horizontally and discharge at ends of river basins to form intermediate flow systems. The rest of the infiltration could flow even deeper and farther and finally discharge to the Gulf of Mexico. This part is called deep or regional flow system. With increasing travel time, the groundwater experiences increasing total dissolved solids and a series of chemical phase transitions from calcium-carbonate/bicarbonate dominated to sodium-chloride-sulphate dominated.

Groundwater flow from the Yegua-Jackson Aquifer was controlled by regional topography and hydrogeologic properties of the system and adjacent formations. Since the shallow portion of the Catahoula Formation is quite sandy, groundwater flow from the Yegua-Jackson to the Jasper aquifers is primarily in shallow portion. Groundwater across the southern domain perimeter in Mexico flows to either the Rio Grande or Gulf of Mexico.

Rivers and streams in the study area most likely act as discharge points for the shallow and intermediate groundwater flow systems, while all three flow systems could end up in the Gulf of Mexico. As described in Section 4 ([Figure 4.4.13](#)), all the springs associated with the Gulf Coast Aquifer System are located at the outcrop areas. This indicates that most of the recharge at the outcrop areas returned to the ground surface after traveling a relatively short distance. Groundwater loss to evapotranspiration occurred at places with shallow water tables, dense vegetation with long roots, and void-rich soils.

## 5.2 Post-Development Conditions (Transient State)

After the 1940s, increasing groundwater pumping had changed the aquifer system in the study area. These changes included falling water levels/aquifer storage, reducing discharge to rivers and springs, and increasing groundwater recharge in general.

Pumping causes water level decline and forms a “cone of depression” around the well, which deepens and extends radially with time. As the cone of depression expands, it induces groundwater to move toward the well and reduces natural groundwater outflow from the area adjacent to the well. Declining water level reduces evapotranspiration, baseflow to rivers, spring flow, and discharge to the Gulf of Mexico. The combination of these parts is called “captured outflow”. When the induced inflow approximates the captured outflow, the cone of depression becomes stable. However, this equilibrium condition will break by increasing pumping, which causes an even larger depression, reverses groundwater flow, and can cause brackish water migration or sea water intrusion. Pumping can also increase groundwater recharge because the rejected recharge under shallow water level conditions is now capable to enter the groundwater system. [Figure 5.1.2](#) shows the schematic flow system under post-development conditions in the study area.

## 5.3 Implementation of Groundwater Recharge

Section 4.3 presents the groundwater recharge rates estimated from stream baseflow. Several factors, such as groundwater withdrawal, evapotranspiration, stream bank storage, and flow into deeper formations, can reduce stream baseflow. As a result, groundwater recharge values based on stream baseflow measurements are likely close to the low end of the actual groundwater recharge. The groundwater recharge values from stream baseflow will serve as starting points and, if necessary, will be adjusted during the numerical model development.

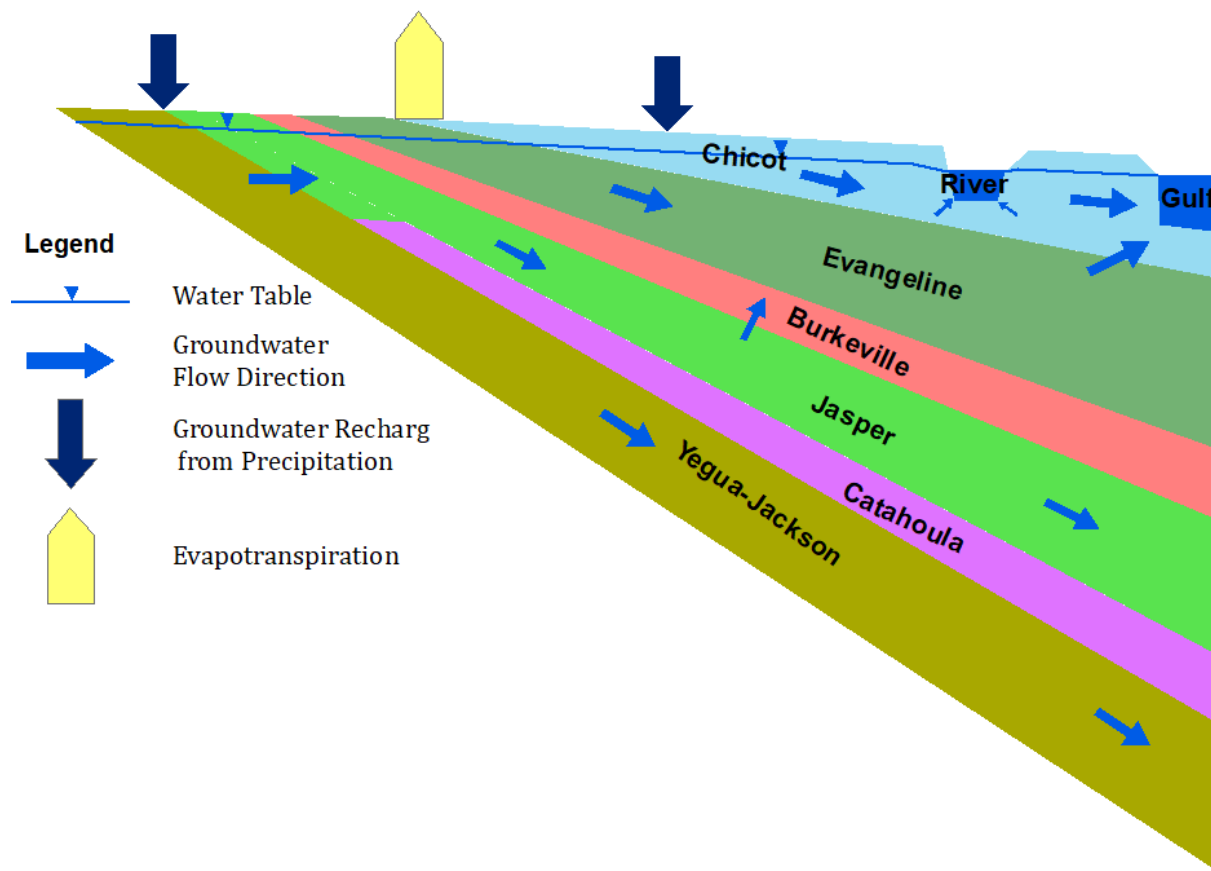


**Figure 5.1.1 Schematic groundwater flow of pre-development conditions.**

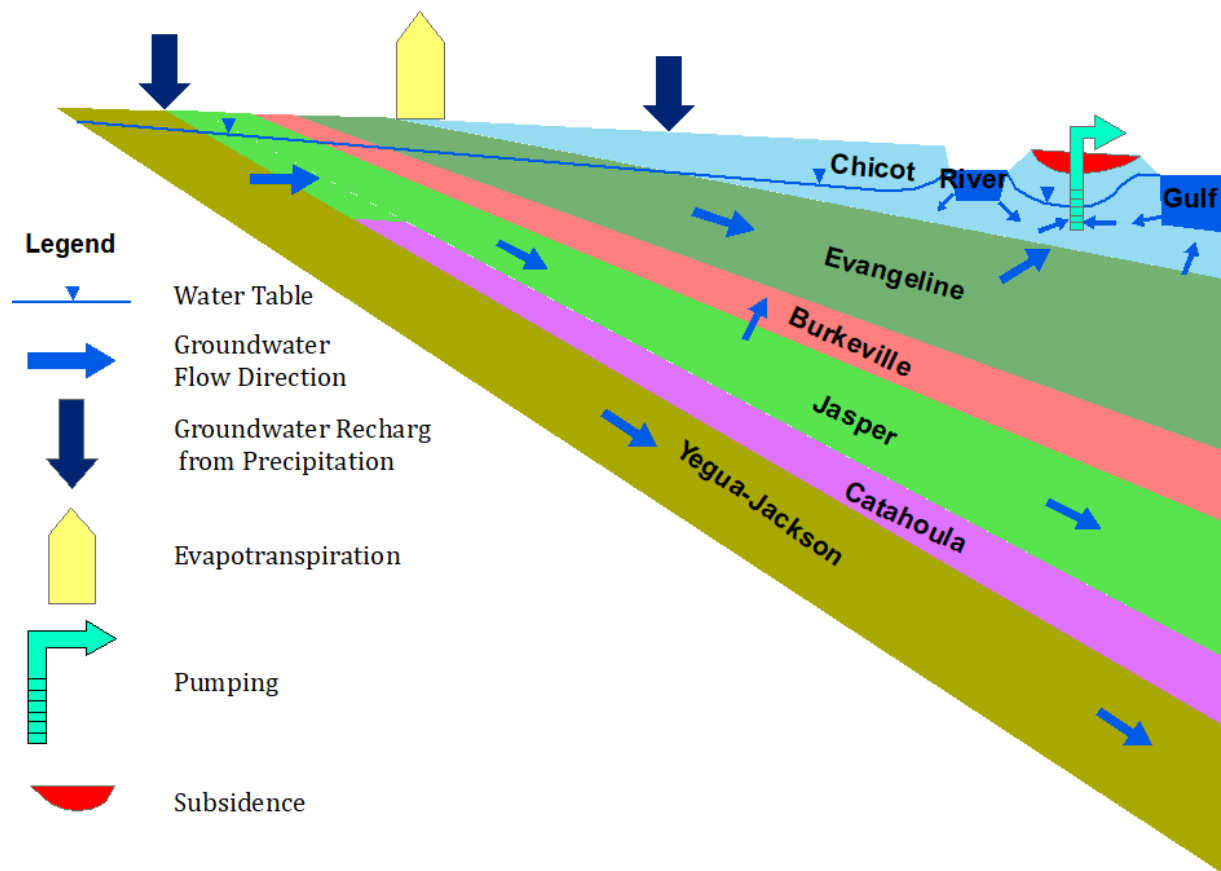


**Figure 5.1.2 Schematic groundwater flow of post-development conditions.**



## 6.0 Future Improvements

Uncertainties exist due to the lack of data for certain areas and the complexity of the study area. One good example is the estimate of sand fraction from geophysical logs. To catch up the continuity or discontinuity of clay and sand units often relies on the density of logs. Unfortunately, much of the study area was covered by a limited number of geophysical logs. One way to compensate this data deficiency is to use seismic profiles. The seismic profiles produce continuous underground geologic information such as depth and thickness of clay or shale units. Water well logs are another good resource, particularly for the shallow portion in the outcrop area. In this study, we have incorporated some of these logs to define the hydrogeologic properties (conductivity and storativity) of model layers. However, logs for new and existing wells are being continuously submitted to TWDB and should be added to the dataset if an update of the framework is warranted in the future.

How to accurately estimate the groundwater recharge continues to be a great challenge for this study. As stated in the previous section, groundwater recharge estimated from stream baseflow (or from chlorine mass balance) is likely lower than the true groundwater recharge. Fortunately, local stakeholders, such as Goliad County Groundwater Conservation District, already started field studies to quantify true groundwater recharge at locations with different top soils and vegetations. These real field data should greatly help us to understand groundwater recharge, not only at these tested locations, but for the whole study area.

Groundwater pumping remains largely uncertain in some counties in the study area. It is expected to improve with refined groundwater use survey methods and involvement of groundwater conservation districts.

The characteristics of faults can be evaluated using tracer tests and pump tests. Tracer test can tell how fast groundwater flows along a fault and its connection with other faults. Pump tests can be used to assess if a fault acts as a barrier by placing a pumping well on one side and the observation well(s) on the other side of the fault.

Research on land subsidence in the study area has been spotty. This can be improved by applying interferometric synthetic-aperture radar (InSAR) images and land surface difference calculation between Light and raDAR (LIDAR) data. Both technologies cover large areas with relative low cost.

The TWDB will update the conceptual model, if warranted, by additional information through the continued stakeholder process and the development of the numerical model. If this occurs, the TWDB will inform the stakeholders.

## Acknowledgments

This conceptual model could not have been done without stakeholder participation. Many stakeholders provided valuable suggestions. These suggestions were evaluated and incorporated into the conceptual model. The central and southern portions of the Gulf Coast Aquifer System groundwater availability model team would like to thank all stakeholders for contributions to the development of this conceptual groundwater flow model.

Special thanks go to:

- Mr. Chris McFarlane and Mr. Landon Yosko of Evergreen Underground Water Conservation District for guiding the field trip to Hordes Creek south of Kenedy and providing core cuttings from their testing well and pumping test result near City of Kenedy;
- Mr. Art Dohmann and Ms. Heather Sumpter of Goliad County Groundwater Conservation District for providing water levels, previous studies, ongoing groundwater recharge study, very constructive discussion of groundwater recharge, surface water/groundwater interaction, and pumping in existing models;
- Mr. Larijai Francis of Corpus Christi Aquifer Storage and Recovery Conservation District for providing information regarding the Lower Nueces River Watershed and revision of Choke Canyon Reservoir groundwater flow model;
- Mr. Andy Garza of Kenedy County Groundwater Conservation District for providing water levels and discussion about groundwater withdrawal in his district;
- Mr. James "Jim" Brasher of Colorado County Groundwater Conservation District for water level data and discussion about irrigation pumping on shallow domestic wells and interaction between Colorado River and nearby groundwater;
- Dr. Steve Young of INTERA, Inc. for providing data (including pumping tests at public supply wells) for several groundwater conservation districts and supporting

information for the Lower Colorado River Basin groundwater flow model for the Chicot and Evangeline aquifers in Colorado, Wharton, and Matagorda counties;

- Mr. Kevin Spencer of R. W. Harden & Associates, Inc. for contributing pumping test data; and
- Mr. David Morgan, Ms. Tina Shearman, and Mr. Terrel Graham of Neighborhood Against Destroying Aquifers for their help and care during the field trip to battle my dehydration.

This conceptual model could not have been done without the leadership from Ms. Cindy Ridgeway (then Manager of Groundwater Availability Modeling Department at TWDB) and Mr. Larry French (Director of Groundwater Division at TWDB). The central and southern portions of the Gulf Coast Aquifer System groundwater availability model team would like to thank Cindy and Larry for their support during the whole process.

## References

- Adidas, E. O., 1991, Ground-Water Quality and Availability in and around Bruni, Webb County, Texas. Texas Water Development Board LP-209, 57 p.
- Alexander, Jr., W. H., B. N. Myers, and O. C. Dale, 1964, Reconnaissance Investigation of the Ground-Water Resources of the Guadalupe, San Antonio, and Nueces River Basins, Texas. Texas Water Commission Bulletin 6409, 124 p.
- Anders, R. B., 1960, Ground-Water Geology of Karnes County, Texas. Texas Board of Water Engineers Bulletin 6007, 107 p.
- Anders, R. B. and E. T. Baker, Jr., 1961, Ground-Water Geology of Live Oak County, Texas. Texas Board of Water Engineers Bulletin 6105, 55 p.
- Arnold, J.G., P.M. Allen, R. Muttiah, and G. Bernhardt. 1995, Automated base flow separation and recession analysis techniques. *Ground Water* 33(6): 1010-1018.
- Baker, Jr., E. T., 1995, Stratigraphic nomenclature and geologic sections of the gulf coastal plain of Texas. U.S. GEOLOGICAL SURVEY Open-File Report 94-461, 34 p.
- Baker, Jr., E.T., 1986, Hydrology of the Jasper Aquifer in the Southeast Texas Coastal Plain: Texas Water Development Board Report 295, 64 p.
- Baker, Jr., E. T., 1979, Stratigraphic and hydrogeologic framework of part of the coastal plain of Texas. Texas Department of Water Resources Report 236, 43 p.
- Baker, Jr., E. T., 1965, Ground-Water Resources of Jackson County, Texas. Texas Water Development Board Report 1, 90 p.
- Baker, R. C. and O. C. Dale, 1964, Ground-Water Resources of the Lower Rio Grande Valley Area, Texas. Geological Survey Water-Supply Paper 1653, 57 p.
- Blandford, T.N., Clause, V., Lewis, A., Standen, A.R., Donnelly, A., Calhoun, K., Botros, F., and Umstot, T., 2021, Conceptual Model Report for the Cross Timbers Aquifer. Texas Water Development Board. 275 p.
- Blum, M.D., and D.M. Price, 1998, Quaternary alluvial plain construction in response to glacioeustatic and climatic controls, Texas Gulf Coastal Plain: *Society of Sedimentary Geology (SEPM) Special Publication No. 59*, p. 31–48.
- Braun, C.L., and Lambert, R.B., 2011, Streamflow, groundwater hydrology, and water quality in the upper Coleto Creek watershed in southeast Texas, 2009–10: U.S. Geological Survey Scientific Investigations Report 2011–5157, 53 p.
- Brown, L. F., Jr., J. L. Brewton, T. J. Evans, J. H. McGowen, W. A. White, C. G. Groat, and W. L. Fisher, 1980, Environmental geologic atlas of the Texas coastal zone–Brownsville-Harlingen area: The University of Texas at Austin, Bureau of Economic Geology, 140 p.
- Bureau of Economic Geology, 1997, Tectonic Map of Texas, The University of Texas at Austin.

- Carr, J.E., Meyer, W.R., Sandeen, W.M., and McLane, I.R., 1985, Digital models for simulation of ground-water hydrology of the Chicot and Evangeline aquifers along the Gulf Coast of Texas: Texas Department of Water Resources, Report 289, 101 p.
- Chowdhury, A. and R. E. Mace, 2007, Groundwater Resource Evaluation and Availability Model of the Gulf Coast Aquifer in the Rio Grande Valley of Texas. Texas Water Development Board Report 368, 119 p.
- Chowdhury, A.H., and M.J. Turco, 2006, Geology of the Gulf Coast aquifer, Texas, in R.E. Mace and others, eds., Aquifers of the Gulf Coast of Texas: Texas Water Development Board Report 365, p. 23–50.
- Chowdhury, A. H., S. Wade, R. E. Mace, and C. Ridgeway, 2004, Groundwater Availability Model of the Central Gulf Coast Aquifer System: Numerical Simulations through 1999 Model Report. Texas Water Development Board, 108 p.
- Christian, B. and Wuerch, D., 2012, Compilation of Results of Aquifer Tests in Texas. Texas Water Development Board Report 365, 106 p.
- Dale, O. C., 1952, Ground-Water Resources of Starr County, Texas. Texas Board of Water Engineers Bulletin 5209, 50 p.
- Dale, O. C. and W. O. George, 1954, Ground-Water Resources of Cameron County, Texas. Texas Board of Water Engineers Bulletin 5403, 66 p.
- Dale, O. C., E. A. Moulder, and T. Arnow, 1957, Ground-Water Resources of Goliad County, Texas. Texas Board of Water Engineers Bulletin 5711, 102 p.
- Dubar, J.R., T.E. Ewing, E.L. Lundelius, Jr., E.G. Otvos, and C.D. Winker, 1991, Quaternary Geology of the Gulf of Mexico Coastal Plain, in R. B. Morrison, ed., Quaternary Non-Glacial Geology of the Conterminous United States: Boulder, Colorado, The Geological Society of America, The Geology of North America, v. K-2, p. 583–610.
- Ewing, T.E., 1991, Structural framework, *in* A. Salvador, ed., The geology of North America: the Gulf of Mexico basin, v. J: Boulder, Colorado, Geological Society of America, p. 31–52.
- Follet, C.R. and R. K. Gabrysch, 1965, Ground-Water Resources of DeWitt County. Texas. Texas Water Commission Bulletin 6518, 113 p.
- Fry, J., Xian, G., Jin, S., Dewitz, J., Homer, C., Yang, L., Barnes, C., Herold, N., and Wickham, J., 2011, Completion of the 2006 National Land Cover Database for the Conterminous United States, PE&RS, Vol. 77(9):858-864.
- Gabrysch, R. K., 1982, Ground-Water Withdrawals and Land-Surface Subsidence in the Houston-Galveston Region, Texas, 1906-80. U. S. Geological Survey Open-File Report 82-571, 68 p.
- Galloway, W.E., 2005, Gulf of Mexico Basin depositional record of Cenozoic North American drainage basin evolution: International Association Sedimentologists Special Publication 35, p. 409–423.
- Galloway, W.E., D.G. Bebout, W.L. Fisher, R. Cabrera-Castro, J.E. Lugo-Rivera, and T.M. Scott, 1991, Cenozoic, in A. Salvador, ed., The geology of North America: the Gulf of Mexico basin, v. J: Boulder, Colorado, Geological Society of America, p. 245–324.

- Galloway, W.E., L.A. Jirik, R.A. Morton, and J.R. DuBar, 1986, Lower Miocene (Fleming) depositional episode of the Texas Coastal Plain and continental shelf: The University of Texas at Austin, Bureau of Economic Geology Report of Investigations No. 150, 50 p.
- Galloway, W.E., C.D. Henry, and G.E. Smith, 1982, Depositional framework, hydrostratigraphy, and uranium mineralization of the Oakville Sandstone (Miocene), Texas Coastal Plain: The University of Texas at Austin, Bureau of Economic Geology Report of Investigations No. 113, 51 p.
- Hammond, Jr., W.W., 1969, Ground-Water Resources of Matagorda County, Texas. Texas Water Development Board Report 91, 163 p.
- HDR Engineering Inc., INTERA Inc, Geochemical Solutions LLC, and Wellspec, 2019, Corpus Christi Aquifer Storage and Recovery Feasibility Project. TWDB Contract No. 1600011956 (Partners: Corpus Christi Aquifer Storage and Recovery Conservation District and City of Corpus Christi), 639 p.
- HDR, Inc., 2000, A Numerical Groundwater Flow Model of the Gulf Coast Aquifer Along the South Texas Gulf Coast, Draft Report, 61 p.
- HDR Engineering Inc., INTERA Inc., Geochemical Solutions LLC, and Wellspec, 2019, Corpus Christi Aquifer Storage and Recovery Feasibility Project Report.
- Heitmuller, F. T. and B. D. Reece, 2003, Database of Historically Documented Springs and Spring Flow Measurements in Texas. U. S. Geological Survey Open-File Report 03-315, 2 p.
- Hoel, H.D., 1982, Goliad Formation of the south Texas Gulf Coastal Plain: regional genetic stratigraphy and uranium mineralization: Master's thesis, The University of Texas at Austin, 173 p.
- Hosman, R. L., 1996, Regional stratigraphy and subsurface geology of Cenozoic deposits, Gulf Coastal Plain, South-Central United States—Regional aquifer system analysis—Gulf Coastal Plain: U. S. Geological Survey Professional Paper 1416-G, 35 p.
- Hutchison, W. R., M. E. Hill, R. Anaya, M. M. Hassan, W. Oliver, M. Jigmond, S. Wade, and E. Aschenbach, 2011, Groundwater Management Area 16 Groundwater Flow Model, Texas Water Development Board, 306 p.
- Kasmarek, M.C., Ramage, J.K., and Johnson, M.R., 2016, Water-level altitudes 2016 and water-level changes in the Chicot, Evangeline, and Jasper aquifers and compaction 1973–2015 in the Chicot and Evangeline aquifers, HoustonGalveston region, Texas: U. S. Geological Survey Scientific Investigations Map 3365, pamphlet, 16 sheets, scale 1:100,000, <http://dx.doi.org/10.3133/sim3365>.
- Kasmarek, M.C., and Robinson, 2004, Hydrogeology and Simulation of Groundwater Flow and Land-Surface Subsidence in the Northern Part of the Gulf Coast Aquifer System, Texas: United States Geological Society, Scientific Investigation Report 2004-5102.
- Knox, P.R., S.C. Young, W.E. Galloway, E.T. Baker, Jr., and T. Budge, 2006, A stratigraphic approach to Chicot and Evangeline aquifer boundaries, central Texas Gulf Coast: Gulf Coast Association of Geological Societies Transactions, v. 56, p. 371–393.

- Kuiper, L.K., 1994, Nonlinear regression flow model, gulf coast aquifer systems, south-central United States: U.S. Geological Survey Water Resources Investigations Report 93-4020, 171 p.
- Kuchanur, M., V. Uddameri, and D. Cravey, 2003, A Numerical Groundwater Flow Model of the Gulf Coast Aquifer Along the South Texas Gulf Coast, Report to Refugio Groundwater Conservation District, 64 p.
- Larkin T.J., and Bomar, G.W., 1983, Climatic atlas of Texas. Texas Department of Water Resources Report LP-192.
- Lizárraga, J.S., and Wehmeyer, L.L., 2012, Estimation of streamflow gains and losses in the lower San Antonio River watershed, south-central Texas, 2006–10: U. S. Geological Survey Scientific Investigations Report 2012–5073, 34 p.
- Lizárraga, J.S., and Ockerman, D.J., 2010, Simulation of streamflow, evapotranspiration, and groundwater recharge in the lower San Antonio River watershed, south-central Texas, 2000–2007: U. S. Geological Survey Scientific Investigations Report 2010–5027, 41 p.
- Lopez, C. V., Murgulet, D., Douglas A., and Murgulet, V., 2018, Impacts of Temporal and Spatial Variation of Submarine Groundwater Discharge on Nutrient Fluxes to Texas Coastal Embayments, Phase III (Baffin Bay) Final Report, GLO Contract No. 16-060-000-9104 (April 10, 2018) <http://www.glo.texas.gov/coastal-grants/documents/grant-project/16-060-final-report.pdf>
- Loskot, C. L., W. M. Sandeen, and C. R. Follett, 1982, Ground-Water Resources of Colorado, Lavaca, and Wharton Counties, Texas. Texas Department of Water Resources Report 270, 199 p.
- Mace, R.E., S. C. Davidson, E. S. Angle, and W. F. Mullican III, 2006, Aquifers of the Gulf Coast of Texas. Texas Water Development Board Report 365, 304 p.
- Marvin, R.F., G. H. Shafer, and O. C. Dale, 1962, Ground-Water Resources of Victoria and Calhoun Counties, Texas. Texas Board of Water Engineers Bulletin 6202, 147 p.
- Mason, C.C., 1963a, Availability of Ground Water from the Goliad Sand in the Alice Area, Texas. Texas Water Commission Bulletin 6301, 101 p.
- Mason, C.C., 1963b, Ground-Water Resources of Refugio County, Texas. Texas Water Commission Bulletin 6312, 85 p.
- McCoy, W. M., 1990, Evaluation of Ground-Water Resources in the Lower Rio Grande Valley, Texas. Texas Water Development Board Report 316, 48 p.
- Morton, R.A., and Galloway, W.E., 1991, Depositional, tectonic and eustatic controls on hydrocarbon distribution in divergent margin basins: Cenozoic Gulf of Mexico case history: Marine Geology, v. 102, p 239–263.
- Morton, R.A., Jirik, L.A., and Galloway, W.E., 1988, Middle-Upper Miocene depositional sequences of the Texas Coastal Plain and continental shelf: The University of Texas at Austin, Bureau of Economic Geology Report of Investigations No. 174, 40 p.
- Myers, B.N., 1969, Compilation of Results of Aquifer Tests in Texas. Texas Water Development Board Report 98, 532 p.



- Myers, B.N. and O. C. Dale, 1967, Groundwater Resources of Brooks County, Texas. Texas Water Development Board Report 61, 80 p.
- Myers, B.N. and O. C. Dale, 1966, Groundwater Resources of Bee County, Texas. Texas Water Development Board Report 17, 101 p.
- Narasimhan, B., R. Srinivasan, S. Quiring, and J.W. Nielsen-Gammon. 2007, Digital Climatic Atlas of Texas. Texas Water Development Board. TWDB contract # 2005-483-559.
- Natural Resources Conservation Service, 2020, Soil Survey Geographic Database (SSURGO) of National Cartography and Geospatial Center of the U. S. Department of Agriculture. Downloaded from ESRI <https://www.arcgis.com/apps/View/index.html?appid=cdc49bd63ea54dd2977f3f2853e07fff>.
- Panday, S., J. Rumbaugh, W. R. Hutchison, and S. Schorr, 2017, Numerical Model Report: Lower Rio Grande Valley Groundwater Transport Model. Prepared for Texas Water Development Board, 65 p.
- Parsons Engineering Science, Inc., 1999, Surface Water/Groundwater Interaction Evaluation for 22 Texas River Basins, Prepared for Texas Natural Resource Conservation Commission, 201 p.
- Plummer, F. B., 1932, Cenozoic Systems in Texas: Geology of Texas, vol. 1, Stratigraphy, University of Texas Bulletin 3232, p. 519–818.
- Price, W.A., 1934, Lissie Formation and Beaumont Clay in south Texas: American Association of Petroleum Geologists Bulletin, v. 18, p. 948–959.
- PRISM Climate Group, 2018, Oregon State University, <http://prism.oregonstate.edu> (downloaded in March 2018).
- Prudic, D. E., 1991, Estimates of Hydraulic Conductivity from Aquifer-Test Analyses and Specific-Capacity Data, Gulf Coast Regional Aquifer Systems, South-Central United States. U.S. Geological Survey Water-Resources Investigations Report 90-4121, 38 p.
- Rayner, F.A., 1958, Records of Water-Level Measurements in Jackson, Matagorda, and Wharton Counties, Texas, 1934 to April 1958. Texas Board of Water Engineers Bulletin 5804, 49 p.
- Ratzlaff, K. W., 1980, Land-Surface Subsidence in the Texas Coastal Region. U. S. Geological Survey Open-File Report 80-969, 23 p.
- Rogers, L.T., 1967, Availability and Quality of Ground Water in Fayette County, Texas. Texas Water Development Board Report 56, 85 p.
- Ryder, P.D., 1988, Hydrogeology and predevelopment flow in the Texas gulf coast aquifer systems. U. S. Geological Survey Water-Resources Investigations Report 87-4248, 109 p.
- Ryder, P. D. and A. F. Ardis, 1991, Hydrology of the Texas Gulf Coast Aquifer Systems. U. S. Geological Survey Open-File Report 91-64, 147 p.
- Sandeen, W. M., 1972, Ground-Water Resources of Washington County, Texas. Texas Water Development Board Report 162, 105 p.

- Scanlon, B., R. Reedy, G. Strassberg, Y. Huang, and G. Senay, 2012, Estimation of Groundwater Recharge to the Gulf Coast Aquifer in Texas, USA. Prepared by the Bureau of Economic Geology for Texas Water Development Board, 128p.
- Scanlon, B., K. Keese, N. Bonal, N. Deeds, V. Kelley, and M. Litvak, 2005, Evapotranspiration Estimates with Emphasis on Groundwater Evapotranspiration in Texas. Prepared for the Texas Water Development Board, 123 p.
- Sellards, E. H., W. S. Adkins, and F. B. Plummer, 1932, The Geology of Texas, Volume I, Stratigraphy: The University of Texas at Austin, Bureau of Economic Geology, 1007 p.
- Shafer, G. H., 1974, Ground-Water Resources of Duval County, Texas. Texas Water Development Board Report 181, 117 p.
- Shafer, G. H., 1970, Ground-Water Resources of Aransas County, Texas. Texas Water Development Board Report 124, 81 p.
- Shafer, G.H., 1968, Ground-Water Resources of Nueces and San Patricio Counties, Texas. Texas Water Development Board Report 73, 129 p.
- Shafer, G. H. and E. T. Baker, Jr., 1973, Ground-Water Resources of Kleberg, Kenedy, and Southern Jim Wells Counties, Texas. Texas Water Development Board Report 173, 153 p.
- Slade, Jr., R. M., J. T. Bentley, and D. Michaud, 2002, Results of Streamflow Gain-Loss Studies in Texas, with Emphasis on Gains from and Losses to Major and Minor Aquifers. U. S. Geological Survey Open-File Report 02-068, 136 p.
- Solis, R. F., 1981, Upper Tertiary and Quaternary depositional systems, central Coastal Plain, Texas—Regional geology of the coastal aquifer and potential liquid-waste repositories: The University of Texas at Austin, Bureau of Economic Geology Report of Investigations 108, 89 p.
- Stearman, J, 1960, Water Levels in Observation Wells in Cameron, Hidalgo, and Starr Counties, Texas, 1950-1959. Texas Board of Water Engineers Bulletin 6008, 14 p.
- Swartz, B.W., 1957, Records of Water Levels in Aransas and San Patricio Counties, Texas. Texas Board of Water Engineers Bulletin 5703, 32 p.
- TNRIS, 2018, Maps & Data at [http://www.tnris.org/get-data?quicktabs\\_maps\\_data=1#quicktabs-maps\\_data](http://www.tnris.org/get-data?quicktabs_maps_data=1#quicktabs-maps_data).
- TWDB, 2019a, Measured groundwater levels (downloaded in January 2019 <http://www.twdb.texas.gov/groundwater/data/gwdbrrpt.asp>).
- TWDB, 2019b, Groundwater analytical data (downloaded in April 20 <http://www.twdb.texas.gov/groundwater/data/gwdbrrpt.asp>).
- TWDB, 2018, Brackish Resources Aquifer Characterization System (BRACS) database (downloaded in January 2018 <http://www.twdb.texas.gov/innovativewater/bracs/database.asp>).
- University of Texas at Austin, 2018, Bureau of Economic Geology Geologic Atlas of Texas (GAT) (downloaded February 2018).

- Uddameri, V. and M. Kuchanur, 2006, A Multi-county Groundwater Availability Model for the Gulf Coast Aquifer in the Coastal Bend Region of South Texas, Texas A&M University-Corpus Christi: Corpus Christi. p. 63.
- Uranium Energy Corp (UEC), 2008, Goliad Project Production Area Authorization Application for: Production Area-1 (PA-1), 320 p.
- U.S. Census Bureau, 2020, TIGER/Line® Shapefiles Pre-joined with Demographic Data at <https://www.census.gov/geo/maps-data/data/tiger-line.html>.
- U.S. Department of Agriculture, 2020, National Agricultural Statistics Service, CropScape-Cropland Data Layer. <http://nassgeodata.gmu.edu/CropScape/>.
- Vandertulip, J. J., L. L. McDaniels, and C. O. Rucker, 1964, Water-Supply Limitations on Irrigation from the Rio Grande in Starr, Hidalgo, Cameron, and Willacy Counties, Texas. Texas Water Commission Bulletin 6413, 84 p.
- Verbeek, E.R., 1979, Surface faults in the Gulf Coastal Plain between Victoria and Beaumont, Texas: Tectonophysics, v. 52, p. 373–375.
- Waterstone Environmental Hydrology and Engineering, Inc., 2003, Groundwater Availability of the Central Gulf Coast Aquifer: Numerical Simulations to 2050 Central Gulf Coast, Texas. Prepared for the Texas Water Development Board, 158 p. <http://www.twdb.texas.gov/groundwater/models/gam/glfc c/Waterstone Conceptual Report.pdf?d=2202.000000048429>
- Weiss, J. S., 1992, Geohydrologic units of the coastal lowlands aquifer system, south-central United States. U. S. Geological Survey Professional Paper 1416-C, 32 p.
- Weiss, J. S., 1987, Determining dissolved-solids concentrations in mineralized ground water of the gulf coast aquifer systems, using electric logs, in Vecchioli, John, and Johnson, A.I, eds., Regional Aquifer Systems of the United States, Aquifers of the Atlantic and Gulf Coastal Plain. American Water Resources Association, Monograph Series, no. 9, p. 139-150.
- Wermund, 1996, Physiography of Texas: The University of Texas at Austin, Bureau of Economic Geology. <http://www.beg.utexas.edu/UTopia/images/pagesizemaps/physiography.pdf>.
- Wet Rock Groundwater Services, LLC, 2017, Aquifer Test – City of Kenedy Test Well Project, 59 p.
- Williamson, A. K. and H. F. Grubb, 2001, Ground-Water Flow in the Gulf Coast Aquifer System, South-Central United States. U. S. Geological Survey Professional Paper 1416-F, 191 p.
- Winker, C. D., and R.T. Buffler, 1988, Paleogeographic evolution of early deep-water Gulf of Mexico and margins, Jurassic to middle Cretaceous (Comanchean): American Association of Petroleum Geologists Bulletin, v. 72, p. 318–346.
- Winker, C.D., 1982, Cenozoic shelf margins, northwestern Gulf of Mexico: Gulf Coast Association of Geological Societies Transactions, vol. 32, p. 427–448.
- Wood, L.A., R.K. Gabrysch, and R. Marvin, 1963, Reconnaissance investigation of the ground-water resources of the Gulf Coast region, Texas: Texas Water Commission Bulletin 6305, 114 p.

- Young, S. C., 2016, Estimates of Land Subsidence in GMA 15 Based on Ground Surface Elevation Data and Model Results. Prepared for Calhoun County GCD, Coastal Bend GCD, Coastal Plains GCD, Pecan Valley GCD, Refugio GCD, Texana GCD, and Victoria County GCD, 130 p.
- Young, S. C., M. Jigmond, N. Deeds, J. Blainey, T. E. Ewing, and D. Banerj, 2016, Final Report: Identification of Potential Brackish Groundwater Production Areas – Gulf Coast Aquifer System, TWDB Contract Number 1600011947, 664 p.
- Young, S. C., J. Pinkard, R L. Bassett, and A. Chowdhury, 2014, Hydrogeochemical Evaluation of the Texas Gulf Coast Aquifer System and Implications for Developing Groundwater Availability Models, 375 p. Texas Water Development Board. TWDB contract #: 1148301233.  
[http://www.twdb.texas.gov/publications/reports/contracted\\_reports/doc/1148301233.pdf](http://www.twdb.texas.gov/publications/reports/contracted_reports/doc/1148301233.pdf).
- Young, S. C., T. Ewing, S. Hamlin, E. Baker, and D. Lupton, 2012, Final Report – Updating the Hydrogeologic Framework for the Northern Portion of the Gulf Coast Aquifer, 285 p. Texas Water Development Board. TWDB contract #: 1004831113.  
[http://www.twdb.texas.gov/publications/reports/contracted\\_reports/doc/1004831113\\_GulfCoast.pdf](http://www.twdb.texas.gov/publications/reports/contracted_reports/doc/1004831113_GulfCoast.pdf).
- Young, S.C., P. R. Knox, E. Baker, S. Hamlin, B. Galloway, and N. Deeds, 2010, Hydrostratigraphy of the Gulf Coast Aquifer from the Brazos River to the Rio Grande, 213 p. Texas Water Development Board. TWDB contract #: 0804830795.  
[http://www.twdb.texas.gov/publications/reports/contracted\\_reports/doc/0804830795\\_Gulf\\_coast\\_hydrostratigraphy\\_wcover.pdf](http://www.twdb.texas.gov/publications/reports/contracted_reports/doc/0804830795_Gulf_coast_hydrostratigraphy_wcover.pdf).
- Young, S. C., P. Knox, T. Budge, and N. Deeds, 2009, Development of the LCRB Groundwater Flow Model for the Chicot and Evangeline Aquifers in Colorado, Wharton, and Matagorda counties. LSWP Report Prepared by the URS Corporation for the Lower Colorado River Authority, 184 p.
- Young, S. C., P. R. Knox, T. Budge, V. Kelley, N. Deeds, W. E. Galloway, and E. T. Baker, Jr., 2006, Stratigraphy, lithology, and hydraulic properties of the Chicot and Evangeline aquifers in the LSWP study area, Central Texas Coast, *in* R.E. Mace and others, eds., *Aquifers of the Gulf Coast of Texas*: Texas Water Development Board Report 365, p. 129–138.

## **Appendix A: Groundwater Level Hydrographs**

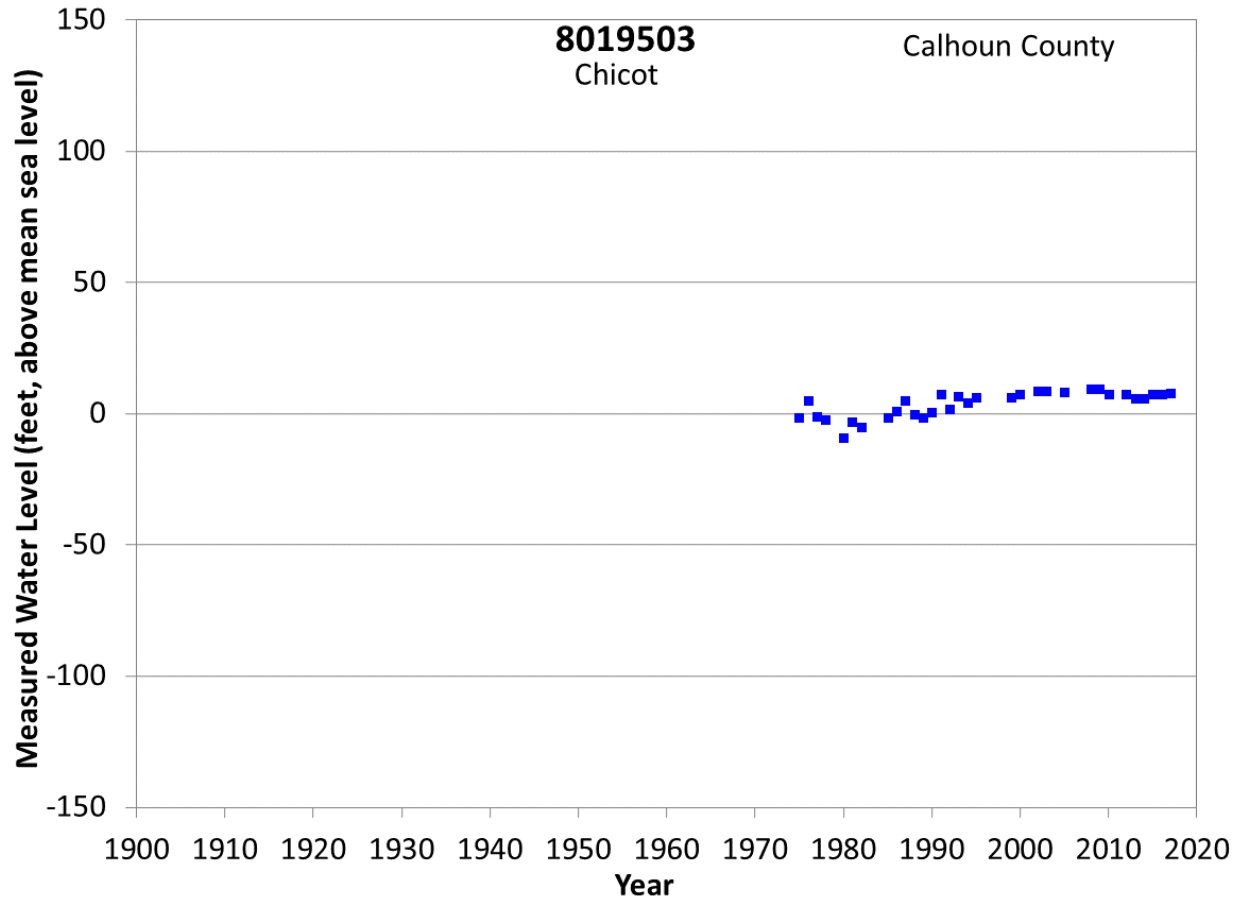


**Figure A1 Groundwater level hydrograph at State Well 8019503.**

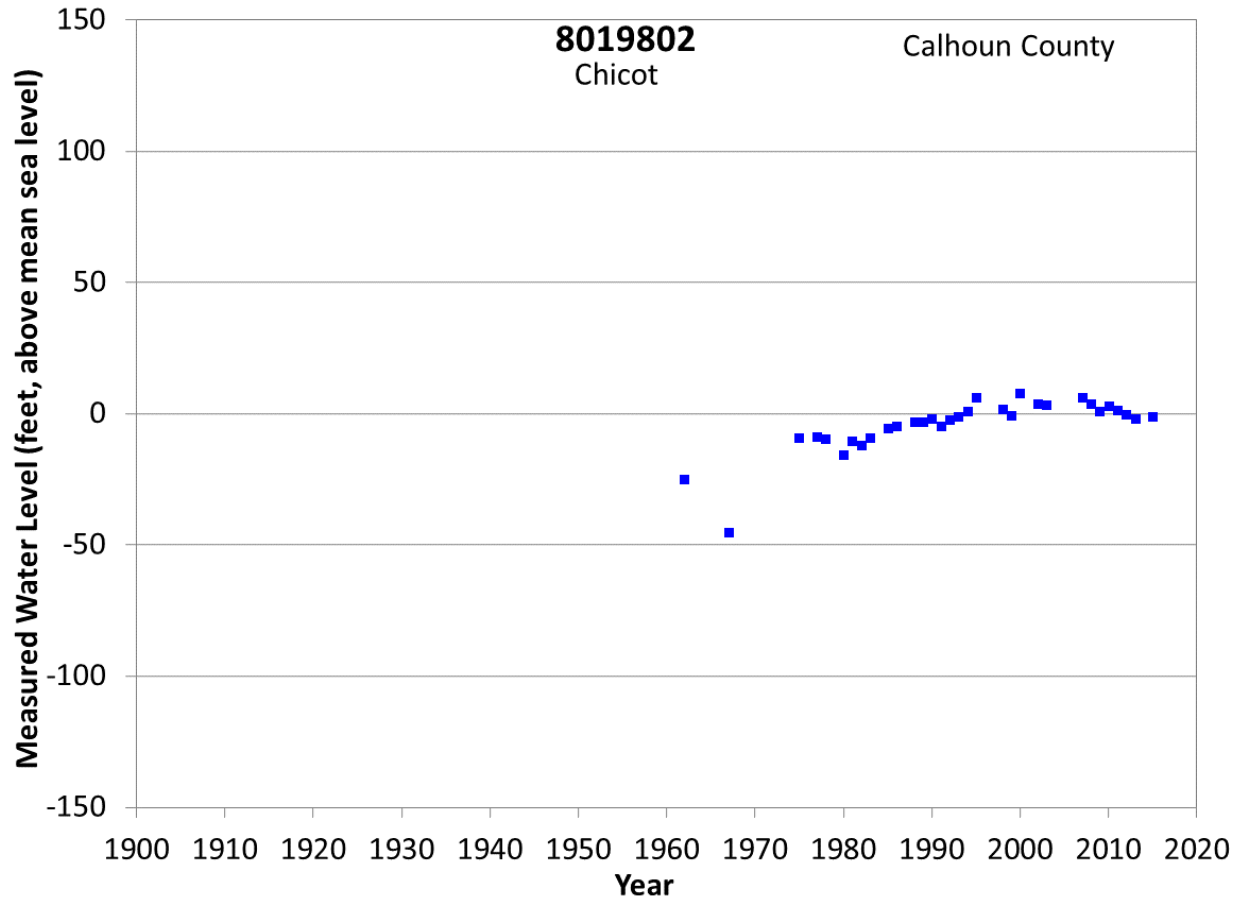


**Figure A2 Groundwater level hydrograph at State Well 8019802.**

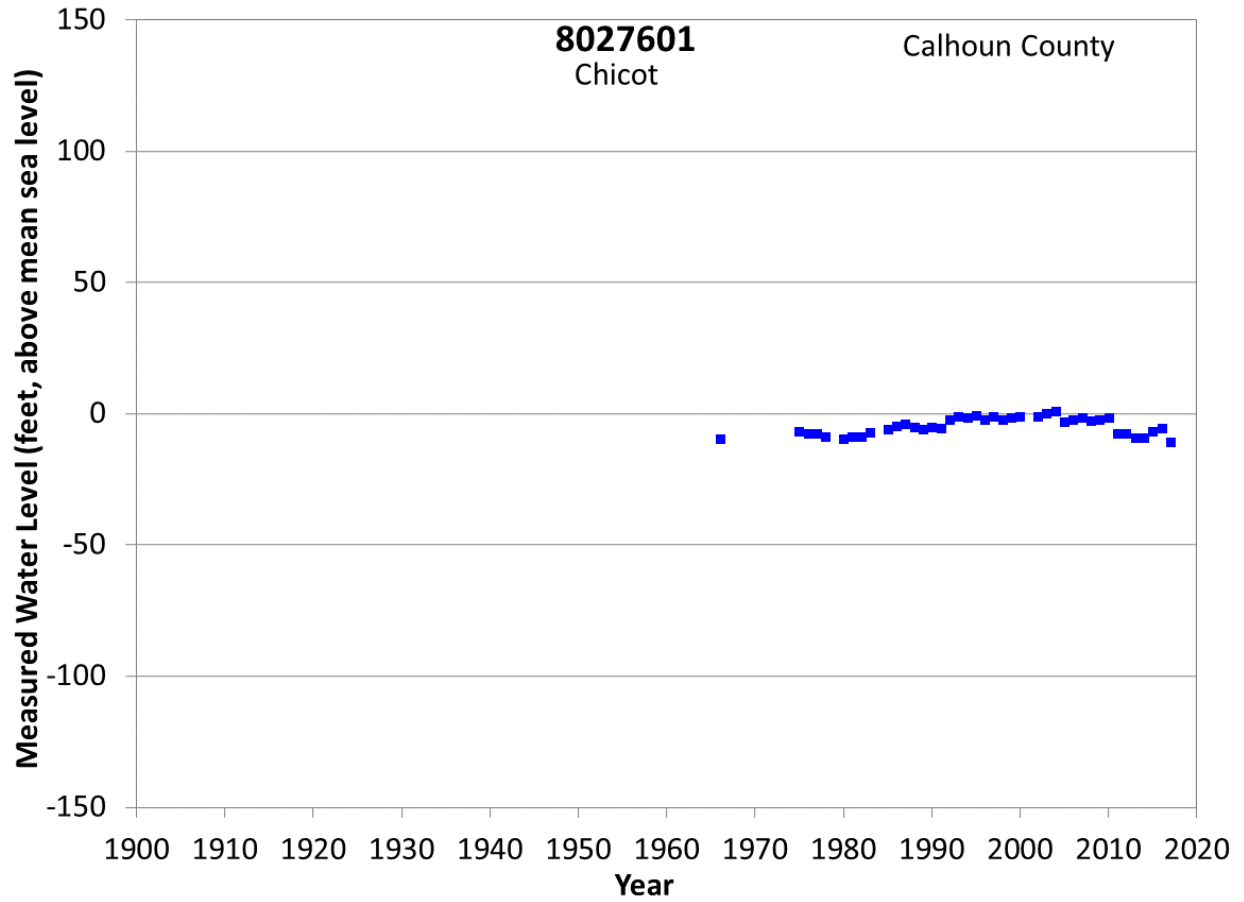


**Figure A3 Groundwater level hydrograph at State Well 8027601.**



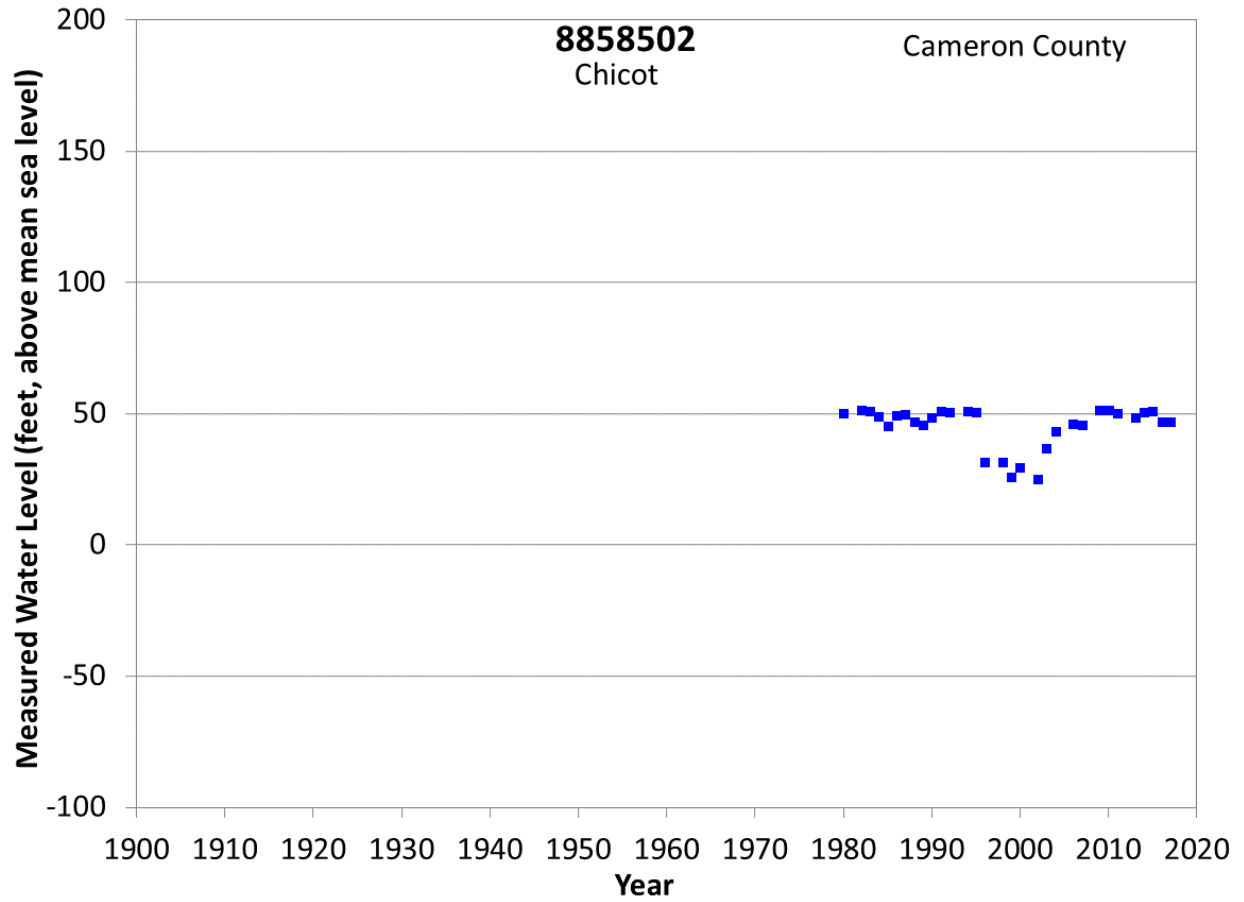


**Figure A4 Groundwater level hydrograph at State Well 8858502.**

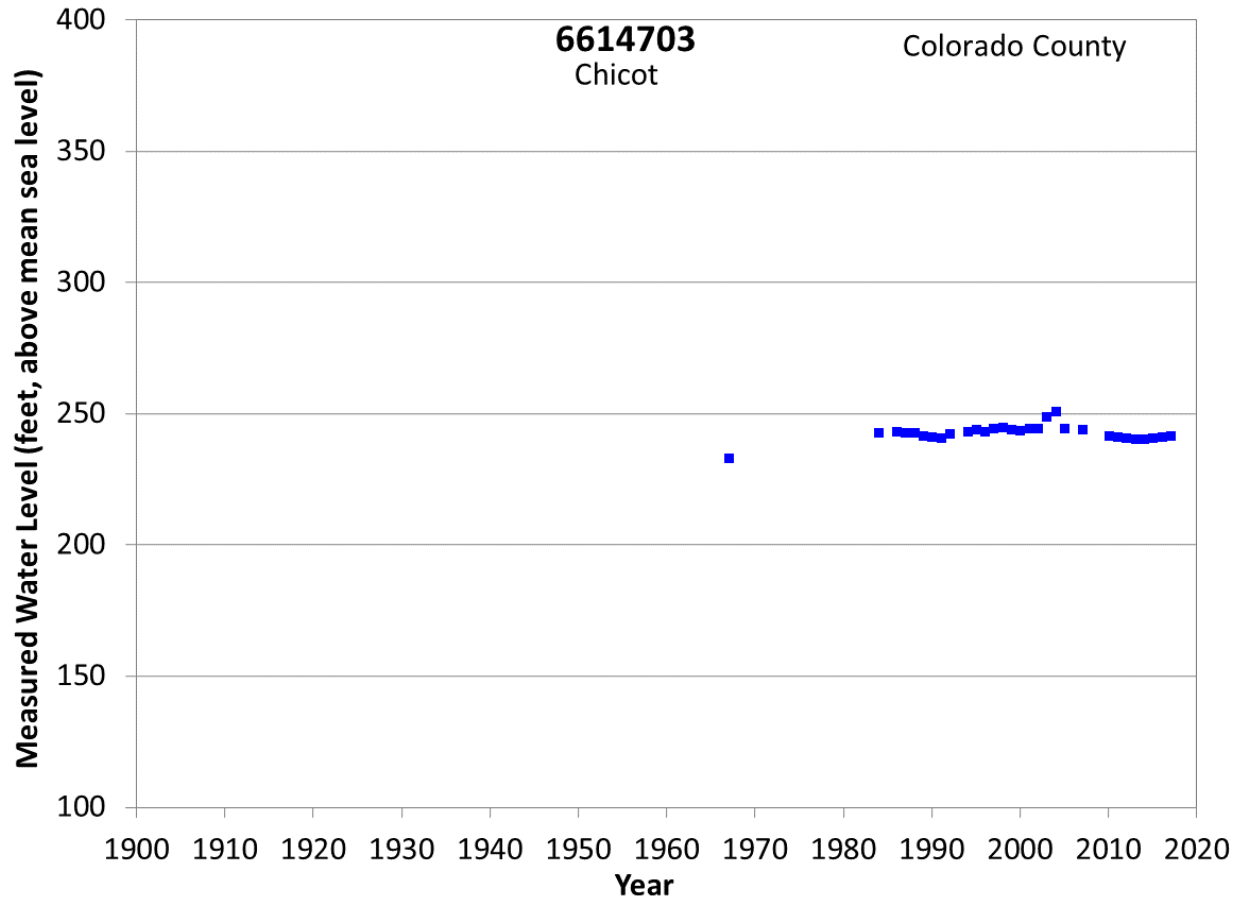


**Figure A5 Groundwater level hydrograph at State Well 6614703.**

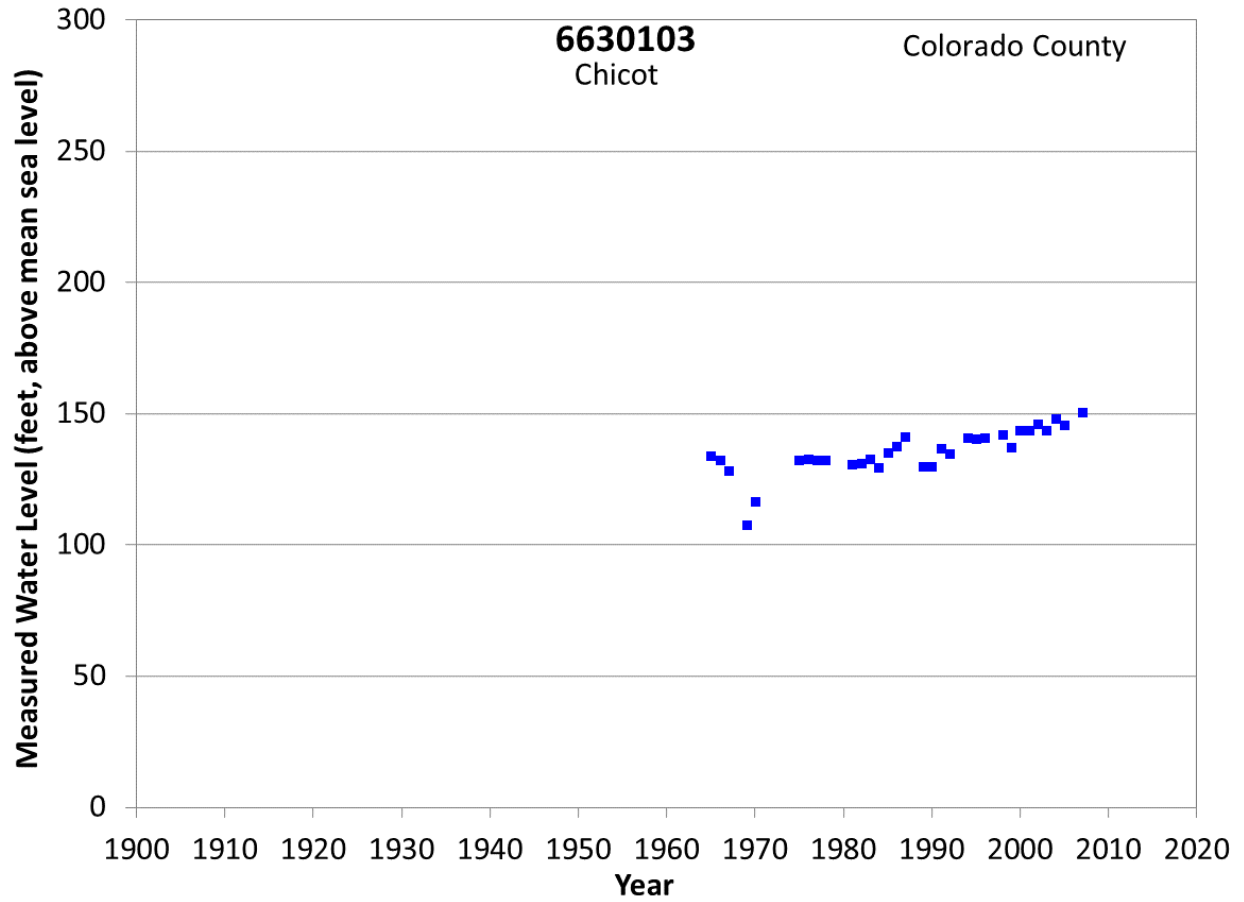


**Figure A6 Groundwater level hydrograph at State Well 6630103.**

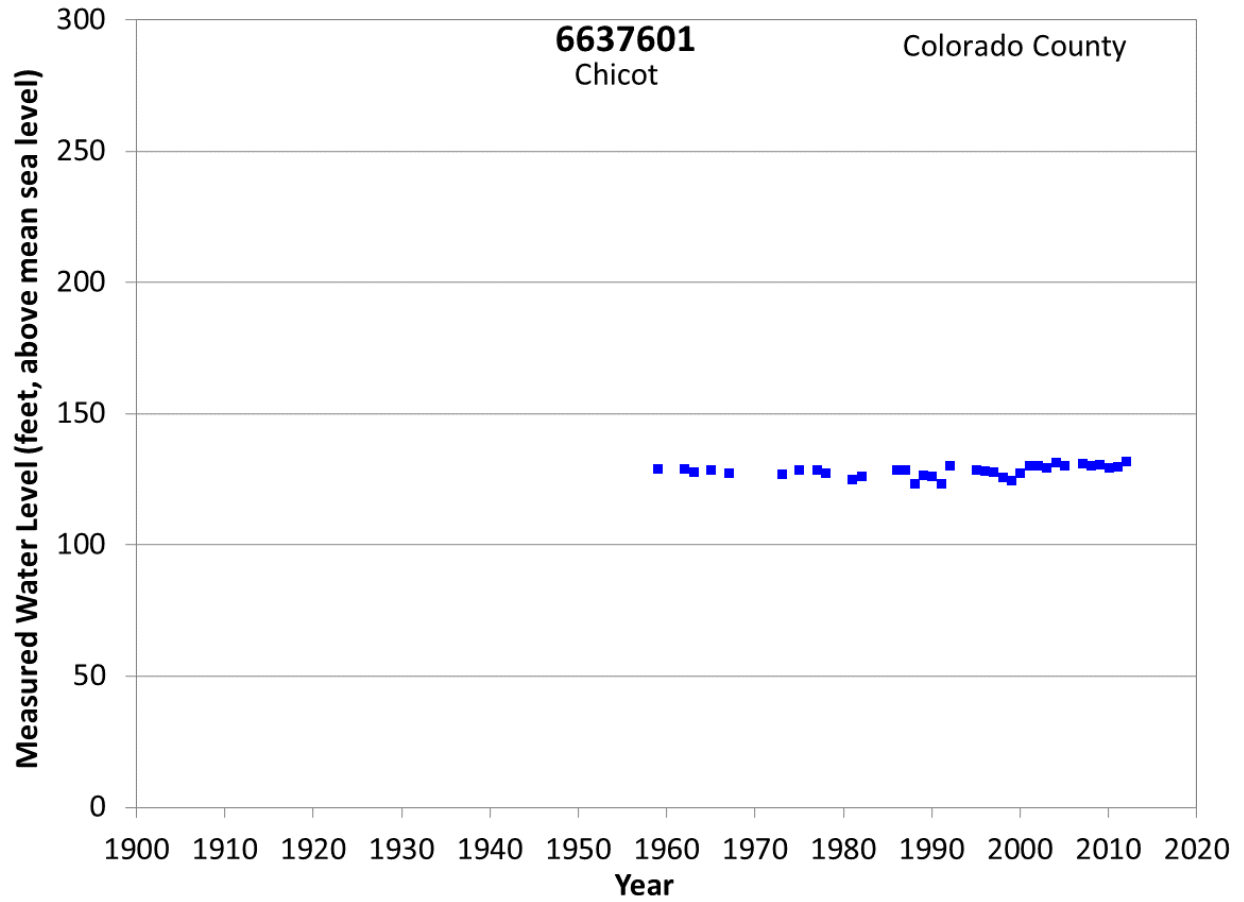


**Figure A7 Groundwater level hydrograph at State Well 6637601.**

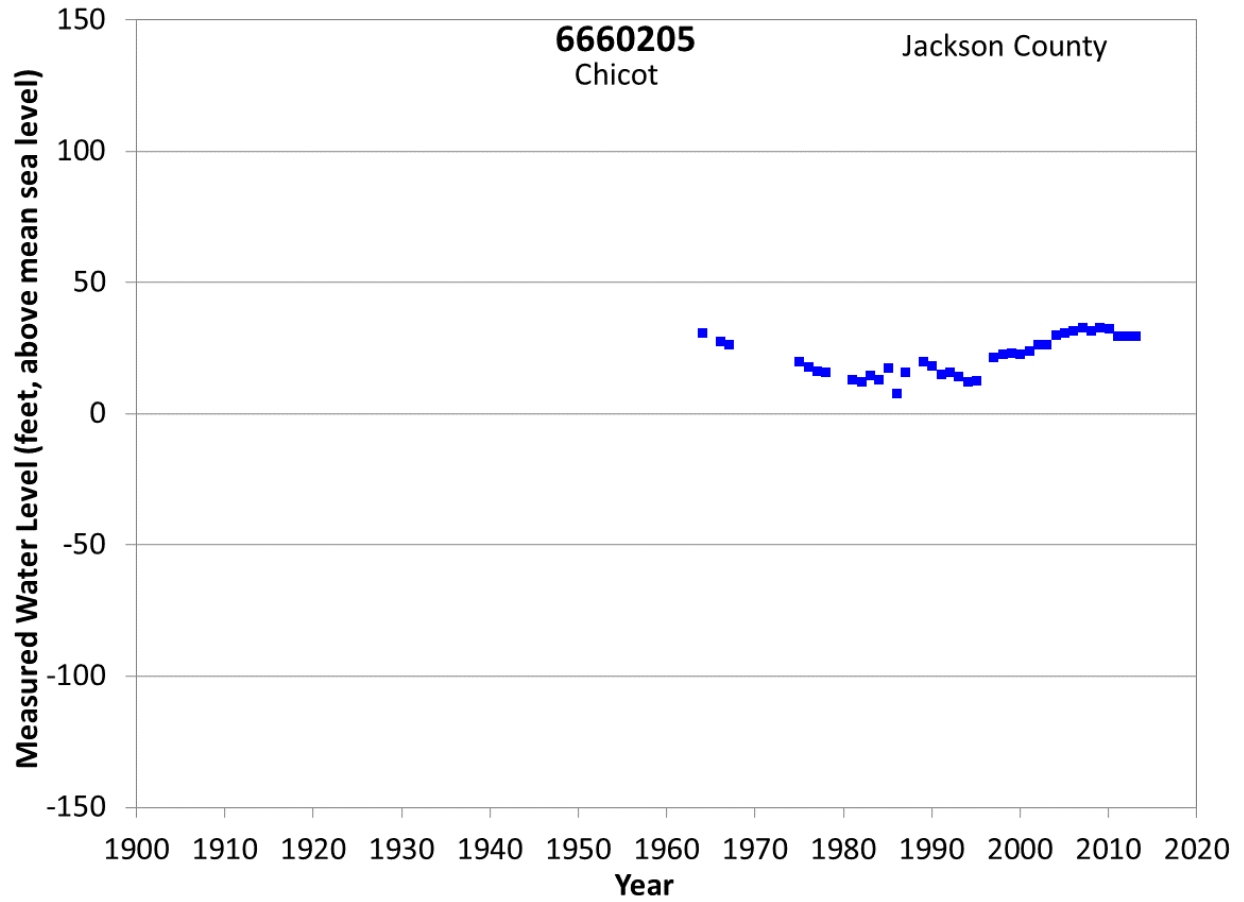


**Figure A8 Groundwater level hydrograph at State Well 6660205.**

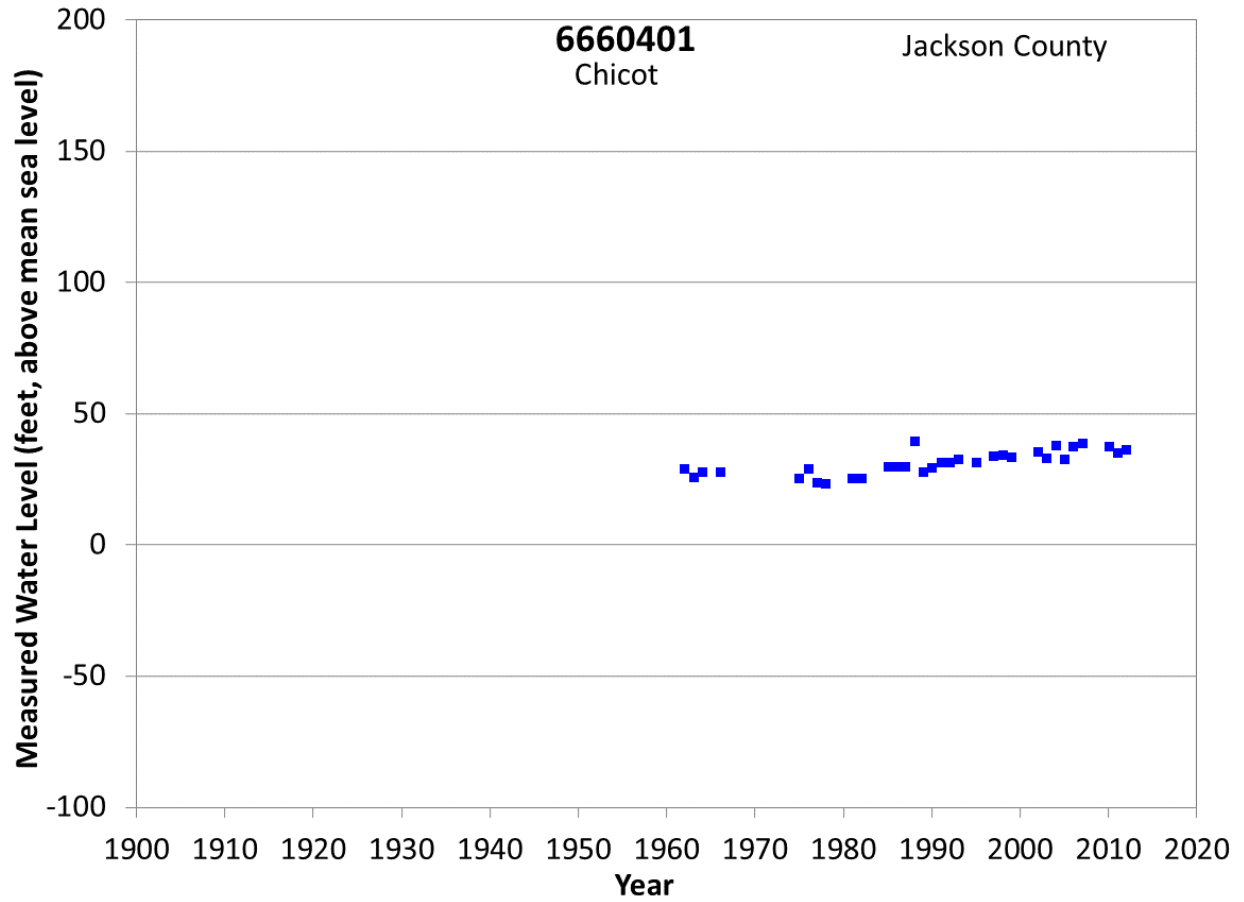


**Figure A9 Groundwater level hydrograph at State Well 6660401.**

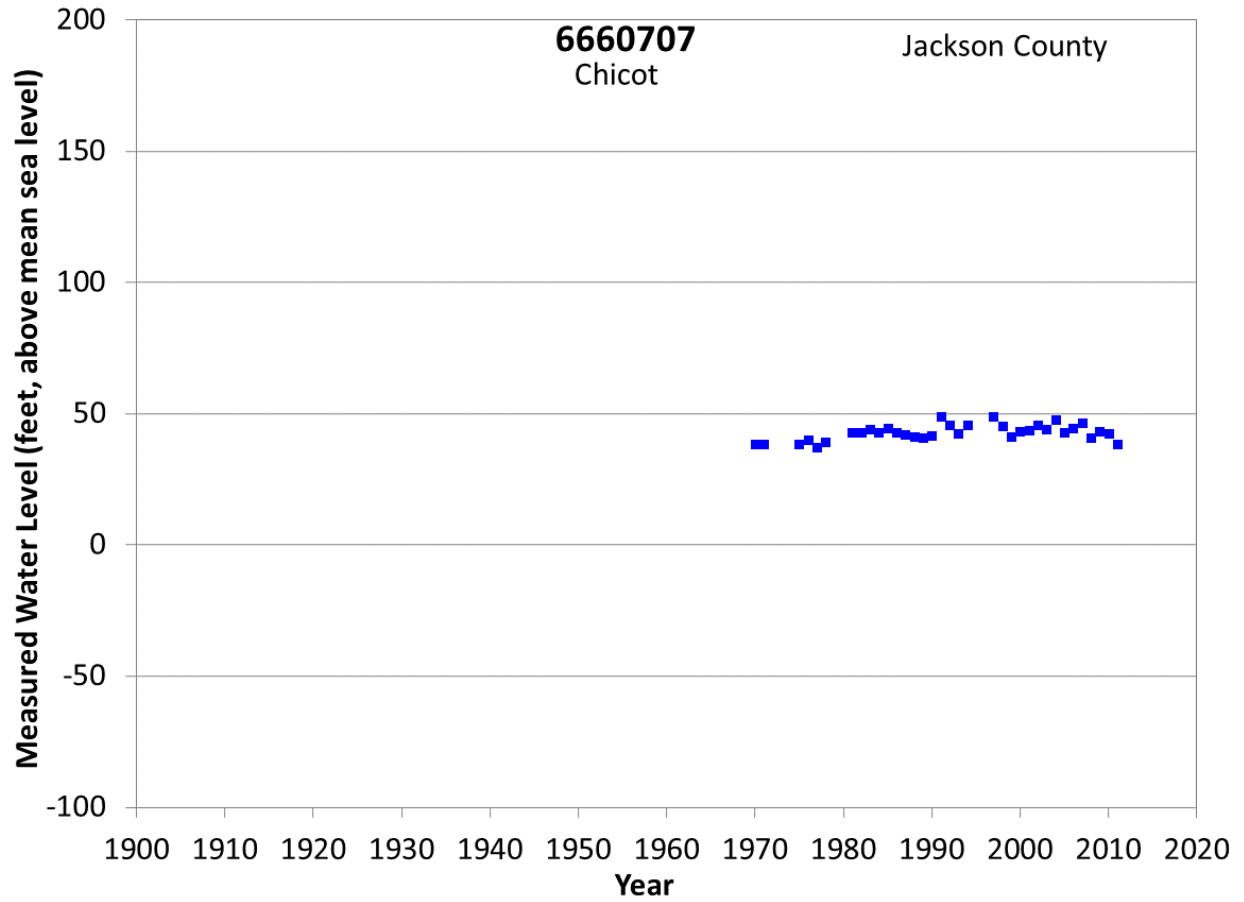


**Figure A10 Groundwater level hydrograph at State Well 6660707.**

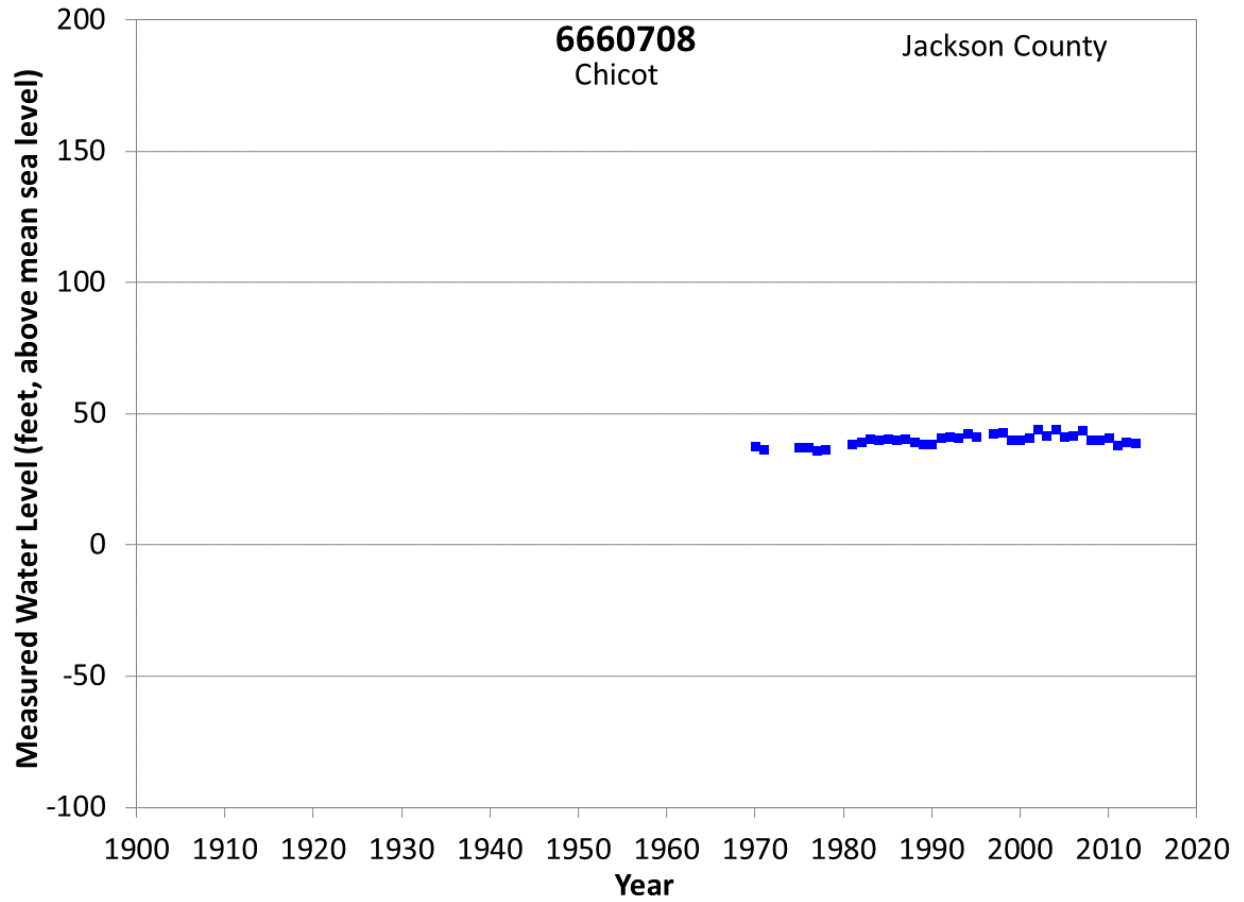


**Figure A11 Groundwater level hydrograph at State Well 6660708.**



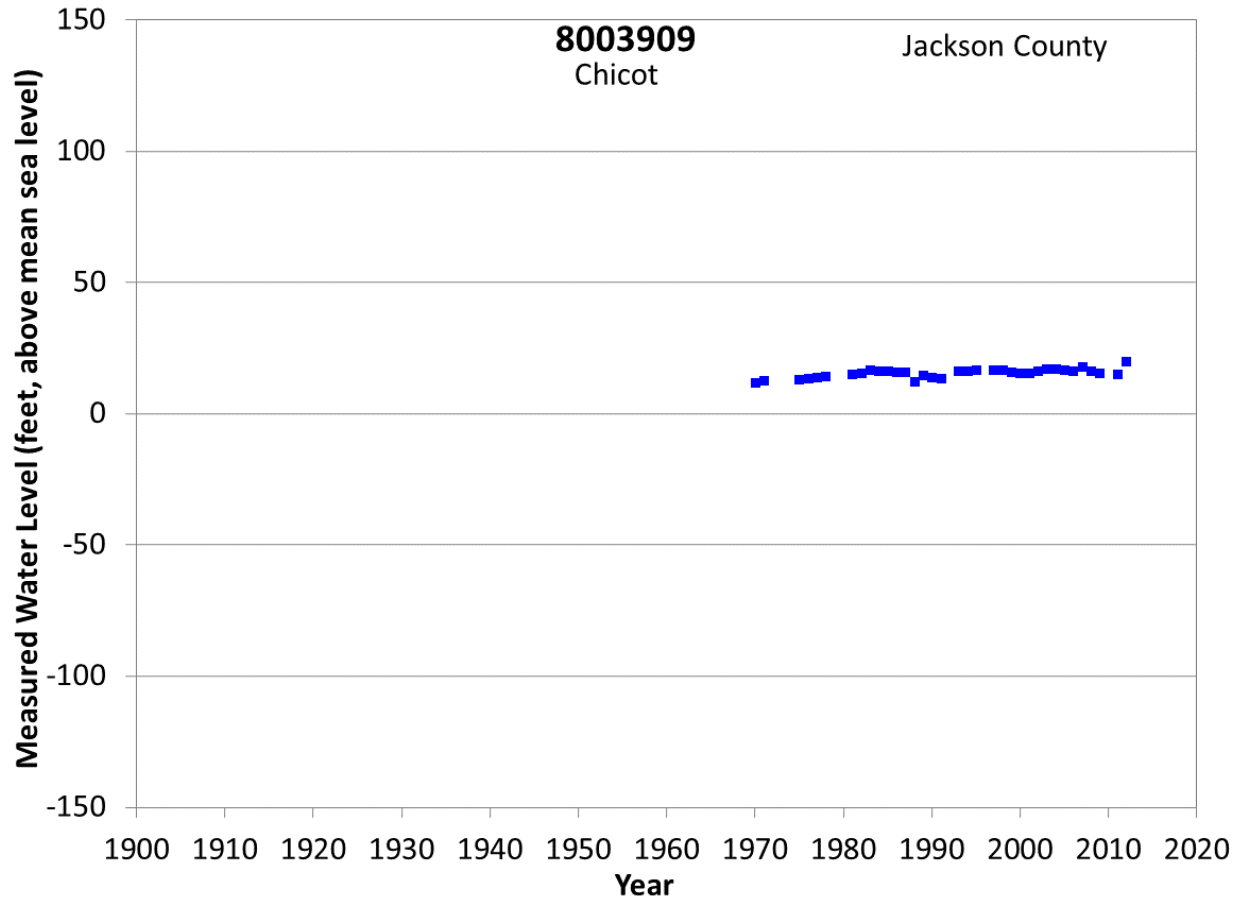


**Figure A12 Groundwater level hydrograph at State Well 8003909.**

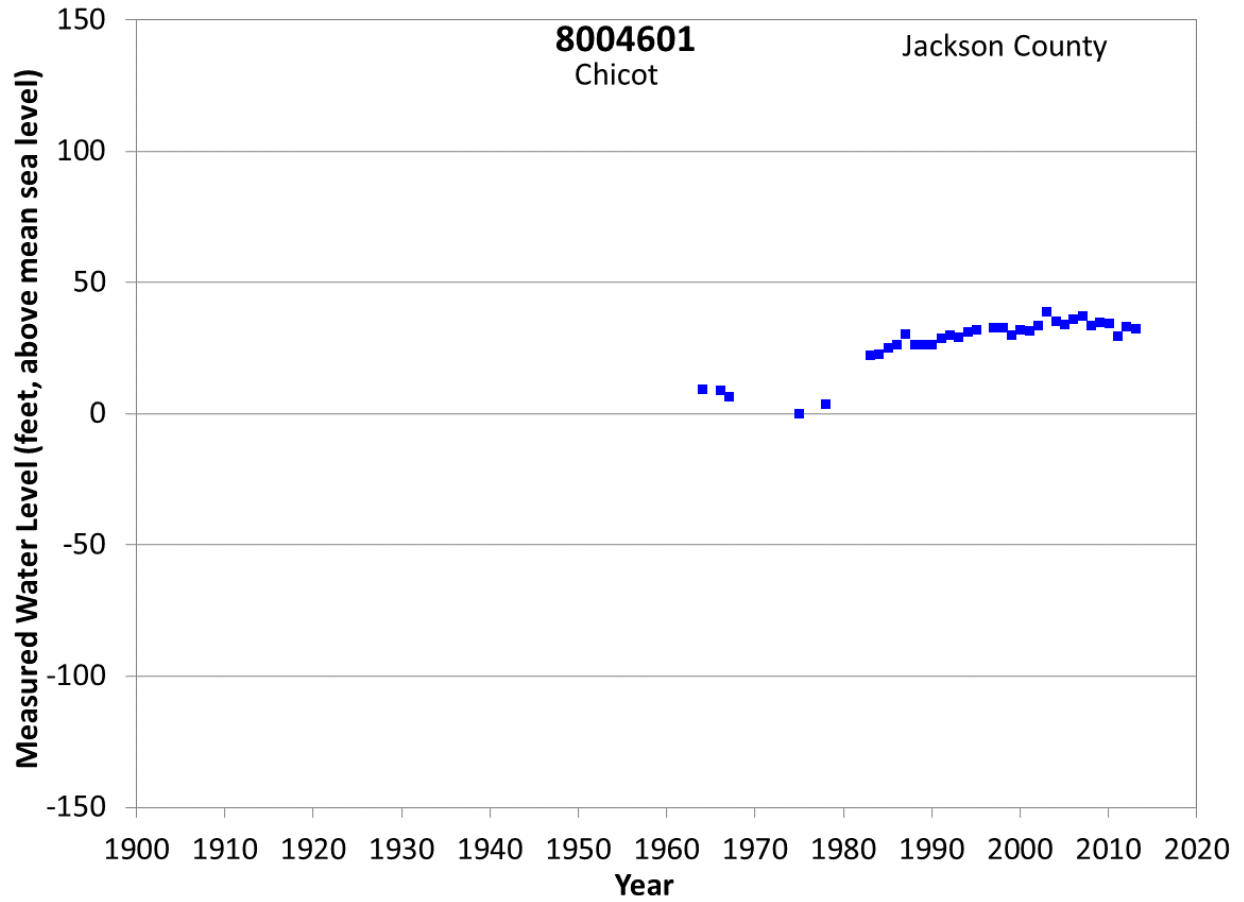


**Figure A13 Groundwater level hydrograph at State Well 8004601.**

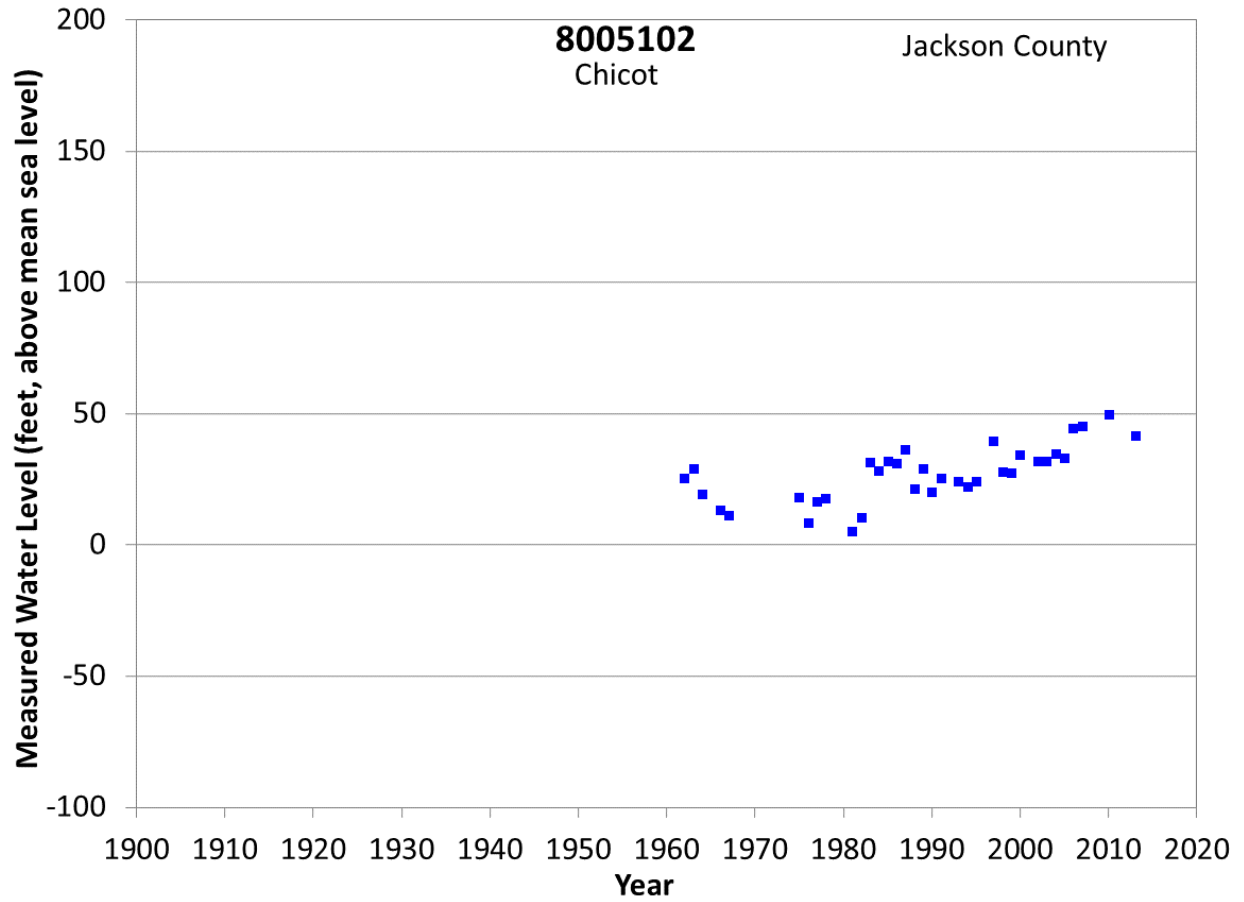


**Figure A14 Groundwater level hydrograph at State Well 8005102.**

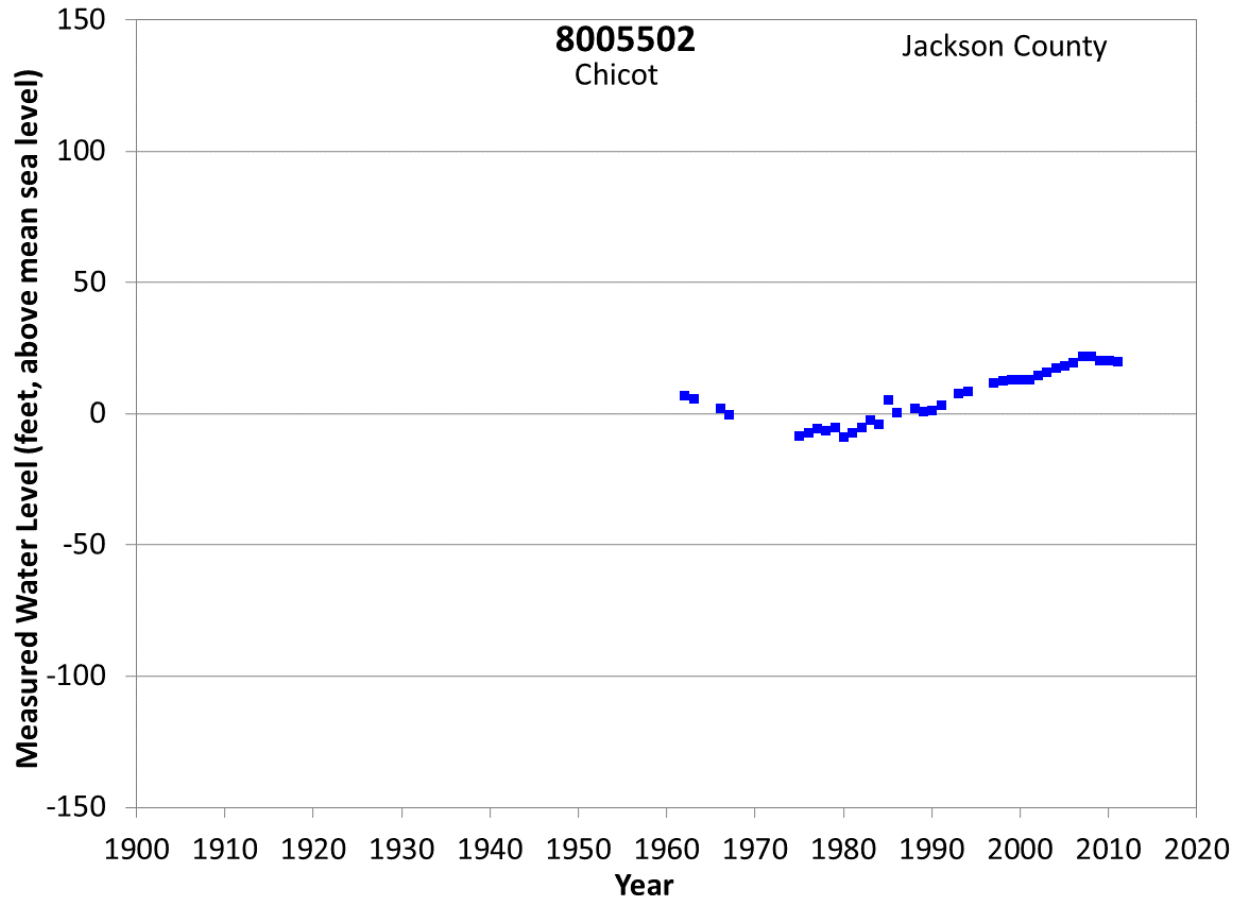


**Figure A15 Groundwater level hydrograph at State Well 8005502.**

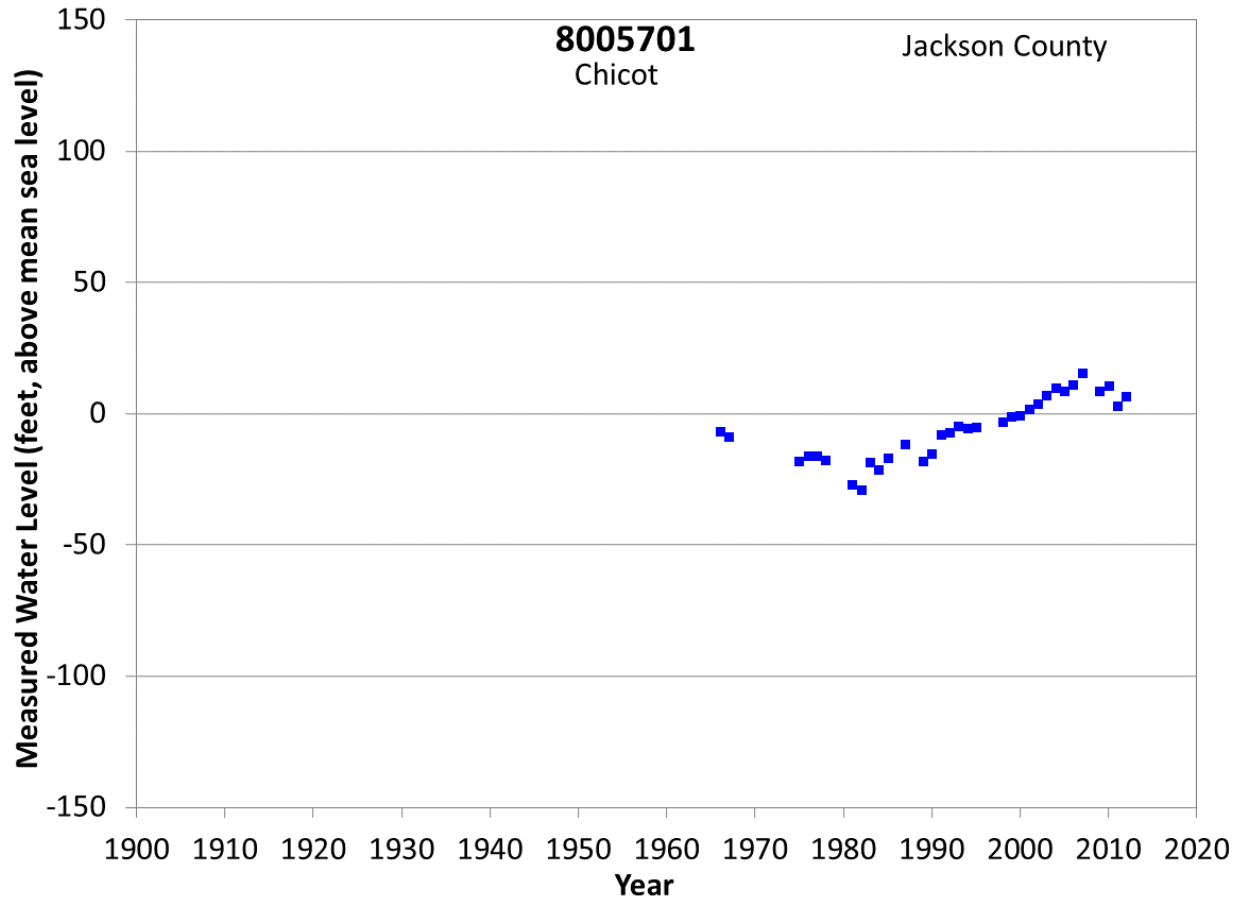


**Figure A16 Groundwater level hydrograph at State Well 8005701.**

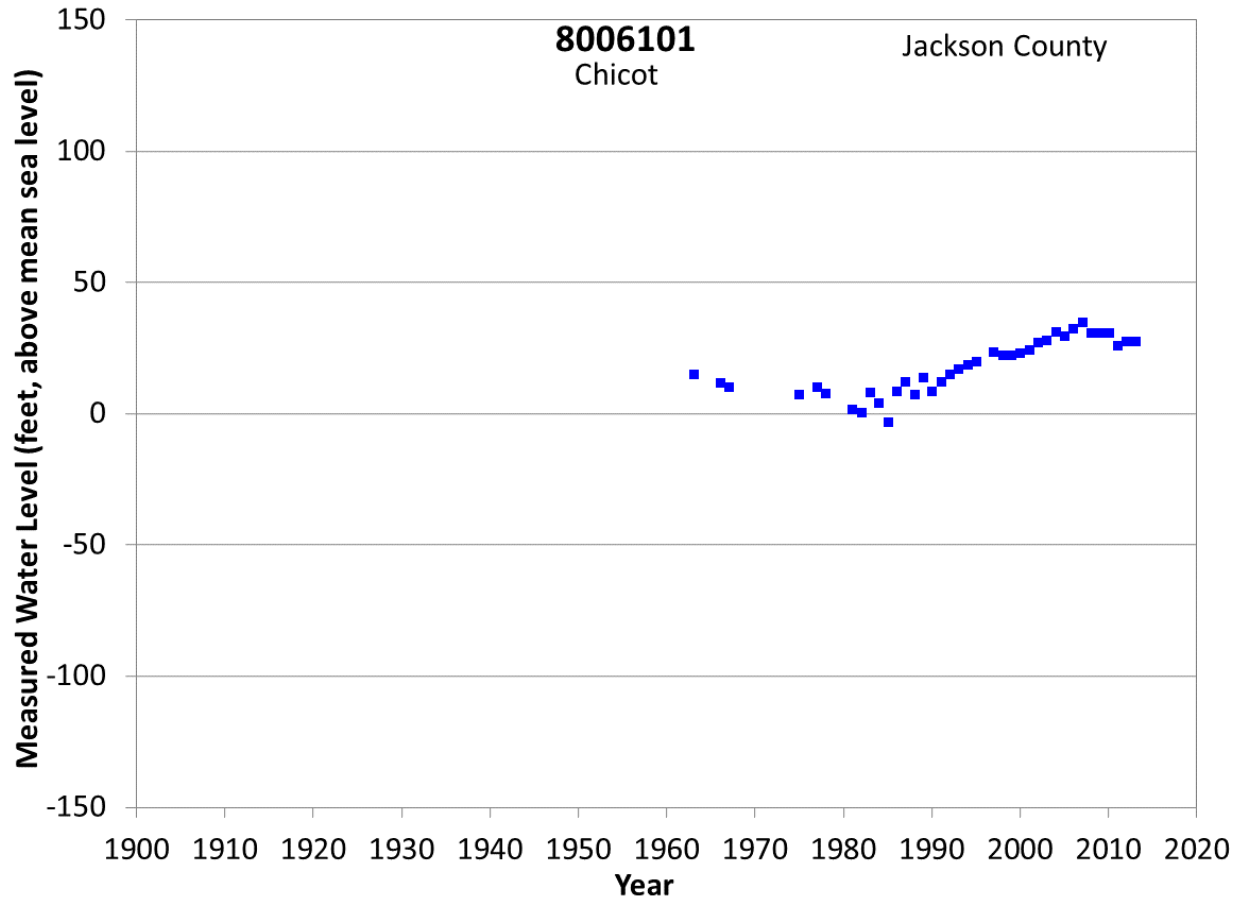


**Figure A17 Groundwater level hydrograph at State Well 8006101.**

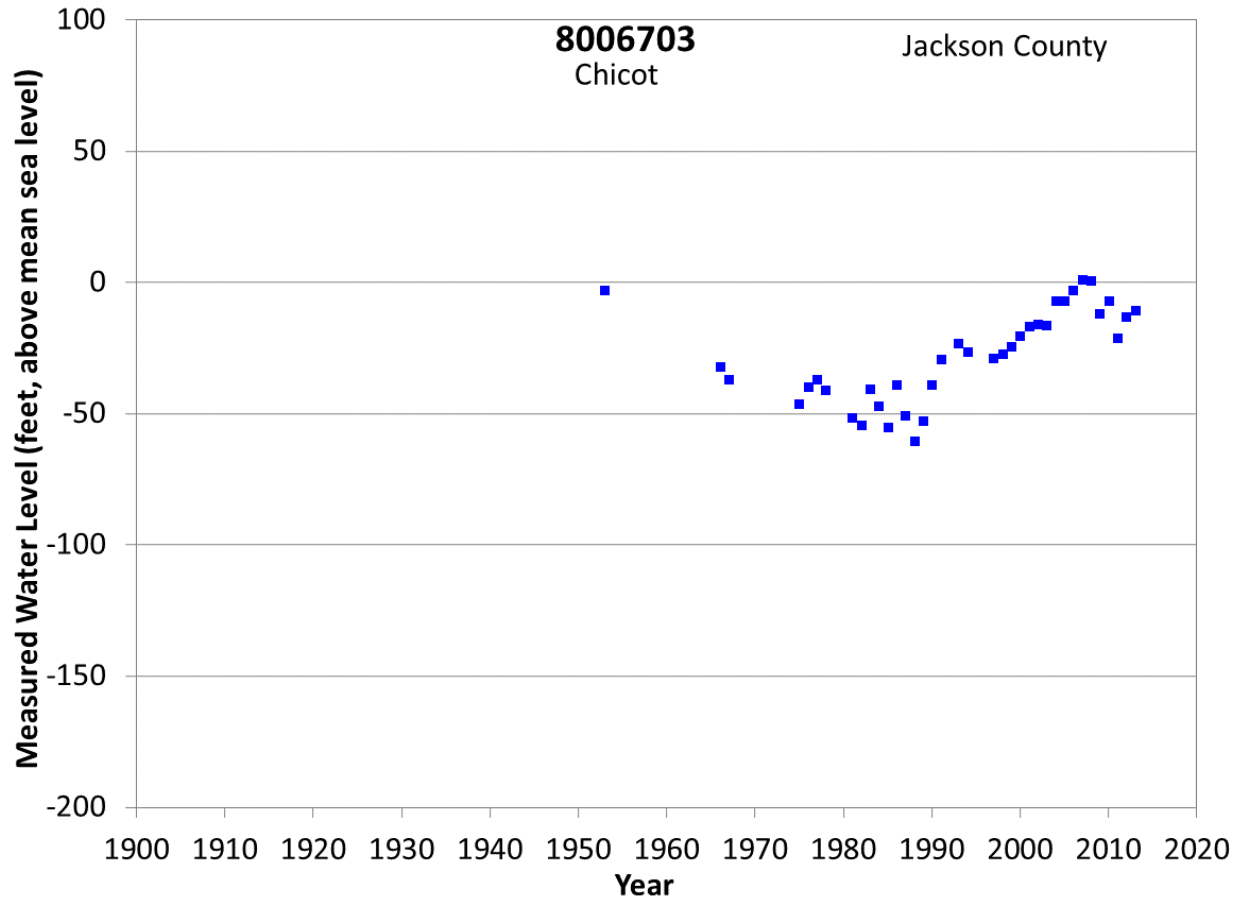


**Figure A18 Groundwater level hydrograph at State Well 8006703.**

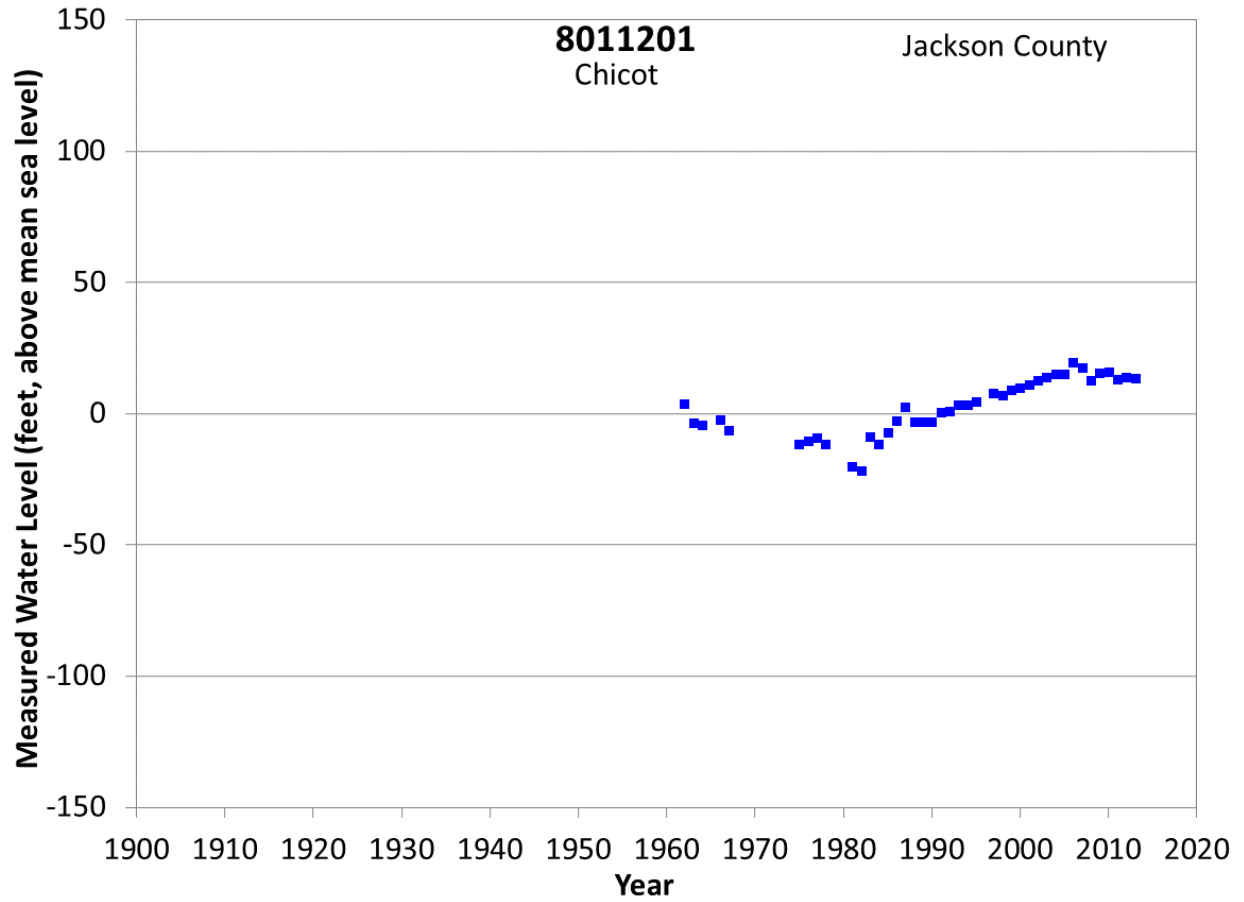


**Figure A19 Groundwater level hydrograph at State Well 8011201.**



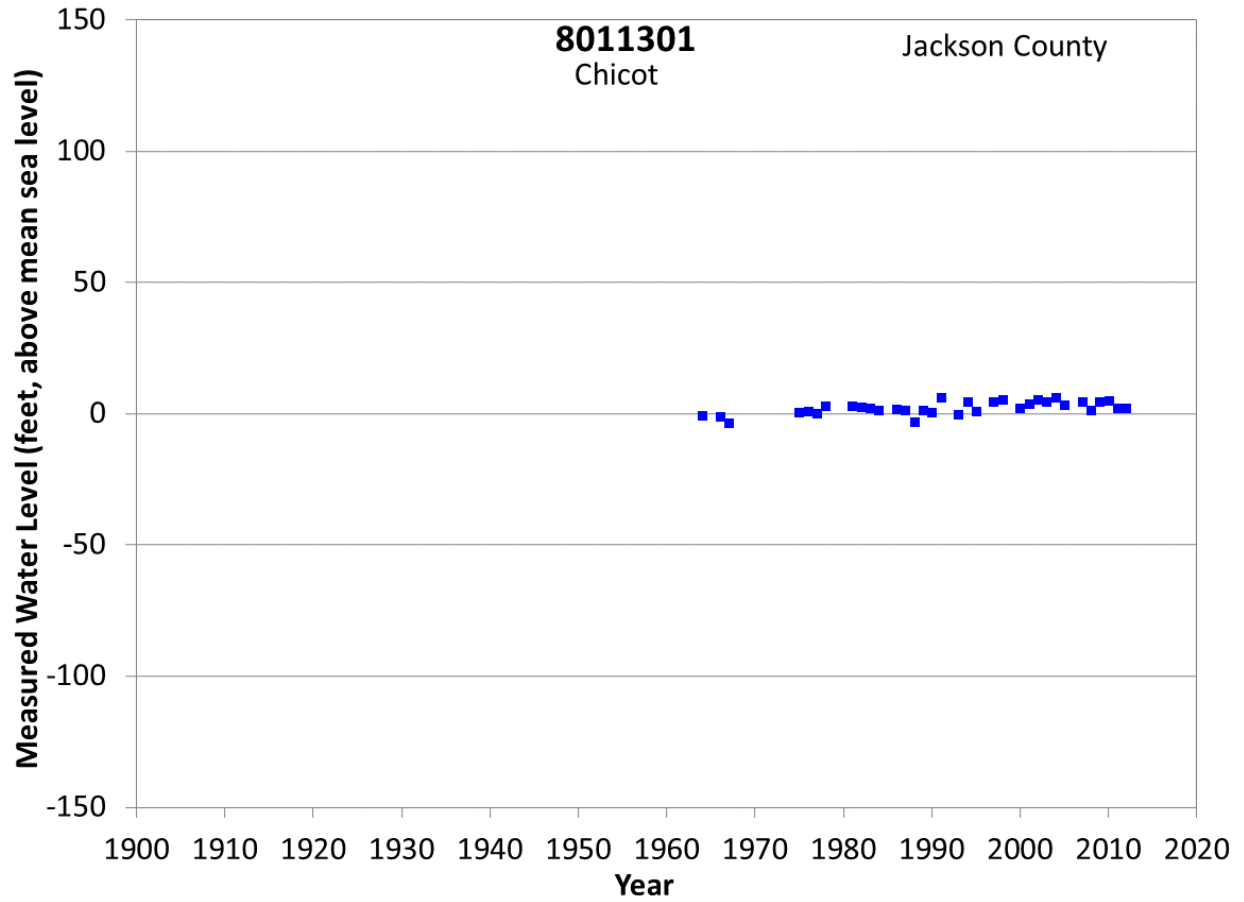


**Figure A20 Groundwater level hydrograph at State Well 8011301.**

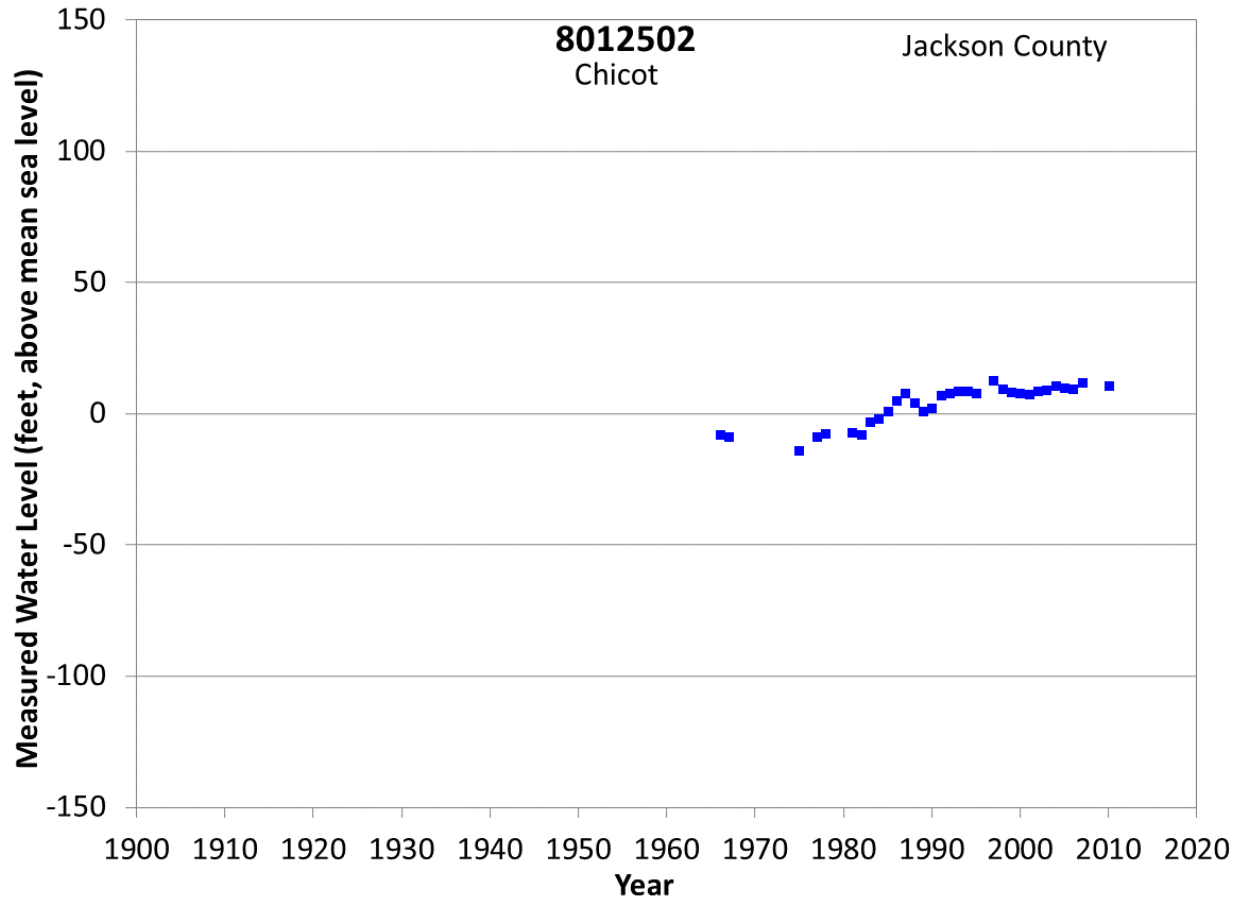


**Figure A21 Groundwater level hydrograph at State Well 8012502.**

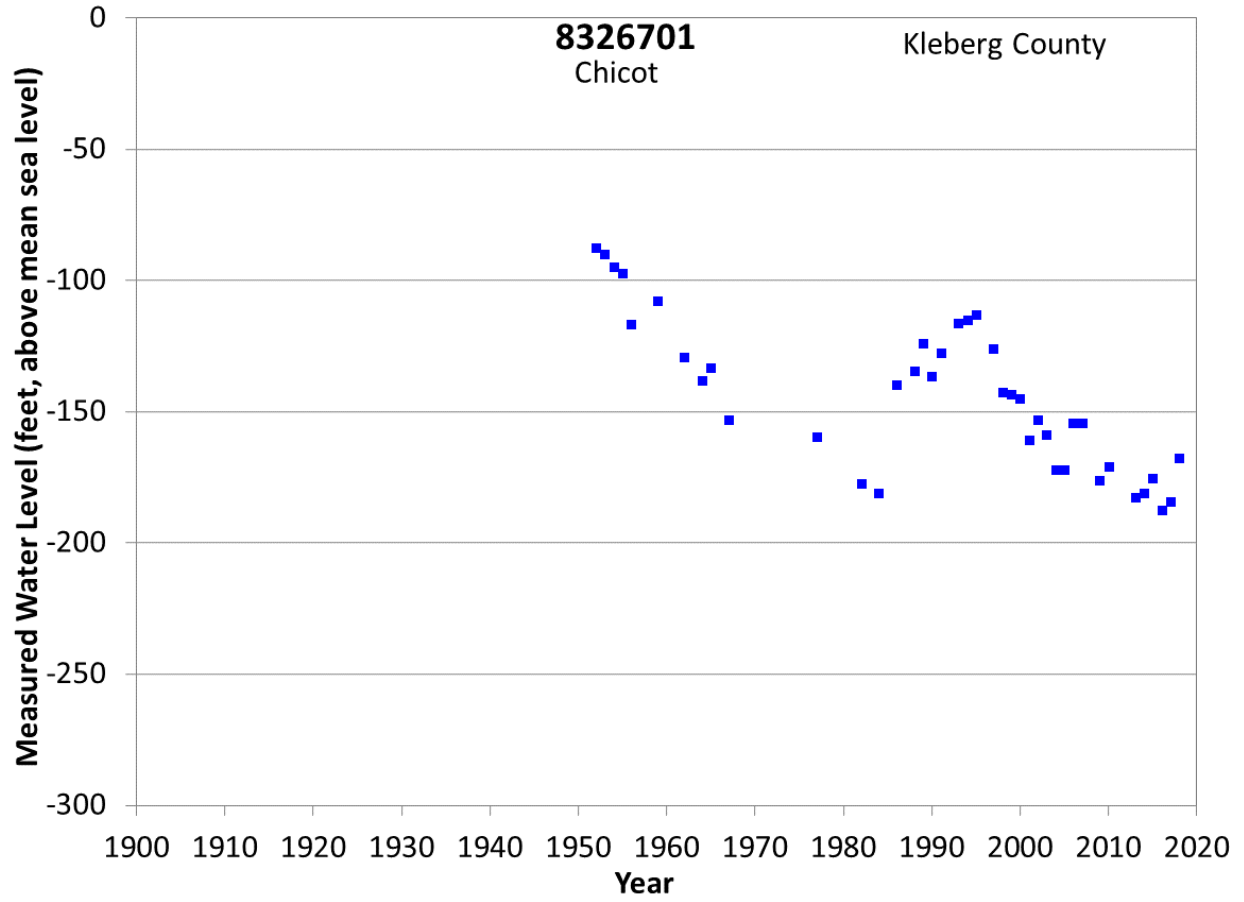


**Figure A22 Groundwater level hydrograph at State Well 8326701.**

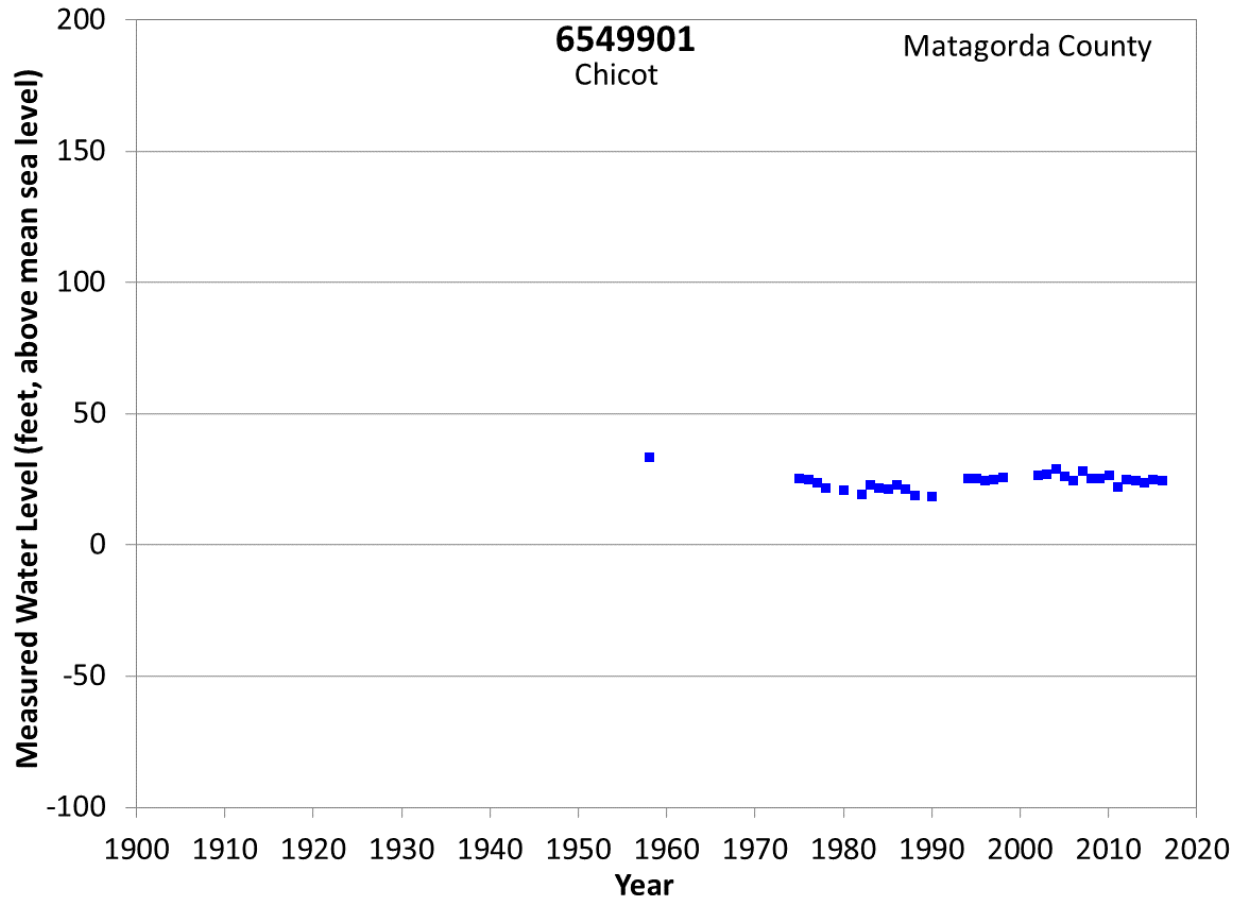


**Figure A23 Groundwater level hydrograph at State Well 6549901.**

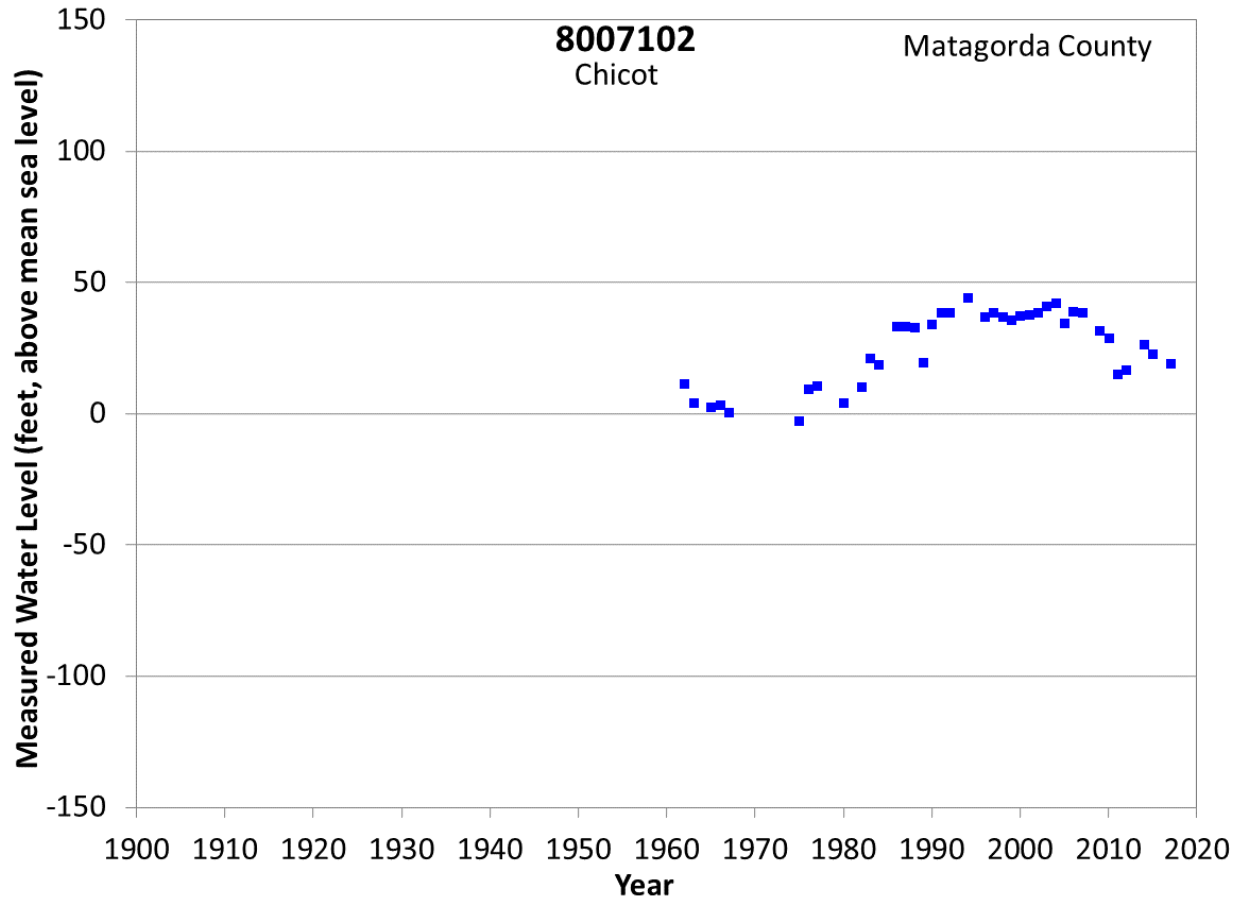


**Figure A24 Groundwater level hydrograph at State Well 8007102.**

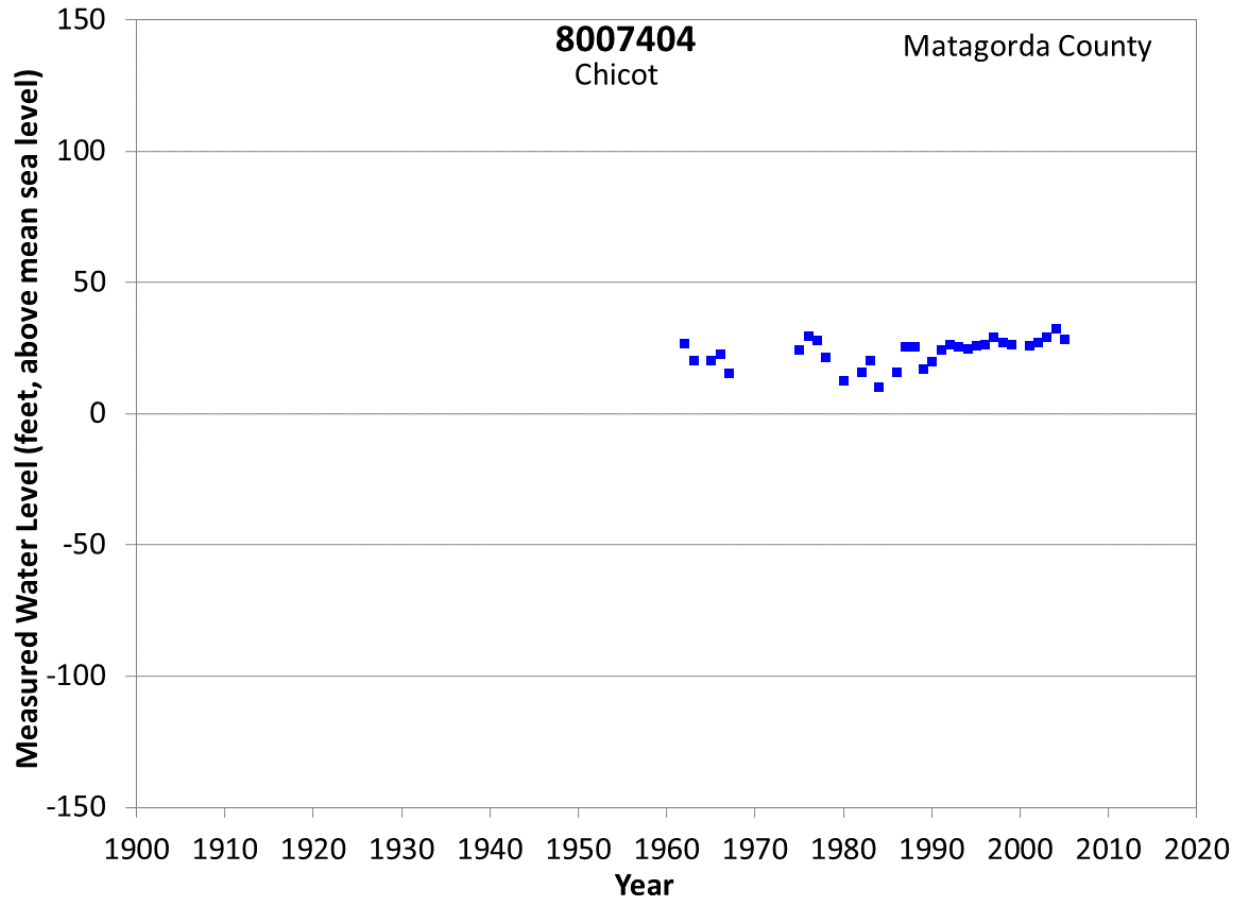


**Figure A25 Groundwater level hydrograph at State Well 8007404.**

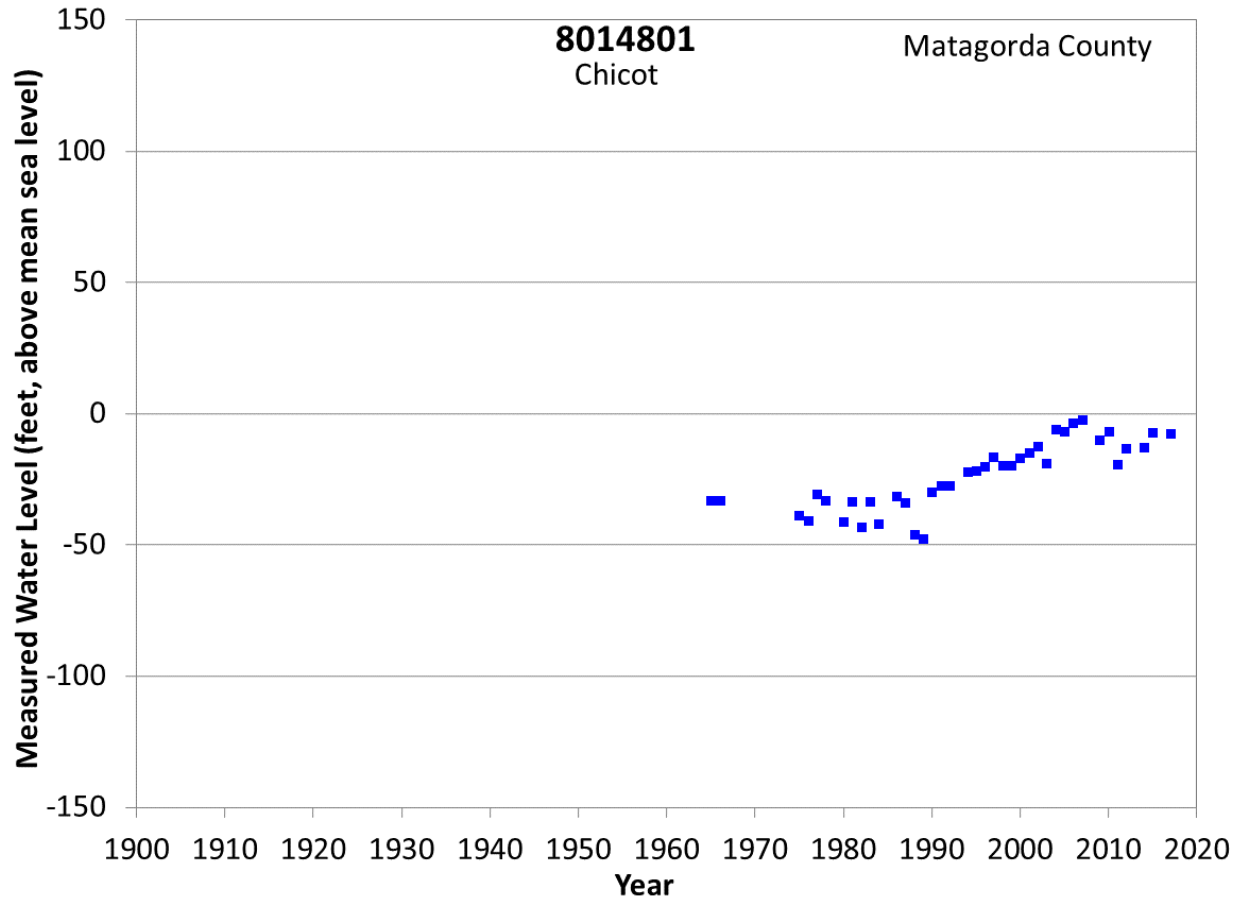


**Figure A26 Groundwater level hydrograph at State Well 8014801.**

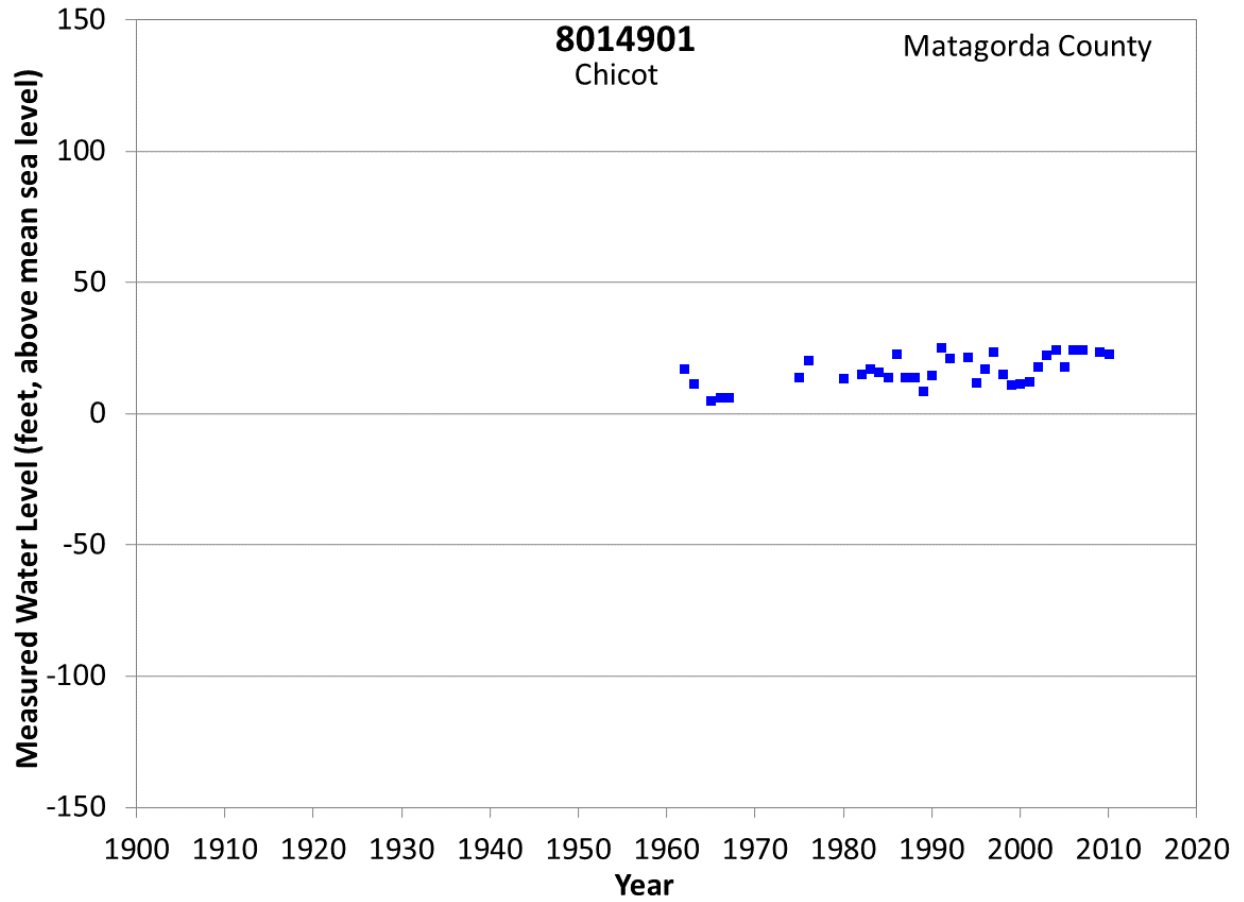


**Figure A27 Groundwater level hydrograph at State Well 8014901.**



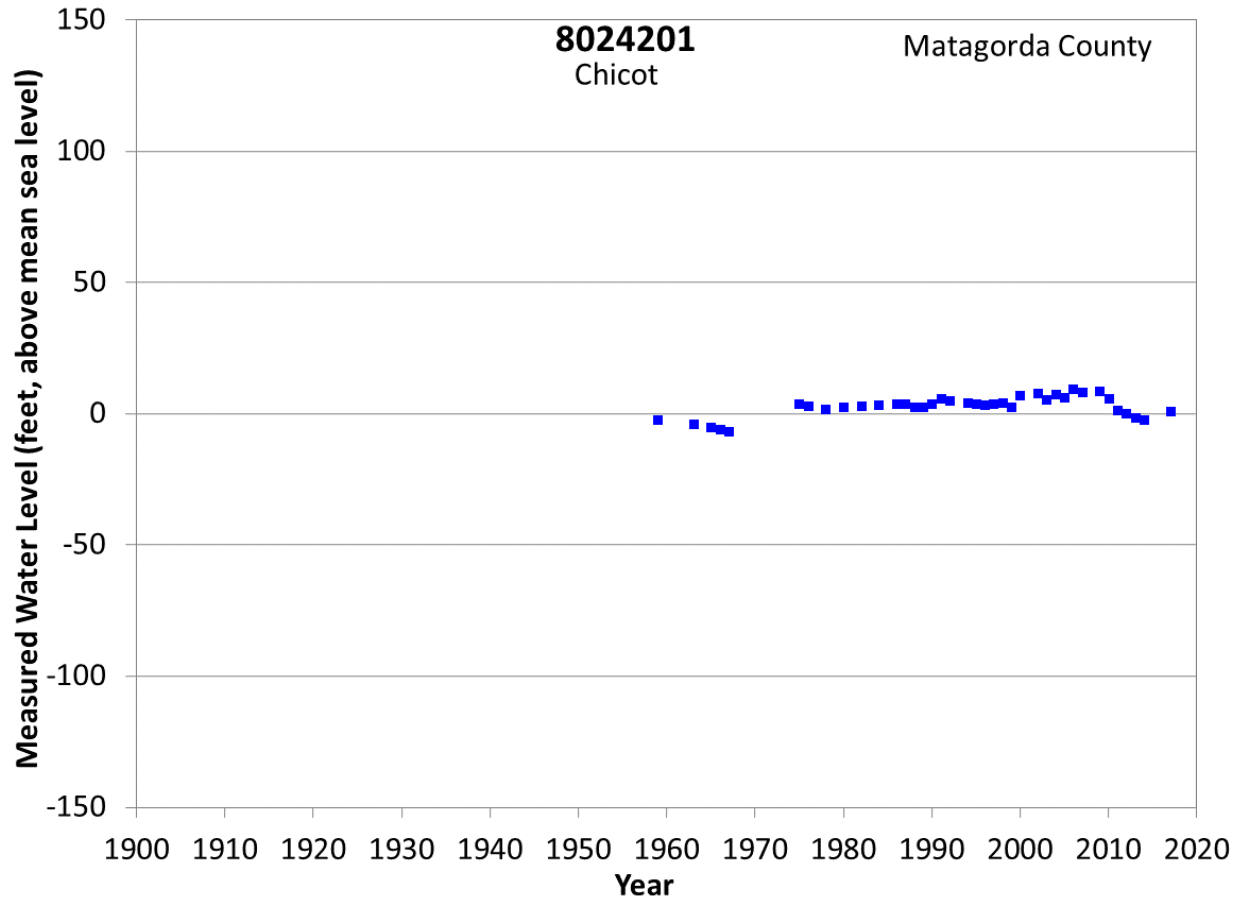


**Figure A28 Groundwater level hydrograph at State Well 8024201.**

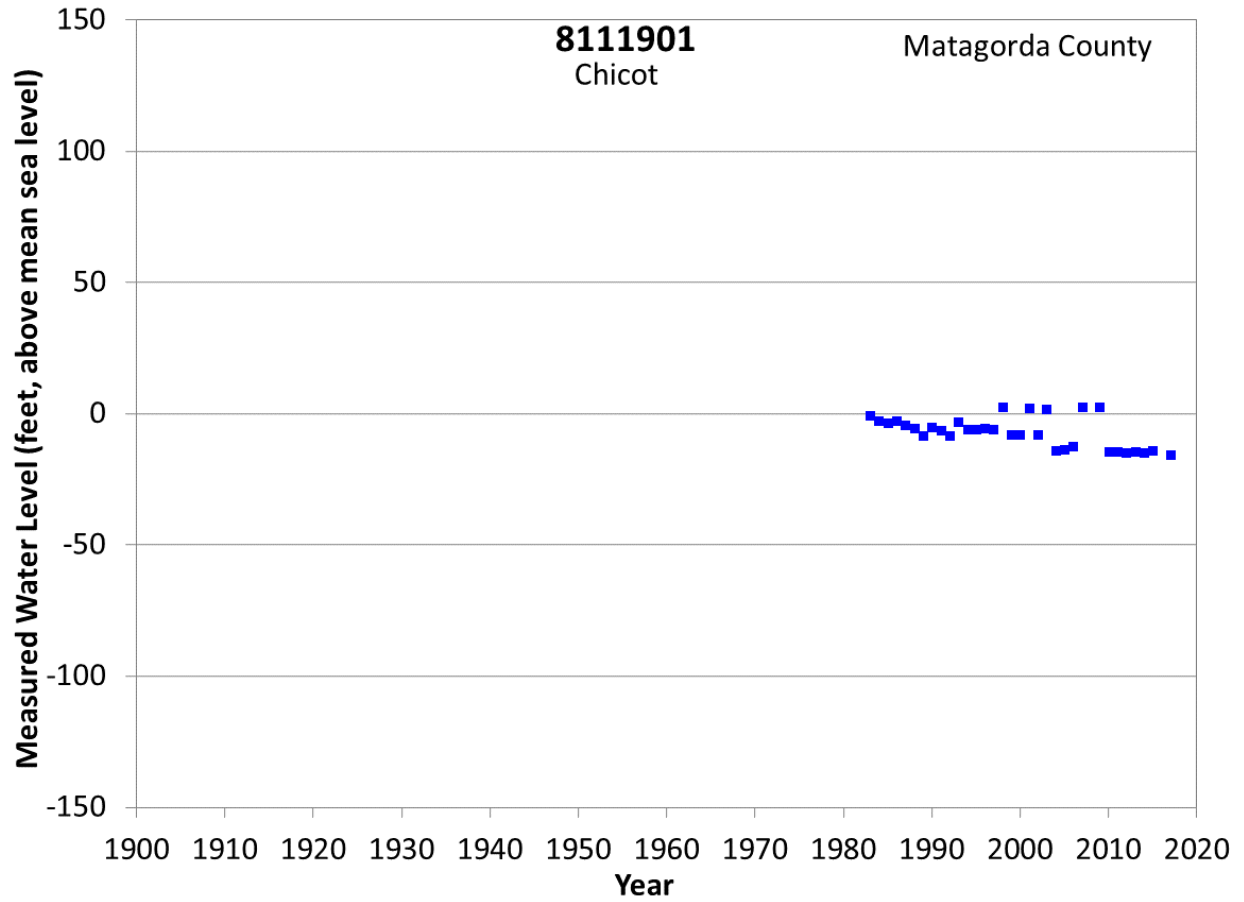


**Figure A29 Groundwater level hydrograph at State Well 8111901.**

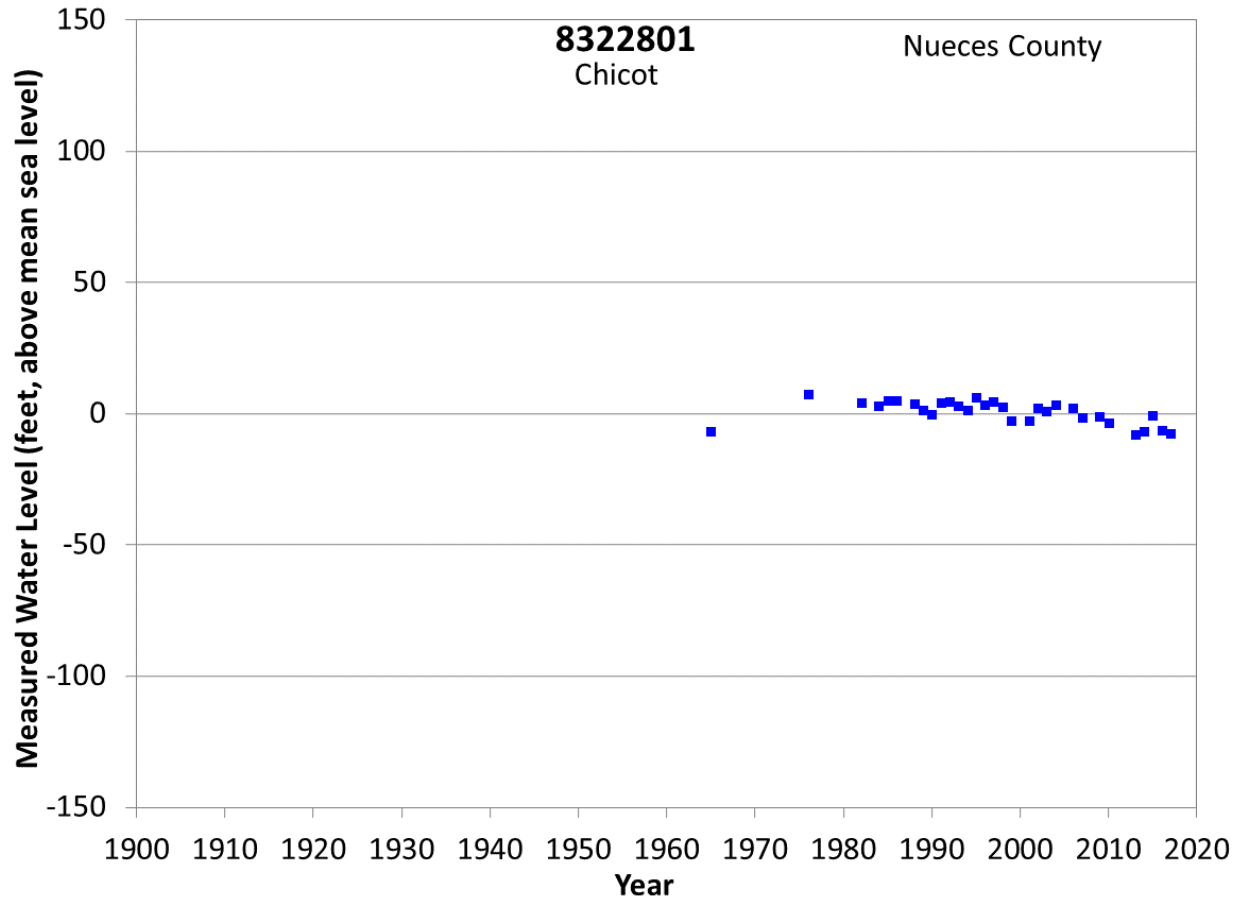


**Figure A30 Groundwater level hydrograph at State Well 8322801.**

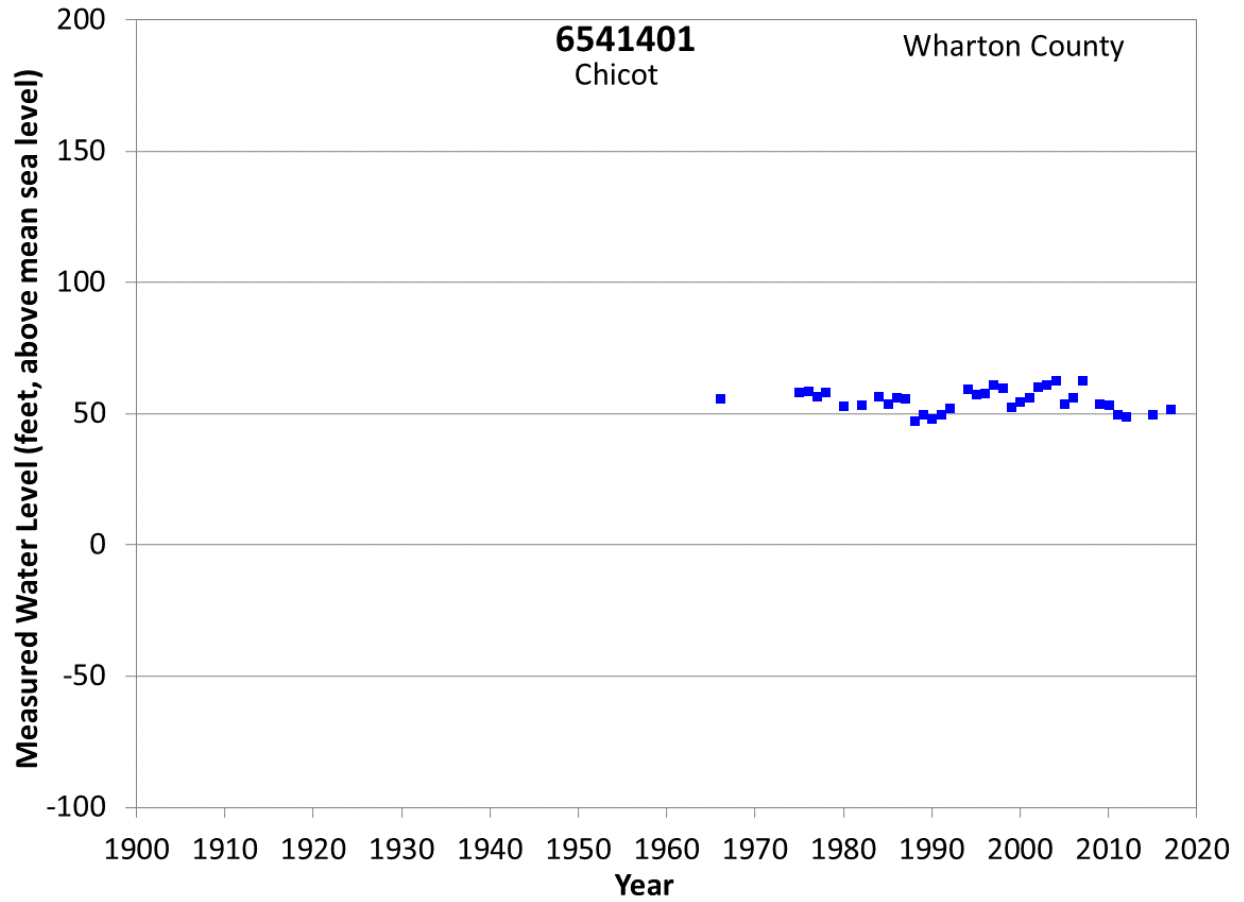


**Figure A31 Groundwater level hydrograph at State Well 6541401.**

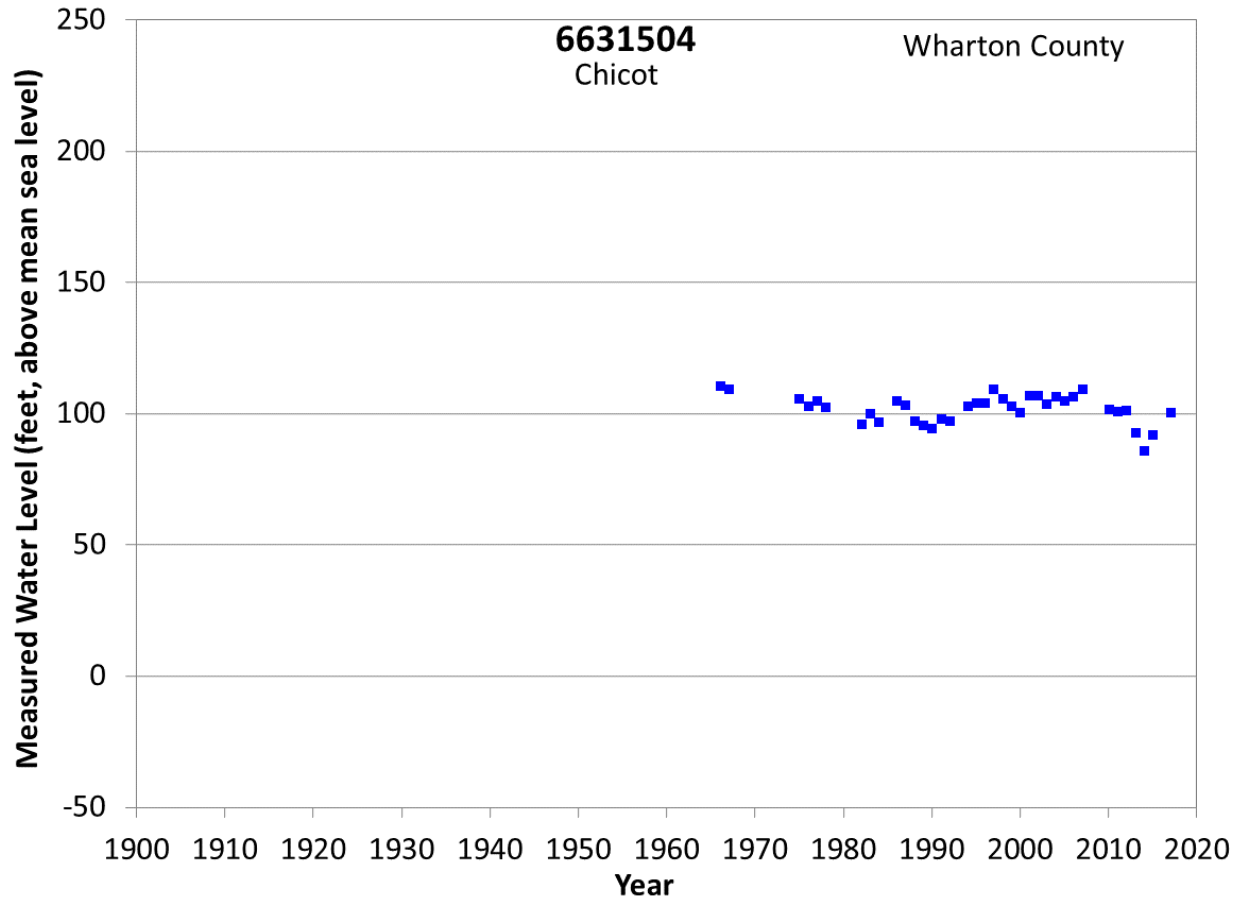


**Figure A32 Groundwater level hydrograph at State Well 6631504.**

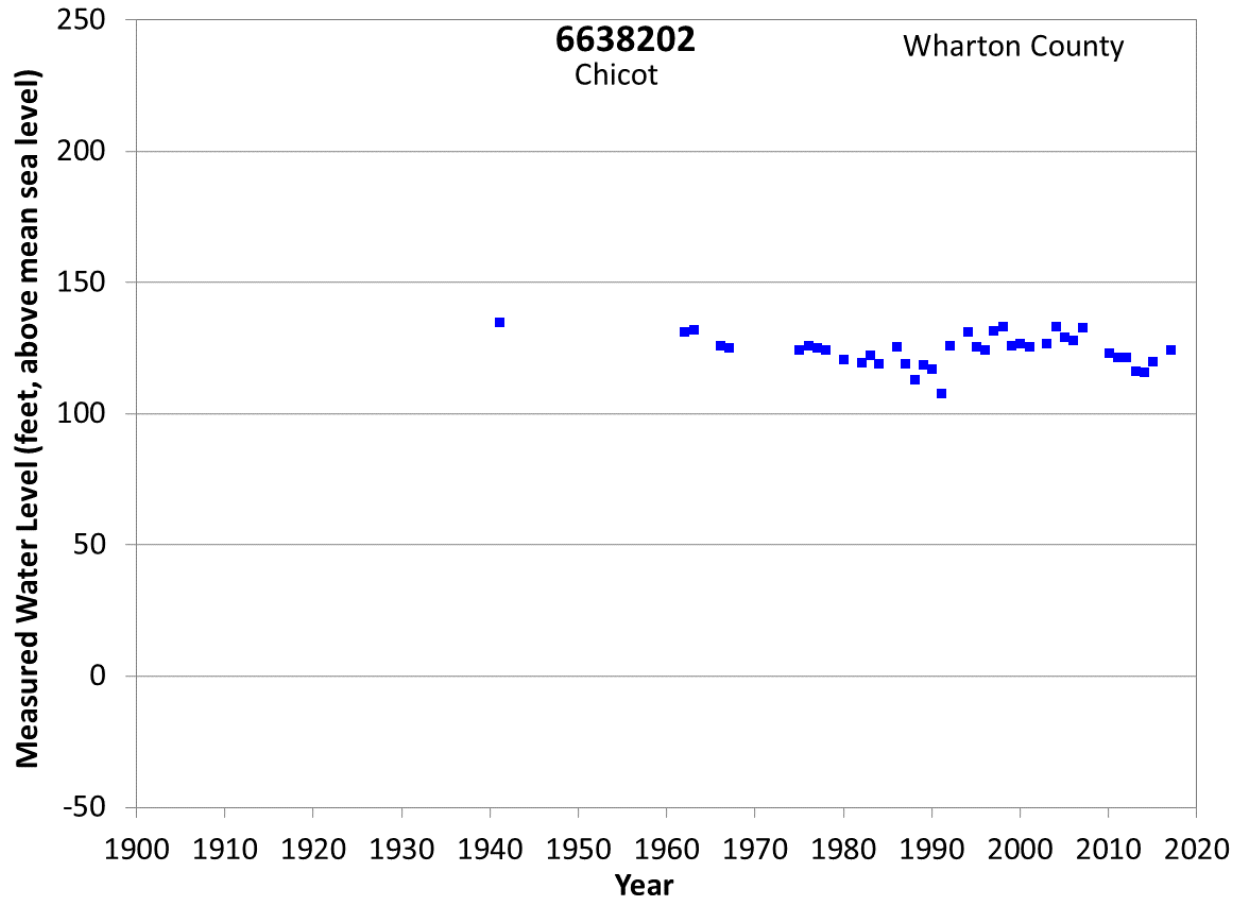


**Figure A33 Groundwater level hydrograph at State Well 6638202.**

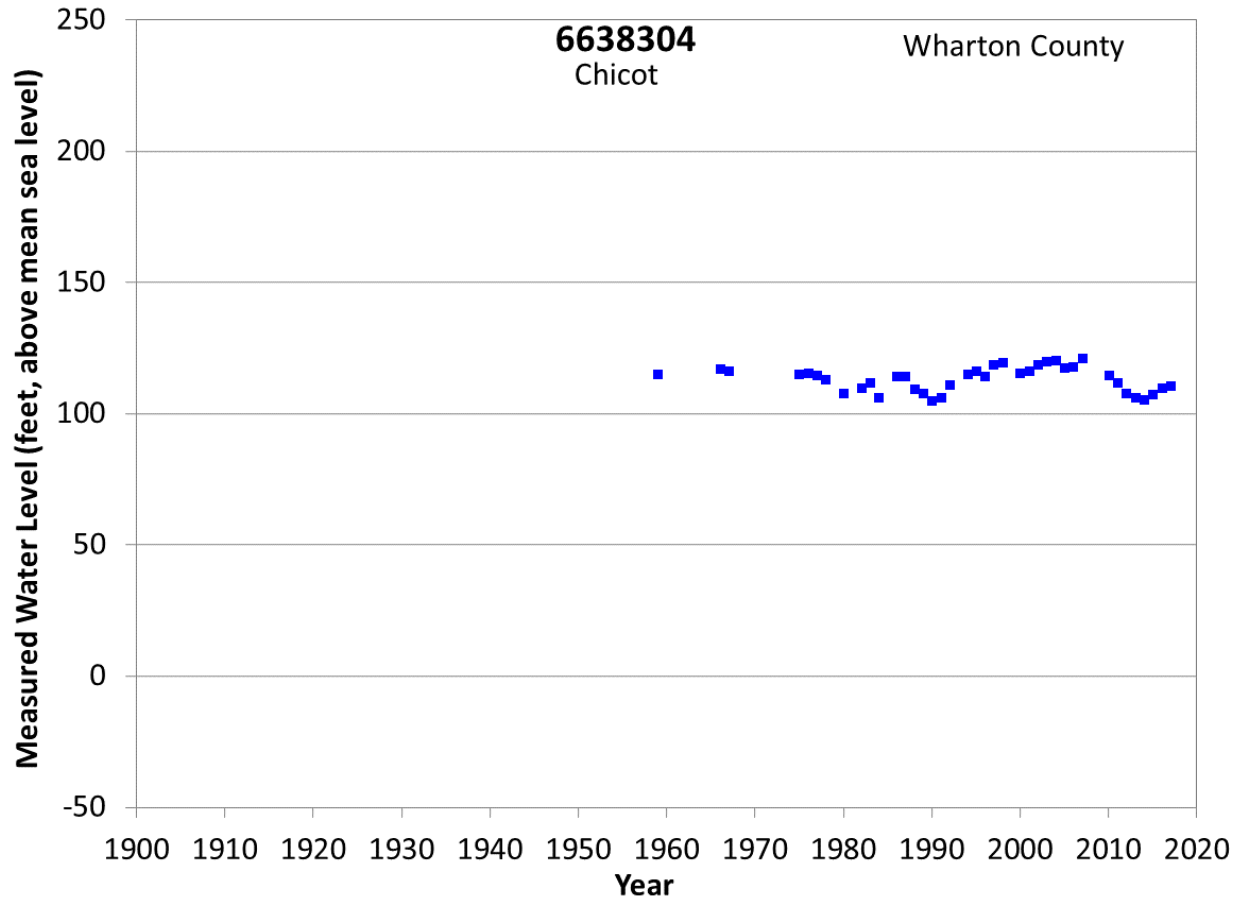


**Figure A34 Groundwater level hydrograph at State Well 6638304.**

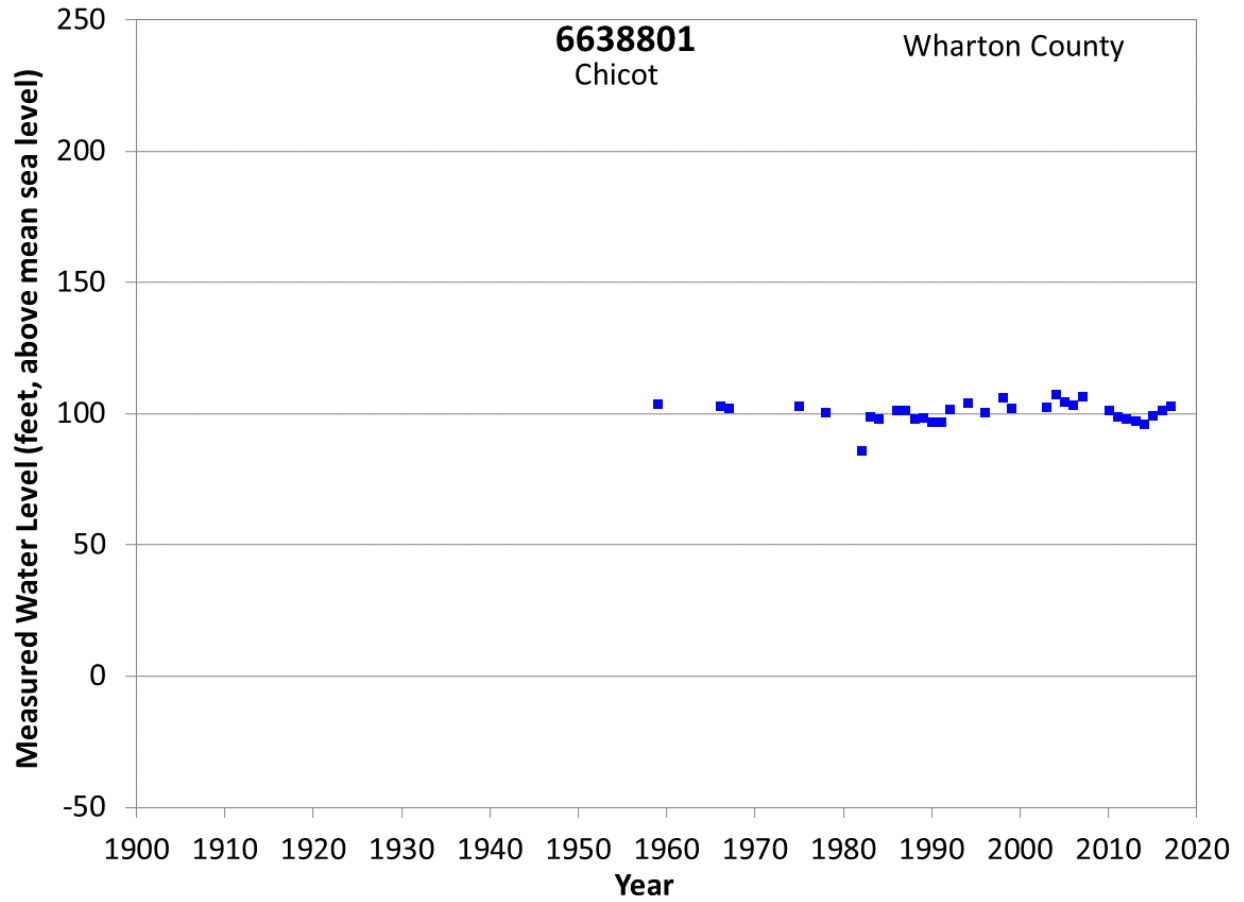


**Figure A35 Groundwater level hydrograph at State Well 6638801.**



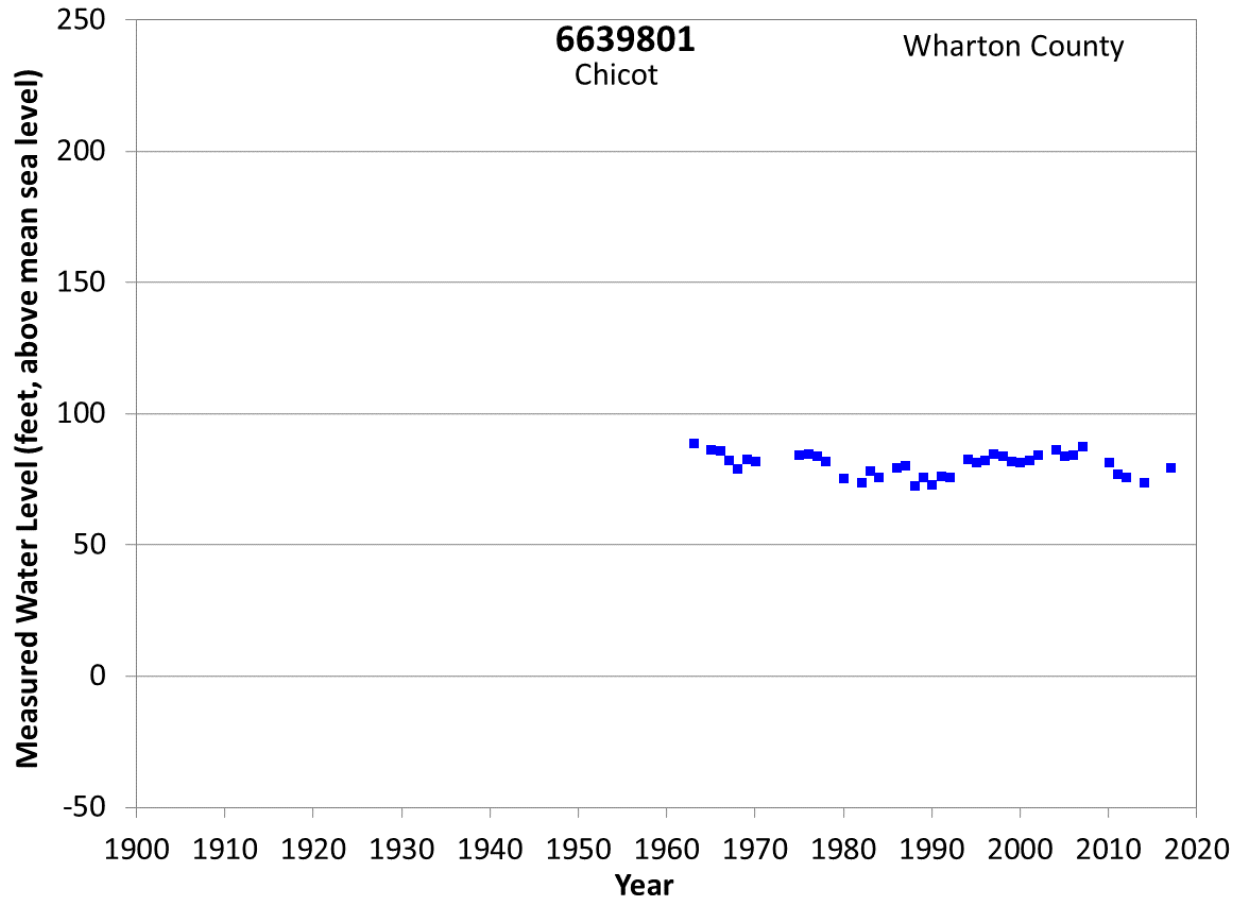


**Figure A36 Groundwater level hydrograph at State Well 6639801.**

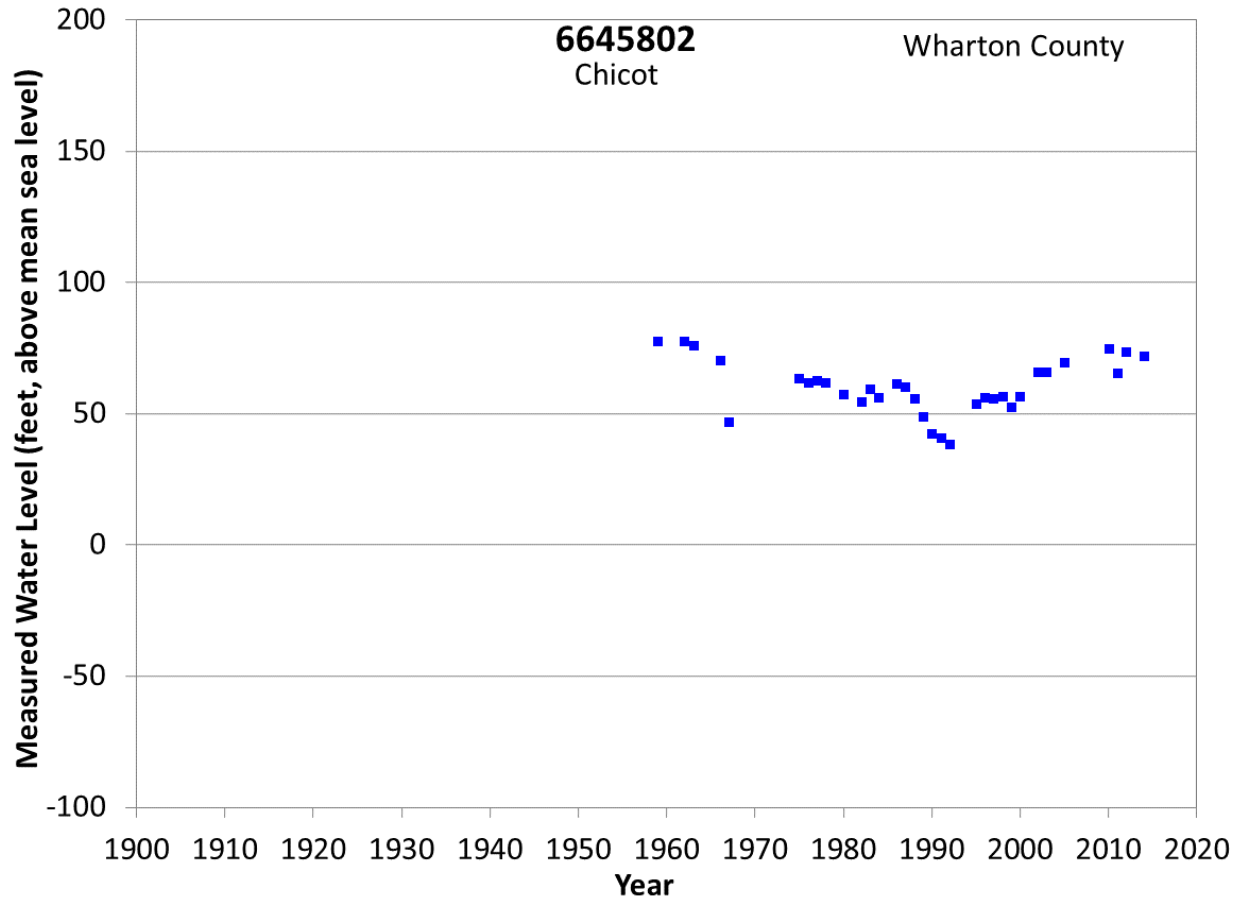


**Figure A37 Groundwater level hydrograph at State Well 6645802.**

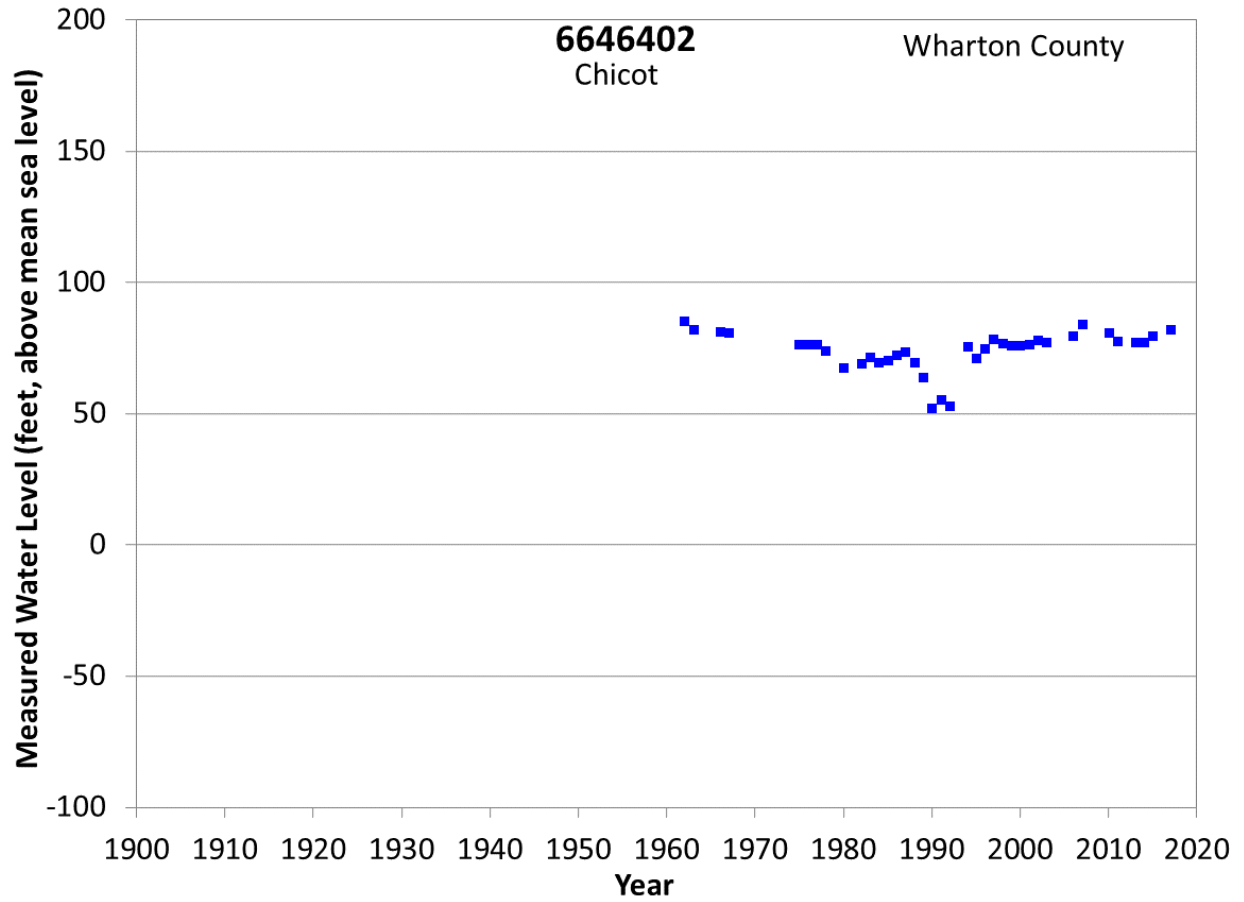


**Figure A38 Groundwater level hydrograph at State Well 6646402.**

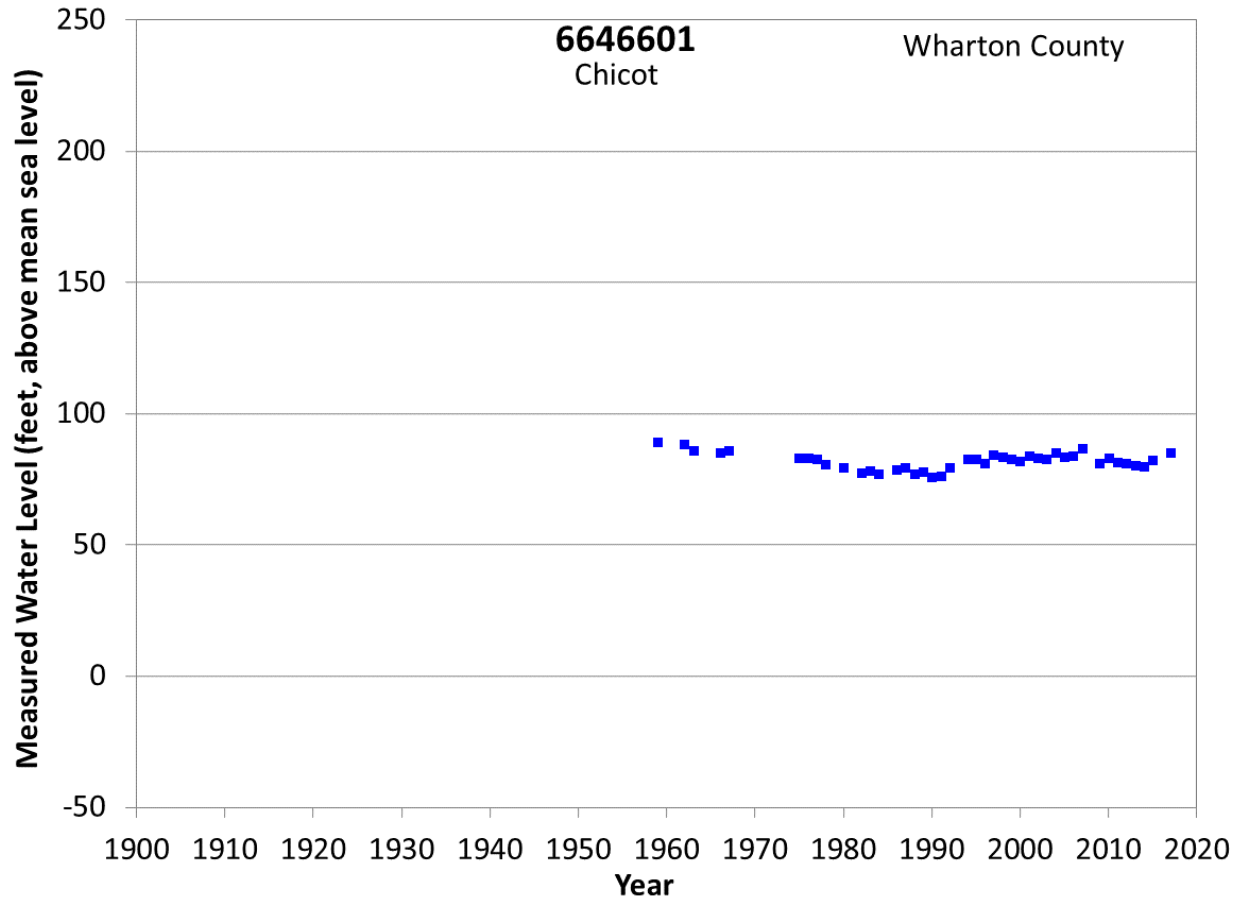


**Figure A39 Groundwater level hydrograph at State Well 6646601.**

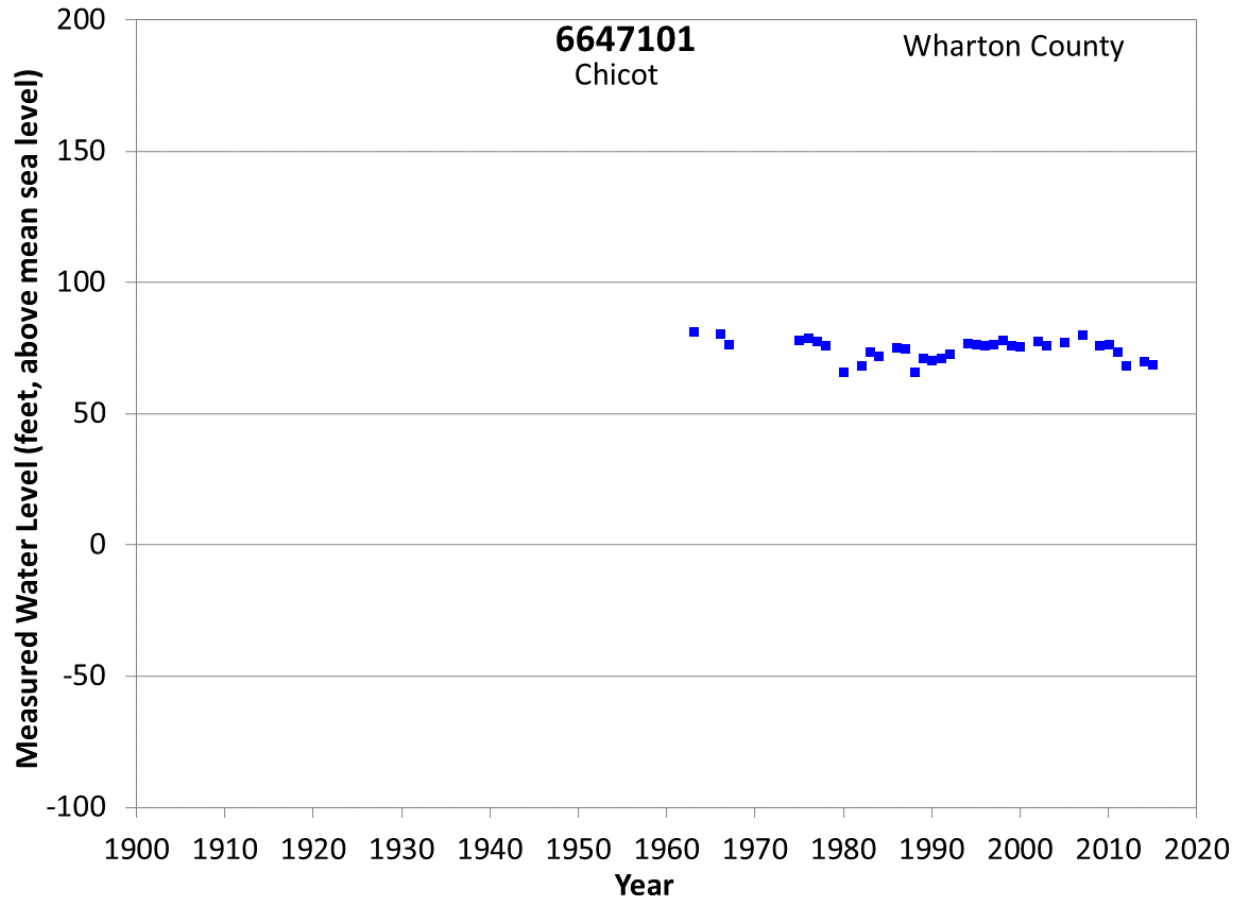


**Figure A40 Groundwater level hydrograph at State Well 6647101.**

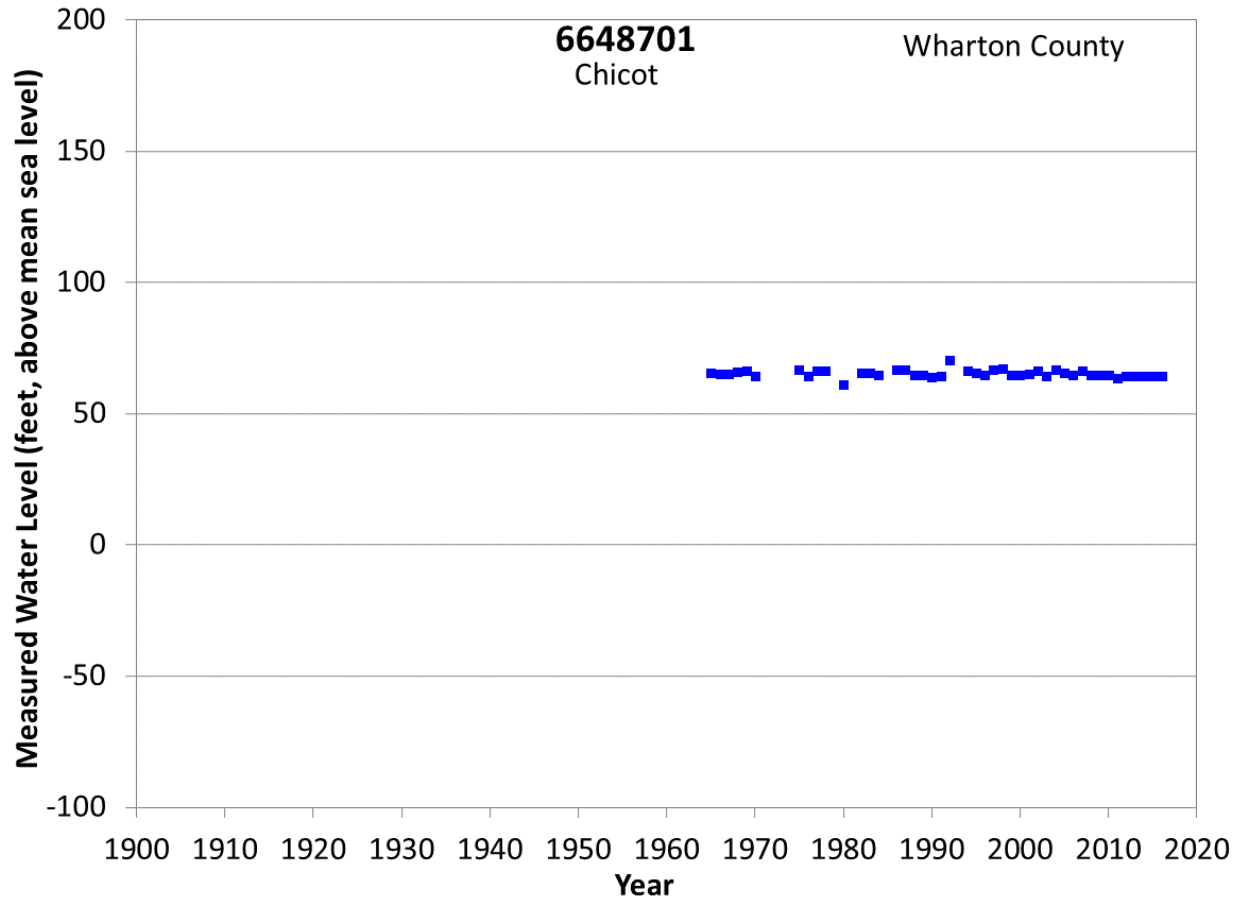


**Figure A41 Groundwater level hydrograph at State Well 6648701.**

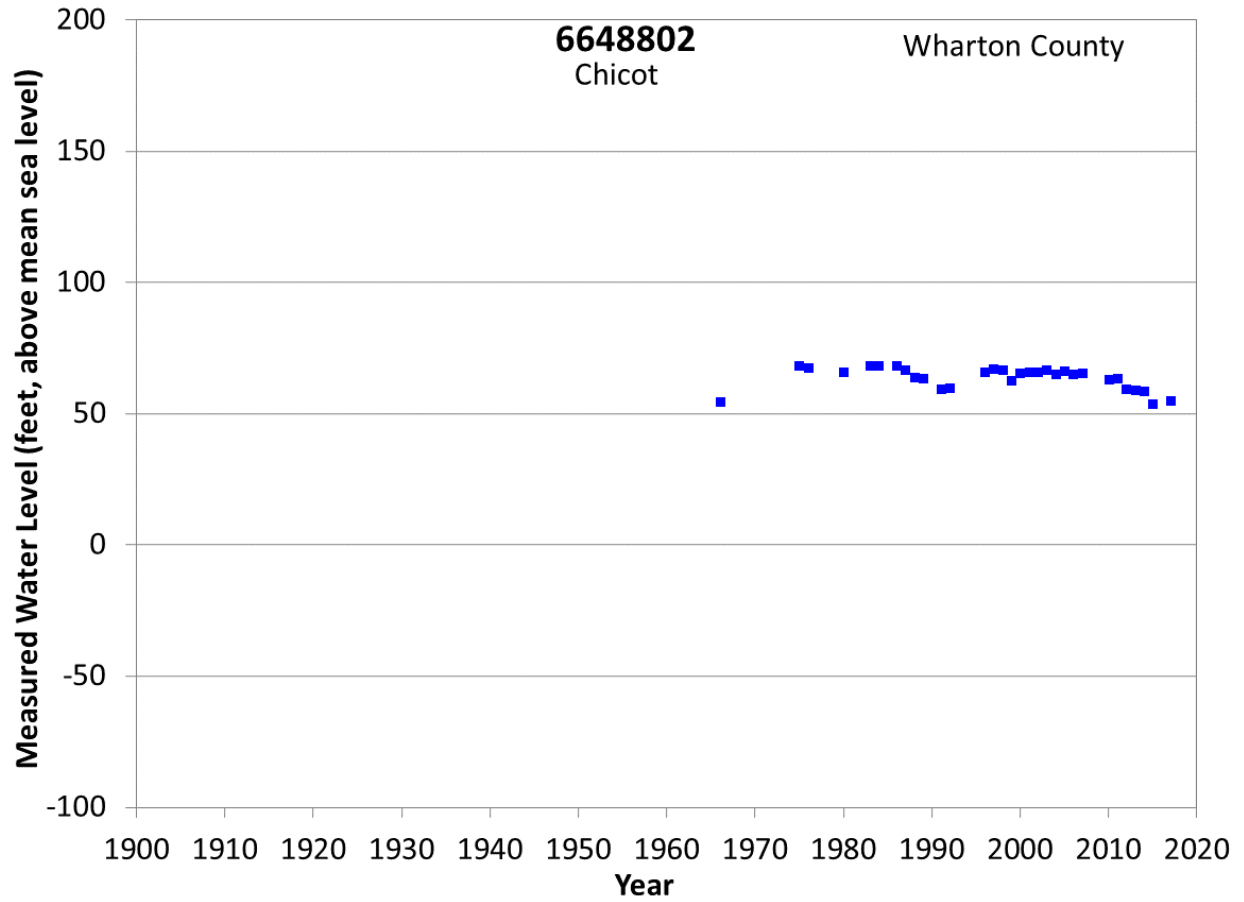


**Figure A42 Groundwater level hydrograph at State Well 6648802.**

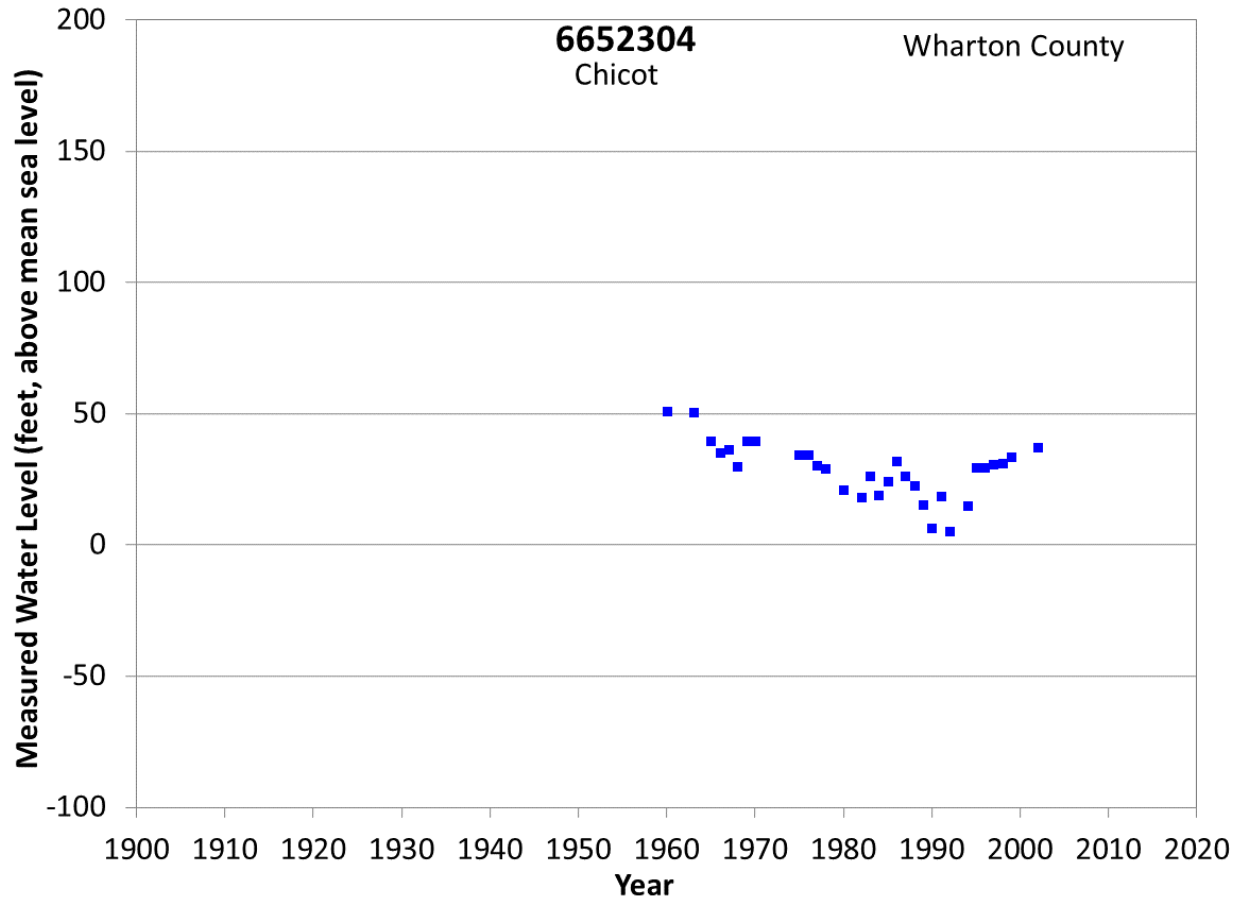


**Figure A43 Groundwater level hydrograph at State Well 6652304.**



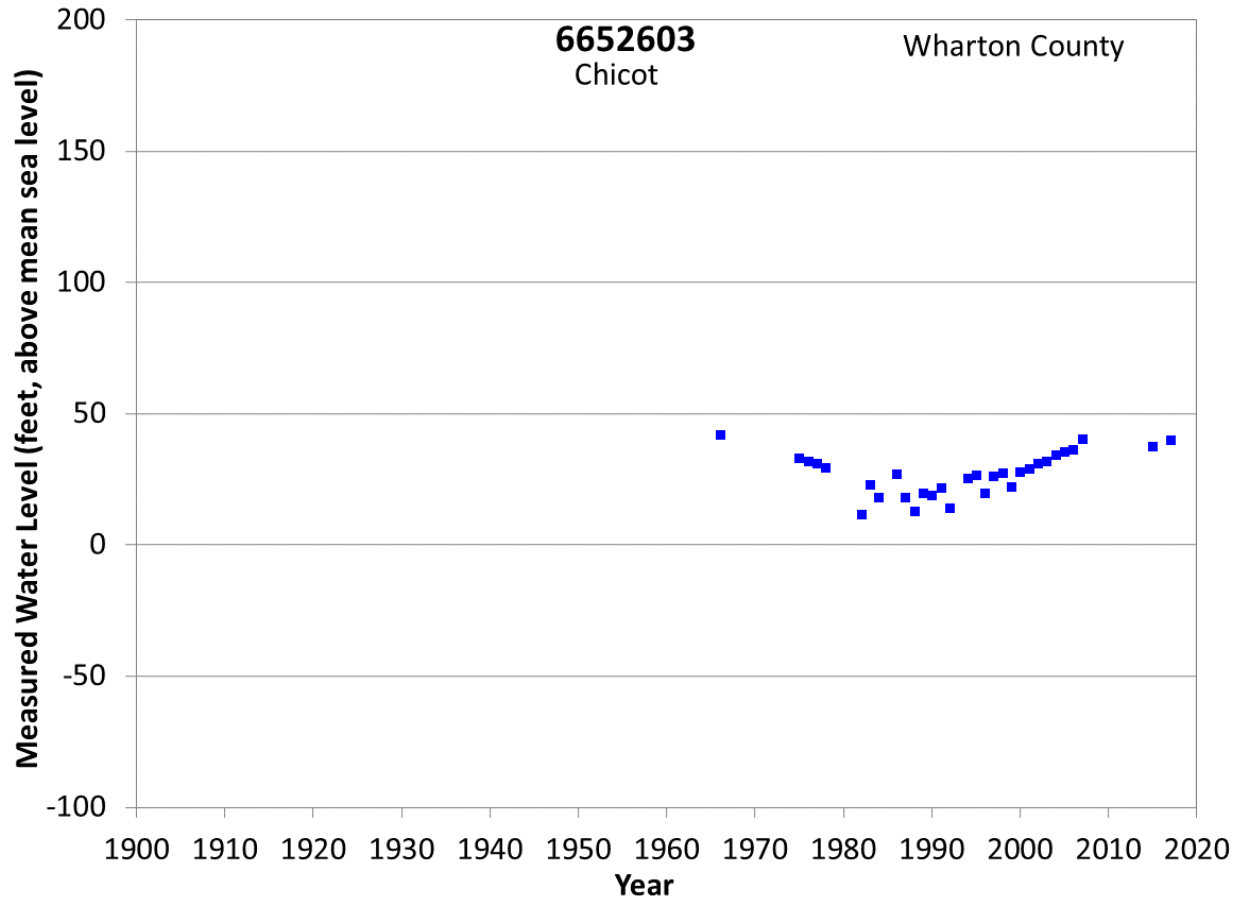


**Figure A44 Groundwater level hydrograph at State Well 6652603.**

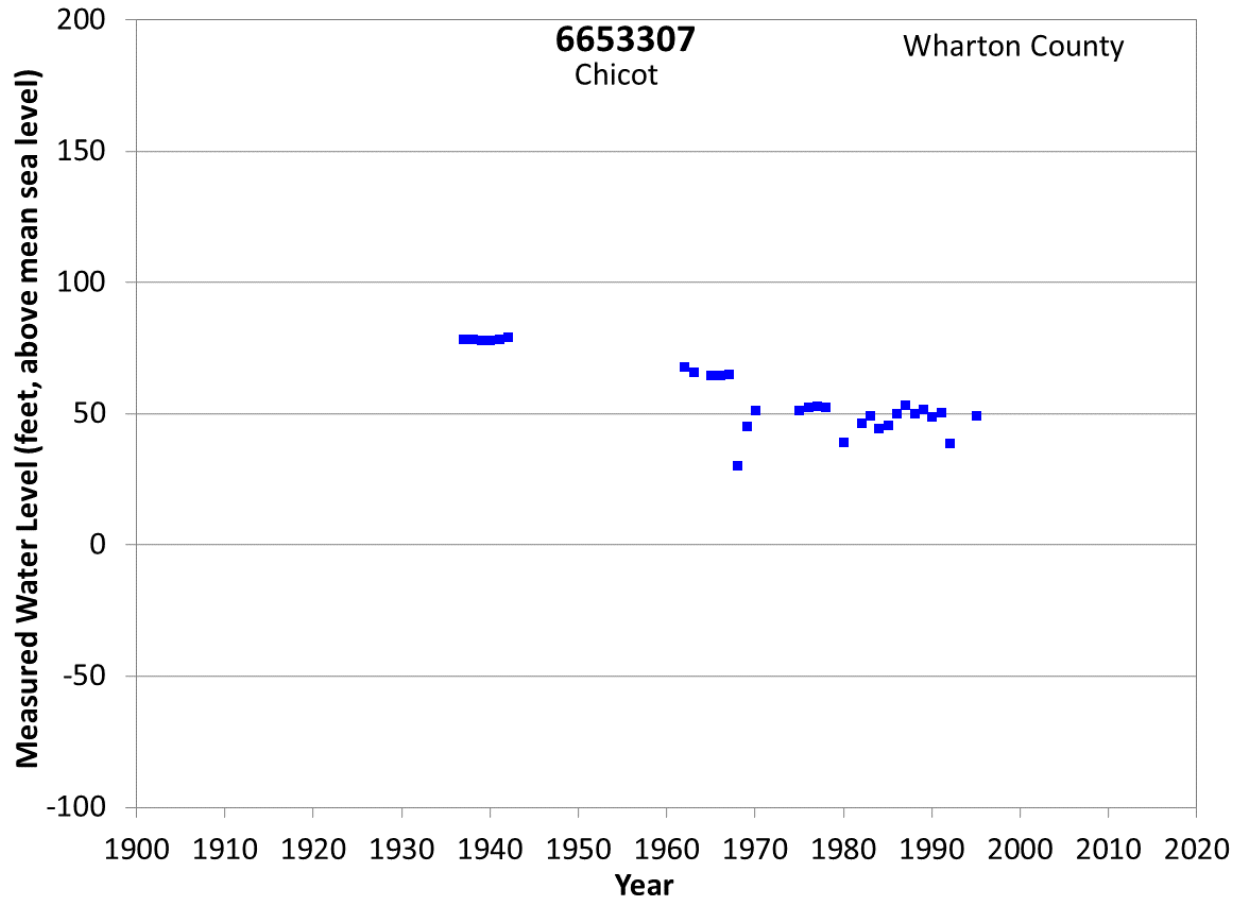


**Figure A45 Groundwater level hydrograph at State Well 6653307.**

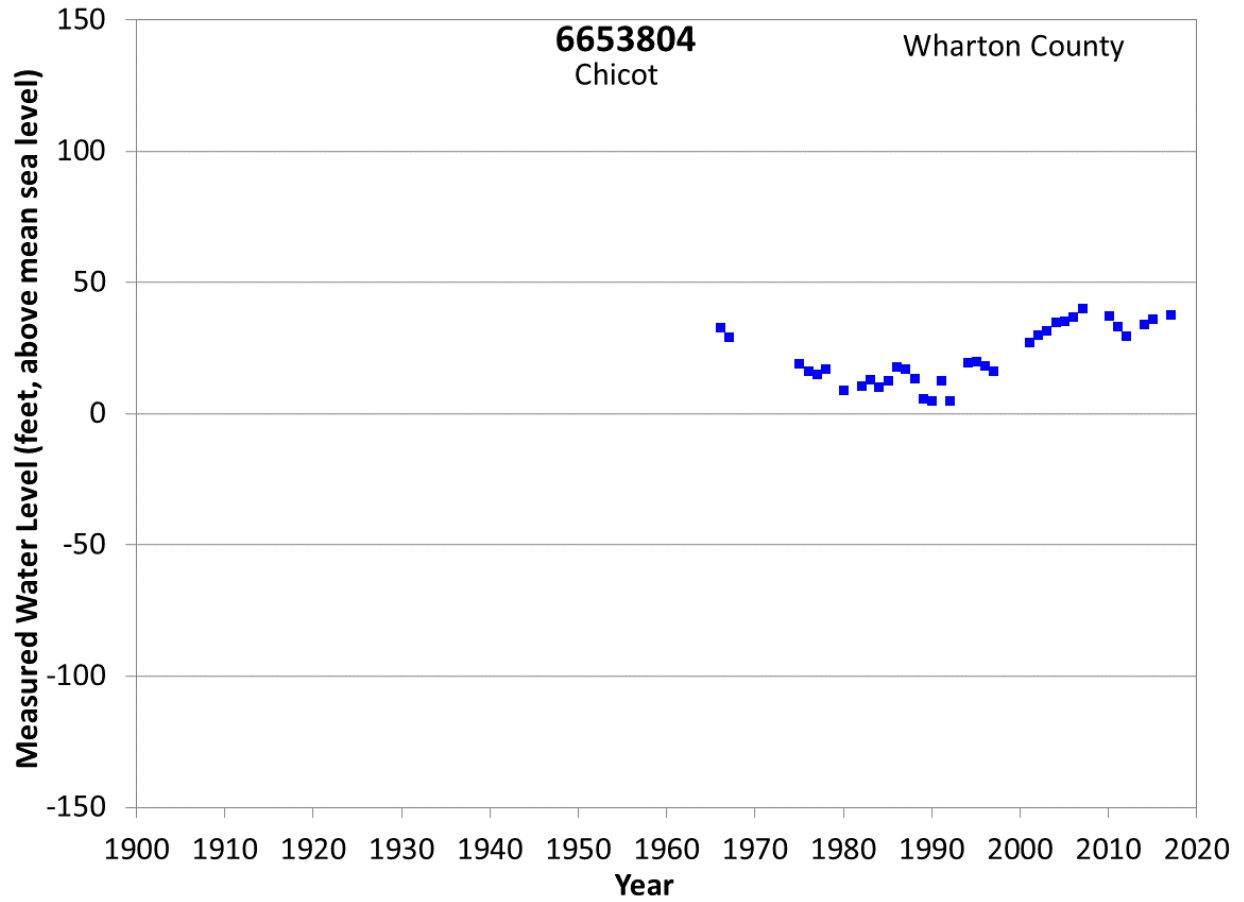


**Figure A46 Groundwater level hydrograph at State Well 6653804.**

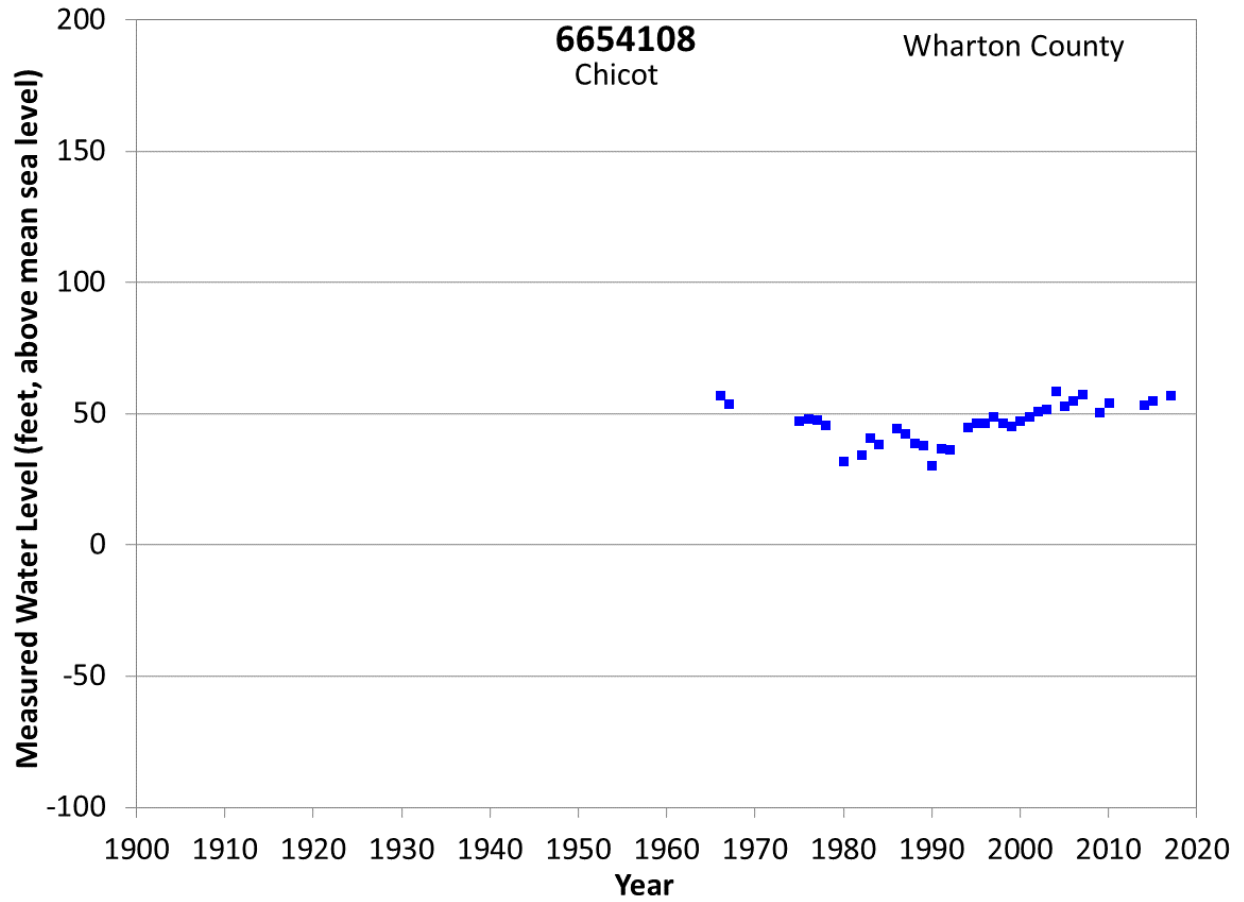


**Figure A47 Groundwater level hydrograph at State Well 6654108.**

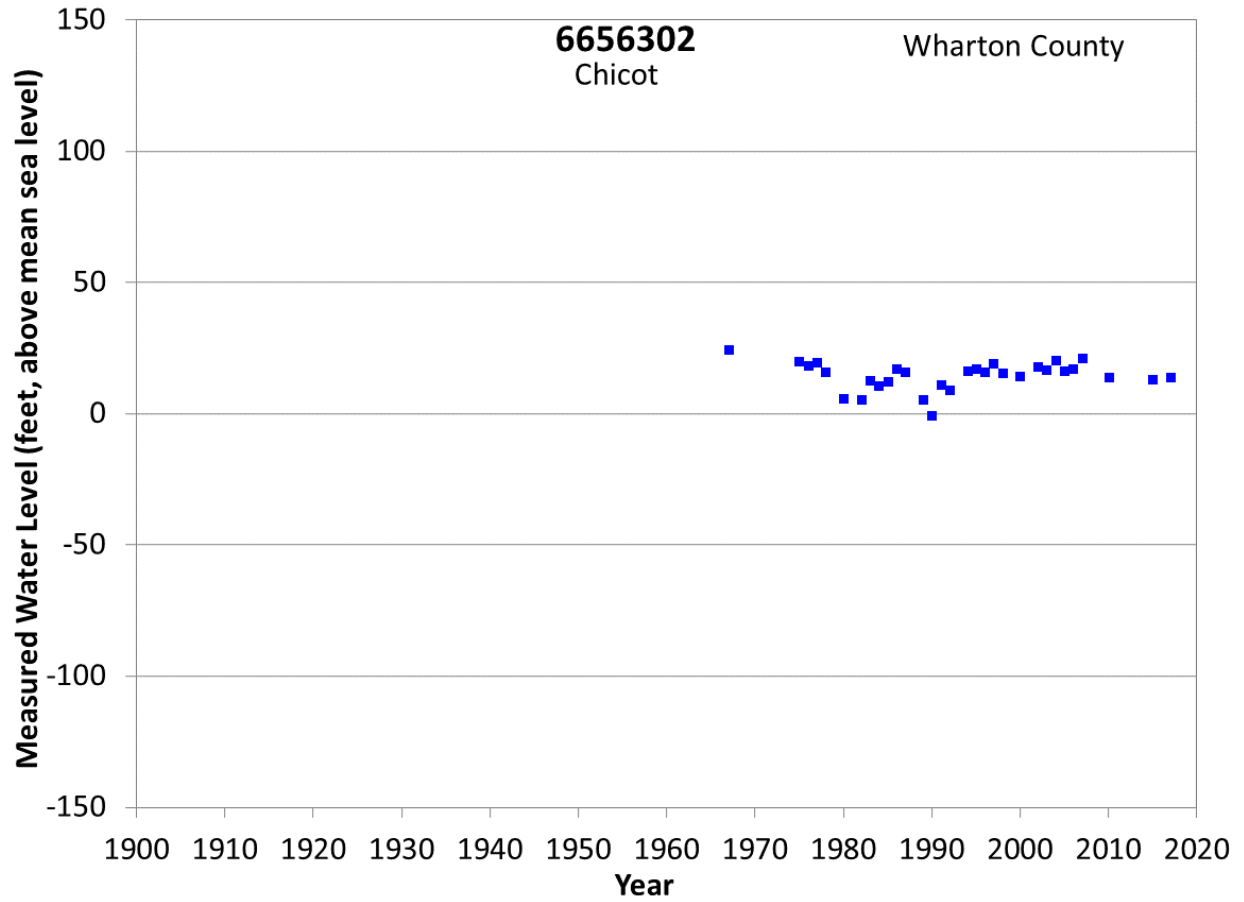


**Figure A48 Groundwater level hydrograph at State Well 6656302.**

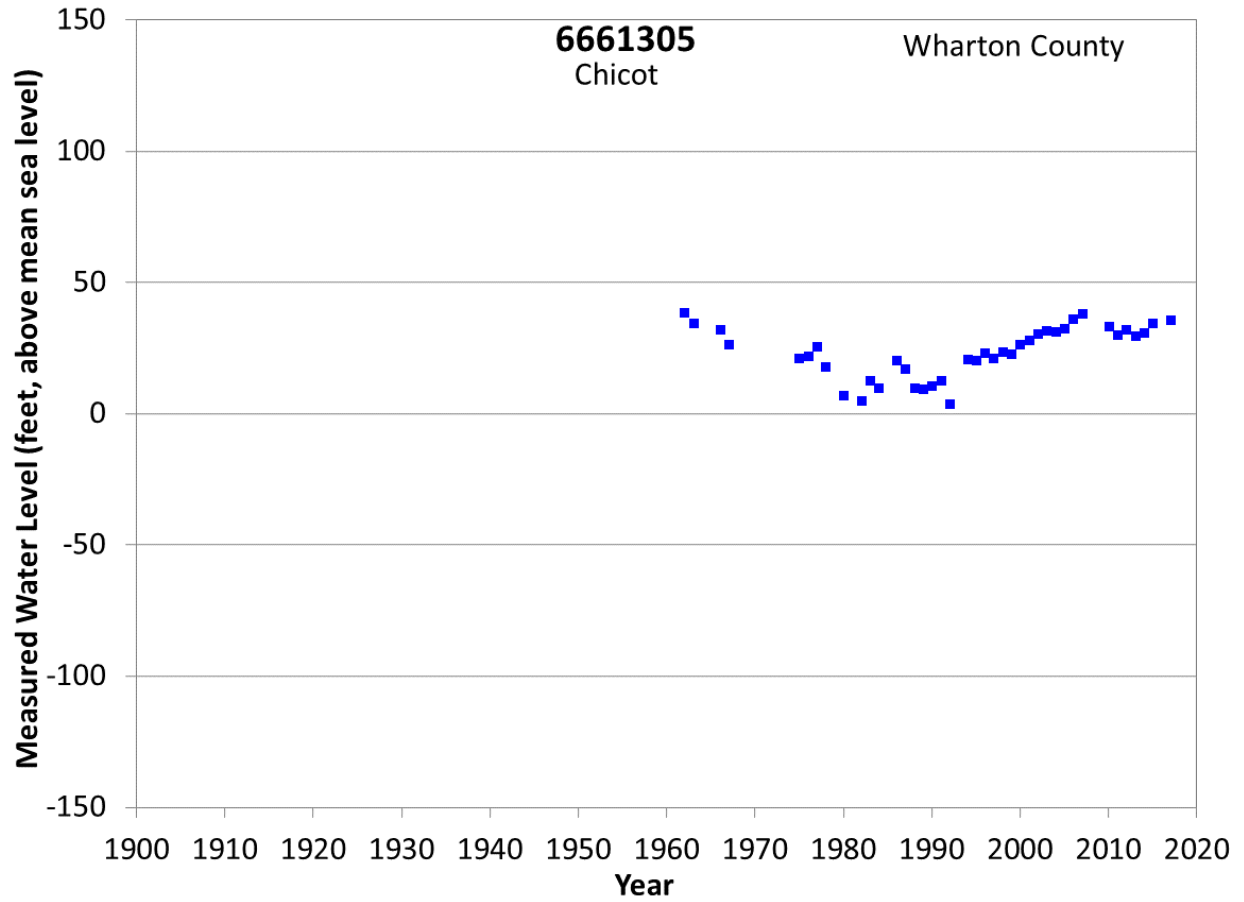


**Figure A49 Groundwater level hydrograph at State Well 6661305.**

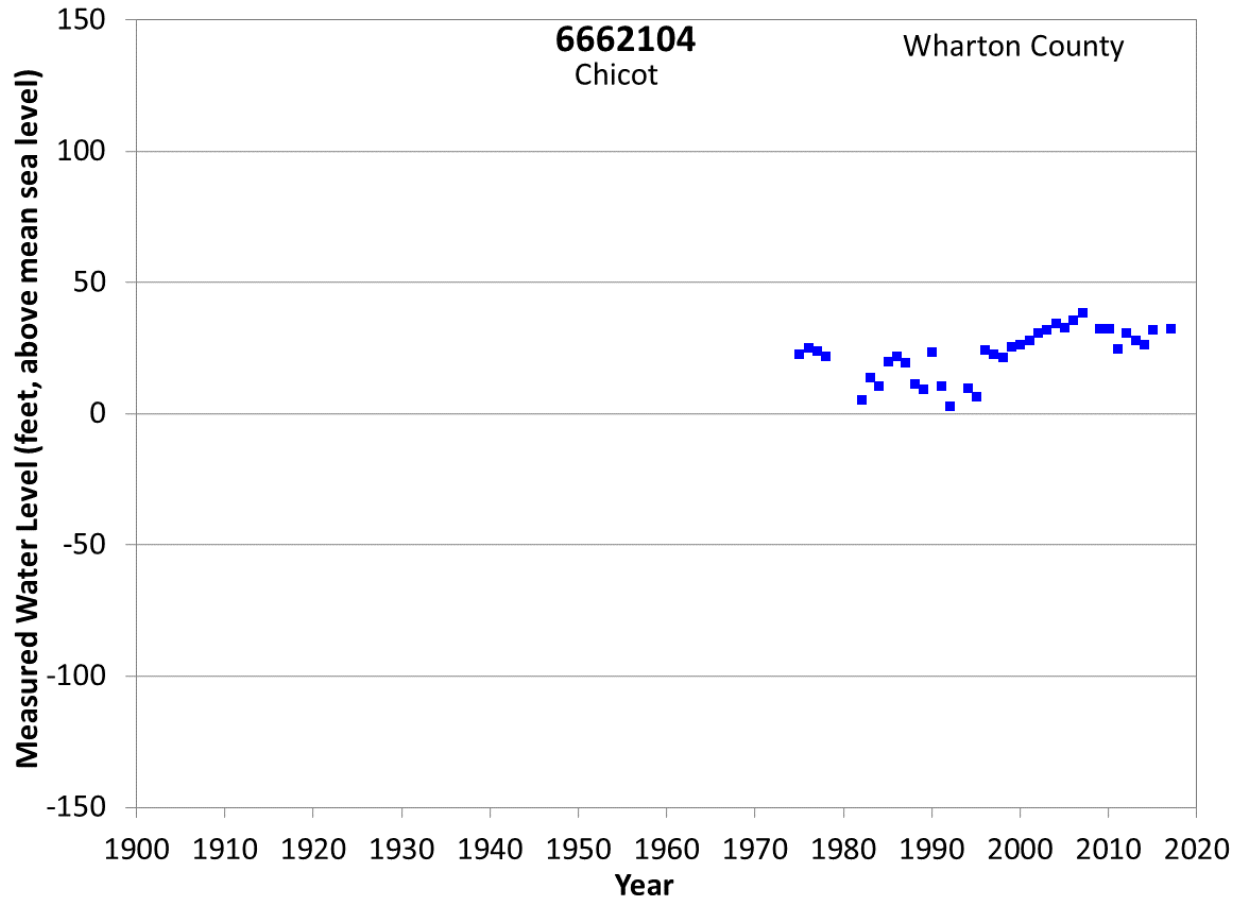


**Figure A50 Groundwater level hydrograph at State Well 6662104.**

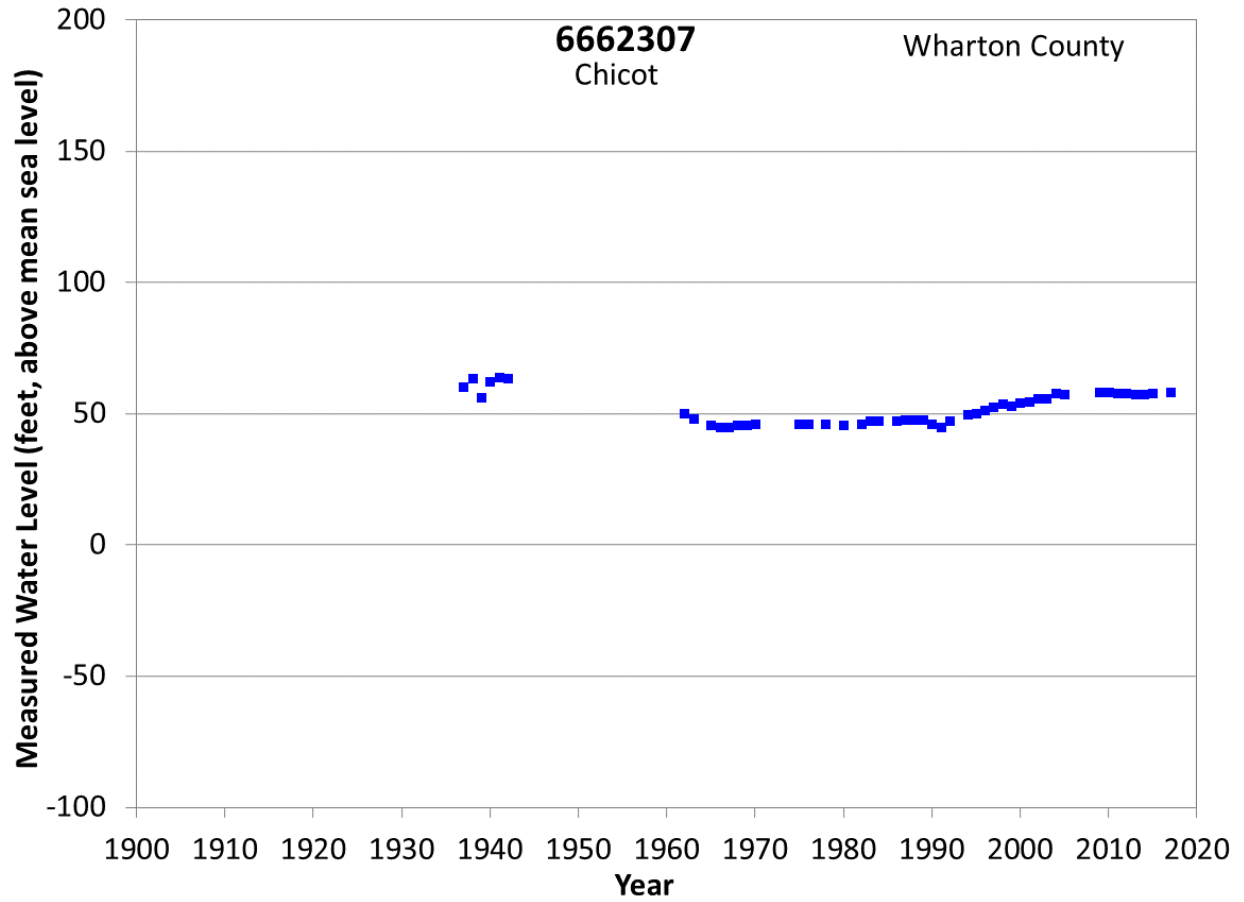


**Figure A51 Groundwater level hydrograph at State Well 6662307.**



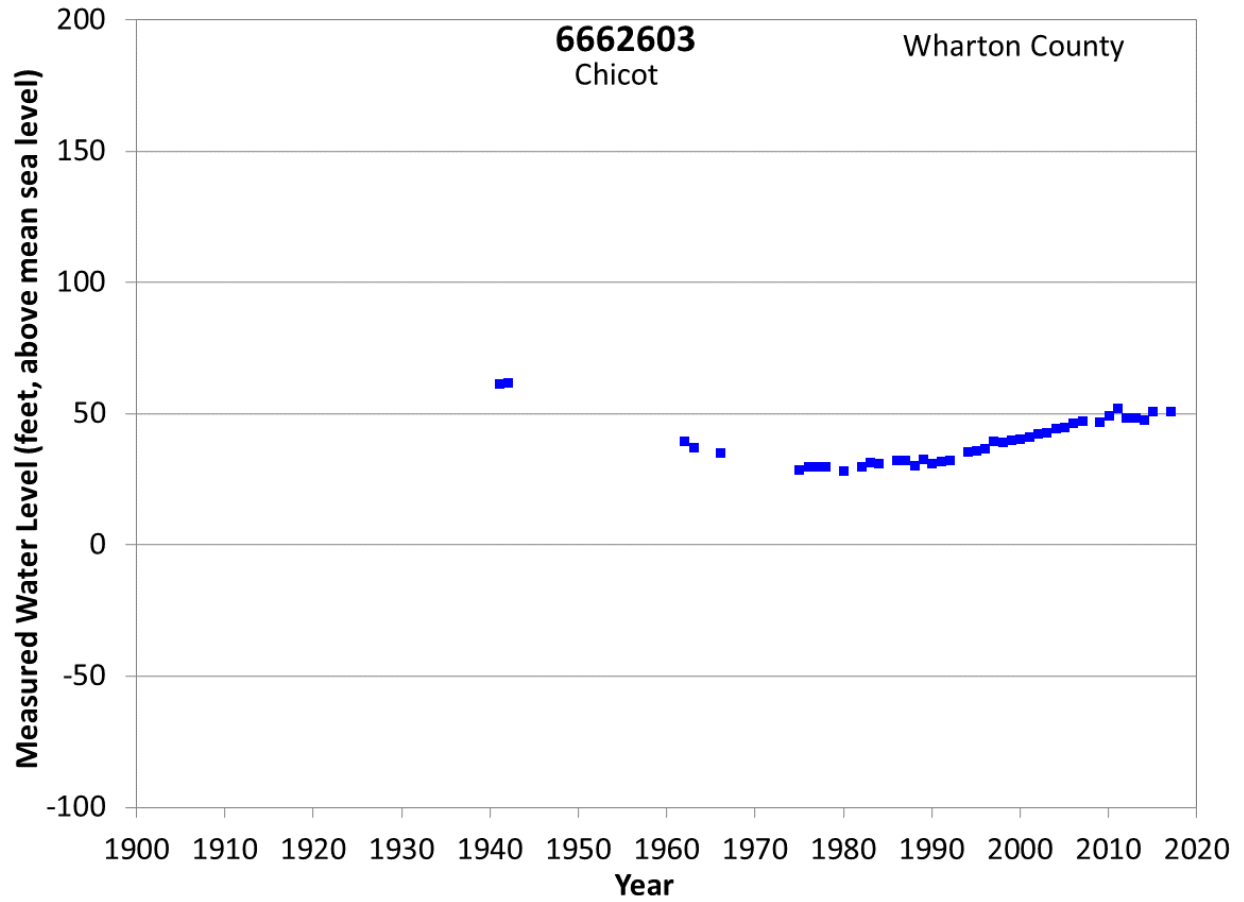


**Figure A52 Groundwater level hydrograph at State Well 6662603.**

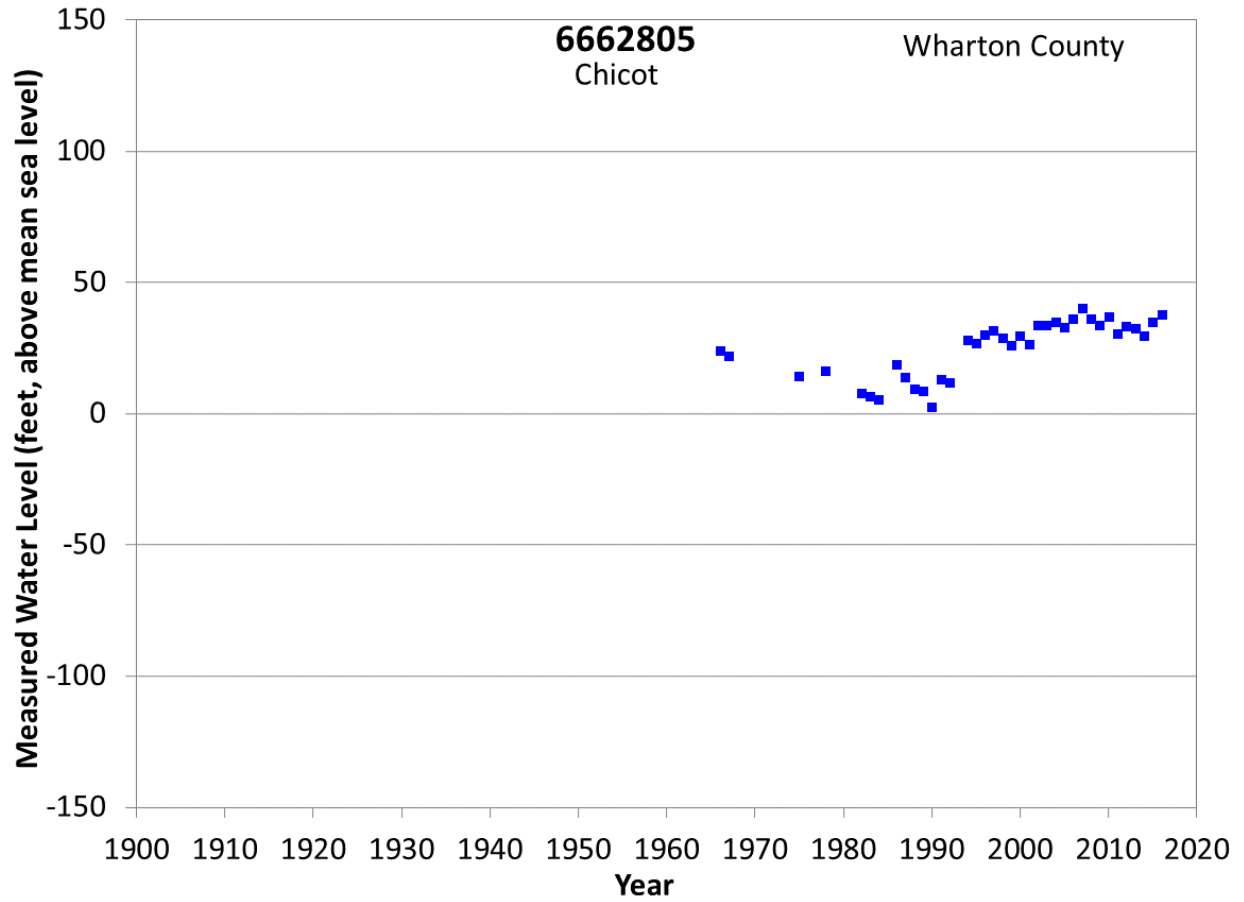


**Figure A53 Groundwater level hydrograph at State Well 6662805.**

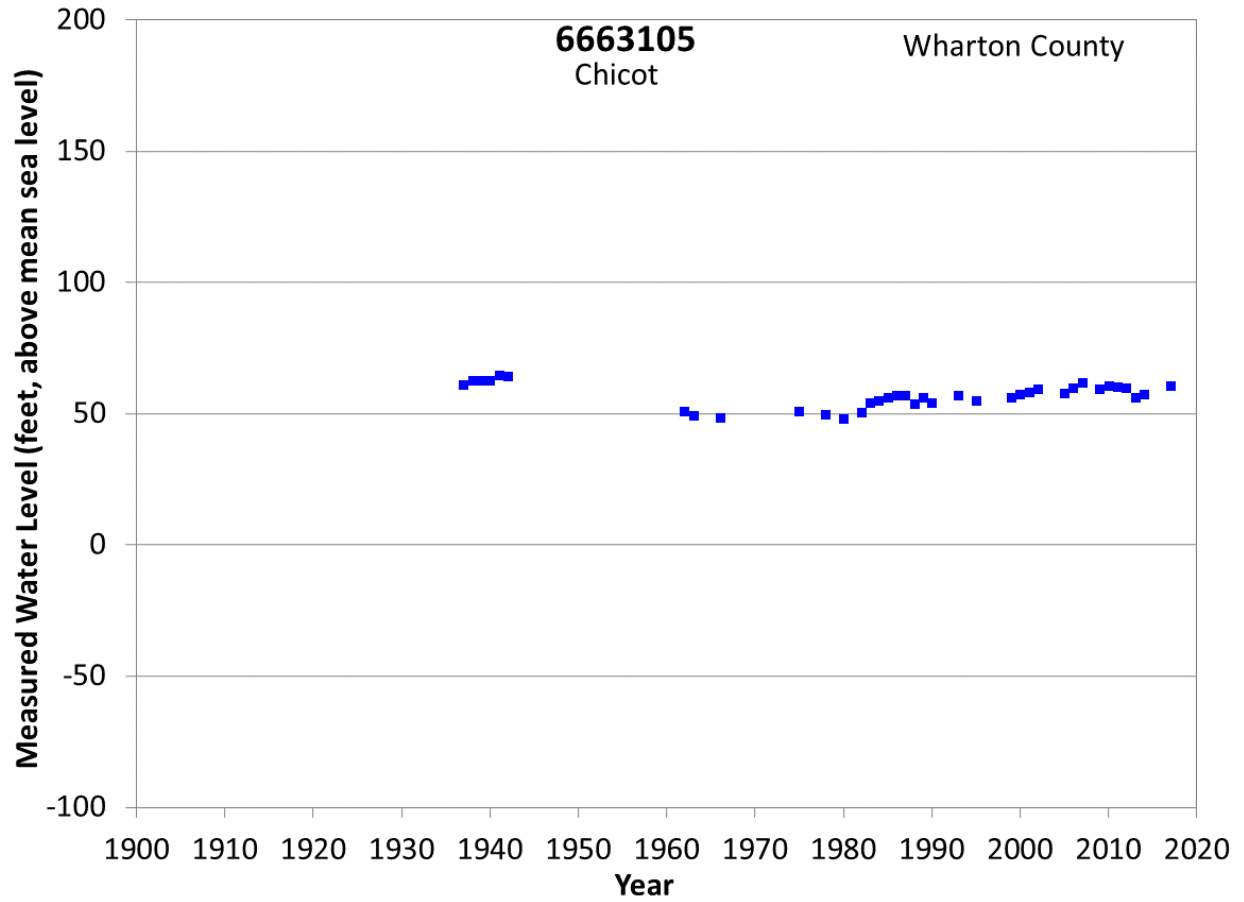


**Figure A54 Groundwater level hydrograph at State Well 6663105.**

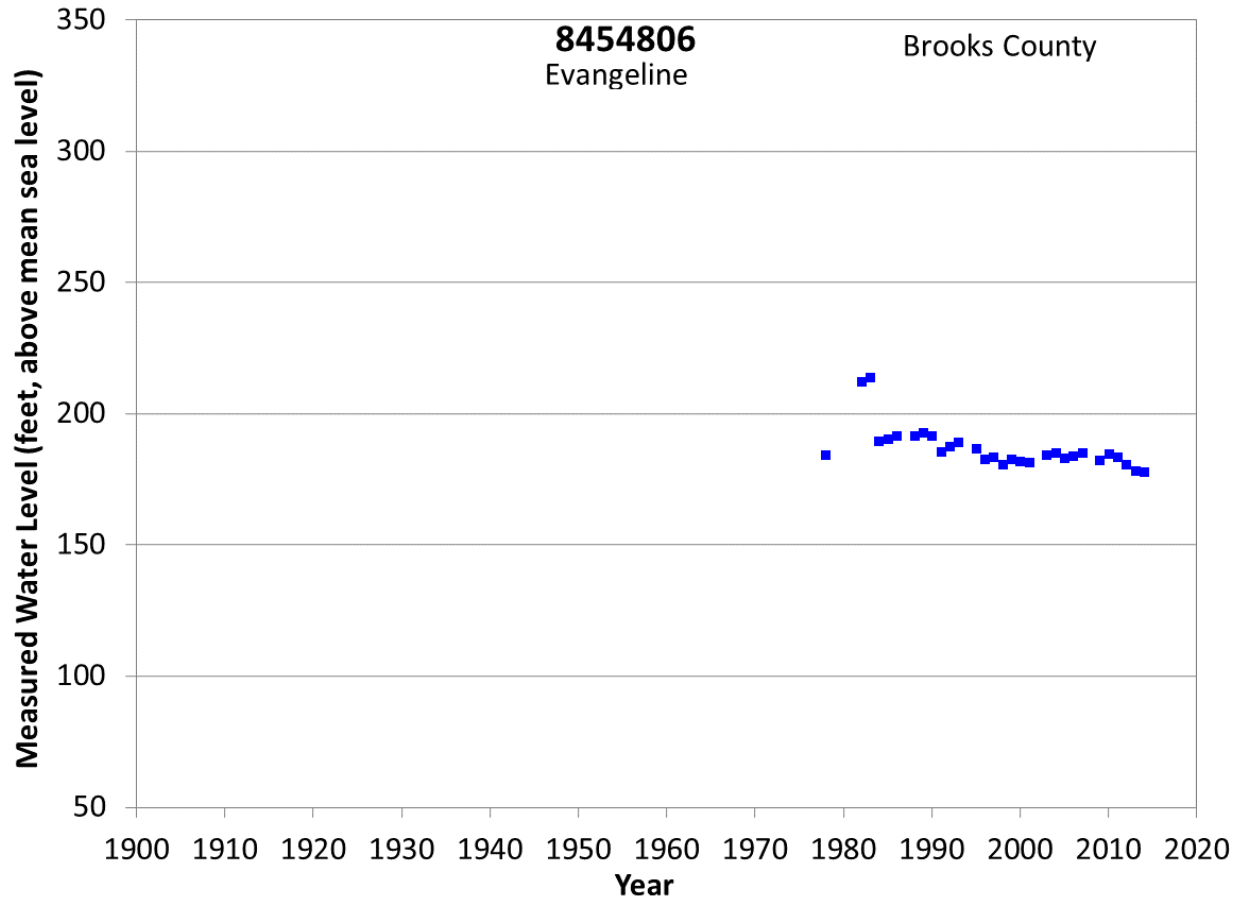


**Figure A55 Groundwater level hydrograph at State Well 8454806.**

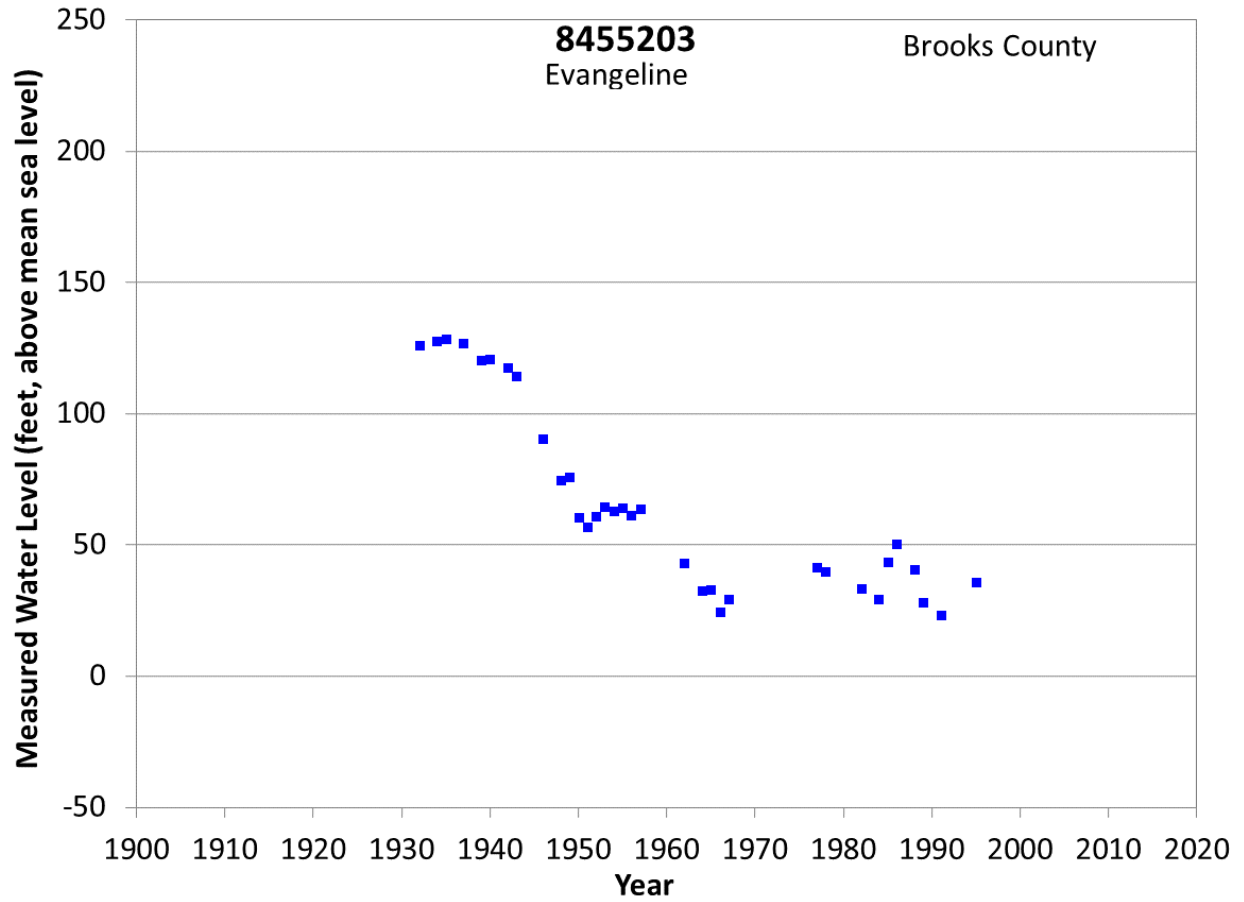


**Figure A56 Groundwater level hydrograph at State Well 8455203.**

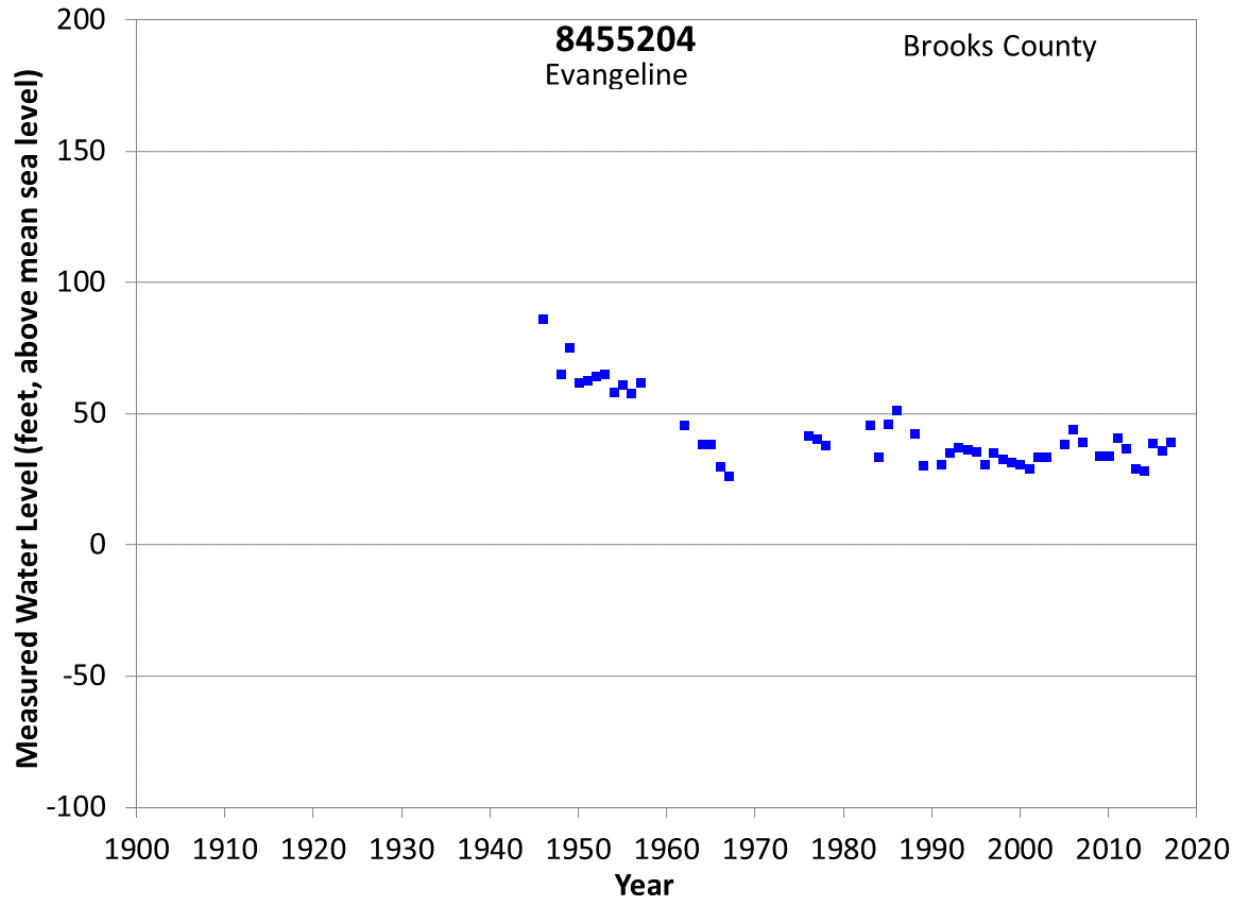


**Figure A57 Groundwater level hydrograph at State Well 8455204.**

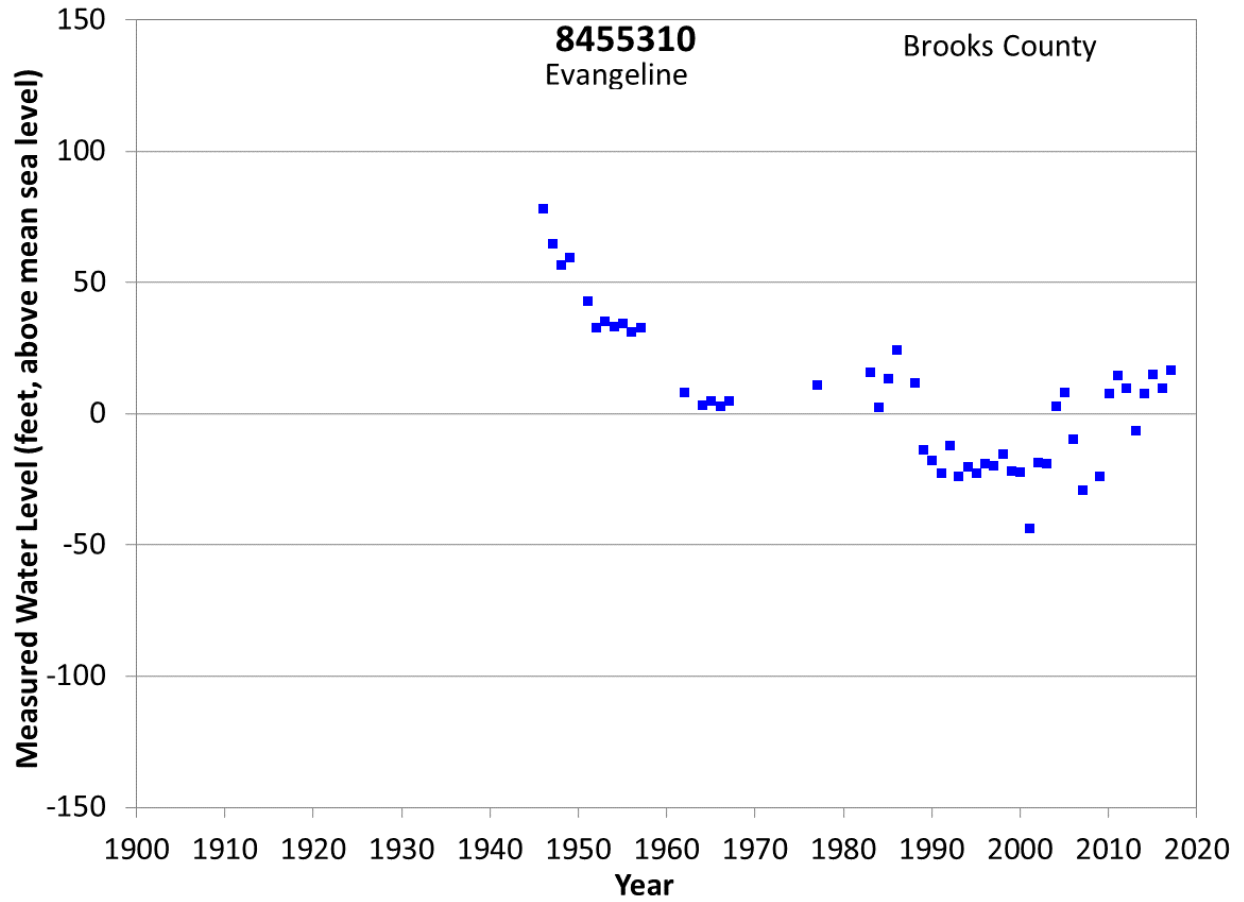


**Figure A58 Groundwater level hydrograph at State Well 8455310.**

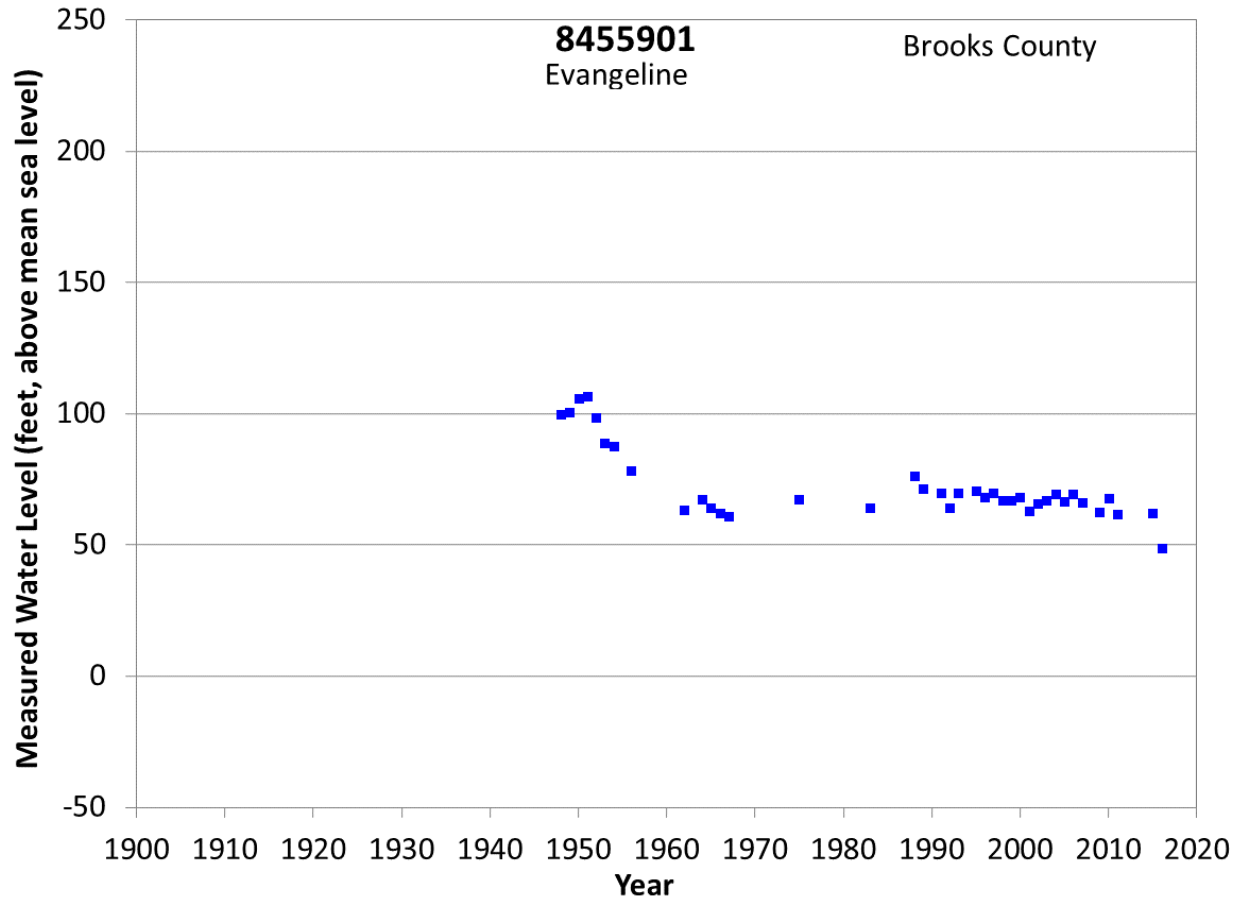


**Figure A59 Groundwater level hydrograph at State Well 8455901.**



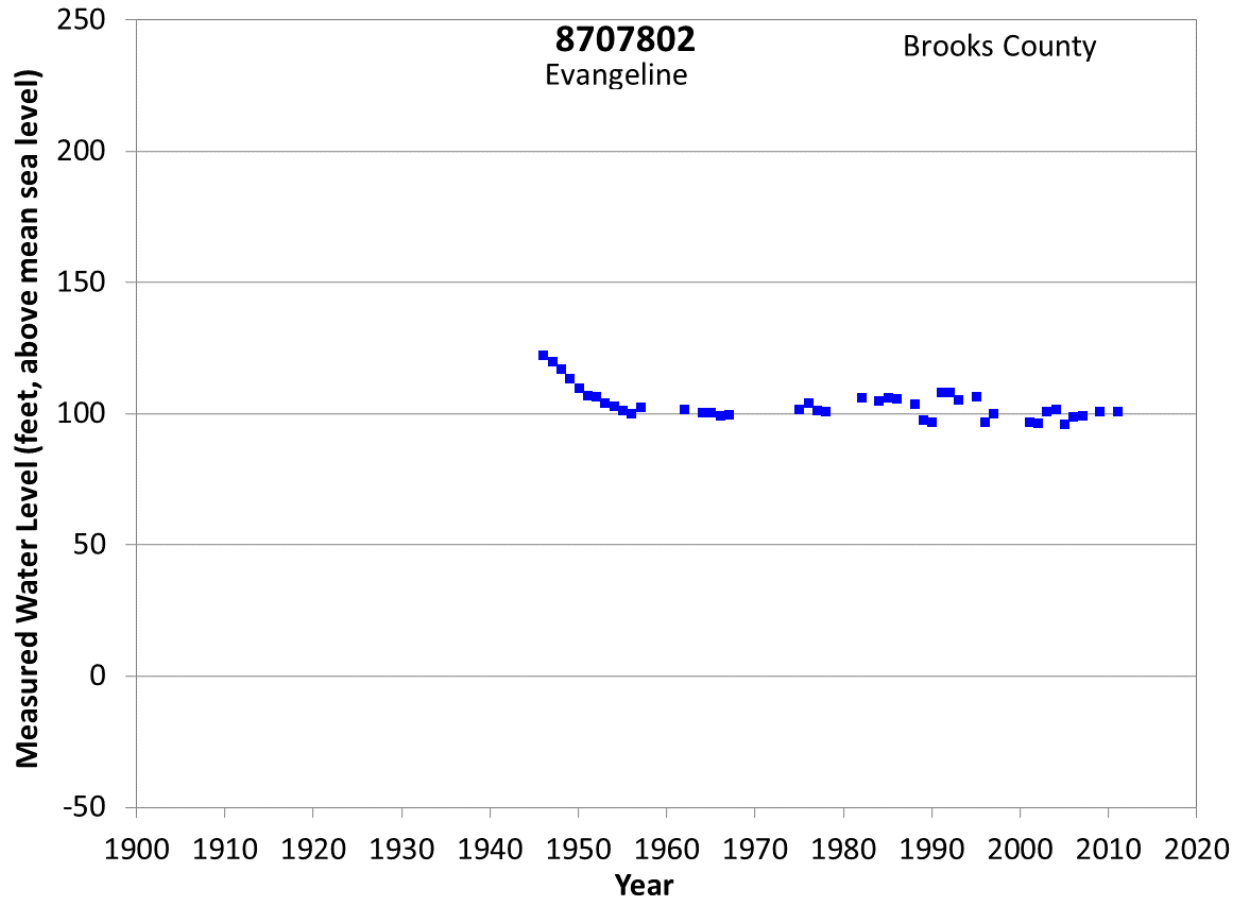


**Figure A60 Groundwater level hydrograph at State Well 8707802.**

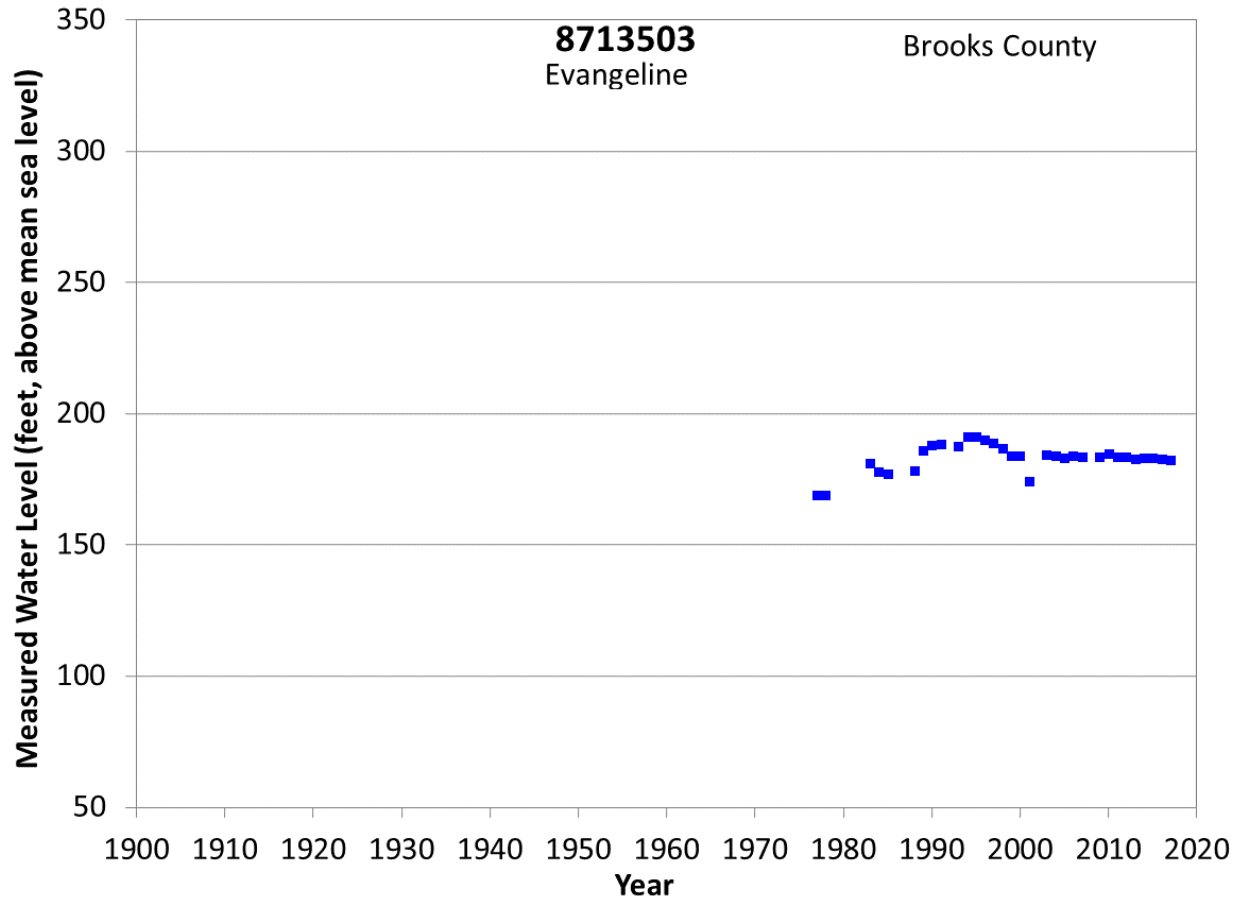


**Figure A61 Groundwater level hydrograph at State Well 8713503.**

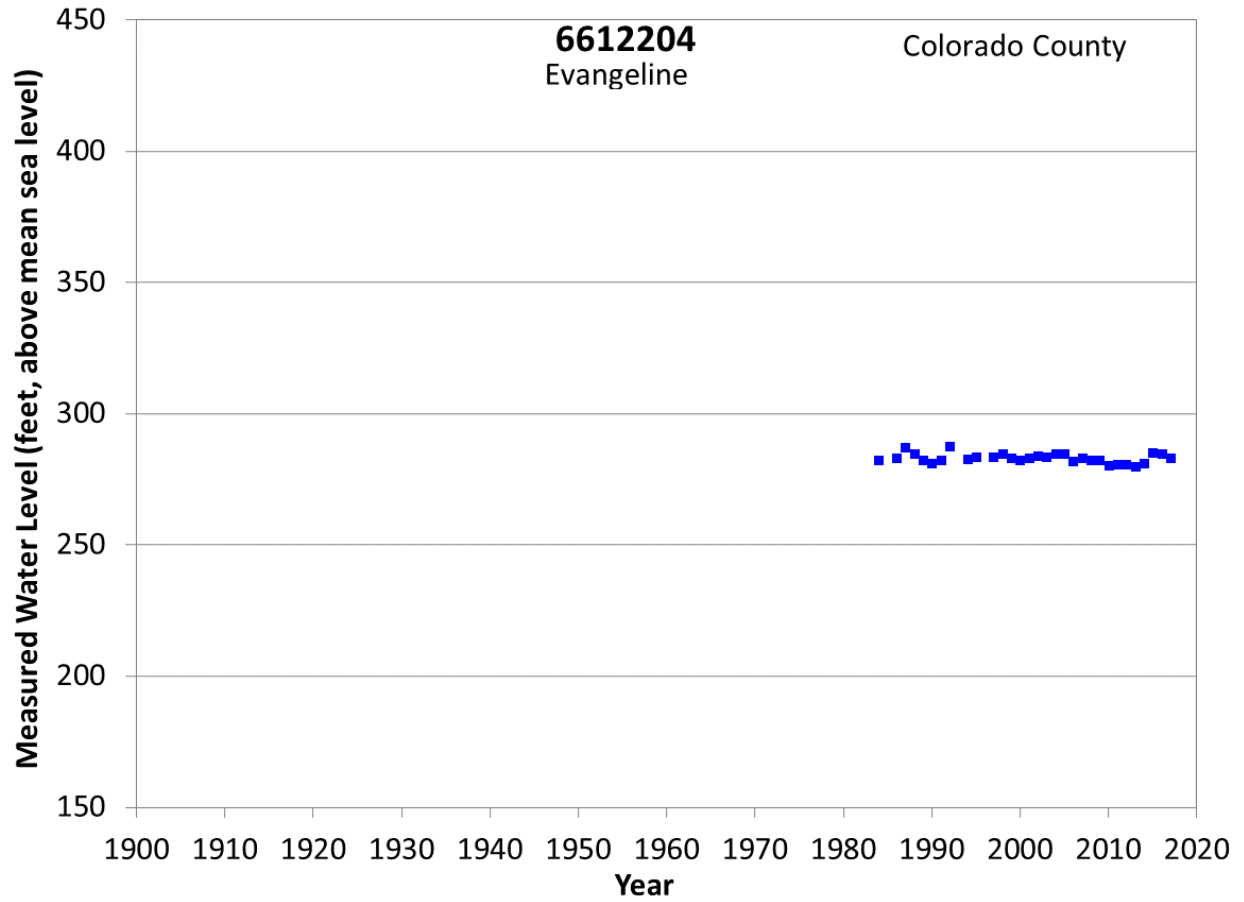


**Figure A62 Groundwater level hydrograph at State Well 6612204.**

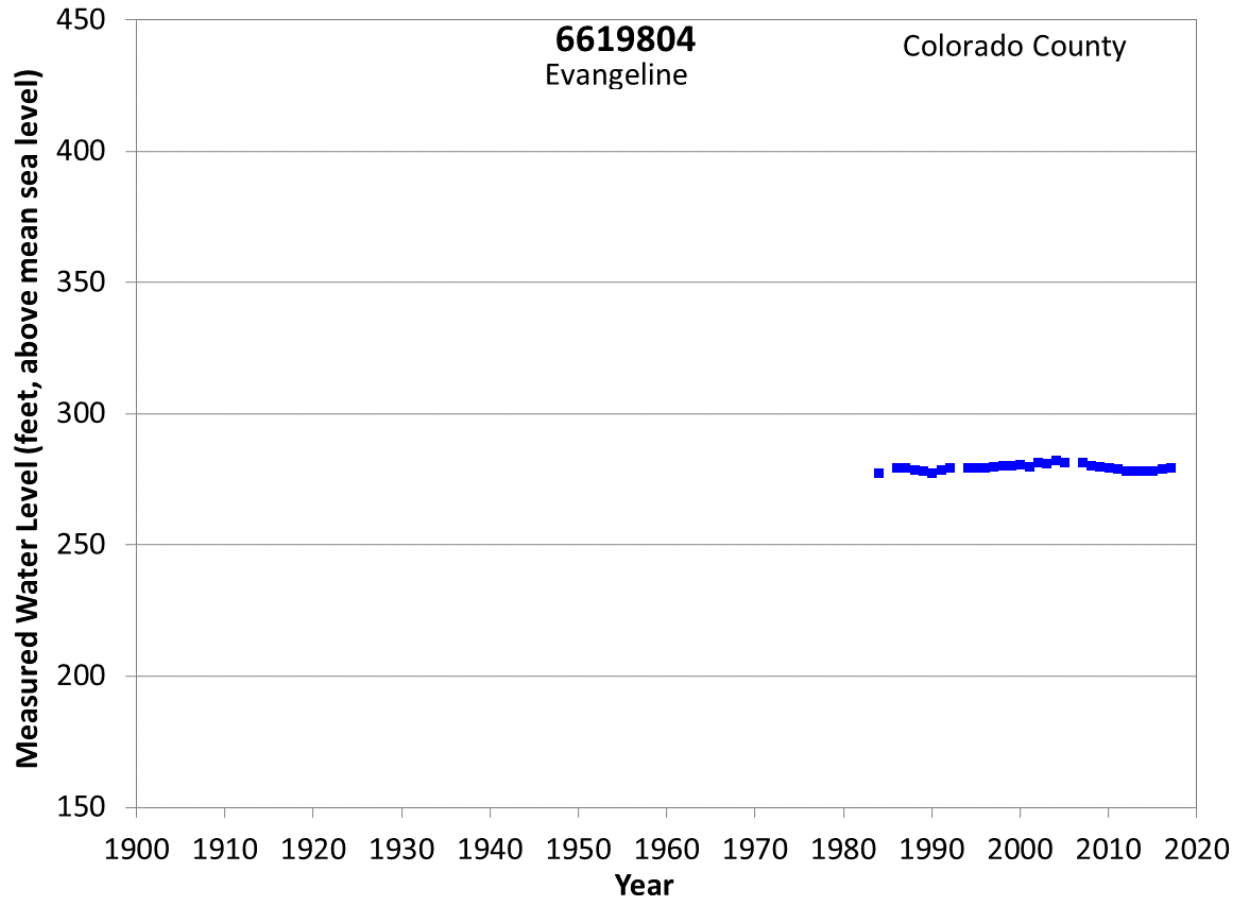


**Figure A63 Groundwater level hydrograph at State Well 6619804.**

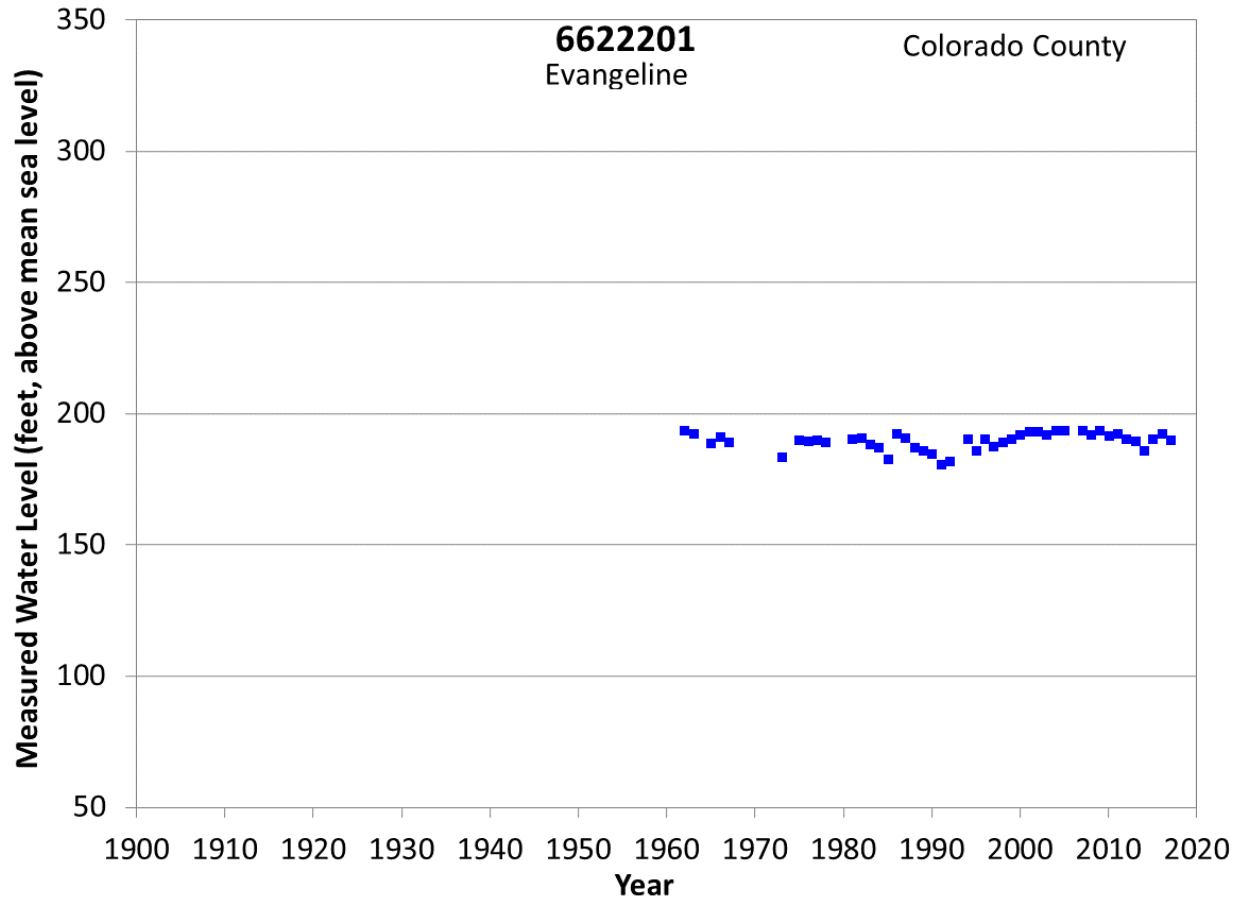


**Figure A64 Groundwater level hydrograph at State Well 6622201.**

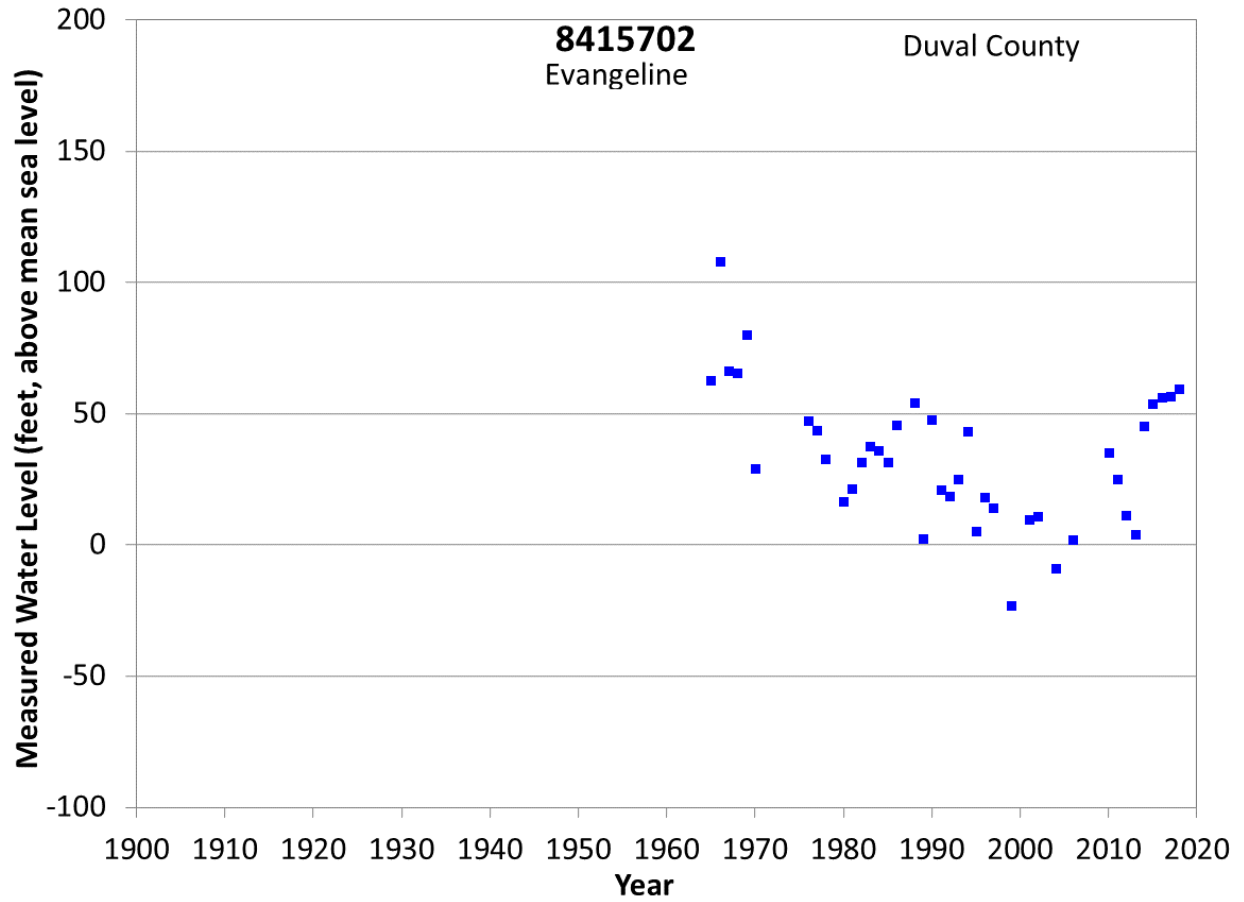


**Figure A65 Groundwater level hydrograph at State Well 8415702.**

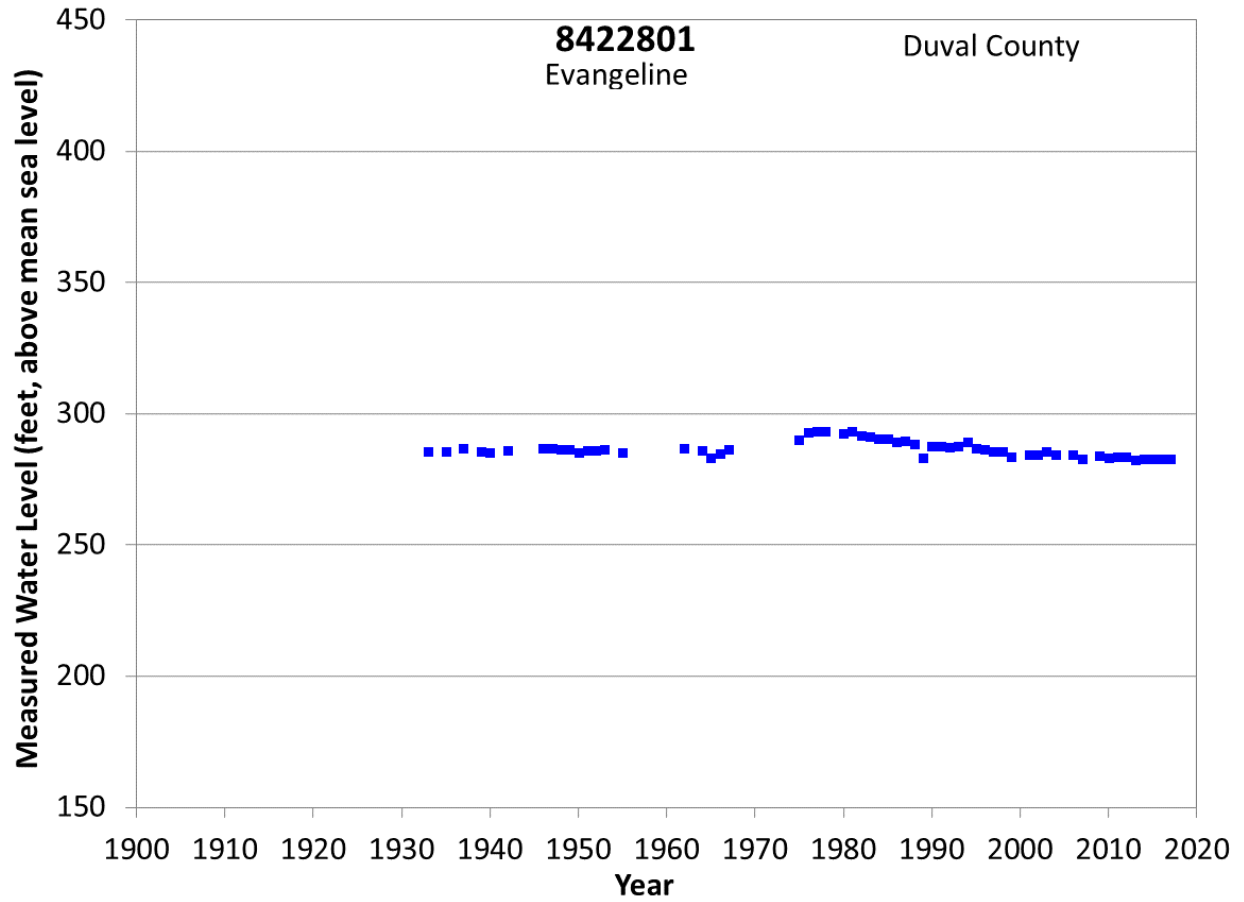


**Figure A66 Groundwater level hydrograph at State Well 8422801.**

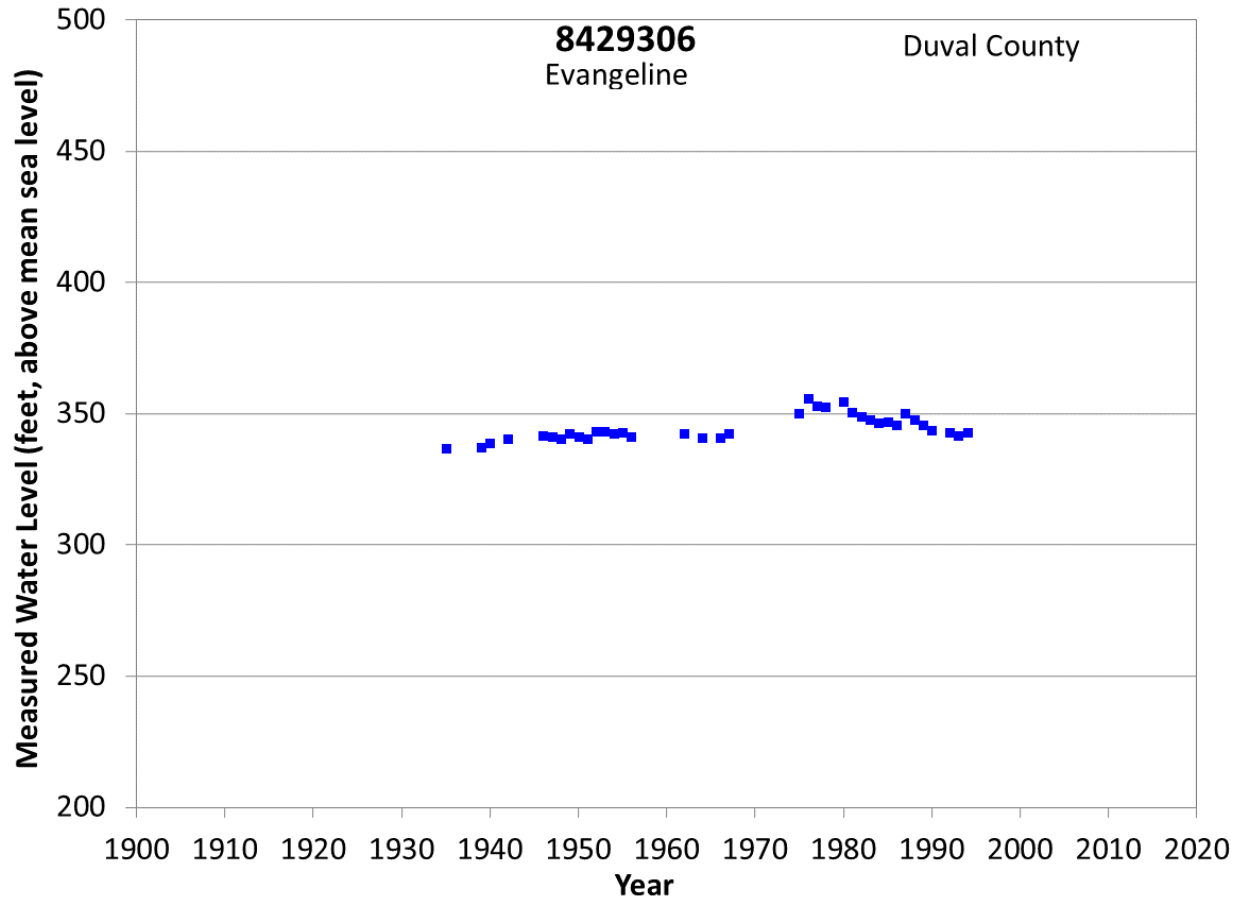


**Figure A67 Groundwater level hydrograph at State Well 8429306.**



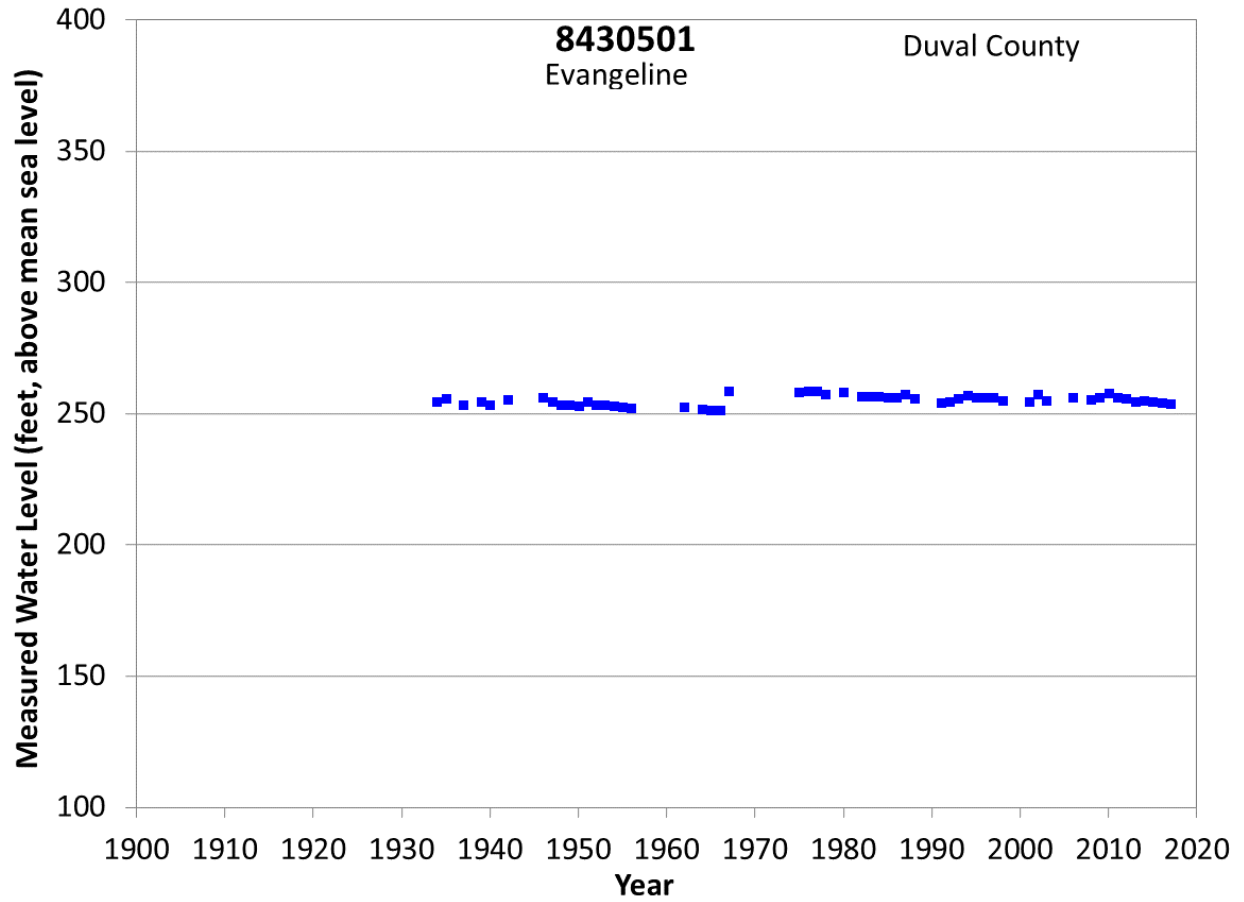


**Figure A68 Groundwater level hydrograph at State Well 8430501.**

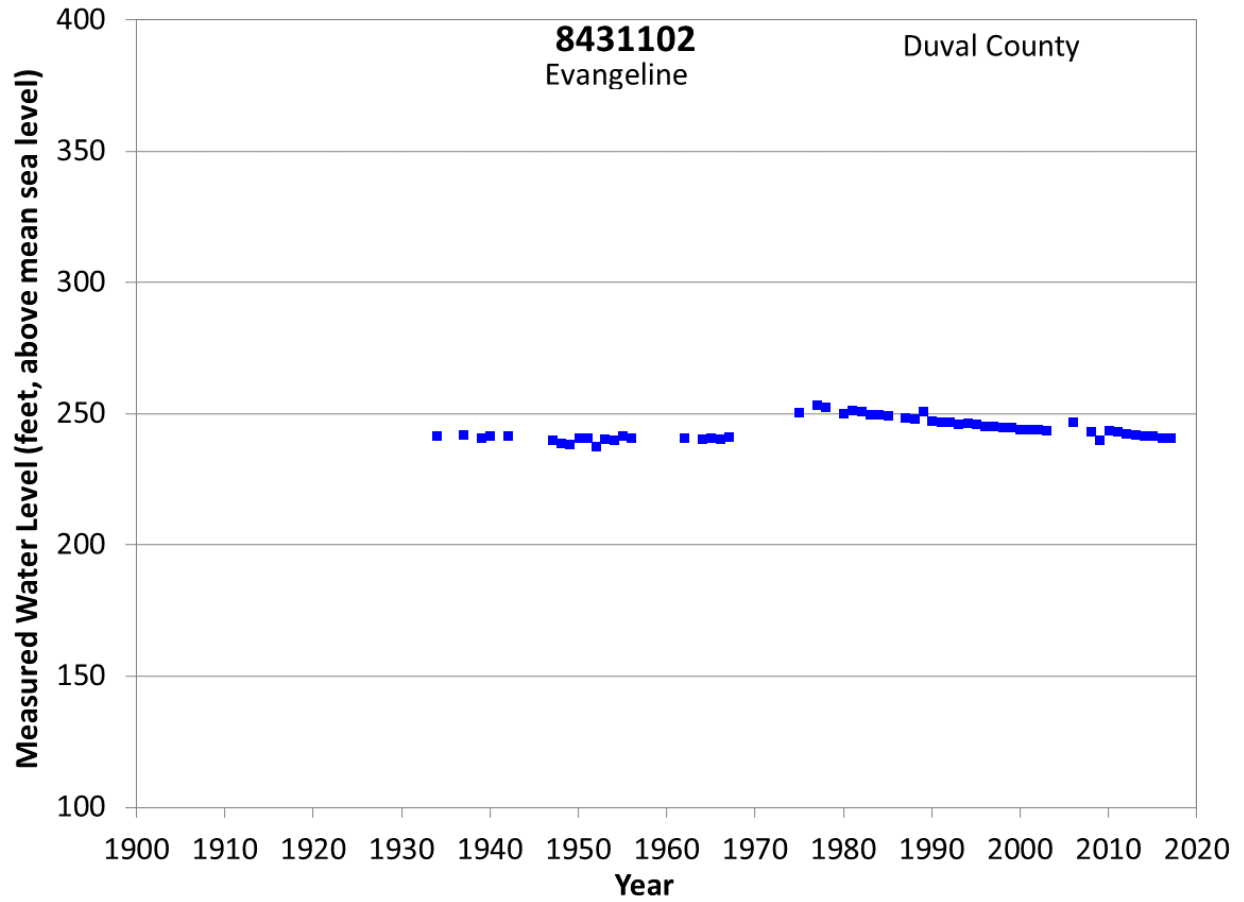


**Figure A69 Groundwater level hydrograph at State Well 8431102.**

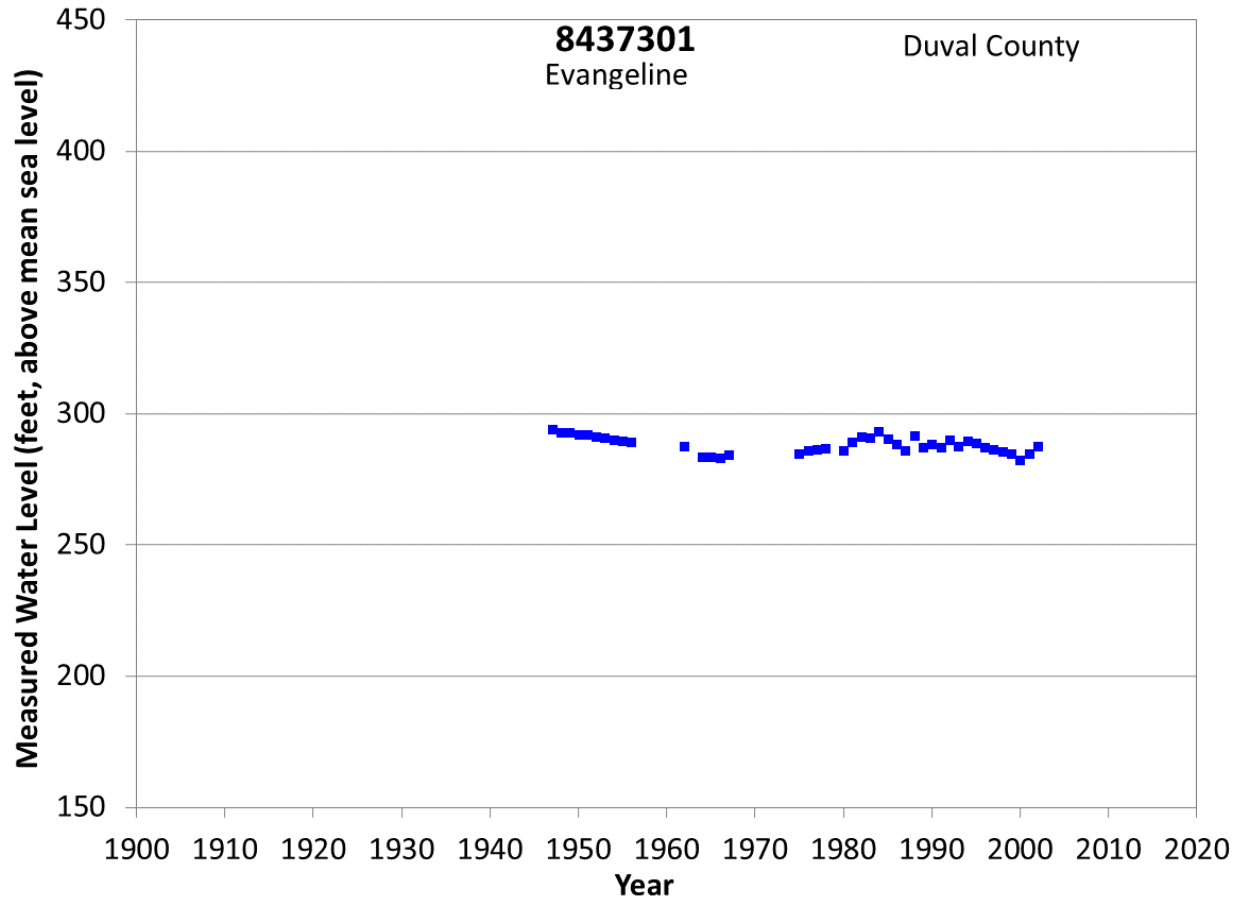


**Figure A70 Groundwater level hydrograph at State Well 8437301.**

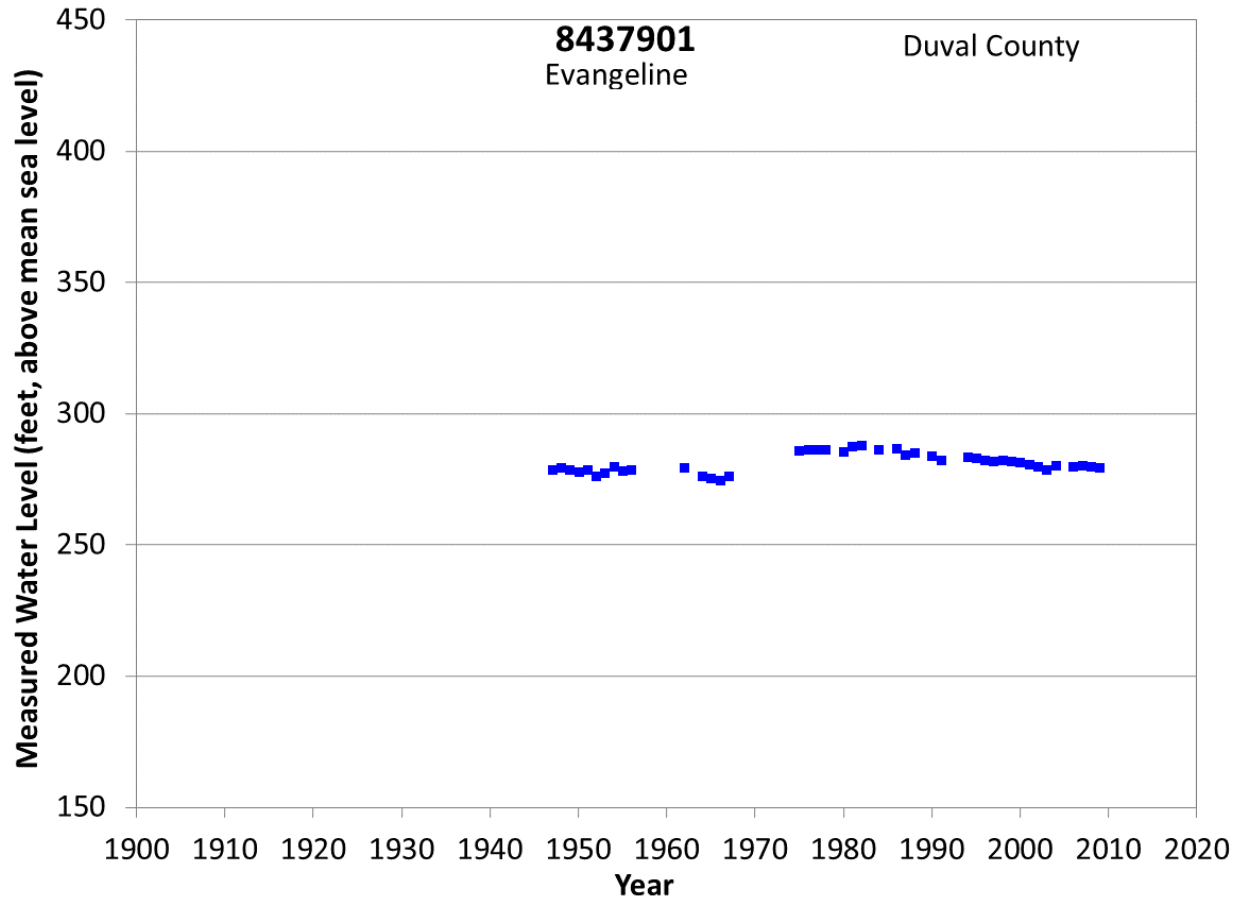


**Figure A71 Groundwater level hydrograph at State Well 8437901.**

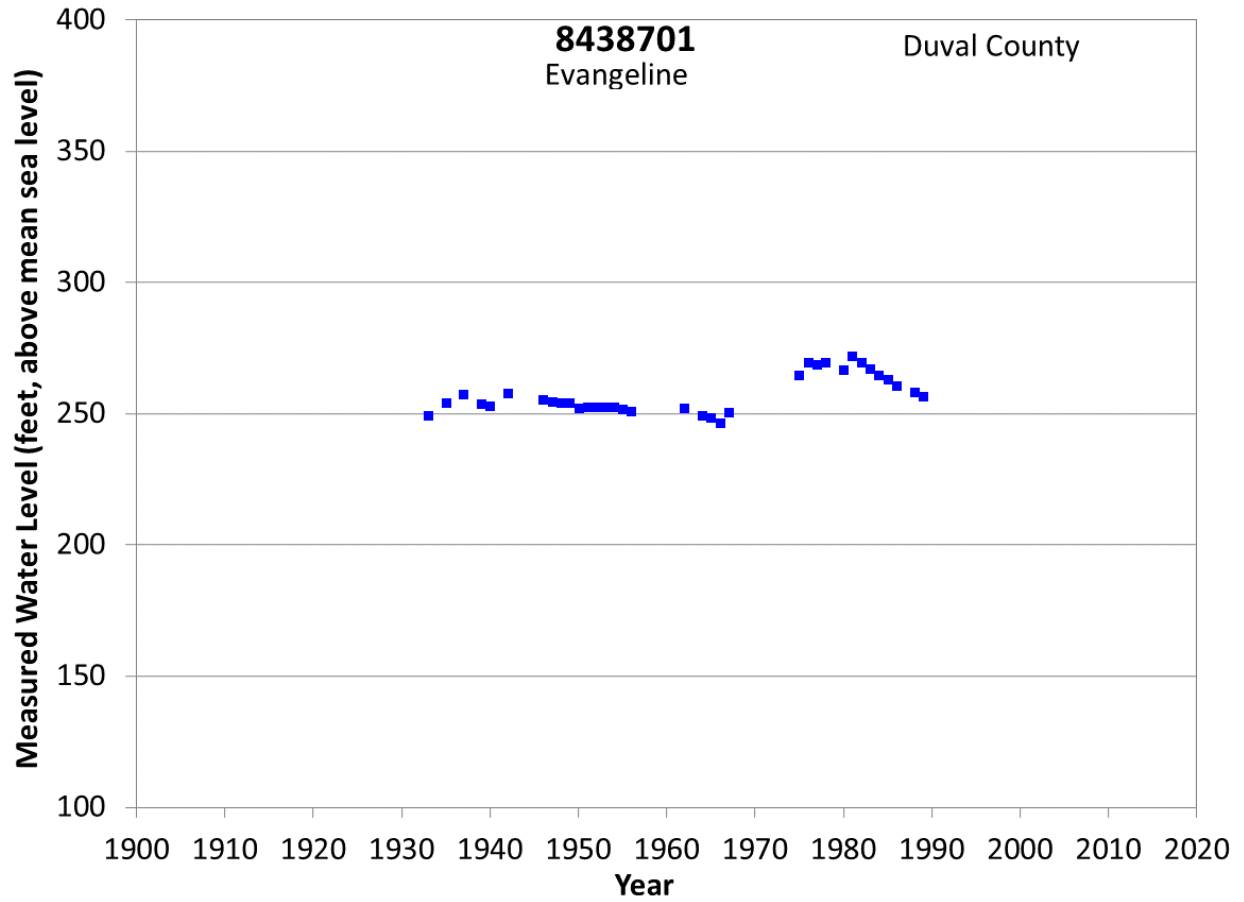


**Figure A72 Groundwater level hydrograph at State Well 8438701.**

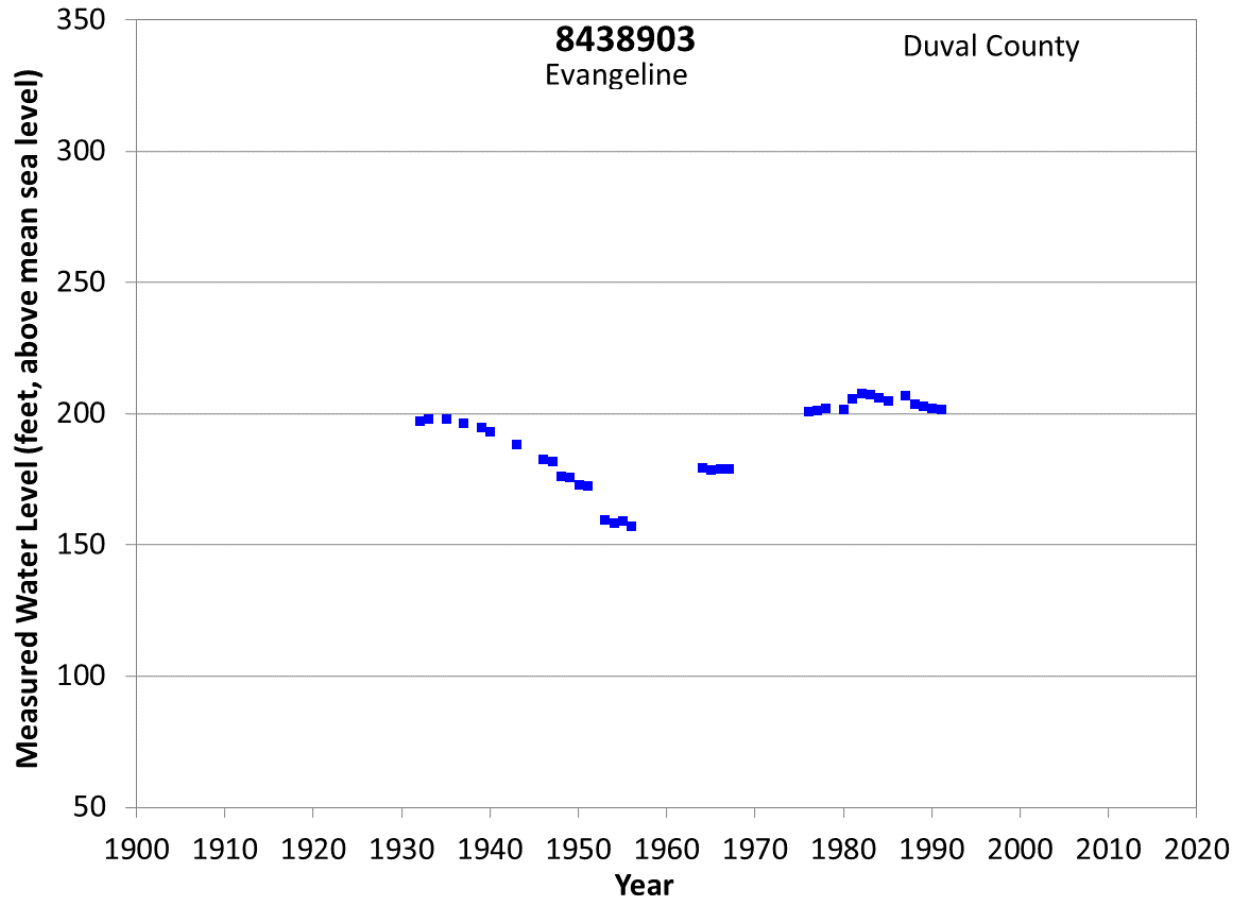


**Figure A73 Groundwater level hydrograph at State Well 8438903.**

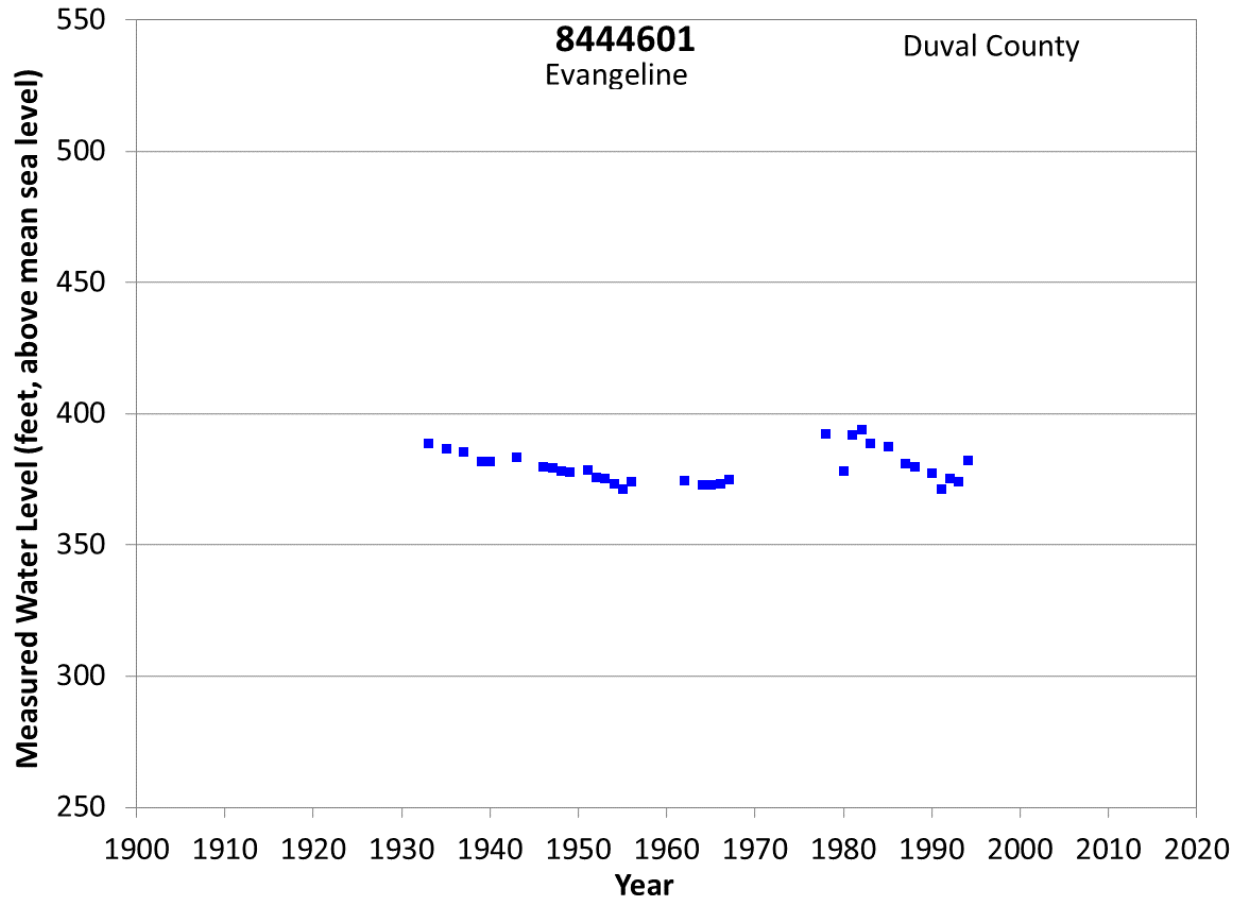


**Figure A74 Groundwater level hydrograph at State Well 8444601.**

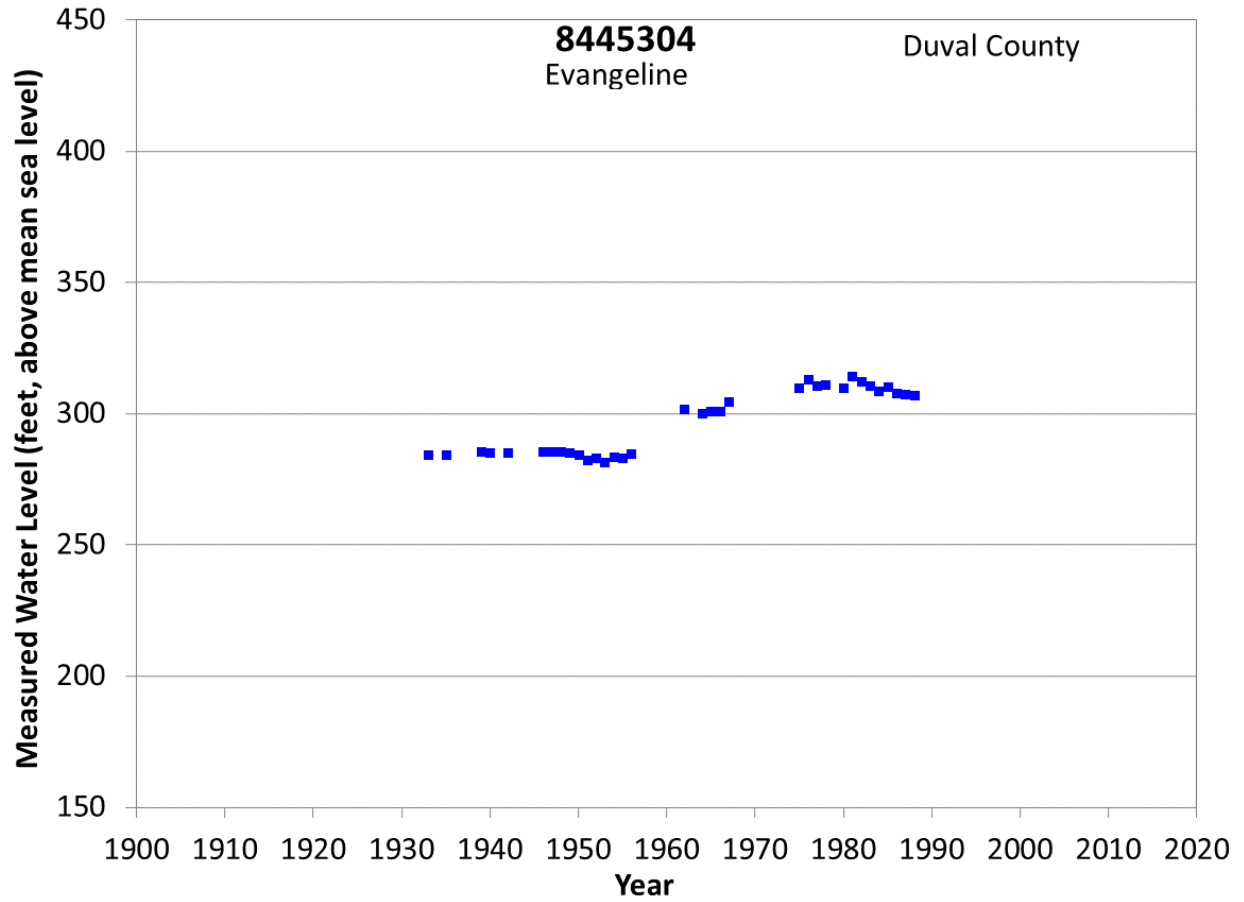


**Figure A75 Groundwater level hydrograph at State Well 8445304.**



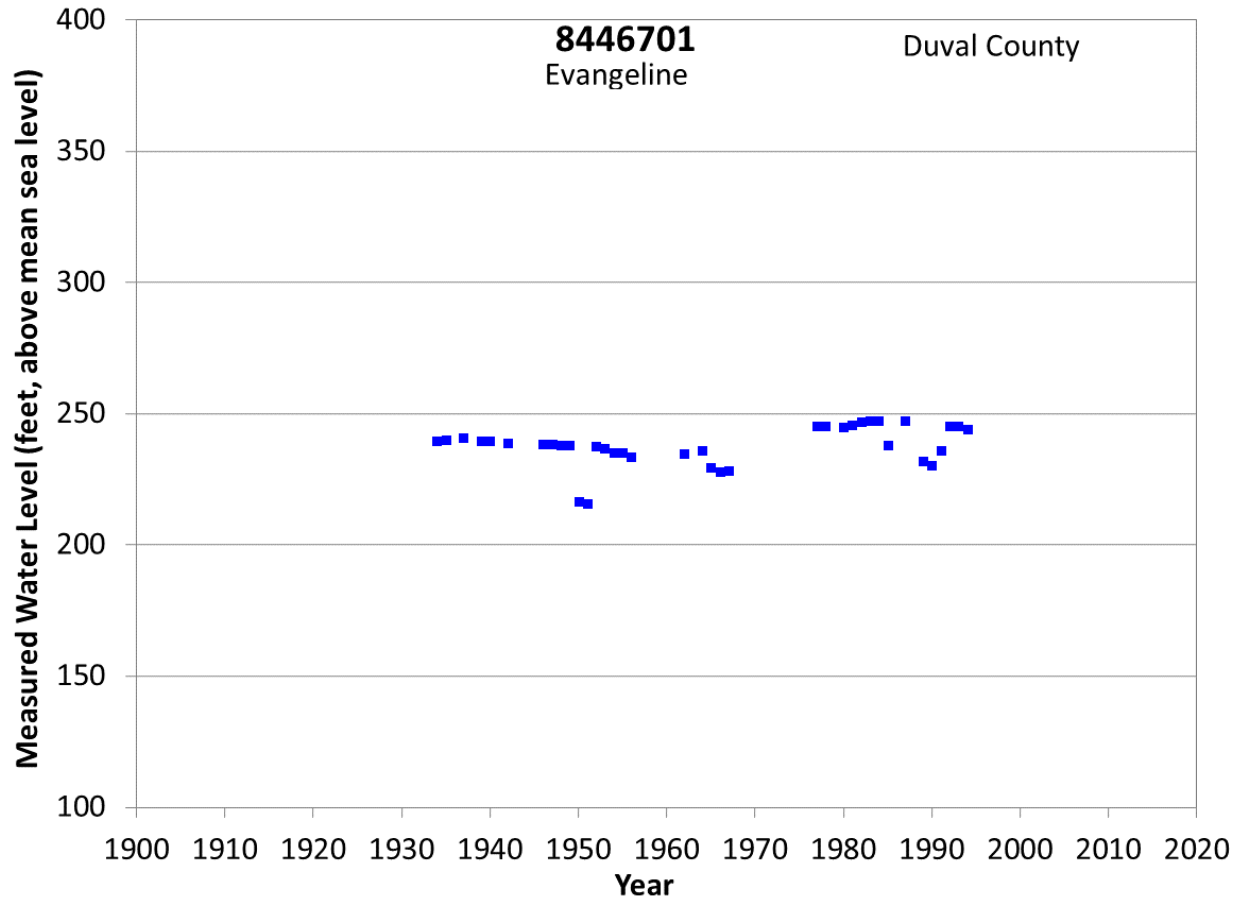


**Figure A76 Groundwater level hydrograph at State Well 8446701.**

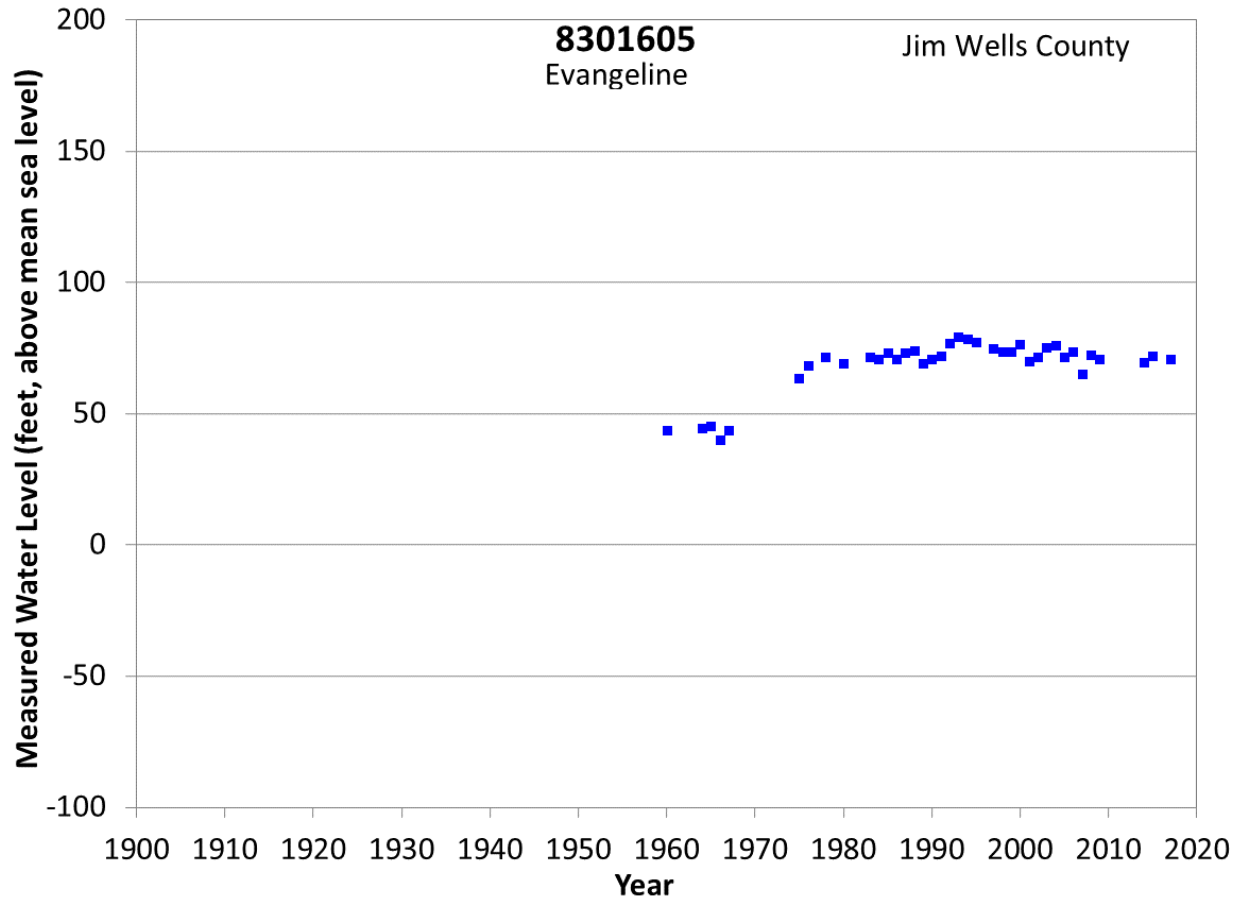


**Figure A77 Groundwater level hydrograph at State Well 8301605.**

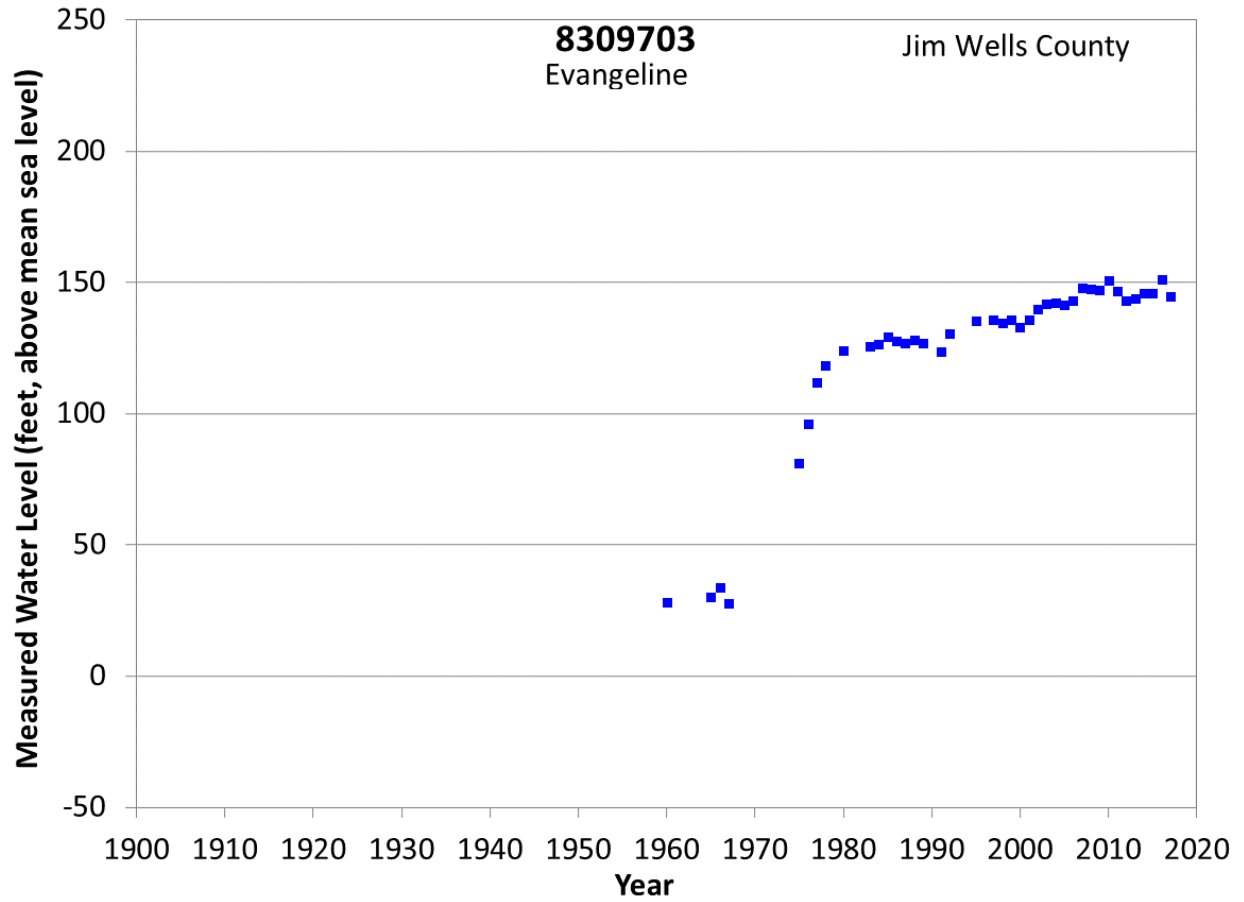


**Figure A78 Groundwater level hydrograph at State Well 8309703.**

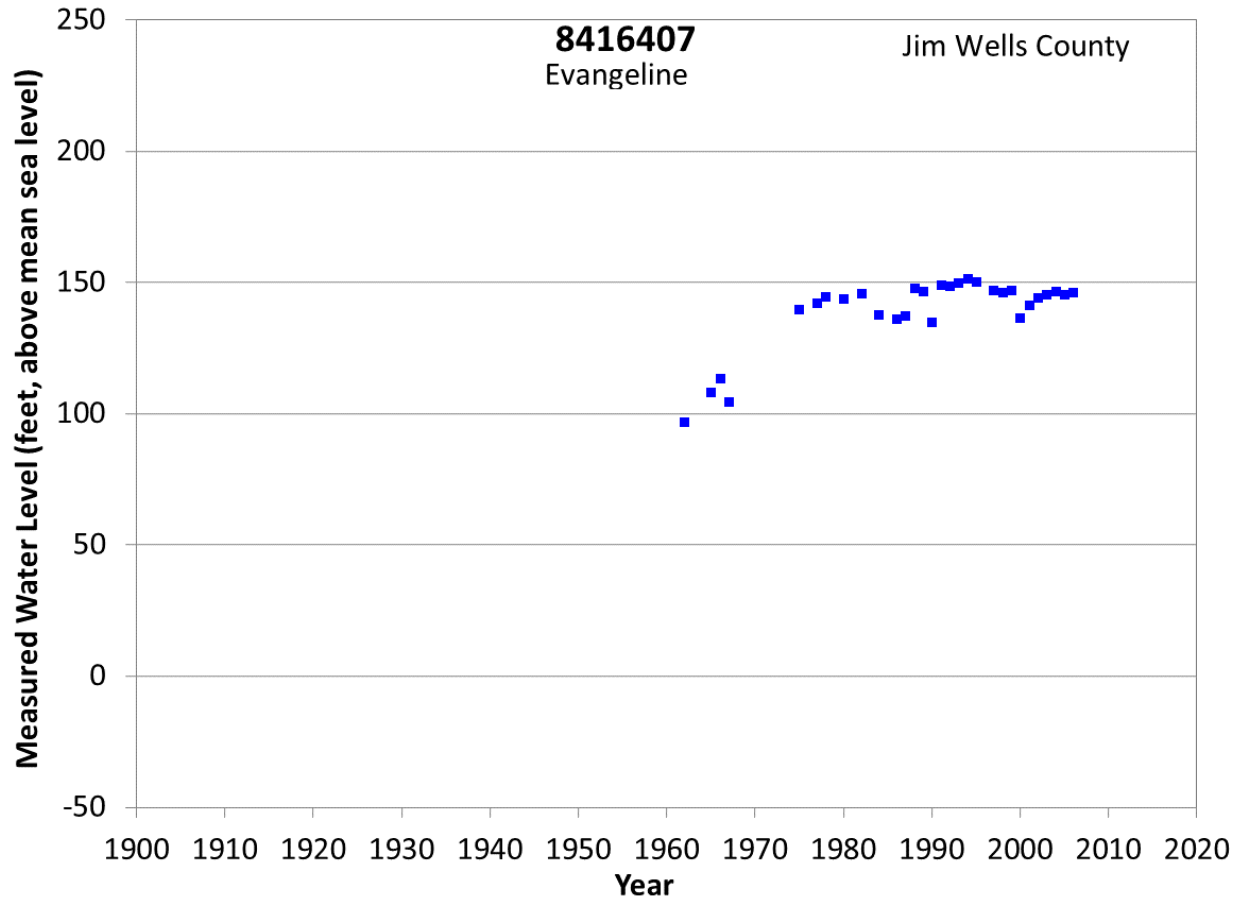


**Figure A79 Groundwater level hydrograph at State Well 8416407.**

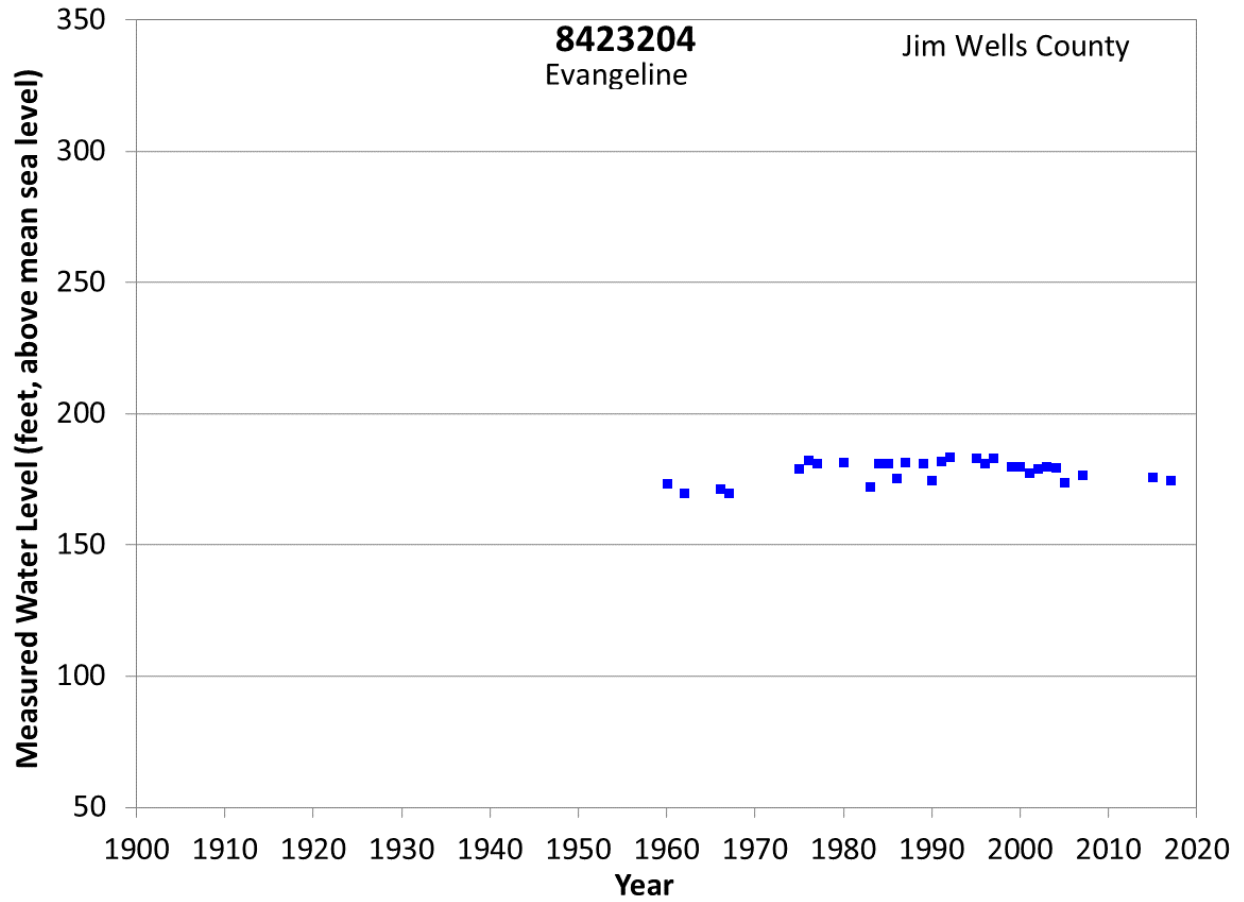


**Figure A80 Groundwater level hydrograph at State Well 8423204.**

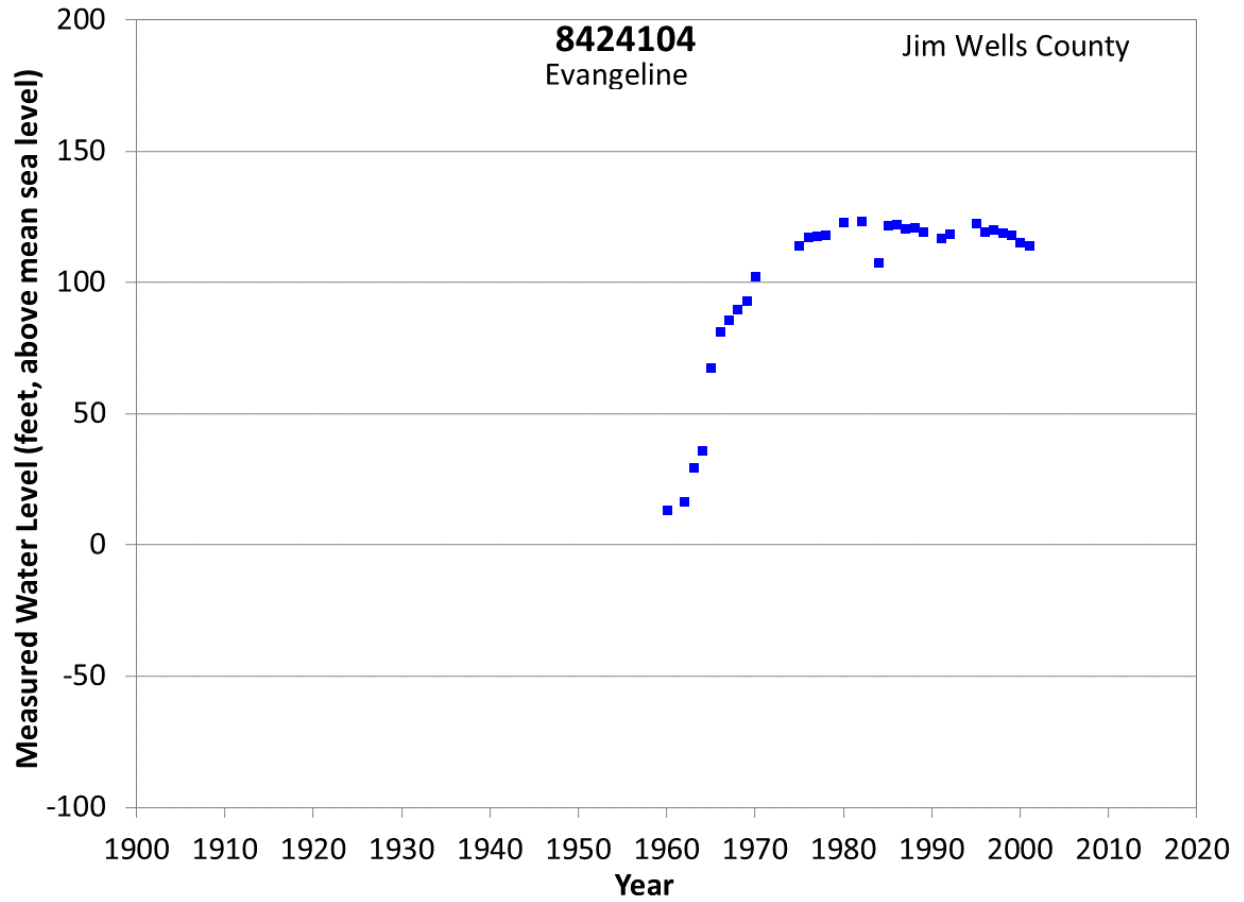


**Figure A81 Groundwater level hydrograph at State Well 8424104.**

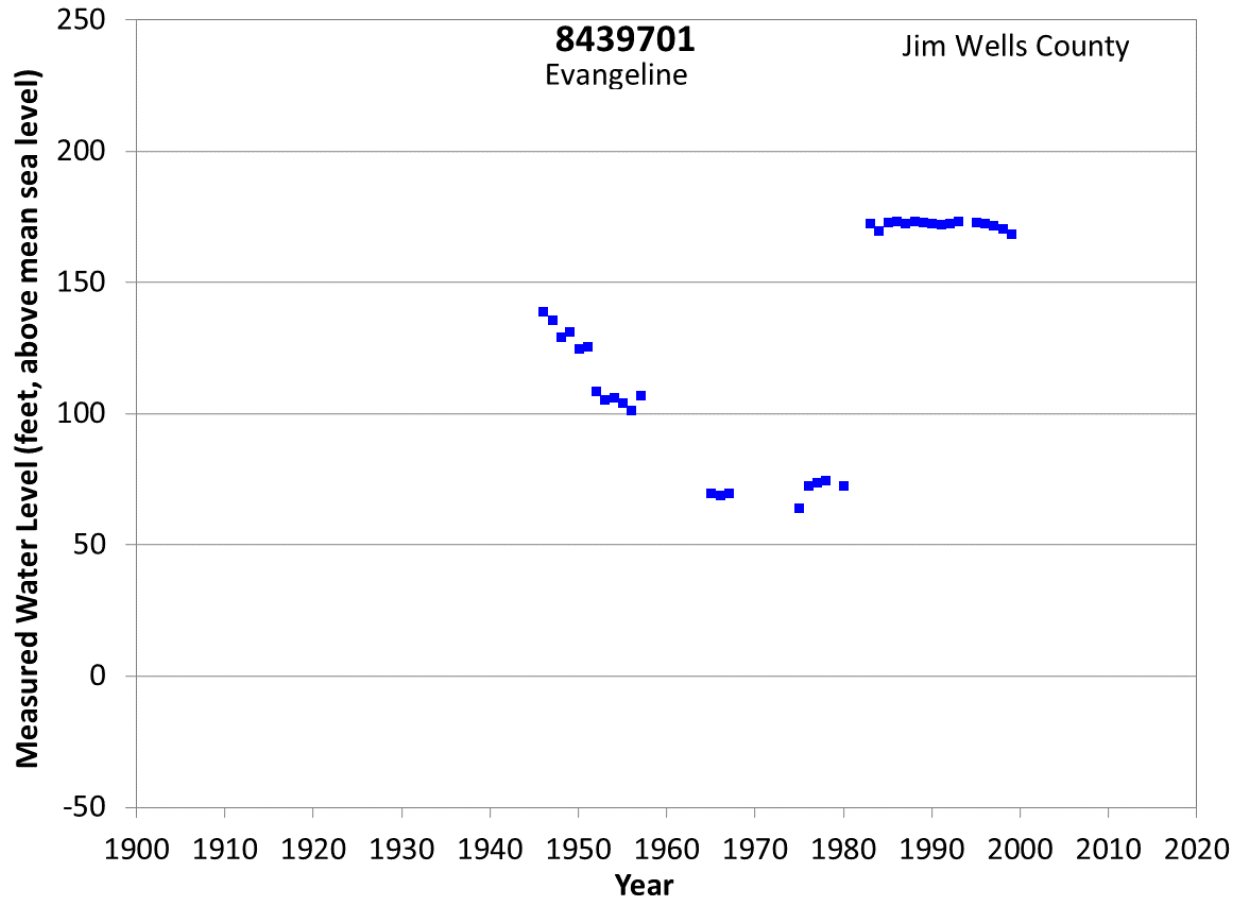


**Figure A82 Groundwater level hydrograph at State Well 8439701.**

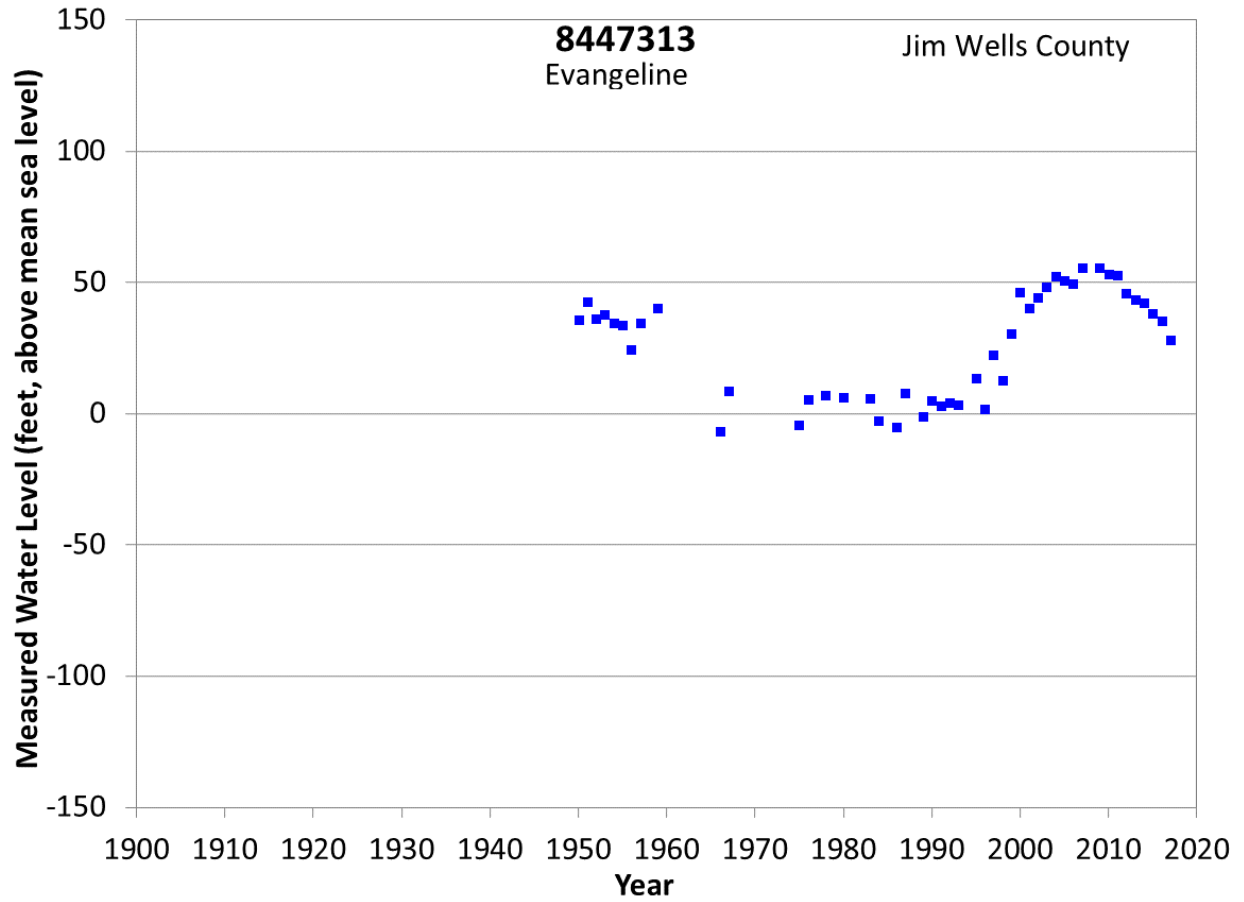


**Figure A83 Groundwater level hydrograph at State Well 8447313.**



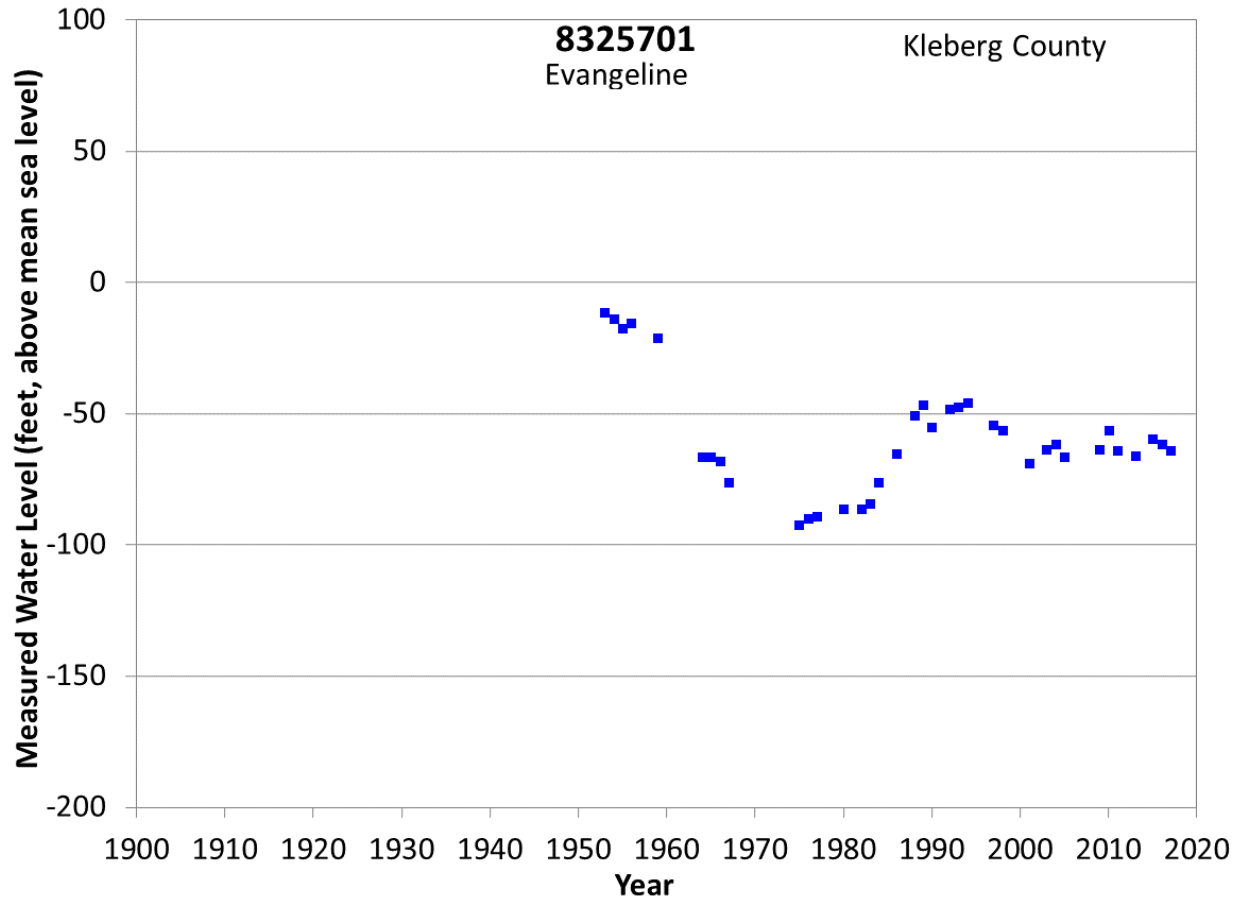


**Figure A84 Groundwater level hydrograph at State Well 8325701.**

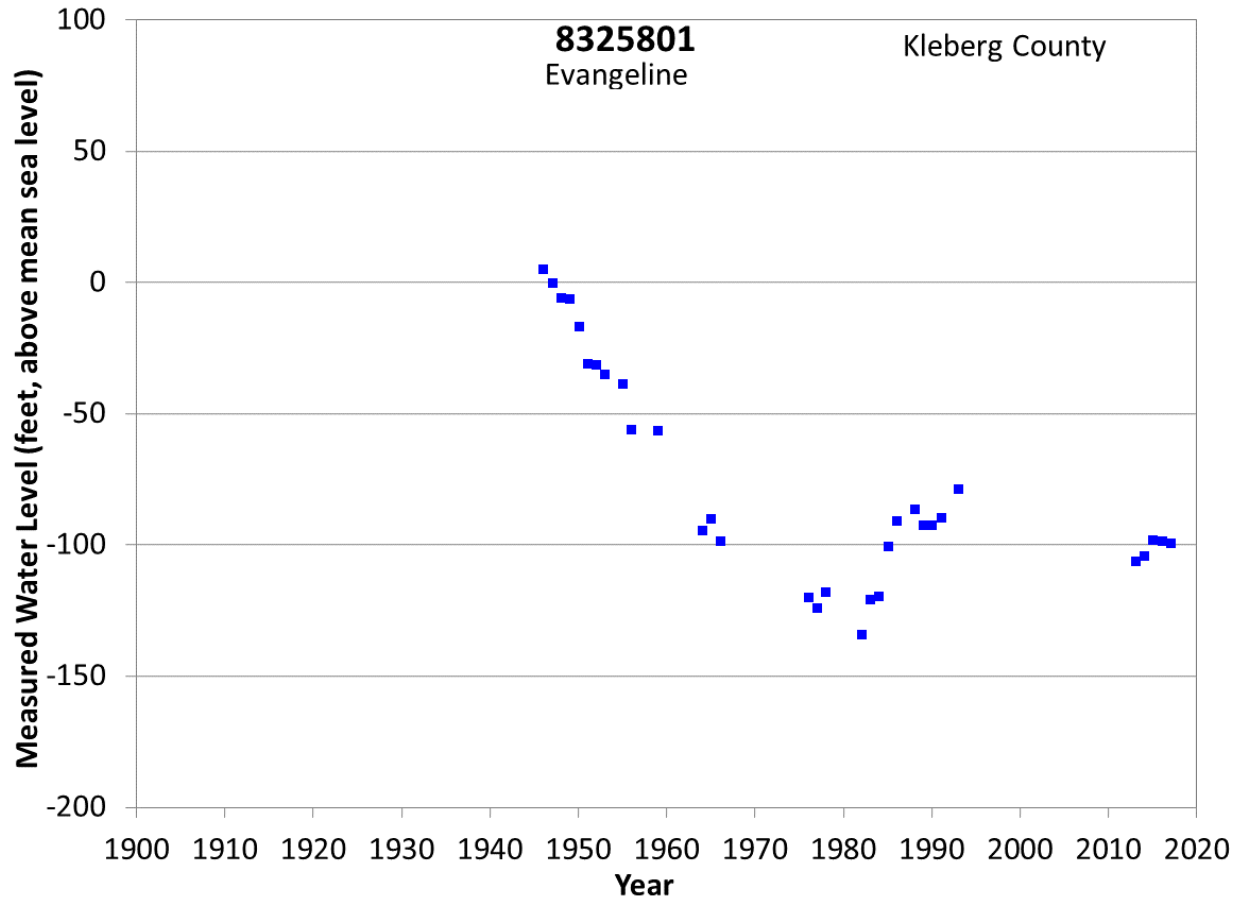


**Figure A85 Groundwater level hydrograph at State Well 8325801.**

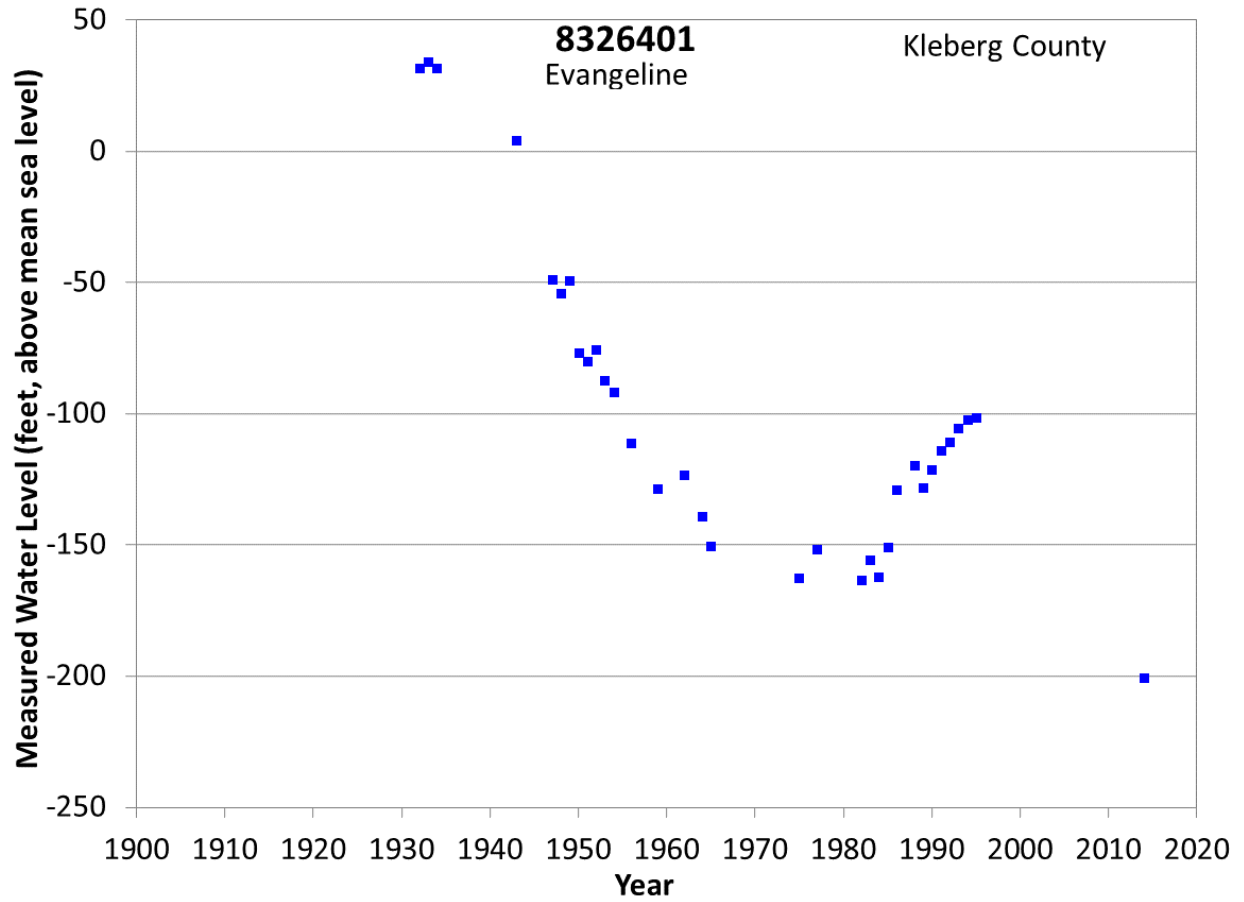


**Figure A86 Groundwater level hydrograph at State Well 8326401.**

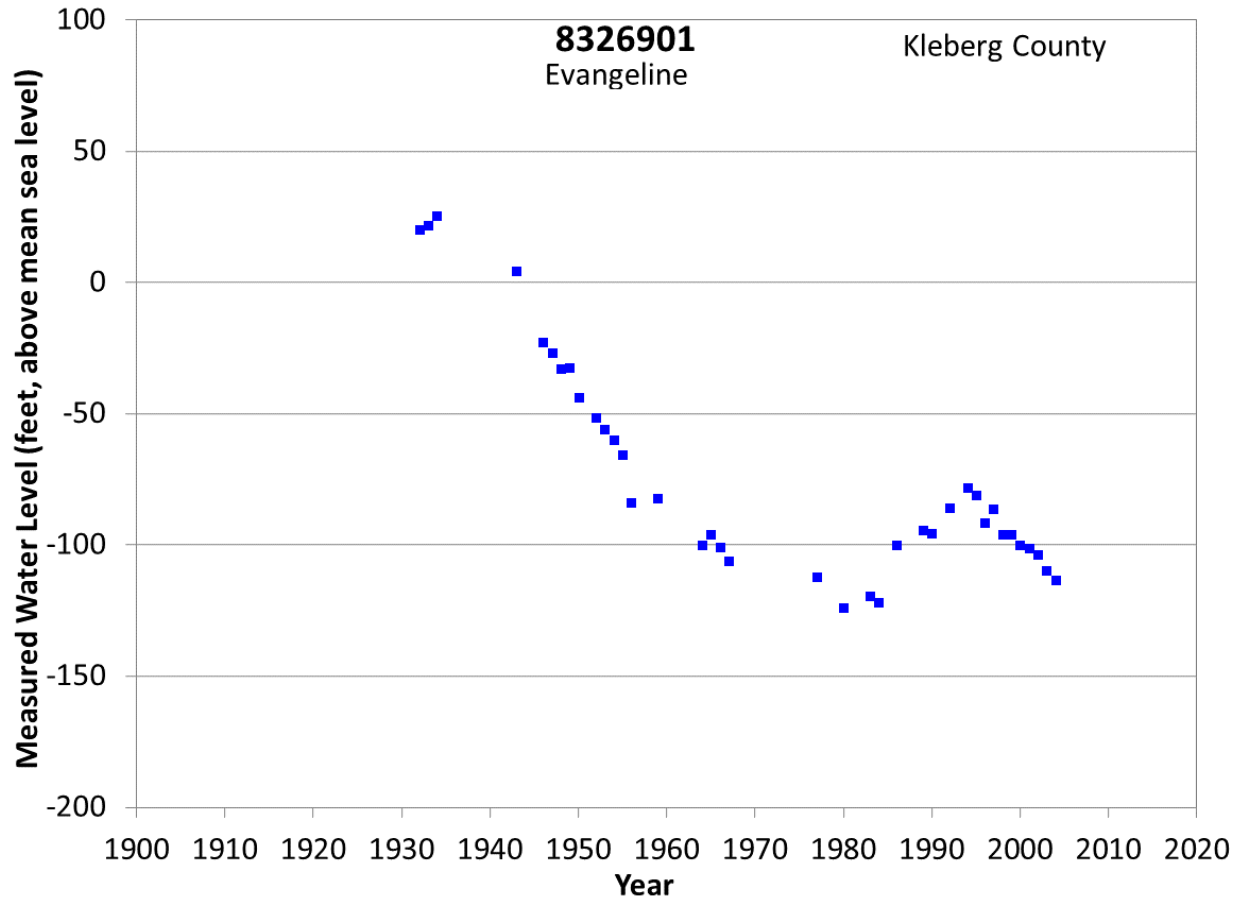


**Figure A87 Groundwater level hydrograph at State Well 8326901.**

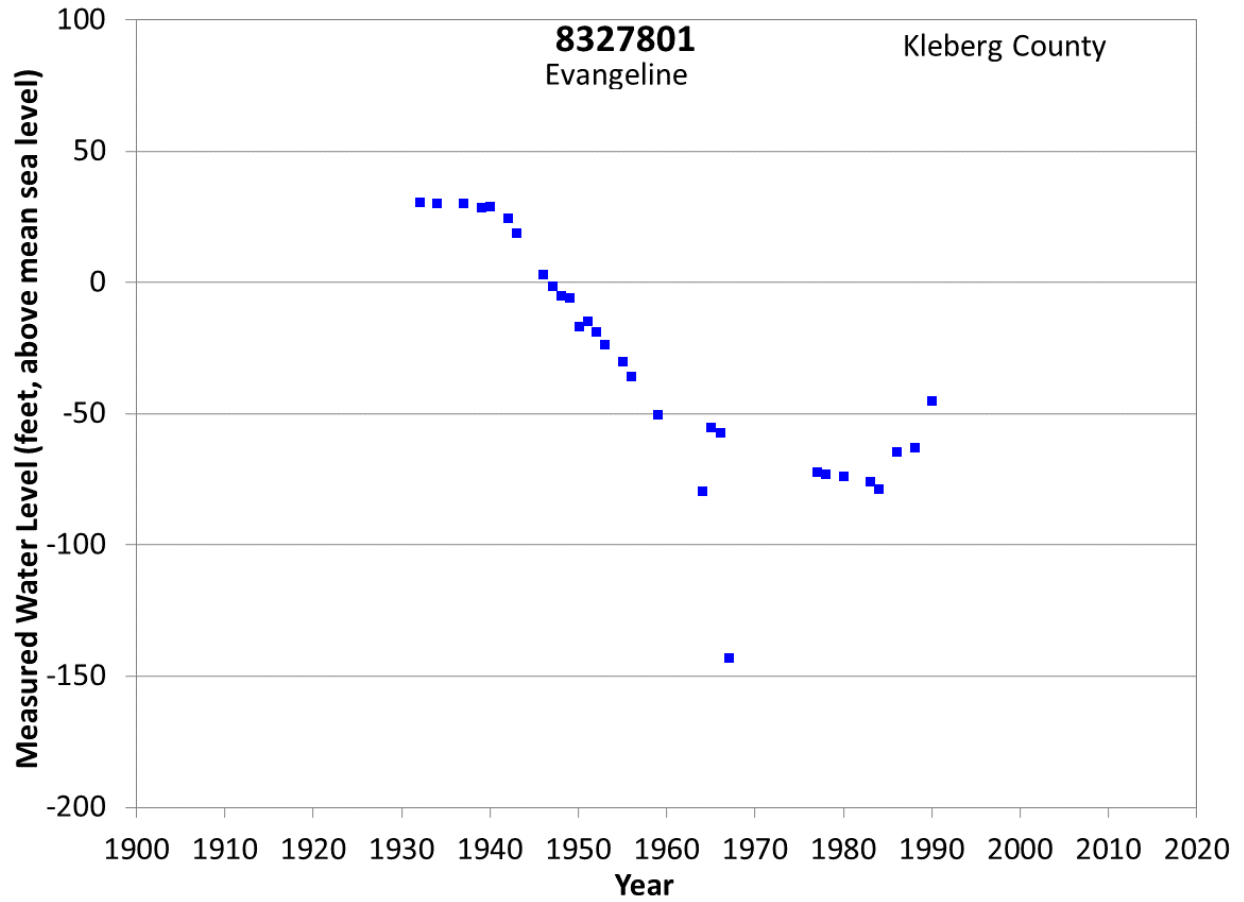


**Figure A88 Groundwater level hydrograph at State Well 8327801.**

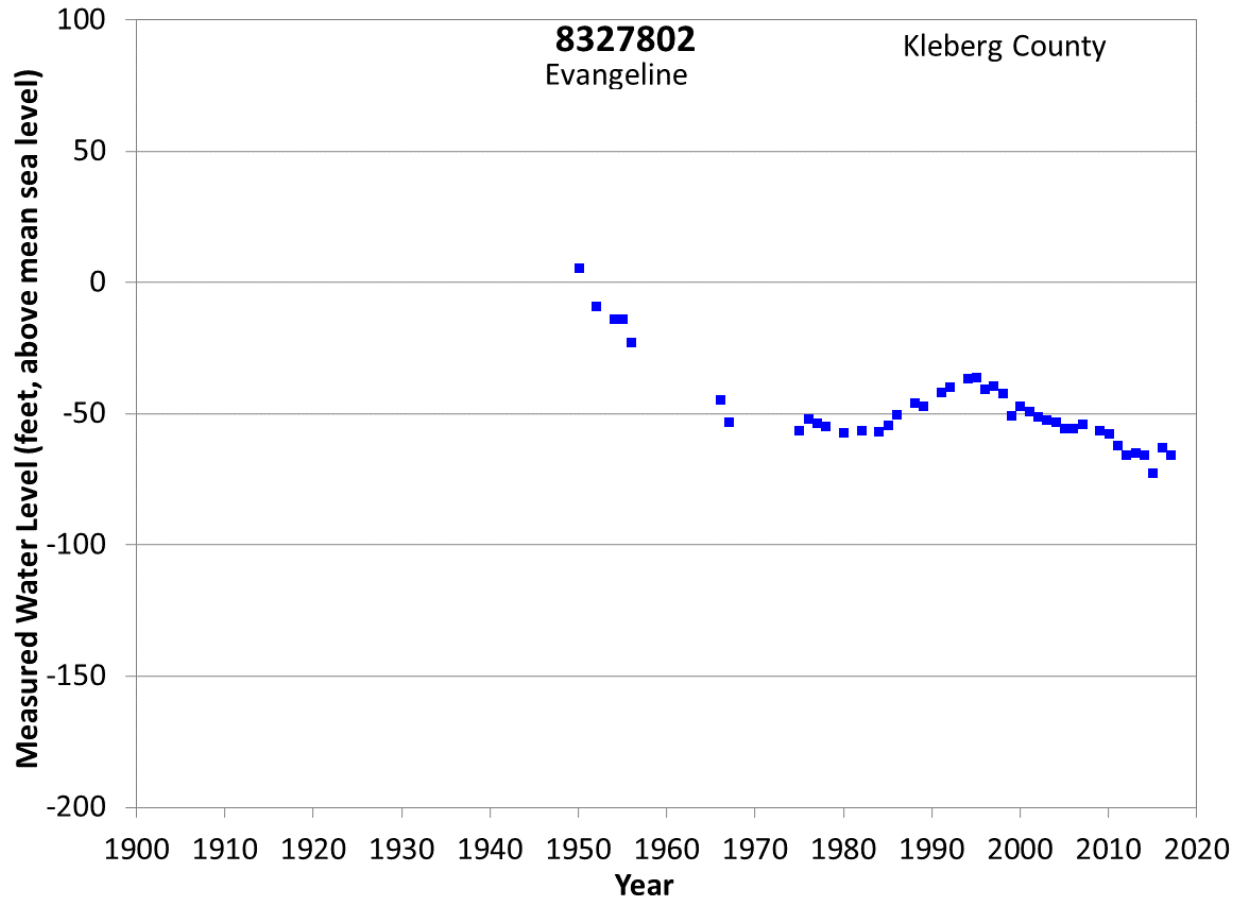


**Figure A89 Groundwater level hydrograph at State Well 8327802.**

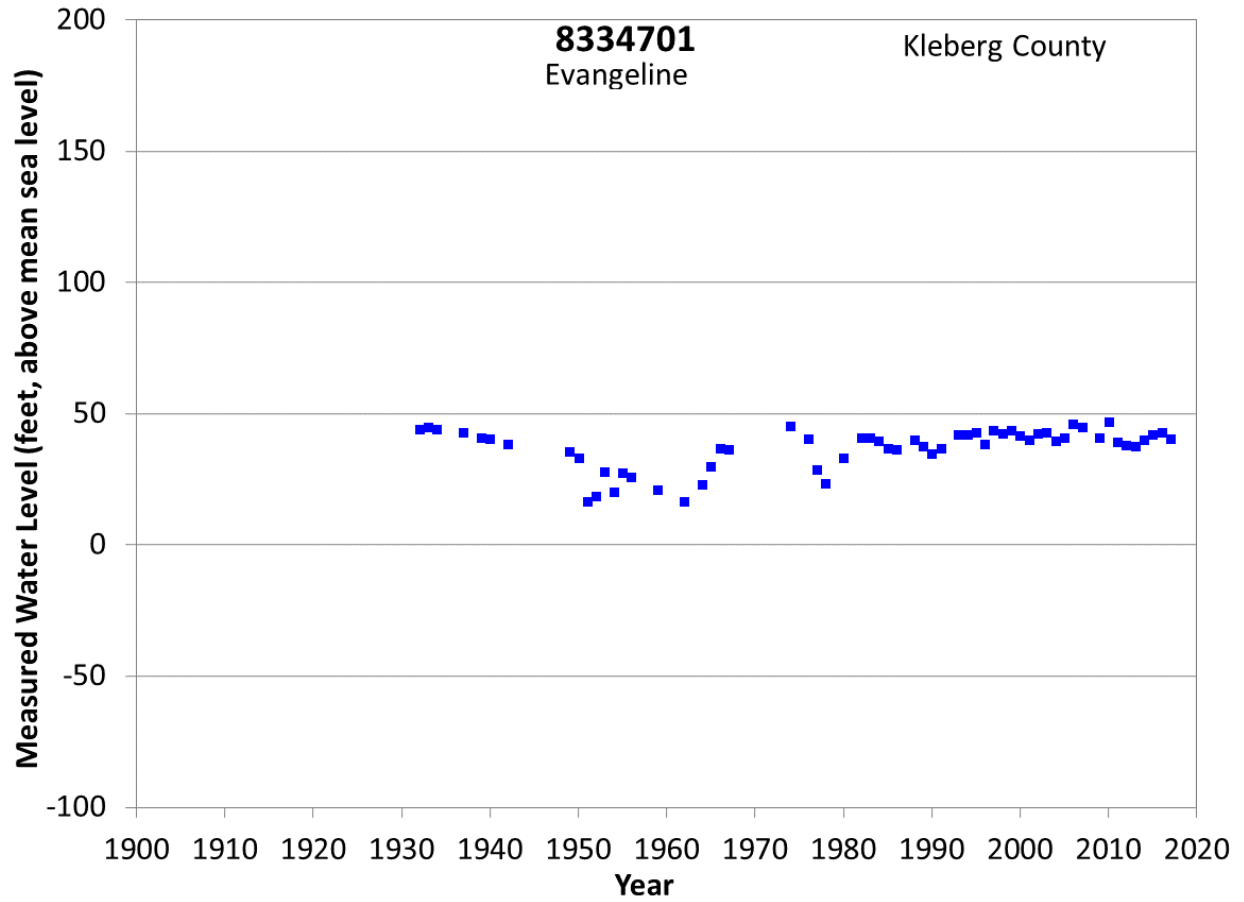


**Figure A90 Groundwater level hydrograph at State Well 8334701.**

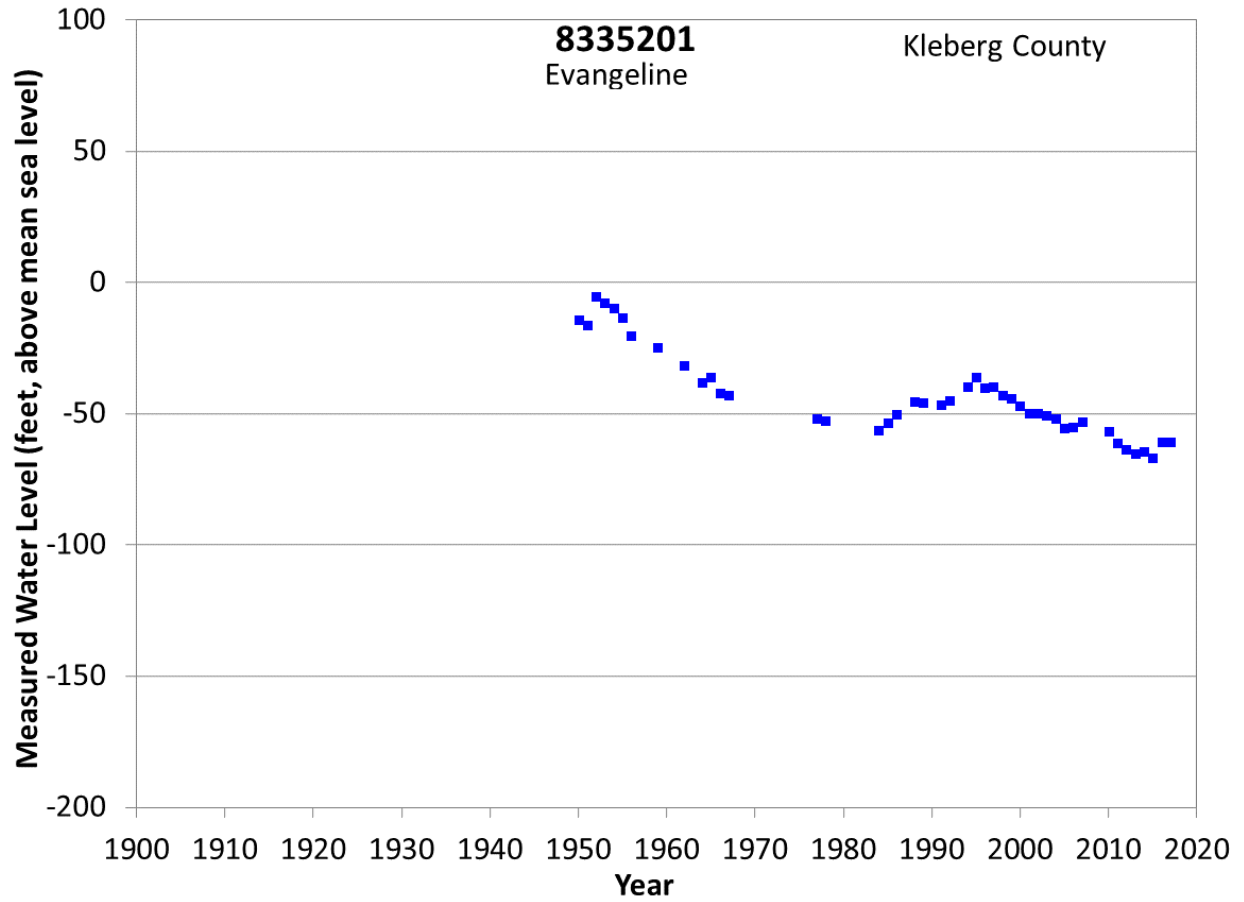


**Figure A91 Groundwater level hydrograph at State Well 8335201.**



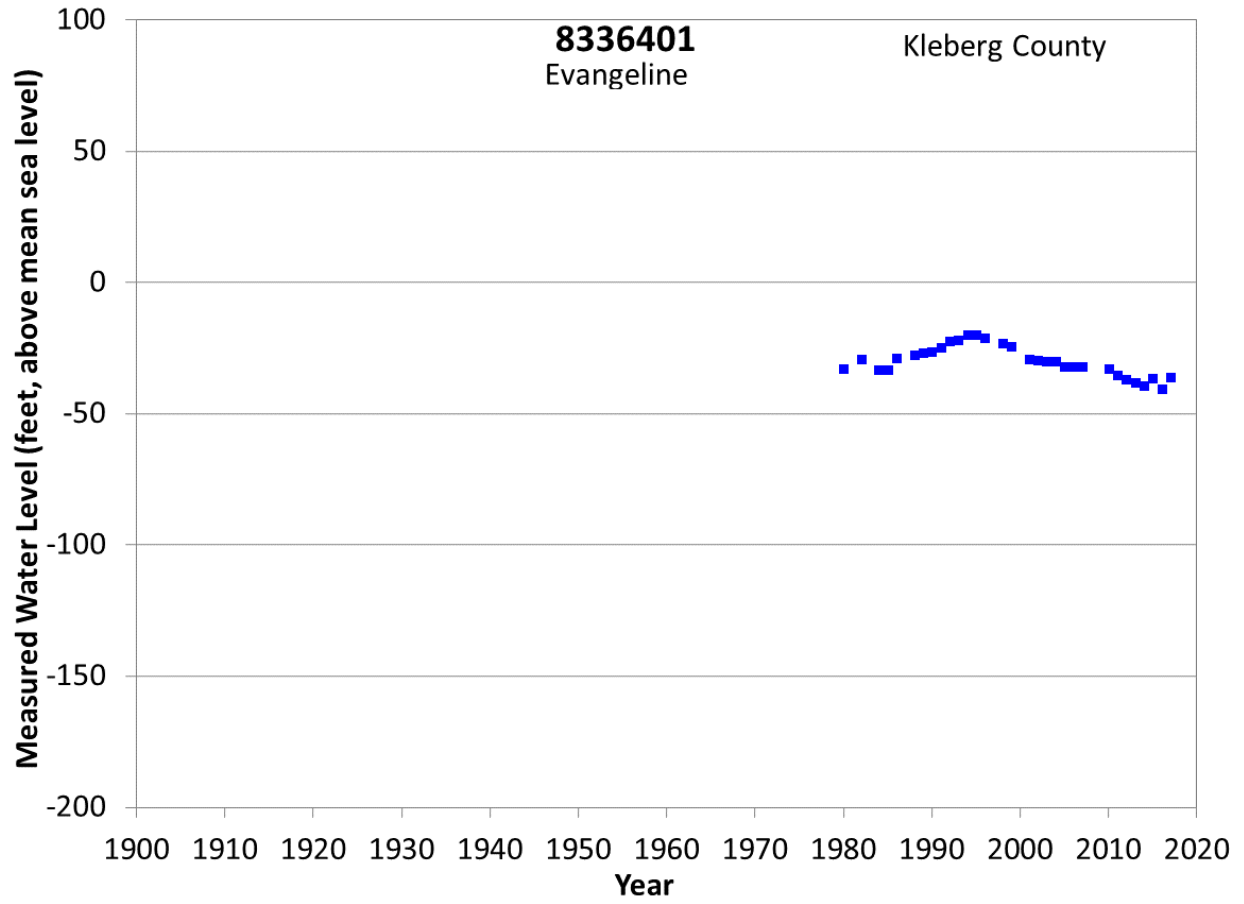


**Figure A92 Groundwater level hydrograph at State Well 8336401.**

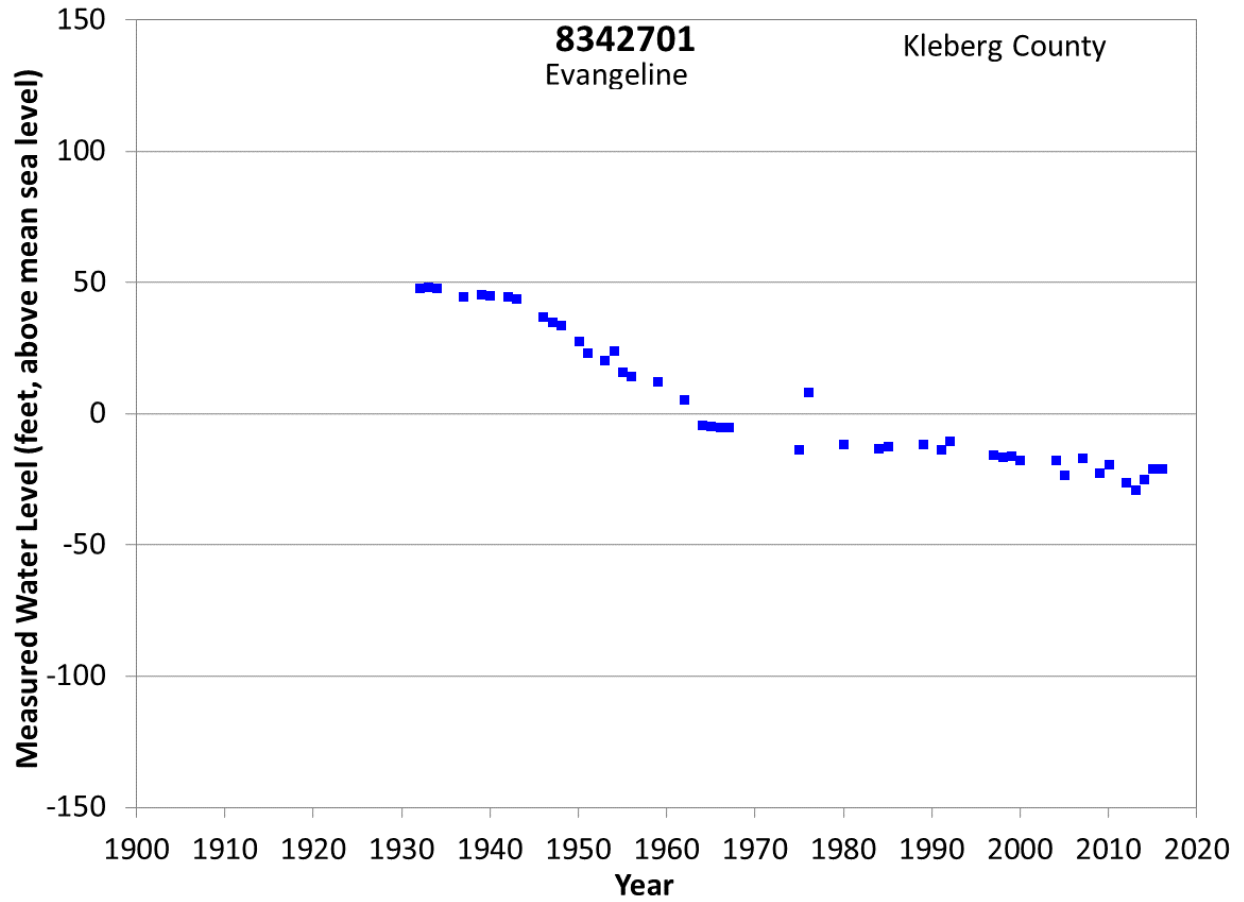


**Figure A93 Groundwater level hydrograph at State Well 8342701.**

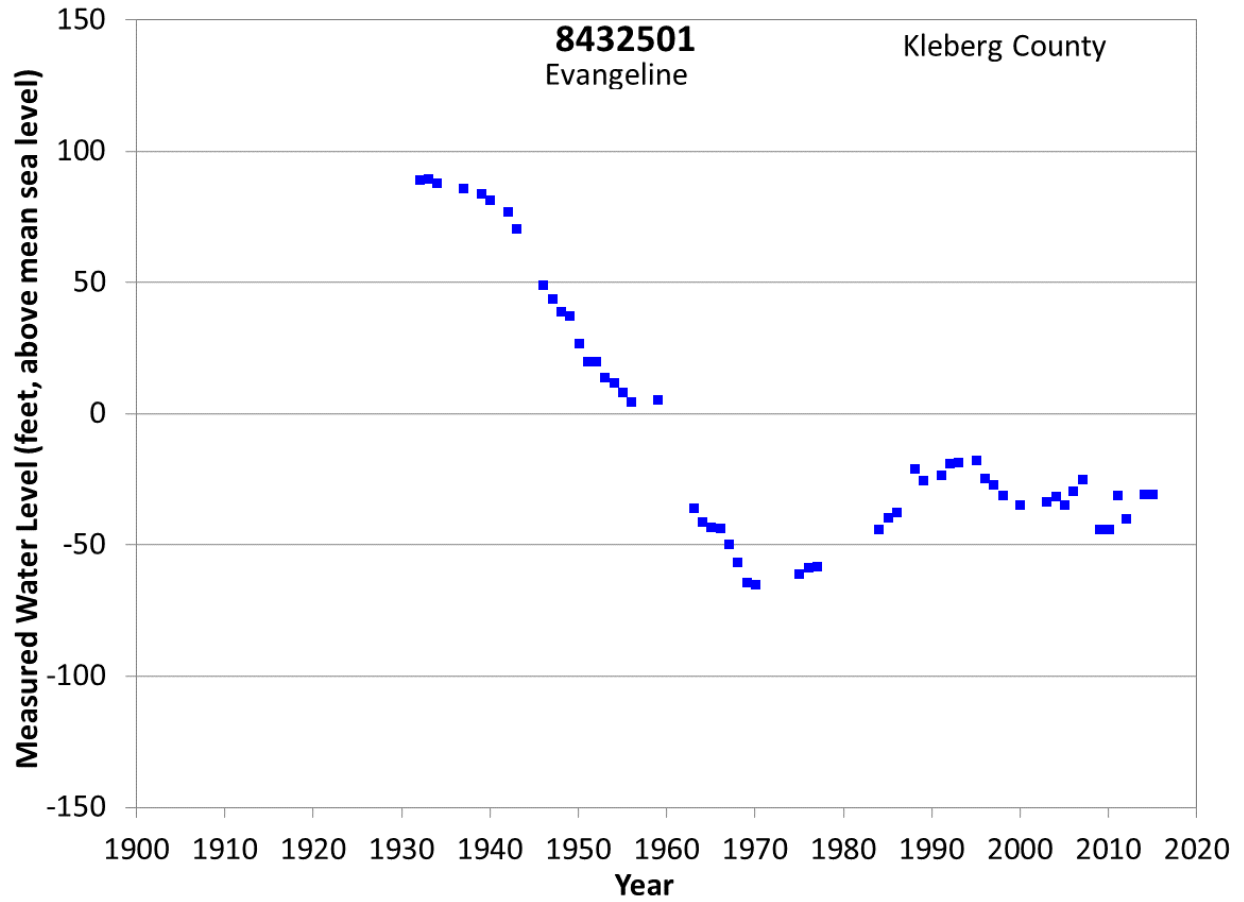


**Figure A94 Groundwater level hydrograph at State Well 8432501.**

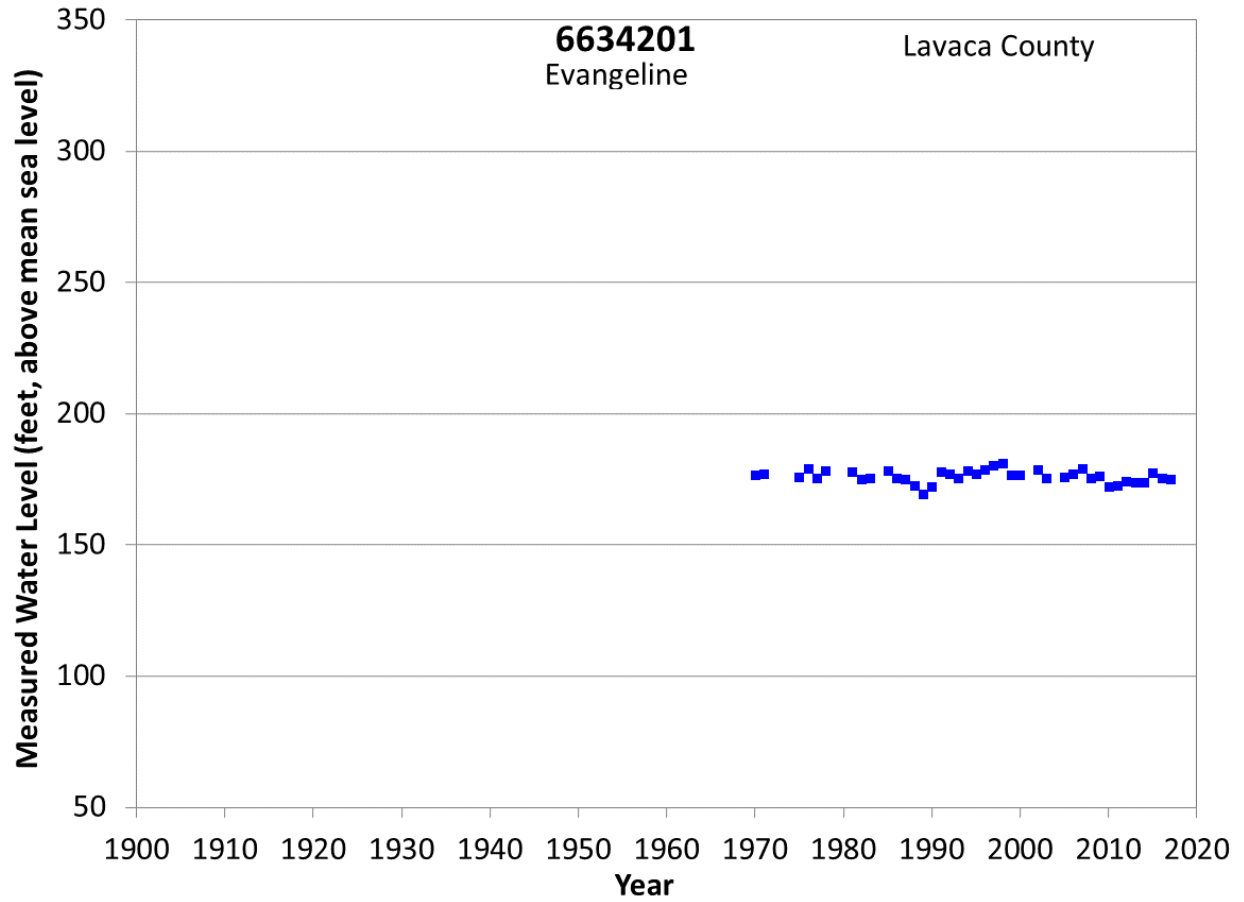


**Figure A95 Groundwater level hydrograph at State Well 6634201.**

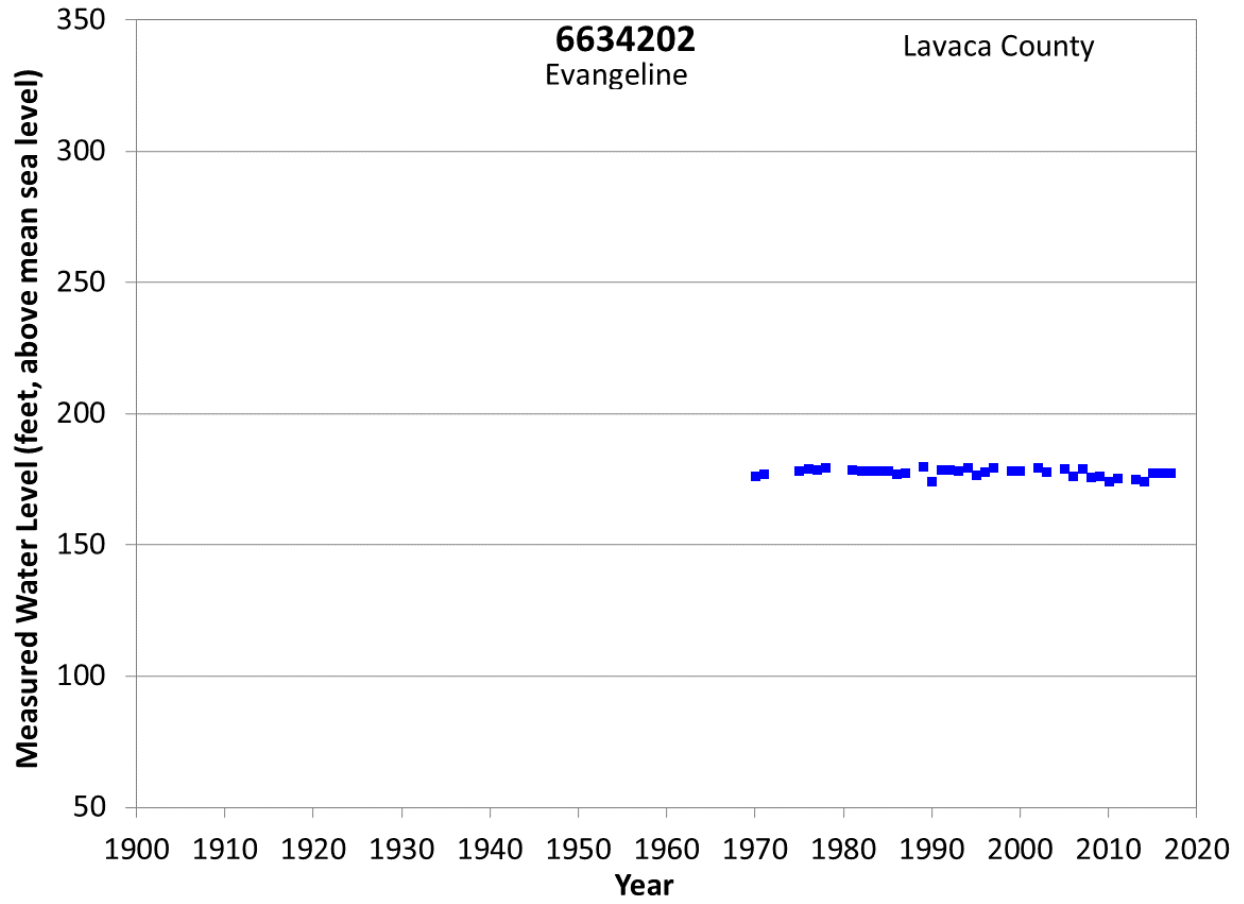


**Figure A96 Groundwater level hydrograph at State Well 6634202.**

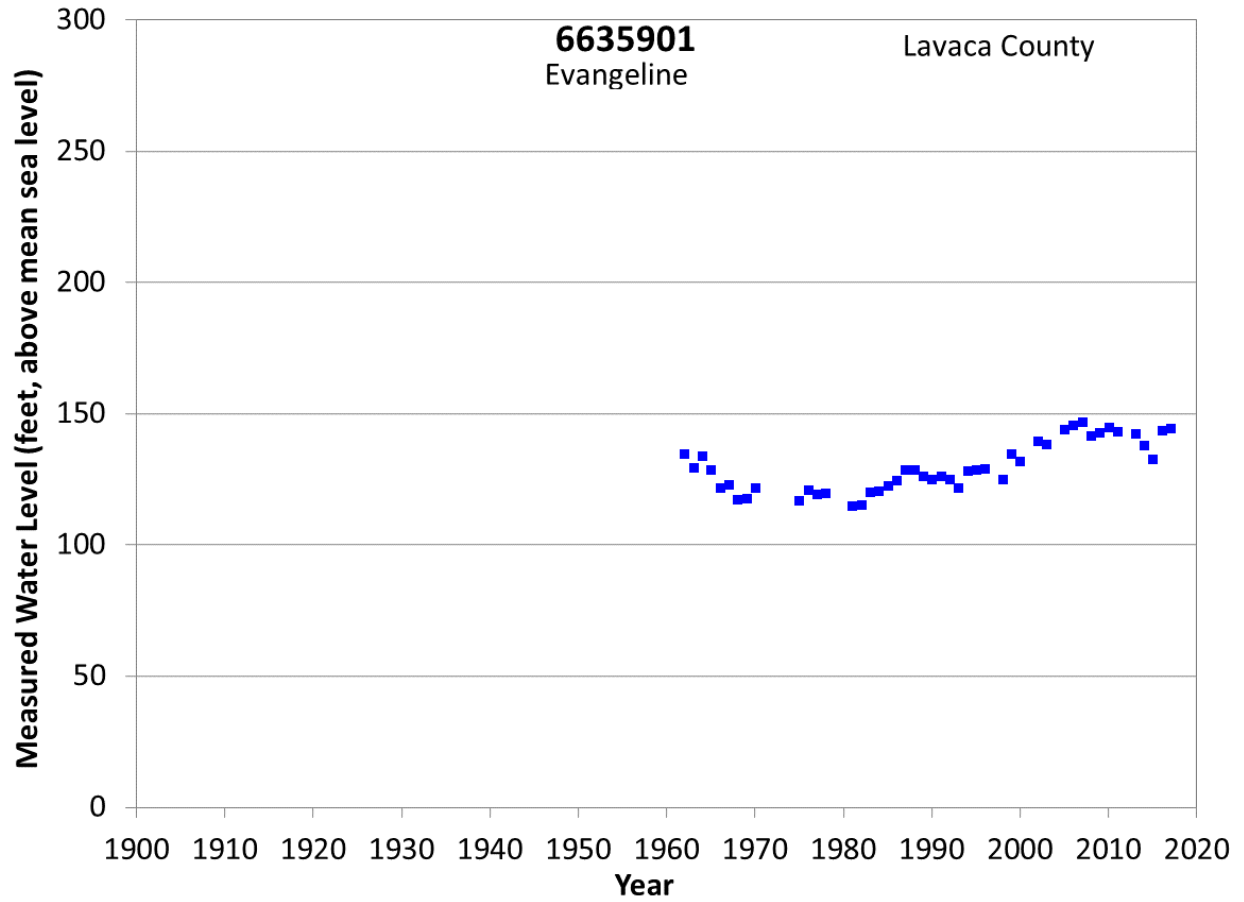


**Figure A97 Groundwater level hydrograph at State Well 6635901.**

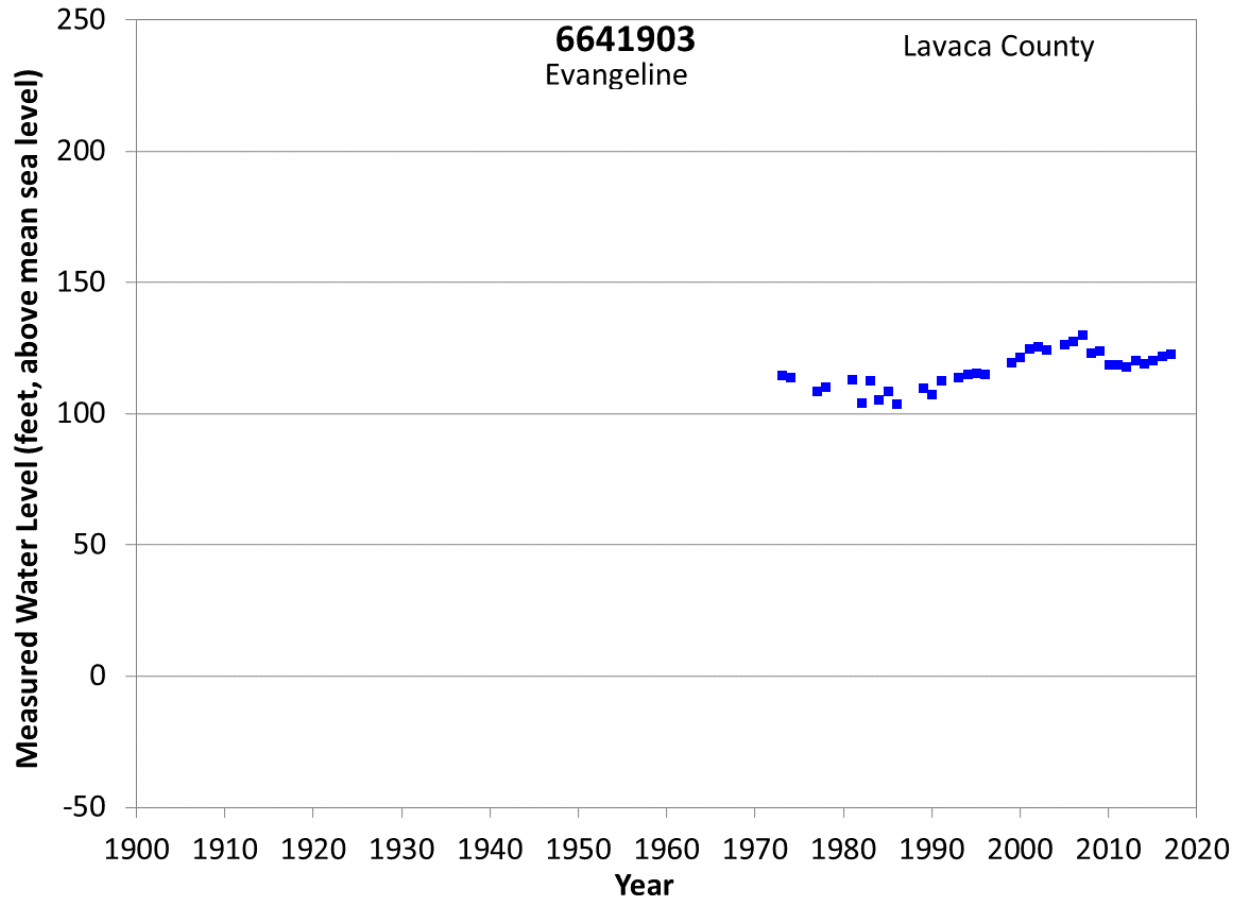


**Figure A98 Groundwater level hydrograph at State Well 6641903.**

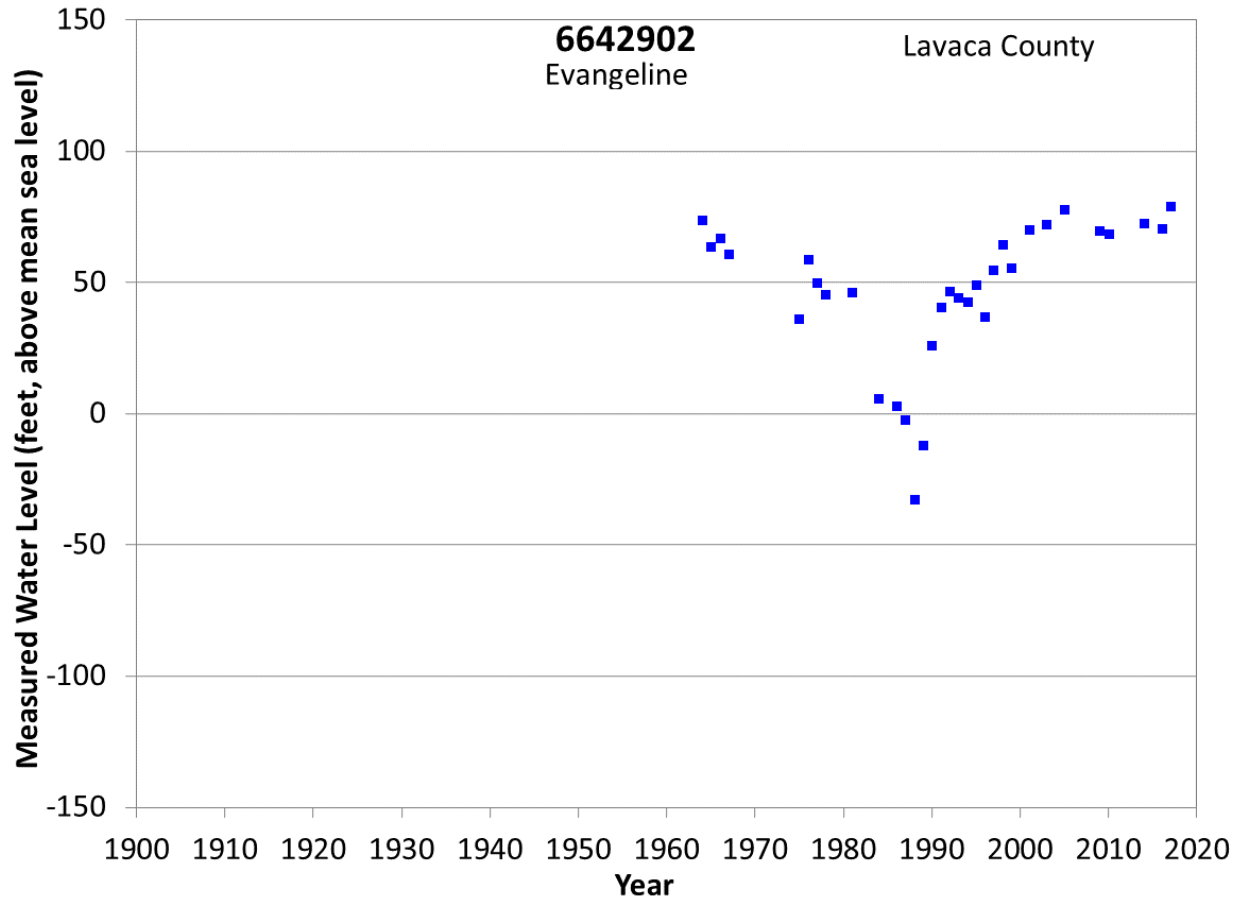


**Figure A99 Groundwater level hydrograph at State Well 6642902.**



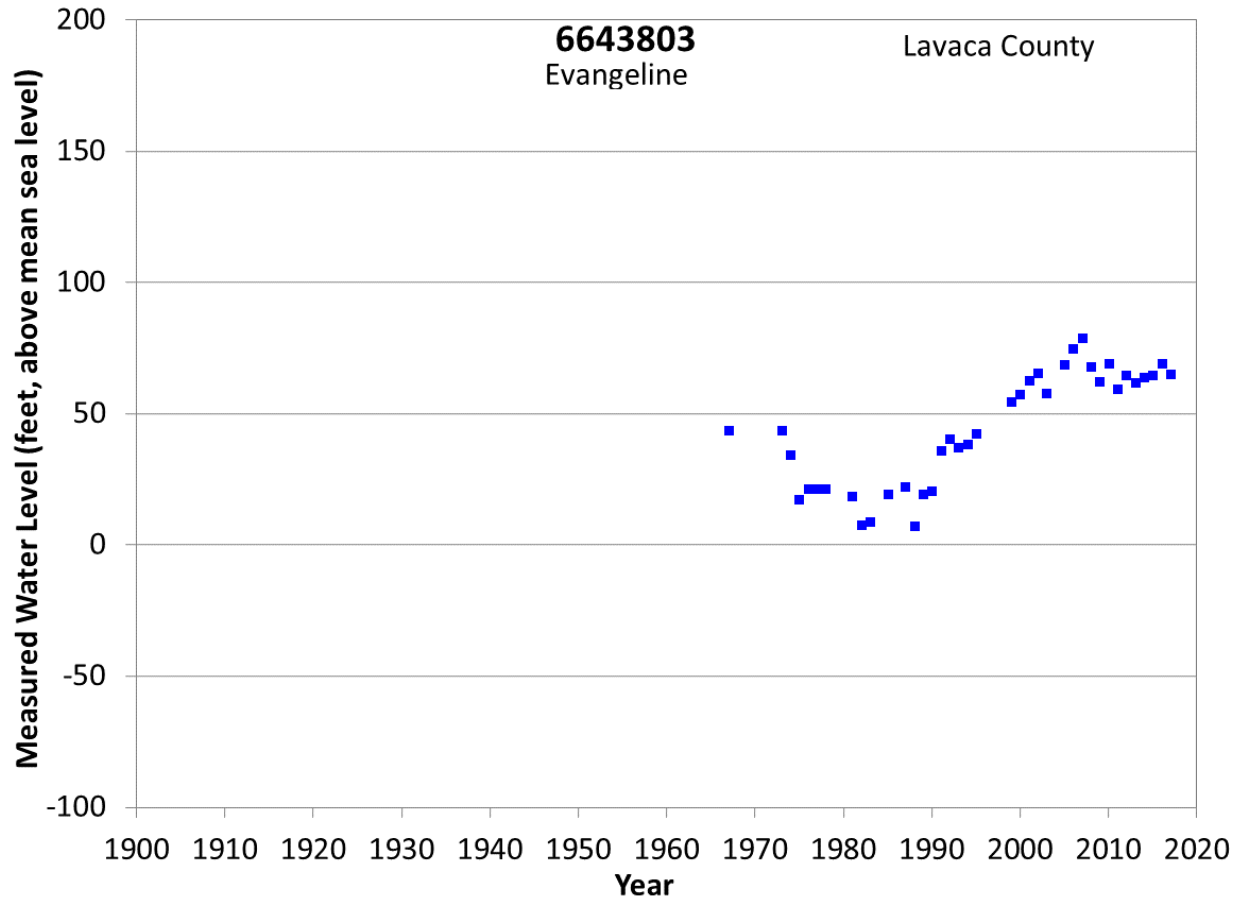


**Figure A100 Groundwater level hydrograph at State Well 6643803.**

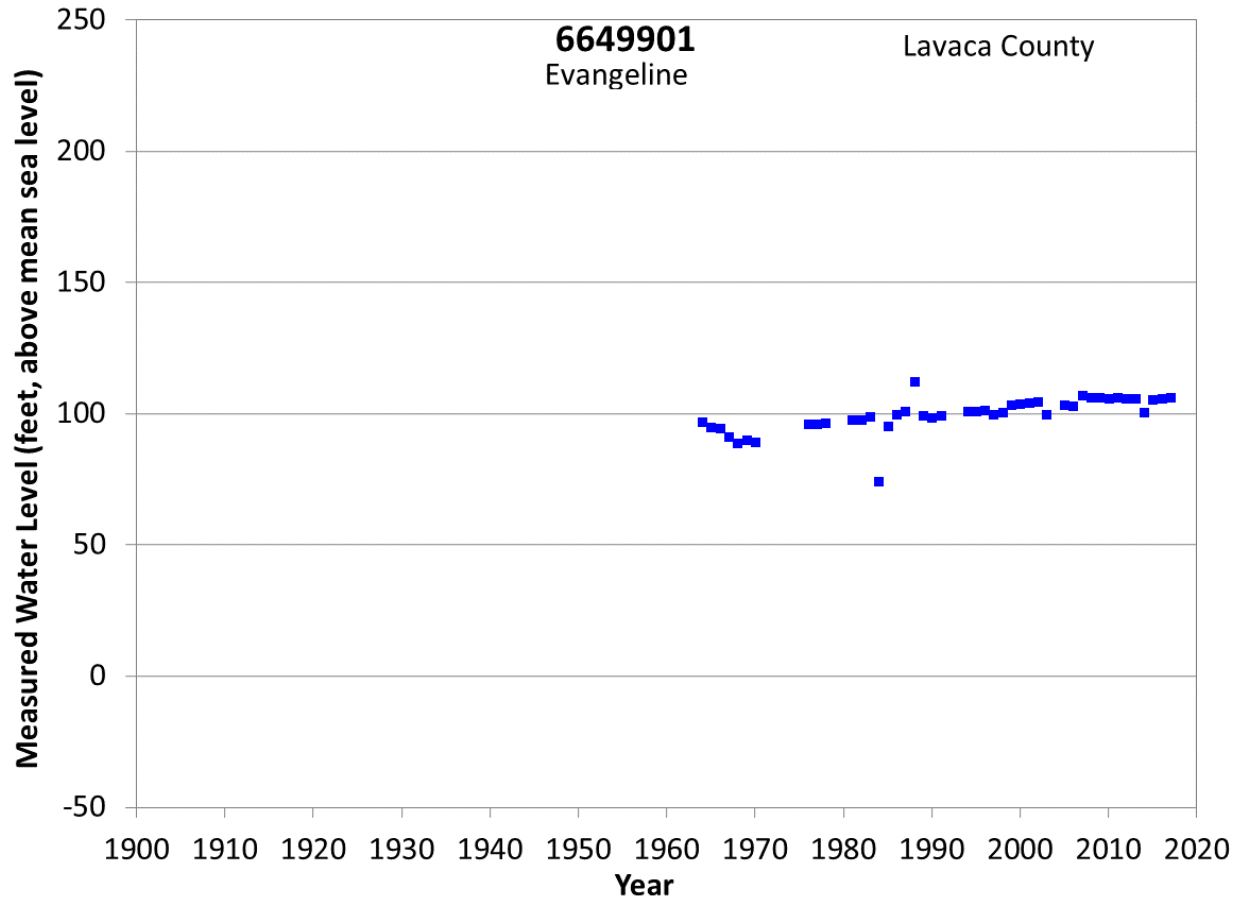


**Figure A101 Groundwater level hydrograph at State Well 6649901.**

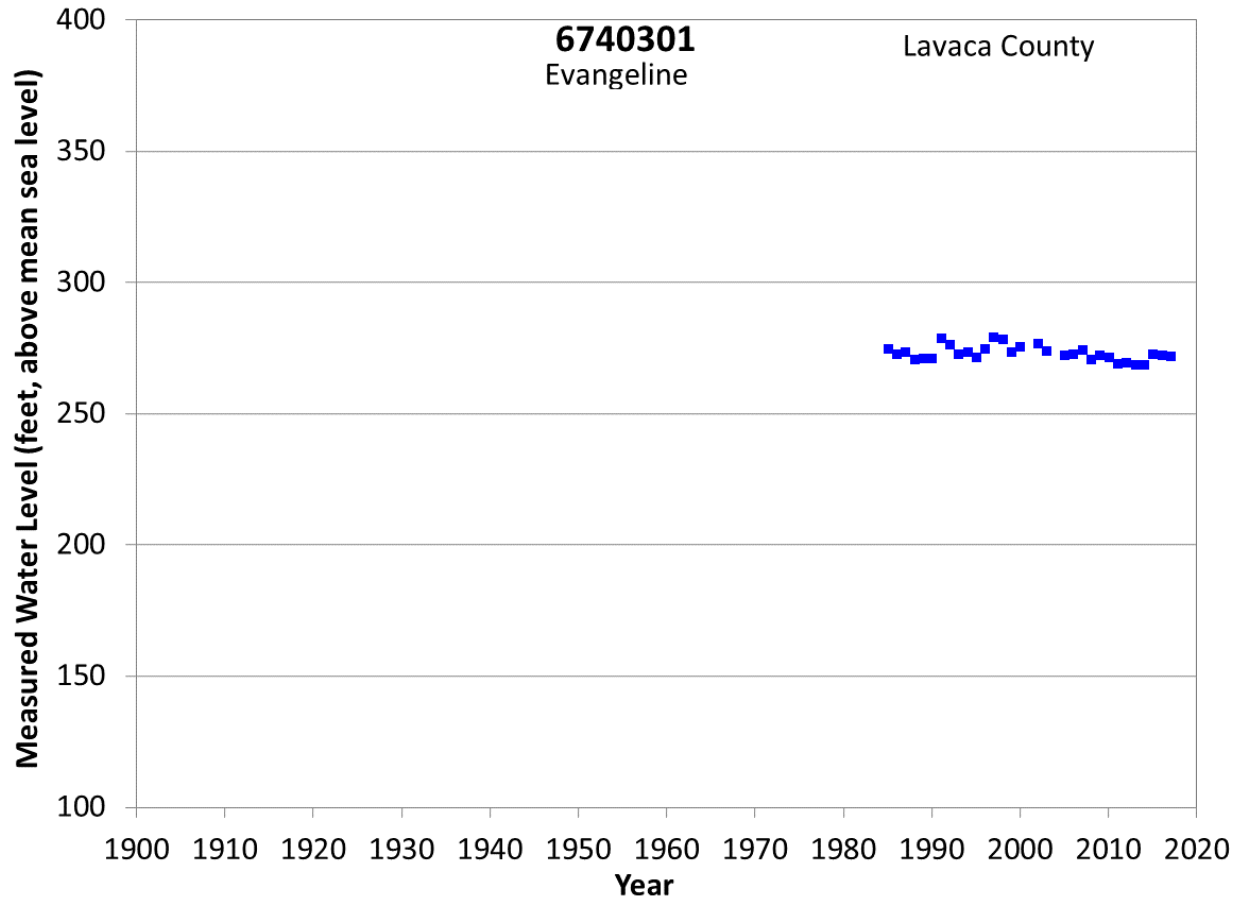


**Figure A102 Groundwater level hydrograph at State Well 6740301.**

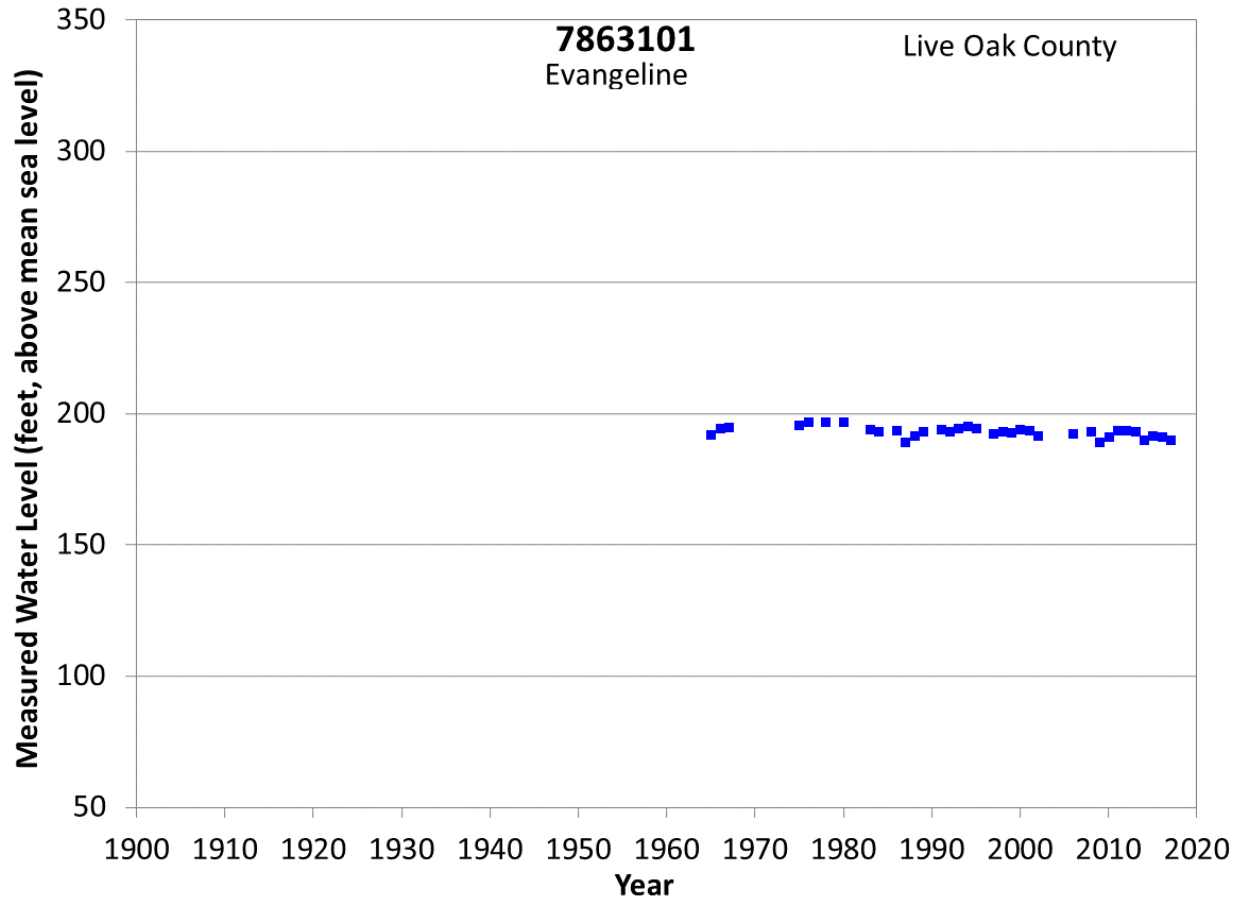


**Figure A103 Groundwater level hydrograph at State Well 7863101.**

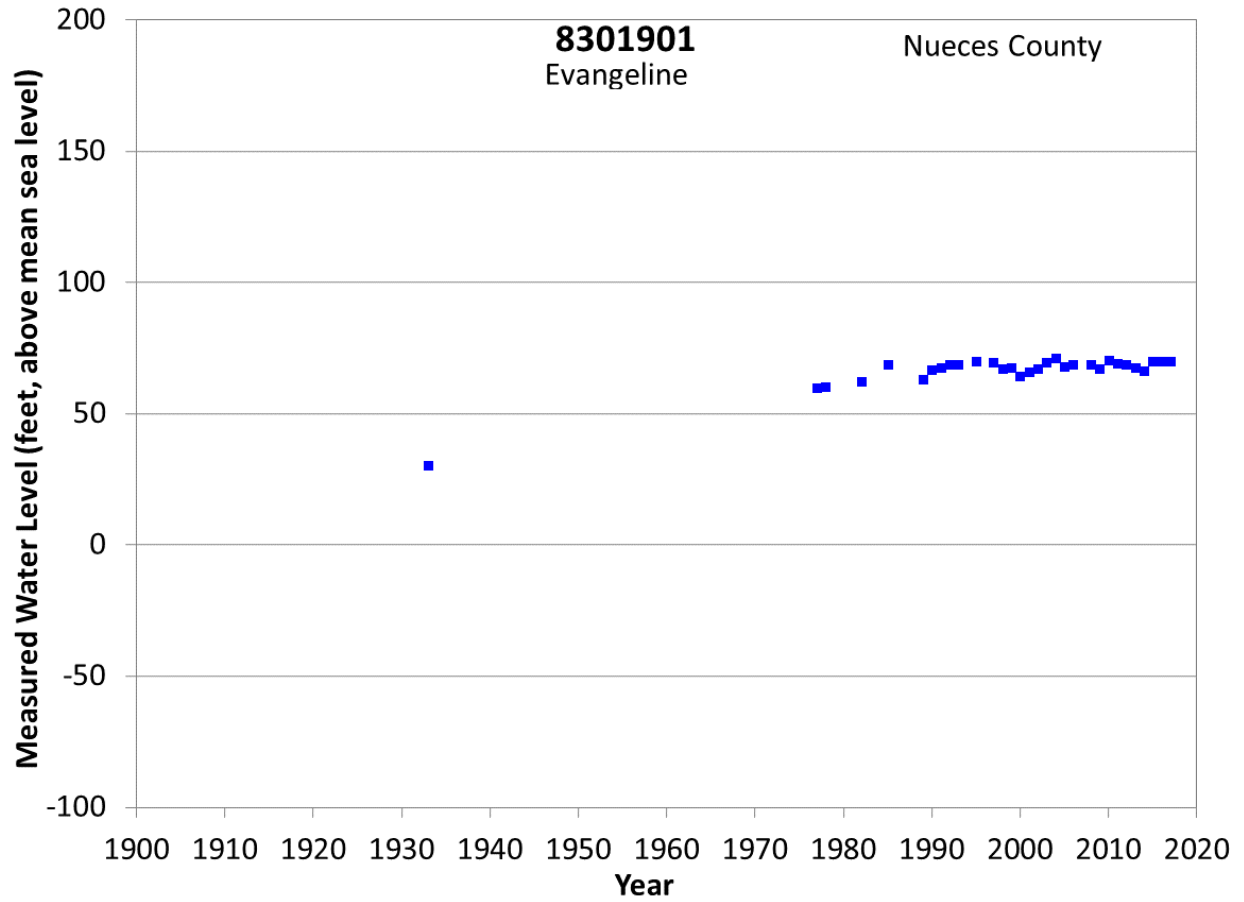


**Figure A104 Groundwater level hydrograph at State Well 8301901.**

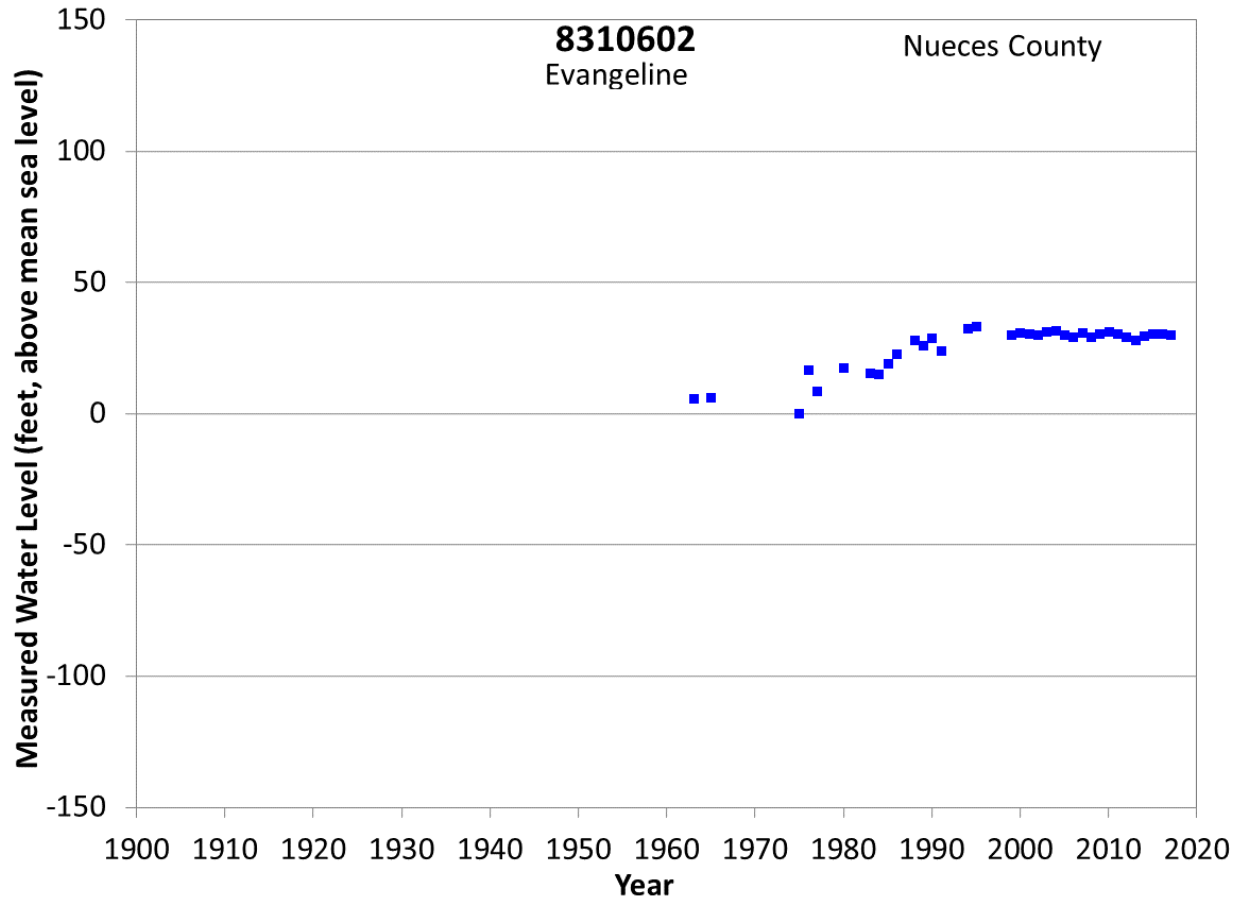


**Figure A105 Groundwater level hydrograph at State Well 8310602.**

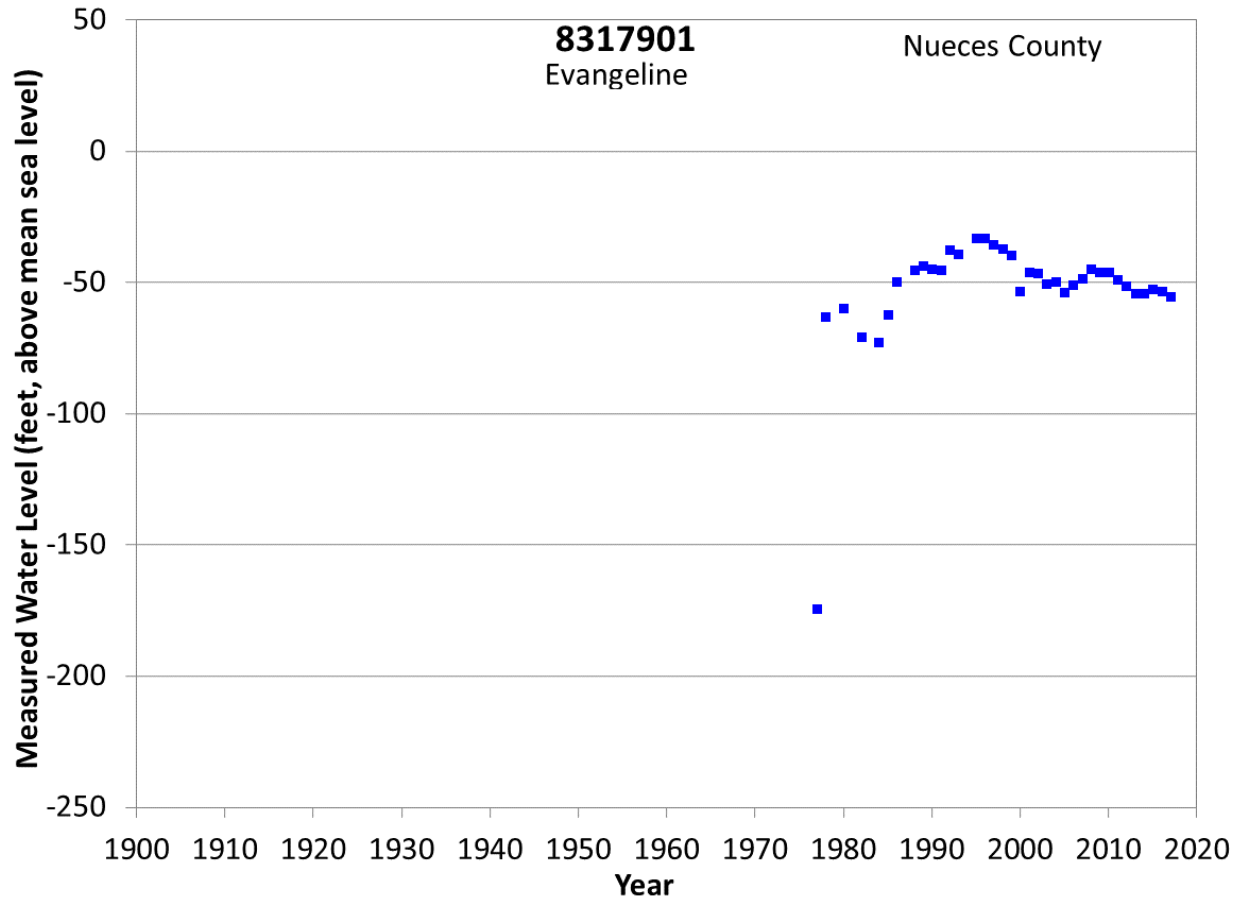


**Figure A106 Groundwater level hydrograph at State Well 8317901.**

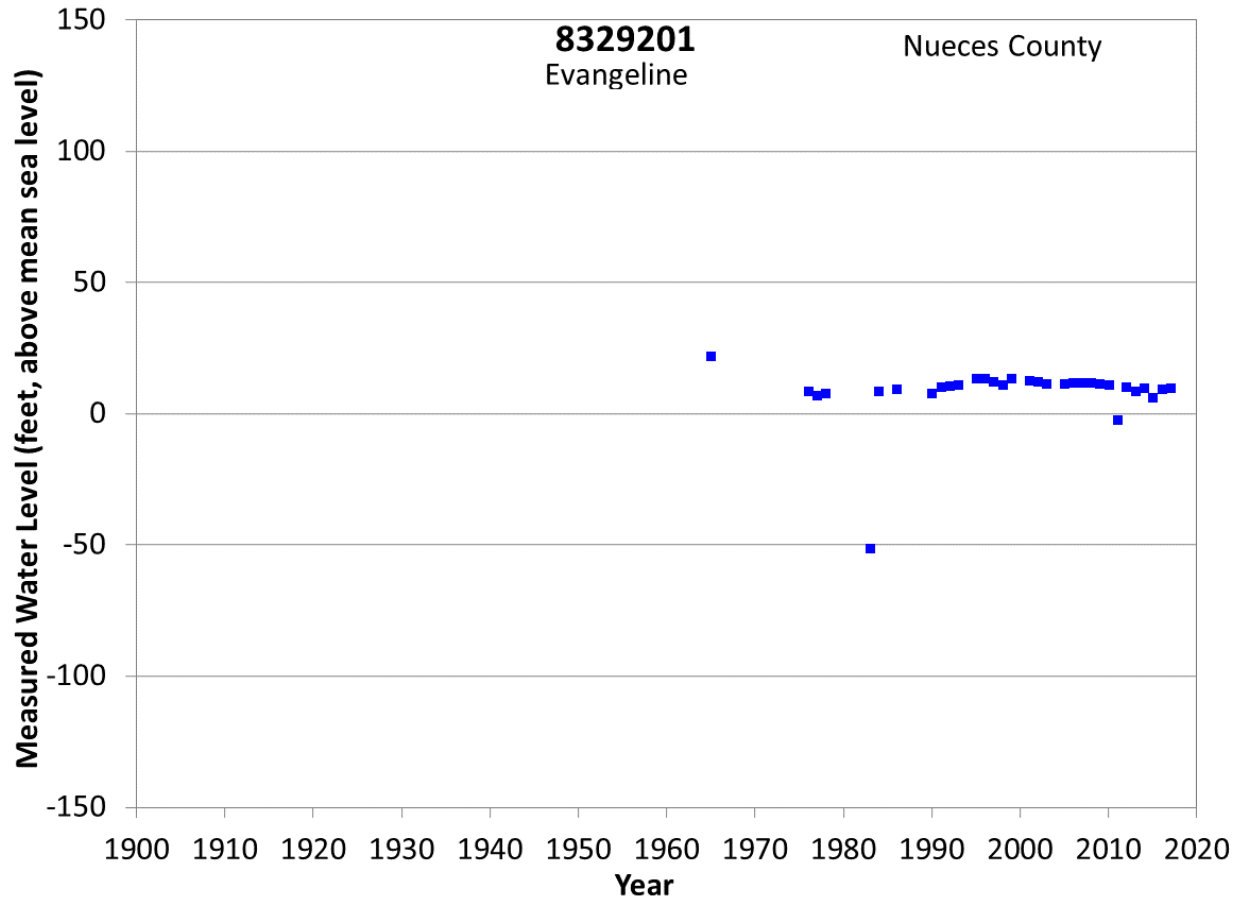


**Figure A107 Groundwater level hydrograph at State Well 8329201.**



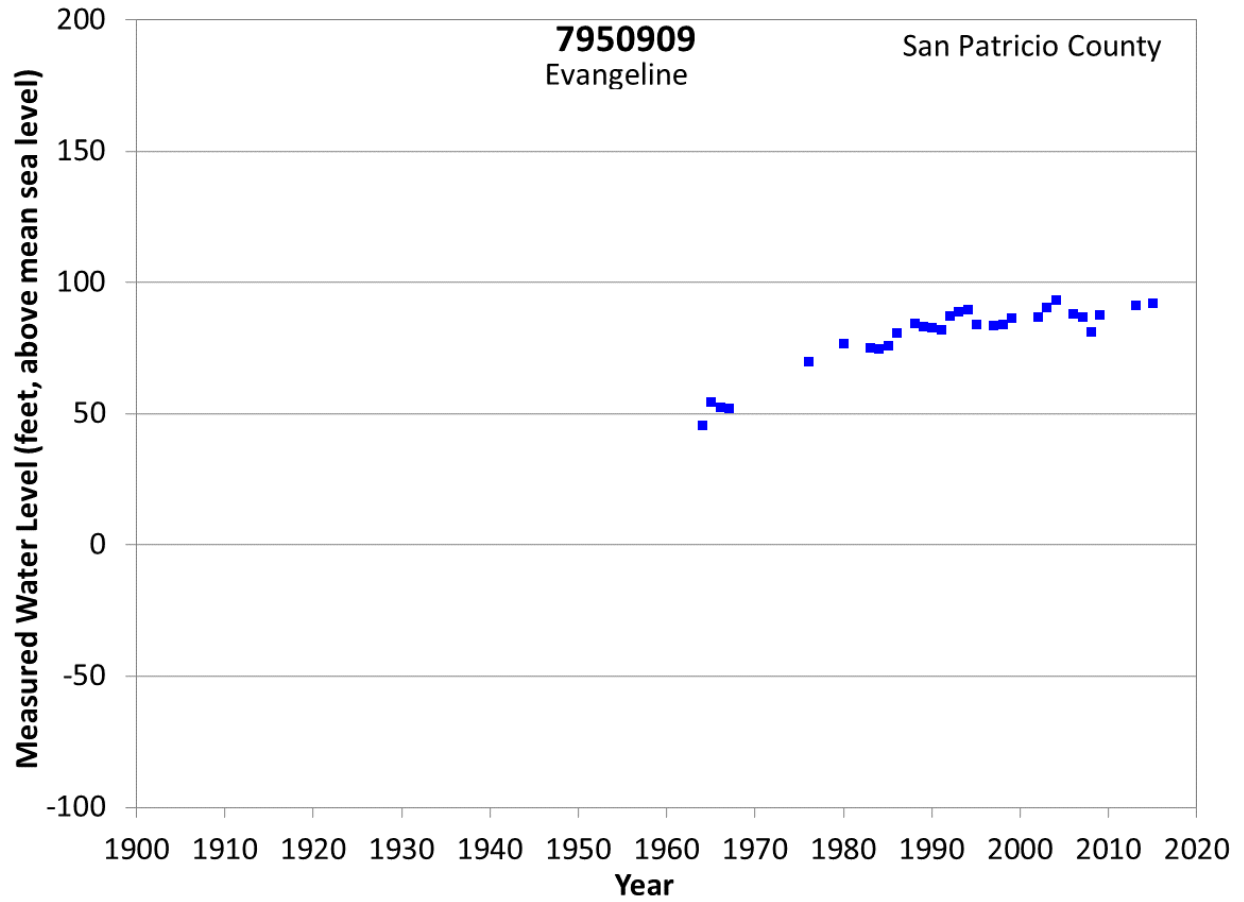


**Figure A108 Groundwater level hydrograph at State Well 7950909.**

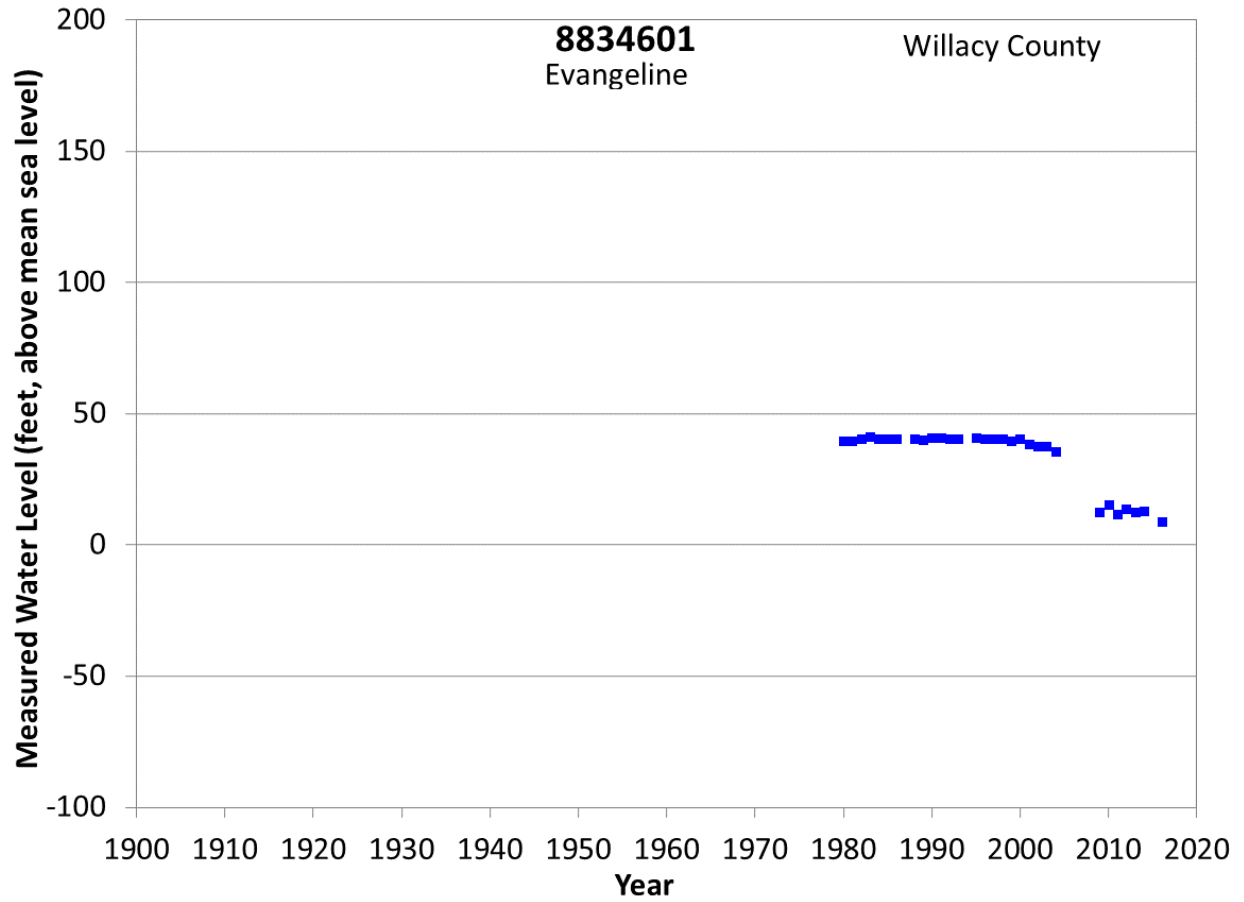


**Figure A109 Groundwater level hydrograph at State Well 8834601.**

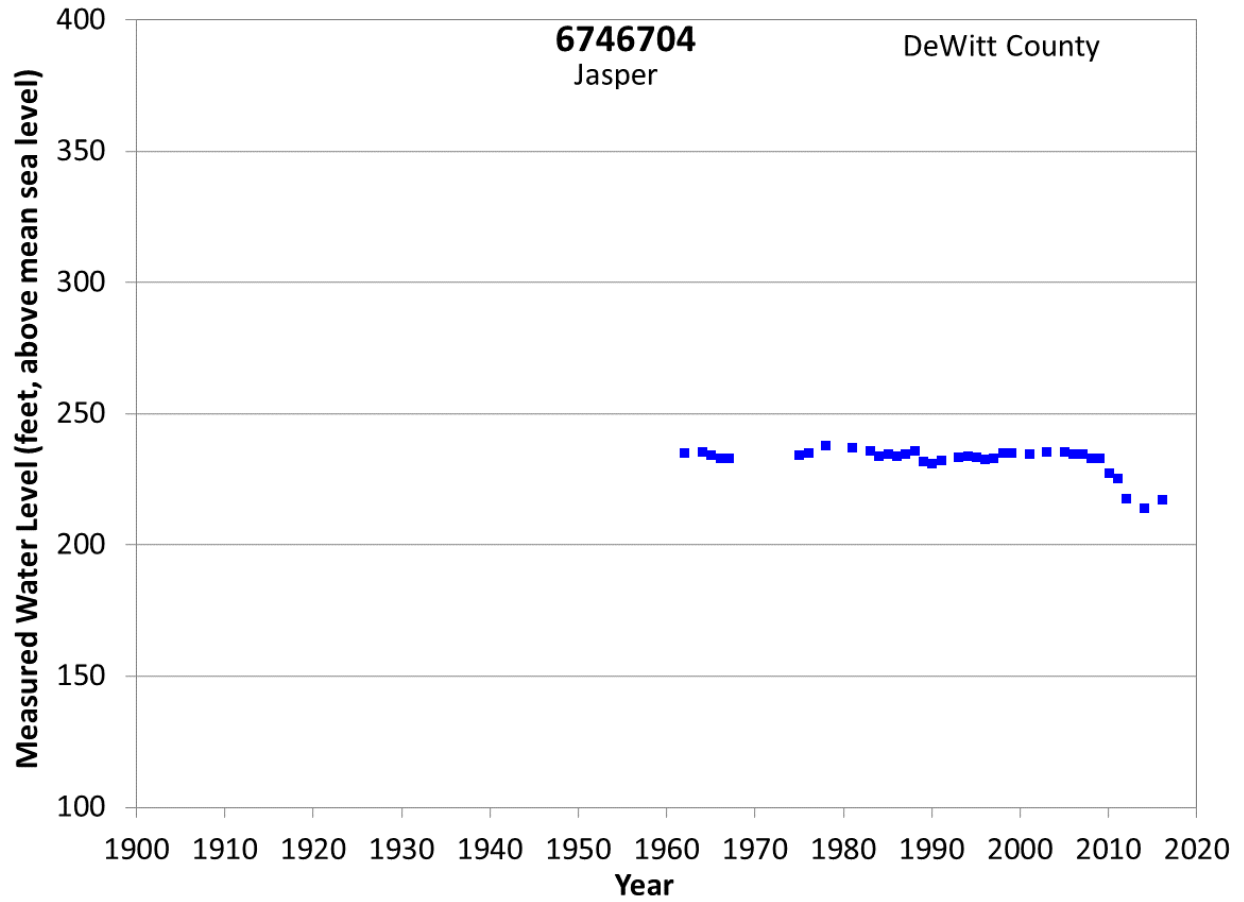


**Figure A110 Groundwater level hydrograph at State Well 6746704.**

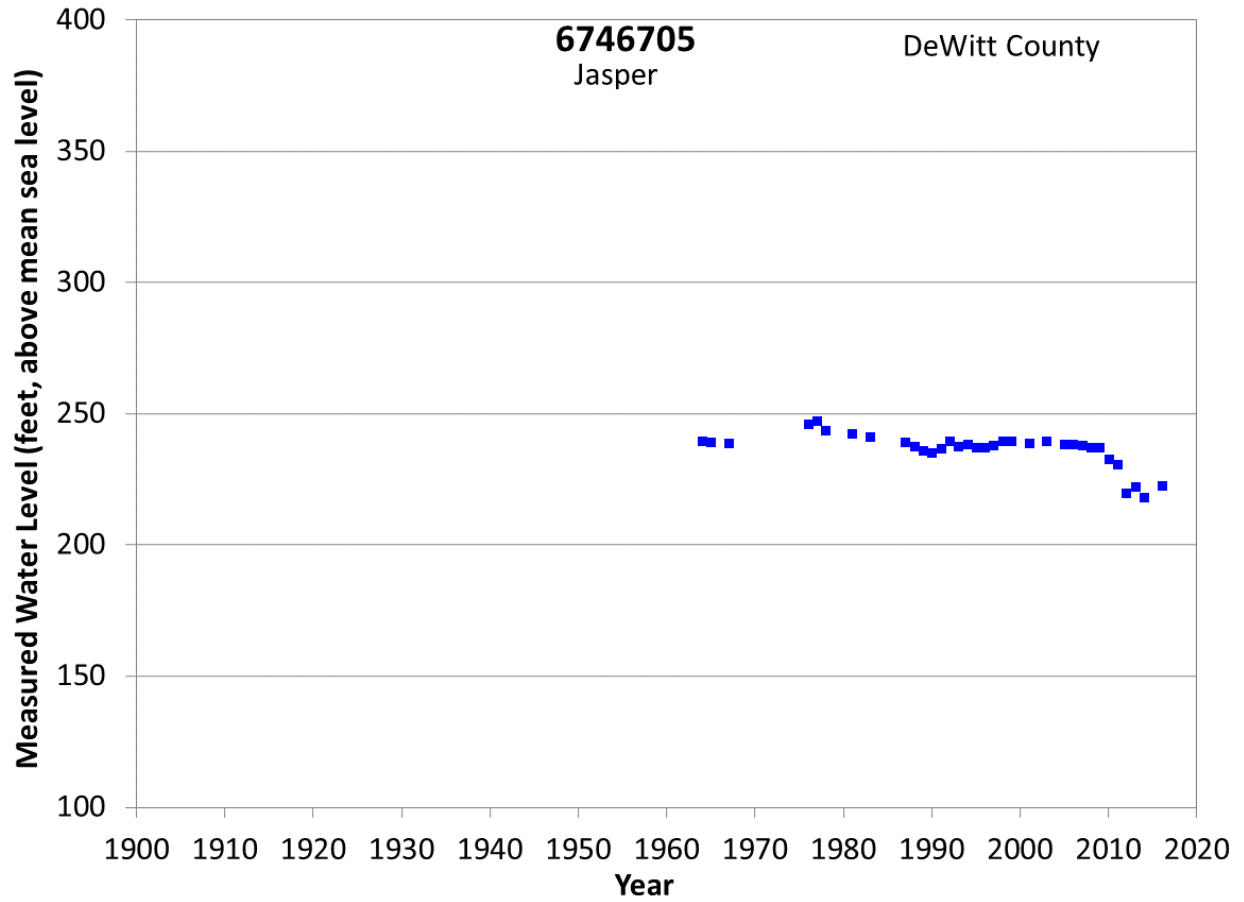


**Figure A111 Groundwater level hydrograph at State Well 6746705.**

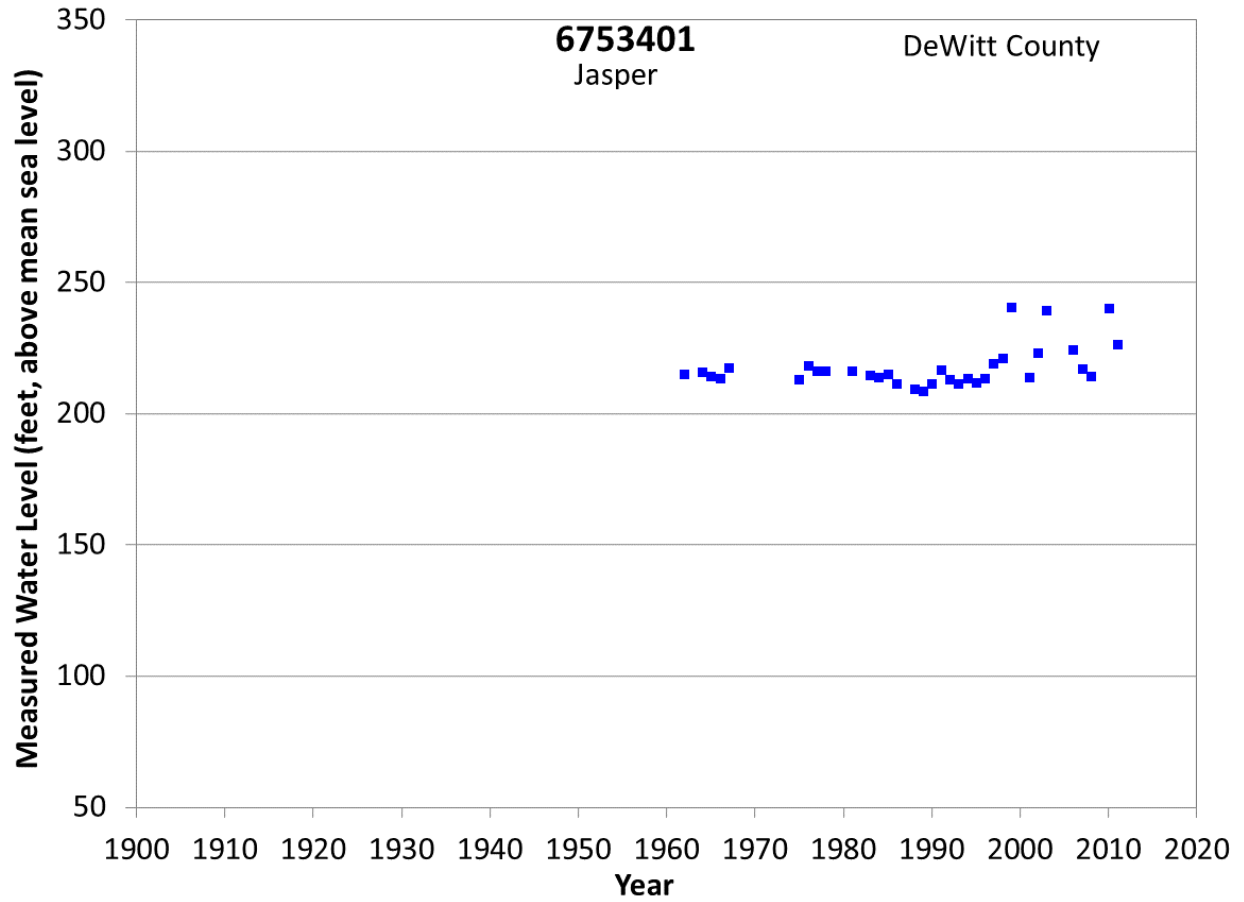


**Figure A112 Groundwater level hydrograph at State Well 6753401.**

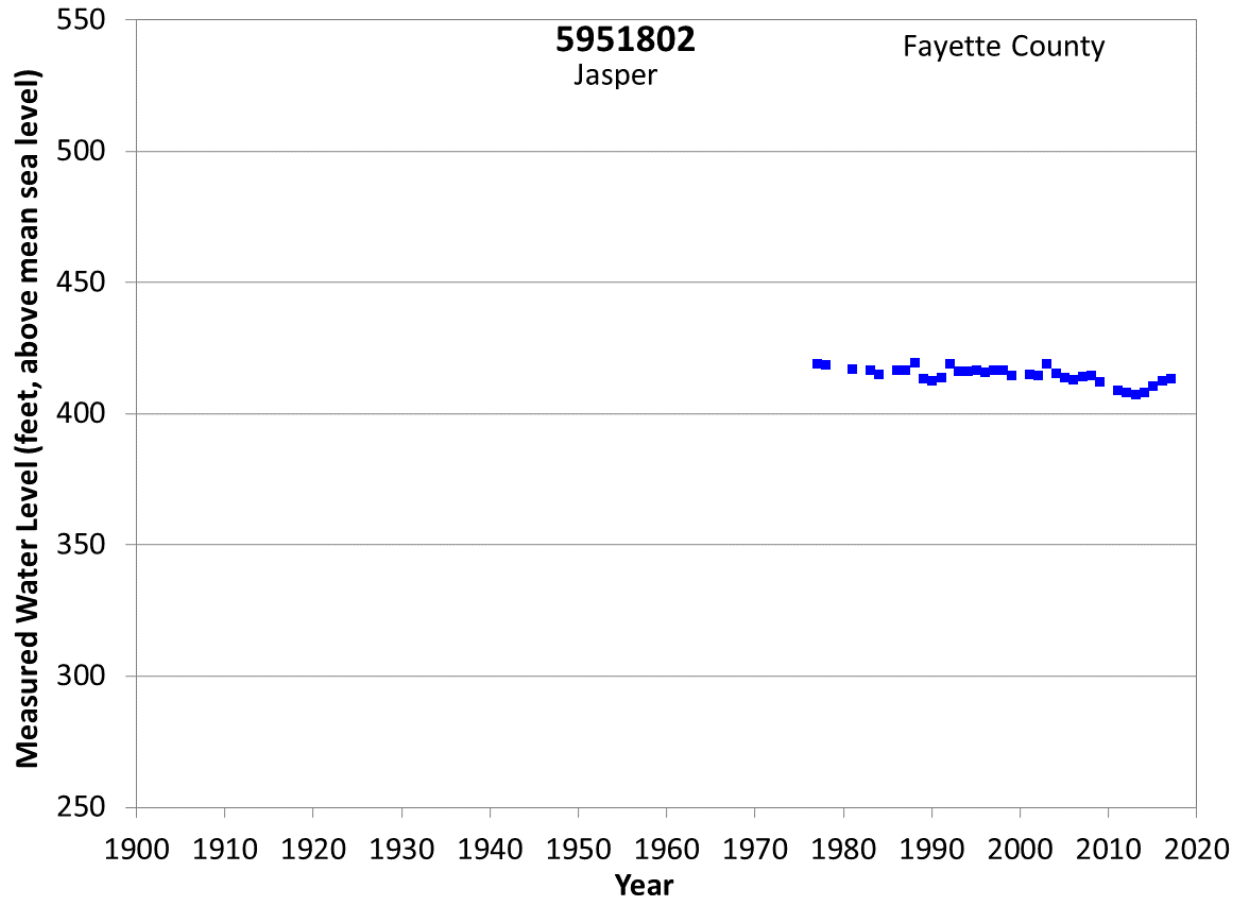


**Figure A113 Groundwater level hydrograph at State Well 5951802.**

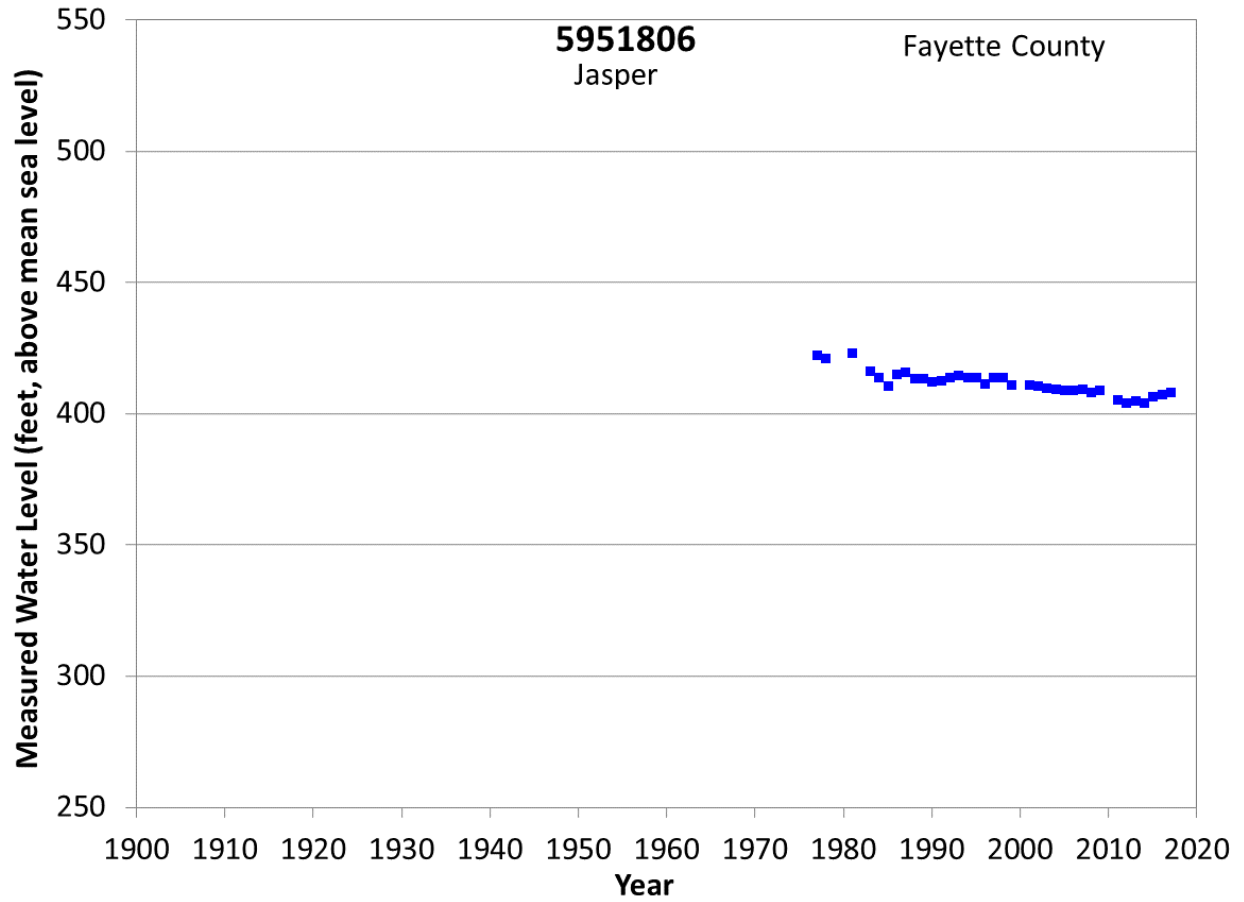


**Figure A114 Groundwater level hydrograph at State Well 5951806.**

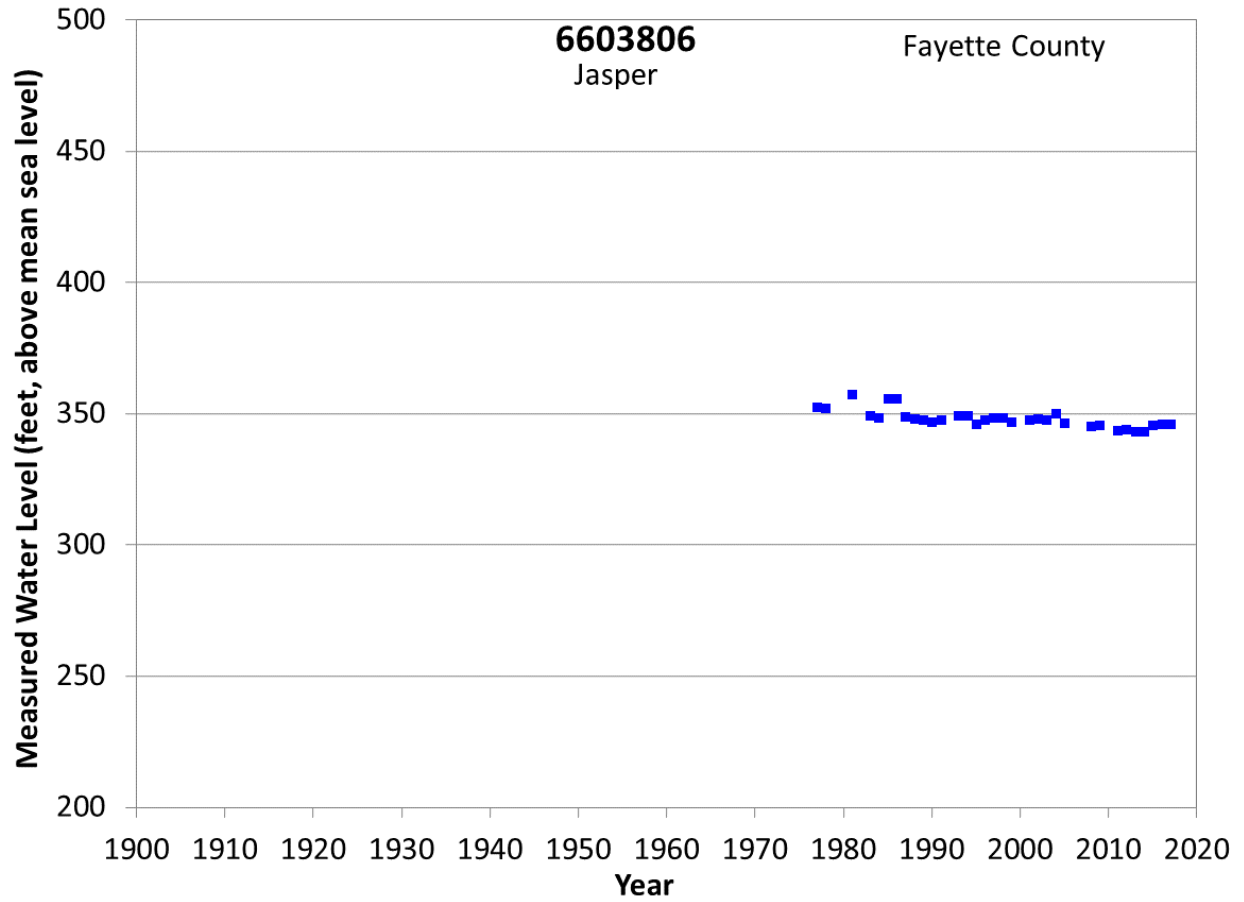


**Figure A115 Groundwater level hydrograph at State Well 6603806.**



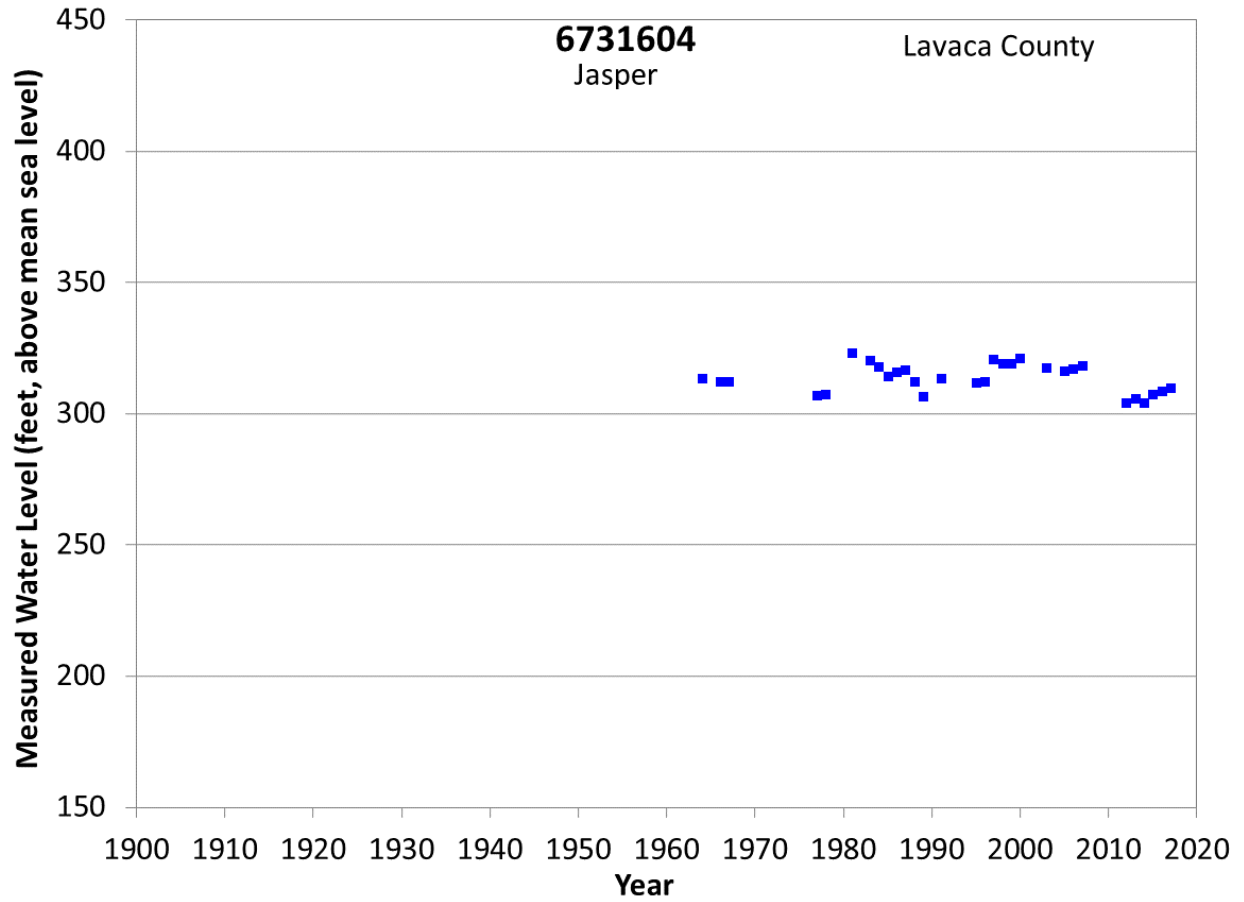


**Figure A116 Groundwater level hydrograph at State Well 6731604.**

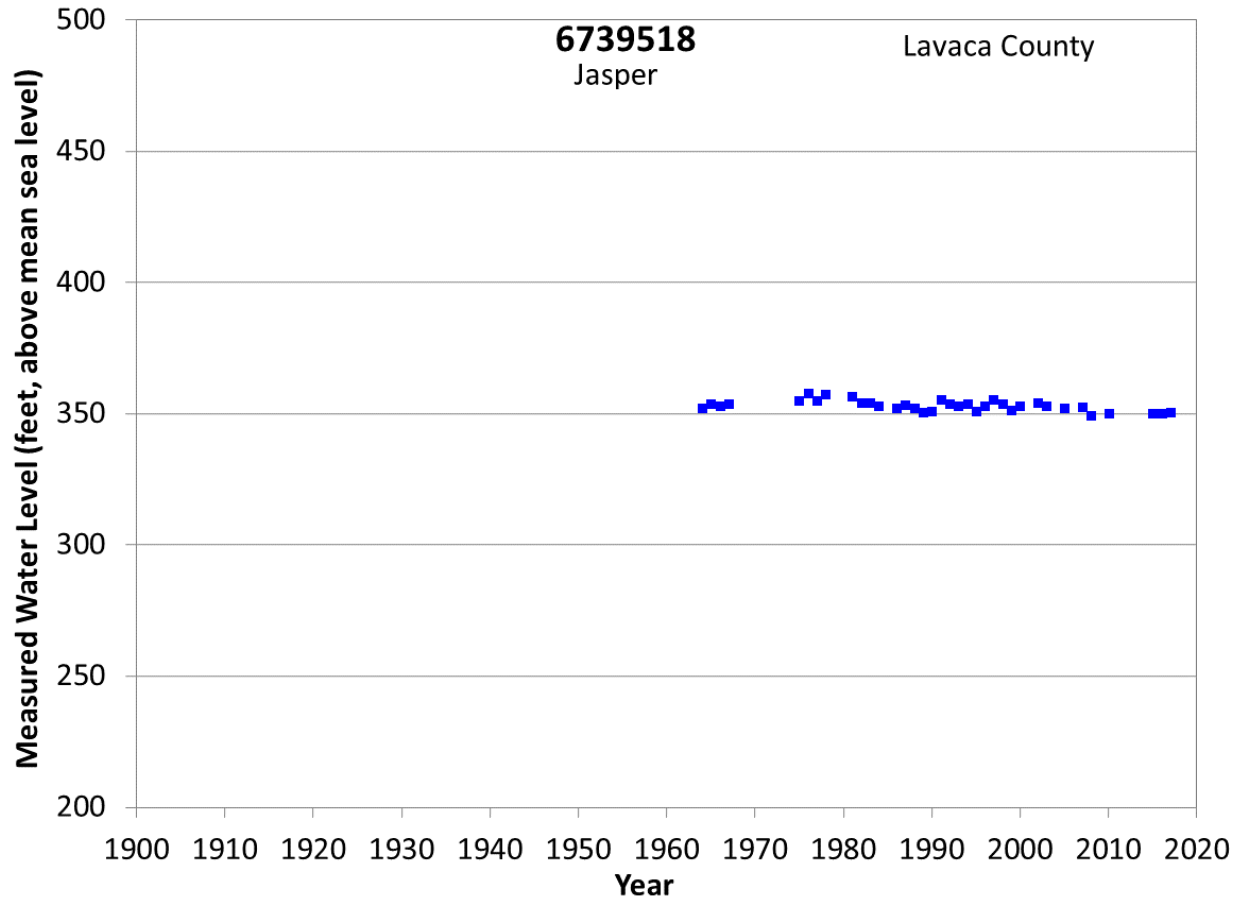


**Figure A117 Groundwater level hydrograph at State Well 6739518.**

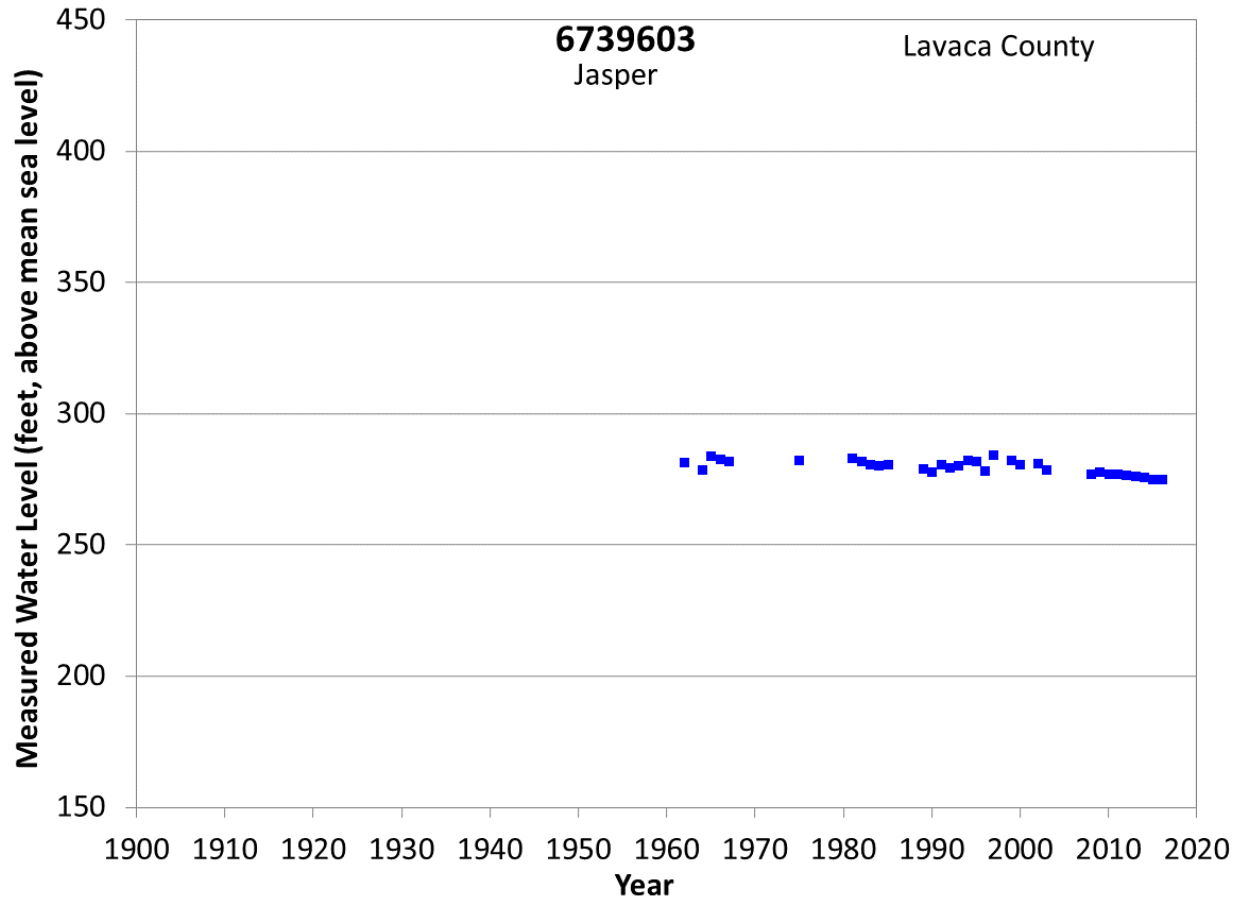


**Figure A118 Groundwater level hydrograph at State Well 6739603.**

## **Appendix B: Groundwater Level at Well Clusters to Show Cross Formation Flow**

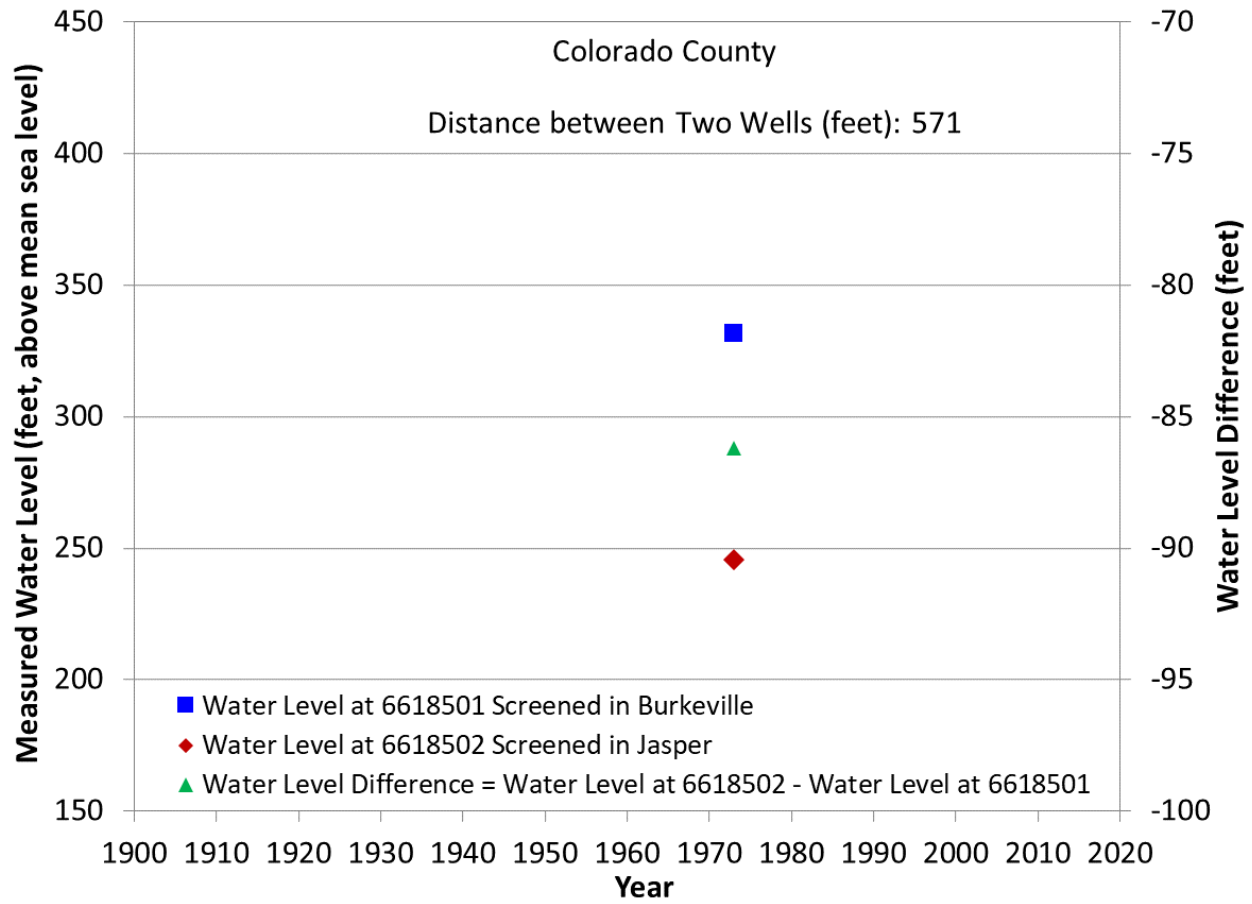


**Figure B1 Groundwater levels at State Well 6618501 and State Well 6618502.**

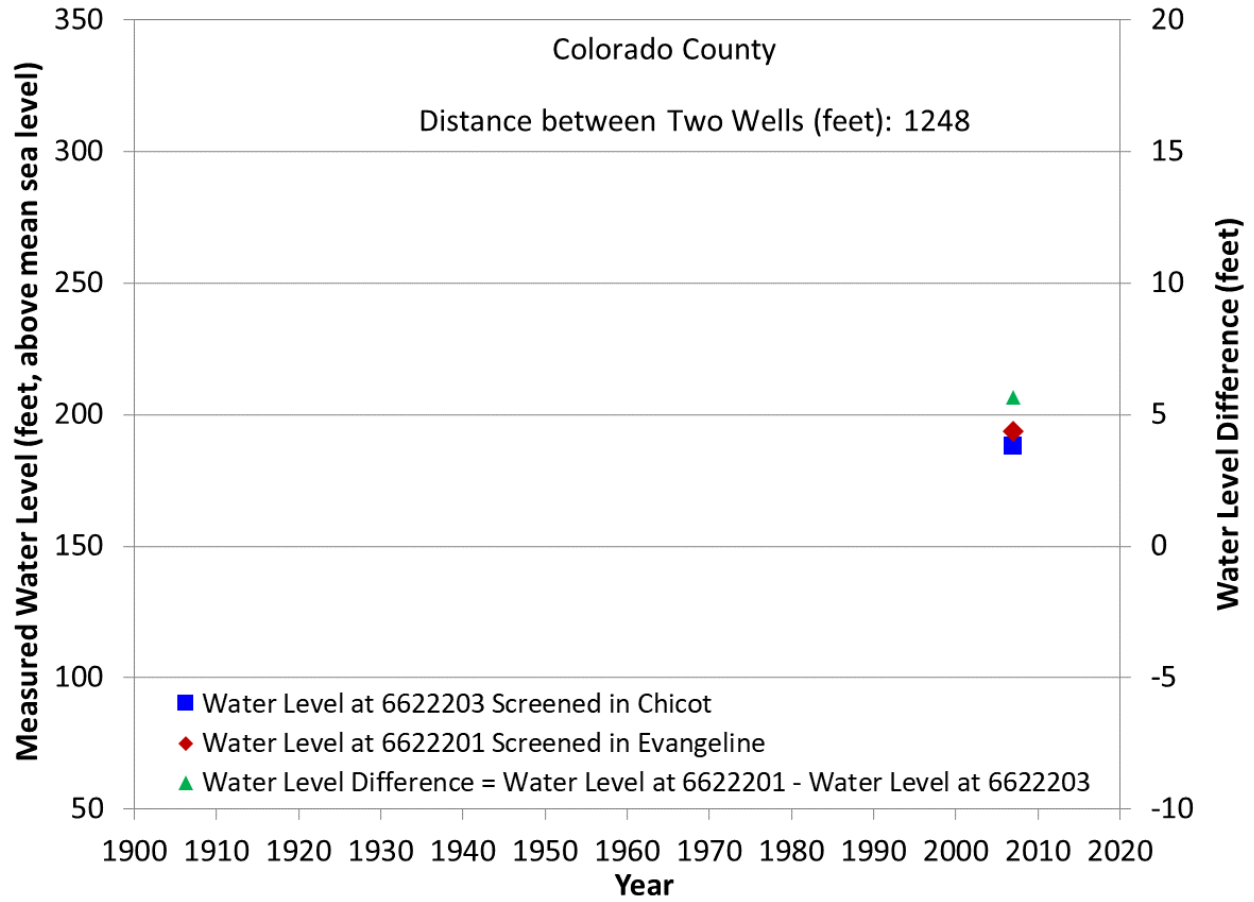


**Figure B2 Groundwater levels at State Well 6622203 and State Well 6622201.**

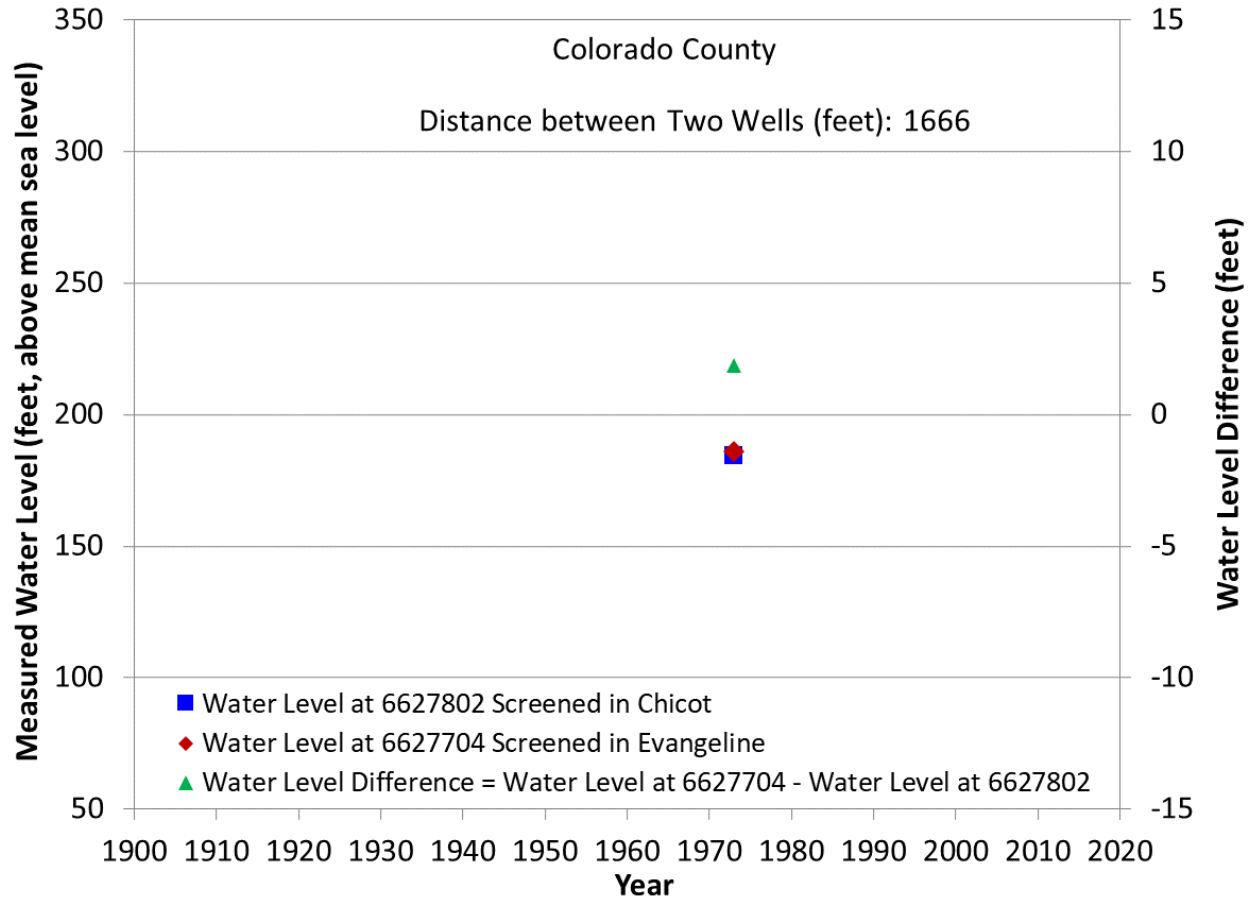


**Figure B3 Groundwater levels at State Well 6627802 and State Well 6627704.**

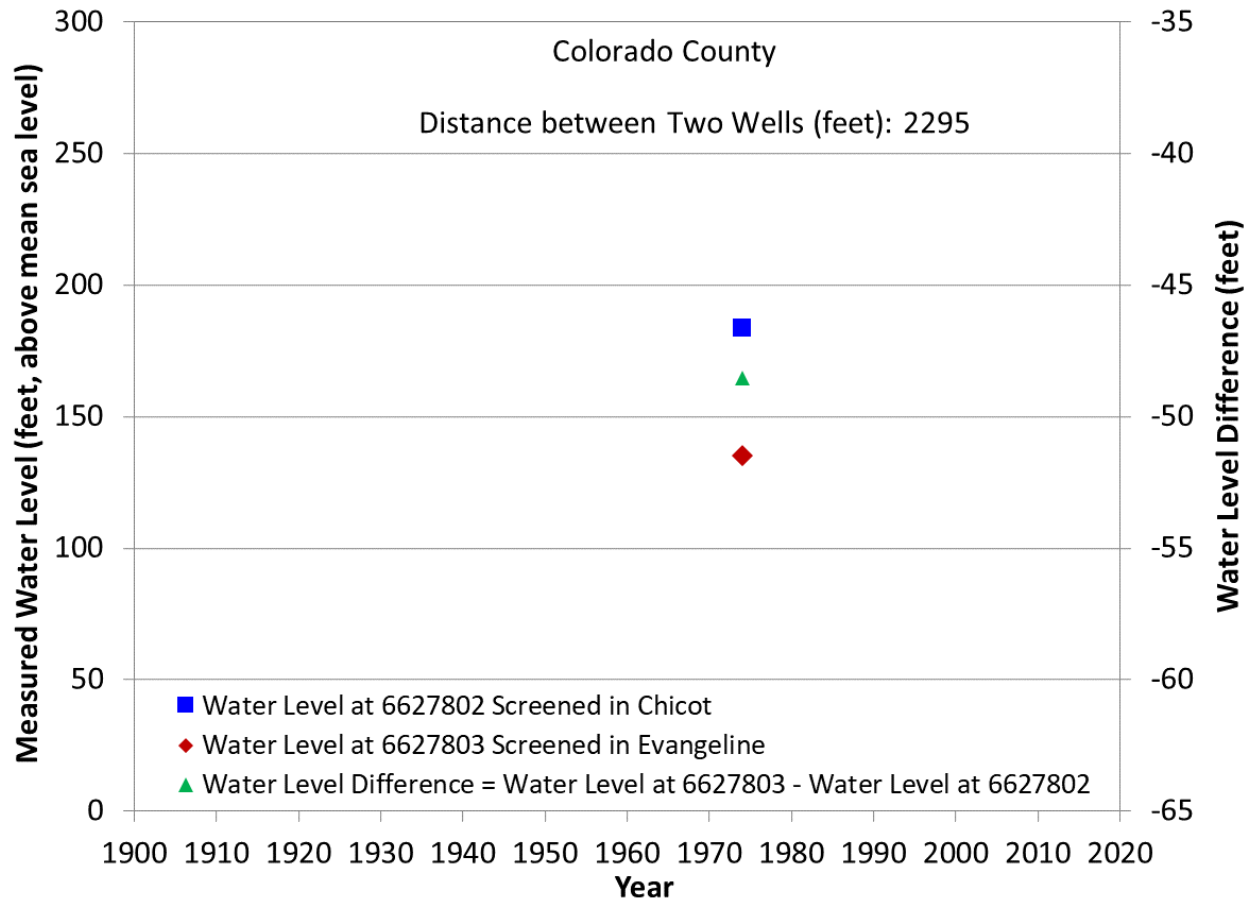


**Figure B4 Groundwater levels at State Well 6627802 and State Well 6627803.**



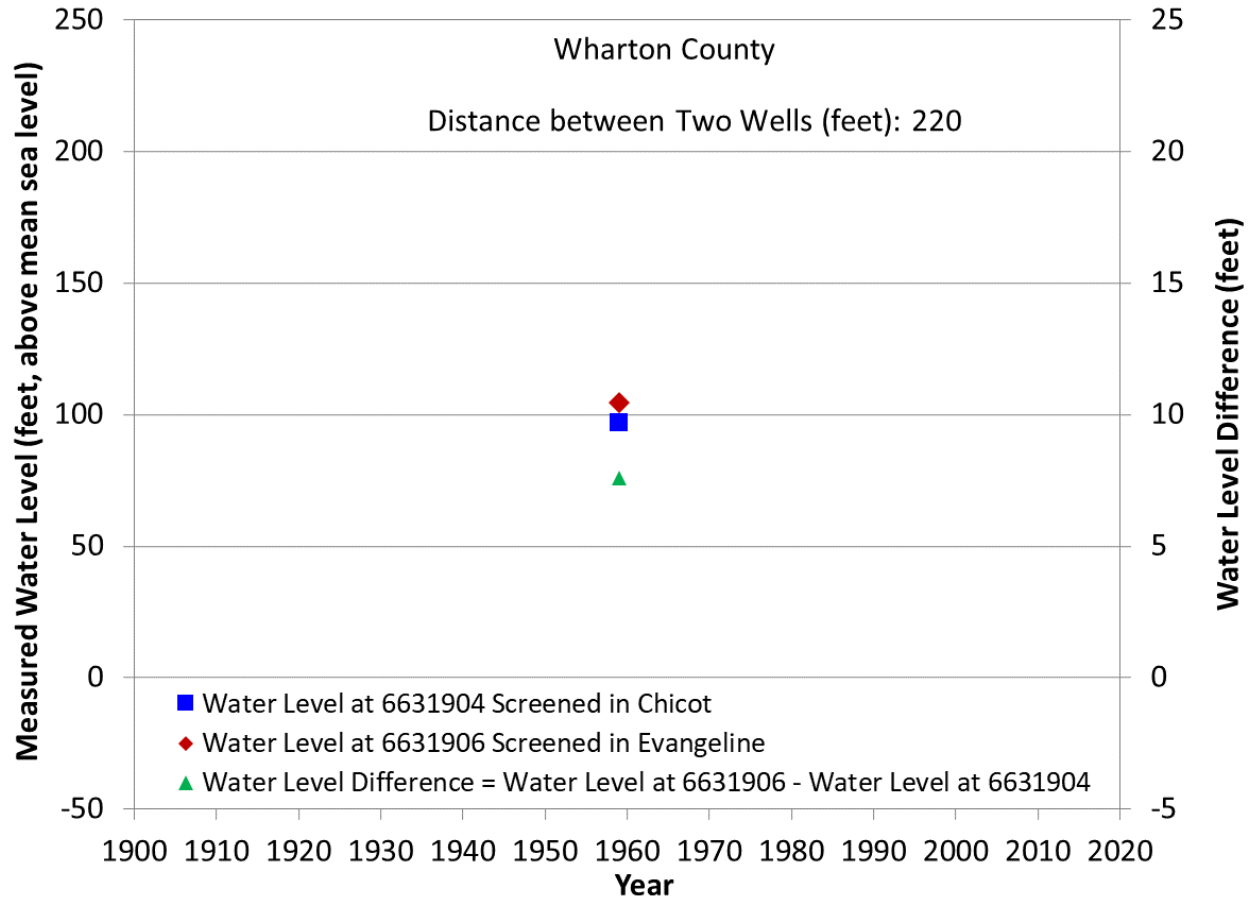


**Figure B5 Groundwater levels at State Well 6631904 and State Well 6631906.**

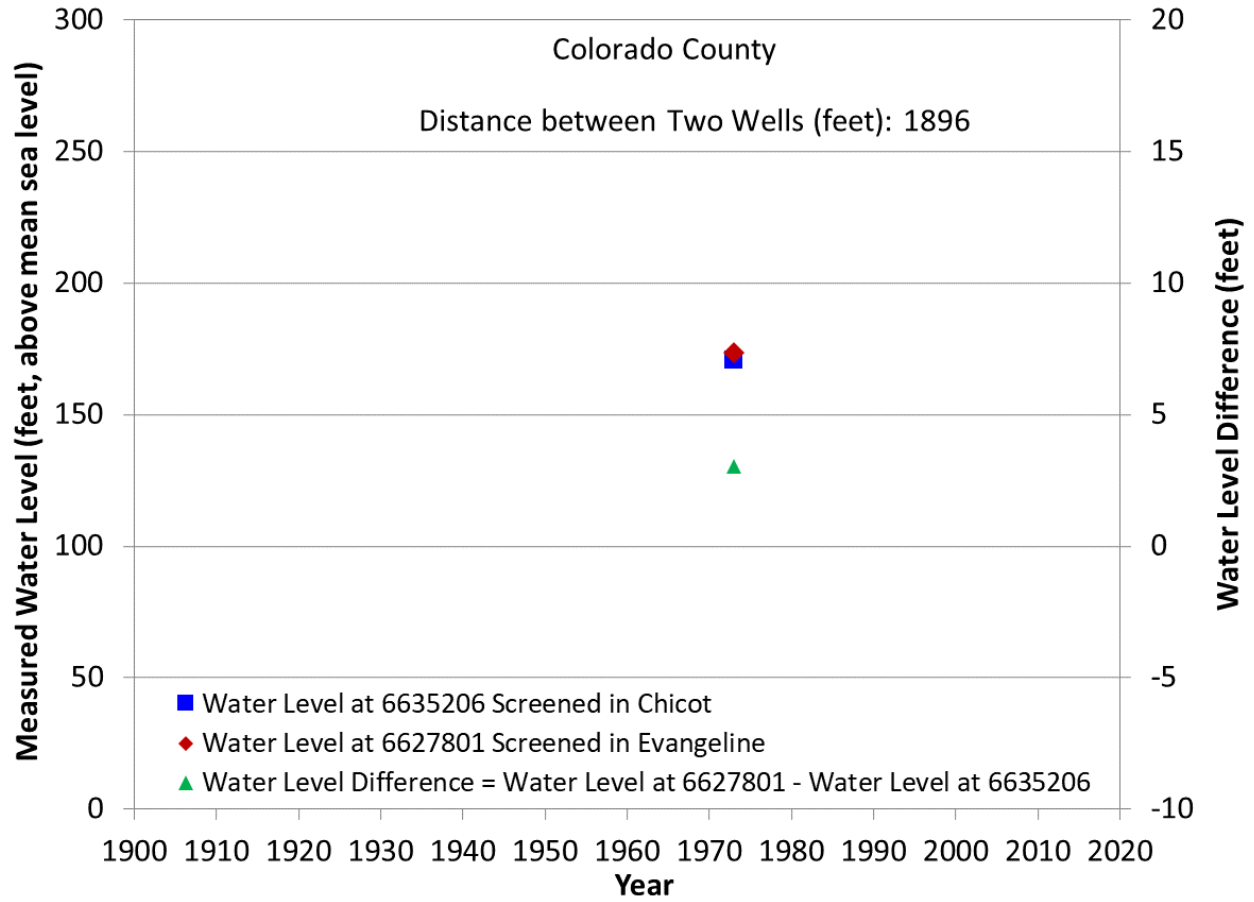


**Figure B6 Groundwater levels at State Well 6635206 and State Well 6627801.**

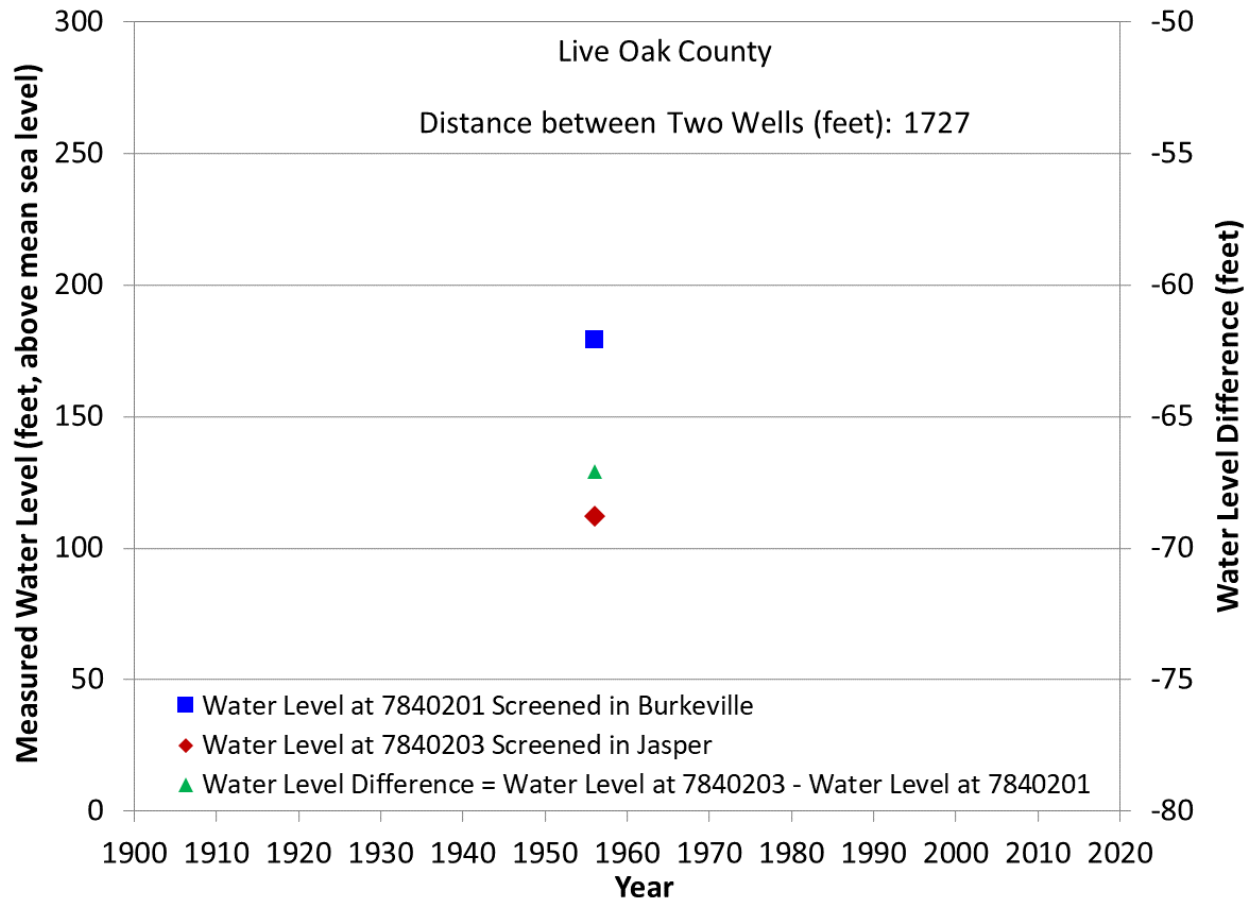


**Figure B7 Groundwater levels at State Well 7840201 and State Well 7840203.**

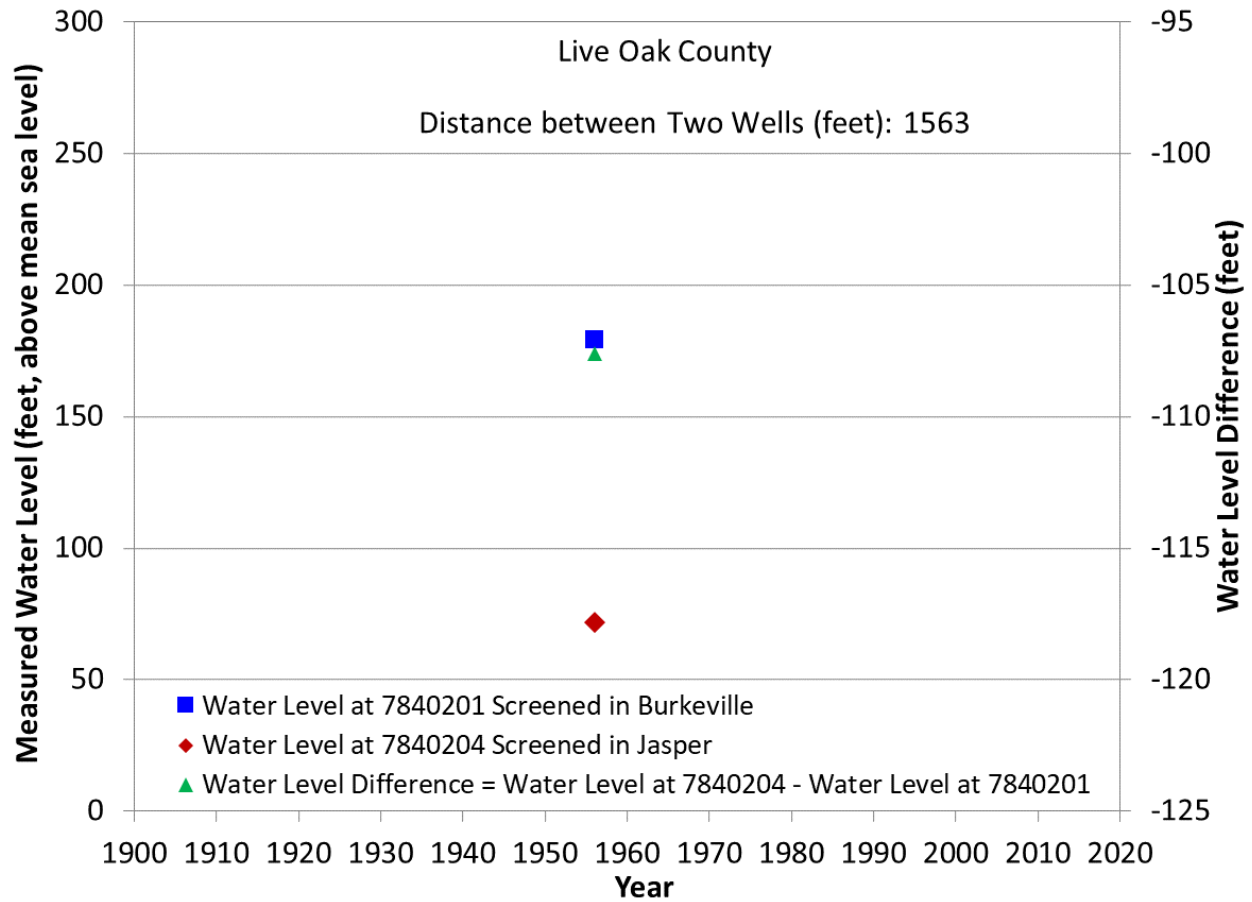


**Figure B8 Groundwater levels at State Well 7840201 and State Well 7840204.**

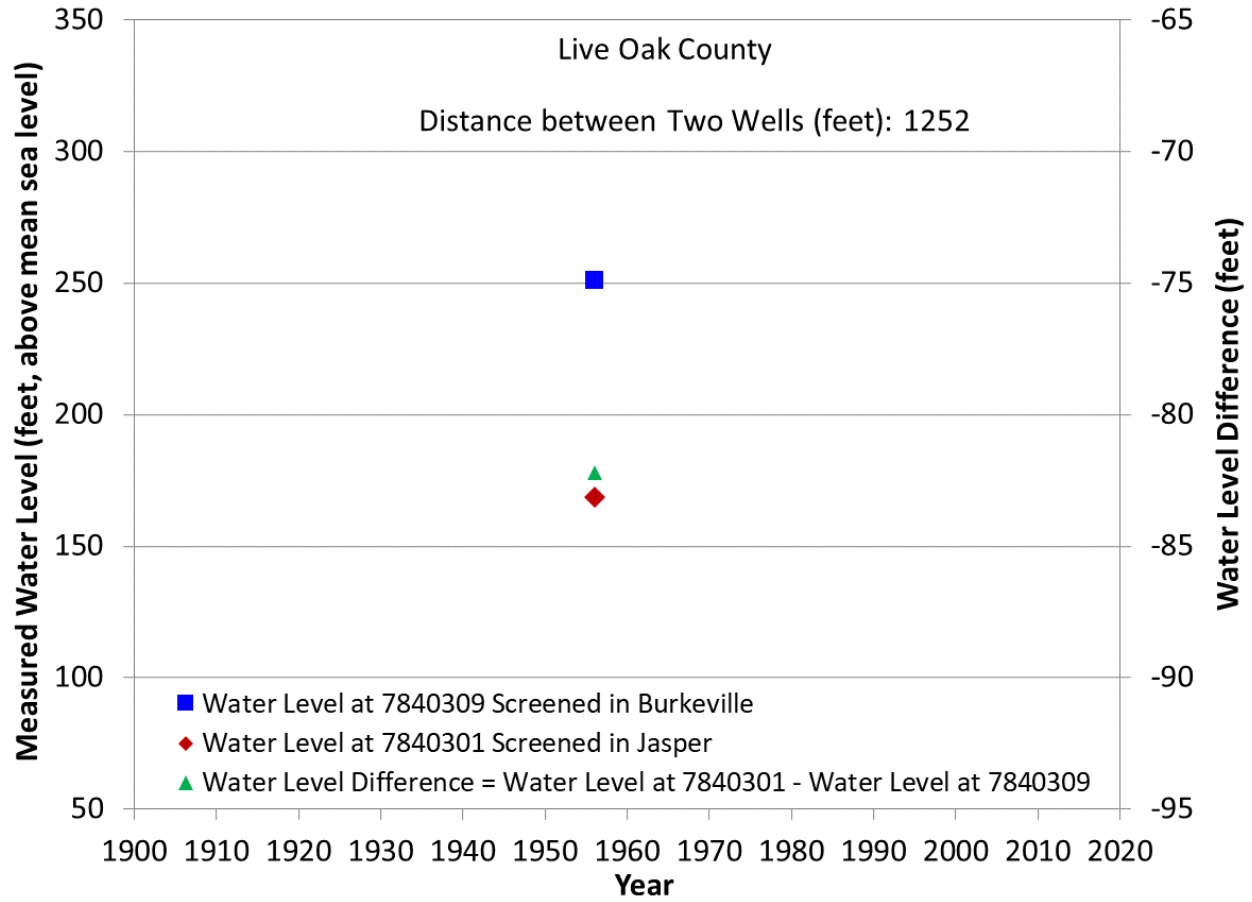


**Figure B9 Groundwater levels at State Well 7840309 and State Well 7840301.**

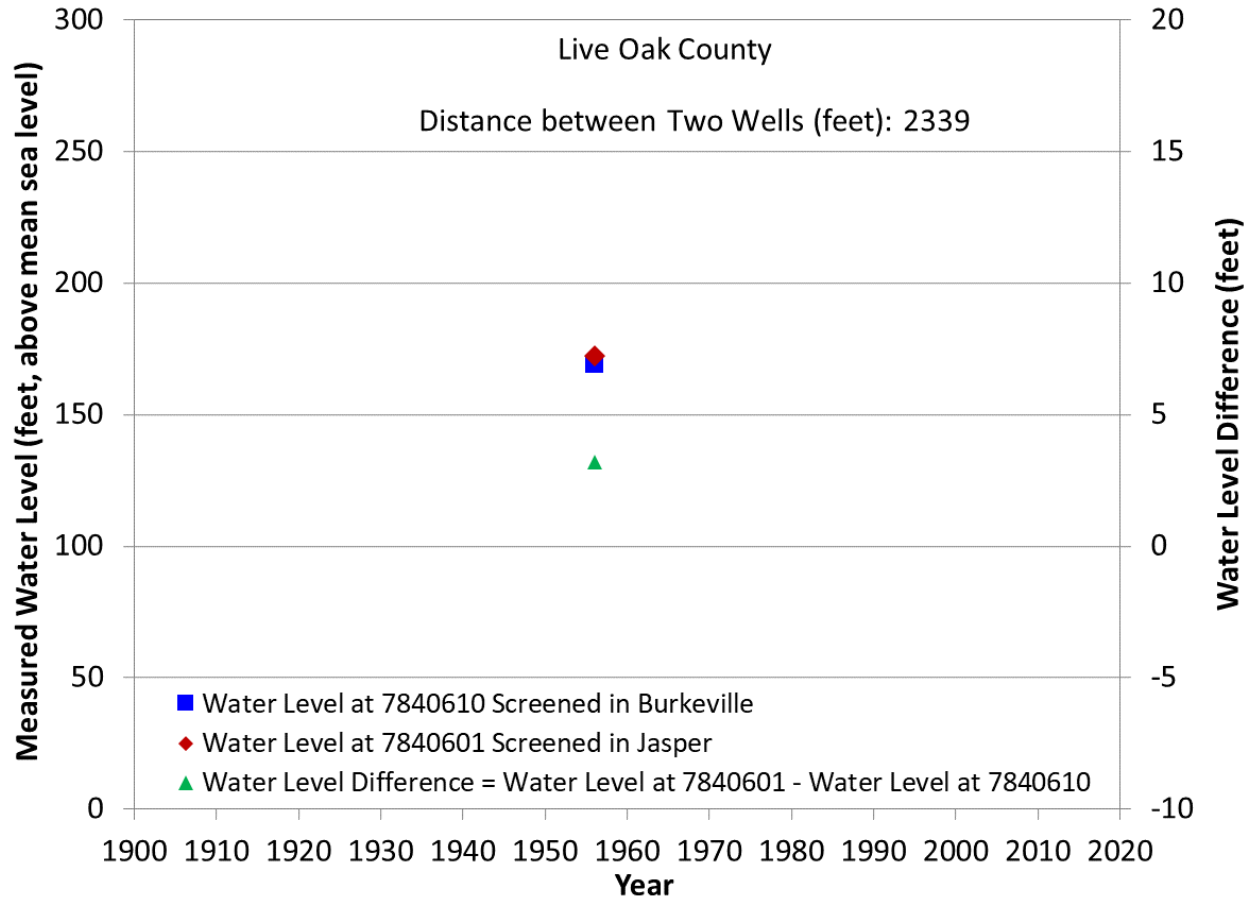


**Figure B10 Groundwater levels at State Well 7840610 and State Well 7840601.**

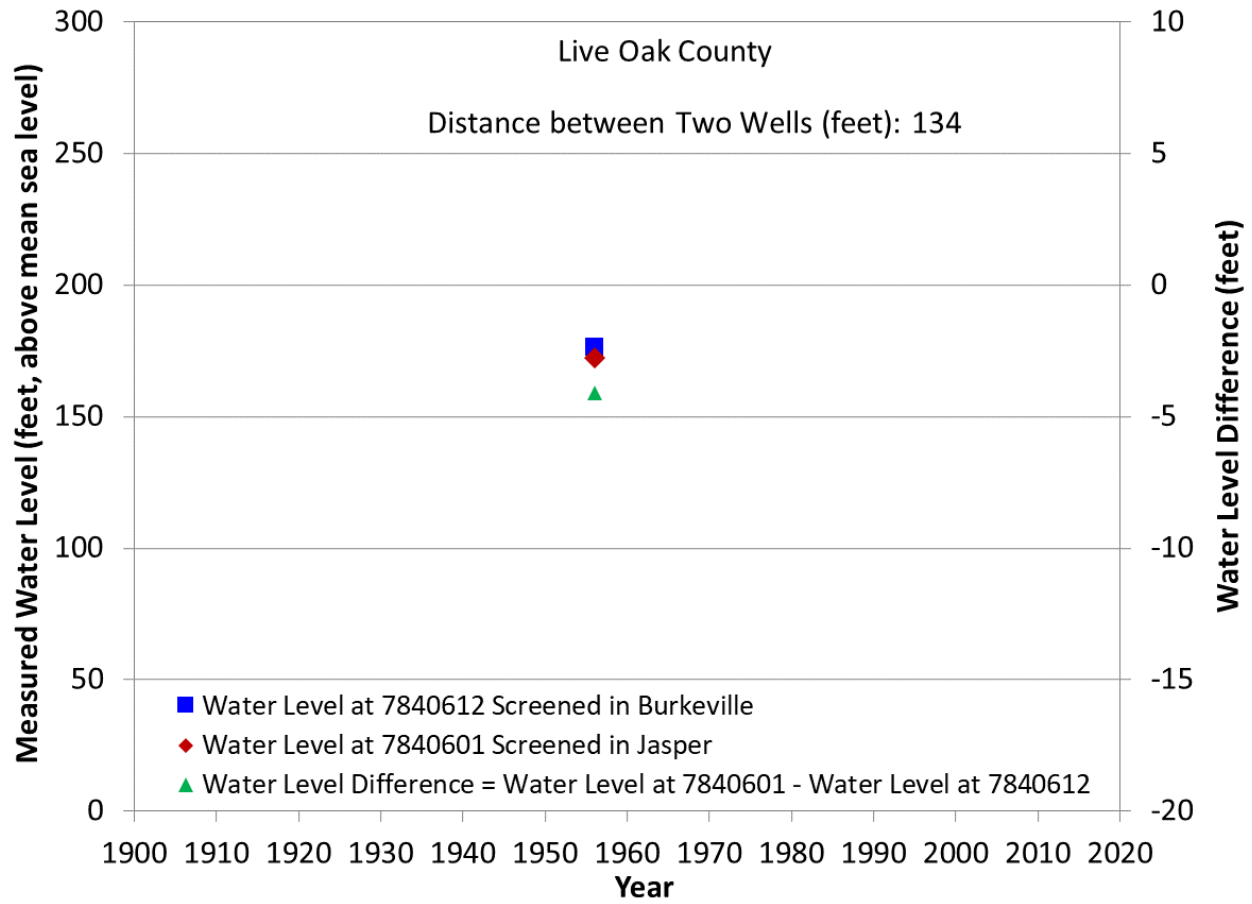


**Figure B11 Groundwater levels at State Well 7840612 and State Well 7840601.**

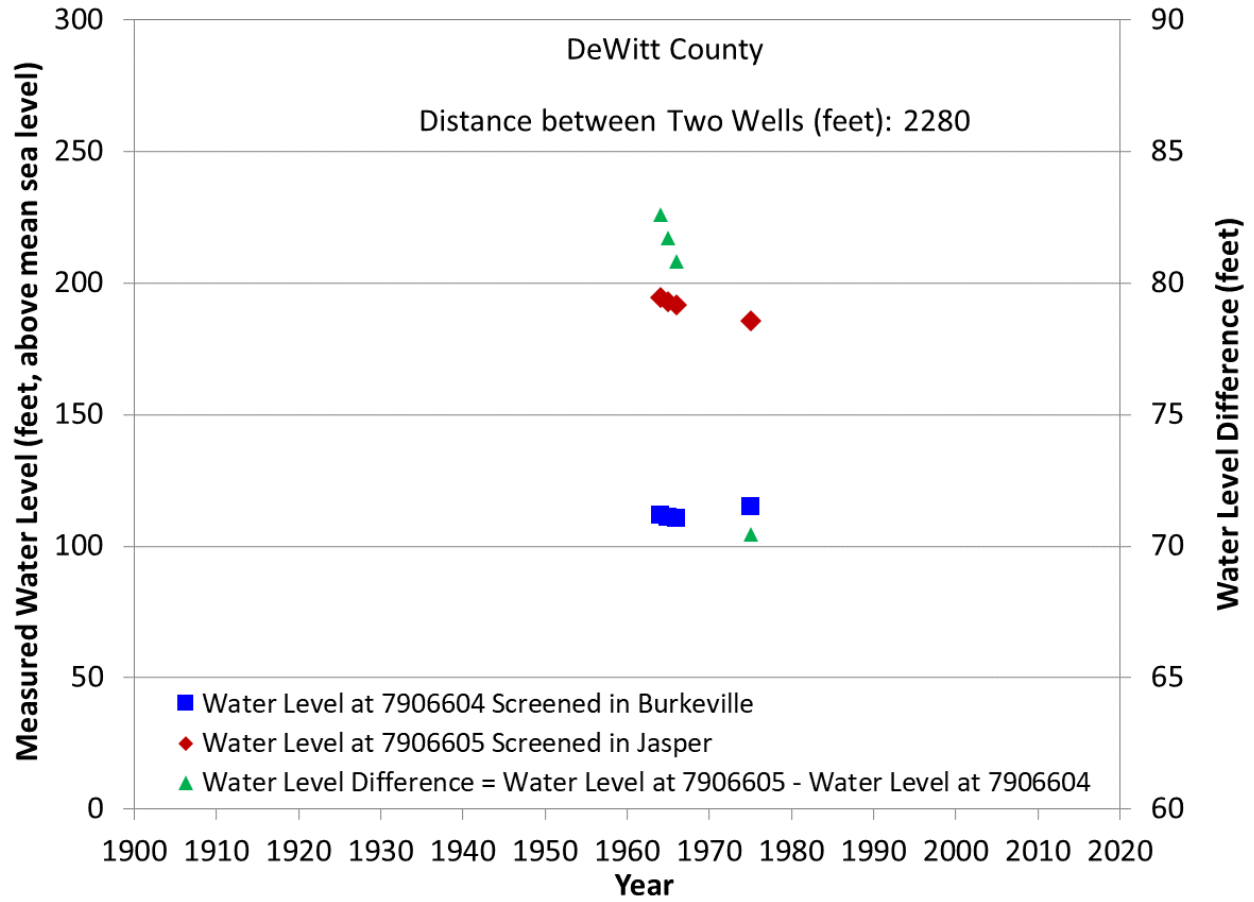


**Figure B12 Groundwater levels at State Well 7906604 and State Well 7906605.**



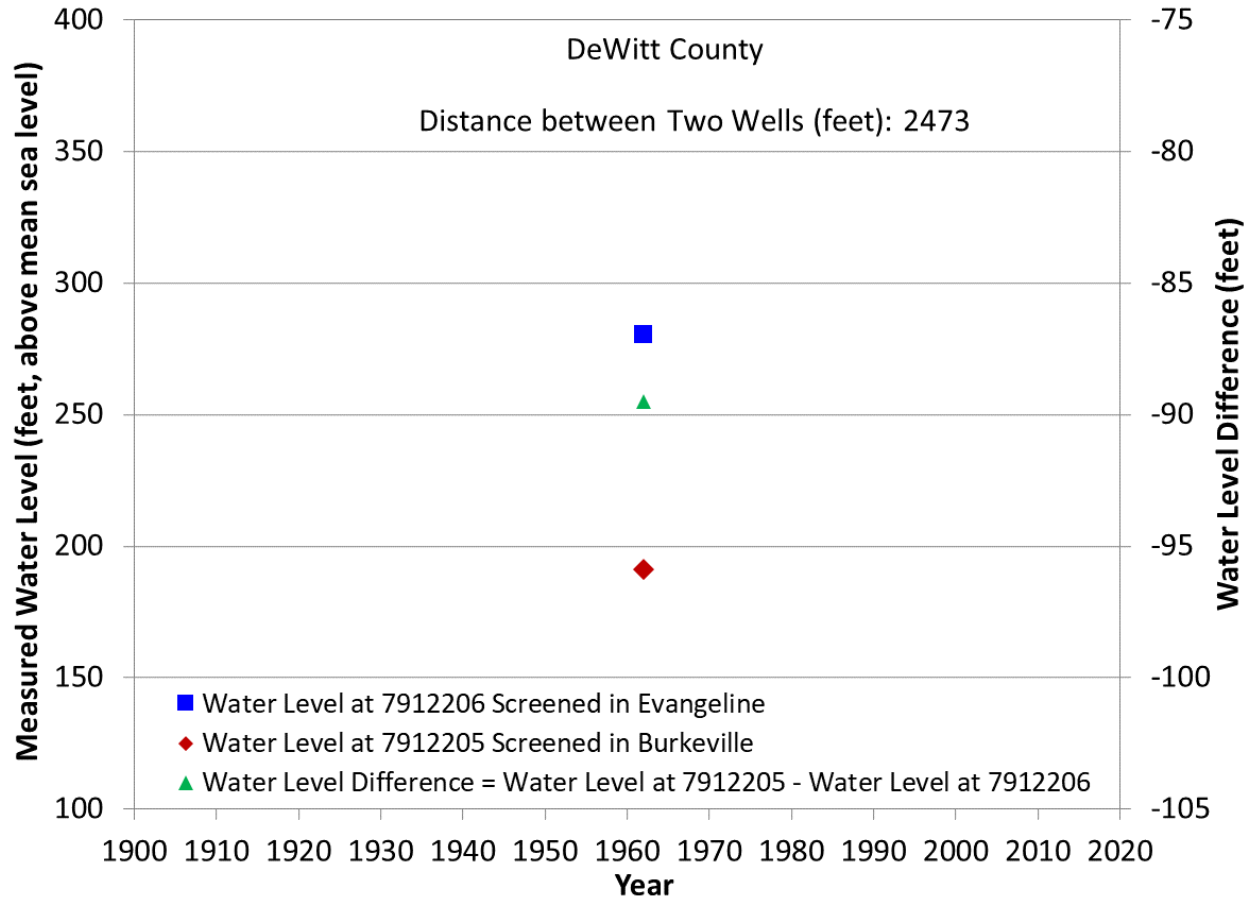


**Figure B13 Groundwater levels at State Well 7912206 and State Well 7912205.**

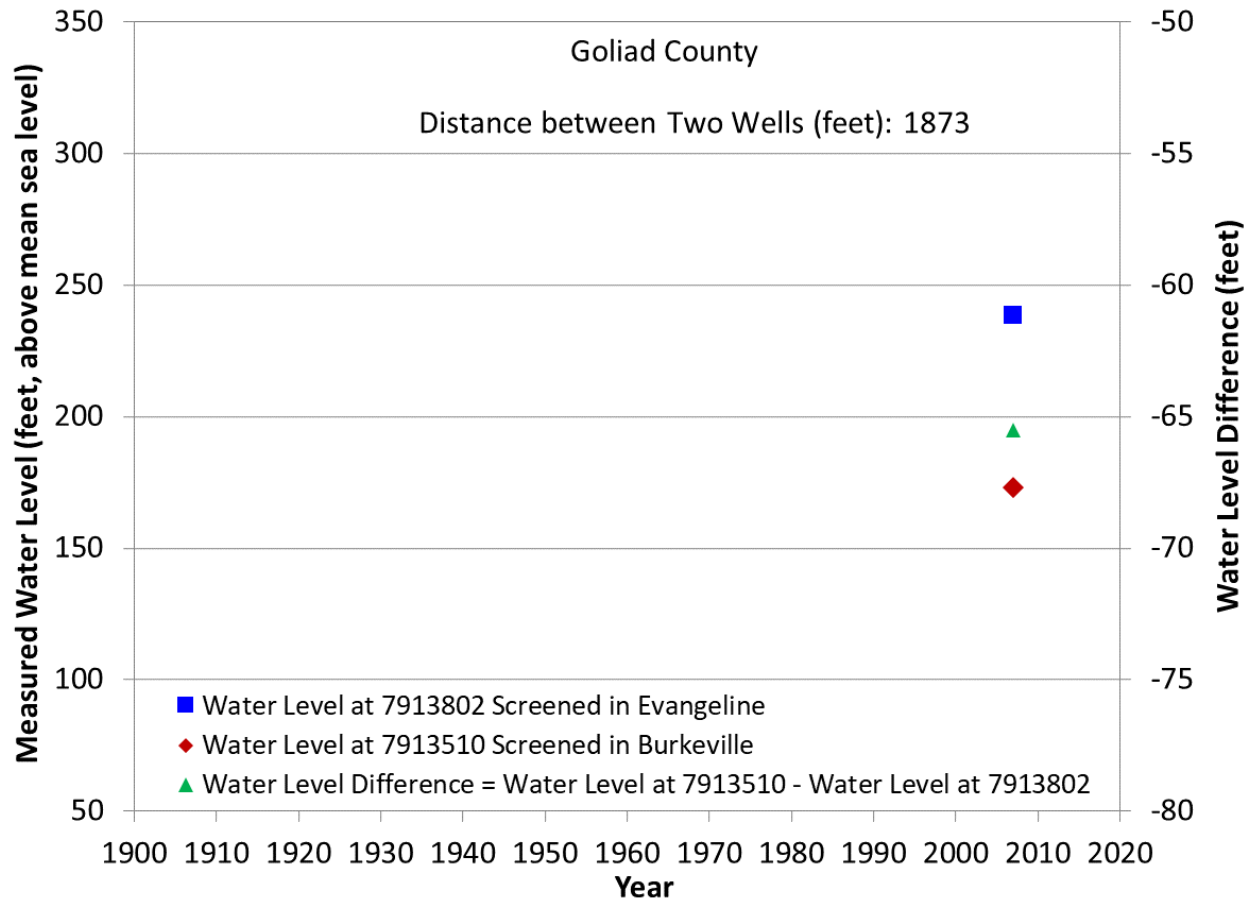


**Figure B14 Groundwater levels at State Well 7913802 and State Well 7913510.**

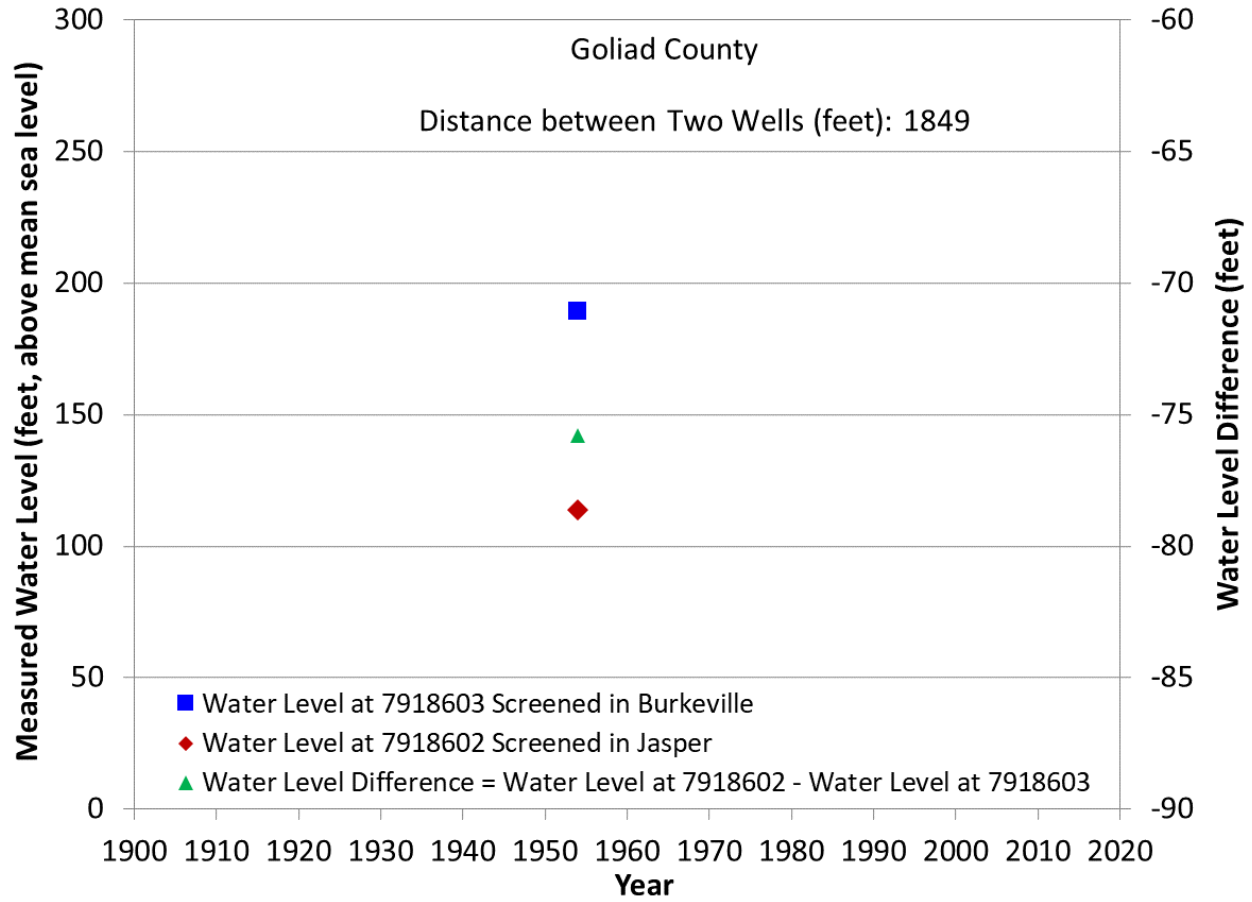


**Figure B15 Groundwater levels at State Well 7918603 and State Well 7918602.**

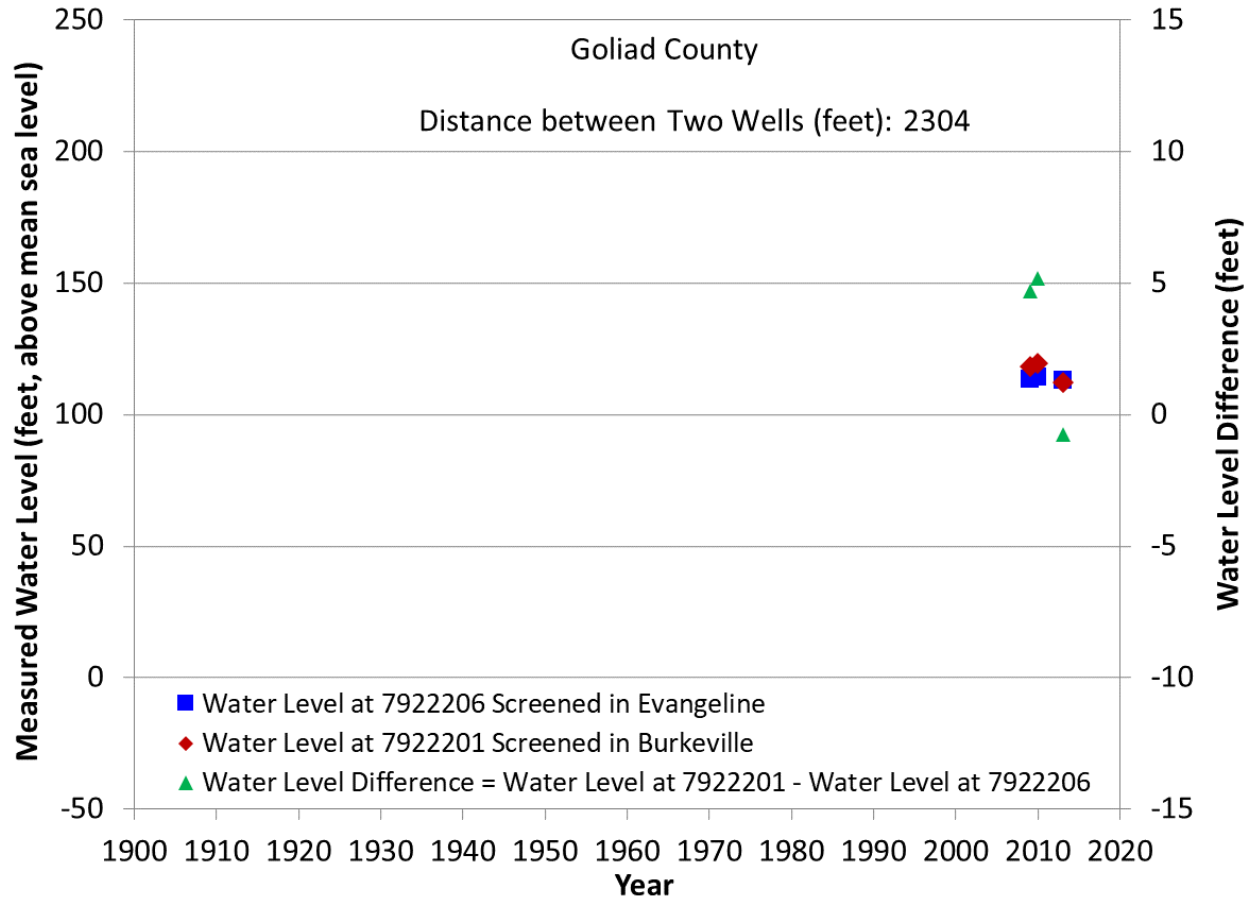


**Figure B16 Groundwater levels at State Well 7922206 and State Well 7922201.**

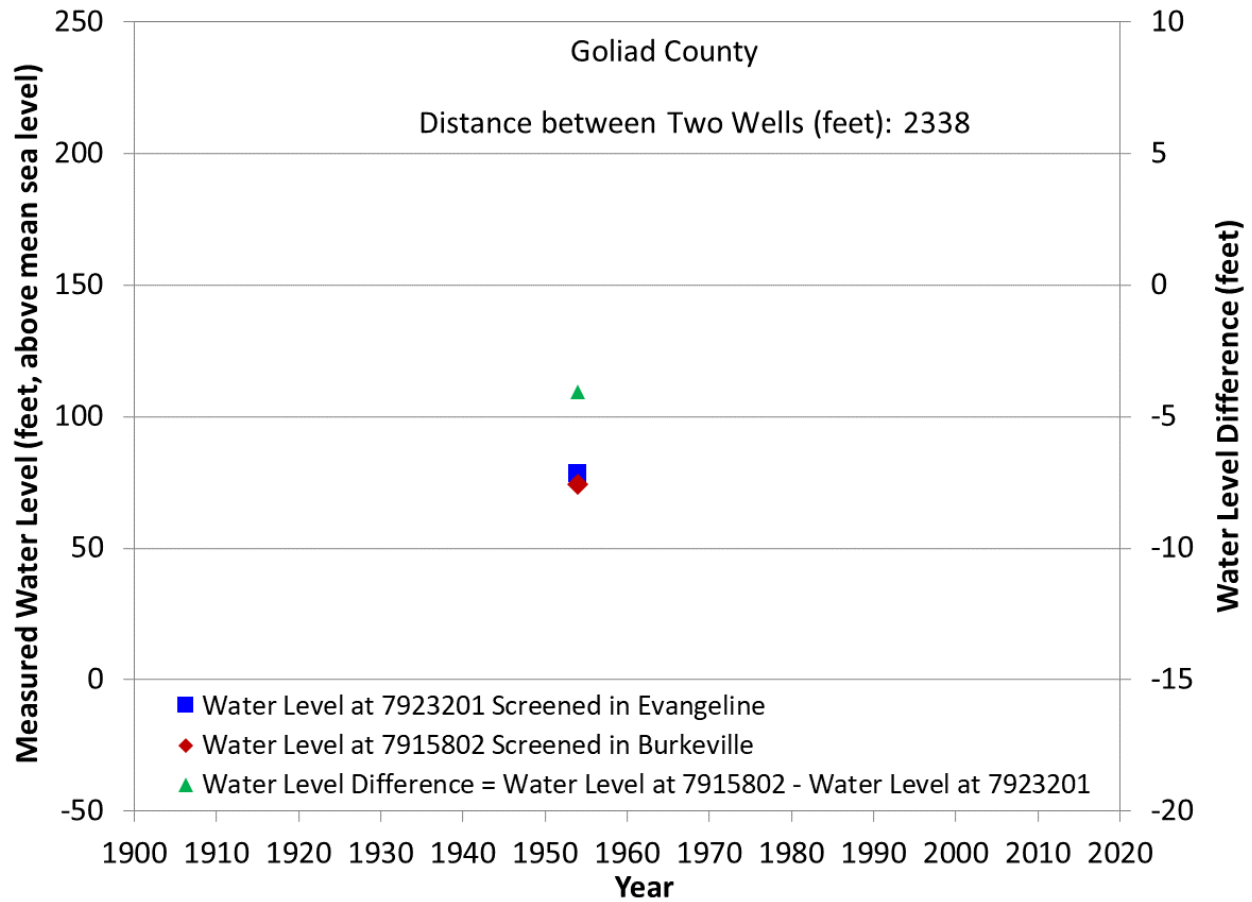


**Figure B17 Groundwater levels at State Well 7923201 and State Well 7915802.**

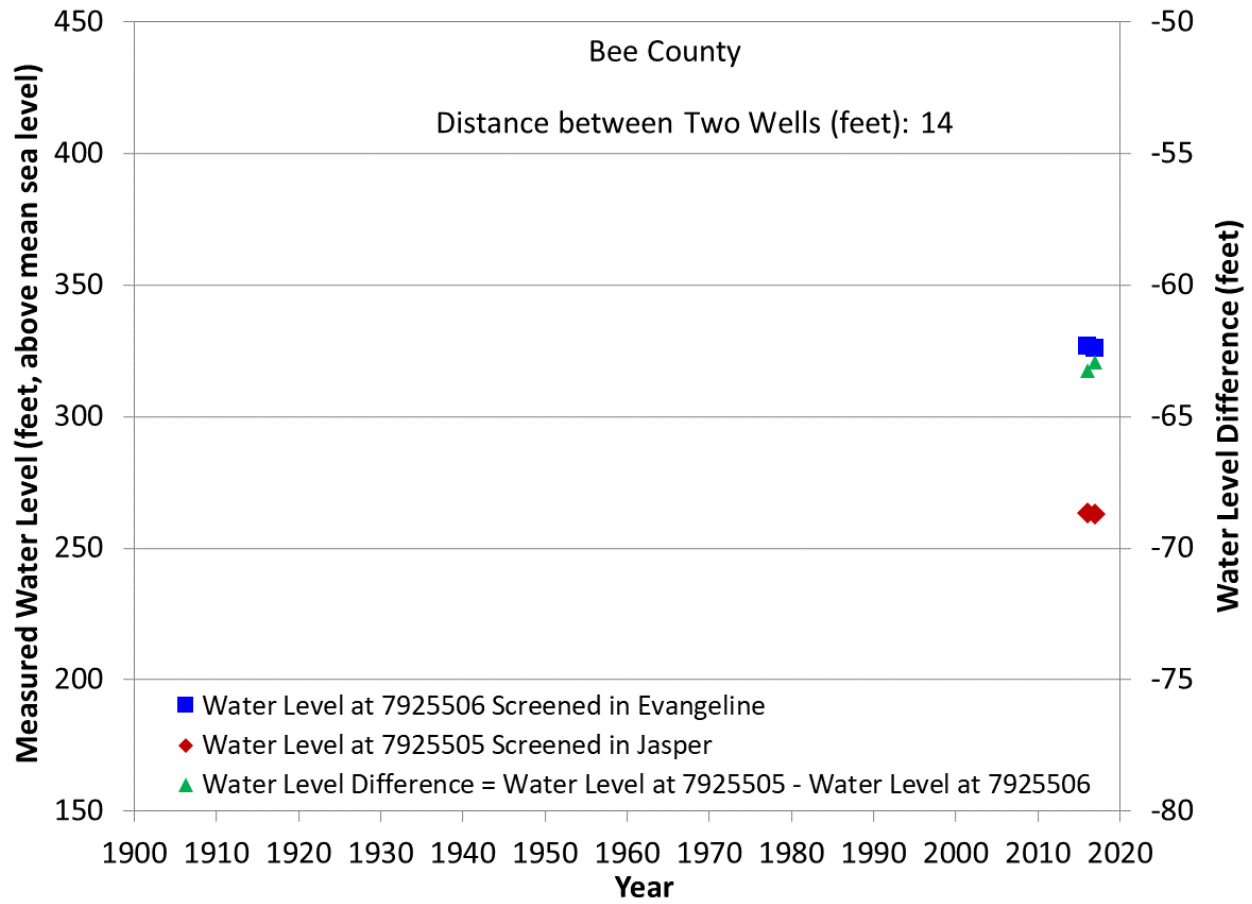


**Figure B18 Groundwater levels at State Well 7925506 and State Well 7925505.**

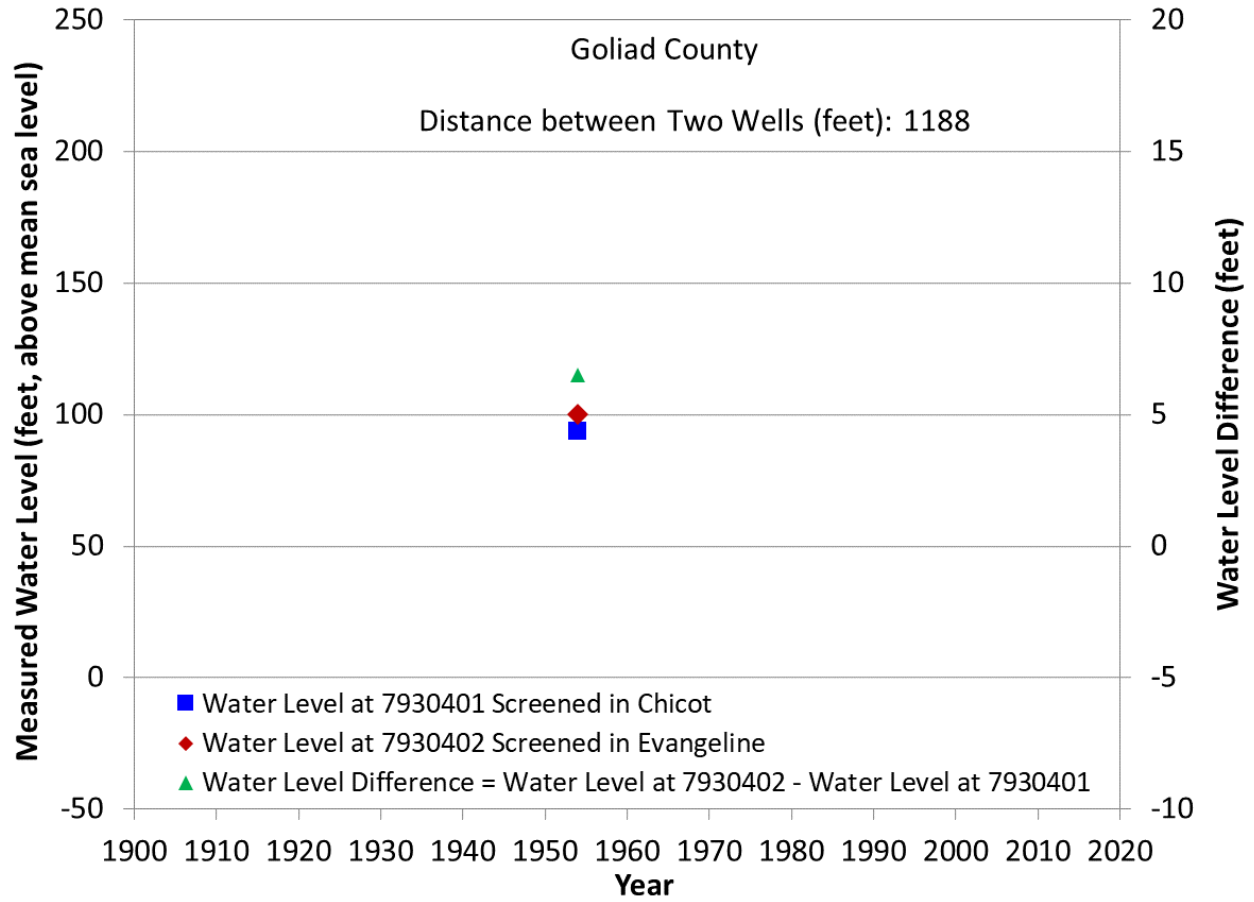


**Figure B19 Groundwater levels at State Well 7930401 and State Well 7930402.**

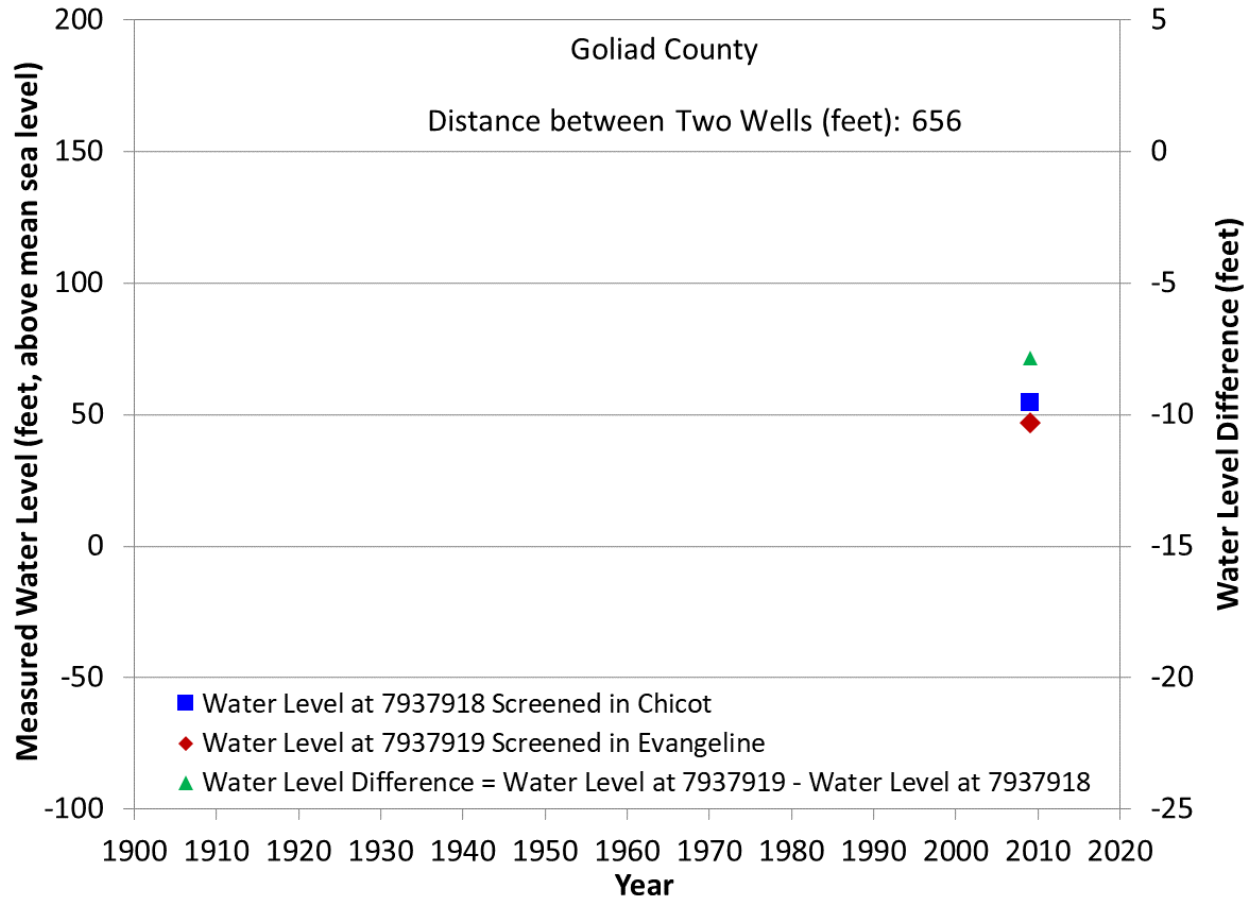


**Figure B20 Groundwater levels at State Well 7937918 and State Well 7937919.**



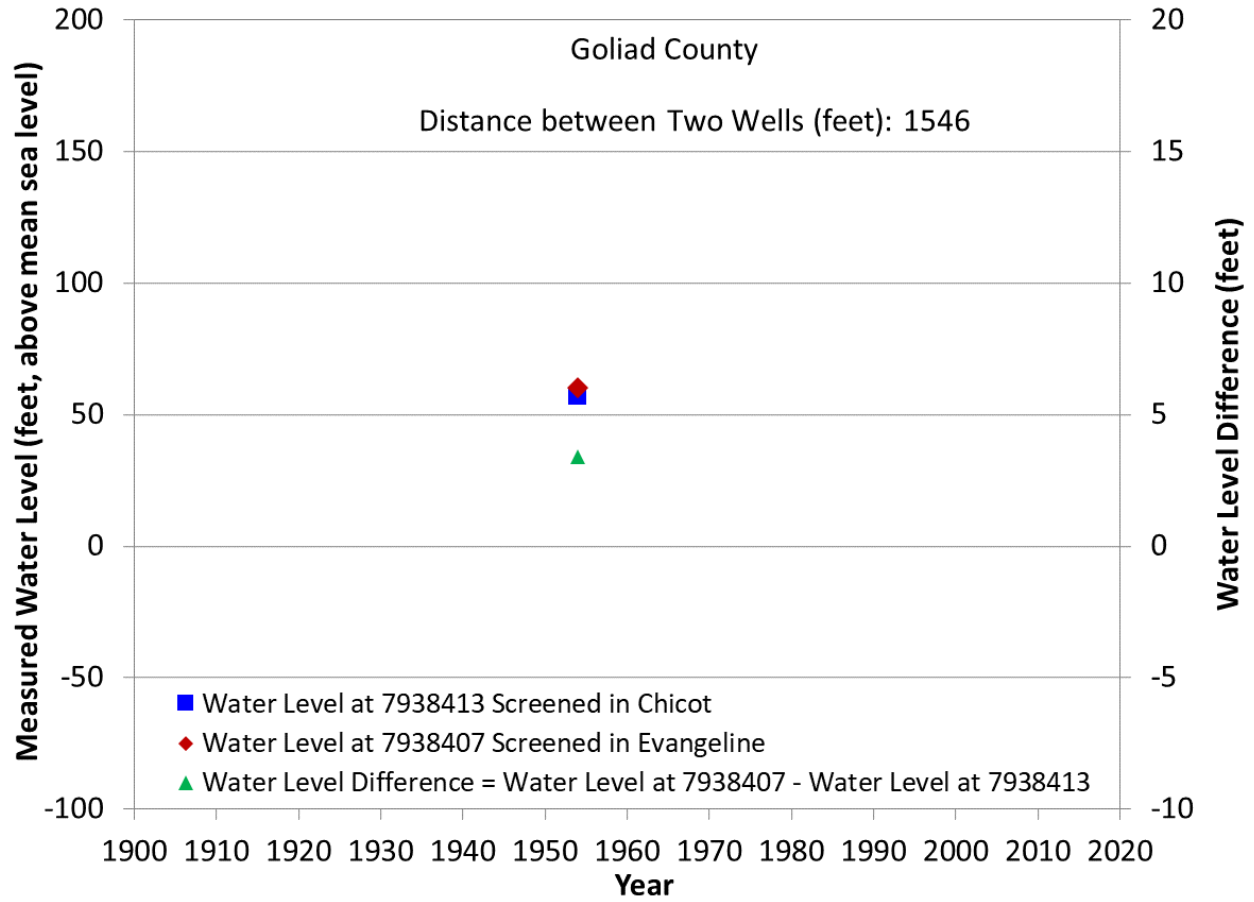


**Figure B21 Groundwater levels at State Well 7938413 and State Well 7938407.**

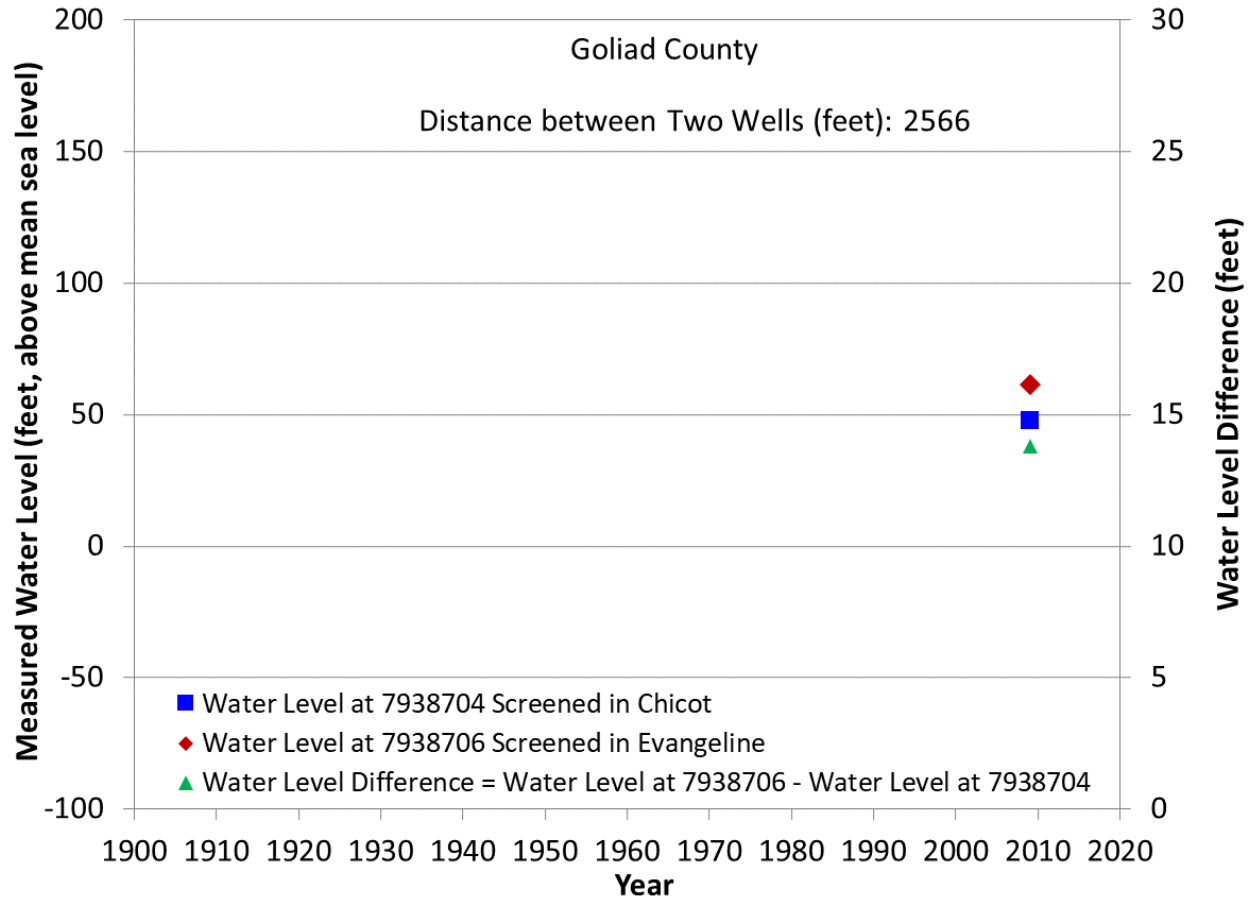


**Figure B22 Groundwater levels at State Well 7938704 and State Well 7938706.**

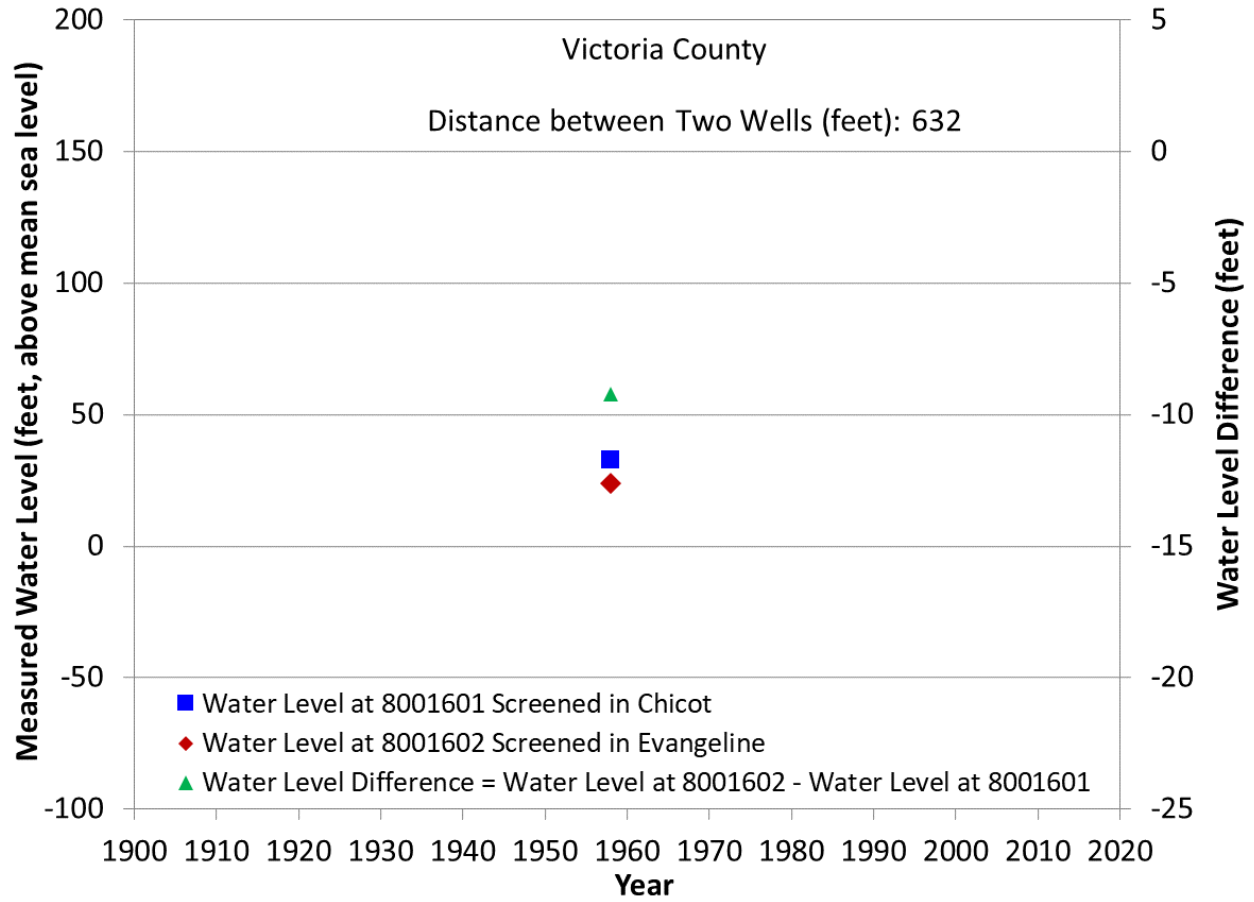


**Figure B23 Groundwater levels at State Well 8001601 and State Well 8001602.**

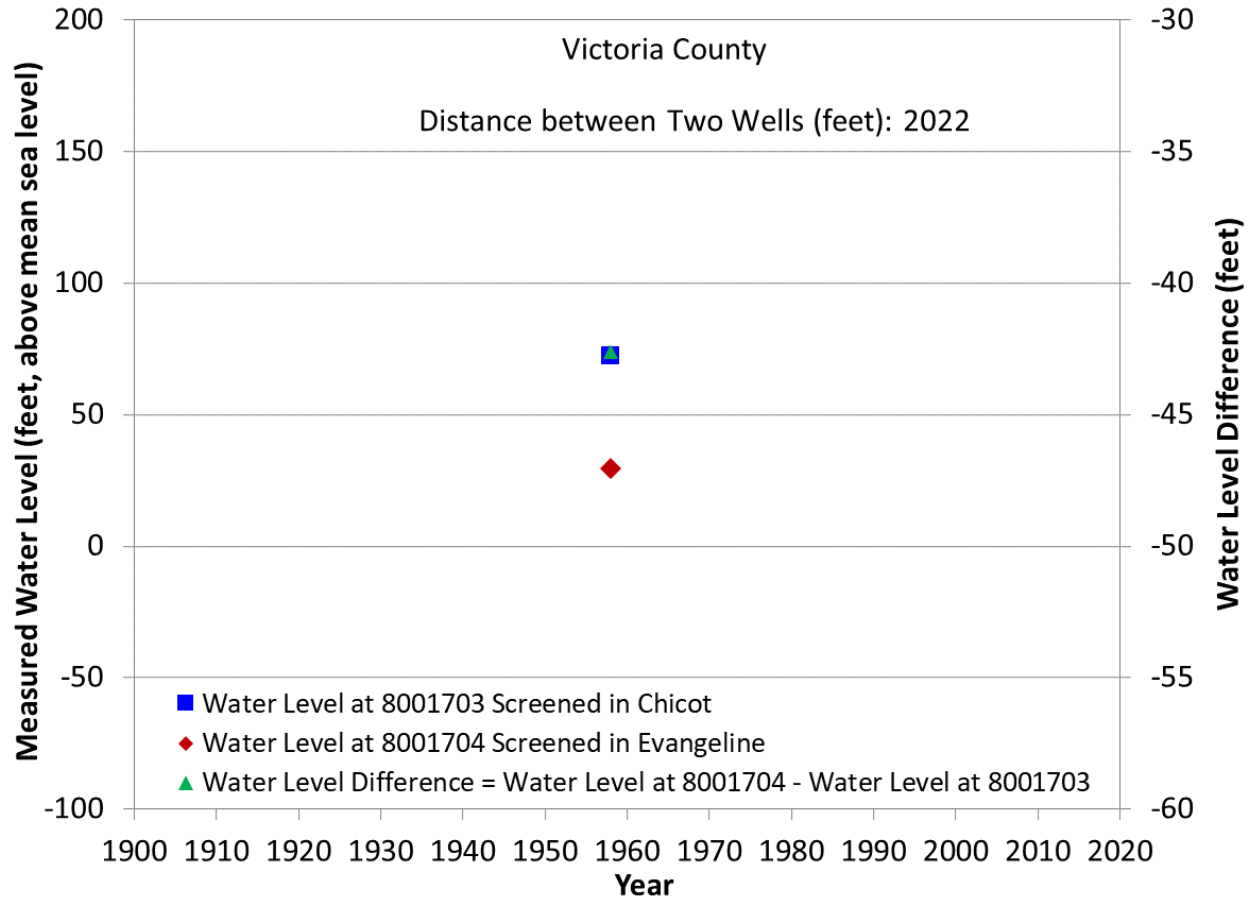


**Figure B24 Groundwater levels at State Well 8001703 and State Well 8001704.**

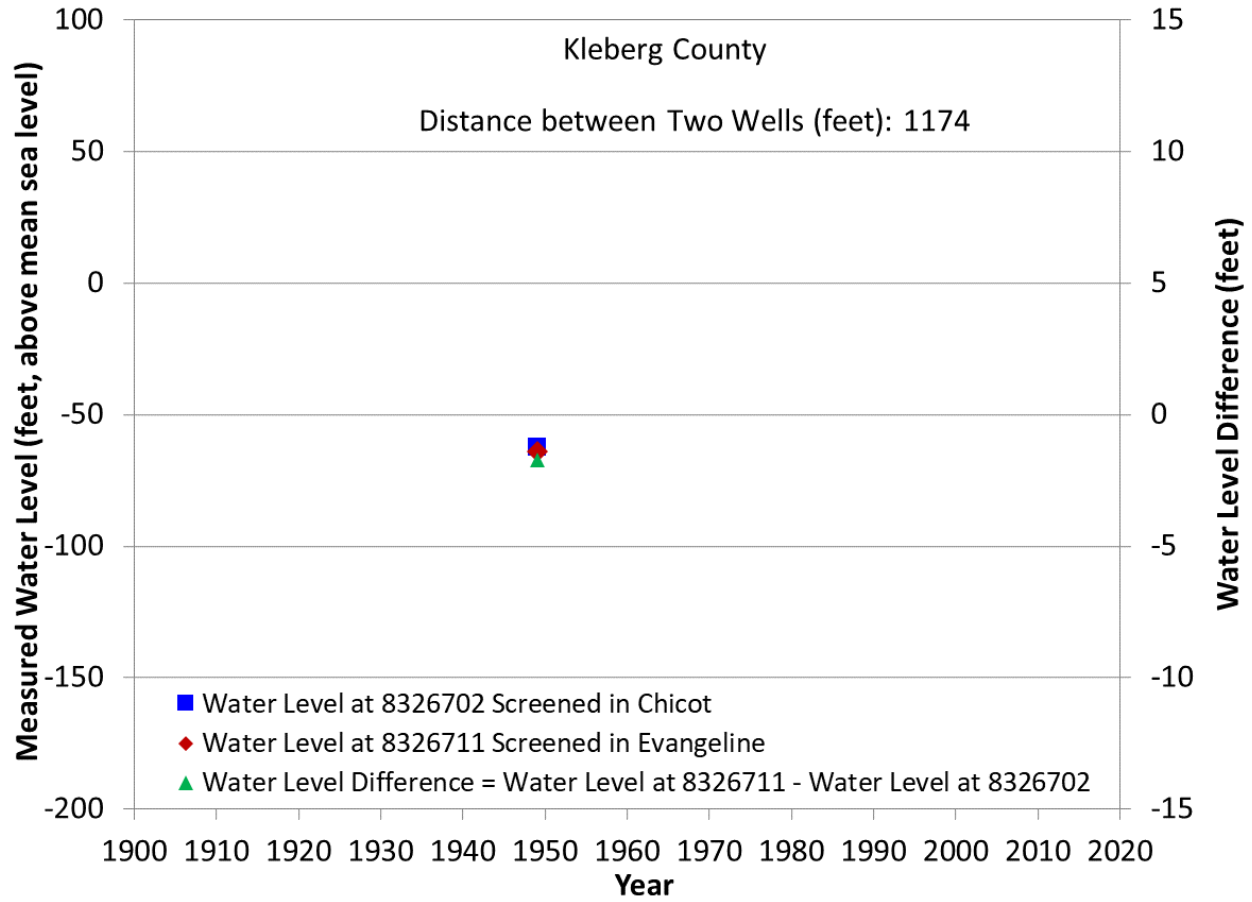


**Figure B25 Groundwater levels at State Well 8326702 and State Well 8326711.**

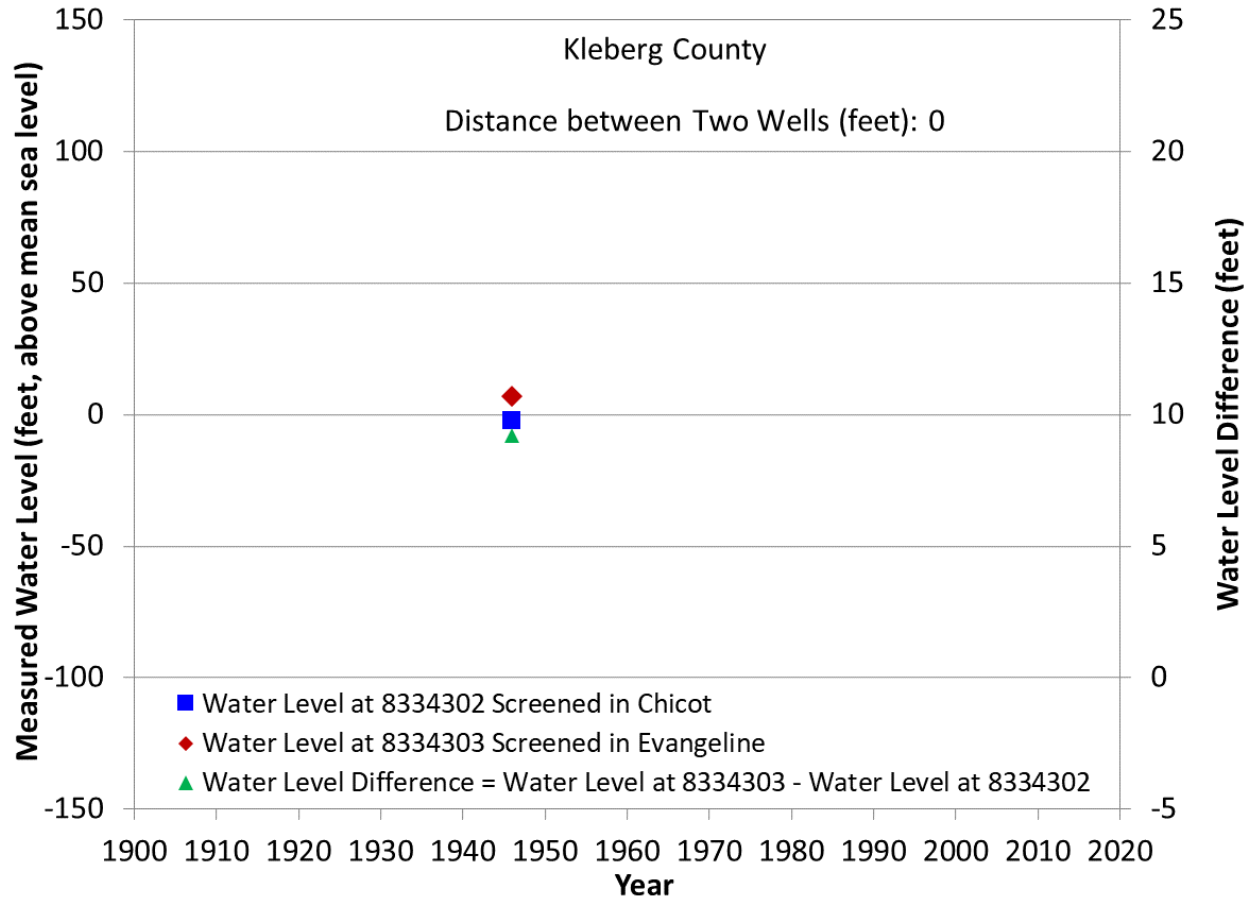


**Figure B26 Groundwater levels at State Well 8334302 and State Well 8334303.**

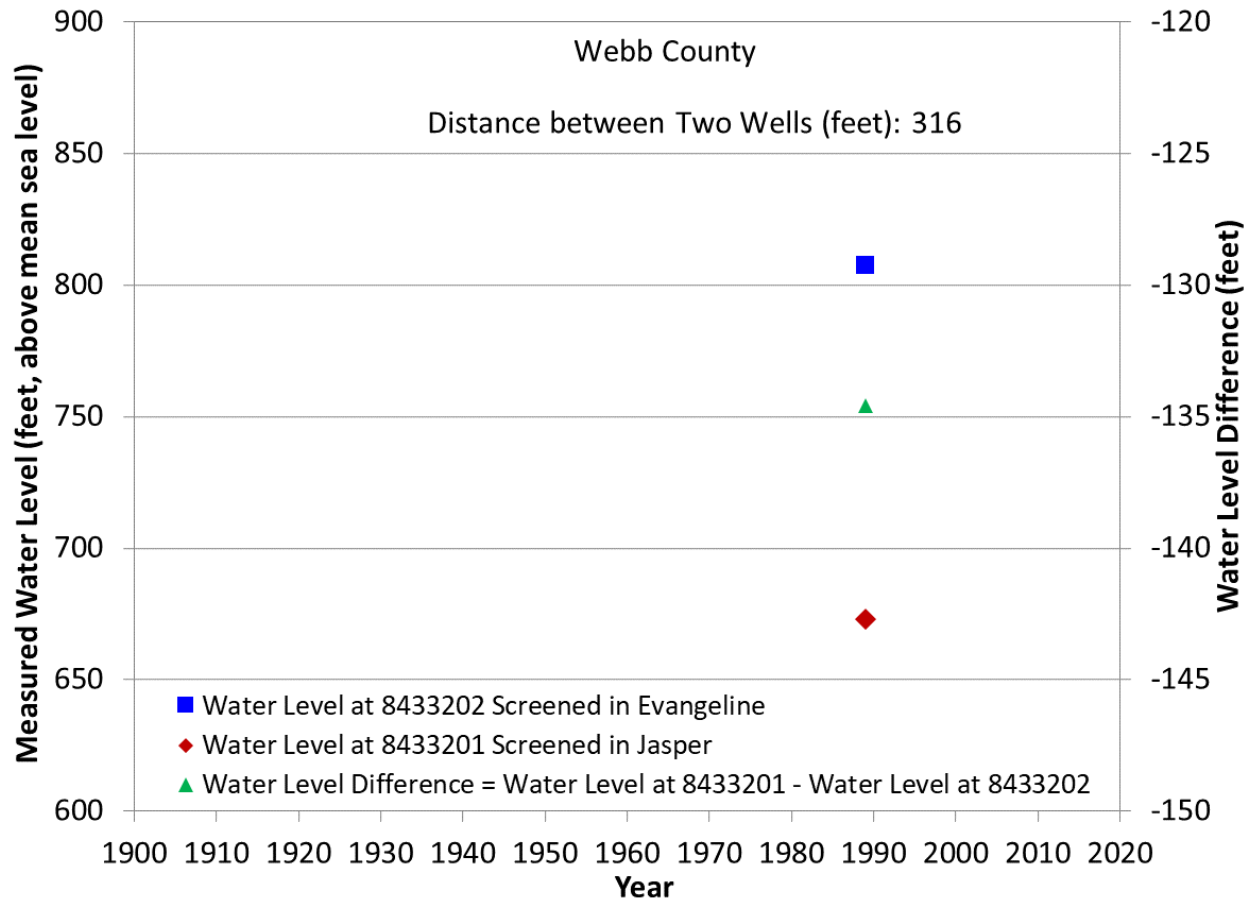


**Figure B27 Groundwater levels at State Well 8433202 and State Well 8433201.**

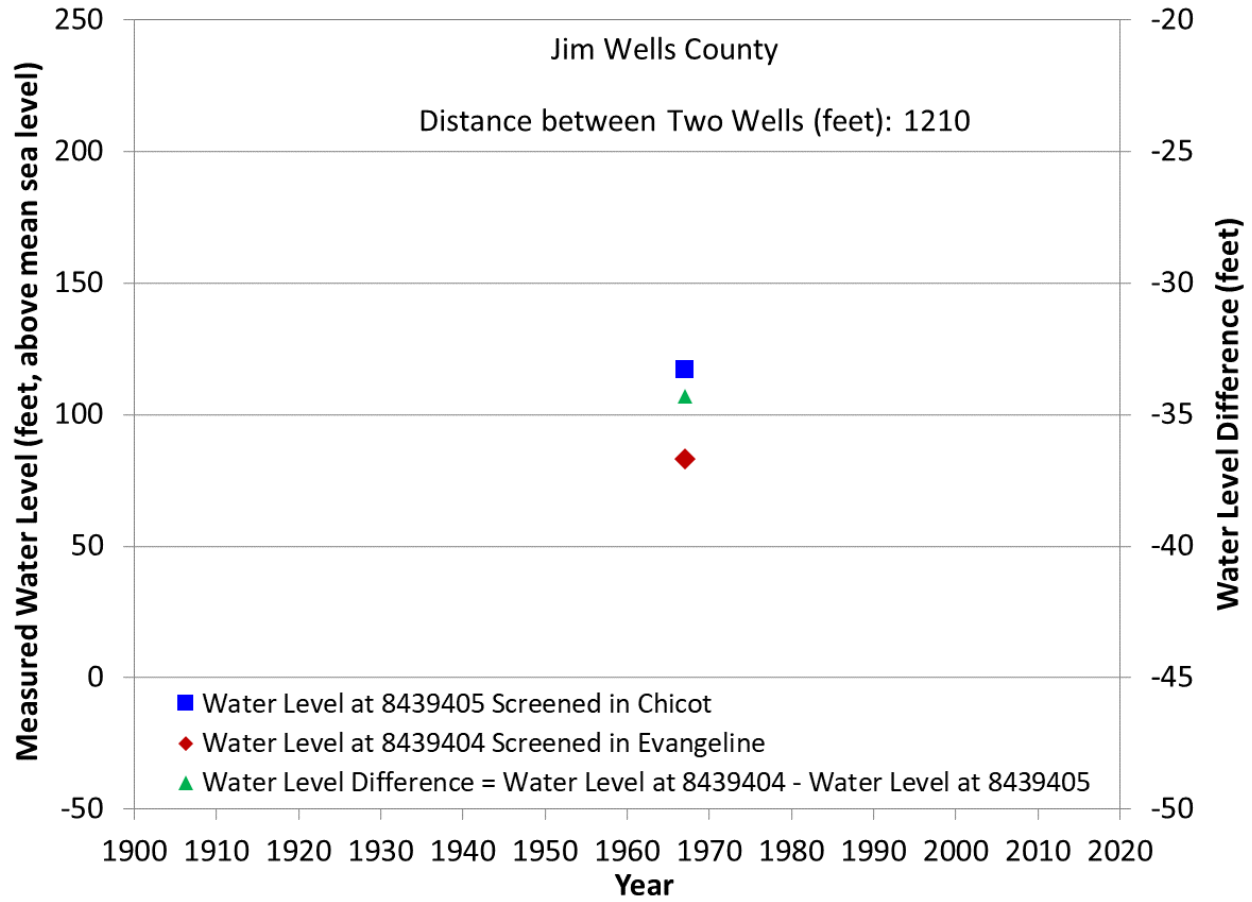


**Figure B28 Groundwater levels at State Well 8439405 and State Well 8439404.**



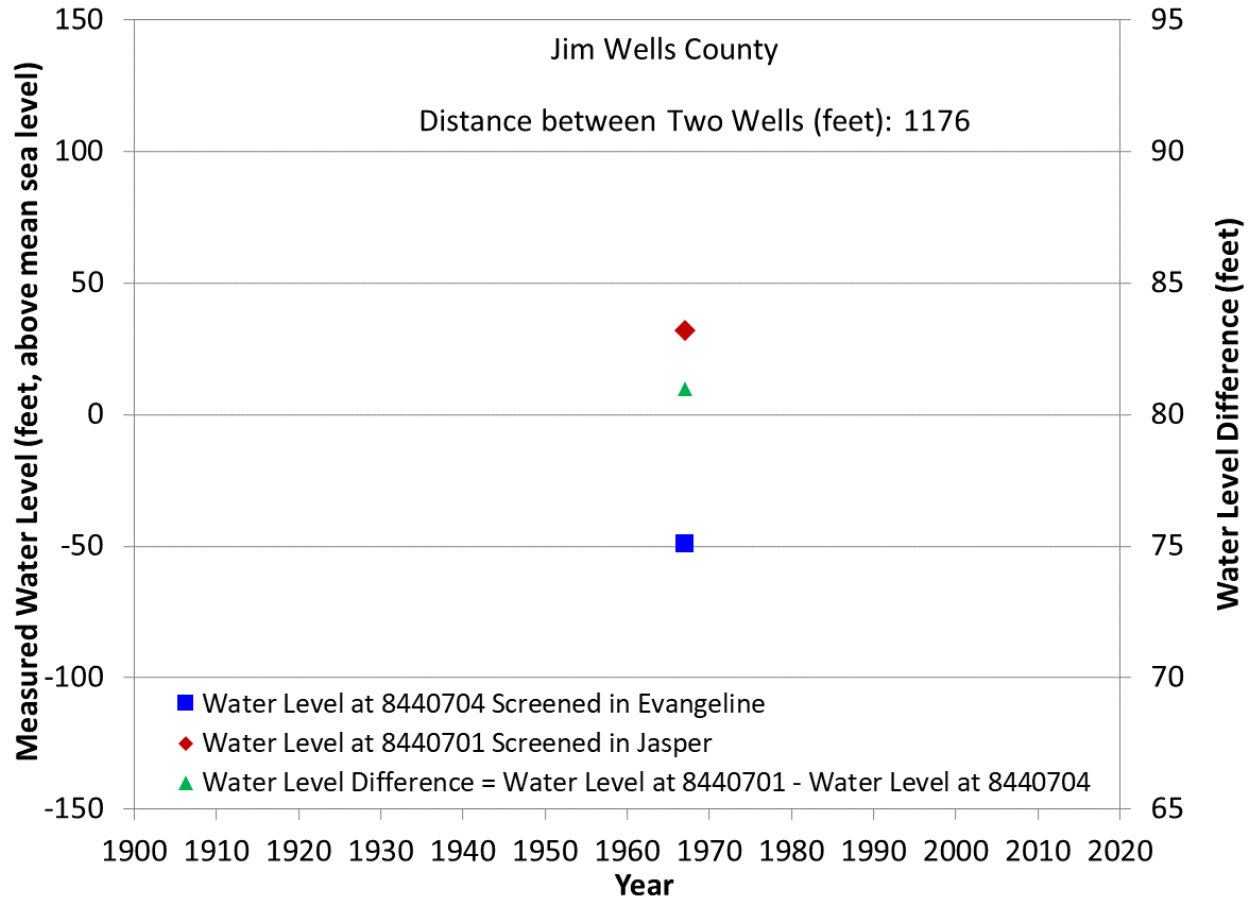


**Figure B29 Groundwater levels at State Well 8440704 and State Well 8440701.**

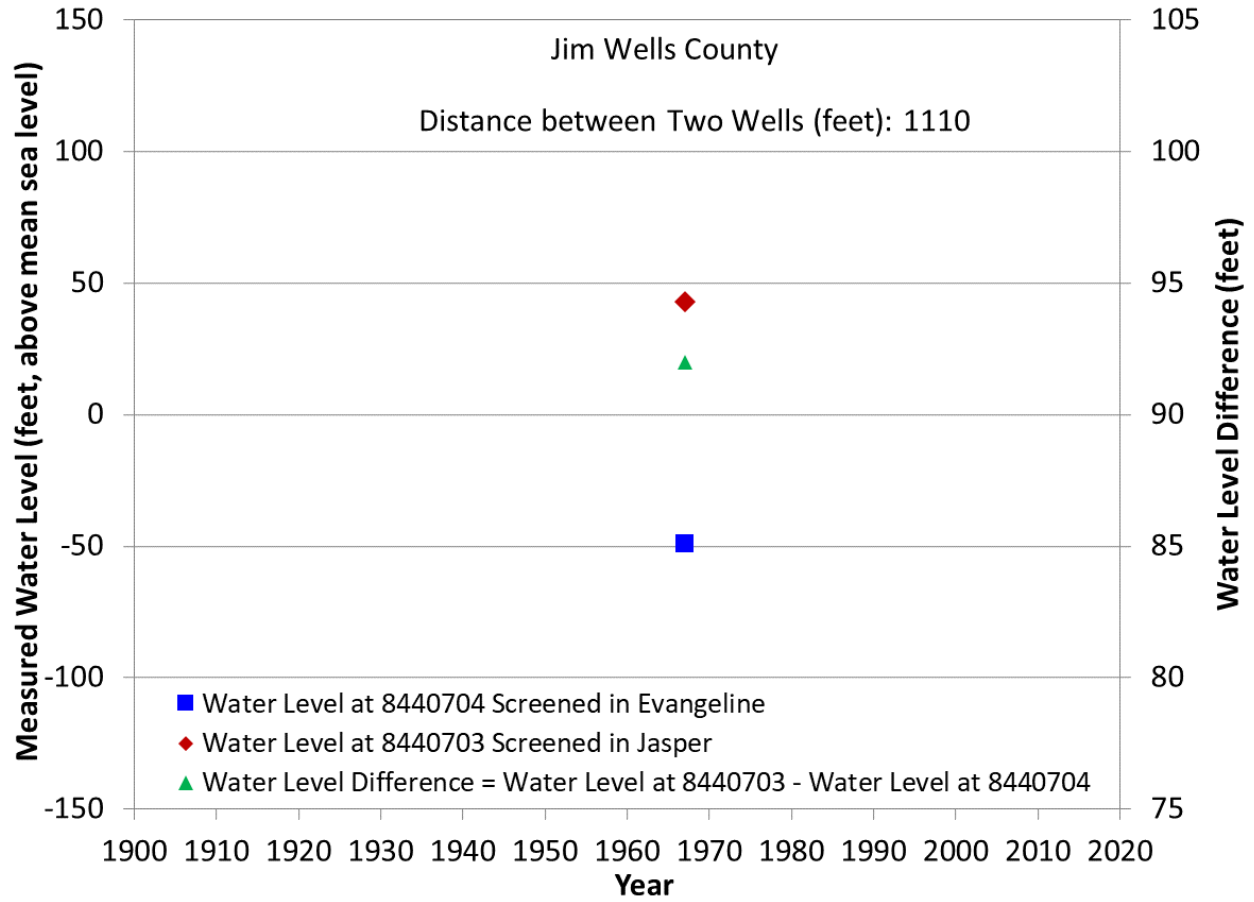


**Figure B30 Groundwater levels at State Well 8440704 and State Well 8440703.**

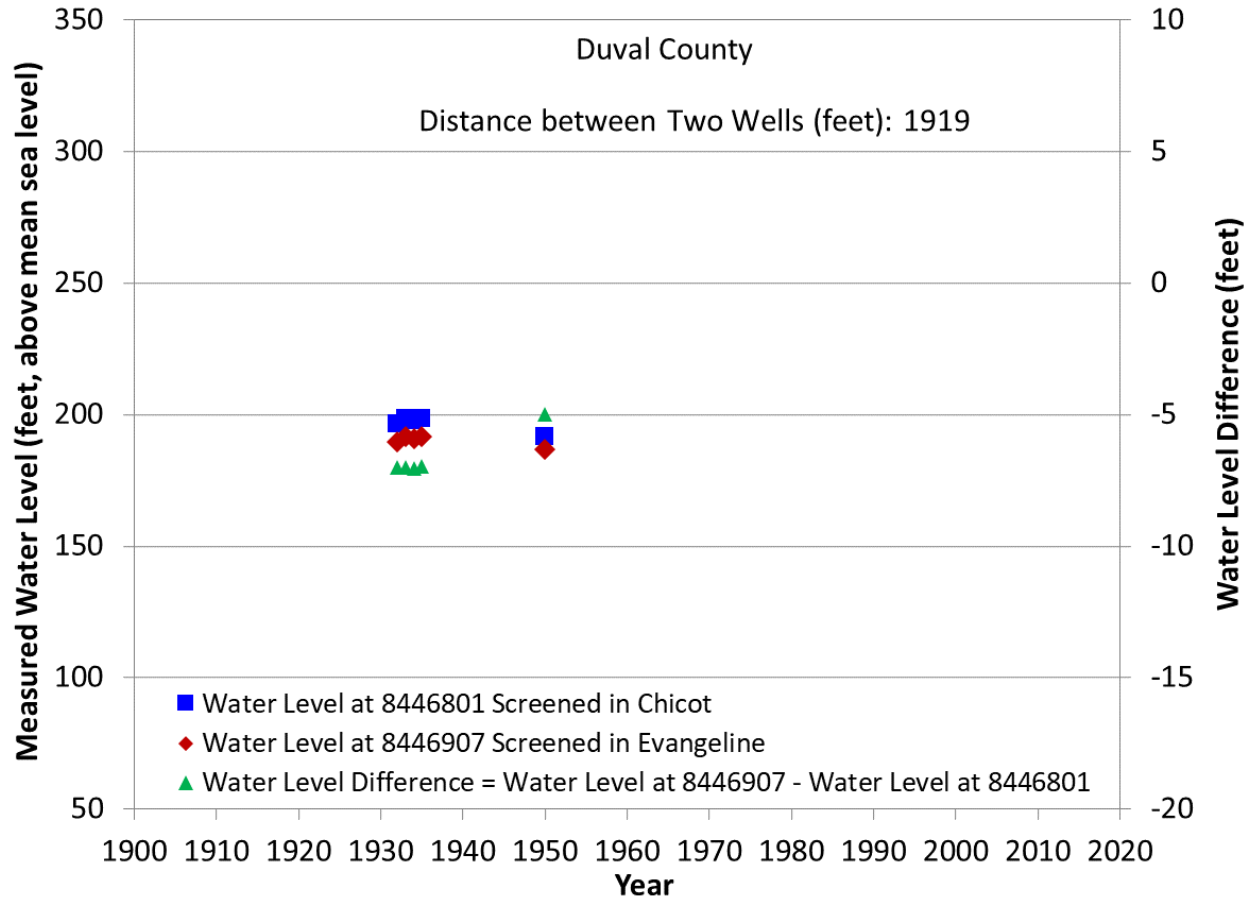


**Figure B31 Groundwater levels at State Well 8446801 and State Well 8446907.**

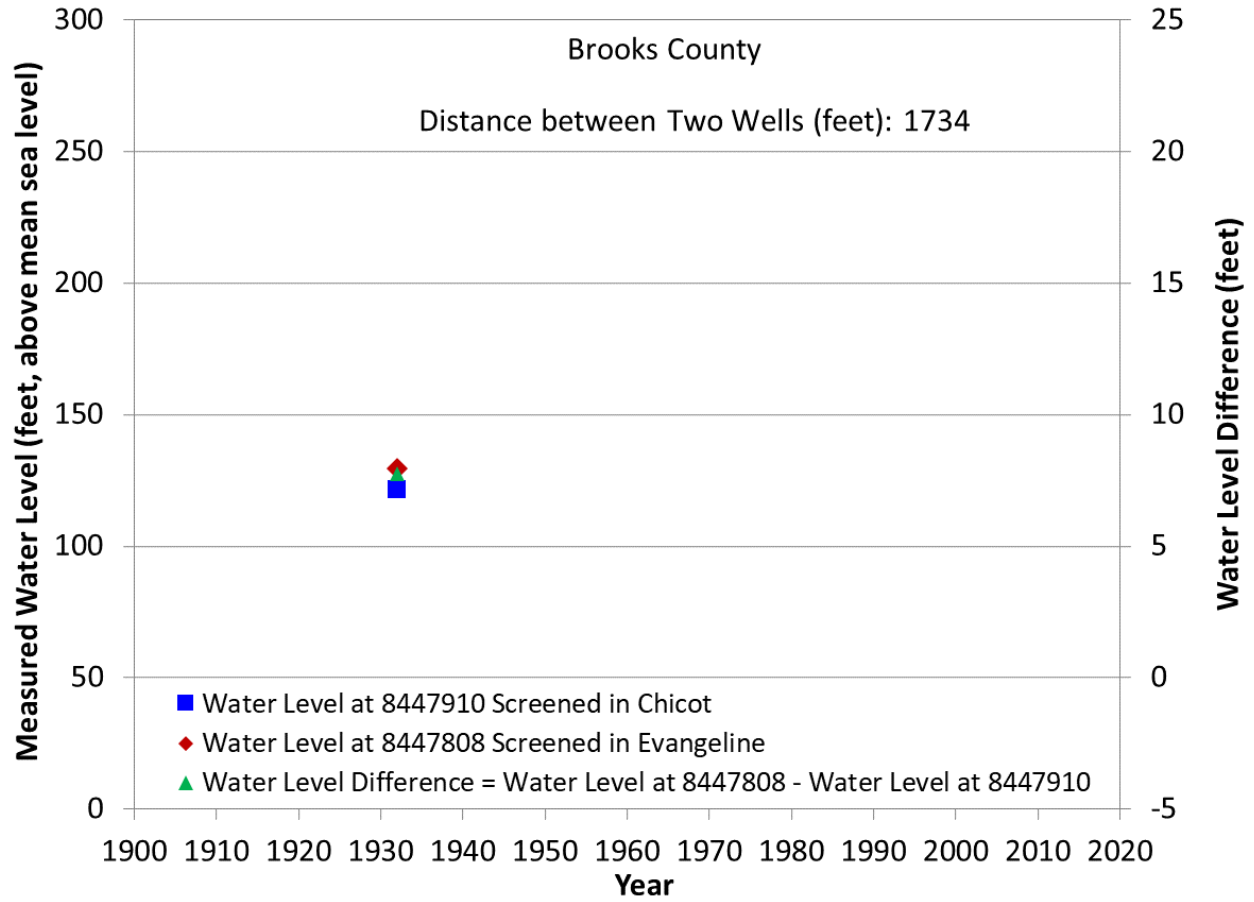


**Figure B32 Groundwater levels at State Well 8447910 and State Well 8447808.**

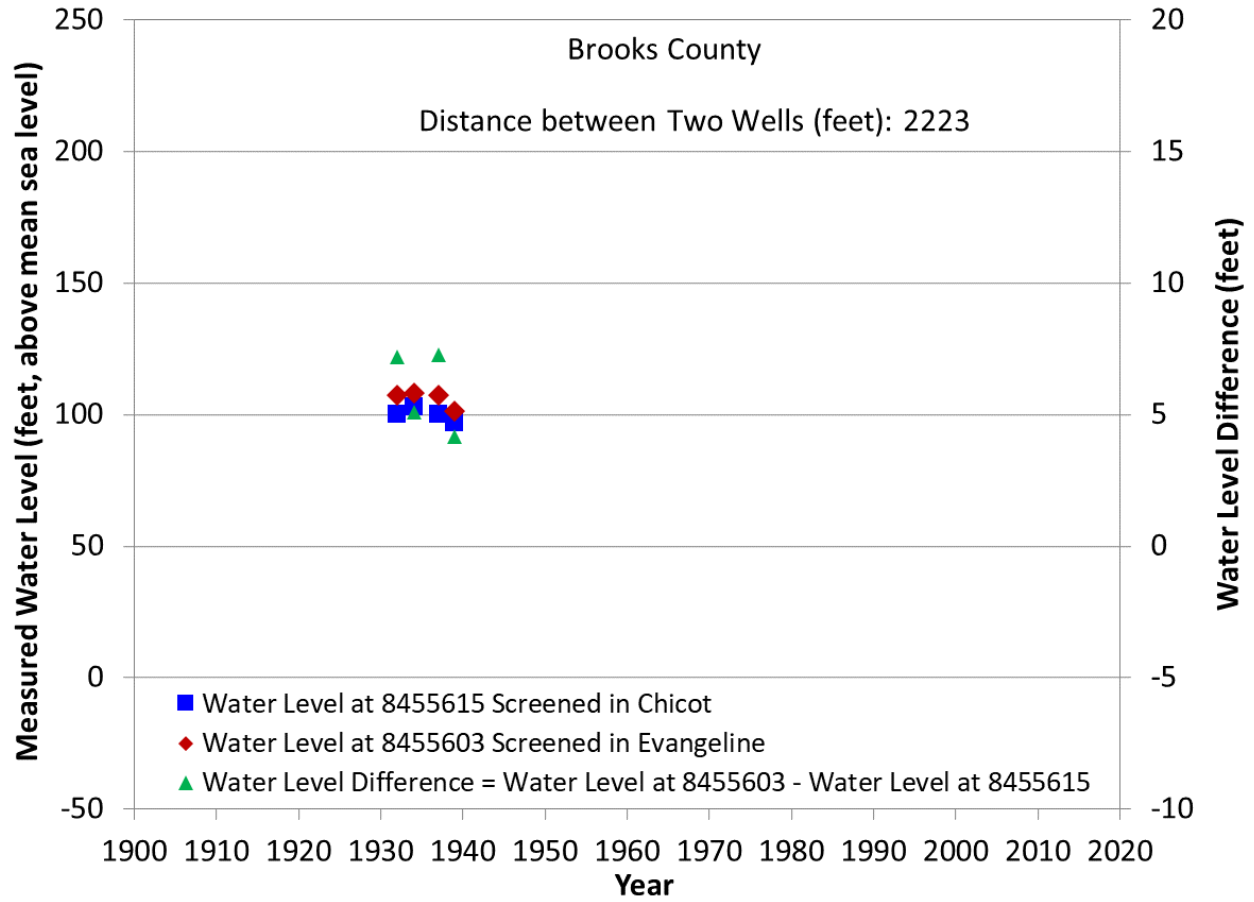


**Figure B33 Groundwater levels at State Well 8455615 and State Well 8455603.**

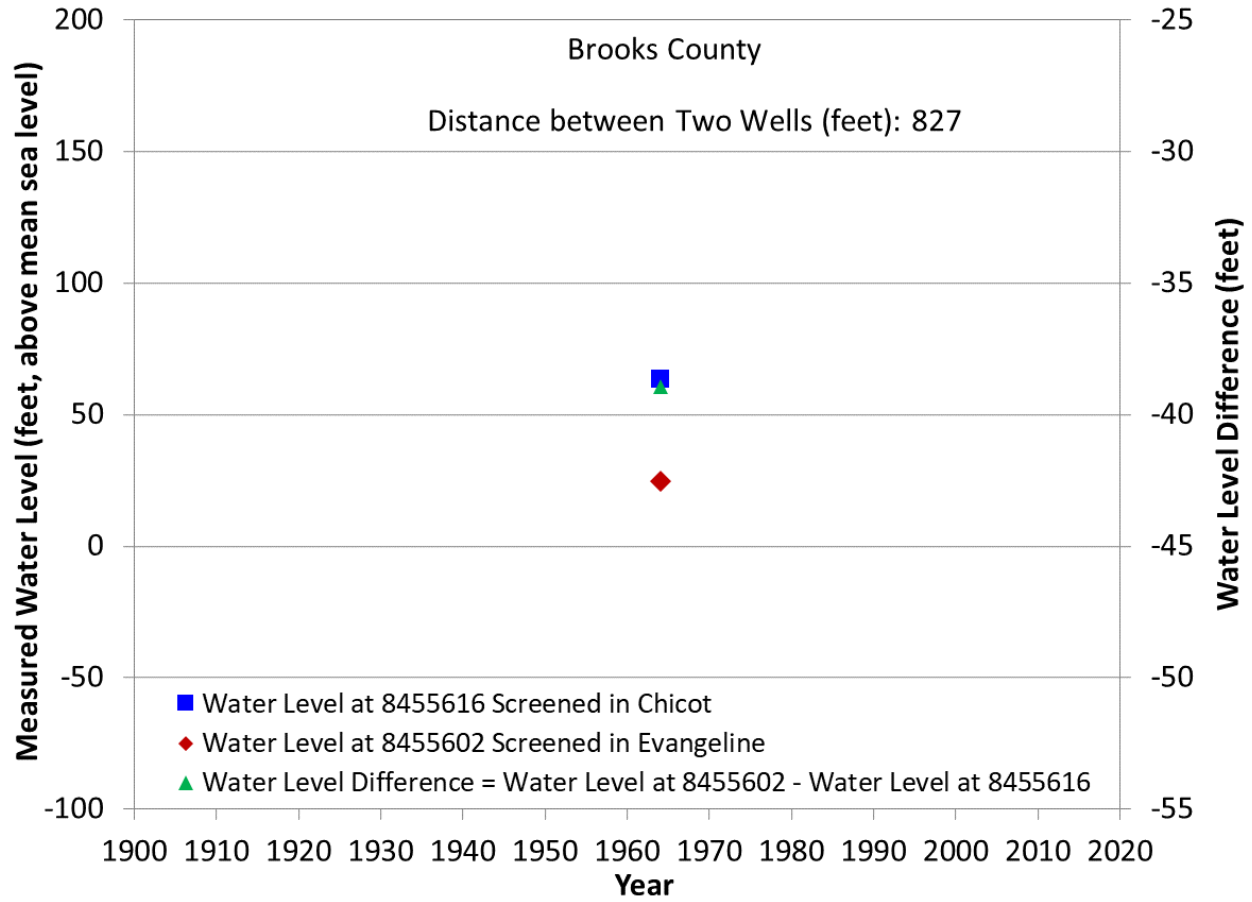


**Figure B34 Groundwater levels at State Well 8455616 and State Well 8455602.**

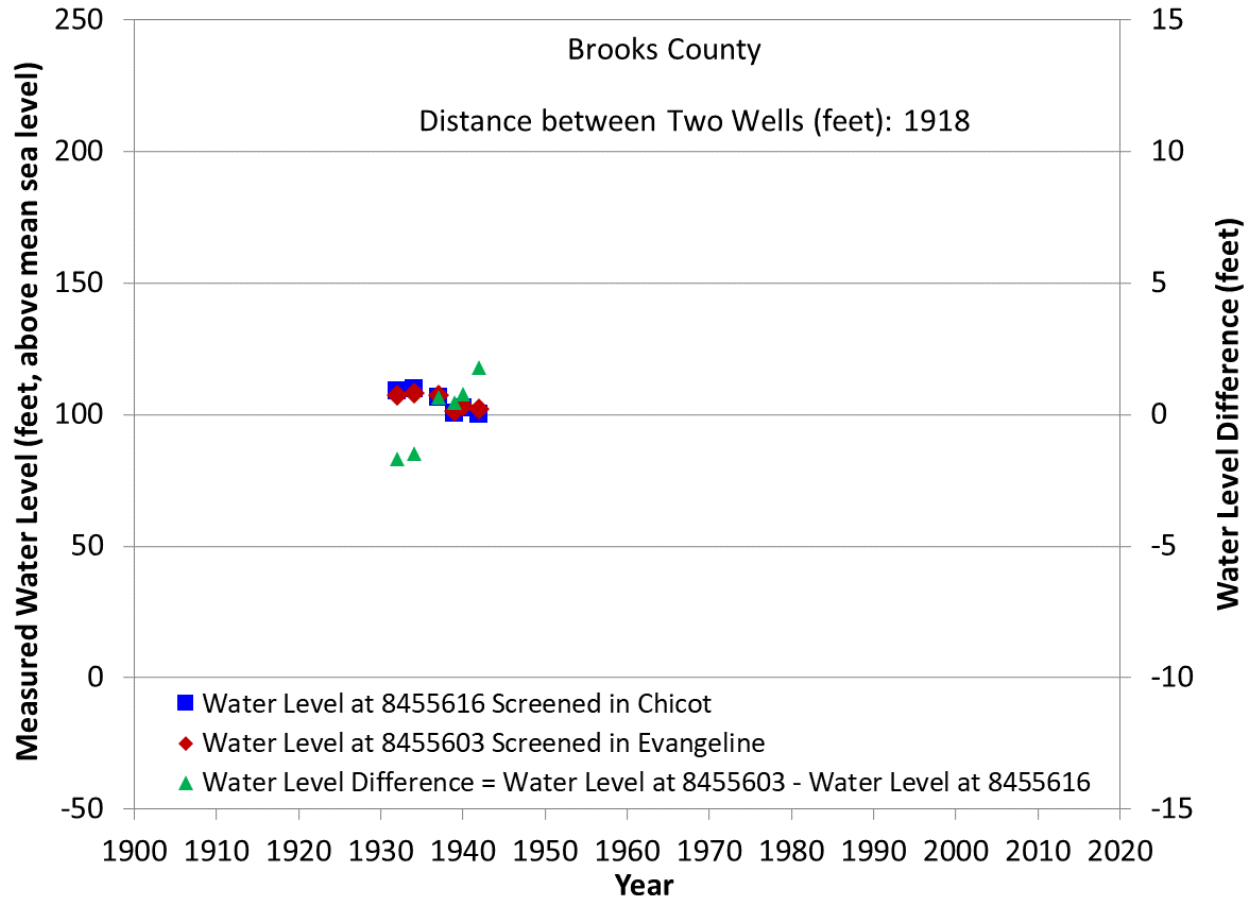


**Figure B35 Groundwater levels at State Well 8455616 and State Well 8455603.**

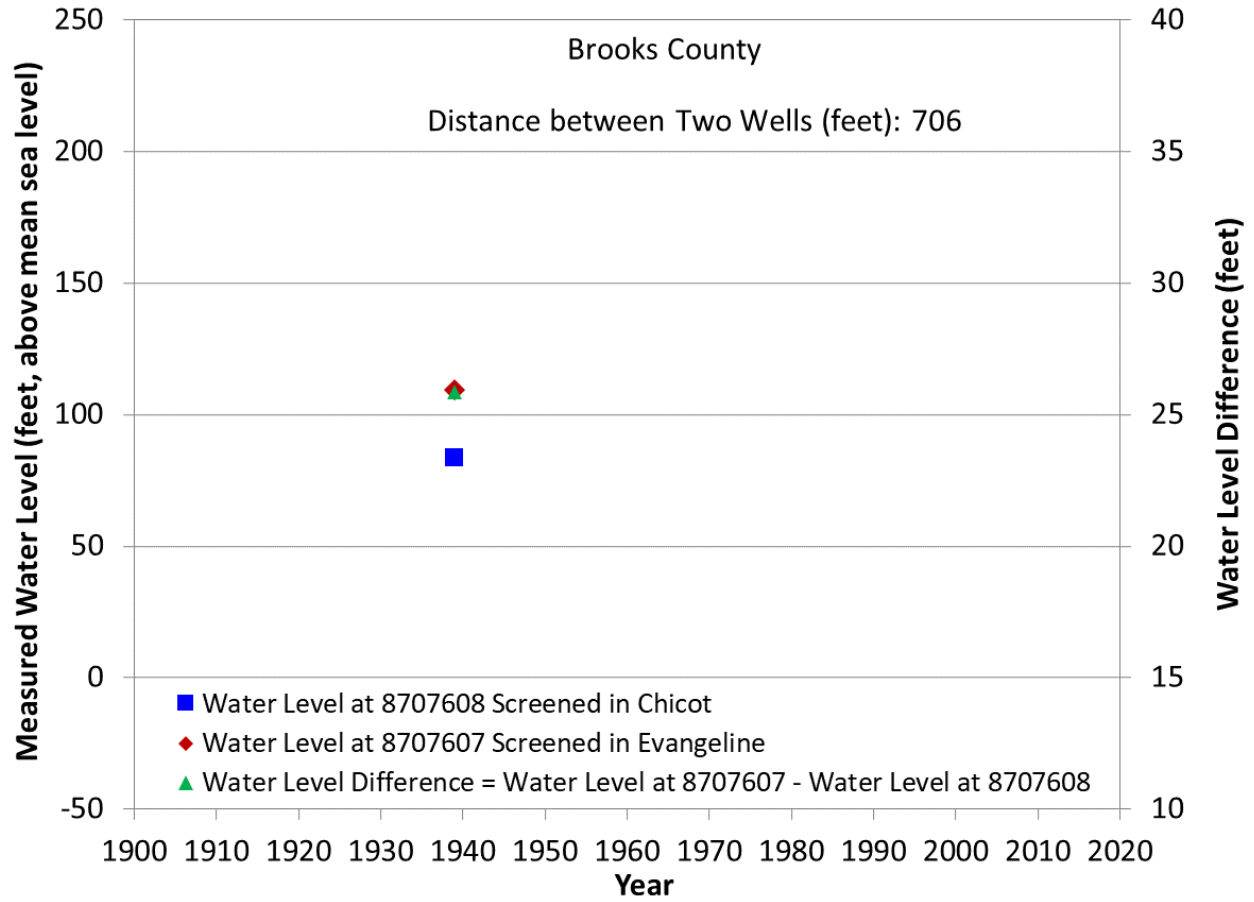


**Figure B36 Groundwater levels at State Well 8707608 and State Well 8707607.**



**Appendix C: Estimated Groundwater Recharge from Stream Baseflow-Precipitation Correlation for Years between 1981 and 2014**

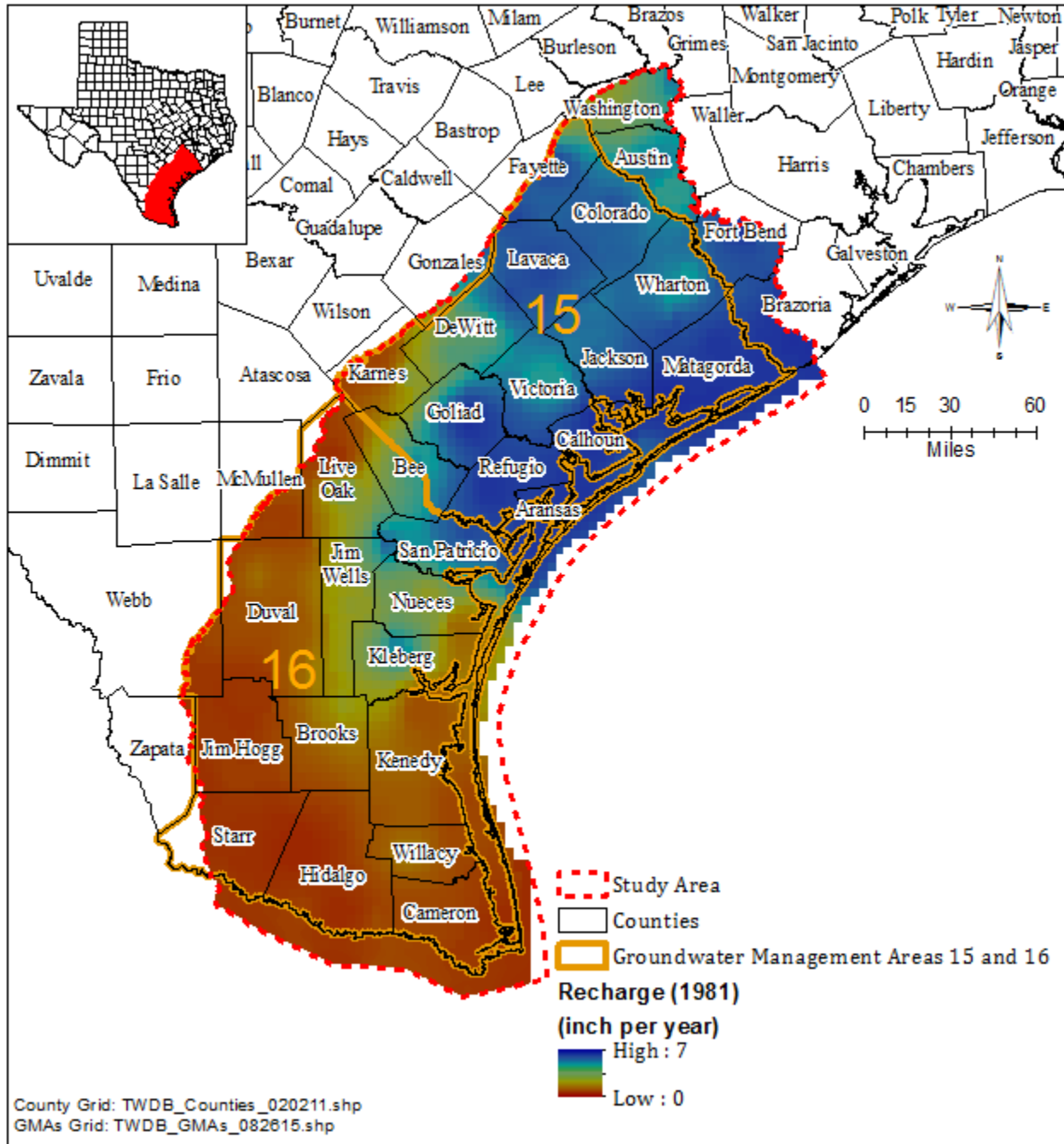
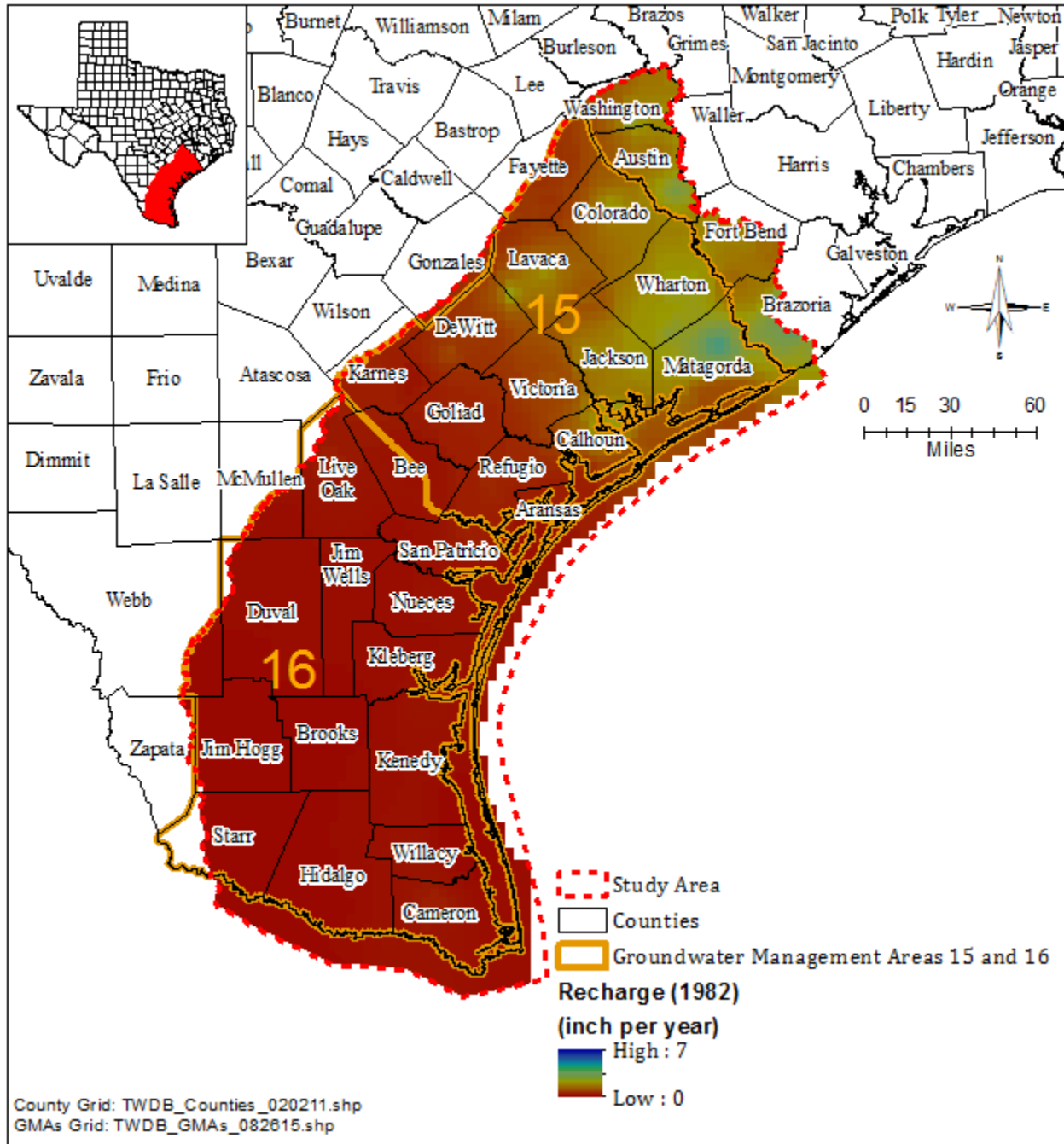
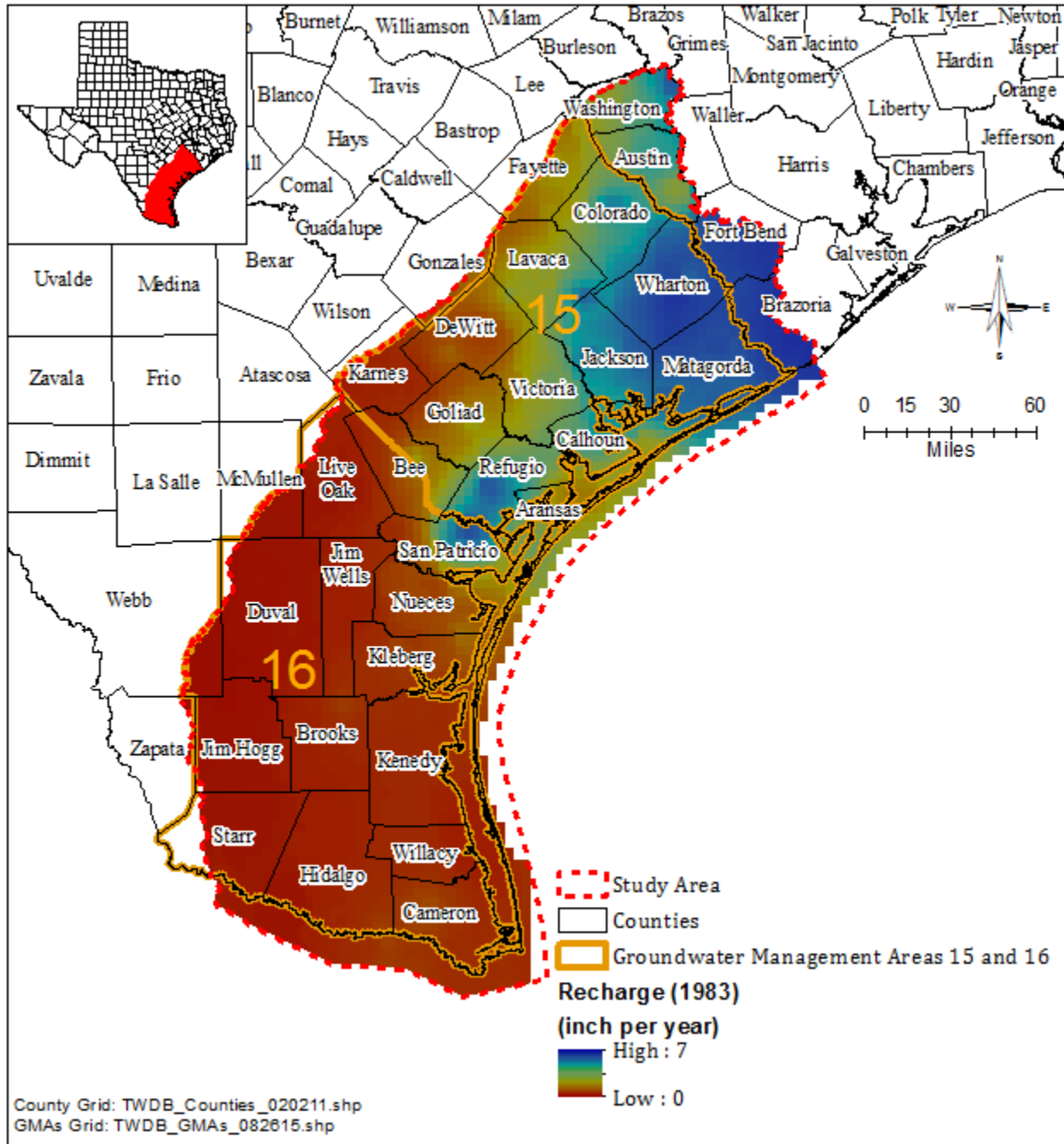


Figure C1 Estimated groundwater recharge from stream baseflow-precipitation correlation (1981).



**Figure C2 Estimated groundwater recharge from stream baseflow-precipitation correlation (1982).**



**Figure C3 Estimated groundwater recharge from stream baseflow-precipitation correlation (1983).**

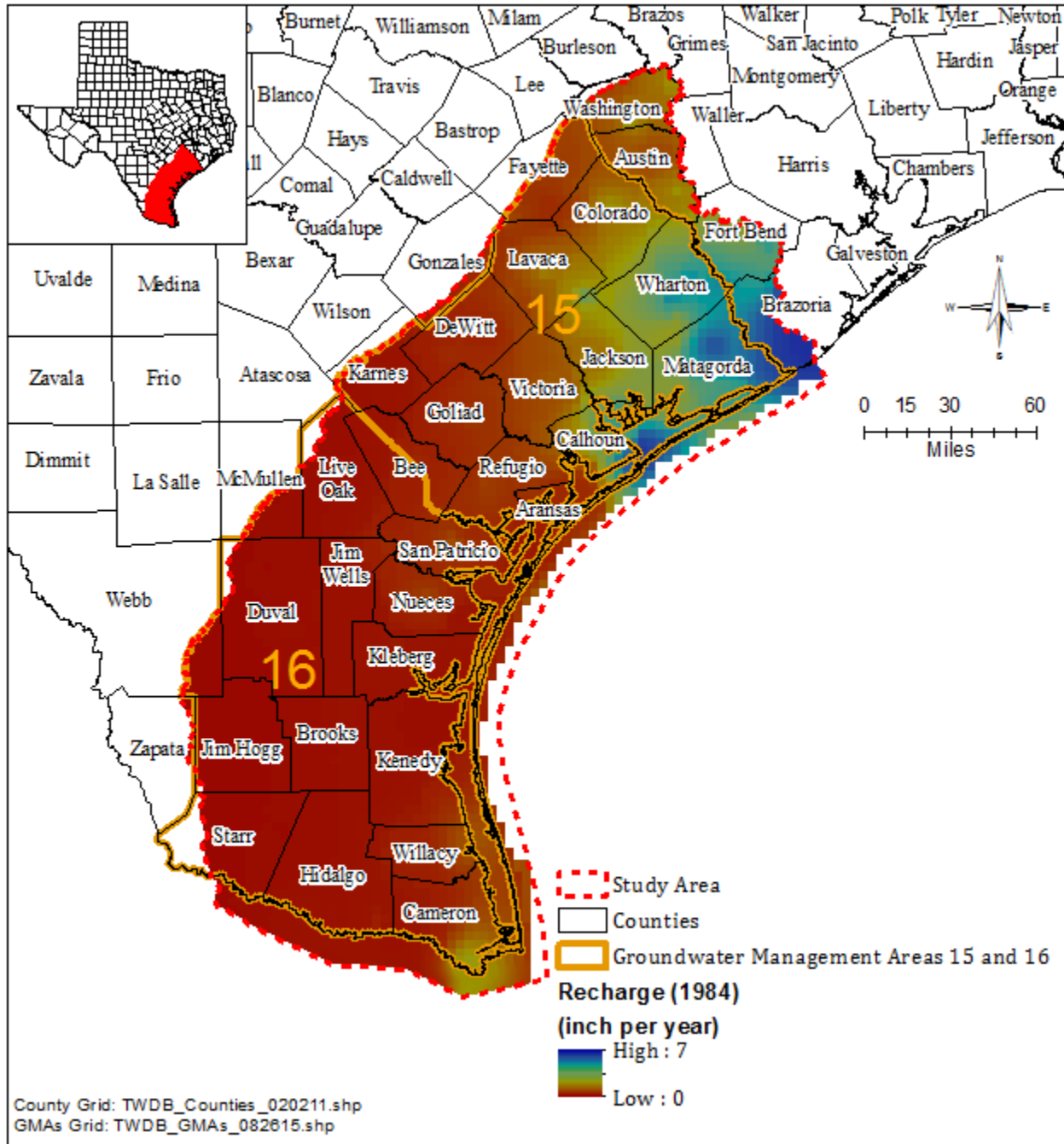
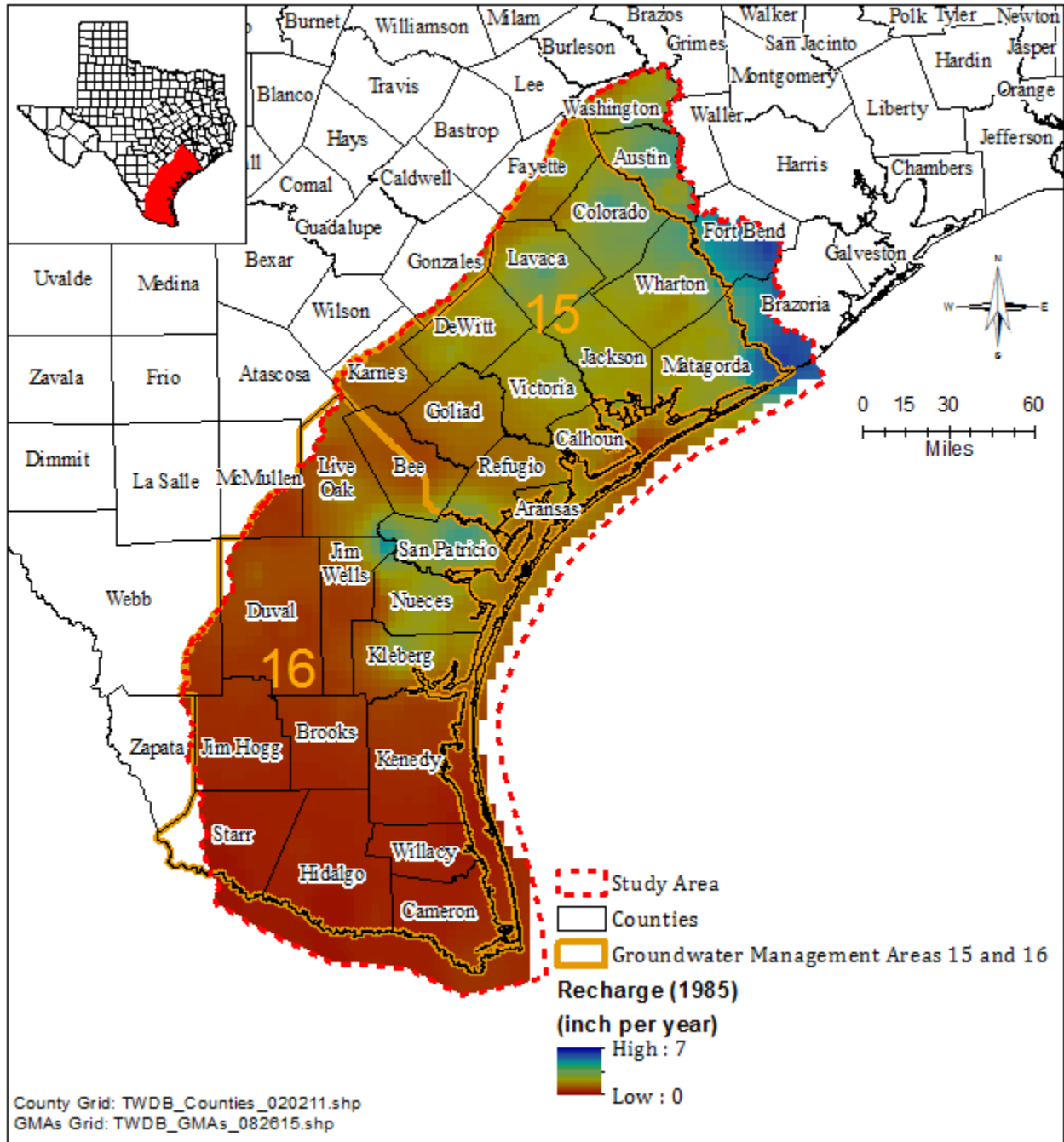
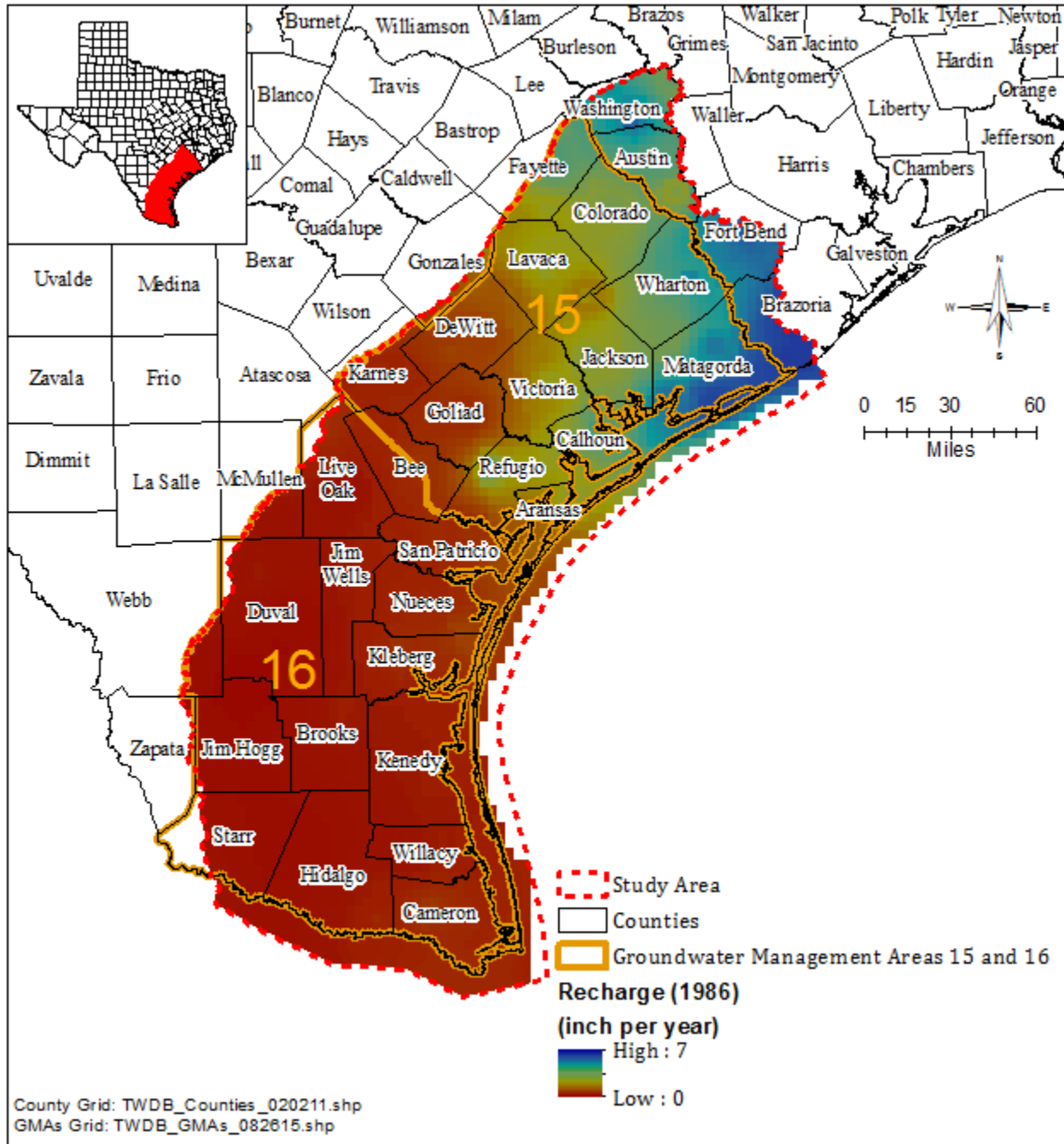


Figure C4 Estimated groundwater recharge from stream baseflow-precipitation correlation (1984).



**Figure C5 Estimated groundwater recharge from stream baseflow-precipitation correlation (1985).**



**Figure C6 Estimated groundwater recharge from stream baseflow-precipitation correlation (1986).**

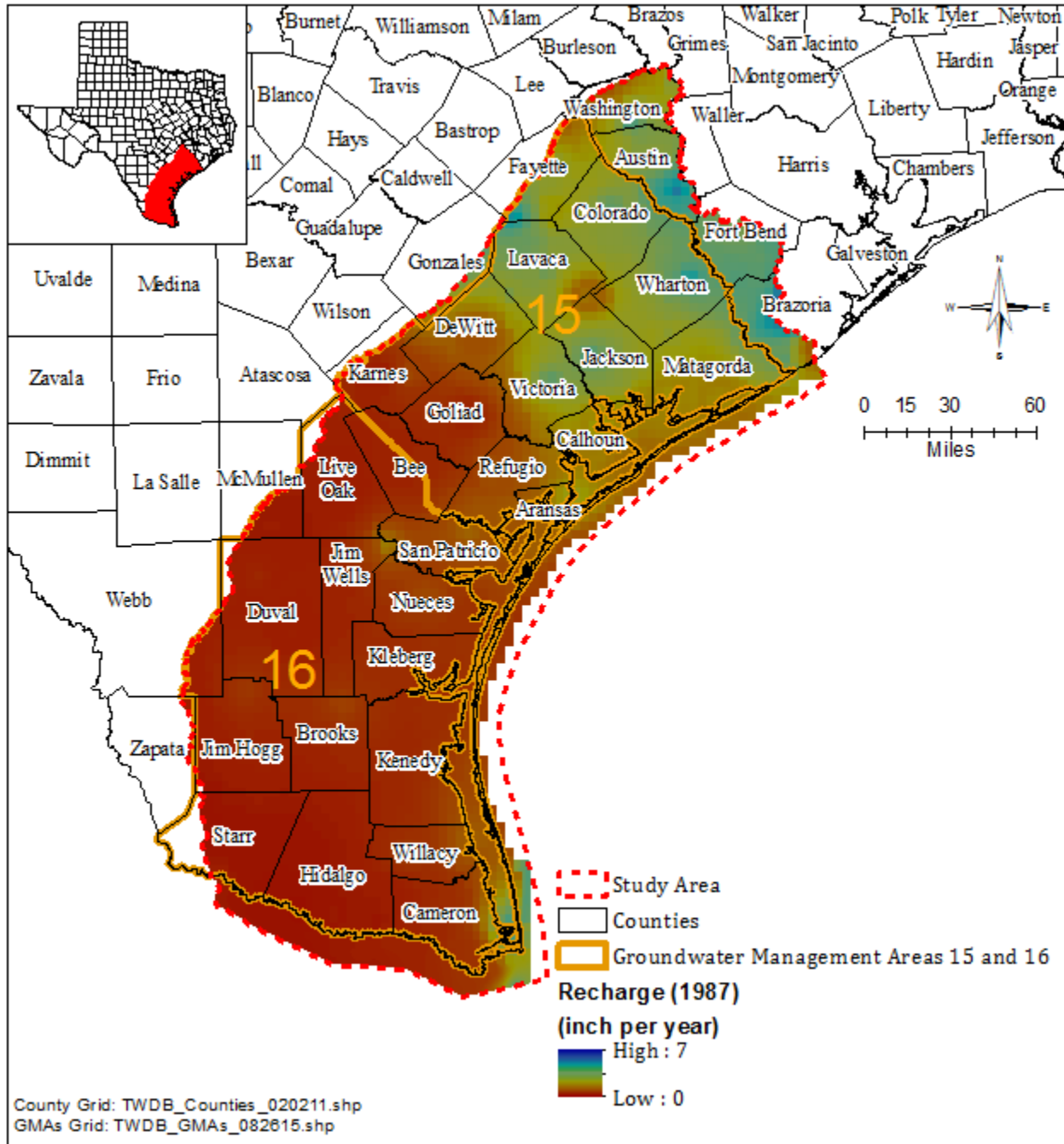


**Figure C7 Estimated groundwater recharge from stream baseflow-precipitation correlation (1987).**



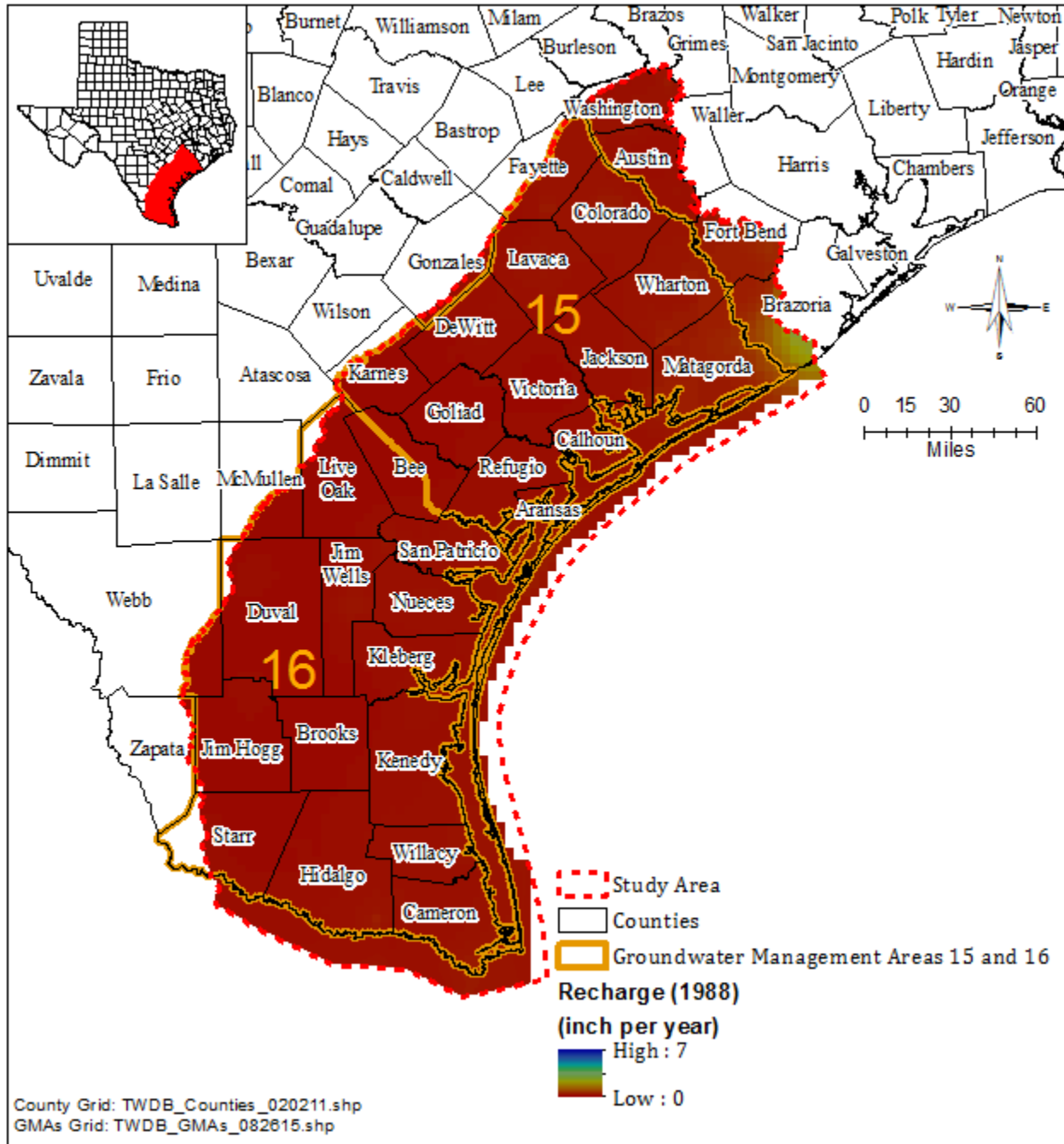
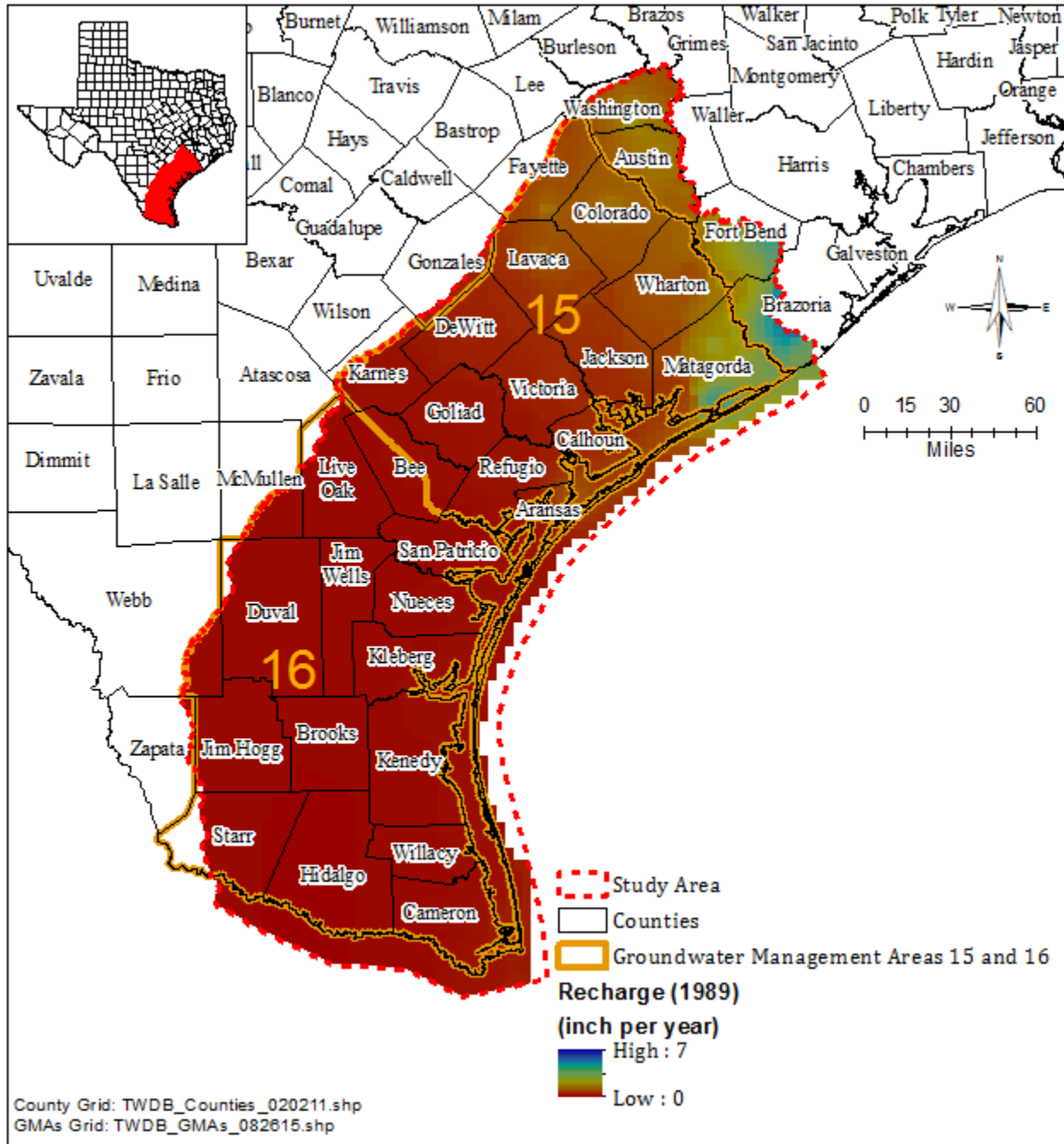
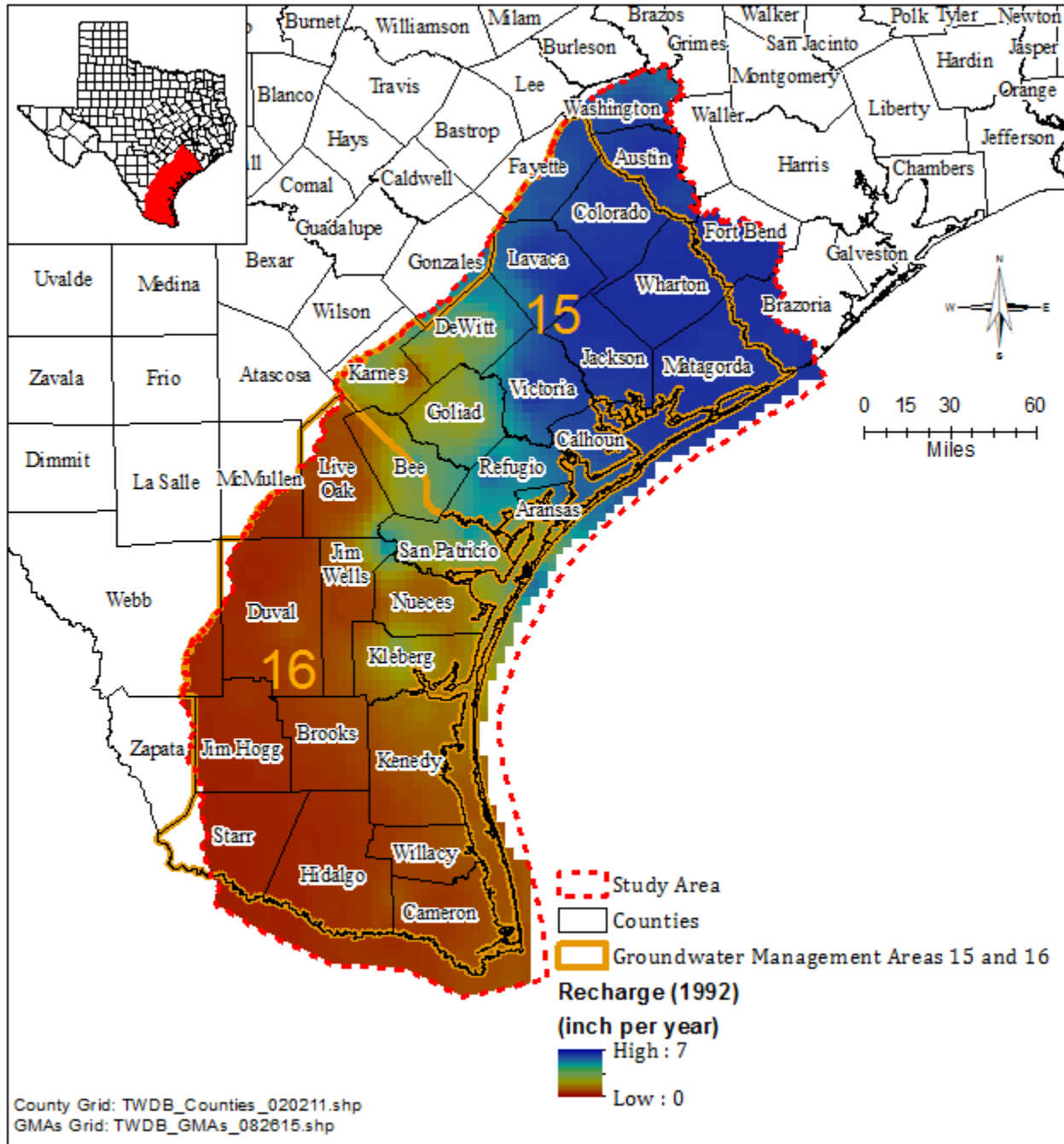


Figure C8 Estimated groundwater recharge from stream baseflow-precipitation correlation (1988).



**Figure C9 Estimated groundwater recharge from stream baseflow-precipitation correlation (1989).**





**Figure C11 Estimated groundwater recharge from stream baseflow-precipitation correlation (1992).**

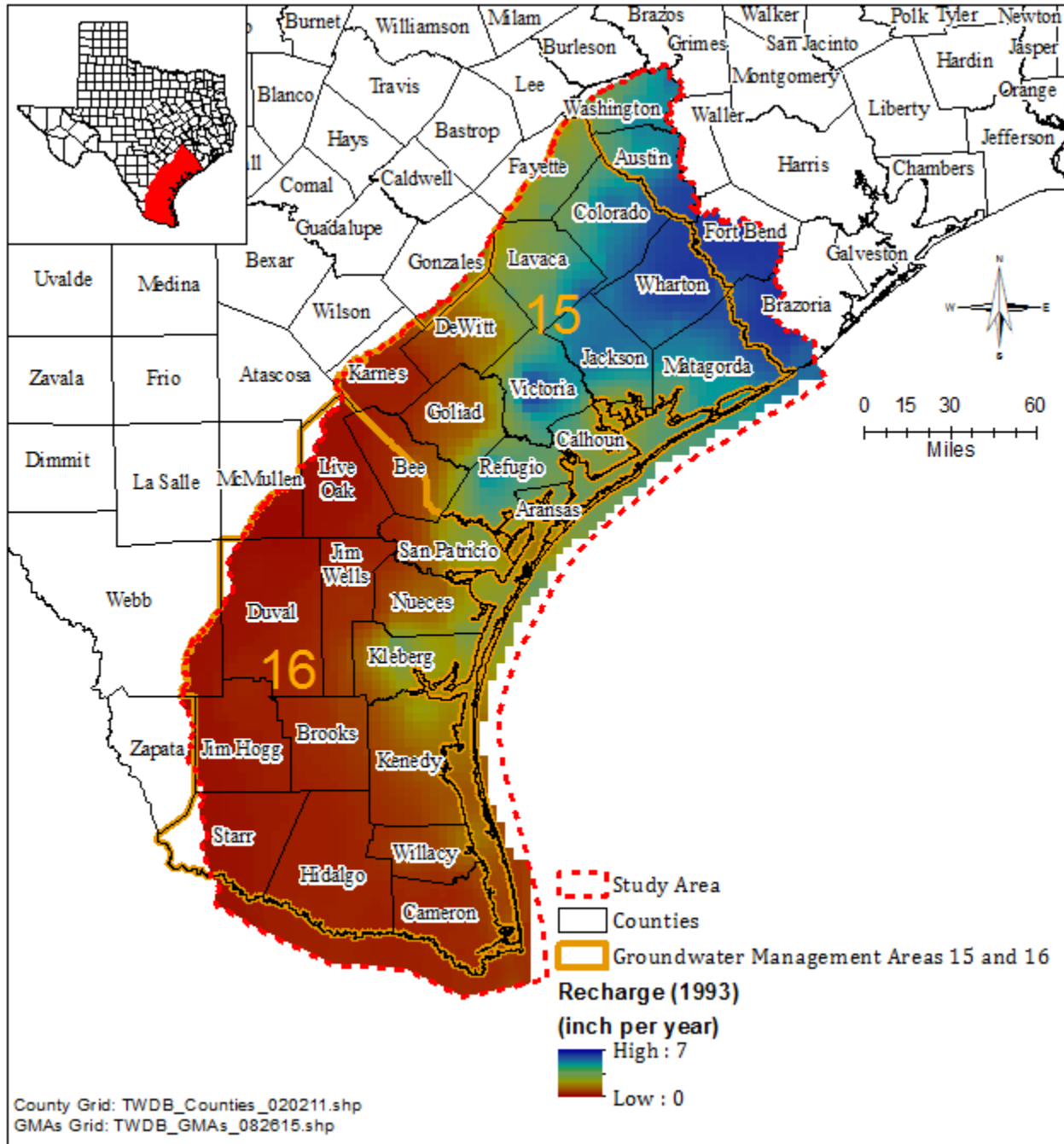


**Figure C12 Estimated groundwater recharge from stream baseflow-precipitation correlation (1993).**

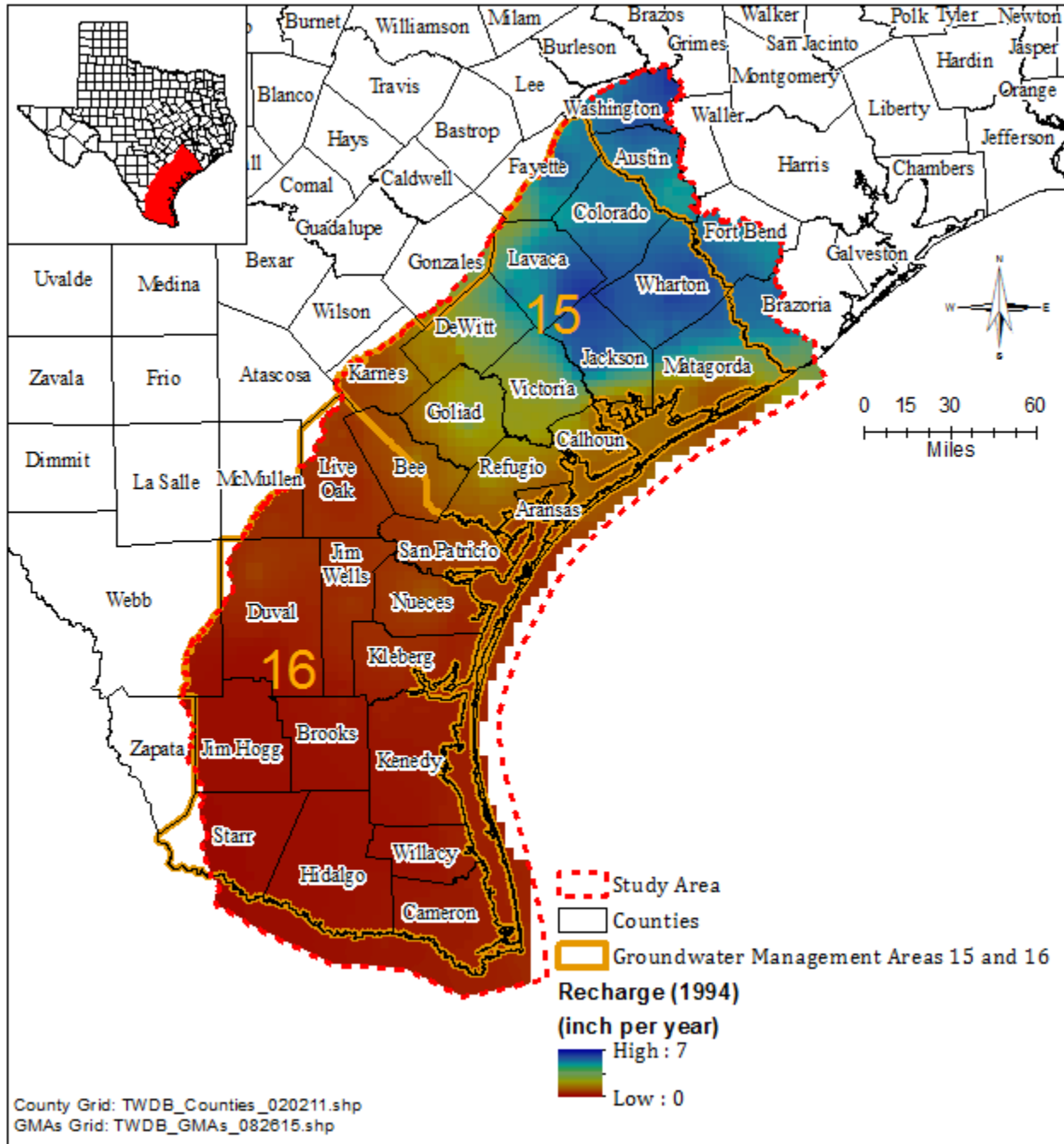


**Figure C13 Estimated groundwater recharge from stream baseflow-precipitation correlation (1994).**

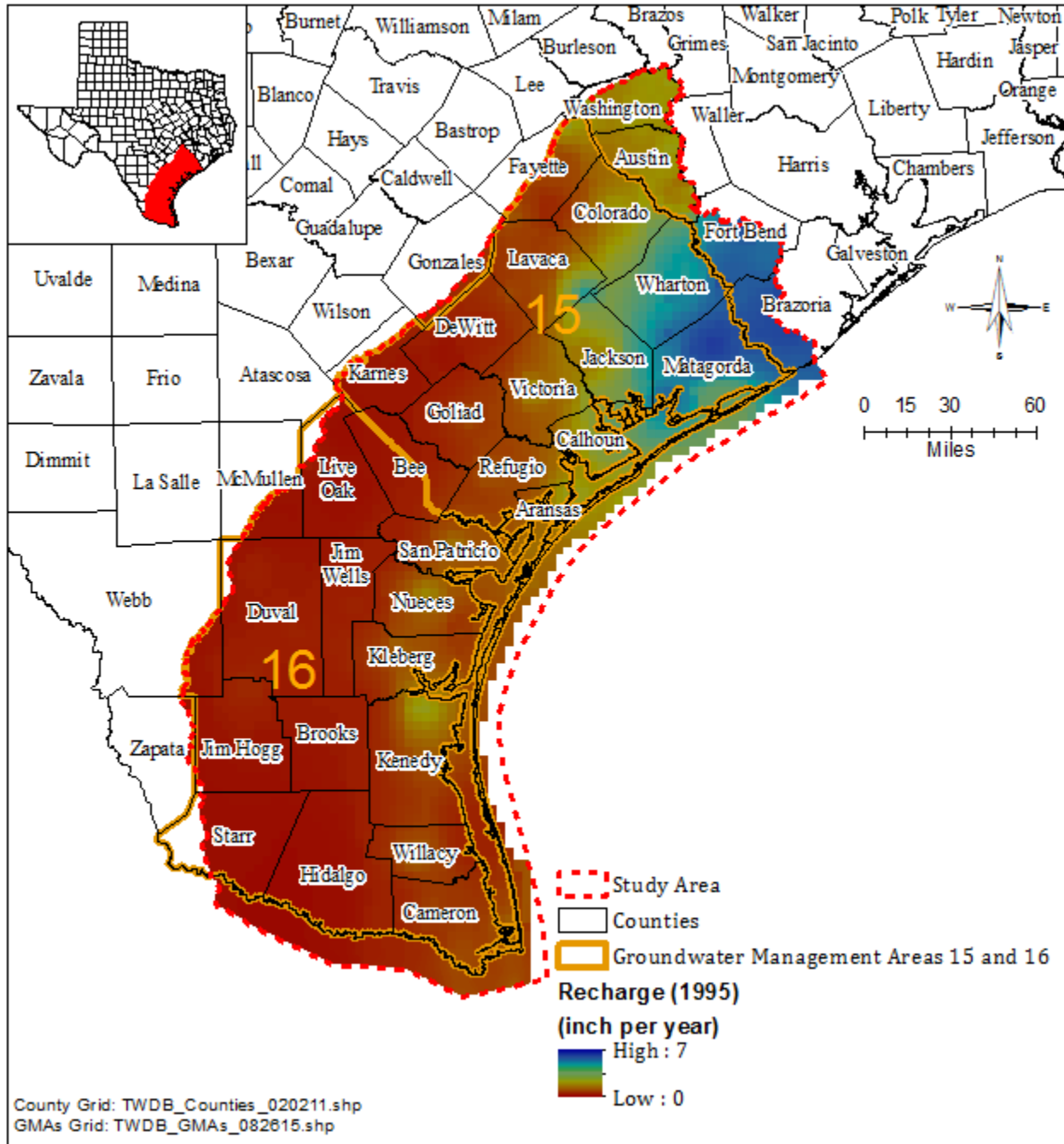


**Figure C14 Estimated groundwater recharge from stream baseflow-precipitation correlation (1995).**

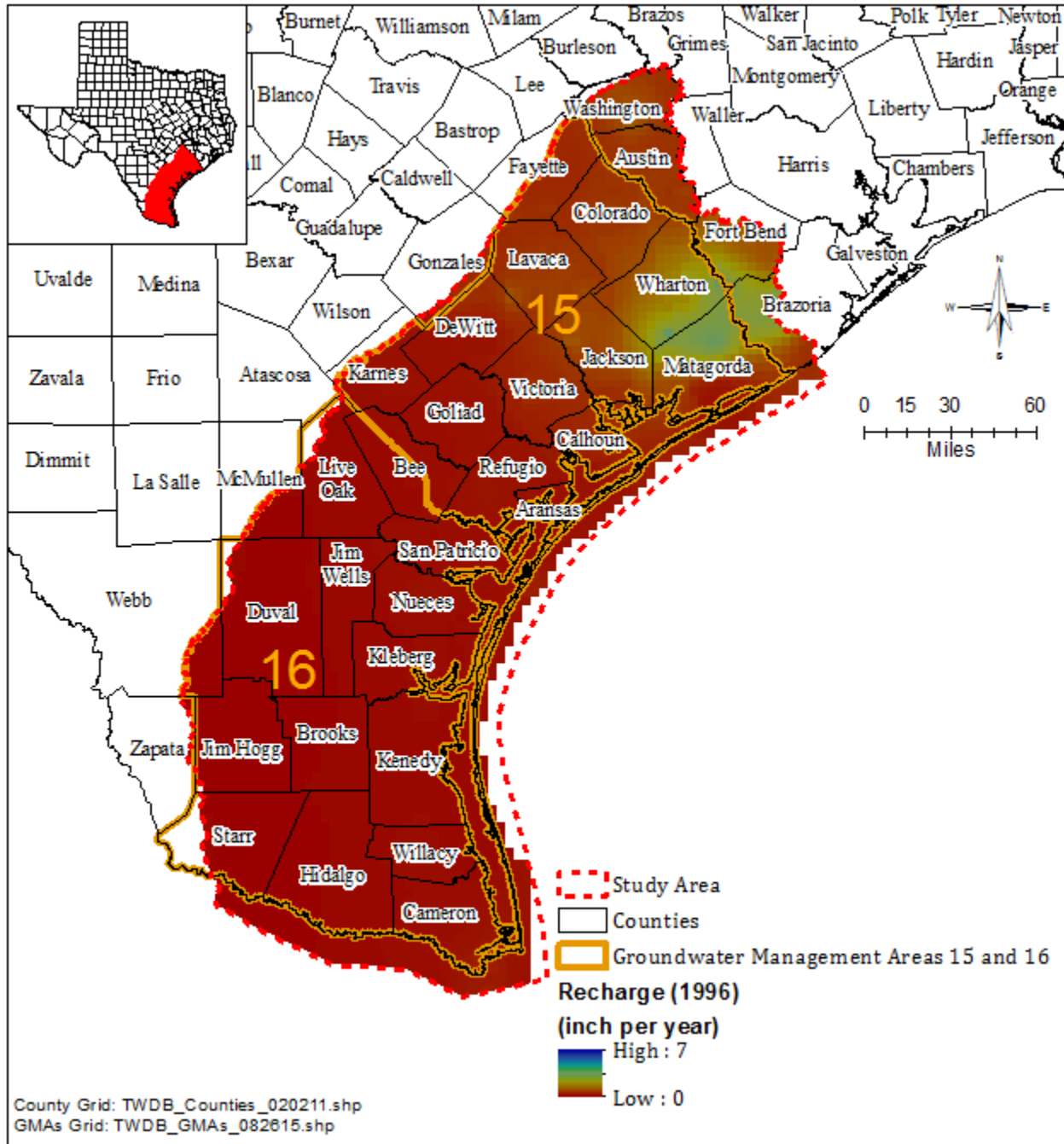


Figure C15 Estimated groundwater recharge from stream baseflow-precipitation correlation (1996).



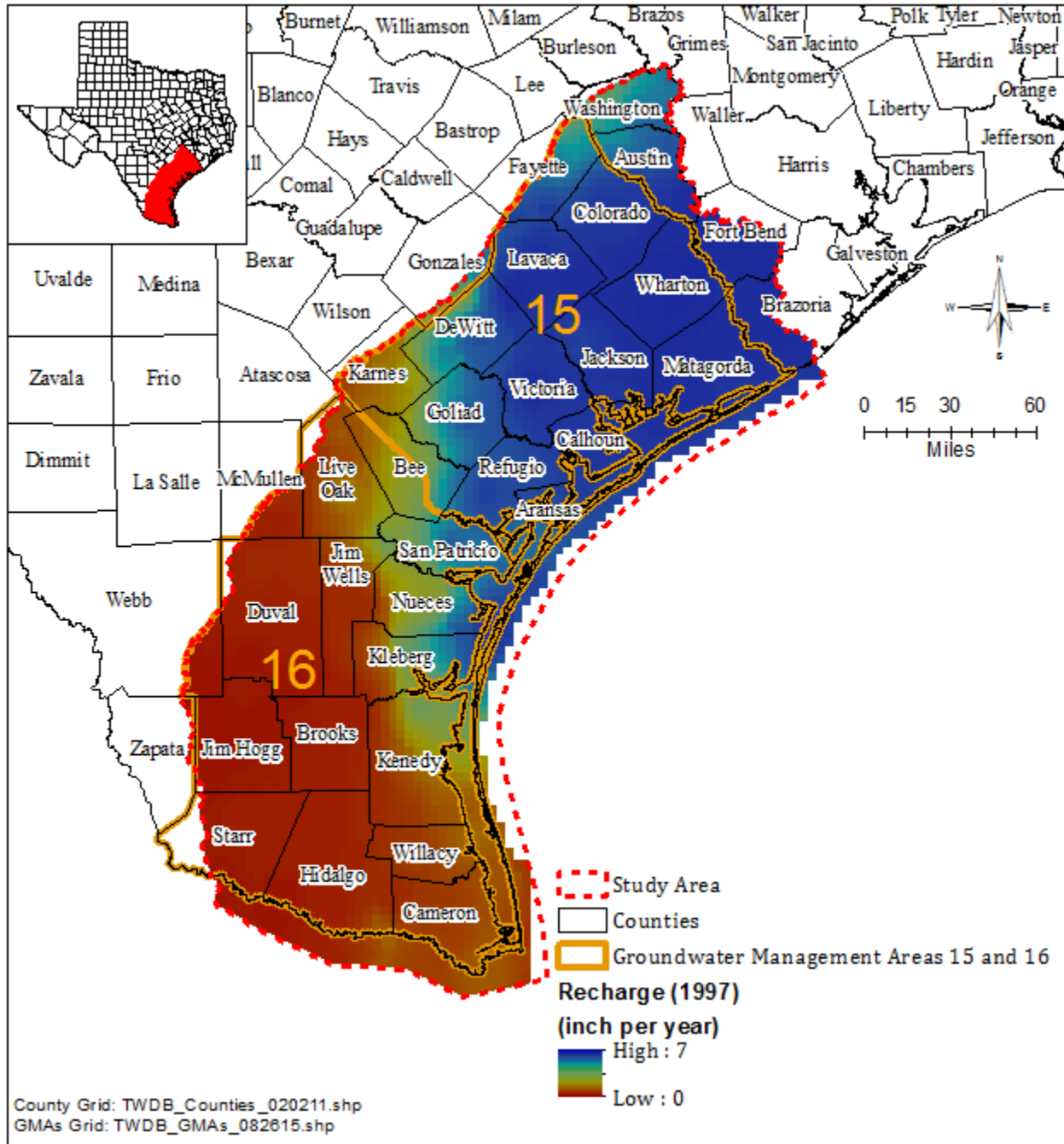
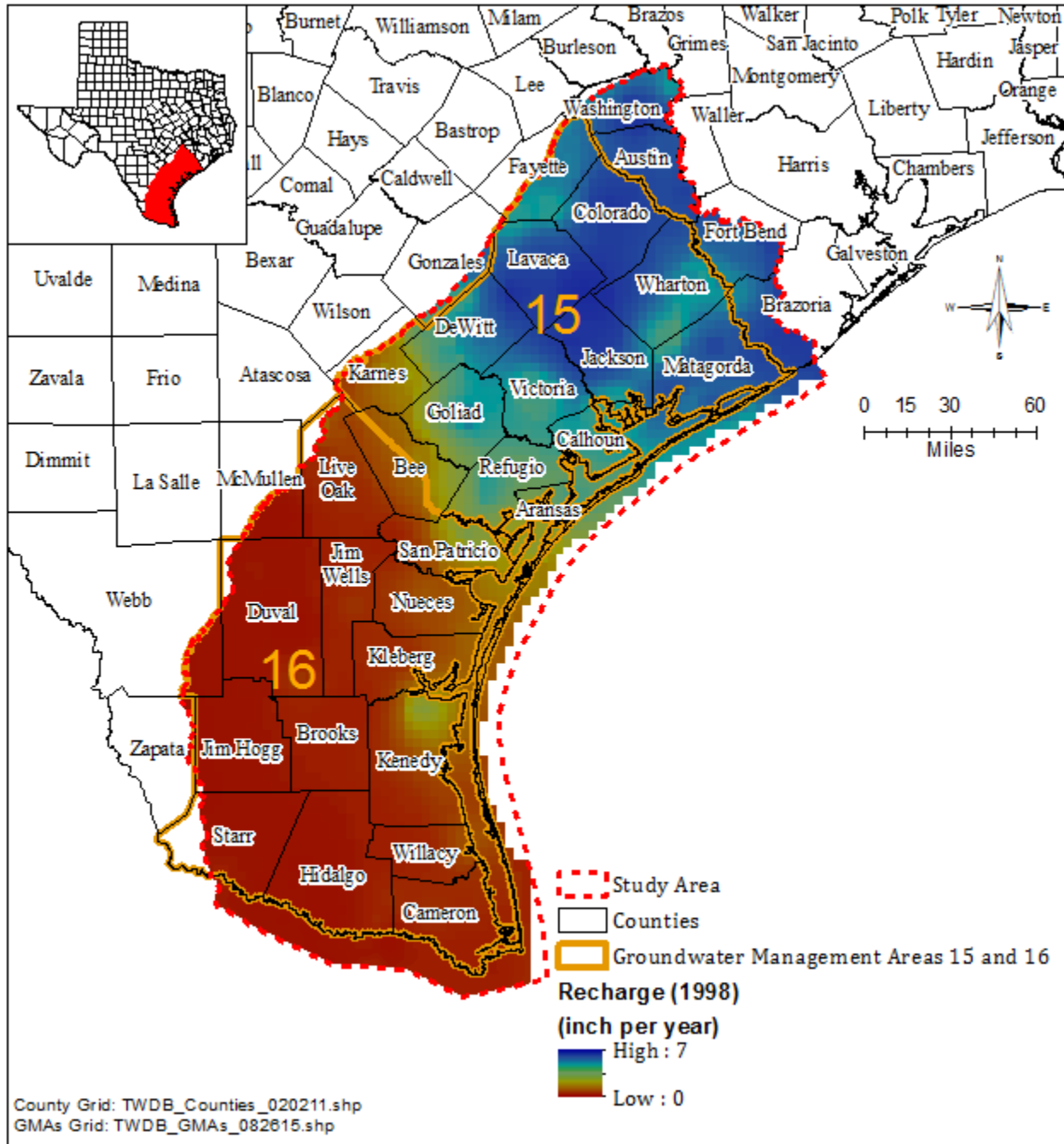


Figure C16 Estimated groundwater recharge from stream baseflow-precipitation correlation (1997).



**Figure C17 Estimated groundwater recharge from stream baseflow-precipitation correlation (1998).**

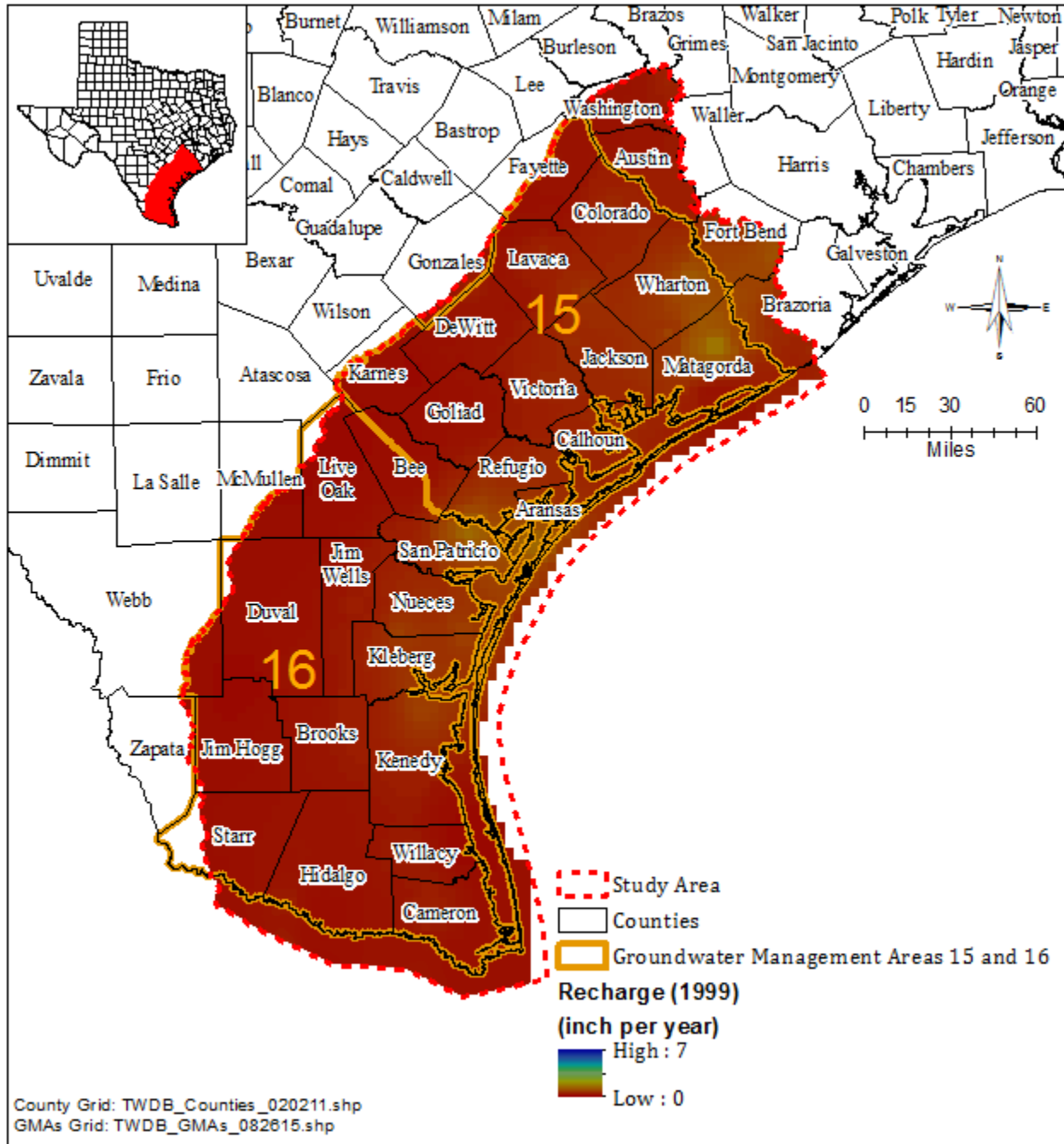
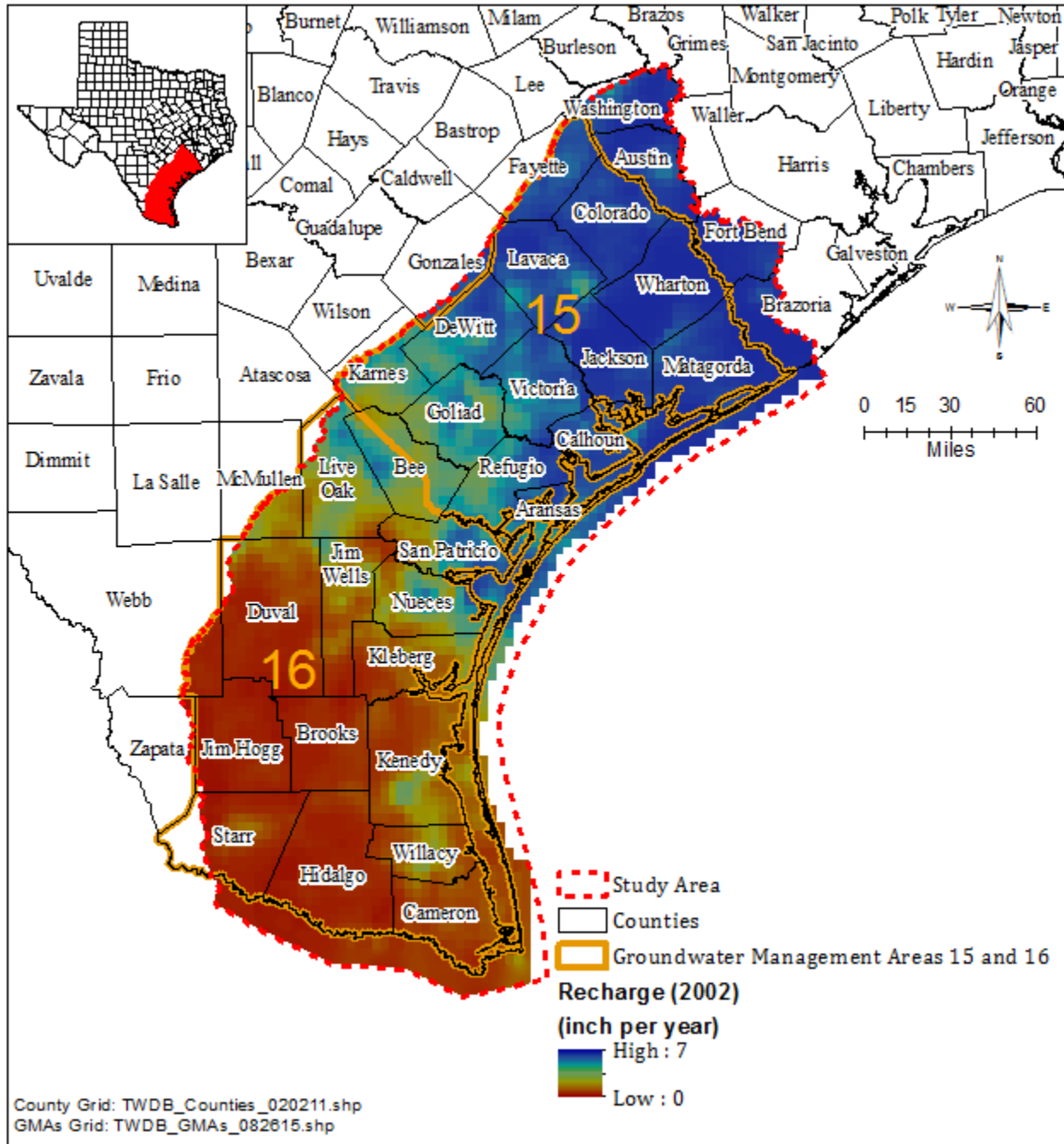
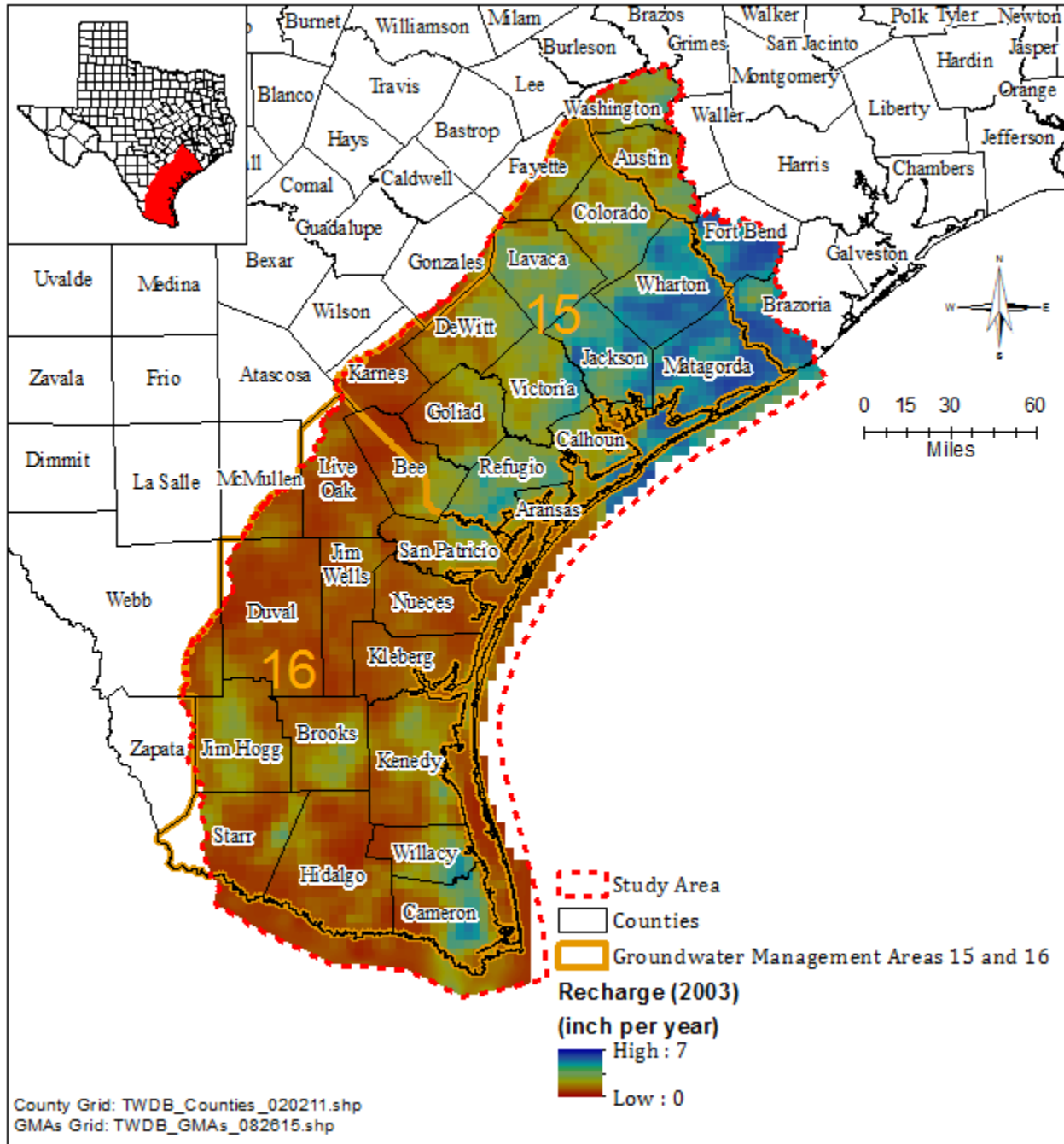


Figure C18 Estimated groundwater recharge from stream baseflow-precipitation correlation (1999).





**Figure C20 Estimated groundwater recharge from stream baseflow-precipitation correlation (2002).**



**Figure C21 Estimated groundwater recharge from stream baseflow-precipitation correlation (2003).**

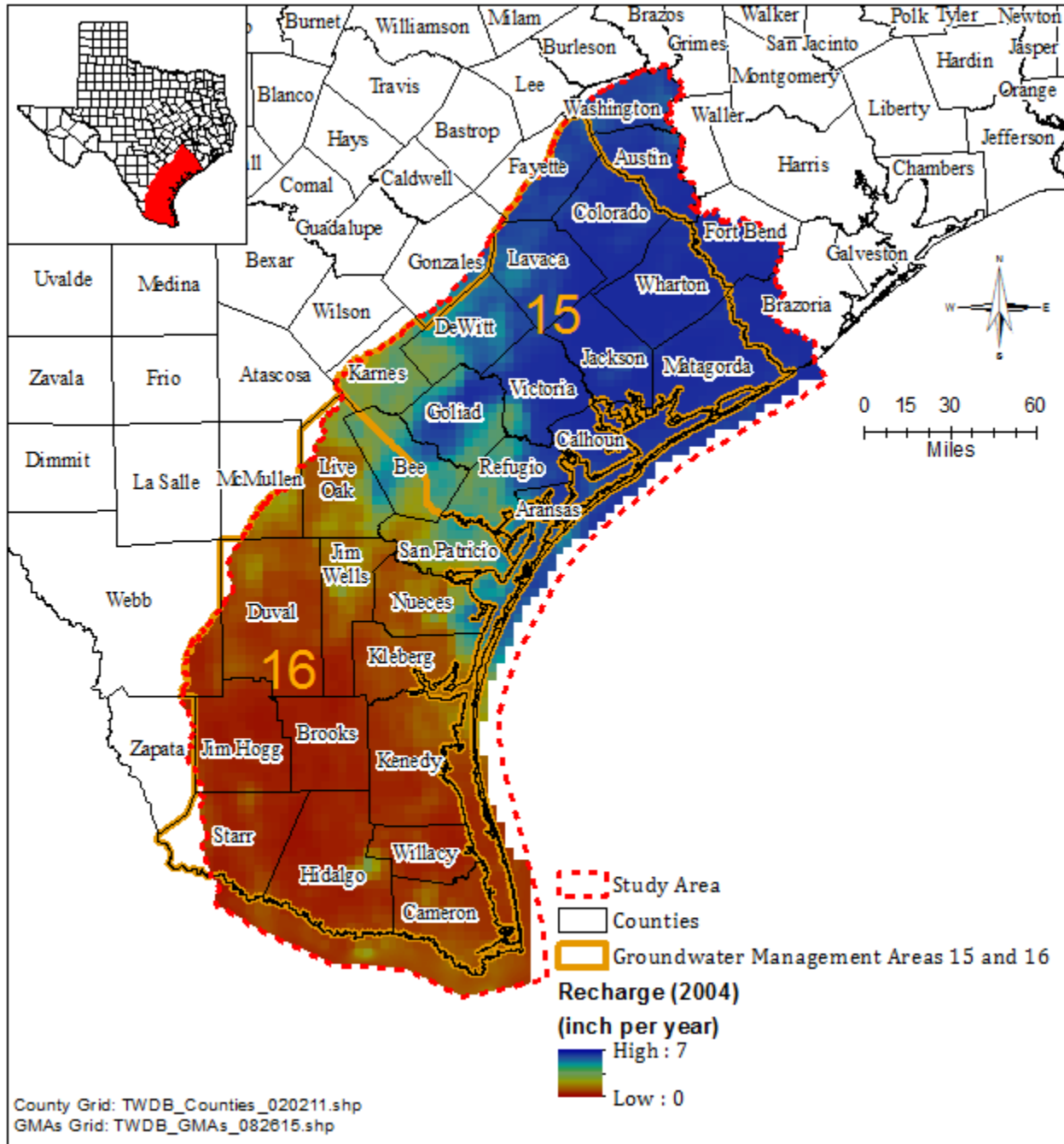


**Figure C22 Estimated groundwater recharge from stream baseflow-precipitation correlation (2004).**

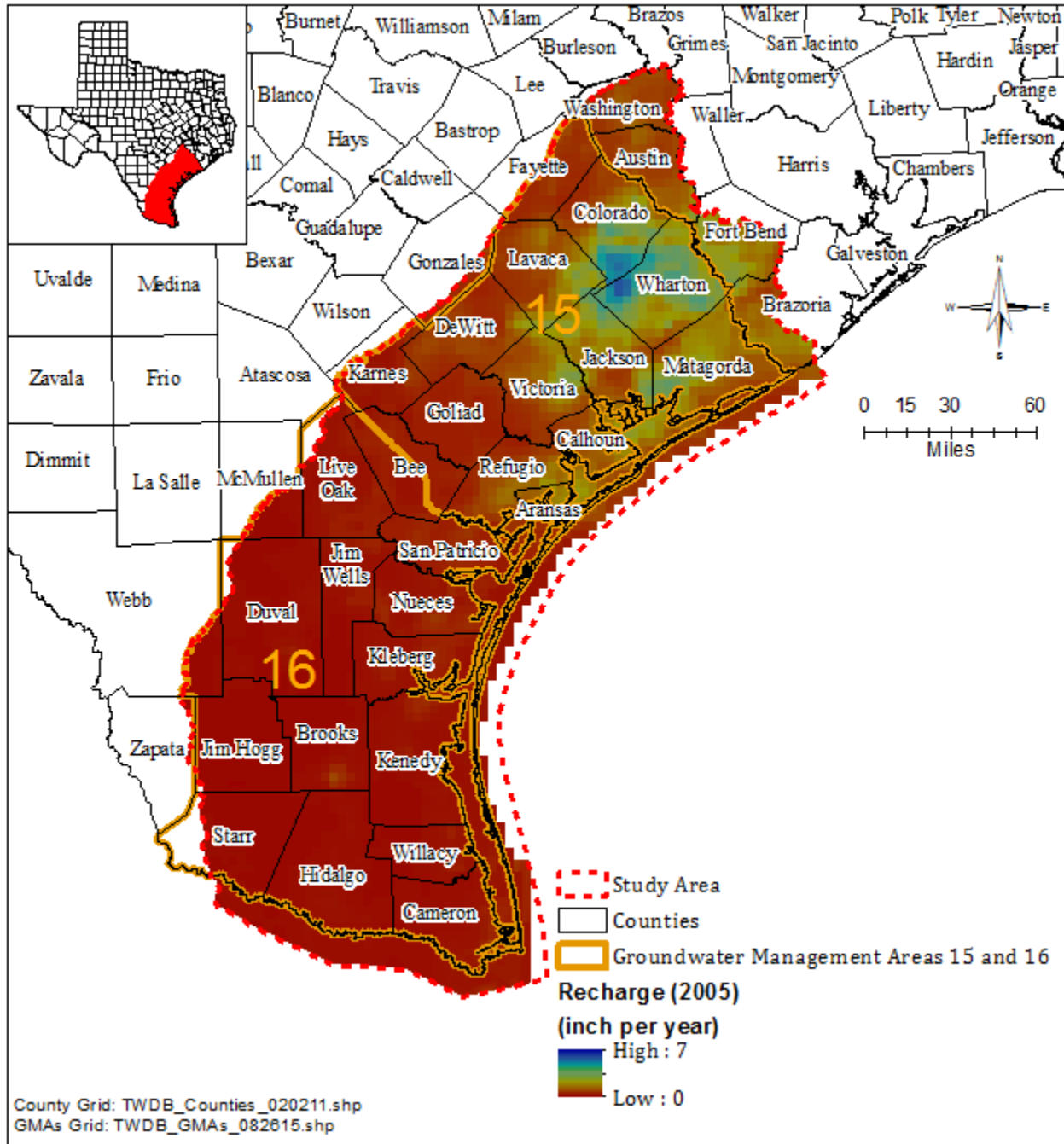


**Figure C23 Estimated groundwater recharge from stream baseflow-precipitation correlation (2005).**



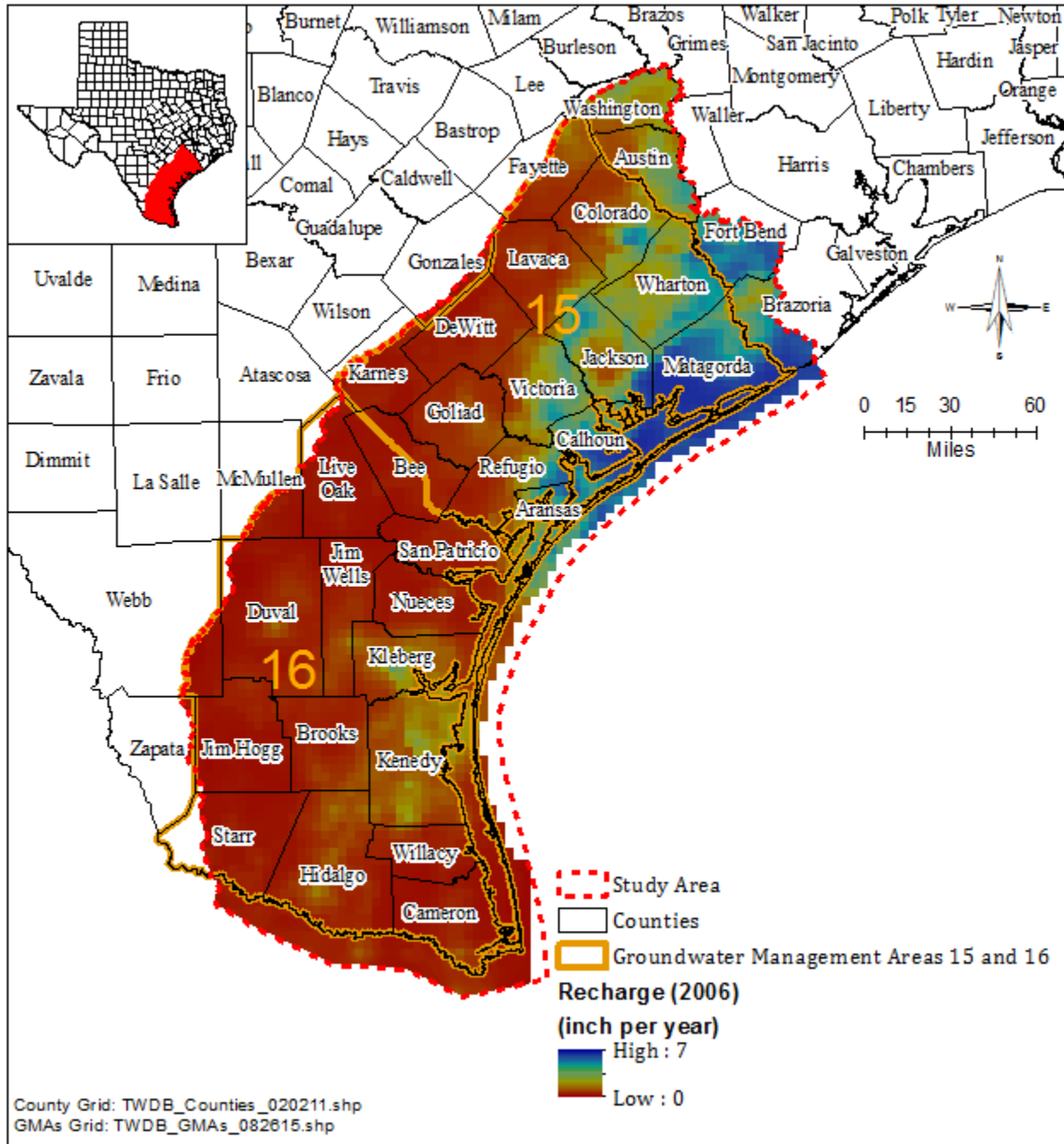


**Figure C24 Estimated groundwater recharge from stream baseflow-precipitation correlation (2006).**

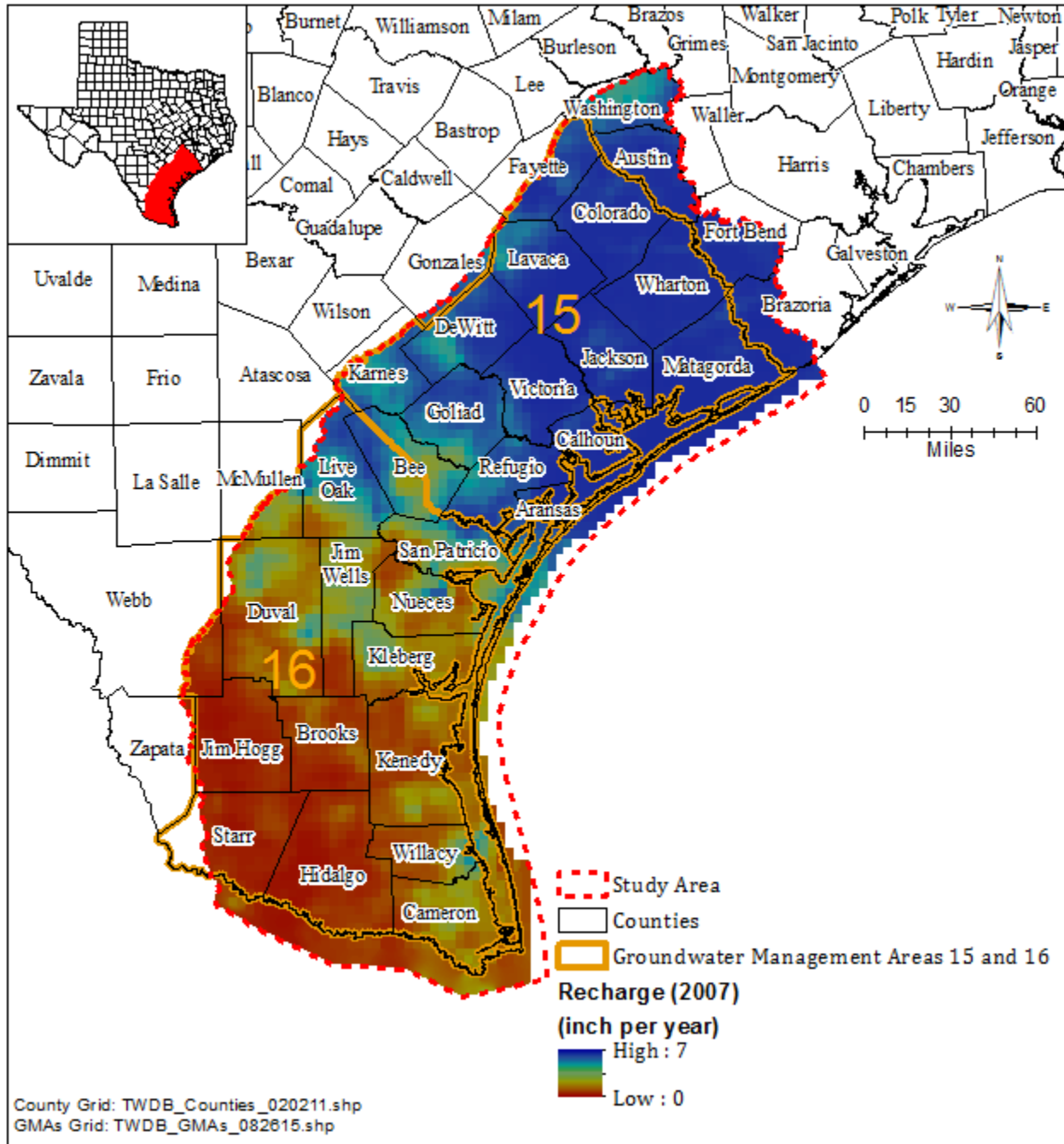


**Figure C25 Estimated groundwater recharge from stream baseflow-precipitation correlation (2007).**

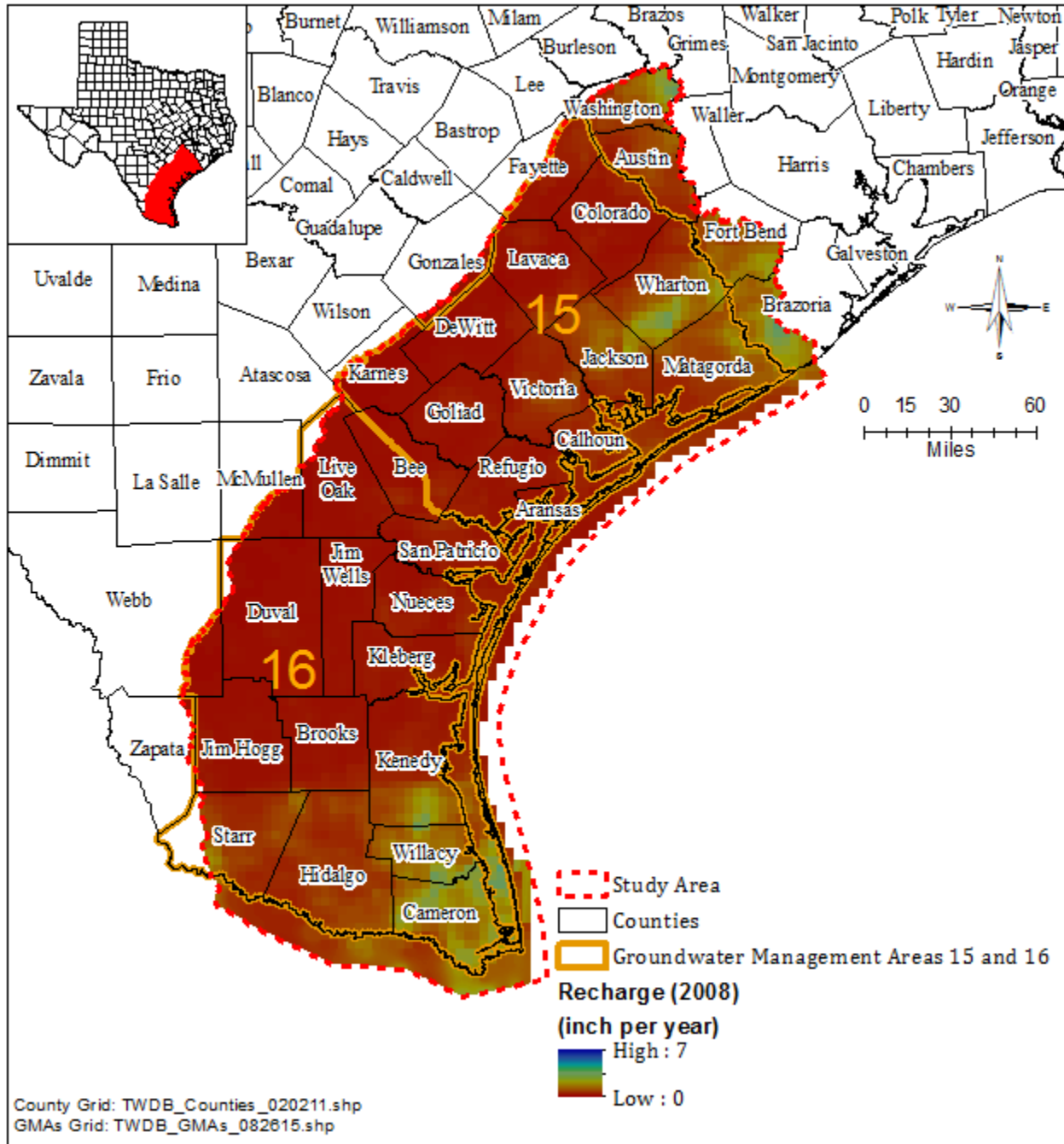
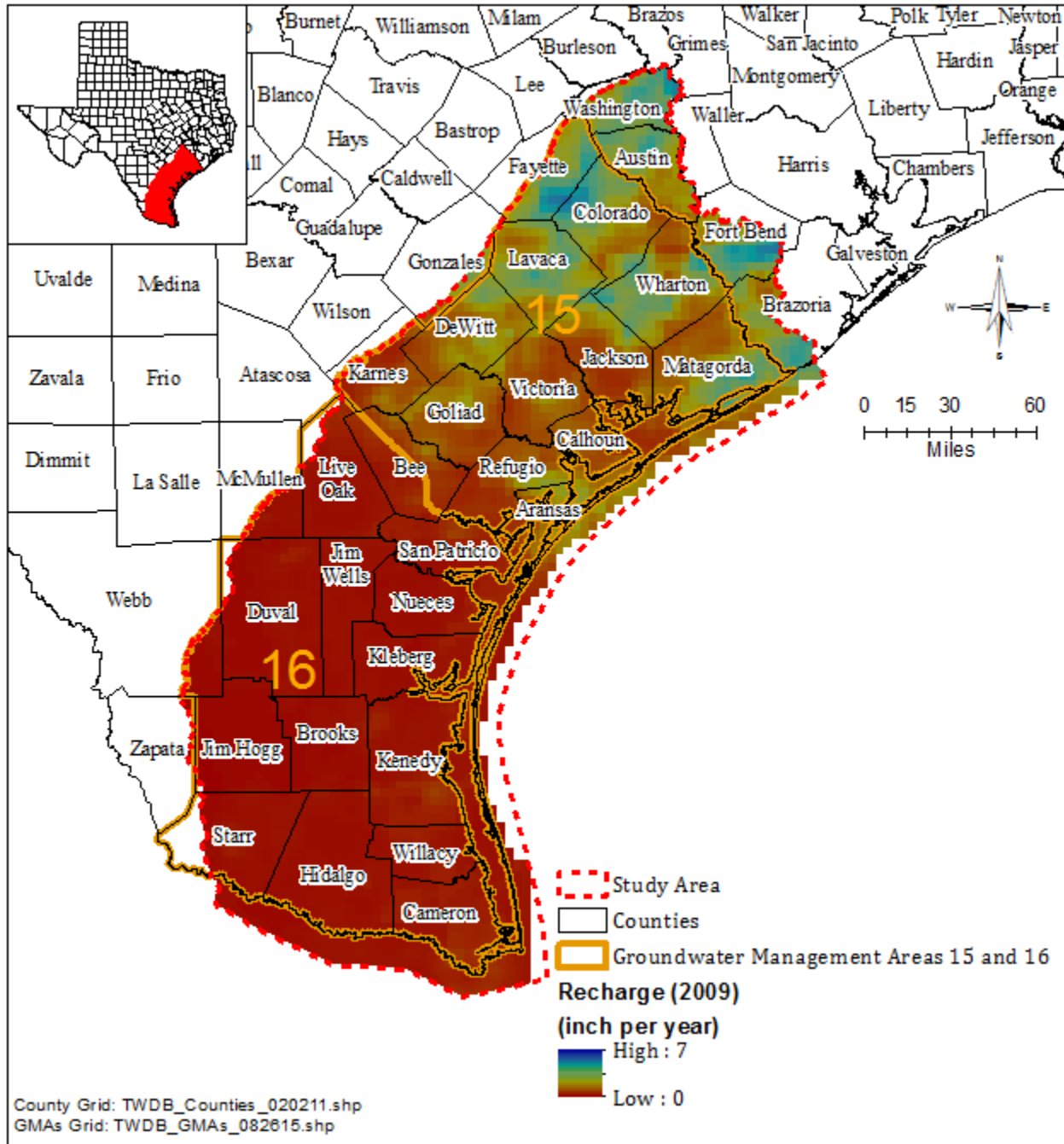
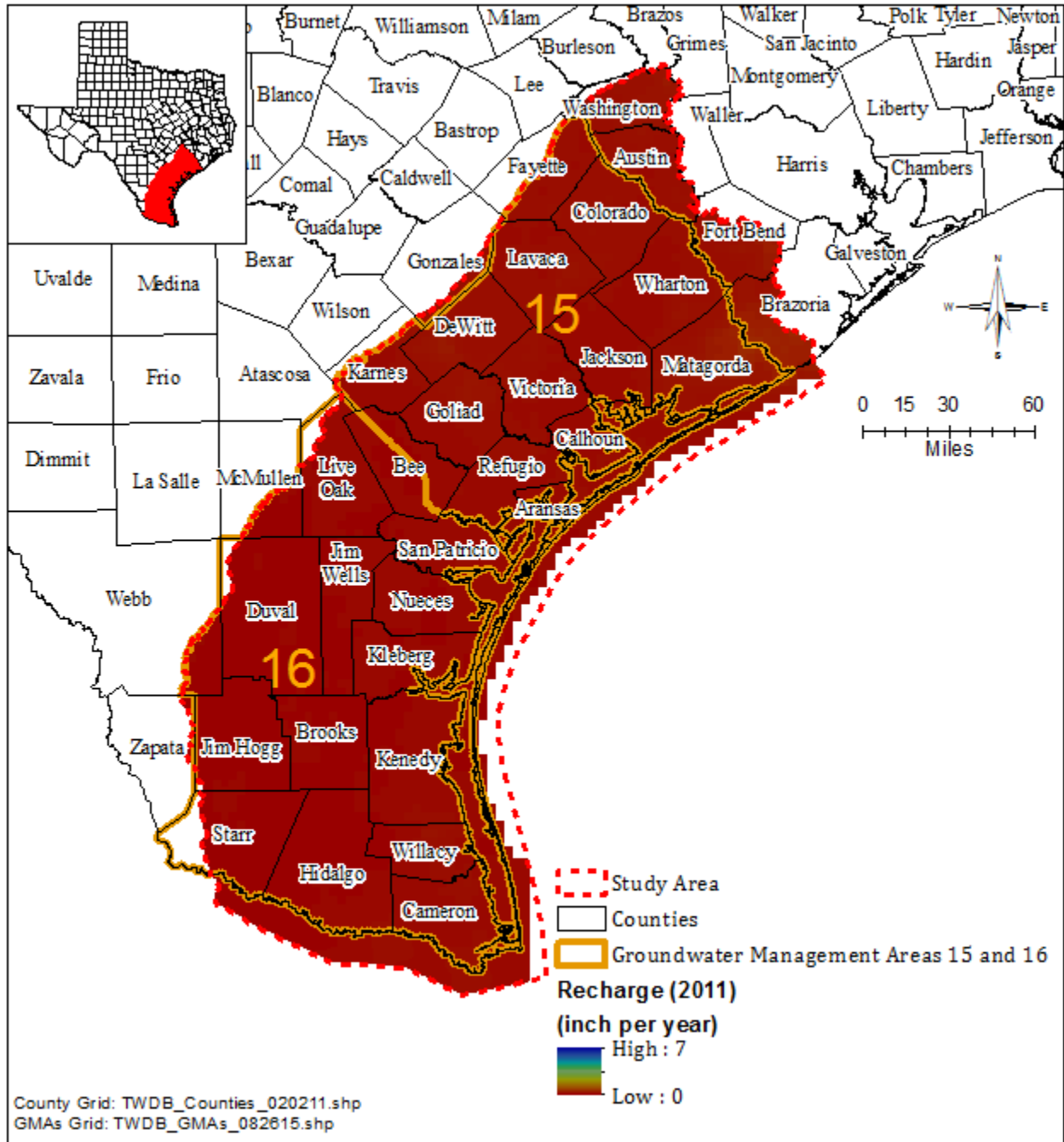


Figure C26 Estimated groundwater recharge from stream baseflow-precipitation correlation (2008).



**Figure C27 Estimated groundwater recharge from stream baseflow-precipitation correlation (2009).**



**Figure C28 Estimated groundwater recharge from stream baseflow-precipitation correlation (2011).**

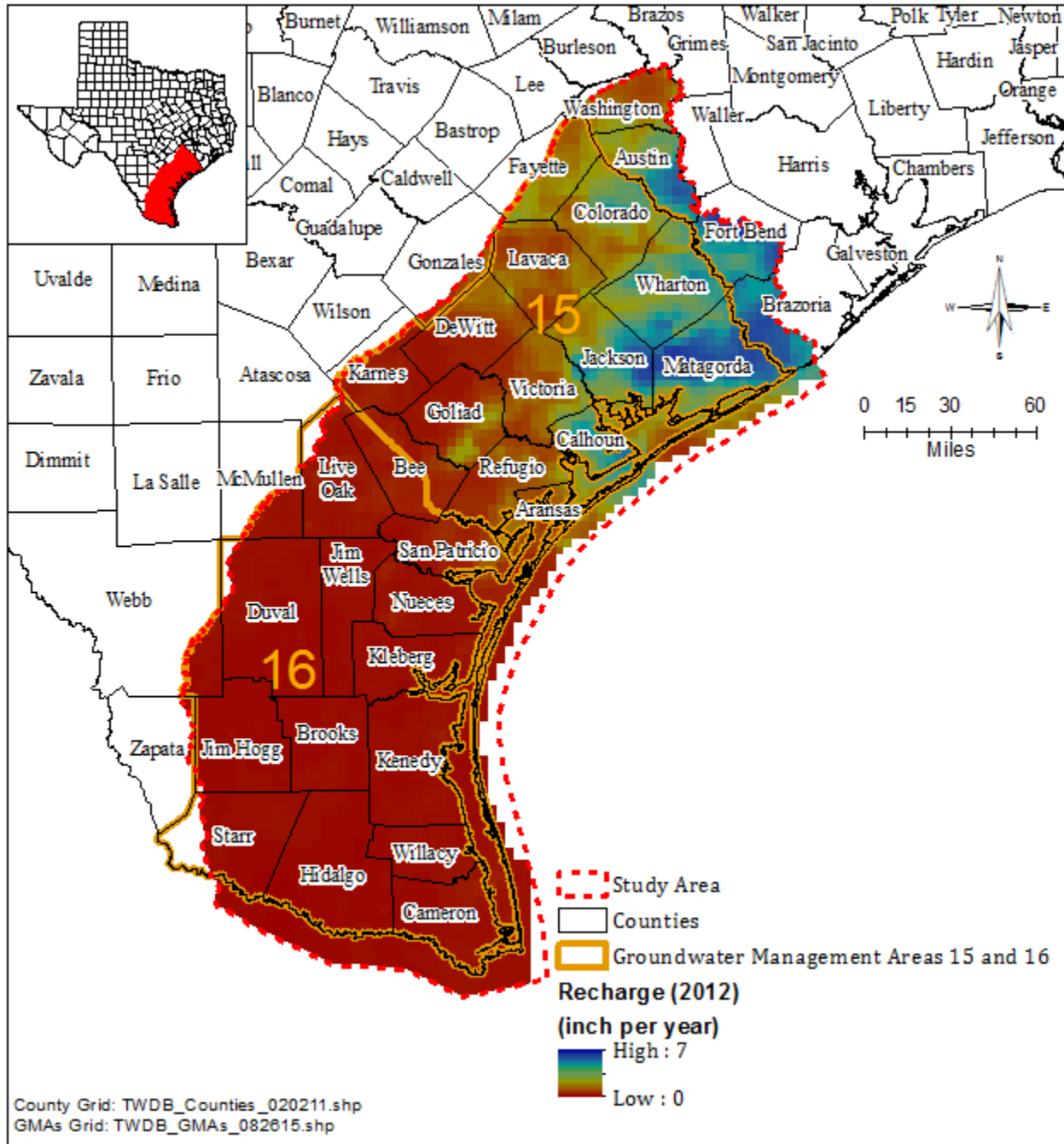


**Figure C29 Estimated groundwater recharge from stream baseflow-precipitation correlation (2012).**

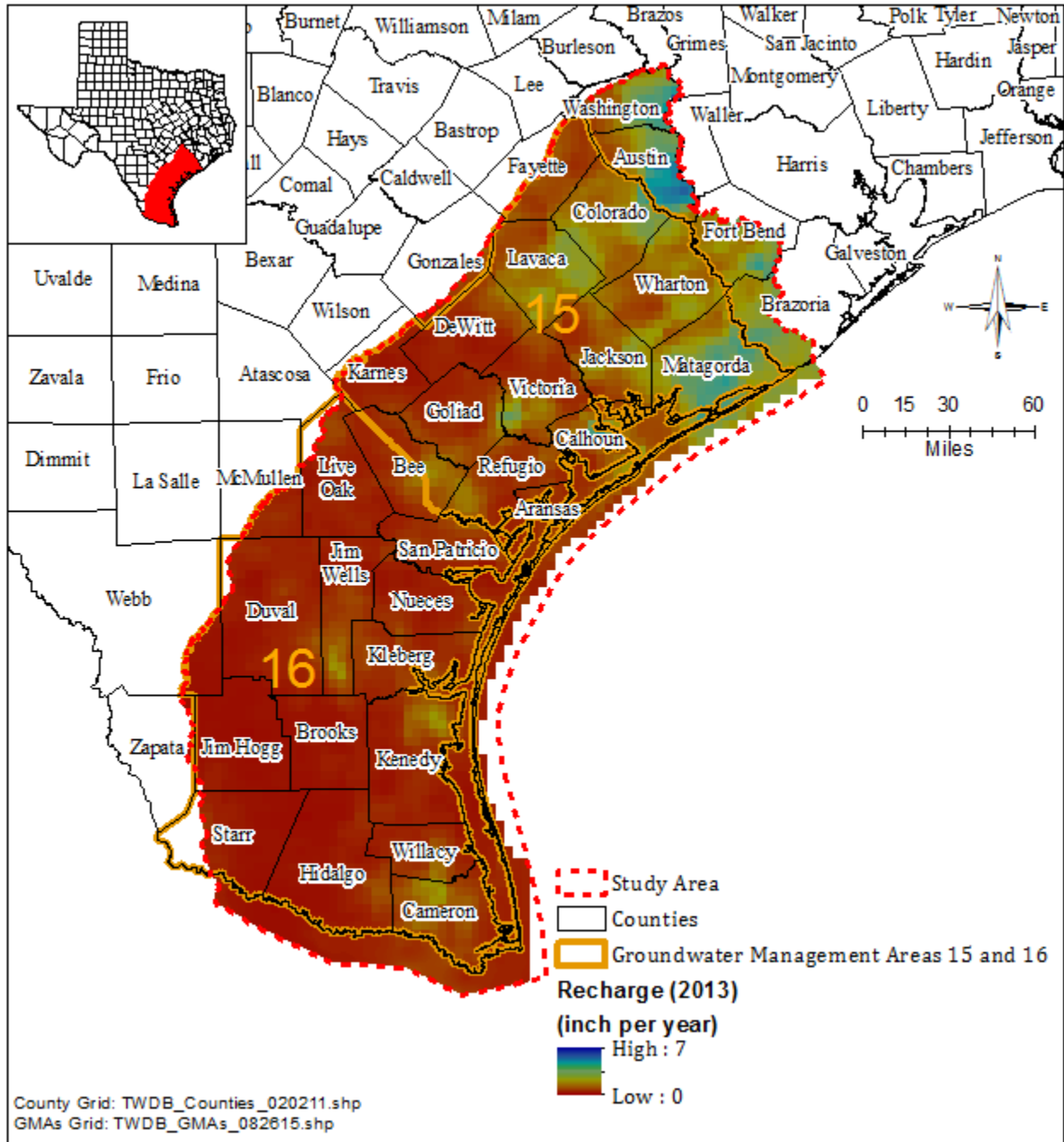


**Figure C30 Estimated groundwater recharge from stream baseflow-precipitation correlation (2013).**

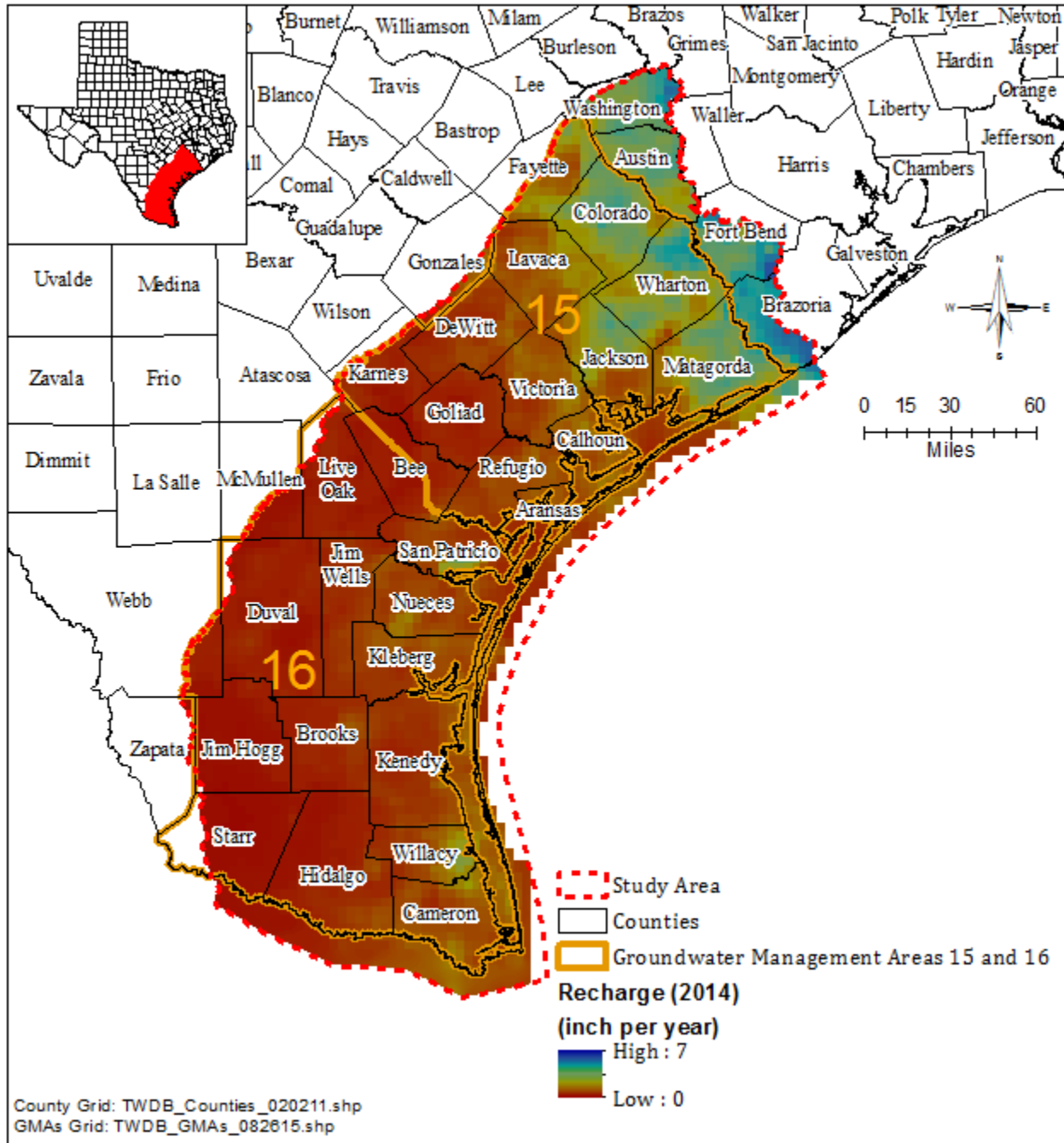


**Figure C31 Estimated groundwater recharge from stream baseflow-precipitation correlation (2014).**



## **Appendix D: Summary of Stream Gain or Loss**

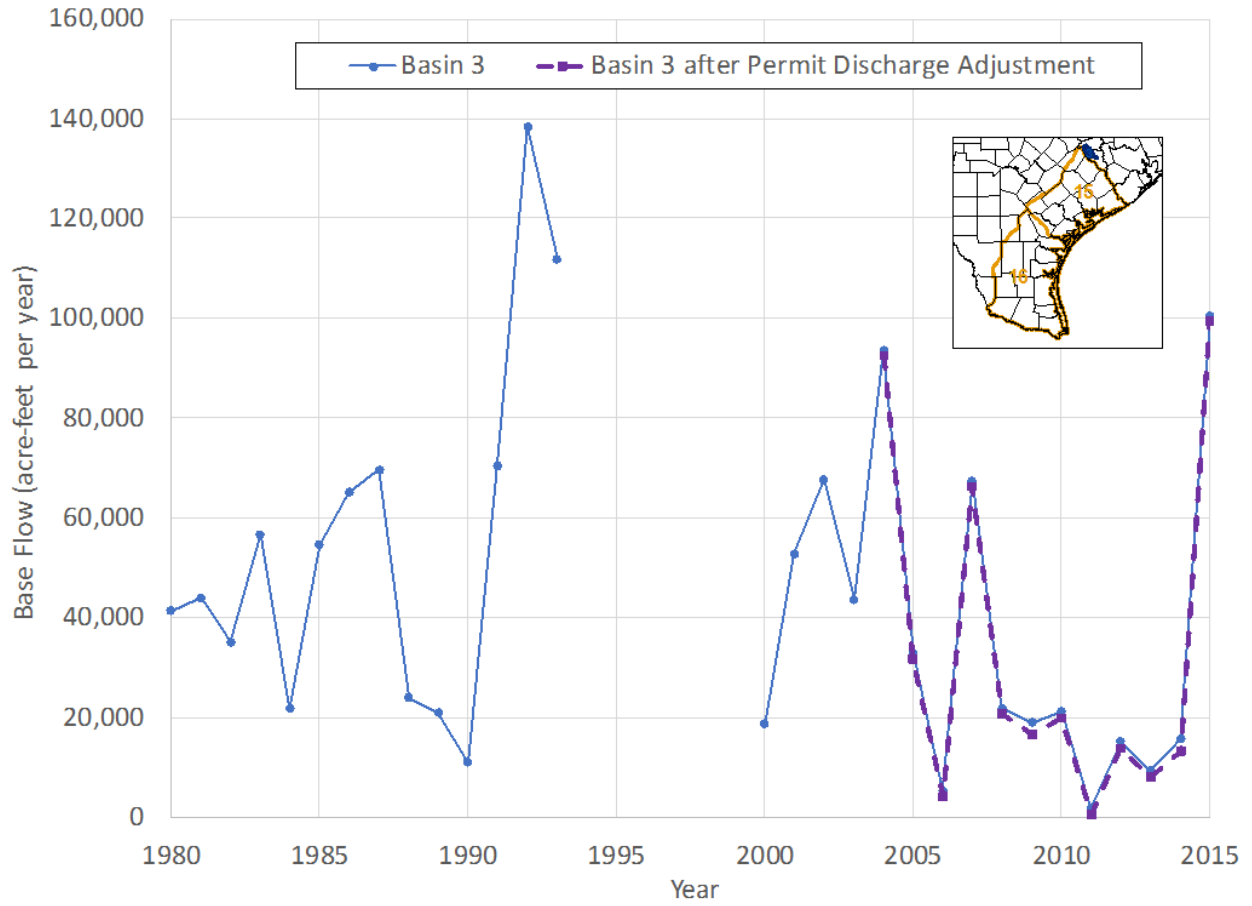


**Figure D1 Stream gain or loss at Basin 3.**

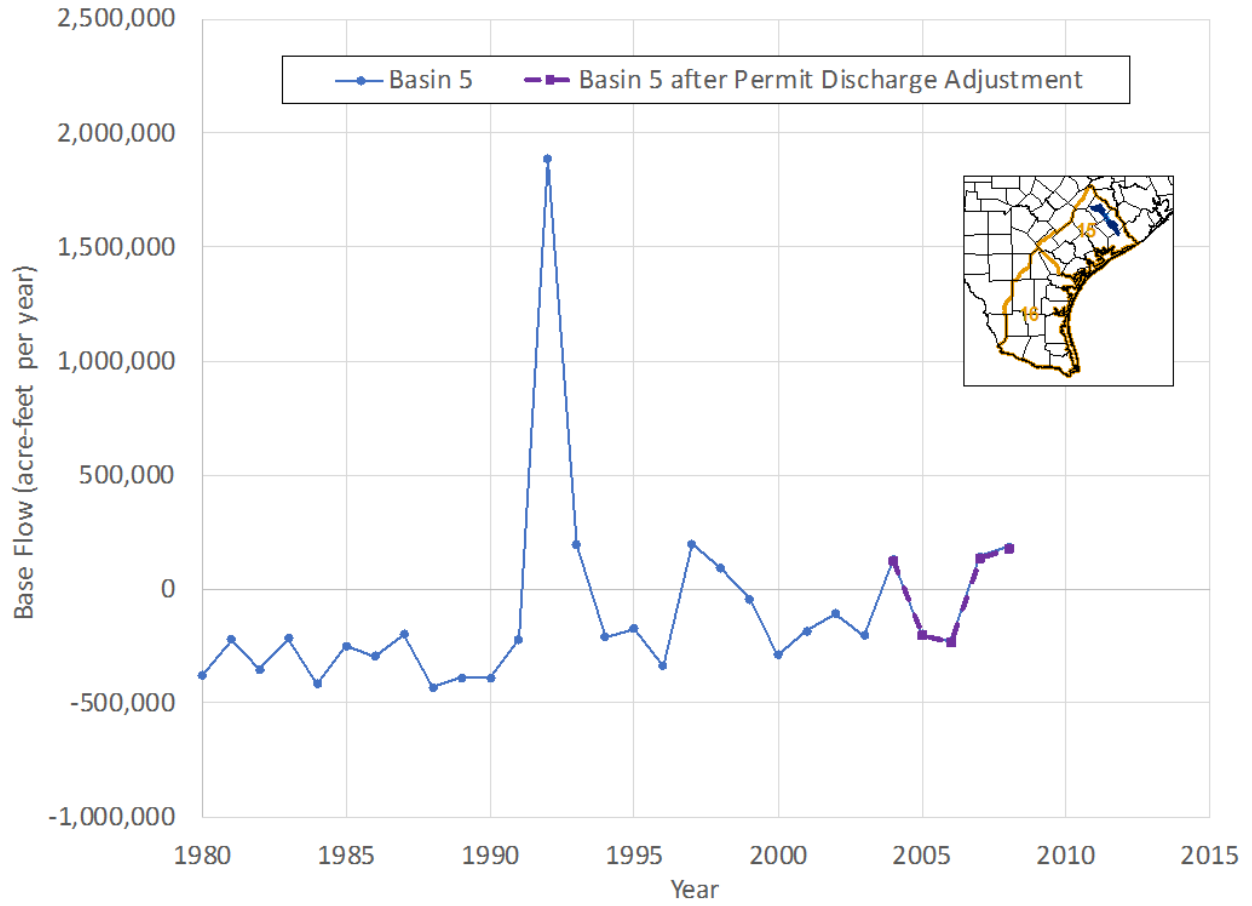


**Figure D2 Stream gain or loss at Basin 5.**

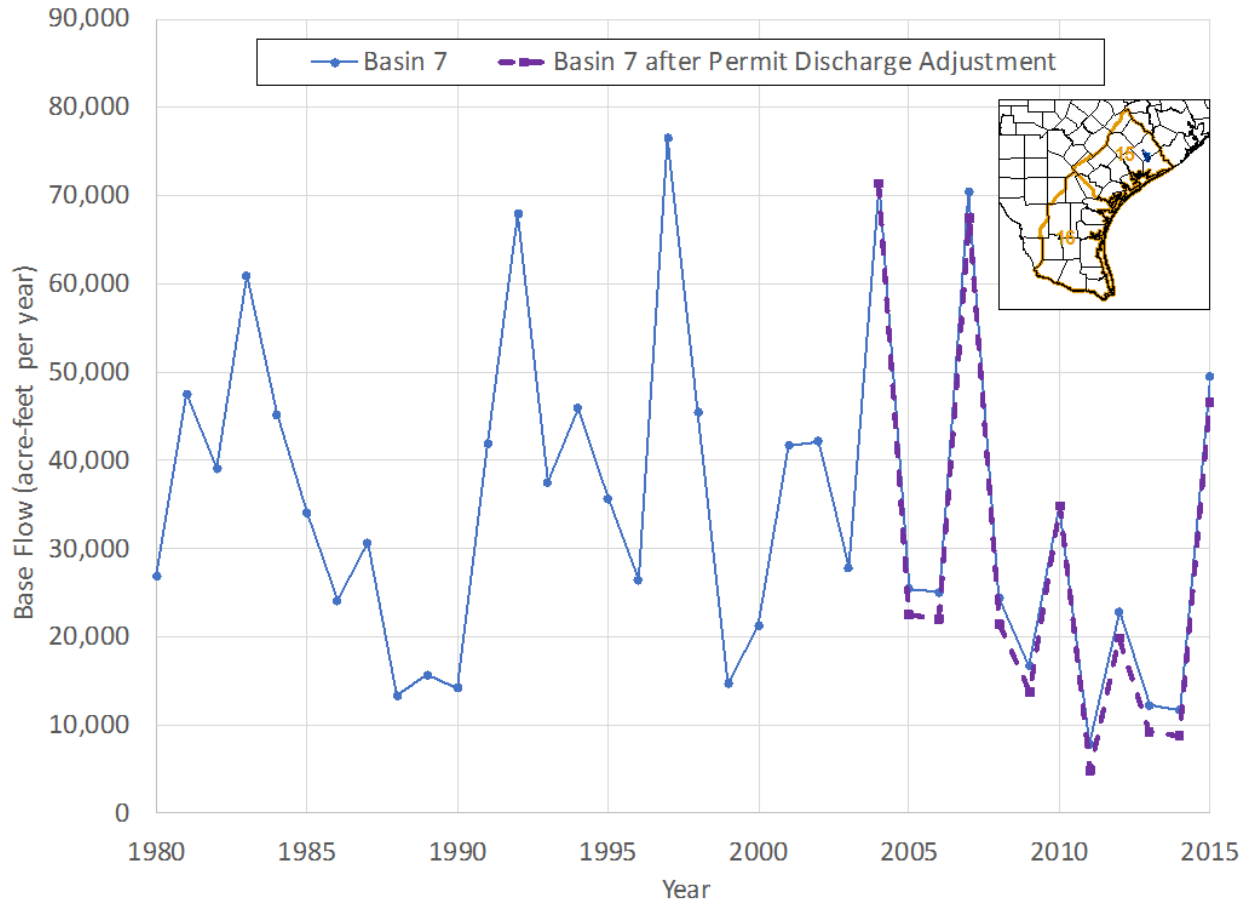


**Figure D3 Stream gain or loss at Basin 7.**

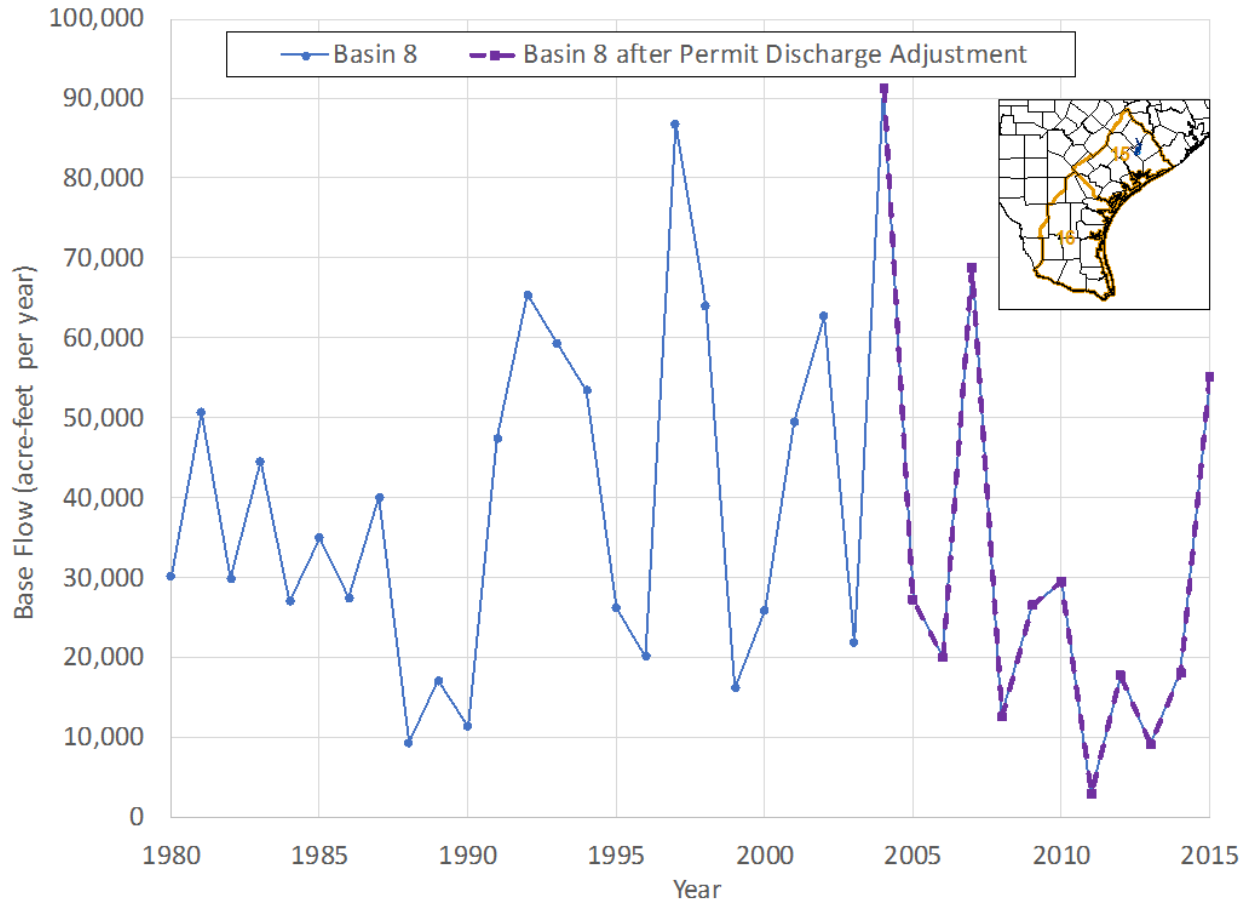


**Figure D4 Stream gain or loss at Basin 8.**

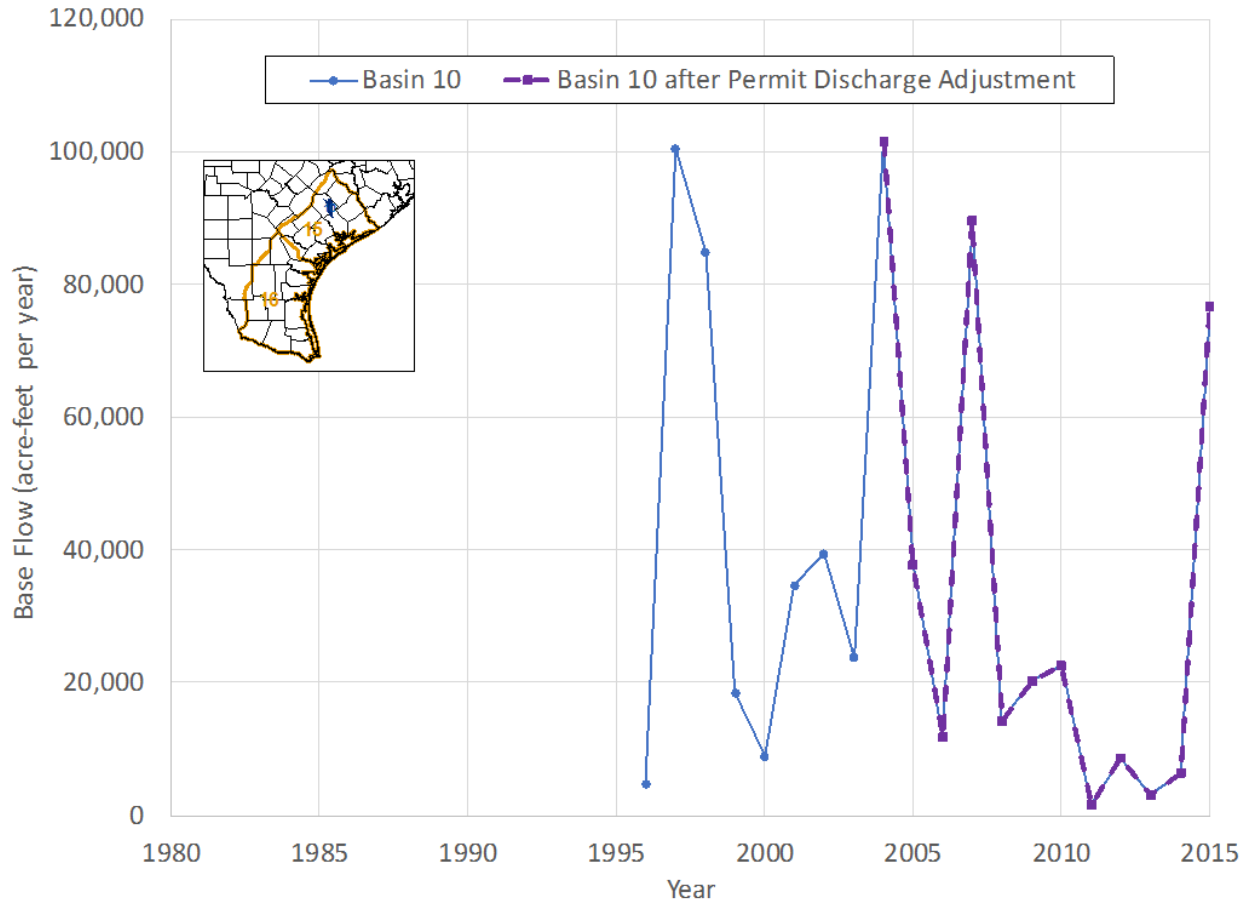


**Figure D5 Stream gain or loss at Basin 10.**

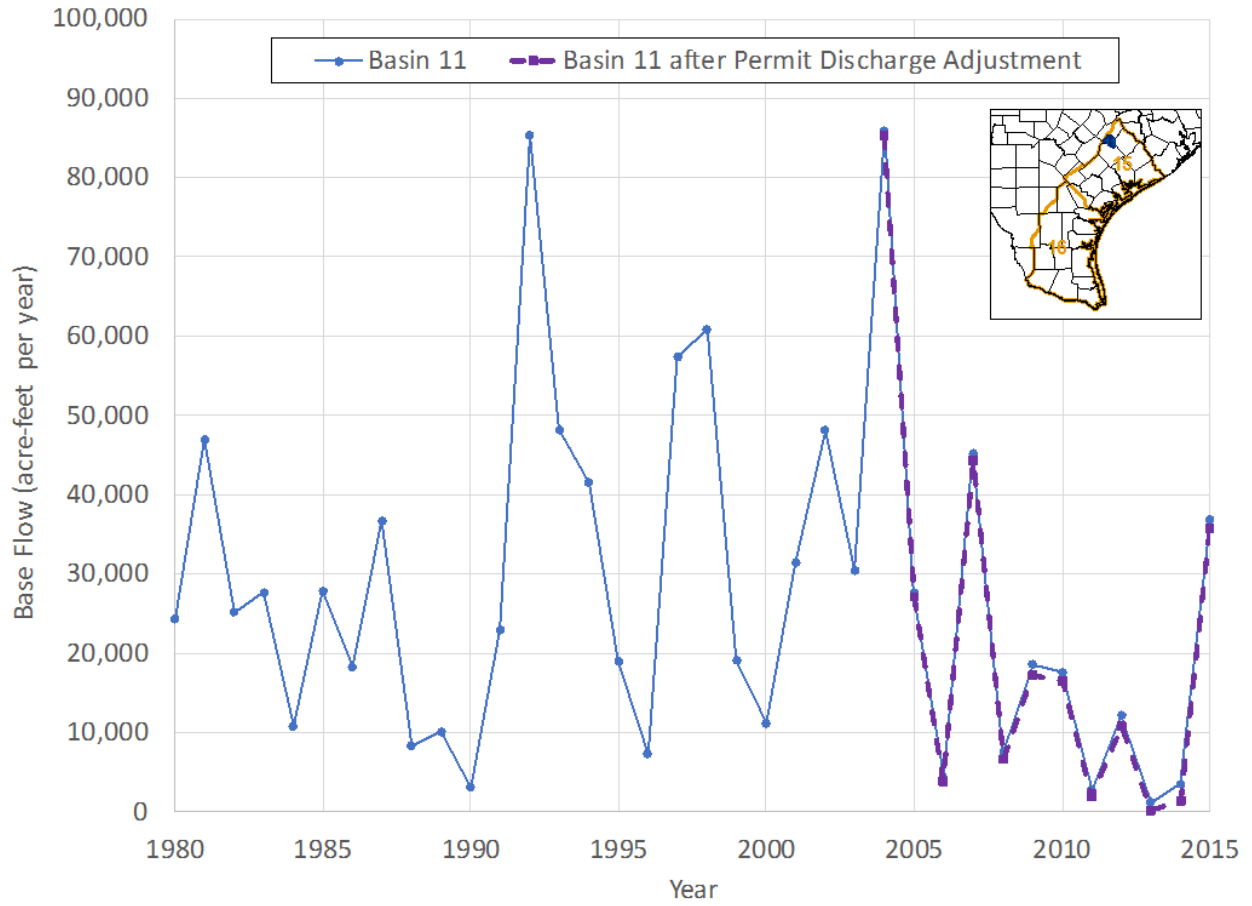


**Figure D6 Stream gain or loss at Basin 11.**

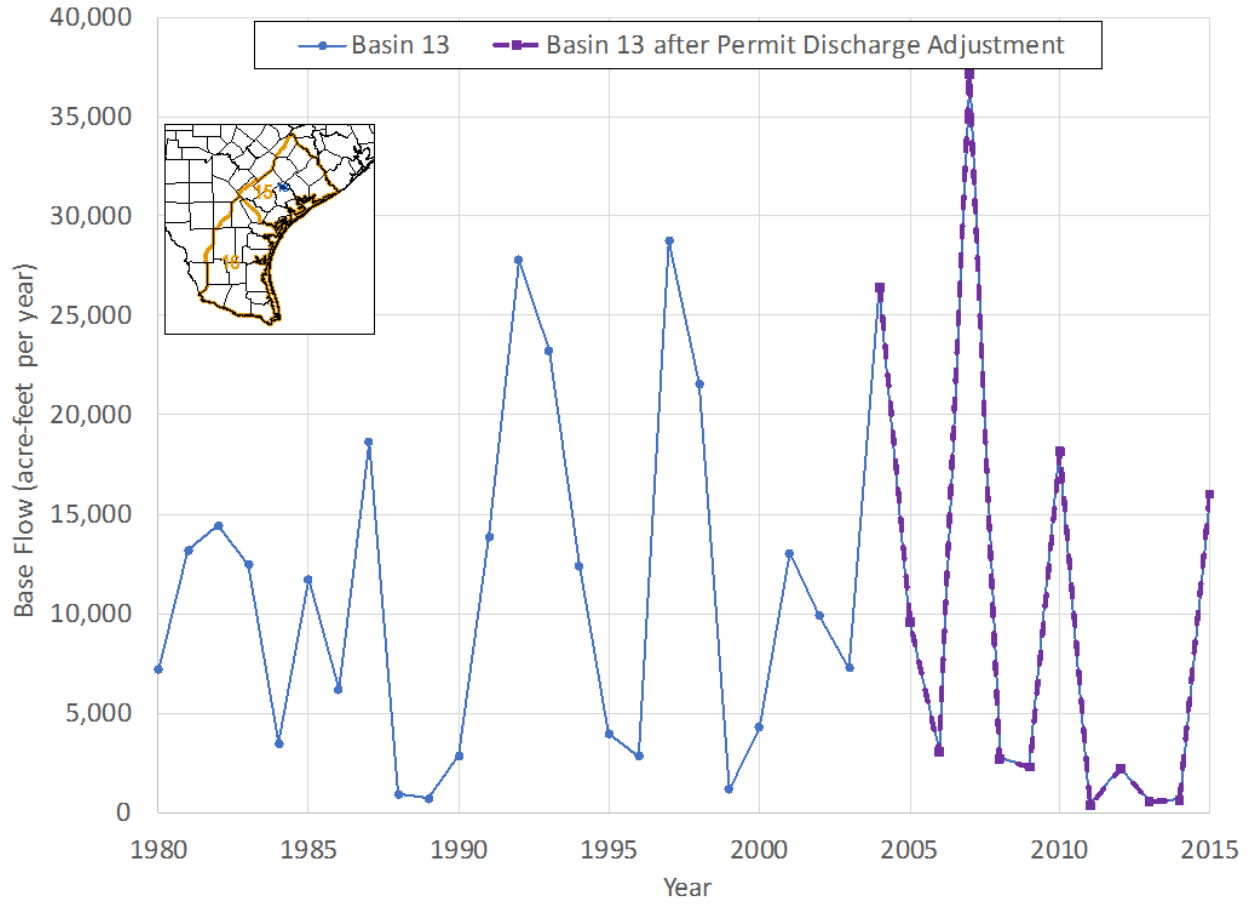


**Figure D7 Stream gain or loss at Basin 13.**



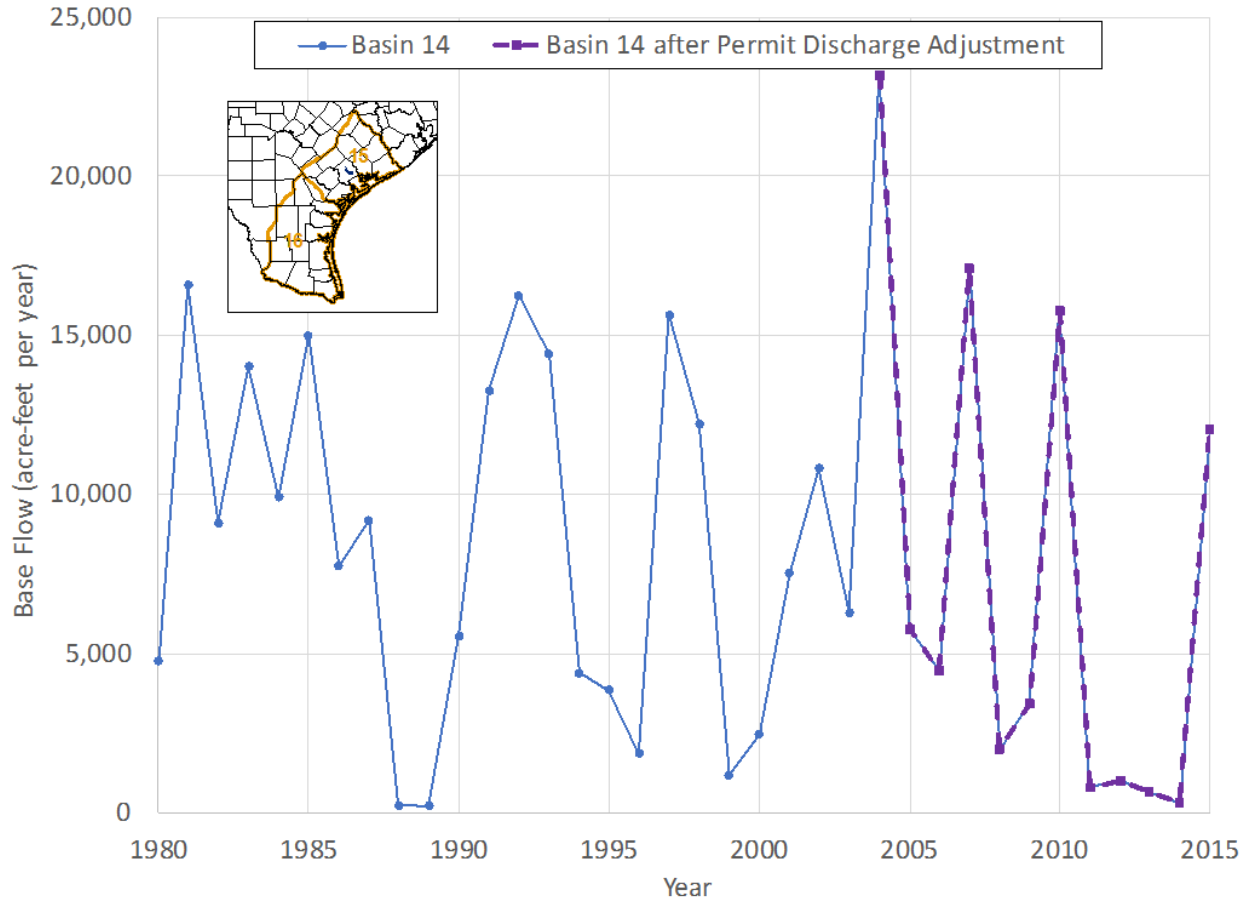


**Figure D8 Stream gain or loss at Basin 14.**

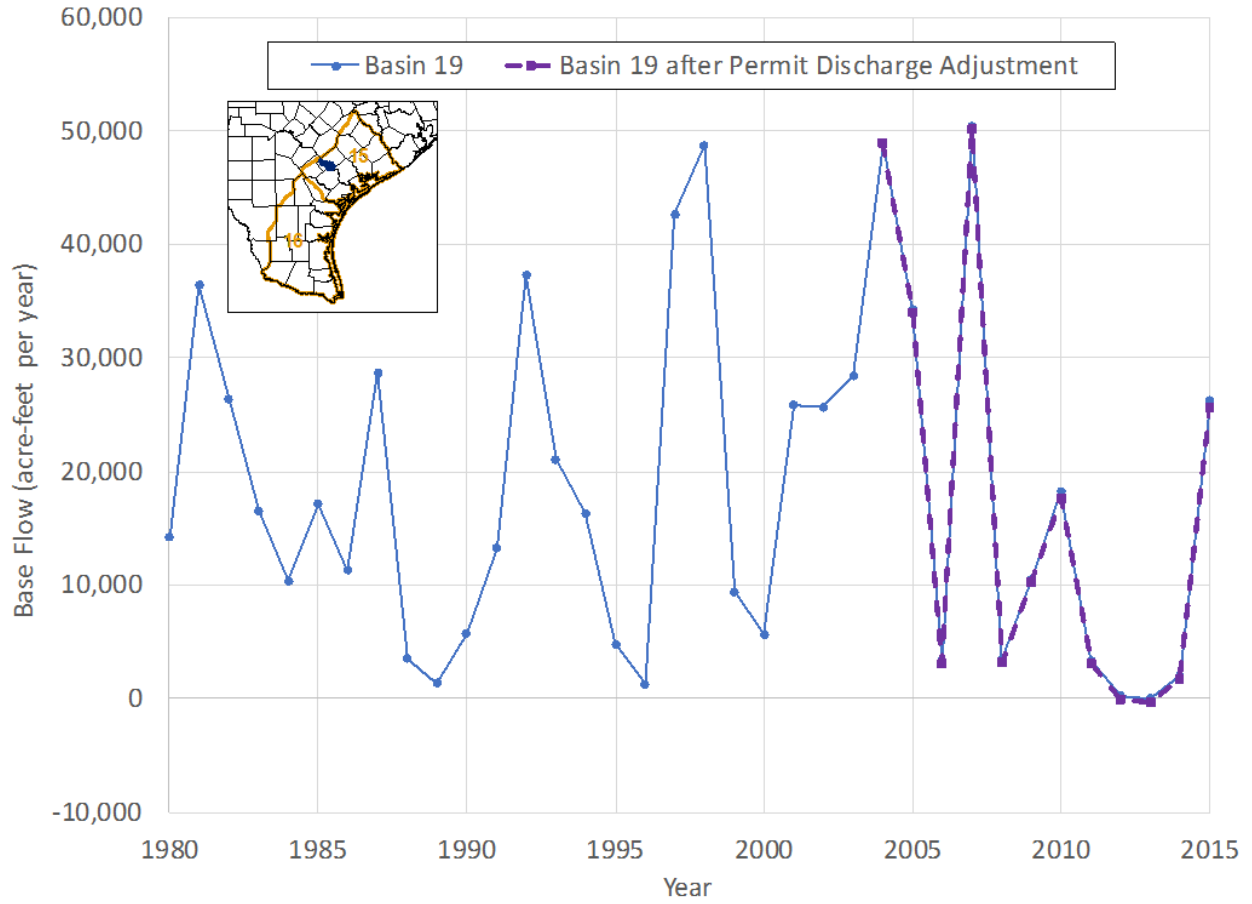


**Figure D9 Stream gain or loss at Basin 19.**

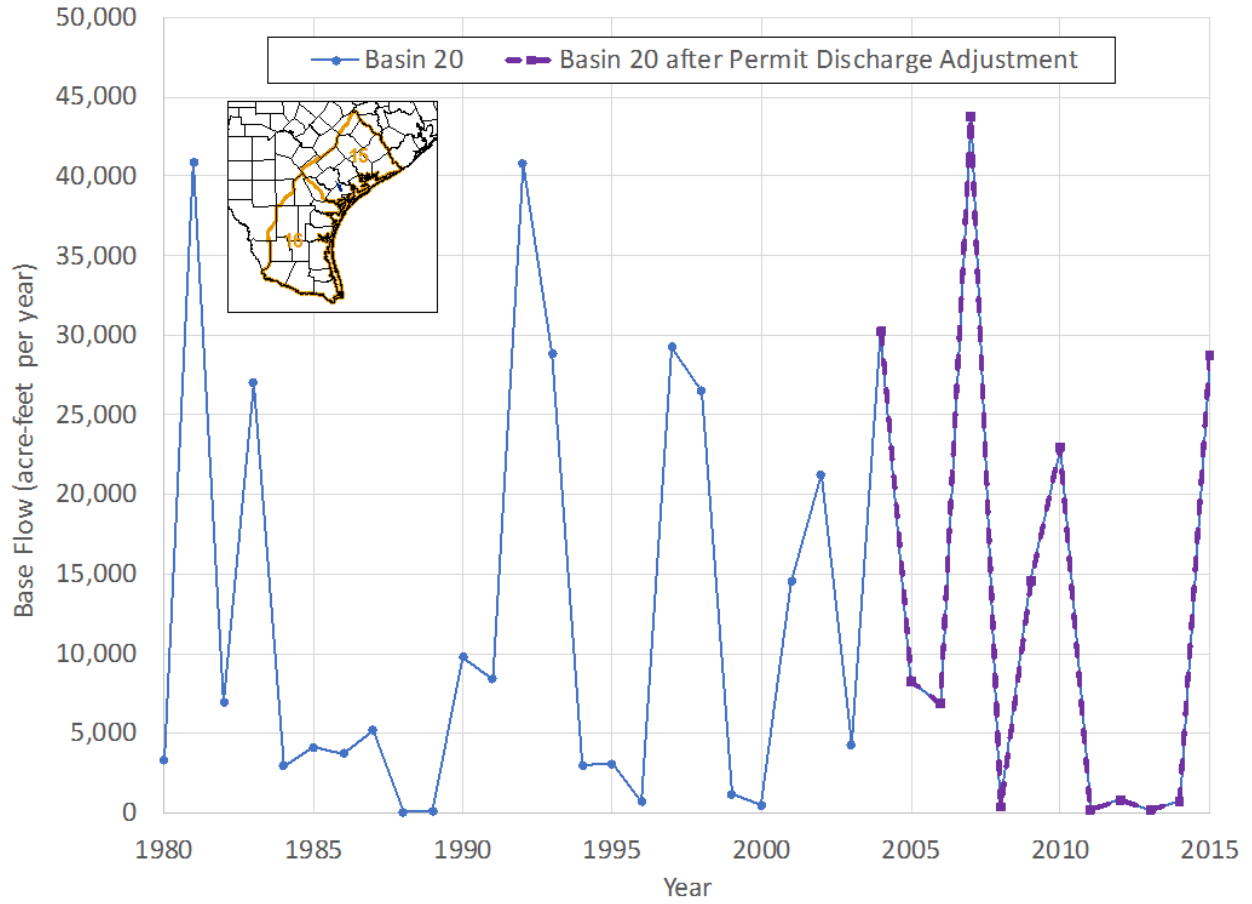


**Figure D10 Stream gain or loss at Basin 20.**

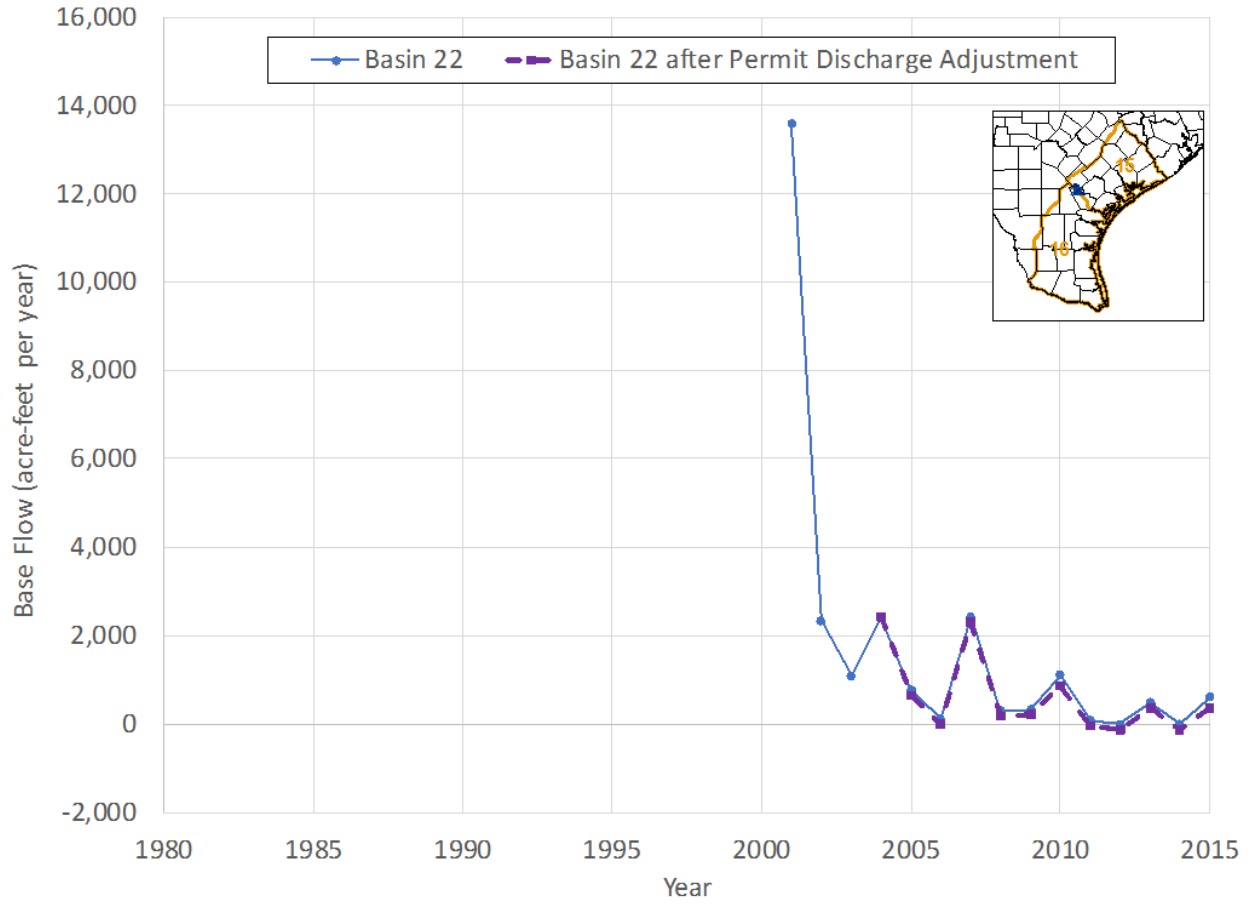


**Figure D11 Stream gain or loss at Basin 22.**

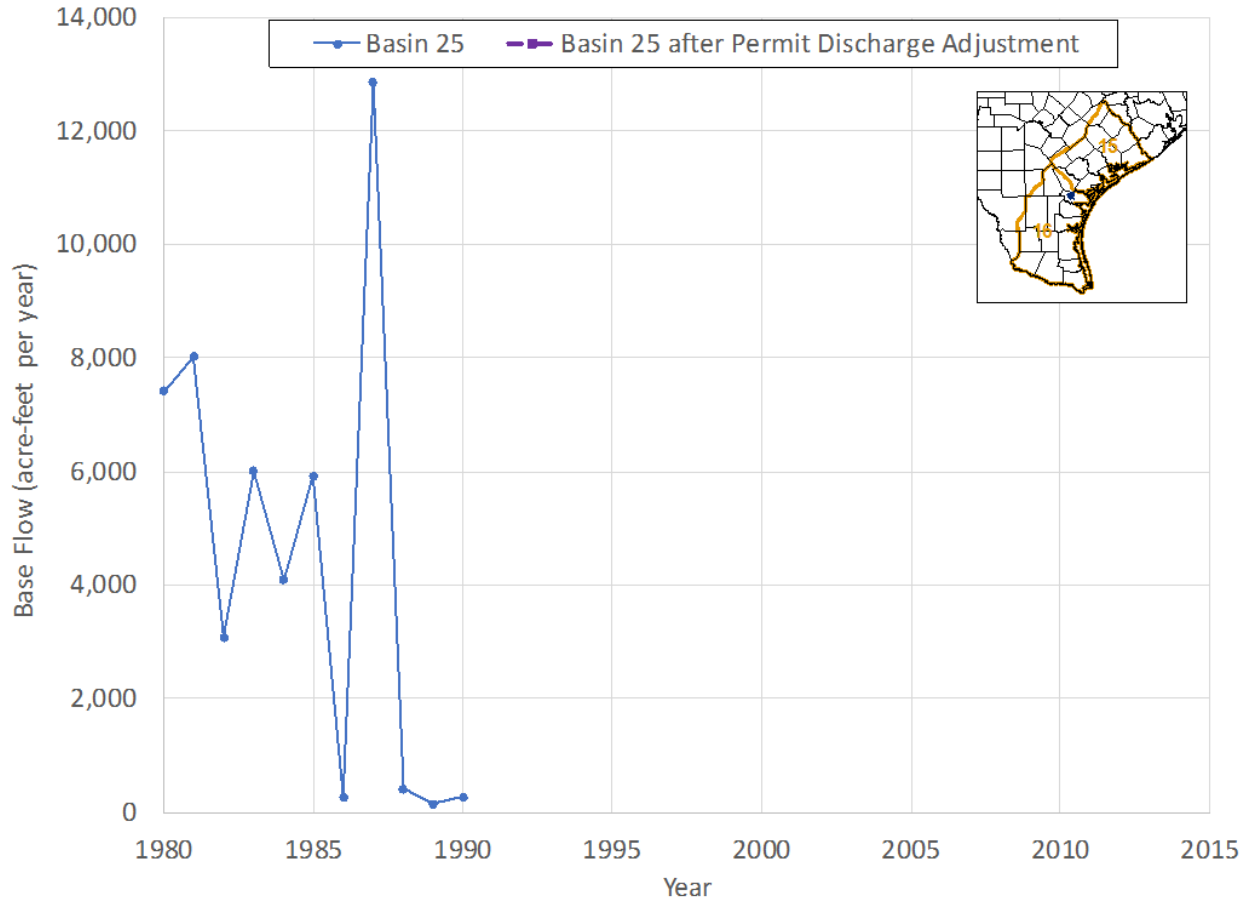


**Figure D12 Stream gain or loss at Basin 25.**

## **Appendix E: Summary of Hydraulic Conductivity and Storativity/Specific Yield Values**

**Table E1 Summary of hydraulic conductivity values from pumping tests.**

Well ID	County	Latitude	Longitude	Hydrogeologic Unit	Screen Top (feet below ground)	Screen Bottom (feet below ground)	Hydraulic Conductivity (feet per day)
Not Available	Aransas	27.93194444	-97.145	Chicot	30	160	60.16
6615903	Austin	29.780833	-96.155278	Chicot	251	315	20.99
6606602	Austin	29.950556	-96.259723	Burkeville	647	725	26.07
6606613	Austin	29.950834	-96.262501	Burkeville	617	834	2.67
5961803	Austin	30.021389	-96.440278	Jasper	674	725	36.50
7934902	Bee	28.405001	-97.752501	Evangelina	526	622	12.43
7943103	Bee	28.337222	-97.746667	Evangelina	96	770	5.40
7943104	Bee	28.337222	-97.746667	Evangelina	95	770	5.78
7943105	Bee	28.337222	-97.746667	Evangelina	96	770	5.93
7943106	Bee	28.337222	-97.746667	Evangelina	73	770	3.68
7943401	Bee	28.332222	-97.745556	Evangelina	340	835	10.29
7818503	Bee	28.67083333	-97.79444444	Jasper	727	907	28.88
7918503	Bee	28.667778	-97.796945	Jasper	727	907	9.80
7935702	Bee	28.399445	-97.737222	Jasper	1428	1590	49.33
6543707	Brazoria	29.2905556	-95.7322222	Chicot	210	250	10.73
6552708	Brazoria	29.160556	-95.621111	Chicot	90	220	19.83
6558617	Brazoria	29.077222	-95.755556	Chicot	130	170	108.86
6559405	Brazoria	29.071111	-95.744445	Chicot	120	160	94.69
6559406	Brazoria	29.065556	-95.738889	Chicot	137	177	83.52
6559429	Brazoria	29.071111	-95.744445	Chicot	120	160	137.30
8104201	Brazoria	28.989167	-95.583055	Chicot	450	490	2.61
Not Available	Brazoria	29.14222222	-95.64555556	Chicot	525	663	7.34
8455307	Brooks	27.225555	-98.147778	Evangelina	675	705	54.28
8455308	Brooks	27.225	-98.130278	Evangelina	675	705	54.37
8455309	Brooks	27.236389	-98.156667	Evangelina	694	755	23.45
8455310	Brooks	27.2302778	-98.1558333	Evangelina	686	749	22.73
8456203	Brooks	27.223611	-98.052223	Evangelina	645	680	70.59
8456501	Brooks	27.182778	-98.079444	Evangelina	560	600	50.53
8463304	Brooks	27.088334	-98.148056	Evangelina	548	600	32.62
8019702	Calhoun	28.648889	-96.723889	Chicot	200	350	23.35
8019703	Calhoun	28.648611	-96.7225	Chicot	201	355	24.91
8019704	Calhoun	28.646111	-96.723889	Chicot	197	365	18.38
8019802	Calhoun	28.6269972	-96.679	Chicot	162	238	35.70
8020801	Calhoun	28.663889	-96.559445	Chicot	254	365	46.26
8020802	Calhoun	28.663889	-96.563334	Chicot	254	369	45.19

Conceptual Model Report: Central and Southern Portions of the Gulf Coast Aquifer System in Texas

Well ID	County	Latitude	Longitude	Hydrogeologic Unit	Screen Top (feet below ground)	Screen Bottom (feet below ground)	Hydraulic Conductivity (feet per day)
8020803	Calhoun	28.659445	-96.550834	Chicot	250	359	58.82
8026603	Calhoun	28.558056	-96.778055	Chicot	185	269	76.47
Not Available	Calhoun	28.3325	-96.45861111	Chicot	270	310	71.93
8851909	Cameron	26.139722	-97.628889	Chicot	182	237	18.76
8851910	Cameron	26.134167	-97.632778	Chicot	163	217	23.48
8858301	Cameron	26.101945	-97.762778	Chicot	158	166	1002.67
8858302	Cameron	26.0908333	-97.7563889	Chicot	150	166	200.53
8858306	Cameron	26.094445	-97.762501	Chicot	159	169	735.29
8858312	Cameron	26.098889	-97.764723	Chicot	156	163	951.87
8858313	Cameron	26.086389	-97.762778	Chicot	146	219	195.19
8858314	Cameron	26.094722	-97.758612	Chicot	160	168	802.14
6620505	Colorado	29.700556	-96.559723	Evangelina	162	288	6.86
6620507	Colorado	29.698334	-96.543334	Evangelina	151	316	11.34
6620602	Colorado	29.7053694	-96.5377583	Evangelina	195	295	10.00
6620902	Colorado	29.64	-96.502501	Evangelina	293	767	3.34
6621301	Colorado	29.715278	-96.415001	Evangelina	400	800	8.50
6627905	Colorado	29.519444	-96.658334	Evangelina	564	615	8.82
6628303	Colorado	29.604445	-96.511112	Evangelina	276	836	8.34
6629104	Colorado	29.598889	-96.475555	Evangelina	282	933	13.83
6635304	Colorado	29.470278	-96.625833	Evangelina	695	820	13.48
6636103	Colorado	29.468611	-96.623889	Evangelina	695	816	12.33
6747909	DeWitt	29.274444	-97.158334	Evangelina	40	79	120.32
6755601	DeWitt	29.203612	-97.156112	Evangelina	88	234	14.97
6756901	DeWitt	29.129167	-97.031389	Evangelina	118	234	2.67
6747403	DeWitt	29.314167	-97.245834	Jasper	130	170	16.15
6747911	DeWitt	29.277222	-97.151945	Jasper	294	782	5.95
6747912	DeWitt	29.277778	-97.160834	Jasper	262	590	9.05
6754814	DeWitt	29.131667	-97.301112	Jasper	186	590	12.42
6760903	DeWitt	29.0177778	-97.5225	Jasper	210	570	7.89
7904301	DeWitt	28.981667	-97.504445	Jasper	880	972	49.68
7904402	DeWitt	28.921389	-97.611389	Jasper	925	1080	30.88
8421601	Duval	27.701389	-98.393056	Evangelina	256	349	3.70
8421603	Duval	27.701667	-98.388611	Evangelina	268	380	2.67
8421801	Duval	27.663334	-98.435	Evangelina	250	635	2.90
8429309	Duval	27.588611	-98.404445	Evangelina	332	607	4.17
8429310	Duval	27.589167	-98.406112	Evangelina	322	596	4.32
8446702	Duval	27.285278	-98.335	Evangelina	140	280	9.55



Conceptual Model Report: Central and Southern Portions of the Gulf Coast Aquifer System in Texas

Well ID	County	Latitude	Longitude	Hydrogeologic Unit	Screen Top (feet below ground)	Screen Bottom (feet below ground)	Hydraulic Conductivity (feet per day)
5960405	Fayette	30.053612	-96.624444	Jasper	490	595	11.56
6610501	Fayette	29.826111	-96.809723	Jasper	411	491	6.81
6617601	Fayette	29.685556	-96.916112	Jasper	154	262	27.93
6617602	Fayette	29.685556	-96.914445	Jasper	177	270	10.40
6525106	Fort Bend	29.6030556	-95.9716667	Chicot	360	400	12.62
6526601	Fort Bend	29.572222	-95.763889	Chicot	317	347	113.64
6526602	Fort Bend	29.557501	-95.781944	Chicot	150	400	57.69
6533502	Fort Bend	29.435	-95.953889	Chicot	72	590	32.53
6533802	Fort Bend	29.378611	-95.9275	Chicot	315	356	35.40
6533803	Fort Bend	29.3797222	-95.9269444	Chicot	315	353	47.32
6533804	Fort Bend	29.381111	-95.936111	Chicot	122	143	69.58
6534901	Fort Bend	29.416389	-95.755556	Chicot	85	617	52.26
6526406	Fort Bend	29.542778	-95.846111	Evangeline	968	1160	51.84
6527506	Fort Bend	29.558889	-95.688334	Evangeline	1652	1922	2.23
8755503	Hidalgo	26.199167	-98.170833	Chicot	258	318	51.11
8747207	Hidalgo	26.340834	-98.178333	Evangeline	162	665	4.28
8747208	Hidalgo	26.344445	-98.172222	Evangeline	363	667	5.93
8747209	Hidalgo	26.341667	-98.170833	Evangeline	321	648	12.01
8762302	Hidalgo	26.100556	-98.260278	Evangeline	188	296	11.55
6652907	Jackson	29.136945	-96.529722	Chicot	130	490	17.11
6660205	Jackson	29.106112	-96.543611	Chicot	97	224	98.13
6660505	Jackson	29.0775	-96.558334	Chicot	135	316	85.83
6660603	Jackson	29.069444	-96.502223	Chicot	64	274	53.07
6660608	Jackson	29.080278	-96.507501	Chicot	112	234	57.22
6660609	Jackson	29.078055	-96.507501	Chicot	42	180	135.63
6660703	Jackson	29.018611	-96.584167	Chicot	132	513	20.45
6661702	Jackson	29.011667	-96.483889	Chicot	127	315	94.92
6661803	Jackson	29.018333	-96.431389	Chicot	105	317	53.48
8004505	Jackson	28.949722	-96.544722	Chicot	275	295	62.66
8004612	Jackson	28.951112	-96.511945	Chicot	190	230	49.20
8005301	Jackson	28.991667	-96.391111	Chicot	40	292	123.08
8005310	Jackson	28.989722	-96.390834	Chicot	115	210	97.59
8005507	Jackson	28.943889	-96.447222	Chicot	178	795	22.33
8005701	Jackson	28.905278	-96.498889	Chicot	120	429	18.98
8006101	Jackson	28.997778	-96.363612	Chicot	85	550	54.34
8006102	Jackson	28.969167	-96.367778	Chicot	104	364	76.27
8006104	Jackson	28.969167	-96.367222	Chicot	50	215	96.42

Conceptual Model Report: Central and Southern Portions of the Gulf Coast Aquifer System in Texas

Well ID	County	Latitude	Longitude	Hydrogeologic Unit	Screen Top (feet below ground)	Screen Bottom (feet below ground)	Hydraulic Conductivity (feet per day)
8006703	Jackson	28.877778	-96.335	Chicot	154	590	24.20
8006704	Jackson	28.8875	-96.367778	Chicot	146	430	49.33
8011201	Jackson	28.8669444	-96.6783333	Chicot	119	572	15.64
8012502	Jackson	28.809723	-96.548889	Chicot	90	330	63.64
8013404	Jackson	28.825833	-96.467222	Chicot	150	510	34.49
8013901	Jackson	28.79	-96.384722	Chicot	140	775	17.51
8014103	Jackson	28.835278	-96.360834	Chicot	200	752	21.66
8014401	Jackson	28.823889	-96.361667	Chicot	150	710	31.28
8021201	Jackson	28.725	-96.4444444	Chicot	412	467	60.83
8021213	Jackson	28.7252778	-96.4480556	Chicot	415	476	30.35
8021214	Jackson	28.7211111	-96.4522222	Chicot	360	455	88.66
8021601	Jackson	28.686111	-96.385278	Chicot	317	635	29.01
8022501	Jackson	28.699445	-96.323333	Chicot	288	370	33.56
G1200022B	Jackson	28.7238884	-96.41638947	Chicot	590	610	168.28
G1200027B	Jackson	28.705196	-96.37855	Chicot	290	310	93.45
G1200028B	Jackson	28.69805556	-96.37583333	Chicot	370	400	57.53
6660613	Jackson	29.041945	-96.513056	Evangelina	730	850	23.79
6660902	Jackson	29.041111	-96.513334	Evangelina	1185	1291	14.30
6660907	Jackson	29.035834	-96.507501	Evangelina	752	1028	1.68
8003301	Jackson	28.9825	-96.645834	Evangelina	970	1195	28.26
8003303	Jackson	28.971944	-96.654445	Evangelina	955	1308	25.12
8443504	Jim Hogg	27.311667	-98.674167	Jasper	806	1408	1.68
8443512	Jim Hogg	27.295834	-98.687778	Jasper	827	1383	3.58
8301508	Jim Wells	27.955556	-97.939167	Evangelina	630	746	9.36
8301509	Jim Wells	27.956945	-97.941111	Evangelina	550	817	11.10
8408801	Jim Wells	27.898889	-98.049445	Evangelina	585	630	10.10
8416804	Jim Wells	27.765001	-98.065834	Evangelina	321	841	2.01
8416805	Jim Wells	27.770833	-98.054167	Evangelina	395	850	1.63
8416807	Jim Wells	27.761112	-98.051667	Evangelina	320	856	3.74
8424101	Jim Wells	27.712223	-98.123333	Evangelina	400	800	2.63
8424102	Jim Wells	27.736667	-98.101389	Evangelina	320	750	1.74
8424203	Jim Wells	27.731667	-98.076111	Evangelina	390	780	2.47
8424204	Jim Wells	27.730555	-98.069444	Evangelina	400	810	2.01
8424401	Jim Wells	27.706112	-98.123333	Evangelina	1850	1900	18.98
8447313	Jim Wells	27.3530556	-98.1265389	Evangelina	427	568	11.23
8448103	Jim Wells	27.35171873	-98.1250325	Evangelina	427	568	9.67
House Well	Karnes	28.70918528	-97.73234222	Burkeville	147	200	2.82

Conceptual Model Report: Central and Southern Portions of the Gulf Coast Aquifer System in Texas

Well ID	County	Latitude	Longitude	Hydrogeologic Unit	Screen Top (feet below ground)	Screen Bottom (feet below ground)	Hydraulic Conductivity (feet per day)
PVC Well	Karnes	28.71035222	-97.71035222	Burkeville	222	327	3.77
246250	Karnes	28.796389	-97.799445	Jasper	300	360	12.99
301931	Karnes	28.780141	-97.81212	Jasper	600	650	27.30
7816609	Karnes	28.8219444	-98.0111111	Jasper	384	503	7.08
7903703	Karnes	28.906945	-97.728611	Jasper	208	377	17.42
7903704	Karnes	28.881389	-97.712778	Jasper	156	190	39.32
7903705	Karnes	28.881667	-97.713056	Jasper	101	156	24.00
7903707	Karnes	28.881111	-97.712778	Jasper	155	210	13.41
7910402	Karnes	28.816389	-97.842778	Jasper	268	417	12.43
7910403	Karnes	28.801389	-97.8425	Jasper	564	634	25.46
7910405	Karnes	28.815834	-97.848889	Jasper	334	396	29.95
7910406	Karnes	28.8122167	-97.8500917	Jasper	90	416	6.89
7910811	Karnes	28.785	-97.8261111	Jasper	580	635	39.74
7910812	Karnes	28.765834	-97.808889	Jasper	123	143	16.91
7911901	Karnes	28.789167	-97.6325	Jasper	510	565	16.58
7911902	Karnes	28.79	-97.631944	Jasper	515	590	14.71
8326702	Kleberg	27.523055	-97.858612	Chicot	360	606	30.61
8341803	Kleberg	27.254723	-97.936389	Evangelina	512	638	34.75
6642502	Lavaca	29.296667	-96.812223	Evangelina	747	845	8.00
6657201	Lavaca	29.100556	-96.917778	Evangelina	234	584	17.11
6748703	Lavaca	29.265556	-97.119722	Burkeville	320	430	24.00
6747608	Lavaca	29.307501	-97.131944	Jasper	894	1030	37.84
7949501	Live Oak	28.179722	-97.918889	Evangelina	200	425	16.58
7950403	Live Oak	28.188611	-97.839167	Evangelina	300	461	19.52
7950404	Live Oak	28.192222	-97.838056	Evangelina	300	460	23.66
7950407	Live Oak	28.180833	-97.850278	Evangelina	300	460	20.05
7848401	Live Oak	28.326667	-98.120278	Jasper	348	501	48.06
7848402	Live Oak	28.330833	-98.120278	Jasper	50	500	8.39
MW17	Live Oak	28.41306501	-98.13783805	Jasper	60	180	24.93
MW18	Live Oak	28.41885867	-98.13150435	Jasper	120	180	26.56
MW19	Live Oak	28.4232188	-98.12629315	Jasper	110	170	57.11
PZ14	Live Oak	28.39705106	-98.13289034	Jasper	132	192	13.03
PZ2	Live Oak	28.40865968	-98.14685	Jasper	128	215	19.42
294215	Matagorda	28.715278	-96.219167	Chicot	545	705	22.51
6549901	Matagorda	29.145278	-95.893334	Chicot	300	355	87.97
6557702	Matagorda	29.008889	-95.997778	Chicot	331	553	6.15
6557801	Matagorda	29.036389	-95.933055	Chicot	51	530	45.19

Conceptual Model Report: Central and Southern Portions of the Gulf Coast Aquifer System in Texas

Well ID	County	Latitude	Longitude	Hydrogeologic Unit	Screen Top (feet below ground)	Screen Bottom (feet below ground)	Hydraulic Conductivity (feet per day)
6557902	Matagorda	29.016389	-95.893334	Chicot	329	440	43.75
6557904	Matagorda	29.0175	-95.8930556	Chicot	526	641	32.86
6558107	Matagorda	29.090556	-95.8475	Chicot	75	202	185.27
6558108	Matagorda	29.087778	-95.851667	Chicot	150	275	92.65
6558803	Matagorda	29.016389	-95.795	Chicot	91	215	528.07
6663802	Matagorda	29.001112	-96.184445	Chicot	240	760	49.24
6663902	Matagorda	29.011667	-96.147778	Chicot	63	240	100.67
6664702	Matagorda	29.023889	-96.084722	Chicot	566	856	29.81
6664802	Matagorda	29.009445	-96.050834	Chicot	410	670	23.83
8007322	Matagorda	28.990278	-96.156945	Chicot	237	480	25.71
8007404	Matagorda	28.937222	-96.228333	Chicot	192	744	68.45
8007501	Matagorda	28.954723	-96.203612	Chicot	220	820	31.72
8008302	Matagorda	28.98	-96.013889	Chicot	530	630	32.01
8008701	Matagorda	28.887778	-96.107778	Chicot	300	600	10.56
8014605	Matagorda	28.807501	-96.2775	Chicot	247	865	56.32
8014608	Matagorda	28.800556	-96.289445	Chicot	243	870	48.13
8015102	Matagorda	28.871111	-96.221389	Chicot	506	634	61.23
8015201	Matagorda	28.861112	-96.195278	Chicot	353	878	56.15
8015301	Matagorda	28.853056	-96.144445	Chicot	145	570	55.21
8015502	Matagorda	28.813889	-96.167778	Chicot	244	776	21.79
8016301	Matagorda	28.862223	-96.018611	Chicot	615	800	67.51
8016305	Matagorda	28.863334	-96.018333	Chicot	632	819	75.03
8023101	Matagorda	28.747222	-96.236667	Chicot	190	776	18.98
8023301	Matagorda	28.740556	-96.148056	Chicot	200	770	18.58
8023402	Matagorda	28.702778	-96.216112	Chicot	544	586	125.40
8023403	Matagorda	28.701945	-96.214445	Chicot	542	578	141.95
8101101	Matagorda	28.979722	-95.975	Chicot	560	760	65.78
8101102	Matagorda	28.98	-95.9752778	Chicot	777	1020	28.48
8101110	Matagorda	28.9825	-95.966389	Chicot	760	1020	35.46
8101201	Matagorda	28.981944	-95.951112	Chicot	778	1033	18.04
8101405	Matagorda	28.956667	-95.971389	Chicot	798	1032	22.62
8101601	Matagorda	28.952223	-95.909445	Chicot	218	660	50.67
8101802	Matagorda	28.875555	-95.946389	Chicot	150	520	21.26
8109202	Matagorda	28.840834	-95.954167	Chicot	240	470	45.33
8109401	Matagorda	28.807501	-95.984445	Chicot	189	366	33.42
8109504	Matagorda	28.802501	-95.939167	Chicot	170	721	44.25
8109904	Matagorda	28.760278	-95.899445	Chicot	361	482	95.86

Conceptual Model Report: Central and Southern Portions of the Gulf Coast Aquifer System in Texas

Well ID	County	Latitude	Longitude	Hydrogeologic Unit	Screen Top (feet below ground)	Screen Bottom (feet below ground)	Hydraulic Conductivity (feet per day)
8109905	Matagorda	28.758612	-95.899445	Chicot	364	491	60.70
8110902	Matagorda	28.755556	-95.769167	Chicot	280	296	88.84
8111604	Matagorda	28.807501	-95.648611	Chicot	480	558	30.35
8117404	Matagorda	28.691945	-95.968055	Chicot	320	410	14.01
G1610013C	Matagorda	28.69203949	-95.96803284	Chicot	320	410	54.03
G1610129A	Matagorda	28.85882778	-96.16040556	Chicot	407	423	5.81
8326511	Nueces	27.575278	-97.8225	Chicot	56	700	0.98
Site #1: TW-450	Nueces	27.758255	-97.489061	Chicot	410	450	16.90
Site #1: TW-650	Nueces	27.758255	-97.489061	Chicot	570	650	5.94
8326508	Nueces	27.598889	-97.823889	Evangelina	855	895	15.37
8326509	Nueces	27.569167	-97.822778	Evangelina	817	950	5.75
7954203	Refugio	28.238334	-97.327778	Chicot	180	270	3.57
7954802	Refugio	28.164167	-97.307501	Chicot	282	300	240.64
7954803	Refugio	28.147222	-97.307223	Chicot	78	331	4.62
7946604	Refugio	28.298611	-97.271944	Evangelina	578	864	21.12
7946608	Refugio	28.299722	-97.271111	Evangelina	800	875	29.28
G1960001E	Refugio	28.313317	-97.270051	Evangelina	424	880	2.98
8307829	San Patricio	27.893056	-97.183055	Chicot	50	182	3.07
8307835	San Patricio	27.893889	-97.183055	Chicot	20	180	3.11
8307836	San Patricio	27.893889	-97.183055	Chicot	21	181	3.28
7951705	San Patricio	28.135	-97.723055	Evangelina	280	751	7.43
7958201	San Patricio	28.1016667	-97.8227778	Evangelina	224	509	8.69
7958502	San Patricio	28.049445	-97.825833	Evangelina	168	288	13.50
219948	Victoria	28.784478	-97.043394	Chicot	230	250	40.72
8010701	Victoria	28.775	-96.872222	Chicot	160	450	37.03
8017505	Victoria	28.6777778	-96.9519444	Chicot	241	447	18.49
8019501	Victoria	28.689722	-96.706112	Chicot	158	324	31.15
G2350006B	Victoria	28.688642	-96.821285	Chicot	425	490	35.54
53809	Victoria	28.881536	-97.172294	Evangelina	235	255	49.06
7907902	Victoria	28.893611	-97.135278	Evangelina	425	835	7.14
7916602	Victoria	28.8127778	-97.0102778	Evangelina	400	990	23.61
7916614	Victoria	28.811112	-97.02	Evangelina	460	1048	9.73
7916615	Victoria	28.81229	-97.001839	Evangelina	400	1044	16.76
7916903	Victoria	28.781667	-97.009723	Evangelina	420	755	29.36
7916904	Victoria	28.782222	-97.004445	Evangelina	420	850	20.81
7916905	Victoria	28.789445	-97.013889	Evangelina	410	830	22.53

Conceptual Model Report: Central and Southern Portions of the Gulf Coast Aquifer System in Texas

Well ID	County	Latitude	Longitude	Hydrogeologic Unit	Screen Top (feet below ground)	Screen Bottom (feet below ground)	Hydraulic Conductivity (feet per day)
8009103	Victoria	28.851112	-96.991111	Evangeline	640	1124	15.77
8009401	Victoria	28.803334	-96.991111	Evangeline	439	749	28.59
8009402	Victoria	28.803334	-96.991389	Evangeline	818	993	46.59
8009404	Victoria	28.820833	-96.986667	Evangeline	425	1010	21.05
8009406	Victoria	28.821111	-96.984167	Evangeline	442	1000	31.82
8009411	Victoria	28.816112	-96.9925	Evangeline	406	1020	12.34
8017905	Victoria	28.6475	-96.895278	Evangeline	784	996	88.46
5946802	Washington	30.272222	-96.308056	Jasper	243	446	3.61
5952702	Washington	30.154723	-96.618611	Jasper	180	275	22.46
5953901	Washington	30.158056	-96.395834	Jasper	58	320	6.84
5953902	Washington	30.158334	-96.395556	Jasper	58	185	14.32
5953903	Washington	30.158612	-96.395278	Jasper	61	182	14.56
5953911	Washington	30.161945	-96.388889	Jasper	73	528	5.35
5953915	Washington	30.1663889	-96.3841667	Jasper	75	810	2.58
5953916	Washington	30.161389	-96.380833	Jasper	120	990	1.93
5954902	Washington	30.140556	-96.256112	Jasper	747	778	0.80
6541928	Wharton	29.256667	-95.901667	Chicot	369	579	119.15
6541933	Wharton	29.250834	-95.890834	Chicot	340	580	88.99
6549111	Wharton	29.228055	-95.978611	Chicot	430	520	89.13
6631901	Wharton	29.539722	-96.144167	Chicot	100	135	212.00
6631902	Wharton	29.538334	-96.156112	Chicot	40	52	2127.90
6631903	Wharton	29.535	-96.150556	Chicot	40	405	29.28
6640607	Wharton	29.431667	-96.028333	Chicot	300	426	48.51
6640804	Wharton	29.397222	-96.074722	Chicot	243	298	82.47
6645201	Wharton	29.351389	-96.441389	Chicot	0	257	115.00
6645804	Wharton	29.269167	-96.456667	Chicot	110	388	59.09
6646402	Wharton	29.3069444	-96.3480556	Chicot	100	366	120.59
6648902	Wharton	29.2825	-96.012778	Chicot	10	105	192.37
6648904	Wharton	29.255556	-96.008612	Chicot	95	370	89.57
6655103	Wharton	29.235834	-96.228889	Chicot	260	500	59.00
6661302	Wharton	29.1088889	-96.4094444	Chicot	400	528	96.31
6661305	Wharton	29.1041667	-96.4083333	Chicot	134	599	41.04
6661309	Wharton	29.109167	-96.409445	Chicot	95	350	52.10
6662313	Wharton	29.1186111	-96.2716667	Chicot	406	480	69.89
6662709	Wharton	29.010001	-96.355278	Chicot	200	785	64.00
6662713	Wharton	29.010556	-96.354445	Chicot	200	690	90.00
6662904	Wharton	29.020555	-96.256389	Chicot	162	573	43.58

Conceptual Model Report: Central and Southern Portions of the Gulf Coast Aquifer System in Texas

<b>Well ID</b>	<b>County</b>	<b>Latitude</b>	<b>Longitude</b>	<b>Hydrogeologic Unit</b>	<b>Screen Top (feet below ground)</b>	<b>Screen Bottom (feet below ground)</b>	<b>Hydraulic Conductivity (feet per day)</b>
6663201	Wharton	29.123055	-96.182222	Chicot	116	594	55.35
6663504	Wharton	29.0472222	-96.1677778	Chicot	167	682	63.50
6665103	Wharton	29.23361111	-96.23027778	Chicot	264	500	44.79
G2410008C	Wharton	29.108931	-96.40522	Chicot	404	600	17.39
6631906	Wharton	29.5325	-96.144722	Evangeline	860	990	12.97
6654601	Wharton	29.206389	-96.280555	Evangeline	690	1085	29.01
6654603	Wharton	29.194445	-96.270833	Evangeline	790	1265	14.30
6654621	Wharton	29.187778	-96.258889	Evangeline	710	1020	45.29
8827801	Willacy	26.502778	-97.688611	Evangeline	1000	1165	1.56

**Table E2. Summary of hydraulic conductivity values from pumping tests and specific capacity tests.**

(Due to its large size, this table is included in a separate EXCEL file: Table E2. Summary of hydraulic conductivity values from pumping and specific capacity tests.xlsx)



**Table E3. Summary of storativity and specific yield values from pumping tests.**

(Due to its large size, this table is included in a separate EXCEL file: Table E3. Summary of S and Sy values from pumping tests.xlsx)

## **Appendix F: Hydrograph of Total Dissolved Solids**

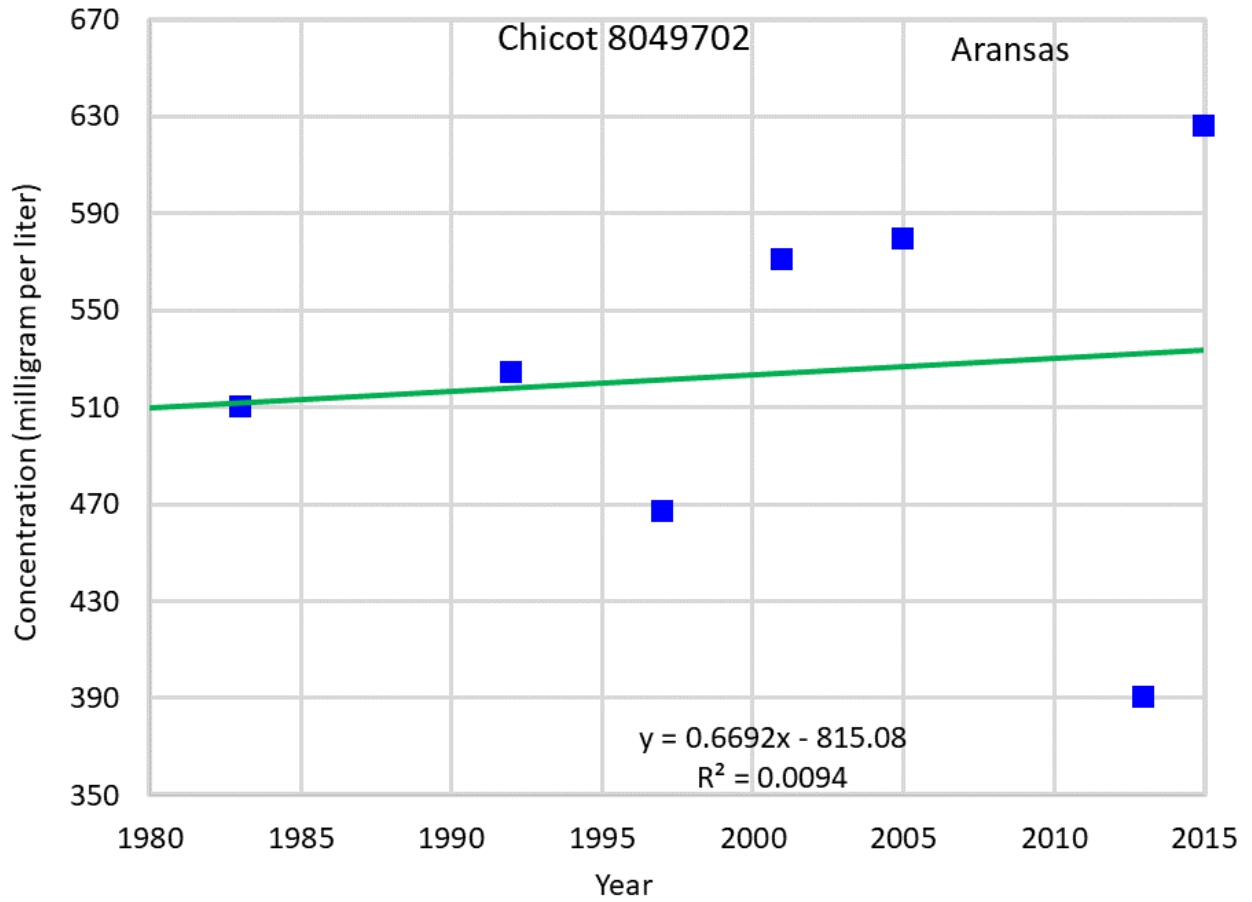


**Figure F1 Hydrograph of total dissolved solids at State Well 8049702.**

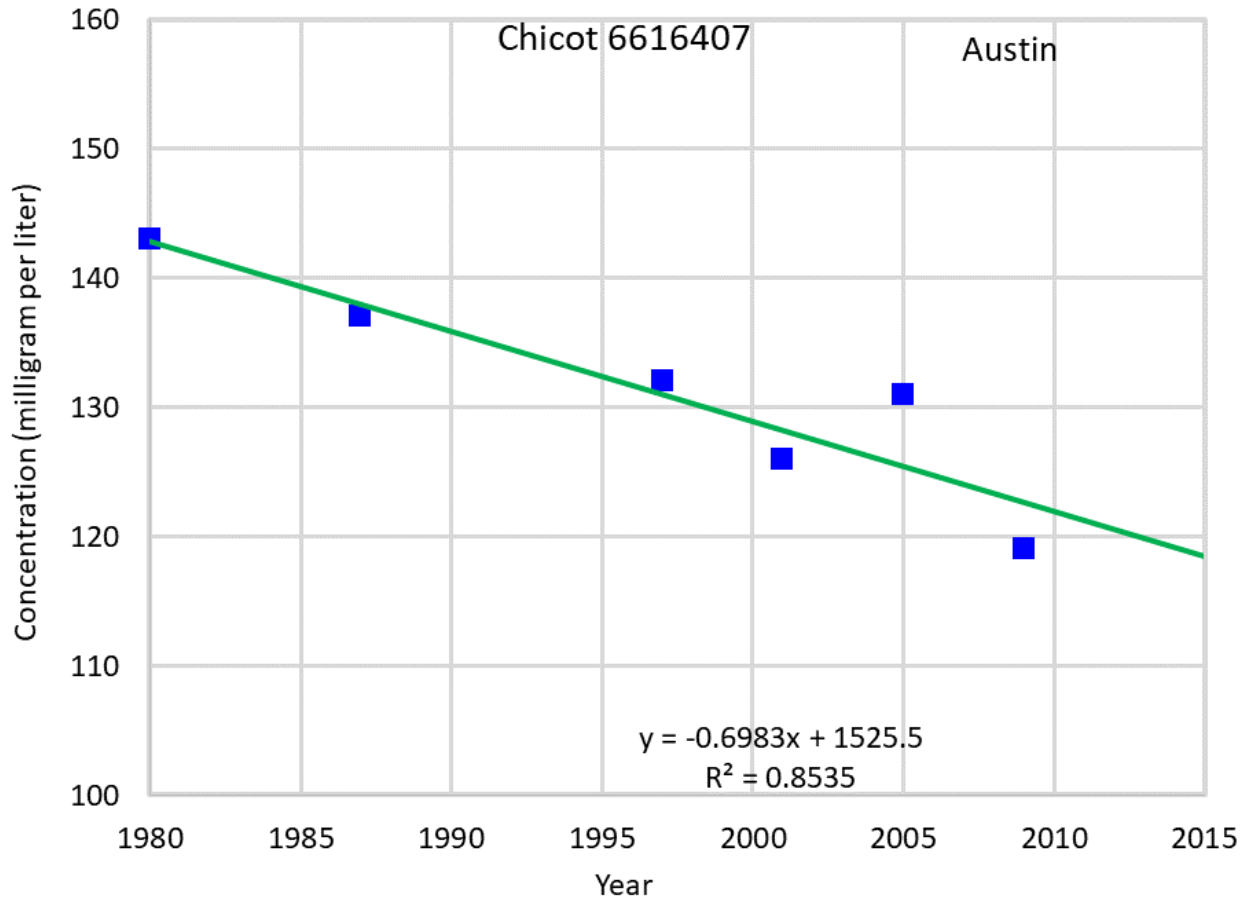


**Figure F2 Hydrograph of total dissolved solids at State Well 6616407.**

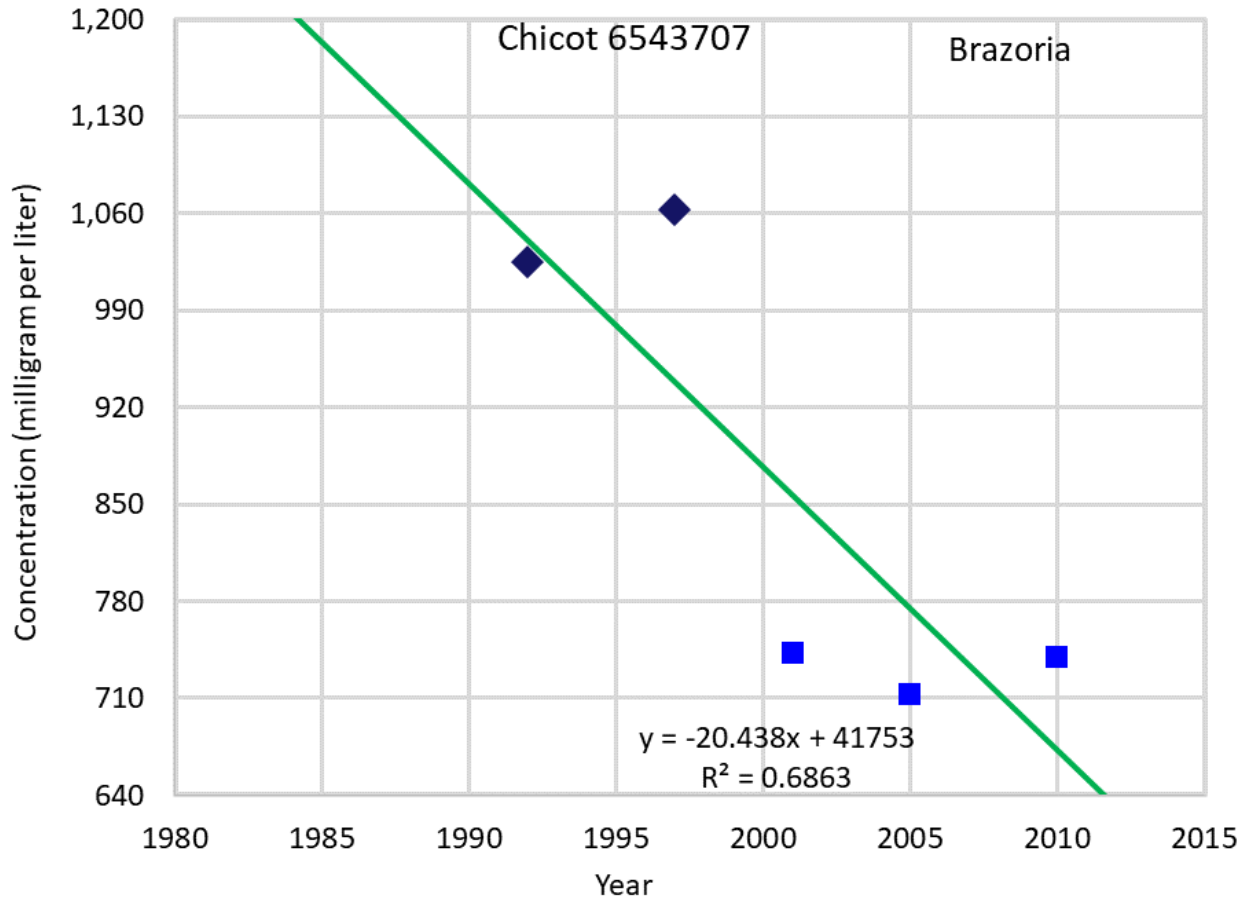


**Figure F3 Hydrograph of total dissolved solids at State Well 6543707.**

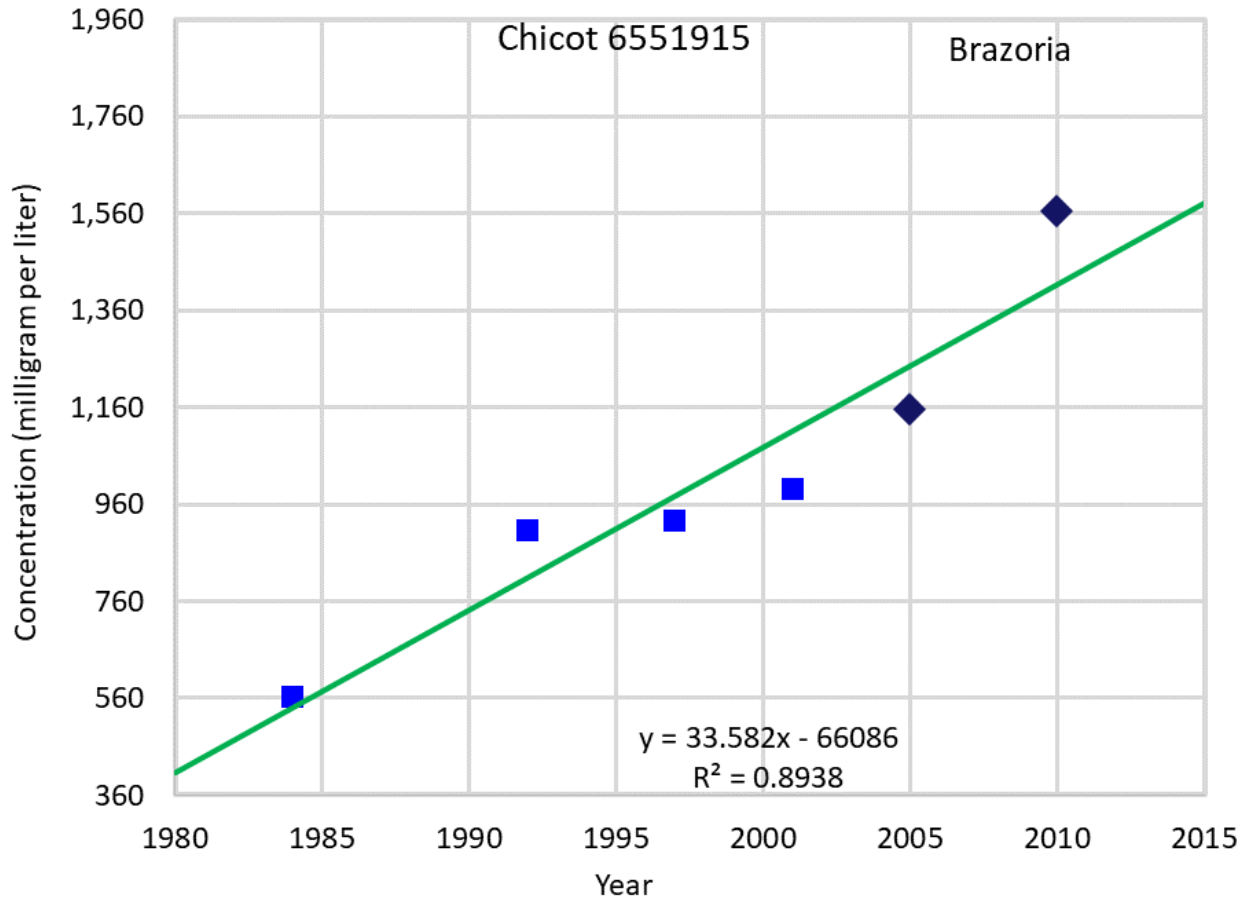


**Figure F4 Hydrograph of total dissolved solids at State Well 6551915.**

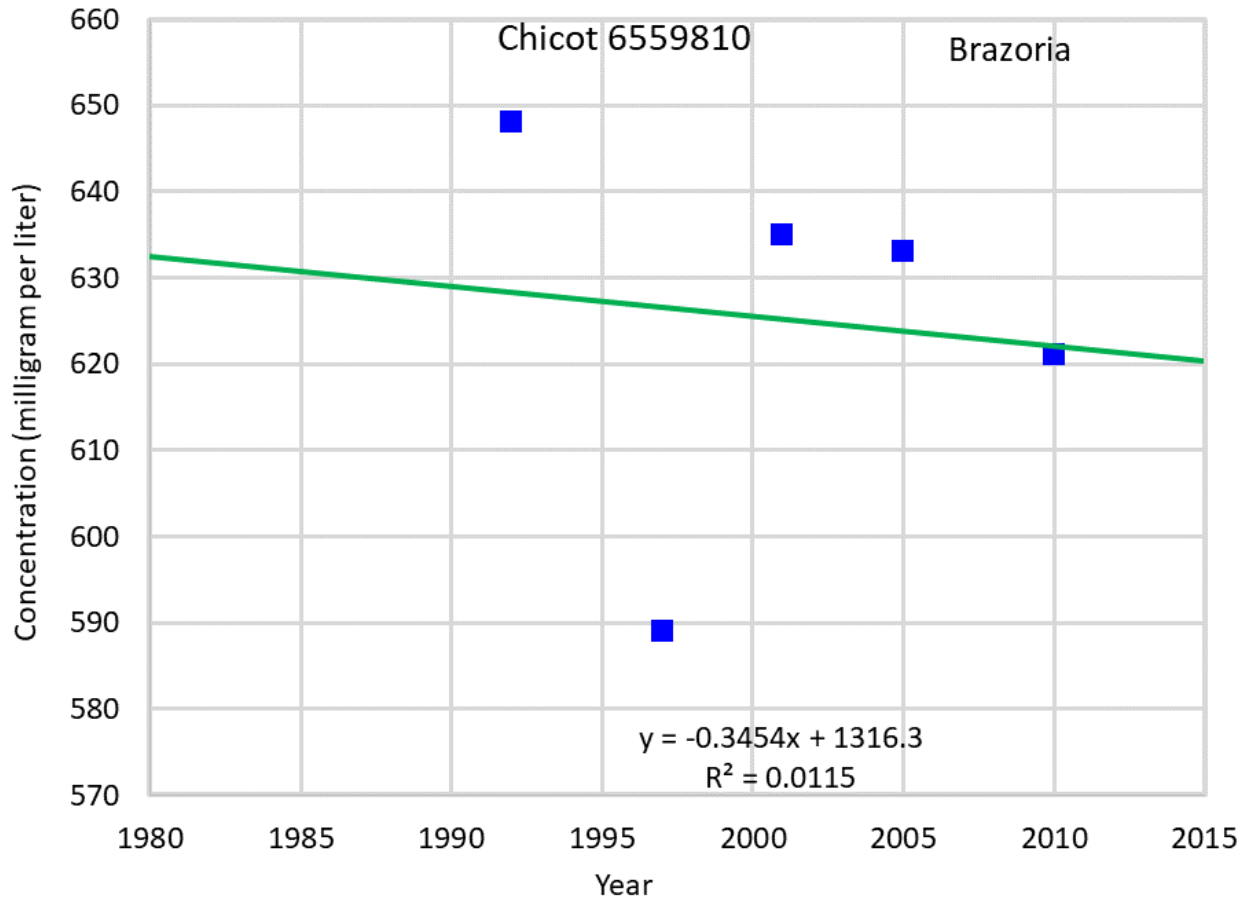


**Figure F5 Hydrograph of total dissolved solids at State Well 6559810.**

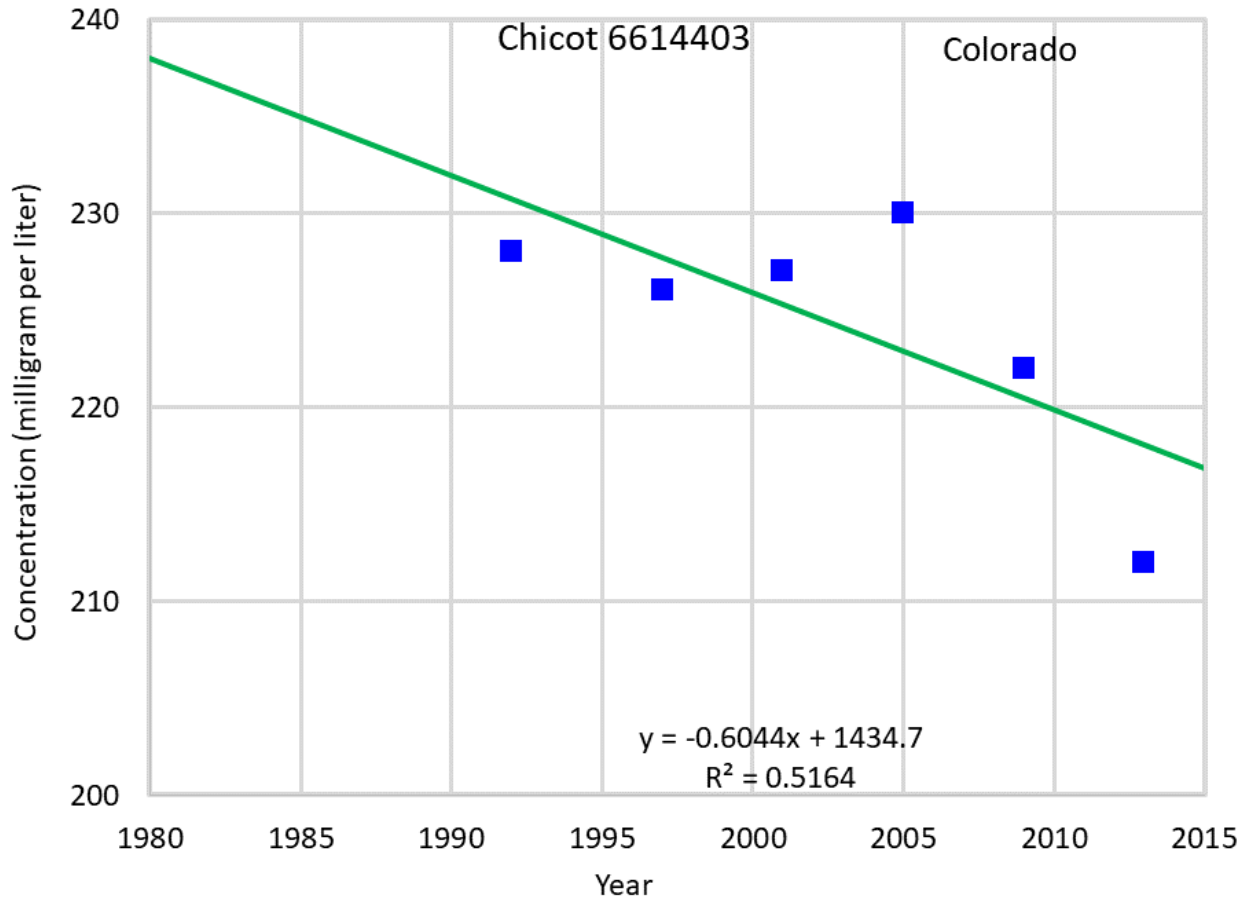


**Figure F6 Hydrograph of total dissolved solids at State Well 6614403.**



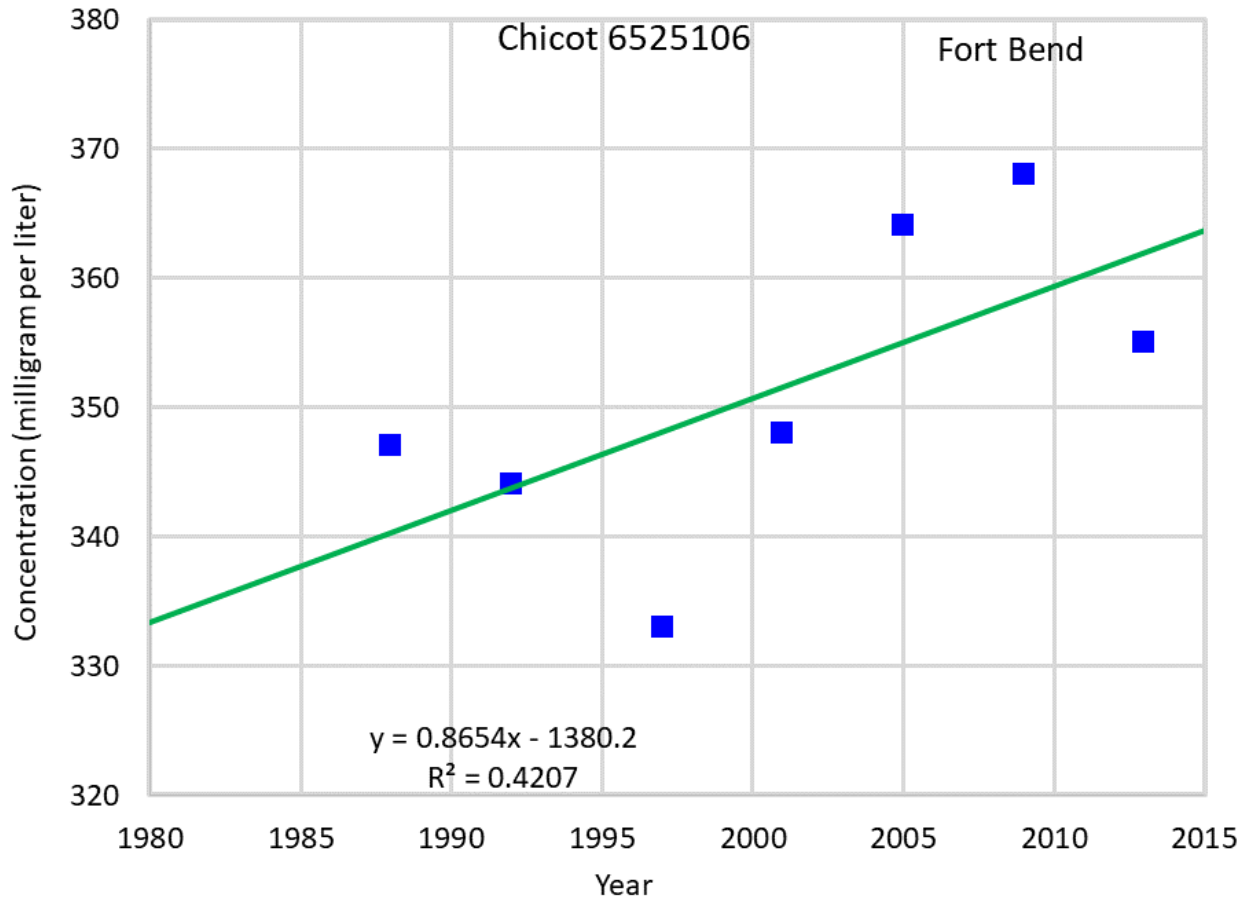


**Figure F7 Hydrograph of total dissolved solids at State Well 6525106.**

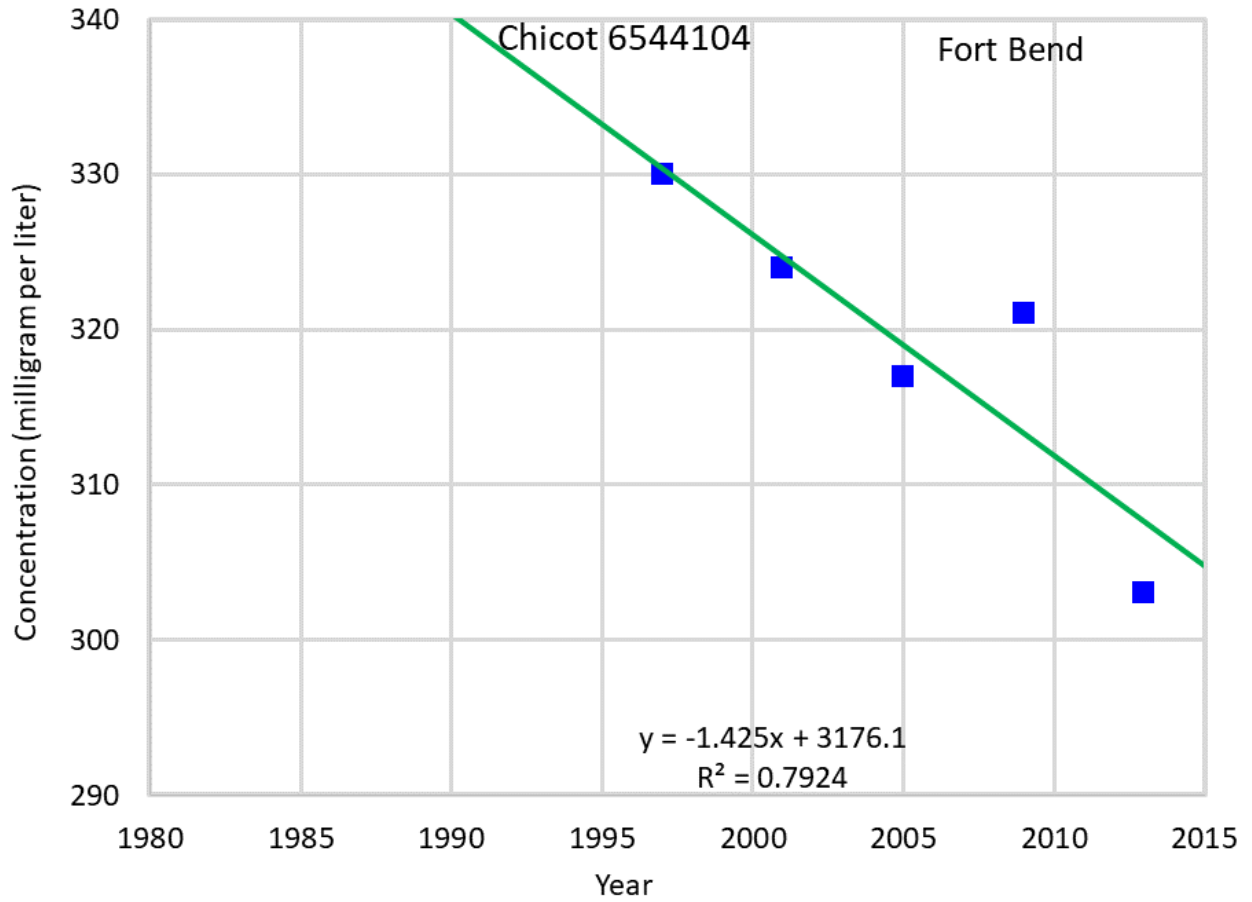


**Figure F8 Hydrograph of total dissolved solids at State Well 6544104.**

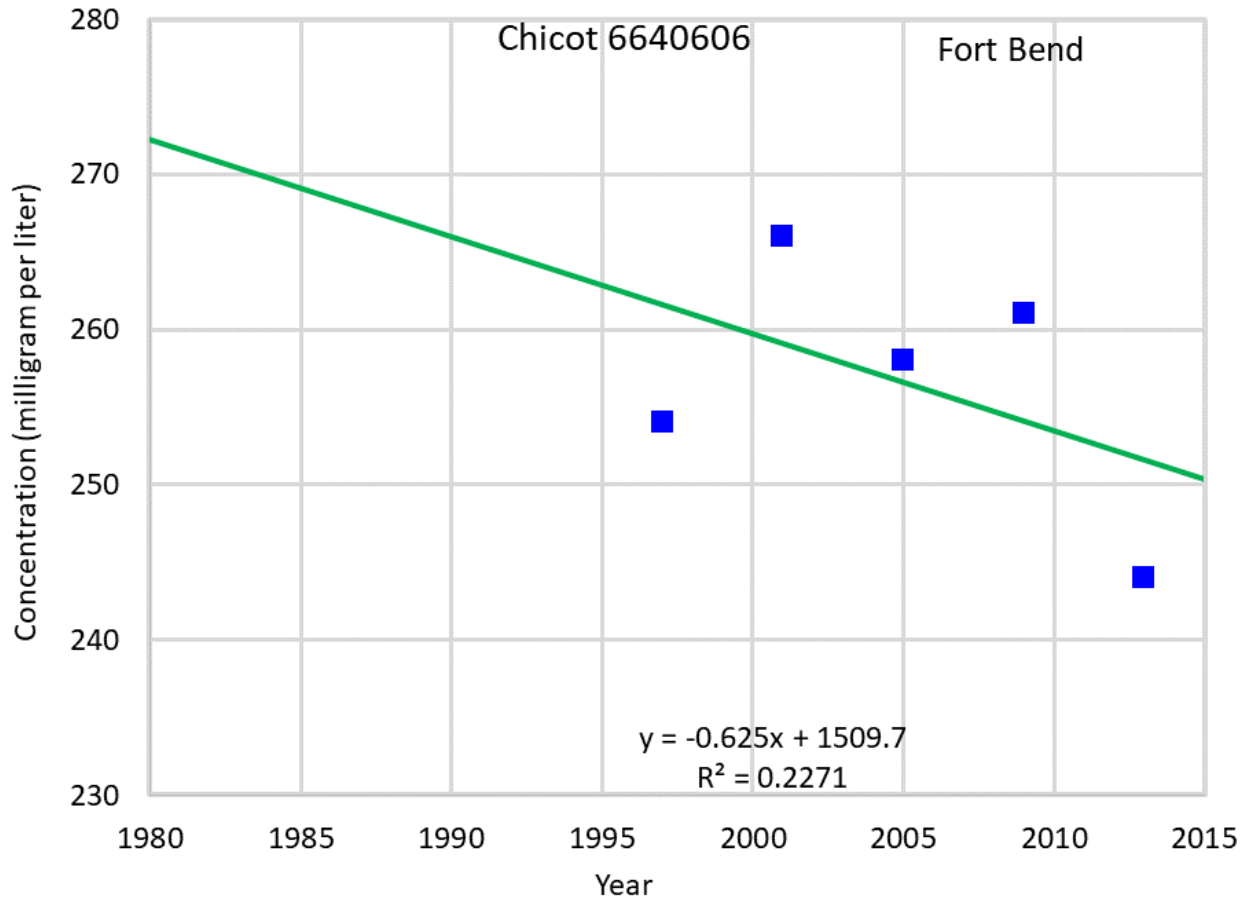


**Figure F9 Hydrograph of total dissolved solids at State Well 6640606.**

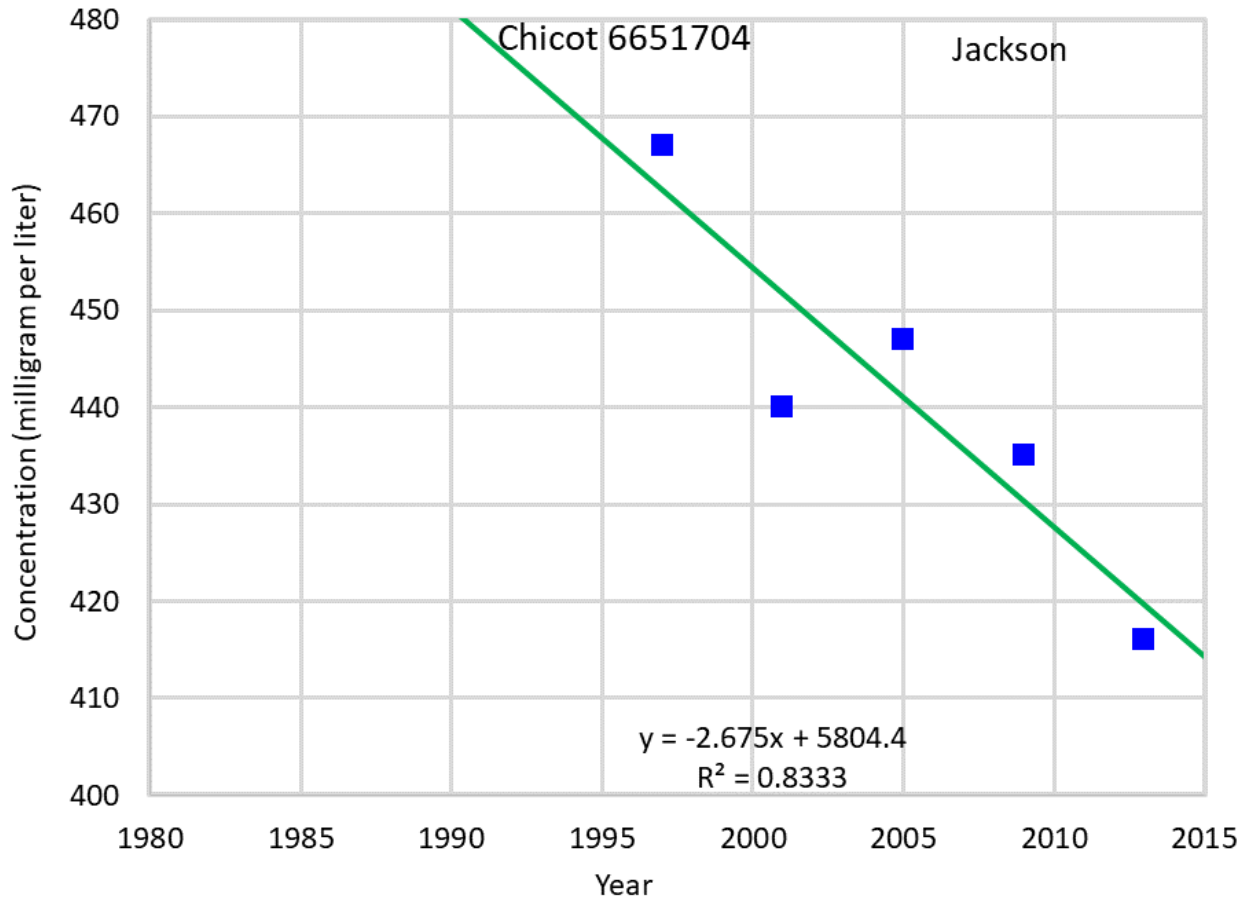


**Figure F10 Hydrograph of total dissolved solids at State Well 6651704.**

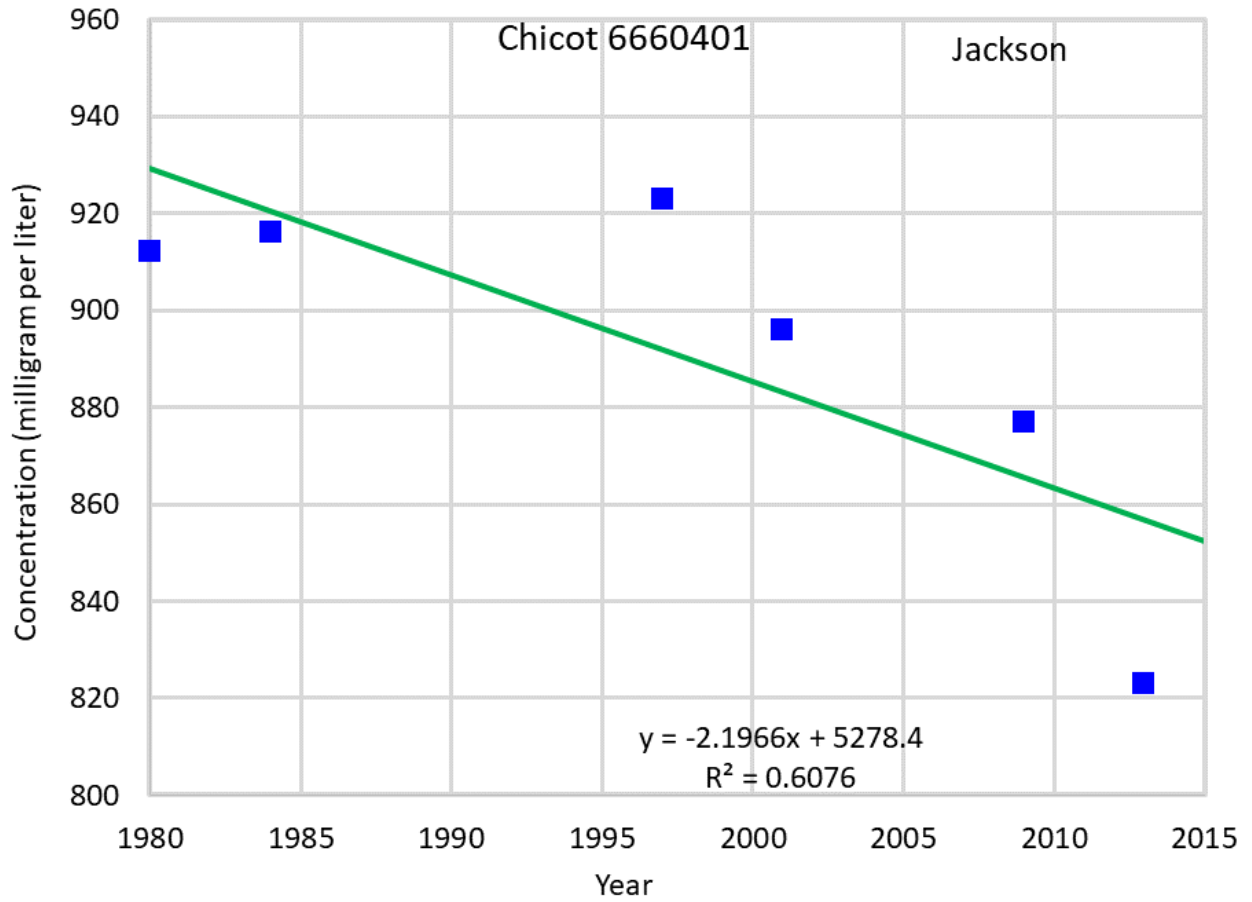


**Figure F11 Hydrograph of total dissolved solids at State Well 6660401.**

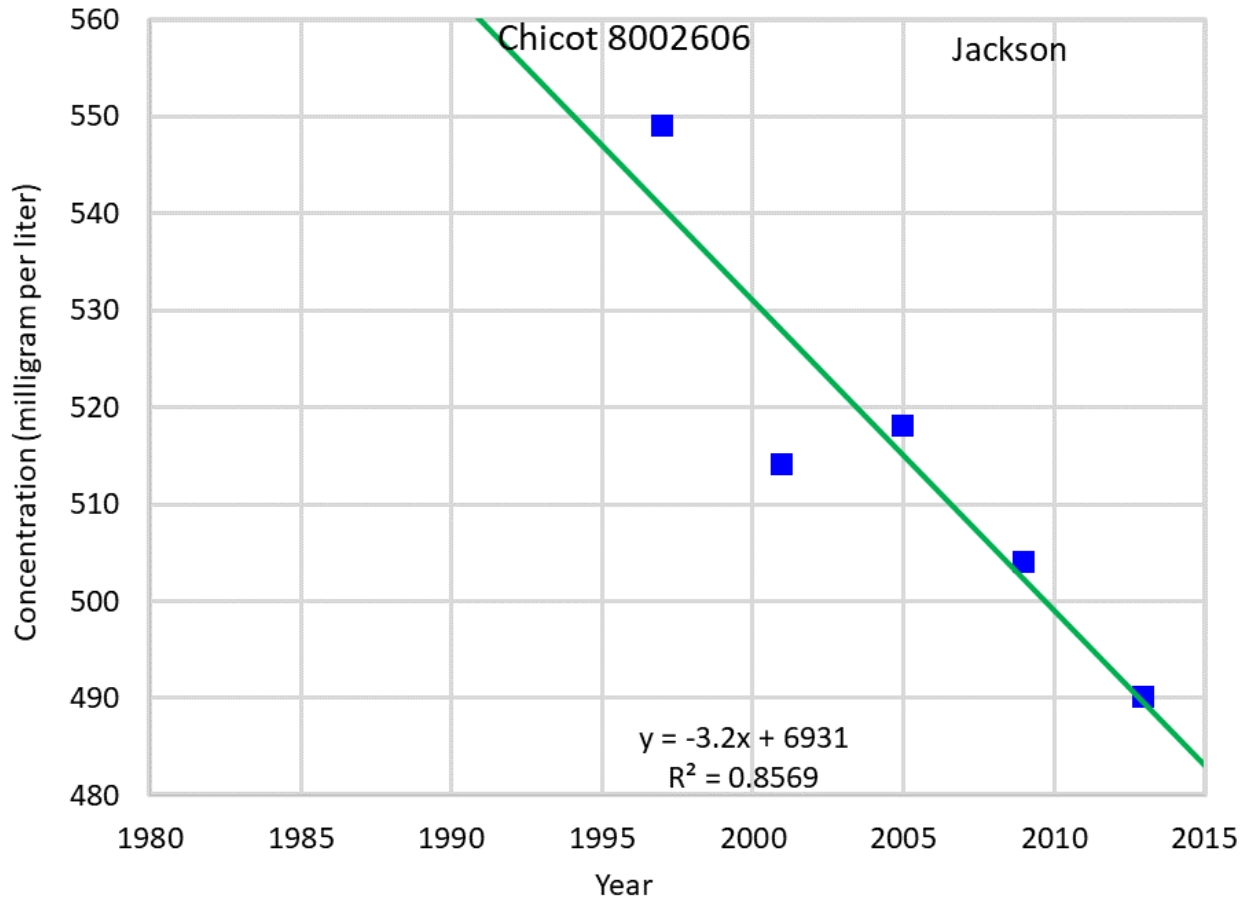


**Figure F12 Hydrograph of total dissolved solids at State Well 8002606.**

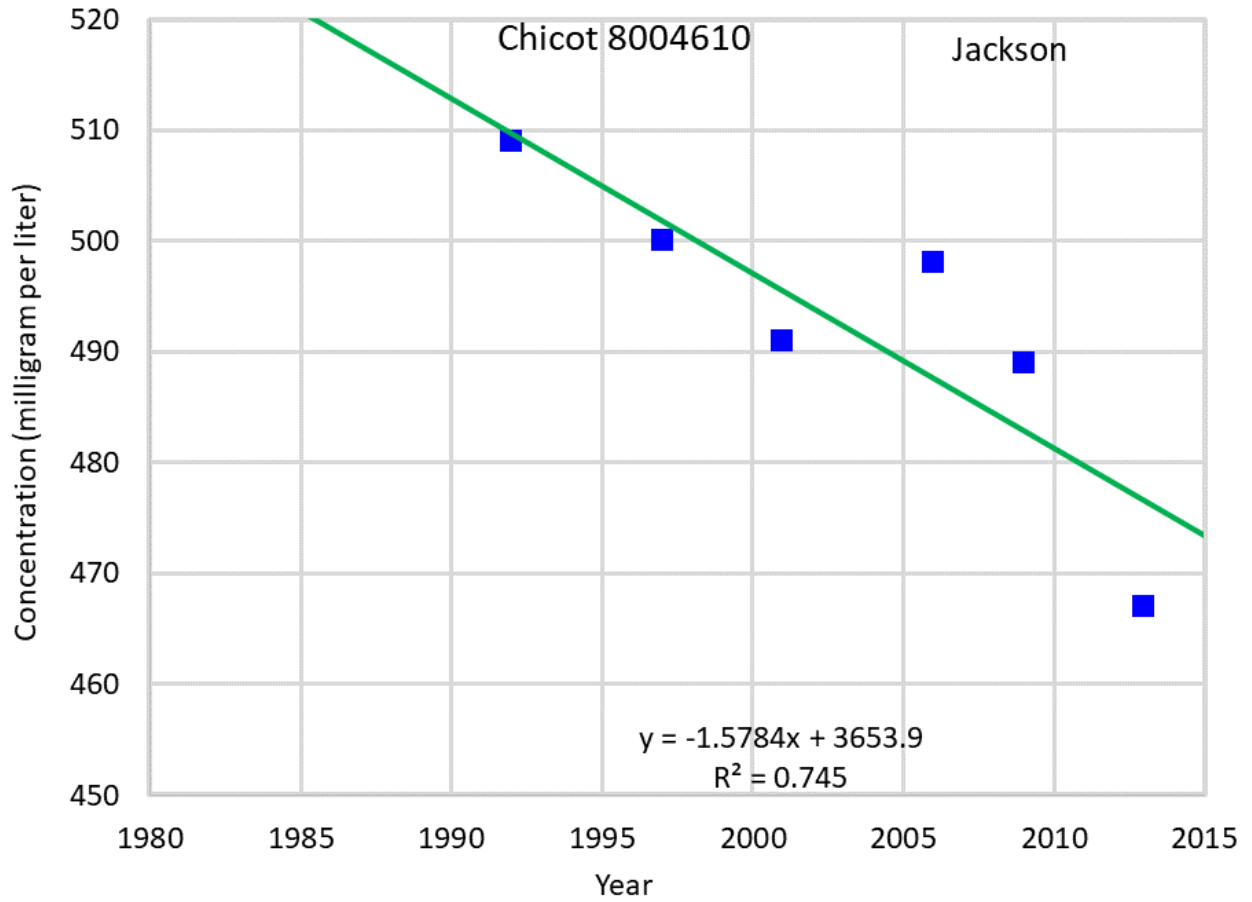


**Figure F13 Hydrograph of total dissolved solids at State Well 8004610.**

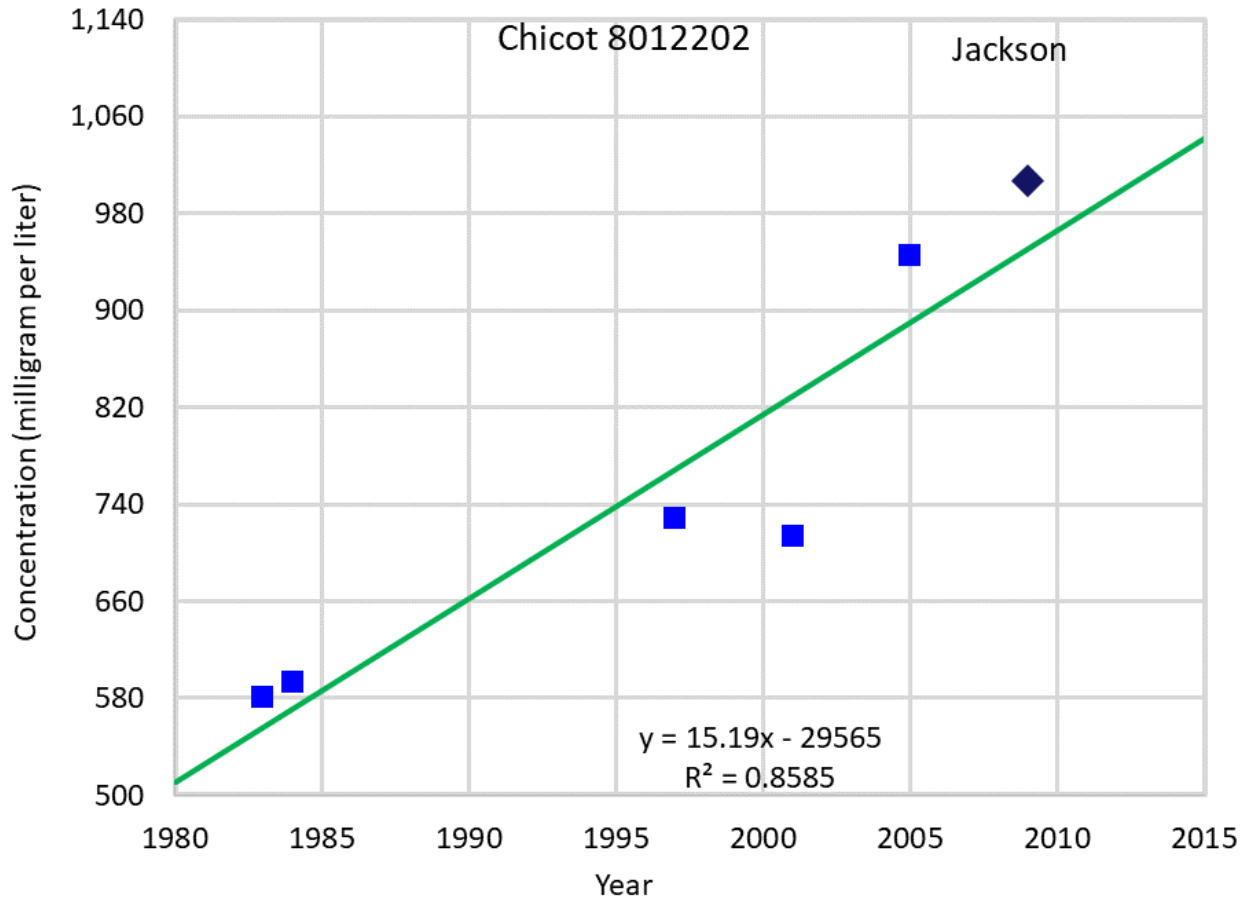


**Figure F14 Hydrograph of total dissolved solids at State Well 8012202.**



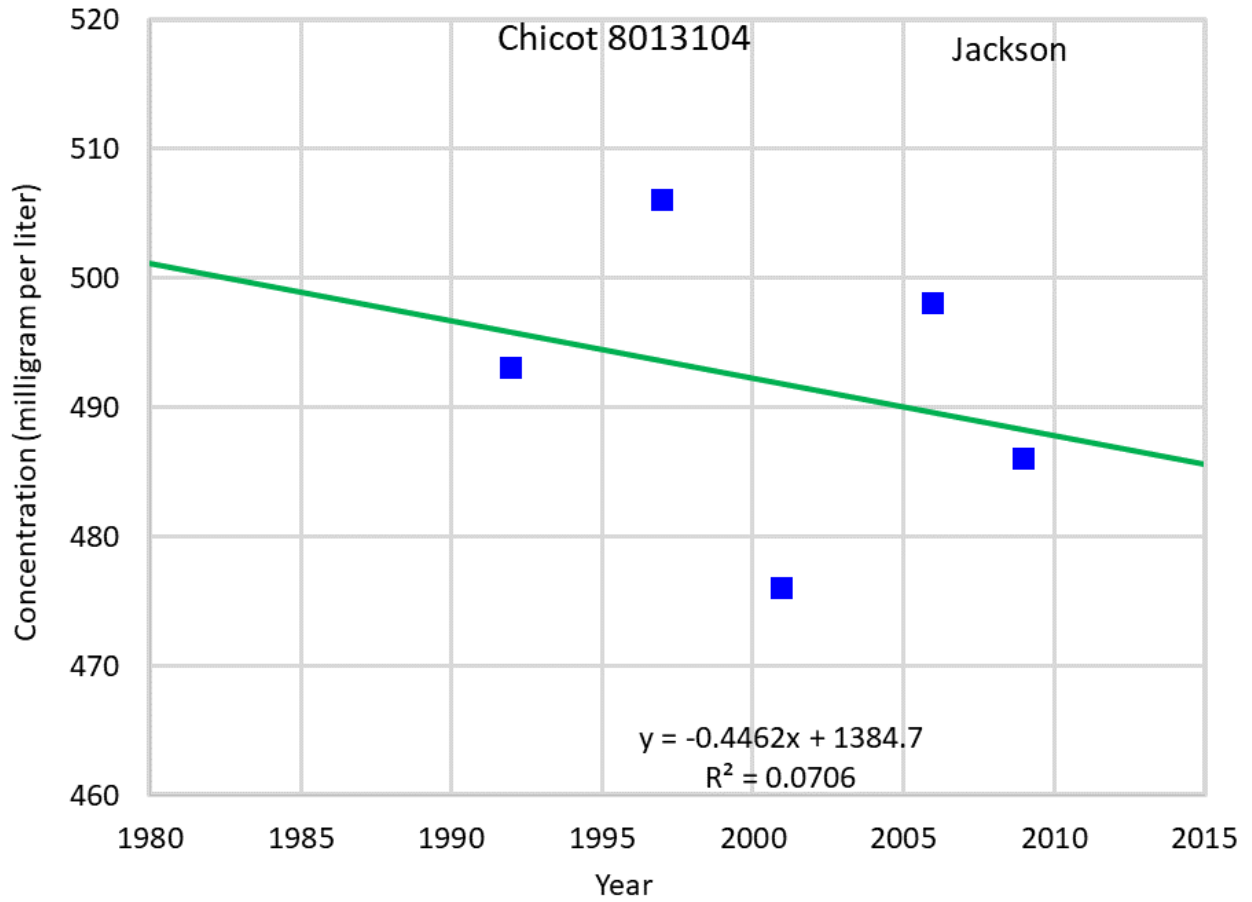


**Figure F15 Hydrograph of total dissolved solids at State Well 8013104.**

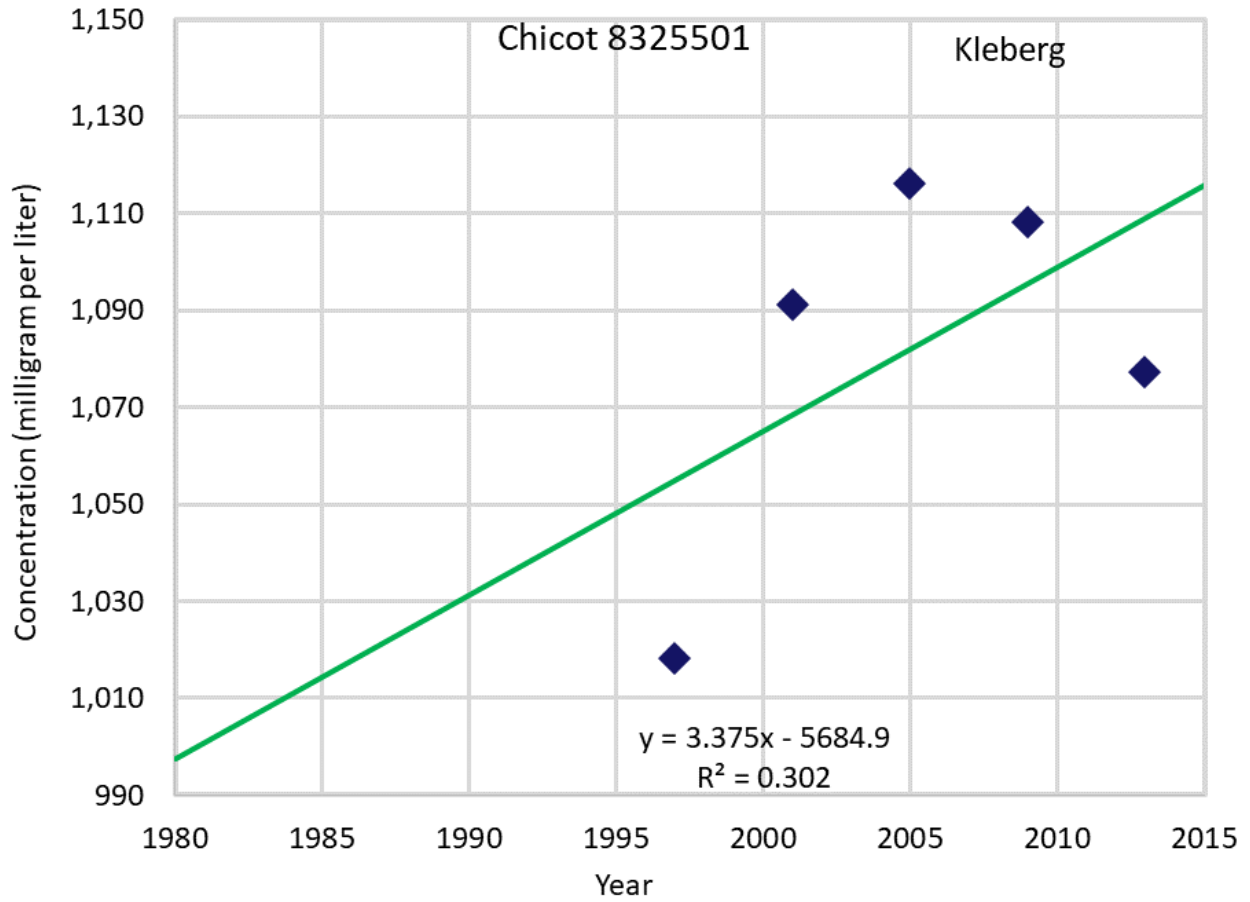


**Figure F16 Hydrograph of total dissolved solids at State Well 8325501.**

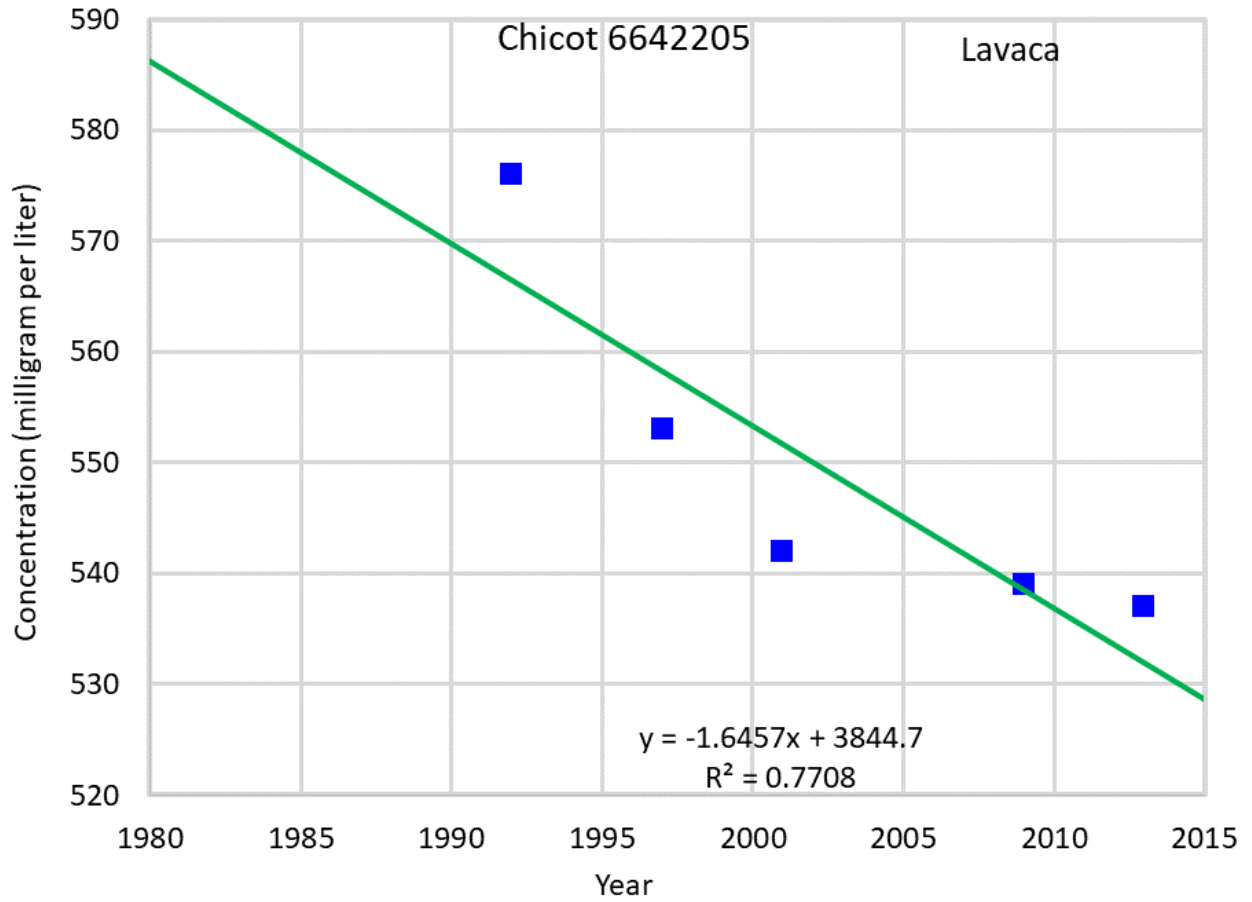


**Figure F17 Hydrograph of total dissolved solids at State Well 6642205.**

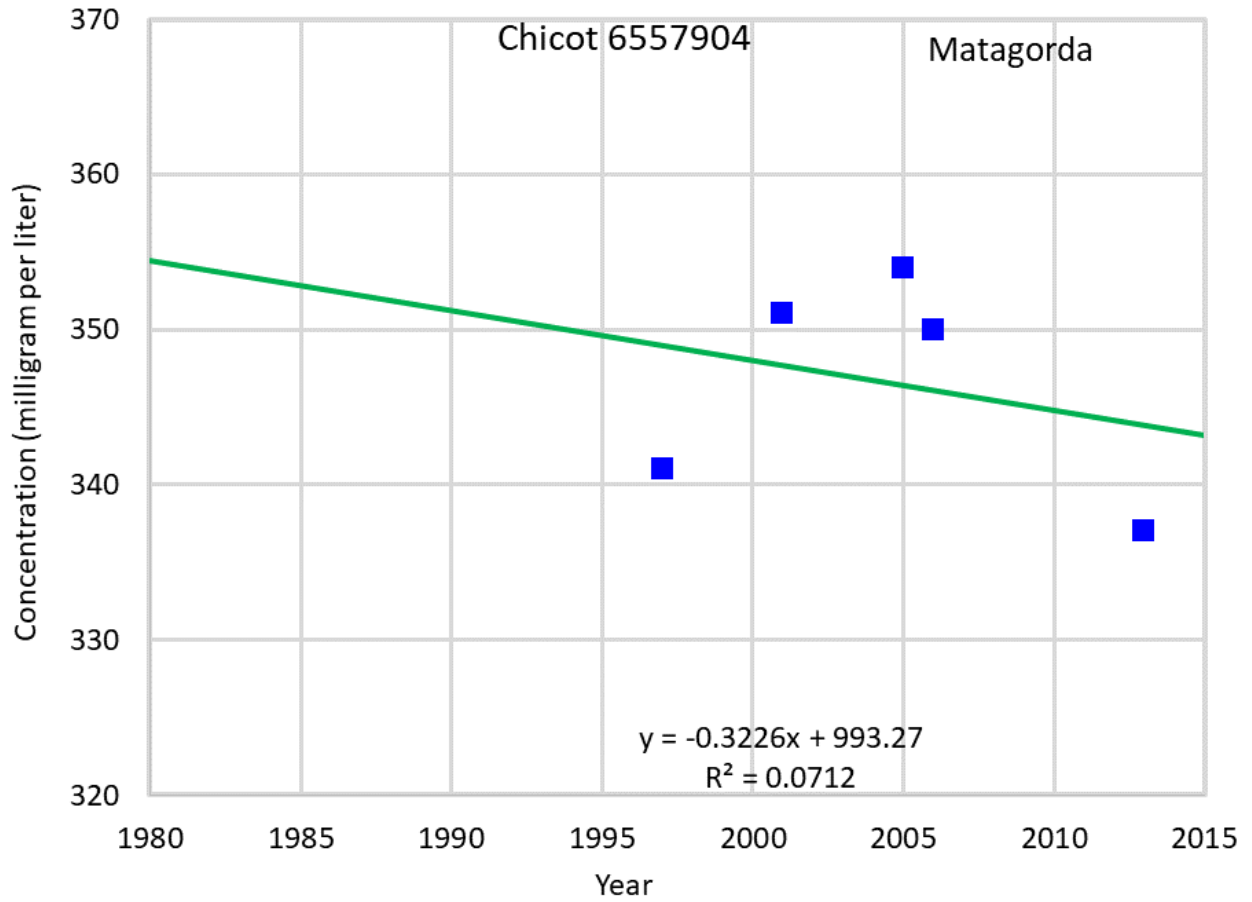


**Figure F18 Hydrograph of total dissolved solids at State Well 6557904.**

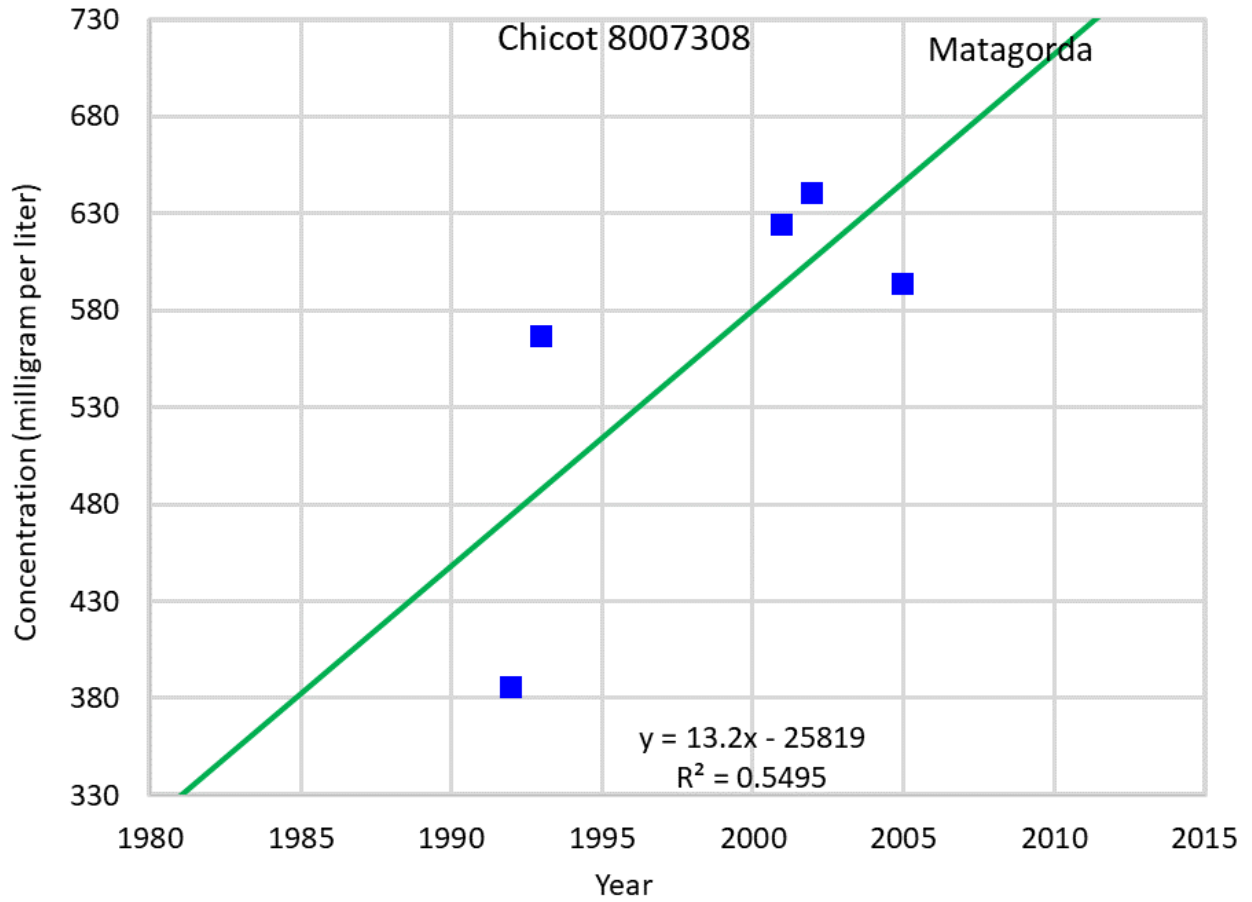


**Figure F19 Hydrograph of total dissolved solids at State Well 8007308.**

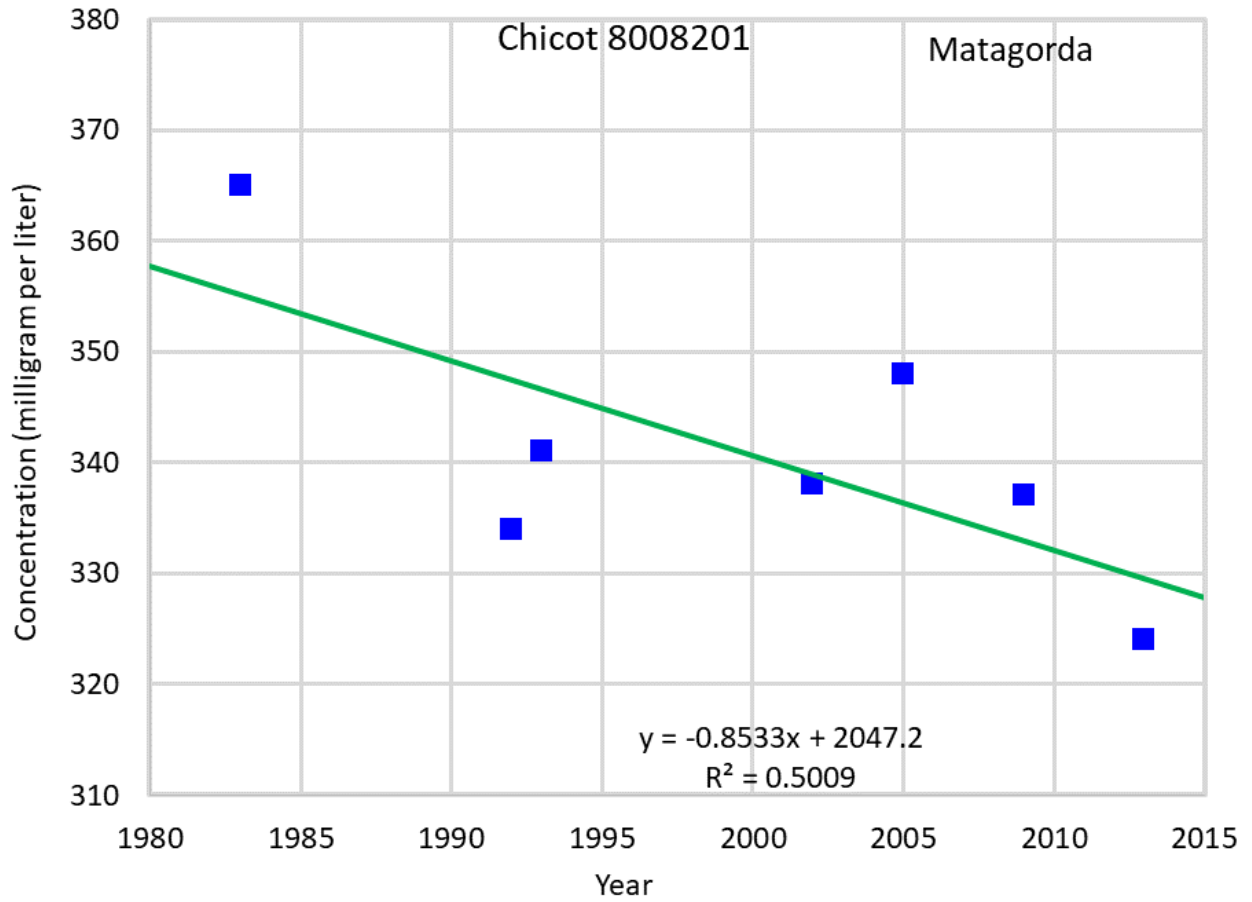


**Figure F20 Hydrograph of total dissolved solids at State Well 8008201.**

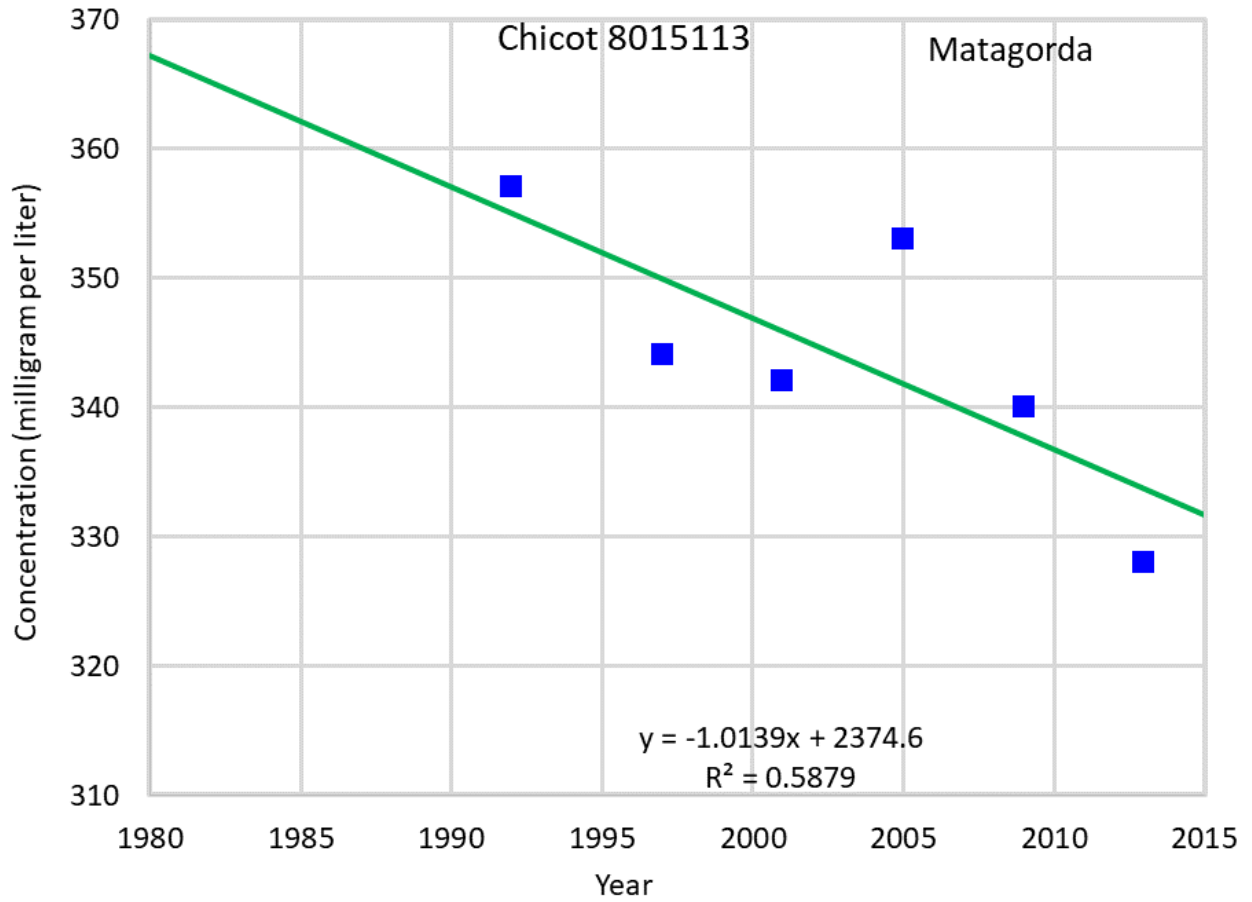


**Figure F21 Hydrograph of total dissolved solids at State Well 8015113.**

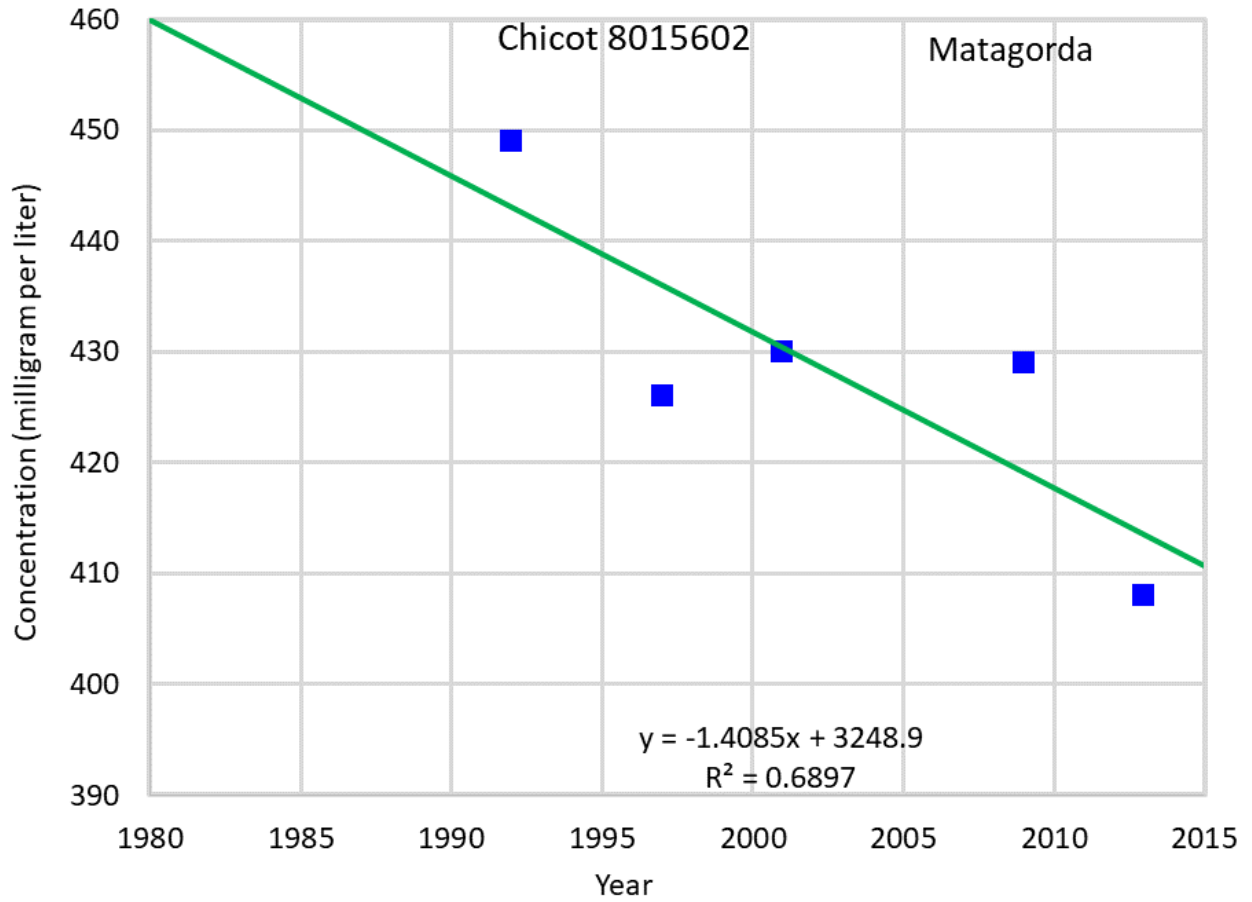


**Figure F22 Hydrograph of total dissolved solids at State Well 8015602.**



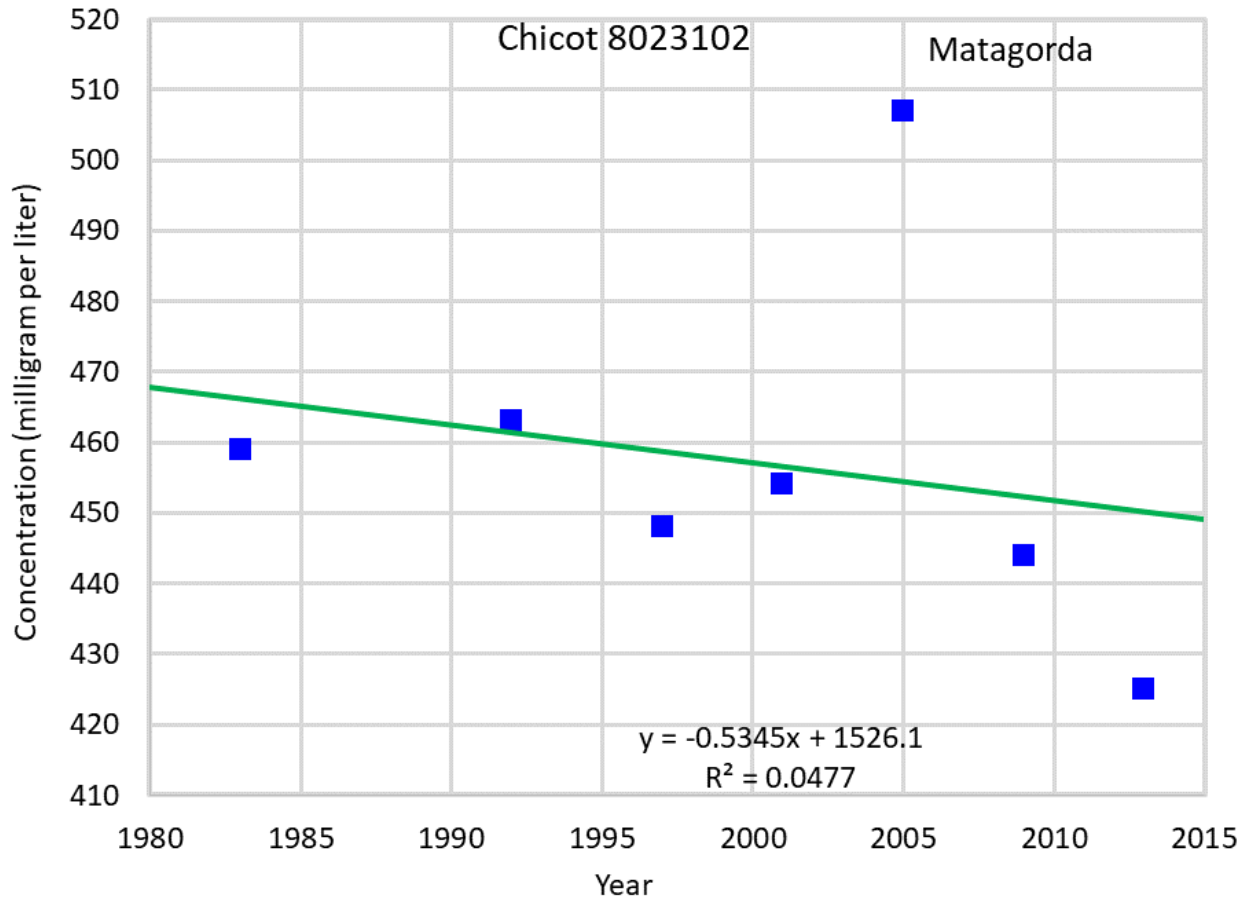


**Figure F23 Hydrograph of total dissolved solids at State Well 8023102.**

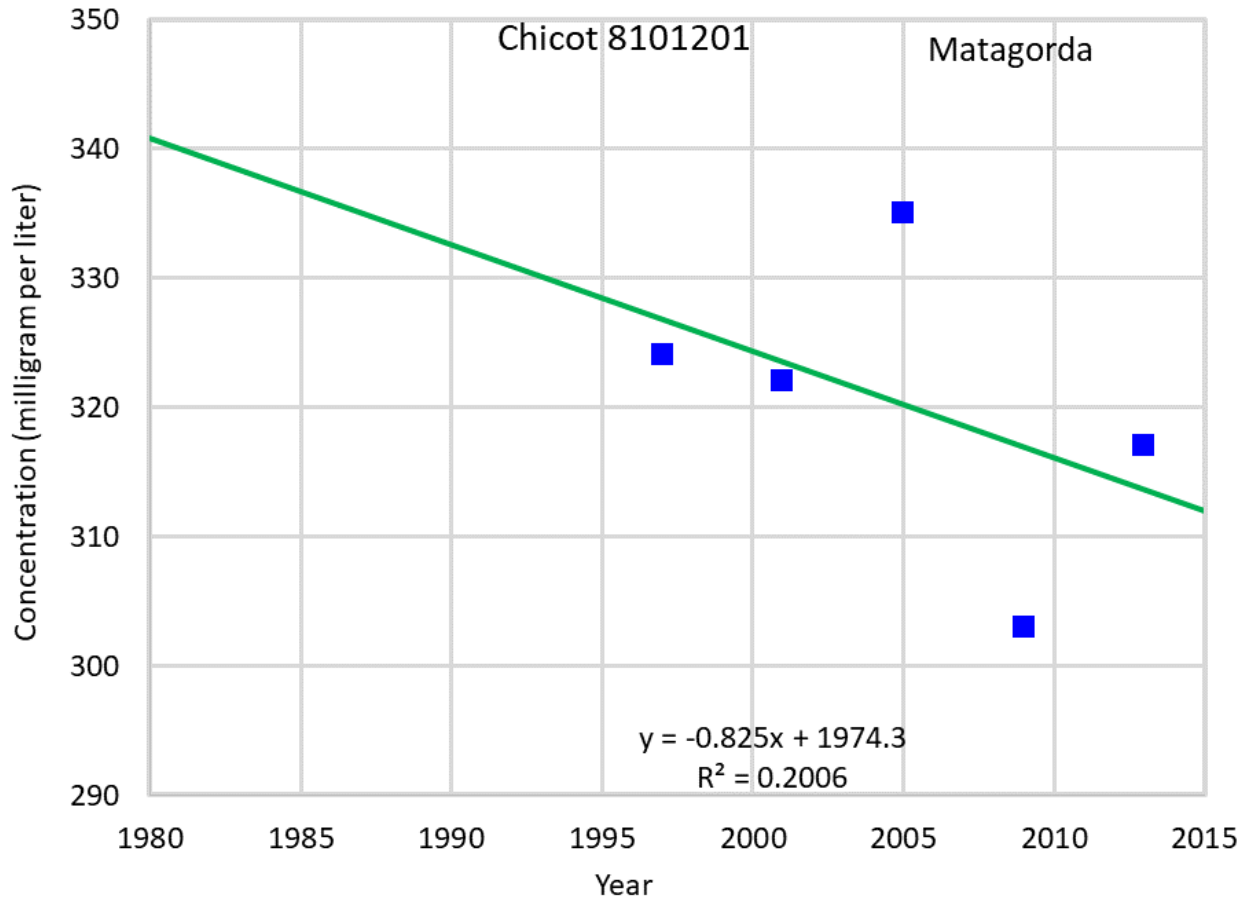


**Figure F24 Hydrograph of total dissolved solids at State Well 8101201.**

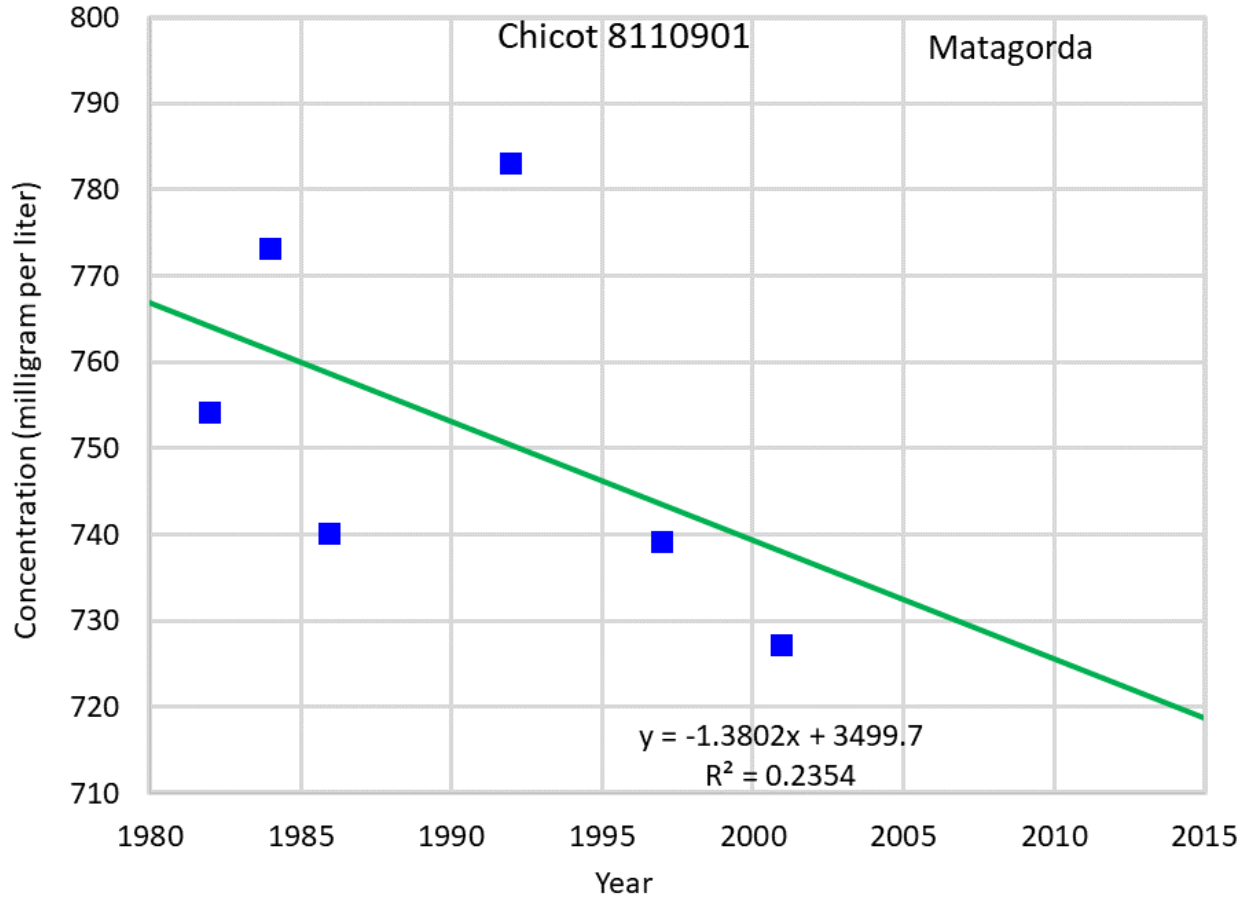


**Figure F25 Hydrograph of total dissolved solids at State Well 8110901.**

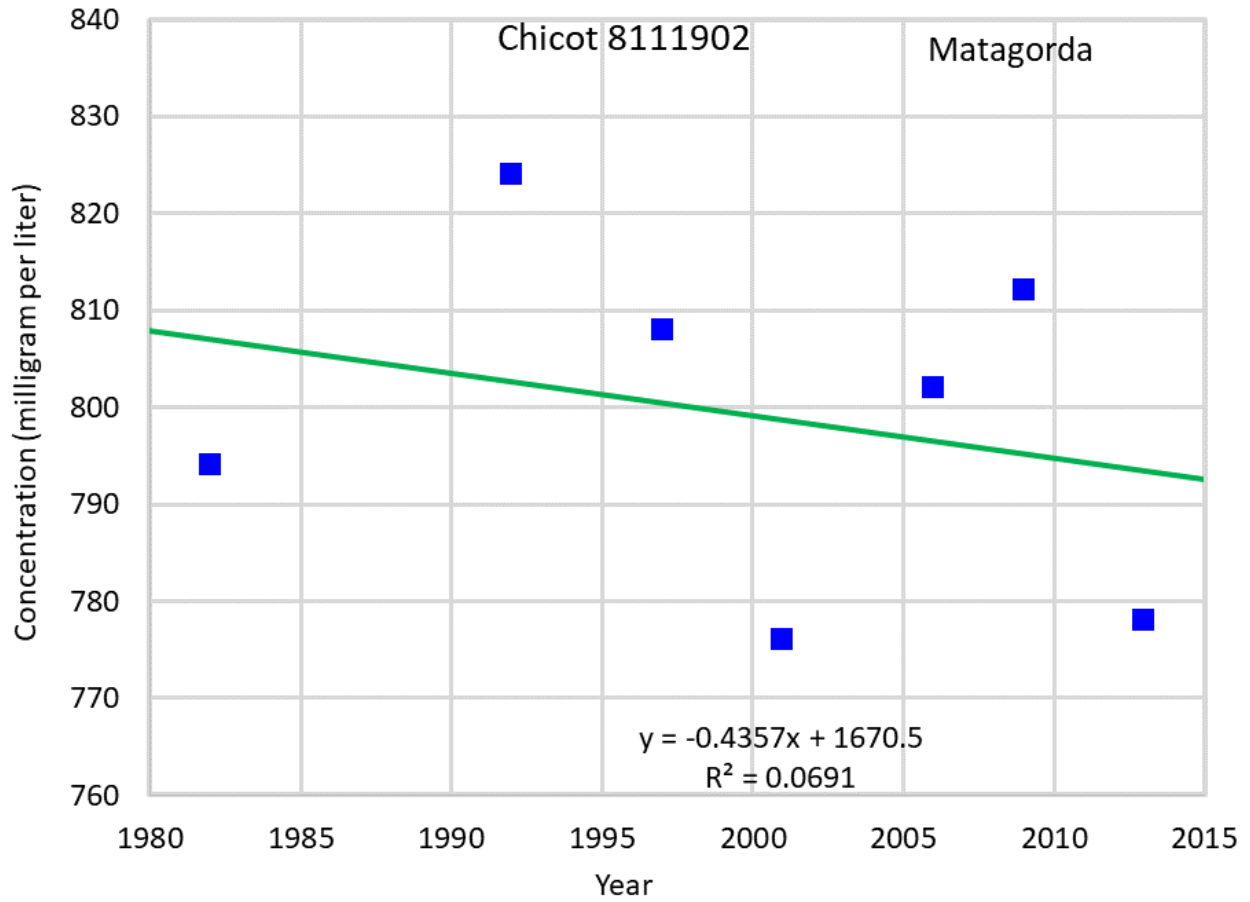


**Figure F26 Hydrograph of total dissolved solids at State Well 8111902.**

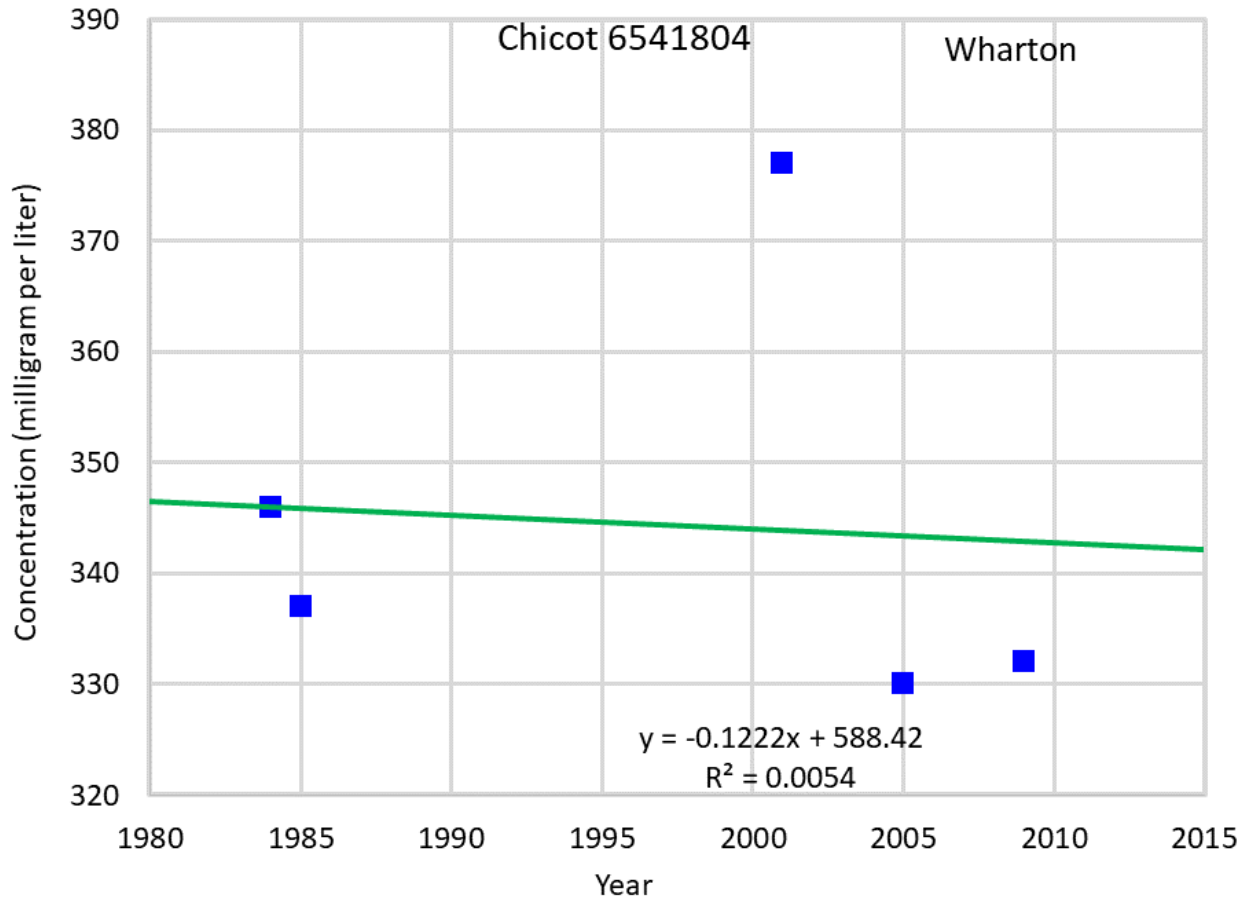


**Figure F27 Hydrograph of total dissolved solids at State Well 6541804.**

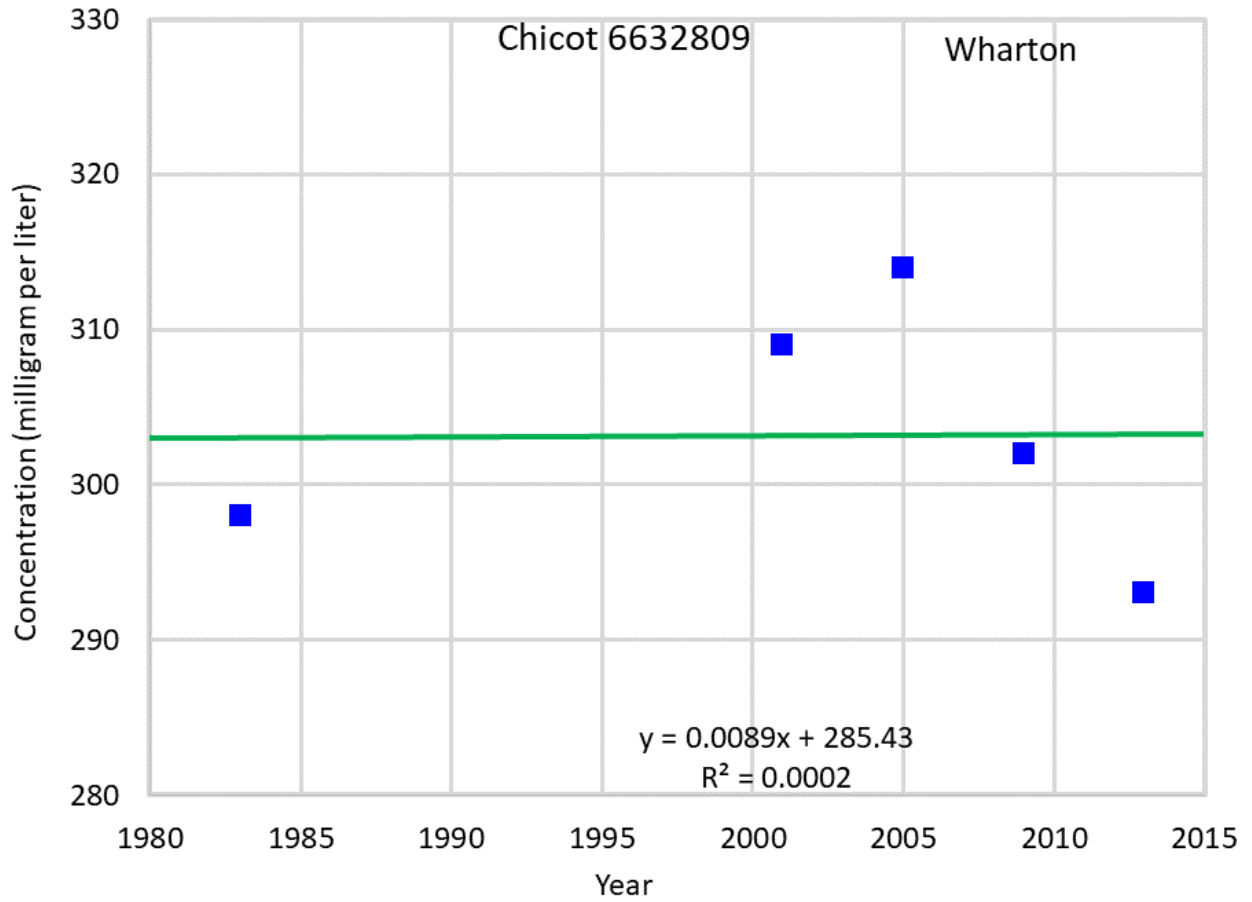


**Figure F28 Hydrograph of total dissolved solids at State Well 6632809.**

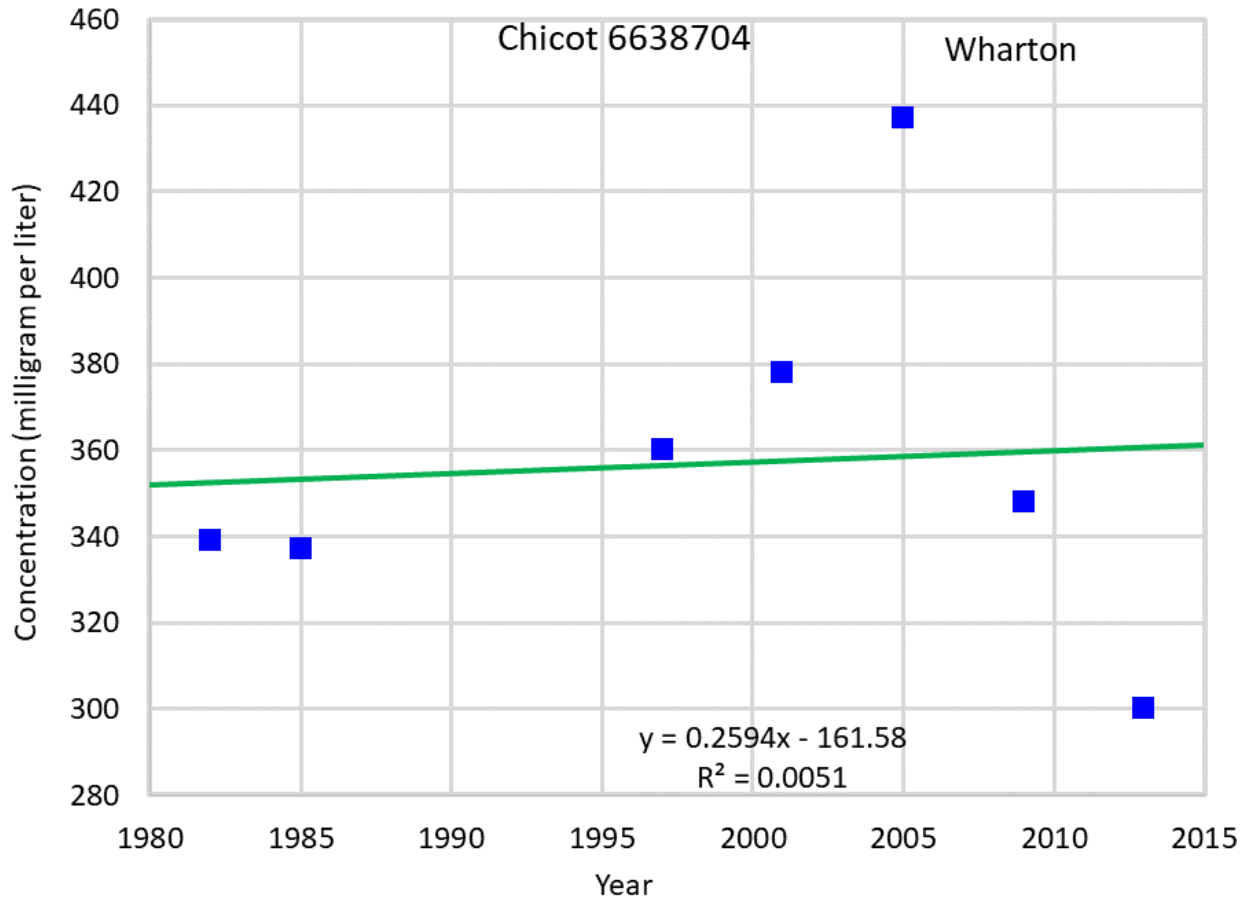


**Figure F29 Hydrograph of total dissolved solids at State Well 6638704.**

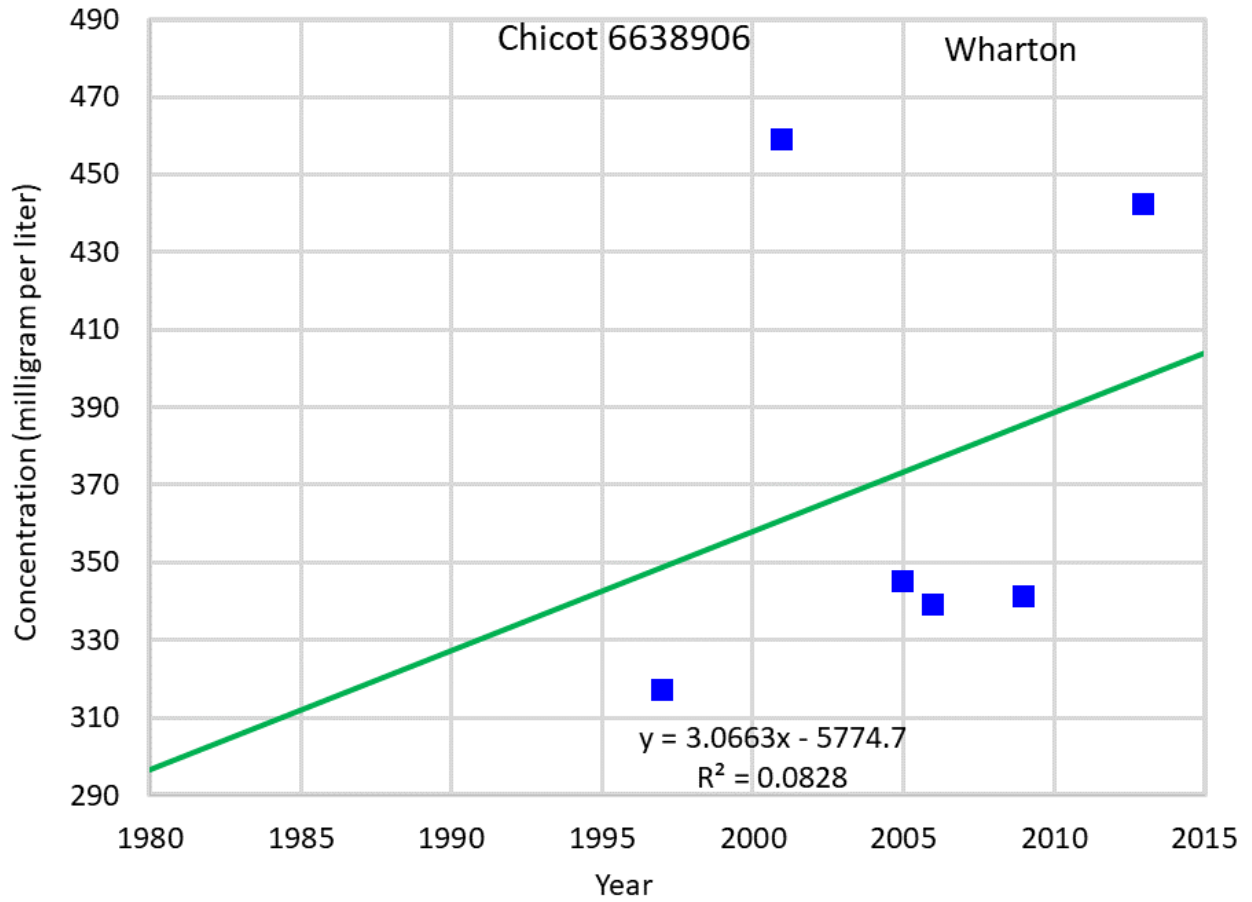


**Figure F30 Hydrograph of total dissolved solids at State Well 6638906.**



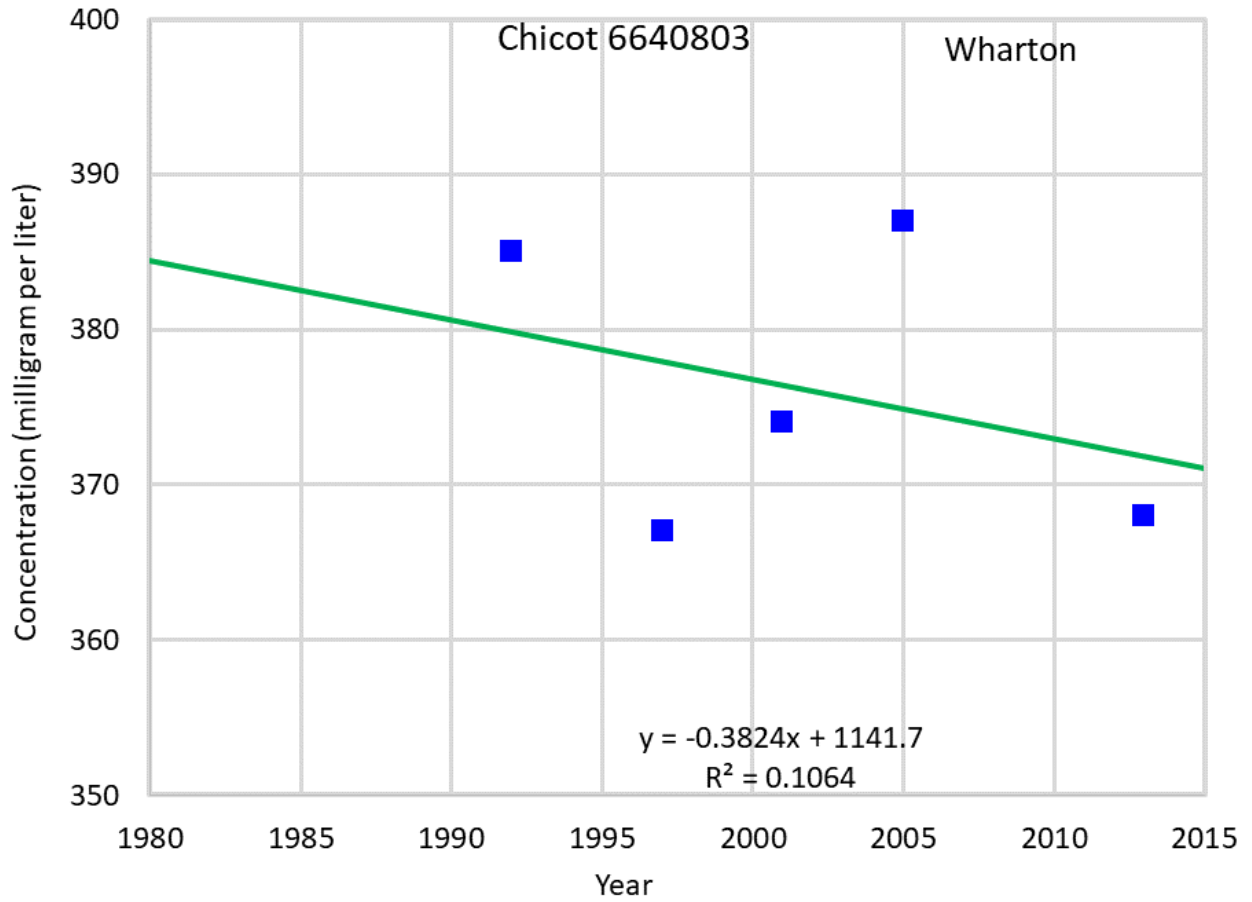


**Figure F31 Hydrograph of total dissolved solids at State Well 6640803.**

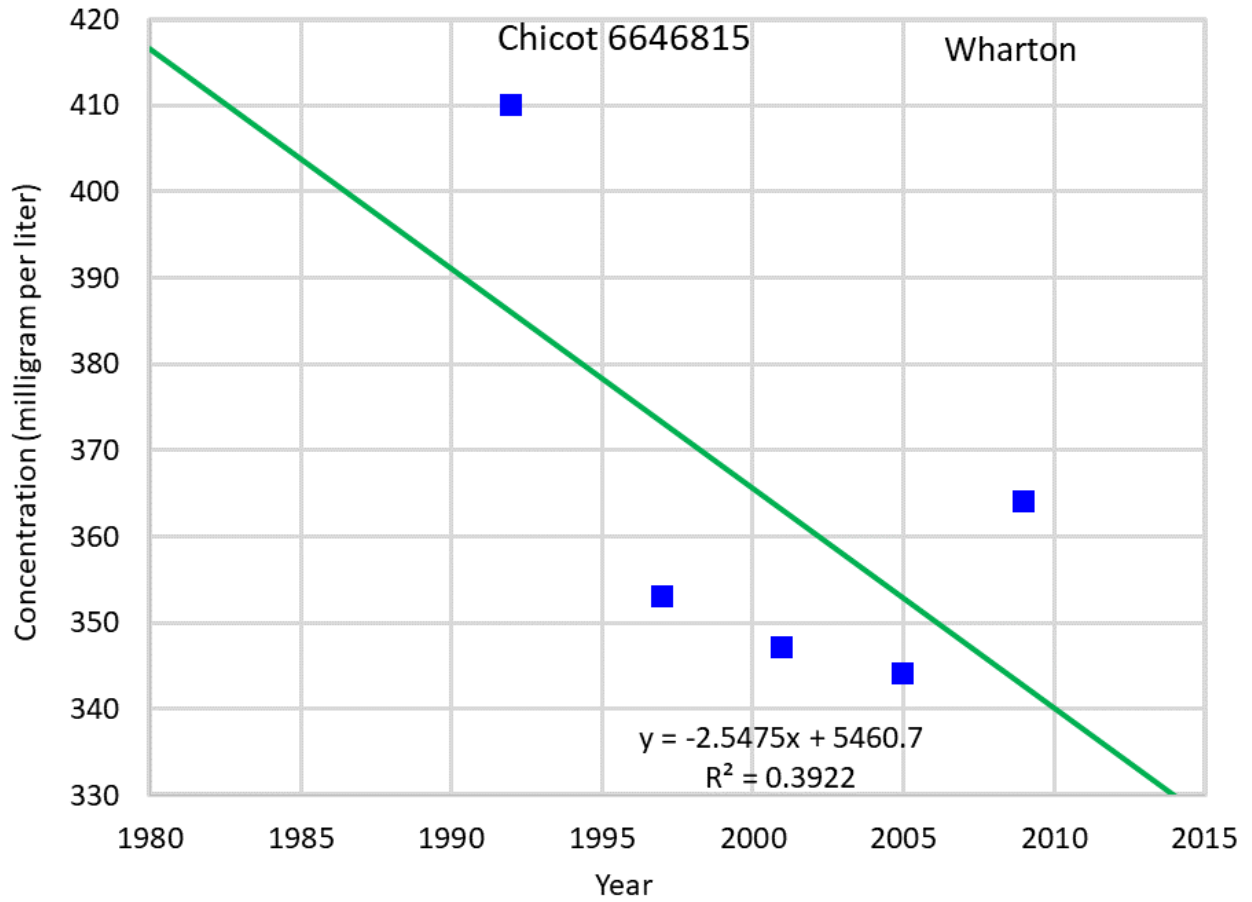


**Figure F32 Hydrograph of total dissolved solids at State Well 6646815.**

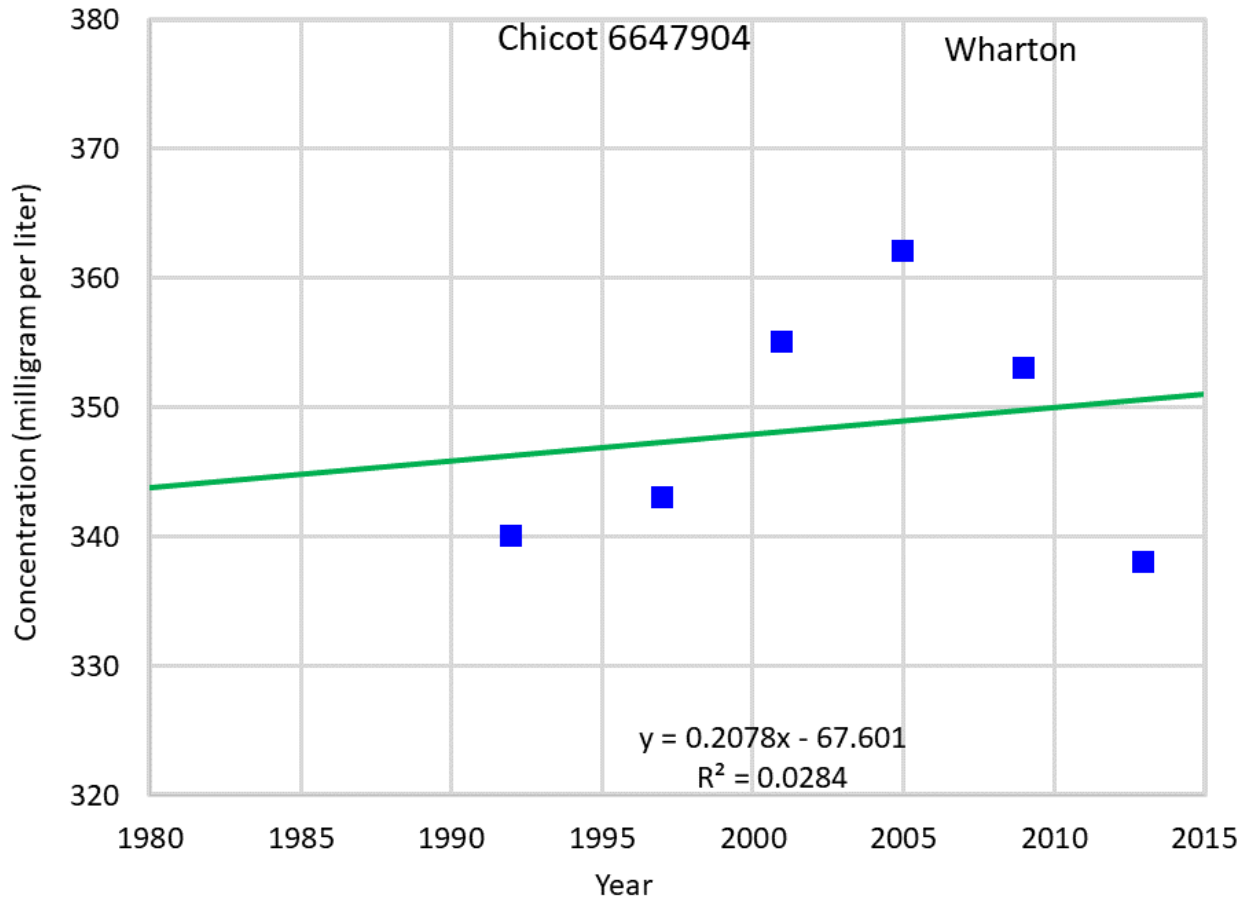


**Figure F33 Hydrograph of total dissolved solids at State Well 6647904.**

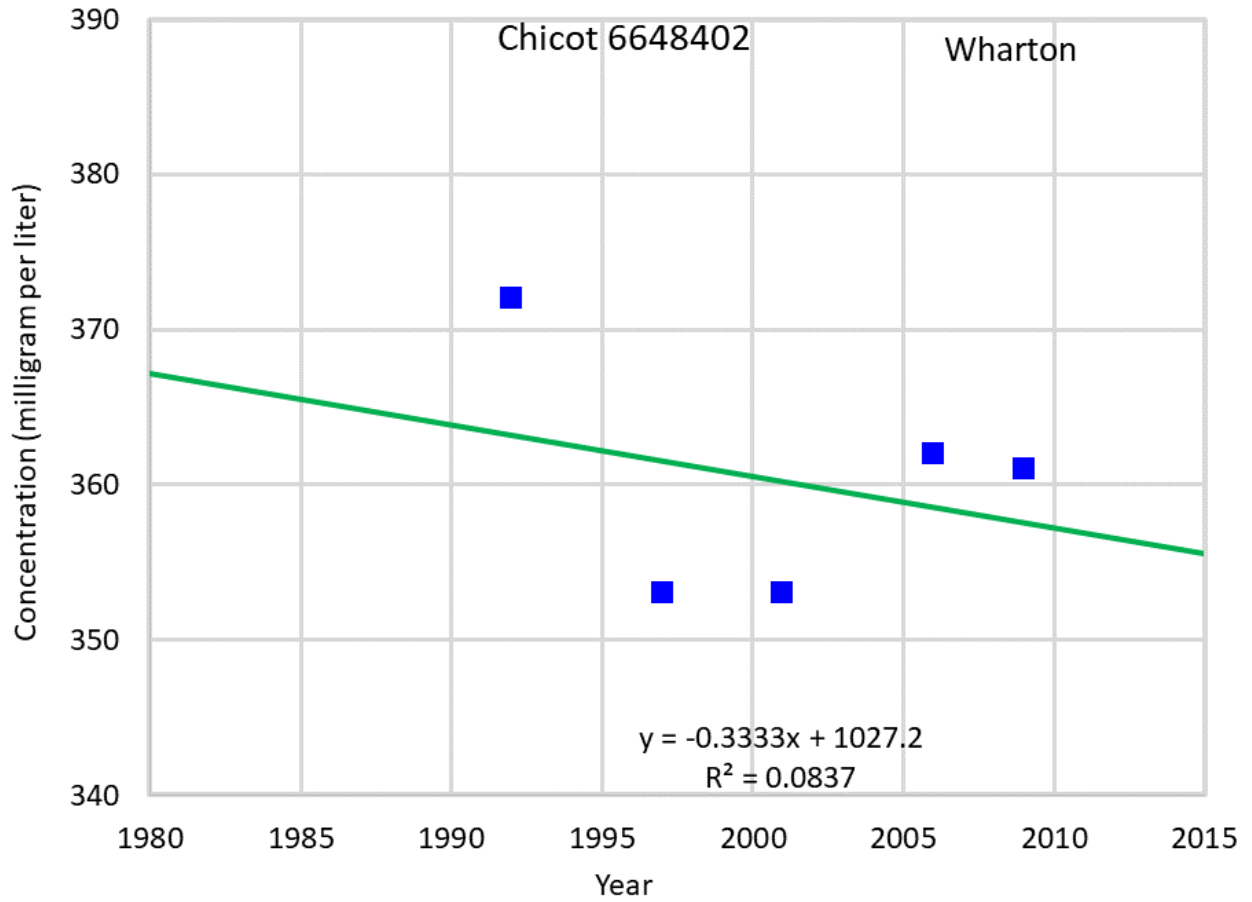


**Figure F34 Hydrograph of total dissolved solids at State Well 6648402.**

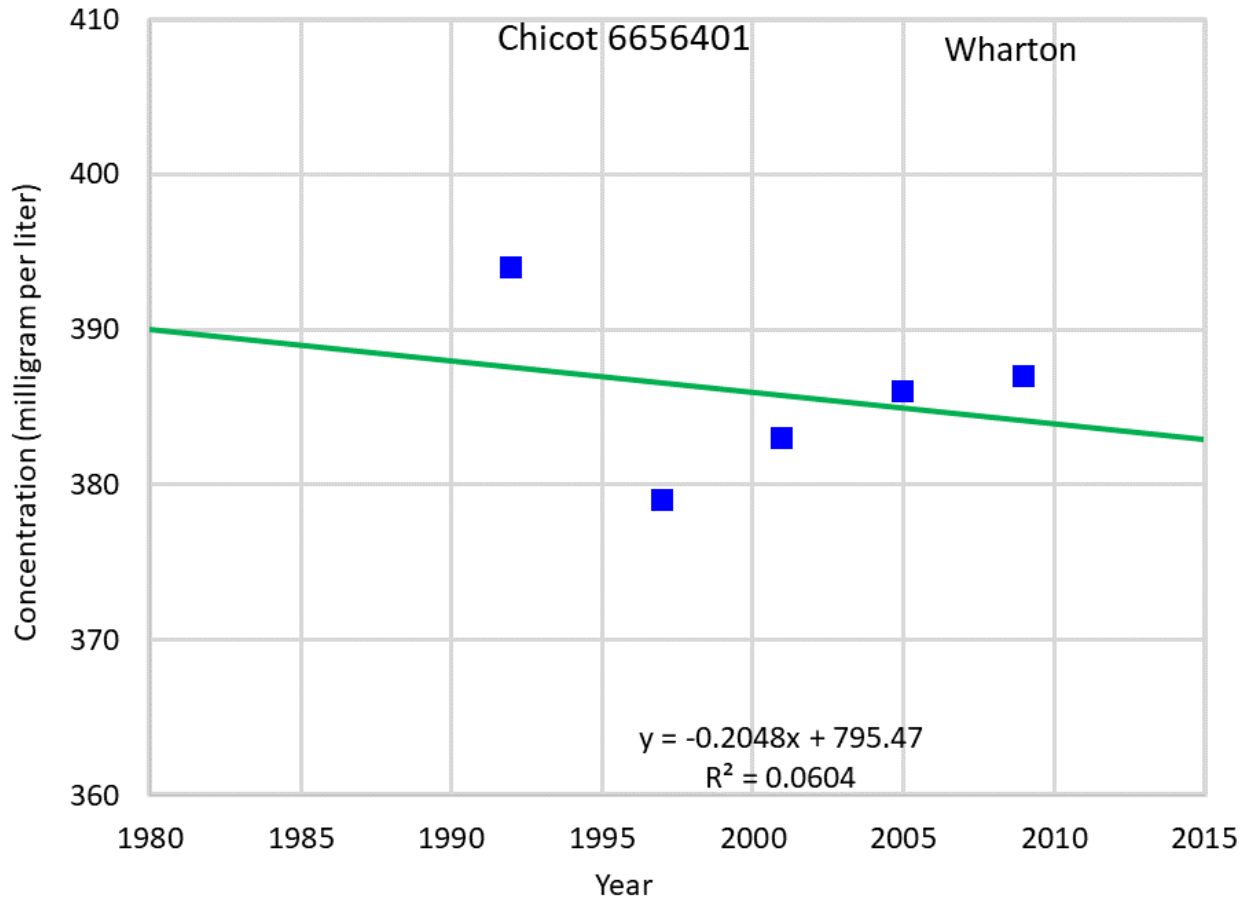


**Figure F35 Hydrograph of total dissolved solids at State Well 6656401.**

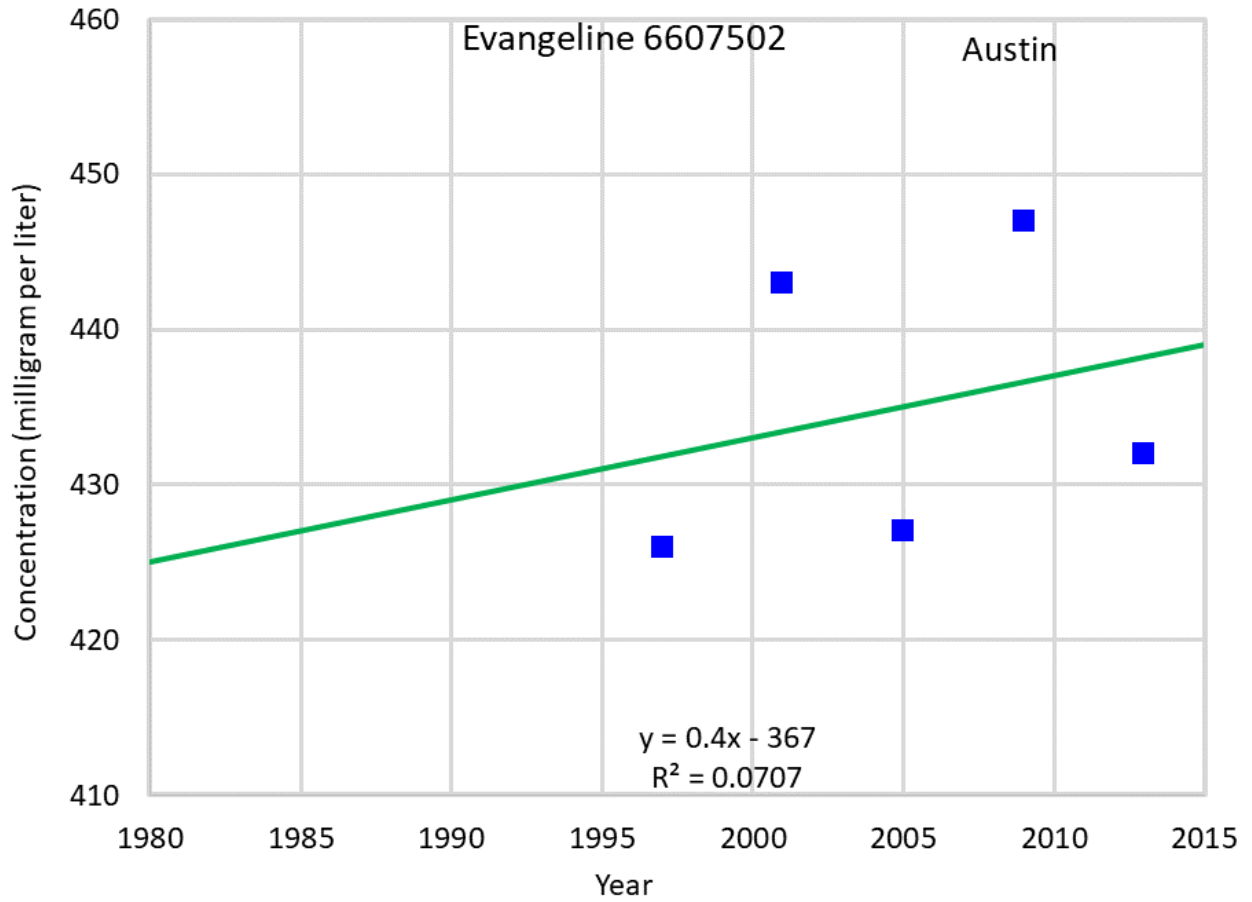


**Figure F36 Hydrograph of total dissolved solids at State Well 6607502.**

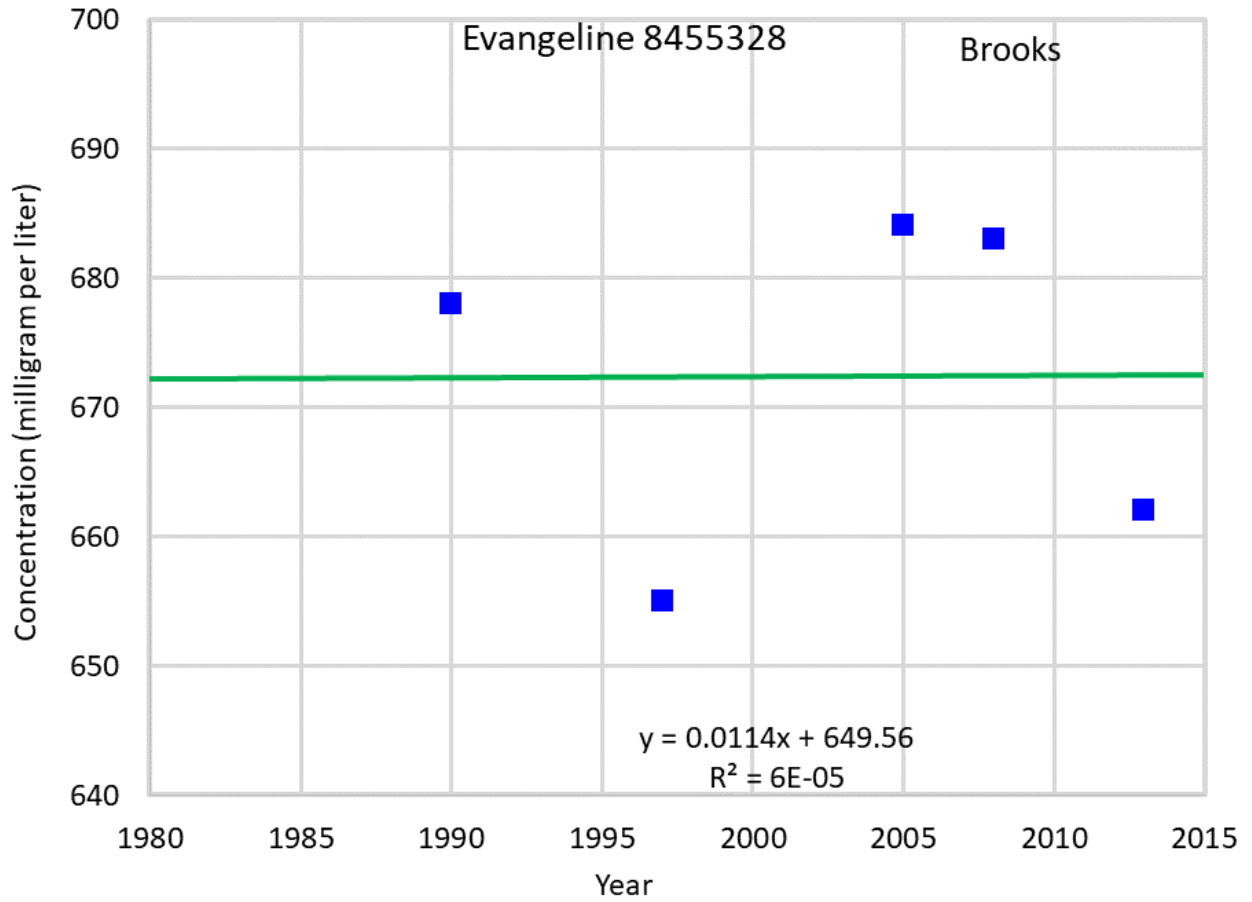


**Figure F37 Hydrograph of total dissolved solids at State Well 8455328.**

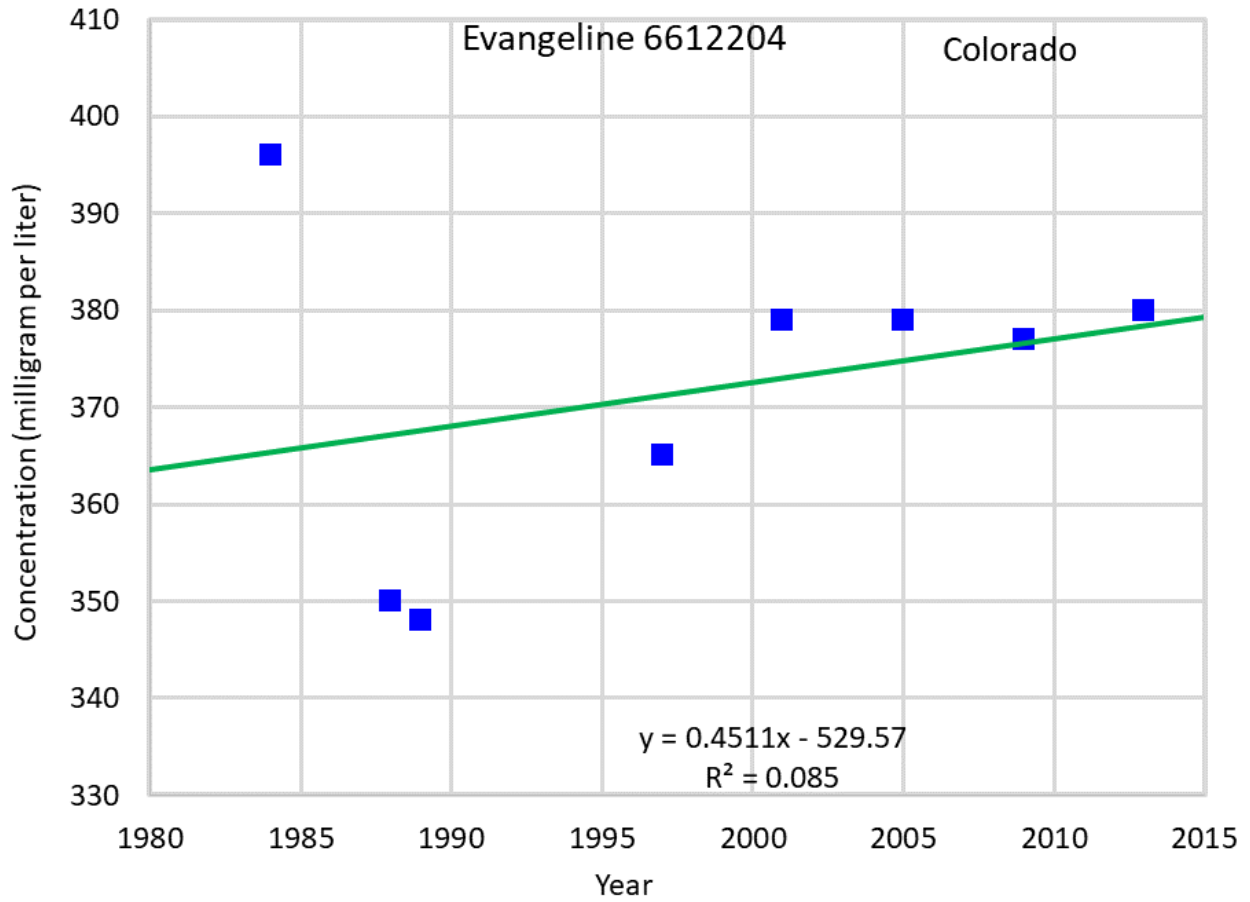


**Figure F38 Hydrograph of total dissolved solids at State Well 6612204.**



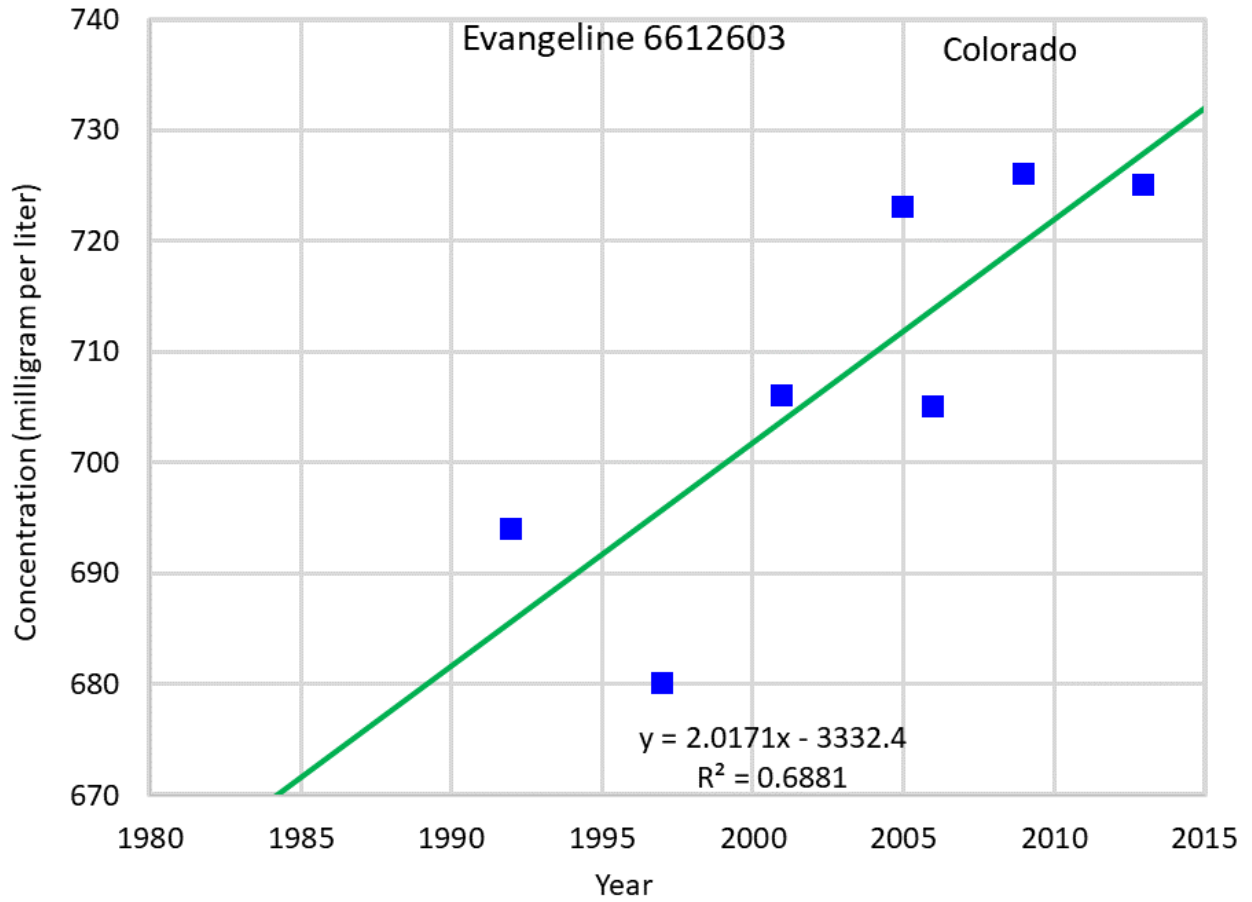


**Figure F39 Hydrograph of total dissolved solids at State Well 6612603.**

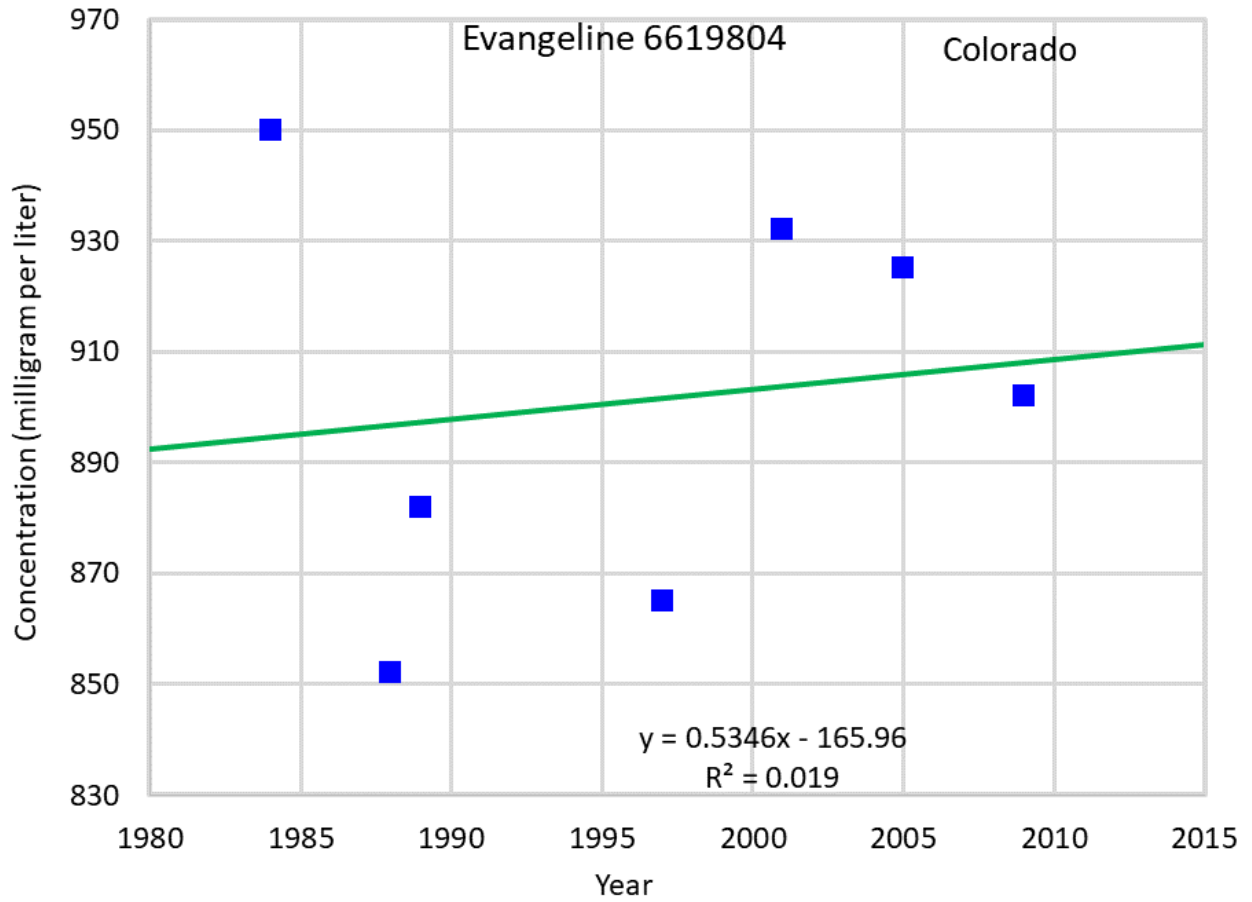


**Figure F40 Hydrograph of total dissolved solids at State Well 6619804.**

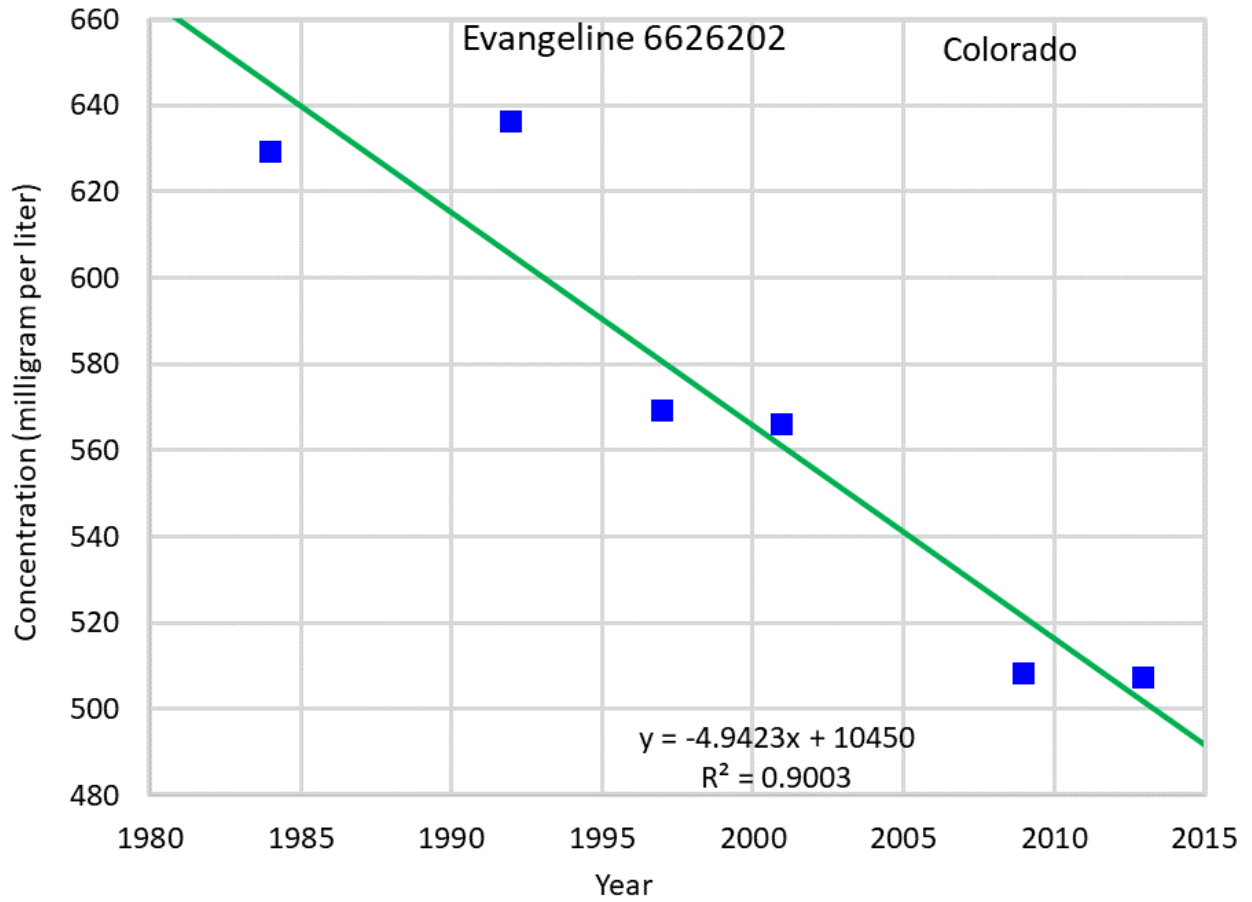


**Figure F41 Hydrograph of total dissolved solids at State Well 6626202.**

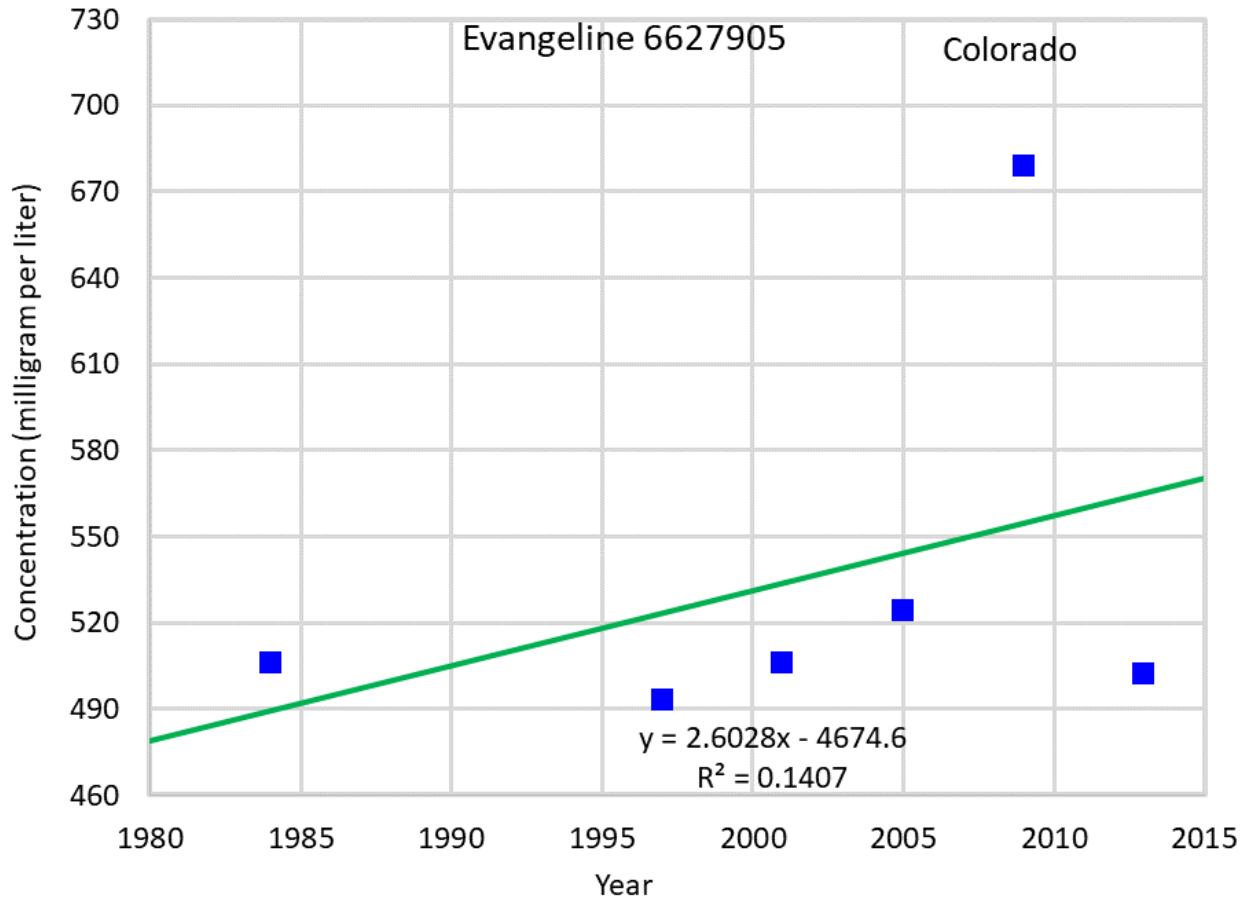


**Figure F42 Hydrograph of total dissolved solids at State Well 6627905.**

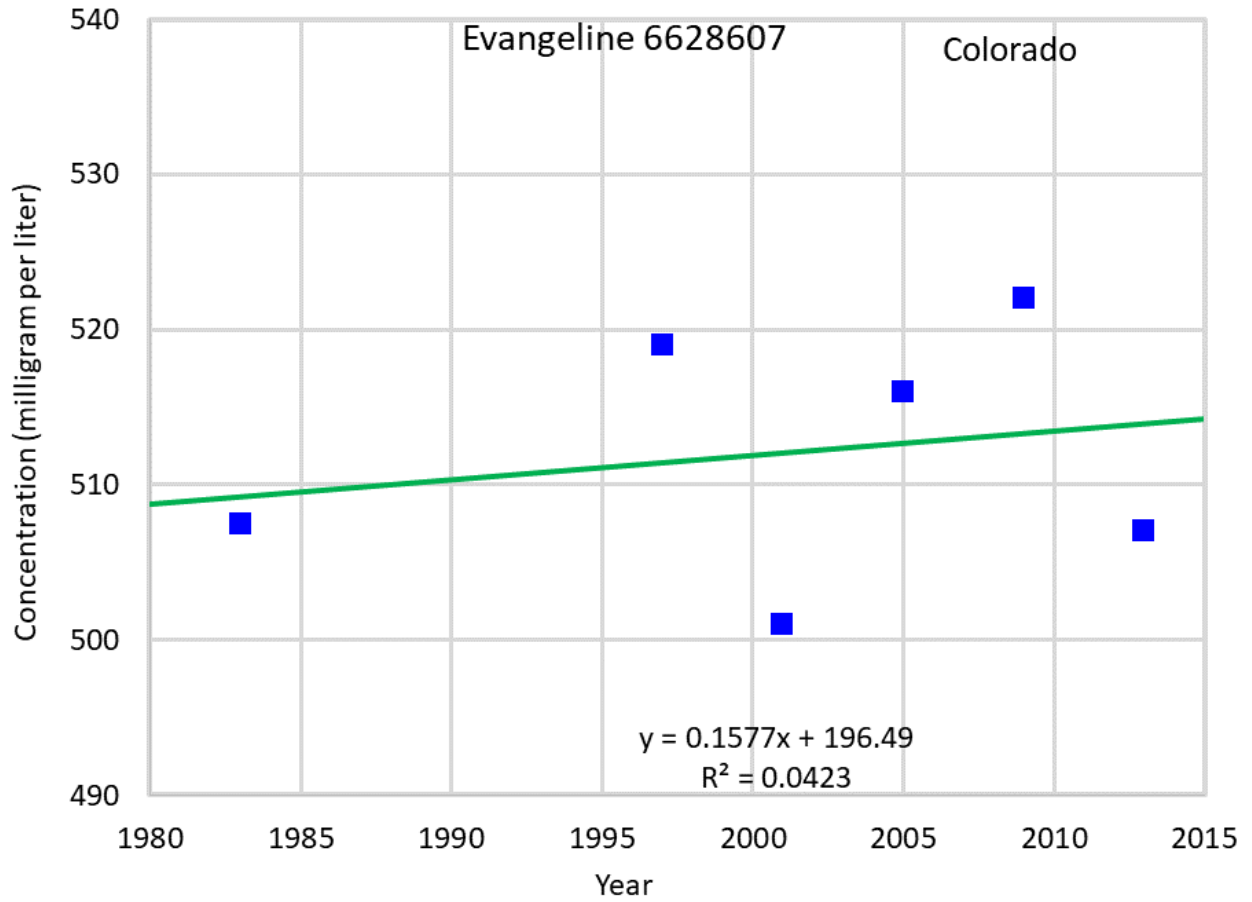


**Figure F43 Hydrograph of total dissolved solids at State Well 6628607.**

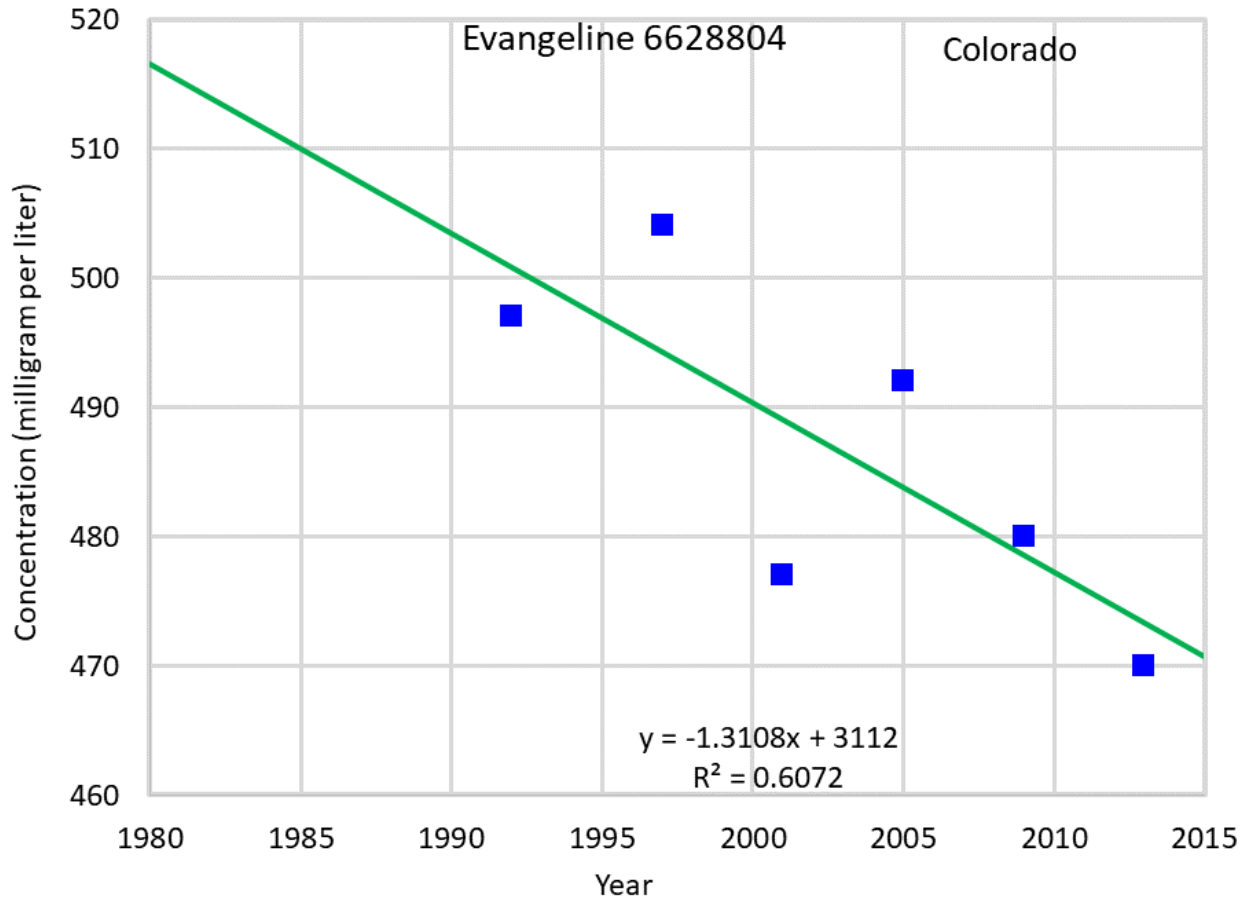


**Figure F44 Hydrograph of total dissolved solids at State Well 6628804.**

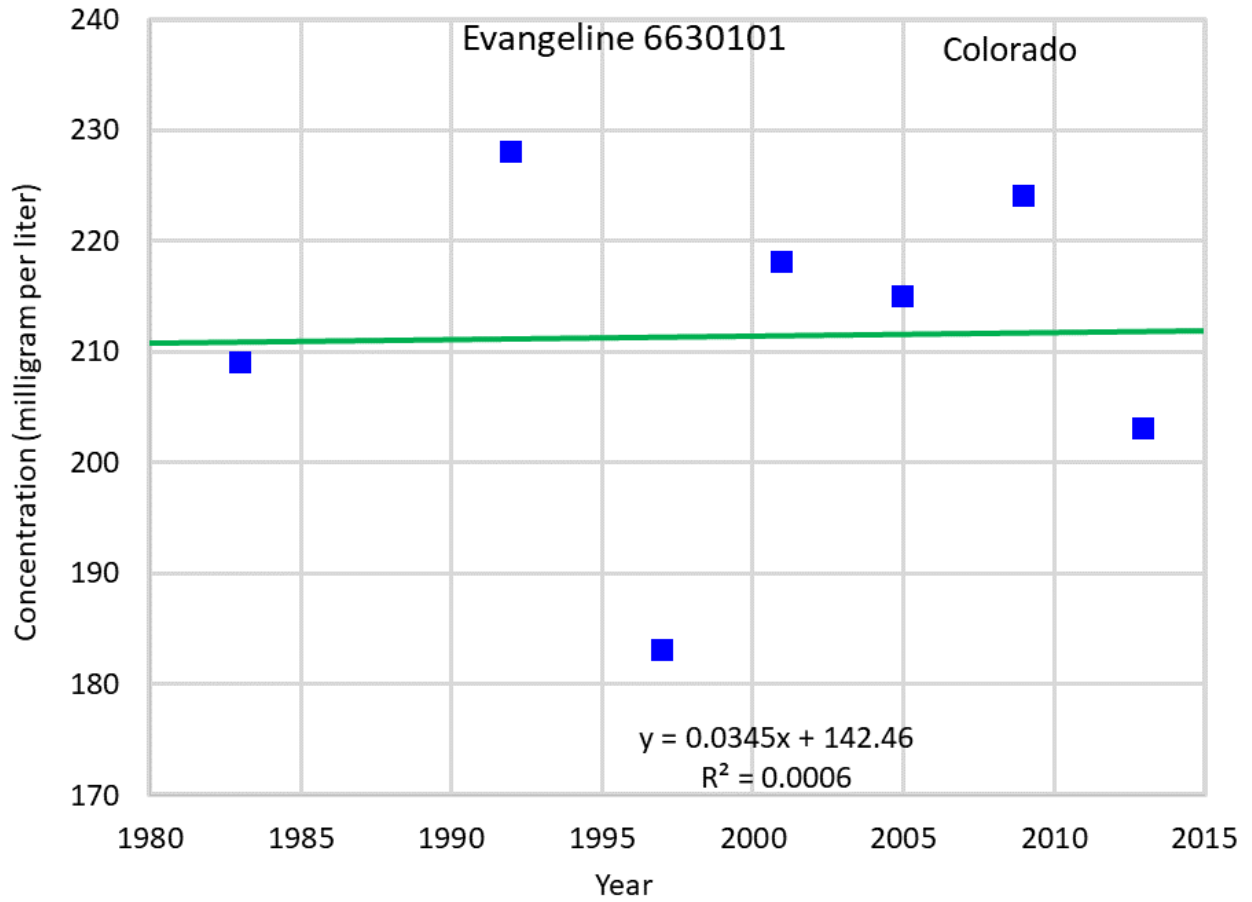


**Figure F45 Hydrograph of total dissolved solids at State Well 6630101.**

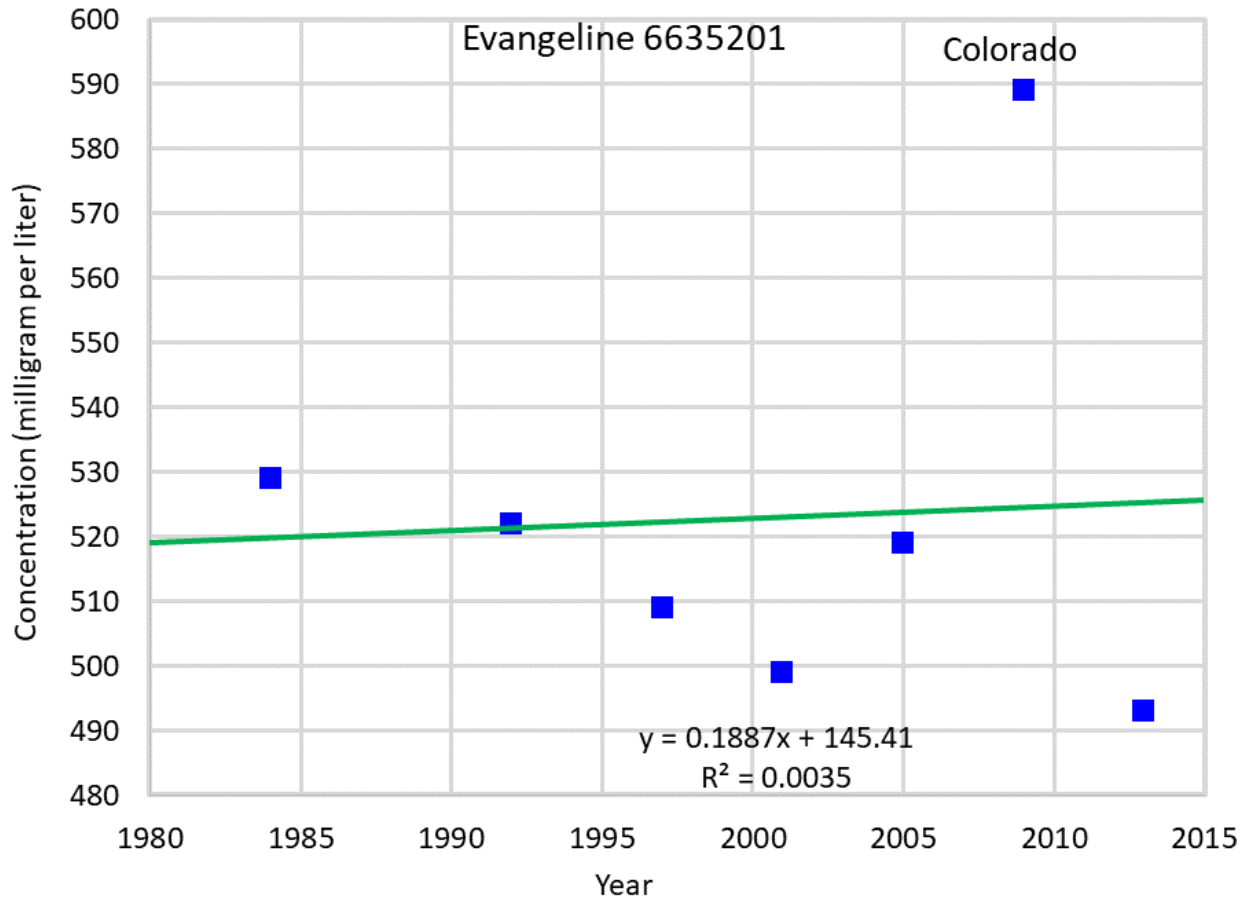


**Figure F46 Hydrograph of total dissolved solids at State Well 6635201.**



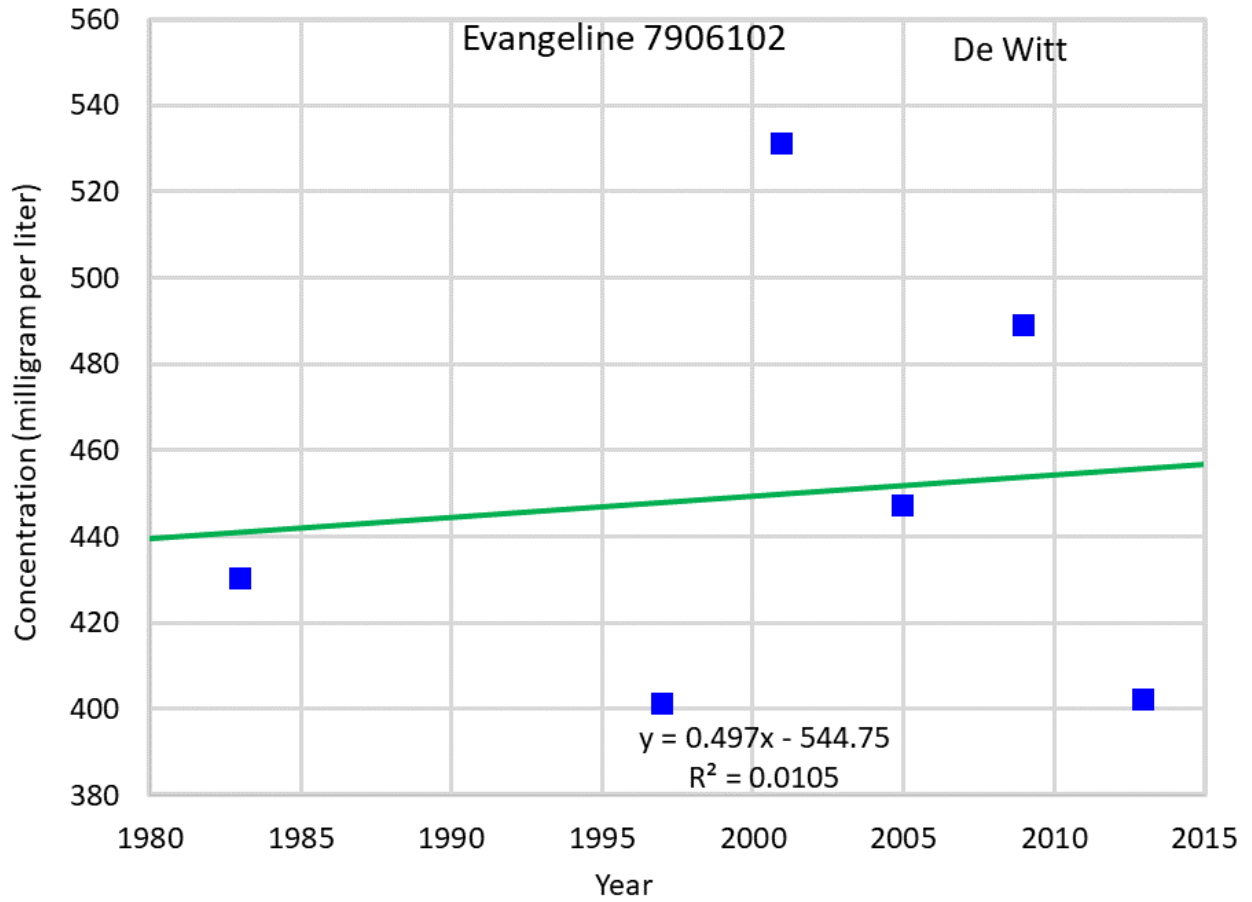


**Figure F47 Hydrograph of total dissolved solids at State Well 7906102.**

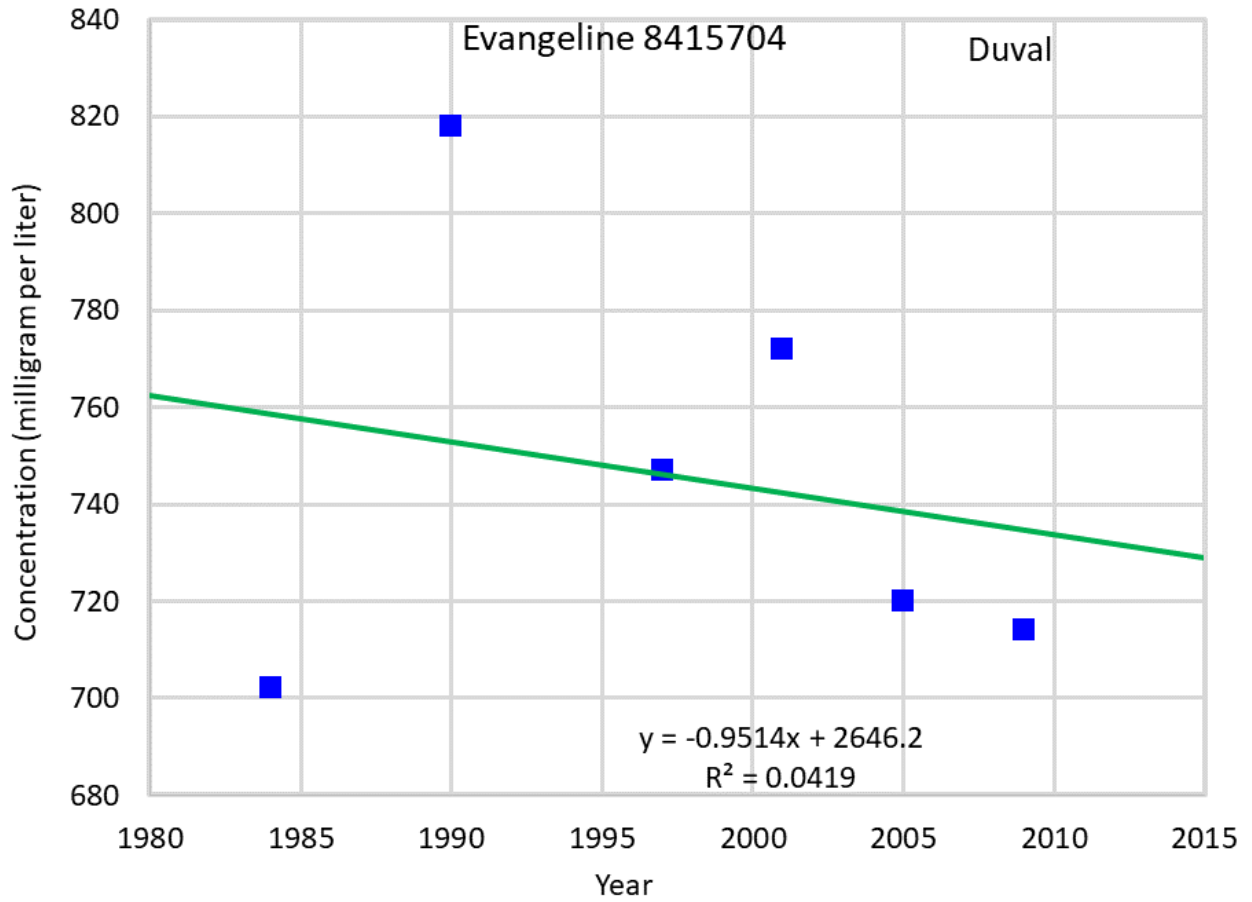


**Figure F48 Hydrograph of total dissolved solids at State Well 8415704.**

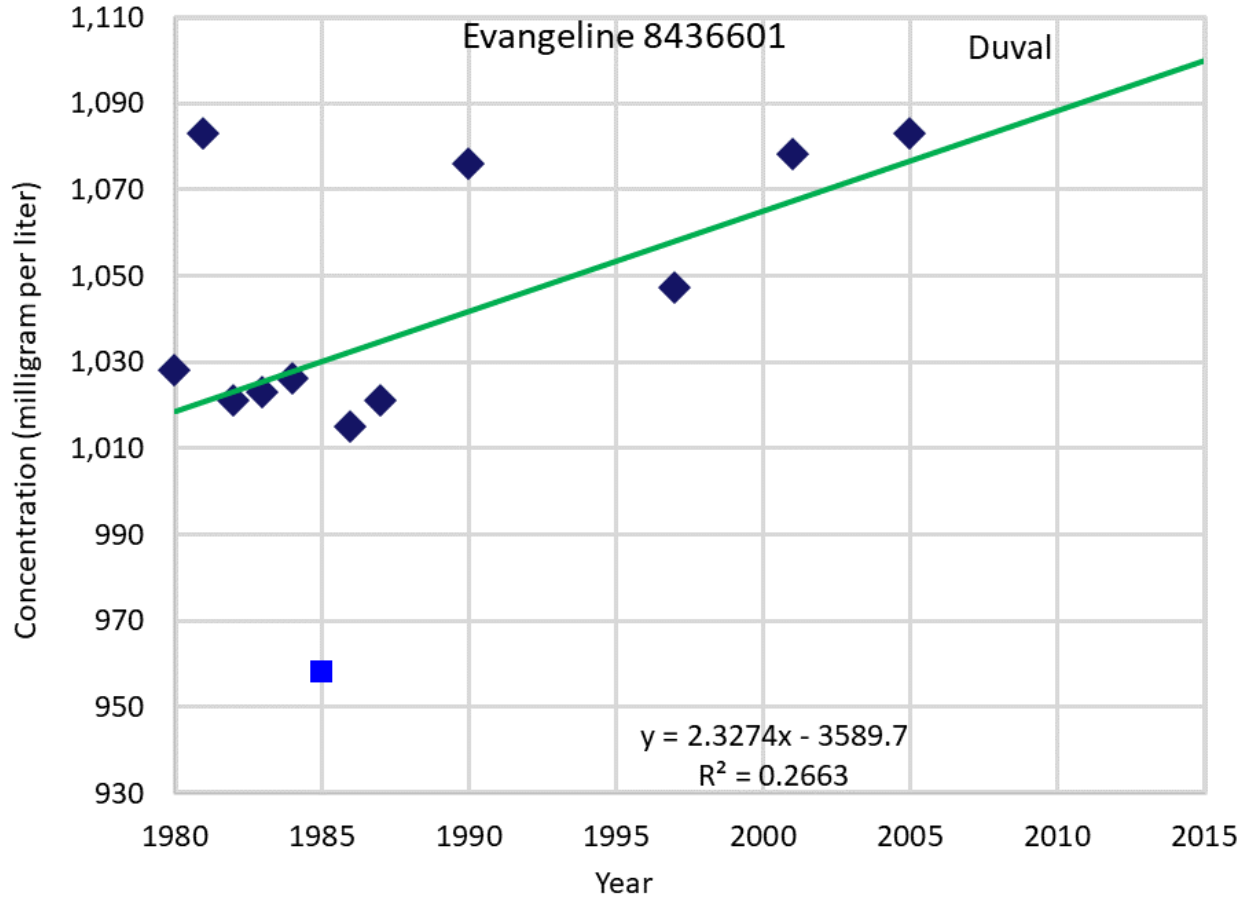


**Figure F49 Hydrograph of total dissolved solids at State Well 8436601.**

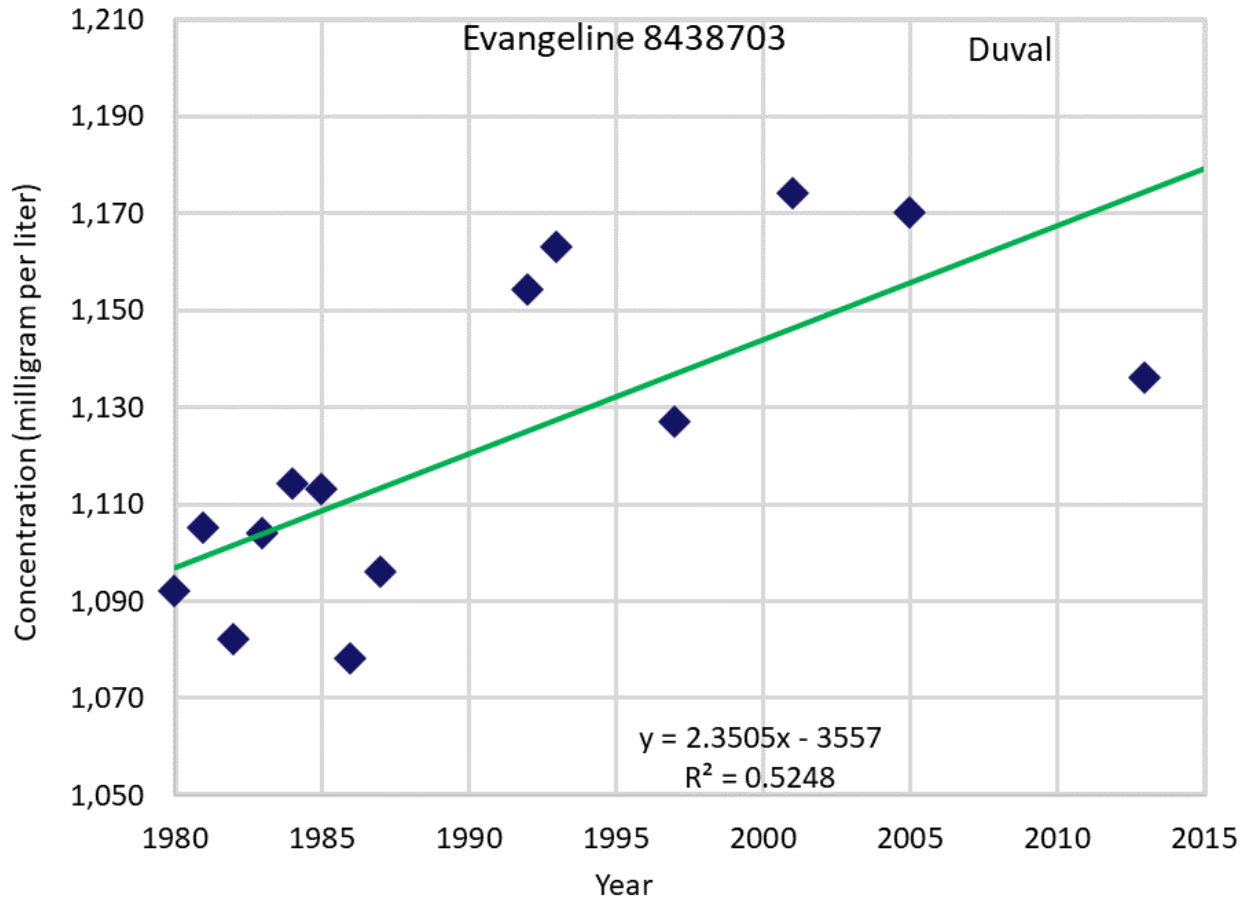


**Figure F50 Hydrograph of total dissolved solids at State Well 8438703.**

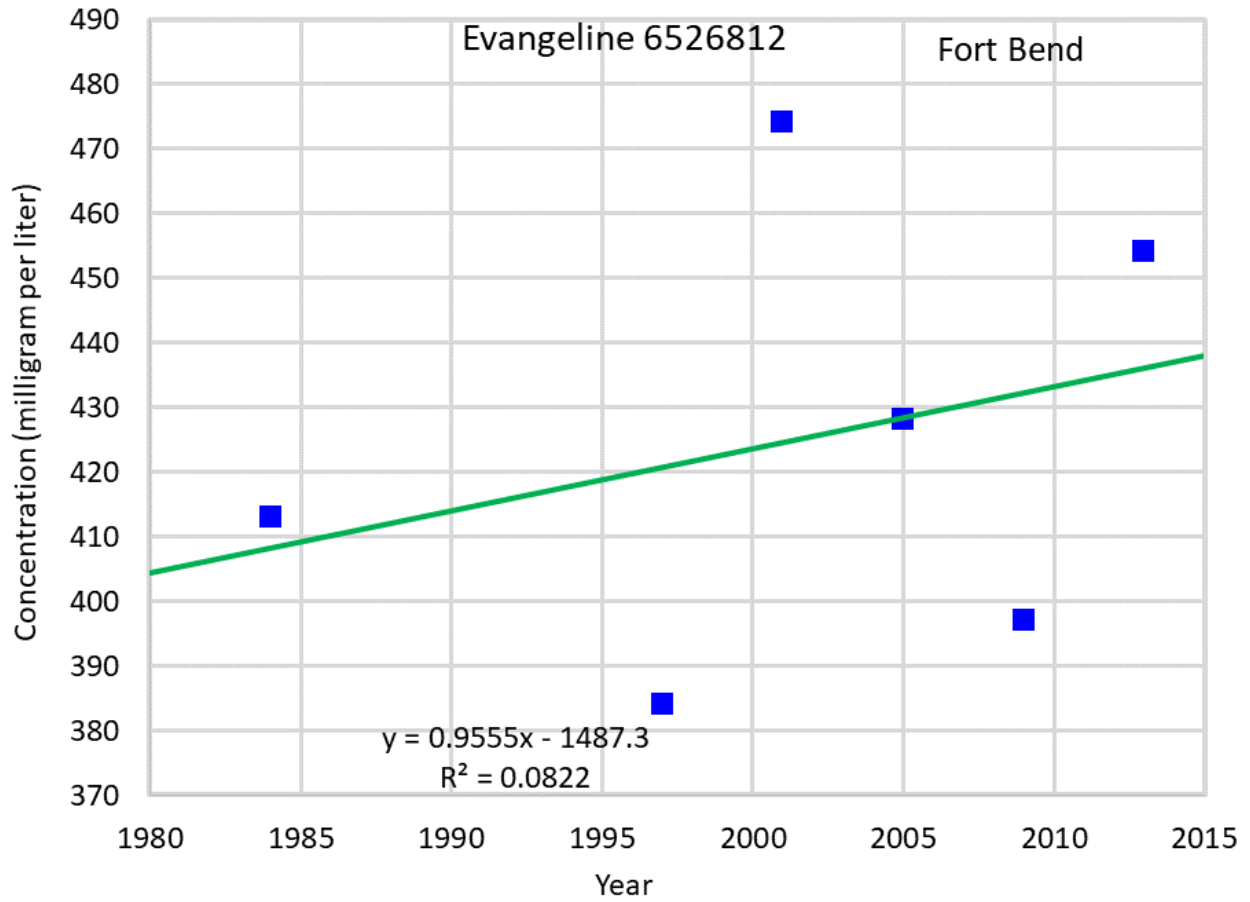


**Figure F51 Hydrograph of total dissolved solids at State Well 6526812.**

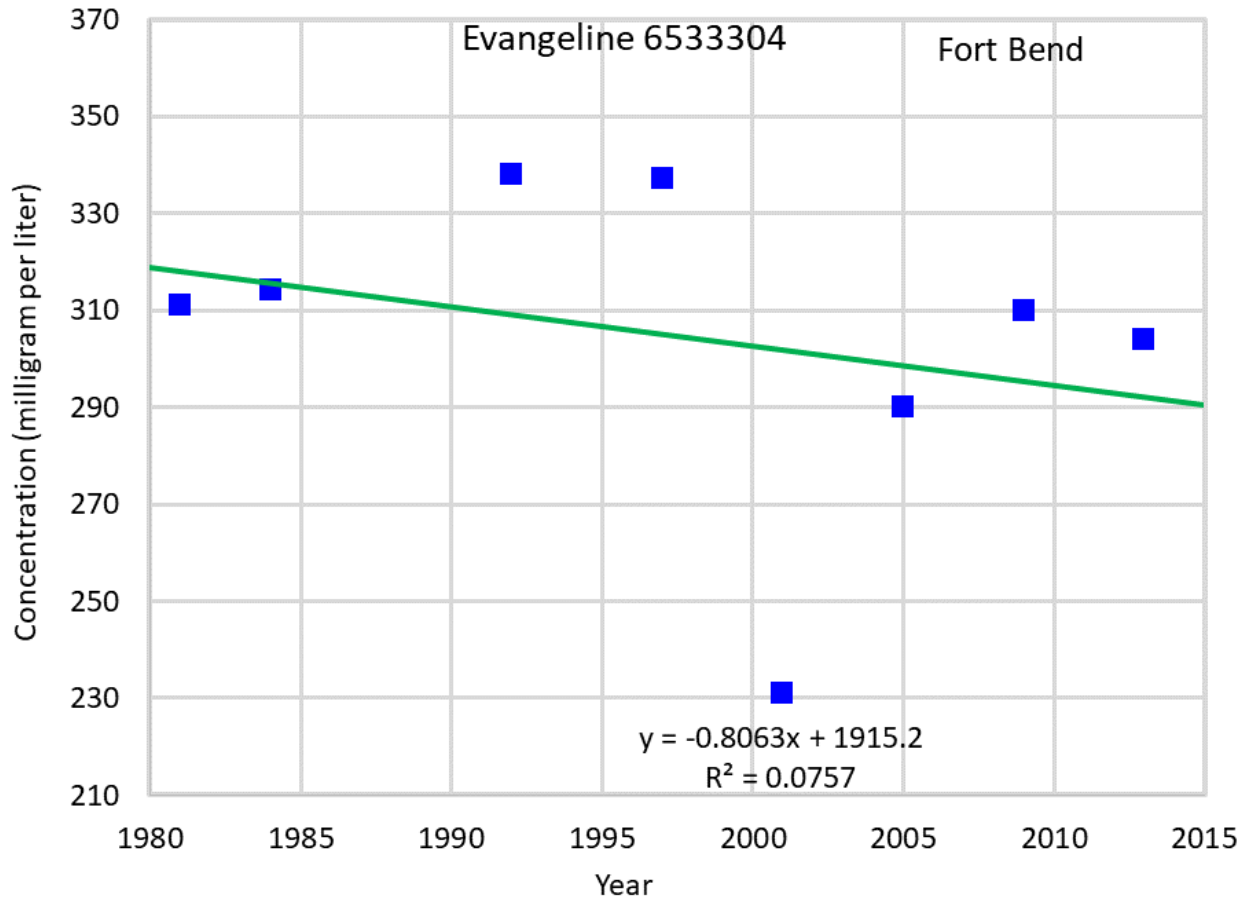


**Figure F52 Hydrograph of total dissolved solids at State Well 6533304.**

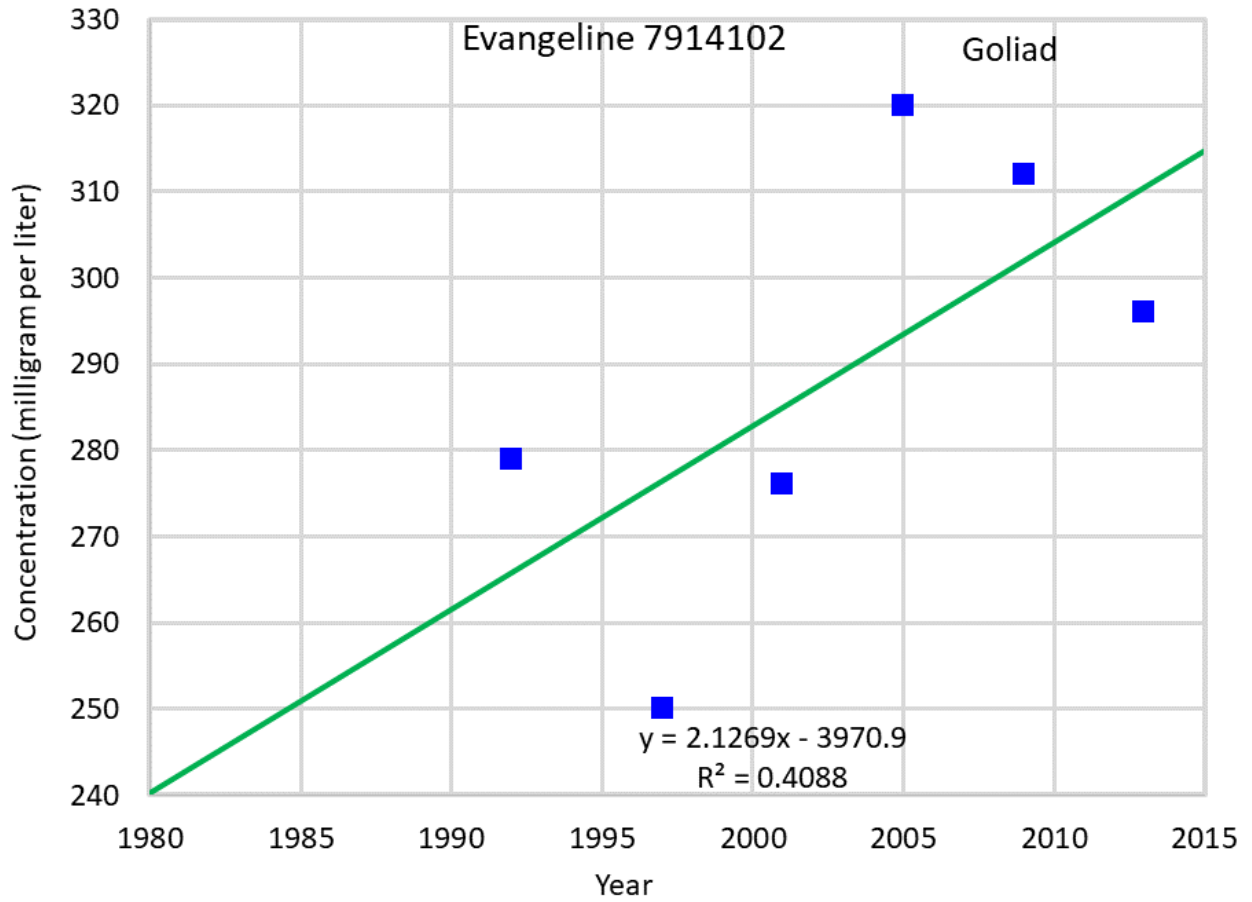


**Figure F53 Hydrograph of total dissolved solids at State Well 7914102.**

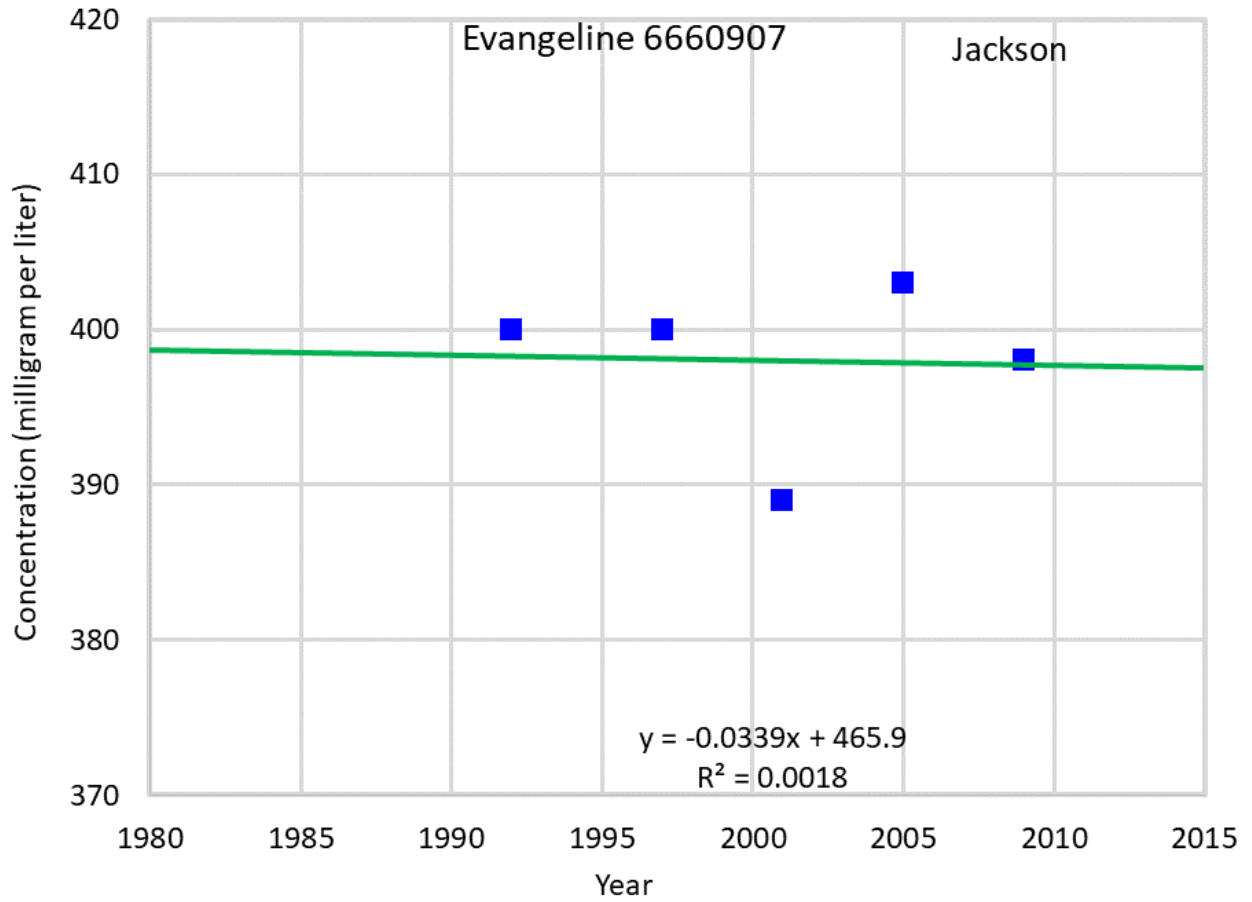


**Figure F54 Hydrograph of total dissolved solids at State Well 6660907.**



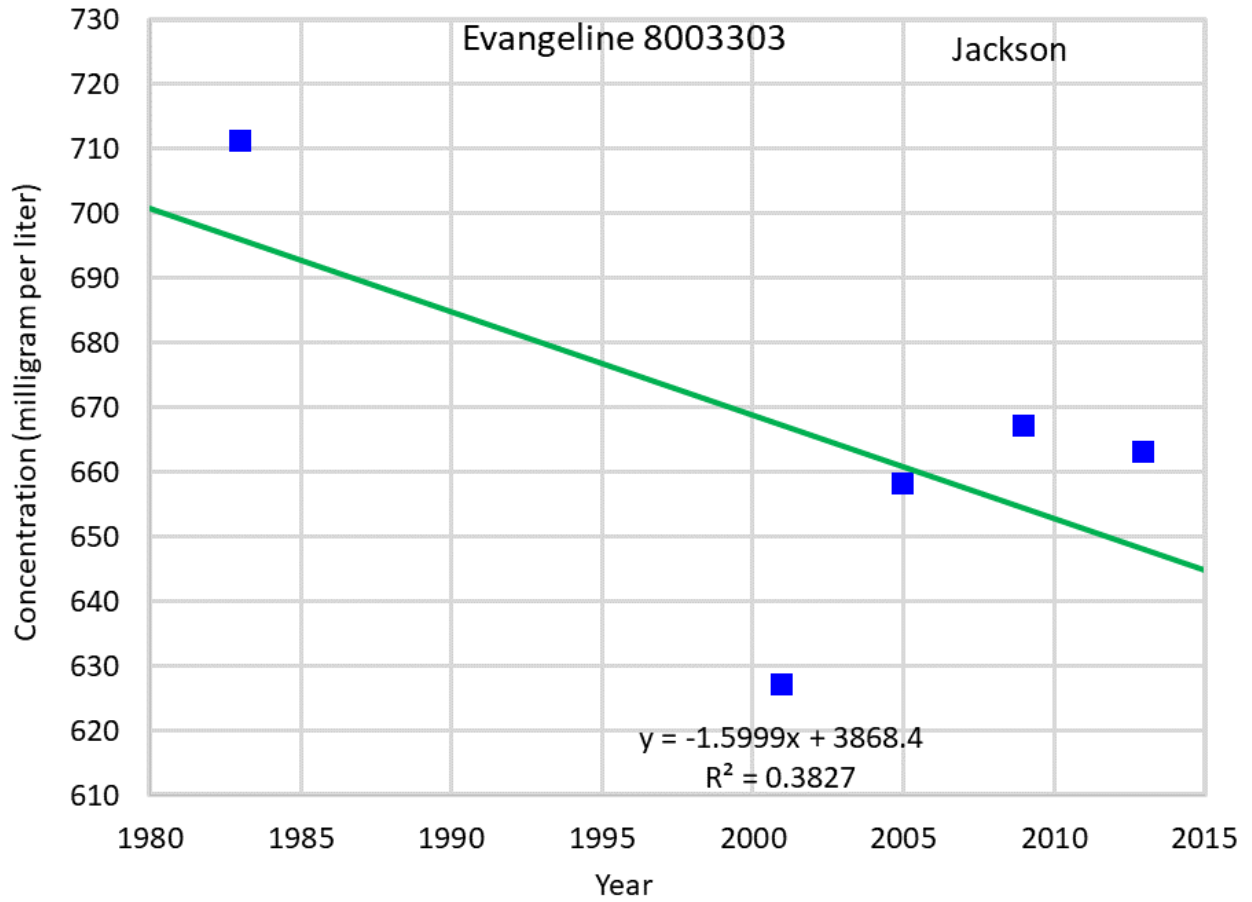


**Figure F55 Hydrograph of total dissolved solids at State Well 8003303.**

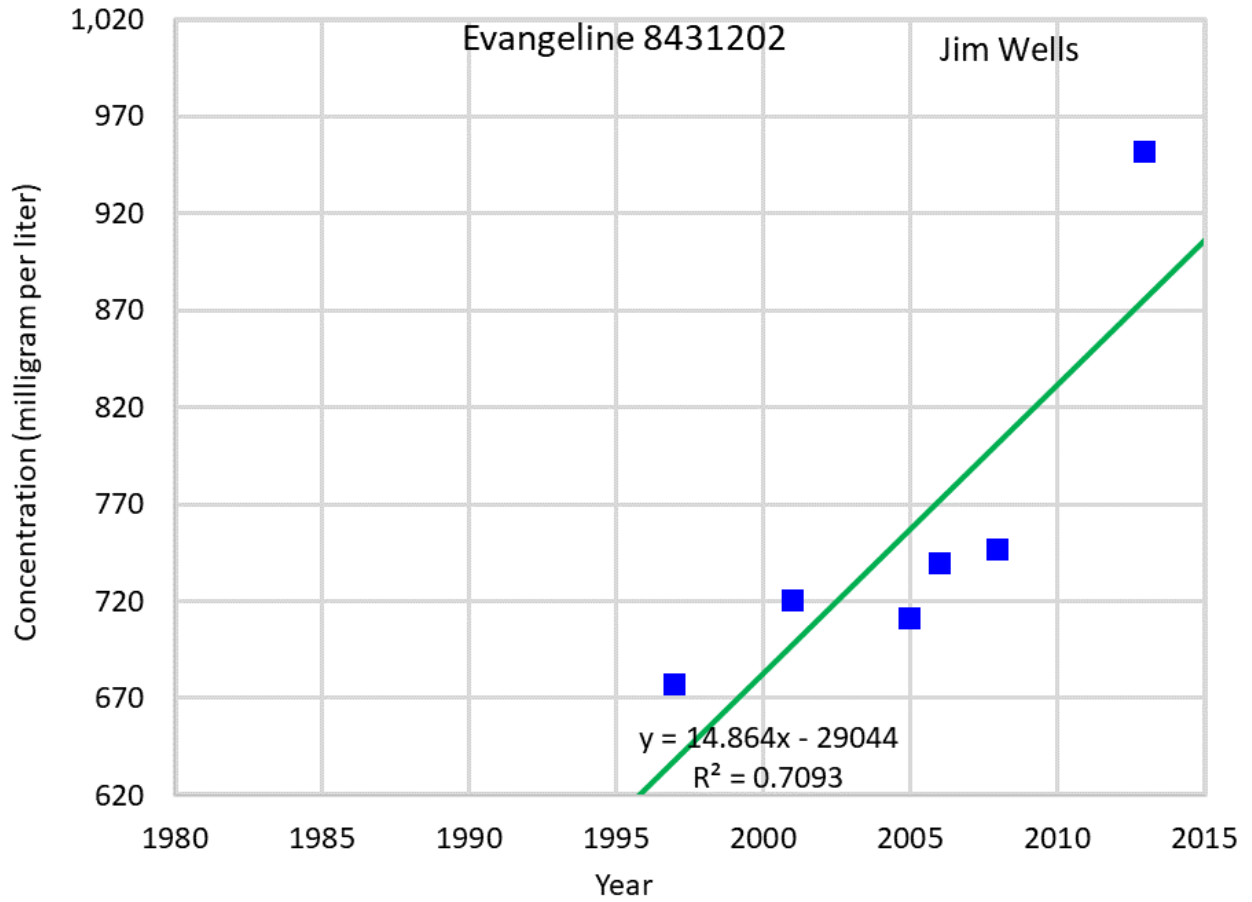


**Figure F56 Hydrograph of total dissolved solids at State Well 8431202.**

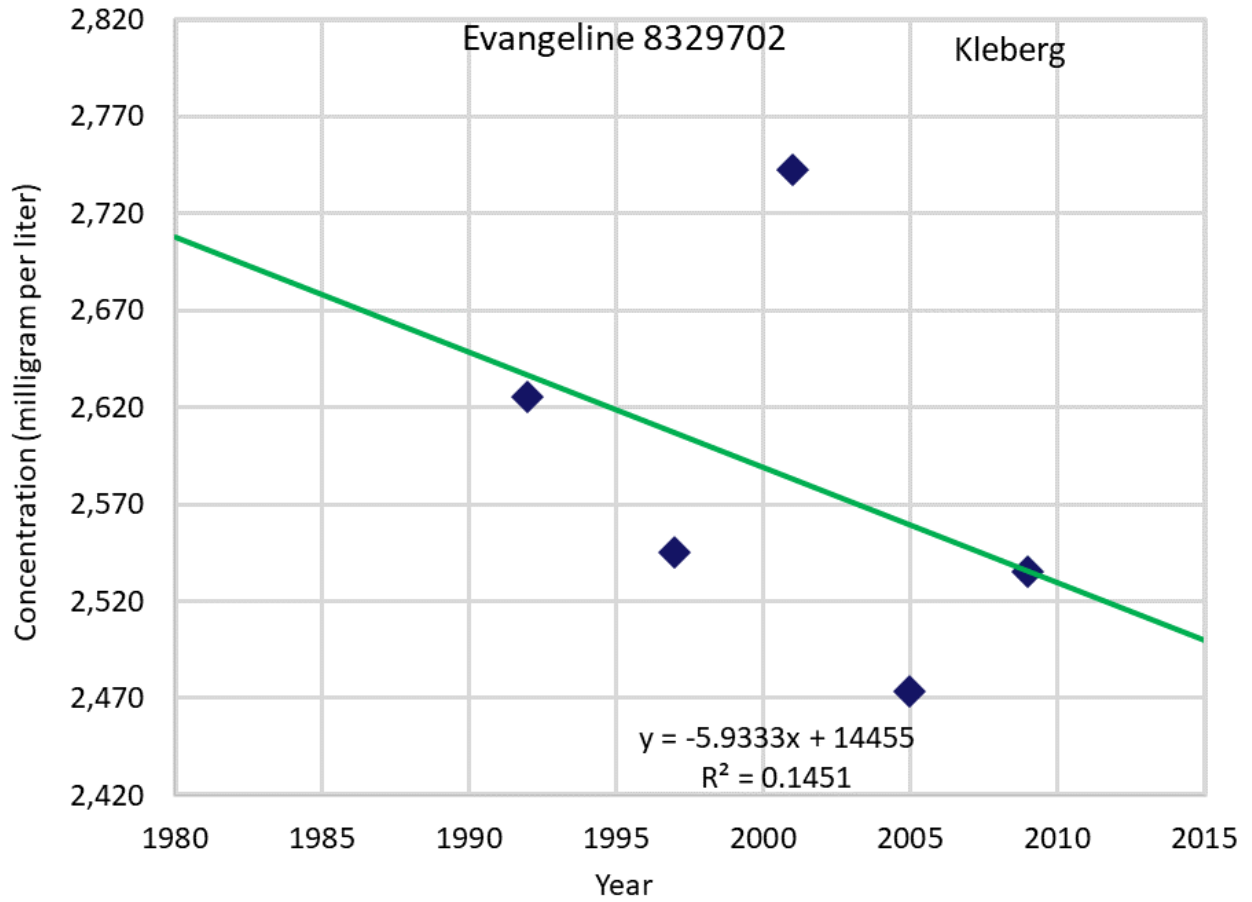


**Figure F57 Hydrograph of total dissolved solids at State Well 8329702.**

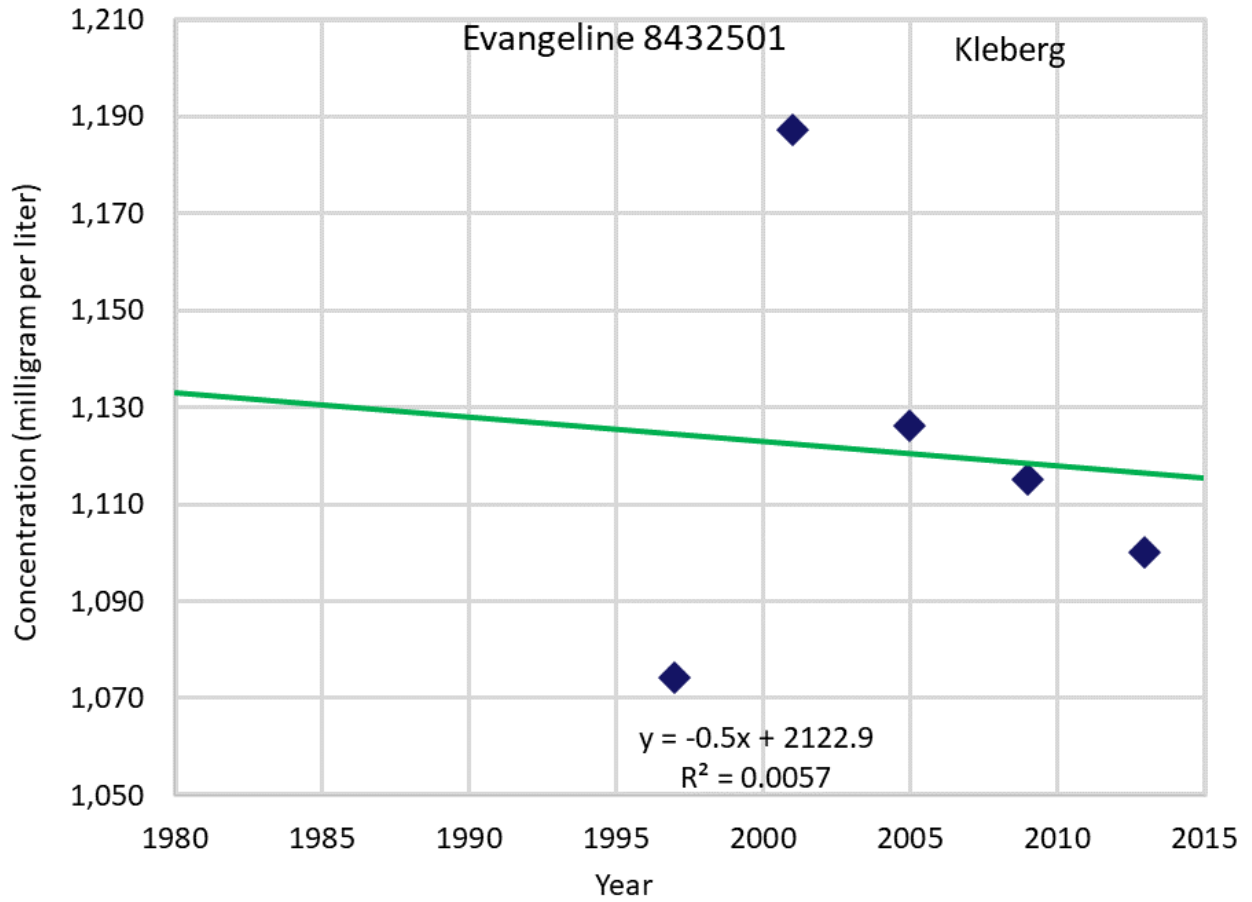


**Figure F58 Hydrograph of total dissolved solids at State Well 8432501.**

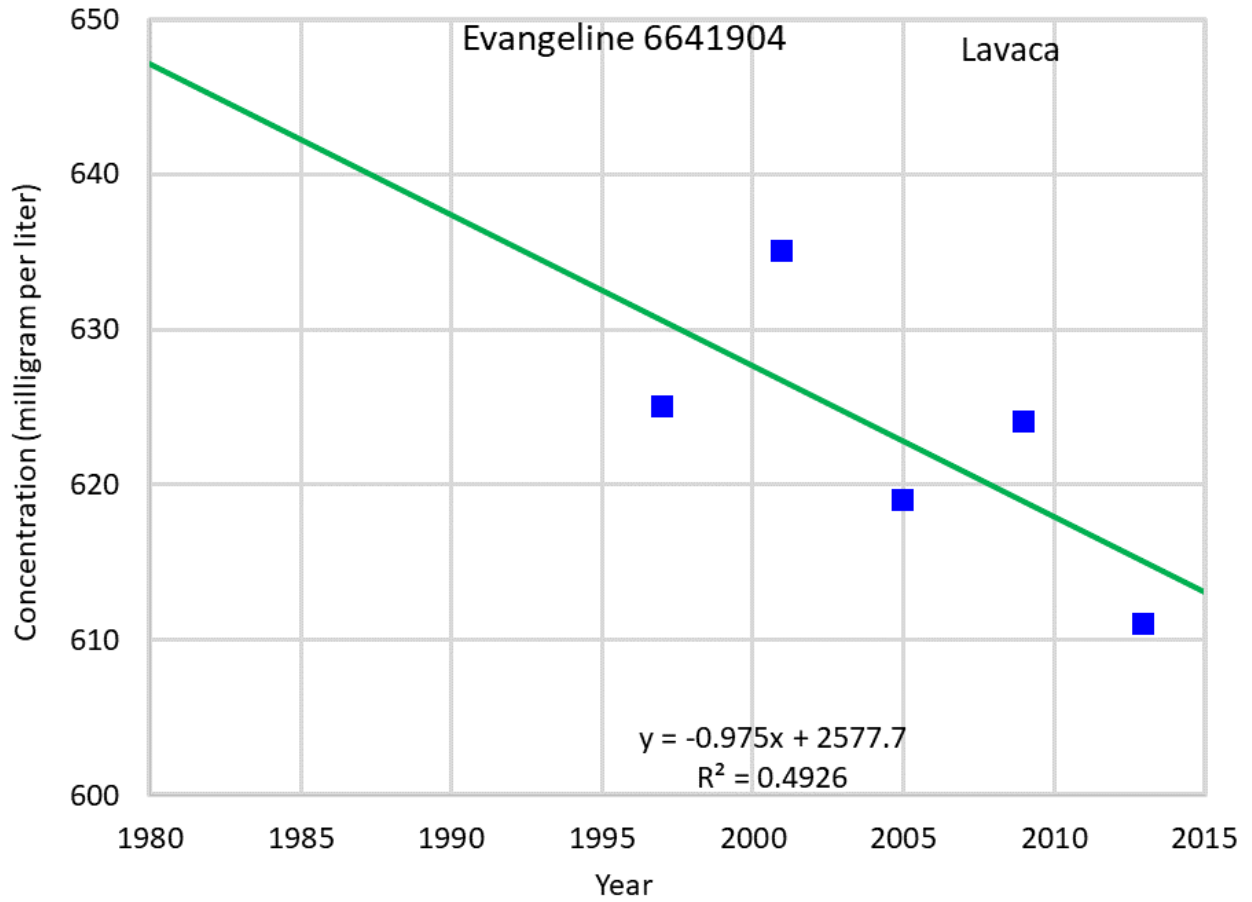


**Figure F59 Hydrograph of total dissolved solids at State Well 6641904.**

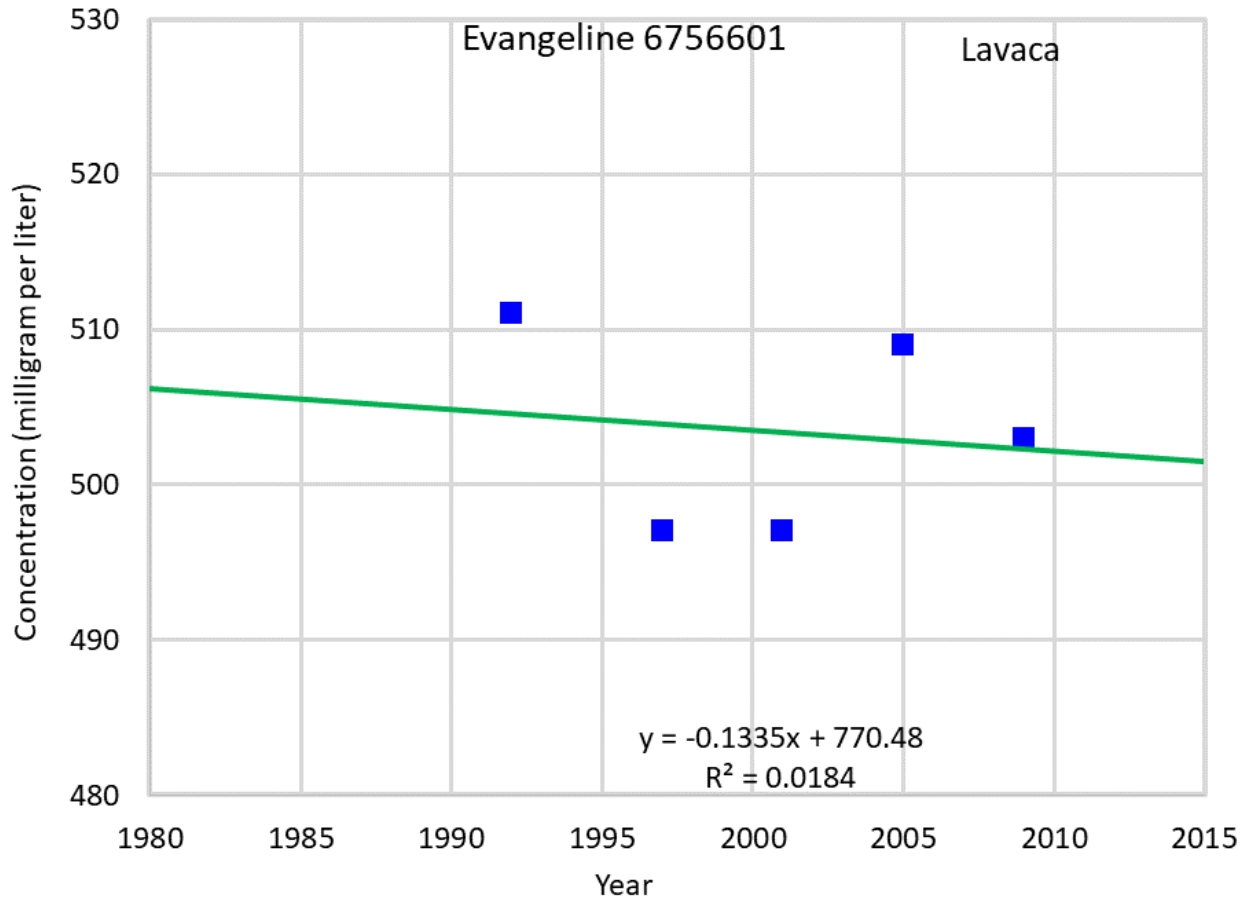


**Figure F60 Hydrograph of total dissolved solids at State Well 6756601.**

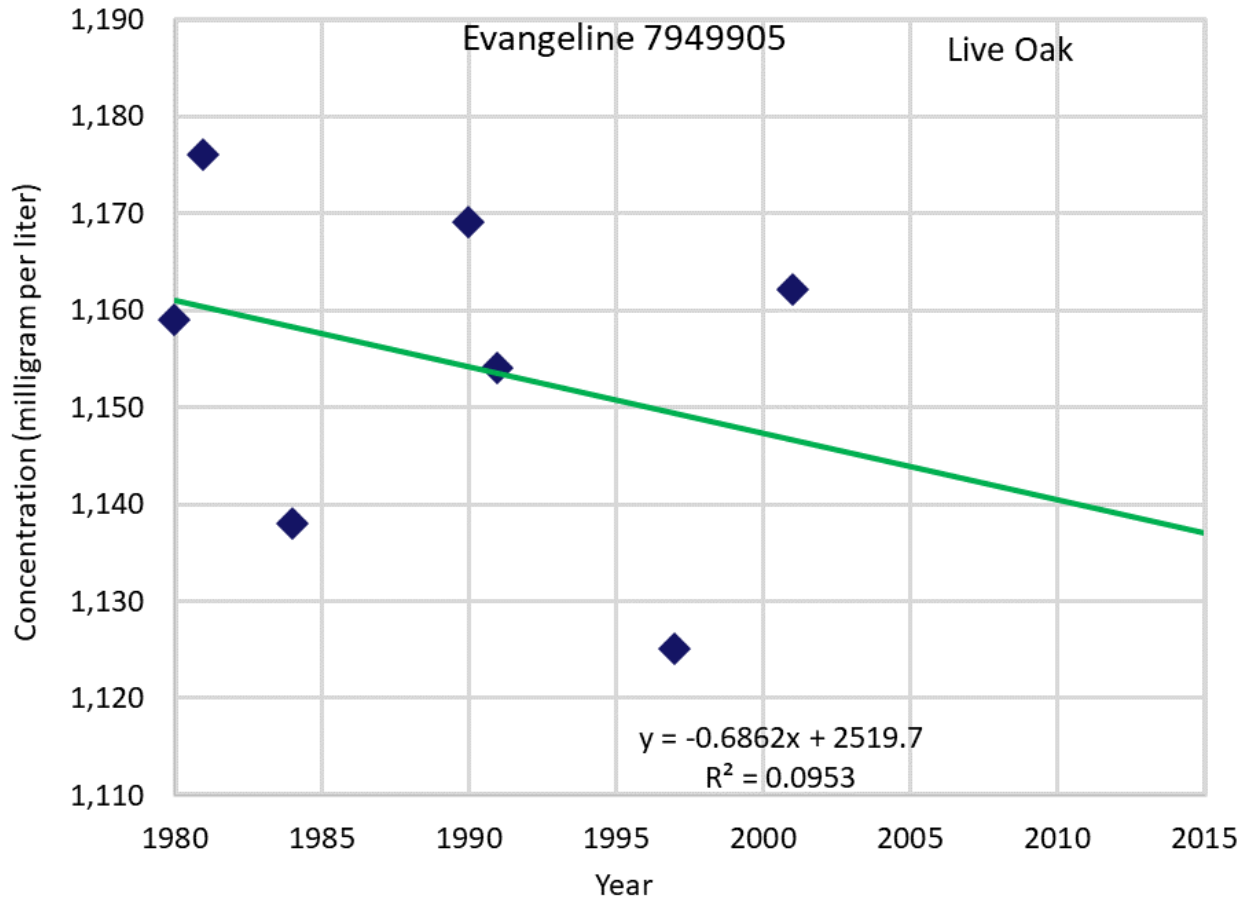


**Figure F61 Hydrograph of total dissolved solids at State Well 7949905.**

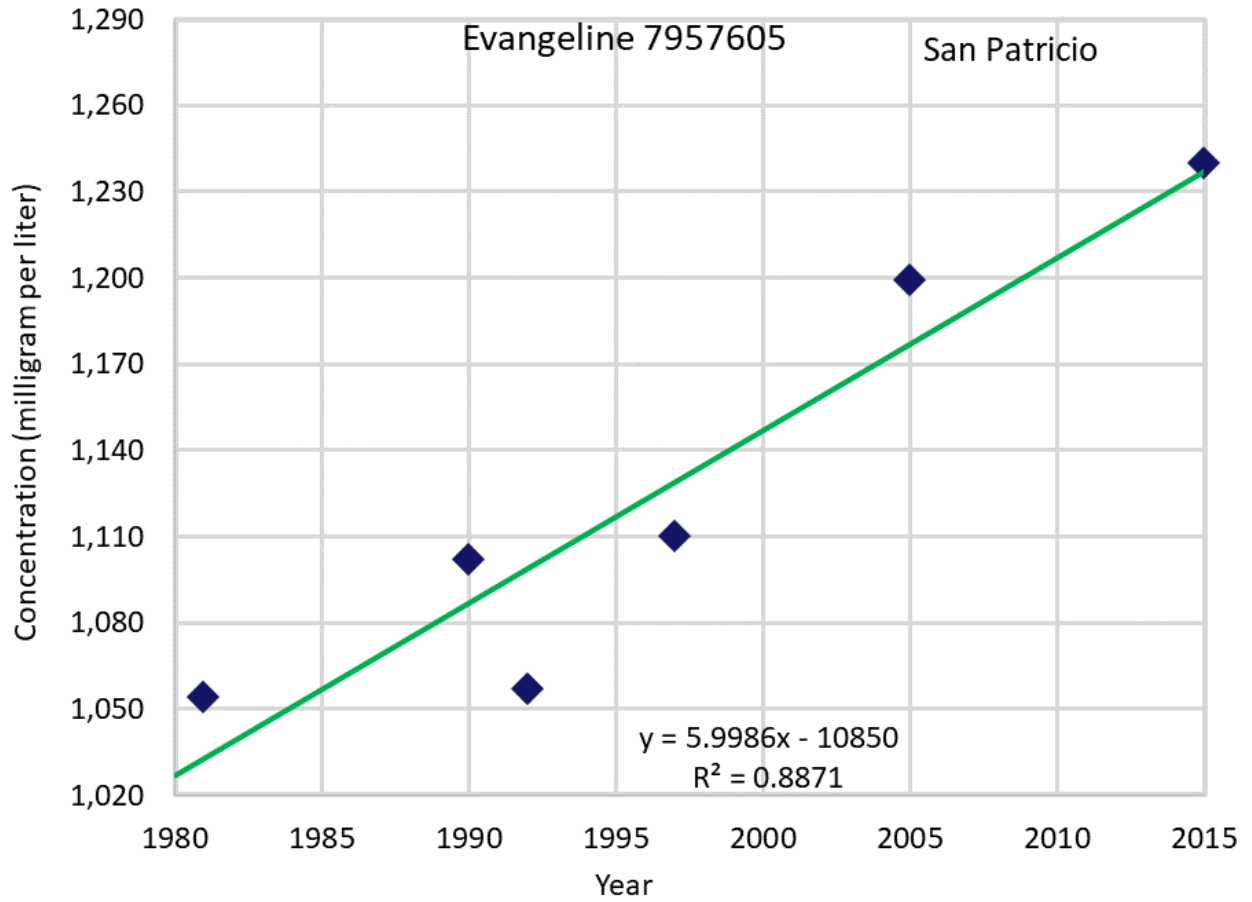


**Figure F62 Hydrograph of total dissolved solids at State Well 7957605.**



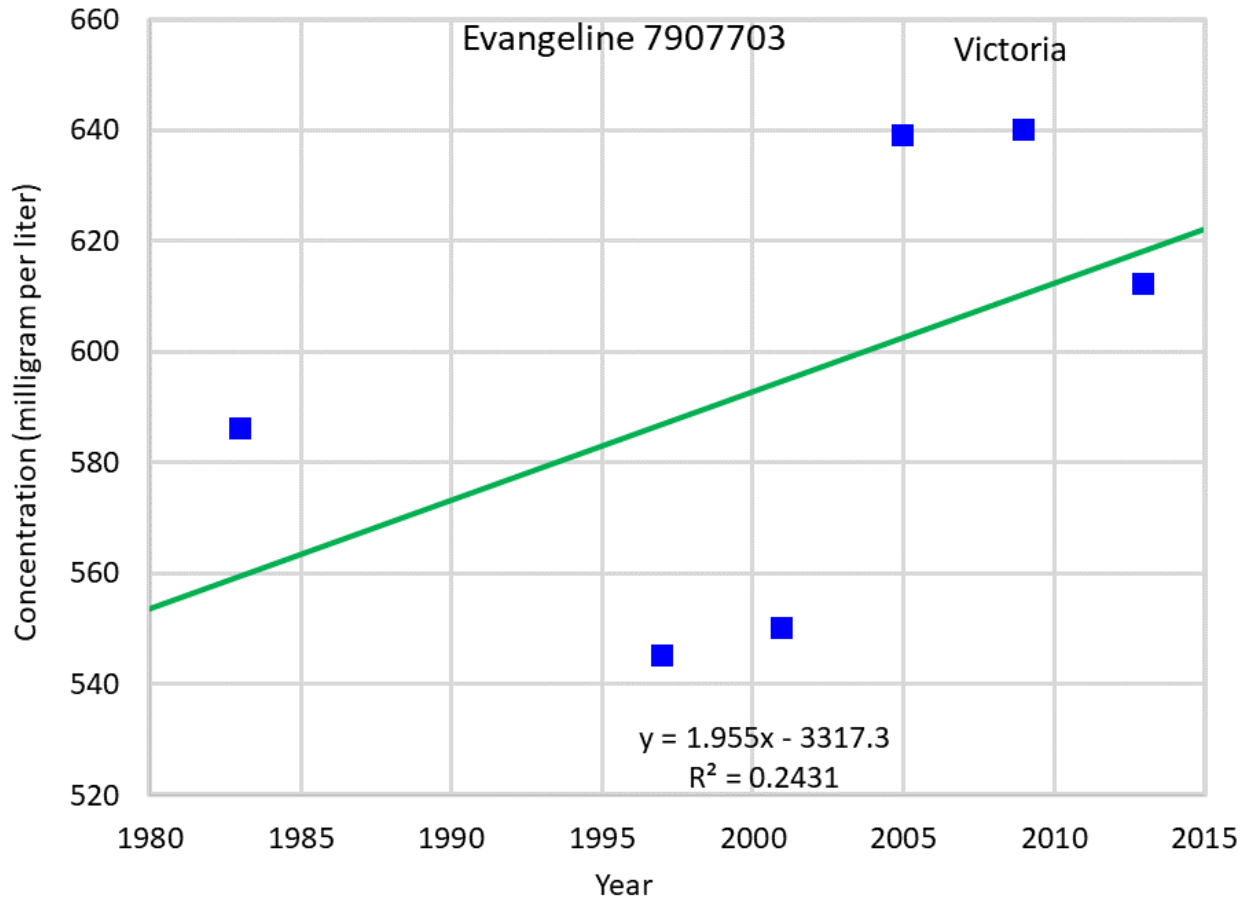


**Figure F63 Hydrograph of total dissolved solids at State Well 7907703.**

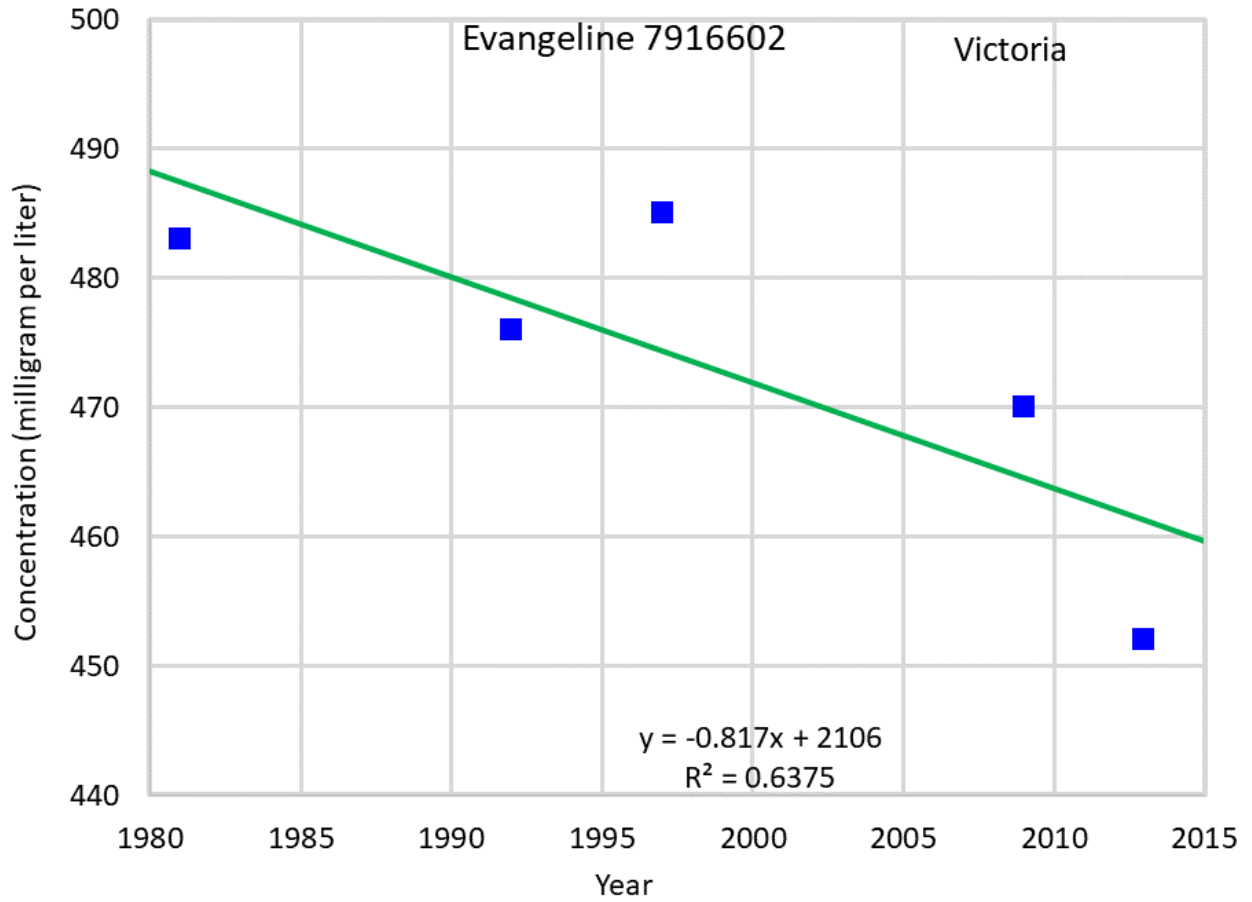


**Figure F64 Hydrograph of total dissolved solids at State Well 7916602.**

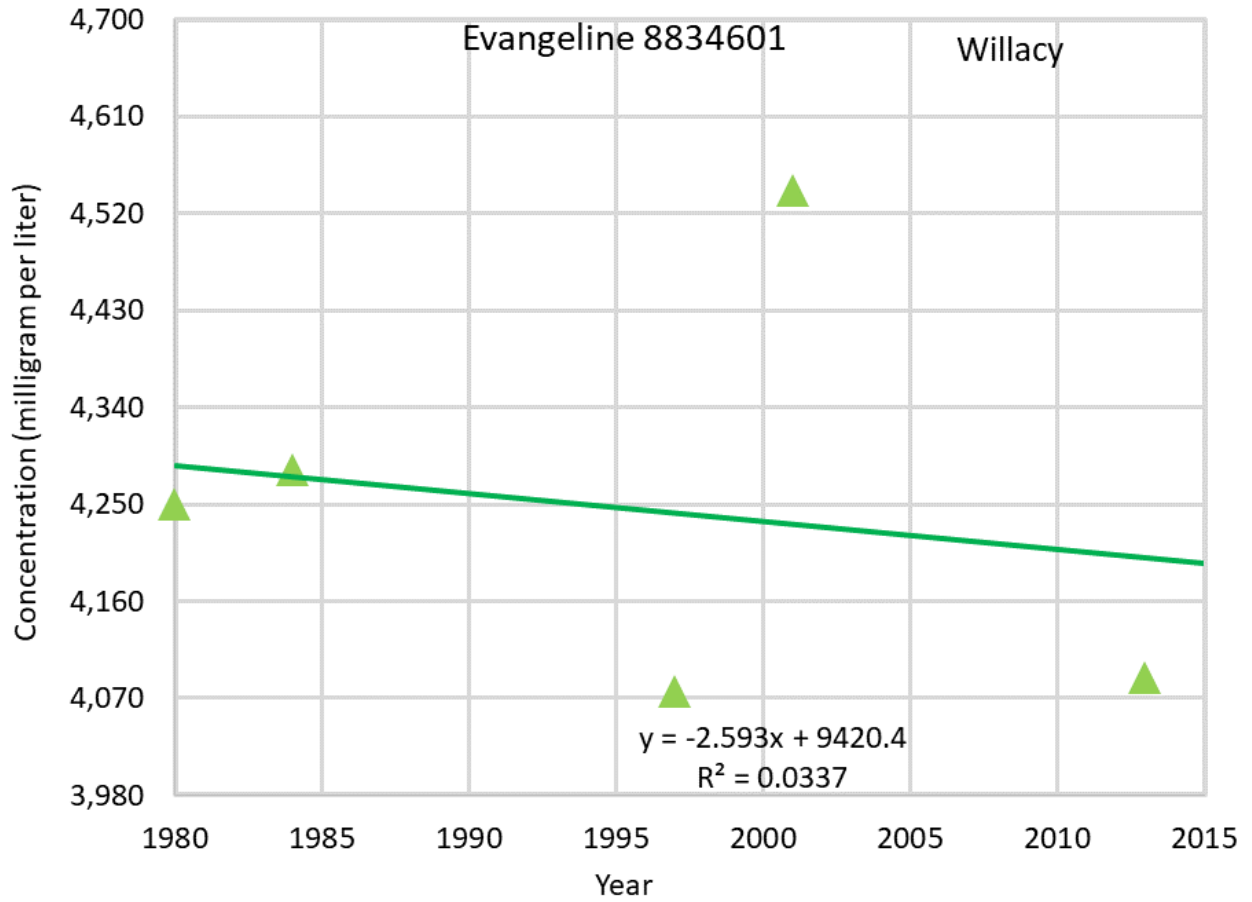


**Figure F65 Hydrograph of total dissolved solids at State Well 8834601.**

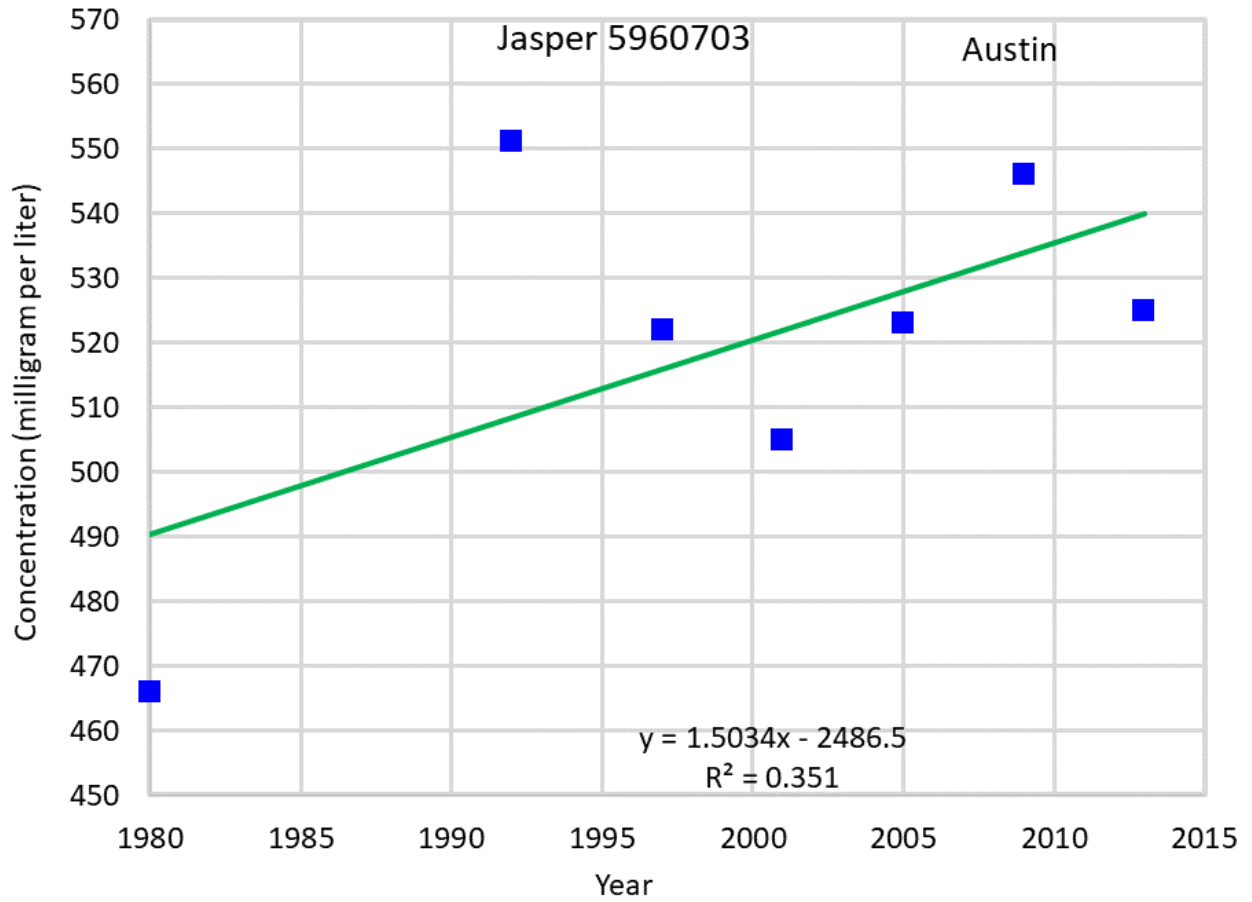


**Figure F66 Hydrograph of total dissolved solids at State Well 5960703.**

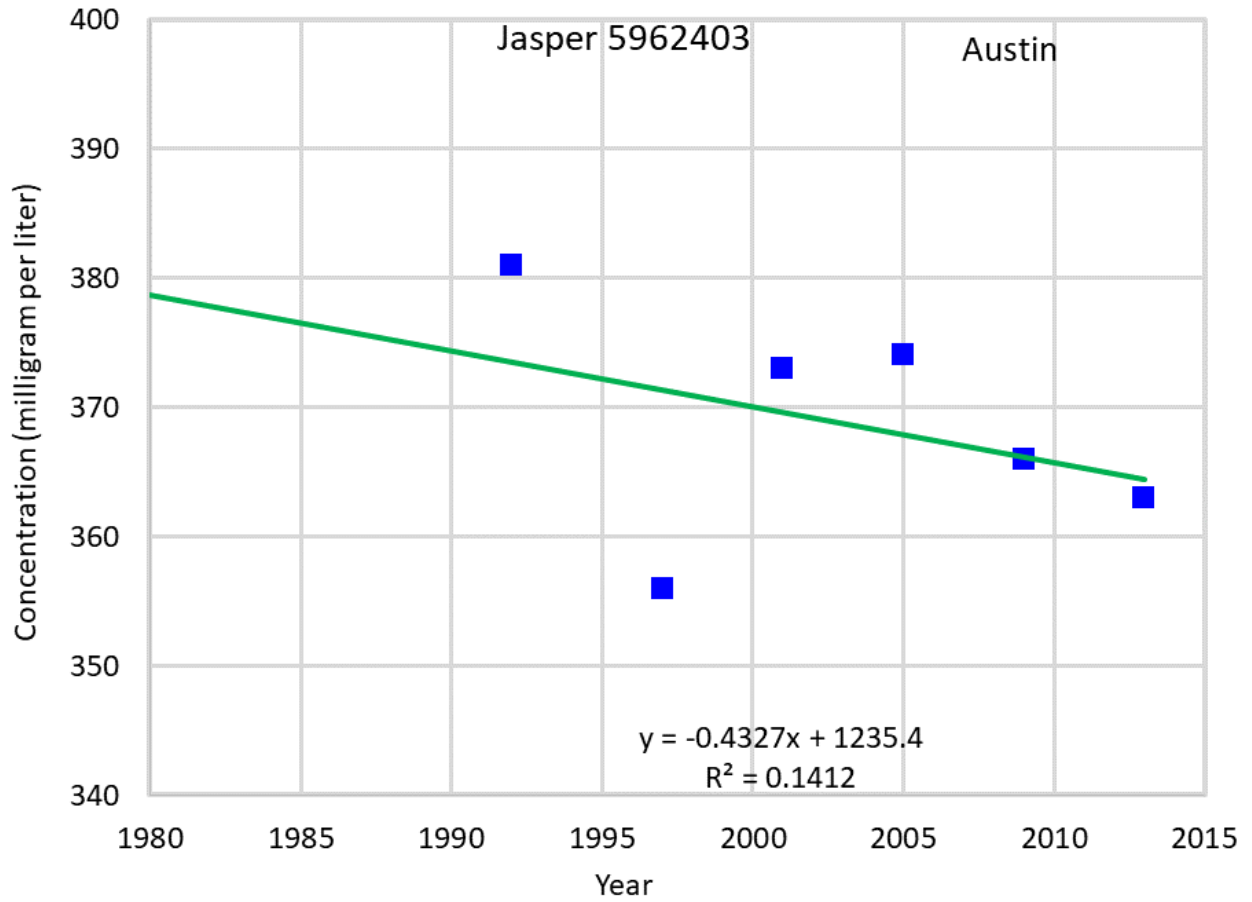


**Figure F67 Hydrograph of total dissolved solids at State Well 5962403.**

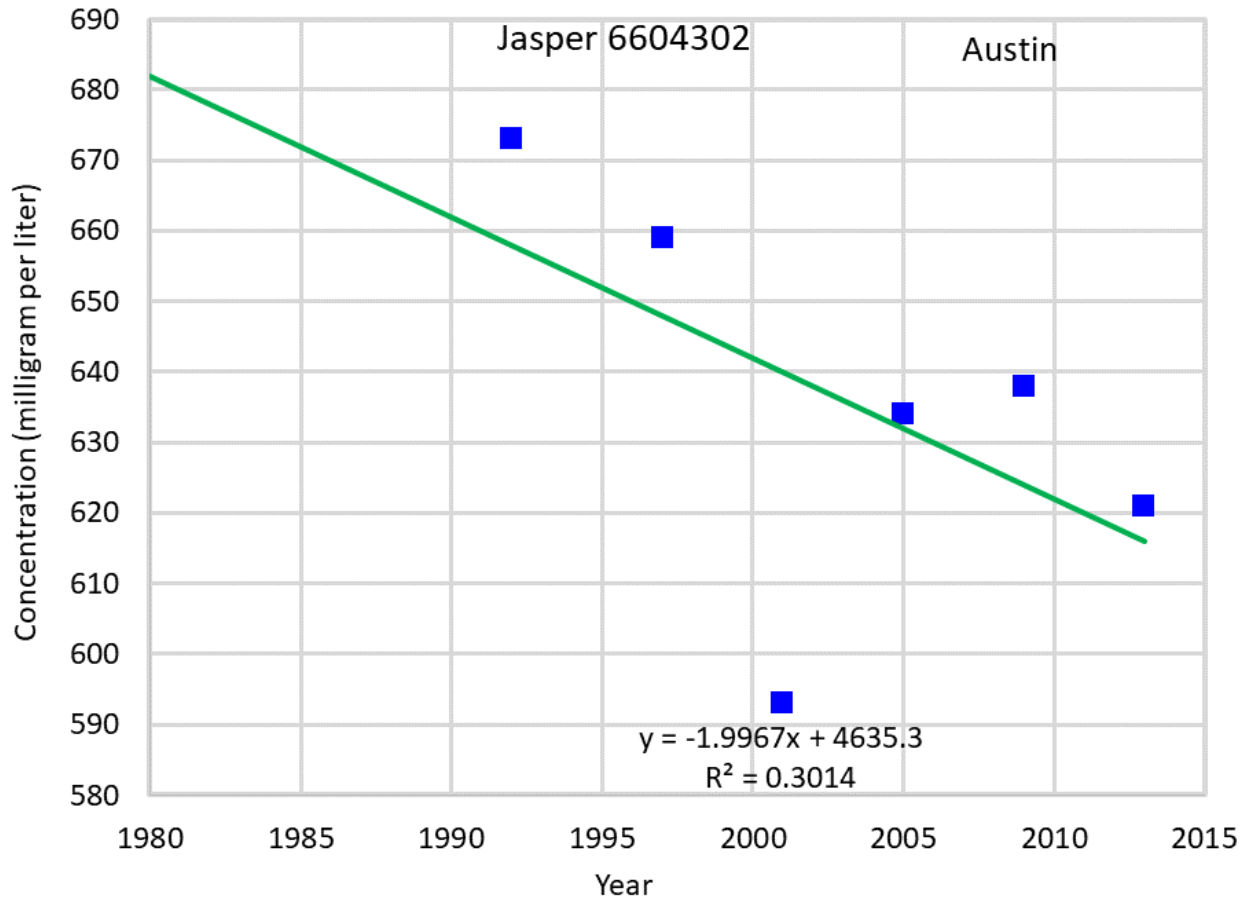


**Figure F68 Hydrograph of total dissolved solids at State Well 6604302.**

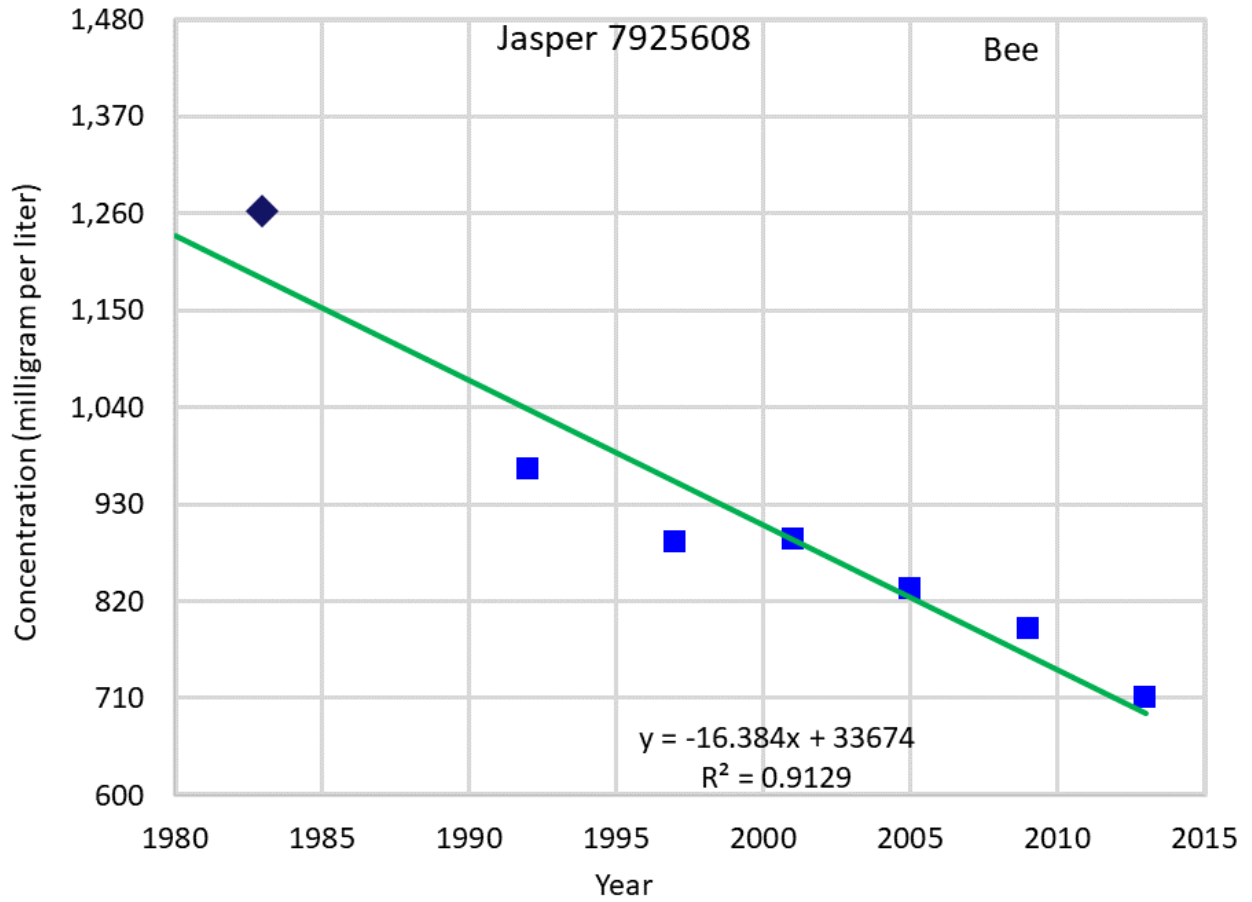


**Figure F69 Hydrograph of total dissolved solids at State Well 7925608.**

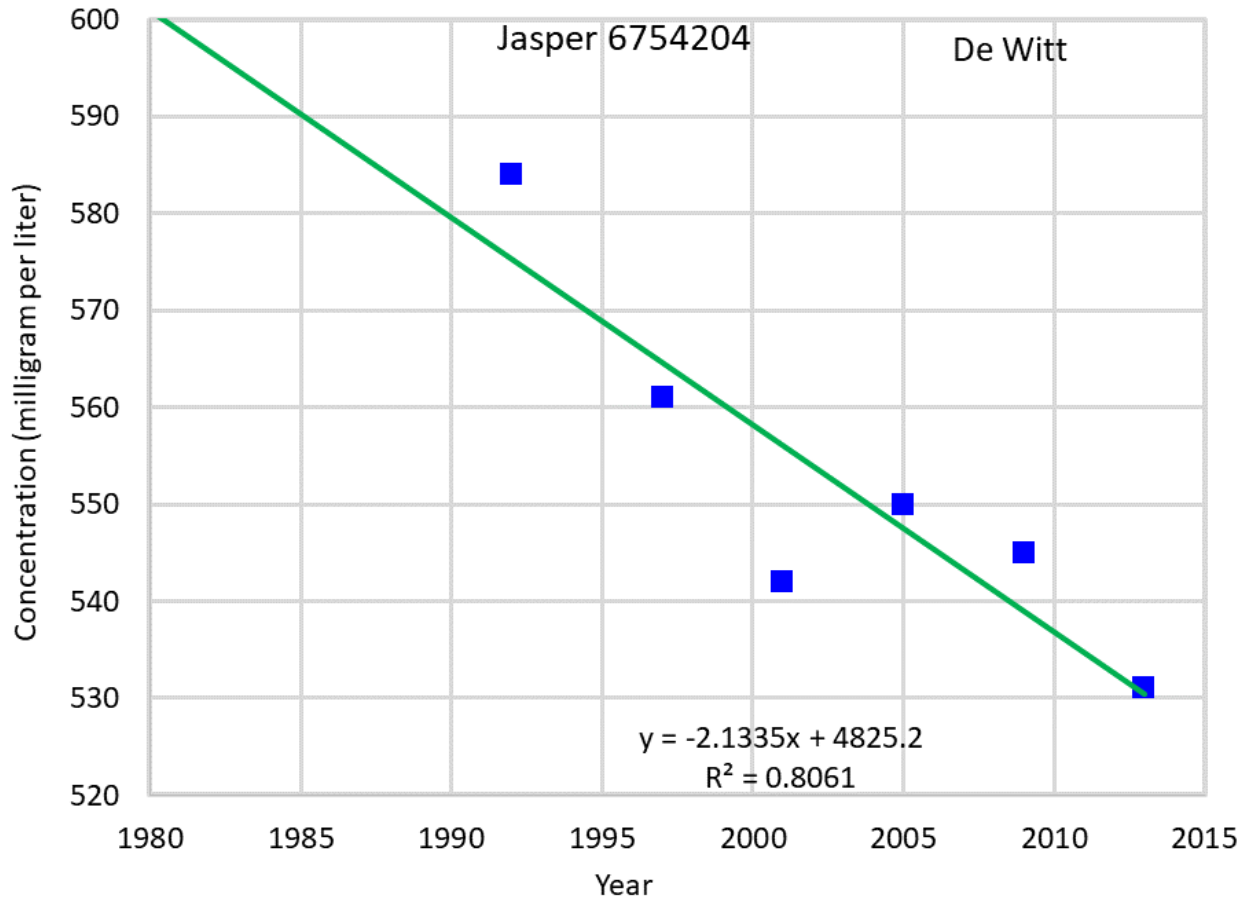


**Figure F70 Hydrograph of total dissolved solids at State Well 6754204.**



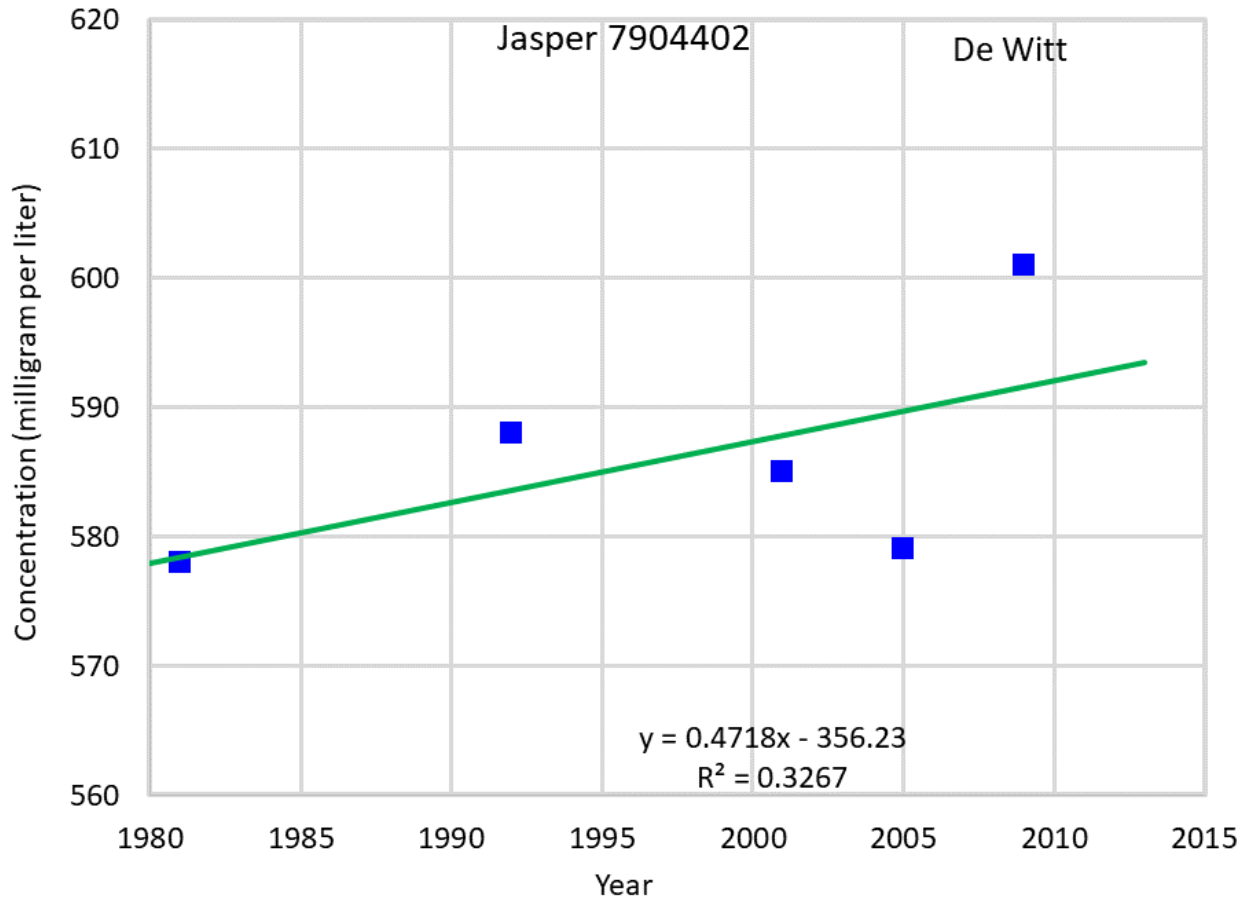


**Figure F71 Hydrograph of total dissolved solids at State Well 7904402.**

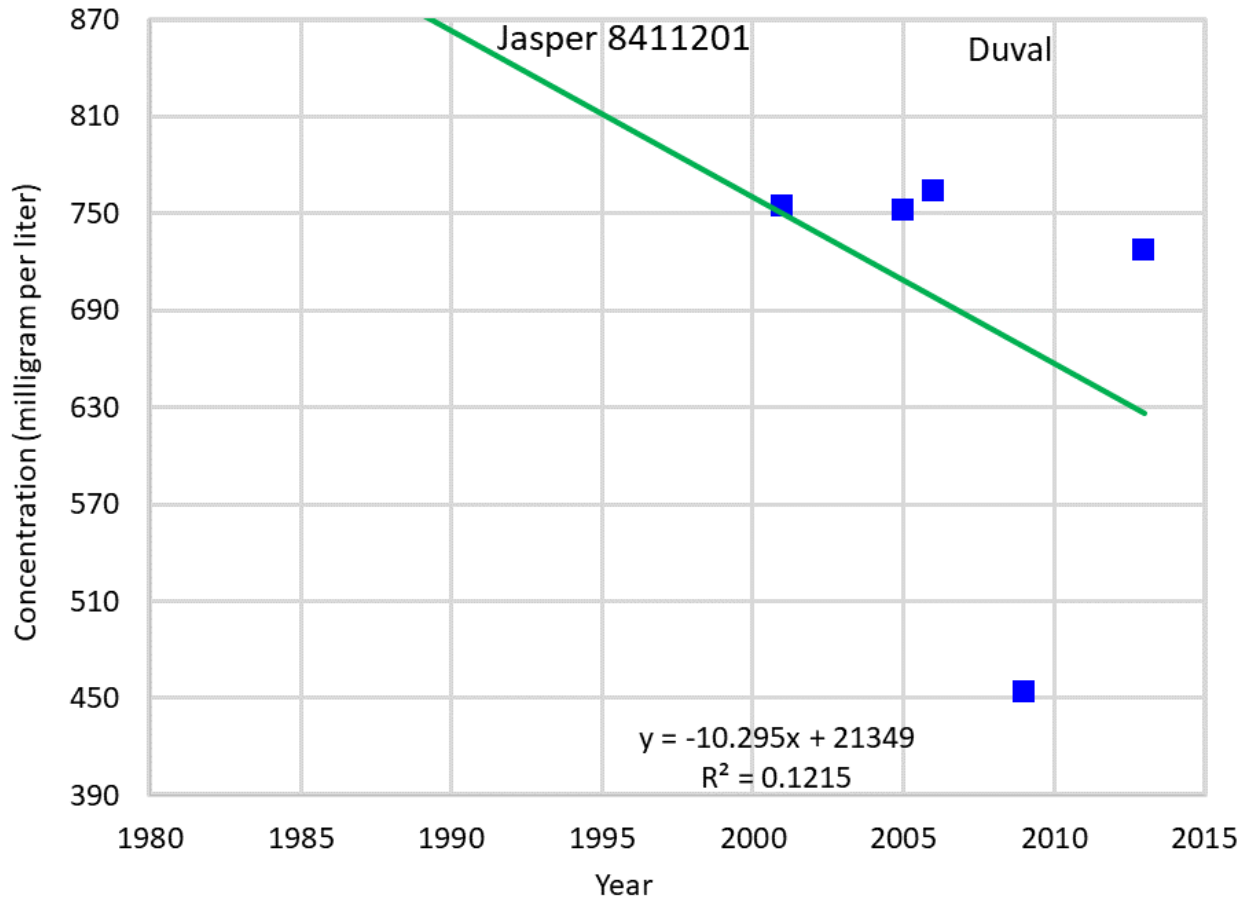


**Figure F72 Hydrograph of total dissolved solids at State Well 8411201.**

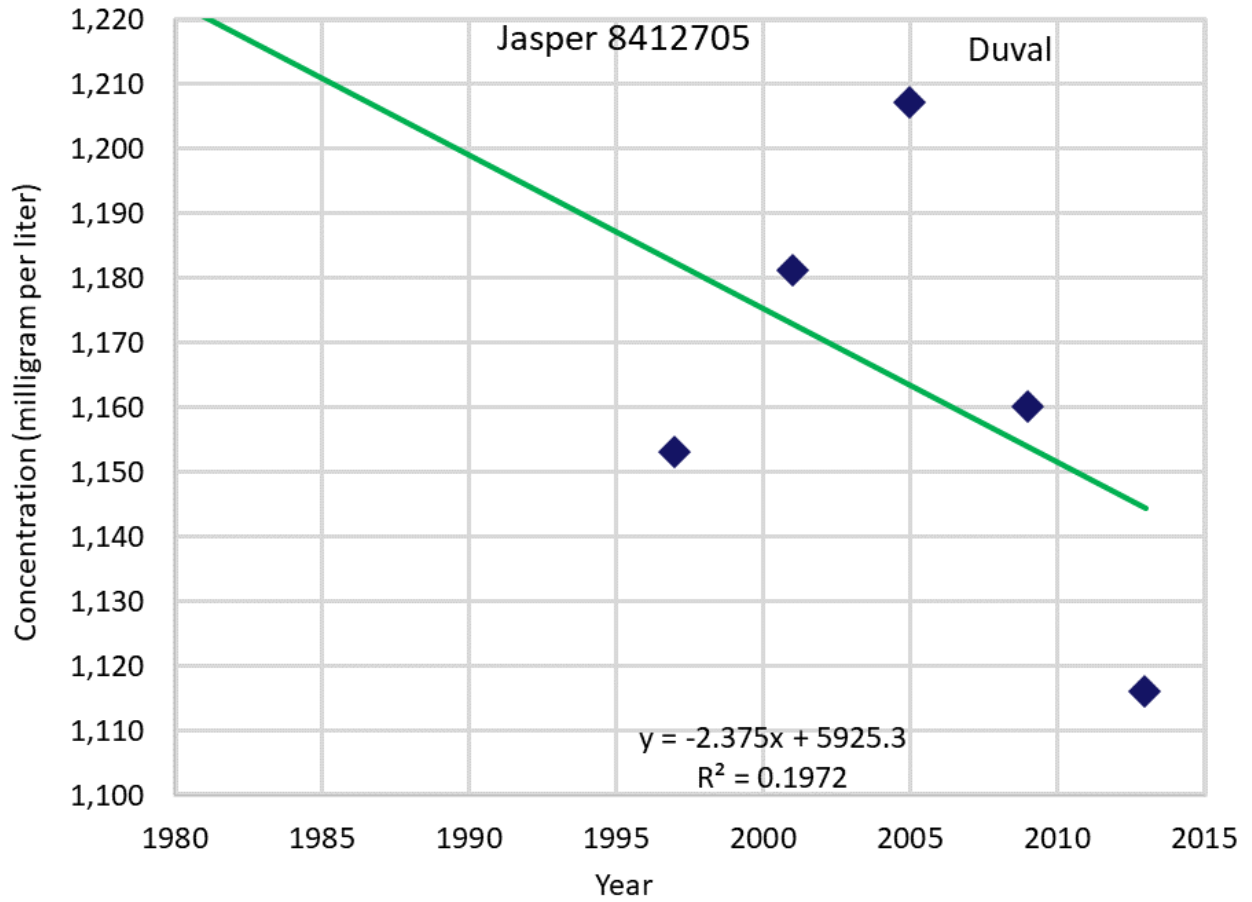


**Figure F73 Hydrograph of total dissolved solids at State Well 8412705.**

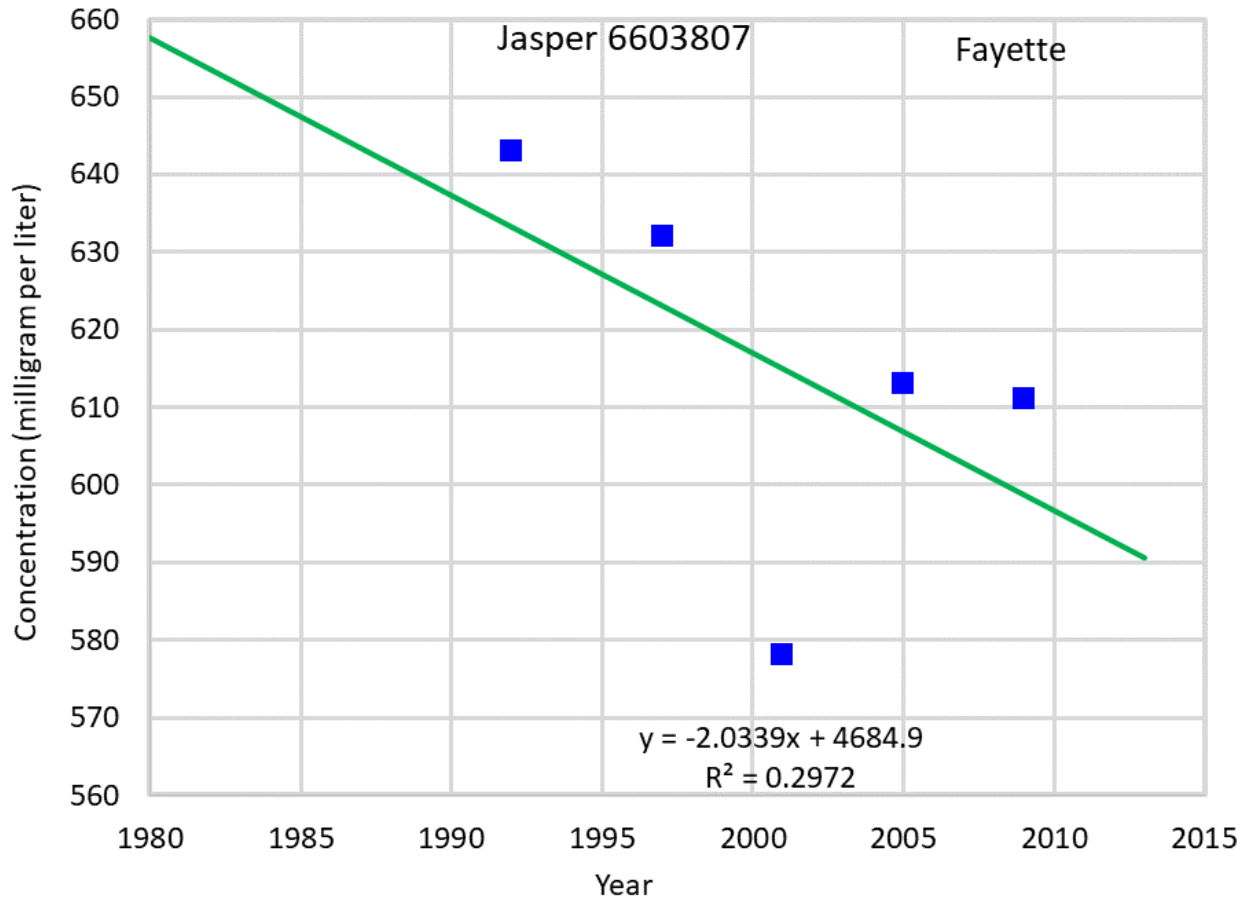


**Figure F74 Hydrograph of total dissolved solids at State Well 6603807.**

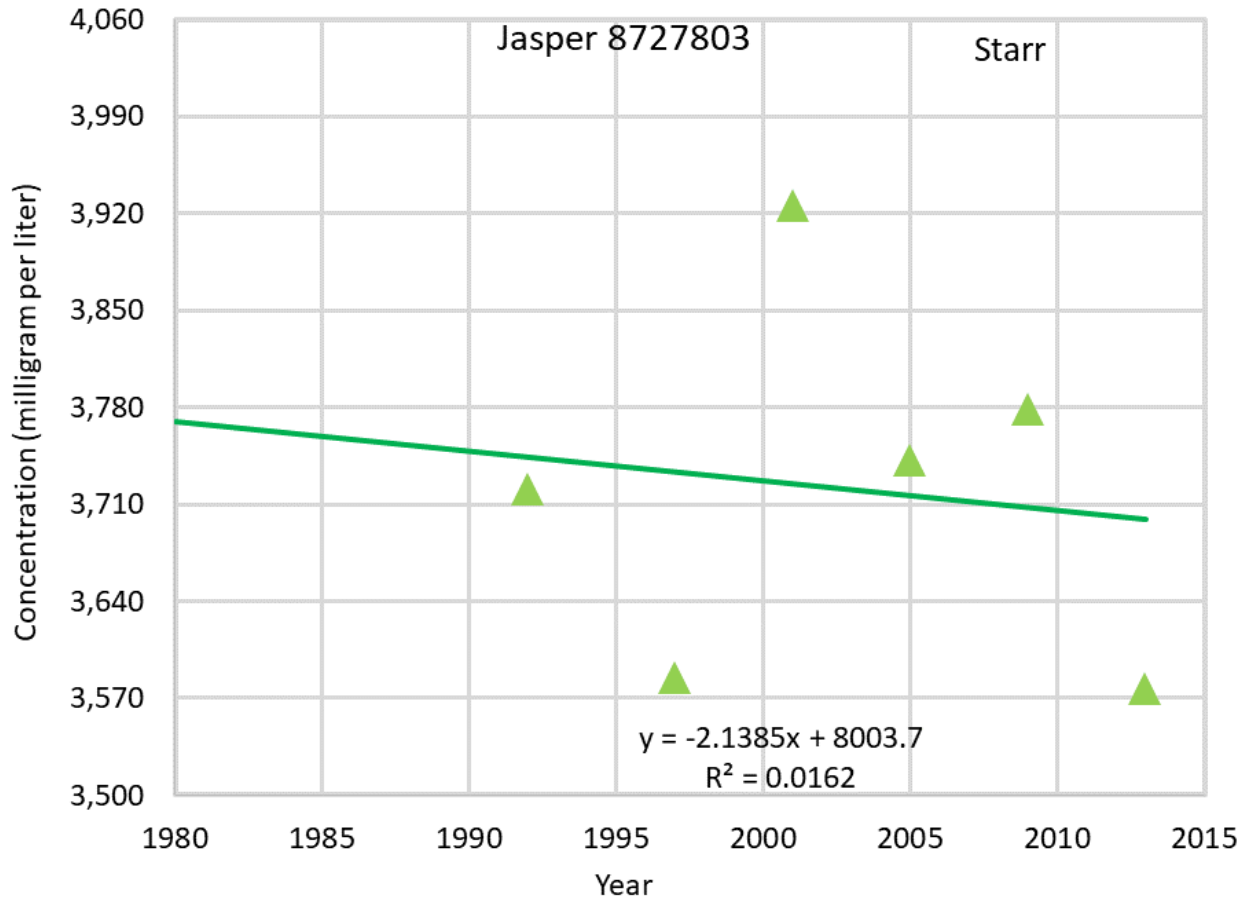


**Figure F75 Hydrograph of total dissolved solids at State Well 8727803.**

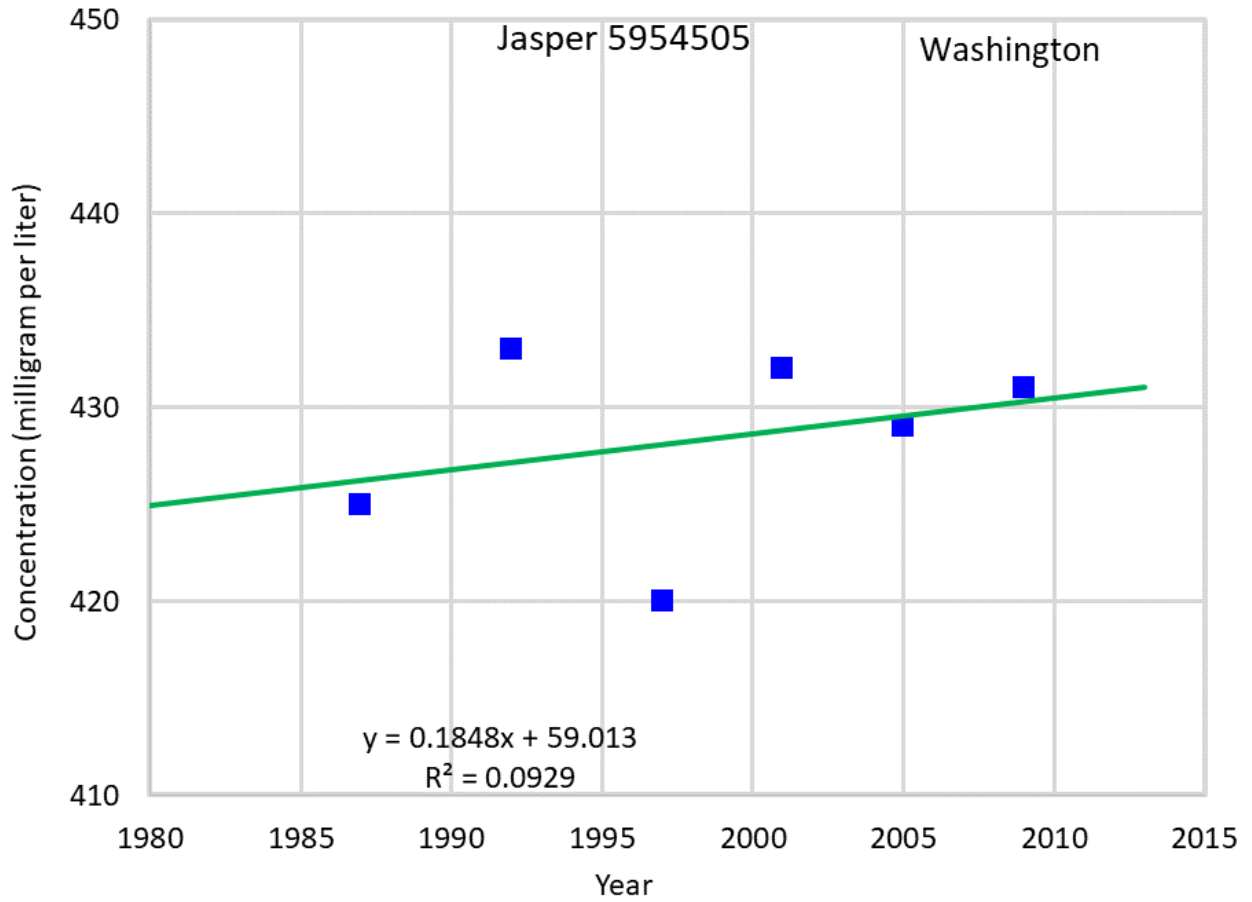


**Figure F76 Hydrograph of total dissolved solids at State Well 5954505.**